Scientific and Technical Aerospace Reports

STAR

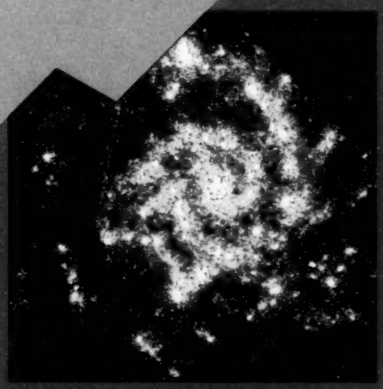

An Abstract Journal

NASA STI PROGRAM SCIENTIFIC & TECHNICAL INFORMATION

Volume 30, Number 21
November 8, 1992
N92-30233 to N92-31237

Scientific and Technical Aerospace Reports

Scientific and Technical Aerospace Reports (STAR) is an abstract journal that provides comprehensive coverage of worldwide aerospace-related reports. It is a major product of the International Aerospace Database managed by the NASA Scientific and Technical Information (STI) Program. The coverage includes reports on aeronautics, space, and supporting disciplines. *STAR* lists current, publicly available reports entered into the NASA STI Database during the 2-week period preceding publication. A typical citation and abstract appear on page viii. They explain how to read the items that are announced in this journal.

NASA sponsors a companion journal, *International Aerospace Abstracts (IAA)* (*NOVA* for internal NASA use) that lists abstracts of the open literature on aerospace subjects available worldwide. *IAA* is available for sale through the AIAA.

Entries found in *STAR* and *IAA* are available through NASA's online service, RECON, as the International Aerospace Database and through DIALOG as the Aerospace Database.

Information on aerospace and related subjects is gathered by the NASA STI Program through national and international agreements and exchanges and is made available to the NASA community as well as to the public in many forms through various outlets. The section on NASA STI Program Products and Services contains additional information.

For further information please contact:
NASA Center for AeroSpace Information (CASI)
P.O. Box 8757
Baltimore, Maryland 21240-0757
(301) 621-0390

US ISSN 0036-8741

Volume 30 Number 21 / November 8, 1992

TABLE OF CONTENTS

AERONAUTICS For related information see also *Astronautics.*

01 AERONAUTICS (GENERAL) **3573**

02 AERODYNAMICS **3573**
Includes aerodynamics of bodies, combinations, wings, rotors, and control surfaces; and internal flow in ducts and turbomachinery. For related information see also *34 Fluid Mechanics and Heat Transfer.*

03 AIR TRANSPORTATION AND SAFETY **3577**
Includes passenger and cargo air transport operations; and aircraft accidents. For related information see also *16 Space Transportation* and *85 Urban Technology and Transportation.*

04 AIRCRAFT COMMUNICATIONS AND NAVIGATION **3579**
Includes digital and voice communication with aircraft; air navigation systems (satellite and ground based); and air traffic control. For related information see also *17 Space Communications, Spacecraft Communications, Command and Tracking* and *32 Communications and Radar.*

05 AIRCRAFT DESIGN, TESTING AND PERFORMANCE **3579**
Includes aircraft simulation technology. For related information see also *18 Spacecraft Design, Testing and Performance* and *39 Structural Mechanics.* For land transportation vehicles see *85 Urban Technology and Transportation.*

06 AIRCRAFT INSTRUMENTATION **3581**
Includes cockpit and cabin display devices; and flight instruments. For related information see also *19 Space craft Instrumentation* and *35 Instrumentation and Photography.*

07 AIRCRAFT PROPULSION AND POWER **3581**
Includes prime propulsion systems and systems components, e.g., gas turbine engines and compressors; and onboard auxiliary power plants for aircraft. For related information see also *20 Spacecraft Propulsion and Power, 28 Propellants and Fuels,* and *44 Energy Production and Conversion.*

08 AIRCRAFT STABILITY AND CONTROL **3583**
Includes aircraft handling qualities; piloting; flight controls; and autopilots. For related information see also *05 Aircraft Design, Testing and Performance.*

09 RESEARCH AND SUPPORT FACILITIES (AIR) **3584**
Includes airports, hangars and runways; aircraft repair and overhaul facilities; wind tunnels; shock tubes; and aircraft engine test stands. For related information see also *14 Ground Support Systems and Facilities (Space).*

ASTRONAUTICS For related information see also *Aeronautics.*

12 ASTRONAUTICS (GENERAL) ..... **N.A.**
For extraterrestrial exploration see *91 Lunar and Planetary Exploration.*

13 ASTRODYNAMICS ..... **N.A.**
Includes powered and free-flight trajectories; and orbital and launching dynamics.

14 GROUND SUPPORT SYSTEMS AND FACILITIES (SPACE) **3585**
Includes launch complexes, research and production facilities; ground support equipment, e.g., mobile transporters; and simulators. For related information see also *09 Research and Support Facilities (Air).*

15 LAUNCH VEHICLES AND SPACE VEHICLES **3586**
Includes boosters; operating problems of launch/space vehicle systems; and reusable vehicles. For related information see also *20 Spacecraft Propulsion and Power.*

16 SPACE TRANSPORTATION **3586**
Includes passenger and cargo space transportation, e.g., shuttle operations; and space rescue techniques. For related information see also *03 Air Transportation and Safety* and *18 Spacecraft Design, Testing and Performance.* For space suits see *54 Man/System Technology and Life Support.*

17 SPACE COMMUNICATIONS, SPACECRAFT COMMUNICATIONS, COMMAND AND TRACKING . **3587**
Includes telemetry; space communications networks; astronavigation and guidance; and radio blackout. For related information see also *04 Aircraft Communications and Navigation* and *32 Communications and Radar.*

N.A.—no abstracts were assigned to this category for this issue.

18 SPACECRAFT DESIGN, TESTING AND PERFORMANCE **3587**
Includes satellites; space platforms; space stations; spacecraft systems and components such as thermal and environmental controls; and attitude controls. For life support systems see *54 Man/System Technology and Life Support.* For related information see also *05 Aircraft Design, Testing and Performance, 39 Structural Mechanics,* and *16 Space Transportation.*

19 SPACECRAFT INSTRUMENTATION **3588**
For related information see also *06 Aircraft Instrumentation* and *35 Instrumentation and Photography.*

20 SPACECRAFT PROPULSION AND POWER **3588**
Includes main propulsion systems and components, e.g., rocket engines; and spacecraft auxiliary power sources. For related information see also *07 Aircraft Propulsion and Power, 28 Propellants and Fuels, 44 Energy Production and Conversion,* and *15 Launch Vehicles and Space Vehicles.*

CHEMISTRY AND MATERIALS

23 CHEMISTRY AND MATERIALS (GENERAL) ..... **N.A.**

24 COMPOSITE MATERIALS **3590**
Includes physical, chemical, and mechanical properties of laminates and other composite materials. For ceramic materials see *27 Nonmetallic Materials.*

25 INORGANIC AND PHYSICAL CHEMISTRY **3593**
Includes chemical analysis, e.g., chromatography; combustion theory; electrochemistry; and photochemistry. For related information see also *77 Thermodynamics and Statistical Physics.*

26 METALLIC MATERIALS **3597**
Includes physical, chemical, and mechanical properties of metals, e.g., corrosion; and metallurgy.

27 NONMETALLIC MATERIALS **3601**
Includes physical, chemical, and mechanical properties of plastics, elastomers, lubricants, polymers, textiles, adhesives, and ceramic materials. For composite materials see *24 Composite Materials.*

28 PROPELLANTS AND FUELS **3607**
Includes rocket propellants, igniters and oxidizers; their storage and handling procedures; and aircraft fuels. For related information see also *07 Aircraft Propulsion and Power, 20 Spacecraft Propulsion and Power,* and *44 Energy Production and Conversion.*

29 MATERIALS PROCESSING **3608**
Includes space-based development of products and processes for commercial application. For biological materials see *55 Space Biology.*

ENGINEERING For related information see also *Physics.*

31 ENGINEERING (GENERAL) **3612**
Includes vacuum technology; control engineering; display engineering; cryogenics; and fire prevention.

32 COMMUNICATIONS AND RADAR **3613**
Includes radar; land and global communications; communications theory; and optical communications. For related information see also *04 Aircraft Communications and Navigation* and *17 Space Communications, Spacecraft Communications, Command and Tracking.* For search and rescue see *03 Air Transportation and Safety,* and *16 Space Transportation.*

33 ELECTRONICS AND ELECTRICAL ENGINEERING **3622**
Includes test equipment and maintainability; components, e.g., tunnel diodes and transistors; microminiaturization; and integrated circuitry. For related information see also *60 Computer Operations and Hardware* and *76 Solid-State Physics.*

34 FLUID MECHANICS AND HEAT TRANSFER **3627**
Includes boundary layers; hydrodynamics; fluidics; mass transfer and ablation cooling. For related information see also *02 Aerodynamics* and *77 Thermodynamics and Statistical Physics.*

35 INSTRUMENTATION AND PHOTOGRAPHY **3636**
Includes remote sensors; measuring instruments and gauges; detectors; cameras and photographic supplies; and holography. For aerial photography see *43 Earth Resources and Remote Sensing.* For related information see also *06 Aircraft Instrumentation* and *19 Spacecraft Instrumentation.*

36 LASERS AND MASERS **3656**
Includes parametric amplifiers. For related information see also *76 Solid-State Physics.*

37 MECHANICAL ENGINEERING **3658**
Includes auxiliary systems (nonpower); machine elements and processes; and mechanical equipment.

38 QUALITY ASSURANCE AND RELIABILITY **3660**
Includes product sampling procedures and techniques; and quality control.

39 STRUCTURAL MECHANICS **3661**
Includes structural element design and weight analysis; fatigue; and thermal stress. For applications see *05 Aircraft Design, Testing and Performance* and *18 Spacecraft Design, Testing and Performance.*

GEOSCIENCES For related information see also *Space Sciences.*

42 GEOSCIENCES (GENERAL) ..... **N.A.**

43 EARTH RESOURCES AND REMOTE SENSING **3666**
Includes remote sensing of earth resources by aircraft and spacecraft; photogrammetry; and aerial photography. For instrumentation see *35 Instrumentation and Photography.*

44 ENERGY PRODUCTION AND CONVERSION **3670**
Includes specific energy conversion systems, e.g., fuel cells; global sources of energy; geophysical conversion; and windpower. For related information see also *07 Aircraft Propulsion and Power, 20 Spacecraft Propulsion and Power,* and *28 Propellants and Fuels.*

45 ENVIRONMENT POLLUTION **3672**
Includes atmospheric, noise, thermal, and water pollution.

46 GEOPHYSICS **3675**
Includes aeronomy; upper and lower atmosphere studies; ionospheric and magnetospheric physics; and geomagnetism. For space radiation see *93 Space Radiation.*

47 METEOROLOGY AND CLIMATOLOGY **3678**
Includes weather forecasting and modification.

48 OCEANOGRAPHY **3681**
Includes biological, dynamic, and physical oceanography; and marine resources. For related information see also *43 Earth Resources and Remote Sensing.*

LIFE SCIENCES

51 LIFE SCIENCES (GENERAL) **3683**

52 AEROSPACE MEDICINE **3684**
Includes physiological factors; biological effects of radiation; and effects of weightlessness on man and animals.

53 BEHAVIORAL SCIENCES **3686**
Includes psychological factors; individual and group behavior; crew training and evaluation; and psychiatric research.

54 MAN/SYSTEM TECHNOLOGY AND LIFE SUPPORT **3688**
Includes human engineering; biotechnology; and space suits and protective clothing. For related information see also *16 Space Transportation.*

55 SPACE BIOLOGY ..... **N.A.**
Includes exobiology; planetary biology; and extraterrestrial life.

MATHEMATICAL AND COMPUTER SCIENCES

59 MATHEMATICAL AND COMPUTER SCIENCES (GENERAL) **3689**

60 COMPUTER OPERATIONS AND HARDWARE **3689**
Includes hardware for computer graphics, firmware, and data processing. For components see *33 Electronics and Electrical Engineering.*

61 COMPUTER PROGRAMMING AND SOFTWARE **3691**
Includes computer programs, routines, algorithms, and specific applications, e.g., CAD/CAM.

62 COMPUTER SYSTEMS **3698**
Includes computer networks and special application computer systems.

63 CYBERNETICS **3700**
Includes feedback and control theory, artificial intelligence, robotics and expert systems. For related information see also *54 Man/System Technology and Life Support.*

64 NUMERICAL ANALYSIS **3701**
Includes iteration, difference equations, and numerical approximation.

65 STATISTICS AND PROBABILITY **3707**
Includes data sampling and smoothing; Monte Carlo method; and stochastic processes.

66 SYSTEMS ANALYSIS **3708**
Includes mathematical modeling; network analysis; and operations research.

67 THEORETICAL MATHEMATICS **3709**
Includes topology and number theory.

PHYSICS For related information see also *Engineering.*

70 PHYSICS (GENERAL) **3710**
For precision time and time interval (PTTI) see *35 Instrumentation and Photography;* for geophysics, astrophysics or solar physics see *46 Geophysics, 90 Astrophysics,* or *92 Solar Physics.*

71 ACOUSTICS **3711**
Includes sound generation, transmission, and attenuation. For noise pollution see *45 Environment Pollution.*

72 ATOMIC AND MOLECULAR PHYSICS **3711**
Includes atomic structure, electron properties, and molecular spectra.

73 NUCLEAR AND HIGH-ENERGY PHYSICS **3717**
Includes elementary and nuclear particles; and reactor theory. For space radiation see *93 Space Radiation.*

74 OPTICS **3719**
Includes light phenomena and optical devices. For lasers see *36 Lasers and Masers.*

75 PLASMA PHYSICS **3722**
Includes magnetohydrodynamics and plasma fusion. For ionospheric plasmas see *46 Geophysics.* For space plasmas see *90 Astrophysics.*

76 SOLID-STATE PHYSICS **3727**
Includes superconductivity. For related information see also *33 Electronics and Electrical Engineering* and *36 Lasers and Masers.*

77 THERMODYNAMICS AND STATISTICAL PHYSICS **3731**
Includes quantum mechanics; theoretical physics; and Bose and Fermi statistics. For related information see also *25 Inorganic and Physical Chemistry* and *34 Fluid Mechanics and Heat Transfer.*

SOCIAL SCIENCES

80 SOCIAL SCIENCES (GENERAL) **3732**
Includes educational matters.

81 ADMINISTRATION AND MANAGEMENT **3732**
Includes management planning and research.

82 DOCUMENTATION AND INFORMATION SCIENCE **3734**
Includes information management; information storage and retrieval technology; technical writing; graphic arts; and micrography. For computer documentation see *61 Computer Programming and Software.*

83 ECONOMICS AND COST ANALYSIS ..... **N.A.**
Includes cost effectiveness studies.

84 LAW, POLITICAL SCIENCE AND SPACE POLICY **3735**
Includes NASA appropriation hearings; aviation law; space law and policy; international law; international cooperation; and patent policy.

85 URBAN TECHNOLOGY AND TRANSPORTATION **3736**
Includes applications of space technology to urban problems; technology transfer; technology assessment; and surface and mass transportation. For related information see *03 Air Transportation and Safety, 16 Space Transportation,* and *44 Energy Production and Conversion.*

SPACE SCIENCES For related information see also *Geosciences*.

88 SPACE SCIENCES (GENERAL) **3736**

89 ASTRONOMY **3739**
Includes radio, gamma-ray, and infrared astronomy; and astrometry.

90 ASTROPHYSICS **3740**
Includes cosmology; celestial mechanics; space plasmas; and interstellar and interplanetary gases and dust. For related information see also *75 Plasma Physics*.

91 LUNAR AND PLANETARY EXPLORATION **3741**
Includes planetology; and manned and unmanned flights. For spacecraft design or space stations see *18 Spacecraft Design, Testing and Performance*.

92 SOLAR PHYSICS **3742**
Includes solar activity, solar flares, solar radiation and sunspots. For related information see *93 Space Radiation*.

93 SPACE RADIATION **3743**
Includes cosmic radiation; and inner and outer earth's radiation belts. For biological effects of radiation see *52 Aerospace Medicine*. For theory see *73 Nuclear and High-Energy Physics*.

GENERAL

Includes aeronautical, astronautical, and space science related histories, biographies, and pertinent reports too broad for categorization; histories or broad overviews of NASA programs.

99 GENERAL **3744**

SUBJECT INDEX **I-1**

PERSONAL AUTHOR INDEX **I-77**

CORPORATE SOURCE INDEX **I-87**

CONTRACT NUMBER INDEX **I-101**

REPORT NUMBER INDEX **I-105**

ACCESSION NUMBER INDEX **I-113**

APPENDIX **A-1**

TYPICAL CITATION AND ABSTRACT

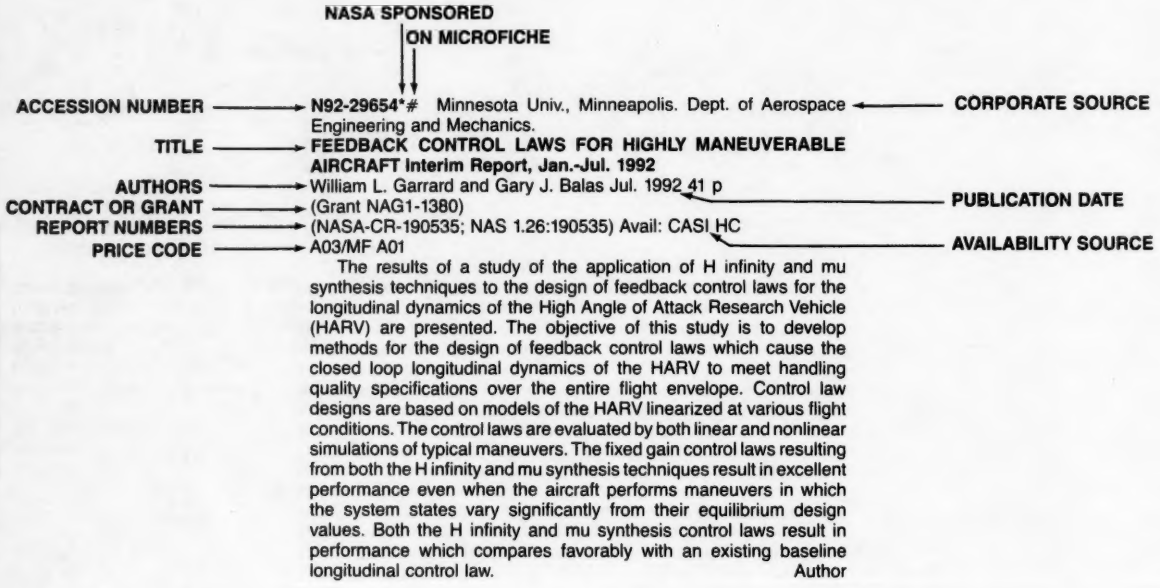
NASA SPONSORED
ON MICROFICHE
ACCESSION NUMBER
N92-29654*# Minnesota Univ., Minneapolis. Dept. of Aerospace Engineering and Mechanics.
CORPORATE SOURCE
TITLE
FEEDBACK CONTROL LAWS FOR HIGHLY MANEUVERABLE AIRCRAFT Interim Report, Jan.-Jul. 1992
AUTHORS
William L. Garrard and Gary J. Balas Jul. 1992 41 p
PUBLICATION DATE
CONTRACT OR GRANT
(Grant NAG1-1380)
REPORT NUMBERS
(NASA-CR-190535; NAS 1.26:190535) Avail: CASI HC
AVAILABILITY SOURCE
PRICE CODE
A03/MF A01
The results of a study of the application of H infinity and mu synthesis techniques to the design of feedback control laws for the longitudinal dynamics of the High Angle of Attack Research Vehicle (HARV) are presented. The objective of this study is to develop methods for the design of feedback control laws which cause the closed loop longitudinal dynamics of the HARV to meet handling quality specifications over the entire flight envelope. Control law designs are based on models of the HARV linearized at various flight conditions. The control laws are evaluated by both linear and nonlinear simulations of typical maneuvers. The fixed gain control laws resulting from both the H infinity and mu synthesis techniques result in excellent performance even when the aircraft performs maneuvers in which the system states vary significantly from their equilibrium design values. Both the H infinity and mu synthesis control laws result in performance which compares favorably with an existing baseline longitudinal control law.
Author

VOLUME 30 NUMBER 21 / NOVEMBER 8, 1992

Scientific and Technical Aerospace Reports

A Semimonthly Publication of the National Aeronautics and Space Administration

01 AERONAUTICS (GENERAL)

N92-30253# North Carolina Agricultural and Technical State Univ., Greensboro.
MODEL ANALYSIS AND EXPERT SYSTEM DEVELOPMENT FOR PLANNING AND SCHEDULING TELEOPERATIONS FOR AIRCRAFT TURNAROUND FUNCTIONS, VOLUME 1 Final Report, Jun. 1988 - Jul. 1991
Eui H. Park and Celestine A. Ntuen Feb. 1992 98 p
(Contract F33615-88-C-3400)
(AD-A251037; WL-TR-91-3107-Vol-1) Avail: CASI HC A05/MF A02

This report summarizes the results of a 3-year effort to study the planning and scheduling of aircraft turnaround functions using an expert system to minimize the turnaround time. This effort established the feasibility of using expert system technology to model aircraft turnaround functions in a teleoperated environment. The model 'opportunistically' generates schedules based on aircraft turnaround functions (refueling, weapons loading, aircraft inspection, maintenance, etc.) and personnel assignments and automation technologies. The model is conceptualized for a dynamic environment. Thus, it is possible for the model to consult its knowledge base in order to identify scheduling strategies to maximize aircraft turnaround efficiency for a particular function.
GRA

N92-30258# North Carolina Agricultural and Technical State Univ., Greensboro.
MODEL ANALYSIS AND EXPERT SYSTEM DEVELOPMENT FOR PLANNING AND SCHEDULING TELEOPERATIONS FOR AIRCRAFT TURNAROUND FUNCTIONS. VOLUME 2: TOP USER'S GUIDE Final Report, Jul. 1988 - Jul. 1991
Eui H. Park and Celestine A. Ntuen Feb. 1992 48 p
(Contract F33615-88-C-3400)
(AD-A251083; WL-TR-91-3107-Vol-2) Avail: CASI HC A03/MF A01

This report summarizes the results of a 3-year effort to study the planning and scheduling of aircraft turnaround functions using an expert system to minimize the turnaround time. This effort established the feasibility of using expert system technology to model aircraft turnaround functions in a teleoperated environment. The model opportunistically generates schedules based on aircraft turnaround functions (refueling, weapons loading, aircraft inspection, maintenance, etc.) and personnel assignments and automation technologies. The model is conceptualized for a dynamic environment. Thus, it is possible for the model to consult its knowledge base in order to identify scheduling strategies to maximize aircraft turnaround efficiency for a particular function.
GRA

N92-30675# Messerschmitt-Boelkow-Blohm G.m.b.H., Munich (Germany, F.R.). Military Aircraft Div.
NUMERICAL OPTIMIZATION IN GERMANY: A NON-EXHAUSTIVE SURVEY ON CURRENT ACTIVITIES WITH EMPHASIS ON AERONAUTICS
Luciano Fornasier Oct. 1991 21 p Presented at the 3rd Internatiaonal Conference on Inverse Design Concept and 1991
(MBB/FE211/S/PUB/474; ETN-92-91906) Copyright Avail: CASI HC A03/MF A01

Without claim to completeness, some recent progresses achieved in development and application of numerical optimization methods are presented. With emphasis lying on aeronautical problems, the activities in the field of aerodynamic design by Computational Fluid Dynamics (CFD) methods, structural optimization and determination of optimal flight trajectories are surveyed. As the reviewed methods show different levels of mathematical background, capability, maturity and applicability, the need for a stronger exchange of information and experience between the different disciplines emerges as a key factor for increasing the impact of numerical optimization strategies in the design process.
ESA

02 AERODYNAMICS

Includes aerodynamics of bodies, combinations, wings, rotors, and control surfaces; and internal flow in ducts and turbomachinery.

For related information see also *34 Fluid Mechanics and Heat Transfer.*

N92-30239# Lowell Univ., MA.
SELECTION OF OPENING MODEL FOR PARACHUTE SCALING STUDIES Final Report, Jan. 1990 - Jun. 1991
Eugene E. Niemi, Jr. Mar. 1992 50 p
(AD-A250882; NATICK-TR-92/009) Avail: CASI HC A03/MF A01

This report consists of a summary of work to program an existing parachute opening dynamics theory for use with research into the scaling laws governing relationships between model and full-scale parachutes during the opening phase. The theory forms a basis to which modifications can be made to predict the opening dynamics of small-scale models. The object is eventually to be able to predict canopy stiffness effects on opening behavior.
GRA

N92-30295*# National Aeronautics and Space Administration. Langley Research Center, Hampton, VA.
VALIDATION OF THREE-DIMENSIONAL INCOMPRESSIBLE SPATIAL DIRECT NUMERICAL SIMULATION CODE: A COMPARISON WITH LINEAR STABILITY AND PARABOLIC STABILITY EQUATION THEORIES FOR BOUNDARY-LAYER TRANSITION ON A FLAT PLATE
Ronald D. Joslin, Craig L. Streett, and Chau-Lyan Chang (High Technology Corp., Hampton, VA.) Jul. 1992 49 p
(RTOP 505-59-50-01)
(NASA-TP-3205; L-17026; NAS 1.60:3205) Avail: CASI HC A03/MF A01

Spatially evolving instabilities in a boundary layer on a flat plate are computed by direct numerical simulation (DNS) of the incompressible Navier-Stokes equations. In a truncated physical domain, a nonstaggered mesh is used for the grid. A Chebyshev-collocation method is used normal to the wall; finite difference and compact difference methods are used in the streamwise direction; and a Fourier series is used in the spanwise

Runge-Kutta schemes are used to the time-splitting method. The influence-matrix technique is used to solve the pressure equation. At the outflow boundary, the buffer-domain technique is used to prevent convective wave reflection or upstream propagation of information from the boundary. Results of the DNS are compared with those from both linear stability theory (LST) and parabolized stability equation (PSE) theory. Computed disturbance amplitudes and phases are in very good agreement with those of LST (for small inflow disturbance amplitudes). A measure of the sensitivity of the inflow condition is demonstrated with both LST and PSE theory used to approximate inflows. Although the DNS numerics are very different than those of PSE theory, the results are in good agreement. A small discrepancy in the results that does occur is likely a result of the variation in PSE boundary condition treatment in the far field. Finally, a small-amplitude wave triad is forced at the inflow, and simulation results are compared with those of LST. Again, very good agreement is found between DNS and LST results for the 3-D simulations, the implication being that the disturbance amplitudes are sufficiently small that nonlinear interactions are negligible. Author

N92-30298*# Pratt and Whitney Aircraft, East Hartford, CT. Commercial Engine Business.

ULTRA HIGH BYPASS NACELLE AERODYNAMICS INLET FLOW-THROUGH HIGH ANGLE OF ATTACK DISTORTION TEST Final Report

Michael J. Larkin and Paul S. Schweiger Jul. 1992 73 p
(Contract NAS3-25952; RTOP 535-03-10)
(NASA-CR-189149; NAS 1.26:189149; PWA-6354) Avail: CASI HC A04/MF A01

A flow-through inlet test program was conducted to evaluate inlet test methods and determine the impact of the fan on inlet separation when operating at large angles of attack. A total of 16 model configurations of approximately 1/6 scale were tested. A comparison of these flow-through results with powered data indicates the presence of the fan increased separation operation 3 degrees to 4 degrees over the flow through inlet. Rods and screens located at the fan face station, that redistribute the flow, achieved simulation of the powered-fan results for separation angle of attack. Concepts to reduce inlet distortion and increase angle of attack capability were also evaluated. Vortex generators located on the inlet surface increased inlet angle of attack capability up to 2 degrees and reduced inlet distortion in the separated region. Finally, a method of simulating the fan/inlet aerodynamic interaction using blockage sizing method has been defined. With this method, a static blockage device used with a flow-through model will approximate the same inlet onset of separation angle of attack and distortion pattern that would be obtained with an inlet model containing a powered fan. Author

N92-30367# Sandia National Labs., Albuquerque, NM.

JOINT COMPUTATIONAL AND EXPERIMENTAL AERODYNAMICS RESEARCH ON A HYPERSONIC VEHICLE

W. L. Oberkampf, D. P. Aeschliman, and M. M. Walker 1992 35 p Presented at the Advisory Group for Aerospace Research and Development (AGARD) Fluid Dynamics Panel Symposium on Theoretical and Experimental Methods in Hypersonic Flows, Torino (Italy), 5-7 May 1992
(Contract DE-AC04-76DP-00789)
(DE92-013439; SAND-92-0919C; CONF-920534-2) Avail: CASI HC A03/MF A01

A closely coupled computational and experimental aerodynamics research program was conducted on a hypersonic vehicle configuration at Mach 8. Aerodynamic force and moment measurements and flow visualization results were obtained in the Sandia National Laboratories hypersonic wind tunnel for laminar boundary layer conditions. Parabolized and iterative Navier-Stokes simulations were used to predict flow fields and forces and moments on the hypersonic configuration. The basic vehicle configuration is a spherically blunted 10 degree cone with a slice parallel with the axis of the vehicle. On the slice portion of the vehicle, a flap can be attached so that deflection angles of 10, 20, and 30 degrees can be obtained. Comparisons are made between experimental and computational results to evaluate quality of each and to identify areas where improvements are needed. This extensive set of high-quality experimental force and moment measurements is recommended for use in the calibration and validation of computational aerodynamics codes. DOE

N92-30392*# Maryland Univ., College Park. Dept. of Aerospace Engineering.

NAVIER-STOKES COMPUTATIONS OF A VISCOUS OPTIMIZED WAVERIDER M.S. Thesis

Naruhisa Takashima Jun. 1992 102 p
(Grant NAG1-1192; RTOP 505-59-40-10)
(NASA-CR-189658; NAS 1.26:189658; UM-AERO-92-08) Avail: CASI HC A06/MF A02

The performance of a Mach 6 viscous optimized waverider was calculated using the 3-D Navier-Stokes equations. The Mach 6 viscous optimized waverider was generated using MAXWARP, a code developed at the University of Maryland. The computations were performed using CFL3D, an implicit upwind-biased finite-volume algorithm developed at NASA Langley. Results show that good agreement was found between the calculated performance by MAXWARP and results from the Mach 6 Navier-Stokes computation. Furthermore, off-design performance of the Mach 6 optimized waverider was computed at Mach 4 and 8. The performance at these Mach numbers compared well with the performance of the viscous optimized waveriders specifically designed for these Mach numbers. Finally, contours of different flow parameters in the cross-flow plane were examined for the three calculations. The results indicate that the flow gradients are relatively small within the captured flow, and the variation itself is well behaved; thus, making the waverider configuration a promising choice for an engine/airframe design, especially for cruise-type applications. Author

N92-30393*# National Aeronautics and Space Administration. Langley Research Center, Hampton, VA.

PROGRESS IN UNSTRUCTURED-GRID METHODS DEVELOPMENT FOR UNSTEADY AERODYNAMIC APPLICATIONS

John T. Batina Jul. 1992 13 p Presented at the 7th IMACS International Conference on Computer Methods for Partial Differential Equations, New Brunswick, NJ, 22-24 Jun. 1992
(RTOP 505-63-50-12)
(NASA-TM-107643; NAS 1.15:107643) Avail: CASI HC A03/MF A01

The development of unstructured-grid methods for the solution of the equations of fluid flow and what was learned over the course of the research are summarized. The focus of the discussion is on the solution of the time-dependent Euler equations including spatial discretizations, temporal discretizations, and boundary conditions. An example calculation with an implicit upwind method using a CFL number of infinity is presented for the Boeing 747 aircraft. The results were obtained in less than one hour CPU time on a Cray-2 computer, thus, demonstrating the speed and robustness of the capability. Additional calculations for the ONERA M6 wing demonstrate the accuracy of the method through the good agreement between calculated results and experimental data for a standard transonic flow case. Author

N92-30394*# National Aeronautics and Space Administration. Langley Research Center, Hampton, VA.

TWO-DIMENSIONAL AERODYNAMIC CHARACTERISTICS OF SEVERAL POLYGON-SHAPED CROSS-SECTIONAL MODELS APPLICABLE TO HELICOPTER FUSELAGES

Henry L. Kelley, Cynthia A. Crowell, and John C. Wilson Aug. 1992 30 p
(DA Proj. 1L2-36003-D-313; RTOP 505-59-36-01)
(NASA-TP-3233; L-16951; NAS 1.60:3233;
AVSCOM-TR-92-B-002) Avail: CASI HC A03/MF A01

A wind-tunnel investigation was conducted to determine 2-D aerodynamic characteristics of nine polygon-shaped models applicable to helicopter fuselages. The models varied from 1/2 to 1/5 scale and were nominally triangular, diamond, and rectangular

in shape. Side force and normal force were obtained at increments of angle of flow incidence from -45 to 90 degrees. The data were compared with results from a baseline UH-60 tail-boom cross-section model. The results indicate that the overall shapes of the plots of normal force and side force were similar to the characteristic shape of the baseline data; however, there were important differences in magnitude. At a flow incidence of 0 degrees, larger values of normal force for the polygon models indicate an increase in fuselage down load of 1 to 2.5 percent of main-rotor thrust compared with the baseline value. Also, potential was indicated among some of the configurations to produce high fuselage side forces and yawing moments compared with the baseline model. Author

N92-30514# European Space Agency, Paris (France).
COMPUTATION OF UNSTEADY TRANSONIC FLOWS USING AN IMPLICIT CENTERED EULER SOLVER WITHOUT ARTIFICIAL VISCOSITY
Anne-Sophie Sens (Office National d'Etudes et de Recherches Aerospatiales, Paris, France) Mar. 1992 105 p Transl. into ENGLISH of Calcul d'Ecoulements Transsoniques Instationnaires par Resolution Implicite Centree des Equations d'Euler sans Viscosite Artificielle (Paris, France, ONERA), Sep. 1990 98 p Original language document was announced as N91-12633
(ESA-TT-1235; ONERA-NT-1990-8; ETN-92-91709) Avail: CASI HC A06/MF A02

The numerical simulation of unsteady transonic flows is presented. The solution of the Euler equations using an extension of Lerat's second order accurate, centered implicit scheme is used. When applied as an unsteady method for determining steady solutions, the scheme has the advantage of working without artificial viscosity, and the aim of this study is to extend this property to the case of truly unsteady problems. The approximations are developed in one dimension. The two timestep scheme is extended to two dimensions following the approach of Lerat and Sides for the steady case. A stability result on the scalar case is given. The method is applied to the computation of the unsteady transonic flow around an airfoil in rigid body motion. A three dimensional validation of the two timestep method is proposed for the problem of the swept wing oscillating in translation between parallel walls. ESA

N92-30570*# National Aeronautics and Space Administration. Langley Research Center, Hampton, VA.
A GRIDLESS EULER/NAVIER-STOKES SOLUTION ALGORITHM FOR COMPLEX TWO-DIMENSIONAL APPLICATIONS
John T. Batina Jun. 1992 25 p
(RTOP 505-63-50-12)
(NASA-TM-107631; NAS 1.15:107631) Avail: CASI HC A03/MF A01

The development of a gridless computational fluid dynamics (CFD) method for the solution of the two-dimensional Euler and Navier-Stokes equations is described. The method uses only clouds of points and does not require that the points be connected to form a grid as is necessary in conventional CFD algorithms. The gridless CFD approach appears to resolve the problems and inefficiencies encountered with structured or unstructured grid methods. As a result, the method offers the greatest potential for accurately and efficiently solving viscous flows about complex aircraft configurations. The method is described in detail, and calculations are presented for standard Euler and Navier-Stokes cases to assess the accuracy and efficiency of the capability. Author

N92-30676# Messerschmitt-Boelkow-Blohm G.m.b.H., Munich (Germany, F.R.). Military Aircraft Div.
CFD CONTRIBUTIONS DURING HYPERSONIC AIRPLANE INTAKE DESIGN
N. C. Bissinger and A. Eberle Jul. 1991 28 p
(MBB/FE213/S/PUB/459; ETN-92-91907) Copyright Avail: CASI HC A03/MF A01

Numerical elements of an advanced Computational Fluid Dynamics (CFD) code regarding computational speed and accuracy are addressed. With increasing Mach number of high speed vehicles there is a growing need for the design people to get information on the steadily growing complexity of the flows outside and inside these airplanes. Results of several calculations performed to gain insight into the flow in hypersonic intakes are presented. ESA

N92-30691*# National Aeronautics and Space Administration. Langley Research Center, Hampton, VA.
IMPLICIT UPWIND-EULER SOLUTION ALGORITHMS FOR UNSTRUCTURED-GRID APPLICATIONS
John T. Batina Jul. 1992 9 p Presented at the First European Computational Dynamics Conference, Brussels, Belgium, 7-11 Sep. 1992
(RTOP 505-63-50-12)
(NASA-TM-107645; NAS 1.15:107645) Avail: CASI HC A02/MF A01

The development of implicit upwind algorithms for the solution of the three-dimensional, time-dependent Euler equations on unstructured tetrahedral meshes is described. The implicit temporal discretization involves either a two-sweep Gauss-Seide relaxation procedure, a two-sweep Point-Jacobi relaxation procedure, or a single-sweep Point-Implicit procedure; the upwind spatial discretization is based on the flux-difference splitting of Roe. Detailed descriptions of the three implicit solution algorithms are given, and calculations for the Boeing 747 transport configuration are presented to demonstrate the algorithms. Advantages and disadvantages of the implicit algorithms are discussed. A steady-state solution for the 747 configuration, obtained at transonic flow conditions using a mesh of over 100,000 cells, required less than one hour of CPU time on a Cray-2 computer, thus demonstrating the speed and robustness of the general capability. Author

N92-30713# Aeronautical Research Inst. of Sweden, Stockholm. Aerodynamics Dept.
MATGRID, A PROGRAM FOR GENERATION OF C-H AND C-O TOPOLOGY GRIDS AROUND WING/BODY CONFIGURATIONS: SOFTWARE DESCRIPTION DOCUMENT
Lars G. Tysell and Sven G. Hedman Dec. 1991 101 p Sponsored by Swedish Board for Technical Development
(FFA-TN-1990-20; ETN-92-91704) Avail: CASI HC A06/MF A02

The software description of MATGRID is given. MATGRID is a computer program for generation of C-H or C-O topology grids for the discretization of flow fields around configurations consisting of a wing alone or a wing and a fuselage. MATRICS (Multicomponent Aircraft Transonic Inviscid Computation System) and MATGRID together form a system of computer programs for the calculation of the flow at cruise condition around wing/body combinations of the type of commercial airliners. The general layout of the program and all major subroutines are described. Also included are subroutine, common block and file cross reference lists, an installation guide, a user's guide, and a mathematical definition document. ESA

N92-30740*# MCAT Inst., San Jose, CA.
NUMERICAL METHODS FOR THE SIMULATION OF COMPLEX MULTI-BODY FLOWS WITH APPLICATIONS FOR THE INTEGRATED SPACE SHUTTLE VEHICLE Progress Report
William M. Chan Apr. 1992 42 p
(Contract NCC2-654)
(NASA-CR-190045; NAS 1.26:190045; MCAT-92-009) Avail: CASI HC A03/MF A01

The following papers are presented: (1) numerical methods for the simulation of complex multi-body flows with applications for the Integrated Space Shuttle vehicle; (2) a generalized scheme for 3-D hyperbolic grid generation; (3) collar grids for intersecting geometric components within the Chimera overlapped grid scheme; and (4) application of the Chimera overlapped grid scheme to simulation of Space Shuttle ascent flows. For individual titles, see N92-30741 through N92-30742.

N92-30741*# MCAT Inst., San Jose, CA.
NUMERICAL METHODS FOR THE SIMULATION OF COMPLEX MULTI-BODY FLOWS WITH APPLICATIONS FOR THE INTEGRATED SPACE SHUTTLE VEHICLE
William M. Chan *In its* Numerical Methods for the Simulation of Complex Multi-Body Flows with Applications for the Integrated Space Shuttle Vehicle Apr. 1992 5 p (For primary document see N92-30740 21-02)
Avail: CASI HC A01/MF A01

This project forms part of the long term computational effort to simulate the time dependent flow over the integrated Space Shuttle vehicle (orbiter, solid rocket boosters (SRB's), external tank (ET), and attach hardware) during its ascent mode for various nominal and abort flight conditions. Due to the limitations of experimental data such as wind tunnel wall effects and the difficulty of safely obtaining valid flight data, numerical simulations are undertaken to supplement the existing data base. This data can then be used to predict the aerodynamic behavior over a wide range of flight conditions. Existing computational results show relatively good overall comparison with experiments but further refinement is required to reduce numerical errors and to obtain finer agreements over a larger parameter space. One of the important goals of this project is to obtain better comparisons between numerical simulations and experiments. In the simulations performed so far, the geometry has been simplified in various ways to reduce the complexity so that useful results can be obtained in a reasonable time frame due to limitations in computer resources. In this project, the finer details of the major components of the Space Shuttle are modeled better by including more complexity in the geometry definition. Smaller components not included in early Space Shuttle simulations will now be modeled and gridded. Author

N92-30742*# MCAT Inst., San Jose, CA.
APPLICATION OF THE CHIMERA OVERLAPPED GRID SCHEME TO SIMULATION OF SPACE SHUTTLE ASCENT FLOWS
Pieter G. Buning (National Aeronautics and Space Administration. Ames Research Center, Moffett Field, CA.), Steven J. Parks (Lockheed Engineering and Sciences Co., Houston, TX.), William M. Chan, and Kevin J. Renze (Iowa State Univ. of Science and Technology, Ames.) *In its* Numerical Methods for the Simulation of Complex Multi-Body Flows with Applications for the Integrated Space Shuttle Vehicle Apr. 1992 7 p Presented at the 4th International Symposium on Computational Fluid Dynamics, Davis, CA, 9-12 Sep. 1991 (For primary document see N92-30740 21-02)
Avail: CASI HC A02/MF A01

Several issues relating to the application of Chimera overlapped grids to complex geometries and flowfields are discussed. These include the addition of geometric components with different grid topologies, gridding for intersecting pieces of geometry, and turbulence modeling in grid overlap regions. Sample results are presented for transonic flow about the Space Shuttle launch vehicle. Comparisons with wind tunnel and flight measured pressures are shown. Author

N92-30747*# National Aeronautics and Space Administration. Langley Research Center, Hampton, VA.
TRAJECTORY FITTING IN FUNCTION SPACE WITH APPLICATION TO ANALYTIC MODELING OF SURFACES
Raymond L. Barger Jul. 1992 15 p
(RTOP 505-59-53-01)
(NASA-TP-3232; L-17054; NAS 1.60:3232) Avail: CASI HC A03/MF A01

A theory for representing a parameter-dependent function as a function trajectory is described. Additionally, a theory for determining a piecewise analytic fit to the trajectory is described. An example is given that illustrates the application of the theory to generating a smooth surface through a discrete set of input cross-section shapes. A simple procedure for smoothing in the parameter direction is discussed, and a computed example is given. Application of the theory to aerodynamic surface modeling is demonstrated by applying it to a blended wing-fuselage surface. Author

N92-30909*# National Aeronautics and Space Administration. Langley Research Center, Hampton, VA.
DIRECT SIMULATION OF HIGH-SPEED MIXING LAYERS
H. S. Mukunda, B. Sekar (General Electric Co., Cincinnati, OH.), M. H. Carpenter, J. Philip Drummond, and Ajay Kumar Jul. 1992 63 p
(RTOP 505-62-40-06)
(NASA-TP-3186; L-16929; NAS 1.60:3186) Avail: CASI HC A04/MF A01

A computational study of a nonreacting high-speed mixing layer is performed. A higher order algorithm with sufficient grid points is used to resolve all relevant scales. In all cases, a temporal free-stream disturbance is introduced. The resulting flow is time-sampled to generate a statistical cross section of the flow properties. The studies are conducted at two convective Mach numbers, three free-stream turbulence intensities, three Reynolds numbers, and two types of initial profiles-hyperbolic tangent (tanh) and boundary layer. The boundary-layer profile leads to more realistic predictions of the transition processes. The predicted transition Reynolds number of 0.18 x 10(exp 6) compares well with experimental data. Normalized vortex spacings for the boundary-layer case are about 3.5 and compare favorably with the 1.5 to 2.5 found in experimental measurements. The tanh profile produces spacings of about 10. The growth rate of the layer is shown to be moderately affected by the initial disturbance field, but comparison with experimental data shows moderate agreement. For the boundary-layer case, it is shown that noise at the Strouhal number of 0.007 is selectively amplified and shows little Reynolds number dependence. Author

N92-30947# Advisory Group for Aerospace Research and Development, Neuilly-Sur-Seine (France). Fluid Dynamics Panel.
VORTEX FLOW AERODYNAMICS [L'AERODYNAMIQUE DES ECOULEMENTS TOURBILLONNAIRES]
J. H. B. Smith (Royal Aircraft Establishment, Farnborough, England), J. F. Campbell (National Aeronautics and Space Administration. Langley Research Center, Hampton, VA.), and A. D. Young, ed. Apr. 1992 27 p Presented at the Fluid Dynamics Panel Symposium, Scheveningen, The Netherlands, 1-4 Oct. 1990
(AGARD-AR-299; ISBN-92-835-0670-7) Copyright Avail: CASI HC A03/MF A01

The principal emphasis of the meeting was to be on the understanding and prediction of separation-induced vortex flows and their effects on vehicle performance, stability, control, and structural design loads. This report shows that a substantial amount of the papers covering this area were received from a wide range of countries, together with an attendance that was even more diverse. In itself, this testifies to the current interest in the subject and to the appropriateness of the Panel's choice of topic and approach. An attempt is made to summarize each paper delivered, and to relate the contributions made in the papers and in the discussions to some of the important aspects of vortex flow aerodynamics. This reveals significant progress and important clarifications, but also brings out remaining weaknesses in predictive capability and gaps in understanding. Where possible, conclusions are drawn and areas of continuing concern are identified. Author

N92-30977*# Iowa State Univ. of Science and Technology, Ames. Coll. of Engineering.
DEVELOPMENT OF A 3-D UPWIND PNS CODE FOR CHEMICALLY REACTING HYPERSONIC FLOWFIELDS Final Report, 1 Feb. 1988 - 31 Jan. 1992
J. C. Tannehill and G. Wadawadigi 31 Jan. 1992 29 p
(Grant NAG2-502; ERI Proj. 3051)
(NASA-CR-190182; NAS 1.26:190182; CFD-26) Avail: CASI HC A03/MF A01

Two new parabolized Navier-Stokes (PNS) codes were developed to compute the three-dimensional, viscous, chemically

reacting flow of air around hypersonic vehicles such as the National Aero-Space Plane (NASP). The first code (TONIC) solves the gas dynamic and species conservation equations in a fully coupled manner using an implicit, approximately-factored, central-difference algorithm. This code was upgraded to include shock fitting and the capability of computing the flow around complex body shapes. The revised TONIC code was validated by computing the chemically-reacting (M(sub infinity) = 25.3) flow around a 10 deg half-angle cone at various angles of attack and the Ames All-Body model at 0 deg angle of attack. The results of these calculations were in good agreement with the results from the UPS code. One of the major drawbacks of the TONIC code is that the central-differencing of fluxes across interior flowfield discontinuities tends to introduce errors into the solution in the form of local flow property oscillations. The second code (UPS), originally developed for a perfect gas, has been extended to permit either perfect gas, equilibrium air, or nonequilibrium air computations. The code solves the PNS equations using a finite-volume, upwind TVD method based on Roe's approximate Riemann solver that was modified to account for real gas effects. The dissipation term associated with this algorithm is sufficiently adaptive to flow conditions that, even when attempting to capture very strong shock waves, no additional smoothing is required. For nonequilibrium calculations, the code solves the fluid dynamic and species continuity equations in a loosely-coupled manner. This code was used to calculate the hypersonic, laminar flow of chemically reacting air over cones at various angles of attack. In addition, the flow around the McDonnel Douglas generic option blended-wing-body was computed and comparisons were made between the perfect gas, equilibrium air, and the nonequilibrium air results. Author

N92-31122# Virginia Polytechnic Inst. and State Univ., Blacksburg. Dept. of Aerospace and Ocean Engineering.
AN EXPERIMENTAL STUDY OF THE RELATIONSHIP BETWEEN VELOCITY AND PRESSURE FLUCTUATIONS IN A WING-BODY JUNCTION Technical Report, 1 Dec. 1990 - 24 Jan. 1992
M. C. Rife, W. J. Davenport, and R. L. Simpson 25 Jan. 1992 231 p
(Contract N00014-90-J-1909)
(AD-A249628; VPI-AOE-188) Avail: CASI HC A11/MF A03

Velocity and pressure fluctuations were measured in a wind tunnel in the plane of symmetry in front of a wing-body junction at an approach free velocity of U(sub ref) = 28.3 m/s and momentum thickness Reynolds number R(sub e(theta)) = 6900. The cylindrical wing shape was a 3.2 elliptical nose attached to a NACA 0020 tail at maximum thickness. A two component laser Doppler anemometer was used to make the velocity measurements. Pressure measurements were made at two locations upstream of the wing by a pair of Sennheiser microphones. A relationship between the velocity and the pressure was determined to reveal the bimodal structure of the flow field. Histograms and power spectra of both quantities are presented along with cross-spectra and cross-correlations. The velocity power spectra revealed spectral slopes of -1 throughout the entire flow field. Author

N92-31157*# Stanford Univ., CA. Dept. of Aeronautics and Astronautics.
NONLINEAR AERODYNAMICS AND THE DESIGN OF WING TIPS Final Report, 1 Apr. 1991 - 31 Mar. 1992
Ilan Kroo and Sean Wakayama Apr. 1992 17 p
(Contract NCC2-683)
(NASA-CR-190649; NAS 1.26:190649) Avail: CASI HC A03/MF A01

This report describes results of research conducted from April 1991 through March 1992. The general objective was to improve an existing wing optimization method, and apply the method to specific problems of interest. The method, while a valuable tool for wing tip design studies, can be applied to more general problems, and has been applied to some of these other problems during its development. Specific goals that were accomplished are listed and explained in more detail in the report. First, improvements were made to the portability and control flow of the existing code. The major iteration loop dealing with structural design was sped up and an alternate approach, using the optimizer to do structural sizing, was studied. Second, analysis methods were improved in the areas of structural and high lift modeling. The structural method was revised to give total wing weight and verified against data for particular commercial aircraft. The high lift analysis was improved to provide reasonable estimates of C(sub L max) in the flaps down condition. These improvements enabled making wing area a design variable, where it had been a fixed variable in the original method. Third, the method was applied to the design of wings for a Learjet. Rough studies were done to determine the effects of laminar flow design on wing shape. Finally, studies on wingtip shape were begun. Author

N92-31171# Purdue Univ., West Lafayette, IN. School of Aeronautics and Astronautics.
EXTENSION OF THE INTEGRAL EQUATION FORMULATION OF LINEARIZED TIME DEPENDENT SUBSONIC FLOW Final Report, 3 May 1990 - 3 Sep. 1991
Marc H. Williams Feb. 1992 38 p
(Contract F33615-90-C-3206)
(AD-A250654; WL-TR-91-3120) Avail: CASI HC A03/MF A01

This report describes the results of a study of the feasibility of extending the time domain formulation of the linearized aerodynamics of flexible bodies that had been developed earlier for planar wings to the general case of arbitrary, complete aircraft configurations. The end products of that study are a formulation of the problem, an exact solution applicable to any geometry, a sample calculation for a simple nonplanar configuration, and some suggestions on how to proceed. The formulation is based on distributions of elementary sources and doublets over the mean solid surface. The problem is first formulated for arbitrary motion, and then specialized to the case of uniform translation. GRA

03 AIR TRANSPORTATION AND SAFETY

Includes passenger and cargo air transport operations; and aircraft accidents.

For related information see also *16 Space Transportation* and *85 Urban Technology and Transportation.*

N92-30395*# National Aeronautics and Space Administration. Lewis Research Center, Cleveland, OH.
LEWIS ICING RESEARCH TUNNEL TEST OF THE AERODYNAMIC EFFECTS OF AIRCRAFT GROUND DEICING/ANTI-ICING FLUIDS
L. James Runyan (Boeing Commercial Airplane Co., Seattle, WA.), Thomas A. Zierten (Boeing Commercial Airplane Co., Seattle, WA.), Eugene G. Hill (Boeing Commercial Airplane Co., Seattle, WA.), and Harold E. Addy, Jr. Aug. 1992 134 p
(RTOP 505-68-11)
(NASA-TP-3238; E-5808; NAS 1.15:3238) Avail: CASI HC A07/MF A02

A wind tunnel investigation of the effect of aircraft ground deicing/anti-icing fluids on the aerodynamic characteristics of a Boeing 737-200ADV airplane was conducted. The test was carried out in the NASA Lewis Icing Research Tunnel. Fluids tested include a Newtonian deicing fluid, three non-Newtonian anti-icing fluids commercially available during or before 1988, and eight new experimental non-Newtonian fluids developed by four fluid manufacturers. The results show that fluids remain on the wind after liftoff and cause a measurable lift loss and drag increase. These effects are dependent on the high-lift configuration and on the temperature. For a configuration with a high-lift leading-edge device, the fluid effect is largest at the maximum lift condition. The fluid aerodynamic effects are related to the magnitude of the fluid surface roughness, particularly in the first 30 percent chord. The experimental fluids show a significant reduction in aerodynamic effects. Author

N92-30418# Messerschmitt-Boelkow-Blohm G.m.b.H., Munich (Germany, F.R.).
THE EUROFAR PROGRAM: AN EUROPEAN OVERVIEW ON ADVANCED VTOL CIVIL TRANSPORTATION SYSTEM
J. Renaud (Aerospatiale, Paris, France), H. Huber, and G. Venn (Westland Helicopters Ltd., Yeovil, England) 1991 12 p Presented at the 17th European Rotorcraft Forum, Berlin, Fed. Republic of Germany, 24-27 Sep. 1991
(MBB-UD-0611-91-PUB; ETN-92-91890) Avail: CASI HC A03/MF A01

Some European overviews on the role which could be devoted to a Vertical Take Off and Landing (VTOL) transportation system based on the tilt rotor, and the conditions of introduction of this aircraft within civil community, are summarized. As regards these issues, the Eurofar approach is based on aircraft design activities, and on studies related to marketing, infrastructure and airspace system. ESA

N92-30474# National Aerospace Lab., Amsterdam (Netherlands). Structures and Materials Div.
EXAMINATION OF AIRCRAFT WARNING AND CAUTION LIGHTS AFTER SHOCK TESTING
W. J. A. Bonnee and H. J. Kolkman 15 Aug. 1989 16 p Presented at the International Symposium for Testing and Failure Analysis, Los Angeles, CA, 6-10 Nov. 1989 Sponsored by Royal Netherlands Air Force
(NLR-TP-89284-U; ETN-92-91525) Avail: CASI HC A03/MF A01

Warning and caution light bulbs recovered after aircraft accidents provide useful information. It is generally assumed that upon impact the filament of an unlit bulb will break without deformation, whereas a hot filament will show extensive elongation. Deviations from this idealized behavior were investigated by shock tests on F-16 warning and caution light bulbs. From the tests it could be concluded that relatively new lamps do not show the idealized behavior described above. This makes it necessary in certain cases to estimate the number of burning hours by a simple scanning electron microscopy (SEM) investigation of the surface morphology of the filament. Besides its age, the behavior of a filament upon impact is also influenced by the direction and especially the duration and maximum g-level of the impact. However, the behavior of a burning lamp is not influenced by deviations from the correct voltage. The above results are included in a recommended procedure for examining light bulbs after aircraft accidents. ESA

N92-30551# Federal Aviation Administration, Washington, DC. Office of Aviation Medicine.
EVALUATION OF HEAD IMPACT KINEMATICS FOR PASSENGERS SEATED BEHIND INTERIOR WALLS Final Report
Van Gowdy and Richard DeWeese May 1992 15 p
(AD-A252651; DOT/FAA/AM-92/20) Avail: CASI HC A03/MF A01

Federal Aviation Regulations for crashworthy seats include the Head Injury Criteria (HIC) as part of the pass-fail performance specifications. For passenger seats located behind interior walls to meet this requirement, the dynamics of head impact with the wall must be evaluated from a system approach. Procedures for conducting system tests and analyzing the head motion of an anthropomorphic test dummy (ATD) are described. Analyses of head kinematics from dynamic impact tests with a lap belt restrained ATD are presented. GRA

N92-30565# Oak Ridge National Lab., TN.
THE ALLOCATION OF CARGO TO CHANNEL MISSIONS
Cheng Liu and G. Harrison 1992 24 p Presented at the Military Airlift Command Transportation and Mobility Modeling Conference, Scott Air Force Base, IL, 3 Apr. 1992
(Contract DE-AC05-84OR-21400)
(DE92-013234; CONF-9204131-1) Avail: CASI HC A03/MF A01

Each month the armed services provide a forecast of tons of cargo by channel to MAC. The purpose of the Channels Allocation Algorithm is to allocate cargo requirements to specific Channel Missions. The objective of the allocation algorithm is to minimize frequency and cargo requirements shortfall. The constraints on the allocation model include flying hours, channel frequencies, mission structure, mission operation days, and aircraft capacity. Cargo requirements shortfall is defined as the tonnage of cargo not moved from the airfields in the United States that are channel staging points to overseas locations. Channel frequencies are defined by the number of times a destination is served by an origin in one month. The mission structures are defined as sets of missions usually in the form of a circuit. Mission operating days are determined by the operating day rules for the month, or they can be input by the user for an individual month. One of the assumptions in this model is that there is only one transshipment allowed between any origin and a destination if there is no mission that actually connects the stations. The transshipment stations are also restricted in that only certain stations can serve as transshipment stations. The Channels Allocation Algorithm consists of two linear programs that incorporate three objectives. The objectives are: (1) to minimize that number of frequency channels not met, (2) to minimize cargo shortfall, and (3) to minimize operating cost. The first linear program minimizes frequency channels not met, subject to the mission structure, number of times the mission operates, and total flying hours available. The second linear program minimizes the fleet operating cost cargo handling cost, and cargo shortfall, subject to frequency channels met by the first linear program, aircraft capacity, and total flying hours available. This document is comprised of viewgraphs.
DOE

N92-30980# Advanced Aviation Concepts, Jupiter, FL.
INTRODUCTION TO COGNITIVE PROCESSES OF EXPERT PILOTS Final Report
Richard J. Adams and K. Anders Ericsson (Colorado Univ., Boulder.) Jun. 1992 50 p
(Contract DTFA01-90-C-00042)
(DOT/FAA/RD-92/12) Avail: CASI HC A03/MF A01

This report addresses the historical problem that a very high percentage of accidents have been classified as involving 'pilot error'. Through extensive research since 1977, the Federal Aviation Administration determined that the predominant underlying cause of these types of accidents involved decisional problems or cognitive information processing. To attack these problems, Aeronautical Decision Making (ADM) training materials were developed and tested for ten years. Since the publication of the ADM training manuals in 1987, significant reductions in human performance error (HPE) accidents have been documented both in the U.S. and world wide. However, shortcomings have been observed in the use of these materials for recurrency training and in their relevance to more experienced pilots. The following discussion defines the differences between expert and novice decision makers from a cognitive information processing perspective, correlates the development of expert pilot cognitive processes with training and experience, and reviews accident scenarios which exemplify those processes. This introductory material is a necessary prerequisite to an understanding of how to formulate expert pilot decision making training innovations.
Author

N92-31159# National Transportation Safety Board, Washington, DC.
AIRCRAFT ACCIDENT REPORT: EXPLOSIVE DECOMPRESSION - LOSS OF CARGO DOOR IN FLIGHT, UNITED AIRLINES FLIGHT 811, BOEING 747-122, N4713U, HONOLULU, HAWAII, FEBRUARY 24, 1989
18 Mar. 1992 119 p Supersedes NTSB/AAR-90/01; N90-21748
(PB92-910402; NTSB/AAR-92/02; NTSB/AAR-90/01) Avail: CASI HC A06/MF A02

This report explains the explosive decompression resulting from the loss of a cargo door in flight on United Airlines flight 811, a Boeing 747-122, near Honolulu, Hawaii, on Feb. 24, 1989. The

safety issues discussed in this report are the design and certification of the B-747 cargo doors, the operation and maintenance to assure the continuing airworthiness of the doors, and emergency response. Recommendations concerning these issues were made to the Federal Aviation Administration, the State of Hawaii, and the U.S. Department of Defense. Author

N92-31193# Army Engineer Waterways Experiment Station, Vicksburg, MS. Geotechnical Lab.
EVALUATION OF GROUNDING AND MOORING POINTS FOR ARMY AIRCRAFT Final Report
Richard H. Grau and David L. Cooksey Apr. 1992 68 p
(AD-A250749; WES/MP/GL-92-10) Avail: CASI HC A04/MF A01

This report presents results of tests conducted to evaluate the load capacity of aircraft mooring and grounding points. Both existing mooring points located at a military installation and newly designed systems were evaluated. Specifically, this report documents laboratory and field investigations on mooring systems to evaluate their ability to withstand anticipated forces applied by a moored Army aircraft during a 100-knot wind. GRA

N92-31211# Computer Resource Management, Inc., Herndon, VA.
NATIONAL AIRSPACE SYSTEM. AIR DEFENSE AND LAW ENFORCEMENT SURVEILLANCE OPERATIONAL CONCEPT NAS-SR-135
William Trent, Thomas Pickerell, and Harold Nelson, Jr. Jul. 1992 29 p
(Contract DTFA01-91-Y-01004)
(DOT/FAA/SE-92/3) Avail: CASI HC A03/MF A01

This operational concept describes the Air Defense and Law Enforcement Surveillance system which will be in place upon implementation of the Federal Aviation Administration (FAA) National Airspace System (NAS) Plan. Air Defense and Law Enforcement Surveillance includes those activities necessary to provide for the detection of aircraft throughout an Air Defense Identification Zone and Distant Early Warning Identification Zone, as well as to ascertain aircraft position, velocity, and identity of unauthorized intruders. The objective is to describe the relationship between subsystems, facilities, information, and operators/users involved in requirements stated in the National Airspace System Requirement Specification (NAS-SR-1000). Several types of block diagrams are used to illustrate systems' connectivity and operational flow. Scenarios are also derived to describe the process from a user's perspective. This concept, and the other seven operational concepts, will complete the description of the system requirements as described in the NASSRS. Author

04 AIRCRAFT COMMUNICATIONS AND NAVIGATION

Includes digital and voice communication with aircraft; air navigation systems (satellite and ground based); and air traffic control.

For related information see also *17 Space Communications, Spacecraft Communications, Command and Tracking* and *Communications and Radar.*

N92-30978*# Douglas Aircraft Co., Inc., Long Beach, CA.
EVALUATION OF MICROWAVE LANDING SYSTEM APPROACHES IN A WIDE-BODY TRANSPORT SIMULATOR Final Report
L. G. Summers and J. B. Feather Washington NASA. Langley Research Center Jun. 1992 153 p
(Contract NAS1-18028; RTOP 505-66-41-66)
(NASA-CR-4450; NAS 1.26:4450; MDC-91K0792) Avail: CASI HC A08/MF A02

The objective of this study was to determine the suitability of flying complex curved approaches using the microwave landing system (MLS) with a wide-body transport aircraft. Fifty pilots in crews of two participated in the evaluation using a fixed-base simulator that emulated an MD-11 aircraft. Five approaches, consisting of one straight-in approach and four curved approaches, were flown by the pilots using a flight director. The test variables include the following: (1) manual and autothrottles; (2) wind direction; and (3) type of navigation display. The navigation display was either a map or a horizontal situation indicator (HSI). A complex wind that changed direction and speed with altitude, and included moderate turbulence, was used. Visibility conditions were Cat 1 or better. Subjective test data included pilot responses to questionnaires and pilot comments. Objective performance data included tracking accuracy, position error at decision height, and control activity. Results of the evaluation indicate that flying curved MLS approaches with a wide-body transport aircraft is operationally acceptable, depending upon the length of the final straight segment and the complexity of the approach. Author

05 AIRCRAFT DESIGN, TESTING AND PERFORMANCE

Includes aircraft simulation technology.

For related information see also *18 Spacecraft Design, Testing and Performance* and *39 Structural Mechanics.*For land transportation vehicles see *85 Urban Technology and Transportation.*

N92-30304*# California Univ., Davis. Dept. of Mechanical, Aeronautical and Materials Engineering.
MODELING AND ANALYSIS METHODOLOGY FOR AEROELASTICALLY TAILORED CHORDWISE DEFORMABLE WINGS Final Report
Lawrence W. Rehfield, Stephen Chang, and Peter J. Zischka Jul. 1992 80 p
(Contract NAS1-18754; RTOP 510-02-12-08)
(NASA-CR-189620; NAS 1.26:189620) Avail: CASI HC A05/MF A01

Structural concepts have been created which produce chordwise camber deformation that results in enhanced lift. A wing box can be tailored to utilize each of these with composites. In attempting to optimize the aerodynamic benefits, we have found there are two optimal designs that are of interest. There is a weight optimum which corresponds to the maximum lift per unit structural weight. There is also a lift optimum that corresponds to maximum absolute lift. New structural models, the basic deformation mechanisms that are utilized and typical analytical results are presented. It appears that lift enhancements of sufficient magnitude can be produced to render this type of wing tailoring of practical interest. Experiments and finite element correlations are performed which confirm the validity of the theoretical models utilized. Author

N92-30424# Messerschmitt-Boelkow-Blohm G.m.b.H., Munich (Germany, F.R.). Aircraft Div.
MULTIDISCIPLINARY OPTIMIZATION OF FIBER COMPOSITE AIRCRAFT STRUCTURES
H. A. Eschenauer (Siegen Univ.,, Germany, F.R.), G. Schuhmacher (Siegen Univ.,, Germany, F.R.), and W. Hartzheim 12 Dec. 1991 15 p Presented at the NATO/DFG Advanced Study Institute on Optimization of Large Structural Systems, Berchtesgaden, Fed. Republic of Germany, 23 Sep. - 4 Oct. 1991
(MBB/FW321/S/PUB/476; ETN-92-91902) Copyright Avail: CASI HC A03/MF A01

The application of a method of structural optimization to find optimal layouts of fiber composite structures in aircraft contruction is addressed. The goal of the optimization process is to minimize the structural weight and, simultaneously, to fulfill multidisciplinary constraints concerning failure criteria, stability requirements, dynamic responses, areroelastic efficiencies and flutter speeds. Considering these requirements, the optimal values for the layer thickness and the fiber orientations of composite structures must be determined. This problem can efficiently be solved by structural optimization methods. The model formulation in structural optimization is described in general as well as the special

optimization model and the structural and sensitivity analysis for fiber composite structures. An application example demonstrated the performance of the whole procedure. This example shows that the structural optimization method is very useful to increase the efficiency of the design process as well as the quality and performance of aircraft structures. ESA

N92-30752*# National Aeronautics and Space Administration. Langley Research Center, Hampton, VA.
ON-LINE ANALYSIS CAPABILITIES DEVELOPED TO SUPPORT THE AFW WIND-TUNNEL TESTS
Carol D. Wieseman, Sherwood T. Hoadley, and Sandra M. McGraw (Lockheed Engineering and Sciences Co., Hampton, VA.) Jul. 1992 11 p Presented at the AIAA Dynamic Specialists' Conference, Dallas, TX, 16-17 Apr. 1992 Previously announced in IAA as A92-35656
(RTOP 505-63-50-15)
(NASA-TM-107651; NAS 1.15:107651) Avail: CASI HC A03/MF A01

A variety of on-line analysis tools were developed to support two active flexible wing (AFW) wind-tunnel tests. These tools were developed to verify control law execution, to satisfy analysis requirements of the control law designers, to provide measures of system stability in a real-time environment, and to provide project managers with a quantitative measure of controller performance. Descriptions and purposes of the developed capabilities are presented along with examples. Procedures for saving and transferring data for near real-time analysis, and descriptions of the corresponding data interface programs are also presented. The on-line analysis tools worked well before, during, and after the wind tunnel test and proved to be a vital and important part of the entire test effort. Author

N92-30878# Goldsworthy Engineering, Inc., Springville, UT.
ORGANIC MATRIX COMPOSITE HELICOPTER INTERNAL/EXTERNAL CARGO PALLET SYSTEM (OMC INTEX) Final Report, Jul. 1986 - Jun. 1990
Rob J. Sjostedt and Donna K. Dawson Apr. 1992 95 p
(Contract DAAJ02-86-C-0009)
(AD-A251127; PC-86-08; USAAVSCOM-TR-92-D-2) Avail: CASI HC A05/MF A01

This report describes the development of an OMC INTEX Cargo Pallet System relative to the Army's changing cargo handling requirements. Design, fabrication, and testing of three prototype pallets are discussed. The end result was a full-scale OMC pallet that passed all specified tests, including ultimate hoist and flight testing. The pallet was designed for automated pultrusion processing, which will offer cost effective fabrication of OMC pallets in production quantities. GRA

N92-31165# Federal Aviation Administration, Atlantic City, NJ.
HELICOPTER NIGHTTIME PARKING TEST RESULTS - UH-1 Technical Report, Jan. - Aug. 1989
Rosanne M. Weiss May 1992 67 p
(DOT/FAA/CT-TN92/1) Avail: CASI HC A04/MF A01

Flight tests were previously conducted at the Federal Aviation Administration (FAA) Technical Center to examine issues regarding rotortip separation in ground maneuver areas at heliports. Technical Note DOT/FAA/CT-TN88/30, 'Heliport Surface Maneuvering Test Results', details the results of those tests. However, those tests were conducted under visual flight conditions (VFR) daylight conditions. Given the limitations of scoptic vision, it was determined that nighttime testing was needed to determine whether pilot parking separation performance and perception deteriorates under night, low ambient light conditions. This report documents the results of nighttime parking tests conducted at the Technical Center between Jan. - Aug. 1989. Over 100 parking maneuvers were conducted using a UH-1H helicopter. All were conducted under head, tail, and crosswind conditions, with an unlit and a lit obstacle and without an obstacle in place. Pilot subjective data in reference to these maneuvers were collected via post-maneuver ratings and post-flight questionnaire. Data collection and analysis methodology and objective as well as subjective issues are discussed. Statistical and graphical analysis of pilot performance and perception data and subjective input are provided. Conclusions are drawn about the considerations that must be given to parking space size at heliports permitting nighttime operations. Author

N92-31174*# National Aeronautics and Space Administration. Langley Research Center, Hampton, VA.
AN ANALYTICAL AND EXPERIMENTAL INVESTIGATION OF FLUTTER SUPPRESSION VIA PIEZOELECTRIC ACTUATION
Jennifer Heeg Jul. 1992 13 p Presented at the AIAA 33rd Structures, Structural Dynamics, and Materials Conference, Dallas, TX, 13-15 Apr. 1992
(RTOP 505-63-50-15)
(NASA-TM-107653; NAS 1.15:107653) Avail: CASI HC A03/MF A01

The objective of this research was to analytically and experimentally study the capabilities of adaptive material plate actuators for suppressing flutter. Piezoelectrics are materials which are characterized by their ability to produce voltage when subjected to a mechanical strain. The converse piezoelectric effect can be utilized to actuate a structure by applying a voltage. For this investigation, a two degree of freedom wind-tunnel model was designed, analyzed, and tested. The model consisted of a rigid wing and a flexible mount system which permitted translational and rotational degrees of freedom. Actuators, made of piezoelectric material were affixed to leaf springs on the mount system. Command signals, applied to the piezoelectric actuators, exerted control over the closed-loop damping and stiffness properties. A mathematical aeroservoelastic model was constructed using finite element and stiffness properties. A mathematical aeroservoelastic model was constructed using finite element methods, laminated plate theory, and aeroelastic analysis tools. A flutter suppression control law was designed, implemented on a digital control computer, and tested to conditions 20 percent above the passive flutter speed of the model. The experimental results represent the first time that adaptive materials have been used to actively suppress flutter. It demonstrates that small, carefully-placed actuating plates can be used effectively to control aeroelastic response. Author

N92-31208*# G and C Systems, Inc., San Juan Capistrano, CA.
HIGH-SPEED CIVIL TRANSPORT ISSUES AND TECHNOLOGY PROGRAM Final Report
Marie D. Hewett Washington NASA May 1992 118 p Prepared in cooperation with PRC Kentron, Inc., Edwards, CA
(Contracts NAS2-12722; ATD-91-GNC-7102; RTOP 505-64-20)
(NASA-CR-186020; H-1795; NAS 1.26:186020) Avail: CASI HC A06/MF A02

A strawman program plan is presented, consisting of technology developments and demonstrations required to support the construction of a high-speed civil transport. The plan includes a compilation of technology issues related to the development of a transport. The issues represent technical areas in which research and development are required to allow airframe manufacturers to pursue an HSCT development. The vast majority of technical issues presented require flight demonstrated and validated solutions before a transport development will be undertaken by the industry. The author believes that NASA is the agency best suited to address flight demonstration issues in a concentrated effort. The new Integrated Test Facility at NASA Dryden Flight Research Facility is considered ideally suited to the task of supporting ground validations of proof-of-concept and prototype system demonstrations before night demonstrations. An elaborate ground hardware-in-the-loop (iron bird) simulation supported in this facility provides a viable alternative to developing an expensive fill-scale prototype transport technology demonstrator. Drygen's SR-71 assets, modified appropriately, are a suitable test-bed for supporting flight demonstrations and validations of certain transport technology solutions. A subscale, manned or unmanned flight demonstrator is suitable for flight validation of transport technology solutions, if appropriate structural similarity relationships can be established. The author contends that developing a full-scale prototype transport

technology demonstrator is the best alternative to ensuring that a positive decision to develop a transport is reached by the United States aerospace industry. Author

06 AIRCRAFT INSTRUMENTATION

Includes cockpit and cabin display devices; and flight instruments.

For related information see also *19 Spacecraft Instrumentation* and *35 Instrumentation and Photography.*

N92-30524# TRW, Inc., Beavercreek, OH. Military Electronics and Avionics Div.
A MODEL OF THE ADA AVIONICS REAL-TIME SYSTEM: AN EXAMPLE OF THE BENEFITS OF THE HARDWARE/SOFTWARE CODESIGN APPROACH IN DEVELOPMENT OF REAL-TIME SYSTEMS Final Report
B. E. Clark, F. G. Gray, J. T. Morrison, and T. S. White Mar. 1992 174 p Prepared in cooperation with EPA, Research Triangle Park, NC; and Virginia Polytechnic Inst., Blacksburg, VA
(Contract F33615-87-D-1452)
(AD-A248893; WL-TR-92-1022) Avail: CASI HC A08/MF A02

The Ada Avionics Real-Time System (AARTS) Operating System (AOS) is the OS and management system under development for the PAVE PILLAR architecture. The AOS, in its current version, was modeled in the Architectural Design and Assessment Systems (ADAS) along with the hardware and applications being exercised in the Avionics Directorate's Integrated test bed. The report describes the model, the results of simulation executions, and methods for expansion of the model to architectures larger than that of the integrated test bed. GRA

N92-30965*# Douglas Aircraft Co., Inc., Long Beach, CA.
HIGH SPEED RESEARCH SYSTEM STUDY. ADVANCED FLIGHT DECK CONFIGURATION EFFECTS
Jay R. Swink and Richard T. Goins Jun. 1992 85 p
(Contract NAS1-19345)
(NASA-CR-189650; NAS 1.26:189650) Avail: CASI HC A05/MF A01

In mid-1991 NASA contracted with industry to study the high-speed civil transport (HSCT) flight deck challenges and assess the benefits, prior to initiating their High Speed Research Program (HSRP) Phase 2 efforts, then scheduled for FY-93. The results of this nine-month effort are presented, and a number of the most significant findings for the specified advanced concepts are highlighted: (1) a no nose-droop configuration; (2) a far forward cockpit location; and (3) advanced crew monitoring and control of complex systems. The results indicate that the no nose-droop configuration is critically dependent upon the design and development of a safe, reliable, and certifiable Synthetic Vision System (SVS). The droop-nose configuration would cause significant weight, performance, and cost penalties. The far forward cockpit location, with the conventional side-by-side seating provides little economic advantage; however, a configuration with a tandem seating arrangement provides a substantial increase in either additional payload (i.e., passengers) or potential downsizing of the vehicle with resulting increases in performance efficiencies and associated reductions in emissions. Without a droop nose, forward external visibility is negated and takeoff/landing guidance and control must rely on the use of the SVS. The technologies enabling such capabilities, which de facto provides for Category 3 all-weather operations on every flight independent of weather, represent a dramatic benefits multiplier in a 2005 global ATM network: both in terms of enhanced economic viability and environmental acceptability. Author

07 AIRCRAFT PROPULSION AND POWER

Includes prime propulsion systems and systems components, e.g., gas turbine engines and compressors; and onboard auxilliary power plants for aircraft.

For related information see also *20 Spacecraft Propulsion and Power, 28 Propellants and Fuels,* and *44 Energy Production and Conversion.*

N92-30303# Galaxy Scientific Corp., Mays Landing, NJ.
STATISTICS ON AIRCRAFT GAS TURBINE ENGINE ROTOR FAILURES THAT OCCURRED IN US COMMERCIAL AVIATION DURING 1989 Final Report
E. R. Chapdelaine (Federal Aviation Administration, Atlantic City, NJ.), B. C. Fenton (Federal Aviation Administration, Atlantic City, NJ.), R. A. Delucia (Naval Air Propulsion Test Center, Trenton, NJ.), and M. Muller Jun. 1992 26 p
(Contract DTFA03-89-C-0043)
(DOT/FAA/CT-92/5) Avail: CASI HC A03/MF A01

Presented here is statistical information relating to gas turbine engine rotor failures which occurred during 1989 in U.S. commercial aviation service use. Four hundred and thirty-five failures occurred in 1989. Rotor fragments were generated in 156 of the failures, and of these 24 were uncontained. The predominant failure involved blade fragments, 87 percent of which were contained. Eight disk failures occurred and six were uncontained. Thirty-six percent of the 435 failures occurred during the takeoff and climb stages of flight. This service data analysis is prepared on a calendar-year basis and published yearly. The data are useful in support of flight safety analyses, proposed regulatory actions, certification standards, and cost benefit analyses. Author

N92-30518*# National Aeronautics and Space Administration. Hugh L. Dryden Flight Research Facility, Edwards, CA.
THRUST STAND EVALUATION OF ENGINE PERFORMANCE IMPROVEMENT ALGORITHMS IN AN F-15 AIRPLANE
Timothy R. Conners Jul. 1992 23 p Presented at the 28th AIAA-SAE-ASME-ASEE Joint Propulsion Conference, Nashville, TN, 6-8 Jul. 1992
(RTOP 533-02-36)
(NASA-TM-104252; H-1842; NAS 1.15:104252; AIAA Paper 92-3747) Avail: CASI HC A03/MF A01

An investigation is underway to determine the benefits of a new propulsion system optimization algorithm in an F-15 airplane. The performance seeking control (PSC) algorithm optimizes the quasi-steady-state performance of an F100 derivative turbofan engine for several modes of operation. The PSC algorithm uses an onboard software engine model that calculates thrust, stall margin, and other unmeasured variables for use in the optimization. As part of the PSC test program, the F-15 aircraft was operated on a horizontal thrust stand. Thrust was measured with highly accurate load cells. The measured thrust was compared to onboard model estimates and to results from posttest performance programs. Thrust changes using the various PSC modes were recorded. Those results were compared to benefits using the less complex highly integrated digital electronic control (HIDEC) algorithm. The PSC maximum thrust mode increased intermediate power thrust by 10 percent. The PSC engine model did very well at estimating measured thrust and closely followed the transients during optimization. Quantitative results from the evaluation of the algorithms and performance calculation models are included with emphasis on measured thrust results. The report presents a description of the PSC system and a discussion of factors affecting the accuracy of the thrust stand load measurements. Author

N92-30569*# Quest Integrated, Inc., Kent, WA.
A NEW UNSTEADY MIXING MODEL TO PREDICT NO(x) PRODUCTION DURING RAPID MIXING IN A DUAL-STAGE COMBUSTOR
Suresh Menon Apr. 1992 59 p
(Contract NAS3-26242; RTOP 324-02-00)

(NASA-CR-189155; NAS 1.26:189155; QUEST-TR-534) Avail: CASI HC A04/MF A01

An advanced gas turbine engine to power supersonic transport aircraft is currently under study. In addition to high combustion efficiency requirements, environmental concerns have placed stringent restrictions on the pollutant emissions from these engines. A combustor design with the potential for minimizing pollutants such as NO(x) emissions is undergoing experimental evaluation. A major technical issue in the design of this combustor is how to rapidly mix the hot, fuel-rich primary zone product with the secondary diluent air to obtain a fuel-lean mixture for combustion in the second stage. Numerical predictions using steady-state methods cannot account for the unsteady phenomena in the mixing region. Therefore, to evaluate the effect of unsteady mixing and combustion processes, a novel unsteady mixing model is demonstrated here. This model has been used to study multispecies mixing as well as propane-air and hydrogen-air jet nonpremixed flames, and has been used to predict NO(x) production in the mixing region. Comparison with available experimental data show good agreement, thereby providing validation of the mixing model. With this demonstration, this mixing model is ready to be implemented in conjunction with steady-state prediction methods and provide an improved engineering design analysis tool.

Author

N92-30753*# Pennsylvania State Univ., University Park. Dept. of Electrical and Computer Engineering.

FINITE DIFFERENCE TIME DOMAIN MODELING OF STEADY STATE SCATTERING FROM JET ENGINES WITH MOVING TURBINE BLADES Progress Report, 25 Sep. 1991 - 25 Mar. 1992

Deirdre A. Ryan, H. Scott Langdon, John H. Beggs, David J. Steich, Raymond J. Luebbers, and Karl S. Kunz 4 May 1992 35 p

(Grant NAG1-1350)
(NASA-CR-190290; NAS 1.26:190290) Avail: CASI HC A03/MF A01

The approach chosen to model steady state scattering from jet engines with moving turbine blades is based upon the Finite Difference Time Domain (FDTD) method. The FDTD method is a numerical electromagnetic program based upon the direct solution in the time domain of Maxwell's time dependent curl equations throughout a volume. One of the strengths of this method is the ability to model objects with complicated shape and/or material composition. General time domain functions may be used as source excitations. For example, a plane wave excitation may be specified as a pulse containing many frequencies and at any incidence angle to the scatterer. A best fit to the scatterer is accomplished using cubical cells in the standard cartesian implementation of the FDTD method. The material composition of the scatterer is determined by specifying its electrical properties at each cell on the scatterer. Thus, the FDTD method is a suitable choice for problems with complex geometries evaluated at multiple frequencies. It is assumed that the reader is familiar with the FDTD method.

Author

N92-30972*# National Aeronautics and Space Administration. Lewis Research Center, Cleveland, OH.

NAVIER-STOKES ANALYSIS AND EXPERIMENTAL DATA COMPARISON OF COMPRESSIBLE FLOW WITHIN DUCTS

G. J. Harloff (Sverdrup Technology, Inc., Brook Park, OH.), B. A. Reichert, J. R. Sirbaugh (Sverdrup Technology, Inc., Brook Park, OH.), and S. R. Wellborn (Iowa State Univ. of Science and Technology, Ames.) Jul. 1992 7 p Presented at the 13th International Conference on Numerical Methods in Fluid Dynamics, Rome (Italy), 6-10 Jul. 1992

(Contract NAS3-25266; RTOP 505-62-52)
(NASA-TM-105796; E-7226; NAS 1.15:105796) Avail: CASI HC A02/MF A01

Many aircraft employ ducts with centerline curvature or changing cross-sectional shape to join the engine with inlet and exhaust components. S-ducts convey air to the engine compressor from the intake and often decelerate the flow to achieve an acceptable Mach number at the engine compressor by increasing the cross-sectional area downstream. Circular-to-rectangular transition ducts are used on aircraft with rectangular exhaust nozzles to connect the engine and nozzle. To achieve maximum engine performance, the ducts should minimize flow total pressure loss and total pressure distortion at the duct exit. Changes in the curvature of the duct centerline or the duct cross-sectional shape give rise to streamline curvature which causes cross stream pressure gradients. Secondary flows can be caused by deflection of the transverse vorticity component of the boundary layer. This vortex tilting results in counter-rotating vortices. Additionally, the adverse streamwise pressure gradient caused by increasing cross-sectional area can lead to flow separation. Vortex pairs have been observed in the exit planes of both duct types. These vortices are due to secondary flows induced by pressure gradients resulting from streamline curvature. Regions of low total pressure are produced when the vortices convect boundary layer fluid into the main flow. The purpose of the present study is to predict the measured flow field in a diffusing S-duct and a circular-to-rectangular transition duct with a full Navier-Stokes computer program, PARC3D, and to compare the numerical predictions with new detailed experimental measurements. The work was undertaken to extend previous studies and to provide additional CFD validation data needed to help model flows with strong secondary flow and boundary layer separation. The S-duct computation extends the study of Smith et al, and Harloff et al, which concluded that the computation might be improved by using a finer grid and more advanced turbulence models. The present study compares results for both the Baldwin-Lomas and k-epsilon turbulence models and is conducted with a refined grid. For the transition duct, two inlet conditions were considered, the first with straight flow and the second with swirling flow. The first case permits examination of the effects of the geometric transition on the flow field, while the second case includes the rotational flow effect characteristic of a gas turbine engine.

Author

N92-30998*# National Aeronautics and Space Administration. Lewis Research Center, Cleveland, OH.

PRELIMINARY DYNAMIC TESTS OF A FLIGHT-TYPE EJECTOR

Colin K. Drummond Jul. 1992 22 p Presented at the 28th Joint Propulsion Conference, Nashville, TN, 6-9 Jul. 1992; sponsored by AIAA, SAE, ASME, and ASEE

(RTOP 505-62-30)
(NASA-TM-105814; E-7245; NAS 1.15:105814) Copyright Avail: CASI HC A03/MF A01

A thrust augmenting ejector was tested to provide experimental data to assist in the assessment of theoretical models to predict duct and ejector fluid-dynamic characteristics. Eleven full-scale thrust augmenting ejector tests were conducted in which a rapid increase in the ejector nozzle pressure ratio was effected through a unique facility, bypass/burst-disk subsystem. The present work examines two cases representative of the test performance window. In the first case, the primary nozzle pressure ration (NPR) increased 36 percent from one unchoked (NPR = 1.29) primary flow condition to another (NPR = 1.75) over a 0.15 second interval. The second case involves choked primary flow conditions, where a 17 percent increase in primary nozzle flowrate (from NPR = 2.35 to NPR = 2.77) occurred over approximately 0.1 seconds. Although the real-time signal measurements support qualitative remarks on ejector performance, extracting quantitative ejector dynamic response was impeded by excessive aerodynamic noise and thrust stand dynamic (resonance) characteristics. It does appear, however, that a quasi-steady performance assumption is valid for this model with primary nozzle pressure increased on the order of 50 lb(sub f)/s. Transient signal treatment of the present dataset is discussed and initial interpretations of the results are compared with theoretical predictions for a similar Short Takeoff and Vertical Landing (STOVL) ejector model.

Author

N92-31164*# Advanced Control Technology, Inc., Northridge, CA.

CRYOGENIC MAGNETIC BEARING TEST FACILITY (CMBTF) Final Report

Feb. 1992 67 p
(Contract NAS3-25572; RTOP 590-21-31)
(NASA-CR-189087; NAS 1.26:189087) Avail: CASI HC A04/MF A01

The Cryogenic Magnetic Bearing Test Facility (CMBTF) was designed and built to evaluate compact, lightweight magnetic bearings for use in the SSME's (space shuttle main engine) liquid oxygen and liquid hydrogen turbopumps. State of the art and tradeoff studies were conducted which indicated that a hybrid permanent magnet bias homopolar magnetic bearing design would be smaller, lighter, and much more efficient than conventional industrial bearings. A test bearing of this type was designed for the test rig for use at both room temperature and cryogenic temperature (-320 F). The bearing was fabricated from state-of-the-art materials and incorporated into the CMBTF. Testing at room temperature was accomplished at Avcon's facility. These preliminary tests indicated that this magnetic bearing is a feasible alternative to older bearing technologies. Analyses showed that the hybrid magnetic bearing is one-third the weight, considerably smaller, and uses less power than previous generations of magnetic bearings. Author

N92-31172*# National Aeronautics and Space Administration. Lewis Research Center, Cleveland, OH.
TRENDS IN AEROPROPULSION RESEARCH AND THEIR IMPACT ON ENGINEERING EDUCATION
Louis A. Povinelli, Bruce A. Reichert, and Arthur J. Glassman (Toledo Univ., OH.) Jun. 1992 7 p Presented at the ASEE 1992 Annual Conference, Toledo, OH, 21-25 Jun. 1992
(RTOP 505-62-52)
(NASA-TM-105682; E-7061; NAS 1.15:105682) Avail: CASI HC A02/MF A01

This presentation is concerned with the trends in aeropropulsion both in the U.S. and abroad and the impact of these trends on the educational process in our universities. In this paper, we shall outline the new directions for research which may be of interest to educators in the aeropropulsion field. Awareness of new emphases, such as emission reductions, noise control, maneuverability, speed, etc., will have a great impact on engineering educators responsible for restructuring courses in propulsion. The information presented herein will also provide some background material for possible consideration in the future development of propulsion courses. In describing aeropropulsion, we are concerned primarily with air-breathing propulsion; however many observations apply equally as well to rocket engine systems. Aeropropulsion research needs are primarily motivated by technologies required for advanced vehicle systems and frequently driven by external requirements such as economic competitiveness, environmental concern and national security. In this presentation, vehicle based research is first described, followed by a discussion of discipline and multidiscipline research necessary to implement the vehicle-focused programs. The importance of collaboration in research and the training of future researchers concludes this presentation. Author

08 AIRCRAFT STABILITY AND CONTROL

Includes aircraft handling qualities; piloting; flight controls; and autopilots.

For related information see also *05 Aircraft Design, Testing and Performance.*

N92-30323# Oklahoma Univ., Norman. School of Aerospace Mechanical and Nuclear Engineering.
INFLUENCE OF STRUCTURAL AND AERODYNAMIC MODELING ON FLUTTER ANALYSIS AND STRUCTURAL OPTIMIZATION Interim Report, Jun. - Dec. 1990
Alfred G. Striz Jun. 1991 77 p
(Contract F33615-87-C-3228)
(AD-A248487; ASIAC-1090.10; WL-TR-91-3064) Avail: CASI HC A05/MF A01

The influences of structural and aerodynamic modeling on the flutter analysis and multidisciplinary optimization of fully built-up finite element wing models in an aeroelastic environment are not yet well understood. Therefore, the dynamic aeroelastic and optimization capabilities in the Automated STRuctural Optimization System (ASTROS) were used to evaluate the flutter behavior and the behavior of structural optimization with flutter constraints of various representative fully built-up finite element wing models in subsonic and supersonic flow. ASTROS was used as a tool to calculate flutter speeds and frequencies and to minimize the weight of these wing models in subsonic and supersonic flow under given flutter and frequency constraints to determine the effect that these modeling factors have. GRA

N92-30439# Messerschmitt-Boelkow-Blohm G.m.b.H., Munich (Germany, F.R.). Helicopter Div.
RESONANCE AND CONTROL RESPONSE TESTS USING A CONTROL SIMULATION DEVICE
Hubert Mueller 1991 11 p Presented at the 17th European Rotorcraft Forum, Berlin, Fed. Republic of Germany, 24-27 Sep. 1991
(MBB-UD-0608-91-PUB; ETN-92-91888) Avail: CASI HC A03/MF A01

Prototypes of the light twin helicopter, the BO 108, are addressed. Both aircrafts are equipped with a stimulation device for main rotor control inputs. Many kinds of collective or cyclic inputs can be chosen in a computer menu. It is possible to select the longitudinal and lateral signals separately or in combination. Each input is of an accuracy which no pilot can offer. Thus, a better response analysis can be done if the helicopter's motion is also measured. The different components of the stimulation system and their functions and performance are described. Examples of ground and flight testing are presented for various subjects like ground and air resonance, flight mechanical control response and engine characteristics. For comparison, diagrams of former helicopter testing with manual control inputs are shown and discussed. ESA

N92-30922*# Oregon State Univ., Corvallis. Dept. of Electrical and Computer Engineering.
NONLINEAR STABILITY AND CONTROL STUDY OF HIGHLY MANEUVERABLE HIGH PERFORMANCE AIRCRAFT, PHASE 2 Annual Report
R. R. Mohler 20 Aug. 1992 68 p
(Grant NAG1-1081)
(NASA-CR-190667; NAS 1.26:190667; OSU-ECE-NASA-92-02)
Avail: CASI HC A04/MF A01

This research should lead to the development of new nonlinear methodologies for the adaptive control and stability analysis of high angle-of-attack aircraft such as the F18 (HARV). The emphasis has been on nonlinear adaptive control, but associated model development, system identification, stability analysis and simulation is performed in some detail as well. Various models under investigation for different purposes are summarized in tabular form. Models and simulation for the longitudinal dynamics have been developed for all types except the nonlinear ordinary differential equation model. Briefly, studies completed indicate that nonlinear adaptive control can outperform linear adaptive control for rapid maneuvers with large changes in alpha. The transient responses are compared where the desired alpha varies from 5 degrees to 60 degrees to 30 degrees and back to 5 degrees in all about 16 sec. Here, the horizontal stabilator is the only control used with an assumed first-order linear actuator with a 1/30 sec time constant. Author

N92-31175*# National Aeronautics and Space Administration. Langley Research Center, Hampton, VA.
PRELIMINARY SUBSONIC AERODYNAMIC MODEL FOR SIMULATION STUDIES OF THE HL-20 LIFTING BODY
E. Bruce Jackson and Christopher I. Cruz Aug. 1992 68 p
(RTOP 505-64-40-01)
(NASA-TM-4302; L-16956; NAS 1.15:4302) Avail: CASI HC A04/MF A01

A nonlinear, six-degree-of-freedom aerodynamic model for an early version of the HL-20 lifting body is described and compared with wind tunnel data upon which it is based. Polynomial functions describing most of the aerodynamic parameters are given and tables of these functions are presented. Techniques used to arrive at these functions are described. Basic aerodynamic coefficients were modeled as functions of angles of attack and sideslip. Vehicle lateral symmetry was assumed. Compressibility (Mach) effects were ignored. Control-surface effectiveness was assumed to vary linearly with angle of deflection and was assumed to be invariant with the angle of sideslip. Dynamic derivatives were obtained from predictive aerodynamic codes. Landing-gear and ground effects were scaled from Space Shuttle data. The model described is provided to support pilot-in-the-loop simulation studies of the HL-20. By providing the data in tabular format, the model is suitable for the data interpolation architecture of many existing engineering simulation facilities. Because of the preliminary nature of the data, however, this model is not recommended for study of the absolute performance of the HL-20. Author

09 RESEARCH AND SUPPORT FACILITIES (AIR)

Includes airports, hangars and runways; aircraft repair and overhaul facilities; wind tunnels; shock tubes; and aircraft engine test stands.

For related information see also *14 Ground Support Systems and Facilities (Space).*

N92-30329# Army Electronic Proving Ground, Fort Huachuca, AZ.

ANTENNA PATTERN MEASUREMENT FACILITIES Final Report

16 May 1991 96 p

(AD-A248964) Avail: CASI HC A05/MF A01

The test operations procedure (TOP) is an overview of procedures for testing antennas using the automated data acquisition and analysis system (ADAAS) at the Antenna Test Facility (ATF), US Army Electronic Proving Ground, Fort Huachuca, Arizona. The ATF has two test ranges: an outdoor compact range and an arc range. The Compact Range uses a parabolic reflector to collimate radio frequency energy in order to simulate far-field testing. A large hydraulic positioner moves the test antenna through azimuth and elevation arcs to allow testing of an entire hemisphere of coverage. The Arc Range operates in the near field using uncollimated RF. It uses a turntable to rotate the test item through the desired range of azimuth; a probe antenna moving along the vertical arc structure provides elevation coverage. The combination provides full hemispherical coverage. The TOP describes procedures for measuring antenna gain; locations of beams, lobes, and nulls; and other antenna characteristics. It contrasts the capabilities of the two ranges and provides guidelines to help the user select the right range for a particular test. GRA

N92-30508*# National Aeronautics and Space Administration. Lewis Research Center, Cleveland, OH.

SMALL ENGINE COMPONENTS TEST FACILITY COMPRESSOR TESTING CELL AT NASA LEWIS RESEARCH CENTER

Richard A. Brokopp and Robert S. Gronski (Sverdrup Technology, Inc., Brook Park, OH.) Jul. 1992 13 p Proposed for presentation at the 17th AIAA Aerospace Ground Testing Conference, Nashville, TN, 6-8 Jul. 1992

(RTOP 505-62-84)

(NASA-TM-105685; E-7064; NAS 1.15:105685; AIAA Paper 92-3980) Avail: CASI HC A03/MF A01

LeRC has designed and constructed a new test facility. This facility, called the Small Engine Components Tests Facility (SECTF), is used to test gas turbines and compressors at conditions similar to actual engine conditions. The SECTF is comprised of a compressor testing cell and a turbine testing cell. Only the compressor testing cell is described. The capability of the facility, the overall facility design, the instrumentation used in the facility, and the data acquisition system are discussed in detail. Author

N92-30547# IIT Research Inst., Lanham, MD.

DEVELOPMENT STATISTICS FOR THE UH-1 ADA FEASIBILITY STUDY

Jan. 1992 152 p

(AD-A252404) Avail: CASI HC A08/MF A01

This document describes data collection and analysis techniques that were applied to an Ada software redevelopment of the UH-1 Flight Simulator (FS). It presents results for the following subject areas: the application of function point analysis to estimate trainer size; the application of Ada COCOMO, SoftCost Ada, and SASET models to estimate schedule and efforts; and the application of AdaMAT/D to evaluate trainer quality. The report also describes results of a project profile study to characterize aspects of the development environment. GRA

N92-30621# Army Cold Regions Research and Engineering Lab., Hanover, NH.

POTENTIAL AIRFIELD SITES IN ANTARCTICA FOR WHEELED AIRCRAFT

Charles Swithinbank Dec. 1991 70 p

(AD-A249503; CRREL-SR-91-24) Avail: CASI HC A04/MF A01

This is a report on a search for possible or potential airfield sites in Antarctica, using aerial photographs and satellite images supplemented by other data. A few sites are on ice-free ground but the majority are on inland blue ice fields. Earlier studies of potential airfields on Antarctic glacier ice are referenced. The attraction of a well-chosen blue-ice runway is that construction and maintenance costs are almost nil. A number of sites have been found suitable for the operation of unmodified transport aircraft on wheels. An inland icefield site on Mill Glacier (85 deg 09 min S, 167 deg 12 min E) is in use for wheel landings by LC-130 aircraft; another at Patriot Hills (80 deg 19 min S, 81 deg 16 min W) is in use for wheel landings by DC-6 aircraft. GRA

N92-30769# Advisory Group for Aerospace Research and Development, Neuilly-Sur-Seine (France). Flight Mechanics Panel.

TECHNICAL EVALUATION REPORT ON THE FLIGHT MECHANICS PANEL SYMPOSIUM ON PILOTED SIMULATION EFFECTIVENESS [L'EFFICACITE DE LA SIMULATION PILOTEE]

A. G. Barnes (Barnes, A. G., Lytham Saint Annes, England) Apr. 1992 17 p In FRENCH Symposium held in Brussels, Belgium, 14-17 Oct. 1991

(AGARD-AR-315; ISBN-92-835-0669-3) Copyright Avail: CASI HC A03/MF A01

This report evaluates the AGARD Flight Mechanics Panel Symposium on Piloted Simulator Effectiveness, held from 14 to 17 Oct. 1991, in Brussels, Belgium. The intention of the Symposium was to assess the benefits and the future potential of flight simulation in contributing to aircraft development, skill training, and mission training, for both fixed wing and rotary wing aircraft. In particular, contributors were asked to compare the results of simulated and real tasks. The papers were wide ranging and of high quality; several new ideas emerged. The technology of flight simulation has greatly improved since the last symposium on this topic, in 1985. The emphasis of work related to fixed wing aircraft has shifted towards systems integration. A greater contribution to helicopter design and clearance is also evident. Although new visual display devices show great promise for military flight training at high speed, low level, they are not yet fully proven, and it is recommended that an early return is made to the topic of pilot training. Simulator validation and fidelity are also of growing importance. Author

N92-30777# Federal Aviation Administration, Washington, DC. Office of Aviation Policy and Plans.
ALLOCATION AND RECOVERY OF FEDERAL AIRPORT AND AIRWAY COSTS, 1991 Final Report
Daniel E. Taylor Feb. 1992 24 p
(AD-A249436; FAA/APO-210; FAA/APO-91-4) Avail: CASI HC A03/MF A01

This report presents estimates of the allocation and recovery of federal airport and airway system costs. Estimates for 1991 were constructed using an econometric model that attributes fixed, joint, and marginal airspace system costs to aviation user groups. Two methods are used to allocate FAA costs. First, a full cost allocation attributes direct costs to each user and allocates all remaining joint and overhead costs among users. Second, a minimum cost allocation estimate is made for general aviation based on the concept of avoidable costs. The results of the full cost allocation indicate that about 62 percent of FAA costs in 1991 are attributable to air carriers. General aviation and the public sector accounted for 26 and 12 percent of FAA costs, respectively. GRA

N92-30849# Army Missile Command, Redstone Arsenal, AL. Weapons Science Directorate.
DESIGN AND CONSTRUCTION OF A HELMHOLTZ COIL MAGNETIC TEST CELL Final Report, Jun. - Oct. 1991
Darryl Holder Feb. 1992 18 p
(AD-A249944; AD-E951786; AMSMI/TR-RD-WS-92-1) Avail: CASI HC A03/MF A01

A Helmholtz coil magnetic cell was designed and constructed in order to properly test various systems of interest which involve sensing a magnetic environment as part of their normal function. The electric current feed to the coil is provided by a low impedance, close-spaced busbar assembly so that nonsolenoidal magnetic fields are kept to a minimum. Based on the calibration run described in this report, the Helmholtz coil is seen to provide a usable magnetic field for the testing of smaller items. A more precise calibration and an impulse driver circuit designed to exactly simulate the required drive current waveform would substantially increase the ability to perform tests on an absolute basis. As it stands, this Helmholtz coil and its driver circuit is quite useful for a number of testing purposes. Author (GRA)

N92-30897# Arnold Engineering Development Center, Arnold Air Force Station, TN.
FUTURE AEROSPACE GROUND TEST FACILITY REQUIREMENTS FOR THE ARNOLD ENGINEERING DEVELOPMENT CENTER
Mark E. Kirchner (Boeing Co., Mercer Island, WA.), Judson R. Baron (Massachusetts Inst. of Tech., Cambridge.), Seymour M. Bogdonoff (Princeton Univ., NJ.), Donald I. Carter (Rockwell International Corp., El Segundo, CA.), Lana M. Couch (National Aeronautics and Space Administration. Langley Research Center, Hampton, VA.), Arthur E. Fanning (Boeing Commercial Airplane Co., Seattle, WA.), William H. Heiser (Tennessee Univ. Space Inst., Tullahoma.), Bernard L. Koff (Pratt and Whitney Aircraft, West Palm Beach, FL.), Robert E. Melnik (Grumman Aerospace Corp., Bethpage, NY.), and Stephen C. Mercer (General Dynamics Corp., Fort Worth, TX.) et al 1992 78 p Prepared in cooperation with Air Force Academy, CO
(Contract F40650-90-C-0061)
Avail: CASI HC A05/MF A01

Arnold Engineering Development Center (AEDC) was conceived at the close of World War II, when major new developments in flight technology were presaged by new aerodynamic and propulsion concepts. During the past 40 years, AEDC has played a significant part in the development of many aerospace systems. The original plans were extended through the years by some additional facilities, particularly in the area of propulsion testing. AEDC now has undertaken development of a master plan in an attempt to project requirements and to plan for ground test and computational facilities over the coming 20 to 30 years. This report was prepared in response to an AEDC request that the National Research Council (NRC) assemble a committee to prepare guidance for planning and modernizing AEDC facilities for the development and testing of future classes of aerospace systems as envisaged by the U.S. Air Force. Author

N92-30976# Federal Aviation Administration, Atlantic City, NJ.
GNAS MAINTENANCE CONTROL CENTER (GMCC) DESIGN QUALIFICATION TEST AND EVALUATION (DQT/E) TEST PROCEDURES
Richard Van Suetendael Jun. 1992 159 p
(DOT/FAA/CT-TN91/40) Avail: CASI HC A08/MF A02

This document presents the procedures used for Design Qualification Test and Evaluation (DQT&E) testing of the General National Airspace System (GNAS) Maintenance Control Center (GMCC). The Test Director conducted DQT&E testing at the Federal Aviation Administration (FAA) Technical Center, Atlantic City International Airport, N.J. The purpose of the test is to verify that the phase 1 and phase 2 GMCC design requirements are met. Author

N92-31192# Department of the Navy, Washington, DC.
THRUST TEST FIXTURE Patent Application
Christopher F. Hillenbrand, inventor (to Navy) 27 Nov. 1991 9 p
(AD-D015259; US-Patent-Appl-SN-800785) Avail: CASI HC A02/MF A01

The invention relates generally to test fixtures for measuring the thrust developed by a device which includes some sort of of rotating propeller or impeller designed to draw a fluid medium in one end of the device and eject the fluid medium out of the opposite end of the device. The device to be tested is supported from a beam by two parallel links so the thrust direction remains perpendicular to the direction of gravity. Each link is connected to the beam by a tension transducer also oriented perpendicular to the direction of gravity. The aim of the present invention is to provide a test fixture for evaluating the thrust output of submersible devices of the type used in subsurface remotely controlled vehicles. GRA

12 ASTRONAUTICS (GENERAL)

For extraterrestrial exploration see *91 Lunar and Planetary Exploration.*

No abstracts in this category.

13 ASTRODYNAMICS

Includes powered and free-flight trajectories; and orbital and launching dynamics.

No abstracts in this category.

14 GROUND SUPPORT SYSTEMS AND FACILITIES (SPACE)

Includes launch complexes, research and production facilities; ground support equipment, e.g., mobile transporters; and simulators.

For related information see also *09 Research and Support Facilities (Air).*

N92-30307*# National Aeronautics and Space Administration. Lewis Research Center, Cleveland, OH.
THREE-DIMENSIONAL LASER WINDOW FORMATION
Vincent G. Verhoff Jul. 1992 12 p

(RTOP 505-62-84)
(NASA-RP-1280; E-6096; NAS 1.61:1280) Avail: CASI HC A03/MF A01

The NASA Lewis Research Center has developed and implemented a unique process for forming flawless three-dimensional laser windows. These windows represent a major part of specialized, nonintrusive laser data acquisition systems used in a variety of compressor and turbine research test facilities. This report discusses in detail the aspects of three-dimensional laser window formation. It focuses on the unique methodology and the peculiarities associated with the formation of these windows. Included in this discussion are the design criteria, bonding mediums, and evaluation testing for three-dimensional laser windows. Author

15 LAUNCH VEHICLES AND SPACE VEHICLES

Includes boosters; operating problems of launch/space vehicle systems; and reusable vehicles.

For related information see also *20 Spacecraft Propulsion and Power.*

N92-30310*# National Aeronautics and Space Administration. Lewis Research Center, Cleveland, OH.
AN ELECTROMECHANICAL ACTUATION SYSTEM FOR AN EXPENDABLE LAUNCH VEHICLE
Linda M. Burrows and Mary Ellen Roth Aug. 1992 7 p Presented at the 27th Intersociety Energy Conversion Engineering Conference, San Diego, CA, 3-7 Aug. 1992; sponsored by SAE, ACS, AIAA, ASME, IEEE, AIChE, and ANS
(RTOP 506-41-41)
(NASA-TM-105774; E-7202; NAS 1.15:105774) Avail: CASI HC A02/MF A01

A major effort at the NASA Lewis Research Center in recent years has been to develop electro-mechanical actuators (EMA's) to replace the hydraulic systems used for thrust vector control (TVC) on launch vehicles. This is an attempt ot overcome the inherent inefficiencies and costs associated with the existing hydraulic structures. General Dynamics Space Systems Division, under contract to NASA Lewis, is developing 18.6 kW (25 hp), 29.8 kW (40 hp), and 52.2 kW (70 hp) peak EMA systems to meet the power demands for TVC on a family of vehicles developed for the National Launch System. These systems utilize a pulse population modulated converter and field-oriented control scheme to obtain independent control of both the voltage and frequency. These techniques allow an induction motor to be operated at its maximum torque at all times. At NASA Lewis, we are building on this technology to develop our own in-house system capable of meeting the peak power requirements for an expendable launch vehicle (ELV) such as the Atlas. Our EMA will be capable of delivering 22.4 kW (30 hp) peak power with a nominal of 6.0 kW (8 hp). This system differs from the previous ones in two areas: (1) the use of advanced control methods, and (2) the incorporation of built-in-test. The advanced controls are essential for minimizing the controller size, while the built-in-test is necessary to enhance the system reliability and vehicle health monitoring. The ultimate goal of this program is to demonstrate an EMA which will be capable of self-test and easy integration into other projects. This paper will describe the effort underway at NASA Lewis to develop an EMA for an Atlas class ELV. An explanation will be given for each major technology block, and the status of each major technology block and the status of the overall program will be reported. Author

N92-30715 Elliott-Automation Space and Advanced Military Systems Ltd., Camberley (England).
EASAMS' ARIANE 5 ON-BOARD SOFTWARE EXPERIENCE
Steven Andrew Birnie 1991 40 p Presented at the 2nd Ada in Aerospace Symposium, Rome, Italy
(D308/TN/001; ETN-92-91716) Avail: EASAMS System Engineering G.m.b.H., Max-Eyth-Str. 60, W-7996 Meckenbeuren, Fed. Republic of Germany

The design and development of the prototype flight software for the Ariane 5 satellite launch vehicle is considered. This was specified as being representative of the eventual real flight program in terms of timing constraints and target computer loading. The usability of HOOD (Hierarchical Object Oriented Design) and Ada for development of such preemptive multitasking computer programs was verified. Features of the prototype development included: design methods supplementary to HOOD for representation of concurrency aspects; visibility of Ada enumerated type literals across HOOD parent-child interfaces; deterministic timings achieved by modification of Ada delays; and linking of interrupts to Ada task entries. ESA

N92-31160*# National Aeronautics and Space Administration. Langley Research Center, Hampton, VA.
REAL-TIME SIMULATION MODEL OF THE HL-20 LIFTING BODY
E. Bruce Jackson, Christopher I. Cruz, and W. A. Ragsdale (Unisys Corp., Hampton, VA.) Jul. 1992 423 p
(RTOP 505-64-52-01)
(NASA-TM-107580; NAS 1.15:107580) Avail: CASI HC A18/MF A04

A proposed manned spacecraft design, designated the HL-20, has been under investigation at Langley Research Center. Included in that investigation are flight control design and flying qualities studies utilizing a man-in-the-loop real-time simulator. This report documents the current real-time simulation model of the HL-20 lifting body vehicle, known as version 2.0, presently in use at NASA Langley Research Center. Included are data on vehicle aerodynamics, inertias, geometries, guidance and control laws, and cockpit displays and controllers. In addition, trim case and dynamic check case data is provided. The intent of this document is to provide the reader with sufficient information to develop and validate an equivalent simulation of the HL-20 for use in real-time or analytical studies. Author

16 SPACE TRANSPORTATION

Includes passenger and cargo space transportation, e.g., shuttle operations; and space rescue techniques.

For related information see also *03 Air Transportation and Safety* and *18 Spacecraft Design, Testing and Performance.* For space suits see *54 Man/System Technology and Life Support.*

N92-30382*# National Aeronautics and Space Administration. Lyndon B. Johnson Space Center, Houston, TX.
DEBRIS/ICE/TPS ASSESSMENT AND INTEGRATED PHOTOGRAPHIC ANALYSIS FOR SHUTTLE MISSION STS-45
Gregory N. Katnik, Scott A. Higginbotham, and J. Bradley Davis 24 Mar. 1992 176 p LIMITED REPRODUCIBILITY: More than 20% of this document may be affected by color photographs Original contains color illustrations
(NASA-TM-107545; NAS 1.15:107545) Avail: CASI HC A09/MF A02; 89 functional color pages

The Debris Team has developed and implemented measures to control damage from debris in the Shuttle operational environment and to make the control measures a part of routine launch flows. These measures include engineering surveillance during vehicle processing and closeout operations, facility and flight hardware inspections before and after launch, and photographic analysis of mission events. Photographic analyses of mission imagery from launch, on-orbit, and landing provide significant data in verifying proper operation of systems and evaluating anomalies. In addition to the Kennedy Space Center (KSC) Photo/Video Analysis, reports from Johnson Space Center, Marshall Space Flight Center, and Rockwell International-Downey are also included to provide an integrated assessment of each Shuttle mission. Author

N92-30440# Messerschmitt-Boelkow-Blohm G.m.b.H., Munich (Germany, F.R.).
PROGRESS IN THE DEVELOPMENT OF THE HERMES EVAPORATORS
C. Goehre (Erno Raumfahrttechnik G.m.b.H. Bremen, Germany, F.R.), R. Bohlen (Erno Raumfahrttechnik G.m.b.H. Bremen, Germany, F.R.), Bernhard J. G. Leidinger (Erno Raumfahrttechnik G.m.b.H. Bremen, Germany, F.R.), R. Mueller (Erno Raumfahrttechnik G.m.b.H. Bremen, Germany, F.R.), P. Mueller-Remmers (Erno Raumfahrttechnik G.m.b.H. Bremen, Germany, F.R.), and R. Rohr (Erno Raumfahrttechnik G.m.b.H. Bremen, Germany, F.R.) 1991 7 p Presented at the 4th European Symposium on Space Environmental Control Systems, Florence, Italy, 21-25 Oct. 1991
(MBB-UO-0164-91-PUB; ETN-92-91892) Avail: CASI HC A02/MF A01

The results of the first development approaches of the three waste heat rejection evaporators for the Hermes spaceplane are presented. These are the Water Evaporator Assembly (WEA), the Ammonia Boiler Assembly (ABA), and the Hydraulic Thermal Control Assembly (HTCA). Some important development activities, in particular tests of the technology demonstration models for WEA and ABA are summarized. Tests with these first evaporator prototypes of WEA and ABA showed, that the requirements for the flight unit can be met and certain problems have to be solved. In HTCA, sample tests are envisaged up to now. ESA

N92-30958# RAND Corp., Santa Monica, CA.
SPACE TRANSPORTATION SYSTEMS, LAUNCH SYSTEMS, AND PROPULSION FOR THE SPACE EXPLORATION INITIATIVE: RESULTS FROM PROJECT OUTREACH
T. Garber, J. Hiland, D. Orletsky, B. Augenstein, and M. Miller 1991 205 p Sponsored by NASA. Marshall Space Flight Center
(Contract F49620-86-C-0008)
(NASA-CR-190345; NAS 1.26:190345; N-3283-AF/NASA) Avail: CASI HC A10/MF A03

A number of transportation and propulsion options for Mars exploration missions are analyzed. As part of Project Outreach, RAND received and evaluated 350 submissions in the launch vehicle, space transportation, and propulsion areas. After screening submissions, aggregating those that proposed identical or nearly identical concepts, and eliminating from further consideration those that violated known physical princples, we had reduced the total number of viable submissions to 213. In order to avoid comparing such disparate things as launch vehicles and electric propulsion systems, six broad technical areas were selected to categorize the submissions: space transportation systems; earth-to-orbit (ETO) launch systems; chemical propulsion; nuclear propulsion; low-thrust propulsion; and other. To provide an appropriate background for analyzing the submissions, an extensive survey was made of the various technologies relevant to the six broad areas listed above. We discuss these technologies with the intent of providing the reader with an indication of the current state of the art, as well as the advances that might be expected within the next 10 to 20 years. Author

17 SPACE COMM., SPACECRAFT COMM., COMMAND & TRACKING

Includes telemetry; space communications networks; astronavigation and guidance; and radio blackout.

For related information see also *04 Aircraft Communications and Navigation* and *32 Communications and Radar.*

N92-30383*# National Aeronautics and Space Administration. Lewis Research Center, Cleveland, OH.
THE ACTS MULTIBEAM ANTENNA
Frank A. Regier Apr. 1992 12 p
(RTOP 679-40-00)
(NASA-TM-105645; E-7000; NAS 1.15:105645) Avail: CASI HC A03/MF A01

The Advanced Communications Technology Satellite (ACTS) to be launched in 1993 introduces several new technologies including a multibeam antenna (MBA) operating at Ka-band. The satellite is introduced briefly, and then the MBA, consisting of electrically similar 30 GHz received and 20 GHz transmit offset Cassegrain systems utilizing orthogonal linear polarizations, is described. Dual polarization is achieved by using one feed assembly for each polarization in conjunction with nested front and back subreflectors, the gridded front subreflector acting as a window for one polarization and a reflector for the other. The antennas produce spot beams with approximately 0.3 deg beamwidth and gains of approximately 50 dbi. High surface accuracy and high edge taper produce low sidelobe levels and high cross-polarization isolation. A brief description is given of several Ka-band components fabricated for ACTS. These include multiflare antenna feedhorns, beam-forming networks utilizing latching ferrite waveguide switches, a 30 GHz high mobility electron transmitter (HEMT) low-noise amplifier and a 20 GHz TWT power amplifier. Author

N92-30709*# Notre Dame Univ., IN. Dept. of Electrical Engineering.
BANDWIDTH EFFICIENT CCSDS CODING STANDARD PROPOSALS Semiannual Status Report
Daniel J. Costello, Jr., Lance C. Perez, and Fu-Quan Wang May 1992 71 p
(Grant NAG5-557)
(NASA-CR-190317; NAS 1.26:190317) Avail: CASI HC A04/MF A01

The basic concatenated coding system for the space telemetry channel consists of a Reed-Solomon (RS) outer code, a symbol interleaver/deinterleaver, and a bandwidth efficient trellis inner code. A block diagram of this configuration is shown. The system may operate with or without the outer code and interleaver. In this recommendation, the outer code remains the (255,223) RS code over GF(2 exp 8) with an error correcting capability of t = 16 eight bit symbols. This code's excellent performance and the existence of fast, cost effective, decoders justify its continued use. The purpose of the interleaver/deinterleaver is to distribute burst errors out of the inner decoder over multiple codewords of the outer code. This utilizes the error correcting capability of the outer code more efficiently and reduces the probability of an RS decoder failure. Since the space telemetry channel is not considered bursty, the required interleaving depth is primarily a function of the inner decoding method. A diagram of an interleaver with depth 4 that is compatible with the (255,223) RS code is shown. Specific interleaver requirements are discussed after the inner code recommendations. Author

18 SPACECRAFT DESIGN, TESTING AND PERFORMANCE

Includes satellites; space platforms; space stations; spacecraft systems and components such as thermal and environmental controls; and attitude controls.

For life support systems see *54 Man/System Technology and Life Support.* For related information see also *05 Aircraft Design, Testing and Performance, 39 Structural Mechanics,* and *16 Space Transportation.*

N92-30257# Ballistic Research Labs., Aberdeen Proving Ground, MD.
DEVELOPMENT OF DIAGNOSTICS FOR ELECTROMAGNETIC ARMOR APPLICATIONS Final Report, Apr. 1989 - Jan. 1991
Charles R. Hummer and Clinton E. Hollandsworth Jun. 1992 36 p
(DA Proj. 1L1-61102-AH-43)
(AD-A251074; BRL-TR-3358) Avail: CASI HC A03/MF A01

A test stand consisting of an electrified-plate assembly coupled to a small capacitor bank has been assembled, tested, and used to develop diagnostic instrumentation to be exploited in future range experiments in the general area of electromagnetic

technology applied to terminal ballistics. A 1.2-m-long air gun is used to propel a length of copper wire through small holes in the electrified-plate assembly to simulate the switch-closure action important to some planned range experiments. Instrumentation to measure the relevant currents and voltages was developed and used to characterize the switch-closing action. The test stand was used to calibrate the diagnostics, test their immunity to noise, and measure their time response. The velocity of the wire was determined by optical means. Using this velocity, the features observed with the diagnostics were then correlated with the position of the wire in the test stand. GRA

N92-30315*# National Aeronautics and Space Administration. Lyndon B. Johnson Space Center, Houston, TX.
SPACE STATION TRASH REMOVAL SYSTEM Patent Application
Andrew J. Petro, inventor (to NASA) 22 May 1992 15 p
(NASA-Case-MSC-21723-1; NAS 1.71:MSC-21723-1; US-Patent-Appl-SN-887001) Avail: CASI HC A03/MF A01

A trash removal system for space stations is described. The system is comprised of a disposable trash bag member and an attached, compacted large, lightweight inflatable balloon element. When the trash bag member is filled, the astronaut places the bag member into space through an airlock. Once in the vacuum of space, the balloon element inflates. Due to the large cross-sectional area of the balloon element relative to its mass, the combined balloon element and the trash bag member are slowed by atmospheric drag to a much greater extent than the Space Station's. The balloon element and bag member lose altitude and re-enter the atmosphere, and the elements and contents are destroyed by aerodynamic heating. The novelty of this system is in the unique method of using the vacuum of space and aerodynamic heating to dispose of waste material with a minimum of increase in orbital debris. NASA

N92-30628# Systems Science and Software, La Jolla, CA.
DATA ANALYSIS SUPPORT FOR THE SHUTTLE POTENTIAL AND RETURN ELECTRON EXPERIMENT (SPREE) ON THE TETHERED SATELLITE SYSTEM 1 (TSS-1) FLIGHT Scientific Report No. 1
T. T. Luu, V. A. Davis, J. R. Lilley, and I. Katz 24 Jun. 1991 126 p
(Contract F19628-90-C-0133)
(AD-A248943; AD-E200987; SSS-DPR-91-2194; PL-TR-91-2194) Avail: CASI HC A07/MF A02

This study describes the interactions between the Tethered Satellite System (TSS-1) and the ionosphere. The objective is to increase the understanding of the structure and current characteristics of high-voltage sheaths in the ionosphere. The investigations described here include a determination of the tether current and voltages, an evaluation of the shuttle orbiter ion collection, the ion current detected by the SPREE instrumentation, and the effect of the subsatellite thrusters on the surrounding neutral densities. GRA

N92-30736*# National Aeronautics and Space Administration. Langley Research Center, Hampton, VA.
A CONCEPTUAL DESIGN OF A LARGE APERTURE MICROWAVE RADIOMETER GEOSTATIONARY PLATFORM
Paul A. Garn (Science and Technology Corp., Hampton, VA.), James L. Garrison, and Rachel Jasinski (Flight Mechanics and Control, Inc., Hampton, VA.) Jun. 1992 38 p
(RTOP 506-49-21-02)
(NASA-TM-107577; NAS 1.15:107577) Avail: CASI HC A03/MF A01

A conceptual design of a Large Aperture Microwave Radiometer (LAMR) Platform has been developed and technology areas essential to the design and on-orbit viability of the platform have been defined. Those technologies that must be developed to the requirement stated here for the LAMR mission to be viable include: advanced radiation resistant solar cells, integrated complex structures, large segmented reflector panels, sub 3 kg/m(exp 2) areal density large antennas, and electric propulsion systems. Technology areas that require further development to enhance the capabilities of the LAMR platform (but are not essential for viability) include: electrical power storage, on-orbit assembly, and on-orbit systems checkout and correction. Author

N92-31225*# POD Associates, Inc., Albuquerque, NM.
ENVIRONMENT MODELLING IN NEAR EARTH SPACE: PRELIMINARY LDEF RESULTS
C. R. Coombs, D. R. Atkinson, J. D. Wagner, L. B. Crowell, M. Allbrooks, and A. J. Watts *In* Lunar and Planetary Inst., Twenty-Third Lunar and Planetary Science Conference 1992 p 7-11 (For primary document see N92-31222 21-88)
Avail: CASI HC A01/MF A01

19 SPACECRAFT INSTRUMENTATION

For related information see also *06 Aircraft Instrumentation* and *35 Instrumentation and Photography.*

N92-30301*# National Aeronautics and Space Administration. Lewis Research Center, Cleveland, OH.
DEVELOPMENT OF AND FLIGHT RESULTS FROM THE SPACE ACCELERATION MEASUREMENT SYSTEM (SAMS)
Richard DeLombard, Brian D. Finley (Sverdrup Technology, Inc., Brook Park, OH.), and Charles R. Baugher (National Aeronautics and Space Administration. Marshall Space Flight Center, Huntsville, AL.) Jan. 1992 12 p Presented at the 30th Aerospace Science Meeting and Exhibit, Reno, NV, 6-9 Jan. 1992; sponsored in part by AIAA Previously announced in IAA as A92-28189
(RTOP 694-03-OH)
(NASA-TM-105652; E-7018; NAS 1.15:105652; AIAA Paper 92-0354) Avail: CASI HC A03/MF A01

Described here is the development of and the flight results from the Space Acceleration Measurement System (SAMS) flight units used in the Orbiter middeck, Spacelab module, and the Orbitercargo bay. The SAMS units are general purpose microgravity accelerometers designed to support a variety of science experiments with microgravity acceleration measurements. A total of six flight units have been fabricated; four for use in the Orbiter middeck and Spacelab module, and two for use in the Orbiter cargo bay. The design of the units is briefly described. The initial two flights of SAMS units on STS-40 (June 1991) and STS-43 (August 1991) resulted in 371 megabytes and 2.6 gigabytes of data respectively. Analytical techniques developed to examine this quantity of acceleration data are described and sample plots of analyzed data are illustrated. Future missions for the SAMS units are listed. Author

20 SPACECRAFT PROPULSION AND POWER

Includes main propulsion systems and components, e.g., rocket engines; and spacecraft auxilliary power sources.

For related information see also *07 Aircraft Propulsion and Power, 28 Propellants and Fuels, 44 Energy Production and Conversion,* and *15 Launch Vehicles and Space Vehicles.*

N92-30308*# National Aeronautics and Space Administration. Lewis Research Center, Cleveland, OH.
NEP SYSTEMS ENGINEERING EFFORTS IN FY-92: PLANS AND STATUS
Michael P. Doherty and James H. Gilland (Sverdrup Technology, Inc., Brook Park, OH.) Aug. 1992 10 p Presented at the Nuclear Technologies for Space Exploration Conference, Jackson Hole, WY, 16-19 Aug. 1992; sponsored in part by American Nuclear Society
(Contract NAS3-25266; RTOP 593-72-00)
(NASA-TM-105775; E-7203; NAS 1.15:105775) Avail: CASI HC A02/MF A01

A system engineering effort has been initiated by NASA in

FY-92 to define, address, and resolve issues associated with the use of Nuclear Electric Propulsion (NEP) for megawatt (MW) space propulsion applications associated with the Space Exploration Initiative (SEI). It is intended that key technical issues will be addressed by activities conducted in the early years of a project in NEP, with the objective of resolving such issues. Also, in response to more recent programmatic direction, a concept definition activity for 100 kilowatt NEP is being initiated. This paper will present key issues associated with megawatt NEP, and the plans and status for their resolution, and present the scope and rationale for the 100 kilowatt concept definition activity. Author

N92-30818*# National Aeronautics and Space Administration. Lewis Research Center, Cleveland, OH.
NUCLEAR ELECTRIC PROPULSION DEVELOPMENT AND QUALIFICATION FACILITIES
D. S. Dutt (Westinghouse Hanford Co., Richland, WA.), K. Thomassen (Lawrence Livermore National Lab., CA.), J. Sovey, and Mario Fontana (Oak Ridge National Lab., TN.) Nov. 1991 11 p Presented at the 9th Symposium on Space Nuclear Power Systems, Albuquerque, NM, 13-16 Jan. 1992
(Contract DE-AC06-87RL-10930)
(NASA-TM-105521; NAS 1.15:105521; DE92-004262; WHC-SA-1402; CONF-920104-23) Avail: CASI HC A03/MF A01

This paper summarizes the findings of a Tri-Agency panel consisting of members from the National Aeronautics and Space Administration (NASA), U.S. Department of Energy (DOE), and U.S. Department of Defense (DOD) that were charged with reviewing the status and availability of facilities to test components and subsystems for megawatt-class nuclear electric propulsion (NEP) systems. The facilities required to support development of NEP are available in NASA centers, DOE laboratories, and industry. However, several key facilities require significant and near-term modification in order to perform the testing required to meet a 2014 launch date. For the higher powered Mars cargo and piloted missions, the priority established for facility preparation is: (1) a thruster developmental testing facility, (2) a thruster lifetime testing facility, (3) a dynamic energy conversion development and demonstration facility, and (4) an advanced reactor testing facility (if required to demonstrate an advanced multiwatt power system). Facilities to support development of the power conditioning and heat rejection subsystems are available in industry, federal laboratories, and universities. In addition to the development facilities, a new preflight qualifications and acceptance testing facility will be required to support the deployment of NEP systems for precursor, cargo, or piloted Mars missions. Because the deployment strategy for NEP involves early demonstration missions, the demonstration of the SP-100 power system is needed by the early 2000's. Author

N92-30981*# Alabama A & M Univ., Normal.
NUMERICAL INVESTIGATIONS IN THE BACKFLOW REGION OF A VACUUM PLUME Semiannual Technical Report, Oct. 1991 - May 1992
Goang-Shin Liaw May 1992 37 p
(Grant NAG8-201)
(NASA-CR-190515; NAS 1.26:190515) Avail: CASI HC A03/MF A01

The objective of this research is to numerically simulate the vacuum plume flow field in the backflow region of a low thrust nozzle exit. In space applications, the low thrust nozzles are used as a propulsion device to control the vehicle attitude, or to maneuver the vehicle flight trajectory. When the spacecraft is deployed in the orbit or cruising in a planetary mission, the vacuum plume is created behind the nozzle exit (so called backflow region), by the exhausting gas of the propulsion system or by venting internal gas to the extremely low density ambient. The low density vacuum plume flow regions cover the continuum, transitional and free molecular flow regimes, which were characterized by the Knudsen number K(sub n), K(sub n) = lambda(sub m)/L where lambda(sub m) is the mean free path of the gas molecules and L is the characteristic length of the flow field. The transitional regime is defined by 0.01 is less than or equal to K(sub n) is less than or equal to 10. The conventional Navier-Stokes equations are valid only in the flow region close to the nozzle exit since the validity of the Navier-Stokes equations fails asymptotically as the Knudsen number increases. The vacuum plume characteristics prediction is primarily a problem of transitional aerodynamics. Author

N92-30989*# Valparaiso Univ., IN. Electrical and Computer Engineering.
DEVELOPMENT OF SOFTWARE TO IMPROVE AC POWER QUALITY ON LARGE SPACECRAFT
L. Alan Kraft 31 Dec. 1991 29 p
(Grant NAG3-1254)
(NASA-CR-190569; NAS 1.26:190569) Avail: CASI HC A03/MF A01

To insure the reliability of a 20 kHz, alternating current (AC) power system on spacecraft, it is essential to analyze its behavior under many adverse operating conditions. Some of these conditions include overloads, short circuits, switching surges, and harmonic distortions. Harmonic distortions can become a serious problem. It can cause malfunctions in equipment that the power system is supplying, and, during distortions such as voltage resonance, it can cause equipment and insulation failures due to the extreme peak voltages. To address the harmonic distortion issue, work was begun under the 1990 NASA-ASEE Summer Faculty Fellowship Program. Software, originally developed by EPRI, called HARMFLO, a power flow program capable of analyzing harmonic conditions on three phase, balanced, 60 Hz AC power systems, was modified to analyze single phase, 20 kHz, AC power systems. Since almost all of the equipment used on spacecraft power systems is electrically different from equipment used on terrestrial power systems, it was also necessary to develop mathematical models for the equipment to be used on the spacecraft. The modelling was also started under the same fellowship work period. Details of the modifications and models completed during the 1990 NASA-ASEE Summer Faculty Fellowship Program can be found in a project report. As a continuation of the work to develop a complete package necessary for the full analysis of spacecraft AC power system behavior, deployment work has continued through NASA Grant NAG3-1254. This report details the work covered by the above mentioned grant. Author

N92-31012# Oak Ridge National Lab., TN.
POTASSIUM RANKINE CYCLE POWER CONVERSION SYSTEMS FOR LUNAR-MARS SURFACE POWER
R. S. Holcomb 1992 6 p Presented at the 27th Intersociety Energy Conversion Engineering Conference, San Diego, CA, 3-7 Aug. 1992
(Contract DE-AC05-84OR-21400)
(DE92-015102; CONF-920801-4) Avail: CASI HC A02/MF A01

The potassium Rankine cycle has good potential for application to nuclear power systems for surface power on the moon and Mars. A substantial effort on the development of the power conversion was carried out in the 1960's which demonstrated successful operation of components made of stainless steel at moderate temperatures. This technology could be applied in the near term to produce a 360 kW(e) power system by coupling a stainless steel power conversion system to the SP-100 reactor. Improved performance could be realized in later systems by utilizing niobium or tantalum refractory metal alloys in the reactor and power conversion system. The design characteristics and estimated mass of power systems for each of three technology levels are presented. DOE

N92-31204# Los Alamos National Lab., NM.
THERMOHYDRAULIC MODELING OF NUCLEAR THERMAL ROCKETS: THE KLAXON CODE
M. L. Hall, W. J. Rider, and M. W. Cappiello 1992 12 p Presented at the Nuclear Technologies for Space Exploration, Jackson, WY, 16-19 Aug. 1992
(Contract W-7405-eng-36)
(DE92-015274; LA-UR-92-1674; CONF-920803-8) Avail: CASI HC A03/MF A01

The hydrogen flow from the storage tanks, through the reactor core, and out the nozzle of a Nuclear Thermal Rocket is an integral design consideration. To provide an analysis and design tool for this phenomenon, the KLAXON code is being developed. A shock-capturing numerical methodology is used to model the gas flow (the Harten, Lax, and van Leer method, as implemented by Einfeldt). Preliminary results of modeling the flow through the reactor core and nozzle are given in this paper. DOE

23 CHEMISTRY AND MATERIALS (GENERAL)

No abstracts in this category.

24 COMPOSITE MATERIALS

Includes physical, chemical, and mechanical properties of laminates and other composite materials.

For ceramic materials see *27 Nonmetallic Materials.*

N92-30251# Ohio State Univ., Columbus.
FINITE ELEMENT ANALYSIS OF LAMINATED COMPOSITE AXISYMMETRIC SOLIDS. VOLUME 1: THEORY AND APPLICATIONS Final Report, 1 Oct. 1987 - 30 Aug. 1988
R. S. Sandhu, W. E. Wolfe, and R. A. Dandan Aug. 1991 168 p
(Contract F33615-85-C-3213)
(AD-A250808; WL-TR-91-3020-Vol-1) Avail: CASI HC A08/MF A02

A finite element program is developed to analyze a composite laminate structure axisymmetric geometry and loading. Circumferential displacement is considered in addition to the radial and axial. The fiber orientation may be oblique to the axis. Thus, each nodal point has three degrees of freedom and the procedure models the complete state of stress and strain. The program is verified by application to cross-ply and angle-ply coupons. A segment of a large radius axisymmetric ring under uniform radial pressure is equivalent to a free-edge delamination coupon. The stress field from the axisymmetric analysis is compared with the results of a higher order finite element analysis of a free-edge delamination coupon. Additionally, the computer program has the capability to solve a variety of problems including tubular angle-ply specimens, nozzles, etc. GRA

N92-30318# Florida Univ., Gainesville. Dept. of Electrical Engineering.
DEVELOPMENT OF ULTRA-LOW NOISE, HIGH SENSITIVITY PLANAR METAL GRATING COUPLED AlGaAs/GaAs MULTIQUANTUM WELL IR DETECTORS FOR FOCAL PLANE ARRAY STARING IR SENSOR SYSTEMS Quarterly Progress Report No. 2, 1 Nov. 1991 - 31 Jan. 1992
Max N. Yoder 1 Feb. 1992 31 p
(Contract N00014-91-J-1976)
(AD-A246122) Avail: CASI HC A03/MF A01

During this reporting period (11-01-91 to 1-31-92), we have continued the study of the performance characteristics of the metal grating coupled bound-to-miniband (BTM) and step-bound-to-miniband (SBTM) transition multiquantum well (MQW)/superlattice (SL) barrier infrared (IR) detectors formed on the GaAs and InP substrates for 8-12 micrometer focal plane arrays and image sensor applications. Specific tasks performed are reported: (1) designed and grew several (BTM) GaAs- and (SBTM) InGaAs-based QWIP (quantum well infrared photodetector) structures by MBE technique, (2) fabricated the metal grating couplers on the QWIP's described in (1) with different granting periodicities (1.1, 3.2, 5, 7.2, and 10 micrometers) and patterns (line and cross gratings), (3) performed theoretical and experimental study of the light coupling quantum efficiency vs. grating periodicities for the QWIP's, and (4) performed a theoretical and experimental study of the dark current vs. temperature for the GaAs QWIP's. Detailed results are discussed in Section 3. GRA

N92-30414# Technische Univ., Delft (Netherlands).
LOW-VELOCITY IMPACT LOADING ON FIBRE REINFORCED ALUMINUM LAMINATES (ARALL) AND OTHER AIRCRAFT SHEET MATERIALS Ph.D. Thesis
Arie Vlot 1991 577 p Sponsored by Netherlands Foundation for Technical Research
(ETN-92-91613) Avail: CASI HC A25/MF A06

The impact properties of new aircraft materials play an important role for the design and certification of aircraft structures. Low velocity impact tests were carried out on monolithic aluminum alloys, various types of Arall laminates and thermoplastic composites. The damage resistance, the image tolerance (residual strength after impact damage) and residual strength of the various materials are compared. In the literature only dynamic linear elastic models and a static nonlinear elastic model are available. A Non Linear Elastic Impact Model (NOLEIM) was developed, which is able to calculate the force time, velocity time and deflection time curves accurately. The calculations of this model were compared with experimental and finite element results. A static Elasto Plastic Impact Model (EPIM) was derived which is able to calculate deflection energy and force deflection curves. ESA

N92-30521# Los Alamos National Lab., NM.
ON RECRYSTALLIZATION IN METAL MATRIX COMPOSITES
W. J. Poole, J. D. Embury (McMaster Univ., Hamilton, Ontario), S. P. Silvetti (Cordoba National Univ., Argentina), and U. F. Kocks 1992 7 p Proposed for presentation at the 1992 Recrystallization, San Sebastian (Spain), 31 Aug. - 4 Sep. 1992
(Contract W-7405-eng-36)
(DE92-011364; LA-UR-92-898; CONF-920857-2) Avail: CASI HC A02/MF A01

The plane strain deformation of model continuous fiber composites such as Cu-W provides a vehicle for the study of the macroscopic effects of second phase particles on the strain distribution in the matrix and its possible effects on subsequent recrystallization behavior. By using metallographic studies based both on optical gridding methods and low temperature recrystallization, the pattern of flow enforced by the fibers can be quantified and related to the spatial distribution of recrystallization events. DOE

N92-30528# Nottingham Univ. (England). Dept. of Theoretical Mechanics.
WAVE PROPAGATION AND VIBRATION OF FIBRE-REINFORCED LAMINATES Final Report, 1 Sep. 1988 - 30 Sep. 1991
W. A. Green, E. R. Green, and G A. Rogerson Feb. 1992 73 p
(Grant AF-AFOSR-0353-88)
(AD-A252101; WL-TR-92-3043) Avail: CASI HC A04/MF A01

Theoretical predictions are presented of the response of fiber-composite laminated plates to an impulse load. The cases considered were symmetric arrangements of four, six and eight plies of laminate consisting of straight parallel elastic fibers embedded in an isotropic elastic matrix. Analytical solutions allow the determination of the displacements and stress variation throughout the laminate at any time. The graphs presented show the variation of stresses and displacements along the plate surfaces and at the ply interfaces at fixed times. The analytical solutions illustrate the variation in the nature of the transmission with the direction of propagation and with ply lay-up. Surface impacts will initiate Rayleigh type surface waves propagating with a specified range of angles on any laminate. Outside this range of angles, the existence of the surface wave depends on the overall laminate depth. The study of these wave effects has thrown light on the way in which stress waves are channelled in the various layers of

the laminate and on the manner in which this channelling is dependent on the angle between the fiber direction and the propagation direction in each layer. GRA

N92-30573 Department of the Navy, Washington, DC.
METHOD OF BONDING CARBON-CARBON AND METAL MATRIX COMPOSITE STRUCTURES Patent
Amarnath P. Divecha, inventor (to Navy), William A. Ferrando, inventor (to Navy), Philip W. Hesse, inventor (to Navy), and Subhash D. Karmarkan, inventor (to Navy) 31 Mar. 1992 3 p Filed 1 Jul. 1991
(AD-D015299; US-Patent-5,100,049; US-Patent-Appl-SN-724084; US-Patent-Class-228-198) Avail: US Patent and Trademark Office

A method of bonding two carbon/carbon composite pieces or a carbon/carbon composite piece and a graphite/aluminum metal matrix composite piece together are presented. This procedure is accomplished by: (1) forming a uniform coating of molten AgNO3 on the surfaces to be bonded at a temperature above the melting point of AgNO3 but below the decomposition temperature of AgNO3; (2) placing the molten AgNO3 coated surfaces to be bonded into contact with each other; and (3) decomposing the molten AgNO3 to form a silver metal layer bonding the pieces together. If a graphite/aluminum metal matrix composite piece is being bonded, a silver diffusion step may be added at the end of the process to strengthen the silver bond to the metal cladding or metal matrix of the metal matrix composite piece. Author

N92-30639# Delaware Univ., Newark. Center for Composite Materials.
CENTER FOR COMPOSITES MANUFACTURING SCIENCE, RELIABILITY, AND MAINTAINABILITY TECHNOLOGY Final Report
Tsu-Wei Chou and Roy L. McCullough 30 Jan. 1992 17 p
(Contracts DAAL03-86-K-0170; DAAL03-86-G-0193; DAAL03-86-G-0194)
(AD-A248661; ARO-24614.22-MS-UIR; ARO-24615.1-MS-UIE; ARO-24616.1-MS-UIF) Avail: CASI HC A03/MF A01

The ARO/URI Center of Excellence was established to address the fundamental issues involved in the manufacturing science, reliability, and maintainability of composite structures for future Army systems. The program strongly emphasized building in quality, long life, predictable and reliable performance, durability, and lower life-cycle costs, with a minimum reliance on repair or rejection of poor quality after manufacturing. Research was initially conducted in the following areas: (1) Cure characterization and monitoring; (2) On-line intelligent nondestructive evaluation for in-process control; (3) Process simulation; (4) Computer-aided manufacturing for filament winding; (5) Structure-property relationships of textile structural composites; (6) Mechanics of thick-section laminates; (7) Structural performance and durability; and (8) Integrated engineering for durable structures. The material forms examined included thick-section laminates and textile woven forms; both thermoset and thermoplastic-matrix materials were investigated. GRA

N92-30641# Air Force Inst. of Tech., Wright-Patterson AFB, OH.
THERMAL STRESS EVALUATION OF A SYMMETRICALLY LAMINATED COMPOSITE PLATE M.S. Thesis
Darren Knipp 23 Oct. 1991 61 p
(AD-A249450; AFIT/CI/CIA-91-102) Avail: CASI HC A04/MF A01

The purpose of this investigation is to determine the in-plane thermal stresses for a symmetrically laminated, 50 inch x 12 inch x 0.19 inch composite plate with temperature dependent material properties. For this study only in-plane stresses are investigated. The in-plane equations of motion are solved exactly using a stress function. The resulting compatibility equation is solved approximately using the Galerkin method. This investigation also serves as proof of concept for the variational method. This method produces accurate results while being less rigorous in a computational sense than the high degree of freedom finite element model required to solve the same problem. Variations with lamina orientation and multiple layered laminates are investigated. Results are given in terms of the in-plane force resultant. The baseline case for this study was aluminum and the in-plane force resultant at the center of the plate was calculated to be 60.251 lb/in. The exact solution for the in-plane force resultant at the center of the plate is 59.667 lb/in, a difference of less than 1 percent. Based on these results, additional investigations were accomplished for composite plates. The results from this study will be used as parametric data by NASA-Dryden in verifying finite-element codes and will aid in experimental analysis of thermal loading on composite plates. GRA

N92-30690# Messerschmitt-Boelkow-Blohm G.m.b.H., Munich (Germany, F.R.). Military Aircraft Div.
INFLUENCE OF VARIOUS CARBON FIBRE TYPES ON THE MECHANICAL PERFORMANCE AND DAMAGE TOLERANCE OF COMPOSITES
Josef Walter Vilsmeier and Guenter Herrmann (Badische Anilin- und Soda-Fabrik A.G., Ludwigshafen am Rhein, Germany, F.R.) 21 Jan. 1992 16 p
(MBB/FE202/S/PUB/477; ETN-92-91904) Copyright Avail: CASI HC A03/MF A01

To evaluate the role of different fibers with respect to the damage tolerance behavior, commercially available fibers, two standard and five intermediate modulus fibers were selected and prepregged with the same high performance resin. Compression after impact, fracture toughness for mode 1 and 2 (G(sub (c)) and G(sub 2c)), and edge delamination strength were evaluated. To compare the overall performance of the different materials, additional unidirectional and multidirectional properties were tested. The results showed that improved damage tolerance may induce drawbacks in other important material properties. The discussion of the results showed that G(sub 2c) and Multidirectional Interlaminar Shear (MD-ILS) seem to be good indicators for improved damage tolerance behavior. This was demonstratred for the G30-500, G40-800 and IM7 fibers, showing better damage tolerance values than the T300, T800 and Apollo fibers. The edge dalamination test is no indicator for improved damage tolerance behavior. ESA

N92-30711*# Advanced Technology Materials, Inc., Danbury, CT.
FABRICATION OF MULTIFILAMENT CONDUCTORS: CVD PROCESSING OF HIGH Tc SUPERCONDUCTING COMPOSITE FIBERS Final Report, 14 May 1990 - 14 May 1992
Peter S. Kirlin May 1992 20 p
(Contract NAS8-38485)
(NASA-CR-184344; NAS 1.26:184344) Avail: CASI HC A03/MF A01

The primary purpose of this project was to demonstrate the feasibility of Organo-Metallic Chemical Vapor Deposition (OMCVD) for production of BiSrCaCuO high-temperature superconductor coated wire. In order to carry out this objective, a low-pressure CVD reactor was designed with the capability to deposit continuously on a moving wire or fiber substrate. Substrate wire makes two passes through the reactor so that higher effective deposition rates can be achieved, leading to higher coated wire production rates. Ten to twenty foot lengths of superconductor precursor coated wire were produced in this way. Several significant obstacles were encountered and overcome during this project. Accumulating enough coated wire for analysis and fragility of the coatings, particularly before annealing, were both problems. Run-to-run reproducibility was also an issue. ATM's proprietary delivery system for low volatility source reactants worked quite well for Sr and Ca, but the Bi and Cu were delivered from bubblers, and the coatings showed substantial variations in these two elements from run to run. The main use of this specific work is a feasibility demonstration of low-pressure CVD on a continuously moving substrate with complex oxides. Coated wires several tens of feet in length were produced, with formation of the 2212 phase of BSCCO and a superconducting transition at 71 K. More generally, thin film coated wires have applications in superconducting magnets

and power storage systems. Thin films have to date shown better flux pinning and thus J(sub c)S than bulk HTSC materials. Small filaments, i.e. wires, are preferred for winding magnets and dealing with alternating or rapidly changing currents, since they greatly reduce inductance losses. Therefore it seems likely that a combination of these strengths, thin films and fine wires, will be important in eventual commercialization of high temperature superconducting composite (HTSC) wires. Author

N92-30779*# National Aeronautics and Space Administration. Lewis Research Center, Cleveland, OH.
METAL MATRIX COMPOSITE ANALYZER (METCAN) USER'S MANUAL, VERSION 4.0
H.-J. Lee, P. K. Gotsis, P. L. N. Murthy, and D. A. Hopkins Mar. 1992 176 p
(RTOP 510-01-50)
(NASA-TM-105244; E-6571; NAS 1.15:105244) Avail: CASI HC A09/MF A02

The Metal Matrix Composite Analyzer (METCAN) is a computer code developed at Lewis Research Center to simulate the high temperature nonlinear behavior of metal matrix composites. An updated version of the METCAN User's Manual is presented. The manual provides the user with a step by step outline of the procedure necessary to run METCAN. The preparation of the input file is demonstrated, and the output files are explained. The sample problems are presented to highlight various features of METCAN. An overview of the geometric conventions, micromechanical unit cell, and the nonlinear constitutive relationships is also provided. Author

N92-30809# Oak Ridge National Lab., TN.
THE EFFECT OF NEUTRON IRRADIATION ON THE STRUCTURE AND PROPERTIES OF CARBON-CARBON COMPOSITE MATERIALS
T. D. Burchell, W. P. Eatherly, and J. P. Strizak 1992 2 p Presented at the 16th Annual Symposium of American Society of Testing and Materials (ASTM), Denver, CO, 21-22 Jun. 1992
(Contract DE-AC05-84OR-21400)
(DE92-011670; CONF-920673-3-Extd-Abst) Avail: CASI HC A01/MF A01

Carbon-carbon composites applications, in tokamak fusion energy devices, are discussed in this short paper. The effects of neutron damage to graphite and its dimensional stability is also examined. H.A.

N92-30815# Houston Univ., TX. Dept. of Mechanical Engineering.
NONDESTRUCTIVE CHARACTERIZATION OF TWO-PHASE METAL-MATRIX MATERIALS Final Report, Jun. 1988 - Oct. 1991
Kamel Salama Dec. 1991 102 p
(Contract DAAL03-88-K-0096)
(AD-A249912; ARO-25397.9-MS) Avail: CASI HC A06/MF A02

The major goal of this program is to study methods for the nondestructive characterization of the mechanical properties of two-phase metal-matrix composites such as discontinuous SiC-reinforced aluminum alloys. The methods to be studied are based on the physical nonlinear elastic behavior of solids and utilize measurements of the elastic as well as the acoustoelastic constants. The objectives are to establish both experimentally and theoretically relationships between those parameters which can be measured nondestructively and the percentages of the second phase in two-phase systems. Mechanical properties of these systems are derived from the presence of reinforcement second phase in the matrix. GRA

N92-30871# Georgia Inst. of Tech., Atlanta. School of Chemical Engineering.
PRECURSOR STRUCTURE-FIBER PROPERTY RELATIONSHIPS IN POLYACRYLONITRILE-BASED CARBON FIBERS Final Report, 1 Jun. 1989 - 30 Apr. 1992
Agaram S. Abhiraman 30 Apr. 1992 50 p
(Contract N00014-89-J-1855)
(AD-A249888; GIT-E-19-673) Avail: CASI HC A03/MF A01

This report describes fundamental studies pertaining to two critical aspects in the production of PAN-based carbon fibers: (1) the formation of a stabilized precursor fiber; and (2) the evolution of structure and properties in carbonization. Important new results pertaining to accelerated stabilization and the interactive evolution of structure and mechanical properties in axial tension as well as compression, during carbonization were obtained. Based on the work reported here and our earlier studies, inferences were drawn regarding direction for future research, focused specifically on improving axial compressive performance and reducing the cost of carbon fibers. GRA

N92-30874# California Univ., Irvine. Dept. of Mechanical and Aerospace Engineering.
MECHANICAL BEHAVIOR AND PROCESSING OF ALUMINUM METAL MATRIX COMPOSITES Final Report, 1 Jan. 1989 - 31 Dec. 1991
E. J. Lavernia and F. A. Mohamed 21 Feb. 1992 231 p
(Contract DAAL03-89-K-0027)
(AD-A249918; ARO-26439.48-MS) Avail: CASI HC A11/MF A03

The objectives of the present three year research program were threefold. First the program sought to explore the potential of using spray atomization and deposition to process aluminum metal matrix composites, not only with improved mechanical properties, but also with specifications suitable for applications of interest to the Army; these applications include light weight armor vehicles, helicopter engines, and other structural components. Second, the research program sought to develop an in-depth understanding of the various physical phenomena that occur during spray atomization and deposition of aluminum metal matrix composites. Third, the program sought to provide insight into the fundamental mechanisms governing the elevated temperature deformation behavior, not only of metal matrix composites processed by spray atomization and deposition, but also of metal matrix composites in general. GRA

N92-30906*# Virginia Polytechnic Inst. and State Univ., Blacksburg. Dept. of Engineering Science and Mechanics.
NUMERICAL ANALYSIS OF THE IOSIPESCU SPECIMEN FOR COMPOSITE MATERIALS
H. Ho, M. Y. Tsai, J. Morton, and G. L. Farley (Army Aerostructures Directorate, Hampton, VA.) [1992] 40 p
(Grant NAG1-1053)
(NASA-CR-190658; NAS 1.26:190658) Avail: CASI HC A03/MF A01

A finite element analysis of the Iosipescu shear tests for unidirectional and cross-ply composites is presented. It is shown that an iterative analysis procedure must be used to model the fixture-specimen kinematics. The correction factors which are needed to compensate for the nonuniformity of stress distribution in calculating shear modulus are shown to be dependent on the material orthotropic ratio and the finite element loading models. Test section strain distributions representative of typical graphite-epoxy specimens are also presented. Author

N92-30969# Messerschmitt-Boelkow-Blohm G.m.b.H., Munich (Germany, F.R.).
DEVELOPMENT OF HARDNESS CYCLES FOR FIBER BOUND MATERIALS, USING DSC: FROM LABORATORY SPECIMENS TO COMPLEX HIGH DUTY STRUCTURAL MEMBERS [ENTWICKLUNG VON HAERTEZYKLEN FUER FASERVERBUNDWERKSTOFFE (FVW) MITTELS DSC: VOM REINHARZPRUEFKOERPER ZUR FERTIGUNG VON KOMPLEXEN HOCHLEISTUNGSBAUTEILEN]
Klaus Schmidtke, G. Wachinger, and A. Keller 1991 30 p In GERMAN Presented at Fachtagung Thermische Analyse fuer die Kunststoffe- und Kautschukindustrie, Wuerzburg, Fed. Republic of Germany, 18-19 Sep. 1991

(MBB-Z-0409-91-PUB; ETN-92-91898) Avail: CASI HC A03/MF A01

It is shown that the hardening of fiber bound structural members is often very complicated, when using 'one shot bounding'. The problems of fabricating structural members with great layer thickness are explained, taking a helicopter rotor head system as an example. The DSC investigation processes which can be used for developing hardness cycles, are described. The transfer from laboratory to production scale is represented in detail, with regard to material effects, and optimization of hardness cycles. ESA

N92-30986*# National Aeronautics and Space Administration. Lewis Research Center, Cleveland, OH.
ISOTHERMAL AGING EFFECTS ON PMR-15 RESIN
Kenneth J. Bowles, Douglas Jayne (Case Western Reserve Univ., Cleveland, OH.), and Todd A. Leonhardt (Sverdrup Technology, Inc., Brook Park, OH.) Jul. 1992 22 p
(RTOP 510-01-50)
(NASA-TM-105648; E-7007; NAS 1.15:105648) Avail: CASI HC A03/MF A01

Specimens of PMR-15 polyimide neat resin were aged in air at temperatures of 288, 316, and 343 C. Weight losses and dimensional changes were monitored during the course of the exposure time. Physical changes were also observed by optical and electron microscopy. It was found that polyimide polymer degradation occurred within a thin surface layer that developed and grew during thermal aging. The cores of the polymer specimens were protected from oxidative degradation, and they were relatively unchanged by the thermal treatment. Surface cracking was observed at 343 C and was probably due to an interaction between voids and stresses that developed in the surface layer. Author

N92-31005# Dayton Univ. Research Inst., OH.
EVALUATION OF CHARACTERIZATION TECHNIQUES FOR CARBON-CARBON COMPOSITES Interim Report, Jun. 1990 - Jun. 1991
William Ragland May 1992 83 p
(Contract F33615-91-C-5618)
(AD-A252693; UDR-TR-92-25; WL-TR-92-4027) Avail: CASI HC A05/MF A01

Characterization techniques for organic/inorganic composites are well established and documented; however, this is not the case regarding carbon-carbon composites. Due to expansion of the Materials Directorate in-house carbon-carbon composite research effort, the knowledge to characterize these complex composite structures is essential to their development. This report describes both existing techniques and techniques developed in the Materials Directorate to characterize carbon-carbon composites. GRA

N92-30270*# Idaho Univ., Moscow. Dept. of Forest Products.
DESIGNING, ENGINEERING, AND TESTING WOOD STRUCTURES
Thomas M. Gorman *In* NASA. Langley Research Center, National Educators' Workshop: Update 1991. Standard Experiments in Engineering Materials Science and Technology Jun. 1992 p 121-128 (For primary document see N92-30263 21-29)
Avail: CASI HC A02/MF A03

N92-30287*# East Carolina Univ., Greenville, NC. Dept. of Construction Management.
AN EXPERIMENT ON THE USE OF DISPOSABLE PLASTICS AS A REINFORCEMENT IN CONCRETE BEAMS
Mostafiz R. Chowdhury *In* NASA. Langley Research Center, National Educators' Workshop: Update 1991. Standard Experiments in Engineering Materials Science and Technology Jun. 1992 p 315-327 (For primary document see N92-30263 21-29)
Avail: CASI HC A03/MF A03

25 INORGANIC AND PHYSICAL CHEMISTRY

Includes chemical analysis, e.g., chromatography; combustion theory; electrochemistry; and photochemistry.

For related information see also *77 Thermodynamics and Statistical Physics.*.

N92-30241# SETS Technology, Inc., Mililani, HI.
HYPERSPECTRAL GAS ANALYSIS SYSTEM (HyGAS), PHASE 1 Final Report, Jun. - Dec. 1991
28 Jan. 1992 17 p
(Contract DACA76-91-C-0013)
(AD-A251026; TEC-0005-Phase-1) Avail: CASI HC A03/MF A01

The overall objectives for phase 1 were to develop the conceptual design for a Hyperspectral Gas Analysis System (HyGAS) for gas detection and identification and to show the feasibility and applicability of this system for real time, spectrum data-base-referenced, processing of high spectral resolution image data, and hyperspectral data of gases in a tactical environment. It is concluded that a Hyperspectral Gas Analysis System (HyGAS) can be designed and built which would provide for real time identification and analysis of gas spectra from hyperspectral and ultraspectral imaging sensors. GRA

N92-30245# Bowling Green State Univ., OH. Center for Photochemical Sciences.
VIBRATIONAL OVERTONE SPECTROSCOPY OF GASEOUS METALLOCENES
C. Olsen, T. VanMarter, S. Hassoon, and D. L. Snavely 20 May 1992 5 p
(Contract N00014-88-K-0664)
(AD-A251088; TR-10) Avail: CASI HC A01/MF A01

The vibrational overtone spectra of ferrocene, acetylferrocene, ruthenocene, and cyclopentadienyltitanium trichloride has been recorded in the third overtone region of the C-H stretch vibration. All of the spectra display four peaks in this region which, by comparison to the overtone spectrum of gaseous cyclopentadiene, appear where the C-H olefinic overtone vibration absorbs. The pattern of the absorption spectrum does not vary upon change of the metal (iron, ruthenium, or titanium) or the ligand (chloride or acetylcyclopentadienyl). Author (GRA)

N92-30256# Stanford Univ., CA. High Temperature Gasdynamics Lab.
TURBULENT REACTING FLOWS AND SUPERSONIC COMBUSTION Annual Technical Report, 15 Feb. 1991 - 14 Feb. 1992
C. T. Bowman, R. K. Hanson, M. G. Mungal, and W. C. Reynolds 15 Mar. 1992 30 p
(Grant AF-AFOSR-0151-90)
(AD-A251065; AFOSR-92-0456TR) Avail: CASI HC A03/MF A01

An experimental and computational investigation of supersonic non-reacting and combustion flows is in progress. The principal objective of the research is to gain a more fundamental understanding of mixing and chemical reaction in supersonic flows. The research effort comprises three inter-related elements: (1) an experimental study of mixing and combustion in a supersonic plane mixing layer; (2) development of laser-induced fluorescence techniques for time-resolved two-dimensional imaging of species concentration, temperature, velocity, and pressure; and (3) numerical simulations of compressible reacting flows. The specific objectives and the status of the research of each of these program elements are summarized in this report. GRA

N92-30344# Lehigh Univ., Bethlehem, PA.
PERFORATED MONOLAYERS
S. L. Regen 1992 5 p
(Contract DE-FG02-85ER-13403)
(DE92-011632; DOE/ER-13403/4) Avail: CASI HC A01/MF A01

Our research over this past grant period has focused on (1) developing methods for making in situ permeation measurements at the air-water interface, (2) defining the structural and conformational behavior of selected calix(4)arenes, (3) defining the metal complexation properties of certain upper-rim functionalized calix(4)arenes, and (4) synthesizing a broad series of polymerizable calixarenes, to be used for constructing perforated monolayers and multilayers. DOE

N92-30369# Sandia National Labs., Livermore, CA.
A PULSE COMBUSTION-BASED VOC DESTRUCTION TECHNIQUE
T. T. Bramlette, J. O. Keller, M. A. Allendorf, and P. K. Barr 1992 10 p Presented at the Engineering and Technology Conference on Waste Management and Environmental Restoration, San Juan (Puerto Rico), 9-11 Apr. 1992
(Contract DE-AC04-76DR-00789)
(DE92-013563; SAND-92-8429C; CONF-920466-11) Avail: CASI HC A02/MF A01

We describe a recently initiated project to develop and demonstrate a novel technique for volatile organic compound (VOC) destruction that relies upon the unique characteristics of pulse combustors to effect a two-stage (thermal and catalytic) destruction process. The concept exploits both the high combustion intensity (energy release rate per unit volume) in the pulse combustor combustion chamber and the acoustic resonance in the pulse combustor tailpipe. High combustion intensity results from rapid fluid dynamic mixing, and will lead to compact, transportable designs; acoustic resonance results in significantly increased mass transport to the catalyst material, leading to high destruction efficiencies. The operation of a pulse combustor and its unique characteristics are described and illustrated with experimental data and theoretical calculations. The new pulse combustion-based VOC destruction system is discussed, and results from a preliminary feasibility study are presented. DOE

N92-30422# Messerschmitt-Boelkow-Blohm G.m.b.H., Munich (Germany, F.R.).
ANISOTROPIC SILICON ETCHING TECHNIQUES
Helmut Seidel and Ralf Voss 1991 12 p Presented at Micro System Technologies, Berlin, Fed. Republic of Germany, 29 Oct. - 1 Nov. 1991
(MBB-Z-0413-91-PUB; ETN-92-91900) Avail: CASI HC A03/MF A01

The main properties of anisotropic alkaline silicon etchants, such as anisotropy, influence of dopants, electrochemical, and photoelectrochemical behavior are summarized. A general unifying model is proposed, giving at least a qualitative explanation of all observed phenomena. ESA

N92-30632# Northwestern Univ., Evanston, IL. Dept. of Materials Science and Engineering.
NUCLEATION AND GROWTH OF DIAMOND ON CARBON-IMPLANTED SINGLE CRYSTAL COPPER
T. P. Ong, F. Xiong, R. P. Chang, and C. W. White Apr. 1992 40 p
(Contract N00014-89-J-1848)
(AD-A249021; TR-8) Avail: CASI HC A03/MF A01

The nucleation and growth of diamond crystals on single crystal copper surfaces was studied. Microwave plasma enhanced chemical vapor deposition (MPECVD) was used for diamond nucleation and growth. Prior to diamond nucleation, the single crystal copper surface is modified by carbon ion implantation at an elevated temperature (-820 C). This procedure leads to the formation of a graphite film on the copper surface, resulting in the great enhancement of diamond crystallite nucleation. A simple lattice model has been constructed to describe the mechanism of diamond nucleation on graphite as the group of zone axes (111) parallel to the group of zone axes (0001) and the group of zone axes (110) parallel to the group of zone axes (1120). This leads to a good understanding of diamond growth on carbon-implanted copper surfaces. GRA

N92-30645# Arkansas Univ., Fayetteville. Dept. of Physics.
COMBUSTION DIAGNOSTICS BY PHOTO-DEFLECTION SPECTROSCOPY Final Report, Oct. 1984 - Sep. 1988
Rajendra Gupta Mar. 1992 98 p
(Contract F33615-84-K-2437)
(AD-A250802; WL-TR-92-2023) Avail: CASI HC A05/MF A02

Experimental and theoretical investigations of photoacoustic deflection spectroscopy (PADS) and photo thermal deflection spectroscopy (PDTS) have been carried out for the application of these techniques to combustion diagnostics. The investigations have been two-pronged: (1) To determine the range of applicability of these techniques to combustion diagnostics, and (2) to develop a good theoretical and experimental understanding of these techniques so that quantitative measurements can be made. Both techniques (PADS and PTDS) are very useful for combustion diagnostics and absolute measurements of the species concentrations. Also, simultaneous measurements of species concentrations, local temperature, and flow velocity can be made. With these techniques the most stringent tests of the theoretical models of combustion can be done. PTDS is about an order of magnitude more sensitive than PADS, and therefore PTDS was chosen for a thorough theoretical and experimental investigation. The results showed a good agreement between the theory and the experiment. Where disagreement existed, reasons for the discrepancies were determined. GRA

N92-30717# Delaware Univ., Newark. Center for Catalytic Science and Technology.
DESIGN OF A HIGH ACTIVITY AND SELECTIVITY ALCOHOL CATALYST
H. C. Foley and G. A. Mills 2 Jan. 1992 8 p
(Contract DE-FG22-90PC-90291)
(DE92-013918; DOE/PC-90291/T5) Avail: CASI HC A02/MF A01

Research continues with a view to gaining a better understanding of the secondary dehydration of methanol to dimethyl ether on both the native gamma-alumina surface and our alumina-supported rhodium/molybdenum catalyst. This reaction is important since ethers as well as alcohols are considered to be and are used as octane boosters in reformulated gasoline. Hence, an understanding of the properties of our catalyst which control this chemistry is essential. DOE

N92-30749# Sandia National Labs., Albuquerque, NM.
HIGH-TEMPERATURE IGNITION OF PROPANE WITH MTBE AS AN ADDITIVE: SHOCK-TUBE EXPERIMENTS AND MODELING
J. A. Gray and C. K. Westbrook (Lawrence Livermore National Lab., CA.) 1991 23 p Presented at the 24th International Symposium on Combustion, Sydney (Australia), 5-10 Jul. 1992
(Contracts DE-AC04-76DR-00789; W-7405-eng-48)
(DE92-006679; SAND-91-8721; CONF-920707-9) Avail: CASI HC A03/MF A01

Ignition of propane has been studied in a shock tube and by computational modeling to determine the effect of methyl tert-butyl ether (MTBE) as a fuel additive. MTBE and isobutene were added in amounts up to 25 percent of the fuel to propane-oxygen-argon mixtures in shock-tube experiments covering a range of temperatures between 1450 and 1800 K. Ignition delays were measured from chemiluminescence at 432 nm due to excited CH radicals. The temperature dependence of the ignition rates was analyzed to yield Arrhenius parameters of E(sub a)(approximately)40 kcal/mol and log (A)(approximately) 9.0 sec(exp -1) for the overall reaction. Reactions involving MTBE and its decomposition products were combined with an established propane mechanism in a numerical model to describe the kinetic interaction of this additive with a typical hydrocarbon fuel. The experiments and the kinetic model both show that MTBE and isobutene retard propane ignition with nearly equal efficiency. The kinetic model demonstrates that isobutene kinetics are responsible for inhibition by both MTBE and isobutene, and the specific elementary reactions which produce this behavior are identified. DOE

N92-30773# Clemson Univ., SC. Dept. of Chemical Engineering.
SUPERCRITICAL FLUID EXTRACTION: A NEW PROCESS FOR PRODUCING HIGH-PERFORMANCE, LOW-COST CARBON FIBERS
Mark C. Thies 1 Apr. 1992 12 p
(Contract DAAL03-89-K-0067)
(AD-A249407; ARO-26591.5-MS) Avail: CASI HC A03/MF A01

Supercritical fluid (SCF) extraction was investigated for the production of the mesophase pitch used to spin high-performance carbon fibers. A bench-scale, continuous-flow apparatus was designed and constructed for fractionating petroleum pitch with SCF solvents at temperatures and pressures to 400 C and 350 bar, respectively. A heat-soaked, isotropic petroleum pitch was fractionated with supercritical toluene in a region of liquid-liquid equilibrium at temperatures and pressures from 300-380 C and 30-140 bar, respectively. Bottom-phase pitch fractions produced at 340 C, 70 bar, and a toluene-to-pitch ratio of 3:1 consist of a 100 percent bulk mesophase. This mesophase was used to produce carbon fibers with strengths and moduli (3.3 and 820 GPa, respectively) equal to or better than the best pitch-based fibers currently available. Since SCF extraction can be used to produce mesophase on a continuous basis, production costs could be as low as $0.50/lb. For high production rates of carbon fiber, this processing technique would have a significant cost advantage over alternative methods for producing mesophase. GRA

N92-30793# Texas Univ., Austin. Dept. of Chemistry.
SURFACE-MEDIATED PHOTOCATALYSIS Final Report, 29 Mar. 1991 - 28 Feb. 1992
Marye A. Fox 4 Feb. 1992 3 p
(Contract DAAL03-91-G-0103)
(AD-A249906; ARO-28298.4-CH) Avail: CASI HC A01/MF A01

Three areas were investigated: (1) application of esr spectroscopy, time-resolved diffuse reflectance absorption, and emission spectroscopy to establish mechanisms in photocatalytic oxidative degradations of organic molecules; (2) exploration of controlled oxidation chemistry for new heteroatom-containing organic molecules; and (3) synthesis and characterization of new quantized semiconductor-support systems. Sufficient work was completed to demonstrate that photocatalytic oxidation on irradiated semiconductor surfaces is a useful route for degradation of various organic materials under constrained, highly controlled conditions. GRA

N92-30814# California Univ., Berkeley.
ADVANCED CONCEPTS FOR CONTROLLED COMBUSTION IN ENGINES Final Report
A. K. Oppenheim 15 Dec. 1991 11 p
(Contract DAAL03-87-K-0123)
(AD-A249911; ARO-25245.15-EG) Avail: CASI HC A03/MF A01

Studies carried out at the University of California, Berkeley, over a period of four years were concerned with fluid mechanical properties of turbulent pulsed jet plumes - systems that are of particular relevance to the initiation and control of combustion in engines. The eventual purpose of this program was to provide a rational background for a fundamental refinement of stratified charge diesel engines - the development of a combustion system where the formation of pollutants is minimized, fuel economy is maximized, and fuel tolerance is optimized. The results demonstrated that this goal is attainable by means of appropriate Pulsed Jet Combustion (PJC) generators. The exothermic process of combustion is executed thereby in the form of a fireball taking place in a stratified charge generated by turbulent plumes of a PJC system. GRA

N92-30821# Pittsburgh Univ., PA. Surface Science Center.
INTERACTION OF ATOMIC HYDROGEN WITH THE SURFACE METHYL GROUP ON Si(100): REMOVAL OF SURFACE CARBON
C. C. Cheng, S. R. Lucas, H. Gutleben, W. J. Choyke, and J. T. Yates, Jr. 6 Mar. 1992 27 p
(Contract N00014-82-K-0280)
(AD-A249062; TR-42) Avail: CASI HC A03/MF A01

The interaction of atomic hydrogen with an overlayer derived from methyl iodide on the Si(100) surface has been studied using Auger electron spectroscopy (AES) and temperature programmed desorption (TPD) mass spectroscopy. Efficient removal of surface iodine by reaction with atomic hydrogen is observed. However, experiments with large exposures of atomic hydrogen also show the depletion of surface carbon. In contrast to the almost non-activated behavior observed for the extraction of halogen by an Eley-Rideal process producing the hydrogen halides, the carbon removal rate decreases with increasing temperatures (T greater than or equal to 450 K). The depletion of surface carbon by atomic hydrogen correlates well with H-etching on the Si(100) surface in which SiH4(g) is evolved, and is shown to be due to CH3SiH3(g) production during H-etching. In addition, isotopic exchange of the deuterium from CD(sub 3)(a) with hydrogen atoms supplied from the gas phase is also observed; this is found to be the most rapid kinetic process for the interaction of atomic hydrogen with the surface methyl group on Si(100). Finally, the selectivity of the H-induced reaction for two types of adsorbates, the methyl group and the halogen, is discussed. GRA

N92-30835# Rutgers - The State Univ., New Brunswick, NJ. Dept. of Mechanical and Aerospace Engineering.
TWO-COLOR INFRARED DIGITAL IMAGING FOR DETERMINATION OF IN-CYLINDER TEMPERATURE AND SPECIES DURING COMPRESSION AND COMBUSTION PERIODS OF DI DIESEL ENGINE
K. T. Rhee, H. Jiang, and Y. I. Jeong 13 Jan. 1992 23 p
(Contract DAAL03-91-G-0188)
(AD-A249812; ARO-28316.1-EG) Avail: CASI HC A03/MF A01

In order to determine the spatial and temporal distributions of temperature and species in a direct injection-type (DI) diesel engine combustion chamber, development of a new high-speed two-color infrared (IR) digital data system has been conducted. Among the other performed experimental work tasks is the modification of the engine cylinder head in order to accommodate a new optical access assembly. In an attempt to compare the measurement from this work with predictions made by a computational method, the KIVA II code has been placed according to our engine specifications. New analytical radiation heat transfer computer programs were developed to evaluate our IR system performance. Upon completion of the detailed design, the key system components of the IR apparatus have been fabricated and tested, including optical elements and the new electronic packages. At present the mechanical parts composing the assembly are under construction. Our test of the new optical access installed in the engine apparatus exhibits satisfactory results. Preliminary measurements will be obtained soon. We are in the process of compiling some computational results from the KIVA II operation. According to our results to date, due to many limitations with the code, it appears to be difficult to achieve a realistic evaluation of those results using our measurements from the present experiment. Analysis of our IR system performance using newly developed computer programs suggests that the background radiations (e.g. from the cylinder wall) may not be significant enough to affect the accuracy of measurements from the gaseous mixtures. GRA

N92-30875# Northwestern Univ., Evanston, IL. Dept. of Chemistry.
RESONANCE RAMAN SPECTROSCOPIC STUDIES OF TRANS DIOXORHENIUM(V)TETRAPYRIDYL SPECIES
Christopher S. Johnson, Carolyn Mottley, and Joseph T. Hupp 28 Apr. 1992 16 p Prepared in cooperation with Marquette University, Department of Chemistry, Milwaukee, WI
(Contract N00014-91-J-1035)
(AD-A249919; TR-10) Avail: CASI HC A03/MF A01

Resonance Raman spectra for several trans-dioxo rhenium(V)tetrapyridyl species were obtained. Excitation in the visible region (ligand-field (L-F) absorption) leads to modest enhancement of Raman scattering, chiefly for metal-oxo modes.

The observations are qualitatively consistent with an earlier luminescence study, which clearly demonstrated that L-F excitation induces displacements in O = Re = O coordinates. Excitation in the near LTV leads to much stronger scattering, but only for pyridyl and metal-pyridyl vibrations; metal-oxo scattering is essentially absent. These experiments clearly establish the metal-to-pyridine charge-transfer nature of the intense near-LTV absorption. They also reinforce the assignment of dxy (orthogonal to the O = Re = O core) as the sole occupied d orbital in the ground-state species. In this respect, the trans complexes contrast with related cis species for which p(oxo) orbitals must interact with all three (Re) orbitals, and for which substantial v (O = Re = O) enhancement upon charge-transfer excitation is therefore observed. Finally, this report corrects an earlier observation elsewhere in which normal Raman scattering from solvent (CH3CN) was mistakenly ascribed to scattering from trans-dioxorhenium(V)tetrapyridine. GRA

N92-30879# Midwest Research Inst., Golden, CO. National Renewable Energy Lab.
PHOTODEGRADATION EFFECTS IN MATERIALS EXPOSED TO HIGH FLUX SOLAR AND SOLAR SIMULATED RADIATION
A. Ignatiev (Houston Univ., TX.) Apr. 1992 21 p
(Contract DE-AC02-83CH-10093)
(DE91-002147; NREL/TP-253-4282) Avail: CASI HC A03/MF A01

This report contains study results about photodegradation effects in materials exposed to high flux solar and solar simulated radiation. The studies show that high flux photoirradiation of materials can result in significant changes in the stability of materials. Photodesorption and photo-enhanced oxidation were determined to be the major mechanisms. These mechanisms were shown to affect, in extremely adverse ways, the expected thermal stability of solar relevant materials, especially stainless steels. (It is expected that related high temperature alloy steels will be similarly affected.) An analytical expression was generated to predict the flux behavior of the steels using (number sign)304 as a prototypical stainless steel system. DOE

N92-30882# Midwest Research Inst., Golden, CO. National Renewable Energy Lab.
SYNTHESIS OF CRESOLS AND XYLENOLS FROM BENZENE AND METHANOL
H. W. Prengle, Jr. (Houston Univ., TX.), F. A. Bricout (Houston Univ., TX.), and S. Alam (Houston Univ., TX.) Apr. 1992 39 p
(Contract DE-AC02-83CH-10093)
(DE91-002143; NREL/TP-253-4278) Avail: CASI HC A03/MF A01

The objective of the work is to compare two processes for manufacturing cresols and xylenols: (1) a conventional catalytic process; and (2) a photothermal catalytic process, in order to determine the relative process economics. The products are used primarily as chemical intermediates for manufacture of antioxidants, pesticides, polymerization inhibitors, resins, and other products. The market is approximately 500 million pounds per year. This report is the second of two reports, presenting results of a process evaluation for manufacturing the products by a photothermal catalytic process. DOE

N92-30883# Lawrence Livermore National Lab., CA.
METHANE TO LIQUID
B. E. Watkins, R. N. Shock, and R. T. Taylor 1992 8 p Presented at the US DOE Contractor Review Meeting on Natural Gas Research and Development, Morgantown, WV, 5-6 May 1992
(Contract W-7405-eng-48)
(DE92-001277; DOE/NBM-92001277; CONF-920584-3) Avail: CASI HC A02/MF A01

We are investigating the structure/activity relationships of the bacterial enzyme methane monooxygenase, which catalyzes the specific oxidation of methane to methanol. We then utilize this information to design and synthesize inorganic coordination complexes that mimic the function of the native enzyme but are more robust and have higher catalytic site density. We envision these catalysts to be useful in process catalytic reactors in the conversion of methane in natural gas to liquid methanol. DOE

N92-30899# Westinghouse Savannah River Co., Aiken, SC.
FIBER-OPTIC RAMAN SPECTROSCOPY AT THE SAVANNAH RIVER SITE: USES AND TECHNIQUES
S. E. Nave, P. E. ORourke, R. A. Malstrom, and W. S. Prather 1992 16 p Presented at the ANATECH 1992, Atlanta, GA, 30 Apr. 1992
(Contract DE-AC09-89SR-18035)
(DE92-013971; WSRC-MS-92-131; CONF-9204151-1) Avail: CASI HC A03/MF A01

Remote detection of analyte concentrations is a valuable tool at Savannah River Site for online control of chemical processes and environmental remediation. Vibrational spectral information obtained by Raman or infrared spectroscopy is useful for detecting a large number of analytes. In the case of liquids and for transmission and detection of the light via fiber-optic cables, Raman has an advantage over infrared spectroscopy since the transmitted and detected light is in the visible or near IR and is not attenuated like IR in these media. The design and performance of several probes and sample cell configurations for Raman spectroscopy are discussed. DOE

N92-31006# UOP, Inc., Des Plaines, IL.
THE DEVELOPMENT OF PRECIPITATED IRON CATALYSTS WITH IMPROVED STABILITY
H. Abrevaya May 1992 27 p
(Contract DE-AC22-87PC-79812)
(DE92-014625; DOE/PC-79812/T2) Avail: CASI HC A03/MF A01

The objective of this program is to identify the chemical principles governing the deactivation of precipitated iron catalysts during Fischer-Tropsch synthesis and to use these chemical principles in the design of catalysts suitable for slurry reactors. The performance targets are 88 percent CO+H2 conversion with less than 1 percent deactivation/day for 1 month and a methane and ethane selectivity of no more than 7 percent (based on hydrocarbons and oxygenates only) at a space velocity of at least 2 normal liters per hr per gram iron (NL/hr/gFe) using a synthesis gas with 0.5-1.0 H2:CO ratio in a slurry reactor. DOE

N92-31161*# University of Eastern Kentucky, Richmond. Dept. of Physics and Astronomy.
ANALYSIS, REVIEW, AND DOCUMENTATION OF THE ACTIVATION DATA FROM LDEF MATERIAL Final Technical Report
C. E. Laird Jul. 1992 74 p
(NASA Order H-08071D)
(NASA-CR-184356; NAS 1.26:184356) Avail: CASI HC A04/MF A01

Samples removed from Long Duration Exposure Facility (LDEF-1) are being studied at various laboratories to determine the specific activity(pCi/kg) produced in orbit by exposure to protons and neutrons in near-Earth orbit. These activities are being corrected for efficiency, self-attenuation, and background. The activities and associated gamma-ray spectra are being collected, analyzed, documented and reviewed by faculty and graduate students at Eastern Kentucky University. The currently available activation results have been tabulated and reviewed in this report. Approximately 500 spectra have been accumulated for future archival and analysis. The effect of the changing satellite orbit on the activation is reported herein and was calculated using more recent estimates of the flux of Van Allen belt protons. Author

N92-31178# Electrochemical Society, Inc., Pennington, NJ.
PROCEEDINGS OF THE 181ST ELECTROCHEMICAL SOCIETY, INC. MEETING PROGRAM Annual Report, Apr. - Sep. 1992
K. M. Kadish and R. S. Ruoff 28 Apr. 1991 125 p Meeting held in St. Louis, MO, 17-22 May 1992
(Contract N00014-92-J-1413)
(AD-A249729) Avail: CASI HC A06/MF A02

The Fullerene Symposium is organized with the intention of providing a forum for the presentation of the latest developments on these fascinating new allotropes of carbon. Papers on recent advances or on the state of the field are solicited in the following areas: fundamental understanding of the physical properties and structures; synthesis and separation; chemical reactions and new derivative; charge transfer reactions and electrochemistry; conductivity and super conductivity; possible applications; and new directions. GRA

N92-31184# Oak Ridge National Lab., TN.
LASER MASS SPECTROMETRY FOR BIOPOLYMERS
K. Tang (Vanderbilt Univ., Nashville, TN.), S. L. Allman, and C. H. Chen 1992 5 p Presented at the 6th International Symposium on Resonance Ionization Spectroscopy and Its Applications, Santa Fe, NM, 24-29 May 1992
(Contract DE-AC05-84OR-21400)
(DE92-015238; CONF-920574-3) Avail: CASI HC A01/MF A01

Various matrix materials were used for laser desorption of biological molecules which include large polypeptides and oligonucleotides. Both matrix assisted laser desorption ionization (MALDI) and matrix assisted desorption with post-ionization (MADPI) have been used. Detection sensitivity of femtomole of both oligomer and protein has been achieved. Both positive and negative ions were observed with little fragmentation. DOE

N92-31196# Oak Ridge National Lab., TN.
A MINIATURE CARBON FURNACE FOR MASS SPECTROSCOPY
J. P. Young and R. W. Shaw 1992 4 p Presented at the 6th International Symposium on Resonance Ionization Spectroscopy and Its Applications, Santa Fe, NM, 24-29 May 1992
(Contract DE-AC05-84OR-21400)
(DE92-014460; CONF-920574-2) Avail: CASI HC A01/MF A01

A miniature carbon (graphite) disposable tube furnace has been designed and built for use in resonance ionization mass spectrometry. This furnace is an excellent source for generating atoms to be subsequently ionized by optical or thermal means. The complete furnace assembly is very small, less than 4 cm(exp 2). Electrical connections to the carbon are simple, and no water cooling is required. DOE

N92-30668*# Cambridge Univ. (England). Dept. of Engineering.
STATISTICS FOR LAMINAR FLAMELET MODELING
R. S. Cant, C. J. Rutland (Wisconsin Univ., Madison.), and A. Trouve (Stanford Univ., CA.) *In* Stanford Univ., Studying Turbulence Using Numerical Simulation Databases. 3: Proceedings of the 1990 Summer Program Dec. 1990 p 271-279 (For primary document see N92-30648 21-34)
Avail: CASI HC A02/MF A03; 2 functional color pages

N92-30669*# General Motors Research Labs., Warren, MI.
THE INFLUENCE OF LEWIS NUMBER AND NONHOMOGENEOUS MIXTURE ON PREMIXED TURBULENT FLAME STRUCTURE
D. C. Haworth and T. J. Poinsot (Stanford Univ., CA.) *In* Stanford Univ., Studying Turbulence Using Numerical Simulation Databases. 3: Proceedings of the 1990 Summer Program Dec. 1990 p 281-298 (For primary document see N92-30648 21-34)
Avail: CASI HC A03/MF A03; 2 functional color pages

N92-30670*# Wisconsin Univ., Madison.
PRE-MIXED FLAME SIMULATIONS FOR NON-UNITY LEWIS NUMBERS
C. J. Rutland and A. Trouve (Stanford Univ., CA.) *In* Stanford Univ., Studying Turbulence Using Numerical Simulation Databases. 3: Proceedings of the 1990 Summer Program Dec. 1990 p 299-309 (For primary document see N92-30648 21-34)
Avail: CASI HC A03/MF A03; 2 functional color pages

26 METALLIC MATERIALS

Includes physical, chemical, and mechanical properties of metals, e.g., corrosion; and metallurgy.

N92-30513# European Space Agency, Paris (France).
DETERMINATION OF PAIR POTENTIALS BY ANALYSIS OF DIFFUSE SCATTERING OF THE LOCAL FIELD IN Pd3V AND Ni3V
Francine Solal (Office National d'Etudes et de Recherches Aerospatiales, Paris, France) Mar. 1992 109 p Transl. into ENGLISH of Etude par Diffuse de l'Ordre Local dans Pd3V et Ni3V: Determination de Potentiels de Paire (Paris, France, ONERA), Dec. 1989 87 p Original language document was announced as N91-11117
(ESA-TT-1228; ONERA-NT-1989-7; ETN-92-91708) Avail: CASI HC A06/MF A02

The neutron and x-ray diffuse scattering experiments in Pd3V are discussed. A change in local order between the disorded state, characterized by diffuse intensity maxima at (100) points of reciprocal space, and the ordered phase D0(sub 22), built on (1 1/2 0) concentration waves in the FCC lattice, was observed. Concerning the Ni3V alloy, no such change appears on the local order. At intermediate temperatures, approximate statistical models are necessary to describe order properties. The change in local order observed implies a breakdown of the simplest of these models: the 'one side mean field' theory. The Cluster Variation Method (CVM) reveals the existence of two regimes, corresponding to Pd3V and Ni3V. To account quantitatively for experimental data, it was necessary to use a CVM approximation including pair interactions up to the fourth neighbor, in agreement with electronic structure calculations. A set of such interactions for both alloys is proposed. ESA

N92-30534# Syracuse Univ., NY.
MBE GROWN COPPER-ALUMINUM ALLOY FILMS Final Technical Report, Aug. 1987 - Dec. 1989
Philipp Kornreich May 1992 18 p
(Contract F30602-81-C-0169)
(AD-A252486; RL-TR-92-112) Avail: CASI HC A02/MF A01

This document reports on the design and construction of a Molecular Beam Epitaxy system to grow and characterize aluminum/copper films, for electromigration studies. The growth of Al/Cu films in an evaporation system and reduction of the oxygen content of these films is discussed. Also, a novel approach to the modeling of electromigration in circuit metallization is presented. GRA

N92-30588# Massachusetts Inst. of Tech., Cambridge. Dept. of Materials Science and Engineering.
SUPERCONDUCTIVITY AND MAGNETISM IN RAPIDLY SOLIDIFIED PEROVSKITES
R. C. OHandley and G. Kalonji 1991 12 p
(Contract DE-FG02-84ER-45174)
(DE92-014081; DOE/ER-45174/T4) Avail: CASI HC A03/MF A01

The report is divided into six parts, reflecting major thrusts of our work since 1987. The six areas are: molecular orbital theory of high (Tc) superconductivity; rapid solidification processing of oxide superconductors; time dependent magnetic and superconducting properties of these inhomogeneous materials; excess Gd in Gd(1+x)Ba(2-x)Cu3O(7-delta) perovskites; rapid solidification and directional annealing to achieve high Jc; and Mossbauer studies of T = Fe, Co, and Ni site selection in YBa2(CuT)3O(7-delta) and GdBa2(CuT)3O(7-delta). DOE

N92-30759# Army Materials Technology Lab., Watertown, MA.
CORROSION OF HIGH DENSITY KINETIC ENERGY PENETRATOR MATERIALS Final Report
Chester V. Zabielski and Milton Levy Apr. 1992 30 p
(AD-A249439; MTL-TR-92-17) Avail: CASI HC A03/MF A01

The corrosion behavior of DU-3/4 percent Ti and DU-2 percent Mo alloys was assessed by electrochemical polarization techniques and exposure to both 5 percent salt fog at 35 C and a 95 percent

relative humidity at 45 C. The efficacy of an ion vapor deposited aluminum coating in mitigating the corrosion of these alloys was also assessed. GRA

N92-30785# Helsinki Univ. of Technology, Espoo (Finland). Lab. of Foundry Engineering.
EFFECTS OF IMPURITIES ON THE MECHANICAL BEHAVIOUR OF PRIMARY AND SECONDARY CAST ALUMINUM ALLOYS
J. E. Eklund, C. J. Chen, and J. J. Vuorinen 1991 33 p
(PB92-180652; VAL-6/1991) Avail: CASI HC A03/MF A01

The effects of impurities on the mechanical behavior of aluminium-silicon (7 percent) and aluminum-copper (4 percent) cast alloys were studied. A comparisonal viewpoint between primary and secondary materials was adopted because of the different production methods of these materials. The aim was, accordingly, to determine the usability of secondary casting ingots as raw materials for aluminum castings. GRA

N92-30787# Florida Univ., Gainesville. Dept. of Physics.
X RAY SCATTERING STUDIES OF NON-EQUILIBRIUM ORDERING PROCESSES
S. E. Nagler 1992 22 p
(Contract DE-FG05-86ER-45280)
(DE92-014006; DOE/ER-45280/T4) Avail: CASI HC A03/MF A01

This report summarizes the major results obtained under U.S. DOE Grant Number FG05-90ER45280 from the dates November 1, 1989 through October 31, 1992 inclusive. The principal work includes x-ray scattering studies of phase transition kinetics in binary alloy order-disorder transitions, block co-polymer crystallization, and charge density wave solids under applied electric fields, and studies of magnetic excitations in low dimensional quantum systems. DOE

N92-30834# Edgerton, Germeshausen and Grier, Inc., Idaho Falls, ID.
PROCEEDINGS OF A BERYLLIUM TECHNOLOGY WORKSHOP
Glen R. Longhurst Dec. 1991 239 p Workshop held in Clearwater Beach, FL, 20 Nov. 1991
(Contract DE-AC07-76ID-01570)
(DE92-012312; EGG-FSP-10017; CONF-9111209) Avail: CASI HC A11/MF A03

This report discusses the following topics: beryllium in the ITER blanket; mechanical testing of irradiated beryllium; tritium release measurements on irradiated beryllium; beryllium needs for plasma-facing components; thermal conductivity of plasma sprayed beryllium; beryllium research at the INEL; Japanese beryllium research activities for in-pile mockup tests on ITER; a study of beryllium bonding of copper alloy; new production technologies; thermophysical properties of a new ingot metallurgy beryllium product line; implications of beryllium: steam interactions in fusion reactors; and a test program for irradiation embrittlement of beryllium at JET. DOE

N92-30858# Ames Lab., IA.
NDE CHARACTERIZATION OF THE MICROSTRUCTURE AND MECHANICAL PROPERTIES OF Al-Li ALLOYS
L. J. H. Brasche, J. E. Shield, L. S. Chumbley, and O. Buck 1991 10 p Presented at the Symposium on Nondestructive Evaluation (NDE) and Material Properties, New Orleans, LA, Feb. 1991
(Contract W-7405-eng-82)
(DE92-012154; IS-M-685; CONF-9102170-1) Avail: CASI HC A02/MF A01

Development of NDE techniques sensitive to changes in microstructure should be useful in predicting the mechanical properties of an alloy. This would not only improve quality control on the production line but also insure inservice reliability. In the present case, a binary AL-Li alloy and a commercial Al 2090 alloy were heat treated to achieve different microstructures followed by a series of nondestructive NDE measurements as well as uniaxial tension tests. Correlations between mechanical properties and NDE measurements will be presented, including error analysis for specified confidence levels. Techniques for the nondestructive detection of the deleterious T(sub 1) phase in Al 2090 will also be discussed in connection with TEM observations. The general premise of this work is that knowledge of the microstructural features is necessary in order to develop a successful nondestructive detection plan. DOE

N92-30864# Texas Univ., Austin. Dept. of Chemistry.
DEVELOPMENT OF PRACTICAL MO TECHNIQUES FOR PREDICTION OF THE PROPERTIES AND BEHAVIOR OF MATERIALS Final Report, 1 Nov. 1988 - 30 Apr. 1991
Michael J. Dewar and Marye A. Fox 4 Dec. 1991 12 p
(Grant AF-AFOSR-0179-89)
(AD-A247218; AFOSR-92-0115TR) Avail: CASI HC A03/MF A01

Our object was to provide chemists with theoretical procedures that could serve as practical adjuncts to experiment in studies of chemical problems, in particular studies of reactions and reaction mechanisms. We succeeded for the elements which have sp valence shells and main group elements where d AO's serve only as polarization functions, but attempts to extend this approach to elements with spd valence shells all failed. We had no experience of ab initio programming so we wrote a general program from scratch. Full scale parameterization for the organic elements (CHON) is now in progress. Computer programs were written for treating biradicals in procedures for correlation between the unpaired electrons. Proportionality factors were found by matching the singlet-triplet separations in carbene and singlet-triplet separations were then calculated for large numbers of other carbenes. AM1 parameters were optimized for aluminum, sulfur, germanium, tin, and mercury. We developed a new version of the DEWARPI procedure in which geometries are found by minimizing the total energy. We developed a new version of the AMPAC program at QCPE (AMPAC2.1) for a very effective method for finding transition states. GRA

N92-30865# Allied-Signal Aerospace Co., Kansas City, MO.
PROCESS MODELING AND DEVELOPMENT FOR THREE AXISYMMETRIC NET SHAPE FORGINGS
A. S. El-Gizawy (Missouri Univ., Columbia.) Mar. 1992 77 p
(Contract DE-AC04-76DP-00613)
(DE92-012111; KCP-613-4501) Avail: CASI HC A05/MF A01

The results of dynamic material modeling experiments are reported on aluminum alloys 6061 and 7050, and steel alloy 4340. This information was used to accurately describe the variables in the various constitutive equations used in computer modeling programs. A description of the experimental equipment used to deform the specimens and gather data was given. Previously reported work regarding computer modeling of interface friction and the forging process was reviewed. Using dynamic flow models, three different axisymmetric parts were analyzed for their potential for being produced by net shape or near net shape forging processes. Two aluminum alloy parts were recommended as potential candidates while the steel part was not a potential candidate. Recommendations for processing conditions were also given. DOE

N92-30872# Israel Inst. of Metals, Haifa.
LASER INDUCED REACTION FOR PRE-BOND SURFACE PREPARATION OF ALUMINUM ALLOYS Annual Report, Mar. 1991 - Mar. 1992
M. Rotel, J. Zahavi, A. Buchman, and H. Dodiuk Mar. 1992 38 p
(Grant AF-AFOSR-0148-91)
(AD-A249916; Rept-524-679; AFOSR-91-0148; EOARD-TR-92-07) Avail: CASI HC A03/MF A01

Irradiation of the Al alloy 2024/T3 with an excimer laser was carried out under various experimental conditions (laser energy and number of pulses). Surface analysis of the treated alloy was carried out by FTIR, SEM, and AUGER. The laser treated metal adherends were bonded with rubber modified epoxy adhesive, and the resultant shear strength (SLS) was measured. Fracture surfaces were analyzed by SEM. The results show clearly that laser prebond

treatment of the neat adherend's surface improved significantly the adhesion strength. Improvement of 600 percent of the adhesion shear strength was achieved with laser energy of about 0.2 J/P/sq cm, compared to the adhesion strength of the untreated neat Al alloy. The value of the adhesion strength after optimal laser treatment even exceeds that of conventional unsealed chromic anodized treatment. GRA

N92-30877# Pacific Northwest Lab., Richland, WA.
RECENT IMPROVEMENTS IN SIZE EFFECTS CORRELATIONS FOR DBTT AND UPPER SHELF ENERGY OF FERRITIC STEELS
A. S. Kumar (Missouri Univ., Rolla.), B. S. Louden (Missouri Univ., Rolla.), F. A. Garner, and M. L. Hamilton Jan. 1992 24 p Presented at the ASTM International Symposium on Small Specimen Test Techniques and Their Applications to Nuclear Reactor Vessel Thermal Annealing and Plant Life Extension, New Orleans, LA, 29-31 Jan. 1992
(Contract DE-AC06-76RL-01830)
(DE92-014703; PNL-SA-19683; CONF-920146-3) Avail: CASI HC A03/MF A01

Currently available correlations for the effects of specimen size on the USE were developed for relatively ductile steels and will not serve as well when the steels become embrittled. Size effects correlations were developed recently for the impact properties of less ductile HT9 to be applied to other initially more ductile steels as they lose their ductility during irradiation. These new correlations successfully predict the ductile brittle transition temperature (DBTT) and the upper shelf energy (USE) of full size Charpy specimens based on subsize specimen data. The new DBTT and the USE correlations were tested against published experimental data on other ferritic steels and shown to perform successfully at lower USE particularly when both precracked and notched only specimens were employed. DOE

N92-30888# Oak Ridge National Lab., TN.
INVESTIGATION OF JOINING TECHNIQUES FOR ADVANCED AUSTENITIC ALLOYS
C. D. Lundin (Tennessee Univ., Knoxville.), C. Y. P. Qiao (Tennessee Univ., Knoxville.), Y. Kikuchi (Tennessee Univ., Knoxville.), C. Shi (Tennessee Univ., Knoxville.), and T. P. S. Gill (Tennessee Univ., Knoxville.) May 1991 180 p
(Contract DE-AC05-84OR-21400)
(DE92-015545; ORNL/Sub-88-07685/02) Avail: CASI HC A09/MF A02

Modified Alloys 316 and 800H, designed for high temperature service, have been developed at Oak Ridge National Laboratory. Assessment of the weldability of the advanced austenitic alloys has been conducted at the University of Tennessee. Four aspects of weldability of the advanced austenitic alloys were included in the investigation. DOE

N92-31010# Pacific Northwest Lab., Richland, WA.
A COMPARATIVE EIS STUDY ON CERMET AND PLATINUM ANODES FOR THE ELECTROLYTIC PRODUCTION OF ALUMINUM
C. F. Windisch, Jr. May 1992 8 p Presented at the 181st Meeting of the Electrochemical Society, Inc., St. Louis, MO, 17-22 May 1992
(Contract DE-AC06-76RL-01830)
(DE92-015091; PNL-SA-20305; CONF-920514-4) Avail: CASI HC A02/MF A01

Electrochemical impedance spectra (EIS) of NiO-NiFe2O4-Cu cermet anodes in alumina-saturated molten cryolite at anodic potentials above the decomposition potential of alumina exhibited a loop with a characteristic frequency of about 1 Hz. A similar feature was observed using platinum anodes under the same experimental conditions. Analysis of these data suggests the loop was due to gas bubbling. Features associated with charge-transfer processes were not sufficiently resolved to determine the corrosion properties of the cermet anode. DOE

N92-31110# Army Lab. Command, Watertown, MA. Material Technology Lab.
ELLIPSOMETRIC STUDY OF OXIDE FILMS FORMED ON LDEF METAL SAMPLES Final Report
Wolfgang Franzen, Judith S. Brodkin, Louise C. Sengupta, and Paul L. Sagalyn Feb. 1992 24 p Previously announced as N92-24833
(AD-A249856; MTL-TR-92-2) Avail: CASI HC A03/MF A01

The optical constants of samples of six different metals (Al, Cu, Ni, Ta, W, and Zr) exposed to space on the long duration exposure facility (LDEF) were studied by variable angle spectroscopic ellipsometry. Measurements were also carried out on portions of each sample which were shielded from direct exposure by a metal bar. A least-squares fit of the data using an effective medium approximation was then carried out, with thickness and composition of surface films formed on the metal substrates as variable parameters. The analysis revealed that exposed portions of the Cu, Ni, Ta, and Zr samples are covered with porous oxide films ranging in thickness from 500 to 1000 A. The 410 A thick film of Al203 on the exposed Al sample is practically free of voids. Except for Cu, the shielded portions of these metals are covered by thin nonporous oxide films characteristic of exposure to air. The shielded part of the Cu sample has a much thicker porous coating of CU20. The tungsten data could not be analyzed. GRA

N92-31112# Oak Ridge National Lab., TN.
IMPURITY SEGREGATION TO GRAIN BOUNDARIES AND DEFECTS IN AIN
D. L. Callahan (Rice Univ., Houston, TX.), E. A. Kenik (Rice Univ., Houston, TX.), and K. B. Alexander 1992 3 p Presented at the Annual Meeting of the Electron Microscopy Society (EMS) of America, Boston, MA, 16-21 Aug. 1992
(Contract DE-AC05-84OR-21400)
(DE92-011667; CONF-920819-13) Avail: CASI HC A01/MF A01

The technological development of aluminum nitride (AIN) substrates is driven to a large extent towards the economical production of high thermal conductivity sintered ceramics for substrate applications. Stringent demands on matrix purity combined with the practical necessity of sintering additives have led to extensive analyses of property-controlling matrix defect structures and of the role of additives in both matrix purification and sintering. Of particular interest are defects such as inversion domain boundaries (IDB's) and grain boundaries which may serve as segregation sites for the dominant impurities in AIN, particularly oxygen. Quantitative methods of analytical electron microscopy are applied to the analysis of chemical segregation in electronic grade AIN. DOE

N92-31119# Lawrence Livermore National Lab., CA.
THEORETICAL STUDY OF PHASE STABILITY IN Ni-Al AND Ni-Ti ALLOYS
M. Sluiter, P. E. A. Turchi, F. J. Pinski (Cincinnati Univ., OH.), and G. M. Stocks (Oak Ridge National Lab., TN.) 22 Oct. 1991 21 p Presented at the International Phase Diagram Symposium, Cincinnati, OH, Oct. 1991
(Contract W-7405-eng-48)
(DE92-014776; UCRL-JC-108775; CONF-9110252-2) Avail: CASI HC A03/MF A01

The thermodynamic stability of the bcc and fcc based ordered phases in Ni-Ti and Ni-Al has been studied with a highly accurate first-principles electronic structure method. The occurrence of a martensitic transformation in Ni-Al B2 ordered intermetallic alloys is discussed with relation to the existence of intermediate structures between bcc and fcc based phases. It is shown that closely related ordered structures can exist on fcc and bcc lattices in the composition range where the transformation occurs. The Ni-rich side of the Ni-Al phase diagram has been computed and a comparison with a recent assessment is made. In addition, the rather unusual appearance of the NiTi B2 ordered structure in the phase diagram is discussed. DOE

N92-31124# Lawrence Livermore National Lab., CA.
STABILITY OF METALLIC SUPERLATTICES
P. E. A. Turchi and M. Sluiter Nov. 1991 6 p Presented at the Optical Society of America (OSA) Meeting, Jackson Hole, WY, 2-5 Mar. 1992
(Contract W-7405-eng-48)
(DE92-011526; UCRL-JC-108838; CONF-9203130-1) Avail: CASI HC A02/MF A01

An approach is presented for the study of the thermodynamic stability properties of artificial superlattices. General expressions are derived for the configurational energy as a function of the superlattice parameters, and also for the interfacial energy. Finally, the relationship between some artificial superlattices and naturally occurring ordered phases are briefly discussed. DOE

N92-31125# Lawrence Livermore National Lab., CA.
STABILIZATION OF FACE-CENTERED-CUBIC TITANIUM
A. F. Jankowski and M. A. Wall Nov. 1991 8 p Presented at the Annual Fall Meeting of the Materials Research Society, Boston, MA, 2-6 Dec. 1991
(Contract W-7405-eng-48)
(DE92-011530; UCRL-JC-107793; CONF-911202-75) Avail: CASI HC A02/MF A01

The artificial layering of metals, by vapor deposition, can bring about changes in the physical and structural characteristics of metals. These changes are responsible for the metals having properties that are significantly different from their original bulk properties. The stabilization of such phases often occurs when the component layers are constructed on a nanometric scale. The sequential layering of nickel and titanium has produced the formation of a previously unreported, face-centered-cubic (f.c.c.) phase of titanium. DOE

N92-31138# Lawrence Livermore National Lab., CA.
SELF-CONSISTENT-FIELD KKR-CPA CALCULATIONS IN THE ATOMIC-SPHERE APPROXIMATIONS
P. P. Singh, A. Gonis, and D. deFontaine (California Univ., Berkeley.) 3 Dec. 1991 8 p Presented at the Annual Fall Meeting of the Materials Research Society, Boston, MA, 2-6 Dec. 1991
(Contracts W-7405-eng-48; DE-AC03-76SF-00098)
(DE92-011525; UCRL-JC-108753; CONF-911202-73) Avail: CASI HC A02/MF A01

We present a formulation of the Korringa-Kohn-Rostoker coherent potential approximation (KKR-CPA) for the treatment of substitutionally disordered alloys within the KKR atomic-sphere approximations (ASA). This KKR-ASA-CPA represents the first step toward the implementation of a full cell potential CPA, and combines the accuracy of the KKR-CPA method with the flexibility of treating complex crystal structures. The accuracy of this approach was tested by comparing the self-consistent-field (SCF) KKR-ASA-CPA calculations of Cu-Pd alloys with experimental results and previous SCF-KKR-CPA calculations. DOE

N92-31163# Japan Atomic Energy Research Inst., Tokyo.
FILLER METAL DEVELOPMENT FOR HASTELLOY ALLOY XR
Katsutoshi Watanabe, Hajime Nakajima, and Kensho Sahira Nov. 1991 72 p In JAPANESE
(DE92-782044; JAERI-M-91-189) Avail: CASI HC A04/MF A01

In order to develop the filler metal for Hastelloy alloy XR structure with thick wall, the weldability and high temperature strength properties of Hastelloy alloy XR weldment were investigated using the filler metals, which were alloy-designed on the basis of multiple regression analysis. The former was examined through the chemical analysis in the deposited metal, bend test, FISCO cracking test, optical microscopy, and hardness measurement. The latter was investigated by means of tensile and creep test. It was found from these results that the crack susceptibility in the weldment was apparent to be lowered without degrading the high temperature strength properties. Therefore, it is concluded that these filler metals possess excellent performance as the filler metal for Hastelloy alloy XR structure with thick wall. DOE

N92-31177# Sandia National Labs., Albuquerque, NM.
PHASE TRANSFORMATIONS IN WELDMENTS: NEW MATERIALS AND NEW PERSPECTIVES
M. J. Cieslak 1992 12 p Presented at the 3rd International Conference on Trends in Welding Research, Gatlinburg, TN, 1 Jun. 1992
(Contract DE-AC04-76DP-00789)
(DE92-016231; SAND-92-1233C; CONF-9206173-3) Avail: CASI HC A03/MF A01

The last decade has offered many challenges to the welding metallurgist: new types of materials requiring welded construction, describing the microstructural evolution of traditional materials, and explaining non-equilibrium microstructures arising from rapid thermal cycle weld processing. In this paper, the author will briefly review several advancements made in these areas, often citing specific examples of where new insights were required to describe new observations, and to show how traditional physical metallurgy methods can be used to describe transformation phenomena in advanced, non-traditional materials. The paper will close with comments and suggestions as to the needs required for continued advancement in the field. DOE

N92-31186# Delaware Univ., Newark. Dept. of Physics and Astronomy.
FUNDAMENTAL STUDIES OF STRONGLY MAGNETIC RARE EARTH-TRANSITION METAL ALLOYS
D. J. Sellmyer (Nebraska Univ., Lincoln.) and G. C. Hadjipanayis 1992 11 p
(Contracts DE-FG02-90ER-45413; DE-FG02-86ER-45262)
(DE92-015916; DOE/ER-45413/2) Avail: CASI HC A03/MF A01

The goal of this project is to advance our understanding of new phases and microstructures of rare-earth and transition-metal alloys and compounds. In particular, we investigate several classes of materials which are expected to have high magnetizations and coercivities, which are necessary conditions for high performance permanent magnet and related applications. Hard and semi-hard magnetic materials form the basis of much of the electric power and information storage industries, and the discovery of new and less expensive materials with outstanding properties is of great interest. DOE

N92-31218# Westinghouse Savannah River Co., Aiken, SC.
THERMODYNAMIC EVAPORATION OF HIGHLY VOLATILE COMPONENTS IN THE VACUUM DEGASSING OF MELTED ALUMINUM ALLOYS
G. S. Makarov 1992 9 p Transl. into ENGLISH from Teknologiya Legkikh Splavov (USSR), v. 5, 1970 p 31-36
(Contract DE-AC09-89SR-18035)
(DE92-015315; WSRC-TR-146) Avail: CASI HC A02/MF A01

Based on thermodynamic analysis, the vapor tension of the volatile components over double aluminum alloys was determined. Vacuum degassing of aluminum alloys creates conditions for the evaporation of alloyed components or admixtures that have a high power tension. The process for the elimination of these substances is subjected to the same principles as the process for the evacuation of hydrogen. Substantial losses of the highly volatile components are possible in instances when their vapor tension exceeds the sum of the external pressures, preventing the formation of the vapor phase in the melt. DOE

N92-30266*# Purdue Univ., West Lafayette, IN. Dept. of Mechanical Engineering Technology.
ELEMENTARY METALLOGRAPHY
Sayyed M. Kazem *In* NASA. Langley Research Center, National Educators' Workshop: Update 1991. Standard Experiments in Engineering Materials Science and Technology Jun. 1992 p 57-64 (For primary document see N92-30263 21-29)
Avail: CASI HC A02/MF A03

N92-30269*# Youngstown State Univ., OH. Dept. of Materials Engineering.
Cu-Zn BINARY PHASE DIAGRAM AND DIFFUSION COUPLES

Robert A. McCoy *In* NASA. Langley Research Center, National Educators' Workshop: Update 1991. Standard Experiments in Engineering Materials Science and Technology Jun. 1992 p 111-118 (For primary document see N92-30263 21-29)
Avail: CASI HC A02/MF A03

N92-30272*# Intermet Technology, Georgetown, PA.
EXPERIMENTS WITH THE LOW MELTING INDIUM-BISMUTH ALLOY SYSTEM
Richard P. Krepski *In* NASA. Langley Research Center, National Educators' Workshop: Update 1991. Standard Experiments in Engineering Materials Science and Technology Jun. 1992 p 143-147 Sponsored in part by NSF Prepared in cooperation with Geneva Coll., Beaver Falls, PA (For primary document see N92-30263 21-29)
Copyright Avail: CASI HC A01/MF A03

N92-30276*# Ohio Northern Univ., Ada. Dept. of Mechanical Engineering.
Be-Cu PRECIPITATION HARDENING EXPERIMENT
Richard L. Cowan *In* NASA. Langley Research Center, National Educators' Workshop: Update 1991. Standard Experiments in Engineering Materials Science and Technology Jun. 1992 p 189-193 (For primary document see N92-30263 21-29)
Avail: CASI HC A01/MF A03

N92-30291*# Purdue Univ., West Lafayette, IN. Dept. of Mechanical Engineering Technology.
INTRODUCTORY HEAT-TRANSFER
Edward L. Widener *In* NASA. Langley Research Center, National Educators' Workshop: Update 1991. Standard Experiments in Engineering Materials Science and Technology Jun. 1992 p 377-382 (For primary document see N92-30263 21-29)
Avail: CASI HC A02/MF A03

N92-30292*# Purdue Univ., West Lafayette, IN. Dept. of Mechanical Engineering Technology.
HEAT-TREATING OF MATERIALS
Edward L. Widener *In* NASA. Langley Research Center, National Educators' Workshop: Update 1991. Standard Experiments in Engineering Materials Science and Technology Jun. 1992 p 383-387 (For primary document see N92-30263 21-29)
Avail: CASI HC A01/MF A03

27 NONMETALLIC MATERIALS

Includes physical, chemical, and mechanical properties of plastics, elastomers, lubricants, polymers, textiles, adhesives, and ceramic materials.

For composite materials see *24 Composite Materials*.

N92-30244# Carnegie-Mellon Univ., Pittsburgh, PA. Dept. of Chemistry.
EPOXIDES AS ACTIVATORS FOR GRAFTING OF POLY(TETRAHYDROFURAN) FROM POLY(METHYLPHENYLSILYLENE)
Krzysztof Matyjaszewski and Jeffrey S. Hrkach 25 May 1992 8 p
(Contract N00014-90-J-1186)
(AD-A251086; TR-32) Avail: CASI HC A02/MF A01

Epoxides have been found as efficient activators for initiation of the cationic polymerization of tetrahydrofuran by trimethylsilyl trifluoromethanesulfonate. They can also activate partially triflate polysilane and lead to grafting of the polyTHF from polysilanes.
GRA

N92-30250# Florida Univ., Gainesville. Dept. of Chemistry.
TEMPERATURE EFFECT ON THE LANGMUIR-BLODGETT POLYMERIZATION OF 2-PENTADECYLANILINE
R. Bodalia and R. S. Duran 19 May 1992 4 p Submitted for publication
(Contract N00014-91-J-1655)
(AD-A250803; TR-7) Avail: CASI HC A01/MF A01

The effect of temperature on the Langmuir-Blodgett polymerization of 2-pentadecylaniline (C-15 aniline) was studied at an aqueous sulfuric acid/air interface using (NH4)S208 as an initiator. Isotherms of 2-pentadecylaniline on a 0.1 M H2SO4 subphase at different temperatures show that the mean molecular area at the surface pressure onset increases with the temperature. Stability and the rate of polymerization of C-15 aniline at an aqueous sulfuric acid/air interface were influenced considerably by the temperature. The stability of C-15 aniline at the interface increases with decreasing temperature at constant surface pressure. The time required to complete the polymerization reaction decreases with increasing temperature at a constant surface pressure.
GRA

N92-30313*# National Aeronautics and Space Administration. Langley Research Center, Hampton, VA.
POLYIMIDES CONTAINING THE CYCLOBUTENE-3,4-DIONE MOIETY Patent Application
Terry L. St.Clair, inventor (to NASA) 3 Mar. 1992 12 p
(NASA-Case-LAR-14753-1; NAS 1.71:LAR-14753-1; US-Patent-Appl-SN-845090) Avail: CASI HC A03/MF A01

In the present invention, linear aromatic polyimides containing the cyclobutene-3,4-dione moiety were produced from the reaction of a substituted or unsubstituted 1,2-bis(4-aminoanilino) cyclobutene-3,4-dione (SQDA) with various aromatic dianhydrides. These polymers had high molecular weights and their glass transition temperatures (Tgs) were greater than 500 C. Despite the very high Tg, these polymers exhibited excellent adhesion to glass. In addition, the films of these polyimides increased in flexibility with increasing cure temperatures. The novelty of this invention lies in the linear aromatic polyimide containing the cyclobutene-3,4-dione moiety. The presence of this moiety causes such changes in properties as Tgs greater than 500 C, excellent adhesion to glass, and increased flexibility with increasing cure temperatures.
NASA

N92-30326# North Carolina State Univ., Raleigh. Dept. of Materials Science and Engineering.
COMPUTER-CONTROLLED ION BEAM SPUTTER-DEPOSITION OF SUPERCONDUCTING OXIDE FILMS Final Report, 1 Jul. 1988 - 31 Dec. 1991
Orlando H. Auciello, Angus I. Kingon, and Robert F. Davis 31 Dec. 1991 102 p
(Contract N00014-88-K-0525)
(AD-A248495) Avail: CASI HC A06/MF A02

The system developed can be used to produce multicomponent and/or multilayered structures. Computer-controlled growth of multicomponent materials can be accomplished by sequentially sputtering from elemental targets. Layered structures can be obtained by sequentially sputtering from different multicomponent targets. Sputtering targets are mounted on a motor-driven rotating holder for sequential, in situ positioning in front of the ion beam. The thickness of each individual material layer is monitored by a quartz crystal resonator. The computer program uses feedback control from the quartz crystal monitor to turn the ion beam on and off, and to position the appropriate target in front of the ion beam. This system can be utilized in three basic configurations: with multiple elemental (or single cation) targets, for growing multicomponent oxide films (multiple cations) of any chosen composition, e.g., Y, Cu, and BaF targets for YBa2Cu3O7-sigma film growth; and with multiple elemental or compound targets, for growing multiple film layers, such as YBa2Cu3O7-(sigma)/MgO layers.
GRA

N92-30342# Rockwell International Science Center, Thousand Oaks, CA.
TRANSFORMATION TOUGHENING OF CERAMICS Final Report, 15 Jan. 1989 - 14 Jan. 1992
D. B. Marshall Mar. 1992 150 p
(Contract F49620-89-C-0031)
(AD-A248903; SC71002.FR; AFOSR-92-0236TR) Avail: CASI HC A07/MF A02

The results of a three-year study, aimed at developing a

fundamental understanding of transformation toughening in ceramics and using that understanding to design and fabricate new microstructures with improved properties, are described. A new class of materials with dual scale (laminar) microstructures and greatly enhanced fracture toughness was developed and tested; increases in fracture toughness from 5 to 18 MFA m(exp 1/2) were measured. These new microstructures were designed by combining micromechanics modeling of the effects of zone shape on toughness with direct measurements of transformation zone characteristics (which provided critical testing of the theoretical modeling) and measurements of transformation thermodynamics. To fabricate these microstructures a new colloidal processing method, which allowed construction of multilayered structures with layer thicknesses as small as 10 microns, was developed. The direct transformation zone measurements included Raman microprobe spectroscopy to measure the distribution of transformed phases within the zones, and moire interferometry and high resolution strain mapping (by digital image correlation) to measure directly the transformation strains that are responsible for toughening. Calculations of crack tip shielding indicated modifications to transformation zone shapes that would increase the toughening. GRA

N92-30346# Indiana Univ.-Purdue Univ., Indianapolis. Dept. of Chemistry.
SYNTHESIS AND REACTIVITY OF 1-METHYL-E-ETHYNYLPYRIDINIUM TRIFLATE
Martel Zeldin, Slawomir Rubinsztajn, and Wilmer K. Fife 15 May 1992 6 p
(Contract N00014-91-J-1434)
(AD-A250638; TR-16) Avail: CASI HC A02/MF A01

1-Methyl-4-ethynylpyridinium triflate has been prepared by treatment of 4-ethynylpyridine with methyl triflate in methylene chloride. This new active acetylenic monomer trimerized to trisl, 3,5-(1-methylpyridinium-4-yl) benzene triflate when heated in aqueous solution. The new compounds were isolated and characterized. GRA

N92-30399# Lawrence Livermore National Lab., CA.
SHOCK-INDUCED MARTENSITIC TRANSFORMATION OF HIGHLY ORIENTED GRAPHITE TO DIAMOND
D. Erskine and W. Nellis Mar. 1992 8 p Presented at the Material Research Society Spring Meeting, San Francisco, CA, 27 Apr. - 2 May 1992 Revised
(Contract W-7405-eng-48)
(DE92-014787; UCRL-JC-109293-Rev-1; CONF-920402-15-Rev-1) Avail: CASI HC A02/MF A01

Shock-wave profiles of highly ordered pyrolytic graphite shocked normal to the basal plane of the graphite crystal structure have been measured. For graphite with sufficient orientational order, a martensitic transformation to a diamond-like phase is observed with a transition onset pressure 19.6 +/ 0.7 GPa, the stability limit of the graphite structure under shock compression. The minimum overpressure required for the transformation is not more than 6 GPa. DOE

N92-30402# Atomic Energy of Canada Ltd., Chalk River (Ontario).
NONDESTRUCTIVE EVALUATION OF CERAMIC COMPONENTS BY GAMMA RAY CT
S. Rokugawa (Nippon Kokan K. K., Kawasaki, Japan), S. Usui (Nippon Kokan K. K., Kawasaki, Japan), and B. D. Sawicka Sep. 1991 18 p Presented at the 5th International Symposium on Nondestructive Characterization of Materials, Karuizawa (Japan), 27-30 May 1991
(DE92-626843; AECL-10461; CONF-910572) Avail: CASI HC A03/MF A01

Results of gamma ray computed tomography (CT) examination of ceramic parts in various stages of the manufacturing process are presented. The ceramic samples were prepared by injection-molding and examined in three stages: before sintering and after HIPing. CT tests were performed at AECL Research, Chalk River Laboratories. The uniformity of the material distribution in ceramic parts was measured by measuring density gradients in CT images, with an accuracy of between 0.2 and 0.5 percent in various scans. The results demonstrate that the CT technique is very useful, particularly for monitoring changes in material distribution during various stages of the fabrication process and for providing comparisons between technologically different processes. DOE

N92-30409# Nebraska Univ., Lincoln.
THE ELECTRIC FIELD DEPENDENCE OF THE LASER INDUCED HOLOGRAPHIC GRATING RELAXATION OF PHOTOREFRACTIVE POLYMER
C. H. Wang, R. J. Ma, X. Q. Zhang, Stephen Ducharme, and J. M. Takacs 1992 10 p
(AD-A252641; Rept-18) Avail: CASI HC A02/MF A01

Laser induced holographic grating relaxation (HGR), electro-optical (EO), and second harmonic generation (SHG) studies have been carried out in a guest/host system subject to an external electric field with and without the presence of a hole transport agent. The guest is NNI, which has moderate second order nonlinear optical (NLO) coefficient, the host is PMMA, and the hole transport agent is DEH. In the presence of DEH, the lifetime of the cis isomer of NNI detected by using the HGR technique is lengthened by the application of an electric field of moderate strength. The field dependence effect is not observed when DEH is absent in the sample. The result is interpreted as due to the stabilization of the cis-isomer by the electric field polarized DEH. The data obtained from SHG and EO measurements appear to corroborate the HGR result. GRA

N92-30502# National Inst. for Fusion Science, Nagoya (Japan).
REVIEW OF HIGH Z MATERIALS FOR PSI APPLICATIONS
Tetsuo Tanabe (Osaka Univ., Japan), Nobuaki Noda, and Hiroo Nakamura (Japan Atomic Energy Research Inst., Naka.) Jun. 1992 49 p Presented at the 10th International Conference on Plasma Surface Interactions in Controlled Fusion Devices, Monterey, CA, 30 Mar. - 3 Apr. 1992 Submitted for publication
(NIFS-152; ISSN-0915-633X) Avail: CASI HC A03/MF A01

Application of carbon based low Z materials of plasma facing materials (PFM) has significantly improved plasma parameters in large tokamaks. There are, however, serious concerns of erosion, neutron damage, etc. for application of low Z materials in future D-T burning machine. To apply high Z metals to PFM, there are several issues to be solved; high Z impurity production by sputtering, their accumulation in plasma center, and high radiation loss. Because of these concerns high Z metals are not widely employed nor planned to be used in the present large tokamaks. Since our efforts were concentrated to optimize the low Z materials, few systematic investigations for high Z materials in a tokamak were done; thus, the data base lacks information concerning impacts on the plasma core. In order to employ high Z material as PFM in the near future, material properties related to impurity production and hydrogen recycling are reviewed and discussed. Author

N92-30539*# National Aeronautics and Space Administration. Lyndon B. Johnson Space Center, Houston, TX.
ABLATIVE SHIELDING FOR HYPERVELOCITY PROJECTILES Patent Application
Michelle A. Rucker, inventor (to NASA) 21 May 1992 16 p
(NASA-Case-MSC-21884-1; NAS 1.71:MSC-21884-1;
US-Patent-Appl-SN-887674) Avail: CASI HC A03/MF A01

A hypervelocity projectile shield which includes a hollow semi-flexible housing fabricated from a plastic like, or otherwise transparent membrane which is filled with a fluid (gas or liquid) is presented. The housing has a inlet valve, similar to that on a tire or basketball, to introduce an ablating fluid into the housing. The housing is attached by a Velcro mount or double-sided adhesive tape to the outside surface of a structure to be protected. The housings are arrayed in a side-by-side relationship for complete coverage of the surface to be protected. In use, when a hypervelocity projectile penetrates the outer wall of a housing it is broken up and then the projectile is ablated as it travels through the fluid, much like a meteorite 'burns up' as it enters the earth's

atmosphere, and the housing is deflated. The deflated housing can be easily spotted for replacement, even from a distance. Replacement is then accomplished by simply pulling a deflated housing off the structure and installing a new housing. NASA

N92-30544# Sandia National Labs., Albuquerque, NM.
MOLECULAR WEIGHT DEPENDENCE OF DOMAIN STRUCTURE IN SILICA-SILOXANE MOLECULAR COMPOSITES
Tamara A. Ulibarri, Greg Beaucage, Dale W. Schaefer, Bernard J. Olivier, and Roger A. Assink 1992 7 p Presented at the Material Research Society Spring Meeting, San Francisco, CA, 27 Apr. - 2 May 1992
(Contract DE-AC04-76DP-00789)
(DE92-015046; SAND-91-2539C; CONF-920402-20) Avail: CASI HC A02/MF A01

A detailed investigation of the molecular weight dependence of silica growth in in situ filled polydimethyl siloxane/tetraethyl orthosilicate (PDMS/TEOS) materials was conducted using small angle neutron scattering (SANS). Composite materials were produced by using TEOS to simultaneously produce the glassy filler phase and to crosslink linear, hydroxyl terminated PDMS of variable molecular weight M. Correlated domains of glassy filler were produced. The morphology of the in situ filled material showed a definite dependence on the molecular weight of the precursor polymer. The scale, R, of the glassy domains follows de Gennes' description of phase separation in a crosslinked system (R(alpha)M(exp 1/2)). DOE

N92-30553# Colorado State Univ., Fort Collins. Dept. of Chemistry.
TEMPLATE-SYNTHESIS: A METHOD FOR ENHANCING THE IONIC AND ELECTRONIC CONDUCTIVITY IN ELECTRONICALLY CONDUCTIVE POLYMERS
Charles R. Martin, Leon S. VanDyke, and Zhihua Cai 16 Apr. 1992 11 p
(Contract N00014-82-K-0612)
(AD-A248806; TR-66) Avail: CASI HC A03/MF A01

Template-synthesis entails the synthesis of an electronically conductive polymer (or other material) within the pores of a microporous membrane. The membranes used have cylindrical pores of equivalent pore diameter; as a result, polymeric fibers are obtained, where the diameters of the fibers are determined by the diameter of the pores in the template membrane. We show in this paper that template-synthesized polypyrrole fibers show faster rates of charge transport, during electrochemical undoping, and dramatically higher electronic conductivity than conventional forms (e.g. electrochemically-synthesized film) of this polymer.
GRA

N92-30594# Rutgers - The State Univ., Piscataway, NJ. Dept. of Mechanics and Materials Science.
A NEW CLASS OF FERROELECTRIC POLYMERS: THE ODD-NUMBERED NYLONS Technical Report, 1 Jun. 1991 - 31 May 1992
B. A. Newman, J. I. Scheinbeim, J. W. Lee, and Y. Takase Jun. 1992 9 p
(Contract N00014-80-C-0795)
(AD-A252268; TR-24) Avail: CASI HC A02/MF A01

The thermal stability of the piezoelectric response of a new class of ferroelectric polymer, the odd-numbered nylons, has been studied and the behavior compared with the thermal stability of piezoelectricity in poly(vinylidene fluoride). FTIR absorbance spectroscopy and an x-ray diffraction study show that under high applied electric fields, a 90 degree dipole switching mechanism orients amide dipoles in the field direction prior to 1800 switching under repeated reversals of field. GRA

N92-30623# Rensselaer Polytechnic Inst., Troy, NY. Dept. of Chemistry.
STUDIES OF THERMAL DECOMPOSITION OF THE 1:1 R3Al:en ADDUCT (R = Me, Et; en = ETHYLENEDIAMINE): SYNTHESIS AND STRUCTURE OF A NOVEL INTERMEDIATE Al((HNCH2CH2NH)AlMe2)3
Zhiping Jiang, Leonard V. Interrante, Daekeun Kwon, Fook S. Tham, and Rudolph Kullnig 25 May 1992 36 p
(Contract N00014-91-J-1917)
(AD-A251061) Avail: CASI HC A03/MF A01

The research activity in this area has been enhanced recently by the discovery that such organoaluminum-nitrogen compounds have potential utility as precursors to aluminum nitride, a refractory ceramic material of much current interest for both electronic and structural applications. Such precursors offer the prospect of improvements in processability, by virtue of the volatility, solubility, and/or thermoplasticity characteristic of molecular systems. The factors influencing the formation of chelated monomers versus open chain dimers in organoaluminum amides derived from the reaction of a 1:1 ratio of R3A1 with various diamines of the type, HRN(CH2)(n)NR'R' (R = H, Me, Et, Ph; R', R' = Me, Et), have been investigated by Beachley and coworkers. They found that the equilibria between the monomer and dimer forms were influenced by steric effects due to the R, R', and R' substituents, as well as the ligand base strength and the chelate ring size.
GRA

N92-30626# Oak Ridge National Lab., TN.
EFFECT OF BENDING ON THE ROOM-TEMPERATURE TENSILE STRENGTHS OF STRUCTURAL CERAMICS
M. G. Jenkins 1992 8 p Presented at the 7th Society for Experimental Mechanics International Congress on Experimental Mechanics, Las Vegas, NV, 8-11 Jun. 1992
(Contract DE-AC05-84OR-21400)
(DE92-015196; CONF-9206187-2) Avail: CASI HC A02/MF A01

Results for nearly fifty, room-temperature tensile tests conducted on two advanced, monolithic silicon nitride ceramics are evaluated for the effects of bending and application of various Weibull statistical analyses. Two specimen gripping systems (straight collet and tapered collet) were evaluated for both success in producing gage section failures and tendency to minimize bending at failure. Specimen fabrication and grinding technique considerations are briefly reviewed and related to their effects on successful tensile tests. Ultimate tensile strengths are related to the bending measured at specimen failure, and the effects of the gripping system on bending are discussed. Finally, comparisons are made between the use of censored and uncensored data sample sets for determining the maximum likelihood estimates of the Weibull parameters from the tensile strength distributions.
DOE

N92-30635# Laser Science, Inc., Ames, IA.
SOLID LUBRICATION OF LASER GROWN FLUORINATED DIAMOND THIN FILMS Final Report, 1 Jul. - 31 Dec. 1991
Bruce Janvrin, Madhav Rao, Deli Gong, Arul Molian, and P. Molian 21 Jan. 1992 66 p
(Contract DAAL03-91-C-0041)
(AD-A249485; ARO-29043.1-MS-SBI) Avail: CASI HC A04/MF A01

A laser chemical vapor deposition process was developed to grow fluorinated diamond thin films on bearing material substrates including SiC and 440C stainless steel. The type of laser, carbon feedstock, laser-precursor gas interactions, and deposition conditions were established. Analysis of laser grown films revealed that the films deposited on SiC consisted of a mixture of diamond and graphite while the films on 440C steel were composed of diamond, diamond-like carbon, and graphite. The presence of significant amounts of C-F compounds both in the surface and subsurface layers was also identified. Tribological tests (ball-on-disc and pin-on-disc) of laser grown films in an ambient environment indicated a friction coefficient in the range of 0.1 to 0.3 depending on the wear couple, sliding speed, and load. These tests confirmed

the effectiveness of these films as solid lubricants for moving mechanical assemblies in space structures. Fluorination of carbon films has the following attributes: passivation of the surface of diamond/graphite films from absorption of water or oxygen; reduction of surface energy needed for shearing of the film during solid lubrication; and protection from corrosive environments.
GRA

N92-30685# Department of the Navy, Washington, DC.
METHOD OF SYNTHESIZING HIGH QUALITY, DOPED DIAMOND AND DIAMONDS AND DEVICES OBTAINED THEREFROM Patent Application
Art Morrish, inventor (to Navy) and Keith Snail, inventor (to Navy) 20 Aug. 1991 28 p
(AD-D015267; US-Patent-Appl-SN-747321; Navy-Case-73546)
Avail: CASI HC A03/MF A01

Diamond crystals and films having a well-controlled amount of dopant are synthesized by incorporating a dopant into a deposition species formed from a gaseous source of carbon and a gaseous source of hydrogen. Flame and/or plasma deposition may be used. Various apparatuses for carrying out the growth of the doped diamond are also disclosed.
GRA

N92-30695# Tennessee Univ., Knoxville. Dept. of Chemistry.
STUDY OF THE SURFACE PROPERTIES OF CERAMIC MATERIALS BY CHROMATOGRAPHY
G. Guiochon Mar. 1992 22 p
(Contract DE-FG05-88ER-13859)
(DE92-011129; DOE/ER-13859/31) Avail: CASI HC A03/MF A01

Most fundamental research on adsorption assumes adsorbent surfaces to be homogeneous. Material chemists have been able to design and prepare a variety of adsorbents with a highly homogeneous surface. These adsorbents are widely used in chromatography and in adsorption studies, contributing to further anchor the idea that homogeneous surfaces are the most frequent case. In reality, many common materials used as finely divided powders such as pigments, fillers, ceramics, or involved in industrial procedures such as adhesion, have inhomogeneous surfaces, and this fact explains difficulties and troubles in predicting their properties and usefulness. The main result of work is a practical method which permits the detailed study of the chemical properties of non-homogeneous surfaces.
DOE

N92-30744# Oak Ridge National Lab., TN.
NONDESTRUCTIVE TESTING OF CERAMICS FOR VEHICULAR ADVANCED HEAT ENGINES
R. W. McClung and D. R. Johnson 1992 3 p Presented at the 1992 American Society for Nondestructive Testing (ASNT) Spring Conference, Orlando, FL, 30 Mar. - 3 Apr. 1992
(Contract DE-AC05-84OR-21400)
(DE92-010471; CONF-9203108-1) Avail: CASI HC A01/MF A01

Transportation is the largest petroleum user in the United States, accounting for about two-thirds of the total use. Of this, over 80 percent of the transportation fuels are consumed in roadway vehicles. The need for improvements in transportation fuel efficiency is clear. As one approach toward the solution of this problem, there has been expanded research into new automotive propulsion systems. One phase of this development has been concerned with advanced heat engines such as the automotive gas turbine and low-heat rejection diesel engine. The improved energy efficiency depends on the ability of such engines to operate at very high temperatures by using high-temperature structural materials. Advanced structural ceramics are the materials of choice. However, current limitations in reliability of advanced ceramics have required extensive research and development to overcome the problems. A major program is being funded by the Department of Energy, Office of Transportation Technologies. Nondestructive testing (NDT) is a vital part of that program. Development and application of advanced NDT are being performed by several ceramics producers, engine fabricators, research and development organizations, and NDT companies. Advanced and improved techniques are being studied for examination of ceramics at all stages of fabrication: from the starting raw materials, through intermediate stages, to the final finished product.
DOE

N92-30758# Army Materials Technology Lab., Watertown, MA.
PRESSURE DENSIFICATION
George E. Gazza Mar. 1992 15 p
(AD-A249438; MTL-TR-92-15) Avail: CASI HC A03/MF A01

Densification of ceramics can be achieved using a variety of techniques that are based on the application of external force. These techniques include uniaxial hot pressing, hot isostatic pressing, gas pressure sintering, and various modifications. A general overview of the issues, approaches, and parameters used in pressure-assisted densification processes is provided in this article. First, pressure densification theory is described in terms that are not intended to over simplify complex processes, but to simply outline some models and parameters used for the analysis and interpretation of densification behavior. Second, the various densification techniques are described using approaches and results from densification studies. These approaches continue to be examined and modified in order to provide further understanding of the densification processes and to produce ceramic component materials of suitable quality for emerging and expanding markets.
GRA

N92-30788# National Inst. of Standards and Technology, Gaithersburg, MD.
STUDIES ON THE MELT FLOW RATE OF THE SRM 1473: A LOW DENSITY POLYETHYLENE RESIN
J. R. Maurey and C. M. Guttman Apr. 1992 20 p
(PB92-181080; NISTIR-4627) Avail: CASI HC A03/MF A01

The melt flow rate of SRM 1473, a low density polyethylene, was determined to be 1.29 g/10 min at 190 C under a load of 2.16 kg using the ASTM method D 1238-89. The average results from 42 determinations on samples with a standard deviation of a single measurement of 0.020 g/10 min. A small but measurable drift from the first timed extrudate to the third timed extrudate was observed.
GRA

N92-30792# Lawrence Livermore National Lab., CA.
MICROSCOPIC THEORY OF THG AND ELECTRO-ABSORPTION IN CONJUGATED POLYMERS
D. Guo (Arizona Univ., Tucson.), S. Mazumdar (Arizona Univ., Tucson.), and S. N. Dixit Feb. 1992 12 p Presented at the Optical Probes of Conjugated Polymers Conference, Snowbird, UT, 19-22 Aug. 1991
(Contract W-7405-eng-48)
(DE92-014786; UCRL-JC-109730; CONF-9108168-3) Avail: CASI HC A03/MF A01

We develop a physical, intuitive description of optical nonlinearity in conjugated polymers within a completely general microscopic theoretical model. It is shown that third harmonic generation and electro-absorption give complimentary information on the electronic structures of (pi)-conjugated systems.
DOE

N92-30794# South Carolina Univ., Columbia. Dept. of Chemistry.
POLYMERIZATION OF 1-BROMO-4-LITHIOBENZENE IN THF. A ROUTE TO SOLUBLE POLYPHENYLENES
James M. Tour, Eric B. Stephens, and Joanna F. Davis 25 Apr. 1992 11 p
(Contract N00014-89-J-3062)
(AD-A249926; TR-8) Avail: CASI HC A03/MF A01

A synthesis of polyphenylene is described that involves the room temperature polymerization of 1-bromo-4-lithiobenzene in THF. The polymerization was complete within 2 hours to afford 65 percent yield of an ether insoluble fraction of brominated polyphenylene that was soluble in THF, CH2C12, and CHC13. Analysis of the initially formed polymers showed that there was a high bromide content with approximately one bromide for every three aryl rings. Debromination of the material was achieved by treatment with butyllithium and quenching with water. The

pre-quenched polymer had no lithiated aromatic rings and LiH appeared to be present in significant amounts upon completion of the polymerization. GRA

N92-30795# South Carolina Univ., Columbia. Dept. of Chemistry.
EXTENDED ORTHOGONALLY FUSED CONDUCTING OLIGOMERS FOR MOLECULAR ELECTRONIC DEVICES
James M. Tour, Ruilian Wu, and Jeffry S. Schumm 25 Apr. 1992 10 p
(Contract N00014-89-J-3062)
(AD-A249927; TR-7) Avail: CASI HC A02/MF A01

Described is an approach to orthogonally fused conjugated organic compounds that may act as molecular switching devices. Four thiophene trimers are added in a single operation to spiro-fused cores to afford the target molecules. A spiro-fused thiophene-based monomer system is converted to a spiro-fused heptamer that is 25 A long. The synthesis of a mixed phenylene-thiophene system is described that provides a spiro-fused octamer that is 30 A long. In each case, alkyl substituents on the thiophenes afford soluble materials. Trimethylsilyl end groups flank each orthogonally fused system. Organopalladium- and organonickel-catalyzed procedures are used extensively for the synthesis of the orthogonally fused compounds. GRA

N92-30796# South Carolina Univ., Columbia. Dept. of Chemistry.
SYNTHESIS OF ORTHOGONALLY FUSED CONDUCTING OLIGOMERS FOR MOLECULAR ELECTRONIC DEVICES
James M. Tour, Ruilian Wu, and Jeffry Schumm 25 Apr. 1992 8 p
(Contract N00014-89-J-3062)
(AD-A249929; TR-11) Avail: CASI HC A02/MF A01

Described is an approach to orthogonally fused conjugated organic compounds that may act as molecular switching devices. Four thiophene trimers are added in a single operation to spiro-fused cores to afford the target molecules. A spiro-fused thiophene-based monomer system is converted to a spiro-fused heptamer that is 25 A long. The synthesis of a mixed phylene-thiophene system is described that provides a spiro-fused octamer that is 30 A long. In each case, alkyl substituents on the thiophenes afford soluble materials. Trimethylsilyl end groups flank each orthogonally fused system. Organopalladium- and organonickel-catalyzed procedures are used extensively for the synthesis of the orthogonally fused compounds. GRA

N92-30804# Sandia National Labs., Albuquerque, NM.
NUMERICAL SIMULATION OF THE DYNAMIC BEHAVIOR OF THE POLYMERIC GELS
D. Segalman, W. Witkowski, D. Adolf, and M. Shahinpoor (New Mexico Univ., Albuquerque.) 1992 4 p Presented at the 1st International Conference on Intelligent Materials, Oiso-Machi, Japan, 23-25 Mar. 1992
(Contract DE-AC04-76DP-00789)
(DE92-011358; SAND-92-0193C; CONF-9203127-1) Avail: CASI HC A01/MF A01

Theoretical models have been formulated describing the dynamic behavior of the swelling and contracting of polyelectrolyte gels. This paper presents a method of weighted residuals approach to solving the governing system of equations by finite element analysis. The modulation of the imbibition of solvent by a spherical gel is studied. DOE

N92-30816# South Carolina Univ., Columbia. Dept. of Chemistry.
THERMOSET PRECURSOR TO MONOLITHIC CARBON GLASS PREPARED BY THE Pd/Cu-CATALYZED ALKYNYLATION OF POLYPHENYLENES
Eric B. Stephens and James M. Tour 25 Apr. 1992 8 p
(Contract N00014-89-J-3062)
(AD-A249920; TR-12) Avail: CASI HC A02/MF A01

The functionalization of (bromophenyl)oligophenylene with several alkynes is described. The bromide groups on the oligomer were replaced with terminal alkynes using a Pd/Cu catalyst system. Substitution of nearly all the original bromide locations was achieved. The functionalized oligomers, freely soluble in THF, exhibited high char yields on thermolysis to 900 C under a nitrogen atmosphere. Several of the functionalized oligomers flowed on heating. The oligomer that was functionalized with phenylacetylene exhibited a well-defined melting point at 190 C and acetylenic coupling did not take place until 310 C. The hot oligomer flowed to form a monolith of glassy carbon. Depending on the alkyne used, a range of densities from 1.39-1.95 g/cc could be obtained in the final carbon glass. The structure/property relationships and the material applications are discussed. GRA

N92-30817# South Carolina Univ., Columbia. Dept. of Chemistry.
ELECTROOXIDATION OF SOLUBLE ALPHA,ALPHA-COUPLED THIOPHENE OLIGOMERS
J. Guay, A. Diaz, R. Wu, J. M. Tour, and L. H. Dao 25 Apr. 1992 9 p
(Contract N00014-89-J-3062)
(AD-A249928; TR-10) Avail: CASI HC A02/MF A01

The electro-oxidation of alpha,alpha-coupled thiophene oligomers with terminal trimethylsilyl and P-methyl groups was studied in methylene chloride at room temperature. The oligomers with 4, 5, and 7 thiophene rings undergo two stepwise oxidations to produce the radical cation and dication, respectively, as confirmed by Vis/Nir esr spectra. The redox waves are chemically reversible and are well-separated (ca. 200 mV) in the cyclic voltammogram. It is suggested that the same electrochemical behavior should be observed with the next higher oligomers or in the n-conjugated segments of polythiophene. Thus the broad featureless voltammogram observed with films of polythiophene is not an inherent property of the polymer segments but may reflect complications from the solid state nature of the film. GRA

N92-30830# Sandia National Labs., Albuquerque, NM.
THERMALLY ACTIVATED REJUVENATION OF FERROELECTRIC PROPERTIES IN ELECTRICALLY FATIGUED LEAD ZIRCONATE TITANATE CERAMICS
W. Y. Pan (New Mexico Inst. of Mining and Technology, Socorro.), C. F. Yue (New Mexico Inst. of Mining and Technology, Socorro.), K. W. Lin (New Mexico Inst. of Mining and Technology, Socorro.), and B. A. Tuttle 1992 15 p Presented at the 25th Anniversary Meeting of the Dielectric Society with the 2nd European Conference on Applications of Polar Dielectrics and International Workshop on Integrated Ferroelectrics, London, England, 12-15 Apr. 1992
(Contract DE-AC04-76DP-00789)
(DE92-012634; SAND-92-0864C; CONF-920445-1) Avail: CASI HC A03/MF A01

Thermally activated rejuvenation of ferroelectric properties is investigated for modified lead zirconate titanate ferroelectric ceramics that have been electrically fatigued. The extent of rejuvenation for the ferroelectric polarization increases with both increasing temperature and increasing time of the post-fatigue thermal anneal. For an insufficient post-fatigue thermal anneal, the ferroelectric ceramic sample exhibits incomplete restoration of ferroelectric properties and an increased fatigue rate compared to the virgin sample. Complete rejuvenation of ferroelectric properties occurs when the fatigued ferroelectric ceramic is thermally annealed well above the ferroelectric-paraelectric phase transition temperature for many hours. The thermal rejuvenation of fatigue is explained by the thermally stimulated decoupling between the spontaneous polarization and either defects or space charge. DOE

N92-30838# Colorado State Univ., Fort Collins. Dept. of Chemistry.
INFRARED INVESTIGATIONS OF PRISTINE, DOPED AND PARTIALLY-DOPED POLYPYRROLE
J. Lei, W. Liang, and Charles R. Martin 8 May 1992 29 p
(Contract N00014-82-K-0612)
(AD-A250644) Avail: CASI HC A03/MF A01

It is well known that pristine (i.e. undoped) polypyrrole is not air-stable. As a result, it is difficult to obtain spectral data for the pristine polymer. Indeed, there are only two reports of infrared (IR) absorption spectra for the pristine material in the literature and, in both cases, the polymer seems to have undergone some air oxidation. It would be highly desirable to have reliable and reproducible IR spectra for the pristine form of this important polymer. We have designed a novel IR spectroelectrochemical cell which allows for electrochemical synthesis and IR and electrochemical analyses of thin polypyrrole films, while rigorously protecting these films from air. We present here IR spectra, obtained with this cell, for doped, partially doped and pristine polypyrrole. GRA

N92-30847# Los Alamos National Lab., NM.
THEORY OF SUBLINEAR POWER DEPENDENCE FOR MICROWAVE HEATING IN SOME CERAMIC MATERIALS
V. M. Kenkre (New Mexico Univ., Albuquerque.), M. Kus (New Mexico Univ., Albuquerque.), and J. D. Katz 1992 7 p Presented at the Material Research Society Spring Meeting, San Francisco, CA, 27 Apr. - 2 May 1992
(Contract W-7405-eng-36)
(DE92-015147; LA-UR-92-1558; CONF-920402-29) Avail: CASI HC A02/MF A01

A sublinear dependence of the microwave heating rate on the incident microwave power implying a saturation effect appears to have been observed recently. We present simple model calculations to address this observation on the basis of an idea of spatial confinement of the absorbing charges in grain boundary regions. Two natural lengths exist in this model: the spatial extent of the confining region, and the maximum distance an absorbing charge travels under the combined action of damping and of the oscillating microwave field. We suggest that a mismatch of these lengths results in the observed saturation, and more generally, in the observed decrease in absorption efficiency. DOE

N92-30857# Sandia National Labs., Albuquerque, NM.
COMPUTATIONAL SIMULATION OF DIAMOND CHEMICAL VAPOR DEPOSITION IN PREMIXED C2H2/O2/H2 AND CH4/O2 STRAINED FLAMES
E. Meeks (Sandia Labs., Livermore, CA.), R. J. Kee (Sandia Labs., Livermore, CA.), D. S. Dandy (Sandia Labs., Livermore, CA.), and M. E. Coltrin 1992 26 p Presented at the 1992 Spring Meeting of the Western States Section of the Combustion Institute, Corvallis, OR, 23-24 Mar. 1992
(Contract DE-AC04-76DR-00789)
(DE92-012144; SAND-92-8462C; WSS/CI-92-6; CONF-9203140-1) Avail: CASI HC A03/MF A01

We have modeled combustion synthesis of CVD diamond in a stagnation-flow reactor under atmospheric conditions. In this configuration a premixed flat flame flows over a flat deposition substrate that lies perpendicular to the flow and parallel to the burner face. Optimal growth conditions occur when the flame is lifted from the burner surface and stabilized at the deposition surface. A similarity transformation for the stagnation flow field reduces the governing equations to a one-dimensional boundary value problem, thus, significantly simplifying the computational task. The simulations include elementary gas-phase and surface chemistry as well as multicomponent molecular transport in the flame gas. Due to increased flame temperature and stability, the C2H2 flames produce much higher growth rates than the CH4 flames. DOE

N92-30866# Allied-Signal Aerospace Co., Kansas City, MO.
INTERFACE FRICTION, LUBRICANTS, AND THEIR INFLUENCE ON METAL FLOW
A. S. El-Gizawy (Missouri Univ., Columbia.) Mar. 1992 33 p
(Contract DE-AC04-76DP-00613)
(DE92-012112; KCP-613-4504) Avail: CASI HC A03/MF A01

In precision forging, interface friction between the workpiece and the die has a significant effect on material flow and the character of die filling. Hot forming lubricants differ dramatically in their ability to reduce friction and aid die filling depending on the temperature at which they are used and the material being forged. The ring compression test was used to evaluate a variety of lubricants at a number of temperatures. The test involves forging a flat ring. The change in internal diameter during reduction in ring height provides a sensitive measure of interface friction. FORTRAN programs were developed to predict the variation in the internal diameter of the rings with the percentage of height reduction for different friction factors. Friction factors estimated by evaluation of the exact energy balance equation were reported to be most accurate and were recommended as better than previously published calibration curves. DOE

N92-30873# Cornell Univ., Ithaca, NY.
APPROACHES TO POLYMER CURING AND IMAGING VIA THE IN SITU GENERATION OF A CATALYST
Jean M. Frechet 20 Apr. 1992 11 p
(Contract N00014-91-J-1338)
(AD-A249917; TR-9) Avail: CASI HC A03/MF A01

The in situ photogeneration of catalytic species such as acids, bases, or free radicals from soluble organic precursors can be used in polymer curing or in photoresist processes. Convenient photoprecursors of acids include iodonium and sulfonium salts as well as a large number of halogenated aromatic compounds, sulfonate esters, etc. The photogeneration of amine is possible from a variety of active carbamates, while hydroxide or alkoxide bases can be obtained by irradiation of hydrox or alkoxy derivatives of triphenylmethane. Specially designed polymers that include acid or base sensitive groups were prepared, mainly for use as imaging and resist materials for microlithography. For example a photosensitive polyimide can be formulated from a polyamic acid derivative and a photoprecursor of base. Of particular interest are systems that incorporate chemical amplification. In these systems the initial radiation induced process, photogeneration of the acid or base catalyst within the polymer film, is followed by a cascade of reactions affecting the polymer. Overall this leads to highly sensitive photopolymer formulations in which the effective quantum yield is many times higher than that of the original photoevent. GRA

N92-31141# Harvard Univ., Cambridge, MA. Dept. of Chemistry.
FROM MINERALS TO MATERIALS: A FACILE SYNTHETIC ROUTE TO PRECERAMIC POLYMERS FOR ALUMINUM OXIDE
Allen W. Apblett, Christopher C. Landry, Mark W. Mason, and Andrew R. Barron 12 May 1992 9 p
(Contract N00014-91-J-1934)
(AD-A250351) Avail: CASI HC A02/MF A01

Reaction of boehmite (Al(O)(OH))(n) with an excess of carboxylic acid (HO2CR) results in the formation of the carboxy substituted alumoxanes, (Al(O)(x)(OH)(y)(O2CR)(z))(n) where 2x + y + z = 3 and R = alkyl substituents. The alumoxanes were fully characterized by SEM, elemental analysis, IR, and multinuclear NMR spectroscopy. The physical properties of the alumoxanes are highly dependent on the identity of R, and range from insoluble crystalline powders, e.g. R = CH3, to powders which readily form solutions or gels in hydrocarbon solvents, e.g. R = C5H11. All of the alumoxanes decompose under mild thermolysis to yield gamma-alumina. GRA

N92-31146# EG and G Rocky Flats, Inc., Golden, CO.
A METHOD FOR REGENERATING ION EXCHANGE RESIN
Masahiro Ogihara, Kenichi Ichikawa, and Takeshi Idemizu Dec. 1991 9 p Transl. into ENGLISH of Japanese Patent No. HEI-3-154642 (2 Jul. 1991)
(Contract DE-AC34-90DP-62349)
(DE92-015312; RFP-Trans-525) Avail: CASI HC A02/MF A01

This invention is comprised of a method for regenerating ion exchange resin consisting of a mixed resin. The mixed resin contains a granular cation exchange resin and anion exchange resin contaminated during condensation treatment in steam power generating plants. The mixed resin is separated into cation exchange resin and anion exchange resin, and the separated cation exchange resin is regenerated by immersion in aqueous acidic

solution for more than 5 hours. It also consists of a method for regenerating ion exchange resin according to claim 1. The aqueous acidic solution is sulfuric acid, hydrochloric acid, or nitric acid solution. DOE

N92-31207# Colorado State Univ., Fort Collins. Dept. of Chemistry.
POLYPHOSPHAZENES BEARING POLYMERIZABLE PYRROLE, THIOPHENE AND FURAN SIDE GROUPS: SYNTHESIS AND CHEMICAL OXIDATION
Harry R. Allcock, Jeffrey A. Dodge, Leon S. VanDyke, and Charles R. Martin 30 Apr. 1992 56 p
(Contract N00014-82-K-0612)
(AD-A249747; CSU-TR-68) Avail: CASI HC A04/MF A01

The synthesis and chemical oxidation of linear poly(organophosphazenes) that bear polymerizable, heterocyclic side groups is described. The polymers were prepared for use as precursors to electronically conductive materials. GRA

N92-30264*# Oak Ridge National Lab., TN.
STRUCTURAL CERAMICS
Douglas F. Craig *In* NASA. Langley Research Center, National Educators' Workshop: Update 1991. Standard Experiments in Engineering Materials Science and Technology Jun. 1992 p 3-43 (For primary document see N92-30263 21-29)
Avail: CASI HC A03/MF A03

N92-30265*# Battelle Pacific Northwest Labs., Richland, WA.
TEMPERED GLASS AND THERMAL SHOCK OF CERAMIC MATERIALS
L. Roy Bunnell *In* NASA. Langley Research Center, National Educators' Workshop: Update 1991. Standard Experiments in Engineering Materials Science and Technology Jun. 1992 p 45-53 (For primary document see N92-30263 21-29)
(Contract DE-AC06-76RL-01830)
Avail: CASI HC A02/MF A03

N92-30267*# New Mexico Univ., Albuquerque. Dept. of Mechanical Engineering.
CERAMIC PROCESSING: EXPERIMENTAL DESIGN AND OPTIMIZATION
Martin W. Weiser, David N. Lauben, and Philip Madrid *In* NASA. Langley Research Center, National Educators' Workshop: Update 1991. Standard Experiments in Engineering Materials Science and Technology Jun. 1992 p 67-95 (For primary document see N92-30263 21-29)
Avail: CASI HC A03/MF A03

N92-30279*# College of Western New England, Springfield, MA.
DETERMINING SIGNIFICANT MATERIAL PROPERTIES: A DISCOVERY APPROACH
Alan K. Karplus *In* NASA. Langley Research Center, National Educators' Workshop: Update 1991. Standard Experiments in Engineering Materials Science and Technology Jun. 1992 p 223-231 (For primary document see N92-30263 21-29)
Avail: CASI HC A02/MF A03

N92-30285*# Northeastern Univ., Boston, MA. School of Engineering Technology.
STRESS-STRAIN CHARACTERISTICS OF RUBBER-LIKE MATERIALS: EXPERIMENT AND ANALYSIS
David J. Allen *In* NASA. Langley Research Center, National Educators' Workshop: Update 1991. Standard Experiments in Engineering Materials Science and Technology Jun. 1992 p 301-305 (For primary document see N92-30263 21-29)
Avail: CASI HC A01/MF A03

28 PROPELLANTS AND FUELS

Includes rocket propellants, igniters, and oxidizers; their storage and handling procedures; and aircraft fuels.

For related information see also *07 Aircraft Propulsion and Power, 20 Spacecraft Propulsion and Power,* and *44 Energy Production and Conversion.*

N92-30321# Naval Air Development Center, Warminster, PA. Air Vehicle and Crew Systems Technology Dept.
IN-SERVICE EVALUATION OF 2090 ALUMINUM-LITHIUM ALLOY ON F/A-18 AIRCRAFT Interim Report, Feb. 1988 - Jun. 1991
J. Kozol, E. S. Tankins, J. J. Thompson, and C. E. Neu 1 Aug. 1991 31 p
(AD-A248472; NADC-91078-60) Avail: CASI HC A03/MF A01

Al-Li alloys can provide reduced weight and increased stiffness as replacements for conventional aluminum alloy aircraft components. A study was conducted to compare the performance of 2090 Al-Li and 7075 Al alloys in-service on Navy aircraft, during shipboard exposure and in laboratory accelerated tests. Results from this investigation indicated that no additional maintenance was required during in-service exposure and that the corrosion behavior of the two alloys in laboratory tests and during shipboard exposure was comparable. GRA

N92-30341# Coordinating Research Council, Inc., Atlanta, GA.
EFFECT OF VOLATILITY AND OXYGENATES ON DRIVEABILITY AT INTERMEDIATE AMBIENT TEMPERATURES
Mar. 1992 140 p
(AD-A248902; CRC-578) Avail: CASI HC A07/MF A02

Recent regulations reduce summertime fuel front-end volatility by limiting fuel Reid vapor pressure (RVP) to values considerably less than past commercial practices. There has been some concern that such reduced-RVP fuels may lead to degraded driveability, especially in areas with long distribution lead times and low tank turnover rates. In those areas, significant volumes of these fuels may be sold in cool spring weather in order to ensure that the RVP regulations are met at the start of the summer control period. The 1989 CRC driveability program investigated the independent effects of front-end volatility and mid-range volatility on cold-start and warmup driveability of late model vehicles at intermediate ambient temperatures. Front-end volatility was measured by RVP, and mid-range volatility was measured by the temperature at which 50 percent of the fuel is evaporated (T50). Volatility ranges investigated were those that may be required of future summertime fuels. GRA

N92-30767# Southwest Research Inst., San Antonio, TX.
LASER INDUCED FLUORESCENCE DETECTION OF GUMS IN JET FUELS Final Report, Jul. 1990 - May 1992
David W. Naegeli and Ralph H. Hill May 1992 59 p
(Contract F33615-90-C-2050)
(AD-A252685; SWRI-03-3685; WL-TR-92-2015) Avail: CASI HC A04/MF A01

The current method (ASTM D381) of determining the concentration of gums in jet fuels is a lengthy procedure requiring a large sample size. Because gum formation is believed to be an important step in the formation of deposits in fuel systems used in jet aircraft, a non-intrusive method of performing spatially resolved measurements of gum concentration in high temperature flow systems is a desired research tool. The present study was conducted to determine the feasibility of using laser-induced fluorescence (LIF) to monitor gum concentration in jet fuel. The study revealed several effects, such as aging and the interference of other fluorophores with gum fluorescence, which require further investigation before LIF is to be considered a quantitative technique for measuring gums in jet fuels. However, this study showed that the formation of gums in jet fuels is detectable by LIF. The results show that gum formation in some fuels correlates strongly with LIF while for other fuels the results are ambiguous. GRA

N92-30904# Pittsburgh Univ., PA. Dept. of Chemical and Petroleum Engineering.
A NOVEL PROCESS FOR METHANOL SYNTHESIS
J. W. Tierney and I. Wender 1992 11 p
(Contract DE-FG22-89PC-89786)
(DE92-015798; DOE/PC-89786/T12) Avail: CASI HC A03/MF A01

A bench-scale reactor is being used to study the conversion of synthesis gas to methanol (MeOH) by a novel process. In previous reports, we provided evidence that the reaction takes place in two steps. A molecule of MeOH is first carbonylated to form methyl formate (MeF) which then reacts with H2 to form two molecules of MeOH. The second reaction occurs on the surface of a heterogeneous catalyst such as copper chromite, while the first reaction requires a homogenous catalyst such as potassium methoxide (KOMe) and takes place in a non-equilibrium region in the vicinity of the heterogeneous catalyst. A synergism between the two catalysts enhances the rate of MeOH formation. In this quarter, we studied the effect of reaction conditions on the rate of formation of MeF and the effect of CO2 concentration in the feed gas on the rate of MeOH synthesis. Kinetic studies were also initiated and rate expressions were examined. DOE

N92-31202# Los Alamos National Lab., NM.
MODELING INITIATION OF EXPLOSIVES BY PROJECTILE IMPACT
R. J. Yactor 1992 15 p Presented at the 18th International Pyrotechnics Seminar, Breckenridge, CO, 13-17 Jul. 1992
(Contract W-7405-eng-36)
(DE92-015210; LA-UR-92-1476; CONF-920796-5) Avail: CASI HC A03/MF A01

A shock initiation model was developed for the initiation of bare or clad explosives impacted by flat or hemispherical-tipped projectiles. The model requires Hugoniot data for the unreacted explosive, cladding material and projectile material, and the shock run distance to detonation as function of the shock pressure imparted to the explosive. Model results are compared to experimental data for flat and hemispherical-tipped steel projectiles impacting bare and clad PBX 9404 explosive. DOE

29 MATERIALS PROCESSING

Includes space-based development of products and processes for commercial applications.
For biological materials see *55 Space Biology.*

N92-30263*# National Aeronautics and Space Administration. Langley Research Center, Hampton, VA.
NATIONAL EDUCATORS' WORKSHOP: UPDATE 1991. STANDARD EXPERIMENTS IN ENGINEERING MATERIALS SCIENCE AND TECHNOLOGY
James E. Gardner, comp., James A. Jacobs, comp. (Norfolk State Univ., VA.), and James O. Stiegler, comp. (Oak Ridge National Lab., TN.) Washington Jun. 1992 369 p Workshop held in Oak Ridge, TN, 12-14 Nov. 1991; sponsored by NASA, DOE, Norfolk State Univ., and NIST
(RTOP 505-63-50-01)
(NASA-CP-3151; L-17099; NAS 1.55:3151) Avail: CASI HC A16/MF A03

Given here is a collection of experiments presented and demonstrated at the National Educators' Workshop: Update 91, held at the Oak Ridge National Laboratory on November 12-14, 1991. The experiments related to the nature and properties of engineering materials and provided information to assist in teaching about materials in the education community. For individual titles, see N92-30264 through N92-30294.

N92-30264*# Oak Ridge National Lab., TN.
STRUCTURAL CERAMICS **c27**
Douglas F. Craig *In* NASA. Langley Research Center, National Educators' Workshop: Update 1991. Standard Experiments in Engineering Materials Science and Technology Jun. 1992 p 3-43 (For primary document see N92-30263 21-29)
Avail: CASI HC A03/MF A03

This presentation gives a brief history of the field of materials sciences and goes on to expound the advantages of the fastest growing area in that field, namely ceramics. Since ceramics are moving to fill the demand for lighter, stronger, more corrosion resistant materials, advancements will rely more on processing and modeling from the atomic scale up which is made possible by advanced analytical, computer, and processing techniques. All information is presented in viewgraph format. H.A.

N92-30265*# Battelle Pacific Northwest Labs., Richland, WA.
TEMPERED GLASS AND THERMAL SHOCK OF CERAMIC MATERIALS **c27**
L. Roy Bunnell *In* NASA. Langley Research Center, National Educators' Workshop: Update 1991. Standard Experiments in Engineering Materials Science and Technology Jun. 1992 p 45-53 (For primary document see N92-30263 21-29)
(Contract DE-AC06-76RL-01830)
Avail: CASI HC A02/MF A03

A laboratory experiment is described that shows students the different strengths and fracture toughnesses between tempered and untempered glass. This paper also describes how glass is tempered and the materials science aspects of the process. H.A.

N92-30266*# Purdue Univ., West Lafayette, IN. Dept. of Mechanical Engineering Technology.
ELEMENTARY METALLOGRAPHY **c26**
Sayyed M. Kazem *In* NASA. Langley Research Center, National Educators' Workshop: Update 1991. Standard Experiments in Engineering Materials Science and Technology Jun. 1992 p 57-64 (For primary document see N92-30263 21-29)
Avail: CASI HC A02/MF A03

Materials and Processes 1 (MET 141) is offered to freshmen by the Mechanical Engineering Department at Purdue University. The goal of MET 141 is to broaden the technical background of students who have not had any college science courses. Hence, applied physics, chemistry, and mathematics are included and quantitative problem solving is involved. In the elementary metallography experiment of this course, the objectives are: (1) introduce the vocabulary and establish outlook; (2) make qualitative observations and quantitative measurements; (3) demonstrate the proper use of equipment; and (4) review basic mathematics and science. H.A.

N92-30267*# New Mexico Univ., Albuquerque. Dept. of Mechanical Engineering.
CERAMIC PROCESSING: EXPERIMENTAL DESIGN AND OPTIMIZATION **c27**
Martin W. Weiser, David N. Lauben, and Philip Madrid *In* NASA. Langley Research Center, National Educators' Workshop: Update 1991. Standard Experiments in Engineering Materials Science and Technology Jun. 1992 p 67-95 (For primary document see N92-30263 21-29)
Avail: CASI HC A03/MF A03

The objectives of this paper are to: (1) gain insight into the processing of ceramics and how green processing can affect the properties of ceramics; (2) investigate the technique of slip casting; (3) learn how heat treatment and temperature contribute to density, strength, and effects of under and over firing to ceramic properties; (4) experience some of the problems inherent in testing brittle materials and learn about the statistical nature of the strength of ceramics; (5) investigate orthogonal arrays as tools to examine the effect of many experimental parameters using a minimum number of experiments; (6) recognize appropriate uses for clay based ceramics; and (7) measure several different properties important to ceramic use and optimize them for a given application. H.A.

N92-30268*# University of the Pacific, Stockton, CA.
IMPACT TESTING OF WELDED SAMPLES **c39**

Calvin D. Lundeen *In* NASA. Langley Research Center, National Educators' Workshop: Update 1991. Standard Experiments in Engineering Materials Science and Technology Jun. 1992 p 99-102 (For primary document see N92-30263 21-29)
Avail: CASI HC A01/MF A03

The objective of this paper is to demonstrate how welding practice and joint design affect the performance of the joint. Also demonstrated is the importance of weld inspection to ensure quality welds. H.A.

N92-30269*# Youngstown State Univ., OH. Dept. of Materials Engineering.
Cu-Zn BINARY PHASE DIAGRAM AND DIFFUSION COUPLES c26

Robert A. McCoy *In* NASA. Langley Research Center, National Educators' Workshop: Update 1991. Standard Experiments in Engineering Materials Science and Technology Jun. 1992 p 111-118 (For primary document see N92-30263 21-29)
Avail: CASI HC A02/MF A03

The objectives of this paper are to learn: (1) what information a binary phase diagram can yield; (2) how to construct and heat treat a simple diffusion couple; (3) how to prepare a metallographic sample; (4) how to operate a metallograph; (5) how to correlate phases found in the diffusion couple with phases predicted by the phase diagram; (6) how diffusion couples held at various temperatures could be used to construct a phase diagram; (7) the relation between the thickness of an intermetallic phase layer and the diffusion time; and (8) the effect of one species of atoms diffusing faster than another species in a diffusion couple. H.A.

N92-30270*# Idaho Univ., Moscow. Dept. of Forest Products.
DESIGNING, ENGINEERING, AND TESTING WOOD STRUCTURES c24

Thomas M. Gorman *In* NASA. Langley Research Center, National Educators' Workshop: Update 1991. Standard Experiments in Engineering Materials Science and Technology Jun. 1992 p 121-128 (For primary document see N92-30263 21-29)
Avail: CASI HC A02/MF A03

The objective of this paper is to introduce basic structural engineering concepts in a clear, simple manner while actively involving students. This project emphasizes the fact that a good design uses materials efficiently. The test structure in this experiment can easily be built and has various design options. Even when the structure is loaded to collapsing, only one or two pieces usually break, leaving the remaining pieces intact and reusable. H.A.

N92-30271*# Texas A&M Univ., College Station. Dept. of Mechanical Engineering.
COMPUTER VISION IN MICROSTRUCTURAL ANALYSIS c61

Malur N. Srinivasan, W. Massarweh, and C. L. Hough *In* NASA. Langley Research Center, National Educators' Workshop: Update 1991. Standard Experiments in Engineering Materials Science and Technology Jun. 1992 p 131-139 (For primary document see N92-30263 21-29)
Avail: CASI HC A02/MF A03

The following is a laboratory experiment designed to be performed by advanced-high school and beginning-college students. It is hoped that this experiment will create an interest in and further understanding of materials science. The objective of this experiment is to demonstrate that the microstructure of engineered materials is affected by the processing conditions in manufacture, and that it is possible to characterize the microstructure using image analysis with a computer. The principle of computer vision will first be introduced followed by the description of the system developed at Texas A&M University. This in turn will be followed by the description of the experiment to obtain differences in microstructure and the characterization of the microstructure using computer vision. D.R.D.

N92-30272*# Intermet Technology, Georgetown, PA.
EXPERIMENTS WITH THE LOW MELTING INDIUM-BISMUTH ALLOY SYSTEM c26

Richard P. Krepski *In* NASA. Langley Research Center, National Educators' Workshop: Update 1991. Standard Experiments in Engineering Materials Science and Technology Jun. 1992 p 143-147 Sponsored in part by NSF Prepared in cooperation with Geneva Coll., Beaver Falls, PA (For primary document see N92-30263 21-29)
Copyright Avail: CASI HC A01/MF A03

The following is a laboratory experiment designed to create an interest in and to further understanding of materials science. The primary audience for this material is the junior high school or middle school science student having no previous familiarity with the material, other than some knowledge of temperature and the concepts of atoms, elements, compounds, and chemical reactions. The objective of the experiment is to investigate the indium-bismuth alloy system. Near the eutectic composition, the liquidus is well below the boiling point of water, allowing simple, minimal hazard casting experiments. Such phenomena as metal oxidation, formation of intermetallic compound crystals, and an unusual volume increase during solidification could all be directly observed. A key concept for students to absorb is that properties of an alloy (melting point, mechanical behavior) may not correlate with simple interpolation of properties of the pure components. Discussion of other low melting metals and alloys leads to consideration of environmental and toxicity issues, as well as providing some historical context. Wetting behavior can also be explored. D.R.D.

N92-30273*# Ball State Univ., Muncie, IN. Dept. of Industry and Technology.
A SENIOR MANUFACTURING LABORATORY FOR DETERMINING INJECTION MOLDING PROCESS CAPABILITY c31

Jerry L. Wickman and David Plocinski *In* NASA. Langley Research Center, National Educators' Workshop: Update 1991. Standard Experiments in Engineering Materials Science and Technology Jun. 1992 p 151-158 (For primary document see N92-30263 21-29)
Avail: CASI HC A02/MF A03

The following is a laboratory experiment designed to further understanding of materials science. This subject material is directed at an upper level undergraduate/graduate student in an Engineering or Engineering Technology program. It is assumed that the student has a thorough understanding of the process and quality control. The format of this laboratory does not follow that which is normally recommended because of the nature of process capability and that of the injection molding equipment and tooling. This laboratory is instead developed to be used as a point of departure for determining process capability for any process in either a quality control laboratory or a manufacturing environment where control charts, process capability, and experimental or product design are considered important topics. Author

N92-30274*# Arizona State Univ., Tempe. Dept. of Manufacturing and Industrial Technology.
LABORATORY EXPERIMENTS FROM THE TOY STORE c39

H. T. McClelland *In* NASA. Langley Research Center, National Educators' Workshop: Update 1991. Standard Experiments in Engineering Materials Science and Technology Jun. 1992 p 161-168 (For primary document see N92-30263 21-29)
Avail: CASI HC A02/MF A03

The following is a laboratory experiment designed to further understanding of materials science. This material could be taught to a typical student of materials science or manufacturing at the high school level or above. The objectives of this experiment are as follows: (1) to qualitatively demonstrate the concepts of elasticity, plasticity, and the strain rate and temperature dependence of the mechanical properties of engineering materials; (2) to qualitatively demonstrate the basics of extrusion including material flow, strain rate dependence of defects, lubrication effects, and the making of hollow shapes by extrusion (the two parts may be two separate experiments done at different times when the respective subjects are covered); and (3) to demonstrate the importance of qualitative

observations and the amount of information which can be gathered without quantitative measurements. D.R.D.

N92-30275*# State Univ. of Southeast Missouri, Cape Girardeau. Dept. of Physics.

DIELECTRIC BEHAVIOR OF SEMICONDUCTORS AT MICROWAVE FREQUENCIES **c33**

Jai N. Dahiya *In* NASA. Langley Research Center, National Educators' Workshop: Update 1991. Standard Experiments in Engineering Materials Science and Technology Jun. 1992 p 171-185 (For primary document see N92-30263 21-29)
Avail: CASI HC A03/MF A03

A cylindrical microwave resonant cavity in TE(011) (Transverse Electric) mode is used to study the dielectric relaxation in germanium and silicon. The samples of these semiconductors are used to perturb the electric field in the cavity, and Slater's perturbation equations are used to calculate the real and imaginary parts of the dielectric constant. The dielectric loss of germanium and silicon is studied at different temperatures, and Debye's equations are used to calculate the relaxation time at these temperatures. Author

N92-30276*# Ohio Northern Univ., Ada. Dept. of Mechanical Engineering.

Be-Cu PRECIPITATION HARDENING EXPERIMENT **c26**

Richard L. Cowan *In* NASA. Langley Research Center, National Educators' Workshop: Update 1991. Standard Experiments in Engineering Materials Science and Technology Jun. 1992 p 189-193 (For primary document see N92-30263 21-29)
Avail: CASI HC A01/MF A03

The following is a laboratory experiment designed to further a student's understanding of materials science. The student performing this experiment should have a knowledge of binary phase diagrams. The objectives of this experiment are as follows: (1) to give the student a hands-on approach to changing materials properties through heat treatment of a specimen; (2) to quantify the amount of strengthening obtained in the specimen; and (3) to encourage the student to speculate about the structural changes that have occurred in the material to cause the changes in strength. D.R.D.

N92-30277*# Oak Ridge National Lab., TN. Committee on Terminology.

STANDARD TERMINOLOGY IN THE LABORATORY AND CLASSROOM **c82**

Richard A. Strehlow *In* NASA. Langley Research Center, National Educators' Workshop: Update 1991. Standard Experiments in Engineering Materials Science and Technology Jun. 1992 p 197-210 (For primary document see N92-30263 21-29)
(Contract DE-AC05-84OR-21400)
Avail: CASI HC A03/MF A03

Each of the materials produced by modern technologists is associated with a family of immaterials--all the concepts of substance, process, and purpose. It is concepts that are essential to transfer knowledge. It is concepts that are the stuff of terminology. Terminology is standardized today by companies, standards organizations, governments, and other groups. Simply described, it is the pre-negotiation of the meanings of terms. Terminology has become a key issue in businesses, and terminology knowledge is essential in understanding the modern world. The following is a introductory workshop discussing the concepts of terminology and methods of its standardization. Author

N92-30278*# Oak Ridge National Lab., TN. Metals and Ceramics Div.

SCIENCE IN ACTION: AN INTERDISCIPLINARY SCIENCE EDUCATION PROGRAM **c80**

Linda L. Horton *In* NASA. Langley Research Center, National Educators' Workshop: Update 1991. Standard Experiments in Engineering Materials Science and Technology Jun. 1992 p 213-216 (For primary document see N92-30263 21-29)
(Contract DE-AC05-84OR-21400)
Avail: CASI HC A01/MF A03

Science in Action is an education outreach program for pre-collegiate students. It is based on the concept that, in order to interest students in science, they must see science and scientists at work. The program encompasses the full range of scientific disciplines - the core sciences, engineering, and mathematics. A unique aspect of the program is the involvement and support of scientists and engineers representing local professional societies, industries, business, and academic institutions. An outline of the program is given. Author

N92-30279*# College of Western New England, Springfield, MA.

DETERMINING SIGNIFICANT MATERIAL PROPERTIES: A DISCOVERY APPROACH **c27**

Alan K. Karplus *In* NASA. Langley Research Center, National Educators' Workshop: Update 1991. Standard Experiments in Engineering Materials Science and Technology Jun. 1992 p 223-231 (For primary document see N92-30263 21-29)
Avail: CASI HC A02/MF A03

The following is a laboratory experiment designed to further understanding of materials science. The experiment itself can be informative for persons of any age past elementary school, and even for some in elementary school. The preparation of the plastic samples is readily accomplished by persons with resonable dexterity in the cutting of paper designs. The completion of the statistical Design of Experiments, which uses Yates' Method, requires basic math (addition and subtraction). Interpretive work requires plotting of data and making observations. Knowledge of statistical methods would be helpful. The purpose of this experiment is to acquaint students with the seven classes of recyclable plastics, and provide hands-on learning about the response of these plastics to mechanical tensile loading. Author

N92-30280*# North Carolina Agricultural and Technical State Univ., Greensboro. Dept. of Manufacturing Systems.

MECHANISM OF SLIP AND TWINNING **c76**

Mansur Rastani *In* NASA. Langley Research Center, National Educators' Workshop: Update 1991. Standard Experiments in Engineering Materials Science and Technology Jun. 1992 p 235-243 (For primary document see N92-30263 21-29)
Avail: CASI HC A02/MF A03

The objectives are to: (1) demonstrate the mechanisms of deformation in body centered cubic (BCC), face centered cubic (FCC), and hexagonal close-packed (HCP)-structure metals and alloys and in some ceramics as well; (2) examine the deformed microstructures (slip lines and twin boundaries) in different grains of metallic and ceramic specimens; and (3) study visually the deformed macrostructure (slip and twin bands) of metals and alloys. Some of the topics covered include: deformation behavior of materials, mechanisms of plastic deformation, slip bands, twin bands, ductile failure, intergranular fracture, shear failure, slip planes, crystal deformation, and dislocations in ceramics. Author

N92-30281*# Oak Ridge National Lab., TN. Metals and Ceramics Div.

THE MICROSCOPIC WORLD: A DEMONSTRATION OF ELECTRON MICROSCOPY FOR YOUNGER STUDENTS **c80**

Linda L. Horton *In* NASA. Langley Research Center, National Educators' Workshop: Update 1991. Standard Experiments in Engineering Materials Science and Technology Jun. 1992 p 247-249 (For primary document see N92-30263 21-29)
(Contract DE-AC05-84OR-21400)
Avail: CASI HC A01/MF A03

The purpose is to excite students about the importance of scientific investigation and demonstrate why they should look at things in greater detail, extending beyond superficial examination. The topics covered include: microscopy, scanning electron microscopes, high magnification, and the scientific method. Author

N92-30282*# Loyola Coll., Baltimore, MD. Dept. of Electrical Engineering and Engineering Science.
AN AUTOMATED SYSTEM FOR CREEP TESTING c39
F. Xavier Spiegel and Bernard J. Weigman *In* NASA. Langley Research Center, National Educators' Workshop: Update 1991. Standard Experiments in Engineering Materials Science and Technology Jun. 1992 p 253-262 (For primary document see N92-30263 21-29)
Avail: CASI HC A02/MF A03

A completely automated data collection system was devised to measure, analyze, and graph creep versus time using a PC, a 16 channel multiplexed analog to digital converter, and low friction potentiometers to measure length. The sampling rate for each experiment can be adjusted in the software to meet the needs of the material tested. Data is collected and stored on a diskette for permanent record and also for later data analysis on a different machine. Author

N92-30283*# Loyola Coll., Baltimore, MD.
FIVE EXPERIMENTS IN MATERIALS SCIENCE FOR LESS THAN $10.00 c39
F. Xavier Spiegel *In* NASA. Langley Research Center, National Educators' Workshop: Update 1991. Standard Experiments in Engineering Materials Science and Technology Jun. 1992 p 263-266 (For primary document see N92-30263 21-29)
Avail: CASI HC A01/MF A03

Diffusion, twinning, fatigue, acoustic emission, and aging can be studied using readily available materials and the household oven. Each experiment can be expanded to a more extensive investigation of the properties of the material investigated, as well as other materials, and offers an opportunity for the student to learn about the relationship between engineering, science, society, and politics. Author

N92-30284*# Purdue Univ., West Lafayette, IN. School of Technology.
ISOTROPIC THIN-WALLED PRESSURE VESSEL EXPERIMENT c39
Nancy L. Denton and Vernon S. Hillsman *In* NASA. Langley Research Center, National Educators' Workshop: Update 1991. Standard Experiments in Engineering Materials Science and Technology Jun. 1992 p 291-298 (For primary document see N92-30263 21-29)
Avail: CASI HC A02/MF A03

The objectives are: (1) to investigate the stress and strain distributions on the surface of a thin walled cylinder subject to internal pressure and/or axial load; and (2) to relate stress and strain distributions to material properties and cylinder geometry. The experiment, supplies, and procedure are presented. Author

N92-30285*# Northeastern Univ., Boston, MA. School of Engineering Technology.
STRESS-STRAIN CHARACTERISTICS OF RUBBER-LIKE MATERIALS: EXPERIMENT AND ANALYSIS c27
David J. Allen *In* NASA. Langley Research Center, National Educators' Workshop: Update 1991. Standard Experiments in Engineering Materials Science and Technology Jun. 1992 p 301-305 (For primary document see N92-30263 21-29)
Avail: CASI HC A01/MF A03

The objectives are: (1) to demonstrate tensile testing of materials and the application of the concepts of stress and strain; and (2) to yield a mathematical relationship between stress and strain for many artificial rubbers and plastics. The experiment, supplies, and procedure are presented. Author

N92-30286*# Iowa State Univ. of Science and Technology, Ames. Dept. of Materials Science and Engineering.
DEMONSTRATION OF MAGNETIC DOMAIN BOUNDARY MOVEMENT USING AN EASILY ASSEMBLED VIDEOCAM-MICROSCOPE SYSTEM c70
John W. Patterson *In* NASA. Langley Research Center, National Educators' Workshop: Update 1991. Standard Experiments in Engineering Materials Science and Technology Jun. 1992 p 309-312 (For primary document see N92-30263 21-29)
Avail: CASI HC A01/MF A03

The objectives are to build and demonstrate a low cost and highly flexible TV microscope facility and then use it to view the motion of magnetic domain boundaries as the local magnetic field is varied. The expense of an optical microscope and the videocam adapters sold for them is largely avoided by using the facility described below. The equipment, supplies, and procedure are presented. Author

N92-30287*# East Carolina Univ., Greenville, NC. Dept. of Construction Management.
AN EXPERIMENT ON THE USE OF DISPOSABLE PLASTICS AS A REINFORCEMENT IN CONCRETE BEAMS c24
Mostafiz R. Chowdhury *In* NASA. Langley Research Center, National Educators' Workshop: Update 1991. Standard Experiments in Engineering Materials Science and Technology Jun. 1992 p 315-327 (For primary document see N92-30263 21-29)
Avail: CASI HC A03/MF A03

Illustrated here is the concept of reinforced concrete structures by the use of computer simulation and an inexpensive hands-on design experiment. The students in our construction management program use disposable plastic as a reinforcement to demonstrate their understanding of reinforced concrete and prestressed concrete beams. The plastics used for such an experiment vary from plastic bottles to steel reinforced auto tires. This experiment will show the extent to which plastic reinforcement increases the strength of a concrete beam. The procedure of using such throw-away plastics in an experiment to explain the interaction between the reinforcement material and concrete, and a comparison of the test results for using different types of waste plastics are discussed. A computer analysis to simulate the structural response is used to compare the test results and to understand the analytical background of reinforced concrete design. This interaction of using computers to analyze structures and to relate the output results with real experimentation is found to be a very useful method for teaching a math-based analytical subject to our non-engineering students. Author

N92-30288*# Maryland Univ., College Park. Materials and Nuclear Engineering Unit.
STRUCTURE, PROCESSING, AND PROPERTIES OF POTATOES c77
Isabel K. Lloyd, Kimberly R. Kolos, Edmond C. Menegaux, Huy Luo, Richard H. McCuen, and Thomas M. Regan *In* NASA. Langley Research Center, National Educators' Workshop: Update 1991. Standard Experiments in Engineering Materials Science and Technology Jun. 1992 p 331-359 Sponsored in part by NSF (For primary document see N92-30263 21-29)
Avail: CASI HC A03/MF A03

The objective of this experiment and lesson intended for high school students in an engineering or materials science course or college freshmen is to demonstrate the relation between processing, structure, and thermodynamic and physical properties. The specific objectives are to show the effect of structure and structural changes on thermodynamic properties (specific heat) and physical properties (compressive strength); to illustrate the first law of thermodynamics; to compare boiling a potato in water with cooking it in a microwave in terms of the rate of structural change and the energy consumed to 'process' the potato; and to demonstrate compression testing. Author

N92-30289*# Ventura Coll., CA. Dept. of Engineering.
COMPUTER INTEGRATED LABORATORY TESTING c61
Charles C. Dahl *In* NASA. Langley Research Center, National Educators' Workshop: Update 1991. Standard Experiments in Engineering Materials Science and Technology Jun. 1992 p 363-365 (For primary document see N92-30263 21-29)
Avail: CASI HC A01/MF A03

The objective is the integration of computers into the Engineering Materials Science Laboratory course, where existing test equipment is not computerized. The first lab procedure is to

demonstrate and produce a material phase change curve. The second procedure is a demonstration of the modulus of elasticity and related stress-strain curve, plastic performance, maximum and failure strength. The process of recording data by sensors that are connected to a data logger which adds a time base, and the data logger in turn connected to a computer, places the materials labs into a computer integrated mode with minimum expense and maximum flexibility. The sensor signals are input into a spread sheet for tabular records, curve generation, and graph printing. Author

N92-30290*# Texas A&M Univ., College Station. Dept. of Mechanical Engineering.
MECHANICAL PROPERTIES OF BRITTLE MATERIALS c39
L. R. Cornwell and H. R. Thornton *In* NASA. Langley Research Center, National Educators' Workshop: Update 1991. Standard Experiments in Engineering Materials Science and Technology Jun. 1992 p 369-373 (For primary document see N92-30263 21-29)
Avail: CASI HC A01/MF A03

Brittle materials are difficult to tensile test because of gripping problems. They either crack in conventional grips or they are crushed. Furthermore, they may be difficult to make into tensile specimens having, for example, threated ends or donut shapes. To overcome the problem, simple rectangular shapes can be used in bending (i.e., a simple beam) in order to obtain the modulus of rupture and the elastic modulus. The equipment necessary consists of a fixture for supporting the specimens horizontally at two points, these points contact points being rollers which are free to rotate. The force necessary to bend the specimen is produced by a tup attached to the crosshead of an Instron machine. Here, the experimental procedure is explained. Author

N92-30291*# Purdue Univ., West Lafayette, IN. Dept. of Mechanical Engineering Technology.
INTRODUCTORY HEAT-TRANSFER c26
Edward L. Widener *In* NASA. Langley Research Center, National Educators' Workshop: Update 1991. Standard Experiments in Engineering Materials Science and Technology Jun. 1992 p 377-382 (For primary document see N92-30263 21-29)
Avail: CASI HC A02/MF A03

The objective is to introduce some concepts of thermodynamics in existing heat-treating experiments using available items. The specific objectives are to define the thermal properties of materials and to visualize expansivity, conductivity, heat capacity, and the melting point of common metals. The experimental procedures are described. Author

N92-30292*# Purdue Univ., West Lafayette, IN. Dept. of Mechanical Engineering Technology.
HEAT-TREATING OF MATERIALS c26
Edward L. Widener *In* NASA. Langley Research Center, National Educators' Workshop: Update 1991. Standard Experiments in Engineering Materials Science and Technology Jun. 1992 p 383-387 (For primary document see N92-30263 21-29)
Avail: CASI HC A01/MF A03

The objective was to introduce those solid state transformations of material structures known as 'heat treatments' and to emphasize the commercial importance of common processes for metals as well as non-metals. Experimental procedures are explained for annealing, quenching, hardening, and temper. Author

N92-30293*# Brigham Young Univ., Provo, UT. Dept. of Manufacturing Engineering and Engineering Technology.
MEASURING THE SURFACE TENSION OF SOAP BUBBLES c34
Carl D. Sorensen *In* NASA. Langley Research Center, National Educators' Workshop: Update 1991. Standard Experiments in Engineering Materials Science and Technology Jun. 1992 p 391-395 (For primary document see N92-30263 21-29)
Avail: CASI HC A01/MF A03

The objectives are for students to gain an understanding of surface tension, to see that pressure inside a small bubble is larger than that inside a large bubble. These concepts can be used to explain the behavior of liquid foams as well as precipitate coarsening and grain growth. Equipment, supplies, and procedures are explained. Author

N92-30294*# Brigham Young Univ., Provo, UT. Dept. of Manufacturing Engineering and Engineering Technology.
MEASURING THE WEIBULL MODULUS OF MICROSCOPE SLIDES c39
Carl D. Sorensen *In* NASA. Langley Research Center, National Educators' Workshop: Update 1991. Standard Experiments in Engineering Materials Science and Technology Jun. 1992 p 397-406 (For primary document see N92-30263 21-29)
Avail: CASI HC A02/MF A03

The objectives are that students will understand why a three-point bending test is used for ceramic specimens, learn how Weibull statistics are used to measure the strength of brittle materials, and appreciate the amount of variation in the strength of brittle materials with low Weibull modulus. They will understand how the modulus of rupture is used to represent the strength of specimens in a three-point bend test. In addition, students will learn that a logarithmic transformation can be used to convert an exponent into the slope of a straight line. The experimental procedures are explained. Author

N92-30971*# National Aeronautics and Space Administration. Marshall Space Flight Center, Huntsville, AL.
A REDUCED GRAVITY FIBER PULLING APPARATUS
D. S. Tucker Jul. 1992 14 p
(NASA-TM-103594; NAS 1.15:103594) Avail: CASI HC A03/MF A01

A reduced gravity fiber pulling apparatus (FPA) was constructed in order to study the effects of gravity on glass fiber formation. The apparatus was specifically designed and built for use on NASA's KC-135 aircraft. To date, four flights have been completed during which E-glass fiber was successfully produced in simulated lunar gravity. Author

31 ENGINEERING (GENERAL)

Includes vacuum technology; control engineering; display engineering; cryogenics; and fire prevention.

N92-30378*# National Aeronautics and Space Administration. Goddard Space Flight Center, Greenbelt, MD.
CABLE COMPLIANCE
J. Kerley, W. Eklund (NSI Technology Services Corp., Greenbelt, MD.), R. Burkhardt (NSI Technology Services Corp., Greenbelt, MD.), and P. Rossoni Jun. 1992 138 p
(NASA-TP-3216; NAS 1.60:3216; Rept-92B00026) Avail: CASI HC A07/MF A02

The object of the investigation was to solve mechanical problems using cable-in-bending and cable-in-torsion. These problems included robotic contacts, targets, and controls using cable compliance. Studies continued in the use of cable compliance for the handicapped and the elderly. These included work stations, walkers, prosthetic knee joints, elbow joints, and wrist joints. More than half of these objects were met, and models were made and studies completed on most of the others. It was concluded that the many different and versatile solutions obtained only opened the door to many future challenges. Author

N92-30411# National Materials Advisory Board, Washington, DC.
BEAM TECHNOLOGIES FOR INTEGRATED PROCESSING
Mar. 1992 103 p
(Contracts MDA903-89-K-0078; MDA972-92-C-0028)
(AD-A252647; NMAB-461) Avail: CASI HC A06/MF A01

Beam technologies offer opportunities for application in many manufacturing schemes. Various beam technologies are reviewed, and applications to electronics and engineered materials are identified. Examples of existing manufacturing processes are

described. Recommendations for R and D efforts are developed for enhancing the understanding of the operation and capabilities of beam technologies and their applications. GRA

N92-30441# Messerschmitt-Boelkow-Blohm G.m.b.H., Munich (Germany, F.R.).
LIQUID DROPLET RADIATOR: DESIGN CONCEPTS AND DEVELOPMENT LOGIC
Alois Koeppl (Erno Raumfahrttechnik G.m.b.H. Bremen, Germany, F.R.) and Bernhard Leidinger, J. G. (Erno Raumfahrttechnik G.m.b.H. Bremen, Germany, F.R.) 1991 19 p Presented at the 1st European Symposium on Fluids in Space, Ajaccio, France, 18-22 Nov. 1991
(MBB-UO-0165-91-PUB; ETN-92-91893) Avail: CASI HC A03/MF A01

Liquid Droplet Radiators (LDRs), which stand out for their high efficiency compared to that of conventional radiators are addressed. The waste heat is radiated from the cooling fluid directly to the surrounding space. The actual radiator consists of a sheet of droplets of the cooling fluid. The droplets carrying the waste heat emanate from a droplet generator, transfer the waste heat to space by radiation, and are collected in a droplet collector afterwards. From there the fluid is pumped back, absorbs waste heat in a heat exchanger or cold plate, and returns to the droplet generator. First studies showed important open problems despite extensive literature on the LDR. The result of these studies, a preliminary sizing of an LDR for a heat rejection capability of 20 kW and the deduced development logic are presented. ESA

N92-30692*# National Aeronautics and Space Administration. Lewis Research Center, Cleveland, OH.
MICROGRAVITY VIBRATION ISOLATION: OPTIMAL PREVIEW AND FEEDBACK CONTROL
R. D. Hampton (Virginia Univ., Charlottesville.), C. R. Knospe (Virginia Univ., Charlottesville.), C. M. Grodsinsky, P. E. Allaire (Virginia Univ., Charlottesville.), and D. W. Lewis (Virginia Univ., Charlottesville.) May 1992 25 p
(NASA-TM-105673; E-7042; NAS 1.15:105673) Avail: CASI HC A03/MF A01

In order to achieve adequate low-frequency vibration isolation for certain space experiments an active control is needed, due to inherent passive-isolator limitations. Proposed here are five possible state-space models for a one-dimensional vibration isolation system with a quadratic performance index. The five models are subsets of a general set of nonhomogeneous state space equations which includes disturbance terms. An optimal control is determined, using a differential equations approach, for this class of problems. This control is expressed in terms of constant, Linear Quadratic Regulator (LQR) feedback gains and constant feedforward (preview) gains. The gains can be easily determined numerically. They result in a robust controller and offers substantial improvements over a control that uses standard LQR feedback alone. Author

N92-30754*# Micro Craft, Inc., Huntsville, AL.
INTEGRATION MOCKUP AND PROCESS MATERIAL MANAGEMENT SYSTEM Final Report
Adas James Verble, Jr. 27 Feb. 1992 56 p Original contains color illustrations
(Contract NAS8-36412)
(NASA-CR-184319; NAS 1.26:184319; MC-PY-92-011) Avail: CASI HC A04/MF A01; 28 functional color pages

Work to define and develop a full scale Space Station Freedom (SSF) mockup with the flexibility to evolve into future designs, to validate techniques for maintenance and logistics and verify human task allocations and support trade studies is described. This work began in early 1985 and ended in August, 1991. The mockups are presently being used at MSFC in Building 4755 as a technology and design testbed, as well as for public display. Micro Craft also began work on the Process Material Management System (PMMS) under this contract. The PMMS simulator was a sealed enclosure for testing to identify liquids, gaseous, particulate samples, and specimen including, urine, waste water, condensate, hazardous gases, surrogate gasses, liquids, and solids. The SSF would require many trade studies to validate techniques for maintenance and logistics and verify system task allocations; it was necessary to develop a full scale mockup which would be representative of current SSF design with the ease of changing those designs as the SSF design evolved and changed. The tasks defined for Micro Craft were to provide the personnel, services, tools, and materials for the SSF mockup which would consist of four modules, nodes, interior components, and part task mockups of MSFC responsible engineering systems. This included the Engineering Control and Life Support Systems (ECLSS) testbed. For the initial study, the mockups were low fidelity, soft mockups of graphics art bottle, and other low cost materials, which evolved into higher fidelity mockups as the R&D design evolved, by modifying or rebuilding, an important cost saving factor in the design process. We designed, fabricated, and maintained the full size mockup shells and support stands. The shells consisted of cylinders, end cones, rings, longerons, docking ports, crew airlocks, and windows. The ECLSS required a heavier cylinder to support the ECLSS systems test program. Details of this activity will be covered. Support stands were designed and built for each module to sufficiently move and rotate each module. Secondary structures such as floors, ceilings, bulkheads, standoffs, racks, etc. were developed and built.
Author

N92-30887# Sandia National Labs., Albuquerque, NM.
FRAGMENT HAZARD ZONE ANALYSES FOR EXPLOSIVE TEST FACILITIES
M. G. Vigil May 1992 70 p
(Contract DE-AC04-76DP-00789)
(DE92-015391; SAND-92-0243) Avail: CASI HC A04/MF A01

The analytical procedures for establishing the fragment hazard zone for explosive test facilities are presented. Environment, safety, and health regulations require that a hazard zone analysis be conducted for every explosive test facility. Analyses are presented for explosively driven missile fragment trajectories resultant from cased explosive configurations. Fragment trajectory parameter data are presented in graphical form for three different fragment materials (aluminum, steel, and tantalum), initial velocities between 0.6 to 4.3 mm/micron, and for various geometries. This trajectory information is used, as an example, to determine the safe distance or hazard zone for the Area 2 explosive test facility at Sandia National Laboratories. DOE

N92-30273*# Ball State Univ., Muncie, IN. Dept. of Industry and Technology.
A SENIOR MANUFACTURING LABORATORY FOR DETERMINING INJECTION MOLDING PROCESS CAPABILITY
Jerry L. Wickman and David Plocinski *In* NASA. Langley Research Center, National Educators' Workshop: Update 1991. Standard Experiments in Engineering Materials Science and Technology Jun. 1992 p 151-158 (For primary document see N92-30263 21-29)
Avail: CASI HC A02/MF A03

32 COMMUNICATIONS AND RADAR

Includes radar; land and global communications; communications theory; and optical communications.

For related information see also *04 Aircraft Communications and Navigation* and *17 Space Communications, Spacecraft Communications, Command and Tracking.* For search and rescue see *03 Air Transportation and Safety,* and *16 Space Transportation.*

N92-30246# Bowling Green State Univ., OH. Center for Photochemical Sciences.
PHOTODISSOCIATION OF AZULENE UNDER UV-LASER IRRADIATION AT 325 NM
S. Hassoon, D. L. Snavely, and I. Oref 18 May 1992 9 p
(Contract N00014-88-K-0664)
(AD-A251093; TR-8) Avail: CASI HC A02/MF A01

UV-laser photodissociation of azulene at 325 nm is reported. The photodissociation reaction occurs by a two photon absorption process producing acetylene. The quantum yield for acetylene produced by irradiation of neat azulene and azulene/argon mixtures is reported. The quantum yield of acetylene produced after irradiation of peat azulene at its normal vapor pressure is approximately 5.85 +/- 1.46 x 1O(exp -6). GRA

N92-30300*# Space Systems/Loral, Palo Alto, CA. Communications System Lab.
TECHNICAL AND ECONOMIC FEASIBILITY OF INTEGRATED VIDEO SERVICE BY SATELLITE Final Report
Kent M. Price, R. K. Garlow (Communications Satellite Corp., Clarksburg, MD.), T. R. Henderson (Communications Satellite Corp., Clarksburg, MD.), Robert K. Kwan, and L. W. White (Communications Satellite Corp., Clarksburg, MD.) Mar. 1992 119 p
(Contract NAS3-25092; RTOP 144-50-50)
(NASA-CR-189210; NAS 1.26:189210) Avail: CASI HC A06/MF A02

The trends and roles of satellite based video services in the year 2010 time frame are examined based on an overall network and service model for that period. Emphasis is placed on point to point and multipoint service, but broadcast could also be accommodated. An estimate of the video traffic is made and the service and general network requirements are identified. User charges are then estimated based on several usage scenarios. In order to accommodate these traffic needs, a 28 spot beam satellite architecture with on-board processing and signal mixing is suggested. Author

N92-30348# Department of the Army, Washington, DC.
WAVEGUIDE POLARIZER USING LOCALIZED SURFACE PLASMONS Patent Application
Mark J. Bloemer, inventor (to Army) 20 Dec. 1991 18 p
(AD-D015258; US-Patent-Appl-SN-811279) Avail: CASI HC A03/MF A01

Surface plasmon resonance in small particles of metal is employed to polarize light propagating in a waveguide. An ion-exchanged glass waveguide is provided with a 50 Angstrom (5 nm) mass thick layer of silver which is deposited on the waveguide. The ion-exchanged glass waveguide having the specified layer of silver is annealed at 2000 C for 1 minute causing the silver film to bead, much like water droplets on a waxed car. The silver microparticles have a nonspherical shape with their major axes parallel to the surface of the waveguide and their minor axis perpendicular to the surface of the waveguide. When light from a HeNe laser at a wavelength of 633 nm is prism-coupled into the waveguide with the field of laser beam parallel to the major axes of the spheroids (TE polarization) the laser light is strongly absorbed and the TM light is passed. By orienting the microparticles with the major axes perpendicular to surface, TM light will be absorbed and TE light will pass. Thus, changing the orientation of the nonspherical particles by 90 degrees changes the polarization state absorbed. The microparticles can be placed in the core of the waveguide, in the cladding, or on the cladding. All that is required of the microparticle location is that the electromagnetic field propagating in the waveguide extend to where the particles are located. The waveguide material is not limited to planar glass waveguides. Especially attractive are waveguide materials of optical fibers and III-V semiconductor compounds. For optical fiber waveguide materials, the particles can be deposited directly onto the cladding, or part of the cladding can be removed before deposition of the particles. GRA

N92-30354# Technische Univ., Delft (Netherlands). Faculty of Technical Mathematics and Information.
SIGNAL MATCHING BY DYNAMIC PROGRAMMING
P. L. Vermeer and J. A. H. Alkemade (Shell Exploration and Production Lab., Rijswijk , Netherlands) 1992 95 p
(Rept-92-01; ISSN-0922-5641; ETN-92-91853) Copyright Avail: CASI HC A05/MF A01

A method for the matching of mutually deformed signals is considered. The signals may be shifted, stretched, or compressed with respect to each other. The deformation is determined by minimization of a distance measure between the signals. The minimization algorithm is based on dynamic programming. Application to the correlation of well logs is of special interest. ESA

N92-30361# Beleidscommissie Remote Sensing, Delft (Netherlands).
RESULTS OF THE 1989 EXPERIMENT WITH A POLARIMETRIC MULTIFREQUENCY SAR
J. S. Groot (Physics and Electronics Lab. TNO, The Hague, Netherlands) and A. C. vandenBroek (Physics and Electronics Lab. TNO, The Hague, Netherlands) Mar. 1992 91 p
(BCRS Proj. TE-1.17)
(BCRS-91-33; ISBN-90-5411-016-3; ETN-92-91881) Avail: CASI HC A05/MF A01

In August 1989, a single day measurement campaign was conducted with two airborne imaging radars, the Dutch X band Side Looking Airborne Radar (SLAR) and the P/L/C band polarimetric Synthetic Aperture Radar (SAR). Test sites were the Flevopolder and the Veluwe (agricultural and forested areas, respectively) in the Netherlands. Ground activities included the deployment of several calibration devices like different sized trihedrals, dihedrals, and PARC's (active calibrators). An extensive experiment description is presented. Relevant details of the two radar systems and the calibration devices used are given. The calibration of the SLAR and SAR data is described. The calibrated data is used to investigate its potential for the classification of agricultural crop types. Several quantities are extracted from the data, which are used to do this. Examples are the copolarization phase difference distribution, the degree of polarization, and copolarized signatures. It appears to be quite possible to discriminate bare soil fields from vegetated fields using polarimetric quantities like the HH/VV (Horizontal Horizontal/Vertical Vertical) phase difference distribution and the degree of polarization. However, discrimination between fields with different crop types is much more difficult probably due to interference of features not related to the crop type, such as soil moisture, soil roughness, lodging, etc. ESA

N92-30391*# National Aeronautics and Space Administration. Pasadena Office, CA.
DOUBLE-LOOP FREQUENCY-SELECTED SURFACES FOR MULTIFREQUENCY DIVISION MULTIPLEXING IN A DUAL-REFLECTOR ANTENNA Patent Application
Te-Kao Wu, inventor (to NASA) (Jet Propulsion Lab., California Inst. of Tech., Pasadena.) 24 Jun. 1992 38 p
(Contract NAS7-918)
(NASA-Case-NPO-18701-1-CU; NAS 1.71:NPO-18701-1-CU; US-Patent-Appl-SN-909501) Avail: CASI HC A03/MF A01

A multireflector antenna utilizes a frequency-selective surface (FSS) in a subreflector to allow signals in two different radio frequency (RF) bands to be selectively reflected back into a main reflector and to allow signals in other RF bands to be transmitted through it to the main reflector for primary focus transmission. A first approach requires only one FSS at the subreflector which may be an array of double-square-loop conductive elements. A second approach uses two FSS's at the subreflector which may be an array of either double-square-loop (DSL) or double-ring (DR). In the case of DR elements, they may be advantageously arranged in a triangular array instead of the rectangular array for the DSL elements. NASA

N92-30407# Naval Research Lab., Washington, DC.
NUMERICAL SIMULATION OF THE ELECTROMAGNETIC INSTABILITY OF AN INTENSE BEAM IN A QUADRUPOLE FOCUSING SYSTEM Interim Report
J. Krall, C. M. Tang, and T. Swyden (FM Technologies, Inc., Fairfax, VA.) 15 Jun. 1992 17 p
(ARPA Order 7781)
(AD-A252275; NRL/MR/4790-92-6984) Avail: CASI HC A02/MF A01

Discrete quadrupole focusing systems are subject to an electromagnetic instability wherein the growing transverse motion of the beam interacts with the quadrupole field and the TE11, waveguide mode. We study this via three-dimensional particle simulation. We find evidence of the instability with growth rates and frequencies in reasonable agreement with theory. The instability is found to saturate at a low amplitude, however, it has no discernable effect on the macroscopic properties of the beam. GRA

N92-30408# Texas A&M Univ., College Station. Dept. of Electrical Engineering.
RADIATION, SCATTERING, AND GUIDANCE OF ELECTROMAGNETIC FIELDS BY ARBITRARILY SHAPED STRUCTURES EMBEDDED IN LAYERED DIELECTRIC MEDIA
Quarterly Progress Report, 1 Apr. - 30 Jun. 1992
K. A. Michalski 30 Jun. 1992 1 p
(Contract N00014-90-J-1197)
(AD-A252621) Avail: CASI HC A02/MF A01

The work on the waveguide-excited microstrip patch antenna for millimeter-wave applications has entered the final phase. An experimental validation of the analysis and its computer implementation was done in X-band, to reduce the effect of fabrication tolerances on the results. The computed and measured reflection coefficient results for a rectangular and a circular patch were found to be in close agreement. A paper on this research will be presented during the upcoming IEEE AP-S/URSI Symposium in Chicago. We have also continued to make progress in the research related to three-dimensional microstrip discontinuities and in the analysis of single and coupled integrated dielectric waveguides. GRA

N92-30448# Utrecht State Univ. (Netherlands). Dept. of Computer Science.
A PARADIGM FOR ASYNCHRONOUS COMMUNICATION AND ITS APPLICATION TO CONCURRENT CONSTRAINT PROGRAMMING
Frank S. deBoer (Technische Univ., Eindhoven, Netherlands), Joost N. Kok, Catuscia PalamiDessi (Center for Mathematics and Computer Science, Amsterdam, Netherlands), and Jan J. M. M. Rutten (Center for Mathematics and Computer Science, Amsterdam, Netherlands) Dec. 1991 37 p
(RUU-CS-91-46; ISSN-0924-3275; ETN-92-91812) Avail: CASI HC A03/MF A01

A general semantic theory of the asynchronous communication mechanism of concurrent logic and concurrent constraint languages is developed. The main characteristic of these languages, from the point of view of the communication mechanism, is that processes interact by querying and updating some common data structure. Abstraction from the specific features of the underlying data structure is carried out by means of a uniform language where actions are interpreted as transformations in an abstract set of states. Suspension and failure in this framework are viewed as special states. This approach shows that there exists a basic similarity between concurrent logic (constraint) languages and either languages based in asynchronous communication, like dataflow and asynchronous Communicating Sequential Processes (CSP). The intention is to capture languages based on asynchronous communication as instances of the paradigm, such an instance being determined by a specific set of states and interpretation of the actions. The computational model of the paradigm is described by a transition system in the style of Plotkin's Structural Operational Semantics (SOS). A compositional model is presented that is based on reactive sequences, i.e., sequences of pairs of states. ESA

N92-30532# Institute for Defense Analyses, Alexandria, VA.
HIGH FREQUENCY COMMUNICATIONS UNDER ADVERSE CONDITIONS Final Report
Herbert M. Federhen Dec. 1991 72 p
(Contract MDA903-89-C-0003)
(AD-A252199; AD-E501529; IDA-P-2598; IDA/HQ-91-38244)
Avail: CASI HC A04/MF A01

This paper discusses both ground-wave and sky-wave HF propagation and derives the equation describing the performance of a radio link when interference or jamming is present. Various techniques are then discussed to improve the link performance under these conditions. The most promising are shown to be directional antennas and spread-spectrum modulation, and these are discussed in great detail. GRA

N92-30583# Army Electronic Proving Ground, Fort Huachuca, AZ.
COMPACT RANGE TEST APPLICATIONS, PHASE 2 Methodology Investigation, Oct. 1990 - Oct. 1991
Francis L. Davis Jan. 1992 54 p
(AD-A248790; USAEPG-FR-1420-Phase-2) Avail: CASI HC A04/MF A01

Georgia Tech Research Institute (GTRI) has designed and fabricated a large outdoor Compact Antenna Range for the U.S. Army Electronic Proving Ground (USAEPG). This range enables USAEPG to test antenna systems of large ground vehicles or aircraft that weigh up to 70 tons and are up to 50 feet in size over a frequency range of 6 to 40 GHz. Ongoing investigation and study are being conducted to determine the compatibility and adaptability of this antenna pattern measurement range to measure other system parameters such as target return signals and system responses to specialized electromagnetic environments. GRA

N92-30637# Naval Research Lab., Washington, DC.
GLINT ERRORS DERIVED FROM THE PARTIAL DERIVATIVES OF THE ECHO SIGNAL PHASE FOR A DISTRIBUTED SCATTERER
Victor C. Chen 1 May 1992 29 p
(AD-A249499; NRL/MR/4440-92-6978) Avail: CASI HC A03/MF A01

This report extends the study of radar measurements from a point scatterer to a distributed scatterer. The measurement is based on partial derivatives of the echo-signal phase. The study is aimed at developing an understanding of what kind of radar information can be measured from echo-signal and formulating glint errors caused by a distributed scatterer. The importance of the phase was shown in signal and image processing. Basic radar measurements can also be obtained from the echo-signal phase. Unlike the measuring of target information from a point scatterer, for a distributed scatterer we must account for the measurement errors caused by the dimension and the orientation of a distributed scatterer. These are called glint errors. In this report, we describe how to measure radar information from the partial derivatives of the echo-signal phase with respect to frequency, time, and spatial position. We derive the expressions of range, range-rate, angle, and angle-rate glint errors for a distributed scatterer, and give an insight into these glint errors. GRA

N92-30703# Los Alamos National Lab., NM.
PROCESSING AEROSOLS AND FILAMENTS IN A TM010 MICROWAVE CAVITY AT 2.45 GHz
G. J. Vogt and W. P. Unruh 1992 8 p Presented at the Material Research Society Spring Meeting, San Francisco, CA, 27 Apr. - 2 May 1992
(Contract W-7405-eng-36)
(DE92-013536; LA-UR-92-1289; CONF-920402-5) Avail: CASI HC A02/MF A01

As part of the development of generic microwave processes for spray-drying of homogeneous complex metal oxide powders and for inorganic fiber processing, we have investigated the use of 2.45 GHz microwaves in a high-Q single-mode TM(sub 010) (transverse magnetic) cavity coupled directly to aerosols and fibers. Aqueous and ethanol aerosols of ferric nitrate solutions have been successfully dried at 1.8 kW of cavity power for a loaded Q greater than 6000 in flowing nitrogen gas. Similarly, we have observed extremely rapid heating rates in the TM(sub 010) cavity for small-diameter confined cylinders of water and lossy inorganic fibers. These observations suggest using 2.45 GHz microwave power for drying, calcining, and sintering extruded ceramic filaments. Droplet modeling indicates that the large dielectric shielding for spherical droplets can significantly limit the coupling

of 2.45 GHz microwave with spherical aerosols, but not with fibers. Experimental observations on the microwave interactions with ferric nitrate aerosols and with ceramic filaments in the TM(sub 010) cavity are described. DOE

N92-30721# Naval Command, Control and Ocean Surveillance Center, San Diego, CA.
A NEW MATRIX FORMULATION OF CLASSICAL ELECTRODYNAMICS. PART 1: VACUUM Final Report
R. P. Bocker and B. R. Frieden (Arizona Univ., Tucson.) Mar. 1992 42 p
(AD-A249643; NRAD-TD-2259) Avail: CASI HC A03/MF A01

Presented in this paper is a new matrix representation of classical electromagnetic theory. The basis of this representation is a space-time, eight-by-eight differential matrix operator. This matrix operator is initially formulated from the differential form of the Maxwell field equations in vacuum. The resulting matrix formulation of Maxwell's equations allows simple and direct derivation of the electromagnetic wave and charge continuity equations, the Lorentz conditions and definition of the electromagnetic potentials, the Lorentz and Coulomb gauges, the electromagnetic potential wave equations, and Poynting's conservation of energy theorem. A four-dimensional Fourier transform of the matrix equations casts them into an eight-dimensional transfer theorem. The transfer function has an inverse, and this allows the equations to be inverted. This inversion expresses the fields directly in terms of the charge and current source distributions, i. e., without the need for calculating intermediary potentials. This inversion formula is new, for the general scenario of space- and time-dependent sources. A simple pedagogical example is included illustrating use of the formulation. GRA

N92-30755# Rand Graduate Inst. for Policies Study, Santa Monica, CA.
THE RISE OF ACTIVE-ELEMENT PHASED-ARRAY RADAR
Ike Chang 1991 14 p
(RAND-P-7747-RGS) Avail: CASI HC A03/MF A01

The War in the Persian Gulf has recently underscored the vast leverage of advanced electronics to U.S. military power. Advanced electronics will likely play an even greater role in the U.S. military in the future. Under declining budgets, the U.S. forces are experiencing drastic reductions in manpower and resources. To offset these reductions, the military has turned to high technology in general as a force multiplier. In terms of projecting air power, a key force multiplier involves the use of electronic sensors for reconnaissance, surveillance, and tracking. One type of sensor for tactical aircraft, fire control radar, has proven to be a crucial element in establishing air superiority over potential adversaries in war. The advantages, history of development, and enabling technologies of a superior and emerging technology for fire control radars are discussed. Author

N92-30760# Rome Lab., Griffiss AFB, NY.
FOREIGN SURVEILLANCE RADAR UPGRADE ANALYSIS Report, Dec. 1990 - Dec. 1991
Steven D. Farr Feb. 1992 41 p
(AD-A249440; RL-TR-92-34) Avail: CASI HC A03/MF A01

This report details an example of the work required to predict the functionality of future systems based on improvements in computer technology. Areas of analysis include CPU load, bus load, memory load, I/O load, target report delay, and probability of target loss associated with the upgraded radar. The analysis scenario provides an example of how queuing theory and probability can be applied for the purpose of assessing future threats. GRA

N92-30761# Massachusetts Inst. of Tech., Lexington. Lincoln Lab.
ON THE RADIAL COMPONENT OF THE ELECTRIC FIELD FOR A MONOPOLE PHASED ARRAY ANTENNA FOCUSED IN THE NEAR ZONE
Alan J. Fenn 10 Jan. 1992 27 p
(Contract F19628-90-C-0002)
(AD-A249441; TR-944; ESD-TR-944) Avail: CASI HC A03/MF A01

The near-zone radial and principal spherical components of the electric field for a linear phased array antenna that is focused at one to two aperture diameters in the near zone are investigated. The phased array antenna, consisting of thin monopole elements, is analyzed by using the method of moments. A theoretical formulation is described and computer simulation results are presented. The results show that the radial component is negligible in the focused near-field region, which allows the principal component to be accurately computed from knowledge of only the tangential electric field on the focal plane. GRA

N92-30762# Massachusetts Inst. of Tech., Lexington. Lincoln Lab.
MAXIMUM LIKELIHOOD DETECTION OF ELECTRO-OPTIC MOVING TARGETS
Stephen C. Pohlig 16 Jan. 1992 56 p
(Contract F19628-90-C-0002)
(AD-A249442; TR-940; ESD-TR-91-174) Avail: CASI HC A04/MF A01

The description of a maximum likelihood algorithm to detect moving targets in electro-optic data is presented. The algorithm is based on processing image data that are modeled as temporally stationary and spatially nonstationary Gaussian samples. Algorithm performance is evaluated in terms of the probabilities of false alarm and detection. A comparison of theoretical and experimental probability distributions for single normalized pixels shows good agreement for different clutter backgrounds (stellar, sky, mountains, and desert). Similarly, a comparison of theoretical and experimental false alarm probabilities also shows good agreement. These results validate using theoretical models to predict performance. A binary integration version of this algorithm is described and evaluated in terms of false alarm and detection probabilities. This version is suboptimum and is compared with the optimum algorithm to determine the performance loss. A processing architecture concept is also described. GRA

N92-30863# Massachusetts Inst. of Tech., Lexington. Lincoln Lab.
MULTIFREQUENCY MEASUREMENTS OF RADAR GROUND CLUTTER AT 42 SITES. VOLUME 3: APPENDIX E
J. B. Billingsley and John F. Larrabee 15 Nov. 1991 758 p
(Contract F19628-90-C-0002)
(AD-A246988; MIT-TR-916-Vol-3; ESD-TR-91-176) Avail: CASI HC A99/MF A06

This report determines how ground clutter strength varies with RF frequency from VHF to X-band in ground-sited radar. This determination is accomplished by providing extensive empirical results from multifrequency clutter measurements conducted at 42 different sites widely dispersed over the North American continent. These results indicate that the frequency dependence of ground clutter strength depends upon terrain type and can vary, for example, from a strongly decreasing function of frequency in forest to a strongly increasing function of frequency in farmland. Five major terrain categories are defined that encompass this dependence, namely, urban, mountains, forest, farmland, and desert. Within each terrain category, results are also shown to be dependent upon the relief or roughness of the terrain and upon the depression angle at which the terrain is illuminated. The depression angle dependence is important, even for the very low angles (typically within a degree of grazing incidence) and small (typically fractional) variations in angle that occur in ground-sited radar. This report presents specific clutter strength results at each of five frequencies (VHF, UHF, L-, S-, and X-band) from each of the 42 sites at which measurements were conducted. The report then combines results from similar sites to obtain the general dependence of clutter strength versus frequency for each terrain category. GRA

N92-30869# Naval War Coll., Newport, RI. Dept. of Operations.
STEALTH: A REVOLUTIONARY CHANGE TO AIR WARFARE Final Report
Kevin J. Kennedy 13 Feb. 1992 54 p
(AD-A249880) Avail: CASI HC A04/MF A01

'Stealth, A Revolutionary Change To Warfare' highlights the unique capabilities stealth weapons bring to the battlefield and asserts they offer new and valuable options to the commander. It suggests these capabilities must be completely understood to be fully effective. With a focus at the doctrinal level, the paper claims the following: stealth assets take away from the absolute primacy of aerospace control (air superiority) and in many cases, allows force application to became the primary task. The claim is also made that stealth assets expand and enhance the potential opportunities for effective use of air power across the spectrum of warfare to include the force presence role. These and other changes will impact air warfare at all levels. Capitalizing on stealth requires the following: (1) a recognition of unique stealth attributes; (2) fully embracing these attributes through Air Force doctrinal changes; and (3) a fresh look for potential applications in all operational planning. GRA

N92-30876# Naval Ocean Systems Center, San Diego, CA. Research, Development, Test, and Evaluation Div.
EVAPORATION DUCT EFFECTS AT MILLIMETER WAVELENGTHS
K. D. Anderson Mar. 1992 16 p Previously announced as N90-21914
(AD-A250239) Avail: CASI HC A03/MF A01

The evaporation duct strongly influences low-altitude over-the-horizon propagation at millimeter wavelengths. Results from more than 2000 hours of propagation and meteorological measurements made at 94 GHz on a 40.6 km over-horizon, over-water path along the southern California coast show that the average received power was 63 dB greater than d for propagation in a nonducting, or standard, atmosphere; 90 percent of the measurements were at least 55 dB greater than diffraction. A numerical model of transmission loss based on the observed surface meteorology is discussed and results are compared to measured transmission loss. On average, modeling results underestimate observations by only 10 dB. In addition, results from modeling based on an independent climatology of evaporation duct heights for the area are shown to be adequate for most propagation assessment purposes. The reliability and reasonable accuracy of the numerical model provides a strong justification for utilizing the technique to assess millimeter wave communication and radar systems operating in many, if not all, ocean regions. GRA

N92-30923*# Jet Propulsion Lab., California Inst. of Tech., Pasadena.
PROCEEDINGS OF THE WORKSHOP ON ADVANCED NETWORK AND TECHNOLOGY CONCEPTS FOR MOBILE, MICRO, AND PERSONAL COMMUNICATIONS
Lori Paul, ed. 15 Sep. 1991 325 p Workshop held in Pasadena, CA, 30-31 May 1991
(Contract NAS7-918; RTOP 650-60-15-01-00)
(NASA-CR-190459; NAS 1.26:190459; JPL-Publ-91-35) Avail: CASI HC A14/MF A03

The Workshop on Advanced Network and Technology Concepts for Mobile, Micro, and Personal Communications was held at NASA's JPL Laboratory on 30-31 May 1991. It provided a forum for reviewing the development of advanced network and technology concepts for turn-of-the-century telecommunications. The workshop was organized into three main categories: (1) Satellite-Based Networks (L-band, C-band, Ku-band, and Ka-band); (2) Terrestrial-Based Networks (cellular, CT2, PCN, GSM, and other networks); and (3) Hybrid Satellite/Terrestrial Networks. The proceedings contain presentation papers from each of the above categories. For individual titles, see N92-30924 through N92-30946.

N92-30924*# Ministry of Posts and Telecommunications, Tokyo (Japan). Communications Research Lab.
ADVANCED MOBILE SATELLITE COMMUNICATIONS SYSTEM USING Ka AND MM-WAVE BANDS IN JAPAN'S R AND D SATELLITE PROJECT
Shunkichi Isobe, Shingo Ohmori, Naokazu Hamamoto, and Minoru Yamamoto *In* JPL, Proceedings of the Workshop on Advanced Network and Technology Concepts for Mobile, Micro, and Personal Communications 15 Sep. 1991 p 15-19 (For primary document see N92-30923 21-32)
Avail: CASI HC A01/MF A03

Communications Research Laboratory (CRL) studied an advanced mobile satellite communications system using Ka and millimeter-wave bands in the R&D Satellite project. The project started in 1990 and the satellite will be launched in 1997. On-board multi-beam interconnecting is one of basic functions to realize one-hop connection among Very Small Aperture Terminals (VSATs), mobile, and hand-held terminals in future mobile satellite communications system. An Intermediate Frequency (IF) filter bank and regenerative transponder are suitable for this function. The transponder configuration of an advanced mobile communications mission of the R&D Satellite for experiment is shown. High power transmitters of Ka and millimeter-wave bands, a 3x3 IF filter band and Single Channel Per Carrier/Time Division Multiplexing (SCPC/TDM) regenerative MODEMS, which will be boarded on the R&D Satellite, are being developed for the purpose of studying the feasibility of advanced mobile communications system. Author

N92-30925*# American Mobile Satellite Corp., Washington, DC.
DESIGN OF THE AMERICAN MOBILE SATELLITE SYSTEM
Charles Kittiver *In* JPL, Proceedings of the Workshop on Advanced Network and Technology Concepts for Mobile, Micro, and Personal Communications 15 Sep. 1991 p 21-40 (For primary document see N92-30923 21-32)
Avail: CASI HC A03/MF A03

This paper presents an overview of the American Mobile Satellite Corporation (AMSC) Mobile Satellite System (MSS). A summary of the mobile satellite (MSAT) design and overall performance is provided. The design and components of both the forward link and return link transponders are described in detail. The design and operation of a unique hybrid matrix amplifier that offers flexible power distribution is outlined. The conceptual design and performance of three types of land mobile antennas are described. Author

N92-30926*# Motorola, Inc., Schaumburg, IL. Satellite Communications.
LEO SATELLITE-BASED TELECOMMUNICATION NETWORK CONCEPTS
John G. Aiken, Peter A. Swan, and Ray J. Leopold *In* JPL, Proceedings of the Workshop on Advanced Network and Technology Concepts for Mobile, Micro, and Personal Communications 15 Sep. 1991 p 41-53 (For primary document see N92-30923 21-32)
Avail: CASI HC A03/MF A03

Design considerations are discussed for Low Earth Orbit (LEO) satellite based telecommunications networks. The satellites are assumed to be connected to each other via intersatellite links. They are connected to the end user either directly or through gateways to other networks. Frequency reuse, circuit switching, packet switching, call handoff, and routing for these systems are discussed by analogy with terrestrial cellular (mobile radio) telecommunication systems. Author

N92-30927*# Ministry of Posts and Telecommunications, Tokyo (Japan). Communications Research Lab.
EXPERIMENTAL MILLIMETER-WAVE PERSONAL SATELLITE COMMUNICATIONS SYSTEM
Yoshiaki Suzuki, Shigeru Kimura, Masaaki Shimada, Masato Tanaka, and Yasuhiro Takahashi *In* JPL, Proceedings of the Workshop on Advanced Network and Technology Concepts for

Mobile, Micro, and Personal Communications 15 Sep. 1991 p 55-64 (For primary document see N92-30923 21-32)
Avail: CASI HC A02/MF A03

Communications Research Laboratory (CRL) has investigated an advanced millimeter (mm)-wave satellite communications system for personal use. Experiments in mm-wave personal satellite communication are to be conducted for 3 years using Japan's Engineering Test Satellite VI (ETS-VI). This paper describes an experimental mm-wave (43/38 GHz) personal satellite communication system, including an onboard transponder and an earth terminal. The on-board transponder is almost completed, and the ground experiment system is still in the design stage. The transponder employs advanced mm-wave solid state technology. It uses 38 GHz high power solid state amplifiers to accelerate the development of mm-wave solid state devices which are indispensable to personal earth terminals. The transponder consists of a 43 GHz receiver with a built-in low noise amplifier, an IF filter section with very narrow bandwidth to improve the carrier-to-noise power ratio of the weak personal communication signal, and two high power amplifiers using newly developed high power Gallium Arsenide (GaAs) metal-semiconductor field effect transistors (MESFETs). Author

N92-30928*# Jet Propulsion Lab., California Inst. of Tech., Pasadena.
Ka-BAND MOBILE AND PERSONAL SYSTEMS DEVELOPMENT AT JPL
K. Dessouky, P. Estabrook, T. Jedrey, and M. K. Sue *In its* Proceedings of the Workshop on Advanced Network and Technology Concepts for Mobile, Micro, and Personal Communications 15 Sep. 1991 p 65-77 (For primary document see N92-30923 21-32)
Avail: CASI HC A03/MF A03

Expanding the commercial applications of space is one of the primary goals of NASA. Throughout the eighties NASA has pursued this objective by sponsoring and undertaking the development of system concepts, enabling high risk technologies, and actual proof of concept demonstration hardware. In the mobile and personal arena, or the so-called low data rate applications area, JPL is NASA's lead center. JPL's focus of activities has been the Mobile Satellite-Experiment (MSAT-X) project, which developed mobile communication technologies at L-band, and its present successors, which aim to expand the mobile arena by exploiting Ka-band.
Author

N92-30929*# Communications Satellite Corp., Clarksburg, MD.
PERSONAL COMMUNICATIONS VIA ACTS SATELLITE HBR TRANSPONDERS
Russell J. F. Fang *In* JPL, Proceedings of the Workshop on Advanced Network and Technology Concepts for Mobile, Micro, and Personal Communications 15 Sep. 1991 p 79-97 (For primary document see N92-30923 21-32)
Avail: CASI HC A03/MF A03

The concept of a fully meshed network of briefcase-sized terminals is presented for personal communications over Ka-band satellite transponders. In this concept, undesirable double-hop delays are avoided for voice communications. The bandwidth and power resources of the transponder are efficiently shared by users in a simple demand-assigned manner via code-division multiple access (CDMA). Voice, data, and facsimile are statistically multiplexed at each terminal. In order to minimize terminal costs, frequency-precorrected, and level-preadjusted continuous-wave tones are sent from the central network control station in each beam so that the terminals in each down-link beam can use these pilots as references for antenna acquisition and tracking, as reliable frequency sources, and as indicators of signal fade for up-link power control (ULPC). The potential CDMA 'near-far' problem due to up-link fades is mitigated by using ULPC. Quasi-burst mode transmission is employed to minimize the potential clock and pseudorandom number code synchronization. Author

N92-30930*# Ellipsat Corp., Washington, DC.
THE ELLIPSO (TM) SYSTEM: ELLIPTICAL LOW ORBITS FOR MOBILE COMMUNICATIONS AND OTHER OPTIMUM SYSTEM ELEMENTS
David Castiel *In* JPL, Proceedings of the Workshop on Advanced Network and Technology Concepts for Mobile, Micro, and Personal Communications 15 Sep. 1991 p 101-117 (For primary document see N92-30923 21-32)
Avail: CASI HC A03/MF A03

On 5 Nov. 1990, Ellipsat filed with the FCC the first application to provide voice communication services via low earth orbiting (LEO) satellites. The proposed system, ELLIPSO, aims at achieving end-user costs comparable to those in the cellular industry. On 3 Jun. 1991 Ellipsat filed for the second complement of its system. Ellipsat was also the first company to propose combined position determination and mobile voice services via low-earth orbiting satellites. Ellipsat is still the only proponent of elliptical orbits for any commercial system in the United States. ELLIPSO uses a spectrum efficient combination of FDMA and CDMA techniques. Ellipsat's strategy is to tailor required capacity to user demand, reduce initial system costs and investment risks, and allow the provision of services at affordable end-user prices. ELLIPSO offers optimum features in all the components of its system, elliptical orbits, small satellites, integrated protocol and signalling system, integrated end-user electronics, novel marketing approach based on the cooperation with the tenets of mobile communications, end-user costs that are affordable, and a low risk approach as deployment is tailored to the growth of its customer base. The efficient design of the ELLIPSO constellation and system allows estimated end-user costs in the $.50 per minute range, five to six times less than any other system of comparable capability.
Author

N92-30931*# Telesat Canada, Gloucester (Ontario).
SHARP SYSTEM FOR PERSONAL COMMUNICATIONS
K. M. Sundara Murthy *In* JPL, Proceedings of the Workshop on Advanced Network and Technology Concepts for Mobile, Micro, and Personal Communications 15 Sep. 1991 p 119-124 (For primary document see N92-30923 21-32)
Avail: CASI HC A02/MF A03

The application of the stationary high altitude relay platform (SHARP) concept orignally developed by the Department of Communications to provide a wide range of personal communications services is addressed. The inherent merits of SHARP are ideally suited to personal communications particularly to overcome some of the limitations of the geostationary satellites (GEOS) and low earth orbit satellite systems (LEOS) when used in personal communications environment. An overview of the SHARP concept is presented, and some of its merits are outlined. High level networking concepts are presented for typical cases as applicable to personal communications. Author

N92-30932*# National Aeronautics and Space Administration. Lewis Research Center, Cleveland, OH.
CHARACTERISTICS OF A FUTURE AERONAUTICAL SATELLITE COMMUNICATIONS SYSTEM
Philip Y. Sohn, Alan Stern (General Electric Co., Princeton, NJ.), and Fred Schmidt (Ball Corp., Bloomfield, CO.) *In* JPL, Proceedings of the Workshop on Advanced Network and Technology Concepts for Mobile, Micro, and Personal Communications 15 Sep. 1991 p 125-152 Previously announced as N91-23102 (For primary document see N92-30923 21-32)
Avail: CASI HC A03/MF A03

A possible operational system scenario for providing satellite communications services to the future aviation community was analyzed. The system concept relies on a Ka-band (20/30 GHz) satellite that utilizes Multibeam Antenna (MBA) technology. The aircraft terminal uses an extremely small aperture antenna as a result of using this higher spectrum at Ka-band. The satellite functions as a relay between the aircraft and the ground stations. The ground stations function as interfaces to the existing terrestrial networks such as the Public Service Telephone Network (PSTN). Various system tradeoffs are first examined to ensure optimized

system parameters. High level performance specifications and design approaches are generated for the space, ground, and aeronautical elements in the system. Both technical and economical issues affecting the feasibility of the studied concept are addressed with the 1995 timeframe in mind. Author

N92-30933*# Communications Research Centre, Ottawa (Ontario). Dept. of Communications.
AN INTEGRATED Ka/Ku-BAND PAYLOAD FOR PERSONAL, MOBILE AND PRIVATE BUSINESS COMMUNICATIONS
Edward J. Hayes and J. Malcolm Keelty (Spar Aerospace Ltd., Montreal, Quebec) *In* JPL, Proceedings of the Workshop on Advanced Network and Technology Concepts for Mobile, Micro, and Personal Communications 15 Sep. 1991 p 153-164 (For primary document see N92-30923 21-32)
Avail: CASI HC A03/MF A03

The Canadian Department of Communications has been studying options for a government-sponsored demonstration payload to be launched before the end of the century. A summary of the proposed system concepts and network architectures for providing an advanced private business network service at Ku-band and personal and mobile communications at Ka-band is presented. The system aspects addressed include coverage patterns, traffic capacity, and grade of service, multiple access options as well as special problems, such as Doppler in mobile applications. Earth terminal types and the advanced payload concept proposed in a feasibility study for the demonstration mission are described. This concept is a combined Ka-band/Ku-band payload which incorporates a number of advanced satellite technologies including a group demodulator to convert single-channel-per-carrier frequency division multiple access uplink signals to a time division multiplex downlink, on-board signal regeneration, and baseband switching to support packet switched data operation. The on-board processing capability of the payload provides a hubless VSAT architecture which permits single-hop full mesh interconnectivity. The Ka-band and Ku-band portions of the payload are fully integrated through an on-board switch, thereby providing the capability for fully integrated services, such as using the Ku-band VSAT terminals as gateway stations for the Ka-band personal and mobile communications services. Author

N92-30934*# National Aeronautics and Space Administration. Lewis Research Center, Cleveland, OH.
A PERSONAL COMMUNICATIONS NETWORK USING A Ka-BAND SATELLITE
L. C. Palmer (Hughes Network Systems, Inc., Germantown, MD.), A. Stern (General Electric Co., Princeton, NJ.), and P. Y. Sohn *In* JPL, Proceedings of the Workshop on Advanced Network and Technology Concepts for Mobile, Micro, and Personal Communications 15 Sep. 1991 p 165-176 (For primary document see N92-30923 21-32)
(Contract AC-90-695)
Avail: CASI HC A03/MF A03

The feasibility of portable communications terminals that can provide 4.8-kbps voice communications to a hub station via a Ka-band geosynchronous satellite was investigated. Tradeoffs are examined so that the combined system of the hub and gateway earth stations, the satellite, and the personal terminals can provide a competitive service in terms of cost, availability, and quality. A baseline system is described using a spacecraft with approximately 140 spot beams that cover CONUS with 5-watt power amplifiers in each beam. Satellite access in both the forward and return directions uses Frequency Division Multiple Access/Code Division Multiple Access (FDMA/CDMA) with a chip rate of 2.5 Mchip/sec. An experiment is recommended using the Advanced Communications Technology Satellite (ACTS) to demonstrate some of the features of the portable terminal concept. Author

N92-30935*# Communications Research Centre, Ottawa (Ontario).
EHF (28/19 GHz) PERSONAL COMMUNICATIONS SATELLITE TERMINAL DEVELOPMENT
Corey Pike *In* JPL, Proceedings of the Workshop on Advanced Network and Technology Concepts for Mobile, Micro, and Personal Communications 15 Sep. 1991 p 177-188 (For primary document see N92-30923 21-32)
Avail: CASI HC A03/MF A03

The concept of communicating on a personal basis using a small terminal has been investigated globally from many different applications and technology perspectives. Applications range from terrestrial handheld communicators for paging, cellular, zone voice/data networks, etc., to satellite terminals of pocket dimensions for voice/low speed data or similar terminals using larger antennas for VSAT, news gathering (30 cm), and video (1.2 m). A brief status of some developments in the satellite personal communications at CRC will be presented. Author

N92-30936*# GTE Government Systems Corp., Waltham, MA. Mobile Communications.
CELLULAR: TOWARD PERSONAL COMMUNICATIONS
Stuart Heffernan *In* JPL, Proceedings of the Workshop on Advanced Network and Technology Concepts for Mobile, Micro, and Personal Communications 15 Sep. 1991 p 191-195 (For primary document see N92-30923 21-32)
Avail: CASI HC A01/MF A03

The cellular industry is one of the fastest growing segment of the telecommunications industry. With an estimated penetration rate of 20 percent in the near future, cellular is becoming an ubiquitous telecommunications service in the U.S. In this paper we will examine the major advancements in the cellular industry: customer equipment, cellular networks, engineering tools, customer support, and nationwide seamless service. Author

N92-30937*# PacTel Corp., Walnut Creek, CA.
CAPACITY AND INTERFERENCE IN A PCS SYSTEM
William C. Y. Lee *In* JPL, Proceedings of the Workshop on Advanced Network and Technology Concepts for Mobile, Micro, and Personal Communications 15 Sep. 1991 p 197-206 (For primary document see N92-30923 21-32)
Avail: CASI HC A02/MF A03

In order to increase the capacity of a Personal Communication Service (PCS) system, the PCS system environment needs to be understood. The PCS system environment is briefly described in this paper. Because the frequency reuse concept is used to increase the capacity of PCS, the cochannel cells created cause cochannel interference. There are two approaches to reduce cochannel interference. One is the microcell approach (within the existing system) and the other is the reduction of cochannel cell separation approach (developing a new system). In-building communications using PCS systems has been addressed. Also, the Intelligent Network (IN) is described to show its importance. The cellular system has great potential to be the future PCS system. Author

N92-30938*# Motorola, Inc., Arlington Heights, IL. Radio-Telephone Systems Group.
THE PAN-EUROPEAN DIGITAL CELLULAR (GSM) SYSTEM
Valy Lev and Michael Kotzin *In* JPL, Proceedings of the Workshop on Advanced Network and Technology Concepts for Mobile, Micro, and Personal Communications 15 Sep. 1991 p 209-218 (For primary document see N92-30923 21-32)
Avail: CASI HC A02/MF A03

This paper presents an overview of the Pan-American Cellular System (GSM). Much of the information is generic to the GSM architecture and operation, as defined in ETSI Recommendations 1 to 12. Author

N92-30939*# City Coll. of the City Univ. of New York, NY. Dept. of EECS.
DIRECT SEQUENCE SPREAD SPECTRUM CDMA IN SHARED SPECTRUM APPLICATIONS
Donald L. Schilling, Laurence B. Milstein (California Univ., San Diego, La Jolla.), Raymond L. Pickholtz (George Washington Univ., Washington, DC.), and Frank Miller (Millicom, Inc., New York, NY.) *In* JPL, Proceedings of the Workshop on Advanced Network and Technology Concepts for Mobile, Micro, and Personal

Communications 15 Sep. 1991 p 219-226 Submitted for publication Sponsored in part by SCS Mobilecom, Inc.; and Millicom, Inc. (For primary document see N92-30923 21-32)
Avail: CASI HC A02/MF A03

Personal Communication Network (PCN) is an entirely wireless communication system with the capability of assessing the wired telephone system to reach anyone processing only a wired telephone. It is expected to compete with the existing mobile cellular system which connects directly to the wired telephone system. While many PCN systems employ TDMA technology, the PCN system described here uses Broadband CDMA (BCDMA(sup SM)) which is capable of sharing the spectrum with other users and which is extremely resistant to fading caused by multipath.
Author

N92-30940*# Department of Defense, Fort Meade, MD.
TOWARD A NORTH AMERICAN STANDARD FOR MOBILE DATA SERVICES
Richard A. Dean and Allen H. Levesque (GTE Government Systems Corp., Waltham, MA.) *In* JPL, Proceedings of the Workshop on Advanced Network and Technology Concepts for Mobile, Micro, and Personal Communications 15 Sep. 1991 p 229-239 (For primary document see N92-30923 21-32)
Avail: CASI HC A03/MF A03

The rapid introduction of digital mobile communications systems is an important part of the emerging digital communications scene. These developments pose both a potential problem and a challenge. On one hand, these separate market driven developments can result in an uncontrolled mixture of analog and digital links which inhibit data modem services across the mobile/Public Switched network (PSTN). On the other hand, the near coincidence of schedules for development of some of these systems, i.e., Digital Cellular, Mobile Satellite, Land Mobile Radio, and ISDN, provides an opportunity to address interoperability problems by defining interfaces, control, and service standards that are compatible among these new services. In this paper we address the problem of providing data services interoperation between mobile terminals and data devices on the PSTN. The expected data services include G3 Fax, asynchronous data, and the government's STU-3 secure voice system, and future data services such as ISDN. We address a common architecture and a limited set of issues that are key to interoperable mobile data services. We believe that common mobile data standards will both improve the quality of data service and simplify the systems for manufacturers, data users, and service providers. Author

N92-30941*# Florence Univ. (Italy). Dipt. di Ingegneria Elettronica.
ISSUES FOR THE INTEGRATION OF SATELLITE AND TERRESTRIAL CELLULAR NETWORKS FOR MOBILE COMMUNICATIONS
Enrico DelRe, Ignazio Mistretta (Telespazio, S.p.A., Rome, Italy), Francesco DelliPriscoli (Telespazio, S.p.A., Rome, Italy), and Franco Settimo (Centro Studi e Laboratori Telecomunicazioni, Turin, Italy) *In* JPL, Proceedings of the Workshop on Advanced Network and Technology Concepts for Mobile, Micro, and Personal Communications 15 Sep. 1991 p 241-262 (For primary document see N92-30923 21-32)
Avail: CASI HC A03/MF A03

Satellite and terrestrial cellular systems naturally complement each other for land mobile communications, even though present systems have been developed independently. The main advantages of the integrated system are a faster wide area coverage, a better management of overloading traffic conditions, an extension to geographical areas not covered by the terrestrial network and, in perspective, the provision of only one integrated system for all mobile communications (land, aeronautical, and maritime). To achieve these goals, as far as possible the same protocols of the terrestrial network should be used also for the satellite network. Discussed here are the main issues arising from the requirements of the main integrated system. Some results are illustrated, and possible future improvements due to technical solutions are presented. Author

N92-30942*# Radio Satellite Corp., Long Beach, CA.
THE RADIOSAT (SM) NETWORK
Gary K. Noreen *In* JPL, Proceedings of the Workshop on Advanced Network and Technology Concepts for Mobile, Micro, and Personal Communications 15 Sep. 1991 p 265-272 (For primary document see N92-30923 21-32)
Avail: CASI HC A02/MF A03

The RadioSat network under development by radio Satellite Corporation will use mobile satellite (MSAT) technology to provide diverse personal communications, broadcast, and navigation services. The network will support these services simultaneously for integrated mobile radios throughout Canada and the United States. The RadioSat network takes advantage of several technological breakthroughs, all coming to fruition by the time the first MSAT satellite is launched in 1994. The most important of these breakthroughs is the enormous radiated power of each MSAT spacecraft - orders of magnitude greater than the radiated power of previous L-band spacecraft. Another important breakthrough is the development of advanced digital audio compression algorithms, enabling the transmission of broadcast quality music at moderate data rates. Finally, continuing dramatic increases in VLSI capabilities permit the production of complex, multi-function mobile satellite radios in very large quantities at prices little more than those of conventional car radios. In addition to performance breakthroughs and their economic implications to RadioSat, the design of the RadioSat network is reviewed. Author

N92-30943*# National Communications System, Arlington, VA.
NATIONAL TRANSPORTABLE TELECOMMUNICATIONS CAPABILITY
Kenneth B. Boheim and Beverly Bach (Bell Atlantic Mobile Systems, Bedminster, NJ.) *In* JPL, Proceedings of the Workshop on Advanced Network and Technology Concepts for Mobile, Micro, and Personal Communications 15 Sep. 1991 p 273-285 (For primary document see N92-30923 21-32)
Avail: CASI HC A03/MF A03

The chance to integrate two emerging telecommunications technologies together, the Ku-band satellite communication (SATCOM) and cellular, offered the unique opportunity to package a truly stand-alone capability to reconstitute telecommuications service. Terrestrial cellular telephone services have proven to be an essential tool for dealing with local emergencies to the extent that they survive and remain operable, as in the San Francisco earthquake. Cellular telephones can provide emergency coordinators the flexibility of wireless mobility in the field via the Public Switched Network (PSN) to coordinate emergency services. However, not all areas are covered by cellular service; existing cellular and PSN service availability could be limited by the congestion and competition for the dial tone that occurs in emergencies. It was realized that a critical need exists for a rapidly deployable stand-alone cellular capability coupled with alternate connectivity to bypass congested or damaged PSN links. Existing commercial Ku-band satellite communications have provided alternate routing links in some cases to support emergency communications. An emergency operational capability was conceived that integrates these technologies into a rapidly deployable and transportable package that provides both local and long distance telephone services to an area that has suffered widespread telecommunications outages or has been totally isolated from the world. Author

N92-30944*# Multi-Technology Analysis and Research Corp., Washington, DC.
THE MARCOR GPS MOBILE DATA SYSTEM
Martin Rothblatt *In* JPL, Proceedings of the Workshop on Advanced Network and Technology Concepts for Mobile, Micro, and Personal Communications 15 Sep. 1991 p 287-295 (For primary document see N92-30923 21-32)
Avail: CASI HC A02/MF A03

Market research revealed several key demands for an Automatic Vehicle Location (AVL) Global Positioning System (GPS) radio. The demands were for minimization of urban building blockage, easy programmability to minimize mobile data

transmission costs, high accuracy for street map level coordination, interface capability with non-digital Specialized Mobile Radios (SMR), and a selling price close to that of alternatives such as Signposts and Loran-C. A team of experts was assembled to surmount these challenges and deliver a GPS radio for $500 to $1000, which operates at high accuracy in an urban environment and is plug-compatible with nearly all vehicle radios. Among the engineering and production breakthroughs described here are a unique Simultrac (Trademark) approach to satellite tracking, enabling up to eight GPS satellites to be used for position determination with a 2-channel receiver, and a receiver-in-a-microphone design. A powerful Application Specific Integrated Circuit (ASIC) allowed GPS to be brought within easy reach of millions of AVL users such as bus, taxi, and delivery vehicle fleets. Author

N92-30945*# Jet Propulsion Lab., California Inst. of Tech., Pasadena.
DIRECT BROADCAST SATELLITE-RADIO: PORTABLE AND MOBILE RECEPTION TRADE-OFFS
Nasser Golshan *In its* Proceedings of the Workshop on Advanced Network and Technology Concepts for Mobile, Micro, and Personal Communications 15 Sep. 1991 p 297-325 (For primary document see N92-30923 21-32)
Avail: CASI HC A03/MF A03

There has been considerable international effort in the areas of system studies, system development, and regulatory work for a Direct Broadcast Satellite Radio (DBS-R). An important milestone will be the 1992 World Radio Administrative Conference (WARC 1992) consideration of frequency allocation in the 500 - 3000 MHz range for such a service. There is an interagency agreement between Voice of America and the National Aeronautics and Space Administration for a coordinated program in DBS-R. This program includes seven tasks: systems tradeoff studies, propagation measurements, satellite experiment and demonstration, receiver development, market studies, regulatory studies, and WARC preparations. The findings of ongoing work under the first task, systems tradeoff studies, are discussed. Topics covered include digital bit rate and audio quality, propagation considerations and link margin estimates for portable reception, link margin estimates for mobile reception, coverage, and satellite size and cost estimates for a regional DBS-R coverage example. Author

N92-30946*# AfriSpace, Inc., Washington, DC.
BROADCAST SATELLITE SERVICE: THE INTERNATIONAL DIMENSION
Noah Samara *In* JPL, Proceedings of the Workshop on Advanced Network and Technology Concepts for Mobile, Micro, and Personal Communications 15 Sep. 1991 p 327-334 (For primary document see N92-30923 21-32)
Avail: CASI HC A02/MF A03

The dawn of the 1990's has witnessed the birth of a new satellite service - satellite sound broadcasting. This new service is characterized by digital transmission at data rates up to 256 kb/s from satellites in geostationary orbit to small, low-cost, mobile and portable receivers. The satellite sound broadcasting service is a logical step beyond navigation satellite service, such as that provided by the GPS Navstar system. The mass market appeal of satellite sound broadcasting in the area of lightsat technology and low-cost digital radios has greatly facilitated the financing of this type of space service. Author

N92-31007# Lawrence Livermore National Lab., CA.
ELECTRON SCATTERING AND ELECTROMAGNETIC RESPONSE PROPERTIES OF METAL CLUSTERS
V. V. Kresin (California Univ., Berkeley.) Dec. 1991 10 p Presented at the WE-Heraeus Seminar, Bad Honnef (Germany), 19-22 Nov. 1991
(Contract W-7405-eng-48)
(DE92-014715; UCRL-JC-109212; CONF-9111226-1) Avail: CASI HC A02/MF A01

The response of metal clusters to inelastic electron impact and to external electromagnetic radiation is discussed. The delocalized valence electrons play a decisive role in determining the response properties. First, a description and interpretation of an inelastic electron scattering experiment are given, and a connection to electromagnetic response studies is pointed out. Secondly, a summary of a theoretical analytical description of the response properties of metal clusters is presented. Finally, the effect of non-sphericity on the electronic properties of clusters is analyzed. DOE

N92-31129# Oregon Univ., Eugene. Dept. of Psychology.
PROCEEDINGS OF THE SYLVIA BEACH LANGUAGE COMPREHENSION CONFERENCE Final Technical Report, 15 Apr. 1990 - 14 Apr. 1992
Morton A. Gernsbacher 16 Apr. 1992 25 p Conference held in 1991
(Grant AF-AFOSR-0272-90)
(AD-A250488; AFOSR-92-0348TR) Avail: CASI HC A03/MF A01

A conference was held for internationally-known scholars in the field of language comprehension. It was a small, intense, two-and-a-half day conference in which participants had the opportunity to interact both formally and informally. Each participant gave a 30-minute talk overviewing the current state of his or her research. A thirty-minute round-table talk discussion followed each set of two talks. GRA

N92-31130# Mitre Corp., Bedford, MA.
PERFORMANCE OF GROUND-BASED HIGH-FREQUENCY RECEIVING ARRAYS WITH ELECTRICALLY-SMALL GROUND PLANES
M. M. Weiner Sep. 1991 70 p
(Mitre RP-91260)
(AD-A250489; MTR-11277) Avail: CASI HC A04/MF A01

Electrically-small ground planes degrade the performance of ground-based high-frequency receiving arrays because the arrays are more susceptible to earth multipath, ground losses, and external currents on element feed cables. Performance degradations include a reduction in element directive gain near the horizon, distortion of the element azimuthal pattern, an increase in the system internal noise factor, and increases in the array factor root-mean-squared (rms) phase error and beam-pointing errors. The advantage of electrically-small ground planes is their relatively low cost of construction and maintenance. Author (GRA)

N92-31150*# National Aeronautics and Space Administration. Langley Research Center, Hampton, VA.
FLEXIBLE HEATING HEAD FOR INDUCTION HEATING APPARATUS AND METHOD Patent Application
Robert H. Coultrip, inventor (to NASA) (Inductron Corp., Yorktown, VA.), Carl E. Copeland, inventor (to NASA) (Inductron Corp., Yorktown, VA.), Robert L. Fox, inventor (to NASA), Samuel D. Jr. Johnson, inventor (to NASA) (Inductron Corp., Yorktown, VA.), W. Morris Phillips, inventor (to NASA) (Inductron Corp., Yorktown, VA.), and John D. Buckley, inventor (to NASA) 31 Oct. 1991 17 p
(NASA-Case-LAR-14679-2; US-Patent-Appl-SN-790731) Avail: CASI HC A03/MF A01

An induction heating head includes: a length of wire having first and second opposite ends and being wound in a flat spiral shape to form an induction coil; a capacitor connected to the first and second ends of the wire, the induction coil and capacitor defining a tank circuit; and a flexible, elastomeric body molded to encase the induction coil. When a susceptor is placed in juxtaposition to the body, and the tank circuit is powered, the susceptor is inductively heated. NASA

N92-31156*# Arizona State Univ., Tempe. Coll. of Engineering and Applied Science.
ADVANCED ELECTROMAGNETIC METHODS FOR AEROSPACE VEHICLES Semiannual Progress Report, 1 Jan. - 30 Jun. 1992
Constantine A. Balanis, Weimin Sun, El-Budawy El-Sharawy, James T. Aberle, Craig R. Birtcher, Jian Peng, and Panayiotis A. Tirkas 30 Jun. 1992 63 p

(Grant NAG1-1082)
(NASA-CR-190650; NAS 1.26:190650; TRC-EM-CAB-9203)
Avail: CASI HC A04/MF A01

The Advanced Helicopter Electromagnetics (AHE) Industrial Associates Program continues its research on variety of main topics identified and recommended by the Advisory Task Force of the program. The research activities center on issues that advance technology related to helicopter electromagnetics. While most of the topics are a continuation of previous works, special effort has been focused on some of the areas due to recommendations from the last annual conference. The main topics addressed in this report are: composite materials, and antenna technology. The area of composite materials continues getting special attention in this period. The research has focused on: (1) measurements of the electrical properties of low-conductivity materials; (2) modeling of material discontinuity and their effects on the scattering patterns; (3) preliminary analysis on interaction of electromagnetic fields with multi-layered graphite fiberglass plates; and (4) finite difference time domain (FDTD) modeling of fields penetration through composite panels of a helicopter. Author

N92-31180# Massachusetts Univ., Amherst. Dept. of Electrical and Computer Engineering.
MODIFICATION OF 95 GHz RADAR SOURCE MODULE FOR LOW PHASE NOISE OPERATION Final Report
Robert E. McIntosh Nov. 1991 9 p
(Contract DAAL03-90-G-0232)
(AD-A249793; ARO-28584.1-GS-EQ) Avail: CASI HC A02/MF A01

This report describes the results of a modification to the University of Massachusetts 95 GHz polarimetric radar. This modification was done to reduce problems caused by phase noise originating from the radar's millimeter-wave oscillator. GRA

N92-31212# Computer Technology Associates, Inc., McKee City, NJ. English Creek Center.
AERONAUTICAL MOBILE SATELLITE SERVICE (AMSS) CAPACITY ANALYSIS AND PROTOCOL PERFORMANCE SIMULATION RESULTS
Thomas F. Dehel Jul. 1992 75 p Sponsored by FAA
(DOT/FAA/CT-TN90/64) Avail: CASI HC A04/MF A01

The Federal Aviation Administration (FAA) is supporting the development of standards for the use of satellite communications in aviation. As part of this support, the FAA has conducted an analysis and simulation of the Aeronautical Mobile Satellite Service (AMSS) to determine the capacity of this system to meet data requirements and to determine the message transit delay of the system under a range of conditions. The results show that a minimum AMSS ground station (which can receive four 600 bits per second (bps) R-channels and transmit on one 600 bps P-channel) will be able to support about 60 aircraft with a message (e.g., ADS position report) update rate of 5 minutes. The transit delay results show that, under the system projected bit error rate of 1 x 10 exp -5 and 15 percent channel occupancy, the transit delay will be 75 seconds or less for 99.9 percent of the messages and 40 seconds or less for 99 percent of the messages. Voice call setup delays were also determined; the transit delay time for a voice call setup message is 48 seconds or less for 99.9 percent of the calls. However, if the system bit error rate (BER) drops to the lower end of the expected range (i.e., 1 x 10 exp -4), then the probability of delivery of data messages drops below 99.9 percent. Author

33 ELECTRONICS AND ELECTRICAL ENGINEERING

Includes test equipment and maintainability; components, e.g., tunnel diodes and transistors; microminiaturization; and integrated circuitry.

For related information see also *60 Computer Operations and Hardware* and *76 Solid-State Physics.*

N92-30249# Boston Univ., MA. Dept. of Mathematics.
MATHEMATICAL MODELS OF NON-LINEAR MECHANICAL AND ELECTRICAL SYSTEMS AND THEIR QUALITATIVE BEHAVIOR Final Report, 15 Jul. - 14 Oct. 1991
Mark Levi 14 Oct. 1991 4 p
(Grant AF-AFOSR-0296-91)
(AD-A248847; AFOSR-92-0228TR) Avail: CASI HC A01/MF A01

A series of numerical experiments, which were carried out with Michael Henderson at IBM (Yorktown), uncovered a very puzzling phenomenon of phase repulsion. This effect consists of the following: when two (identical) oscillators interact, their phases actually repel: one oscillator wants to be slightly ahead or slightly behind the other; this happens despite the apparently synchronizing effect of the coupling. This phase-repulsion phenomenon was totally unexpected and a full explanation remains to be given. The principal investigator (PI) did provide an explanation in a simple case, based on estimates (he would like to find a more universal explanation of this apparently basic effect). The PI expects phase repulsion to play an interesting role in large networks of coupled oscillators. GRA

N92-30332# New Mexico Univ., Albuquerque. Dept. of Electrical Engineering and Computer Science.
BACKWARD-WAVE OSCILLATOR INVESTIGATIONS IN THE RAMAN REGIME Final Report
Edl Schamiloglu and John Gahl 29 Feb. 1992 71 p
(Grant AF-AFOSR-0393-89)
(AD-A250738; AFOSR-92-0266TR) Avail: CASI HC A04/MF A01

The short-pulse backward-wave oscillator (BWO) experiment utilizes a 600-700 KeV, 1-4 KA electron beam to generate microwave radiation due to the interaction with sinusoidally-rippled wall slow wave structures. GRA

N92-30370# Sandia National Labs., Albuquerque, NM.
ABSOLUTE SEEBECK THERMOELECTRIC CHARACTERISTICS: PRINCIPLES, SIGNIFICANCE, AND APPLICATIONS
R. P. Reed 1991 6 p Presented at the 7th International Symposium on Temperature: Its Measurement and Control in Science and Industry, Toronto (Canada), 28 Apr. - 1 May 1992
(Contract DE-AC04-76DP-00789)
(DE92-013684; SAND-91-1015C; CONF-920423-4) Avail: CASI HC A02/MF A01

The absolute Seebeck coefficient is to transport property of individual materials. Absolute properties for pairs of dissimilar materials combine in simple thermocouples to produce an effective relative Seebeck coefficient. The less familiar absolute properties are particularly useful in analysis and in materials research. Generic absolute Seebeck characteristics are known for many materials. Nevertheless, more accurate characteristics for specific primary standardized reference materials like Cu, Pb, W, and especially Pt-67, are needed for authoritative reference. Such characteristics should be formally approved by a recognized standards body for universal reference use. DOE

N92-30389*# National Aeronautics and Space Administration. Langley Research Center, Hampton, VA.
A METHOD OF MAKING A SINGLE LAYER MULTI-COLOR LUMINESCENT DISPLAY Patent Application
James B. Robertson, inventor (to NASA) 24 Mar. 1992 13 p
(NASA-Case-LAR-14811-1; NAS 1.71:LAR-14811-1;
US-Patent-Appl-SN-858176) Avail: CASI HC A03/MF A01

The invention is a method of forming a multi-color luminescent display including the steps of depositing on an insulator substrate a smooth single layer of host material which itself may be a phosphor with the properties to host varying quantities of different impurities and introducing one or more of said different impurities into selected areas of the single layer of host material via an appropriately positioned mask as by thermal diffusion or ion-implantation to form a pattern of phosphors of different colors in the single layer of host material such that the top surface of the host layer remains smooth. Red phosphors are formed by adding impurities selected from the group consisting of Sm, SmF3, Eu, EuF3, and ZnS:MnTbF3 to a ZnS host; green phosphors by adding impurities selected from the group consisting of Tb and TbF3 to a ZnS host; and blue phosphors by adding impurities selected from the group consisting of Tm, Al, Ag, and Mg to a ZnS host. NASA

N92-30397*# National Aeronautics and Space Administration. Lewis Research Center, Cleveland, OH.

COMPARISON OF HIGH TEMPERATURE, HIGH FREQUENCY CORE LOSS AND DYNAMIC B-H LOOPS OF A 2V-49Fe-49Co AND A GRAIN ORIENTED 3Si-Fe ALLOY

W. R. Wieserman (Pittsburgh Univ., Johnstown, PA.), G. E. Schwarze, and J. M. Niedra (Sverdrup Technology, Inc., Cleveland, OH.) Aug. 1992 9 p Presented at the 27th Intersociety Energy Conversion Engineering Conference, San Diego, CA, 3-7 Aug. 1992; sponsored by SAE, ACS, AIAA, ASME, IEEE, AIChE, and ANS

(RTOP 590-13-31)

(NASA-TM-105791; E-7221; NAS 1.15:105791) Avail: CASI HC A02/MF A01

The design of power magnetic components such as transformers, inductors, motors, and generators, requires specific knowledge about the magnetic and electrical characteristics of the magnetic materials used in these components. Limited experimental data exists that characterizes the performance of soft magnetic materials for the combined conditions of high temperature and high frequency over a wide flux density range. An experimental investigation of a 2V-49-Fe-49Co (Supermendur) and a grain oriented 3 Si-Fe (Magnesil) alloy was conducted over the temperature range of 23 to 300 C and frequency range of 0.1 to 10 kHz. The effects of temperature, frequency, and maximum flux density on the core loss and dynamic B-H loops for sinusoidal voltage excitation conditions are examined for each of these materials. A comparison of the core loss of these two materials is also made over the temperature and frequency range investigated. Author

N92-30427*# National Aeronautics and Space Administration. Lewis Research Center, Cleveland, OH.

WIRING FOR AEROSPACE APPLICATIONS

J. L. Christian, Jr., J. E. Dickman, R. W. Bercaw, I. T. Myers, A. N. Hammoud (Sverdrup Technology, Inc., Brook Park, OH.), M. Stavnes (Sverdrup Technology, Inc., Brook Park, OH.), and J. Evans (National Aeronautics and Space Administration, Washington, DC.) Jul. 1992 9 p Presented at the 1992 Power Electronics Specialist Conference, Toledo (Spain), 29 Jun. - 3 Jul. 1992; sponsored by IEEE

(RTOP 323-57-4A)

(NASA-TM-105777; E-7204; NAS 1.15:105777) Avail: CASI HC A02/MF A01

In this paper, the authors summarize the current state of knowledge of arc propagation in aerospace power wiring and efforts by the National Aeronautics and Space Administration (NASA) towards the understanding of the arc tracking phenomena in space environments. Recommendations will be made for additional testing. A database of the performance of commonly used insulating materials will be developed to support the design of advanced high power missions, such as Space Station Freedom and Lunar/Mars Exploration. Author

N92-30503# Technische Univ., Berlin (Germany, F.R.). Fachbereich Elektrotechnik.

COMPARISON OF SIGNAL PROCESSING METHODS FOR ESTIMATION OF NETWORK IMPEDANCE FOR REMOTE PROTECTION Ph.D. Thesis [VERGLEICH VON SIGNALVERARBEITUNGSMETHODEN ZUR BESTIMMUNG DER NETZIMPENDANZ FUER DEN DISTANZSCHUTZ]

Thomas Reck 1991 180 p In GERMAN

(ETN-92-91686) Avail: CASI HC A09/MF A02

The improvement of selectivity and velocity of the protection systems in energy supply networks is investigated. The structure and the functioning of the electronic distance protection relay in an analog switching technique are described, and calculation possibilities for asymmetric defects are presented. A network short circuit model was developed to depict the influence of nonlinear and nonideal signal distortions. Comparative examinations of several impedance identification processes in the frequency and time areas are carried out. The linear differential equation for a condition model is solved by filtering and with linear estimation processes based on the least squares method and recursive processes. Autoregressive and moving average formulations for perturbation models are presented. The difference in convergence behavior of the studied processes is found to be neglectable. ESA

N92-30537# California Univ., Los Angeles.

EVIDENCE FOR THE DEPENDENCE OF THE SPUTTER YIELD OF GRAPHITE ON ION BOMBARDMENT FLUENCE Technical Report, 1 Jun. 1991 - 31 May 1992

E. J. Snyder, D. A. Baugh, R. S. Williams, E. A. Eklund, and M. S. Anderson 31 May 1992 16 p

(Contract N00014-90-J-1178)

(AD-A252500; TR-19) Avail: CASI HC A02/MF A01

The scanning tunneling microscope (STM) and the atomic force microscope (AFM) were both used to study the evolution of the morphology of graphite (0001) surfaces etched with 5 keV Ar+ ions as a function of both ion beam flux and fluence. STM and AFM topographs collected after ion beam exposure show surface features that increase in average size as a function of ion beam fluence, but which have a non-monotonic dependence on ion beam flux. Furthermore, the surface roughness does not follow a square root dependence with respect to the ion fluence, as expected for a stochastic process. One explanation for this behavior is that the sputter yield for graphite is a function of the ion beam fluence. GRA

N92-30542*# National Aeronautics and Space Administration. Pasadena Office, CA.

HYBRIDIZATION OF DETECTOR ARRAY AND INTEGRATED CIRCUIT FOR READOUT Patent Application

Eric R. Fossum, inventor (to NASA) (Jet Propulsion Lab., California Inst. of Tech., Pasadena.) and Frank J. Grunthaner, inventor (to NASA) (Jet Propulsion Lab., California Inst. of Tech., Pasadena.) 29 Apr. 1992 18 p

(Contract NAS7-918)

(NASA-Case-NPO-18062-1-CU; NAS 1.71:NPO-18062-1-CU; US-Patent-Appl-SN-877966) Avail: CASI HC A03/MF A01

A process is explained for fabricating a detector array in a layer of semiconductor material on one substrate and an integrated readout circuit in a layer of semiconductor material on a separate substrate in order to select semiconductor material for optimum performance of each structure, such as GaAs for the detector array and Si for the integrated readout circuit. The detector array layer is lifted off its substrate, laminated on the metallized surface on the integrated surface, etched with reticulating channels to the surface of the integrated circuit, and provided with interconnections between the detector array pixels and the integrated readout circuit through the channels. The adhesive material for the lamination is selected to be chemically stable to provide electrical and thermal insulation and to provide stress release between the two structures fabricated in semiconductor materials that may have different coefficients of thermal expansion. NASA

N92-30590# Allied-Signal Aerospace Co., Kansas City, MO.
PRINTED TRANSFORMER PROCESS/PRODUCT IMPROVEMENTS
R. R. Penniston Jun. 1992 46 p
(Contract DE-AC04-76DP-00613)
(DE92-014760; KCP-613-4701) Avail: CASI HC A03/MF A01

Production yields for the printed transformer were averaging 10-20 percent for the two years previous to the body of work. Areas of production contributing to poor performance included machining, imaging, and plating. Process improvements in each area were identified. Implementation of these improvements had begun when a more serious problem with the function of the units was identified. Excessive next assembly electrical failures were occurring due to a stress failure in the transformer lead. The balance of work performed against this project dealt with the improvements in processing transformers with a thicker lead. After all improvements were implemented, production yields at the transformer level rose to 70 percent. DOE

N92-30598# Pennsylvania State Univ., University Park. Materials Research Lab.
RELAXOR FERROELECTRICS FOR ELECTROSTRICTIVE TRANSDUCER Quarterly Report, Sep. 1991 - 31 Jan. 1992
Thomas R. Shrout and Sei-Joo Jang 31 Jan. 1992 32 p
(Contract N00014-90-J-4077)
(AD-A248671) Avail: CASI HC A03/MF A01

The objective of this program is to investigate the potential of electrostrictive actuator materials for use in NAVY-type sonar. The anticipated performance requirements for such materials is summarized in the following: Operating temperature range 0-30 C; High sensitivity; Large E-field induced strain; Minimal hysteresis and low loss; Frequency of operation; and Mechanically stiff (low compliance). Additional requirements include operational E-field strain under prestress, and duty cycles. GRA

N92-30617# Stanford Univ., CA. Center for Materials Research.
GROWTH AND EVALUATION OF NONLINEAR OPTICAL MATERIALS FOR LASER APPLICATIONS: BARIUM BORATE, LITHIUM BORATE, AND SILVER GALLIUM SELENIDE Report, 1 Aug. 1990 - 31 Jan. 1992
Robert S. Feigelson, Roger K. Route, Ekkes Brueck, N. H. Kim, and H. Lee 31 Jan. 1992 3 p
(Contract N00014-90-J-4092)
(AD-A248861) Avail: CASI HC A01/MF A01

A major goal of this program is to develop processes that industry can use to grow large high quality B-barium borate (BBO) and lithium triborate (LBO) crystals with good yield. High optical quality single crystals of both are currently being grown by modified top-seeded solution growth (TSSG) methods using sodium oxide and boric oxide, respectively, as solvents. This advanced TSSG growth technology has been transferred to both INRAD, Inc. and Cleveland Crystals, Inc. during the course of the program. The development of a phenomenological model which accurately predicts the growth rate in these systems has allowed us to grow cylindrical boules of both in multi-centimeter lengths, which has not previously been possible by the TSSG method. The crystal growth process is also being monitored by a high resolution weight sensing system which verifies system parameters. Development of a control algorithm using the growth rate model and real time weight sensing is being pursued in order to develop a totally automatic diameter control process. Additional research has focused on reducing the density of solvent inclusions in flux-grown barium borate by optimizing forced convective stirring in the melts and by understanding the effects of melt chemistry. GRA

N92-30619# Dayton Univ., OH.
EVALUATION OF DOPED POLYETHYLENE OXIDE AS SOLID ELECTROLYTE FOR POLYMER BATTERIES Final Report, 1 Aug. - 31 Oct. 1991
A. K. Sircar, P. T. Weissman, and B. Kumar Feb. 1992 59 p
(Contract F33615-87-C-2714)
(AD-A249501; UDR-TR-91-135; WL-TR-91-2139) Avail: CASI HC A04/MF A01

This report presents results of an investigation on the preparation and characterization of polyethylene oxide (PEO) and lithium tetrafluoroborate (LiBF4) complexes for application as solid electrolytes in polymer batteries. AC conductivity and permittivity (dielectric constant) were measured as functions of frequency, temperature, and concentration of lithium tetrafluoroborate (LiBF4) in polyethylene oxide (PEO) films. Differential Scanning Calorimetry (DSC) was used to trace changes of the morphology of the polymeric medium. Thermogravimetry (TG) and derivative thermogravimetry (DTG) were used to follow the decomposition of components and to define the maximum temperature limits for these measurements. Infrared Spectroscopy monitored structural evolution as the O:Li ratio in the polymer complex was varied. Thin films of a complex (O:Li = 8) were used to assemble Li/Polymer/Li Cell for electrochemical characterization. The study showed that the relationship of dopant concentration to electrical properties is rather complex. Degree of ion-pairing, dissociation of ions on dilution, changes in the morphology of the polymeric medium, and variations in viscosity and its consequence on ion mobility were considered to explain the data. An optimum in room conductivity occurred in a complex with O:Li ratio of 8. GRA

N92-30630# Pennsylvania Univ., Philadelphia. Dept. of Physics.
FIRST-PRINCIPLES COMPUTATIONAL STUDIES OF ALKALI-DOPED C60 FULLERIDES Final Technical Report, 1 Jan. 1991 - 1 Jan. 1992
Steven C. Erwin 6 Apr. 1992 10 p
(Contract N00014-91-J-1265)
(AD-A249018) Avail: CASI HC A02/MF A01

The discovery of superconductivity at 18 K in a potassium-doped fullerene solid, K(sub x)C60, is reported. This marked a major turning point in the young history of the C60 molecule 'buckminsterfullerene': from a hypothetical molecule (1985), to small-scale (mg) production of crystalline powders (1988), to large-scale synthesis (1990), to a material with the highest transition temperature of any molecular superconductor. This history represents only one of many research lines. Concurrently with the work at AT and T on partial doping, researchers at the Laboratory for Research on the Structure of Matter at the University of Pennsylvania were doping solid C60 to saturation with potassium. The resulting pure phase, K6C60, was characterized by x-ray diffraction in Apr. 1991: the lattice was body-centered cubic, with the C60 molecules essentially undistorted, orientationally ordered, and each surrounded by a cage of 24 K atoms. Nothing was known about the electronic structure at this early stage. GRA

N92-30678# Polytechnic Univ., Farmingdale, NY.
NONEQUILIBRIUM BEHAVIOR OF CARRIERS IN SEMICONDUCTORS SUBJECTED TO STRONG SPACE-TIME VARYING FIELDS Final Technical Report, 1 Dec. 1989 - 30 Nov. 1991
Erich E. Kunhardt Dec. 1991 83 p
(Grant AF-AFOSR-0069-90)
(AD-A246961; AFOSR-92-0095TR) Avail: CASI HC A05/MF A01

During this funding period, the macrokinetic theory for electron transport (developed for semiconductors during the previous funding period) was implemented for multivalley semiconductors. The model was applied to GaAs subjected to rapidly varying (in time) fields. The set of material parameters used was obtained by minimizing the error between calculated and measured transport parameters over the range of values of the applied field for which experimental results are available. An experimental facility for investigating the transient dynamics of high power semiconducting switches was established. GRA

N92-30683# Defence Research Establishment, Ottawa (Ontario).
THE TEMPERATURE DEPENDENCE OF A LARGE DYNAMIC RANGE PHOTODETECTOR STRUCTURE

Robert J. Inkol Dec. 1991 25 p
(AD-A247667; DREO-TN-91-35) Avail: CASI HC A03/MF A01

A recently developed photodetector circuit exploits the exponential voltage-to-current characteristic of a MOSFET operated in the subthreshold region to achieve a logarithmic steady state response. This paper analyzes the temperature dependence of the circuit operation and presents experimental results demonstrating the capabilities and limitations of the model. GRA

N92-30702# Institut National Polytechnique, Grenoble (France). Lab. de Modelisation et Calcul.

CONTRIBUTION OF PARALLELISM TO SOLVING A LOAD DISTRIBUTION PROBLEM IN ELECTRIC NETWORKS Ph.D. Thesis [CONTRIBUTION DU PARALLELISME A LA RESOLUTION D'UN PROBLEME DE REPARTITION DE CHARGE DANS LES RESEAUX ELECTRIQUES]

Jean-Yves Blanc 1991 211 p In FRENCH
(ETN-92-91668) Avail: CASI HC A10/MF A03

The parallelization of a load distribution problem in electric networks which corresponds mathematically to successive solving of linear systems with close matrices is addressed. A solution in a sequential framework is presented and a parallelization on several types of architecture (vector Multiple Instruction Multiple Data Stream (MIMD), massively parallel Single Instruction Multiple Data Stream (SIMD), and reconfigurable topology MIMD) is proposed. The target machines are studied and theoretically modeled. Several ideas for parallelization are considered. An interesting finding is that the best solution methods (i.e. the fastest) are different according to the parallel machine considered. ESA

N92-30729# Technische Univ., Delft (Netherlands).

QUANTUM INTERFERENCE AND CONFINEMENT EFFECTS IN NARROW CHANNEL Si-MOSFET's Ph.D. Thesis

Jianrong Gao 1991 120 p
(ETN-92-91742) Avail: CASI HC A06/MF A02

Weak localization, universal conductance fluctuations and quantum confinement effects are reviewed. Fabrication processes developed to realize the narrow channel devices required for transport studies are presented. The temperature dependence of universal fluctuations in the magnetoconductance, together with weak localization measurements in single narrow channel Metal Oxide Semiconductor Field Effect Transistors (MOSFET's) are described. The temperature dependence of universal fluctuations in the conductance is presented as a function of Fermi energy in the same devices. Measurements of one dimensional confinement effects in the magnetoconductance of multiple quantum wires in Si-MOSFETs including the first observation of the magnetic depopulation of one dimensional subbands in a Si quantum wire device are given. For individual titles, see N92-30730 through N92-30732.

N92-30730# Technische Univ., Delft (Netherlands). Delft Inst. for Microelectronics and Submicron Technology.

TEMPERATURE DEPENDENCE OF UNIVERSAL CONDUCTANCE FLUCTUATIONS IN NARROW Si INVERSION LAYERS

Jianrong Gao, J. Caro, A. H. Verbruggen, S. Radelaar, and J. Middelhoek (Universiteit Twente, Enschede, Netherlands) *In its* Quantum Interference and Confinement Effects in Narrow Channel Si-MOSFET's 1991 p 39-56 Repr. from Phys. Rev. B, v. 40, 1989 p 11,676 (For primary document see N92-30729 21-33)
Avail: CASI HC A03/MF A02

The temperature dependence of magnetoconductance fluctuations in narrow mesoscopic silicon inversion layers (lengths 4.3 micrometers, width 0.14 and 0.43 micrometers) was studied. The magnitude and magnetic correlation length of the fluctuations was measured in the temperature range T = 0.2 to 4.2 K and for magnetic fields up to 3 T. Weak localization experiments were performed for an independent determination of the inelastic diffusion length L(sub in). When L(sub in) exceeds the channel width W (quasi one dimensional) the experimental temperature dependence of the fluctuation amplitude and magnetic correlation length is very well described by the theory for universal conductance fluctuations of Lee and Stone. In the case of L(sub in) less than W (quasi two dimensional) a good agreement with this theory is found for the temperature dependence of the fluctuation amplitude. ESA

N92-30731# Technische Univ., Delft (Netherlands). Delft Inst. for Microelectronics and Submicron Technology.

ONE-DIMENSIONAL SUBBAND EFFECTS IN THE CONDUCTANCE OF MULTIPLE QUANTUM WIRES IN Si-MOSFET'S

Jianrong Gao, C. deGraaf, J. Caro, S. Radelaar, M. Offenberg (Technische Hochschule, Aachen, Germany, F.R.), V. Lauer (Technische Hochschule, Aachen, Germany, F.R.), J. Singleton (Nijmegen Univ., Netherlands), T. J. B. M. Janssen (Nijmegen Univ., Netherlands), and J. A. A. J. Perenboom (Nijmegen Univ., Netherlands) *In its* Quantum Interference and Confinement Effects in Narrow Channel Si-MOSFET's 1991 p 71-80 Repr. from Phys. Rev. B, v. 41, 1990 p 12,315 (For primary document see N92-30729 21-33)
Avail: CASI HC A02/MF A02

The electrical transport in narrow (60 to 80 nm), parallel multiple quantum wires in Si Metal Oxide Semiconductor Field Effect Transistors (MOSFETs) was studied at 0.2 K as a function of gate voltage in zero magnetic field and in fields up to 20 T. The conductance of the multiple wires as a function of gate voltage shows well resolved structures due to successive population of one dimensional subbands. In addition, quantum oscillations in the gate voltage derivative of the conductance as a function of magnetic field show, for the first time in a Si MOSFET, characteristics due to magnetic depopulation of one dimensional subbands. ESA

N92-30732# Technische Univ., Delft (Netherlands). Delft Inst. for Microelectronics and Submicron Technology.

ENHANCEMENT OF WEAK LOCALIZATION IN A Si LATERAL SUPERLATTICE DEVICE

Jianrong Gao, J. Caro, C. deGraaf, S. Radelaar, and K. Heyers (Technische Hochschule, Aachen, Germany, F.R.) *In its* Quantum Interference and Confinement Effects in Narrow Channel Si-MOSFET's 1991 p 81-93 Submitted for publication (For primary document see N92-30729 21-33)
Avail: CASI HC A03/MF A02

It is found, for the first time, that Weak Localization (WL) in a Lateral Superlattice (LSL) is considerably enhanced compared to the homogeneous two dimensional case. The enhancement increases with the strength of the potential modulation and its maximum value deduced from the experiments is 2.3. This superlattice effect in the WL was studied by measuring the low field magnetoconductance of a superlattice Metal Oxide Semiconductor Field Effect Transmitter (MOSFET) in dependence of the strength of the potential modulation. The results qualitatively agree with a recent theory of WL in a LSL. By varying the gate voltage over a wide range a clear cross over from one dimensional WL in the quantum wire mode of the device to two dimensional WL in the superlattice mode was observed. ESA

N92-30757*# Motorola, Inc., Chandler, AZ. Strategic Electronics Div.

SOFTWARE BREADBOARD STUDY Final Report

C. Nuckolls and Mark Frank 31 Jan. 1990 177 p
(Contract JPL-958596)
(NASA-CR-190473; JPR-9950-1370; NAS 1.26:190473) Avail: CASI HC A09/MF A02

The overall goal of this study was to develop new concepts and technology for the Comet Rendezvous Asteroid Flyby (CRAF), Cassini, and other future deep space missions which maximally conform to the Functional Specification for the NASA X-Band Transponder (NXT), FM513778 (preliminary, revised July 26, 1988). The study is composed of two tasks. The first task was to investigate a new digital signal processing technique which involves the processing of 1-bit samples and has the potential for significant size, mass, power, and electrical performance improvements over conventional analog approaches. The entire X-band receiver

tracking loop was simulated on a digital computer using a high-level programming language. Simulations on this 'software breadboard' showed the technique to be well-behaved and a good approximation to its analog predecessor from threshold to strong signal levels in terms of tracking-loop performance, command signal-to-noise ratio and ranging signal-to-noise ratio. The successful completion of this task paves the way for building a hardware breadboard, the recommended next step in confirming this approach is ready for incorporation into flight hardware. The second task in this study was to investigate another technique which provides considerable simplification in the synthesis of the receiver first LO over conventional phase-locked multiplier schemes and in this approach, provides down-conversion for an S-band emergency receive mode without the need of an additional LO. The objective of this study was to develop methodology and models to predict the conversion loss, input RF bandwidth, and output RF bandwidth of a series GaAs FET sampling mixer and to breadboard and test a circuit design suitable for the X and S-band down-conversion applications. Author

N92-30764# Sandia National Labs., Albuquerque, NM.
ANALYSIS OF A DIGITAL RF MEMORY IN A SIGNAL-DELAY APPLICATION
D. A. Jelinek Mar. 1992 31 p
(Contract DE-AC04-76DP-00789)
(DE92-013457; SAND-92-0448) Avail: CASI HC A03/MF A01

Laboratory simulation of the approach of a radar fuze towards a target is an important factor in our ability to accurately measure the radar's performance. This simulation is achieved, in part, by dynamically delaying and attenuating the radar's transmitted pulse and sending the result back to the radar's receiver. Historically, the device used to perform the dynamic delay has been a limiting factor in the evaluation of a radar's performance and characteristics. A new device has been proposed that appears to have more capability than previous dynamic delay devices. This device is the digital RF memory. This report presents the results of an analysis of a digital RF memory used in a signal-delay application. DOE

N92-30807# Sandia National Labs., Albuquerque, NM.
TESTING OF DOUBLE-LAYER CAPACITORS FOR HIGH RELIABILITY APPLICATIONS
N. H. Clark 1992 4 p Presented at the 35th International Power Sources Symposium, Cherry Hill, NJ, 22-23 Jun. 1992
(Contract DE-AC04-76DP-00789)
(DE92-011384; SAND-92-0736C; CONF-920669-4) Avail: CASI HC A01/MF A01

Double Layer Capacitors (DLCs) have been used mainly for computer memory backup in consumer products during the last ten years. Their high capacitance density along with maintenance-free operation makes them suited for these applications. In recent years users, mostly military customers, have expressed interest in using them in high reliability applications both for backup power and pulse power applications. To meet this need developers have pursued technologies that use carbon and mixed metal oxides as the electrode material to produce high reliability DLCs. In this paper, the carbon based DLCs were manufactured by Evans Co. and the Mixed Metal Oxide (MMO) DLCs by Pinnacle Research Inc. There are few published data on their reliability in adverse environments. This paper demonstrates their environmental stability in temperature, shock, vibration and linear acceleration. The purpose of this paper is to review the available test data for both types of DLCs under these stress conditions. The data for this paper was generated by Sandia National Laboratories, General Electric Neutron Devices Division, Motorola Company and Evans Company. DOE

N92-30813# California Univ., Berkeley. Lawrence Berkeley Lab.
PROPERTIES OF CMOS DEVICES AND CIRCUITS FABRICATED ON HIGH-RESISTIVITY, DETECTOR-GRADE SILICON
S. Holland Nov. 1991 5 p Presented at the IEEE Nuclear Science Symposium, Santa Fe, NM, 5-9 Nov. 1991
(Contract DE-AC03-76SF-00098)
(DE92-011727; LBL-31596; CONF-911106-93) Avail: CASI HC A01/MF A01

A complementary metal oxide semiconductor (CMOS) process that is compatible with silicon p-i-n radiation detectors has been developed and characterized. A total of twelve mask layers are used in the process. The NMOS device is formed in a retrograde well while the PMOS device is fabricated directly in the high-resistivity silicon. Isolation characteristics are similar to a standard foundary CMOS process. Circuit performance using 3 micro-m design rules has been evaluated. The measured propagation delay and power-delay product for a 51-stage ring oscillator was 1.5 nano-s and 43 fJ, respectively. Measurements on a simple cascode amplifier results in a gain-bandwidth product of 200 MHz at a bias current of 15 micro-A. The input-referred noise of the cascode amplifier is 20 nV/(radical)Hz at 1 MHz. DOE

N92-30836# Raytheon Co., Lexington, MA. Research Div.
RF VACUUM MICROELECTRONICS Quarterly Progress Report No. 1, 1 Jan. - 31 Mar. 1992
Alan Palevsky 23 Apr. 1992 6 p
(Contract MDA972-91-C-0032; ARPA Order 8162)
(AD-A249814; RAY/RD/S-4752) Avail: CASI HC A02/MF A01

The status of research and development on field emission array cathodes for RF vacuum microelectronics is presented. The dc emission characteristics have improved. Designs for high frequency circuits are complete and are being fabricated. GRA

N92-30842# Kansas State Univ., Manhattan.
ELECTRIC VEHICLE SITE OPERATOR PROGRAM
1992 106 p
(Contract DE-FC07-91ID-13074)
(DE92-014591; DOE/ID-13074/T3) Avail: CASI HC A06/MF A02

Kansas State University, with funding support from federal, state, public, and private companies, is participating in the Department of Energy's Electric Vehicle Site Operator Program. Through participation is this program, Kansas State is demonstrating, testing, and evaluating electric or hybrid vehicle technology. This participation will provide organizations the opportunity to examine the latest EHV prototypes under actual operating conditions. KSU proposes to purchase one electric or hybrid van and four electric cars during the first two years of this five year program. KSU has purchased one G-Van built by Conceptor Industries, Toronto, Canada and has initiated a procurement order to purchase two Soleq 1992 Ford EVcort stationwagons. DOE

N92-30851# Naval Research Lab., Washington, DC.
NANOSCIENCE AND NANOTECHNOLOGY
William M. Tolles 5 May 1992 87 p
(AD-A250376; NRL/MR/1003-92-6989) Avail: CASI HC A05/MF A01

This document reviews the research area of nanoscience/nanotechnology, both within and outside of NRL. Rapid developments in frontiers related to miniaturization have taken place in the last several years, in microelectronics and microelectronic devices, optical materials, biotechnology, structural materials, tunneling tip microscopy (and the field of proximal probes), and microelectromechanical systems (MEMS). Important developments are expected for electronics and computers, sensors, materials, biological behavior, and a number of devices. An overview of these areas is preliminary to examining priorities for investment in this field. This document is an attempt to provide an overview of these diverse efforts, particularly where the Naval Research Laboratory has significant interests. GRA

N92-30901# Indiana Univ., Bloomington.
HIGH RESOLUTION ELECTRON ENERGY LOSS STUDIES OF SURFACE VIBRATIONS
L. L. Kesmodel May 1992 10 p

(Contract DE-FG02-84ER-45147)
(DE92-014608; DOE/ER-45147/7) Avail: CASI HC A02/MF A01

New experimental studies of the surface vibrational properties of materials with high-resolution electron energy loss spectroscopy (EELS) are reported. This document summarizes recent progress on the following: surface phonon dispersion measurements on copper (001) and silver (001) and (111); oxygen adsorption on ultrathin films of cobalt and nickel, and aluminum on silicon (111); and copper-oxide based superconductors. DOE

N92-30902*# National Aeronautics and Space Administration. Marshall Space Flight Center, Huntsville, AL.
A STUDY OF ENHANCING CRITICAL CURRENT DENSITIES (J(SUB c)) AND CRITICAL TEMPERATURE (T(SUB c)) OF HIGH-TEMPERATURE SUPERCONDUCTORS Final Report
Marcus Vlasse Aug. 1992 43 p
(Proj. 90-N26)
(NASA-TM-103595; NAS 1.15:103595) Avail: CASI HC A03/MF A01

The development of pure phase 123 and Bi-based 2223 superconductors has been optimized. The pre-heat processing appears to be a very important parameter in achieving optimal physical properties. The synthesis of pure phases in the Bi-based system involves effects due to oxygen partial pressure, time, and temperature. Orientation/melt-sintering effects include the extreme c-axis orientation of Yttrium 123 and Bismuth 2223, 2212, and 2201 phases. This orientation is conductive to increasing critical currents. A procedure was established to substitute Sr for Ba in Y-123 single crystals. Author

N92-31004# Massachusetts Inst. of Tech., Cambridge. Research Lab. of Electronics.
FOCUSED ION BEAM IMPLANTATION Final Report, 1 Aug. 1988 - 31 Dec. 1991
John Melngailis 17 Mar. 1992 27 p
(Contract DAAL03-88-K-0108)
(AD-A249662; ARO-26051.5-EL) Avail: CASI HC A03/MF A01

The goals of this research program were to develop devices fabricated by focused ion beam implantation, such as tunable Gunn diodes, GaAs MESFET'S, silicon MOSFET's or other novel devices, and to advance the focused ion beam technology. All the goals were reached and are reported in this report. GRA

N92-31107# Los Alamos National Lab., NM.
PROCEEDINGS, PHENOMENOLOGY AND APPLICATIONS OF HIGH TEMPERATURE SUPERCONDUCTORS
K. S. Bedell 1991 527 p Presented at the Phenomenology and Applications of High Temperature Superconductivity, Los Alamos, NM, 22-24 Aug. 1991
(Contract W-7405-eng-36)
(DE92-011133; LA-UR-92-922; CONF-9108140) Avail: CASI HC A23/MF A04

Phenomenology and Applications of High Temperature Superconductors, The Los Alamos Symposium: 1991, was sponsored by the Los Alamos National Laboratory, Center for Materials Science, the Advanced Studies Program on High Temperature Superconductivity Theory (ASP), and the Exploratory Research and Development Center. This is the second symposium in the series. High Temperature Superconductivity, The Los Alamos Symposium: 1989, also published by Addison Wesley, focused on the cutting-edge theoretical and experimental issues in high temperature superconductors. This symposium, with its focus on the phenomenology and applications of high temperature superconductors, gives a complementary review of the aspects of the field closely related to the impact of high temperature superconductors on technology. The objective of ASP is to advance the field on a broad front with no specific point of view by bringing a team of leading academic theorists into a joint effort with the theoretical and experimental scientists of a major DOE national laboratory. The ASP consisted of fellows led by Robert Schrieffer (UCSB and now FSU) joined by David Pines (University of Illinois), Elihu Abrahams (Rutgers), Sebastian Doniach (Stanford), and Maurice Rice (ETH, Zurich) and theoretical and experimental staff of Los Alamos National Laboratory. This synergism of academic, laboratory, theoretical, and experimental research produced a level of interaction and excitement that would not be possible otherwise. This publication and the previous one in the series are just examples of how this approach to advancing science can achieve significant contributions. DOE

N92-31144# Allied-Signal Aerospace Co., Kansas City, MO.
TRANSFER SOLDERING EVALUATION
G. A. Becka May 1992 180 p
(Contract DE-AC04-76DP-00613)
(DE92-015160; KCP-613-4749) Avail: CASI HC A09/MF A02

Transfer soldering is a hand-soldering technique used to complete printed wiring board (PWB) or wire-to-terminal joints. The technique consists of carrying enough molten solder on a soldering iron tip to fill the connection. This evaluation compares PWB solder joints made by transfer soldering to those made by the conventional technique (as defined in documents such as MIL-STD-2000). Physical and metallurgical properties were compared between the two techniques. Also the potential degradation from thermal cycling of joints made by the two techniques was compared. Results from these tests confirm that there is no difference in reliability between transfer-soldered joints and conventional hand-soldered joints. DOE

N92-31210# Louisiana State Univ., Baton Rouge. Dept. of Physics and Astronomy.
QUANTUM TRANSPORT, NOISE AND NON-LINEAR DISSIPATIVE EFFECTS IN ONE- AND TWO-DIMENSIONAL SYSTEMS AND ASSOCIATED SUB-MICRON AND NANOSTRUCTURE DEVICES Final Report, 1 Oct. 1989 - 31 Dec. 1991
R. F. OConnell 1992 11 p
(Contract N00014-86-J-1124)
(AD-A250895) Avail: CASI HC A03/MF A01

The underlying theme of most of our research has been transport and noise phenomena in sub-micron systems and devices. This subject is of interest for both basic and technological reasons. It is now well-recognized that many interesting quantum phenomena come into play in the so-called mesoscopic regime. Whereas in the past we placed emphasis on the development of optimum techniques, our present thrust has been geared toward applications of same. The main thrust of the research was concerned with semiconductor quantum wires, and special emphasis was placed on analyzing the relevant experiments. GRA

N92-30275*# State Univ. of Southeast Missouri, Cape Girardeau. Dept. of Physics.
DIELECTRIC BEHAVIOR OF SEMICONDUCTORS AT MICROWAVE FREQUENCIES
Jai N. Dahiya *In* NASA. Langley Research Center, National Educators' Workshop: Update 1991. Standard Experiments in Engineering Materials Science and Technology Jun. 1992 p 171-185 (For primary document see N92-30263 21-29)
Avail: CASI HC A03/MF A03

34 FLUID MECHANICS AND HEAT TRANSFER

Includes boundary layers; hydrodynamics; fluidics; mass transfer; and ablation cooling.

For related information see also *02 Aerodynamics* and *77 Thermodynamics and Statistical Physics.*

N92-30297*# National Aeronautics and Space Administration. Lewis Research Center, Cleveland, OH.
NUMERICAL SOLUTION OF A THREE-DIMENSIONAL CUBIC CAVITY FLOW BY USING THE BOLTZMANN EQUATION
Danny P. Hwang Jul. 1992 17 p Presented at the 18th International Symposium on Rarefied Gas Dynamics, Vancouver,

British Columbia, 26-31 Jul. 1992; sponsored in part by British Columbia Univ. Original contains color illustrations
(RTOP 505-62-20)
(NASA-TM-105693; E-7080; NAS 1.15:105693) Avail: CASI HC A03/MF A01; 2 functional color pages

A three-dimensional cubic cavity flow has been analyzed for diatomic gases by using the Boltzmann equation with the Bhatnagar-Gross-Krook (B-G-K) model. The method of discrete ordinate was applied, and the diffuse reflection boundary condition was assumed. The results, which show a consistent trend toward the Navier-Stokes solution as the Knudson number is reduced, give us confidence to apply the method to a three-dimensional geometry for practical predictions of rarefied-flow characteristics. The CPU time and the main memory required for a three-dimensional geometry using this method seem reasonable.
Author

N92-30358# Technische Univ., Delft (Netherlands). Faculty of Technical Mathematics and Information.
THE DIFFRACTION OF SHORT FREE SURFACE WATER WAVES, A UNIFORM EXPANSION
A. J. Hermans 1992 27 p
(Rept-92-06; ISSN-0922-5641; ETN-92-91858) Copyright Avail: CASI HC A03/MF A01

A mathematical tool to improve the optimal design of ship forms is provided. It is common practice that hull forms are designed such that they have minimal wave resistance in calm water. A theory is described by which the effect of short waves may be incorporated. The basic tool used is the ray theory. The appropriate free surface condition is shown and the standard ray method, well known in geometric optics, is formulated in the fluid region and at the free surface. After an elimination process, the eikonal equation and the transport equation are obtained. The characteristic equations for the nonlinear eikonal equations are derived, keeping in mind that the characteristics (rays) are not perpendicular to the wave fronts, due to the influence of the double body potential generated by the slow forward speed of the ship, which is assumed to be a good approximation for the steady potential. Numerical integration of the ray equations lead to the ray pattern. After some manipulations the amplitude may be computed just as well. The second order mean force or added resistance is calculated.
ESA

N92-30372# Technische Univ., Delft (Netherlands). Faculty of Technical Mathematics and Information.
GLOBAL EXISTENCE FOR A SEMILINEAR ELLIPTIC-PARABOLIC PDE SYSTEM
Shuanhu Li 1991 17 p
(Rept-91-70; ISSN-0922-5641; ETN-92-91820) Copyright Avail: CASI HC A03/MF A01

An elliptic-parabolic PDE (Partial Differential Equation) system arising from a two dimensional groundwater flow problem is studied. It describes the mixing of fresh and salt water with dominant molecular diffusion. An approach based on L(sup p) - L(sup q) a priori estimates for solutions and the inverse function theorem is used. Global existence and uniqueness are derived. ESA

N92-30373# Technische Univ., Delft (Netherlands). Faculty of Technical Mathematics and Information.
FINITE VOLUME DISCRETIZATION OF THE INCOMPRESSIBLE NAVIER-STOKES EQUATIONS IN GENERAL COORDINATES ON STAGGERED GRIDS
P. Wesseling, A. Segal, J. vanKan, C. W. Oosterlee, and C. G. M. Kassels 1991 13 p Presented at the 4th International Symposium on Computational Fluid Dynamics, Davis, CA, Sep. 1991
(Rept-91-71; ISSN-0922-5641; ETN-92-91821) Copyright Avail: CASI HC A03/MF A01

Using standard tensor notation, a coordinate invariant finite volume discretization of the incompressible Navier-Stokes equations is derived in staggered grids in general coordinates. No effort is made to avoid Christoffel symbols. The metric quantities are approximated in a specific way, satisfying a certain geometric identity. It is shown that instead of the contravariant velocity components U(sup alpha), the quantities V(sup alpha) = (square root of g)(U(sup alpha)) should be used as unknowns, where the square root of g is the Jacobian of the mapping. Satisfactory accuracy is obtained on reasonably smooth grids. ESA

N92-30380*# Nevada Univ., Reno. Engineering Research and Development Center.
NUMERICAL INVESTIGATIONS IN THREE-DIMENSIONAL INTERNAL FLOWS Semiannual Status Report, 1 Jan. - 30 Jun. 1992
William C. Rose 30 Jun. 1991 24 p
(Contract NCC2-507)
(NASA-CR-190498; NAS 1.26:190498) Avail: CASI HC A03/MF A01

In previous efforts, a two-dimensional full Navier-Stokes (FNS) code (SCRAM2D) was used in a design process that involved parametric modifications of the inlet geometry to arrive at what appeared to be an optimum inlet flowfield that produced a uniform flow at the exit in a very short distance. In these previous studies, the technologies for determining the contours with a 'man-in-the-loop' approach for both the ramp and cowl of the inlet were demonstrated, and nearly shock-free exiting flowfields were shown to be obtainable. The resulting two-dimensional compression contours were then used with swept sidewalls to form a three-dimensional inlet. Then the three-dimensional Navier-Stokes code (SCRAM3D) was used to investigate the inlet's three-dimensional flow. One of the major difficulties encountered in the previous studies was that associated with the relatively long time required to obtain a solution using even the 2D FNS code in the design process. Since one of the goals of high-speed inlet design is to produce inputs to the overall aircraft design in a timely manner, it was proposed for this year's research to examine 2D and 3D viscous flow solver techniques alternative to the NFS codes used to date. Areas of the inlet particularly identified for code speed up are those associated with the forebody and external flow ramp systems of the inlet. In these areas, parabolized, or space-marched, Navier-Stokes codes were proposed to be investigated for their applicability in the design process developed previously. This report describes the results of an investigation into the use of two other codes for analyzing the forebody and inlet ramp systems of high-speed inlets. Author

N92-30387*# National Aeronautics and Space Administration. Langley Research Center, Hampton, VA.
CONTROL AND AUGMENTATION OF PASSIVE POROSITY THROUGH TRANSPIRATION CONTROL Patent Application
Daniel W. Banks, inventor (to NASA), Richard M. Wood, inventor (to NASA), and Steven X. S. Bauer, inventor (to NASA) 22 May 1992 11 p
(NASA-Case-LAR-14682-1; NAS 1.71:LAR-14682-1; US-Patent-Appl-SN-887002) Avail: CASI HC A03/MF A01

A device for controlling pressure loading of a member caused by a fluid moving past the member or the member moving through a fluid is presented. The device consists of a porous skin mounted over the solid surface of the member and separated from the solid surface by a plenum. Fluid from an area exerting high pressure on the member may enter the plenum through the porous surface and exit into an area exerting a lower pressure on the member, thus, controlling pressure loading of the member. A transpirational control device controls the conditions within the plenum, thus, controlling the side force and yaw moment on the forebody.
NASA

N92-30390*# National Aeronautics and Space Administration. Langley Research Center, Hampton, VA.
METHOD OF MEASURING CROSS-FLOW VORTICES BY USE OF AN ARRAY OF HOT-FILM SENSORS Patent Application
Naval K. Agarwal, inventor (to NASA) (Analytical Services and Materials, Inc., Hampton, VA.), Dal V. Maddalon, inventor (to NASA), and Siva M. Mangalam, inventor (to NASA) (Analytical Services and Materials, Inc., Hampton, VA.) 7 Jan. 1991 15 p

(NASA-Case-LAR-14824-1-SB; NAS 1.71:LAR-14824-1-SB; US-Patent-Appl-SN-823805) Avail: CASI HC A03/MF A01

The invention is a method for measuring the wavelength of cross-flow vortices of air flow having streamlines of flow traveling across a swept airfoil. The method comprises providing a plurality of hot-film sensors. Each hot-film sensor provides a signal which can be processed, and each hot-film sensor is spaced in a straight-line array such that the distance between successive hot-film sensors is less than the wavelength of the cross-flow vortices being measured. The method further comprises determining the direction of travel of the streamlines across the airfoil and positioning the straight-line array of hot film sensors perpendicular to the direction of travel of the streamlines, such that each sensor has a spanwise location. The method further comprises processing the signals provided by the sensors to provide root-mean-square values for each signal, plotting each root-mean-square value as a function of its spanwise location, and determining the wavelength of the cross-flow vortices by noting the distance between two maxima or two minima of root-mean-square values. NASA

N92-30438# Worcester Polytechnic Inst., MA.
KINETIC THEORY AND BOUNDARY CONDITIONS FOR FLOWS OF HIGHLY INELASTIC SPHERES
M. W. Richman 1991 28 p
(Contract DE-AC22-91PC-90185)
(DE92-012645; DOE/PC-90185/T4) Avail: CASI HC A03/MF A01

In this quarter we accomplished two milestones. First, we qualitatively compared the approximate solutions for gravity-driven granular flows down bumpy inclines obtained by Richman and Marciniec (1990) to the experimental results for the same flows obtained by Johnson and Jackson (1990). The comparison was made by employing the reparameterized solutions of Richman and Marciniec (1990) and by analyzing several angles of inclination, coefficients of restitution, and boundary geometries. Next, we obtained exact numerical solutions of the equations of motion that were solved approximately by Richman and Marciniec (1990). We found that there are flow rates at which two flows are possible. Of the two, the less massive is more dilute, more thermalized, and faster than its more massive counterpart. In addition, we found that the approximate results obtained by Richman and Marciniec (1990) for the same flows are in reasonable agreement with the numerical solutions. The numerical work is outlined in detail in the report. DOE

N92-30453# Technische Univ., Delft (Netherlands). Faculty of Technical Mathematics and Information.
FLOW OF FRESH AND SALT WATER IN AN AQUIFER WITH INJECTION FROM THE TOP
Philippe Blanc 1991 21 p Sponsored by Swiss National Science Foundation
(Rept-91-68; ISSN-0922-5641; ETN-92-91818) Copyright Avail: CASI HC A03/MF A01

A given Cauchy problem is studied in relation to the evolution in time of the interface between fresh and salt water flow. A model for the flow in a horizontal homogeneous aquifer of a given constant thickness is considered. The definition of a parabolic type problem is given and the uniqueness of its solution is proved. Two existence results are proved by parabolic regularization. ESA

N92-30454# Technische Univ., Delft (Netherlands). Faculty of Technical Mathematics and Information.
A MULTIGRID METHOD FOR A DISCRETIZATION OF THE INCOMPRESSIBLE NAVIER-STOKES EQUATIONS IN GENERAL COORDINATES
C. W. Oosterlee and P. Wesseling 1991 12 p
(Rept-91-73; ISSN-0922-5641; ETN-92-91823) Copyright Avail: CASI HC A03/MF A01

A discretization for the incompressible Navier-Stokes equations in general coordinates is derived. A staggered grid arrangement is used for the unknowns: contravariant flux components and pressure. The performance of the nonlinear multigrid algorithm, in particular the performance of two smoothing methods, Symmetric Coupled Gauss-Seidel (SCGS) and SCGS/Line Solver (LS), is investigated. ESA

N92-30462# Technische Univ., Delft (Netherlands). Faculty of Technical Mathematics and Information.
A ROBUST MULTIGRID METHOD FOR A DISCRETIZATION OF THE INCOMPRESSIBLE NAVIER-STOKES EQUATIONS IN GENERAL COORDINATES
C. W. Oosterlee and P. Wesseling 1992 23 p
(Rept-92-14; ISSN-0922-5641; ETN-92-91865) Copyright Avail: CASI HC A03/MF A01

The discretization of the incompressible Navier-Stokes equations in general coordinates, and requirements to obtain accuracy, are presented. A survey of smoothing methods is given and the multigrid method and the smoothing method are presented. Test problems and results are presented to show accurate solutions and good convergence rates. Multigrid reduction factors for flows in domains in which stretched cells occur are good, contrary to the reduction factors of the SCGS (Symmetric Coupled Gauss-Seidel) method in these domains. The SCAL (Symmetric Coupled Alternating Lines) smoother is more robust in the variation of underrelaxation factors than the SCGS smoother. ESA

N92-30548# Washington State Univ., Pullman. Dept. of Chemistry.
COEFFICIENTS OF THE SECOND VISCOSITY IN BULK LIQUID HELIUM
Chung-In Um, Chul-Won Jun, and Thomas F. George Jun. 1992 17 p
(Contract N00014-90-J-1193)
(AD-A252421; WSU/92/86; TR-86) Avail: CASI HC A02/MF A01

The coefficients of the second viscosity in bulk liquid helium are evaluated explicitly as a function of temperature via interactions between the anomalous excitation spectrums. The four coefficients of the second viscosity exhibit a T-1 dependence at low temperatures (well below 0.6 K), which is due to three-phonon processes originating from the anomalous dispersion at very low momenta and temperatures. GRA

N92-30560# Mitre Corp., McLean, VA.
CONTINUUM APPROACHES FOR DESCRIBING SOLID-LIQUID FLOW
P. Diamond, J. Harvey, H. Levine, P. Steinhardt, and R. Westervelt Feb. 1992 24 p Sponsored by DOE
(AD-A249028; JSR-91-310) Avail: CASI HC A03/MF A01

Two-phase continuum models have been used to describe the multiphase flow properties of solid-gas and solid-liquid mixtures. The approach is limited in that it requires many fitting functions and parameters to be determined empirically, and it does not provide natural explanations for some of the qualitative behavior of solid-fluid flow. In this report, we explore a more recent single-phase continuum model proposed by Jenkins and Savage (1982) to describe granular flow. Jenkins and McTigue (1989) have proposed a modified model to describe the flow of dense suspensions, and, hence, many of our results can be straight-forwardly extended to this flow regime as well. The solid-fluid mixture is treated as a homogeneous, compressible fluid in which the particle fluctuations about the mean flow are described in terms of an effective temperature. The particle collisions are treated as inelastic. After an introduction in which we briefly comment on the present status of the field, we describe the details of the single-phase continuum model and analyze the microscopic and macroscopic flow conditions required for the approach to be valid. We then derive numerous qualitative predictions which can be empirically verified in small-scale experiments. The flow profiles are computed for simple boundary conditions, plane Couette flow and channel flow. Segregation effects, when there are two (or more) particle sizes are considered. GRA

N92-30604# Ballistic Research Labs., Aberdeen Proving Ground, MD.
VARIATIONAL METHOD IN THE STATISTICAL THEORY OF TURBULENT TWO-PHASE FLOWS Final Technical Report, Jun. 1989 - Sep. 1991
C. K. Zoltani, S. Kovesi-Domokos (Johns Hopkins Univ., Baltimore, MD.), and G. Domokos (Johns Hopkins Univ., Baltimore, MD.) Jun. 1992 36 p
(DA Proj. 1L1-61102-AH-43)
(AD-A252263; BRL-TR-3362) Avail: CASI HC A03/MF A01

Variational principles are introduced in the statistical theory of turbulent two-phase flows. With the help of these principles, correlation functions can be calculated by means of extremizing certain functionals. We carry out a sample calculation of the mean flow profile and correlation functions of a cylindrically symmetric two-phase jet. A Rayleigh-Ritz method is used for the determination of the correlation functions. There is a reasonable agreement between the theoretical calculation and experimental data even with a rather simple choice of the trial functions. GRA

N92-30607# Sandia National Labs., Albuquerque, NM.
MONTE CARLO PARTICLE SIMULATION OF LOW-DENSITY FLUID FLOW ON MIMD SUPERCOMPUTERS
S. Plimpton and T. Bartel 1991 5 p Presented at the Scalable High Performance Computing Conference, Williamsburg, VA, 26-29 Apr. 1992
(Contract DE-AC04-76DP-00789)
(DE92-014618; SAND-91-2787C; CONF-9204106-4) Avail: CASI HC A01/MF A01

Direct Monte Carlo Simulation is a well-established technique for modeling low density fluid flows. The parallel implementation of a general simulation which allows for body-fitted grids, particle weighting, and a variety of surface and flow chemistry models is described. We compare its performance on a 1024-node nCUBE2 to a serial version for the CRAY-YMP. Experiences with load-balancing the computation via graph-based heuristics (Kernighan and Lin) and the newer spectral techniques (Pothen, Simon, and Liou) are also discussed. This is a critical issue since density fluctuations can create orders-of-magnitude differences in computational loads as the simulation progresses. DOE

N92-30616# Stanford Univ., CA. Dept. of Mechanical Engineering.
THE EFFECTS OF FREE STREAM TURBULENCE AND SURFACE CURVATURE ON BOUNDARY LAYER FLOW AND HEAT TRANSFER Final Report, 1 Jan. 1989 - 31 Dec. 1990
P. Bradshaw, J. P. Johnson, and R. J. Moffat 5 Mar. 1992 17 p
(Grant AF-AFOSR-0246-89)
(AD-A248846; AFOSR-92-0258TR) Avail: CASI HC A03/MF A01

The effects of grid-generated, free-stream turbulence up to levels of 7.5 percent were investigated in a low speed water channel. The distribution of turbulent Prandtl number in the flat-wall region was found to be the same in water as in air, contrary to expectations based on the literature. The effect of Prandtl number on wall trace visualizations of heat transfer was investigated with a liquid crystal surface in a water tunnel. Heat transfer images were dominated by events within the sublayer, fluid mechanics visualizations show effects from far out in the boundary layer. A series of experiments were done in a high turbulence air tunnel (16 percent, uniform across the tunnel) to investigate whether or not an abrupt change in flow passage size, with no flow acceleration, would affect heat transfer. A membrane was placed at 1/3 and 1/6 of the passage height in a heat transfer tunnel, reducing the largest possible normal scale of the turbulence by that same ratio. There was no significant change in the distribution of heat transfer on the surface under the membrane. A second investigation involved wake-like turbulence interacting with turbulent boundary layers. A wind tunnel experiment is described where spatially-inhomogeneous turbulence, in the absence of mean-velocity variations, is generated by a graded grid which produces intensity levels of 10 percent at its top and hardly any at its bottom, the part close to a flat wall. GRA

N92-30648*# Stanford Univ., CA. Center for Turbulence Research.
STUDYING TURBULENCE USING NUMERICAL SIMULATION DATABASES. 3: PROCEEDINGS OF THE 1990 SUMMER PROGRAM
Debra Spinks, comp. Dec. 1990 338 p Program held in Stanford, CA, 16 Jul. - 10 Aug. 1990 Original contains color illustrations
(Contract NCC2-460)
(NASA-CR-189475; NAS 1.26:189475) Avail: CASI HC A15/MF A03; 2 functional color pages

Papers that cover the following topics are presented: subgrid scale modeling; turbulence modeling; turbulence structure, transport, and control; small scales mixing; turbulent reacting flows; and turbulence theory. For individual titles, see N92-30649 through N92-30673.

N92-30649*# Politecnico di Torino (Italy).
A DYNAMIC SUBGRID-SCALE EDDY VISCOSITY MODEL
Massimo Germano, Ugo Piomelli (Maryland Univ., College Park.), Parviz Moin (Stanford Univ., CA.), and William H. Cabot (Stanford Univ., CA.) *In* Stanford Univ., Studying Turbulence Using Numerical Simulation Databases. 3: Proceedings of the 1990 Summer Program Dec. 1990 p 5-17 (For primary document see N92-30648 21-34)
Avail: CASI HC A03/MF A03; 2 functional color pages

One major drawback of the eddy viscosity subgrid-scale stress models used in large-eddy simulations is their inability to represent correctly with a single universal constant different turbulent field in rotating or sheared flows, near solid walls, or in transitional regimes. In the present work, a new eddy viscosity model is presented which alleviates many of these drawbacks. The model coefficient is computed dynamically as the calculation progresses rather than input a priori. The model is based on an algebraic identity (Germano 1990) between the subgrid-scale stresses at two different filtered levels and the resolved turbulent stresses. The subgrid-scale stresses obtained using the proposed model vanish in laminar flow and at a solid boundary, and have the correct asymptotic behavior in the near-wall region of a turbulent boundary layer. The results of large-eddy simulations of transitional and turbulent channel flow that use the proposed model are in good agreement with the direct simulation data. Author

N92-30650*# Maryland Univ., College Park.
SUBGRID-SCALE BACKSCATTER IN TRANSITIONAL AND TURBULENT FLOWS
Ugo Piomelli, William H. Cabot (Stanford Univ., CA.), Parviz Moin (Stanford Univ., CA.), and Sangsan Lee (Stanford Univ., CA.) *In* Stanford Univ., Studying Turbulence Using Numerical Simulation Databases. 3: Proceedings of the 1990 Summer Program Dec. 1990 p 19-30 (For primary document see N92-30648 21-34)
Avail: CASI HC A03/MF A03; 2 functional color pages

Most subgrid-scale (SGS) models for large-eddy simulations are absolutely dissipative (that is, they remove energy from the large scales at each point in the physical space). The actual SGS stresses, however, may transfer energy to the large scales (backscatter) at a given location. Direct numerical simulations of turbulent channel flow and compressible isotropic turbulence are used to study the backscatter phenomena. In all flows considered roughly 50 percent of the grid points were experiencing backscatter when a Fourier cutoff filter was used. The backscatter fraction was less with a Gaussian filter, and intermediate with a box filter in physical space. Moreover, the backscatter and forward scatter contributions to the SGS dissipation were comparable, and each was often much larger than the total SGS dissipation. The SGS dissipation (normalized by total dissipation) increased with filter width almost independently of filter type and Reynolds number. The amount of backscatter showed an increasing trend with Reynolds numbers. In the near-wall region of the channel, events characterized by strong Reynolds shear stress correlated fairly

well with areas of high SGS dissipation (both forward and backward). In compressible isotropic turbulence similar results were obtained, independent of fluctuation Mach number. Author

N92-30651*# Institut de Mecanique de Grenoble (France).
A SUBGRID-SCALE MODEL BASED ON THE SECOND-ORDER VELOCITY STRUCTURE FUNCTION
P. Comte, Sangsan Lee (Stanford Univ., CA.), and William H. Cabot (Stanford Univ., CA.) *In* Stanford Univ., Studying Turbulence Using Numerical Simulation Databases. 3: Proceedings of the 1990 Summer Program Dec. 1990 p 31-45 (For primary document see N92-30648 21-34)
Avail: CASI HC A03/MF A03; 2 functional color pages

A series of tests were performed to help extend the use of a subgrid-scale model to compressible and wall-bounded flows. A priori tests were done in the case of the incompressible turbulent channel flow. They showed that a 1-D formulation of the structure-function model is more appropriate, leading to a satisfactory behavior of the model at the walls without requiring any damping function. This model is consistent with the original formulation of Metais & Lesieur (1990). In large-eddy simulations of compressible isotropic turbulence, both models performed well up to an initial rms Mach number of 0.6. Author

N92-30652*# Stanford Univ., CA. Center for Turbulence Research.
ON THE SUBGRID-SCALE MODELING OF COMPRESSIBLE TURBULENCE
Kyle Squires and Otto Zeman *In its* Studying Turbulence Using Numerical Simulation Databases. 3: Proceedings of the 1990 Summer Program Dec. 1990 p 47-59 (For primary document see N92-30648 21-34)
Avail: CASI HC A03/MF A03; 2 functional color pages

A new sub-grid scale model is presented for the large-eddy simulation of compressible turbulence. In the proposed model, compressibility contributions have been incorporated in the sub-grid scale eddy viscosity which, in the incompressible limit, reduce to a form originally proposed by Smagorinsky (1963). The model has been tested against a simple extension of the traditional Smagorinsky eddy viscosity model using simulations of decaying, compressible homogeneous turbulence. Simulation results show that the proposed model provides greater dissipation of the compressive modes of the resolved-scale velocity field than does the Smagorinsky eddy viscosity model. For an initial r.m.s. turbulence Mach number of 1.0, simulations performed using the Smagorinsky model become physically unrealizable (i.e., negative energies) because of the inability of the model to sufficiently dissipate fluctuations due to resolved scale velocity dilations. The proposed model is able to provide the necessary dissipation of this energy and maintain the realizability of the flow. Following Zeman (1990), turbulent shocklets are considered to dissipate energy independent of the Kolmogorov energy cascade. A possible parameterization of dissipation by turbulent shocklets for Large-Eddy Simulation is also presented. Author

N92-30653*# Centre d'Etudes et de Recherches, Toulouse (France). Dept. of Aerothermodynamics.
MODELING THE TURBULENT KINETIC ENERGY EQUATION FOR COMPRESSIBLE, HOMOGENEOUS TURBULENCE
B. Aupoix, G. A. Blaisdell, William C. Reynolds (Stanford Univ., CA.), and Otto Zeman (Stanford Univ., CA.) *In* Stanford Univ., Studying Turbulence Using Numerical Simulation Databases. 3: Proceedings of the 1990 Summer Program Dec. 1990 p 63-74 (For primary document see N92-30648 21-34)
Avail: CASI HC A03/MF A03; 2 functional color pages

The turbulent kinetic energy transport equation, which is the basis of turbulence models, is investigated for homogeneous, compressible turbulence using direct numerical simulations performed at CTR. It is shown that the partition between dilatational and solenoidal modes is very sensitive to initial conditions for isotropic decaying turbulence but not for sheared flows. The importance of the dilatational dissipation and of the pressure-dilatation term is evidenced from simulations and a transport equation is proposed to evaluate the pressure-dilatation term evolution. This transport equation seems to work well for sheared flows but does not account for initial condition sensitivity in isotropic decay. An improved model is proposed. Author

N92-30654*# Stanford Univ., CA.
STRUCTURE OF THREE-DIMENSIONAL TURBULENT BOUNDARY LAYERS
P. Bradshaw and O. Sendstad *In its* Studying Turbulence Using Numerical Simulation Databases. 3: Proceedings of the 1990 Summer Program Dec. 1990 p 75-84 (For primary document see N92-30648 21-34)
Avail: CASI HC A02/MF A03; 2 functional color pages

The changes that occur in the Reynolds-stress-producing motion when a cross-stream pressure gradient is applied to an initially two-dimensional turbulent flow are discussed. Two examples are used: (1) a temporal simulation of a channel flow with crossflow applied by a spanwise pressure gradient for t is greater than 0; and (2) a spatial simulation of the boundary layer on an infinite swept wing. Evidence examined to date suggests that the structural changes in the two cases are similar, but the mechanisms may be significantly different, even if effects peculiar to the viscous wall region are ignored. The results from (2) are provisional, based on too short a time series for accurate statistical averages to be obtained. We treat turbulence 'statistics' (solutions of the Navier-Stokes equations in three space dimensions and time) in the same way as experiments: both have limitations of accuracy but both are acceptable representations of real fluid flows.
Author

N92-30655*# National Aeronautics and Space Administration. Ames Research Center, Moffett Field, CA.
LOW REYNOLDS NUMBER KAPPA-EPSILON MODELING WITH THE AID OF DIRECT SIMULATION DATA
W. Rodi (Karlsruhe Univ., Germany, F.R.) and N. N. Mansour *In* Stanford Univ., Studying Turbulence Using Numerical Simulation Databases. 3: Proceedings of the 1990 Summer Program Dec. 1990 p 85-106 Sponsored in part by Stanford Univ. (For primary document see N92-30648 21-34)
Avail: CASI HC A03/MF A03; 2 functional color pages

The constant C(sub mu) and the near-wall damping function f(sub mu) in the eddy-viscosity relation of the kappa-epsilon model are evaluated from direct numerical simulation (DNS) data for developed channel and boundary layer flow at two Reynolds numbers each. Various existing f(sub mu) model functions are compared with the DNS data, and a new function is fitted to the high-Reynolds-number channel flow data. The epsilon-budget is computed for the fully developed channel flow. The relative magnitude of the terms in the epsilon-equation is analyzed with the aid of scaling arguments, and the parameter governing this magnitude is established. Models for the sum of all source and sink terms in the epsilon-equation are tested against the DNS data, and an improved model is proposed. Author

N92-30656*# National Aeronautics and Space Administration. Ames Research Center, Moffett Field, CA.
ONE-EQUATION NEAR-WALL TURBULENCE MODELING WITH THE AID OF DIRECT SIMULATION DATA
W. Rodi (Karlsruhe Univ., Germany, F.R.) and N. N. Mansour *In* Stanford Univ., Studying Turbulence Using Numerical Simulation Databases. 3: Proceedings of the 1990 Summer Program Dec. 1990 p 107-124 Sponsored in part by Stanford Univ. (For primary document see N92-30648 21-34)
Avail: CASI HC A03/MF A03; 2 functional color pages

The length scales appearing in the relations for the eddy viscosity and dissipation rate in one-equation models were evaluated from direct numerical simulation data for developed channel and boundary-layer flow at two Reynolds numbers each. To prepare the ground for the evaluation, the distribution of the most relevant mean-flow and turbulence quantities is presented and discussed with respect to Reynolds-number influence and to differences between channel and boundary-layer flow. An alternative model is also examined in which bar-(v'(exp 2))(exp

1/2) is used as velocity scale instead of k(exp 1/2). With this velocity scale, the length scales now appearing in the model follow very closely a linear relationship near the wall so that no damping is necessary. For the determination of bar-v'(exp 2) in the context of a one-equation model, a correlation is provided between bar-(v'(exp 2))/k and bar-(u'v')/k. Author

N92-30657*# National Aeronautics and Space Administration. Ames Research Center, Moffett Field, CA.
THE STRUCTURE OF TURBULENT CHANNEL FLOW WITH PASSIVE SCALAR TRANSPORT
Y. Guezennec (Ohio State Univ., Columbus.), D. Stretch (Stanford Univ., CA.), and J. Kim *In* Stanford Univ., Studying Turbulence Using Numerical Simulation Databases. 3: Proceedings of the 1990 Summer Program Dec. 1990 p 127-138 Original contains color illustrations (For primary document see N92-30648 21-34)
Avail: CASI HC A03/MF A03; 2 functional color pages

The simulation of turbulent channel flow, with various passive markers, was examined to investigate the local mechanisms of passive scalar transport. We found significant differences between the local transport of heat and momentum, even when the molecular and turbulent Prandtl numbers are of order one. These discrepancies can be attributed to the role of the pressure. We also found that the heat is a poor marker of the vorticity field outside of the near wall region and that scalar transport over significant distances results from the aggregate effect of many turbulent eddies. Author

N92-30658*# National Aeronautics and Space Administration. Ames Research Center, Moffett Field, CA.
A STUDY OF THE TOPOLOGY OF DISSIPATING MOTIONS IN DIRECT NUMERICAL SIMULATIONS OF TIME-DEVELOPING COMPRESSIBLE AND INCOMPRESSIBLE MIXING LAYERS
J. H. Chen (Sandia National Labs., Albuquerque, NM.), M. S. Chong (Melbourne Univ., Parkville, Australia), J. Soria (Commonwealth Scientific and Industrial Research Organization, Highett, Australia), R. Sondergaard (Stanford Univ., CA.), A. E. Perry (Melbourne Univ., Parkville, Australia), M. Rogers, R. Moser (Stanford Univ., CA.), and B. J. Cantwell (Stanford Univ., CA.) *In* Stanford Univ., Studying Turbulence Using Numerical Simulation Databases. 3: Proceedings of the 1990 Summer Program Dec. 1990 p 139-161 Sponsored in part by CSIRO Original contains color illustrations (For primary document see N92-30648 21-34)
(Contracts DE-AC04-76DP-00789; N00014-90-J-1976)
Avail: CASI HC A03/MF A03; 2 functional color pages

A preliminary investigation of the geometry of flow patterns in numerically simulated compressible and incompressible mixing layers was carried out using 3-D critical point methodology. Motions characterized by high rates of kinetic energy dissipation and/or high enstrophy were of particular interest. In the approach the partial derivatives of the velocity field are determined at every point in the flow. These are used to construct the invariants of the velocity gradient tensor and the rate-of-strain tensor (P, Q, R, and P(sub s), Q(sub s), R(sub s) respectively). For incompressible flow the first invariant is zero. For the conditions of the compressible simulation, the first invariant is found to be everywhere small, relative to the second and third invariants, and so in both cases the local topology at a point is mainly determined by the second and third invariants. The data at every grid point is used to construct scatter plots of Q versus R and Q(sub s) versus R(sub s). Most points map to a cluster near the origin in Q-R space. However, fine scale motions, that is motions which are characterized by velocity derivatives which scale with the square root of R(sub delta), tend to map to regions which lie far from the origin. Definite trends are observed for motions characterized by high enstrophy and/or high dissipation. The observed trends suggest that, for these motions, the second and third invariants of the velocity gradient and rate-of-strain tensors are strongly correlated. The second and third invariants of the rate-of-strain tensor are related by K(-Q(sub s))(exp 3/2), which is consistent with the above scaling of velocity derivatives. The quantity K appears to depend on Reynolds number with an upper limit K = 2(the square root of 3)/9 corresponding to locally axisymmetric flow. For both the compressible and incompressible mixing layer, regions corresponding to high rates of dissipation are found to be characterized by comparable magnitudes of R(sub ij)R(sub ij) and S(sub ij)S(sub ij). For the incompressible mixing layer, regions characterized by the highest values of enstrophy are found to have relatively low strain rates. Author

N92-30659*# Johns Hopkins Univ., Baltimore, MD. Chesapeake Bay Inst.
DIRECT NUMERICAL SIMULATIONS OF STABLY-STRATIFIED SHEARED TURBULENCE: IMPLICATIONS FOR OCEANIC MIXING
E. C. Itsweire, S. E. Holt (Stanford Univ., CA.), J. R. Koseff (Stanford Univ., CA.), and J. H. Ferziger (Stanford Univ., CA.) *In* Stanford Univ., Studying Turbulence Using Numerical Simulation Databases. 3: Proceedings of the 1990 Summer Program Dec. 1990 p 163-180 Sponsored in part by ONR (For primary document see N92-30648 21-34)
Avail: CASI HC A03/MF A03; 2 functional color pages

Direct numerical simulations of the time evolution of homogeneous stably stratified turbulent shear flows have been performed for several Richardson numbers Ri and Reynolds numbers R(sub lambda) in earlier works. The results show excellent agreement with length scale models developed from laboratory experiments to characterize oceanic turbulence. When the Richardson number Ri is less than the stationary value Ri(sub s), the turbulence intensity grows at all scales, and the growth rate appears to be a function of Ri. The size of the vertical density inversions also increases. On the other hand, when Ri is greater than or equal to Ri(sub s) the largest turbulent eddies become vertically constrained by buoyancy when the Ellison (turbulence) scale L(sub E) and the Ozmidov (buoyancy) scale L(sub O) are equal. At this point, the mixing efficiency is maximal and corresponds to a flux Richardson number R(sub f) = 0.20. The vertical mass flux becomes counter-gradient when epsilon = 19(nu)N(exp 2) and vertical density overturns are suppressed in less than half a Brunt-Vaisala period. The results of the simulations were also recast in terms of the Hydrodynamic Phase Diagram introduced in fossil turbulence models. The so-called point of fossilization occurs when epsilon = 4DCN(exp 2); Gibson proposed 13DCN(exp 2). This value is in agreement with indirect laboratory observations and field observations. Finally, the validity of the steady-state models to estimate vertical eddy diffusivities in the oceanic thermocline is discussed. Author

N92-30660*# Cornell Univ., Ithaca, NY. Center for Applied Mathematics.
A NUMERICAL EVALUATION OF THE DYNAMICAL SYSTEMS APPROACH TO WALL LAYER TURBULENCE
Gal Berkooz *In* Stanford Univ., Studying Turbulence Using Numerical Simulation Databases. 3: Proceedings of the 1990 Summer Program Dec. 1990 p 181-189 (For primary document see N92-30648 21-34)
(Grant AF-AFOSR-0226-89)
Avail: CASI HC A02/MF A03; 2 functional color pages

This work attempts to test predictions based on the Dynamical Systems approach to Wall Layer Turbulence. We analyze the Dynamical Systems model for the nonlinear interaction mechanisms between the coherent structures and deduce qualitative behavior as expected. We then test for this behavior in data sets from D.N.S. The agreement is good, given the suboptimal conditions for the test. We discuss implications of this test and work to be done to deepen the understanding of control of turbulent boundary layers. Author

N92-30661*# Florida State Univ., Tallahassee.
RESONANT INSTABILITY OF SUPERSONIC SHEAR LAYERS
C. K. W. Tam and S. K. Lele (Stanford Univ., CA.) *In* Stanford Univ., Studying Turbulence Using Numerical Simulation Databases. 3: Proceedings of the 1990 Summer Program Dec. 1990 p 191-201 (For primary document see N92-30648 21-34)
Avail: CASI HC A03/MF A03; 2 functional color pages

A computer simulation of possible resonant instability of a

supersonic shear layer is carried out. The resonance of two acoustic duct modes of the flow induced by periodic Mach waves generated by a wavy wall is sought. Results of the simulations are reported. Simulations are unable to document a resonant instability and the mixing characteristics remain unchanged. Possible weakness of the present simulations are discussed. A second set of simulations involving a mixing layer separating a supersonic and a subsonic stream were performed. A wavy wall placed adjacent to the supersonic stream to produce a set of periodic Mach waves terminating at the shear layer is modelled. The entire flow field is similar to that of an imperfectly expanded supersonic jet discharging into a subsonic coflowing stream for which enhanced mixing due to the onset of screech (feedback instability) is known to occur. The purpose of these simulations is to see if enhanced mixing and feedback instability would, indeed, take place. Some evidence of feedback oscillations is found in the simulated flow. Author

N92-30662*# National Aeronautics and Space Administration. Ames Research Center, Moffett Field, CA.

LOW ORDER DYNAMICAL MODELS FOR MIXING LAYERS

D. N. Riahi (Illinois Univ., Urbana.), R. D. Moser, and F. Waleffe (Stanford Univ., CA.) *In* Stanford Univ., Studying Turbulence Using Numerical Simulation Databases. 3: Proceedings of the 1990 Summer Program Dec. 1990 p 205-210 (For primary document see N92-30648 21-34)

Avail: CASI HC A02/MF A03; 2 functional color pages

The goal of this project was to investigate the feasibility of developing useful low order dynamical systems to allow one to determine cheaply the effect of various initial conditions on the evolution of mixing layers. A mathematically rigorous approach for a time evolving base flow as found in a mixing layer seems to be the singular value decomposition of the linear operator transforming some initial perturbations into the solution at a given later time. Unfortunately, this is very costly, if at all feasible, and only deals with the linear evolution of a disturbance. A different approach based on weakly nonlinear analysis was attempted, but numerous difficulties were encountered. Several formulations were proposed which may be ill-posed. The reasons for this possible failure of the attempted approach is related to the fundamental limitations of weakly nonlinear analysis. The clarification of these issues is attempted in this report. Author

N92-30663*# National Aeronautics and Space Administration. Ames Research Center, Moffett Field, CA.

NUMERICAL SIMULATION OF LOW PRANDTL NUMBER TURBULENT MIXING

C. Gibson (California Univ., San Diego.), M. Rogers, J. Chasnov (National Aeronautics and Space Administration. Goddard Space Flight Center, Greenbelt, MD.), and J. Petresky (California Univ., San Diego.) *In* Stanford Univ., Studying Turbulence Using Numerical Simulation Databases. 3: Proceedings of the 1990 summer Program Dec. 1990 p 211-224 (For primary document see N92-30648 21-34)

Avail: CASI HC A03/MF A03; 2 functional color pages

Numerical simulations of turbulent mixing of strongly diffusive scalar fields were carried out with and without subgrid-scale modeling of the small-scale strain field. For low Reynolds number flows, when the rate of strain field (determined primarily by the small scales) is fully resolved, the scalar microstructure was found to collapse under Batchelor rate-of-strain scaling even for small Prandtl numbers, in agreement with Kerr. For high Reynolds number flows, when small-scale straining is modeled with a subgrid-scale model, the scalar microstructure follows the Batchelor, Howells, and Townsend predictions that the small-scale rate-of-strain is irrelevant. Author

N92-30664*# National Aeronautics and Space Administration. Ames Research Center, Moffett Field, CA.

LENGTH SCALES AND DISSIPATION OF FINE EDDIES IN A MIXING LAYER

Y. Zohar (University of Southern California, Los Angeles.), R. D. Moser, J. C. Buell (Stanford Univ., CA.), and C. M. Ho (University of Southern California, Los Angeles.) *In* Stanford Univ., Studying Turbulence Using Numerical Simulation Databases. 3: Proceedings of the 1990 Summer Program Dec. 1990 p 225-234 (For primary document see N92-30648 21-34)

Avail: CASI HC A02/MF A03; 2 functional color pages

It has been shown that small scale turbulence is produced by the interactions of the merging spanwise structures (rollers) and the streamwise vortices (ribs). In this study, we examine the dissipation rate of the three dimensional kinetic energy and length scales associated with the dissipation rate in a temporally evolving mixing layer. Author

N92-30665*# Stanford Univ., CA. Center for Turbulence Research.

A FRACTAL TRANSITION IN THE TWO DIMENSIONAL SHEAR LAYER

Javier Jimenez (Universidad Politecnica de Madrid, Spain) and Carlos Martel (Universidad Politecnica de Madrid, Spain) *In its* Studying Turbulence Using Numerical Simulation Databases. 3: Proceedings of the 1990 Summer Program Dec. 1990 p 235-242 (For primary document see N92-30648 21-34)

Avail: CASI HC A02/MF A03; 2 functional color pages

The dependence of product generation with the Peclet and Reynolds number in a numerically simulated, reacting, two dimensional, temporally growing mixing layer is used to compute the fractal dimension of passive scalar interfaces. A transition from a low dimension of 4/3 to a higher one of 5/3 is identified and shown to be associated to the kinematic distortion on the flow field during the first pairing interaction. It is suggested that the structures responsible for this transition are non-deterministic, non-random, inhomogeneous fractals. Only the large scales are involved. No further transition is found for Reynolds numbers up to 20,000. Author

N92-30666*# Sandia National Labs., Albuquerque, NM. Combustion Research Facility.

GEOMETRY OF PREMIXED FLAMES IN THREE-DIMENSIONAL TURBULENCE

William T. Ashurst *In* Stanford Univ., Studying Turbulence Using Numerical Simulation Databases. 3: Proceedings of the 1990 Summer Program Dec. 1990 p 245-253 Sponsored in part by DOE and Stanford Univ. (For primary document see N92-30648 21-34)

Avail: CASI HC A02/MF A03; 2 functional color pages

Constant density premixed flame propagation in three dimensional Navier-Stokes turbulence has been simulated. The zero-thickness flame model of Kerstein has been used. There are two aspects to this study: (1) adjustment of the large-scale strain rate in order to achieve a constant energy system; and (2) determination of flame curvature. The sampled distribution of curvature indicates that in most cases the flame has a cylindrical shape, with one curvature at least three times larger than the other. This implies that realistic chemical reactions in a flame-vortex interaction may be simulated in two dimensions. Author

N92-30667*# Washington Univ., Seattle.

LAMINAR FLAMELET MODELING OF TURBULENT DIFFUSION FLAMES

W. E. Mell, G. Kosaly, O. Planche (Stanford Univ., CA.), T. Poinsot (Stanford Univ., CA.), and J. H. Ferziger (Stanford Univ., CA.) *In* Stanford Univ., Studying Turbulence Using Numerical Simulation Databases. 3: Proceedings of the 1990 Summer Program Dec. 1990 p 255-269 (For primary document see N92-30648 21-34)

Avail: CASI HC A03/MF A03; 2 functional color pages

In modeling turbulent combustion, decoupling the chemistry from the turbulence is of great practical significance. In cases in which the equilibrium chemistry model breaks down, laminar flamelet modeling (LFM) is a promising approach to decoupling. Here, the validity of this approach is investigated using direct numerical simulation of a simple chemical reaction in two-dimensional turbulence. Author

N92-30668*# Cambridge Univ. (England). Dept. of Engineering.
STATISTICS FOR LAMINAR FLAMELET MODELING c25
R. S. Cant, C. J. Rutland (Wisconsin Univ., Madison.), and A. Trouve (Stanford Univ., CA.) *In* Stanford Univ., Studying Turbulence Using Numerical Simulation Databases. 3: Proceedings of the 1990 Summer Program Dec. 1990 p 271-279 (For primary document see N92-30648 21-34)
Avail: CASI HC A02/MF A03; 2 functional color pages

Statistical information required to support modeling of turbulent premixed combustion by laminar flamelet methods is extracted from a database of the results of Direct Numerical Simulation of turbulent flames. The simulations were carried out previously by Rutland (1989) using a pseudo-spectral code on a three dimensional mesh of 128 points in each direction. One-step Arrhenius chemistry was employed together with small heat release. A framework for the interpretation of the data is provided by the Bray-Moss-Libby model for the mean turbulent reaction rate. Probability density functions are obtained over surfaces of the constant reaction progress variable for the tangential strain rate and the principal curvature. New insights are gained which will greatly aid the development of modeling approaches. Author

N92-30669*# General Motors Research Labs., Warren, MI.
THE INFLUENCE OF LEWIS NUMBER AND NONHOMOGENEOUS MIXTURE ON PREMIXED TURBULENT FLAME STRUCTURE c25
D. C. Haworth and T. J. Poinsot (Stanford Univ., CA.) *In* Stanford Univ., Studying Turbulence Using Numerical Simulation Databases. 3: Proceedings of the 1990 Summer Program Dec. 1990 p 281-298 (For primary document see N92-30648 21-34)
Avail: CASI HC A03/MF A03; 2 functional color pages

The structure of a premixed flame front in two-dimensional turbulence is investigated using full numerical simulation including heat release, variable fluid properties, and one-step Arrhenius chemistry. Non-unity Lewis number (Le) effects are described by comparing the local instantaneous turbulent flame structure to the steady one dimensional laminar flame structure for the same thermochemical parameters. Flame surface area, mean reactant consumption rate per unit area of flame, turbulent flame speed, and statistical descriptions of the flame geometry are also reported. Principal findings are that the local flame structure correlates strongly with the local flame curvature, while global properties depend both on strain and on curvature. Preliminary results for cases with nonhomogeneous reactant mixture strength are reported. Here, the emphasis is on the ability of a propagating flame to recover after encountering a fuel-lean pocket in an otherwise homogeneous mixture. Both one dimensional and two dimensional cases are described. Author

N92-30670*# Wisconsin Univ., Madison.
PRE-MIXED FLAME SIMULATIONS FOR NON-UNITY LEWIS NUMBERS c25
C. J. Rutland and A. Trouve (Stanford Univ., CA.) *In* Stanford Univ., Studying Turbulence Using Numerical Simulation Databases. 3: Proceedings of the 1990 Summer Program Dec. 1990 p 299-309 (For primary document see N92-30648 21-34)
Avail: CASI HC A03/MF A03; 2 functional color pages

A principal effect of turbulence on premixed flames in the flamelet region is to wrinkle the flame fronts. For non-unity Lewis numbers (Le), the local flame structure is altered in curved regions. This effect is examined using direct numerical simulations of the three dimensional, constant density, decaying isotropic turbulence with a single step, finite rate chemical reaction. Simulations of Lewis numbers 0.8, 1.0, and 1.2 are compared. The turbulent flame speed, S(sub T), increases as Le decreases. The correlation between S(sub T) and u prime found in previous Le = 1 simulations has a strong Lewis number dependency. The variance of the pdf of the flame curvature increases as Le decreases, indicating that the flames become more wrinkled. A strong correlation between local flame speed and curvature was found. For Le greater than 1, the flame speed increases in regions concave towards the products and decreases in convex regions. The opposite correlation was found for Le less than 1. The mean temperature of the products was also found to vary with Lewis number. For Le = 0.8, it is less than the adiabatic flame temperature and for Le = 1.2 it is greater. Author

N92-30671*# National Aeronautics and Space Administration. Goddard Space Flight Center, Greenbelt, MD.
GENERATION OF LARGE-SCALE DENSITY FLUCTUATIONS BY BUOYANCY
J. R. Chasnov (National Academy of Sciences - National Research Council, Greenbelt, MD.) and R. S. Rogallo *In* Stanford Univ., Studying Turbulence Using Numerical Simulation Databases. 3: Proceedings of the 1990 Summer Program Dec. 1990 p 313-318 (For primary document see N92-30648 21-34)
Avail: CASI HC A02/MF A03; 2 functional color pages

The generation of fluid motion from a state of rest by buoyancy forces acting on a homogeneous isotropic small-scale density field is considered. Nonlinear interactions between the generated fluid motion and the initial isotropic small-scale density field are found to create an anisotropic large-scale density field with spectrum proportional to kappa(exp 4). This large-scale density field is observed to result in an increasing Reynolds number of the fluid turbulence in its final period of decay. Author

N92-30672*# National Aeronautics and Space Administration. Ames Research Center, Moffett Field, CA.
INTERSCALE ENERGY TRANSFER IN NUMERICALLY SIMULATED TURBULENCE
J. A. Domaradzki (University of Southern California, Los Angeles.), R. S. Rogallo, and A. A. Wray *In* Stanford Univ., Studying Turbulence Using Numerical Simulation Databases. 3: Proceedings of the 1990 Summer Program Dec. 1990 p 319-329 (For primary document see N92-30648 21-34)
Avail: CASI HC A03/MF A03; 2 functional color pages

Energy transfer is investigated for flows obtained by direct numerical simulations of low Reynolds number homogeneous shear and isotropic turbulence and by large eddy simulations of high Reynolds number isotropic turbulence. The transfer in spectral space is found to be local, but results from interaction between separated scales. The transfer among small scales is highly intermittent in physical space. The measurements suggest an important correlation between transfer among small scales and the energy of large scales. Author

N92-30673*# Ecole Normale Superieure, Paris (France).
CONTINUOUS WAVELET ANALYSIS OF COHERENT STRUCTURES
M. Farge, Y. Guezennec (Ohio State Univ., Columbus.), C. M. Ho (University of Southern California, Los Angeles.), and C. Meneveau (Johns Hopkins Univ., Baltimore, MD.) *In* Stanford Univ., Studying Turbulence Using Numerical Simulation Databases. 3: Proceedings of the 1990 Summer Program Dec. 1990 p 331-348 (For primary document see N92-30648 21-34)
Avail: CASI HC A03/MF A03; 2 functional color pages

We perform an analysis of planar cuts through three dimensional turbulent fields (planar channel flow and mixing layer) using the 2D continuous wavelet transform. We propose two new diagnostics: (1) a measure of intermittency I(r, vector x), which is the ratio of local energy and average energy at a given scale r; and (2) a local Reynolds number, defined on the local velocity contribution at a given scale, computed from the wavelet transform of the three velocity components, the scale of the transform, and molecular viscosity; this gives a representation of the local non-linearity of the flow viewed in both space and scale. We find, for the analyzed flows, strong small-scale intermittency located in the ejection regions for the channel flow and in the vortex core of the mixing layer. Author

N92-30674# Messerschmitt-Boelkow-Blohm G.m.b.H., Munich (Germany, F.R.). Military Aircraft Div.
CALCULATION OF VISCOUS HYPERSONIC FLOWS IN CHEMICAL NON-EQUILIBRIUM
Christian Mundt Sep. 1991 14 p Presented at the 9th GAMM Conference on Numerical Methods in Fluid Mechanics,

Lausanne, Switzerland, 25-27 Sep. 1991
(MBB/FE211/S/PUB/466; ETN-92-91905) Copyright Avail: CASI HC A03/MF A01

An efficient method which can calculate viscous flows at high Mach and moderate to high Reynolds numbers in chemical nonequilibrium by a solution of the Euler and second order boundary layer equations is presented. This approach is valid for flows showing no strong viscous/inviscid interaction. Thus it is suited for determining the flow at the windward side of reentry vehicles. Applications are discussed together with the modeling of effects of practical interest, such as catalytic walls and wall radiative equilibrium. ESA

N92-30751*# North Carolina State Univ., Raleigh. Dept. of Mechanical and Aerospace Engineering.
REAL GAS FLOW PARAMETERS FOR NASA LANGLEY 22-INCH MACH 20 HELIUM TUNNEL Report, Jun. 1991 - Jun. 1992
Brian R. Hollis Washington NASA. Langley Research Center Aug. 1992 66 p
(Grant NAGw-1072; RTOP 506-40-41-02)
(NASA-CR-4462; NAS 1.26:4462) Avail: CASI HC A04/MF A01

A computational procedure was developed which can be used to determine the flow properties in hypersonic helium wind tunnels in which real gas behavior is significant. In this procedure, a three-coefficient virial equation of state and the assumption of isentropic nozzle flow are employed to determine the tunnel reservoir, nozzle, throat, freestream, and post-normal shock conditions. This method was applied to a range of conditions which encompasses the operational capabilities of the LaRC 22-Inch Mach 20 Helium Tunnel. Results are presented graphically in the form of real gas correction factors which can be applied to perfect gas calculations. Important thermodynamic properties of helium are also plotted versus pressure and temperature. The computational scheme used to determine the real-helium flow parameters was incorporated into a FORTRAN code which is discussed. Author

N92-30765*# National Aeronautics and Space Administration. Ames Research Center, Moffett Field, CA.
INTERSECTING SHOCK-WAVE/TURBULENT BOUNDARY-LAYER INTERACTIONS AT MACH 8.3
M. I. Kussoy (Eloret Corp., Palo Alto, CA.) and K. C. Horstman (Eloret Corp., Palo Alto, CA.) Feb. 1992 68 p
(RTOP 505-59-40)
(NASA-TM-103909; A-92027; NAS 1.15:103909) Avail: CASI HC A04/MF A01

Experimental data for two 3-D intersecting shock-wave/turbulent boundary-layer interaction flows at Mach 8.3 are presented. The test bodies, composed of two sharp fins fastened to a flat-plate test bed, were designed to generate flows with varying degrees of pressure gradient, boundary-layer separation, and turning angle. The data include surface pressure and heat transfer distributions as well as mean flow-field surveys both in the undisturbed and interaction regimes. The data are presented in a convenient form to be used to validate existing or future computational models of these hypersonic flows. Author

N92-30775# Naval Research Lab., Washington, DC.
NEW INSIGHTS INTO LARGE EDDY SIMULATION
J. P. Boris, F. F. Grinstein, E. S. Oran, and R. L. Kolbe 30 Apr. 1992 58 p
(AD-A249424; NRL/MR/4400-92-6979) Avail: CASI HC A04/MF A01

Fluid dynamic turbulence is one of the most challenging computational physics problems because of the extremely wide range of time and space scales involved, the strong nonlinearity of the governing equations, and the many practical and important applications. While most linear fluid instabilities are well understood, the nonlinear interactions among them makes even the relatively simple limit of homogeneous isotropic turbulence difficult to treat physically, mathematically, and computationally. Turbulence is modeled computationally by a two stage bootstrap process. The first stage, Direct Numerical Simulations (DNS), attempts to resolve the relevant physical time and space scales but its application is limited to diffusive flows with a relatively small Reynolds number (Re). Using DNS to provide a database, in turn, allows calibration of phenomenological turbulence models for engineering applications. Large Eddy Simulation (LES) incorporates a form of turbulence modeling applicable when the large-scale flows of interest are intrinsically time dependent, thus throwing common statistical models into question. A promising approach to LES involves the use of high-resolution monotonic computational fluid dynamics algorithms such as the Flux-Corrected Transport or the Piecewise Parabolic Method which have intrinsic subgrid turbulence models coupled naturally to the resolves scales in the computed flow. The physical considerations underlying and evidence supporting this Monotone Integrated LES approach are discussed. GRA

N92-30831# Stanford Univ., CA. Thermosciences Div.
NUMERICAL STUDY OF AXIAL TURBULENT FLOW OVER LONG CYLINDERS
Joao C. Neves, Parviz Moin, and Robert D. Moser Apr. 1992 163 p
(Contract N00014-88-K-0145)
(AD-A250801; SU-TF-54) Avail: CASI HC A08/MF A02

Convex transverse curvature effects in wall bounded turbulent flows are significant if the boundary layer thickness is large compared to the radius of curvature. The curvature affects the inner part of the flow if a+, the cylinder radius in wall units, is small. This flow regime is common in sonar devices towed by long cables. Two direct numerical simulations of transversely curved flows were performed, and statistical and structural data were extracted from the computed flow fields. The effects of the transverse curvature were identified by comparing the present results with those of the plane channel simulation, performed at a similar Reynolds number. As expected, the transversely curved turbulent flow exhibits many features common to the planar flows: near-wall low speed streaks, near-wall inclined shear layers, near-wall streamwise vortices, Reynolds shear stress dominated by second and fourth quadrant events, etc. As the curvature increases, the skin friction increases, the slope of the logarithmic region decreases, and turbulence intensities are reduced. Several turbulence statistics are found to scale with a curvature dependent velocity scale derived from the mean momentum equation. Near the wall, the flow is more anisotropic than in the plane channel with a larger percentage of the turbulent kinetic energy resulting from the streamwise velocity fluctuations. Near-wall streamwise vortices are the strongest sources of pressure fluctuations. As the curvature increases, regions of strong normal vorticity develop near the wall. GRA

N92-30852# Stanford Univ., CA. Dept. of Mechanical Engineering.
INTERACTION OF ISOTROPIC TURBULENCE WITH A SHOCK WAVE Final Report, 1 Jan. 1989 - 31 Dec. 1991
S. Lee, P. Moin, and S. K. Lele Mar. 1992 237 p
(Grant AF-AFOSR-0249-89)
(AD-A250409; AFOSR-92-0408TR) Avail: CASI HC A11/MF A03

As a first step to understand the compressibility effects, interaction of isotropic quasi-incompressible turbulence with a weak shock wave was studied by three-dimensional time-dependent direct numerical simulations. In addition, linear analysis was used to study interaction of isotropic turbulence with shock waves of a wide range of strengths. The effects of the fluctuation Mach number M sub t and the average Mach number M sub 1 superscript u of the upstream turbulence on turbulence statistics were investigated. Both numerical simulations and linear analyses of the interaction show that turbulence is enhanced during the interaction with a shock wave. Turbulent kinetic energy (TKE) and transverse vorticity components are amplified, and turbulent length scales are decreased. The predictions of the linear analyses compare

favorably with simulation results for flows with M sub t less than M sub 1 superscript U-1, which suggests that the amplification mechanism is mainly linear. GRA

N92-30894*# Sverdrup Technology, Inc., Brook Park, OH.
DIRECT COUPLING METHOD FOR TIME-ACCURATE SOLUTION OF INCOMPRESSIBLE NAVIER-STOKES EQUATIONS Final Report
Woo Y. Soh May 1992 20 p
(Contract NAS3-25266; RTOP 505-62-52)
(NASA-CR-189177; E-7041; NAS 1.26:189177) Avail: CASI HC A03/MF A01

A noniterative finite difference numerical method is presented for the solution of the incompressible Navier-Stokes equations with second order accuracy in time and space. Explicit treatment of convection and diffusion terms and implicit treatment of the pressure gradient give a single pressure Poisson equation when the discretized momentum and continuity equations are combined. A pressure boundary condition is not needed on solid boundaries in the staggered mesh system. The solution of the pressure Poisson equation is obtained directly by Gaussian elimination. This method is tested on flow problems in a driven cavity and a curved duct. Author

N92-30903# Sandia National Labs., Albuquerque, NM.
NUMERICAL CALCULATIONS OF TWO-DIMENSIONAL SINGLE AND MULTI-MATERIAL FLOW FIELDS WITH CCICE
A. R. Lopez and R. S. Baty Jan. 1992 45 p
(Contract DE-AC04-76DP-00789)
(DE92-015778; SAND-91-2650) Avail: CASI HC A03/MF A01

This report documents the progress that Sandia National Laboratories has made toward establishing a capability to numerically simulate flow fields around arbitrary bodies for high speed water entry and water exit problems. The two-dimensional, compressible, unsteady, inviscid code, CCICE (Cell Centered Implicit Continuous-fluid Eulerian), developed at Los Alamos National Laboratory (LANL), has been benchmarked for a variety of flow problems. CCICE provides a sufficient description of fluid flows to predict the unsteady pressure forces experienced by vehicles entering or exiting the water. An incompressible version of CCICE, CCMAC (Cell Centered Marker and Cell), has also been benchmarked for a variety of flow problems. CCMAC was obtained from LANL and is a two-dimensional, incompressible, unsteady, inviscid code which can simulate fluid-vehicle interaction in low speed water entry and water exit problems. This report also documents practical information necessary to run the CCICE and CCMAC codes. DOE

N92-30982*# National Aeronautics and Space Administration. Ames Research Center, Moffett Field, CA.
A CFD VALIDATION ROADMAP FOR HYPERSONIC FLOWS
Joseph G. Marvin Apr. 1992 19 p Presented at the 70th Fluid Dynamics Panel Meeting and Symposium on Theoretical and Experimental Methods in Hypersonic Flows, Torino, Italy, 4-8 May 1992
(RTOP 505-59-00)
(NASA-TM-103935; A-92091; NAS 1.15:103935) Avail: CASI HC A03/MF A01

A roadmap for computational fluid dynamics (CFD) code validation is developed. The elements of the roadmap are consistent with air-breathing vehicle design requirements and related to the important flow path components: forebody, inlet, combustor, and nozzle. Building block and benchmark validation experiments are identified along with their test conditions and measurements. Based on an evaluation criteria, recommendations for an initial CFD validation data base are given and gaps identified where future experiments would provide the needed validation data. Author

N92-30293*# Brigham Young Univ., Provo, UT. Dept. of Manufacturing Engineering and Engineering Technology.
MEASURING THE SURFACE TENSION OF SOAP BUBBLES
Carl D. Sorensen *In* NASA. Langley Research Center, National Educators' Workshop: Update 1991. Standard Experiments in Engineering Materials Science and Technology Jun. 1992 p 391-395 (For primary document see N92-30263 21-29)
Avail: CASI HC A01/MF A03

35 INSTRUMENTATION AND PHOTOGRAPHY

Includes remote sensors; measuring instruments and gages; detectors; cameras and photographic supplies; and holography.

For aerial photography see *43 Earth Resources and Remote Sensing.* For related information see also *06 Aircraft Instrumentation,* and *19 Spacecraft Instrumentation.*

N92-30365# Nationaal Inst. voor Kernfysica en Hoge Energiefysica, Amsterdam (Netherlands).
TESTS OF THE PERFORMANCE OF DIFFERENT GAS MIXTURES IN MICROSTRIP GAS COUNTERS
M. Geijsberts, F. G. Hartjes, J. G. Pannekoek, J. Schmitz, and F. Udo Sep. 1991 24 p
(NIKHEF-H/91-23; ETN-92-91621) Avail: CASI HC A03/MF A01

Measurements of the electron drift and diffusion parameters in gas mixtures, suited for application in a microstrip gas counter are described. The aim was to optimize for position resolution, detection efficiency and response time. The measurements were done in mixtures of Ar, CF4, C2H6, Xe, CO2 and DME by using a pulsed ultraviolet laser beam. Results from tests in a particle beam for efficiency and position resolution of the counter using the two gases found to be most promising in laser tests. These two gas mixtures are Xe/DME/CO2 30/30/40 and DME/CO2 60/40. ESA

N92-30412# Aerospace Corp., El Segundo, CA. Technology Operations.
MODELING FAST MODULATION EFFECTS IN CESIUM ATOMIC CLOCKS
John P. Hurrell, Walter A. Johnson, Sarunas K. Karuza, and Frank J. Voit 16 Jun. 1992 13 p
(Contract F04701-88-C-0089)
(AD-A252649; TR-0091(6925-08)-3; SSD-TR-92-15) Avail: CASI HC A02/MF A01

A theory for fast modulation in cesium frequency standards has been developed and expressions derived for frequency offsets produced by Rabi and cavity pulling with square-wave phase modulation. These are compared with equivalent expressions for sine-wave phase modulation. Ratios of the amplitudes of the frequency offsets in the two modulation schemes are calculated for a mono-velocity beam and shown to be in agreement with measurements performed on a commercial standard. This analysis allows a more complete evaluation and comparison of different modulation schemes for cesium atomic beam standards. GRA

N92-30530# Naval Surface Weapons Center, Dahlgren, VA.
ALIGNMENT OF A 3-D SENSOR AND A 2-D SENSOR MEASURING AZIMUTH AND ELEVATION Final Report
Ronald E. Helmick and Theodore R. Rice Apr. 1992 35 p
(AD-A252120; NSWCDD/TR-92/181) Avail: CASI HC A03/MF A01

The problem of aligning two sensors using targets of opportunity is examined in this report, where one of the sensors is a 3-D sensor that measures range, azimuth, and elevation and the other one is a 2-D sensor that measures azimuth and elevation. Both a mathematical model and an alignment algorithm are developed for this problem, where attitude and offset errors in both sensors are included in the formulation. Because of the method used to formulate the problem, it is not possible to determine the individual alignment errors at each sensor. However, it is possible to determine the differences in the respective alignment errors of the two sensors. This is sufficient to align one sensor relative to the other one. For illustrative purposes, the alignment algorithm is

applied to simulated data from two sensors. The algorithm converges within 50 sec to values very close to the actual values of the alignment parameters. Using these values, it is possible to obtain a dramatic 23-fold reduction in the relative error between the tracks generated by the sensors. GRA

N92-30546# California Inst. of Tech., Pasadena. Dept. of Electrical Engineering.
DENSE MODIFIABLE INTERCONNECTIONS UTILIZING PHOTOREFRACTIVE VOLUME HOLOGRAMS Final Report, 1 Nov. 1988 - 28 Feb. 1992
Demetri Psaltis 20 May 1992 10 p
(Grant AF-AFOSR-0045-89)
(AD-A252193; CIT-61430; AFOSR-92-0539TR) Avail: CASI HC A02/MF A01

This report summarizes research efforts on (1) the demonstration of holographic degeneracies in associative memories, (2) the procedure for designing fractal grids for planar holograms, (3) the experimental demonstration of one and two layer neural networks that are designed with such fractal sampling grids, (4) the experimental demonstration of dynamic holographic memories that are capable of an arbitrarily long sequence of adaptations, (5) the optical implementation of the Kanerva's network for hand-written character recognition, (6) the development of an anti-Hebbian local learning algorithm for training multi-layer neural networks, (7) the experimental demonstration of optical radial basis function network, and (8) the demonstration of a two-layer local-representation optical network for real-time face recognition. GRA

N92-30688# Nationaal Inst. voor Kernfysica en Hoge Energiefysica, Amsterdam (Netherlands).
OPTIMIZATION OF THE MICROSTRIP GAS COUNTER
M. H. J. Geijberts, F. G. Hartjes, J. G. Pannekoek, J. Schmitz, and F. Udo Aug. 1991 14 p Presented at the 5th Pisa Meeting on Advanced Detectors, Elba Island, Italy, 26-31 May 1991
(NIKHEF-H/91-21; ETN-92-91619) Avail: CASI HC A03/MF A01

A study to optimize the characteristics of the microstrip gas counter for use as a tracker at the Large Hadron Collider was made. It was found that two of the most important design parameters of the detector are given by the choice of the counter gas and the width of the gas gap. Using measurements with an ultraviolet laser and a particle beam, two most suited mixtures for the counter gas were found, which consist of xenon, dimethylether and CO2. The optimum width of the gas gap was derived. It was found that when a high drift field is chosen in combination with a narrow gas gap, a reliable event tagging can be expected while the resolution still remains at a high level. ESA

N92-30737*# National Aeronautics and Space Administration. Langley Research Center, Hampton, VA.
A STROBOSCOPIC TECHNIQUE FOR USING CCD CAMERAS IN FLOW VISUALIZATION SYSTEMS FOR CONTINUOUS VIEWING AND STOP ACTION PHOTOGRAPHY
John M. Franke, David B. Rhodes, Stephen B. Jones, and Harriet R. Dismond Jun. 1992 10 p
(RTOP 505-59-53-03)
(NASA-TM-107648; NAS 1.15:107648) Avail: CASI HC A02/MF A01

A technique for synchronizing a pulse light source to charge coupled device cameras is presented. The technique permits the use of pulse light sources for continuous as well as stop action flow visualization. The technique has eliminated the need to provide separate lighting systems at facilities requiring continuous and stop action viewing or photography. Author

N92-30822# Sandia National Labs., Albuquerque, NM.
INITIAL LABORATORY EVALUATION OF COLOR VIDEO CAMERAS
P. L. Terry Mar. 1992 30 p
(Contract DE-AC04-76DP-00789)
(DE92-010399; SAND-91-2579) Avail: CASI HC A03/MF A01

Sandia National Laboratories has considerable experience with monochrome video cameras used in alarm assessment video systems. Most of these systems, used for perimeter protection, were designed to classify rather than identify an intruder. Monochrome cameras are adequate for that application and were selected over color cameras because of their greater sensitivity and resolution. The increased emphasis placed on the identification objective of video security systems leads to the need to improve system designs and upgrade existing systems. Color information is useful for identification purposes, and color camera technology is rapidly changing. Thus, Sandia National Laboratories established an ongoing program to evaluate color solid-state cameras. This report describes test parameters and procedures and provides the results of an initial evaluation. DOE

N92-30827# Oak Ridge National Lab., TN.
HIGH-RESOLUTION IMAGING IN THE SCANNING TRANSMISSION ELECTRON MICROSCOPE
S. J. Pennycook and D. E. Jesson Mar. 1992 31 p Presented at the International School on Electron Microscopy in Materials Science, Brindisi, Italy, 7-11 Oct. 1991
(Contract DE-AC05-84OR-21400)
(DE92-010647; CONF-9110359-1) Avail: CASI HC A03/MF A01

The high-resolution imaging of crystalline materials in the scanning transmission electron microscopy (STEM) is reviewed with particular emphasis on the conditions under which an incoherent image can be obtained. It is shown that a high-angle annular detector can be used to break the coherence of the imaging process, in the transverse plane through the geometry of the detector, or in three dimensions if multiphonon diffuse scattering is detected. In the latter case, each atom can be treated as a highly independent source of high-angle scattering. The most effective fast electron states are therefore tightly bound s-type Bloch states. Furthermore, they add constructively for each incident angle in the coherent STEM probe, so that s states are responsible for practically the entire image contrast. Dynamical effects are largely removed, and almost perfect incoherent imaging is achieved. S states are relatively insensitive to neighboring strings, so that incoherent imaging is maintained for superlattice and interfaces, and supercell calculations are unnecessary. With an optimum probe profile, the incoherent image represents a direct image of the crystal projection, with compositional sensitivity built in through the strong dependence of the scattering cross sections on atomic number Z. DOE

N92-30893# Sandia National Labs., Albuquerque, NM.
REPETITIVE HIGH ENERGY PULSED POWER (RHEPP) TEMPERATURE MONITORING SYSTEM UTILIZING LUXTRON FLUOROPTIC SENSORS AND THERMOCOUPLES TECHNICAL REFERENCE MANUAL
G. E. Laderach Jan. 1992 42 p
(Contract DE-AC04-76DP-00789)
(DE92-013461; SAND-91-1624) Avail: CASI HC A03/MF A01

This document describes the Temperature Monitoring System for the RHEPP project at Sandia National Laboratories. The system is designed to operate in the presence of severe repetitive high voltage and electromagnetic fields while providing real time thermal data on component behavior. The thermal data is used in the design and evaluation of the major RHEPP components such as the magnetically switched pulse compressor and the linear induction voltage adder. Particular attention is given to the integration of commercially available hardware and software components with a custom written control program. While this document is intended to be a reference guide, it may also serve as a template for similar applications. DOE

N92-31013*# National Aeronautics and Space Administration. Langley Research Center, Hampton, VA.
SIXTEENTH INTERNATIONAL LASER RADAR CONFERENCE, PART 2

M. Patrick McCormick, ed. Washington Jul. 1992 361 p Conference held in Cambridge, MA, 20-24 Jul. 1992; sponsored by NASA. Langley Research Center, AFOSR, AF Phillips Lab., American Meteorological Society, and the Optical Society of America
(RTOP 665-45-20-21)
(NASA-CP-3158-Pt-2; L-17126-Pt-2; NAS 1.55:3158-Pt-2) Avail: CASI HC A16/MF A03

Given here are extended abstracts of papers presented at the 16th International Laser Radar Conference, held in Cambridge, Massachusetts, July 20-24, 1992. Topics discussed include the Mt. Pinatubo volcanic dust laser observations, global change, ozone measurements, Earth mesospheric measurements, wind measurements, imaging, ranging, water vapor measurements, and laser devices and technology. For individual titles, see N92-31014 through N92-31106.

N92-31014*# Paris VI Univ. (France). Service d'Aeronomie du CNRS.
BOUNDARY LAYER STRUCTURE OVER THE OCEAN OBSERVED BY LEANDRE 1 DURING A TRAMONTANE EVENT **c48**
C. Flamant, J. Pelon, P. Flamant (Ecole Polytechnique, Palaiseau, France), and P. Durand (Toulouse Univ., France) *In* NASA. Langley Research Center, 16th International Laser Radar Conference, Part 2 Jul. 1992 p 381-383 (For primary document see N92-31013 21-35)
Avail: CASI HC A01/MF A03

A new airborne backscatter lidar, has been developed by CNRS (Service d'Aeronomie, (SA) Laboratoire de Meteorologie Dynamique (LMD) and the Institut des Sciences de 1'Univers) in the frame of the LEANDRE research program. It has been qualified on board the ARAT in autumn 1989 and spring 1990 and was involved in its first cooperative campaign during PYREX in October and November 1990. During this campaign, lidar observations of the perturbations induced on tropospheric flow and boundary layer structure were performed, and results are presented. A large number of experiments were performed, for synoptic situation description (meteorological radiosoundings, constant level balloons) and local flow analysis (aircrafts, radars, sodars). For the first time in such an experiment, a lidar has been flown on a research aircraft to perform altitude resolved observations of these perturbations, and we will present here results obtained for deflected flow structure. In the presence of a synoptic northerly flow, part of it is deflected to the east by the Pyrenees, and accelerated over the Mediterranean by the mountain surroundings. In this case, a low level wind is generated (the Tramontane) bringing cold and dry air over the Mediterranean Sea. As the sea is still at a warm temperature in November (around 17 degrees), an Internal Marine Boundary Layer rapidly grows over the first tens of kilometers and stabilizes at about 1 km depth, corresponding to an altitude just below the Lifting Condensation Level. The whole Marine Atmospheric Boundary Layer (MABL) is characterized by highly turbulent motions bringing large humid particles from the surface up to its top. The lidar signal due to scattering by these particles is then representative of the turbulent kinetic energy in this layer. Author

N92-31015*# National Oceanic and Atmospheric Administration, Boulder, CO. Wave Propagation Lab.
LOW-LEVEL ATMOSPHERIC FLOWS STUDIED BY PULSED DOPPLER LIDAR **c46**
Robert M. Banta, Lisa D. Olivier, and R. Michael Hardesty *In* NASA. Langley Research Center, 16th International Laser Radar Conference, Part 2 Jul. 1992 p 385-388 (For primary document see N92-31013 21-35)
Avail: CASI HC A01/MF A03

A pulsed Doppler radar gains a tremendous advantage in studying atmospheric flows when it has the ability to scan. The Wave Propagation Laboratory (WPL) has been operating a scanning, 10.59 micron CO2 system for over 10 years. Recently, the WPL lidar has been a featured instrument in several investigations of mesoscale wind fields in the lowest 3-4 km of the atmosphere. These include four experiments: a study of the initiation and growth of the sea breeze off the coast of California, a study of the snake column of a prescribed forest fire, a study of the nighttime flow over the complex terrain near Rocky Flats, Colorado as it affects the dispersion of atmospheric contaminants, and a study of the wind flow in the Grand Canyon. We have analyzed much data from these experiments, and we have found that the lidar provides new insight into the structure of these flows. Many of these studies took place in rugged or mountainous terrain, thus using one of the major benefits of the lidar: the narrow, 90 microrad beam of the lidar makes it an ideal instrument for studying flow close to topography. Author

N92-31016*# National Aeronautics and Space Administration. Goddard Space Flight Center, Greenbelt, MD.
ON THE EXISTENCE OF CONVECTIVELY PRODUCED GRAVITY WAVES **c46**
Stephen P. Palm (Science Systems and Applications, Inc., Lanham, MD.) and S. H. Melfi *In* NASA. Langley Research Center, 16th International Laser Radar Conference, Part 2 Jul. 1992 p 389-392 (For primary document see N92-31013 21-35)
Avail: CASI HC A01/MF A03

The Boundary Layer Lidar System (BLLS), together with the gustprobe system onboard the NASA Electra has acquired a unique data set which, for the first time, clearly depicts a gravity wave above a convectively driven planetary boundary layer (PBL). In addition, we believe that the data show the development of a trapped gravity wave over a period of about an hour. If this is the case, it would certainly be the first time that such a process has been seen in the atmosphere. We also conclude that the gravity wave, while being initiated by the convection in the PBL, ultimately acts to organize and control scales in the PBL. Author

N92-31017*# National Aeronautics and Space Administration. Goddard Space Flight Center, Greenbelt, MD.
DOPPLER LIDAR WIND MEASUREMENT WITH THE EDGE TECHNIQUE **c47**
C. Laurence Korb and Bruce M. Gentry *In* NASA. Langley Research Center, 16th International Laser Radar Conference, Part 2 Jul. 1992 p 393-396 (For primary document see N92-31013 21-35)
Avail: CASI HC A01/MF A03

The edge technique is a new and powerful method for measuring small frequency shifts. Range resolved lidar measurements of winds can be made with high accuracy and high vertical resolution using the edge technique to measure the Doppler shift of an atmospheric backscattered signal from a pulsed laser. The edge technique can be used at near-infrared or visible wavelengths using well developed solid state lasers and detectors with various edge filters. In the edge technique, the laser frequency is located on the steep slope of the spectral response function of a high resolution optical filter. Due to the steep slope of the edge, very small frequency shifts cause large changes in measured signal. The frequency of the outgoing laser pulse is determined by measuring its location on the edge of the filter. This is accomplished by sending a small portion of the beam to the edge detection setup where the incoming light is split into two channels - an edge filter and an energy monitor channel. The energy monitor signal is used to normalize the edge filter signal for magnitude. The laser return backscattered from the atmosphere is collected by a telescope and directed through the edge detection setup to determine its frequency (location on the edge) in a similar manner for each range element. The Doppler shift, and thus the wind, is determined from a differential measurement of the frequency of the outgoing laser pulse and the frequency of the laser return backscattered from the atmosphere. We have conducted simulations of the performance of an edge lidar system using an injection seeded pulsed Nd:YAG laser at 1.06 microns. The central fringe of a Fabry-Perot etalon is used as a high resolution edge filter to measure the shift of the aerosol return. Author

N92-31018*# Michigan Univ., Ann Arbor. Dept. of Atmospheric, Oceanic and Space Sciences.
TROPOSPHERIC AND STRATOSPHERIC WIND PROFILING WITH A DIRECT DETECTION DOPPLER LIDAR **c47**
Vincent J. Abreu, John E. Barnes, Ken W. Fischer, Wilbert R. Skinner, and Matt J. McGill *In* NASA. Langley Research Center, 16th International Laser Radar Conference, Part 2 Jul. 1992 p 397-400 (For primary document see N92-31013 21-35)
Avail: CASI HC A01/MF A03

The Space Physics Research Laboratory at the University of Michigan has been operating a direct detection, high resolution Doppler Lidar (HRDL) to measure winds in the boundary layer, free troposphere and lower stratosphere. A direct detection Doppler lidar measures the Doppler shift of the aerosol or Rayleigh backscattered signal, from which the wind velocity vector can be retrieved (Benedetti-Michelangeli et al, 1972, 1974; Chanin et al., 1989; Abreu et al., 1992). The system components are shown. The transmitting system is a Continuum NY-60 Nd:YAG laser frequency doubled to a wavelength of 532 nm. The laser is injection seeded for single line mode operation yielding a linewidth of 0.0045 cm(exp -1) (135 MHz) with excellent shot-to-shot frequency stability. The laser produces 60 mJ pulses and operates at a 50 Hz repetition rate for an effective output power of 3.0 W. A description of the University of Michigan's Doppler lidar is given with examples of wind profiles for the boundary layer, free troposphere, and for the lower stratosphere. The system provides a reliable method of remotely measuring the wind. The wind error is smallest in regions of high aerosols. The system also produces aerosol extinction profiles versus altitude which can be determined by the shape of the spectra. The system has been installed in a trailor so that measurements can be made for field campaigns. Winds and aerosol data are available immediately at the site for use in forecasting.
Author

N92-31019*# Coherent Technologies, Inc., Boulder, CO.
ATMOSPHERIC WIND SENSING WITH A 1 AND 2 MICRON COHERENT LIDAR **c47**
R. Milton Huffaker and Sammy W. Henderson *In* NASA. Langley Research Center, 16th International Laser Radar Conference, Part 2 Jul. 1992 p 401-403 (For primary document see N92-31013 21-35)
Avail: CASI HC A01/MF A03

The majority of coherent lidar remote sensing performed to date has utilized carbon dioxide gas laser technology at wavelengths of 9 to 11 microns. However, the use of rapidly developing solid state laser technology and the shorter wavelengths offers many potential advantages. These advantages include low mass, small size, long shelf and operating lifetimes, the absence of consumables, and in many cases, increased atmospheric transmission. The shorter wavelengths of solid state lasers allow velocity measurements having better range resolution for equivalent wind velocity resolution. Coherent Technologies, Inc. has developed a 1.06 and 2.1 micron coherent lidar system for remote wind field measurements. This system is described, and some performance data are given.
Author

N92-31020*# National Oceanic and Atmospheric Administration, Boulder, CO. Wave Propagation Lab.
DESIGN OF A NEAR-IR COHERENT LIDAR FOR HIGH SPATIAL AND VELOCITY RESOLUTION WIND MEASUREMENT **c47**
Christian J. Grund and Madison J. Post *In* NASA. Langley Research Center, 16th International Laser Radar Conference, Part 2 Jul. 1992 p 405-408 (For primary document see N92-31013 21-35)
Avail: CASI HC A01/MF A03

A coherent Doppler lidar based on a CW diode-pumped, injection seeded, Th:YAG laser operating at approx. 2.02 microns is currently under development. This system is optimized for measurements of boundary layer winds with high spatial, temporal, and velocity resolution. Initially, the system will run alongside a new high repetition rate (5-10 kHz) CO2 mini-Master Oscillator Power Amplifier (mini-MOPA) Doppler lidar, which will provide simultaneous range-resolved Differential Absorption Lidar (DIAL) water vapor measurements. Water vapor DIAL operation of the 2 micron system is being considered as a future option. The anticipated specifications and the preliminary design are discussed.
Author

N92-31021*# Colorado Univ., Boulder. Cooperative Inst. for Research in Environment Sciences.
A PULSED CO2 DOPPLER LIDAR FOR BOUNDARY LAYER MONITORING **c46**
Guy N. Pearson *In* NASA. Langley Research Center, 16th International Laser Radar Conference, Part 2 Jul. 1992 p 409-411 (For primary document see N92-31013 21-35)
Avail: CASI HC A01/MF A03

A monostatic, master oscillator power amplifier (MOPA), CO2 pulsed Doppler lidar was constructed and tested. The system is compact (120 x 60 cm), operates at high pulse repetition rates (greater than 1 kHz) and is intended for simultaneous Doppler/Differential Absorption Lidar (DIAL) monitoring of the planetary boundary layer. Details of the system design, hard target calibrations, and aerosol returns are presented.
Author

N92-31022*# Phillips Lab., Hanscom AFB, MA. Optical Environment Div.
A COMPACT HIGH REPETITION RATE CO2 COHERENT DOPPLER LIDAR
S. Alejandro, R. Frelin, B. Dix, and P. McNicholl (Photometrics, Inc., Woburn, MA.) *In* NASA. Langley Research Center, 16th International Laser Radar Conference, Part 2 Jul. 1992 p 413-416 (For primary document see N92-31013 21-35)
Avail: CASI HC A01/MF A03

As part of its program to develop coherent heterodyne detection lidar technology for space, airborne, and ground based applications, the Optical Environment Division of the USAF's Phillips Laboratory developed a compact coherent CO2 TEA lidar system. Although originally conceived as a high altitude balloon borne system, the lidar is presently integrated into a trailer for ground based field measurements of aerosols and wind fields. In this role, it will also serve as a testbed for signal acquisition and processing development for planned future airborne and space based solid state lidar systems. The system has also found significance in new areas of interest to the Air Force such as cloud studies and coherent Differential Absorption Lidar (DIAL) systems.
Author

N92-31023*# National Center for Atmospheric Research, Boulder, CO.
SIMPLIFIED SIGNAL PROCESSING FOR AN AIRBORNE CO2 DOPPLER LIDAR **c36**
R. L. Schwiesow and M. P. Spowart *In* NASA. Langley Research Center, 16th International Laser Radar Conference, Part 2 Jul. 1992 p 417-420 Sponsored in part by NSF (For primary document see N92-31013 21-35)
Avail: CASI HC A01/MF A03

In the development of the National Center for Atmospheric Research (NCAR) airborne infrared lidar system (NAILS), we have emphasized a simple, modular design to suit the instrument to its mission of providing measurements of atmospheric structure and dynamics from an aircraft platform. Based on our research to this point, we believe that a significant simplification of the signal processing approach compared to that now used is possible by using high speed digitization of the signal. The purpose here is to place signal processing in the context of the overall system design and to explore the basis of the alternative technique so that the community can comment on the approach.
Author

N92-31024*# Photometrics, Inc., Woburn, MA.
PHASE NOISE IN PULSED DOPPLER LIDAR AND LIMITATIONS ON ACHIEVABLE SINGLE-SHOT VELOCITY ACCURACY
P. McNicholl and S. Alejandro (Phillips Lab., Hanscom AFB, MA.) *In* NASA. Langley Research Center, 16th International Laser Radar Conference, Part 2 Jul. 1992 p 421-424 (For primary document

see N92-31013 21-35)
Avail: CASI HC A01/MF A03

The smaller sampling volumes afforded by Doppler lidars compared to radars allows for spatial resolutions at and below some sheer and turbulence wind structure scale sizes. This has brought new emphasis on achieving the optimum product of wind velocity and range resolutions. Several recent studies have considered the effects of amplitude noise, reduction algorithms, and possible hardware related signal artifacts on obtainable velocity accuracy. We discuss here the limitation on this accuracy resulting from the incoherent nature and finite temporal extent of backscatter from aerosols. For a lidar return from a hard (or slab) target, the phase of the intermediate frequency (IF) signal is random and the total return energy fluctuates from shot to shot due to speckle; however, the offset from the transmitted frequency is determinable with an accuracy subject only to instrumental effects and the signal to noise ratio (SNR), the noise being determined by the LO power in the shot noise limited regime. This is not the case for a return from a media extending over a range on the order of or greater than the spatial extent of the transmitted pulse, such as from atmospheric aerosols. In this case, the phase of the IF signal will exhibit a temporal random walk like behavior. It will be uncorrelated over times greater than the pulse duration as the transmitted pulse samples non-overlapping volumes of scattering centers. Frequency analysis of the IF signal in a window similar to the transmitted pulse envelope will therefore show shot-to-shot frequency deviations on the order of the inverse pulse duration reflecting the random phase rate variations. Like speckle, these deviations arise from the incoherent nature of the scattering process and diminish if the IF signal is averaged over times greater than a single range resolution cell (here the pulse duration). Apart from limiting the high SNR performance of a Doppler lidar, this shot-to-shot variance in velocity estimates has a practical impact on lidar design parameters. In high SNR operation, for example, a lidar's efficiency in obtaining mean wind measurements is determined by its repetition rate and not pulse energy or average power. In addition, this variance puts a practical limit on the shot-to-shot hard target performance required of a lidar. Author

N92-31025*# Aerospace Corp., Los Angeles, CA.
A COMPARISON OF ULTRA-SENSITIVE COHERENT DETECTION (USCD) AND HETERODYNE DETECTION FOR A WIND SENSING APPLICATION
Sherwin Amimoto, Rolf Gross, Bob Lacy, Lissa Garman-DuValle, and Tom Good *In* NASA. Langley Research Center, 16th International Laser Radar Conference, Part 2 Jul. 1992 p 425-428 (For primary document see N92-31013 21-35)
Avail: CASI HC A01/MF A03

Ultra-Sensitive Coherent Detection (USCT) and conventional heterodyne detection methods were evaluated for use as a space-borne wind sensing system. For this study, we assume that the wind sensing system would be available by the year 2015. Consequently, laser systems and detectors more advanced than those under consideration for near term programs could be included. Three laser candidates under evaluation are Nd-YAG at 1.06 microns, Ho-YAG at 2.1 microns, and CO2 at 9.11 microns. Both heterodyne and USCD detection methods were included. The primary stress is on the optimization of weight and power consumption of the wind sensor portion of the satellite system.
Author

N92-31026*# Massachusetts Inst. of Tech., Lexington.
DIVERSITY IMAGING TECHNIQUES IN LIDAR Abstract Only
K. I. Schultz *In* NASA. Langley Research Center, 16th International Laser Radar Conference, Part 2 Jul. 1992 p 429 (For primary document see N92-31013 21-35)
Avail: CASI HC A01/MF A03

Diversity imaging techniques have been successfully employed in conventional microwave range-Doppler imaging radars to obtain high resolution images of both natural and man-made targets. These techniques allow microwave radars to achieve image resolution which would otherwise require excessively large antennas. Recent advances in coherent laser radar techniques and signal processing have led to the development of range-Doppler imaging laser radars. While much of the theory and signal processing techniques used in microwave radars can be brought to bear on laser radars, the significant difference in wavelength results in issues peculiar to laser radar systems. Both the fundamental concepts and specific applications of diversity imaging techniques applied to laser radar imaging systems will be discussed. Angle, frequency, and bistatic angle degrees of freedom can be employed in a coherent laser radar imaging system to achieve image resolution which exceeds the traditional Rayleigh criterion associated with the receive aperture. In diversity imaging, angle and frequency degrees of freedom can be used to synthesize an effective aperture providing range and Doppler target information. The ability to vary the bistatic angle provides an additional means of synthesizing an effective aperture. Both simulated and experimentally obtained laser radar images of spinning and/or tumbling objects utilizing both angular and frequency diversity will be presented. In coherent laser radar systems, image quality can be dominated by laser speckle effects. In particular, the signal-to-noise ratio (SNR) of a coherent laser radar image is at most unity in the presence of fully developed speckle. Diversity techniques can be utilized to improve the image SNR; simple incoherent averaging of images utilizing temporal and polarization degrees of freedom can significantly improve image SNR. Both the SNR and image resolution (as defined by the synthetic aperture) contribute to image quality. The relationship between the available degrees of freedom and image quality are discussed.
Author

N92-31027*# Shinshu Univ., Nagano (Japan). Faculty of Engineering.
A RANGE-RESOLVED BISTATIC LIDAR USING A HIGH-SENSITIVE CCD-CAMERA
K. Yamaguchi, A. Nomura, Y. Saito, and T. Kano *In* NASA. Langley Research Center, 16th International Laser Radar Conference, Part 2 Jul. 1992 p 431-432 Prepared in cooperation with Meisei Electric Co. Ltd., Moriya, Japan (For primary document see N92-31013 21-35)
Avail: CASI HC A01/MF A03

Until now monostatic type lidar systems have been mainly utilized in the field of lidar measurements of the atmosphere. We propose here a range-resolved bistatic lidar system using a high-sensitive cooled charge coupled device (CCD) camera. This system has the ability to measure the three dimensional distributions of aerosol, atmospheric density, and cloud by processing the image data of the laser beam trajectory obtained by a CCD camera. Also, this lidar system has a feature that allows dual utilization of continuous wave (CW) lasers and pulse lasers. The scheme of measurement with this bistatic lidar is shown. A laser beam is emitted vertically and the image of its trajectory is taken with a remote high-sensitive CCD detector using an interference filter and a camera lens. The specifications of the bistatic lidar system used in the experiments are shown. The preliminary experimental results of our range-resolved bistatic lidar system suggest potential applications in the field of lidar measurements of the atmosphere.
Author

N92-31028*# Lund Inst. of Tech. (Sweden). Dept. of Physics.
FLUORESCENCE LIDAR MULTI-COLOR IMAGING OF VEGETATION **c43**
J. Johansson, E. Wallinder, H. Edner, and S. Svanberg *In* NASA. Langley Research Center, 16th International Laser Radar Conference, Part 2 Jul. 1992 p 433-436 Sponsored in part by Swedish Natural Science Research Council; and the Swedish Space Board (For primary document see N92-31013 21-35)
Avail: CASI HC A01/MF A03

Multi-color imaging of vegetation fluorescence following laser excitation is reported for distances of 50 m. A mobile laser radar system equipped with a Nd:YAG laser transmitter and a 40 cm diameter telescope was used. Image processing allows extraction of information related to the physiological status of the vegetation and might prove useful in forest decline research.
Author

N92-31029*# Hamamatsu Photonics K. K., Ichino (Japan).
A GEODETIC LASER RADAR RANGEFINDER WITH 10(EXP -7) RESOLUTION **c36**
Y. Mizushima, M. Takeichi, Y. Warashima, A. Takeshima, I. Ogawa, K. Ichie, and N. H. Schiller (Hamamatsu Corp., Bridgewater, NJ.) *In* NASA. Langley Research Center, 16th International Laser Radar Conference, Part 2 Jul. 1992 p 437-440 Sponsored in part by Hamamatsu Photonics K. K.; Japan Key Technology Center; and Shizuoka Prefectural Government (For primary document see N92-31013 21-35)
Avail: CASI HC A01/MF A03

A novel geodetic laser radar rangefinder (GLRR) unit utilizing a pair of synchronized 10-psec streak camera systems was developed for displacement measurements of the earth's plates. In order to achieve minimum computing error and assure extremely high spatial resolution, an optical pulse registration clock was developed and used to register a fiducial mark on the time scale of the system. Conventional optical rangefinders have been limited to a relative resolution of 10(exp -6) even for short distances. The system to be reported on today has the capability of measuring a 50km range with an accuracy of 4mm corresponding to a relative resolution of 10(exp -7). With a gain of greater than 3 x 10(exp 3), the system has the capability of detecting extremely weak signals on the order of photon counting. This combined with temporal gating makes daytime measurements comparable in signal-to-noise ratio to nighttime viewing. This is useful for measuring faint signals returning over a range of several tens of kilometers. The present ranging system was designed to observe the mutual displacement of geodetic plates and was employed to measure the boundary between the Philippine and Asian geodetic plates that pass beneath the Suruga Bay near Hamamatsu City, Japan. The system has been in operation for over 3 years. In addition, the system has the ability of producing and detecting optical ranging pulses of several wavelengths simultaneously, making this a complete multicolor system. The basic GLRR system consists of a frequency stabilizing crystal, optical clock, YAG laser, KDP doubling crystal, DK*P tripling crystal, two matched streak cameras (A and B), a control computer, and an output/input periscope system. Author

N92-31030*# National Aeronautics and Space Administration. Goddard Space Flight Center, Greenbelt, MD.
ALTIMETRY AND LIDAR USING AlGaAs LASERS MODULATED WITH PSEUDO-RANDOM CODES
James B. Abshire, Jonathan A. R. Rall, and Serdar S. Manizade (Science Systems and Applications, Inc., Lanham, MD.) *In* NASA. Langley Research Center, 16th International Laser Radar Conference, Part 2 Jul. 1992 p 441-445 (For primary document see N92-31013 21-35)
Avail: CASI HC A01/MF A03

We have demonstrated a prototype laser altimeter and lidar which uses a low power AlGaAs laser modulated with a pseudorandom noise (PN) code, a 20 cm diameter telescope, and a photon counting receiver. Measurements to tree canopies over a 400 m horizontal path show strong signals with 5.3 mW average power and a 6.4 msec averaging time. Computer simulations predict lidar performance for various types of scattering performance. Author

N92-31031*# Defence Research Establishment Valcartier (Quebec).
MULTIPLE SCATTERING TECHNIQUE LIDAR
Luc R. Bissonnette *In* NASA. Langley Research Center, 16th International Laser Radar Conference, Part 2 Jul. 1992 p 447-450 (For primary document see N92-31013 21-35)
Avail: CASI HC A01/MF A03

The Bernouilli-Ricatti equation is based on the single scattering description of the lidar backscatter return. In practice, especially in low visibility conditions, the effects of multiple scattering can be significant. Instead of considering these multiple scattering effects as a nuisance, we propose here to use them to help resolve the problems of having to assume a backscatter-to-extinction relation and specifying a boundary value for a position far remote from the lidar station. To this end, we have built a four-field-of-view lidar receiver to measure the multiple scattering contributions. The system has been described in a number of publications that also discuss preliminary results illustrating the multiple scattering effects for various environmental conditions. Reported here are recent advances made in the development of a method of inverting the multiple scattering data for the determination of the aerosol scattering coefficient. Author

N92-31032*# National Aeronautics and Space Administration. Langley Research Center, Hampton, VA.
MULTIPLE SCATTERING EFFECTS ON SPACEBORNE LIDAR
David M. Winker and Lamont R. Poole *In its* 16th International Laser Radar Conference, Part 2 Jul. 1992 p 451-454 (For primary document see N92-31013 21-35)
Avail: CASI HC A01/MF A03

A semianalytic Monte Carlo code originally developed for oceanographic calculations (Poole et al., 1981) has been modified for use in studying multiple scattering of space-based lidar. The approach is very similar to that described by Kunkel and Weinman (1976). The trajectory of each photon is followed from the transmitter through multiple scattering until the photon is either scattered backward out of the atmosphere, scattered forward into the ground and absorbed, or scattered out the sides of the cloud. The probability that the photon will return directly to the detector is computed and summed over all significant scattering events within the field of view of the detector. Multiple scattering of the lidar pulse causes an apparent increase in the transmittance of the medium. Multiple scattering effects for space-based lidar are more significant than for ground-based lidar due to the much larger beam diameter in the atmosphere. These larger diameters are due not only to the greater range between the lidar and the scattering volume, but also the need to maintain relatively large beam divergences to satisfy eye safety restrictions on the laser irradiance at the Earth's surface. The simulations presented here are for a wavelength of 1064 nm and the Deirmendjian C1 phase function, which yields an extinction coefficient of 17.259/km. We have looked at two cases: a space-based lidar at 296 km observing a C1 cloud 293 km from the lidar and, for comparison purposes, a ground-based lidar looking at a C1 cloud with a base height of either 2 km or 5 km. The C1 size distribution roughly approximates that of stratocumulus or altocumulus clouds (aufm Kampe and Weickmann, 1957). Author

N92-31033*# GKSS-Forschungszentrum Geesthacht (Germany, F.R.).
MEASUREMENT OF MULTIPLE SCATTERING EFFECTS WITH A POLARIZATION RAMAN ELASTIC-BACKSCATTER LIDAR
Ulla Wandinger, Albert Ansmann, Claus Weitkamp, and Walfried Michaelis *In* NASA. Langley Research Center, 16th International Laser Radar Conference, Part 2 Jul. 1992 p 455-458 (For primary document see N92-31013 21-35)
Avail: CASI HC A01/MF A03

A new method for the determination of multiple scattering effects is described. A polarization Raman elastic backscatter lidar is used, which allows the measurement of the depolarization of both the elastically backscattered light and the light Raman scattered from nitrogen molecules. With this technique the depolarization effect due to multiple scattering can be separated from single scattering polarization. Presented here are a short discussion of the idea and a measurement example. Author

N92-31034*# Photometrics, Inc., Woburn, MA.
DETERMINING WATER CLOUD PARTICLE SIZES FROM LIDAR DEPOLARIZATION MEASUREMENTS AND TIME DEPENDENT MULTIPLE SCATTERING COEFFICIENTS **c47**
R. C. Garner and G. G. Koenig (Phillips Lab., Hanscom AFB, MA.) *In* NASA. Langley Research Center, 16th International Laser Radar Conference, Part 2 Jul. 1992 p 459-461 Sponsored in part by AF (For primary document see N92-31013 21-35)
Avail: CASI HC A01/MF A03

We present a technique of extracting water cloud particle

size information from lidar measurements in conjunction with double scattering calculations. In this presentation, we describe the technique and give examples using data taken with the Air Force Phillips Laboratory's (Geophysics Directorate) low altitude Nd:YAG, elastic backscatter lidar. In a related presentation we describe the double scattering lidar model which we developed for this work. The technique uses simultaneous measurements of two orthogonal linear polarization components of lidar returns from water clouds or other media composed of spherical particles. Any depolarization of the incident lidar radiation backscattered by such a media can only be due to multiple scattering. The amount of depolarization is dependent on the extinction coefficient and the single scatter phase matrix, both of which are functions of position in the medium. The phase matrix is dependent on the index of refraction of the particles and the particle size distribution. Our technique is a modification of a procedure presented in Reference 1. There, particle sizes of water clouds are determined from double scattering calculations together with measurements of radiation scattered from volumes outside the lidar receiver's field of view (which can only be multiply scattered radiation). The methodology of our technique is similar but our 'probe' of the scattering phase function (and thus the particle size distribution) is different. Author

N92-31035*# Defence Research Establishment Valcartier (Quebec).

MULTIPLE SCATTERING LIDAR RETURNS FROM STRATUS CLOUDS **c47**

D. L. Hutt and L. R. Bissonnette *In* NASA. Langley Research Center, 16th International Laser Radar Conference, Part 2 Jul. 1992 p 463-466 Prepared in cooperation with Laval Univ. (Quebec) (For primary document see N92-31013 21-35)
Avail: CASI HC A01/MF A03

Multiple scattering lidar returns from stratus clouds were measured using a multi-field-of-view (MFOV) lidar operating at 1.054 microns. The detector consists of four concentric silicon photodiodes which define half-angle fields of view (FOV) of 3.8, 12.5, 25 and 38.5 mrad. The central FOV receives the conventional lidar signal, while the outer FOV's receive only multiply scattered contributions. The ratios of the signals in the outer FOV's to the signal in the central FOV is an indication of the lateral spreading of the scattered component of the laser pulse as it propagates through the cloud. MFOV lidar returns from stratus clouds measured between October 1991 and March 1992 can be divided into two distinct types, those with large multiple scattering ratios and those with small ratios. An example of each type of return is shown. Both measurements were made at an elevation angle of 45 degrees. Clouds with small multiple scattering signals probably have a high concentration of much larger particles on the order of hundreds of micrometers in size. This is a typical size range for suspended ice crystals or precipitations. Stratus clouds often have a high concentration of ice crystals even when there is no precipitation. Large ice crystals would give smaller signals in the outer FOV's because much of the scattered intensity is contained in a narrow diffraction peak with an angular width on the order of milliradians. The result is that for a given extinction, many more orders of scattering are required for the laser pulse to spread out. So far we have not been able to do simulations of MFOV lidar returns from ice crystal clouds because of uncertainties about the phase function of the crystals, particularly the magnitude of the backscatter peak at 180 degrees. On two occasions, MFOV lidar returns measured just prior to snowfall, showed a striking vertical profile. An example is shown. From 900 to 1300m, the multiply scattered signals are negligible compared to the return in the central FOV. Abruptly, at 1300m strong signals begin in the outer FOVs. These results could be explained by the presence of a cloud layer composed of water droplets at a range of 1300m (or 900m above ground) with snow precipitations forming at the bottom of the cloud. By measuring the polarization ratio of lidar signals, Pal and Carswell have observed snow precipitating from a cloud layer composed of water droplets. Based on these results, we believe that analysis of multiple scattering lidar returns can yield important information on the phase of cloud particles. Author

N92-31036*# Eidgenoessische Technische Hochschule, Zurich (Switzerland). Inst. of Atmospheric Physics.

ANALYTICAL MULTIPLE SCATTERING CORRECTION TO THE MIE THEORY: APPLICATION TO THE ANALYSIS OF THE LIDAR SIGNAL

C. Flesia and P. Schwendimann (Defence Procurement and Technology Group, Bern, Switzerland) *In* NASA. Langley Research Center, 16th International Laser Radar Conference, Part 2 Jul. 1992 p 467-470 Prepared in cooperation with Observatoire Cantonal, Neuchatel, Switzerland Sponsored in part by ESA (For primary document see N92-31013 21-35)
Avail: CASI HC A01/MF A03

The contribution of the multiple scattering to the lidar signal is dependent on the optical depth tau. Therefore, the radar analysis, based on the assumption that the multiple scattering can be neglected is limited to cases characterized by low values of the optical depth (tau less than or equal to 0.1) and hence it exclude scattering from most clouds. Moreover, all inversion methods relating lidar signal to number densities and particle size must be modified since the multiple scattering affects the direct analysis. The essential requests of a realistic model for lidar measurements which include the multiple scattering and which can be applied to practical situations follow. (1) Requested are not only a correction term or a rough approximation describing results of a certain experiment, but a general theory of multiple scattering tying together the relevant physical parameter we seek to measure. (2) An analytical generalization of the lidar equation which can be applied in the case of a realistic aerosol is requested. A pure analytical formulation is important in order to avoid the convergency and stability problems which, in the case of numerical approach, are due to the large number of events that have to be taken into account in the presence of large depth and/or a strong experimental noise. Author

N92-31037*# Ecole Polytechnique, Palaiseau (France). Lab. de Meteorologie Dynamique.

AIRBORNE LIDAR AND RADIOMETRIC OBSERVATIONS OF PBL- AND LOW CLOUDS **c47**

P. H. Flamant, R. Valentin, and J. Pelon (Paris VI Univ., France) *In* NASA. Langley Research Center, 16th International Laser Radar Conference, Part 2 Jul. 1992 p 471-473 (For primary document see N92-31013 21-35)
Avail: CASI HC A01/MF A03

Boundary layer- and low altitude clouds over open ocean and continent areas have been studied during several field campaigns since mid-1990 using the French airborne backscatter lidar LEANDRE in conjunction with on-board IR and visible radiometers. LEANDRE is an automatic system, and a modification of the instrumental parameters, when airborne, is computer controlled through an operator keyboard. The vertical range squared lidar signals and instrument status are displayed in real time on two dedicated monitors. The lidar is used either down- or up-looking while the aircraft is flying above or below clouds. A switching of the viewing configuration takes about a minute. The lidar measurements provide a high resolution description of cloud morphology and holes in cloud layers. The flights were conducted during various meteorological conditions on single or multilayer stratocumulus and cumulus decks. Analysis on a single shot basis of cloud top (or bottom) altitude and a plot of the corresponding histogram allows one to determine a probability density function (PDF). The preliminary results show the PDFs for cloud top are not Gaussian and symmetric about the mean value. The skewness varies with atmospheric conditions. An example of results recorded over the Atlantic ocean near Biarritz is displayed, showing: (1) the range squared lidar signals as a function of time (here 100 s corresponds to about 8 km, 60 shots are averaged on horizontal); the Planetary Boundary Layer (PBL) - up to 600 m - is observed at the beginning of the leg as well as on surface returns, giving an indication of the porosity; (2) the cloud top altitude variation between 2.4 to 2.8 km during the 150 to 320 s section; and (3) the corresponding PDF. Similar results are obtained on stratocumulus over land. Single shot measurements can be used also to determine an optical porosity at a small scale as well as a

fractional cloudiness at a larger scale. A comparison of cloud top altitude retrieved from lidar and narrowbeam IR radiometer is conducted to study the scale integration problem. A good agreement within less than 100 m relies on spatial uniformity and an optically thick layer. In the presence of holes, a discrepancy is observed. This is illustrated in figure 2, displaying as a function of time (1) the lidar signals; (2) the target temperature (either clouds or sea surface) retreived from a narrowbeam IR radiometer, 17 C is the sea surface temperature on that day; and (3) the visible flux, linked to cloud albedo, measured by a pyranometer. In preparation of ASTEX, down- and up-looking measurements where conducted on stratocumulus clouds over the Atlantic Ocean near Quimper in Brittany. Depending on the flight pattern orientation with respect to the wind, the top and bottom cloud morphologies are different. Preliminary results are given on cloud morphology, cloud top PDFs, optical porosity, fractional cloudiness, and comparison of lidar and radiometric measurements. Author

N92-31038*# Ecole Polytechnique, Palaiseau (France). Lab. de Meteorologie Dynamique.

ECLIPS AT LMD: PRELIMINARY RESULTS OF PHASE 2 c47

R. Valentin, L. Menenger, S. Elouragini, P. H. Flamant, and J. Pelon (Paris VI Univ., France) *In* NASA. Langley Research Center, 16th International Laser Radar Conference, Part 2 Jul. 1992 p 475-478 (For primary document see N92-31013 21-35)

Avail: CASI HC A01/MF A03

The LMD (Laboratoire de Meteorologie Dynamique) ground-based backscatter lidar station (48 degrees 4 N, 02 degrees 0 E) near Paris was operated daily during the phase 2 of the Experimental Closed Lidar Pilot Study (ECLIPS) from May 22 to June 19, 1991 simultaneously with a radiometric equipment recording the downward short wavelength (SW) and long wavelength (LW) fluxes. A day-by-day summary of the field measurement as a function of universal time (UT) is given. Considering a 5 days week, there are only two days of missing data (05/31 and 06/06) in our record. The nearby meteorological station (10 km away) provides rawindsounding at 00UT and 12UT. During two days, the French airborne lidar LEANDRE was flown over the ground-based station. The airborne equipment looked down while the ground based equipment looked up. The two lidars were operated at 532 nm, and the on-board radiometers were identical to the ones on the ground. The measurements were synchronized with Advanced Very High Resolution Radiometer (AVHIRR) overpasses as required. We also indicate the Meteosat data corresponding to the period of measurements. Two examples of simultaneous ground-based lidar, pygeometer and pyranometer data are displayed. Author

N92-31039*# Paris VI Univ. (France). Service d'Aeronomie du CNRS.

THE 2ND PHASE OF THE LEANDRE PROGRAM: WATER-VAPOR DIAL MEASUREMENT c47

P. Quaglia, D. Bruneau, and J. Pelon *In* NASA. Langley Research Center, 16th International Laser Radar Conference, Part 2 Jul. 1992 p 479-482 (For primary document see N92-31013 21-35)

Avail: CASI HC A01/MF A03

As a follow-on of the backscattered lidar, a differential absorption lidar (LEANDRE 2) is now being developed as part of the LEANDRE program for airborne meteorological studies. The primary measurement objective of LEANDRE 2 is water vapor. Pressure and temperature measurements are aimed at a second stage. The goals are to obtain a horizontal resolution of a few hundred meters for a vertical resolution of less than a hundred meters, with an absolute accuracy of 10 percent for humidity measurement. As compatibility is an important feature between the 2 first phases of LEANDRE, most of the LEANDRE 1 sub-system will be used and adapted for LEANDRE 2. For example, detection electronics, central computer, detectors and telescope will be the same. However, important modifications have to be done on the laser source, and spectral control has to be added. Most of the work is thus devoted to those developments, and the status is presented here. Author

N92-31040*# National Aeronautics and Space Administration. Goddard Space Flight Center, Greenbelt, MD.

ADVANCED RAMAN WATER VAPOR LIDAR

David N. Whiteman, S. Harvey Melfi, Richard A. Ferrare (Universities Space Research Association, Columbia, MD.), Keith A. Evans (Hughes STX, Inc., Lanham, MD.), Luis Ramos-Izquierdo, O. Glenn Staley, Raymond W. DiSilvestre, Inna Gorin, Kenneth R. Kirks (Science Systems and Applications, Inc., Greenbelt, MD.), and William A. Mamakos (Science Systems and Applications, Inc., Greenbelt, MD.) et al *In* NASA. Langley Research Center, 16th International Laser Radar Conference, Part 2 Jul. 1992 p 483-484 Prepared in cooperation with Ressler Associates, Inc., Laurel, MD; University Research Foundation, Greenbelt, MD; and NYMA, Inc., Greenbelt, MD (For primary document see N92-31013 21-35)

Avail: CASI HC A01/MF A03

Water vapor and aerosols are important atmospheric constituents. Knowledge of the structure of water vapor is important in understanding convective development, atmospheric stability, the interaction of the atmosphere with the surface, and energy feedback mechanisms and how they relate to global warming calculations. The Raman Lidar group at the NASA Goddard Space Flight Center (GSFC) developed an advanced Raman Lidar for use in measuring water vapor and aerosols in the earth's atmosphere. Drawing on the experience gained through the development and use of our previous Nd:YAG based system, we have developed a completely new lidar system which uses a XeF excimer laser and a large scanning mirror. The additional power of the excimer and the considerably improved optical throughput of the system have resulted in approximately a factor of 25 improvement in system performance for nighttime measurements. Every component of the current system has new design concepts incorporated. The lidar system consists of two mobile trailers; the first (13m x 2.4m) houses the lidar instrument, the other (9.75m x 2.4m) is for system control, realtime data display, and analysis. The laser transmitter is a Lambda Physik LPX 240 iCC operating at 400 Hz with a XeF gas mixture (351 nm). The telescope is a .75m horizontally mounted Dall-Kirkham system which is bore sited with a .8m x 1.1m elliptical flat which has a full 180 degree scan capability - horizon to horizon within a plane perpendicular to the long axis of the trailer. The telescope and scan mirror assembly are mounted on a 3.65m x .9m optical table which deploys out the rear of the trailer through the use of a motor driven slide rail system. The Raman returns from water vapor (403 nm), nitrogen (383 nm) and oxygen (372 nm) are measured in addition to the direct Rayleigh/Mie backscatter (351). The signal from each of these is split at about a 5/95 ratio between two photomultiplier detectors. The 5 percent detector is used for measurements below about 4.0 km, while the 95 percent detector provides the information above this level. Author

N92-31041*# National Aeronautics and Space Administration. Goddard Space Flight Center, Greenbelt, MD.

WATER VAPOR VARIANCE MEASUREMENTS USING A RAMAN LIDAR c47

K. Evans (Hughes STX, Inc., Lanham, MD.), S. H. Melfi, R. Ferrare (Universities Space Research Association, Columbia, MD.), and D. Whiteman *In* NASA. Langley Research Center, 16th International Laser Radar Conference, Part 2 Jul. 1992 p 485-487 (For primary document see N92-31013 21-35)

Avail: CASI HC A01/MF A03

Because of the importance of atmospheric water vapor variance, we have analyzed data from the NASA/Goddard Raman lidar to obtain temporal scales of water vapor mixing ratio as a function of altitude over observation periods extending to 12 hours. The ground-based lidar measures water vapor mixing ration from near the earth's surface to an altitude of 9-10 km. Moisture profiles are acquired once every minute with 75 m vertical resolution. Data at each 75 meter altitude level can be displayed as a function of time from the beginning to the end of an observation period.

These time sequences have been spectrally analyzed using a fast Fourier transform technique. An example of such a temporal spectrum obtained between 00:22 and 10:29 UT on December 6, 1991 is shown in the figure. The curve shown on the figure represents the spectral average of data from 11 height levels centered on an altitude of 1 km (1 plus or minus .375 km). The spectra shows a decrease in energy density with frequency which generally follows a -5/3 power law over the spectral interval 3x10 (exp -5) to 4x10 (exp -3) Hz. The flattening of the spectrum for frequencies greater than 6x10 (exp -3) Hz is most likely a measure of instrumental noise. Spectra like that shown in the figure are calculated for other altitudes and show changes in spectral features with height. Spectral analysis versus height have been performed for several observation periods which demonstrate changes in water vapor mixing ratio spectral character from one observation period to the next. The combination of these temporal spectra with independent measurements of winds aloft provide an opportunity to infer spatial scales of moisture variance. Author

N92-31042*# Deutsche Forschungs- und Versuchsanstalt fuer Luft- und Raumfahrt, Oberpfaffenhofen (Germany, F.R.). Inst. of Atmospheric Physics.

AIRBORNE REMOTE SENSING OF TROPOSPHERIC WATER VAPOR USING A NEAR INFRARED DIAL SYSTEM **c47**

G. Ehret, C. Kiemle, W. Renger, and G. Simmet *In* NASA. Langley Research Center, 16th International Laser Radar Conference, Part 2 Jul. 1992 p 489-492 (For primary document see N92-31013 21-35)

Avail: CASI HC A01/MF A03

Summarized here are the results of airborne water vapor measurements in the lower middle and upper troposphere using the Differential Absorption Lidar (DIAL) technique in the near infrared. The measurements were performed in July 1990 in Southern Bavaria between Allersberg and Straubing from 20 to 23 UTC taking advantage of night time conditions. The tropospheric H2O profiles were range investigated both horizontally and vertically. With the DIAL system that was used, water vapor measurements in the upper troposphere have been carried out for the first time. To calibrate the H2O-retrievals, effective absorption cross sections of selected H2O lines in terms of altitude around 724 nm were calculated using line parameter data from the literature (B. E. Grossmann et al). The frequency of the on-line measurements was adjusted by the spectra of a Polyacenic Semiconductor (PAS) cell filled with H2O. We found that the calibration error ranged between 0.005 and 0.015 cm(exp -1). The systematic errors of the H2O as a function of altitude were estimated below 7 km and 12 percent accuracy in the upper troposphere. The vertical H2O profile agrees well with in situ measurements in the investigated range between the top of the planetary boundary layer (PBL) up to near the tropopause. Horizontal and vertical H2O profiles are calculated by means of averaging single lidar returns. Typical horizontal resolutions range from 4 km in the lower to 11 km in the upper troposphere with vertical resolutions varying from 0.3 km up to 1 km, respectively, in order to satisfy a 5 - 10 percent accuracy in the statistical error. The measurement sensibility of the water vapor mixing ration in the upper troposphere is 0.01 g/kg. Author

N92-31043*# Deutsche Forschungsanstalt fuer Luft- und Raumfahrt, Oberpfaffenhofen (Germany, F.R.). Inst. of Optoelectronics.

TRIAL OF A SLANT VISUAL RANGE MEASURING DEVICE

J. Streicher, C. Muenkel (Impulsphysik G.m.b.H., Hamburg, Germany, F.R.), and H. Borchardt (Deutscher Wetterdienst, Hamburg, Germany, F.R.) *In* NASA. Langley Research Center, 16th International Laser Radar Conference, Part 2 Jul. 1992 p 493-496 (For primary document see N92-31013 21-35)

Avail: CASI HC A01/MF A03

Each year, fog at airports renders some landing operations either difficult or impossible. The visibility that a pilot of a landing aircraft can expect is in that case the most important information. It could happen that the visibility versus the altitude is constantly decreasing or increasing. However, it is not possible to distinguish this with the existing sensors at an airport. If the visibility is decreasing with the altitude, one has the worst case - ground fog. The standard visibility sensor, the transmissometer, determines only the horizontal visual range, which will be underestimated in comparison with the real visibility a pilot has on his landing approach. Described here is a new technique to measure the slant visual range, making use of a slant scanning device - an eye-safe laser radar. A comparison with commercial visibility sensors shows that it is possible to measure visibilities with the slant looking laser radar in the range from 50 meters up to 2000 meters and even distinguish inhomogenities like ground fog.

Author

N92-31044*# Eidgenoessische Technische Hochschule, Zurich (Switzerland). Inst. of Atmospheric Physics.

LIDAR DEPOLARIZATION BY NONSPHERICAL PARTICLES: POTENTIAL OF COMBINED DEPOLARIZATION/BACKSCATTERING MEASUREMENTS FOR PSC'S CHARACTERIZATION **c46**

C. Flesia, A. Mugnai (Consiglio Nazionale delle Ricerche, Frascati, Italy), L. deSchoulepnikoff, and L. Stefanutti (Consiglio Nazionale delle Ricerche, Florence, Italy) *In* NASA. Langley Research Center, 16th International Laser Radar Conference, Part 2 Jul. 1992 p 497-500 Prepared in cooperation with Observatoire Cantonal, Neuchatel, Switzerland (For primary document see N92-31013 21-35)

Avail: CASI HC A01/MF A03

We analyze the potential of combined backscatter and depolarization information for deriving the optical parameters of Polar Stratospheric Clouds (PSCs) together with the size and physical phase of the cloud particles. In particular, we investigate the influence of particle shape and orientation on the parallel and perpendicular backscattered intensities and on the depolarization ratio under experimental noise conditions, and how the first three moments of the particle size distribution (i.e., particle concentration, mean radius, and standard deviation) may be used to introduce further distinction between type Ia and type Ib PSCs. Author

N92-31045*# National Oceanic and Atmospheric Administration, Boulder, CO. Wave Propagation Lab.

COHERENT CO2 LIDAR: A SUPERIOR SYSTEM FOR OBSERVING CLOUDS?

Wynn L. Eberhard and R. Michael Hardesty *In* NASA. Langley Research Center, 16th International Laser Radar Conference, Part 2 Jul. 1992 p 501-504 (For primary document see N92-31013 21-35)

Avail: CASI HC A01/MF A03

Lidars have long been used to study various parameters of clouds. NOAA's Wave Propagation Laboratory has operated a coherent CO2 lidar for over a decade, using Doppler to study wind fields and turbulence, atmospheric absorption for Differential Absorption Lidar (DIAL) applications, backscatter to investigate aerosol distributions, and backscatter and extinction measurements on clouds. A system under development for our laboratory promises to overcome the older system's problems of large size, frequency instability, and need for continual operator attention. We are also thoroughly evaluating the capabilities of CO2 lidar for observing clouds, including development of some new techniques. CO2 lidar provides a view of clouds different in many ways from that of lidars at other extinction measurements from clouds. This discussion argues in support of the proposition: coherent CO2 lidar can be a superior lidar system for measuring most cloud properties. Author

N92-31046*# Colorado State Univ., Fort Collins. Dept. of Physics.

MEASUREMENT OF AEROSOL PROFILES USING HIGH-SPECTRAL-RESOLUTION RAYLEIGH-MIE LIDAR **c45**

D. A. Krueger, R. J. Alvarez, II, L. M. Caldwell, and C. Y. She *In* NASA. Langley Research Center, 16th International Laser Radar Conference, Part 2 Jul. 1992 p 505-508 (For primary document see N92-31013 21-35)

Avail: CASI HC A01/MF A03

High-spectral-resolution Rayleigh-Mie lidar measurements of vertical profiles (1 to 5 km) of atmospheric pressure and density, as well as aerosol profiles, including backscatter ratio and extinction ratio are reported. These require simultaneous measurement of temperature. Use of the technique does not require any assumptions about the aerosol but does require that the pressure at one altitude is known and that the gas law of the air is known (e.g., an ideal gas). Author

N92-31047*# Florence Univ. (Italy). Dept. of Physics.
LABORATORY SCALED SIMULATION OF LIDAR CLOUD SOUNDING EXPERIMENTS **c47**
G. Zaccanti, P. Bruscaglioni, M. Gurioli (European Lab. for Non-Linear Spectroscopy, Florence, Italy), and P. Sansoni *In* NASA. Langley Research Center, 16th International Laser Radar Conference, Part 2 Jul. 1992 p 509-512 (For primary document see N92-31013 21-35)
Avail: CASI HC A01/MF A03

The results of lidar measurements carried out on laboratory scale models of clouds are presented. Measurements on laboratory scale models are important since one has the knowledge of the relevant parameters of the diffusing medium, such as: scattering and absorption coefficients, phase function, homogeneity, shape, etc. Knowledge of these parameters enables one to use the results to test the reliability of theoretical and numerical investigations. To obtain a laboratory scaled model of a lidar system sounding a cloud, it is necessary to scale down all the geometrical quantities by the same factor to reduce distances of the order of kilometers to the order of meters, keeping the size and the optical depth of the diffusers unchanged. If a time resolution of the order of nanoseconds is necessary for a lidar sounding actual clouds, the corresponding time resolution for the laboratory model should be of the order of picoseconds. It is possible to obtain this resolution by using picosecond laser systems and fast electrooptical detectors like the streak camera. The results of the laboratory measurements showed that the multiple scattering effect strongly depends on the size of the diffusers, as well as on the concentration. The experimental results were compared with the numerical results of a Monte Carlo code. A generally good agreement was obtained. Author

N92-31048*# Max-Planck-Inst. fuer Meteorologie, Hamburg (Germany, F.R.).
AN ALEXANDRITE REGENERATIVE AMPLIFIER FOR WATER VAPOR AND TEMPERATURE MEASUREMENTS **c47**
P.-Y. Thro, J. Boesenberg, and V. Wulfmeyer *In* NASA. Langley Research Center, 16th International Laser Radar Conference, Part 2 Jul. 1992 p 513-516 (For primary document see N92-31013 21-35)
Avail: CASI HC A01/MF A03

The Differential Absorption Lidar (DIAL) technique is a powerful method for determining meteorological parameters, but it requires high quality of the laser source: high energy, very narrow bandwidth, high wavelength stability, and spectral purity. Although many efforts have been made to improve the lasers in view of these aspects, a satisfactory solution has not been demonstrated up to now. We describe a regenerative amplifier, using a Ti:sapphire laser as master oscillator and an alexandrite laser as slave amplifier, which is expected to meet the requirements for water vapor concentration and temperature measurements. Author

N92-31049*# National Aeronautics and Space Administration. Goddard Space Flight Center, Greenbelt, MD.
WAVEMETER MEASUREMENTS OF FREQUENCY STABILITY OF AN INJECTION SEEDED ALEXANDRITE LASER FOR PRESSURE AND TEMPERATURE LIDAR
C. R. Prasad (Universities Space Research Association, Greenbelt, MD.), G. K. Schwemmer, and C. L. Korb *In* NASA. Langley Research Center, 16th International Laser Radar Conference, Part 2 Jul. 1992 p 517-520 (For primary document see N92-31013 21-35)
Avail: CASI HC A01/MF A03

The GSFC pressure-temperature lidar is a differential absorption lidar operating in the oxygen A band absorption region (760 to 770 nm), and utilizes two tunable pulsed alexandrite lasers. For obtaining temperature measurements with an accuracy of less than or = 1 K, it has been determined that the stability of the online laser frequency over a period of time corresponding to a set of measurements, 0.1 to 30 min, has to be better than +/- 0.002/cm. In addition, the requirements on laser spectral bandwidth and spectral purity are less than or = 0.02/cm and greater than or = 99.9 percent, respectively. Injection seeding with a stabilized AlGaAs diode laser was used to achieve the required frequency stability and spectral bandwidth. A high resolution Fizeau wavemeter was employed to determine the frequency stability of the pulsed alexandrite laser and determine its bandwidth, mode structure. We present the results of measurements of the frequency stability and the spectrum of the injection seeded alexandrite laser. Author

N92-31050*# National Aeronautics and Space Administration. Goddard Space Flight Center, Greenbelt, MD.
CONICALLY SCANNED LIDAR TELESCOPE USING HOLOGRAPHIC OPTICAL ELEMENTS
Geary K. Schwemmer and Thomas D. Wilkerson (Maryland Univ., College Park.) *In* NASA. Langley Research Center, 16th International Laser Radar Conference, Part 2 Jul. 1992 p 521-524 (For primary document see N92-31013 21-35)
Avail: CASI HC A01/MF A03

Holographic optical elements (HOE) using volume phase holograms make possible a new class of lightweight scanning telescopes having advantages for lidar remote sensing instruments. So far, the only application of HOE's to lidar has been a non-scanning receiver for a laser range finder. We introduce a large aperture, narrow field of view (FOV) telescope used in a conical scanning configuration, having a much smaller rotating mass than in conventional designs. Typically, lidars employ a large aperture collector and require a narrow FOV to limit the amount of skylight background. Focal plane techniques are not good approaches to scanning because they require a large FOV within which to scan a smaller FOV mirror or detector array. Thus, scanning lidar systems have either used a large flat scanning mirror at which the receiver telescope is pointed, or the entire telescope is steered. We present a concept for a conically scanned lidar telescope in which the only moving part is the HOE which serves as the primary collecting optic. We also describe methods by which a multiplexed HOE can be used simultaneously as a dichroic beamsplitter. Author

N92-31051*# Centre National de la Recherche Scientifique, Verrieres-Le Buisson (France).
OPTICS OF THE OZONE LIDAR ELSA **c74**
J. Porteneuve *In* NASA. Langley Research Center, 16th International Laser Radar Conference, Part 2 Jul. 1992 p 525-527 (For primary document see N92-31013 21-35)
Avail: CASI HC A01/MF A03

In order to study the ozone layer in the Arctic, we have to define a new optical concept for a lidar. It was necessary to build a transportable system with a large collecting surface in a minimum of volume. It was too useful to have a multichannel receptor. A description of the Emettor Receptor System, collecting system, and analysis system is provided. Author

N92-31052*# Centre National de la Recherche Scientifique, Verrieres-Le Buisson (France).
INTERFEROMETERS ADAPTATIONS TO LIDARS
J. Porteneuve *In* NASA. Langley Research Center, 16th International Laser Radar Conference, Part 2 Jul. 1992 p 529-531 (For primary document see N92-31013 21-35)
Avail: CASI HC A01/MF A03

To perform daytime measurements of the density and temperature by Rayleigh lidar, it is necessary to select the wavelength with a very narrow spectral system. This filter is composed by an interference filter and a Fabry Perot etalon. The Fabry Perot etalon is the more performent compound, and it is necessary to build a specific optic around it. The image of the

entrance pupil or the field diaphragm is at the infinite and the other diaphragm is on the etalon. The optical quality of the optical system is linked to the spectral resolution of the system to optimize the reduction of the field of view. The resolution is given by the formula: R = 8(xD/Fd)exp 2 where R = lambda/delta(lambda), x = diameter of the field diaphragm, D = diameter of the reception mirror, F = focal length of the telescope, and d = useful diameter of the etalon. In the Doppler Rayleigh lidars, the PF interferometer is the main part of the experiment and the exact spectral adaptation is the most critical problem. In the spectral adaptation of interferometers, the transmittance of the system will be acceptable if the etalon is exactly adjusted to the wavelength of the laser. It is necessary to work with a monomode laser, and adjust the shift to the bandpass of the interferometer. We are working with an interferometer built with molecular optical contact. This interferometer is put in a special pressure closed chamber.

Author

N92-31053*# Aerospace Corp., Los Angeles, CA.

AN ULTRA-SENSITIVE COHERENT DETECTOR CAPABLE OF SINGLE PHOTON DETECTION FOR LIDAR APPLICATIONS

Sherwin Amimoto, Rolf Gross, Bob Lacy, Lissa Garman-DuValle, and Tom Good *In* NASA. Langley Research Center, 16th International Laser Radar Conference, Part 2 Jul. 1992 p 533-535 (For primary document see N92-31013 21-35)

Avail: CASI HC A01/MF A03

The properties of Ultra-Sensitive Coherent Detectors (USCD's) are nearly that of an ideal detector for lidar applications. Recent progress in the development of USCD's is briefly reviewed, and its imaging capability is demonstrated. These new detectors possess properties with significant improvements over conventional technology. These improvements include a high quantum efficiency of 0.95, gain in excess of 10 exp 13, a narrow bandwidth of 180-300 MHz at 1 micron, imaging capability, and phase conjugation ability. We have constructed a USCD using two Nd:YAG laser amplifiers and a four-wave Brillouin mirror (FWBM) using SnCl4 as the Brillouin medium. Using a 10 Hz repetitively-pulsed single frequency laser, we have shown that the Brillouin medium is free from thermal blooming and from optical breakdown. Author

N92-31054*# Chiba Univ. (Japan). Remote Sensing and Image Research Center.

A HIGH SPEED SIGNAL PROCESSING SYSTEM FOR A DIODE-PUMPED YAG LIDAR

H. Okumura, T. Sugita, H. Matsumoto, N. Takeuchi, and S. Kuwashima (OKK, Inc., Tokyo, Japan) *In* NASA. Langley Research Center, 16th International Laser Radar Conference, Part 2 Jul. 1992 p 537-539 (For primary document see N92-31013 21-35)

Avail: CASI HC A01/MF A03

Usually, in acquisition of the lidar echo signal, a transient recorder has been used. However, in the case of using a high-repetitive laser, such as a diode-pumped YAG laser, as a lidar light source, the acquisition speed of a transient recorder is not fast enough. A system using a sampling and direct accumulation in a clock cycle, before transferring digital data to a computer, is necessary for a fast acquisition, and a new system which equips the necessary functions was developed and is reported. Author

N92-31055*# National Aeronautics and Space Administration. Goddard Space Flight Center, Greenbelt, MD.

PULSED LASER SPECTRAL MEASUREMENT USING A FABRY-PEROT INTERFEROMETER: LIMITS TO RESOLUTION

Anthony Notari (Science and Engineering Services, Inc., Burtonsville, MD.) and Bruce M. Gentry *In* NASA. Langley Research Center, 16th International Laser Radar Conference, Part 2 Jul. 1992 p 541-544 (For primary document see N92-31013 21-35)

Avail: CASI HC A01/MF A03

We are developing a Doppler lidar system using the edge technique to measure atmospheric wind profiles. The edge technique requires a laser with a narrow spectral bandwidth and a high resolution optical filter. The lidar system will use a Nd:YAG laser operating at 1.064 microns and a high resolution Fabry-Perot interferometer for the edge filter. The Doppler shift measurement is made by locating the laser on the edge of the filter's spectral response function. Due to the steep slope on the edge, large changes in the filter transmission will be observed for small changes in frequency. The Doppler shift can be determined from a measurement of this change in filter transmission if the filter spectral response function in the region of the measurement is well known. Recently developed injection seeded solid state lasers have made near transform limited laser output readily available for lidar work. Injection-seeded Nd:YAG laser exhibit single mode output with smooth Gaussian temporal pulse shapes. Results of an experiment we conducted to evaluate the effects of a short Gaussian temporal input pulse on the spectral response of a high resolution Fabry-Perot interferometer are presented. Author

N92-31056*# Massachusetts Inst. of Tech., Lexington. Lincoln Lab.

TUNABLE ELECTRO-OPTIC MODULATORS FOR LIDAR SYSTEMS AND ATMOSPHERIC APPLICATIONS

R. S. Eng, N. W. Harris, C. L. Summers, and B. Lax (Massachusetts Inst. of Tech., Cambridge.) *In* NASA. Langley Research Center, 16th International Laser Radar Conference, Part 2 Jul. 1992 p 545-548 Sponsored in part by AF (For primary document see N92-31013 21-35)

Avail: CASI HC A01/MF A03

In global sensing applications using different types of lidars, the spectral range and fine frequency coverages are often limited because of the finite tunabilities of molecular lasers and the number of molecular species that are available. To overcome the above obstacle, we have proposed new broadband frequency tunable electro-optic (EO) modulators that can cover a wide range from the mid-infrared to the visible as lidar sources in atmospheric sensing applications such as high resolution atmospheric molecular spectroscopy, Differential Absorption Lidar (DIAL), and laser radar imaging. The configuration of the proposed new tunable EO modulators includes an electro-optic active crystal element surrounded by a ferrite tuning element which is placed inside a microwave waveguide. The tuning is provided by an external magnetic field, which is either longitudinal or transverse, and the modulator can be either single sideband type or a double sideband type depending on the application required for the spectral purity of the modulator output. Author

N92-31057*# Science and Engineering Services, Inc., Burtonsville, MD.

INJECTION SEEDED SINGLE MODE ALEXANDRITE RING LASER FOR LIDAR APPLICATIONS

H. Sang Lee and Anthony Notari *In* NASA. Langley Research Center, 16th International Laser Radar Conference, Part 2 Jul. 1992 p 549-552 (For primary document see N92-31013 21-35)

Avail: CASI HC A01/MF A03

Along with many spectroscopic applications, atmospheric lidar measurements require a tunable, narrow band laser with a very high degree of spectral purity. A standing wave pulsed alexandrite laser tuned by injection seeding with an AlGaAs laser diode has demonstrated high stability. The standing wave cavity, however, poses several difficulties in light of the single mode operation and efficient seeding beam into the cavity. In order to overcome these problems and to operate the high power alexandrite laser in a single axial mode with a high spectral purity, a new ring laser system is being developed. The design features of the ring laser and some measurements of the laser characteristics are presented. Author

N92-31058*# Tohoku Univ., Sendai (Japan). Inst. of Technology.

Tm,Ho:YAG LASER WITH TUNABLE RANGE OF 2.08-2.12 MICRONS AND ITS APPLICATIONS TO SPECTROSCOPY c36

Kazuhiro Asai and Toshikazu Itabe (Ministry of Posts and Telecommunications, Tokyo, Japan) *In* NASA. Langley Research Center, 16th International Laser Radar Conference, Part 2 Jul.

1992 p 553-554 (For primary document see N92-31013 21-35)
Avail: CASI HC A01/MF A03

In recent advanced lasers, 2 micron solid-state lasers such as Tm:YAG and Ho:YAG lasers are very attractive for laser radar remote sensing technologies because of eye safety, realizations of all solid-state laser pumped by diode laser and smaller dimension, tunability of lasing wavelength, possibility of coherent detection, etc. Featuring these advantages, 2 micron lasers have been candidated as laser transmitters for use in water vapor Differential Absorption Lidar (DIAL), laser altimeter, Doppler wind sensor, Mie lidar, etc. Characterization of a tunable Cr, Tm, Ho:YAG laser and its applications to spectroscopy concerning absorption and reflectance are reported. Author

N92-31059*# Office National d'Etudes et de Recherches Aerospatiales, Meundon (France).
THEORETICAL SIMULATION OF A 2 MICRON AIRBORNE SOLID STATE LASER ANEMOMETER
Beatrice Imbert and Jean-Pierre Cariou *In* NASA. Langley Research Center, 16th International Laser Radar Conference, Part 2 Jul. 1992 p 555-558 Sponsored in part by the Direction des Constructions Aeronautiques (For primary document see N92-31013 21-35)
Avail: CASI HC A01/MF A03

In the near future, military aircraft will need to know precisely their true airspeed in order to optimize flight conditions. In comparison with classical anemometer probes, an airborne Doppler lidar allows measurement of the air velocity without influence from aircraft aerodynamic disturbance. While several demonstration systems of heterodyne detection using a CO2 laser have been reported, improvements in the technology of solid state lasers have recently opened up the possibility that these devices can be used as an alternative to CO2 laser systems. In particular, a diode pumped Tm:Ho:YAG laser allows a reliable compact airborne system with an eye safe wavelength (lambda = 2.09 microns) to be achieved. The theoretical study of performances of a coherent lidar using a solid state diode pumped Tm:Ho:YAG laser, caled SALSA, for measuring aircraft airspeed relative to atmospheric aerosols is described. A computer simulation was developed in order to modelize the Doppler anemometer in the function of atmospheric propagation and optical design. A clever analysis of the power budget on the detector area allows optical characteristic parameters of the system to be calculated, and then it can be used to predict performances of the Doppler system. Estimating signal to noise ratios (SNR) and heterodyne efficiency provides the available energy of speed measurement as well as a useful measurement of the alignment of the backscattered and reference fields on the detector. Author

N92-31060*# National Aeronautics and Space Administration. Langley Research Center, Hampton, VA.
COMPARISON OF EYE-SAFE SOLID STATE LASER DIAL WITH PASSIVE GAS FILTER CORRELATION MEASUREMENTS FROM AIRCRAFT AND SPACECRAFT **c74**
Robert V. Hess, Leo D. Staton, H. Andrew Wallio, and Liang-Guo Wang (College of William and Mary, Williamsburg, VA.) *In its* 16th International Laser Radar Conference, Part 2 Jul. 1992 p 559-562 (For primary document see N92-31013 21-35)
Avail: CASI HC A01/MF A03

Differential Absorption Lidar (DIAL) using solid state Ti:sapphire lasers finds current application in the NASA/LASE Project for H2O vapor measurements in the approximately = 0.820 micron region for the lower and mid-troposphere and in potential future applications in planned measurements of the approximately = 0.940 micron region where both strong and weak absorption lines enables measurements throughout the troposphere and lower stratosphere. The challenge exists to perform measurements in the eye-safe greater than 1.5 micron region. A comparison between DIAL and passive Gas Filter Correlation Radiometer (GFCR) measurements is made. The essence of the differences in signal to noise ratio for DIAL and passive GFCR measurements is examined. The state of the art of lasers and optical parametric oscillators (OPO's) is discussed. Author

N92-31061*# Ludwig-Maximilians-Univ., Munich (Germany, F.R.). Inst. der Meteorologisches.
LIDAR MULTIPLE SCATTERING: DEPENDENCE ON ATMOSPHERIC PARAMETERS **c47**
Matthias Wiegner *In* NASA. Langley Research Center, 16th International Laser Radar Conference, Part 2 Jul. 1992 p 563-565 (For primary document see N92-31013 21-35)
Avail: CASI HC A01/MF A03

Backscatter lidars are very useful tools in gaining information about the atmosphere. Inversion of backscatter signals can be used to retrieve the spatial distribution of clouds and aerosols, e.g., vertical extensions of clouds and aerosol layers, detection of 'subvisible' cirrus, etc., very accurately compared to passive radiometers. To retrieve extinction coefficient profiles, in general, the so-called lidar equation is solved. This equation describes a laser pulse which propagates through an atmosphere with transmission exp(- integral of sigma(z')dz'), which is scattered singly under 180 degrees towards a receiver, and which is attenuated on its way back again by exp(- integral of sigma(z')dz'). For inversion, further information on optical properties of the scatterers are required (extinction to backscatter ratio). However, it is evident that, at least for optically thick clouds and/or large receiver's field-of-views, this approach may be erroneous because of multiply scattered photons. Several studies were performed to simulate multiple scattering in case of collimated beams or pulses including Monte Carlo, transport, and diffusion theory. Unfortunately, most of the approaches require an enormous amount of computer time. Thus, it is meaningful to elaborate approximate methods, and one such method is discussed. Our method is based on Bissonnett (1988). We have improved the numerical simulation of limited field-of-view detectors, and compared the results to Monte Carlo calculations and an exact model of Altmann (1989). Author

N92-31062*# GKSS-Forschungszentrum Geesthacht (Germany, F.R.).
VERIFICATION MEASUREMENT OF A POLARIZATION RAMAN ELASTIC-BACKSCATTER LIDAR
Christoph Schulze, Ulla Wandinger, Albert Ansmann, Claus Weitkamp, and Walfried Michaelis *In* NASA. Langley Research Center, 16th International Laser Radar Conference, Part 2 Jul. 1992 p 567-570 (For primary document see N92-31013 21-35)
Avail: CASI HC A01/MF A03

By measuring the depolarization of light Raman scattered from a gas of known number density (nitrogen), it is possible to determine the influence of multiple scattering on lidar signals. In order to realize such measurements, linearly polarized laser light is emitted and two components of the nitrogen Raman signals, with E vectors parallel (parallel P sub lambda R) and perpendicular (perpendicular P sub lambda R) to the plane of polarization of the laser light, are measured. The depolarization ratio, delta sub lambda R = perpendicular P sub lambda R/parallel P sub lambda R, is constant if only the Raman scattering process contributes to the signal. Any variation of the depolarization is caused by additional elastic, and, thus, multiple scattering. If the contribution of multiple scattered light to the lidar signals is known, other parameters determined with the systems such as extinction, backscattering, and the depolarization of elastically scattered light, can be corrected for this influence. The lidar system used for the polarization measurements, especially the receiver setup, is described. The calibration of the apparatus and a clear air measurement are discussed. Author

N92-31063*# Photometrics, Inc., Woburn, MA.
TIME AND POLARIZATION DEPENDENT DOUBLE SCATTERING CALCULATIONS OF LIDAR RETURNS FROM WATER CLOUDS **c47**
R. C. Garner *In* NASA. Langley Research Center, 16th International Laser Radar Conference, Part 2 Jul. 1992

p 571-574 Sponsored in part by AF (For primary document see N92-31013 21-35)
Avail: CASI HC A01/MF A03

We describe and present results of a double scattering lidar model which we use to calculate lidar returns from water clouds. The model is used in conjunction with the Phillips Laboratory's (Geophysics Directorate) low altitude Nd:YAG lidar system to determine microphysical properties of water clouds. The model determines the Stokes parameters of the backscattered lidar radiation, from media composed of spherical particles, as a function of time. The Stokes parameters of the radiation of the lidar return are determined, at each time, by considering all radiation which has traveled the same path length from transmitter to receiver while making two successive single scatters. Each single scatter is considered a Mie scatter. We have also developed a Mie scattering program for use with the double scattering model. Each single scatter takes into account the polarization of the incident and scattered radiation. Inputs to the double scattering mode include the receiver area and field of view, the receiver integration time, the extinction coefficient as a function of distance into the cloud, the particle size distribution (assumed independent of position), and the complex index of refraction of the spherical particles. Author

N92-31064*# Science and Technology Corp., Edgewood, MD.
MULTIPLE SCATTERING WAVELENGTH DEPENDENT BACKSCATTERING OF KAOLIN DUST IN THE IR: MEASUREMENTS AND THEORY **c47**
Avishai Ben-David *In* NASA. Langley Research Center, 16th International Laser Radar Conference, Part 2 Jul. 1992 p 575-578 (For primary document see N92-31013 21-35)
(Contract DAAA15-89-D-0007)
Avail: CASI HC A01/MF A03

Knowing the optical properties of aerosol dust is important for designing electro-optical systems and for modeling the effect on propagation of light in the atmosphere. As CO2 lidar technology becomes more advanced and is used for multiwavelength measurements, information on the wavelength dependent backscattering of aerosol dust particles is required. The volume backscattering coefficient of aerosols in the IR is relatively small. Thus, only a few field measurements of backscattering, usually at only a few wavelengths, are reported in the literature. We present spectral field measurements of backscattering of kaolin dust in the 9-11 micron wavelength range. As the quantity of dust increases, multiple scattering contributes more to the measured backscattered signal. The measurements show the effect of the dust quantity of the spectral backscatter measurements. A simple analytical two stream radiative transfer model is applied to confirm the measurements and to give insight to the multiple scattering spectra of backscattering. Author

N92-31065*# Naval Research Lab., Washington, DC. Remote Sensing Div.
AUREOLE LIDAR: DESIGN, OPERATION, AND COMPARISON WITH IN-SITU MEASUREMENTS
William P. Hooper and D. R. Jensen (Naval Command, Control and Ocean Surveillance Center, San Diego, CA.) *In* NASA. Langley Research Center, 16th International Laser Radar Conference, Part 2 Jul. 1992 p 579-580 (For primary document see N92-31013 21-35)
Avail: CASI HC A01/MF A03

In 1986, H. Berber and Hooper examined the signals that could be detected by an airborne lidar flying above the marine boundary layer (MBL). One signal (aureole) formed from laser light returned to the receiver after a reflect off the ocean and forward scatter off the aerosol particles appeared to be both detectable and related to the optical depth of the MBL. Now, research has been directed towards developing a practical instrument to measure the aureole and finding an algorithm to use the information. Unlike the lidar backscatter which typically requires a telescope with a narrow field of view (0.5 mrad), the aureole signal occurs over a wide field of view (50 mrad). To accommodate the totally different needs, a standard commercial Cassegrainian telescope was modified to yield a telescope with two focal planes. The secondary mirror was replaced by a lens, whose front surface was half silvered and curved to match the replaced mirror. Light reflecting off the lens focused behind the primary mirror. The back lens surface was curved to allow unreflected light to focus at the natural focus of the primary mirror. This focal plane which is behind the lens has a wide field of view. To calculate an extinction profile, the aureole optical depth estimate is combined with the lidar backscatter profile. Author

N92-31066*# Defence Research Establishment Valcartier (Quebec).
EFFECT OF ATMOSPHERIC EXTINCTION ON LASER RANGEFINDER PERFORMANCE AT 1.54 AND 0.6 MICRONS **c36**
D. L. Hutt, J.-M. Theriault, V. Larochelle, and D. Bonnier *In* NASA. Langley Research Center, 16th International Laser Radar Conference, Part 2 Jul. 1992 p 581-584 Prepared in cooperation with Laval Univ., Quebec; and Wisconsin Univ., Madison (For primary document see N92-31013 21-35)
Avail: CASI HC A01/MF A03

Extinction of laser rangefinder (LRF) pulses by the atmosphere depends on the wavelength, weather conditions, and aerosol concentration along the optical path. In the IR, extinction is due to absorption by molecular constituents and scattering and absorption by aerosols. The total atmospheric extinction alpha(lambda) is the sum of the molecular and aerosol contributions, alpha(sub m)(lambda)and Alpha(sub a)(lambda). We present simple expressions for alpha(sub m)(lambda) and alpha(sub a)(lambda) for two LRF sources: Er:glass and CO2 which operate at 1.54 and 10.6 microns, respectively. The expressions are based on accepted models of atmospheric aerosols and molecular extinction and give an estimate of alpha(lambda) as a function of standard meteorological parameters, assuming horizontal beam propagation. Signal-to-noise ratios of LRF returns, measured from a reference target under different weather conditions are compared to predictions based on the estimate of alpha(lambda). Author

N92-31067*# Litton Industries, Moorpark, CA. Aero Products Div.
A STUDY OF ATMOSPHERIC OPTICAL SCATTERING PARAMETERS AT 1.5 AND 2 MICRON REGION FOR SOLID STATE DOPPLER LIDAR APPLICATIONS
Eli Margalit, Farzin Amzajerdian, Rodney Benoist, and Richard Dubinsky (Sky Council, Toronto, Ontario) *In* NASA. Langley Research Center, 16th International Laser Radar Conference, Part 2 Jul. 1992 p 585-588 (For primary document see N92-31013 21-35)
Avail: CASI HC A01/MF A03

The increasing interest in the development of an eye-safe, solid state, Doppler lidar for avionic applications has created the need for a quantitative evaluation of atmospheric effects on performance. Theoretical calculations were completed for optical scattering parameters to be compared with the field measurements. Computer codes were developed for the required calculations and designed to be interactive and user friendly in order to support comparison with experimental results and, thus, provide the basis for evaluation of eye-safe Doppler lidar over a wide range of atmospheric conditions and geographical locations. A holmium Doppler lidar operating at 2.09 microns was constructed for atmospheric backscattering, attenuation, and wind velocity measurements. Theoretical calculations and field studies were performed for backscatter coefficients. The selected wavelengths correspond to Er:glass, Tm:YAG, and Tm,Ho:YAG solid state lasers that are suitable for use in an eye-safe Doppler lidar system. Author

N92-31068*# Thomson-TRT Defense, Guyancourt (France).
A CABLE DETECTION LIDAR SYSTEM FOR HELICOPTERS
Benoist Grossmann, Alain Capbern, Martin Defour, and Remi Fertala *In* NASA. Langley Research Center, 16th International Laser Radar Conference, Part 2 Jul. 1992 p 589-592 (For

primary document see N92-31013 21-35)
Avail: CASI HC A01/MF A03

Helicopters in low-level flight are endangered by power lines or telephone wires, especially when flying at night and under poor visibility conditions. In order to prevent 'wire strike', Thomson has developed a lidar system consisting of a pulsed diode laser emitting in the near infrared region (lambda = 0.9 microns). The HOWARD (Helicopter Obstacle Warning and Detection) System utilizes a high repetition rate diode laser (PRE = 20 KHz) along with counter-rotating prisms for laser beam deflection with a total field of view of 30 degrees. This system was successfully field tested in 1991. HOWARD can detect one inch wires at ranges up to 200 meters. We are presently in the process of developing a flyable compact lidar system capable of detection ranges in the order of 400 meters. Author

N92-31069*# Los Alamos National Lab., NM.
LIDAR ANALYSIS TECHNIQUES FOR USE IN THE ATMOSPHERIC BOUNDARY LAYER **c46**
William E. Eichinger, Daniel I. Cooper, Doug Hof, David Holtkamp, Robert Quick, Jr., Joe Tiee, and Robert Karl *In* NASA. Langley Research Center, 16th International Laser Radar Conference, Part 2 Jul. 1992 p 593-596 (For primary document see N92-31013 21-35)
Avail: CASI HC A01/MF A03

There is a growing body of observational and theoretical evidence which suggests that local climate characteristics are associated with variations in the earth's surface. The link between surface variability and local-scale processes must be made if we are to improve our understanding of the feedback mechanisms involved in surface-atmosphere dynamics. However, to understand these interactions, the surface-atmosphere interface must be studied as a large-scale spatial system. Lidars are ideal tools to study the spatial properties of the atmosphere. The described techniques were developed for use with the Los Alamos Water Raman-Lidar, but are applicable to many other types of lidar. The methodology of the analysis of lidar data is summarized in order to determine meteorological parameters in the atmospheric boundary layer. The techniques are not exhaustive but are intended to show the depth and breadth of the information which can be obtained from lidars. Two methods for the computation of water-vapor fluxes were developed. The first uses the fact that the water vapor concentration in the vertical direction follows a logarithmic profile when corrected for atmospheric stability. The second method involves using inertial dissipation techniques in which lidar-derived spatial and temporal power spectra are used to determine the flux. Author

N92-31070*# York Univ. (Ontario). Dept. of Physics and Astronomy.
CORRECTION FOR NONLINEAR PHOTON COUNTING EFFECTS IN LIDAR SYSTEMS
D. P. Donovan, J. A. Whiteway, and A. I. Carswell *In* NASA. Langley Research Center, 16th International Laser Radar Conference, Part 2 Jul. 1992 p 597-600 (For primary document see N92-31013 21-35)
Avail: CASI HC A01/MF A03

Photomultiplier tubes (PMT's) employed in the photon counting (PC) mode of operation are widely used as detectors in lidar systems. In our laboratory, we have developed a versatile Nd:YAG lidar which is used for measurement of both the middle atmosphere and the troposphere. With this system, we encounter a very wide range of signal levels ranging from the extremely weak signals from the top of the mesosphere to the very strong returns from low level clouds. Although the system is capable of operating the PMT's in either the analog detection or photon counting mode, we find that often when we use photon counting we have portions of our lidar return which contain very useful information but are not within the linear operating regime of the PC system. We report the results of our efforts to explore the extent to which such high intensity PC signals can be quantitatively analyzed. In particular, a useful model relating the mean 'true' count rate and the observed count rate is presented and it's application to our system demonstrated. This model takes into account the variation in height of the PMT output pulses and the effect of the pulse height discrimination threshold. Author

N92-31071*# Naval Postgraduate School, Monterey, CA.
HIGH BACKGROUND PHOTON COUNTING LIDAR
W. J. Lentz *In* NASA. Langley Research Center, 16th International Laser Radar Conference, Part 2 Jul. 1992 p 601-604 (For primary document see N92-31013 21-35)
Avail: CASI HC A01/MF A03

Photon counting with lidar returns is usually limited to low light levels, while wide dynamic range is achieved by counting for long times. The broad emission spectrum of inexpensive high-power semiconductor lasers makes receiver filters pass too much background light for traditional photon counting in daylight. Very high speed photon counting is possible, however, at more than 500 MHz which allows the construction of eyesafe lidar operating in the presence of bright clouds. Detector improvements are possible to count to 20 GHz producing a single shot dynamic range of ten decades. Author

N92-31072*# Sparta, Inc., Lexington, MA.
DEVELOPMENT OF A RAMAN LIDAR SIMULATION TOOL Abstract Only
R. J. Grasso and J. R. Hummel *In* NASA. Langley Research Center, 16th International Laser Radar Conference, Part 2 Jul. 1992 p 605 (For primary document see N92-31013 21-35)
Avail: CASI HC A01/MF A03

Raman Lidar is a useful and powerful tool for remote probing of the atmosphere. With Raman Lidars, one can accurately determine the identity and concentration of a particular molecular specie present in the atmosphere. We present the results from a program to develop a simulation capability of Raman Lidar systems for the remote detection of atmospheric gases and/or air polluting hydrocarbons. Our model, which integrates remote Raman spectroscopy with SPARTA's BACKSCAT atmospheric lidar simulation package, permits accurate determination of the performance of a Raman Lidar system. The accuracy with which our model operates is due to the accurate calculation, at any given excitation wavelength, of the differential scattering cross section for the molecular specie under investigation. We show excellent correlation of our calculated cross section data with experimental data from the published literature. In addition, the use of our BACKSCAT package, which provides a user friendly environment to define the operating conditions, provides an accurate calculation of the atmospheric extinction at both the excitation and Raman shifted wavelengths. Our code can be used to accurately predict the performance of a Raman Lidar system, the concentration and identification of a specie in the atmosphere, or the feasibility of making Raman measurements. Author

N92-31073*# Environmental Protection Agency, Las Vegas, NV.
A VARIABLE PHASE FUNCTION APPROACH FOR THE INVERSION OF LIDAR RETURN SIGNALS
V. A. Kovalev and H. Moosmueller (Nevada Univ., Las Vegas.) *In* NASA. Langley Research Center, 16th International Laser Radar Conference, Part 2 Jul. 1992 p 607-610 (For primary document see N92-31013 21-35)
Avail: CASI HC A01/MF A03

A variable phase function is developed. This function may be used for the inversion of lidar data in an iterative process. Numerical simulations of this method were performed successfully, demonstrating fast convergence of the particulate phase function. The method will be used in the future to evaluate extinction and backscattering corrections for an Ultra-Violet Differential Absorption Lidar (UV-DIAL) system measuring tropospheric ozone concentrations. Author

N92-31074*# Ecole Polytechnique, Palaiseau (France). Lab. de Meteorologie Dynamique du CNRS.
A COMPARISON OF LIDAR INVERSION METHODS FOR CIRRUS APPLICATIONS
Salem Elouragini and Pierre H. Flamant *In* NASA. Langley

Research Center, 16th International Laser Radar Conference, Part 2 Jul. 1992 p 611-612 (For primary document see N92-31013 21-35)
Avail: CASI HC A01/MF A03

Several methods for inverting the lidar equation are suggested as means to derive the cirrus optical properties (beta backscatter, alpha extinction coefficients, and delta optical depth) at one wavelength. The lidar equation can be inverted in a linear or logarithmic form; either solution assumes a linear relationship: beta = kappa(alpha), where kappa is the lidar ratio. A number of problems prevent us from calculating alpha (or beta) with a good accuracy. Some of these are as follows: (1) the multiple scattering effect (most authors neglect it); (2) an absolute calibration of the lidar system (difficult and sometimes not possible); (3) lack of accuracy on the lidar ratio k (taken as constant, but in fact it varies with range and cloud species); and (4) the determination of boundary condition for logarithmic solution which depends on signal to noise ration (SNR) at cloud top. An inversion in a linear form needs an absolute calibration of the system. In practice one uses molecular backscattering below the cloud to calibrate the system. This method is not permanent because the lower atmosphere turbidity is variable. For a logarithmic solution, a reference extinction coefficient (alpha(sub f)) at cloud top is required. Several methods to determine alpha(sub f) were suggested. We tested these methods at low SNR. This led us to propose two new methods referenced as S1 and S2. Author

N92-31075*# Atmospheric Sciences Lab., White Sands Missile Range, NM.
TIME AND WAVELENGTH DOMAIN ALGORITHMS FOR CHEMICAL ANALYSIS BY LASER RADAR c36
David L. Rosen and James B. Gillespie *In* NASA. Langley Research Center, 16th International Laser Radar Conference, Part 2 Jul. 1992 p 613-616 (For primary document see N92-31013 21-35)
Avail: CASI HC A01/MF A03

Laser-induced fluorescence (LIF) is a promising technique for laser radar applications. Laser radar using LIF has already been applied to algae blooms and oil slicks. Laser radar using LIF has great potential for remote chemical analysis because LIF spectra are extremely sensitive to chemical composition. However, most samples in the real world contain mixtures of fluorescing components, not merely individual components. Multicomponent analysis of laser radar returns from mixtures is often difficult because LIF spectra from solids and liquids are very broad and devoid of line structure. Therefore, algorithms for interpreting LIF spectra from laser radar returns must be able to analyze spectra that overlap in multicomponent systems. This paper analyzes the possibility of using factor analysis-rank annihilation (FARA) to analyze emission-time matrices (ETM) from laser radar returns instead of excitation-emission matrices (EEM). The authors here define ETM as matrices where the rows (or columns) are emission spectra at fixed times and the columns (or rows) are temporal profiles for fixed emission wavelengths. Laser radar usually uses pulsed lasers for ranging purposes, which are suitable for measuring temporal profiles. Laser radar targets are hard instead of diffuse; that is, a definite surface emits the fluorescence instead of an extended volume. A hard target would not broaden the temporal profiles as would a diffuse target. Both fluorescence lifetimes and emission spectra are sensitive to chemical composition. Therefore, temporal profiles can be used instead of excitation spectra in FARA analysis of laser radar returns. The resulting laser radar returns would be ETM instead of EEM. Author

N92-31076*# Bulgarian Academy of Sciences, Sofia. Inst. of Electronics.
LIDAR RECEIVERS FOR PICOSECOND REMOTE SENSING
D. V. Stoyanov and T. N. Dreischuh *In* NASA. Langley Research Center, 16th International Laser Radar Conference, Part 2 Jul. 1992 p 617-620 (For primary document see N92-31013 21-35)
Avail: CASI HC A01/MF A03

The lidars of picosecond resolution are an attractive tool for remote probing of some highly dynamic objects like sea subsurface waters, small-scale turbulences in the atmosphere, etc. The picosecond lasers are suitable illuminating sources, but the main restrictions are due to the lack of proper receiving methods, combining the both high temporal and amplitude resolution, good sensitivity, short integration time, and wide dynamic range. The methods for short pulse measurements are not suitable for picosecond lidars, operating at low level, with highly dynamic signals. The streak-cameras are of high cost, lower sensitivity, and lower dynamic range (approximately 10(exp 3)). Because of the background, the single quantum regime in photomultipliers (PMT) is ineffective. The sampling of highly dynamic optical signals with resolution less than or equal to 1ns is a serious problem, limiting the application of the high speed PMT-MCP (microchannel plate) in the picosecond lidar systems. The goal of this work is to describe the use of a new photodetection technique which combines the picosecond resolution with the high amplitude resolution, dynamic range, and sensitivity. Author

N92-31077*# Bulgarian Academy of Sciences, Sofia. Inst. of Electronics.
ACOUSTO-OPTIC FILTERING OF LIDAR SIGNALS
G. Kolarov, A. Deleva, and Ts. Mitsev *In* NASA. Langley Research Center, 16th International Laser Radar Conference, Part 2 Jul. 1992 p 621-623 (For primary document see N92-31013 21-35)
Avail: CASI HC A01/MF A03

The predominant part of the noise in lidar receivers is created by the background radiation; therefore, one of the most important elements of the receiving optics is a spectrally selecting filter placed in front of the photodetector. Interference filters are usually used to transmit a given wavelength. Specific properties of the interference filters, such as simple design, reliability, small size, and large aperture, combined with high transmission coefficient and narrow spectral band, make them the preferred spectral device in many cases. However, problems arise in applications such as the Differential Absorption Lidar (DIAL) technique, where fast tuning within a wide spectral region is necessary. Tunable acousto-optical filters (TAOF), used recently in astrophysical observations to suppress the background radiation, can be employed with success in lidar sounding. They are attractive due to the possibility for fast spectral scanning with a narrow transmission band. The TAOF's advantages are fully evident in DIAL lidars where one must simultaneously receive signals at two laser frequencies. Author

N92-31078*# Bulgarian Academy of Sciences, Sofia. Inst. of Electronics.
GROUND-BASED DOPPLER LIDAR OF INCREASED LASER INSTABILITY: CONCEPTION AND DESIGN
D. V. Stoyanov, B. M. Bratanov, V. N. Naboko, and M. D. Angelova *In* NASA. Langley Research Center, 16th International Laser Radar Conference, Part 2 Jul. 1992 p 625-628 (For primary document see N92-31013 21-35)
Avail: CASI HC A01/MF A03

Pulsed CO2 Doppler lidars are effective tools for ground-based atmospheric wind sensing, but the high cost of the lidar transceivers, mainly due to the required high frequency stability (better than 10(exp -9) or 100 KHz), prevents their wide use in meteorology. The best approach to overcome this problem is to develop Doppler lidars that are effective at increased laser instability. This work is based on the results of a new scheme for Doppler lidar detection by the use of frequency synthesis, in a wide fluctuation bandwidth of laser instabilities, is described. A ground-based system, using this approach, is under development in the Institute of Electronics - Bulgarian Academy of Science (BAS). Author

N92-31079*# Bulgarian Academy of Sciences, Sofia. Inst. of Electronics.
ANALYTICAL ESTIMATES OF THE PP-ALGORITHM AT LOW NUMBER OF DOPPLER PERIODS PER PULSE LENGTH c70
M. D. Angelova, E. V. Stoykova, and D. V. Stoyanov *In* NASA. Langley Research Center, 16th International Laser Radar

Conference, Part 2 Jul. 1992 p 629-632 (For primary document see N92-31013 21-35)
Avail: CASI HC A01/MF A03

When discussing the Doppler velocity estimators, it is of significant interest to analyze their behavior at a low number of Doppler periods n(sub D) = 2v(sub r)t(sub s)/lambda is approximately equal to 1 within the resolution cell t(sub s) (v(sub 4) is the radial velocity, lambda is the wavelength). Obviously, at n(sub D) is approximately less than 1 the velocity error is essentially increased. The problem of low n(sub D) arises in the planetary boundary layer (PBL), where higher resolutions are usually required but the signal-to-noise ratio (SNR) is relatively high. In this work analytical expression for the relative root mean square (RMS) error of the PP Doppler estimator at low number of periods for a narrowband Doppler signal and arbitrary model of the noise correlation function is obtained. The results are correct at relatively high SNR. The analysis is supported by computer simulations at various SNR's. Author

N92-31080*# Academia Sinica, Beijing (China). Inst. of Atmospheric Physics.
A CONSIDERABLE EFFECT OF STRATOSPHERIC AEROSOL ON LIDAR-DETECTED OZONE PROFILE AND A THREE-WAVELENGTH INVERSION TECHNIQUE FOR BOTH OZONE AND AEROSOL c45
Jinhuan Qiu *In* NASA. Langley Research Center, 16th International Laser Radar Conference, Part 2 Jul. 1992 p 633-636 (For primary document see N92-31013 21-35)
Avail: CASI HC A01/MF A03

As far as the Differential Absorption Lidar (DIAL) technique is concerned, it is important that the off-line wavelength is close to the on-line wavelength in order to avoid a messy computation of the atmospheric aerosol scattering. However, the two wavelengths of ozone-DIAL are usually considerably different. Usually, an excimer laser of 308nm (on-line) and Raman shifting of 353nm or the third harmonic of a Nd-YAG laser with 355nm (off-line) are selected for measurements of the stratospheric ozone, and there is a difference of 45nm or 47nm between them. Because of the difference there is a difference in the atmospheric scatterings of the two wavelengths. This can cause some error in the retrieved ozone profile if the aerosol scattering is neglected. This paper is devoted to a study of the effect of the stratospheric aerosol on the ozone solution, and a three-wavelength detection technique is proposed for obtaining the more exact ozone profile and the aerosol profile in the stratosphere. Author

N92-31081*# Bulgarian Academy of Sciences, Sofia. Inst. of Electronics.
HIGH-RESOLUTION PROCESSING OF LONG-PULSE-LIDAR DATA
L. L. Gurdev, T. N. Dreischuh, and D. V. Stoyanov *In* NASA. Langley Research Center, 16th International Laser Radar Conference, Part 2 Jul. 1992 p 637-640 (For primary document see N92-31013 21-35)
Avail: CASI HC A01/MF A03

The purpose of this work is to demonstrate the performance of the Fourier-deconvolution technique developed to improve the resolution of the long-pulse coherent lidar power profile, and to take into account the multiplicative fluctuations. The behavior of the error due to the power fluctuations and a method to reduce it are analyzed theoretically and simulated numerically. A processing of real data obtained from the National Oceanic and Atmospheric Administration (NOAA) ground-based Doppler lidar is also presented. Similar problems were investigated using a different approach based on introducing a correction function to the lidar equation. Author

N92-31082*# Academia Sinica, Beijing (China). Inst. of Atmospheric Physics.
LIDAR MEASUREMENTS OF CLOUD EXTINCTION COEFFICIENT DISTRIBUTION AND ITS FORWARD SCATTERING PHASE FUNCTION ACCORDING TO MULTIPLY SCATTERED LIDAR RETURNS c47
Jinhuan Qiu and Qirong Huang *In* NASA. Langley Research Center, 16th International Laser Radar Conference, Part 2 Jul. 1992 p 641-642 (For primary document see N92-31013 21-35)
Avail: CASI HC A01/MF A03

The study of the inversion algorithm for the single scatter lidar equation, for quantitative determination of cloud (or aerosol) optical properties, has received much attention over the last thirty years. Some of the difficulties associated with the solution of this equation are not yet solved. One problem is that a single scatter lidar equation has two unknowns. Because of this, the determination of the far-end boundary value, in the case of Klett's algorithm, is a problem if the atmosphere is optically inhomogeneous. Another difficulty concerns multiple scattering. There is a large error in the extinction distribution solution, in many cases, if only the single scattering component is considered, while neglecting the multiple scattering component. However, the use of multiple scattering in the remote sensing of aerosol or cloud optical properties is promising. In our early study, an inversion method for simultaneous determination of the cloud (or aerosol) Extinction Coefficient Distribution (ECD) and its Forward Scattering Phase Function (FSPF) was proposed according to multiply scattered lidar returns with two fields of view for the receiver. The method is based on a parameterized multiple scatter lidar equation. This paper is devoted to further numerical tests and an experimental study of lidar measurements of cloud ECD and FSPF using this method. Author

N92-31083*# Academy of Sciences (USSR), Tomsk. Inst. of Atmospheric Optics.
MEASUREMENTS OF THE BACKSCATTERING PHASE MATRICES OF CRYSTAL CLOUDS WITH A POLARIZATION LIDAR c47
B. V. Kaul, A. L. Kuznetsov, and E. R. Polovtseva *In* NASA. Langley Research Center, 16th International Laser Radar Conference, Part 2 Jul. 1992 p 643-646 (For primary document see N92-31013 21-35)
Avail: CASI HC A01/MF A03

A polarization technique based on measurements of intensities of the polarized I(parallel) and crosspolarized I(perpendicular) components of scattered radiation is often used in lidar studies of aerosols. The ratio I(perp)/I(para) is related to nonsphericity of scattering particles and it is often called, though unjustified, depolarization. Correct definition of the term has previously been shown to be the value d = 1 - P, where P is the degree of polarization defined in terms of the Stokes parameters. In fact, measurements of I(para) and I(perp) enable one to determine the Stokes parameter Q = I(para) - I(perp), and under the condition U = V = 0 the depolarization is determined by the relationship d = 2 x I(perp)/(I(para) + I(perp)). In 1988 a new cycle of measuring the Stokes parameters of lidar returns from scattering media irradiated with a linearly polarized light was started. Based on the lidar data obtained during the 1988-1990 period, a classification of scattering ensembles was made which reveals five types of the scattering particle ensembles differing by a combination of the Stokes parameters. In the 1990-1991 period, a cycle of measurements of the lidar returns' Stokes parameters was carried out using sounding radiation. Author

N92-31084*# Illinois Univ., Urbana-Champaign. Dept. of Electrical and Computer Engineering.
MEASUREMENT CAPABILITIES OF GIANT LIDARS FOR MIDDLE AND UPPER ATMOSPHERIC APPLICATIONS Abstract Only c48
Chester S. Gardner *In* NASA. Langley Research Center, 16th International Laser Radar Conference, Part 2 Jul. 1992 p 647 (For primary document see N92-31013 21-35)
Avail: CASI HC A01/MF A03

The development and refinement of sophisticated remote sensing techniques during the past three decades have contributed enormously to our knowledge of the atmosphere. Lidar technologies have developed rapidly since the invention of the laser in 1961. Today, sophisticated systems are used to probe composition and

structure throughout the atmosphere from the troposphere into the lower thermosphere and are making important contributions to several global change studies. While the recent advances in lidar technology have been impressive, the accuracy, resolution, and sensitivity of many systems are still limited by signal levels. We review the scientific rationale for developing a major new lidar facility to study the chemistry and dynamics of the Earth's atmosphere. The centerpiece of the facility is to be a 10-meter telescope which serves as the receiving system for several very large lidar systems. We discuss the observational capabilities of the proposed facility with particular emphasis on measurements of temperature, winds, water vapor, and ozone. Author

N92-31085*# Academy of Sciences (USSR), Tomsk. Inst. of Atmospheric Optics.

LIDAR SOUNDING OF OZONE AND AEROSOLS c45

V. E. Zuev *In* NASA. Langley Research Center, 16th International Laser Radar Conference, Part 2 Jul. 1992 p 649 (For primary document see N92-31013 21-35)

Avail: CASI HC A01/MF A03

The present report is devoted to the problem of clarifying the mechanism of interaction of ozone molecules with aerosol particles in the atmosphere. It is necessary to take into account the meteorological conditions and the synoptic situation. We have built a unique lidar facility that provides simultaneous sounding of ozone and aerosols at different heights of the upper troposphere and in the stratosphere. Simultaneous with the retrieval of the standard scattering ratio profiles, data are obtained on the profiles of the microphysical parameters of the aerosols (particle size distribution and particle concentration) using the method of multifrequency lidar sounding developed at the Institute of Atmospheric Optics. Author

N92-31086*# Pennsylvania State Univ., University Park.

ATMOSPHERIC MEASUREMENTS USING THE LAMP LIDAR DURING THE LADIMAS CAMPAIGN c47

C. R. Philbrick, D. B. Lysak, T. D. Stevens, P. A. T. Haris, and Y.-C. Rau *In* NASA. Langley Research Center, 16th International Laser Radar Conference, Part 2 Jul. 1992 p 651-654 Sponsored in part by Army, Navy, and NSF (For primary document see N92-31013 21-35)

Avail: CASI HC A01/MF A03

The results of the LAtitudinal DIstribution of Middle Atmosphere Structure (LADIMAS) experiment have provided a unique data set to improve our understanding of the middle atmosphere. The project included shipboard and rocket range coordinated measurements between 70 deg N to 65 deg S to study the structure, dynamics, and chemistry of the atmosphere. Results on important dynamical processes, such as gravity waves, tidal components, as well as the formation of the layers of meteoric ion and neutral species, were obtained with lidar, digisonde, microwave radiometer, and spectrometers. The cooperative study of the atmosphere was undertaken by researchers from several laboratories, including Penn State University (PSU), University Bonn, University Wuppertal, Lowell University, and others. Several of the parameters studied have never been measured before over such a wide range of latitudes. Instruments were assembled aboard the German research vessel RV POLARSTERN while this vessel was sailing from the Arctic to the Antarctic seas between 8 Oct. 1991 - 2 Jan. 1992. This paper presents an introduction to the data gathered by the PSU investigation with the Lidar Atmospheric Measurements Program (LAMP) lidar. Author

N92-31087*# University of Western Ontario, London. Dept. of Physics.

LIDAR MEASUREMENTS USING LARGE LIQUID MIRROR TELESCOPES

R. J. Sica, S. Sargoytchev, S. Flatt, E. Borra (Laval Univ., Quebec), and L. Girard (Laval Univ., Quebec) *In* NASA. Langley Research Center, 16th International Laser Radar Conference, Part 2 Jul. 1992 p 655-658 (For primary document see N92-31013 21-35)

Avail: CASI HC A01/MF A03

It is a well accepted practice in the discussion of lidars to compare systems by a performance factor given by the product of the transmitter power and receiver aperture. This form of the performance factor reflects the two key parameters that determine the amount of photons recorded from a given range bin; the amount of transmitted photons and the probability of collecting a scattered photon. We are interested in studying the propagation and breaking of gravity waves typically generated in the lower atmosphere. To study these waves requires high temporal and spatial resolution, as they have frequencies as high as 500 mHz and generate turbulent structures with vertical scales of less than 25 m. In the 80 - 100 km region of the atmosphere these measurements are most efficiently obtained by using resonance scattering from sodium atoms deposited by meteors. However, in the 30 - 80 km region, the most efficient scattering arises from molecules (Rayleigh scattering). Since the atmospheric scale height is nominally 7 km, this scattering becomes extremely weak above 60 km. Furthermore, present laser technology limits the power available for Rayleigh-scattering experiments to about 0.5 - 50 W. The transmitter for the lidar system under development at the University of Western Ontario uses a two-beam transmitter to simultaneously measure density perturbations and temperature from both Rayleigh and resonance scattering. Author

N92-31088*# National Inst. for Environmental Studies, Tsukuba (Japan).

SPECTROSCOPIC METHOD FOR EARTH-SATELLITE-EARTH LASER LONG-PATH ABSORPTION MEASUREMENTS USING RETROREFLECTOR IN SPACE (RIS)

Nobuo Sugimoto, Atsushi Minato, and Yasuhiro Sasano *In* NASA. Langley Research Center, 16th International Laser Radar Conference, Part 2 Jul. 1992 p 659-662 (For primary document see N92-31013 21-35)

Avail: CASI HC A01/MF A03

The Retroreflector in Space (RIS) is a single element cube-corner retroreflector with a diameter of 0.5 m designed for earth-satellite-earth laser long-path absorption experiments. The RIS is to be loaded on the Advanced Earth Observing System (ADEOS) satellite which is scheduled for launch in Feb. 1996. The orbit for ADEOS is a sun synchronous subrecurrent polar-orbit with an inclination of 98.6 deg. It has a period of 101 minutes and an altitude of approximately 800 km. The local time at descending node is 10:15-10:45, and the recurrent period is 41 days. The velocity relative to the ground is approximately 7 km/s. In the RIS experiment, a laser beam transmitted from a ground station is reflected by RIS and received at the ground station. The absorption of the intervening atmosphere is measured in the round-trip optical path. Author

N92-31089*# National Aeronautics and Space Administration. Goddard Space Flight Center, Greenbelt, MD.

RAMAN LIDAR MEASUREMENTS OF WATER VAPOR AND AEROSOL/CLOUDS DURING THE FIRE/SPECTRE FIELD CAMPAIGN c47

S. H. Melfi, D. Whiteman, R. Ferrare, K. Evans, J. E. M. Goldsmith (Sandia National Labs., Livermore, CA.), M. Lapp (Sandia National Labs., Livermore, CA.), and S. E. Bisson (Sandia National Labs., Livermore, CA.) *In* NASA. Langley Research Center, 16th International Laser Radar Conference, Part 2 Jul. 1992 p 663-666 Prepared in cooperation with Universities Space Research Association, Columbia, MD; and Hughes STX, Inc., Lanham, MD (For primary document see N92-31013 21-35)

Avail: CASI HC A01/MF A03

Water vapor is one of the most important constituents of the earth's atmosphere. It has a major impact on both atmospheric dynamics and radiative transfer. From a dynamic standpoint, the distribution of water vapor with height determines convective stability which is the major indicator of destructive storm development. Also, water vapor stored in the planetary boundary layer acts as the fuel to intensify severe weather. In regards to radiative transfer, water vapor is the most active IR molecule in the atmosphere. It is more effective in absorbing and emitting IR radiation than either carbon dioxide or methane, and thus plays

an important role in global change. The main objective of FIRE (First ISSCCP (International Satellite Cloud Climatology Project) Regional Experiment) was to study the development and radiative characteristics of cirrus clouds. The SPECTRE (Spectral Radiation Experiment) project was designed to acquire the necessary atmospheric observations to compare radiative measurements with radiative transfer theory, with special emphasis on understanding the water vapor spectral continuum. The FIRE/SPECTRE field campaign was conducted during Nov. - Dec. 1991 in Coffeyville, Kansas. A complete understanding of water vapor, its distribution with height, and its temporal variation was important for both experiments. Author

N92-31090*# National Aeronautics and Space Administration. Goddard Space Flight Center, Greenbelt, MD.

PERFORMANCE MODELING OF DAYTIME RAMAN LIDAR SYSTEMS FOR PROFILING ATMOSPHERIC WATER VAPOR **c47**

J. E. M. Goldsmith and Richard A. Ferrare *In* NASA. Langley Research Center, 16th International Laser Radar Conference, Part 2 Jul. 1992 p 667-670 Prepared in cooperation with Universities Space Research Association, Columbia, MD (For primary document see N92-31013 21-35)
Avail: CASI HC A01/MF A03

We describe results from a comprehensive computer model developed to guide optimization of an ultraviolet Raman lidar system for measuring daytime profiles of atmospheric water vapor. Daytime measurements present added challenges because of the difficulties inherent in detecting Raman signals against solar backgrounds. We are pursuing two concepts for optimizing the daytime performance of a Raman lidar system. The first involves operating the system in the solar blind region of the ultraviolet spectrum. The second concept involves operation of the system in a narrowband, narrow field-of-view mode. Calculations for lidar systems based on both concepts are presented. Author

N92-31091*# GKSS-Forschungszentrum Geesthacht (Germany, F.R.).

BELINDA: BROADBAND EMISSION LIDAR WITH NARROWBAND DETERMINATION OF ABSORPTION. A NEW CONCEPT FOR MEASURING WATER VAPOR AND TEMPERATURE PROFILES

F. A. Theopold, C. Weitkamp, and W. Michaelis *In* NASA. Langley Research Center, 16th International Laser Radar Conference, Part 2 Jul. 1992 p 671-674 (For primary document see N92-31013 21-35)
Avail: CASI HC A01/MF A03

We present a new concept for differential absorption lidar measurements of water vapor and temperature profiles. The idea is to use one broadband emission laser and a narrowband filter system for separation of the 'online' and 'offline' return signals. It is shown that BELINDA offers improvements as to laser emission shape and stability requirements, background suppression, and last and most important a significant reduction of the influence of Rayleigh scattering. A suitably designed system based on this concept is presented, capable of measuring water vapor or temperature profiles throughout the planetary boundary layer. Author

N92-31092*# Paris VI Univ. (France). Service d'Aeronomie du CNRS.

DIAL SIMULATIONS FOR SATELLITE WATER VAPOR PROFILE MEASUREMENTS WITHIN THE BEST PROJECT **c47**

P. Chazette, J. Pelon, and G. Megie *In* NASA. Langley Research Center, 16th International Laser Radar Conference, Part 2 Jul. 1992 p 675-678 (For primary document see N92-31013 21-35)
Avail: CASI HC A01/MF A03

The project BEST has been proposed by several laboratories of the French Space Agency (CNES) as part of the GEWEX program. Its objective is the study of the energy budget of the tropical system, and aims at measuring different components of the water cycle by coupling several observing systems. As part of this, Service d'Aeronomie (SA) proposed to study a Differential Absorption Lidar (DIAL) system to measure tropical water vapor profiles and to determine humidity convergence fields, when coupled with the Doppler wind lidar. We have performed simulation analyses for water vapor measurement from the selected orbit of 400 km. For these simulations, we have adopted an atmospheric model developed at SA. We have optimized, by a Monte Carlo statistical method, the system parameters and evaluated bias and standard deviation of the retrieved water vapor mixing ratio. Author

N92-31093*# National Aeronautics and Space Administration. Langley Research Center, Hampton, VA.

AIRBORNE WATER VAPOR DIAL RESEARCH: SYSTEM DEVELOPMENT AND FIELD MEASUREMENTS **c47**

Noah S. Higdon (ST Systems Corp., Hampton, VA.), Edward V. Browell (ST Systems Corp., Hampton, VA.), Patrick Ponsardin (ST Systems Corp., Hampton, VA.), Thomas H. Chyba (National Academy of Sciences - National Research Council, Hampton, VA.), Benoist E. Grossmann (Thomson-CSF, Paris, France), Carolyn F. Butler (ST Systems Corp., Hampton, VA.), Marta A. Fenn (ST Systems Corp., Hampton, VA.), Shane D. Mayor (ST Systems Corp., Hampton, VA.), Syed Ismail, and William B. Grant *In its* 16th International Laser Radar Conference, Part 2 Jul. 1992 p 679-682 (For primary document see N92-31013 21-35)
Avail: CASI HC A01/MF A03

This paper describes the airborne differential absorption lidar (DIAL) system developed at the NASA Langley Research Center for remote measurement of water vapor (H2O) and aerosols in the lower atmosphere. The airborne H2O DIAL system was flight tested aboard the NASA Wallops Flight Facility (WFF) Electra aircraft in three separate field deployments between 1989 and 1991. Atmospheric measurements were made under a variety of atmospheric conditions during the flight tests, and several modifications were implemented during this development period to improve system operation. A brief description of the system and major modifications will be presented, and the most significant atmospheric observations will be described. Author

N92-31094*# Kyushu Univ., Fukuoka (Japan). Dept. of Electrical Engineering.

ALEXANDRITE LIDAR FOR THE ATMOSPHERIC WATER VAPOR DETECTION AND DEVELOPMENT OF POWERFUL TUNABLE SOURCES IN IR **c47**

M. Uchiumi, M. Maeda, K. Muraoka, and O. Uchino (Meteorological Research Inst., Tsukuba, Japan) *In* NASA. Langley Research Center, 16th International Laser Radar Conference, Part 2 Jul. 1992 p 683-686 (For primary document see N92-31013 21-35)
Avail: CASI HC A01/MF A03

New tunable solid-state lasers, such as alexandrite and Ti-sapphire lasers, provide a powerful technique to detect various molecules in the atmosphere whose absorption bands are in the infrared region. The differential absorption lidar (DIAL) system to measure the tropospheric water vapor has been investigated by many authors, in an early stage, by dye and ruby lasers. Using the alpha band of water vapor, the longest detection range can be obtained with high accuracy, and the alexandrite laser is the most suitable laser for this purpose. In this paper, we describe the detection of water vapor in the atmosphere by an alexandrite lidar, and the development of powerful tunable sources based on Raman lasers in the infrared region. Author

N92-31095*# University of South Florida, Tampa. Dept. of Physics.

EMERGING SOLID-STATE LASER TECHNOLOGY BY LIDAR/DIAL REMOTE SENSING

Dennis Killinger *In* NASA. Langley Research Center, 16th International Laser Radar Conference, Part 2 Jul. 1992 p 687-688 (For primary document see N92-31013 21-35)
Avail: CASI HC A01/MF A03

Significant progress has been made in recent years in the

development of new, solid-state laser sources. This talk will present an overview of some of the new developments in solid-state lasers, and their application toward lidar/DIAL measurements of the atmosphere. Newly emerging lasers such as Ho:YAG, Tm:YAG, OPO, and Ti:Sapphire will be covered, along with the spectroscopic parameters required for differential operational modes of atmospheric remote sensing including Doppler-Windshear lidar, Tunable laser detection of water/CO2, and broad linewidth OPO's for open path detection of pollutant hydrocarbon gases. Additional considerations of emerging laser technology for lidar/DIAL will also be covered. Author

N92-31096*# University of South Florida, Tampa. Dept. of Physics.

COHERENT SUMMATION OF SPATIALLY DISTORTED DOPPLER LIDAR SIGNALS USING A TWO-DIMENSIONAL HETERODYNE DETECTOR ARRAY

Kin Pui Chan and Dennis K. Killinger *In* NASA. Langley Research Center, 16th International Laser Radar Conference, Part 2 Jul. 1992 p 689-690 (For primary document see N92-31013 21-35)

Avail: CASI HC A01/MF A03

We have investigated the improvement in the signal-to-noise ratio for a coherent Doppler lidar through the use of a multi-element heterodyne detector array. Such an array enables the spatial summation of atmospheric refractive turbulence induced speckles, and time varying target speckles. Our recent experiments have shown that the non-coherent summation of the lidar signals from a heterodyne detector array can enhance the heterodyne mixing efficiency and thus the signal-to-noise ratio. In this paper, we expand this work to include the coherent summation of array signals. The digitized heterodyne signals were stored in a personal computer. Fast Fourier transforms were performed on both the non-coherent and coherent summations of the detector array signals. It was found that the coherent summation greatly enhanced the accuracy in the Doppler frequency estimate. A theoretical analysis was performed and indicated good agreement with experimental results. We have also applied these results to the more general lidar applications including atmospheric wind sensing, and have found that in most lidar applications the Doppler frequency estimate is increased through the use of the heterodyne detector array. Author

N92-31097*# Massachusetts Inst. of Tech., Lexington. Lincoln Lab.

THE ROLE OF LASER COHERENCE IN LONG-RANGE VIBRATION MEASUREMENTS

R. S. Eng, C. Freed, R. H. Kingston, K. I. Schultz, A. L. Kachelmyer, and W. E. Keicher *In* NASA. Langley Research Center, 16th International Laser Radar Conference, Part 2 Jul. 1992 p 691-694 Sponsored in part by Navy (For primary document see N92-31013 21-35)

Avail: CASI HC A01/MF A03

In this paper, the temporal coherence effect of a laser oscillator will be critically examined using existing laser frequency stability data in the time domain by first converting them to the frequency domain. We limit our discussion to CO2 lasers. To be more specific, our presentation will include the following items: (1) a review of the definitions and representations of laser oscillator frequency stability; (2) a methodology will be developed for determining the dynamic range of vibration measurements; (3) the methodology will show that the conversion of the laser frequency stability from the time domain to the frequency domain can be performed effectively in the optical region; and (4) because of a finite time delay, the phase noise is reduced for offset frequencies close to the carrier frequency. Author

N92-31098*# Chiba Univ. (Japan). Remote Sensing and Image Research Center.

A PORTABLE LIDAR USING A DIODE-PUMPED YAG LASER

N. Takeuchi, H. Okumura, T. Sugita, H. Matsumoto, and S. Yamaguchi (Nippon Steel Corp., Sagamihara, Japan) *In* NASA. Langley Research Center, 16th International Laser Radar Conference, Part 2 Jul. 1992 p 695-698 (For primary document see N92-31013 21-35)

Avail: CASI HC A01/MF A03

A Mie lidar system is technically established and is used for monitoring air pollution, stratospheric and boundary layer aerosol distribution, plume dispersion, visibility, and the study of atmospheric structure and cloud physics. However, a lidar system is not widely used because of its cumbersome handling and unwieldy portability. Although the author developed a laser diode lidar system based on RM-CW technique, it has a limit of measurement distance. Here we report the development of an all solid Mie lidar system using a diode-pumped Nd:YAG laser and a Si-APD detector. This was constructed as a prototype of a handy lidar system. Author

N92-31099*# GKSS-Forschungszentrum Geesthacht (Germany, F.R.). Inst. fuer Physik.

INVESTIGATIONS ON ATOMIC-VAPOR-FILTER HIGH-SPECTRAL-RESOLUTION LIDAR FOR TEMPERATURE MEASUREMENTS

E. Voss and C. Weitkamp *In* NASA. Langley Research Center, 16th International Laser Radar Conference, Part 2 Jul. 1992 p 699-702 (For primary document see N92-31013 21-35)

Avail: CASI HC A01/MF A03

The temperature measurement by the analysis of Rayleigh scattered laser radiation with atomic vapor filters is investigated in both theory and laboratory experiments. Synthetic air is irradiated with a cw dye laser at 283 nano-meters, and the backscattered spectrum is analyzed with two lead vapor cells in one oven. Temperature measurements are carried out, and the effect of different parameters on the accuracy is investigated. Important aspects for the realization of a lidar are given. Author

N92-31100*# Santa Barbara Research Center, Goleta, CA.

HgCdTe PHOTOMIXERS FOR CO2 LASER RADAR SYSTEMS

Peter R. Bratt *In* NASA. Langley Research Center, 16th International Laser Radar Conference, Part 2 Jul. 1992 p 703-706 (For primary document see N92-31013 21-35)

Avail: CASI HC A01/MF A03

The Santa Barbara Research Center has developed a variety of high speed HgCdTe photodetectors for use in CO2 laser radar systems. These detectors have outstanding performance and can be made available in production quantities. Many of them have been employed in a variety of systems applications over the past ten years. In this paper, we briefly describe the detector technology, summarize the state-of-the-art, and indicate some practical applications. Author

N92-31101*# SRI International Corp., Menlo Park, CA. Geoscience and Engineering Center.

AIRBORNE LIDAR MAPPING OF VERTICAL OZONE DISTRIBUTIONS IN SUPPORT OF THE 1990 CLEAN AIR ACT AMENDMENTS **c45**

Edward E. Uthe, Norman B. Nielsen, and John M. Livingston *In* NASA. Langley Research Center, 16th International Laser Radar Conference, Part 2 Jul. 1992 p 707-710 Sponsored in part by the Lake Michigan Air Directors Consortium (For primary document see N92-31013 21-35)

Avail: CASI HC A01/MF A03

The 1990 Clean Air Act Amendments mandated attainment of the ozone standard established by the U.S. Environmental Protection Agency. Improved photochemical models validated by experimental data are needed to develop strategies for reducing near surface ozone concentrations downwind of urban and industrial centers. For more than 10 years, lidar has been used on large aircraft to provide unique information on ozone distributions in the atmosphere. However, compact airborne lidar systems are needed for operation on small aircraft of the type typically used on regional air quality investigations to collect data with which to develop and validate air quality models. Data presented in this paper will consist of a comparison between airborne differential absorption lidar (DIAL) and airborne in-situ ozone measurements. Also discussed are future plans to improve the airborne

ultraviolet-DIAL for ozone and other gas observations and addition of a Fourier Transform Infrared (FTIR) emission spectrometer to investigate the effects of other gas species on vertical ozone distribution. Author

N92-31102*# National Physical Lab., Teddington (England).
MEASUREMENTS OF FUGITIVE HYDROCARBON EMISSIONS WITH A TUNABLE INFRARED DIAL **c45**
M. J. T. Milton, P. T. Woods, B. W. Jolliffe, N. R. W. Swann, and R. A. Robinson *In* NASA. Langley Research Center, 16th International Laser Radar Conference, Part 2 Jul. 1992 p 711-713 (For primary document see N92-31013 21-35)
Avail: CASI HC A01/MF A03

A tunable infrared differential absorption lidar (DIAL) system has been designed and developed at the National Physics Lab (NPL) which is capable of making measurements throughout the spectral region 3.0 to 4.2 micro-m. It is ideally suited to measuring a range of organic and inorganic species including methane, propane, and butane. The system also has an ultraviolet channel that is capable of making simultaneous measurements of aromatic hydrocarbons such as Toluene and benzene. This paper describes the source and detection system, together with some measurements of fugitive hydrocarbon emissions performed at various petrochemical plants. Author

N92-31103*# European Nuclear Energy Agency, Frascati (Italy).
THE ENEA CO2 LIDAR/DIAL STATION ACTIVITY IN A TROPOSPHERIC REMOTE SENSING PROGRAM
R. Barbini, F. Colao, A. Palucci, and S. Ribezzo *In* NASA. Langley Research Center, 16th International Laser Radar Conference, Part 2 Jul. 1992 p 715-718 (For primary document see N92-31013 21-35)
Avail: CASI HC A01/MF A03

The ENEA CO2 Lidar/Differential Absorption Lidar (DIAL) apparatus has become operational by detecting atmospheric components such as water vapor and ozone, with a useful range of R approx. = 6 km. Range resolved concentrations of the investigated molecules are presented together with a discussion about the techniques adopted for data analysis. Author

N92-31104*# Ship Research Inst., Tokyo (Japan). Ship Equipment and Marine Environment Div.
LIDAR OBSERVATION OF MARINE MIXED LAYER **c47**
Susumu Yamagishi, Hiroshi Yamanouchi, and Masayuki Tsuchiya *In* NASA. Langley Research Center, 16th International Laser Radar Conference, Part 2 Jul. 1992 p 719-722 (For primary document see N92-31013 21-35)
Avail: CASI HC A01/MF A03

Marine mixed layer is known to play an important role in the transportation of pollution exiting ship funnels. The application of a diffusion model is critically dependent upon a reliable estimate of a lid. However, the processes that form lids are not well understood, though considerable progress toward marine boundary layer has been achieved. This report describes observations of the marine mixed layer from the course Ise-wan to Nii-jima with the intention of gaining a better understanding of their structure by a shipboard lidar. These observations were made in the summer of 1991. One interesting feature of the observations was that the multiple layers of aerosols, which is rarely numerically modeled, was encountered. No attempt is yet made to present a systematic analysis of all the data collected. Instead we focus on observations that seem to be directly relevant to the structure of the mixed layer. Author

N92-31105*# National Defence Research Establishment, Linkoeping (Sweden). Dept. of Information Technology.
AEROSOL EXTINCTION MEASUREMENTS WITH CO2-LIDAR **c45**
Arne Hagard and Rolf Persson *In* NASA. Langley Research Center, 16th International Laser Radar Conference, Part 2 Jul. 1992 p 723-725 (For primary document see N92-31013 21-35)
Avail: CASI HC A01/MF A03

With the aim to develop a model for infrared extinction due to aerosols in slant paths in the lower atmosphere we perform measurements with a CO2-lidar. Earlier measurements with a transmissometer along horizontal paths have been used to develop relations between aerosol extinction and meteorological parameters. With the lidar measurements we hope to develop corresponding relations for altitude profiles of the aerosol extinction in the infrared. An important application is prediction of detection range for infrared imaging systems. Author

N92-31106*# BMW-A.G., Munich (Germany, F. R.).
DENSE FOG ON THE HIGHWAY: VISUAL RANGE MONITORING IN CARS? **c47**
W. Hahn, W. Krichbaumer (Deutsche Forschungsanstalt fuer Luft- und Raumfahrt, Oberpfaffenhofen, Germany, F.R.), J. Streicher (Deutsche Forschungsanstalt fuer Luft- und Raumfahrt, Oberpfaffenhofen, Germany, F.R.), and Ch. Werner (Deutsche Forschungsanstalt fuer Luft- und Raumfahrt, Oberpfaffenhofen, Germany, F.R.) *In* NASA. Langley Research Center, 16th International Laser Radar Conference, Part 2 Jul. 1992 p 727-730 (For primary document see N92-31013 21-35)
Avail: CASI HC A01/MF A03

This paper reports on the development of a new sensor. Laser range-finders are currently installed in cars and trucks to measure the distance to a proceeding car (LEICA). A modification of such a sensor to measure visibility was made. The problems that had to be solved were: (1) choice of wavelength with relation to the human eye for visibility measurements; (2) dependency of the wavelength on atmospheric turbidity; (3) laser eye-safety; and (4) influence of multiple scattering at visibilities smaller than 200 m. The wavelength used for lidar sensors in the near infrared presents no real problems because the object to be sensed is fog appearing white which means that scattering from fog is wavelength independent. There are however differences in backscatter-to-extinction ratio for different fog and weather situations. The two solutions to these problems are polarization and multiple scattering. As known from airport operations of a laser ceilometer, one can use this multiple scattering contribution to determine the visibility. Author

N92-31109# Argonne National Lab., IL. High Energy Physics Div.
MECHANICAL DESIGN AND FINITE ELEMENT ANALYSIS OF THE SDC CENTRAL CALORIMETER
V. Guarino, N. F. Hill, J. Nasiatka, D. A. Hoecker, T. D. Hordubay, D. W. Scherbarth, and R. L. Swensrud (Westinghouse Research and Development Center, Pittsburgh, PA.) 1992 8 p Presented at the International Industrial Symposium on the Super Collider, New Orleans, LA, 4-6 Mar. 1992
(Contract W-31109-eng-38)
(DE92-011197; ANL-HEP-CP-92-13; CONF-920331-2) Avail: CASI HC A02/MF A01

When designing scintillating calorimeters for the study of particle interactions resulting from colliding beams, a primary goal is to instrument 100 percent of the available solid angle. In pursuit of this goal the challenge for mechanical designers is to minimize the amount of structural mass and still maintain acceptable engineering standards in the design. Argonne National Laboratory's involvement in the design of a central calorimeter for the SSC started in 1989. Our first proposal was to design a depleted uranium scintillator calorimeter similar to the ZEUS detector presently installed at the HERA electron-proton collider in Hamburg, Germany. Argonne was involved at the time in final assembly of modules for ZEUS that were designed and constructed at ANL. Due to the cost of using depleted uranium, lead was chosen as the absorber material. In collaboration with the Westinghouse Science and Technology Center in Pittsburgh, Pennsylvania, a program was launched to optimize the use of lead or lead alloys in the construction of the calorimeter. A cast lead design for the calorimeter evolved from this effort. Subsequent to this design, further pressure to reduce costs have now dictated a design which contains lead only in the electromagnetic sections of the

calorimeter. The finite element analysis we will present here was done using lead for the HAD1 section of the barrel. DOE

36 LASERS AND MASERS

Includes parametric amplifiers.
For related information see also *76 Solid-State Physics.*

N92-30400# Lawrence Livermore National Lab., CA.
INTERACTION PHYSICS FOR MEGAJOULE LASER FUSION TARGETS
W. L. Kruer Feb. 1992 9 p Presented at the 10th International Workshop on Laser Interaction and Related Plasma Phenomena, Monterey, CA, 11-15 Nov. 1991
(Contract W-7405-eng-48)
(DE92-014796; UCRL-JC-109599; CONF-911131-3) Avail: CASI HC A02/MF A01

Some little-explored interaction phenomena for targets irradiated with megajoule lasers are considered. Simple estimates show that the laser plasma interaction then occurs in a hot (multi-keV) plasma with density much less than the critical density. In such plasmas, Raman and Brillouin scattering into the forward hemisphere are potentially significant. A simple model shows that Raman forward scattering can be saturated at low levels by ponderomotive detuning. Calculations also illustrate a suppression of ponderomotive filamentation by plasma-induced beam smoothing. DOE

N92-30552# Northeast Semiconductor, Inc., Ithaca, NY.
INNOVATIVE TECHNIQUES FOR THE PRODUCTION OF LOW COST 2-D LASER DIODE ARRAYS SUPPLIES OR SERVICES AND PRICES/COSTS Monthly Technical Report No. 6, 1-30 Jun. 1992
30 Jun. 1992 6 p
(Contract N00014-91-C-0222)
(AD-A252665) Avail: CASI HC A02/MF A01

The primary objective of this problem is to develop a low cost, high yielding methodology for processing, packaging, and characterization of MBE grown two dimensional high power laser diode arrays. Projected increases in overall yield of AlGaAs diode lasers would reduce manufacturing cost from the current $10 to $20 per peak watt to below $3 per peak watt. Emphasis will be placed on innovative packaging techniques that will utilize recent advances in diamond heat sinking technology. GRA

N92-30582 Tel-Aviv Univ. (Israel). Dept. of Electron Devices and Materials and Electromagnetic Radiation.
TRANSVERSE PATTERN MODIFICATION IN A STABLE APERTURED LASER RESONATOR M.S. Thesis
Boaz Lissak Jan. 1990 127 p In HEBREW
(ITN-92-85171) Copyright Avail: Tel-Aviv Univ., Exact Sciences Library, Ramat Aviv, 69978, Israel

A very important consideration in the design of a laser resonator system is the transverse field distribution at different locations inside and outside the resonator. This distribution usually differs from that of the ideal Hermite-Gaussian modes due to apertures inevitably present in the resonator. Sometimes these apertures are intentionally placed to suppress higher order modes. The properties of the ideal stable resonator are well known, and their Hermite-Gaussian modes are widely used to analyze a stable resonator, even when the ideal conditions are not well satisfied. One common kind of deviation from the ideal behavior is likely to happen when mirror dimensions are limited or when apertures are present in a resonator. Then, a more accurate analysis is needed. The presence of an aperture inside a cavity may cause deviations from the smooth mode profile expected in stable resonators, manifesting intensity spikes that may damage mirrors and other optical components, or cause nonuniform saturation in the gain medium. In this work, the effects of hard apertures on the transverse mode distribution and on near and far field output distributions are investigated, both theoretically and experimentally. Wavefronts propagating in different directions inside a CO2 laser cavity were measured at the same plane, and found to have different transverse amplitude profiles. Transverse mode modification due to aperture diffraction effects are calculated and measured at planes along the cavity axis. The influence of the intracavity aperture's location and diameter on near field distribution and far field beam quality are calculated and measured. Quantitative figures of merit are introduced to evaluate the departure of the transversal mode patterns from ideal Gaussians. These figures of merit clarify the behavior of the field along the cavity and give guidelines to the resonator designer about the preferred place to insert intensity sensitive intracavity devices. Author (ISA)

N92-30614# Naval Research Lab., Washington, DC.
GENERATION OF STIMULATED BACKSCATTERED HARMONIC RADIATION FROM INTENSE LASER INTERACTIONS WITH BEAMS AND PLASMAS Interim Report
Eric Esarey and Phillip Sprangle 6 Apr. 1992 40 p
(AD-A248782; NRL/MR/4440-92-6786) Avail: CASI HC A03/MF A01

A comprehensive analysis is presented which describes the generation of harmonic radiation by the stimulated backscattering of intense laser fields from electron beams and from plasmas. The dynamics of the intense laser-electron interaction are analyzed using a fully nonlinear, relativistic cold fluid model valid to all orders in the amplitude of the pump laser. In general, the backscattered radiation, from an electron beam or stationary plasma, occurs at odd harmonics of the Doppler shifted incident laser frequency. The strength of the harmonics is strongly dependent on the incident laser intensity. The growth rate and saturation level of the backscattered harmonics are calculated and limitations due to thermal, space charge and collisional effects are discussed. Significant radiation generation at high harmonics requires sufficiently intense pump laser fields and sufficiently cold axial electron distributions. This mechanism may provide a practical method for producing coherent radiation in the XUV regime. GRA

N92-30743# Naval Research Lab., Washington, DC.
NONLINEAR ANALYSIS OF A GRATING FREE-ELECTRON LASER Interim Report
B. Hafizi (Icarus Research, Bethesda, MD.), P. Sprangle, and P. Serafim (Northeastern Univ., Boston, MA.) 31 Mar. 1992 33 p
(AD-A248833; NRL/MR/4790-92-6954) Avail: CASI HC A03/MF A01

A two-dimensional nonlinear model of a grating free-electron laser is formulated that includes the effects of self-field forces, finite beam emittance, energy spread and gyromotion of electrons in a guide magnetic field. The start-oscillation current and energy spread requirement for operation at either 100 Am or at 10 um are determined. The designs call for mildly relativistic (less than 1/2 MV) electron beams. The extraction efficiency is determined by numerical simulation. Three different examples are studied in order to elucidate the nonlinear stage of the interaction. We analyze the examples of an infinitely-thin beam, a finite-thickness beam with laminar flow, and a finite-thickness beam with full transverse motion. For a thick beam we find the interesting result that the effect of electron gyration about the beam axis is to enhance the extraction efficiency as compared to that for a beam with laminar flow. The numerical results for the extraction efficiency are found to be in close agreement with analytical estimates based on a model in which the electrons are trapped in the slow-wave associated with the grating structure. GRA

N92-30774# Boston Univ., MA. Dept. of Chemistry.
TUNABLE SOLID STATE LASERS BASED ON MOLECULAR IONS Final Report, 15 Jul. 1988 - 30 Sep. 1991
A. Lempicki and Cz. Koepke Jan. 1992 146 p
(Contract DAAL03-88-K-0103)
(AD-A249423; ARO-25631.13-PH) Avail: CASI HC A07/MF A02

The main objective of this program was to investigate the possibility of developing tunable solid state lasers based on complexes of Transition Metal Ions in their highest valency state

or equivalently d(sup 0) configuration. This is a class of materials, often referred to as phosphors, with strong absorption bands in the UV and well suited for excimer laser pumping. We have found that, contrary to initial arguments, Excited State Absorption processes are very strong and overlapping the emission spectrum. Indications are that octahedral complexes, rather than tetrahedral may have a greater chance, especially in inorganic glasses. Additionally photochromic effects in BGO are reported, and a study of non-radiative processes in broad band emitters is also reported. The later shows the inadequacy of the present theoretical approach. GRA

N92-30784# Stanford Univ., CA. Lab. of Physics.
RESEARCH STUDIES ON EXTREME ULTRAVIOLET AND SOFT X RAY LASERS
S. E. Harris 10 Jan. 1992 32 p
(Contract MIPR-107-91)
(AD-A249798; ARO-26160.22-PH) Avail: CASI HC A03/MF A01

This report describes studies concerned with the physics of short wavelength lasers and with applications of a new type of quantum mechanical interference. Highlights of this work include the operation of a traveling wave x-ray pump H2 116 nm laser; the development of a new type of depletion spectroscopy for core-excited states; and the proposal of lasers without inversion and related concepts applicable to nonlinear optics. GRA

N92-30805# Los Alamos National Lab., NM.
VUV PRODUCTION FROM A FERRITE-DRIVEN FLASH-PUMPED SYSTEM
R. C. Sze and M. Sentis 1991 11 p Presented at the Lasers 1991, San Diego, CA, 8-13 Dec. 1991
(Contract W-7405-eng-36)
(DE92-011362; LA-UR-92-896; CONF-911296-6) Avail: CASI HC A03/MF A01

The relative spectral emission as a function of wavelength in the 1200-2900 Angstrom region is measured for a vacuum ultraviolet flash device whose discharge is initiated by a high resistance formed-ferrite rod. The device is studied because of its usefulness in the optical pumping of large volume laser systems. DOE

N92-30848# Argonne National Lab., IL.
HIGH FIELD OPTICAL-PUMPING SPIN-EXCHANGE POLARIZED DEUTERIUM SOURCE
A. Zghiche, K. P. Coulter, R. J. Holt, E. R. Kinney, R. S. Kowalczyk, D. H. Potterveld, L. Young, B. Zeidman, and D. K. Toporkov 1991 6 p Presented at the Polarized Target Workshop, Heidelberg, Fed. Republic of Germany, 23-28 Sep. 1991
(Contract W-31109-eng-38)
(DE92-010274; ANL/CP-75202; CONF-9109356-1) Avail: CASI HC A02/MF A01

Recent progress in the performance of laser-driven source of polarized deuterium is described. Optical pumping of potassium atoms followed by spin exchange scattering with deuterium atoms in a high magnetic field and RF transitions in a medium field was found to produce an intense, highly spin-polarized beam of deuterium atoms. In particular, the atomic polarization of deuterium was determined to be 73 percent +/- 3 percent at an intensity of 2.1 x 10(exp 17) Atomsis. The RF transition efficiency was measured and found to be 92 percent +/- 5 percent. DOE

N92-30997# European Space Agency, Paris (France).
NUMERICAL SIMULATION OF CRATER FORMATION HEATING BY LASER BEAM. ANALYSIS OF RADIATION EXCHANGES IN THE CAVITY
Philippe Barillot (Office National d'Etudes et de Recherches Aerospatiales, Paris, France) Mar. 1992 258 p Transl. into ENGLISH of Simulation Numerique de Craterisation d'une Cible sous l'Effet d'un Faisceau Laser. Analyse des Effets Radiatifs dans la Cavite (Paris, France, ONERA), Aug. 1990 215 p Original language document was announced as N91-12925 (ESA-TT-1234; ONERA-NT-1990-5; ETN-92-91746) Avail: CASI HC A12/MF A03

Within the context of laser-material interaction, greater understanding of the drilling process, taking into account the multiple reflections in the cavity, is needed, since it is thought that a sufficiently deep cavity can act as a radiation trap and greatly modify the drilling process. In order to achieve this, modeling of the heating and sublimation of a cylinder illuminated on one of its faces by high power incident radiation was performed. Work done during the modeling process is outlined. The numerical model deals with the multiple reflections inside the cavity during formation. The different approach to the thermal and optical problems allowed them to be studied separately at first. The two models were then brought together in a common code: ARCADES (Ablation and Radiation in a Cavity which is Axisymmetric, Diffuse and (or) Specular). ESA

N92-31115# Lawrence Livermore National Lab., CA.
GENERATION OF A SODIUM GUIDESTAR USING A HIGH POWER DYE LASER
H. Friedman Mar. 1992 6 p Presented at the Nonlinear Optics: Materials, Fundamentals, and Applications, Maui, HI, 17-21 Aug. 1992
(Contract W-7405-eng-48)
(DE92-012696; UCRL-JC-110098; CONF-920853-3) Avail: CASI HC A02/MF A01

Sodium laser guidestars have been proposed as a means to correct for the effects of atmospheric turbulence in large astronomical telescopes. Several groups have produced such guidestars, but as yet, none have been able to close a control loop for an adaptive optics system using this means largely because of the limited power available in the laser system. The effort to utilize a high power laser system developed by LLNL for laser isotope separation, for the generation of a sodium guidestar, is described. The requirements of the laser system are developed by examining the photon signal necessary to achieve sufficient signal to noise in the wavefront detector. The laser system developed for isotope separation is described and the performance characteristics are presented. The beam transport system is discussed and the results that were generated are presented. DOE

N92-31182# Los Alamos National Lab., NM.
REFLECTOR DEVELOPMENT FOR XUV FREE-ELECTRON LASER OSCILLATORS
B. E. Newnam 1992 10 p Presented at the 4th Generation Light Sources Workshop, Stanford, CA, 24-27 Feb. 1992
(Contract W-7405-eng-36)
(DE92-015212; LA-UR-92-1539; CONF-9202111-2) Avail: CASI HC A02/MF A01

The potential for extending FEL oscillators into the extreme ultraviolet below 100 nm has stimulated new resonator mirror concepts and experimental studies of promising reflective materials. Degradation of mirror reflectance by oxide and carbonaceous contaminants can be controlled by proper vacuum environment plus in situ cleaning, and periodic surface renewal. Multifacet mirrors within ring resonators will provide the desired broad-band reflectance and limit beam-induced thermal distortion to a tolerable level. DOE

N92-31023*# National Center for Atmospheric Research, Boulder, CO.
SIMPLIFIED SIGNAL PROCESSING FOR AN AIRBORNE CO2 DOPPLER LIDAR
R. L. Schwiesow and M. P. Spowart *In* NASA. Langley Research Center, 16th International Laser Radar Conference, Part 2 Jul. 1992 p 417-420 Sponsored in part by NSF (For primary document see N92-31013 21-35)
Avail: CASI HC A01/MF A03

N92-31029*# Hamamatsu Photonics K. K., Ichino (Japan).
A GEODETIC LASER RADAR RANGEFINDER WITH 10(EXP -7) RESOLUTION

Y. Mizushima, M. Takeichi, Y. Warashima, A. Takeshima, I. Ogawa, K. Ichie, and N. H. Schiller (Hamamatsu Corp., Bridgewater, NJ.) *In* NASA. Langley Research Center, 16th International Laser Radar Conference, Part 2 Jul. 1992 p 437-440 Sponsored in part by Hamamatsu Photonics K. K.; Japan Key Technology Center; and Shizuoka Prefectural Government (For primary document see N92-31013 21-35)
Avail: CASI HC A01/MF A03

N92-31058*# Tohoku Univ., Sendai (Japan). Inst. of Technology.
Tm,Ho:YAG LASER WITH TUNABLE RANGE OF 2.08-2.12 MICRONS AND ITS APPLICATIONS TO SPECTROSCOPY
Kazuhiro Asai and Toshikazu Itabe (Ministry of Posts and Telecommunications, Tokyo, Japan) *In* NASA. Langley Research Center, 16th International Laser Radar Conference, Part 2 Jul. 1992 p 553-554 (For primary document see N92-31013 21-35)
Avail: CASI HC A01/MF A03

N92-31066*# Defence Research Establishment Valcartier (Quebec).
EFFECT OF ATMOSPHERIC EXTINCTION ON LASER RANGEFINDER PERFORMANCE AT 1.54 AND 0.6 MICRONS
D. L. Hutt, J.-M. Theriault, V. Larochelle, and D. Bonnier *In* NASA. Langley Research Center, 16th International Laser Radar Conference, Part 2 Jul. 1992 p 581-584 Prepared in cooperation with Laval Univ., Quebec; and Wisconsin Univ., Madison (For primary document see N92-31013 21-35)
Avail: CASI HC A01/MF A03

N92-31075*# Atmospheric Sciences Lab., White Sands Missile Range, NM.
TIME AND WAVELENGTH DOMAIN ALGORITHMS FOR CHEMICAL ANALYSIS BY LASER RADAR
David L. Rosen and James B. Gillespie *In* NASA. Langley Research Center, 16th International Laser Radar Conference, Part 2 Jul. 1992 p 613-616 (For primary document see N92-31013 21-35)
Avail: CASI HC A01/MF A03

37 MECHANICAL ENGINEERING

Includes auxiliary systems (nonpower); machine elements and processes; and mechanical equipment.

N92-30316*# National Aeronautics and Space Administration. Lyndon B. Johnson Space Center, Houston, TX.
QUICK ACTING GIMBAL JOINT Patent Application
William B. Wood, inventor (to NASA) and Gary D. Krch, inventor (to NASA) (ILC Dover, Frederica, DE.) 16 Jun. 1992 20 p
(NASA-Case-MSC-21918-1; NAS 1.71:MSC-21918-1; US-Patent-Appl-SN-899536) Avail: CASI HC A03/MF A01

The present invention relates to an adjustable linkage assembly for selectively retaining the position of one member pivotable with respect to another member. More specifically, the invention relates to a linkage assembly commonly referred to as a gimbal joint, and particularly to a quick release or quick acting gimbal joint. The assembly is relatively simple in construction, compact in size, and has superior locking strength in any selected position. The device can be quickly and easily actuated, without separate tooling, by inexperienced personnel or by computer controlled equipment. It also is designed to prevent inadvertent actuation. NASA

N92-30388*# National Aeronautics and Space Administration. Langley Research Center, Hampton, VA.
METHOD FOR REMOTELY POWERING A DEVICE SUCH AS A LUNAR ROVER Patent Application
Russell J. DeYoung, inventor (to NASA), Michael D. Williams, inventor (to NASA), Gilbert H. Walker, inventor (to NASA), Gregory L. Schuster, inventor (to NASA), and Ja H. Lee, inventor (to NASA) 7 Jan. 1992 25 p
(NASA-Case-LAR-14789-1; NAS 1.71:LAR-14789-1; US-Patent-Appl-SN-822457) Avail: CASI HC A03/MF A01

A method of supplying power to a device such as a lunar rover located on a planetary surface is provided. At least one, and preferably three, laser satellites are set in orbit around the planet. Each satellite contains a nuclear reactor for generating electrical power. This electrical power is converted into a laser beam which is passed through an amplifying array and directed toward the device such as a lunar rover. The received laser beam is then converted into electrical power for use by the device. NASA

N92-30396*# National Aeronautics and Space Administration. Lewis Research Center, Cleveland, OH.
DEVELOPMENT OF A FULL-SCALE TRANSMISSION TESTING PROCEDURE TO EVALUATE ADVANCED LUBRICANTS
David G. Lewicki, Harry J. Decker, and John T. Shimski (Naval Air Propulsion Test Center, Trenton, NJ.) Aug. 1992 25 p
(DA Proj. 1L1-62211-A-47-A; RTOP 505-63-36)
(NASA-TP-3265; E-6531; NAS 1.60:3265; AVSCOM-TR-91-C-026)
Avail: CASI HC A03/MF A01

Experimental tests were performed on the OH-58A helicopter main rotor transmission in the NASA Lewis 500-hp Helicopter Transmission Test Stand. The testing was part of a joint Navy/NASA/Army lubrication program. The objective of the program was to develop a separate lubricant for gearboxes and demonstrate an improved performance in life and load-carrying capacity. The goal of the experiments was to develop a testing procedure to fail certain transmission components using a MIL-L-23699 base reference oil, then run identical tests with improved lubricants and demonstrate performance. The tests were directed at failing components that the Navy has had problems with due to marginal lubrication. These failures included mast shaft bearing micropitting, sun gear and planet bearing fatigue, and spiral bevel gear scoring. A variety of tests were performed and over 900 hours of total run time accumulated for these tests. Some success was achieved in developing a testing procedure to produce sun gear and planet bearing fatigue failures. Only marginal success was achieved in producing mast shaft bearing micropitting and spiral bevel gear scoring. Author

N92-30477# National Aerospace Lab., Amsterdam (Netherlands). Space Div.
FLEXIBLE SPACE-BASED ROBOT MODELLING AND REAL-TIME SIMULATION
J. J. M. Prins, P. Dieleman, and P. T. L. M. vanWoerkom 8 Nov. 1989 14 p Presented at the AGARD Flight Mechanics Symposium on Space Vehicle Flight Mechanics, Luxembourg, 13-16 Nov. 1989 Sponsored by Netherlands Agency for Aerospace Programs
(Contract ESA-7222/87/nl)
(NLR-TP-89364-U; ETN-92-91529) Avail: CASI HC A03/MF A01

The Hermes Robot Arm (HERA) is a sophisticated space manipulator system which has to perform tasks ranging from berthing to tool operation in operational modes that range from fully automatic to purely manual. Development and qualification of such a space based manipulator must be supported by computer simulation facilities. A concise description of the HERA Simulation Facility Pilot (HSF-P) is given. It represents the first 'pilot' real-time simulation facility. Design concept, simulation models, and support tools are discussed. ESA

N92-30538# Wisconsin Univ., Madison. Engine Research Center.
DEVELOPMENT OF A MODULAR TRANSIENT CYCLE ANALYSIS PROGRAM FOR THE ADIABATIC DIESEL AND OTHER COMPOUND DIESEL ENGINES Final Technical Report, 30 Jul. 1984 - 30 May 1990
Gary L. Borman, Patrick V. Farrell, David E. Foster, Jay K. Martin, and Phillip S. Myers 17 Jun. 1991 123 p
(Contract DAAE07-84-C-R063)
(AD-A249022) Avail: CASI HC A06/MF A02

This final report covers a broad range of research activities, each of which contributes to the improved application of zero-dimensional engine cycle codes and/or multidimensional computational fluid mechanics (CFM) codes to engine design. Most of the work focused on problems related to in-cylinder heat transfer. GRA

N92-30540*# National Aeronautics and Space Administration. Lyndon B. Johnson Space Center, Houston, TX.
METHOD AND APPARATUS FOR PRELOADING A JOINT BY REMOTELY OPERABLE MEANS Patent Application
Robert O. Shelton, inventor (to NASA) 1 Jun. 1992 21 p
(NASA-Case-MSC-21940-1; NAS 1.71:MSC-21940-1; US-Patent-Appl-SN-892072) Avail: CASI HC A03/MF A01

The invention is a method and apparatus for joining structures, an active structure and a passive structure, and imposing a tensile pre-load on the joint by a remotely operable mechanism comprising a heat contractible joining element. The method and apparatus include mounting on the structure, a probe shaft of material which is transformable from an expanded length to a contracted length when heated to a specific temperature range. The shaft is provided with a probe head which is receivable in a receptacle opening formed in the passive structure, when the active structure is moved into engagement therewith by an appropriate manipulator mechanism. A latching system mounted on the structure adjacent to the receptacle opening captures the probe head, when the probe head is inserted a predetermined amount. A heating coil on the shaft is energizable by remote control for heating the shaft to a temperature range which transforms the shaft to its contracted length, whereby a latching shoulder thereof engages latching elements of the latching system and imposes a tensile preload on the structural joint. Provision is also made for manually adjusting the probe head on the shaft to allow for manual detachment of the structures or manual preloading of the structural joint. NASA

N92-30554# Purdue Univ., West Lafayette, IN. Tribiology Lab.
MODELLING OF HEAVILY LOADED LUBRICATED CONTACTS Final Report, Mar. 1990 - Aug. 1991
Farshid Sadeghi, William D. McClug, Jr., Kyung-Hoon Kim, Kevin Osborn, and Brian Lance Feb. 1992 56 p
(Contract F33615-86-C-2623)
(AD-A248807; WL-TR-91-2120) Avail: CASI HC A04/MF A01

Thermal elastohydrodynamic (EHD) lubrication of rolling/sliding line contacts is investigated to develop an interactive computer program for prediction of lubrication system performance. The user inputs lubricant and mechanical system physical properties as well as operating conditions of load and speed for calculation of contact zone pressure, temperature, traction, and stresses. This program is one of the first to include thermal effects in calculations and, therefore, can more accurately assess the critical tribological performance parameters at high load and speed conditions than previous prediction models. The program is written in the FORTRAN language and utilizes a UNIX operating system for high quality graphic output allowing easy visualization of results. GRA

N92-30571*# National Aeronautics and Space Administration. Lewis Research Center, Cleveland, OH.
DESIGN FEASIBILITY STUDY OF A SPACE STATION FREEDOM TRUSS
Sasan C. Armand and Caroline A. Dohogne (Michigan Univ., Ann Arbor.) Apr. 1992 15 p Original contains color illustrations
(RTOP 474-46-10)
(NASA-TM-105558; E-6882; NAS 1.15:105558) Avail: CASI HC A03/MF A01; 1 functional color page

Here, the focus is on the design and configuration feasibility of the short spacer for the Space Station Program in its launch configuration. The product of this study is being used by Rockwell International (Rocketdyne Division) as they continue their design concept of the current short spacer configuration. It is anticipated that the launch loads will dominate the on-orbit loads and dictate the design configuration of the short spacer. At the present time, the on-orbit loads have not been generated. The structural analysis discussed herein is based on the transient events derived from the Space Transportation System (STS) Interface Control Document (ICD). The transient loading events consist of liftoff loads, landing loads, and emergency landing loads. The quasi-static loading events have been neglected, since the magnitude of the acceleration factors are lower than the transient acceleration factors. The normal mode analyses presented herein are based on the most feasible configurations with acceptable stress ranges. Author

N92-30587# Oak Ridge National Lab., TN.
TRANSPORT PHENOMENA IN WELDS
T. Zacharia, R. J. Toedte, and S. A. David 1992 5 p Presented at the Image 6 Conference, Scottsdale, AZ, 14-17 Jul. 1992
(Contract DE-AC05-84OR-21400)
(DE92-013404; CONF-920795-1) Avail: CASI HC A01/MF A01

Convection is an essential and important part of the mechanism that controls the development of the weld pool. Depending on the direction and the magnitude of molten metal flow in the weld pool, completely different weld geometry, microstructures, and properties can be obtained. The present study focused on the influence of spatial and temporal variation of surface tension on the development of the weld pool. This paper describes the use of scientific visualization to provide a fundamental insight into the complex phenomena, which would otherwise be almost impossible to study and certainly very difficult to understand. DOE

N92-30601# Southwest Research Inst., San Antonio, TX. Dept. of Engine and Vehicle Research.
RINGLESS PISTON EXPERIMENTS. NATURAL GAS ENGINE TECHNOLOGY ADVANCEMENTS Topical Report, Dec. 1989 - Aug. 1991
J. J. Cole Dec. 1991 44 p
(Contract GRI-5089-293-1848)
(PB92-164466; GETA-91-10; SWRI-3178-3.2; GRI-91/0362)
Avail: CASI HC A03/MF A01

A two stroke 250 cc test engine was designed to experimentally evaluate ringless piston operation. The test engine had a crosshead to minimize the side loads on the ringless piston. The crankcase was sealed and it was possible to eliminate oil in the combustion chamber. A ringless molybdenum piston with labyrinth seals was designed and tested. Ringed-to-ringless power ratios greater than 90 percent were achieved by controlling piston-to-liner clearance via cylinder cooling. GRA

N92-30640# Scientific Research Associates, Inc., Glastonbury, CT.
ACTIVE CONTROL OF PRESSURE, SOUND AND VELOCITY OF CENTRIFUGAL PUMPS Final Report
D. G. Tse, J. S. Sabnis, H. McDonald, and James H. Whitelaw Mar. 1992 117 p
(Contract N00014-89-C-0090)
(AD-A249446; R92-920036-F) Avail: CASI HC A06/MF A02

Measurements of velocity, pressure, and sound were obtained in a centrifugal pump with a four blade impeller rotating at speeds between 1470 and 3510 rpm to improve understanding of noise generation and to investigate the feasibility of reducing fluid dynamic noise with active control. The velocity results show flow separation in the region near the shroud wall and at the suction surface of the blades with the flow driven inward by the adverse pressure gradient near the shroud wall. The frequency spectra of the pressure distributions obtained inside the pump casing at 3510 rpm showed a dominant frequency of 50 to 60 dB above the background level associated with the blade passing frequency of approximately 240 Hz. However, the saw-tooth waveform observed in the pressure characteristic also comprised of second and third harmonics of 45 to 55 dB and 35 to 45 dB above the background level and another 8 higher harmonics with diminishing amplitude as the frequency increased. The pressure distribution underwent a circumferential variation which was believed to stem from resonance or suppression of the 11 harmonic frequencies due to circumferential variation of the geometry of the scroll. All the waveforms inside the pump were generated by 11 sinusoids of

different amplitudes. Only the first three harmonics contained sufficient energy to produce a detectable signature in the air-borne noise characteristics. GRA

N92-30722*# National Aeronautics and Space Administration. Lewis Research Center, Cleveland, OH.
FAST METHODS TO NUMERICALLY INTEGRATE THE REYNOLDS EQUATION FOR GAS FLUID FILMS
Florin Dimofte 1992 26 p Presented at the STLE-ASME Joint Tribology Conference, St. Louis, MO, 13-16 Oct. 1991
(RTOP 590-21-11)
(NASA-TM-105415; E-6824; NAS 1.15:105415) Avail: CASI HC A03/MF A01

The alternating direction implicit (ADI) method is adopted, modified, and applied to the Reynolds equation for thin, gas fluid films. An efficient code is developed to predict both the steady-state and dynamic performance of an aerodynamic journal bearing. An alternative approach is shown for hybrid journal gas bearings by using Liebmann's iterative solution (LIS) for elliptic partial differential equations. The results are compared with known design criteria from experimental data. The developed methods show good accuracy and very short computer running time in comparison with methods based on an inverting of a matrix. The computer codes need a small amount of memory and can be run on either personal computers or on mainframe systems. Author

N92-30734*# National Aeronautics and Space Administration. Lewis Research Center, Cleveland, OH.
MAGNETIC BEARINGS FOR FREE-PISTON STIRLING ENGINES
P. W. Curwen (Mechanical Technology, Inc., Latham, NY.), D. P. Fleming, D. K. Rao (Mechanical Technology, Inc., Latham, NY.), and D. S. Wilson (Mechanical Technology, Inc., Latham, NY.) Aug. 1992 8 p Proposed for presentation at the 27th Intersociety Energy Conversion Engineering Conference, San Diego, CA, 3-7 Aug. 1992; sponsored by SAE, ACS, AIAA, ASME, IEEE, AIChE, and ANS
(Contract NAS3-26061; RTOP 590-13-11)
(NASA-TM-105730; E-7091; NAS 1.15:105730) Avail: CASI HC A02/MF A01

The feasibility and efficacy of applying magnetic bearings to free-piston Stirling-cycle power conversion machinery currently being developed for long-term space missions are assessed. The study was performed for a 50-kWe Reference Stirling Space Power Converter (RSSPC) which currently uses hydrostatic gas bearings to support the reciprocating displacer and power piston assemblies. Active magnetic bearings of the attractive electromagnetic type are feasible for the RSSPC power piston. Magnetic support of the displacer assembly would require unacceptable changes to the design of the current RSSPC. However, magnetic suspension of both displacer and power piston is feasible for a relative-displacer version of the RSSPC. Magnetic suspension of the RSSPC power piston can potentially increase overall efficiency by 0.5 to 1 percent (0.1 to 0.3 efficiency points). Magnetic bearings will also overcome several operational concerns associated with hydrostatic gas bearing systems. These advantages, however, are accompanied by a 5 percent increase in specific mass of the RSSPC. Author

N92-30738*# Massachusetts Inst. of Tech., Cambridge. Dept. of Mechanical Engineering.
A DESCRIPTION OF THE RESEARCH FOR PERIOD 3 OF A RESEARCH PROGRAM ON THE PLANNING AND CONTROL FOR SPACE ROBOTIC MANIPULATORS Progress Report, 1 Feb. 1991 - Jan. 1992
Steven Dubowsky Mar. 1992 558 p
(Grant NAG1-801)
(NASA-CR-190243; NAS 1.26:190243) Copyright Avail: CASI HC A24/MF A04

The objective of this research program is to develop control techniques to enable future space robotic systems to meet their mission objectives. This report covers our work during the past year, 1 Feb. 1991 - 31 Jan. 1992 in this three-year research program (1 Aug. 1990 - 31 Jul. 1993). During this past year, we have made very significant progress in our theoretical and analytical work on algorithm development, our simulation studies, and our experimental investigation. This progress is summarized. Author

N92-30860# Argonne National Lab., IL.
VEHICLE/GUIDEWAY INTERACTION FOR HIGH SPEED VEHICLES ON FLEXIBLE GUIDEWAY
Y. Cai, S. S. Chen, D. M. Rote, and H. T. Coffey 1992 42 p Presented at the 1992 Canadian Society for Mechanical Engineering (CSME): Transport 1992+, Montreal (Canada), 1-5 Jun. 1992
(Contract W-31-109-eng-38)
(DE92-013057; ANL/CP-74864; CONF-9206155-1) Avail: CASI HC A03/MF A01

Dynamic interactions between vehicles and guideways of a high speed ground transportation system based on magnetically levitated vehicles are studied with an emphasis on the effects of vehicle and guideway parameters. Two dynamic models for vehicles are presented: first, the vehicle is considered as a moving force traveling on a simply-supported single-span or two-span beam with various speeds; and second, the vehicle is considered as a one dimensional model with two-degrees-of-freedom which represents the primary and secondary suspensions of a vehicle with lumped masses, linear springs, and dampings. The Bernoulli-Euler beam equation is used to model the characteristics of a flexible guideway, and the guideway synthesis is based on a model analysis method. A series of analyses have been performed to understand the response characteristics under different loading conditions and provide some benchmark data for verifications of other comprehensive computer programs and some basic design guidelines for maglev systems. DOE

N92-30948*# National Aeronautics and Space Administration. Lewis Research Center, Cleveland, OH.
MINIMIZATION OF DEVIATIONS OF GEAR REAL TOOTH SURFACES DETERMINED BY COORDINATE MEASUREMENTS
F. L. Litvin (Illinois Univ., Chicago.), C. Kuan (Illinois Univ., Chicago.), J.-C. Wang (Illinois Univ., Chicago.), R. F. Handschuh, J. Masseth (Dana Corp., Fort Wayne, IN.), and N. Maruyama (Nissan Motor Co. Ltd., Yokosuka, Japan) 1992 10 p Proposed for presentation at the 1992 Power Transmission and Gearing Conference, Phoenix, AZ, 13-16 Sep. 1992
(DA Proj. 1L1-62211-A-47A; RTOP 505-63-36)
(NASA-TM-105718; E-7115; NAS 1.15:105718; AVSCOM-TR-92-C-003) Avail: CASI HC A02/MF A01

The deviations of a gear's real tooth surface from the theoretical surface are determined by coordinate measurements at the grid of the surface. A method was developed to transform the deviations from Cartesian coordinates to those along the normal at the measurement locations. Equations are derived that relate the first order deviations with the adjustment to the manufacturing machine-tool settings. The deviations of the entire surface are minimized. The minimization is achieved by application of the least-square method for an overdetermined system of linear equations. The proposed method is illustrated with a numerical example for hypoid gear and pinion. Author

38 QUALITY ASSURANCE AND RELIABILITY

Includes product sampling procedures and techniques; and quality control.

N92-30237# Missouri Univ., Columbia. Dept. of Statistics.
STATISTICAL THEORY ON RELIABILITY Final Report, 15 Jun. 1989 - 14 Dec. 1991
Asit P. Basu 14 Dec. 1991 8 p
(Grant AF-AFOSR-0406-89)
(AD-A250809; AFOSR-92-0358TR) Avail: CASI HC A02/MF A01

Considerable progress was made by the Principal Investigator, Professor Asit Basu, and his collaborators on the areas of tests

for exponentiality, component life length estimation, sequential and influential methods, and Bayesian approaches for reparable systems. All of these results contribute to a better understanding of reliability principles and better techniques for applied reliability practice. GRA

N92-30529# Wright Lab., Wright-Patterson AFB, OH.
CHARACTERIZATION AND ANALYSIS OF DEFECTS IN NONLINEAR OPTICAL MOLECULAR COMPOSITE FILMS Final Report, Sep. 1989 - Apr. 1991
Rajeev Mehta and Charles Y.-C. Lee Apr. 1992 110 p
(AF Proj. 2303)
(AD-A252118; WL-TR-92-4004) Avail: CASI HC A06/MF A01

Recently in our laboratory, improved optical quality films of PBZT were fabricated by extruding low concentration solutions in methane sulphonic acid. The films, even though being extruded from an apparatus that was not designed for optical films, showed a dramatic improvement in the optical quality over those which were used in the previous measurements. The x(sup 3) measurements of these films also indicated that the x(sup 3) values of these films were substantially higher than the previously reported values. However, the films were not of sufficient quality for wave-guiding experiments. This study was to identify the optical defects of the films so that the technique and the equipment can be improved to generate wave-guiding quality films with other NLO polymers. Two classes of defects have been identified and will be described in this report. The equipment modifications being implemented are documented. GRA

N92-30599# Worcester Polytechnic Inst., MA.
ULTRASOUND NDE OF ADHESIVE BOND INTEGRITY: A QUANTITATIVE MEASURE Final Report, 17 Aug. 1990 - 18 Aug. 1991
Rheinhold Ludwig and John M. Sullivan 28 Feb. 1992 84 p
(Contract DAAL04-90-C-0024)
(AD-A248845) Avail: CASI HC A05/MF A01

The objective of this research was to investigate and develop a coupled approach (analytical, numerical and experimental) to the ultrasonic nondestructive evaluation of adhesive bond integrity. Results of these studies were directed toward nondestructive evaluation (NDE) of the integrity of adhesive bonds and bondlines for advanced composites and multi-layered materials by the U.S. Army. Such studies are needed in both the manufacturing phases of products in order to assure quality as well as during the operating lifetime of the products in order to predict water infiltration or bond deterioration and hence prevent failure. The developed multiple-staged model started from a mathematical description of the ultrasound propagation through an inhomogeneous, isotropic or anisotropic solid with appropriate boundary conditions for the transmitter/receiver coupled to the material under test. Analytical solutions were employed to initially test and calibrate the numerical formulations was configured to be flexible and realistic enough to investigate a wide variety of bond configurations on the computer. GRA

N92-30693# Northwestern Univ., Evanston, IL. Center for Quality Engineering and Failure Prevention.
QUANTITATIVE NON-DESTRUCTIVE EVALUATION OF HIGH-TEMPERATURE SUPERCONDUCTING MATERIALS
J. D. Achenbach 14 Jun. 1991 13 p
(Contract DE-FG02-86ER-13484)
(DE92-011615; DOE/ER-13484/4) Avail: CASI HC A03/MF A01

Even though the currently intensive research efforts on high-temperature superconducting materials have not yet converged on a well specified practical material, the indications are that such a material may be quite brittle, anisotropic, and may contain many flaws such as microcracks and voids at grain boundaries. Consequently, practical applications of high temperature superconducting materials will require a very careful strength analysis based on fracture mechanics considerations. Because of the high sensitivity of the strength of such materials to the presence of defects, methods of quantitative non-destructive evaluation may be expected to play an important role in strength determinations. This proposal is concerned with the use of ultrasonic methods to detect and characterize isolated cracks, clusters of microcracks, and microcracks distributed throughout the material. Particular attention was, and will continue to be devoted to relating ultrasonic results to fracture mechanics considerations. DOE

N92-30763# Edgerton, Germeshausen and Grier, Inc., Idaho Falls, ID.
RELIABILITY IN THE DESIGN PHASE
A. S. Siahpush, S. W. Hills, H. Pham, and D. Majumdar (Department of Energy, Idaho Falls, ID.) Dec. 1991 86 p
(Contract DE-AC07-76ID-01570)
(DE92-012217; EGG-ME-9968) Avail: CASI HC A05/MF A01

A study was performed to determine the common methods and tools that are available to calculate or predict a system's reliability. A literature review and software survey are included. The desired product of this developmental work is a tool for the system designer to use in the early design phase so that the final design will achieve the desired system reliability without lengthy testing and rework. Three computer programs were written which provide the first attempt at fulfilling this need. The programs are described and a case study is presented for each one. This is a continuing effort which will be furthered in FY-1992. DOE

N92-31120# Superconducting Super Collider Lab., Dallas, TX.
A STATISTICAL RATIONALE FOR ESTABLISHING PROCESS QUALITY CONTROL LIMITS USING FIXED SAMPLE SIZE, FOR CRITICAL CURRENT VERIFICATION OF SSC SUPERCONDUCTING WIRE
D. A. Pollock, G. Brown, D. W. Capone, II, D. Christopherson, J. M. Seuntjens, and J. Woltz Mar. 1992 8 p Presented at the International Industrial Symposium on the Super Collider, New Orleans, LA, 4-6 Mar. 1992 Submitted for publication
(Contract DE-AC35-89ER-40486)
(DE92-014844; SSCL-Preprint-52; CONF-920331-50) Avail: CASI HC A02/MF A01

The purpose of this paper is to demonstrate a statistical method for verifying superconducting wire process stability as represented by I(sub c). The paper does not propose changing the I(sub c) testing frequency for wire during Phase 1 of the present Vendor Qualification Program. The actual statistical limits demonstrated for one supplier's data are not expected to be suitable for all suppliers. However, the method used to develop the limits and the potential for improved process through their use, may be applied equally. Implementing the demonstrated method implies that the current practice of testing all pieces of wire from each billet, for the purpose of detecting manufacturing process errors (i.e. missing a heat-treatment cycle for a part of the billet, etc.) can be replaced by other less costly process control measures. As used in this paper, process control limits for critical current are quantitative indicators of the source manufacturing process uniformity. The limits serve as alarms indicating the need for manufacturing process investigation. DOE

39 STRUCTURAL MECHANICS

Includes structural element design and weight analysis; fatigue; and thermal stress.

For applications see *05 Aircraft Design, Testing and Performance* and *18 Spacecraft Design, Testing and Performance.*

N92-30309*# Analytical Services and Materials, Inc., Hampton, VA.
A BOUNDARY ELEMENT ALTERNATING METHOD FOR TWO-DIMENSIONAL MIXED-MODE FRACTURE PROBLEMS
I. S. Raju and T. Krishnamurthy Washington NASA. Langley Research Center Aug. 1992 37 p
(Contract NAS1-19317; RTOP 505-63-53-01)

(NASA-CR-4460; NAS 1.26:4460) Avail: CASI HC A03/MF A01

A boundary element alternating method, denoted herein as BEAM, is presented for two dimensional fracture problems. This is an iterative method which alternates between two solutions. An analytical solution for arbitrary polynomial normal and tangential pressure distributions applied to the crack faces of an embedded crack in an infinite plate is used as the fundamental solution in the alternating method. A boundary element method for an uncracked finite plate is the second solution. For problems of edge cracks a technique of utilizing finite elements with BEAM is presented to overcome the inherent singularity in boundary element stress calculation near the boundaries. Several computational aspects that make the algorithm efficient are presented. Finally, the BEAM is applied to a variety of two dimensional crack problems with different configurations and loadings to assess the validity of the method. The method gives accurate stress intensity factors with minimal computing effort. Author

N92-30317*# National Aeronautics and Space Administration. Langley Research Center, Hampton, VA.

A SHEAR SENSITIVE MONOMER-POLYMER LAMINATE STRUCTURE AND METHOD OF USING SAME Patent Application

Jag J. Singh, inventor (to NASA), Abe Eftekhari, inventor (to NASA) (Hampton Univ., VA.), and Devendra S. Parmar, inventor (to NASA) (National Academy of Sciences - National Research Council, Hampton, VA.) 2 Mar. 1992 21 p

(NASA-Case-LAR-14654-1; NAS 1.71:LAR-14654-1; US-Patent-Appl-SN-849612) Avail: CASI HC A03/MF A01

Monomer cholesteric liquid crystals have helical structures which result in a phenomenon known as selective reflection, wherein incident white light is reflected in such a way that its wavelength is governed by the instantaneous pitch of the helix structure. The pitch is dependent on temperature and external stress fields. It is possible to use such monomers in flow visualization and temperature measurement. However, the required thin layers of these monomers are quickly washed away by a flow, making their application time dependent for a given flow rate. the laminate structure according to the present invention comprises a liquid crystal polymer substrate attached to a test surface of an article. A light absorbing coating is applied to the substrate and is thin enough to permit bonding steric interaction between the liquid crystal polymer substrate and an overlying liquid crystal monomer thin film. Light is directed through and reflected by the liquid crystal monomer thin film and unreflected light is absorbed by the underlying coating. The wavelength of the reflected light is indicative of the shear stress experienced by the test surface. Novel aspects of the invention include its firm bonding of a liquid crystal monomer to a model and its use of a coating to reduce interference from light unreflected by the monomer helical structure. NASA

N92-30338# Maryland Univ., College Park. Inst. for Physical Science and Technology.

OPTIMAL SHEAR CORRECTION FACTORS IN HIERARCHICAL PLATE MODELLING Final Report

I. Babuska, J. M. DHarcourt, and C. Schwab 7 Oct. 1991 39 p (Contract N00014-90-J-1030)

(AD-A248899; BN-1129) Avail: CASI HC A03/MF A01

This paper addresses the formulation of hierarchical plate models as an optimal (in a clearly defined sense) numerical method which can be easily implemented and is available in the code MSC/PROBE. Special emphasis is placed on the optimal selection of the shear correction factors. It is shown that different measures of accuracy lead to different optimal choices of these factors. The main tool in the analysis is the Fourier transformation. GRA

N92-30416*# National Aeronautics and Space Administration. Marshall Space Flight Center, Huntsville, AL.

LINEAR ELASTIC FRACTURE MECHANICS PRIMER

Christopher D. Wilson Jul. 1992 77 p

(NASA-TM-103591; NAS 1.15:103591) Avail: CASI HC A05/MF A01

This primer is intended to remove the blackbox perception of fracture mechanics computer software by structural engineers. The fundamental concepts of linear elastic fracture mechanics are presented with emphasis on the practical application of fracture mechanics to real problems. Numerous rules of thumb are provided. Recommended texts for additional reading, and a discussion of the significance of fracture mechanics in structural design are given. Griffith's criterion for crack extension, Irwin's elastic stress field near the crack tip, and the influence of small-scale plasticity are discussed. Common stress intensities factor solutions and methods for determining them are included. Fracture toughness and subcritical crack growth are discussed. The application of fracture mechanics to damage tolerance and fracture control is discussed. Several example problems and a practice set of problems are given. Author

N92-30423# Messerschmitt-Boelkow-Blohm G.m.b.H., Munich (Germany, F.R.). Aircraft Div.

MBB-LAGRANGE: A GENERAL STRUCTURAL RELIABILITY AND OPTIMIZATION STRUCTURAL SYSTEM

Rainer Zotemantel 6 Sep. 1991 21 p Repr. from Reliability and Optimization of Structural Systems 2 (R. Rackwitz u P. Thoft-Christensen) 1991 Presented at the IFIP Conference, Munich, Fed. Republic of Germany, 11-13 Sep. 1991

(MBB/FW321/S/PUB/467; ETN-92-91901) Copyright Avail: CASI HC A03/MF A01

MBB-LAGRANGE is a program system which allows the optimization of general structural systems. The geometry and properties of these structures are idealized by a finite element model with isotropic, orthotropic, anisotropic and composite materials. The design variables and a variety of constraints characterize the optimization model. The design variables are element thicknesses, cross sections, concentrated masses and fiber angles. The design can be restricted with respect to statics (e.g., stresses, displacements), dynamics (natural frequencies, dynamic response) and aeroelastics (efficiencies, flutter speed). In general the aim is to minimize the structure weight subject to the constraints. But often it is necessary to get only a feasible design. The highlights of the program system are: simultaneous optimization, a wide range of mathematical programming algorithms, a modular architecture within computer aided engineering environment. A lot of large scale problems, especially space and aircraft structures, demonstrate the power of MBB-LAGRANGE. ESA

N92-30558# Southwest Research Inst., San Antonio, TX.

CRACK GROWTH PROCESSES AT ELEVATED TEMPERATURES IN ADVANCED MATERIALS Annual Report, 1 Jan. 1991 - 1 Jan. 1992

David L. Davidson, Kwai S. Chan, and James Lankford Feb. 1992 251 p LIMITED REPRODUCIBILITY: Availability: Document partially illegible

(Contract F49620-89-C-0032)

(AD-A249023; SWRI-06-2699/3; AFOSR-92-0241TR) Avail: CASI HC A12/MF A03

Research in this program during the past 3 years has been on fracture studies on intermetallic alloys. Most of the work was focused on alloys based on the intermetallic compounds Ti3Al and TiAl, but some work to characterize alloys based on Nb3Al was also accomplished. The mechanisms controlling fatigue and fracture toughness of these new materials have been determined and compared to similar knowledge for other alloys. For a TiAl alloy with lamellar microstructure, fatigue cracks grew 10 times slower at 800 C in vacuum, and the threshold for the crack growth was higher than for 25 C in air. Growth was intermittent and crack tip opening alternated between blunt and sharp, just as found for other alloys. Crack growth was influenced by the direction of the lamellae relative to the loading axis, especially at low stresses. For crack growth perpendicular to the lamella direction, crack advance was linked to the width of the lamellae. Fatigue crack closure was about the same as for other alloys. Because of

the similarity of crack growth behavior between this and other titanium alloys, a crack tip geometric model previously used for other materials was applied. GRA

N92-30567# Oak Ridge National Lab., TN.
CREEP AND SLOW CRACK GROWTH MECHANISMS RELATED TO MACROSCOPIC CREEP BEHAVIOR OF A SILICON NITRIDE CERAMIC AT ELEVATED TEMPERATURES
M. G. Jenkins, M. K. Ferber, and J. A. Salem (National Aeronautics and Space Administration. Lewis Research Center, Cleveland, OH.) 1992 9 p Presented at the 7th Society for Experimental Mechanics International Congress on Experimental Mechanics, Las Vegas, NV, 8-11 Jun. 1992
(Contract DE-AC05-84OR-21400)
(DE92-015195; CONF-9206187-1) Avail: CASI HC A02/MF A01

Recent tensile creep and creep rupture test results of a hot isostatically pressed silicon nitride at 1150, 1260, and 1370 C were evaluated using microscopy in conjunction with various empirical and mathematical models to provide insight into creep and slow crack growth mechanisms. The stress and temperature sensitivities of the secondary (or minimum) strain rate were used to estimate the stress exponent and activation energy associated with the dominant creep mechanism. Limiting cases for cavity nucleation and growth were applied to establish possible creep damage modes. At 1150 C, creep rupture was controlled by a slow crack growth mechanism. At 1260 and 1370 C, the accumulation of creep damage in the form of grain boundary cavities and cracks dominated the creep rupture behavior. In this temperature regime, the creep rupture life was controlled by the secondary (or minimum) strain rate in accordance with a Monkman-Grant-type relation. DOE

N92-30766# Politecnico di Milano (Italy). Dipartimento di Ingregneria Aerospaziale.
COMPOSITE BEAM ANALYSIS LINEAR ANALYSIS OF NATURALLY CURVED AND TWISTED ANISOTROPIC BEAMS Final Report
Marco Borri, Gian L. Ghiringhelli, and Teodoro Merlini May 1992 88 p
(Contract DAJA45-90-C-0037)
(AD-A252652; R/D-6571-AN-01) Avail: CASI HC A05/MF A01

The aim of this report is to present a consistent theory for the deformation of a naturally curved and twisted anisotropic beam. The proposed formulation naturally extends the classical Saint-Venant approach to the case of curved and twisted anisotropic beams. The mathematical model developed under the assumption of span-wise uniform cross-section, curvature and twist, can take into account any kind of elastic coupling due to the material properties and the curved geometry. The consistency of the presented math-model and its generality about the cross-sectional shape, make it a useful tool even in a preliminary design optimization context such as the aeroelastic tailoring of helicopter rotor blades. The advantage of the present procedure is that it only requires a two-dimensional discretization; thus, very detailed analyses can be performed and interlaminar stresses between laminae can be evaluated. Such analyses would be extremely time consuming if performed with standard finite element codes: that prevents their recursive use as for example when optimizing a beam design. Moreover, as a byproduct of the proposed formulation, one obtains the constitutive law of the cross-section in terms of stress resultant and moment and their conjugate strain measures. This constitutive law takes into account any kind of elastic couplings, e.g., torsion-tension, tension-shear, bending-shear, and constitutes a fundamental input in aeroelastic analyses of helicopter blades. Four simple examples are given in order to show the principal features of the method. GRA

N92-30802# Army Armament Research, Development and Engineering Center, Watervliet, NY.
NONLINEAR STRESS ANALYSIS OF COMPOSITE-JACKETED STEEL CYLINDERS SUBJECTED TO HIGH INTERNAL PRESSURE Final Report
Peter C. Chen Mar. 1992 28 p
(AD-A249500; ARCCB-TR-92009) Avail: CASI HC A03/MF A01

A nonlinear stress analysis of a thick-walled compound tube subjected to high internal pressure is presented. The compound tube is constructed of a steel liner and a graphite-bismaleimide outer shell. Analytical expressions for the stresses, strains, and displacements are derived for all loading ranges up to failure. Numerical results for the stresses and the maximum value that the compound tube can contain without failure are presented. GRA

N92-30823# Oak Ridge National Lab., TN.
ASSESSMENT OF AN IMPROVED MULTIAXIAL STRENGTH THEORY BASED ON CREEP-RUPTURE DATA FOR TYPE 316 STAINLESS STEEL
R. L. Huddleston 1992 9 p Presented at the American Society of Mechanical Engineers Pressure Vessel and Piping Conference, New Orleans, LA, 21-25 Jun. 1992
(Contract DE-AC05-84OR-21400)
(DE92-010431; CONF-920631-16) Avail: CASI HC A02/MF A01

A new multiaxial strength theory incorporating three independent stress parameters was developed and reported by the author in 1984. It was formally incorporated into ASME Code Case N47-29 in 1990. In the earlier paper, the new model was shown to provide significantly more accurate stress-rupture life predictions, than the classical theories of von Mises, Tresca, and Rankine, for the type 304 stainless steel tested at 593 C under different biaxial stress states. Further assessments for other alloys are showing similar results. The current paper provides additional results for type 316 stainless steel specimens tested at 600 C under tension-tension and tension-compression stress states and shows 2 to 3 orders of magnitude reduction in the scatter in predicted versus observed lives. A key feature of the new theory, which incorporates the maximum deviatoric stress, the first invariant of the stress tensor, and the second invariant of the deviatoric stress tensor, is its ability to distinguish between life under tensile versus compressive stress states. DOE

N92-30859# Sandia National Labs., Albuquerque, NM.
A STUDY OF DISCRETE AND CONTINUUM JOINT MODELING TECHNIQUES
J. Jung and S. R. Brown 1992 8 p Presented at the Fractured and Jointed Rock Masses Conference, Lake Tahoe, CA, 3-5 Jun. 1992
(Contract DE-AC04-76DP-00789)
(DE92-012631; SAND-91-1730C; CONF-920633-1) Avail: CASI HC A02/MF A01

This paper presents the results of a numerical and experimental study in which finite element and discrete element techniques were used to analyze a layered polycarbonate plate model subjected to uniaxial compression. Also, the two analysis techniques were used to compute the response of an eight meter diameter drift in jointed-rock. The drift was subjected to in-situ and far-field induced thermal stresses. The finite element analyses used a continuum rock model to represent the jointed-rock. A comparison of the analyses showed that the finite element continuum joint model consistently predicted less joint slippage than did the discrete element analyses, although far-field displacements compared well. DOE

N92-30870# Defence Research Establishment Atlantic, Dartmouth (Nova Scotia).
CROSS SECTIONAL CONSTANTS AND STRESS DISTRIBUTIONS OF THIN-WALLED SECTIONS
Thomas S. Hu Mar. 1992 41 p
(AD-A249886; DREA-TM-92/209) Avail: CASI HC A03/MF A01

The equivalent beam model is widely used for predicting strength and vibration of a ship hull in a preliminary analysis. It can also be used for checking results in a large finite element model and for parametric studies of ship behavior. This method

treats a ship hull as a series of prismatic segments connected together. Each segment has its sectional properties, real and virtual masses. The program SCRAP was developed for calculation of cross sectional constants and estimation of mass properties. It prepares input data files for the finite element programs VAST and TORSON and interprets the analytical results. SCRAP can be only used for some specific sections at the present time. For arbitrarily oriented sections it may give an incorrect shear center and warping constant and thus the wrong stress distributions. This report presents the mathematical derivations of the equations used for the calculation of cross sectional constants and stress distributions of thin-walled sections. As an improvement over the current SCRAP program, these equations are applicable to any shape of cross section, both open and closed, and are independent of the orientation of the cross section. A computer-oriented step-by-step procedure based on these equations is outlined. Several examples are also presented to verify the procedure.
GRA

N92-30963 Materials Research Labs., Maribyrnong (Australia).
PREDICTION OF COINCIDENCE FREQUENCIES FOR A THIN-WALLED, FLUID-FILLED PIPE
R. G. ODonnell and C. L. Sasadeusz 1992 13 p
(MRL-TN-600; AR-006-858) Copyright Avail: Issuing Activity

Outlined here is the role of piping-based noise generation and transmission in naval applications. The nature of turbulence is discussed as well as how it generates acoustic energy. Coincidence between higher order acoustic modes and resonant structural modes is defined. The role of coincidence in determining the efficiency of generating pipe wall vibrations by internal pressure fluctuations is discussed. The inertia effect of contained liquids is discussed. Coincidence data are presented for a 100 mm NB schedule 40 steel pipe. The implications for naval applications are discussed.
Author

N92-30964*# National Aeronautics and Space Administration. Langley Research Center, Hampton, VA.
FASTRAN-2: A FATIGUE CRACK GROWTH STRUCTURAL ANALYSIS PROGRAM
James C. Newman, Jr. Feb. 1992 103 p Revised
(RTOP 505-63-50-04)
(NASA-TM-104159; NAS 1.15:104159) Avail: CASI HC A06/MF A02

FASTRAN-II is a life-prediction code based on the crack-closure concept and is used to predict crack length against cycles from a specified initial crack size to failure for many common crack configurations found in structural components FASTRAN-II is an update of the previous FASTRAN. The life-prediction method used in FASTRAN-II is built around an analytical crack-closure model. The model is based on plasticity-induced fatigue-crack closure and is used to calculate the stress level at which the crack tip becomes fully open during cyclic loading. The applied cyclic loads may be constant-amplitude, variable-amplitude or spectrum loading. Several standardized flight-load spectra (TWIST, Mini-TWIST, FASTAFF, and Felix-28) and other load spectra (Space Shuttle and Gaussian) are included as options. Spectrum loads may also be input by the user as either a list of stress points or a flight-by-flight sequence. The program uses the crack-closure concept to account for load-interaction effects. Tensile or compressive loads can be applied. The program contains seventeen predefined crack configurations; and the user can define one crack configuration. The crack-opening stresses, as a function of load history and crack length, are calculated from the model and the effective stress-intensity factor range, used to correlate fatigue-crack growth rates, may be either elastic or modified for plastic yielding at the crack tip. Ten example problems are included with the user guide to demonstrate the many options in FASTRAN-II. A computer program DKEFF was also developed to analyze laboratory specimen data to obtain the effective stress-intensity factor against crack-growth rate relations used by FASTRAN-II. A user guide for this program is also included and discussed. (Computer programs are available from COSMIC.)
Author

N92-30988*# State Univ. of New York, Binghamton. Dept. of Mechanical and Industrial Engineering.
ACOUSTIC FATIGUE LIFE PREDICTION FOR NONLINEAR STRUCTURES WITH MULTIPLE RESONANT MODES Final Report, Apr. 1989 - Mar. 1992
R. N. Miles Mar. 1992 157 p
(Grant NAG1-978)
(NASA-CR-190471; NAS 1.26:190471) Avail: CASI HC A08/MF A02

This report documents an effort to develop practical and accurate methods for estimating the fatigue lives of complex aerospace structures subjected to intense random excitations. The emphasis of the current program is to construct analytical schemes for performing fatigue life estimates for structures that exhibit nonlinear vibration behavior and that have numerous resonant modes contributing to the response.
Author

N92-31123# Sandia National Labs., Albuquerque, NM.
EULERIAN SIMULATION OF THE PERFORATION OF ALUMINUM PLATES BY NONDEFORMING PROJECTILES
S. A. Silling Mar. 1992 46 p
(Contract DE-AC04-76DP-00789)
(DE92-011515; SAND-92-0493) Avail: CASI HC A03/MF A01

A new algorithm for the treatment of sliding interfaces between solids, with or without friction, in a Eulerian wavecode is described. The algorithm was implemented in the two-dimensional version of the CTH code. The code was used to simulate penetration and perforation of aluminum plates by rigid, conical-nosed tungsten projectiles. Comparison with experimental data is provided.
DOE

N92-31155*# National Aeronautics and Space Administration. Langley Research Center, Hampton, VA.
A DEMONSTRATION OF PASSIVE BLADE TWIST CONTROL USING EXTENSION-TWIST COUPLING
Renee C. Lake, Mark W. Nixon, Matthew L. Wilbur, Jeffrey D. Singleton, and Paul H. Mirick Jun. 1992 11 p Presented at the 33rd Structures, Structural Dynamics and Materials Conference, Dallas, TX, 13-15 Apr. 1992 Previously announced in IAA as A92-34358
(RTOP 505-63-36; DA Proj. 1L1-62211-A-47AB)
(NASA-TM-107642; NAS 1.15:107642;
USAAVSCOM-TR-92-B-010) Avail: CASI HC A03/MF A01

The results from a study aimed at improving the dynamic and aerodynamic characteristics of composite rotor blades through the use of extension-twist coupling are presented. A set of low twist model-scale helicopter rotor blades was manufactured with a view towards demonstrating the passive blade twist control concept. Hover testing of the blades was conducted to measure the change in blade twist as a function of rotor speed. The blades were spun through the 0-800 rpm range, with a corresponding sweep of collective pitch to determine the effect on the blade elastic twist. Hover data were obtained for both a ballasted and unballasted blade configuration in atmospheric conditions, where maximum twist changes of 2.54 and 5.24 degrees were respectively observed. These results compared well with those from a finite element analysis of the blade, which yielded maximum twists of 3.01 and 5.61 degrees for the unballasted and ballasted blade configurations, respectively. The aerodynamic-induced effects on the blade elastic twist, determined by testing a ballasted blade configuration in a near-vacuum condition, were found to be minimal with a maximum twist difference of 0.17 degrees observed between the two test environments. The effect of collective pitch sweep on the elastic twist was minimal.
Author

N92-31214*# National Aeronautics and Space Administration. Langley Research Center, Hampton, VA.
ENVIRONMENTAL FATIGUE OF AN Al-Li-Cu ALLOY. PART 2: MICROSCOPIC HYDROGEN CRACKING PROCESSES
Robert S. Piascik and Richard P. Gangloff (Virginia Univ., Charlottesville.) May 1992 34 p Sponsored in part by Virginia Univ.
(Grant NAG1-745; RTOP 505-63-50-04)

(NASA-TM-107620; NAS 1.15:107620) Avail: CASI HC A03/MF A01

Based on a fractographic analysis of fatigue crack propagation (FCP) in Al-Li-Cu alloy 2090 stressed in a variety of inert and embrittling environments, microscopic crack paths are identified and correlated with intrinsic da/dN-delta K kinetics. FCP rates in 2090 are accelerated by hydrogen producing environments (pure water vapor, moist air, and aqueous NaCl), as defined in Part 1. For these cases, subgrain boundary fatigue cracking (SGC) dominates for delta K values where the crack tip process zone, a significant fraction of the cyclic plastic zone, is sufficiently large to envelop 5 micron subgrains in the unrecrystallized microstructure. SGC may be due to strong hydrogen trapping at T1 precipitates concentrated at sub-boundaries. At low delta K, the plastic zone diameter is smaller than the subgrain size and FCP progresses along (100) planes due to either local lattice decohesion or aluminum-lithium hydride cracking. For inert environments (vacuum, helium, and oxygen), or at high delta K where the hydrogen effect on da/dN is small, FCP is along (111) slip planes; this mode does not transition with increasing delta K and plastic zone size. The SGC and (100) crystallographic cracking modes, and the governing influence of the crack tip process zone volume (delta K), support hydrogen embrittlement rather than a surface film rupture and anodic dissolution mechanism for environmental FCP. Multi-sloped log da/dN-log delta K behavior is produced by changes in process zone hydrogen-microstructure interactions, and not by purely micromechanical-microstructure interactions, in contradiction to microstructural distance-based fatigue models. Author

N92-31215*# National Aeronautics and Space Administration. Langley Research Center, Hampton, VA.
ENVIRONMENTAL FATIGUE OF AN Al-Li-Cu ALLOY. PART 3: MODELING OF CRACK TIP HYDROGEN DAMAGE
Robert S. Piascik and Richard P. Gangloff (Virginia Univ., Charlottesville.) May 1992 42 p Sponsored in part by Virginia Univ.
(Grant NAG1-745; RTOP 505-63-50-04)
(NASA-TM-107619; NAS 1.15:107619) Avail: CASI HC A03/MF A01

Environmental fatigue crack propagation rates and microscopic damage modes in Al-Li-Cu alloy 2090 (Parts 1 and 2) are described by a crack tip process zone model based on hydrogen embrittlement. Da/dN sub ENV equates to discontinuous crack advance over a distance, delta a, determined by dislocation transport of dissolved hydrogen at plastic strains above a critical value; and to the number of load cycles, delta N, required to hydrogenate process zone trap sites that fracture according to a local hydrogen concentration-tensile stress criterion. Transgranular (100) cracking occurs for process zones smaller than the subgrain size, and due to lattice decohesion or hydride formation. Intersubgranular cracking dominates when the process zone encompasses one or more subgrains so that dislocation transport provides hydrogen to strong boundary trapping sites. Multi-sloped log da/dN-log delta K behavior is produced by process zone plastic strain-hydrogen-microstructure interactions, and is determined by the DK dependent rates and proportions of each parallel cracking mode. Absolute values of the exponents and the preexponential coefficients are not predictable; however, fractographic measurements theta sub i coupled with fatigue crack propagation data for alloy 2090 established that the process zone model correctly describes fatigue crack propagation kinetics. Crack surface films hinder hydrogen uptake and reduce da/dN and alter the proportions of each fatigue crack propagation mode. Author

N92-30268*# University of the Pacific, Stockton, CA.
IMPACT TESTING OF WELDED SAMPLES
Calvin D. Lundeen *In* NASA. Langley Research Center, National Educators' Workshop: Update 1991. Standard Experiments in Engineering Materials Science and Technology Jun. 1992 p 99-102 (For primary document see N92-30263 21-29)
Avail: CASI HC A01/MF A03

N92-30274*# Arizona State Univ., Tempe. Dept. of Manufacturing and Industrial Technology.
LABORATORY EXPERIMENTS FROM THE TOY STORE
H. T. McClelland *In* NASA. Langley Research Center, National Educators' Workshop: Update 1991. Standard Experiments in Engineering Materials Science and Technology Jun. 1992 p 161-168 (For primary document see N92-30263 21-29)
Avail: CASI HC A02/MF A03

N92-30282*# Loyola Coll., Baltimore, MD. Dept. of Electrical Engineering and Engineering Science.
AN AUTOMATED SYSTEM FOR CREEP TESTING
F. Xavier Spiegel and Bernard J. Weigman *In* NASA. Langley Research Center, National Educators' Workshop: Update 1991. Standard Experiments in Engineering Materials Science and Technology Jun. 1992 p 253-262 (For primary document see N92-30263 21-29)
Avail: CASI HC A02/MF A03

N92-30283*# Loyola Coll., Baltimore, MD.
FIVE EXPERIMENTS IN MATERIALS SCIENCE FOR LESS THAN $10.00
F. Xavier Spiegel *In* NASA. Langley Research Center, National Educators' Workshop: Update 1991. Standard Experiments in Engineering Materials Science and Technology Jun. 1992 p 263-266 (For primary document see N92-30263 21-29)
Avail: CASI HC A01/MF A03

N92-30284*# Purdue Univ., West Lafayette, IN. School of Technology.
ISOTROPIC THIN-WALLED PRESSURE VESSEL EXPERIMENT
Nancy L. Denton and Vernon S. Hillsman *In* NASA. Langley Research Center, National Educators' Workshop: Update 1991. Standard Experiments in Engineering Materials Science and Technology Jun. 1992 p 291-298 (For primary document see N92-30263 21-29)
Avail: CASI HC A02/MF A03

N92-30290*# Texas A&M Univ., College Station. Dept. of Mechanical Engineering.
MECHANICAL PROPERTIES OF BRITTLE MATERIALS
L. R. Cornwell and H. R. Thornton *In* NASA. Langley Research Center, National Educators' Workshop: Update 1991. Standard Experiments in Engineering Materials Science and Technology Jun. 1992 p 369-373 (For primary document see N92-30263 21-29)
Avail: CASI HC A01/MF A03

N92-30294*# Brigham Young Univ., Provo, UT. Dept. of Manufacturing Engineering and Engineering Technology.
MEASURING THE WEIBULL MODULUS OF MICROSCOPE SLIDES
Carl D. Sorensen *In* NASA. Langley Research Center, National Educators' Workshop: Update 1991. Standard Experiments in Engineering Materials Science and Technology Jun. 1992 p 397-406 (For primary document see N92-30263 21-29)
Avail: CASI HC A02/MF A03

42 GEOSCIENCES (GENERAL)

No abstracts in this category.

43 EARTH RESOURCES AND REMOTE SENSING

Includes remote sensing of earth resources by aircraft and spacecraft; photogrammetry; and aerial photography.

For instrumentation see *35 Instrumentation and Photography.*

N92-30362# Beleidscommissie Remote Sensing, Delft (Netherlands).

THE USE OF TM DATA FOR IDENTIFICATION OF LAND COVER AND FOR DETECTION OF LAND USE CHANGES IN THE ATLANTIC ZONE OF COSTA RICA

J. Huising (Wageningen Agricultural Univ., Netherlands) and M. A. Mulders (Wageningen Agricultural Univ., Netherlands) Feb. 1992 69 p

(BCRS Proj. TO-2.10)

(BCRS-91-36; ISBN-90-5411-026-0; ETN-92-91884) Avail: CASI HC A04/MF A01

A structured approach to land cover mapping, involving different stages of field work and processing of remote sensing data, is presented in order to produce optimum imagery and classification products for land cover mapping of the Atlantic zone of Costa Rica. Three stages were evaluated: image processing in the prefieldwork stage to obtain insight into the overall variation of the scene; small scale reconnaissance fieldwork and processing thereafter, the latter directed towards the production of thematic imagery; medium scale reconnaissance fieldwork; and classification of land cover and land use. Emphasis is laid upon the latter two stages as well as on the detection of land use changes aided by multitemporal Thematic Mapper (TM) data. In the latter stage, the research is focused on testing of training statistics and mapping of spectral classes to derive land use and land cover categories. The use of indices provides an alternative approach to the spectral characterization and mapping of land cover. ESA

N92-30465# Beleidscommissie Remote Sensing, Delft (Netherlands).

PREPARATIONS FOR THE ERS-1 AND TOPEX/POSEIDON SATELLITE ALTIMETRY MISSIONS

M. W. A. vanderKooij (Technische Univ., Delft, Netherlands), M. C. Naeije (Technische Univ., Delft, Netherlands), D. Oskam (Technische Univ., Delft, Netherlands), and K. F. Wakker (Technische Univ., Delft, Netherlands) Jan. 1992 115 p

(BCRS Proj. OP-3.5)

(BCRS-90-28; ISBN-90-5411-017-1; ETN-92-91868) Avail: CASI HC A06/MF A02

Results of a number of separate studies on the processing of Seasat and Geosat satellite altimeter data for the determination of the mean surface, the detection of mesoscale sea surface variability and the modeling of ocean currents are presented. This kind of data analysis provides important information to physical oceanography and in the long run also to meteorology and climatology. The studies were performed during the period Sep. 1988 - Jul. 1990 and had the primary objective to prepare teams for participation in the processing of the ERS-1 and TOPEX/Poseidon altimeter data. A secondary goal was to process altimeter data taken by Seasat in 1978 and by Geosat in the period 1987-1989, and to generate results which could be analyzed by oceanographers. ESA

N92-30466# Beleidscommissie Remote Sensing, Delft (Netherlands).

ON THE REMOTE SENSING OF WATER QUALITY USING THE OPTICAL AIRBORNE SCANNER CAESAR

G. Marees (Nederlands Inst. voor Onderzoek der Zee, Texel.), M. R. Wernand (Nederlands Inst. voor Onderzoek der Zee, Texel.), and J. M. M. Kokke (Rijkswaterstaat, Delft, Netherlands) Nov. 1991 36 p

(BCRS Proj. TO-1.24)

(BCRS-90-30; ISBN-90-5411-008-2; ETN-92-91869) Avail: CASI HC A03/MF A01

An airborne remote sensing experiment was carried out with the spectral scanner CAESAR (CCD (Charge Coupled Device) Airborne Experimental Scanner for Applications in Remote Sensing). The possibilities and limitations of optical airborne remote sensing of the concentration distribution of chlorophyllous and nonchlorophyllous particles and of the dissolved organic materials was investigated. A suitable atmospheric correction procedure for the airborne data was developed and tested. The project is described and results given. It was concluded that the CAESAR imagery of this project is not only quantitatively but also qualitatively unusable for further interpretation purposes. ESA

N92-30467# Beleidscommissie Remote Sensing, Delft (Netherlands).

CAESAR: EVALUATION OF THE DUAL-LOOK CONCEPT

W. J. Looyen (National Aerospace Lab., Amsterdam, Netherlands), W. Verhoef (National Aerospace Lab., Amsterdam, Netherlands) J. G. P. W. Clevers (Wageningen Agricultural Univ., Netherlands), J. T. Lamers (Proefstation voor de Akkerbouw en de Groenteteelt in de Vollegronds, Netherlands), and J. Boerma (Proefstation voor de Akkerbouw en de Groenteteelt in de Vollegronds, Netherlands) Nov. 1991 123 p

(BCRS Proj. TE-1.13)

(BCRS-91-10; ISBN-90-5411-009-0; ETN-92-91871) Avail: CASI HC A06/MF A02

The Dutch CAESAR scanner (Charge Coupled Device Airborne Experimental Scanner for Applications in Remote Sensing) is equipped with a so-called dual look mode. Combining nadir observations with forward looking observations gives information on the directional reflectance of objects on the ground and provides stereoscopic information. A project to study the angle dependent behavior of agricultural crops, to study the impact of the dual look concept on crop classification and the modeling of bidirectional crop reflectance and atmospheric correction, was carried out. Much emphasis was put on crop classification and atmospheric modeling. On 26 Jun. 1989 a CAESAR flight was performed on a cloudless day at the end of a dry period. Spectral measurements were performed by using a hand held radiometer and light interception radiometers. In simulating the dual look effect a SAIL model was used: the SAILH model. This model includes the so-called hot spot effect. A combined vegetation atmosphere model (CAESIM) was developed to study the atmospheric influence on CAESAR measurements. This model was validated against an atmospheric model based on the use of reference targets. It is shown that the CAESAR dual look images provide an important tool to improve crop classifications in a maximum likelihood classification from 83 to 91 . Parameter estimation by bidirectional crop reflectance modeling was carried out. Results indicate the potential of the parameter estimation although, e.g., row effects play an important role. ESA

N92-30468# Beleidscommissie Remote Sensing, Delft (Netherlands).

MONITORING OF DUTCH FOREST WITH LANDSAT-TM Final Report

Dec. 1991 51 p Prepared in cooperation with Environmental Analysis and Remote Sensing, Delft, Netherlands and NAL, Amsterdam, Netherlands

(BCRS Proj. TO-2.17)

(BCRS-91-21; ISBN-90-5411-015-5; ETN-92-91872) Avail: CASI HC A04/MF A01

A study performed to monitor a Dutch forest is outlined. The following questions were addressed: Which changes in timber volume can be detected and possibly quantified with satellite imagery, only clearcut or also thinning? Which changes in vitality of forest stands can be detected? Which methods of analysis are most suitable for these objectives? LANDSAT Thematic Mapper (TM) imagery was used. According to the literature, the mid infrared band (TM5) has a very significant contribution in forestry applications, and this band is not available on SPOT. Scope was restricted to evergreens, Scotch pine in particular. Because of limited funds, the project was carried out retrospectively for the years 1984-1988. This also limited the available ground truth. The

state forestry 'Kootwijk' in the Netherlands was chosen as project area. ESA

N92-30471# Beleidscommissie Remote Sensing, Delft (Netherlands).
VEGETATION CONDITIONS AND YIELD INDICATORS. PART 1: MAIN REPORT Final Report
A. vanDijk (DHV Consultants, Malang, Indonesia), J. A. A. Berkhout (Amsterdam Univ., Netherlands), J. N. Roozekrans (Royal Netherlands Meteorological Inst., De Bilt.), W. Verhoef (National Aerospace Lab., Amsterdam, Netherlands), G. J. A. Nieuwenhuis (Winand Staring Centre, Wageningen, Netherlands), F. J. KutschLojenga (Central Bureau of Statistics, Voorburg, Netherlands), D. Meuldijk (Central Bureau of Statistics, Voorburg, Netherlands), and J. Gunnink (DHV Consultants, Malang, Indonesia) Apr. 1992 215 p 215 p
(Contract EEC-JRC-3444-88-08-ed-isp-NL; BCRS Proj. CO-2.19)
(BCRS-91-26-Pt-1; ISBN-90-5411-012-0; ETN-92-91875) Avail: CASI HC A10/MF A03

The use of NOAA/AVHRR (Advanced Very High Resolution Radiometer) for multiannual indicators, alarm and monitoring was studied. A research project in the Flevopolders (The Netherlands) is outlined and the following conclusions drawn. In Europe the NOAA/AVHRR data can be used for multiannual indicators, alarm and monitoring: the NOAA/AVHRR data can provide quickly discernible visible information on crop conditions and crop production over large areas in a semi operational mode. Convergence of information is important: the results of the crop growth model and the radiometric simulation increase the reliability and accuracy of the crop condition asessment based in NOAA/AVHRR data. ESA

N92-30472# Beleidscommissie Remote Sensing, Delft (Netherlands).
INTERPRETATION OF OPTICAL REMOTE SENSING DATA OVER COASTAL WATERS
G. Marees (Nederlands Inst. voor Onderzoek der Zee, Texel.) and M. R. Wernand (Nederlands Inst. voor Onderzoek der Zee, Texel.) Oct. 1991 115 p
(BCRS Proj. AO-3.3)
(BCRS-91-27; ISBN-90-5411-006-6; ETN-92-91876) Avail: CASI HC A06/MF A02

Optical properties of the Dutch coastal waters were studied. Spectral sea water signatures were analyzed with respect to optical remote sensing applications. The emphasis was on the interpretation of coastal water reflectance spectra in relation to the concentration of suspended and dissolved sea water constituents. From a principal component analysis of the reflectance spectra, it was concluded that maximal two independent sea water constituents can be derived from the spectra. North Sea remote sensing algorithms were developed for the former CZCS (Coastal Zone Color Scanner) and the coming SeaWiFs (Sea Viewing Wide Field of view Scanner) satellite scanners and for the airborne CAESAR (CCD) (Charge Coupled Device) Airborne Experimental Scanner) scanner. The applicability of the visible channel of the NOAA Advanced Very High Resolution Radiometer (AVHRR) weather satellite for mapping water quality parameters was also investigated. ESA

N92-30475# National Aerospace Lab., Amsterdam (Netherlands). Informatics Div.
METEODEC/METEOCRYPT: A DEMONSTRATION OF DATA COMPRESSION AND ENCRYPTION FOR OPERATIONAL REMOTE-SENSING
R. A. Hogendoorn and F. L. G. Kordes 28 Aug. 1989 12 p Presented at the 10th Symposium on Information and Communication Theory in the Benelux, Houhalen, Belgium, 25-26 May 1989
(Contracts ESA-7662/88; ESA-7560/88)
(NLR-TP-89294-U; ETN-92-91526) Avail: CASI HC A03/MF A01

A system for the demonstration of data compression and encryption on Meteosat images is developed. Three topics are described: the selection of the compression algorithm, forward error correction, and the distribution of decryption keys. ESA

N92-30515# European Space Agency, Paris (France).
REGISTRATION OF WINDFALL DAMAGE IN THE EASTERN HUNSRUECK PLATEAU (FEDERAL REPUBLIC OF GERMANY) UTILIZING LANDSAT-TM-DATA: A LANDSCAPE-ECOLOGICAL ANALYSIS FOR PRACTICAL FORESTRY
Johannes Wieczorek (Deutsche Forschungsanstalt fuer Luft- und Raumfahrt, Oberpfaffenhofen, Germany, F.R.) Mar. 1992 144 p Transl. into ENGLISH of Erfassung von Sturmwurfschaeden im Oestlichen Hunsrueck mit Hilfe von LANDSAT-TM-Daten: Eine Landschaftsoekologische Analyse fuer die Forstliche Praxis (Oberpfaffenhofen, Germany, DLR), Jun. 1990 149 p Original language document was announced as N91-21601
(ESA-TT-1253; DLR-FB-90-31; ETN-92-91710) Avail: CASI HC A07/MF A02

Using data from the LANDSAT 5 Thematic Mapper (TM), a mapping of windfall areas in the region of the Eastern Hunsrueck plateau (Germany, F.R.) is carried out. The first step is to make a general exposition of the usefulness of geographical information systems. Subsequently, it is found by classifying the data that the species of tree most heavily affected is the Spruce (Picea abies) grown in monocultures. These results were correlated with digitized soil data. The study showed that it is possible to identify the static wet soils as the soils which, in combination with flatrooting spruce, show the highest potential for windfall damage. ESA

N92-30545# Naval Oceanographic and Atmospheric Research Lab., Bay Saint Louis, MS.
REMOTE SENSING FOR THE LINCOLN SEA WINTEROVER EXPERIMENT Final Report
R. L. Crout, F. M. Fetterer, and A. E. Pressman Mar. 1992 93 p
(AD-A252117; NOARL-TN-231) Avail: CASI HC A05/MF A01

During the Naval Oceanographic and Atmospheric Research Laboratory (NOARL) Winterover experiment of 1989-1990, satellite imagery was processed in order to compare ice parameters derived from the imagery with the acoustic data collected. This effort is a continuation of an investigation of techniques developed during the Lincoln Sea exercise of 1990 (Fetterer et al., 1990). GRA

N92-30704# Los Alamos National Lab., NM.
A ONE-CLASS CLASSIFIER FOR IDENTIFYING URBAN AREAS IN REMOTELY-SENSED DATA
P. M. Kelly (New Mexico Univ., Albuquerque.), D. R. Hush (New Mexico Univ., Albuquerque.), and J. M. White 1992 7 p Presented at the Ideas in Science and Electronics (ISE) Symposium, Albuquerque, NM, 14 May 1992
(Contract W-7405-eng-36)
(DE92-013539; LA-UR-92-1262; CONF-9205141-4) Avail: CASI HC A02/MF A01

For many remote sensing applications, land cover can be determined by using spectral information alone. Identifying urban areas, however, requires the use of texture information since these areas are not generally characterized by a unique spectral signature. We have designed a one-class classifier to discriminate between urban and non-urban data. The advantage in using our classification technique is that principles of both statistical and adaptive pattern recognition are used simultaneously. This prevents new data that is completely dissimilar from the training data from being incorrectly classified. At the same time it allows decision boundary adaptation to reduce classification error in overlap areas of the feature space. Results will be illustrated using a LANDSAT scene of the city of Albuquerque. DOE

N92-30910# Indian Inst. of Tech., Bombay. Centre of Studies in Resources Engineering.
SATELLITE AND RADAR DATA USE IN RAINFALL-RUNOFF MODELS
M. G. Srinivas, ed. Feb. 1992 221 p Workshop held in

Bombay, India, 19-20 Dec. 1990
Avail: CASI HC A10/MF A03

Papers from the proceedings are presented and include: (1) remote sensing applications to rainfall estimation; (2) use of Indian National Satellite (INSAT) data in rainfall estimation; (3) solar-hydrogen energy system for solar belt countries and use of remote sensing; (4) remote sensing satellite data use in run-off studies; (5) digital data integration methods and the Geophysical Information System (GIS); (6) Soil Conservation Service (SCS) method of run-off estimation using remote sensing techniques; (7) remote sensing for rainfall estimation - Space Application Center (SCS) experience; (8) hydrologic modeling and use of remotely sensed data at the Central Water and Power Research Station (CWPRS); (9) estimation of vertical profile of soil moisture through multifrequency microwave data analyses; and (10) digital methods for analyses of satellite imagery. For individual titles, see N92-30911 through N92-30920.

N92-30911# Miami Univ., Coral Gables, FL. Remote Sensing Lab.
REMOTE SENSING APPLICATIONS TO RAINFALL ESTIMATION
H. W. Hiser *In* Indian Inst. of Tech., Satellite and Radar Data Use in Rainfall-Runoff Models Feb. 1992 p 1-12 (For primary document see N92-30910 21-43)
Avail: CASI HC A03/MF A03

Radars, which are active remote sensors, and passive remote sensors aboard satellites have been widely used for rainfall estimation for meteorological and hydrological applications. Most of the radars have been surface based or airborne, but spacecraft radars are likely to be used extensively in the future. The spacecraft passive systems have mostly operated in the visible and IR spectrum as the space scale resolution is improved. Various methods for rainfall estimation are discussed. Author

N92-30912# Indian Meteorological Dept., New Delhi.
USE OF INSAT DATA IN RAINFALL ESTIMATION
A. V. R. Krishna Rao *In* Indian Inst. of Tech., Satellite and Radar Data Use in Rainfall-Runoff Models Feb. 1992 p 13-27 (For primary document see N92-30910 21-43)
Avail: CASI HC A03/MF A03

It is a well known fact that rainfall exhibits large variations both in spatial and temporal scales. The intensity and duration of a particular rainfall event also depend on the type of the weather system that causes it. In addition to these natural variations, the measurement of rainfall by conventional methods is affected from inaccuracies that arise due to effects of terrain, exposure conditions, and the prevailing weather conditions. While the point rainfall measurements from the conventional raingauges suffer from the above errors, estimation of areal precipitation using these observations is subjected to an additional error arising out of the sparseness of the raingauge network. To alleviate these difficulties to some extent, an effective alternative is to resort to some sort of remote sensing. One alternative is to use satellite data in estimating the rainfall. The advantage of using satellite data in rain estimation lies in the fact that the observations are homogenous and estimation can be carried out simultaneously over a large area, and the information can be disseminated to the user, quicker than the conventional observations. The present article describes the technique employed at the Meteorological Data Utilization Center (MDUC) and some of the results of the studies undertaken at this Center. Author

N92-30913# Miami Univ., FL. Clean Energy Research Inst.
SOLAR-HYDROGEN ENERGY SYSTEM FOR SOLAR BELT COUNTRIES AND USE OF REMOTE SENSING
N. Lutfi and T. N. Veziroglu *In* Indian Inst. of Tech., Satellite and Radar Data Use in Rainfall-Runoff Models Feb. 1992 p 28-126 (For primary document see N92-30910 21-43)
Avail: CASI HC A05/MF A03

A solar-hydrogen energy system has been proposed for Pakistan as the best replacement for its present fossil fuel based energy system. The hydrogen is to be produced via photovoltaic-electrolysis. This system would utilize the available, non-agricultural terrain in the Baluchistan region. Additionally, there will be a sea water desalination plant. It is believed that the area under the photovoltaic panels, when coupled with the newly available water, would provide a suitable environment for growing cash crops. This would help to convert the vast tracts of useless desert land into green productive farms. Author

N92-30914# Indian Inst. of Tech., Bombay. Centre of Studies in Resources Engineering.
REMOTE SENSING SATELLITE DATA USE IN RUN-OFF STUDIES
M. G. Srinivas *In its* Satellite and Radar Data Use in Rainfall-Runoff Models Feb. 1992 p 127-135 (For primary document see N92-30910 21-43)
Avail: CASI HC A02/MF A03

Run-off, defined as that portion of the rainfall or snowfall appearing as flow in rivers and streams, is caused by the surface flow from the catchment during and immediately after the rainfall or snowmelt periods and by the underground storages during the remaining time. Values of run-off constitute a basic requirement in the design of water retaining structures (dams, weirs, barrages), flood protection works, river crossings (bridges), etc. Therefore, one of the main objectives in hydrologic research continues to be the modelling of the run-off phenomenon having general validity. Author

N92-30915# Indian Inst. of Tech., Bombay. Centre of Studies in Resources Engineering.
GEOGRAPHIC INFORMATION SYSTEM AND ITS APPLICATIONS
P. Venkatachalam *In its* Satellite and Radar Data Use in Rainfall-Runoff Models Feb. 1992 p 136-147 (For primary document see N92-30910 21-43)
Avail: CASI HC A03/MF A03

Described here are the principles behind the construction of the Geographic Information System (GIS), the development of a regional information system as a case study, and the role of remote sensing data in GIS. Topics covered include data encoding, input processing, data management, data retrieval, data display, the role of data models and structure, vector models, tesselation models, hardware configurations, and the use of GIS to assess surface runoff and soil erosion. Author

N92-30916# National Remote Sensing Agency, Hyderabad (India). Dept. of Space.
SCS METHOD OF RUNOFF ESTIMATION USING REMOTE SENSING TECHNIQUES
P. Srinivas, S. Thiruvengadachari, and M. Ramesha (Karnataka Regional Engineering Coll., Surathkal, India) *In* Indian Inst. of Tech., Satellite and Radar Data Use in Rainfall-Runoff Models Feb. 1992 p 148-161 (For primary document see N92-30910 21-43)
Avail: CASI HC A03/MF A03

The development and validation of a methodological approach to estimate the runoff for hilly basins is attempted. The Soil Conservation Service (SCS) runoff curve numbers (CNs) have been modified to allow for the regional land use pattern obtained from the satellite for hilly basins. Rainfall-runoff data for six consecutive years (1981-1986) were chosen. While the first set of three years (1981-1983) is used for calibrations, the next set of three years (1984-1986) is used for validation. Author

N92-30917# Indian Space Research Organization, Ahmedabad. Meteorology and Oceanography Div.
REMOTE SENSING FOR RAINFALL ESTIMATION: SAC EXPERIENCE
B. M. Rao, S. M. Bhandari, and M. S. Narayanan *In* Indian Inst. of Tech., Satellite and Radar Data Use in Rainfall-Runoff Models Feb. 1992 p 162-176 (For primary document see N92-30910 21-43)
Avail: CASI HC A03/MF A03

Described here are the results of the estimation of the intensity

of rainfall using GOES Very High Resolution Radiometer (VHRR) visible and IR images analyzed using the Grid-History technique. Rainfall ground truth data, simultaneously collected over the Madras region (India) using the Cyclone Detection Radar and raingauge network of the India Meteorological Department (IMD), have been used to compare and establish the feasibility of the satellite based estimation of rainfall over tropical convective situations. Results of satellite-radar comparisons of hourly and daily rainfall distributions over an area of approximately 10(exp 10) to 10(exp 5) square kilometers are presented. Author

N92-30918# Central Water and Power Research Station, Poona (India).
HYDROLOGIC MODELLING AND USE OF REMOTELY SENSED DATA AT CWPRS
F. T. Mathew *In* Indian Inst. of Tech., Satellite and Radar Data Use in Rainfall-Runoff Models Feb. 1992 p 177-178 (For primary document see N92-30910 21-43)
Avail: CASI HC A01/MF A03

The Central Water and Power Research Station (CWPRS), Pune, is actively engaged in applied and basic research in the water resources field. The institution is regularly called upon to advise on a variety of issues pertaining to development and management of water resources. CWPRS experience in computer oriented hydrological modeling dates back for two decades. Rainfall models are frequently used for such processes as: producing streamflow data at ungauged sites; extrapolating short flow records; and projecting flows for hypothetical, future hydrometeorological conditions. Along with these models, the use of remotely sensed data is gaining acceptance in the water resources field. Since remote sensing technology is evolving very fast, more use of the data is anticipated in the future. Author

N92-30919# Indian Inst. of Tech., Bombay. Centre of Studies in Resources Engineering.
ESTIMATION OF VERTICAL PROFILE OF SOIL MOISTURE THROUGH MULTIFREQUENCY MICROWAVE DATA ANALYSIS
K. S. Rao *In its* Satellite and Radar Data Use in Rainfall-Runoff Models Feb. 1992 p 179-203 (For primary document see N92-30910 21-43)
Avail: CASI HC A03/MF A03

An operational model for the retrieval of vertical profile of soil moisture through multifrequency microwave remote sensing is developed based on statistical inversion technique. A three parameter exponential function is used to represent soil moisture profiles. Initially the model is tested with the simulated profile data and corresponding theoretically computed brightness temperature T(sub B), values. The model is also tested using experimental T(sub B) data and experimentally measured profiles. The retrieved profiles are compared with actual field measured profile data. The surface soil moisture and slope near the surface are predicted very accurately using two and three frequency models. The maximum error at deeper depths is about 1 percent. Two and three frequency models give more or less same accuracies. Therefore, two frequency model is recommended for operational applications. Author

N92-30920# Indian Inst. of Tech., Bombay. Centre of Studies in Resources Engineering.
DIGITAL METHODS FOR ANALYSIS OF SATELLITE IMAGERY
G. T. Marathe *In its* Satellite and Radar Data Use in Rainfall-Runoff Models Feb. 1992 p 204-215 (For primary document see N92-30910 21-43)
Avail: CASI HC A03/MF A03

Runoff is one of the major inputs essential for many hydrologic studies. In recent years, satellite images have been increasingly employed as a significant input in the process of runoff estimation. The ability to yield real estimates of landcover over large areas, as compared to point data obtained by ground based methods of data collection, the revisit capability and the computer compatibility are some of the major advantages of remotely sensed data which have found widespread acceptability in runoff estimation procedures. Rainfall is another factor which is crucial in all hydrologic studies. Several methods have been put forward to estimate rainfall from remotely sensed data. The landcover mapping and cloud feature analysis techniques used in runoff and rainfall estimation respectively, are achieved through specific pattern recognition techniques. Even though a large number of such techniques are available, in practice, a finitely small number of techniques are used. Author

N92-30968 Technische Univ., Hanover (Germany, F.R.).
DEVELOPMENT OF THE CULTIVATED LANDSCAPE OF NORTH WEST GERMANY UNDER THE HUMAN INFLUENCE [ENTWICKLUNG DER KULTERLANDSCHAFT NORDWEST DEUTSCHLANDS UNTER DEM EINFLUSS DES MENSCHEN]
Richard Pott 1992 49 p Repr. from Zeitschrift der Universitaet Hannover, Mitteilungsblatt der Hannoverschen Hochschulgemeinschaft, v. 19, no. 1, 1992 p 2-48 In GERMAN (ETN-92-91730)
Avail: Universitaet Hannover,
Universitaetsbibliothek und TIB, Welfengarten 1B, 3000 Hanover 1, Fed. Republic of Germany

The development of the current vegetal landscape in north west Germany from a deciduous forest is described with consideration of geographical, geological, and human influence. The following topics were studied: holocene and post glacial vegetation development; emergence of the beech forests; human settlement origins; neolithic acquisition of land and its effects on environment; agriculture at the bronze and iron ages; Middle Age clearings and modern forest transformations, cultivation of hardwood, and needle wood forests; potential natural forest vegetation and the current forest economy; underwood and open forest economy as extensive forest exploitation; the moor peasantry as landscape and vegetation shape factor; forest and cultivation systems in the low mountain regions; and the current cultivated landscape from an ecological point of view and the evaluation of anthropogenous vegetation and landscape changes. ESA

N92-31139# Coastal Environments, Inc., Baton Rouge, LA.
REMOTE-SENSING SURVEY OF THE ATCHAFALAYA BASIN MAIN CHANNEL, ATCHAFALAYA CHANNEL TRAINING PROJECT, SAINTS MARTIN AND MARY PARISHES, LOUISIANA Final Report
Charles E. Pearson and Allen R. Saltus, Jr. Nov. 1991 118 p (Contract DACW29-88-D-0122)
(AD-A249915; COELMN/PD-90/11) Avail: CASI HC A06/MF A02

A remote sensing survey was conducted at several study areas along the lower Atchafalaya Basin Main Channel and in Bayou Shaffer. Diving and test excavations were conducted on a small number of selected targets. No significant cultural remains were found along the Atchafalaya Basin Main Channel, but a number of partial and complete watercraft were found in Bayou Shaffer. Some of these watercraft represent potentially significant cultural resources. Recommendations for the treatment of vessel remains found in Bayou Shaffer are provided. GRA

N92-31179# Naval Polar Oceanography Center, Washington, DC.
ANTARCTIC ICE CHARTS, 1989 - 1990: ANALYSIS ATLAS Annual Report, Jan. 1989 - Dec. 1990
1992 210 p
(AD-A249730) Avail: CASI HC A10/MF A03

Compilation of the weekly sea ice analyses produced by the Navy/NOAA Joint Ice Center is presented. The Antarctica Ice Charts are produced bi-annually every even numbered year (ie. 1990, 1992 etc.) by June or July. GRA

N92-31028*# Lund Inst. of Tech. (Sweden). Dept. of Physics.
FLUORESCENCE LIDAR MULTI-COLOR IMAGING OF VEGETATION
J. Johansson, E. Wallinder, H. Edner, and S. Svanberg *In* NASA. Langley Research Center, 16th International Laser Radar Conference, Part 2 Jul. 1992 p 433-436 Sponsored in part by Swedish Natural Science Research Council; and the Swedish

Space Board (For primary document see N92-31013 21-35)
Avail: CASI HC A01/MF A03

44 ENERGY PRODUCTION AND CONVERSION

Includes specific energy conversion systems, e.g., fuel cells; global sources of energy; geophysical conversion; and windpower.

For related information see also *07 Aircraft Propulsion and Power, 20 Spacecraft Propulsion and Power,* and *28 Propellants and Fuels.*

N92-30330# Midwest Research Inst., Golden, CO.
DESIGN AND SIMULATION OF LATENT HEAT STORAGE UNITS
N. Shamsundar (Houston Univ., TX.), E. Stein (Houston Univ., TX.), E. Rooz (Houston Univ., TX.), E. Bascaran (Houston Univ., TX.), and T. C. Lee (Houston Univ., TX.) Apr. 1992 64 p
(Contract DE-AC02-83CH-10093)
(DE91-002145; NREL/TP-253-4280) Avail: CASI HC A04/MF A01

This report presents the results of two years of research and development on passive latent heat storage systems. Analytical models have been developed and extended, and a computer code for simulating the performance of a latent heat storage has been developed. The code is intended to be merged into a larger solar energy system simulation code and used for making realistic system studies. Simulation studies using a code which has a flexible and accurate routine for handling the storage subsystem should lead to the development of better systems than those in which storage is added on after the rest of the system has already been selected and optimized. DOE

N92-30426*# National Aeronautics and Space Administration. Lewis Research Center, Cleveland, OH.
HIGH EFFICIENCY THERMAL TO ELECTRIC ENERGY CONVERSION USING SELECTIVE EMITTERS AND SPECTRALLY TUNED SOLAR CELLS
Donald L. Chubb, Dennis J. Flood, and Roland A. Lowe (Cleveland State Univ., OH.) Aug. 1992 12 p Proposed for presentation at the Nuclear Technologies for Space Exploration Conference, Jackson Hole, WY, 16-19 Aug. 1992; sponsored by ANS
(RTOP 506-41-11)
(NASA-TM-105755; E-7166; NAS 1.15:105755) Avail: CASI HC A03/MF A01

Thermophotovoltaic (TPV) systems are attractive possibilities for direct thermal-to-electric energy conversion, but have typically required the use of black body radiators operating at high temperatures. Recent advances in both the understanding and performance of solid rare-earth oxide selective emitters make possible the use of TPV at temperatures as low as 1500 K. Depending on the nature of parasitic losses, overall thermal-to-electric conversion efficiencies greater than 20 percent are feasible. Author

N92-30519# Midwest Research Inst., Golden, CO.
PERSPECTIVE ON PHOTOVOLTAIC AMORPHOUS SILICON
W. Luft, B. Stafford, and B. vonRoedern May 1992 9 p Presented at the 11th Review Meeting of the National Renewable Energy Laboratories: Photovoltaic Advanced Research and Development, Lakewood, CO, 13-15 May 1992
(Contract DE-AC02-83CH-10093)
(DE92-010581; NREL/TP-412-4796; CONF-9205115-2) Avail: CASI HC A02/MF A01

Amorphous silicon is a thin film option that has the potential for a cost-effective product for large-scale utility photovoltaics application. The initial efficiencies for single-junction and multijunction amorphous silicon cells and modules have increased significantly over the past 10 years. The emphasis of research and development has changed to stabilized efficiency, especially that of multijunction modules. NREL has measured 6.3 percent to 7.2 percent stabilized amorphous silicon module efficiencies for U.S. products, and 8.1 percent stable efficiencies have been reported by Fuji Electric. This represents a significant increase over the stabilized efficiencies of modules manufactured only a few years ago. An increasing portion of the amorphous silicon U.S. Government funding is now for manufacturing technology development to reduce cost. The funding for amorphous silicon for photovoltaics by Japan over the last 5 years has been about 50 percent greater than that in the United States, and by Germany in the last 2 to 3 years, more than twice that of the U.S. Amorphous silicon is the only thin-film technology that is selling large-area commercial modules. The cost for amorphous silicon modules is now in the $4.50 range; it is a strong function of plant production capacity and is expected to be reduced to $1.00 to $1.50/W(sub p) for plants with 10 MW/year capacities. DOE

N92-30694# Syracuse Univ., NY. Dept. of Chemistry.
PHOTOCHEMICAL SOLAR ENERGY CONVERSION UTILIZING SEMICONDUCTORS LOCALIZED IN MEMBRANE-MIMETIC SYSTEMS
J. H. Fendler 31 Aug. 1991 15 p
(Contract DE-FG02-86ER-13506)
(DE92-011115; DOE/ER-13506/37) Avail: CASI HC A03/MF A01

Extending the frontiers of colloidal photochemistry and colloidal electrochemistry to solar photochemistry research was the original objective of this research. More recent objectives of this proposal include the examination of semiconductor-particle mediated photoelectron transfer and photoelectric effects in different membrane mimetic systems. Emphasis was placed on developing bilayer lipid membranes and Langmuir-Blodgett films as new membrane-mimetic systems, as well as on the characterization and utilization of these systems. DOE

N92-30808# Sandia National Labs., Albuquerque, NM.
THE STATUS OF RENEWABLE ENERGY TECHNOLOGY
D. G. Schueler 1992 11 p Presented at the Annual Meeting of the Air and Waste Management Association (AWMA), Kansas City, MO, 21-26 Jun. 1992
(Contract DE-AC04-76DP-00789)
(DE92-011386; SAND-92-0523C; CONF-9206114-5) Avail: CASI HC A03/MF A01

Renewable energy technologies convert naturally occurring phenomena into useful energy forms. These technologies use resources that generally are not depleted, such as the direct energy (heat and light) from the sun and the indirect results of its impact on the earth (wind, falling water, heating effects, plant growth), gravitational forces (the tides), and the heat of the Earth's core (geothermal), as the sources from which they produce useful energy. These very large stores of natural energy represent a resource potential that is incredibly massive, and dwarfs that of equivalent fossil energy resources. The magnitude of these resources is, therefore, not a key constraint on energy production. However, they are generally diffuse and not fully accessible, some are intermittent, and all have distinct regional and local variability. It is these aspects of their character that give rise to difficult, but generally solvable, technical, institutional, and economic challenges inherent in development and use of renewable energy resources. This report discusses the technologies and their associated energy source. DOE

N92-30837# Midwest Research Inst., Golden, CO.
YAW DYNAMICS OF HORIZONTAL AXIS WIND TURBINES
A. C. Hansen (Utah Univ., Salt Lake City.) May 1992 175 p
(Contract DE-AC02-83CH-10093)
(DE92-001245; NREL/TP-442-4822) Avail: CASI HC A08/MF A02

Designers of a horizontal axis wind turbine yaw mechanism are faced with a difficult decision. They know that if they elect to use a yaw-controlled rotor then the system will suffer increased initial cost and increased inherent maintenance and reliability problems. On the other hand, if they elect to allow the rotor to freely yaw they know they will have to account for unknown and

random, though bounded, yaw rates. They will have a higher-risk design to trade-off against the potential for cost savings and reliability improvement. The risk of a yaw-free system could be minimized if methods were available for analyzing and understanding yaw behavior. The complexity of yaw behavior has, until recently, discouraged engineers from developing a complete yaw analysis method. The objectives of this work are to (1) provide a fundamental understanding of free-yaw mechanics and the design concepts most effective at eliminating yaw problems, and (2) provide tested design tools and guidelines for use by free-yaw wind systems manufacturers. The emphasis is on developing practical and sufficiently accurate design methods. DOE

N92-30896# Midwest Research Inst., Golden, CO. National Renewable Energy Lab.
UNIFORM FLUX DISH CONCENTRATORS FOR PHOTOVOLTAIC APPLICATION
G. Jorgensen and T. Wendelin May 1992 5 p Presented at the National Solar Energy Conference, Cocoa Beach, FL, 13-18 Jun. 1992
(Contract DE-AC02-83CH-10093)
(DE92-010566; NREL/TP-441-4800; CONF-920678-4) Avail: CASI HC A01/MF A01

Researchers at the National Renewable Energy Laboratory (NREL) have designed a unique and innovative molded dish concentrator capable of producing a uniform flux profile on a flat target plane. Concentration levels of 100-200 suns, which are uniform over an area of several square inches, can be directly achieved for collection apertures of a reasonable size (approximately 1.5 m diameter). Such performance would be immediately applicable to photovoltaic (PV) use. Economic concerns have shown that the proposed approach would be less expensive than Fresnel lens concepts or other dish concentrator designs that require complicated and costly receivers to mix the flux to obtain a uniform distribution. DOE

N92-30949*# Miami Univ., Oxford, OH.
Ni-H2 CELL SEPARATOR MATRIX ENGINEERING Final Report
W. E. Scott 22 Feb. 1992 72 p
(Grant NAG3-1053)
(NASA-CR-190055; NAS 1.26:190055) Avail: CASI HC A04/MF A01

This project was initiated to develop alternative separator materials to the previously used asbestos matrices which were removed from the market for health and environmental reasons. The objective of the research was to find a material or combination of materials that had the following characteristics: (1) resistant to the severe conditions encountered in Ni-H2 cells; (2) satisfactory electrical, electrolyte management, and thermal management properties to function properly; (3) environmentally benign; and (4) capable of being manufactured into a separator matrix. During the course of the research it was discovered that separators prepared from wettable polyethylene fibers along and in combination with potassium titanate pigment performed satisfactory in preliminary characterization tests. Further studies lead to the optimization of the separator composition and manufacturing process. Single ply separator sheets were manufactured with 100 percent polyethylene fibers and also with a combination of polyethylene fibers and potassium titanate pigment (PKT) in the ratio of 60 percent PKT and 40 percent fibers. A pilot paper machine was used to produce the experimental separator material by a continuous, wet laid process. Both types of matrices were produced at several different area densities (grams/sq m).
Author

N92-30970# Messerschmitt-Boelkow-Blohm G.m.b.H., Munich (Germany, F.R.).
INTRODUCTION TO THE EFFICIENCY OF FUEL CELLS [DER WIRKUNGSGRAD VON BRENNSTOFFZELLEN - EINE EINFUEHRUNG]
F. Nitschke 1991 20 p Repr. from MBB Mitteilungen aus dem Zentrallabor, v. 23, 1991 In GERMAN
(MBB-Z-0412-91-PUB; ETN-92-91899) Avail: CASI HC A03/MF A01

Various types of fuel cells are described. Only gaseous fuels are concerned for fuel cells as stationary power stations. The efficiency of fuel cells is defined, with regard to power stations. The emphasis is put on higher and lower thermal value. Thermal value is related to electrical energy. Waste heat need for high temperature fuel cells is discussed. It is shown that losses for the peripheral system, efficiency of coal gasification and external steam reforming are to be taken into account for the calculation of the general efficiency of a power station. The question of the optimal operating range of a fuel cell power station is raised. The various fuel cell technologies are compared. ESA

N92-31113# Morgantown Technology Center, WV.
RESEARCH ISSUES IN MOLTEN CARBONATE FUEL CELLS: PRESSURIZATION
M. C. Williams and T. J. George 1992 7 p Presented at the 27th Intersociety Energy Conversion Engineering Conference, San Diego, CA, 3-7 Aug. 1992
(DE92-011755; DOE/METC-C/92/7014; CONF-920801-2) Avail: CASI HC A02/MF A01

The issue of pressurization is a complex and controversial one involving many engineering design variables. There are among the molten carbonate fuel cell (MCFC) developers and researchers differences in the relative perceived importance of these variables in the MCFC power plant systems determined to be of interest. These variables significantly affect MCFC system economics and commercial viability. While developing at pressure at this time may not be necessary to commercialize the MCFC, there are potential benefits of operating MCFC's at pressure. The advantages and disadvantages of operating the MCFC at pressure are identified. Potential problems are discussed. The large and small power plant system implications of operating at pressure are qualified. Some recommendations are made. The overall goal is to create interest and motivate research in the area. DOE

N92-31117# Hawaii Univ., Honolulu.
TRACE ELEMENT AND ISOTOPE GEOCHEMISTRY OF GEOTHERMAL FLUIDS, EAST RIFT ZONE, KILAUEA, HAWAII
H. B. West, G. A. Delanoy, D. M. Thomas, D. C. Gerlach (Lawrence Livermore National Lab., CA.), B. Chen, P. Takahashi, and D. M. Thomas 1992 32 p
(Contract DE-FG03-85SF-15799)
(DE92-014586; DOE/SF-15799/T14) Avail: CASI HC A03/MF A01

A research program has been undertaken in an effort to better characterize the composition and the precipitation characteristic of the geothermal fluids produced by the HGP-A geothermal well located on the Kilauea East Rift Zone on the island of Hawaii. The results of these studies have shown that the chemical composition of the fluids changed over the production life of the well and that the fluids produced were the result of the mixing of at least two, and possibly three, source fluids. These source fluids were recognized as a sea water composition modified by high temperature water-rock reactions; meteoric recharge; and a hydrothermal fluid that had been equilibriated with high temperature reservoir rocks and magmatic volatiles. Although the major alkali and halide elements show clearly increasing trends with time, only a few of the trace transition metals show a similar trend. The rare earth elements were typically found at low concentrations and appeared to be highly variable with time. Studies of the precipitation characteristics of silica showed that amorphous silica deposition rates were highly sensitive to fluid pH and that increases in fluid pH above about 8.5 could flocculate more than 80 percent of the suspended colloidal silica in excess of its solubility. Addition of transition metal salts were also found to enhance the recovery fractions of silica from solution. The amorphous silica precipitate was also found to strongly scavenge the alkaline earth and transition metal ions naturally present in the brines; mild acid treatments were shown to be capable of removing substantial fractions of the scavenged metals from the silica flocs, yielding a moderately pure gelatinous by-product. Further work on the silica

precipitation process is recommended to improve our ability to control silica scaling from high temperature geothermal fluids or to recover a marketable silica by-product from these fluids prior to reinjection. DOE

N92-31176# Oak Ridge National Lab., TN.
THERMAL ENERGY STORAGE Technical Progress Report, Apr. 1990 - Mar. 1991
J. J. Tomlinson Mar. 1992 41 p
(Contract DE-AC05-84OR-21400)
(DE92-014942; ORNL/TM-12081) Avail: CASI HC A03/MF A01

The Department of Energy (DOE) is supporting development of thermal energy storage (TES) as a means of efficiently coupling energy supplies to variable heating or cooling demands. Uses of TES include electrical demand-side management in buildings and industry, extending the utilization of renewable energy resources such as solar, and recovery of waste heat from periodic industrial processes. Technical progress to develop TES for specific diurnal and industrial applications under Oak Ridge National Laboratory's TES program from April 1990 to March 1992 is reported and covers research in the areas of low temperature sorption, direct contact ice making, latent heat storage plasterboard and latent/sensible heat regenerator technology development. DOE

N92-31188# Department of Energy, Washington, DC. Office of the Deputy Assistant Secretary for Oil, Gas, Shale and Special Technologies.
FUEL CELL SYSTEMS PROGRAM PLAN: FISCAL YEAR 1992
1992 43 p
(DE92-015985; DOE/FE-0260P) Avail: CASI HC A03/MF A01

The goal of the fuel cell program is to increase energy and economic efficiency through the development and commercialization of fuel cell systems which achieve ultrahigh efficiency for power generation (in the 50 to 60 range percent), and environmental benefits in support of the National Energy Strategy (NES) goals of energy security and respecting the environment. The program objectives are to develop and demonstrate cost effective fuel cell power generation which can be successfully commercialized in the 1990's, while meeting NES goals. DOE

N92-31216*# Spectrolab, Inc., Sylmar, CA.
DEVELOPMENT OF ADVANCED SILICON SOLAR CELLS FOR SPACE STATION FREEDOM Final Report
David R. Lillington 9 Aug. 1990 109 p
(Contract NAS3-24672)
(NASA-CR-189215; NAS 1.26:189215; Rept-240-746) Avail: CASI HC A06/MF A02

This report describes the development of large area high efficiency wrapthrough solar cells for Space Station Freedom. The goal of this contract was the development and fabrication of 8 x 8 cm coplanar back contact solar cells with a minimum output of 1.039 watts/cell. The first task in this program was a modeling study to determine the optimum configuration of the cell and to study the effects of surface passivation, substrate resistivity, and back surface field on the BOL and EOL performance. In addition, the optical stack, including the cell cover, AR coatings, and Kapton blanket, was modeled to optimize 'on orbit' operation. The second phase was a manufacturing development phase to develop high volume manufacturing processes for the reliable production of low recombination velocity boron back surface fields, techniques to produce smooth, low leakage wrapthrough holes, passivation, photoresist application methods, and metallization schemes. The final portion of this program was a pilot production phase. Seven hundred solar cells were delivered in this phase. At the end of the program, cells with average efficiencies over 13 percent were being produced with power output in excess of 1.139 watts/cell, thus substantially exceeding the program goal. Author

N92-31221# Morgantown Technology Center, WV.
FUEL CELLS
D. T. Hooie, B. C. Harrington, III, M. J. Mayfield, and E. L. Parsons Jul. 1992 66 p
(DE92-001282; DOE/METC-92-0276) Avail: CASI HC A04/MF A01

The primary objective of DOE's Fossil Energy Fuel Cell program is to fund the development of key fuel cell technologies in a manner that maximizes private sector participation and in a way that will give contractors the opportunity for a competitive posture, early market entry, and long-term market growth. This summary includes an overview of the Fuel Cell program, an elementary explanation of how fuel cells operate, and a synopsis of the three major fuel cell technologies sponsored by the DOE/Fossil Energy Phosphoric Acid Fuel Cell program, the Molten Carbonate Fuel Cell program, and the Solid Oxide Fuel Cell program. DOE

45 ENVIRONMENT POLLUTION

Includes atmospheric, noise, thermal, and water pollution.

N92-30345# State Univ. of New York, Stony Brook. Dept. of Chemistry.
STUDIES OF ATMOSPHERIC MOLECULES BY MULTIPHOTON SPECTROSCOPY
P. M. Johnson Oct. 1991 24 p
(Contract DE-FG02-86ER-13590)
(DE92-012668; DOE/ER-13590/10) Avail: CASI HC A03/MF A01

Carbon dioxide presents a great challenge to spectroscopy because of its propensity toward dissociation in all of its excited states. Multiphoton ionization spectroscopy is usually not applicable to the study of dissociating molecules because the dissociation competes effectively with ionization, resulting in no signal. We reasoned, however, that with high enough laser fluence, ionization could compete with dissociation in the longer lived states, exposing them for study from the continuous spectral background resulting from rapidly dissociating states. We describe the various spectroscopic and photophysical effects found through the multiphoton ionization and multiphoton photoelectron spectra. A recently developed variant of threshold ionization spectroscopy, usually called ZEKE, has shown a great deal of usefulness in providing the same information as traditional photoelectron spectroscopy but with higher resolution and much better signal-to-noise when using standard laboratory lasers. Threshold ionization techniques locate the states of an ion by scanning a light source across the ionization continuum of a neutral and somehow detecting when electrons are produced with no kinetic energy. We chose to develop our capabilities in threshold ionization spectroscopy using aromatic molecules because of their importance and because their electronic structure allows a pump-probe type of excitation scheme which avoids the use of vacuum ultraviolet laser beams. Among aromatics, the azines are noted for their small S(sub 1)-T(sub 1) energy gap which give them unique and interesting photophysical properties. We have continued our work on the multiphoton spectrum of metastable nitrogen produced by an electric discharge in supersonic beam. We have been able to assign more of the lines and simulated their rotational structure, but many peaks remain unassigned. DOE

N92-30374# Pacific Northwest Lab., Richland, WA.
REDUCING GREENHOUSE GAS EMISSIONS IN CZECHOSLOVAKIA
Marie Kostalova (Ministry of Foreign Affairs, Prague, Czechoslovakia), Jiri Suk (Ceskoslovenska Akademie Ved, Prague.), and Stanislav Kolar Dec. 1991 23 p
(Contract DE-AC06-76RL-01830)
(DE92-012354; PNL-SA-20399) Avail: CASI HC A03/MF A01

In this paper are presented important findings on the potential for energy conservation and carbon emissions reduction over the coming decades in Czechoslovakia. The authors describe the state of the energy use in Czechoslovakia today and the measures required to transform its energy system to a market-based economy oriented towards the environmental goal of decreased energy

intensity. This work furthers our understanding of the need for energy efficiency in the newly forming market economies of Eastern and Central Europe. This paper is part of a series of country studies sponsored by the Global Climate Division of the Office of Policy, Planning, and Evaluation, United States Environmental Protection Agency (EPA). We have completed similar studies in Canada, the former Soviet Union, France, Hungary, Italy, Japan, Poland the United Kingdom, and the United States. Research is currently underway or planned in Bulgaria, Romania, and Ukraine. DOE

N92-30425 Ecological Society of America.
THE SUSTAINABLE BIOSPHERE INITIATIVE: AN ECOLOGICAL RESEARCH AGENDA
Jane Lubchenco, Annette M. Olson, Linda B. Brubaker, Stephen R. Carpenter, Marjorie M. Holland, Stephen P. Hubbell, Simon A. Levin, James A. MacMahon, Pamela A. Matson, and Jerry M. Melillo et al 1991 43 p Repr. from Ecology, v. 72, no. 2, Apr. 1991 p 371-412
Copyright Avail: Issuing Activity

In this document, the Ecological Society of America proposes the Sustainable Biosphere Initiative (SBI), an initiative that focuses on the necessary role of ecological science in the wise management of Earth's resources and the maintenance of Earth's life support systems. This document is intended as a call to arms for all ecologists, but it will also serve as a means to communicate with individuals in other disciplines with whom ecologists must join forces to address a common predicament. This document focuses primarily on the acquisition of ecological knowledge. It identifies the ecological research programs of highest priority and recommends steps required to pursue research objectives. The document also lays the groundwork for improving the communication and application of ecological knowledge. The SBI proposes three research priorities: global change; biological diversity; and sustainable ecological systems. H.A.

N92-30494*# Bionetics Corp., Cocoa Beach, FL.
HABITAT MODEL FOR THE FLORIDA SCRUB JAY ON JOHN F. KENNEDY SPACE CENTER
David R. Breininger 18 Feb. 1992 97 p
(Contracts NAS10-10285; NAS10-11624)
(NASA-TM-107543; NAS 1.15:107543) Avail: CASI HC A05/MF A02

The Florida Scrub Jay is endemic to Florida. The John F. Kennedy Space Center (KSC) provides habitat for one of the three largest populations of the Florida Scrub Jay. This threatened bird occupies scrub, slash pine flatwoods, disturbed scrub, and coastal strand on KSC. Densities of Florida Scrub Jays were shown to vary with habitat characteristics but not necessarily with vegetation type. Relationships between Florida Scrub Jay densities and habitat characteristics were used to develop a habitat model to provide a tool to compare alternative sites for new facilities and to quantify environmental impacts. This model is being tested using long term demographic studies of colorbanded Florida Scrub Jays. Optimal habitat predicted by the model has greater than or equal to 50 percent of the shrub canopy comprised of scrub oaks, 20-50 percent open space or scrub oak vegetation within 100 m of a ruderal edge, less than or equal to 15 percent pine canopy cover, a shrub height of 120-170 cm, and is greater than or equal to 100 m from a forest. This document reviews life history, social behavior, food, foraging habitat, cover requirements, characteristics of habitat on KSC, and habitat preferences of the Florida Scrub Jay. Construction of the model and its limitations are discussed. Author

N92-30520# Los Alamos National Lab., NM.
DEVELOPMENT AND TESTING OF AN AIR QUALITY MODEL FOR MEXICO CITY
M. D. Williams, G. Streit, X. Cruz, M. Ruiz, G. Sosa, A. G. Russell, and L. A. McNair 2 Mar. 1992 15 p Presented at the 9th World Clean Air Congress and Exhibition: Towards the Year 2000 - Critical Issues in the Global Environment, Montreal, Ottawa, 30 Aug. - 4 Sep. 1992
(Contract W-7405-eng-36)
(DE92-011238; LA-UR-92-808; CONF-920814-1) Avail: CASI HC A03/MF A01

Los Alamos National Laboratory and Instituto Mexicano del Petroleo have embarked on a joint study of options for improving air quality in Mexico City. The intent is to develop a modeling system which can address the behavior of pollutants in the region so that option for improving Mexico City air quality can be properly evaluated. In February of 1991, the project conducted a field program which yielded a variety of data which is being used to evaluate and improve the models. Normally the worst air quality for both primary and photochemical pollutants occurs in the winter Mexico City. During the field program, measurements included: (1) lidar measurements of aerosol transport and dispersion, (2) aircraft measurements of winds, turbulence, and chemical species aloft, (3) aircraft measurements of earth surface skin temperatures, and (4) tethersonde measurements of wind, temperature and ozone vertical profiles. A three-dimensional, prognostic, higher order turbulence meteorological model (HOTMAC) was modified to include an urban canopy and urban heat sources. HOTMAC is used to drive a Monte-Carlo kernel dispersion code (RAPTAD). HOTMAC also provides winds and mixing heights for the CIT photochemical model which was developed by investigators at the California Institute of Technology and Carnegie Mellon University. DOE

N92-30561# Environmental Protection Agency, Research Triangle Park, NC. Office of Air Quality Planning and Standards.
STATUS OF SELECTED AIR POLLUTION CONTROL PROGRAMS, FEBRUARY 1992
Feb. 1992 179 p
(PB92-171966; EPA/450/2-91/009) Avail: CASI HC A09/MF A02

The collection of status reports was prepared in order to provide a timely summary of selected EPA air pollution control activities to those individuals who are involved with the implementation of these programs. Given here are ozone/carbon monoxide (CO) programs; mobile sources programs; particulate matter nominally 10M and less (PM-10), sulfur dioxide (SO2), and lead programs; New Source Review (NSR); economic programs; emission standards programs; Indian activity programs; mobile sources programs; air toxics programs; acid rain programs; permits programs; chlorofluorocarbons programs; and enforcement programs. Author

N92-30563# National Oceanic and Atmospheric Administration, Washington, DC.
NATIONAL OCEAN POLLUTION PROGRAM: SUMMARY OF FEDERAL PROGRAMS AND PROJECTS: FY 1989 UPDATE
Sep. 1991 339 p
(PB92-187012) Avail: CASI HC A15/MF A03

Information is given on Federal ocean pollution programs. Agency missions and mandates, Federal personnel and facilities, and program descriptions and funding levels are discussed. Author

N92-30602# Environmental Protection Agency, Research Triangle Park, NC. Atmospheric Research and Exposure Assessment Lab.
REPORT OF THE GREAT LAKES AIR TOXICS RESEARCH PRIORITIES WORKSHOP
L. Cupitt, J. Ching, and J. Baker Apr. 1992 49 p
(PB92-166933; EPA/600/R-92/029) Avail: CASI HC A03/MF A01

A three day workshop sponsored by the Environmental Protection Agency (EPA) was held at the University of Minnesota in March, 1991. Nearly 40 scientists and environmental managers from both the U.S. and Canada representing a broad variety of disciplines participated. The objective of the workshop was to discuss the research program required to identify and assess the extent of atmospheric deposition of hazardous air pollutants to the Great Lakes in accordance with Annex 15 of the Great Lakes Water Quality Agreement (1987) and with the Clean Air Amendment

of 1990. The report represents a consensus and prioritization of the research required to meet that objective by the workshop attendees. GRA

N92-30647# Lawrence Livermore National Lab., CA.
TOWARDS THE DEVELOPMENT OF A GLOBAL INVENTORY FOR BLACK CARBON EMISSIONS
J. E. Penner, H. Eddleman, and T. Novakov (California Univ., Berkeley. Lawrence Berkeley Lab.) Mar. 1992 44 p Presented at the 4th International Conference on Carbonaceous Particles in the Atmosphere, Vienna, Austria, 3-5 Apr. 1991
(Contracts W-7405-eng-48; DE-AC03-76SF-00098)
(DE92-013514; UCRL-JC-108523-Rev-1; CONF-9104368-1-Rev-1)
Avail: CASI HC A03/MF A01

We have developed two global inventories for black carbon (BC) emissions using two distinct methods. The first method uses measured ambient concentration ratios of BC and SO2 at locations throughout the world. We demonstrate that BC to SO2 ratios are well correlated at most sites and that distinct ratios of BC to SO2 apply to source areas from economically distinct regions. However, within any one economic region, the ratio of BC to SO2 appears to be relatively constant. These facts are used to construct a global inventory of BC emissions by using previously published inventories for the emissions of sulfur. The derived inventory totals nearly 24 Tg C yr(exp -1). The second method uses estimated emission factors and published fuel production and use statistics for wood and bagasse burning, diesel fuel, and domestic and commercial coal use. The combined global emissions using the second method total 12.6 Tg C yr(exp -1). A comparison of the two inventories shows that the estimated emissions from the ratio method are within a factor of two of those derived from emission factors in regions where the data appear to be reliable. The BC inventory from the ratio method is used in the Lawrence Livermore National Laboratory global chemistry/climate model to simulate the world-wide distribution of BC. The predicted concentrations are compared with available measurements from throughout the world. This comparison also supports the magnitude of the inventory which we derived from the ratio method to within about a factor of two. DOE

N92-30707# Desert Research Inst., Reno, NV. Desert Research Inst.
LINKAGE OF ANTHROPOGENIC AEROSOL TO CLOUDS AND CLIMATE
J. G. Hudson 28 Jan. 1992 11 p
(Contract DE-FG08-90ER-61012)
(DE92-013574; DOE/ER-61012/2) Avail: CASI HC A03/MF A01

This progress report describes the monitoring being done to validate a linkage of anthropogenic aerosol to clouds and climate. Equipment and findings are reported. The equipment construction called for in the original proposal was completed. These instruments are the high temperature processor, the data acquisition system for the direct Royco optical particle counter (OPC), and modifications to the formvar replicator. The main field effort during the past year was the shipboard experiment SEAHUNT (Shiptrail Evolution Above High Updraft Naval Targets). There were also some laboratory and local ambient particle measurements and a surface field program on and near the California coast. The shipboard project was not anticipated in the original proposal but the laboratory and surface measurements were along the lines suggested in the original proposal. DOE

N92-30770# Argonne National Lab., IL. Energy Systems Div.
EMISSIONS OF GREENHOUSE GASES FROM THE USE OF TRANSPORTATION FUELS AND ELECTRICITY
M. A. DeLuchi (California Univ., Davis.) Nov. 1991 142 p
(Contract W-31109-eng-38)
(DE92-012102; ANL/ESD/TM-22-Vol-1) Avail: CASI HC A07/MF A02

This report presents estimates of full fuel-cycle emissions of greenhouse gases from using transportation fuels and electricity. The data cover emissions of carbon dioxide (CO2), methane, carbon monoxide, nitrous oxide, nitrogen oxides, and nonmethane organic compounds resulting from the end use of fuels, compression or liquefaction of gaseous transportation fuels, fuel distribution, fuel production, feedstock transport, feedstock recovery, manufacture of motor vehicles, maintenance of transportation systems, manufacture of materials used in major energy facilities, and changes in land use that result from using biomass-derived fuels. The results for electricity use are in grams of CO2-equivalent emissions per kilowatt-hour of electricity delivered to end users and cover generating plants powered by coal, oil, natural gas, methanol, biomass, and nuclear energy. The transportation analysis compares CO2-equivalent emissions, in grams per mile, from base-case gasoline and diesel fuel cycles with emissions from these alternative-fuel cycles: methanol from coal, natural gas, or wood; compressed or liquefied natural gas; synthetic natural gas from wood; ethanol from corn or wood; liquefied petroleum gas from oil or natural gas; hydrogen from nuclear or solar power; electricity from coal, uranium, oil, natural gas, biomass, or solar energy, used in battery-powered electric vehicles; and hydrogen and methanol used in fuel-cell vehicles. DOE

N92-31121# Lawrence Livermore National Lab., CA.
THE ENVIRONMENTAL DILEMMA OF FOSSIL FUELS
M. C. MacCracken Apr. 1992 11 p Presented at the 6th International Conference on Emerging Nuclear Energy Systems, Monterey, CA, 16-21 Jun. 1991
(Contract W-7405-eng-48)
(DE92-014887; UCRL-JC-106406; CONF-910626-16) Avail: CASI HC A03/MF A01

The increasing atmospheric concentration of carbon dioxide poses an environmental dilemma for fossil fuel energy generation that, unlike other related emissions, cannot be resolved by control technologies alone. Although fossil fuels presently provide the most cost-effective global energy source, and model projections suggest that their use is initiating climatic changes which, while quite uncertain, may induce significant, counter-balancing impacts to water resources, coastal resources, ecological systems, and possibly agricultural production. The climate models indicate that the warming should have begun, and there is some evidence for this occurring, but at a less rapid and more uneven rate than projected. In addition, different climate models are not yet in agreement in their latitudinal or regional predictions, and it will likely require a decade or more for such agreement to develop as high performance computers become available for addressing this 'grand challenge' problem. Thus, in addition to the prospect for climatic change, the uncertainties of the changes and associated impacts contribute to the dilemma of dealing with the issue. Further, the problem is pervasive and international in scope, with different countries and peoples having differing perspectives of technology, development, and environmental responsibility. Dealing with this issue will thus require creativity, commitment, and flexibility. DOE

N92-31153*# Virginia Univ., Charlottesville. Dept. of Environmental Sciences.
TRACE GAS AND AEROSOL TRANSPORTS INTO AND OUT OF THE AMAZON BASIN Semiannual Report, 1 Sep. 1991 - 31 May 1992
Michael Garstang Jul. 1992 165 p
(Contract NCC1-106)
(NASA-CR-190624; NAS 1.26:190624) Avail: CASI HC A08/MF A02

Research under Agreement NCC1-106 during the interim period Oct. 1, 1991 to May 31, 1992 has continued to use the data collected during all three ABLE missions. The work reported on in this interim period includes published papers that cover the topic of global interactions between the rain forest of the Amazon Basin and local regional processes interior to the Basin itself. Author

N92-31181# Department of Energy, Washington, DC.
CHEMISTRY FOR PROTECTION OF THE ENVIRONMENT, 8TH INTERNATIONAL CONFERENCE PROCEEDINGS

W. J. Lacy, ed. 1991 635 p Conference on Chemistry for Protection of the Environment held in Lublin, Poland, 16-18 Sep. 1991
(DE92-014317; CONF-9109358) Avail: CASI HC A99/MF A05

This report presents research programs from the International Conference on the Chemistry for Protection of the Environment. Topics covered include environmental transport, waste minimization, pollution control and prevention, waste management, soil remediation, and health concerns associated with environmental contamination. Individual projects are processed separately for the data bases. DOE

N92-31183# Minnesota Univ., Minneapolis. Dept. of Mechanical Engineering.
ULTRAFINE AEROSOL SIZE DISTRIBUTIONS AND SULFURIC ACID VAPOR PRESSURES: IMPLICATIONS FOR NEW PARTICLE FORMATION IN THE ATMOSPHERE
P. H. McMurry 1992 5 p
(Contract DE-FG02-91ER-61205)
(DE92-015217; DOE/ER-61205/1) Avail: CASI HC A01/MF A01

This project has two components with different but related objectives. One component deals with measurement of H2SO4 vapor pressures in air under temperature and relative humidity conditions similar to those found in the atmosphere. The second deals with measurement of ultrafine aerosol size distributions. Substantial progress has been made on each of these projects. DOE

N92-31046*# Colorado State Univ., Fort Collins. Dept. of Physics.
MEASUREMENT OF AEROSOL PROFILES USING HIGH-SPECTRAL-RESOLUTION RAYLEIGH-MIE LIDAR
D. A. Krueger, R. J. Alvarez, II, L. M. Caldwell, and C. Y. She *In* NASA. Langley Research Center, 16th International Laser Radar Conference, Part 2 Jul. 1992 p 505-508 (For primary document see N92-31013 21-35)
Avail: CASI HC A01/MF A03

N92-31080*# Academia Sinica, Beijing (China). Inst. of Atmospheric Physics.
A CONSIDERABLE EFFECT OF STRATOSPHERIC AEROSOL ON LIDAR-DETECTED OZONE PROFILE AND A THREE-WAVELENGTH INVERSION TECHNIQUE FOR BOTH OZONE AND AEROSOL
Jinhuan Qiu *In* NASA. Langley Research Center, 16th International Laser Radar Conference, Part 2 Jul. 1992 p 633-636 (For primary document see N92-31013 21-35)
Avail: CASI HC A01/MF A03

N92-31085*# Academy of Sciences (USSR), Tomsk. Inst. of Atmospheric Optics.
LIDAR SOUNDING OF OZONE AND AEROSOLS
V. E. Zuev *In* NASA. Langley Research Center, 16th International Laser Radar Conference, Part 2 Jul. 1992 p 649 (For primary document see N92-31013 21-35)
Avail: CASI HC A01/MF A03

N92-31101*# SRI International Corp., Menlo Park, CA. Geoscience and Engineering Center.
AIRBORNE LIDAR MAPPING OF VERTICAL OZONE DISTRIBUTIONS IN SUPPORT OF THE 1990 CLEAN AIR ACT AMENDMENTS
Edward E. Uthe, Norman B. Nielsen, and John M. Livingston *In* NASA. Langley Research Center, 16th International Laser Radar Conference, Part 2 Jul. 1992 p 707-710 Sponsored in part by the Lake Michigan Air Directors Consortium (For primary document see N92-31013 21-35)
Avail: CASI HC A01/MF A03

N92-31102*# National Physical Lab., Teddington (England).
MEASUREMENTS OF FUGITIVE HYDROCARBON EMISSIONS WITH A TUNABLE INFRARED DIAL
M. J. T. Milton, P. T. Woods, B. W. Jolliffe, N. R. W. Swann, and R. A. Robinson *In* NASA. Langley Research Center, 16th International Laser Radar Conference, Part 2 Jul. 1992 p 711-713 (For primary document see N92-31013 21-35)
Avail: CASI HC A01/MF A03

N92-31105*# National Defence Research Establishment, Linkoeping (Sweden). Dept. of Information Technology.
AEROSOL EXTINCTION MEASUREMENTS WITH CO2-LIDAR
Arne Hagard and Rolf Persson *In* NASA. Langley Research Center, 16th International Laser Radar Conference, Part 2 Jul. 1992 p 723-725 (For primary document see N92-31013 21-35)
Avail: CASI HC A01/MF A03

46 GEOPHYSICS

Includes aeronomy; upper and lower atmosphere studies; ionospheric and magnetospheric physics; and geomagnetism.

For space radiation see *93 Space Radiation.*

N92-30417# Danish Meteorological Inst., Copenhagen. Godhavn Geophysical Observatory.
DATA REPORT, 92-2. MAGNETIC RESULTS, 1985-1990
1992 89 p
(ISSN-0907-1695) Avail: CASI HC A05/MF A01

This report presents the results of the geomagnetic measurements carried out at the Godhaven Geophysical Observatory during the years 1985 to 1990. The first section of the report gives coordinates for the observatory and describes the instrumentation and methods of data reduction and distribution. The second part of the report contains tables of monthly and annual mean values and plots of the secular variation for the different magnetic elements. H.A.

N92-30525# UTD, Inc., Newington, VA.
INVESTIGATION OF THE INTERFACE PHENOMENA DUE TO INTERACTION OF HIGH INTENSITY STRESS WAVES WITH GEOLOGIC BOUNDARIES Final Report, 1 Nov. 1990 - 30 Nov. 1991
Ali Amini and Steven I. Majtenyi 30 Nov. 1991 35 p
(Contract F49620-91-C-0008)
(AD-A248992; OSR-9008; AFOSR-92-0235TR) Avail: CASI HC A03/MF A01

During the reporting period a stress-strain relationship was derived for the study of the interface phenomena when a high intensity stress wave impinges on a geologic boundary. The derived relationship was based on the ultimate density concept, i.e., the density of the material increases non-linearly with increasing stresses approaching a limiting value before a polymorphic phase transformation occurs. The derived stress-strain relationship was compared with high pressure data for three rock types. Based on this comparison it was determined that the derived stress-strain relationship modeled material behavior accurately with realistic physical parameters. The relationship was then used in the solution of second order non-linear Partial Differential Equations (PDE) of motion. The method of similarity was used to transform the non-linear PDE to an Ordinary Differential Equation (ODE). The ODE was then solved by standard techniques. The result was a closed form equation for particle displacement profiles in space and time domains including particle velocity acceleration and stress profiles. These profiles will be used in upcoming tasks to determine the role of various parameters in the generation of new waves at interfaces with mediums of finite thickness and the response at interfaces which can be described by a half-space. GRA

N92-30556# Southampton Univ. (England). Dept. of Chemistry.
CHEMIELECTRON AND PHOTOELECTRON SPECTROSCOPIC STUDIES OF IMPORTANCE IN THE UPPER ATMOSPHERE Final Report, 1 Mar. 1989 - 31 Dec. 1991
J. M. Dyke Feb. 1992 9 p

(Grant AF-AFOSR-0351-89)
(AD-A248838; AFOSR-92-0255TR) Avail: CASI HC A02/MF A01

Chemielectron spectroscopy has been used to study the associative and rearrangement ionization reactions of a number of metals with O, O2(X(sup 3) summation(exp -)g) and O2(a(exp 1) delta(sub g)) and other atmospheric species. The spectra obtained have been used to identify the main chemi-ionization channel and to obtain details of the potential surfaces of the reactants and products. Mass spectra, recorded as a function of extraction potential, have also been used to identify primary ions associated with chemi-ionization reactions. The chemi-ionization reactions of oxygen atoms with a number of hydrocarbons have also been studied by chemielectron spectroscopy. Photoelectron spectroscopy has also been used to study in the gas phase the electronic structure of a number of metals and metal oxides which are of importance in the upper atmosphere. Multiphoton spectroscopic studies have also been performed on a number of reactive intermediates. GRA

N92-30708# National Science Foundation, Washington, DC. Div. of Polar Programs.
THE UNITED STATES ANTARCTIC PROGRAM
Vicky Cullen, ed. [1990] 30 p LIMITED REPRODUCIBILITY: More than 20 percent of this document may be affected by color photographs Original contains color illustrations
(NSF-90-97) Avail: CASI HC A03/MF A01; 30 functional color pages

The capabilities, research program, and accomplishments of the U.S. Antarctic Program are discussed. Research in the areas of biology, aeronomy and astrophysics, glaciology, Earth sciences, and ocean and climate systems is reviewed. U.S. research stations and camps are described as well as efforts in the area of environmental preservation. Author

N92-30720# Boston Univ., MA. Center for Space Physics.
MAGNETOSPHERIC STRUCTURE AND DYNAMICS: A MULTISATELLITE APPROACH
W. J. Hughes 9 Apr. 1992 15 p
(Contract F19628-90-K-0003)
(AD-A252326; PL-TR-92-2099; SR-2) Avail: CASI HC A03/MF A01

This report focuses on four areas of scientific investigation in which significant progress has been made during the second year of the contract: electrostatic electron cyclotron harmonic emissions observed by CRRES; the implications of cross tail plasma gradients on the structure of auroral zone; ULF waves excited by storm sudden commencements; and probing flux tube plasma content and distribution using the observed frequencies of field line resonances. Each of these topics is made the subject of one section of this report and has or will result in publication of a scientific paper. Here we summarize the main scientific results and refer the reader to one or more of the publications arising out of our research for fuller details. A complete list of publications arising out of this research is contained in the last section of this report. GRA

N92-30756*# Ohio State Univ., Columbus. Dept. of Geodetic Science and Surveying.
ALTIMETER AND GRAVITY DATA ANALYSIS Final Technical Report, 30 Jun. 1986 - 29 Feb. 1992
Richard H. Rapp Mar. 1992 6 p
(Grant NAG5-781; RF Proj. 765353/718266)
(NASA-CR-190478; NAS 1.26:190478) Avail: CASI HC A02/MF A01

The studies carried out under this grant fell into two broad areas. The first area was the analysis of surface gravity data with the ultimate goal of providing normal equations that could be used in combination with normal equations from the analysis of satellite orbit perturbations to obtain an optimal estimate of the gravitational potential coefficients of the Earth. The second main research activity was the estimation of gravity anomalies in ocean areas from satellite altimeter data. Such anomalies could enable the improved calibration of potential coefficient models derived solely from the analysis of orbital perturbation information. The studies in these two areas are discussed. Author

N92-30868# Air Force Inst. of Tech., Wright-Patterson AFB, OH.
THE CALCULATION OF MID-LATITUDE MERIDIONAL NEUTRAL WINDS FROM AN IMPROVED SERVO MODEL APPROXIMATION METHOD M.S. Thesis
Theodore R. Ballard 1991 139 p
(AD-A249874; AFIT/CI/CIA-91-121) Avail: CASI HC A07/MF A02

A theoretical servo model provided the impetus for a physically more practical version of servo model: the USU servo model. The USU servo model was developed to automatically calculate, with a personal computer, meridional neutral wind of the upper thermosphere for any mid-latitude location from F2-peak layer heights. F2-peak layer heights were input into the USU servo model from three different sources for calculation of meridional neutral winds. The International Reference Ionosphere provided mid-latitude, geomagnetically quiet, monthly averages of F2-layer heights for different solar cycle conditions. The International Reference Ionosphere also provided a means of comparison with ionosonde F2-peak layer height deduced winds. F2-layer heights from different mid-latitude ionosondes were determined by using scaled ionosonde critical frequencies. Millstone Hill incoherent scatter radar provided a means to compare the USU servo model with other neutral wind calculation techniques, including radar-derived winds. Results of this investigation indicate that the USU servo model is a valuable tool in the calculation of mid-latitude meridional neutral winds and compare well with radar-deduced wind data during quiet to moderate geomagnetic activity. GRA

N92-30961*# Lamont-Doherty Geological Observatory, Palisades, NY.
INTER- AND INTRA-PLATE DEFORMATION AT NORTH AMERICAN PLATE BOUNDARIES Final Report, 1 Jul. 1986 - 31 Dec. 1991
John Beavan, Lewis E. Gilbert, and Chris Scholz 20 Jul. 1992 18 p
(Grant NAG5-799)
(NASA-CR-190485; NAS 1.26:190485) Avail: CASI HC A03/MF A01

A geodetic network which spans the region between San Francisco and Lake Tahoe has been measured 5 times completely with triangulation in 1880, 1922, 1929, 1943, 1963. A resurvey with the Global Positioning System (GPS) in 1991 allows the formation of 1 coseismic and 4 interseismic epochs. The data from this network provide a unique opportunity to examine the temporal and spatial evolution of the strain field associated with the 1906 San Francisco earthquake in particular and with the Pacific-North American plate boundary in general. Calculations of strain rate from the network data lead to the following conclusions. (1) There is no resolvable (greater than 0.05 microradians/yr) strain in between Sutter Buttes and the Sierra Nevada. (2) Throughout the time since the 1906 earthquake, a region extending at least as far east as the westernmost Great Valley has been undergoing deformation related to Pac:Nam interaction and the associated earthquake cycle. (3) In the time and space of overlap, our results agree with those from the United States Geological Survey (USGS) trilateration data. Both data sets indicate that strain must be accumulating to the east of Vaca. (4) The San Andreas discrepancy cannot be accommodated in the Great Valley at the 1 sigma level of our results. It is possible to absorb it in that region at the 2 sigma level. (5) Strain rate is elevated in the years following the earthquake and decays slowly with time. It is possible that the rate in the Coast Ranges increases until around 1950 and then decays. With the exception of one epoch, strain rate in the Coast Ranges is consistently fault parallel, shows no sign changes, and is consistent with monotonic strain accumulation. Author

N92-30962*# Utah State Univ., Logan. Center for Atmospheric and Space Sciences.
EFFECT OF WAVE-PARTICLE INTERACTION ON THE OUTFLOW OF IONS AT HIGH LATITUDES Semiannual Progress Report, 1 May - 31 Oct. 1991
Abdallah R. Barakat 31 Oct. 1991 9 p
(Grant NAG5-1546)
(NASA-CR-190560; NAS 1.26:190560) Avail: CASI HC A02/MF A01

The objective of the research is to use the low-frequency wave spectrum measured by the Plasma Wave Instrument on the DE-1 spacecraft to include the wave-particle interaction (WPI) in the different polar wind models that are available at Utah State University. A Monte Carlo technique was used to simulate the ion diffusion in the velocity space due to scattering by the waves. This enabled us to study the effect of WPI on the magnitude as well as the composition of the outflow of the ionospheric ions. In particular, in the first year the 1-D semi-kinetic code developed by Barakat and Schunk (1983) was modified in order to include the effect of the WPI. Author

N92-31008# Los Alamos National Lab., NM.
SMALL SATELLITE RADIATION BUDGET INSTRUMENTATION
P. G. Weber 1992 11 p Presented at the 2nd Small Satellite Technology and Applications Conference, Orlando, FL, 20-24 Apr. 1992
(Contract W-7405-eng-36)
(DE92-011134; LA-UR-92-949; CONF-9204112-1) Avail: CASI HC A03/MF A01

A major diagnostic in understanding the response of the Earth's climate to natural or anthropogenic changes is the radiative balance at the top of the atmosphere. Two classes of measurements may be undertaken: (1) a monitoring of the radiation balance over decade-long long-time scales; and (2) measurements designed to provide a sufficiently complete data set to validate or improve models. This paper discusses some of the important ingredients in obtaining such data and presents a description of some candidate instrumentation for use on a small satellite. DOE

N92-31009# Oak Ridge National Lab., TN.
FIELD STUDIES IN GEOPHYSICAL DIFFRACTION TOMOGRAPHY
Alan J. Witten, S. Scott Stevens, Wendell C. King (Military Academy, West Point, NY.), and James R. Ursic (Environmental Protection Agency, Chicago, IL.) 1992 9 p Presented at the SPIE Symposium on Instrumentation for Magnetospheric Imagery, San Diego, CA, 19-24 Jul. 1992
(Contract DE-AC05-84OR-21400)
(DE92-015084; CONF-920793-2) Avail: CASI HC A02/MF A01

Geophysical diffraction tomography (GDT) is a quantitative, high resolution technique for subsurface imaging. This method has been used in a number of shallow applications to image buried waste, trenches, soil strata, tunnels, synthetic magma chambers, and the buried skeletal remains of seismosaurus, the longest dinosaur ever discovered. The theory associated with the GDT inversion and implementing software have been developed for acoustic and scalar electromagnetic waves for bistatic and monostatic measurements in cross-borehole, offset vertical seismic profiling and reflection geometries. An overview of some signal processing algorithms, a description of the instrumentation used in field studies, and selected imaging results are presented. DOE

N92-31142# Royal Norwegian Council for Scientific and Industrial Research, Kjeller.
[OPERATION, MAINTENANCE AND RESEARCH ACTIVITIES AT THE NORWEGIAN SEISMIC ARRAY (NORSAR), THE NORWEGIAN REGIONAL SEISMIC ARRAY (NORESS), AND THE ARCTIC REGIONAL SEISMIC ARRAY (ARCESS)] Semiannual Report, 1 Apr. - 30 Sep. 1991
Nov. 1991 151 p
(AD-A250403) Avail: CASI HC A08/MF A02

This Semiannual Technical Summary describes the operation, maintenance, and research activities at the Norwegian Seismic Array (NORSAR), the Norwegian Regional Seismic Array (NORESS), and the Arctic Regional Seismic Array (ARCESS) for the period 1 Apr. - 30 Sep. 1991. Statistics are also presented for additional seismic stations, which through cooperative agreements with institutions in the host countries provide continuous data to the NORSAR Data Processing Center (NPDC). GRA

N92-31015*# National Oceanic and Atmospheric Administration, Boulder, CO. Wave Propagation Lab.
LOW-LEVEL ATMOSPHERIC FLOWS STUDIED BY PULSED DOPPLER LIDAR
Robert M. Banta, Lisa D. Olivier, and R. Michael Hardesty *In* NASA. Langley Research Center, 16th International Laser Radar Conference, Part 2 Jul. 1992 p 385-388 (For primary document see N92-31013 21-35)
Avail: CASI HC A01/MF A03

N92-31016*# National Aeronautics and Space Administration. Goddard Space Flight Center, Greenbelt, MD.
ON THE EXISTENCE OF CONVECTIVELY PRODUCED GRAVITY WAVES
Stephen P. Palm (Science Systems and Applications, Inc., Lanham, MD.) and S. H. Melfi *In* NASA. Langley Research Center, 16th International Laser Radar Conference, Part 2 Jul. 1992 p 389-392 (For primary document see N92-31013 21-35)
Avail: CASI HC A01/MF A03

N92-31021*# Colorado Univ., Boulder. Cooperative Inst. for Research in Environment Sciences.
A PULSED CO2 DOPPLER LIDAR FOR BOUNDARY LAYER MONITORING
Guy N. Pearson *In* NASA. Langley Research Center, 16th International Laser Radar Conference, Part 2 Jul. 1992 p 409-411 (For primary document see N92-31013 21-35)
Avail: CASI HC A01/MF A03

N92-31044*# Eidgenoessische Technische Hochschule, Zurich (Switzerland). Inst. of Atmospheric Physics.
LIDAR DEPOLARIZATION BY NONSPHERICAL PARTICLES: POTENTIAL OF COMBINED DEPOLARIZATION/BACKSCATTERING MEASUREMENTS FOR PSC'S CHARACTERIZATION
C. Flesia, A. Mugnai (Consiglio Nazionale delle Ricerche, Frascati, Italy), L. deSchoulepnikoff, and L. Stefanutti (Consiglio Nazionale delle Ricerche, Florence, Italy) *In* NASA. Langley Research Center, 16th International Laser Radar Conference, Part 2 Jul. 1992 p 497-500 Prepared in cooperation with Observatoire Cantonal, Neuchatel, Switzerland (For primary document see N92-31013 21-35)
Avail: CASI HC A01/MF A03

N92-31069*# Los Alamos National Lab., NM.
LIDAR ANALYSIS TECHNIQUES FOR USE IN THE ATMOSPHERIC BOUNDARY LAYER
William E. Eichinger, Daniel I. Cooper, Doug Hof, David Holtkamp, Robert Quick, Jr., Joe Tiee, and Robert Karl *In* NASA. Langley Research Center, 16th International Laser Radar Conference, Part 2 Jul. 1992 p 593-596 (For primary document see N92-31013 21-35)
Avail: CASI HC A01/MF A03

N92-31084*# Illinois Univ., Urbana-Champaign. Dept. of Electrical and Computer Engineering.
MEASUREMENT CAPABILITIES OF GIANT LIDARS FOR MIDDLE AND UPPER ATMOSPHERIC APPLICATIONS Abstract Only
Chester S. Gardner *In* NASA. Langley Research Center, 16th International Laser Radar Conference, Part 2 Jul. 1992 p 647 (For primary document see N92-31013 21-35)
Avail: CASI HC A01/MF A03

N92-31229*# Harvard Univ., Cambridge, MA. Center for Isotope Geochemistry.
THE (146,147)Sm-(142,143)Nd SYSTEMATICS OF EARLY TERRESTRIAL DIFFERENTIATION AND THE LOST CONTINENTS OF THE EARLY EARTH
Charles L. Harper, Jr. and Stein B. Jacobsen *In* Lunar and Planetary Inst., Twenty-Third Lunar and Planetary Science Conference 1992 p 24-28 (For primary document see N92-31222 21-88)
Avail: CASI HC A01/MF A01

47 METEOROLOGY AND CLIMATOLOGY

Includes weather forecasting and modification.

N92-30262# Science and Technology Corp., Hampton, VA.
REGIONAL-SCALE ANALYSIS AND FORECASTING (RAP) REPORT
John C. Burgeson, Christopher R. Redder, Isidore M. Halberstam (ST Systems Corp., Lexington, MA.), and Ralph Shapiro (ST Systems Corp., Lexington, MA.) May 1991 84 p
(Contract F19628-89-C-0167)
(AD-A248384; PL-TR-91-2135; AD-E200940; SR-1) Avail: CASI HC A05/MF A01

The development of the Regional-scale analysis and forecasting (RAP) at the halfway point of the contracted effort is described. The RAP is based on optimum interpolation and rigorous selection by forward stepwise regression of a small subset of the observations available for interpolation to a point. The RAP scheme produces analyses that are nearly as accurate as analyses produced by interpolating the full set of observations to the point. Another unique feature of the RAP is a buddy check that very carefully determines those observations that should be eliminated from affecting the analysis. The scheme used simulated error correlations, which were a function of distance between observations, but will be using error correlation models developed from real data. The correlation models will be stratified by region, season, standard atmospheric levels, forecast lengths, and sensors. The RAP will be used in observing system simulation experiments (OSSEs). The simulated observations will be obtained from perfect FGGE-2b databases after insertion of observation errors. The perfect FGGE-2b observations were derived from a 16-day nature forecast run from the European Center for Medium Range Weather Forecasts (ECMWF). The OSSEs will be used to determine the goodness of RAP and the validity of the developed correlation models. GRA

N92-30340# Dugway Proving Ground, UT.
METHODOLOGY INVESTIGATION, IMPLEMENT REMOTE SENSING Report, Oct. 1990 - Sep. 1991
Christopher A. Biltoft 27 Nov. 1991 49 p
(AD-A248901; DPG-FR-91-713) Avail: CASI HC A03/MF A01

The Dugway Proving Ground radar wind profiler, a ground-based 404.37 MHz Doppler radar, operated continuously through its FY91 evaluation period. The system provides 6-min and hourly wind profiles at 250 m intervals from 500 m to 10 km above ground level. Profiler performance was evaluated using a series of internal measures and through intercomparison with radiosonde-derived wind soundings. Results show profiler measurement precision comparable to that of radiosonde-derived wind data, but with greatly increased temporal resolution. Profiler spectra were examined during periods with strong wind shear, precipitation, and aircraft passage through the radar beams. These conditions caused no significant problems, although data quality was marginal or poor in strong convection or during very dry conditions (dew points below -35 C). A problem with antenna element degradation was discovered, and corrective action was initiated. Automated quality control algorithms were developed for the 6-min profiler data, and formats were developed for inclusion of wind profiler data in test data reports. Shutdown procedures were also developed to eliminate profiler interference with search and rescue satellites. Radar wind profiling is a promising remote sensing technology that offers significant advantages over existing balloon-based wind sounding methods. Once frequency allocation issues are resolved, radar wind profiling is expected to become the preferred method for obtaining ballistic wind data. GRA

N92-30495# National Severe Storms Lab., Norman, OK. National Severe Storms Lab.
ON THE POTENTIAL USE OF THE TERMINAL DOPPLER WEATHER RADAR GUST FRONT DETECTION ALGORITHM ON THE WSR-88D SYSTEM. PART 1: IMPACTS OF RADAR SYSTEM DIFFERENCES Interim Report
Gregory J. Stumpf Sep. 1991 40 p Original contains color illustrations
(Contract DTFA01-80-Y-10524)
(DOT/FAA/NR-92/8,I) Avail: CASI HC A03/MF A01; 9 functional color pages

The feasibility of using the gust front detection algorithm (GFDA) developed for the Terminal Doppler Weather Radar (TDWR) systems on a Next Generation Weather Radar (WSR-88D, formerly NEXRAD) systems is assessed. The data resolution and tilt sequences of the WSR-88D systems are different than TDWR, and the WSR-88D is designated to operate at greater ranges. To test the effect of the decreased data resolution of WSR-88D, TDWR-like data were degraded to the resolution of WSR-88D and the GFDA was tested on this degraded dataset. Also, the GFDA was tested on a gust front which occurred outside the normal 60-km range in which data are processed from TDWR. Results show that the degraded velocity precision of WSR-88D has little effect on the performance of the GFDA. However, the larger sample volume sizes for the WSR-88D system did degrade the performance of the GFDA. The second lowest tilt angle for the WSR-88D tilt sequences is about 0.5 degrees higher than TDWR, and this reduced the maximum range of gust from detectability. These tests show that GFDA's performance on the WSR-88D systems will be acceptable after a few modifications.
Author

N92-30496# National Severe Storms Lab., Norman, OK.
ON THE POTENTIAL USE OF THE TERMINAL DOPPLER WEATHER RADAR GUST FRONT DETECTION ALGORITHM ON THE WSR-88D SYSTEM. PART 2: DETECTING NON-GUST FRONT CONVERGENT WEATHER PHENOMENA Interim Report
Gregory J. Stumpf Oct. 1991 42 p Prepared in cooperation with Oklahoma Univ., Norman Original contains color illustrations
(Contract DTFA01-80-Y-10524)
(DOT/FAA/NR-92/8,II) Avail: CASI HC A03/MF A01; 7 functional color pages

The capability of the Gust Front Detection Algorithm (GFDA) developed for Terminal Doppler Weather Radar (TDWR) systems to detect other types of non-gust front weather phenomena which are associated with patterns of convergence in a Doppler-radar radial velocity field is examined. The potential use of the GFDA as a nowcasting tool, a mesoscale forecasting tool, and as a tool to detect other kinds of aviation hazards besides gust fronts, needs investigation. The phenomena studied include synoptic fronts, sea-breeze fronts, gravity waves, terrain-induced convergence boundaries, old thunderstorm outflow boundaries, and the convergence bands within extratropical cyclones associated with enhanced precipitation. Comparisons of the convergent characteristics of these other phenomena to those of gust fronts are made. In addition, several case studies are presented to demonstrate the ability of the GFDA to detect the non-gust front phenomena. Author

N92-30559# Massachusetts Inst. of Tech., Lexington. Lincoln Lab.
DOPPLER MEAN VELOCITY ESTIMATION: SMALL SAMPLE ANALYSIS AND A NEW ESTIMATOR
Edward S. Chornoboy 25 Mar. 1992 73 p
(Contracts DTFA01-84-Z-02030; F19628-90-C-0002)
(AD-A249024; TR-942) Avail: CASI HC A04/MF A01

Optimal Doppler velocity estimation, under the constraint of small sample size, is explored for a standard Gaussian signal measurement model and thematic maximum likelihood (ML) and Bayes estimation. Because the model considered depends on a vector parameter (velocity, spectrum width, and signal-to-noise ratio (SNR)), the exact formulation of an ML or Bayes solution involves a system of equations that is neither uncoupled nor explicit in form. Historically, iterative methods have been the most suggested approach to solving the required equations. In addition to being computationally intensive, it is unclear whether iterative methods can be constructed to perform well given a small-sample size and low signal strength. This report takes a different approach and seeks to construct approximate (ML and Bayes) estimators based on the notion of using constrained adaptive models to deal with nuisance parameter removal. A Monte Carlo simulation is used to determine small-sample estimator statistics and to demonstrate true performance bounds in the case of known nuisance values. Performance comparisons between these optimal forms and other standard estimators (pulse pair (PP) and a frequency domain wind profiler (WP)) method are presented. Performance sensitivity of the optimal algorithms, with respect to uncertainty in the values of model nuisance parameters, is explored and provides the foundation for the recommendation to seek an adaptive method. GRA

N92-30643# Colorado State Univ., Fort Collins. Dept. of Atmospheric Science.

CLOUDS: THEIR PREDICTION AND SIMULATION Annual Report, 1 Jun. 1991 - 31 Dec. 1991

William R. Cotton 31 Dec. 1991 4 p

(Grant AF-AFOSR-0269-91)

(AD-A250643; AFOSR-92-0280TR) Avail: CASI HC A01/MF A01

Piotr Flatau has nearly completed a new comprehensive two-stream radiative transfer (RT) code which includes cloud water and ice scattering properties. The code is interfaced to the RAMS bulk cloud microphysics module. Several algorithmic improvements have been made to all three major components of the RT package: molecular gases, single scattering properties of clouds, and radiative transfer solver. Reduction and elimination algorithms for the RT solver have been developed. The code has been efficiently written to take advantage of vectorization and parallelization issues. New interfaces to LOWTRAN7 and MODTRAN are also provided. Single scattering properties are included using the anomalous diffraction theory (ADT). A number of members of our research group participated in the FIRE IT Cirrus field experiment in Coffeyville, Kansas (November 12-December 12). This was an extremely successful mission. RAMS was used in a forecasting mode, and data were gathered for future case studies, including data specially tailored for mesoscale modeling during the Intensive Observing Period. We gathered MAPS and NGM data for all the days of the project, collected satellite pictures, and relevant meteorological information. Piotr Flatau and Graeme Stephens also served as mission planning scientists for the NCAR Saberliner aircraft. GRA

N92-30735*# National Aeronautics and Space Administration. Langley Research Center, Hampton, VA.

CORRELATIVE MEASUREMENT OPPORTUNITIES BETWEEN ATLAS-1 AND UARS EXPERIMENTS

Edwin F. Harrison, Fred M. Denn (Lockheed Engineering and Sciences Co., Hampton, VA.), and Gary G. Gibson (Lockheed Engineering and Sciences Co., Hampton, VA.) May 1992 64 p

(RTOP 618-22-31-02)

(NASA-TM-107630; NAS 1.15:107630) Avail: CASI HC A04/MF A01

The first ATmospheric Laboratory for Applications and Science (ATLAS-1) mission was flown aboard the Space Shuttle from March 24 to April 2, 1992. The ATLAS-1 instruments provided a large number of measurements which were coincident with observations from experiments on the Upper Atmosphere Research Satellite (UARS). During the ATLAS-1 mission, simulations were performed to predict when and where coincident measurements between ATLAS and UARS instruments would occur. These predictions were used to develop instrument operation schedules to maximize the correlative opportunities between the two satellites. Results of the simulations provide valuable information for the ATLAS and UARS scientists to compare measurements between various instruments on the two satellites. Author

N92-30867# Air Force Inst. of Tech., Wright-Patterson AFB, OH.

TROPICAL CYCLONE ASYMMETRIES AS REVEALED BY RECENT SATELLITE MICROWAVE BRIGHTNESS TEMPERATURES M.S. Thesis

Jeffrey H. McCoy 1991 148 p

(AD-A249873; AFIT/CI/CIA-91-117) Avail: CASI HC A07/MF A02

Microwave data from the Special Sensor Microwave Imager (SSM/I) were obtained for twenty-nine map times of tropical cyclones from the Northwest Pacific and North Indian Ocean. Automated analysis of 85 GHz vertical polarization (85V GHz) brightness temperatures (Tb's) were conducted by calculating statistics at various radii from a cyclone center. These statistics were correlated against storm traits such as intensity, vortex translation speed, central pressure changes, and direction of vortex movement. The aim of this research was to determine relationships between 85V GHz data and cyclone characteristics, which could lead to the development of forecasting tools using SSM/I data. Anomalies in the 85V GHz Tb fields demonstrated strong correlations to cyclone intensification by highlighting the positions and orientations of the principal rain bands. Such anomalies reveal asymmetries of convection associated with spiraling rainbands and convective eyewalls. This research demonstrated that SSM/I derived TB fields can show patterns of high correlations in the anomalies, as well as portray processes associated with intensification that occur in a tropical cyclone. Since these results were achieved through automatic methods, it is possible to develop forecast nomograms that link SSM/I TB data to cyclone traits. Such tools would be useful in the prediction of tropical cyclones. GRA

N92-31003# Naval Undersea Warfare Center, West Palm Beach, FL.

A STATISTICAL COMPARISON OF AUTEC AND ELEUTHERA ISLAND WIND DATA FOR THE PERIOD 1 APRIL 1989 THROUGH 30 MARCH 1990 Final Report

J. C. Park and J. H. Hinkamp 3 Mar. 1992 42 p

(AD-A248898; NUWC-NPt-TD-10012) Avail: CASI HC A03/MF A01

This document presents a statistical comparison of wind data measured simultaneously on Eleuthera Island and at the Atlantic Undersea Test and Evaluation Center (AUTEC) on Andros Island, Bahamas, for the period 1 April 1989 through 30 March 1990. The statistics calculated and compared include empirical probability distributions, probability densities, conditional probability densities, crosscorrelations, linear correlations, and power spectral estimates. The wind speed and direction data are found to be well correlated; however, the Eleuthera wind speed data exhibit a negative bias relative to the AUTEC data. GRA

N92-31017*# National Aeronautics and Space Administration. Goddard Space Flight Center, Greenbelt, MD.

DOPPLER LIDAR WIND MEASUREMENT WITH THE EDGE TECHNIQUE

C. Laurence Korb and Bruce M. Gentry *In* NASA. Langley Research Center, 16th International Laser Radar Conference, Part 2 Jul. 1992 p 393-396 (For primary document see N92-31013 21-35)

Avail: CASI HC A01/MF A03

N92-31018*# Michigan Univ., Ann Arbor. Dept. of Atmospheric, Oceanic and Space Sciences.

TROPOSPHERIC AND STRATOSPHERIC WIND PROFILING WITH A DIRECT DETECTION DOPPLER LIDAR

Vincent J. Abreu, John E. Barnes, Ken W. Fischer, Wilbert R.

Skinner, and Matt J. McGill *In* NASA. Langley Research Center, 16th International Laser Radar Conference, Part 2 Jul. 1992 p 397-400 (For primary document see N92-31013 21-35)
Avail: CASI HC A01/MF A03

N92-31019*# Coherent Technologies, Inc., Boulder, CO.
ATMOSPHERIC WIND SENSING WITH A 1 AND 2 MICRON COHERENT LIDAR
R. Milton Huffaker and Sammy W. Henderson *In* NASA. Langley Research Center, 16th International Laser Radar Conference, Part 2 Jul. 1992 p 401-403 (For primary document see N92-31013 21-35)
Avail: CASI HC A01/MF A03

N92-31020*# National Oceanic and Atmospheric Administration, Boulder, CO. Wave Propagation Lab.
DESIGN OF A NEAR-IR COHERENT LIDAR FOR HIGH SPATIAL AND VELOCITY RESOLUTION WIND MEASUREMENT
Christian J. Grund and Madison J. Post *In* NASA. Langley Research Center, 16th International Laser Radar Conference, Part 2 Jul. 1992 p 405-408 (For primary document see N92-31013 21-35)
Avail: CASI HC A01/MF A03

N92-31034*# Photometrics, Inc., Woburn, MA.
DETERMINING WATER CLOUD PARTICLE SIZES FROM LIDAR DEPOLARIZATION MEASUREMENTS AND TIME DEPENDENT MULTIPLE SCATTERING COEFFICIENTS
R. C. Garner and G. G. Koenig (Phillips Lab., Hanscom AFB, MA.) *In* NASA. Langley Research Center, 16th International Laser Radar Conference, Part 2 Jul. 1992 p 459-461 Sponsored in part by AF (For primary document see N92-31013 21-35)
Avail: CASI HC A01/MF A03

N92-31035*# Defence Research Establishment Valcartier (Quebec).
MULTIPLE SCATTERING LIDAR RETURNS FROM STRATUS CLOUDS
D. L. Hutt and L. R. Bissonnette *In* NASA. Langley Research Center, 16th International Laser Radar Conference, Part 2 Jul. 1992 p 463-466 Prepared in cooperation with Laval Univ. (Quebec) (For primary document see N92-31013 21-35)
Avail: CASI HC A01/MF A03

N92-31037*# Ecole Polytechnique, Palaiseau (France). Lab. de Meteorologie Dynamique.
AIRBORNE LIDAR AND RADIOMETRIC OBSERVATIONS OF PBL- AND LOW CLOUDS
P. H. Flamant, R. Valentin, and J. Pelon (Paris VI Univ., France) *In* NASA. Langley Research Center, 16th International Laser Radar Conference, Part 2 Jul. 1992 p 471-473 (For primary document see N92-31013 21-35)
Avail: CASI HC A01/MF A03

N92-31038*# Ecole Polytechnique, Palaiseau (France). Lab. de Meteorologie Dynamique.
ECLIPS AT LMD: PRELIMINARY RESULTS OF PHASE 2
R. Valentin, L. Menenger, S. Elouragini, P. H. Flamant, and J. Pelon (Paris VI Univ., France) *In* NASA. Langley Research Center, 16th International Laser Radar Conference, Part 2 Jul. 1992 p 475-478 (For primary document see N92-31013 21-35)
Avail: CASI HC A01/MF A03

N92-31039*# Paris VI Univ. (France). Service d'Aeronomie du CNRS.
THE 2ND PHASE OF THE LEANDRE PROGRAM: WATER-VAPOR DIAL MEASUREMENT
P. Quaglia, D. Bruneau, and J. Pelon *In* NASA. Langley Research Center, 16th International Laser Radar Conference, Part 2 Jul. 1992 p 479-482 (For primary document see N92-31013 21-35)
Avail: CASI HC A01/MF A03

N92-31041*# National Aeronautics and Space Administration. Goddard Space Flight Center, Greenbelt, MD.
WATER VAPOR VARIANCE MEASUREMENTS USING A RAMAN LIDAR
K. Evans (Hughes STX, Inc., Lanham, MD.), S. H. Melfi, R. Ferrare (Universities Space Research Association, Columbia, MD.), and D. Whiteman *In* NASA. Langley Research Center, 16th International Laser Radar Conference, Part 2 Jul. 1992 p 485-487 (For primary document see N92-31013 21-35)
Avail: CASI HC A01/MF A03

N92-31042*# Deutsche Forschungs- und Versuchsanstalt fuer Luft- und Raumfahrt, Oberpfaffenhofen (Germany, F.R.). Inst. of Atmospheric Physics.
AIRBORNE REMOTE SENSING OF TROPOSPHERIC WATER VAPOR USING A NEAR INFRARED DIAL SYSTEM
G. Ehret, C. Kiemle, W. Renger, and G. Simmet *In* NASA. Langley Research Center, 16th International Laser Radar Conference, Part 2 Jul. 1992 p 489-492 (For primary document see N92-31013 21-35)
Avail: CASI HC A01/MF A03

N92-31047*# Florence Univ. (Italy). Dept. of Physics.
LABORATORY SCALED SIMULATION OF LIDAR CLOUD SOUNDING EXPERIMENTS
G. Zaccanti, P. Bruscaglioni, M. Gurioli (European Lab. for Non-Linear Spectroscopy, Florence, Italy), and P. Sansoni *In* NASA. Langley Research Center, 16th International Laser Radar Conference, Part 2 Jul. 1992 p 509-512 (For primary document see N92-31013 21-35)
Avail: CASI HC A01/MF A03

N92-31048*# Max-Planck-Inst. fuer Meteorologie, Hamburg (Germany, F.R.).
AN ALEXANDRITE REGENERATIVE AMPLIFIER FOR WATER VAPOR AND TEMPERATURE MEASUREMENTS
P.-Y. Thro, J. Boesenberg, and V. Wulfmeyer *In* NASA. Langley Research Center, 16th International Laser Radar Conference, Part 2 Jul. 1992 p 513-516 (For primary document see N92-31013 21-35)
Avail: CASI HC A01/MF A03

N92-31061*# Ludwig-Maximilians-Univ., Munich (Germany, F.R.). Inst. der Meteorologisches.
LIDAR MULTIPLE SCATTERING: DEPENDENCE ON ATMOSPHERIC PARAMETERS
Matthias Wiegner *In* NASA. Langley Research Center, 16th International Laser Radar Conference, Part 2 Jul. 1992 p 563-565 (For primary document see N92-31013 21-35)
Avail: CASI HC A01/MF A03

N92-31063*# Photometrics, Inc., Woburn, MA.
TIME AND POLARIZATION DEPENDENT DOUBLE SCATTERING CALCULATIONS OF LIDAR RETURNS FROM WATER CLOUDS
R. C. Garner *In* NASA. Langley Research Center, 16th International Laser Radar Conference, Part 2 Jul. 1992 p 571-574 Sponsored in part by AF (For primary document see N92-31013 21-35)
Avail: CASI HC A01/MF A03

N92-31064*# Science and Technology Corp., Edgewood, MD.
MULTIPLE SCATTERING WAVELENGTH DEPENDENT BACKSCATTERING OF KAOLIN DUST IN THE IR: MEASUREMENTS AND THEORY
Avishai Ben-David *In* NASA. Langley Research Center, 16th International Laser Radar Conference, Part 2 Jul. 1992 p 575-578 (For primary document see N92-31013 21-35)
(Contract DAAA15-89-D-0007)
Avail: CASI HC A01/MF A03

N92-31082*# Academia Sinica, Beijing (China). Inst. of Atmospheric Physics.
LIDAR MEASUREMENTS OF CLOUD EXTINCTION COEFFICIENT DISTRIBUTION AND ITS FORWARD SCATTERING PHASE FUNCTION ACCORDING TO MULTIPLY SCATTERED LIDAR RETURNS
Jinhuan Qiu and Qirong Huang *In* NASA. Langley Research Center, 16th International Laser Radar Conference, Part 2 Jul. 1992 p 641-642 (For primary document see N92-31013 21-35)
Avail: CASI HC A01/MF A03

N92-31083*# Academy of Sciences (USSR), Tomsk. Inst. of Atmospheric Optics.
MEASUREMENTS OF THE BACKSCATTERING PHASE MATRICES OF CRYSTAL CLOUDS WITH A POLARIZATION LIDAR
B. V. Kaul, A. L. Kuznetsov, and E. R. Polovtseva *In* NASA. Langley Research Center, 16th International Laser Radar Conference, Part 2 Jul. 1992 p 643-646 (For primary document see N92-31013 21-35)
Avail: CASI HC A01/MF A03

N92-31086*# Pennsylvania State Univ., University Park.
ATMOSPHERIC MEASUREMENTS USING THE LAMP LIDAR DURING THE LADIMAS CAMPAIGN
C. R. Philbrick, D. B. Lysak, T. D. Stevens, P. A. T. Haris, and Y.-C. Rau *In* NASA. Langley Research Center, 16th International Laser Radar Conference, Part 2 Jul. 1992 p 651-654 Sponsored in part by Army, Navy, and NSF (For primary document see N92-31013 21-35)
Avail: CASI HC A01/MF A03

N92-31089*# National Aeronautics and Space Administration. Goddard Space Flight Center, Greenbelt, MD.
RAMAN LIDAR MEASUREMENTS OF WATER VAPOR AND AEROSOL/CLOUDS DURING THE FIRE/SPECTRE FIELD CAMPAIGN
S. H. Melfi, D. Whiteman, R. Ferrare, K. Evans, J. E. M. Goldsmith (Sandia National Labs., Livermore, CA.), M. Lapp (Sandia National Labs., Livermore, CA.), and S. E. Bisson (Sandia National Labs., Livermore, CA.) *In* NASA. Langley Research Center, 16th International Laser Radar Conference, Part 2 Jul. 1992 p 663-666 Prepared in cooperation with Universities Space Research Association, Columbia, MD; and Hughes STX, Inc., Lanham, MD (For primary document see N92-31013 21-35)
Avail: CASI HC A01/MF A03

N92-31090*# National Aeronautics and Space Administration. Goddard Space Flight Center, Greenbelt, MD.
PERFORMANCE MODELING OF DAYTIME RAMAN LIDAR SYSTEMS FOR PROFILING ATMOSPHERIC WATER VAPOR
J. E. M. Goldsmith and Richard A. Ferrare *In* NASA. Langley Research Center, 16th International Laser Radar Conference, Part 2 Jul. 1992 p 667-670 Prepared in cooperation with Universities Space Research Association, Columbia, MD (For primary document see N92-31013 21-35)
Avail: CASI HC A01/MF A03

N92-31092*# Paris VI Univ. (France). Service d'Aeronomie du CNRS.
DIAL SIMULATIONS FOR SATELLITE WATER VAPOR PROFILE MEASUREMENTS WITHIN THE BEST PROJECT
P. Chazette, J. Pelon, and G. Megie *In* NASA. Langley Research Center, 16th International Laser Radar Conference, Part 2 Jul. 1992 p 675-678 (For primary document see N92-31013 21-35)
Avail: CASI HC A01/MF A03

N92-31093*# National Aeronautics and Space Administration. Langley Research Center, Hampton, VA.
AIRBORNE WATER VAPOR DIAL RESEARCH: SYSTEM DEVELOPMENT AND FIELD MEASUREMENTS
Noah S. Higdon (ST Systems Corp., Hampton, VA.), Edward V. Browell (ST Systems Corp., Hampton, VA.), Patrick Ponsardin (ST Systems Corp., Hampton, VA.), Thomas H. Chyba (National Academy of Sciences - National Research Council, Hampton, VA.), Benoist E. Grossmann (Thomson-CSF, Paris, France), Carolyn F. Butler (ST Systems Corp., Hampton, VA.), Marta A. Fenn (ST Systems Corp., Hampton, VA.), Shane D. Mayor (ST Systems Corp., Hampton, VA.), Syed Ismail, and William B. Grant *In its* 16th International Laser Radar Conference, Part 2 Jul. 1992 p 679-682 (For primary document see N92-31013 21-35)
Avail: CASI HC A01/MF A03

N92-31094*# Kyushu Univ., Fukuoka (Japan). Dept. of Electrical Engineering.
ALEXANDRITE LIDAR FOR THE ATMOSPHERIC WATER VAPOR DETECTION AND DEVELOPMENT OF POWERFUL TUNABLE SOURCES IN IR
M. Uchiumi, M. Maeda, K. Muraoka, and O. Uchino (Meteorological Research Inst., Tsukuba, Japan) *In* NASA. Langley Research Center, 16th International Laser Radar Conference, Part 2 Jul. 1992 p 683-686 (For primary document see N92-31013 21-35)
Avail: CASI HC A01/MF A03

N92-31104*# Ship Research Inst., Tokyo (Japan). Ship Equipment and Marine Environment Div.
LIDAR OBSERVATION OF MARINE MIXED LAYER
Susumu Yamagishi, Hiroshi Yamanouchi, and Masayuki Tsuchiya *In* NASA. Langley Research Center, 16th International Laser Radar Conference, Part 2 Jul. 1992 p 719-722 (For primary document see N92-31013 21-35)
Avail: CASI HC A01/MF A03

N92-31106*# BMW-A.G., Munich (Germany, F. R.).
DENSE FOG ON THE HIGHWAY: VISUAL RANGE MONITORING IN CARS?
W. Hahn, W. Krichbaumer (Deutsche Forschungsanstalt fuer Luft- und Raumfahrt, Oberpfaffenhofen, Germany, F.R.), J. Streicher (Deutsche Forschungsanstalt fuer Luft- und Raumfahrt, Oberpfaffenhofen, Germany, F.R.), and Ch. Werner (Deutsche Forschungsanstalt fuer Luft- und Raumfahrt, Oberpfaffenhofen, Germany, F.R.) *In* NASA. Langley Research Center, 16th International Laser Radar Conference, Part 2 Jul. 1992 p 727-730 (For primary document see N92-31013 21-35)
Avail: CASI HC A01/MF A03

48 OCEANOGRAPHY

Includes biological, dynamic, and physical oceanography; and marine resources.

For related information see also *43 Earth Resources and Remote Sensing.*

N92-30238# Army Cold Regions Research and Engineering Lab., Hanover, NH.
ICE THICKNESS OBSERVATIONS, NORTH AMERICAN ARCTIC AND SUBARCTIC, 1972-1973 AND 1973-1974, PART 8 Special Report
Michael A. Bilello and Roy E. Bates Dec. 1991 132 p (AD-A250830; CRREL-SR-43-Pt-8) Avail: CASI HC A07/MF A02

This eighth in a series of reports on lake and river ice and land-fast sea ice presents ice thickness measurements observed throughout the North American Arctic and subarctic during the 1972-73 and 1973-74 winter seasons. Information on surface ice conditions, dates of first ice, freeze-over and breakup, and detailed measurements of ice thickness across Alaskan rivers are also included. Some reports from the Alaska National Guard network on ice thickness measurements in remote areas of western Alaska are also presented. Analyses were made of maximum observed ice thicknesses reported during the two winters, and isoline maps that show the areal distribution of these values across Canada and Alaska were drawn. GRA

N92-30413 Department of the Navy, Washington, DC.
DIGITAL BOTTOM MAPPING Patent
Anthony P. Passamante, inventor (to Navy), Paul A. Labonski, inventor (to Navy), Nancy J. Harned, inventor (to Navy), Timothy B. Hediger, inventor (to Navy), and John Ambrose, inventor (to Navy) 31 Dec. 1991 14 p Filed 7 Dec. 1990
(AD-D015238; US-Patent-5,077,699; US-Patent-Appl-SN-624014; US-Patent-Class-367-88) Avail: US Patent and Trademark Office

Ocean bottom mapping is carried out by projecting a sonic pulse in the form of a fan-shaped beam from a vessel toward the ocean floor, receiving echoes by an array of sonic detectors extending athwartship, repeatedly taking instantaneous, simultaneous, snapshot-like samples of all the detectors in the array, and, by means of a digital computer, applying a beam-forming transform, such as a Fast Fourier Transform, to the samples, thereby producing a spectrum of amplitudes versus angles. The directions of the floor areas from which the snapshot data emanate are determined from refinement of the peaks in the spectrum of amplitudes, and the distances of the same floor areas from the vessel are determined by the time interval between the pulse and the sample. A bottom profile is constructed from the directions and distances so determined. Two alternative techniques for refining and interpreting spectrum are described. GRA

N92-30470# Beleidscommissie Remote Sensing, Delft (Netherlands).
FEASIBILITY OF EXTRACTING CURRENT PROFILE INFORMATION FROM HF-RADAR SURFACE CURRENT MEASUREMENTS, PART 1 AND 2
C. F. deValk (Delft Hydraulics Lab., Netherlands), R. E. Klein, and H. C. Peters (Rijkswaterstaat, Delft, Netherlands) Dec. 1991 90 p
(BCRS Proj. OP-1.30)
(BCRS-91-23-Pt-1-2; ISBN-90-5411-013-9; ETN-92-91874) Avail: CASI HC A05/MF A01

The need for current information in the Netherlands is outlined and the status of current measuring equipment and hydrodynamic models outlined. With the present means it is difficult to measure currents permanently and in real time in the harsh marine environments. However, recent development of new remote sensing techniques like HF Doppler radar and acoustic Doppler current profilers and the development of hydrodynamic models are very promising modern means to deliver current information. Since one dimensional current models are now readily available that are able to calculate the vertical current profile, the possibility to extrapolate the surface current measured by a HF radar to larger depths with the help of such a one dimensional model was investigated. A feasibility study which made use of available HF radar data gathered in a previous measurement campaign is outlined. The data are suitable, because at some locations current profiles were measured by ships simultaneously with the HF radar data. This offers the possibility to compare the predicted current profiles, produced by the data assimilation procedure, with the actual measured profiles. The numerical and graphical results of this feasibility study are presented. ESA

N92-30593# Arizona State Univ., Tempe. Dept. of Mechanical and Aerospace Engineering.
LABORATORY SIMULATION OF FLUID DYNAMICAL PROCESS RELATED TO WINTER ARCTIC LEADS Final Report
H. J. Fernando 30 Sep. 1991 11 p
(Contract N00014-90-J-1045)
(AD-A252266) Avail: CASI HC A02/MF A01

A comprehensive series of experiments were carried out to investigate the layered convection that occurs in linearly salt-stratified fluids subjected to destabilizing buoyancy fluxes, in particular, heating from below. Unlike previous work, turbulence in the convecting layers was explicitly taken into account in modeling heat and salt transports through these layers. It was shown theoretically that the thicknesses of convecting layers can be parameterized. Accordingly, expressions were derived for thicknesses of the first and the rest of the convecting layers. Experimental results were found to be in good agreement with the proposed predictions. GRA

N92-30739*# Oregon State Univ., Corvallis. Coll. of Oceanography.
EVENT-SCALE RELATIONSHIPS BETWEEN SURFACE VELOCITY, TEMPERATURE AND CHLOROPHYLL IN THE COASTAL OCEAN, AS SEEN BY SATELLITE Final Report, 14 Dec. 1987 - 15 Dec. 1991
P. Ted Strub Dec. 1991 273 p
(Grant NAGw-1251)
(NASA-CR-190266; NAS 1.26:190266) Avail: CASI HC A12/MF A03

The overall goal of this project was to increase our understanding of processes which determine the temporally varying distributions of surface chlorophyll pigment concentration and surface temperature in the California Current System (CCS) on the time-scale of 'events', i.e., several days to several weeks. We also proposed to investigate seasonal and regional differences in these events. Additionally, we proposed to evaluate methods of estimating surface velocities and horizontal transport of pigment and heat from sequences of AVHRR and CZCS images. The four specific objectives stated in the original proposal were to: (1) test surface current estimates made from sequences of both SST and color images using variations of the statistical method of Emery et al. (1986) and estimate the uncertainties in these satellite-derived surface currents; (2) characterize the spatial and temporal relationships of chlorophyll and temperature in rapidly evolving features for which adequate imagery exist and evaluate the contribution of these events to monthly and seasonal averages; (3) use the methods tested in (1) to determine the nature of the velocity fields in the CCS; and (4) compare the currents, temperature, and currents in different seasons and in different geographic regions. Author

N92-30832# Army Cold Regions Research and Engineering Lab., Hanover, NH.
VECTOR ANALYSIS OF ICE FABRIC DATA
Michael G. Ferrick and Kerrn J. Claffey Mar. 1992 22 p
(AD-A250832; CRREL-92-1) Avail: CASI HC A03/MF A01

The mechanical properties of ice are strongly affected by crystal texture and c-axis alignment. Here, we develop a general quantitative method for analysis of uniaxial crystal orientation data. These data are represented as unit vectors from the origin with endpoints on the surface of a unit sphere. An orthogonal least-squares error measure is used to develop equations that define the closest plane and line through the data. The resulting eigenvalue problem is identical to that obtained by other investigators using different methods. However, we identify an implicit assumption in the method, and observe that the error measure represents physical distance and quantifies the goodness-of-fit of the idealized structures to the data. For comparison, a parallel development is presented of classical dependent-variable least squares. A method is developed to transform the data and the results for viewing on Schmidt nets drawn in the best plane and the predominant basal plane of a sample, in addition to the standard xy-plane. Applications of the analysis to sea ice samples include both numerical and Schmidt net presentations of results. GRA

N92-30861# Scripps Institution of Oceanography, La Jolla, CA.
OCEANIC CO2 MEASUREMENTS FOR THE WOCE HYDROGRAPHIC SURVEY IN THE PACIFIC OCEAN, 1990-1991: SHORE BASED ANALYSES DURING LEGS 1-3
C. D. Keeling 1992 10 p
(Contract DE-FG03-90ER-60982)
(DE92-013064; DOE/ER-60982/2) Avail: CASI HC A02/MF A01

During the winter and spring of 1991 we made preparations for sampling on three legs of the U.S. World Ocean Circulation Experiment in the Pacific Ocean. These transects, postponed from an original start date early in 1991, took place between May 31

to October 1. For the project, 1400 0.5 liter Pyrex sampling bottles were used for the collection of sea water. A second major pre-expedition task was the construction of a dual titration cell system of new design, as described in the original proposal and our previous semi-annual report. DOE

N92-31014*# Paris VI Univ. (France). Service d'Aeronomie du CNRS.
BOUNDARY LAYER STRUCTURE OVER THE OCEAN OBSERVED BY LEANDRE 1 DURING A TRAMONTANE EVENT
C. Flamant, J. Pelon, P. Flamant (Ecole Polytechnique, Palaiseau, France), and P. Durand (Toulouse Univ., France) *In* NASA. Langley Research Center, 16th International Laser Radar Conference, Part 2 Jul. 1992 p 381-383 (For primary document see N92-31013 21-35)
Avail: CASI HC A01/MF A03

51 LIFE SCIENCES (GENERAL)

N92-30305*# National Aeronautics and Space Administration. Marshall Space Flight Center, Huntsville, AL.
COMPARISON OF EPIFLUORESCENT VIABLE BACTERIAL COUNT METHODS
E. B. Rodgers and T. L. Huff (Sverdrup Technology, Inc., Huntsville, AL.) Jul. 1992 17 p
(NASA-TM-103592; NAS 1.15:103592) Avail: CASI HC A03/MF A01

Two methods, the 2-(4-Iodophenyl) 3-(4-nitrophenyl) 5-phenyltetrazolium chloride (INT) method and the direct viable count (DVC), were tested and compared for their efficiency for the determination of the viability of bacterial populations. Use of the INT method results in the formation of a dark spot within each respiring cell. The DVC method results in elongation or swelling of growing cells that are rendered incapable of cell division. Although both methods are subjective and can result in false positive results, the DVC method is best suited to analysis of waters in which the number of different types of organisms present in the same sample is assumed to be small, such as processed waters. The advantages and disadvantages of each method are discussed. Author

N92-30368# Arizona State Univ., Tempe.
PHOTOINITIATED ELECTRON TRANSFER IN MULTICHROMOPHORIC SPECIES: SYNTHETIC TETRADS AND PENTADS FEATURING DIQUINONE MOIETIES
30 Apr. 1992 15 p
(Contract DE-FG02-87ER-13791)
(DE92-013472; DOE/ER-13791/37) Avail: CASI HC A03/MF A01

This project involves the design, synthesis, and photophysical study of complex molecular systems engineered to achieve long lived charge separated states by a biomimetic, photoinitiated multistep electron transfer process. The use of these artificial systems to investigate different electron and energy transfer strategies allow the evolution of more efficient molecular devices for the gathering of light energy and its transformation into chemical potential energy. The three major aspects of the work emphasized in the initial proposal are: design and synthesis of molecular devices incorporating new quinone moieties; synthesis and spectroscopic studies of molecular tetrads and pentads featuring modified porphyrin-diquinone linkages; and new photochemical and photophysical investigations of tetrads and pentads, including the development of methods for harvesting the energy stored in long-lived charge separated states. DOE

N92-30531# Pennsylvania State Univ., University Park. Dept. of Chemistry.
VOLTAMMETRIC MEASUREMENT OF OXYGEN IN SINGLE NEURONS USING PLATINIZED CARBON RING ELECTRODES
Yau Y. Lau, Takayuki Abe, and Andrew G. Ewing 10 Jan. 1992 23 p
(Contract N00014-90-J-1161)
(AD-A252191; TR-011) Avail: CASI HC A02/MF A01

Nafion-coated ultrasmall platinum ring electrodes have been implanted in the giant dopamine neuron of the pond snail, Planorbis corneus, and the oxygen concentration inside these single neurons has been estimated. Experimental data suggest that the intracellular oxygen level in the identified dopamine neuron of Planorbis corneus is approximately 0.032 mM. The oxygen concentration immediately outside the cell (approx. 10 micro m away from the cell) is 0.041 mM. Furthermore, staircase voltammetry can be used to monitor dynamic changes in oxygen concentration inside the cell after bathing in Ringer's solution saturated with air/oxygen. Data obtained for intracellular oxygen concentrations suggest that intracellular oxygen consumption is increased following potassium chloride-induced stimulation of these cells. GRA

N92-30829# Nebraska Univ., Lincoln.
ELECTROCHEMICAL AND OPTICAL STUDIES OF MODEL PHOTOSYNTHETIC SYSTEMS
15 Jan. 1992 10 p
(Contract DE-FG02-84ER-13261)
(DE92-010657; DOE/ER-13261/6) Avail: CASI HC A02/MF A01

The objective of this research is to obtain a better understanding of the relationship between the structural organization of photosynthetic pigments and their spectroscopic and electrochemical properties. Defined model systems were studied first. These included the least ordered (solutions) through the most highly ordered (Langmuir-Blodgett (LB) monolayers and self-assembled monolayers) systems containing BChl, BPheo, and UQ. Molecules other than the photosynthetic pigments and quinones were also examined, including chromophores (i.e. surface active cyanine dyes and phthalocyanines) and redox active compounds (methyl viologen (MV) and surfactant ferrocenes), in order to develop the techniques needed to study the photosynthetic components. Because the chlorophylls are photosensitive and labile, it was easier first to develop procedures using stable species. Three different techniques were used to characterize these model systems. These included electrochemical techniques for determining the standard oxidation and reduction potentials of the photosynthetic components as well as methods for determining the heterogeneous electron transfer rate constants for BChl and BPheo at metal electrodes (Pt and Au). Resonance Raman (RR) and surface enhanced resonance Raman (SERR) spectroscopy were used to determine the spectra of the photosynthetic pigments and model compounds. SERRS was also used to study several types of photosynthetic preparations. DOE

N92-31152# Norwegian Defence Research Establishment, Kjeller.
THE PROPERTIES OF THE UPTAKE SYSTEM FOR GLYCINE IN SYNAPTIC VESICLES Thesis
Hege Christensen 20 May 1992 71 p
(ISSN-0800-4412; NDRE/PUBL-92/1001) Avail: CASI HC A04/MF A01

The present study provides evidence for the presence of a temperature sensitive and energy dependent uptake mechanism for glycine in synaptic vesicles isolated from rat spinal cord. The in vitro uptake of glycine in synaptic vesicles was driven by an electrochemical proton gradient generated by a Mg(sup 2+)-ATPase in the vesicle membrane. The properties of the vesicular uptake of glycine in spinal cord were clearly different from those of the plasma membrane uptake of glycine, both with respect to Na(+), Mg(sup 2+) and ATP dependence and the developmental time course. Surprisingly glycine was also taken up by vesicles from whole brain, including cerebral cortex, and the GABA/glycine uptake ratios in different brain regions and spinal cord were similar and very different from the corresponding synaptosomal uptake ratios. These results indicate that glycine was taken up by non-glycinergic vesicles, and the finding that glycine and GABA competitively inhibited each others uptake into vesicles from brain and spinal cord, indicates that GABA and glycine

may be taken up by the same vesicle population. Uptake of glutamate, GABA and glycine in synaptic vesicles from CNS was shown to increase during development, probably in parallel with synaptogenesis, and this indicates a functional role of uptake of the three amino acids by synaptic vesicles in the nerve terminals.
Author

52 AEROSPACE MEDICINE

Includes physiological factors; biological effects of radiation; and effects of weightlessness on man and animals.

N92-30319# Dalhousie Univ., Halifax (Nova Scotia). Dept. of Psychology.
NEUROPHYSIOLOGICAL ANALYSIS OF CIRCADIAN RHYTHM ENTRAINMENT Annual Report, 1 Jan. - 31 Dec. 1991
Benjamin Rusak 31 Dec. 1991 6 p
(Grant AF-AFOSR-0104-90)
(AD-A248466; AFOSR-92-0187TR) Avail: CASI HC A02/MF A01

During the 1991 contract period we published papers on the effects of clorgyline treatment on photic responses of neurons in the circadian entrainment pathway, and on the effects of NMDA neurotransmitter antagonists on photic activation of gene expression in the entrainment pathway. We have completed further studies on regulation of messenger RNA levels for several immediate-early genes (IEG) in suprachiasmatic nucleus (SCN) cells in response to light pulses and on the effects of a non-NMDA antagonist on IEG expression in the SCN; the related manuscripts were accepted for publication. Further studies were completed and submitted for publication or are currently in preparation. These include studies on the following: the effects of different temporal patterns of light exposure on SCN cells and on rhythm phase-shifting; antagonism by serotonin of light effects on cells in the circadian system; the effects of bombesin-like peptides on SCN neuronal activity; the effects of several excitatory amino acids on SCN cells in vitro; the regulation of the melatonin sensitivity rhythm of SCN cells; and the roles of nerve growth factor and muscarinic receptor antagonists in modifying circadian responses to cholinergic agents. The results of these studies were either submitted for publication or are in preparation. GRA

N92-30328# Army Research Inst. of Environmental Medicine, Natick, MA.
THE USE OF TYMPANOMETRY TO DETECT AEROTITIS MEDIA IN HYPOBARIC CHAMBER OPERATIONS Final Report
V. A. Forte, Jr., J. A. Devine, P. B. Rock, and A. Cymerman 31 Jan. 1992 31 p
(AD-A248963) Avail: CASI HC A03/MF A01

Diagnosis and quantification of aerotitis media were performed using a modified commercially-available tympanometer under hypobaric conditions. Subjects were 22 males and 9 females, 22-43 years of age who were tested in each ear with the tympanometer prior to and after exposure, sequentially at the barometric pressure plateaus of 706, 656, 609, 586, 564, and 522 mm Hg, and following an induced ear block during a 1-min descent from 522 to 586 mm Hg. Each Subject was examined once either alone or in pairs during a 90-min exposure. Aerotitis media was detected using tympanometry at simulated altitude as indicated by the difference between measurements made prior to, and during, induced ear blocks as well as following relief of the pressure differential with a Valsalva maneuver. There were no significant differences between pre-and post-hypobaria. Our study suggests that tympanometry can be a valuable tool in managing aerotitis media in the aeromedical environment. GRA

N92-30376# Texas A&M Univ., College Station. Dept. of Biology.
MELATONIN, THE PINEAL GLAND AND CIRCADIAN RHYTHMS Annual Report, 1 Mar. 1991 - 30 Apr. 1992
Vincent M. Cassone 30 Apr. 1992 4 p
(Grant AF-AFOSR-0244-90)
(AD-A250640; AFOSR-92-0413TR) Avail: CASI HC A01/MF A01

This research tests the null hypothesis that the restricted phase of melatonin sensitivity in rats is at least partially due to a coincidence of the time at which exogenous melatonin is administered and the time at which endogenous melatonin begins to rise. Results suggest that the cerebral moiety responding to melatonin (presumably the SCN) responds to it quantally within a very restricted phase, and that this effect is independent of the pineal gland. Pinealectomy had no effect on the binding pattern, affinity or capacity within either the SCN or the pars tuberalis.
GRA

N92-30523# Southeastern Center for Electrical Engineering Education, Inc., Saint Cloud, FL.
OPTIMAL ECG ELECTRODE SITES AND CRITERIA FOR DETECTION OF ASYMPTOMATIC CORONARY ARTERY DISEASE, UPDATE 1990. MULTILEAD ECG CHANGES AT REST, WITH EXERCISE, AND WITH CORONARY ANGIOPLASTY Final Report, 1 Jun. 1989 - 15 Dec. 1990
Ronald H. Selvester, Joseph C. Solomon, Kessag Baron, Helge A. Saetre, and Myrvin H. Ellestad Feb. 1992 62 p Prepared in cooperation with University of Southern California, Downey and Memorial Heart Inst., Long Beach, CA
(Contract F33615-87-D-0609)
(AD-A248613; AL-TR-1991-0029) Avail: CASI HC A04/MF A01

This report presents recent findings from the Selvester-Solomon forward model of the electrophysiology of the human heart simulating infarct and ischemia. This led to a study of a 16-lead ECG at the time of coronary angioplasty. Both the simulations and the angioplasty study (reported in detail in this report) provide evidence that routine screening of apparently healthy aircrews with Hi-Fi rest and exercise 30 lead ECGs will significantly improve the detection of asymptomatic coronary disease. Three ECG recording systems with signal processing of 30 simultaneous leads (30SL) have been developed. These systems record and store on disk up to 2 hr of continuous 3 lead rhythm strips and 10 s epochs of 30SL median beats sampled at 1 ms. Design documents, flow diagrams, schematics, and safety documentation for the 3 ECG mapping systems, and for 3 electrode locator systems designed and fabricated on this contract, are provided. The design of the study at Long Beach Memorial and Armstrong Laboratory is also presented for the follow-on 1 year's contract using 30SL data during exercise (and angioplasty) to define the optimal number of leads and criteria in them for the optimal detection of asymptomatic coronary disease in aircrew persons. GRA

N92-30603# Naval Health Research Center, San Diego, CA.
FEASIBILITY OF A WALK TEST TO ASSESS THE CARDIORESPIRATORY FITNESS OF NAVAL PERSONNEL Final Report
John Pleas and Linda T. Stevens Aug. 1991 17 p
(AD-A250650; NHRC-91-28) Avail: CASI HC A03/MF A01

The feasibility of using a cost-efficient walk test to assess cardiorespiratory fitness among Navy personnel was the major focus of this paper. Studies assessing the ability of pulse rate and 1- and 2-mile timed distance walks to predict maximum oxygen consumption (VO2 max) were reviewed and prediction equations generated from multiple regression analyses were examined. Research findings indicate that a walk test provides a reasonable reliable estimate of VO2 max in a field setting. The strongest evidence in this regard was provided by Kline and colleagues at the University of Massachusetts who developed an equation to estimate VO2 max based on five factors: time to complete a 1-mile walk, average heart rate for the fourth quarter of the mile walk, age, weight and sex. The correlations between measured VO2 max and estimated VO2 max was r=.93 (SE=.325 1/min) when oxygen consumption was not adjusted for body weight and r=.88 (SE=5.0 1/kg min) when oxygen consumption was adjusted for body weight. Correlations ranging from .74 to .93 were obtained in diverse cross-validation groups. Based on a review of the fitness

walking literature, it was concluded that a 1-mile walk test is a valid indicator of cardiorespiratory fitness in the general population. GRA

N92-30605# Aerospace Medical Research Labs., Brooks AFB, TX.
EFFECTS OF PYRIDOSTIGMINE BROMIDE ON A-10 PILOTS DURING EXECUTION OF A SIMULATED MISSION; PERFORMANCE Final Report, Jul. 1984 - Aug. 1991
Rebecca B. Brooks, David C. Hubbard, Samuel G. Schiflett, Robert R. Woodruff, and Arthur E. Harriman May 1992 43 p
(AD-A252309; AL-TR-1992-0005) Avail: CASI HC A03/MF A01

This report documents the performance results of a study that was conducted to determine the effects of pyridostigmine bromide (PYB) (30 mg 3x/day) on pilot performance. Data was collected in an A-10 flight simulator with an Advanced Visual Technology System (AVTS). The subjects were 24 A-10 pilots who were trained on the following simulated tasks over three 55-min sessions: takeoff, patterns, emergency procedure, and landing; air-to-air refueling; conventional low-angle strafing; and low-level ingress to a simulated target and threat area (RED FLAG). Next, during two test sessions, 48 h apart, the pilots were tested using a double-blind procedure on the same tasks in a PYB condition and in a placebo condition. In the two test sessions, 12 of the pilots wore chemical defense ensembles (CDE) and the other 12 wore standard flight gear (SFG). The results indicate that there are no operationally significant effects of pyridostigmine bromide that would preclude an A-10 pilot from accomplishing a tactical mission, including air-to-ground attack, under a chemical warfare threat. GRA

N92-30644# Naval Health Research Center, San Diego, CA.
EXERCISE BEHAVIOR AMONG NAVY RUNNERS AND NON-RUNNERS Final Report
John Pleas Dec. 1991 31 p
(AD-A250651; NHRC-91-43) Avail: CASI HC A03/MF A01

It is generally believed that running is the royal road to fitness. While this may be true for cardiorespiratory fitness, data are unavailable on whether this statement applies to overall fitness. The present study examined physical fitness classifications and the self-reported exercise patterns, weekly kilocalorie expenditure, and social support scores of Navy personnel who either ran, walked, did both or did neither for exercise. Results indicated that runners not only fell into higher fitness categories and expended more kilocalories each week in exercise, but reported higher frequency and duration of exercise, longer involvement in all types of exercise, and greater social support. It is possible that the runners represented a select group of highly motivated fitness-oriented individuals who ascribed to the physical concepts promulgated by the Navy. However, the number of individuals failing the physical readiness test and receiving satisfactory fitness classification remains a physical readiness concern. Consequently, research on short-term and long-term exercise adherence strategies and the role of specific exercise support and general support in facilitating exercise behavior is warranted. GRA

N92-30719# Texas Univ., Galveston. Medical Branch.
SECRETORY MECHANISMS IN OPIOCORTIN CELLS DURING COLD STRESS Final Report, 1 Aug. 1987 - 30 Sep. 1991
Gwen V. Childs 15 Jun. 1992 15 p
(Contract N00014-88-K-0016; NR Proj. RR0-4108)
(AD-A252317) Avail: CASI HC A03/MF A01

The goals of the study were to characterize the sequence of events involved in the hypothalamic-pituitary responses to cold stress. In the hypothalamus, studies focused on Arginine vasopressin neurons and changes in expression of mRNA following cold and novel environment exposure. In the pituitary, studies focused on AVP and CRH target cells, including corticotropes, thyrotropes, and intermediate lobe cells. Changes in size, granulation, expression of mRNA, and binding sites for AVP and CRH were detected. In vitro studies of second messenger effects on CRH and AVP binding provided more clues about mechanisms of action. Finally, a new cell type that changed to a multihormonal corticothyrotrope under the influence of AVP was described. It could provide an efficient means of stimulating both the thyroid and the adrenal. Studies implicating locally produced epidermal growth factor (EGF) as another modulatory agent in the stress response were also done because EGF stimulates corticotropes. Cells producing EGF increased expression of EGF mRNA after exposure to cold. In summary, these studies identified four critical hormones that interact with each other in the control of pituitary responses to cold. These included: AVP, CRH, throtropin in releasing hormone (TRH) and epidermal growth factor. GRA

N92-30745# Cleveland Metropolitan General Hospital, OH. Div. of Cardiology.
TOLERANCE OF BETA BLOCKED HYPERTENSIVES DURING ORTHOSTATIC AND ALTITUDE STRESSES
Steven M. Teague and Jerry R. Hordinsky Apr. 1992 36 p
(Contract DTFA02-86-85098)
(AD-A249904; DOT/FAA/AM-92/19) Avail: CASI HC A03/MF A01

To evaluate the effects of orthostatic, attitude, and pharmacologic stresses upon civil aviation-specific performance, a double-blind, randomized, crossover trial of atenolol, 100mg, was designed and executed. Hypertensive males and females qualifying for the FAA class 3 certificate with mean age of 34 were studied during simulated attitude exposure to 12,500 ft, orthostatic stress, and moderate exercise. Seated lower body negative pressure to -40 mmHg supplied orthostatic stress simulating +2G vertical acceleration. A total of 160 lower body negative pressure tests were performed, 80 at ground and 80 at altitude. Beta-blockade caused a modest impairment in orthostatic tolerance. Five of the 80 lower body negative pressure runs at ground level were marked by intolerance, and all of those responses were in beta-blocked subjects. Of the 80 attitude runs, 30 were terminated for intolerance, of which 18 included beta-blockade. These findings had a Chi-square significance value of P less than .05. The effect of altitude was significant at P less than .01. In a modest exercise protocol (100 watts for 3 minutes) meant to be no more stressful than the exertional requirements of piloting an aircraft during adverse conditions, neither beta-blockade or altitude appeared to limit performance. Quantitative performance on a computerized cognitive battery clearly demonstrated impaired performance during lower body negative pressure stress at altitude. The degree of impairment was significant compared to a learning curve response at the P less than .001 level. The degree of impairment was similar for placebo treated and beta-blocked subjects. GRA

N92-30987* National Aeronautics and Space Administration, Washington, DC.
AEROSPACE MEDICINE AND BIOLOGY: A CONTINUING BIBLIOGRAPHY WITH INDEXES (SUPPLEMENT 363)
Jun. 1992 69 p
(NASA-SP-7011(363); NAS 1.21:7011(363)) Avail: CASI HC A04/MF A01

This bibliography lists 164 reports, articles and other documents introduced into the NASA Scientific and Technical Information System during Jan. 1992. Subject coverage includes aerospace medicine and physiology, life support systems and man/system technology, protective clothing, exobiology and extraterrestrial life, planetary biology, and flight crew behavior and performance. Author

N92-31011# Pacific Northwest Lab., Richland, WA.
THE REVISED INTERNATIONAL COMMISSION ON RADIOLOGICAL PROTECTION (ICRP) DOSIMETRIC MODEL FOR THE HUMAN RESPIRATORY TRACT
W. J. Bair May 1992 5 p Presented at the 8th International Radiation Protection Association World Congress, Vancouver, Ontario, 10-22 May 1992
(Contract DE-AC06-76RL-01830)
(DE92-015092; PNL-SA-20194; CONF-920501-16) Avail: CASI HC A01/MF A01

A task group has revised the dosimetric model of the respiratory

tract used to calculate annual limits on intake of radionuclides. The revised model can be used to project respiratory tract doses for workers and members of the public from airborne radionuclides and to assess past exposures. Doses calculated for specific extrathoracic and thoracic tissues can be adjusted to account for differences in radiosensitivity and summed to yield two values of dose for the respiratory tract that are applicable to the ICRP tissue weighted dosimetry system. DOE

N92-31127# Space and Naval Warfare Systems Command, Washington, DC.
EFFECTS OF MICROWAVE RADIATION ON HUMANS: MONKEYS EXPOSED TO 1.25 GHz PULSED MICROWAVES Final Report, 1 May 1988 - 30 Dec. 1991
Henry Kues 13 Mar. 1992 28 p
(DA Proj. 3M1-61102-BS-15)
(AD-A249997) Avail: CASI HC A03/MF A01

This report is divided into 4 sections: general diagnostic evaluation; fluorophotometry; electroretinography; and histopathologic evaluation. At the end of the report, the results of all aspects of this study are summarized and discussed, and the findings are related to the exposure system. There is also a discussion of these findings in relation to recent observations on humans exposed to microwave radiation. GRA

N92-31143# Virginia Univ., Charlottesville. Dept. of Biology.
CONTROL OF CIRCADIAN BEHAVIOR BY TRANSPLANTED SUPRACHIASMATIC NUCLEI Annual Report, 15 Nov. 1990 - 15 Aug. 1991
Michael Menaker 15 Aug. 1991 4 p
(Grant AF-AFOSR-0098-90)
(AD-A250442; AFOSR-92-0410TR) Avail: CASI HC A01/MF A01

A genetic mutation was found that alters the free running period of the locomotor activity rhythm from the wild-type value of approximately 24 hours to approximately 20 hours in homozygous mutants. Our data suggest the existence of two qualitatively different rhythmic outputs from the circadian oscillators contained with the SCN. One of these outputs stimulates the expression of locomotor activity producing activity rhythm's (which are seen within), and the other suppresses the expression of activity, restricting its appearance to a temporally defined window and thereby defining the boundaries of p'. The idea that one function of a circadian output from the SCN is to suppress activity is novel. GRA

N92-31167*# National Aeronautics and Space Administration. Ames Research Center, Moffett Field, CA.
LIGHT AS A CHRONOBIOLOGIC COUNTERMEASURE FOR LONG-DURATION SPACE OPERATIONS
Alexander Samel, ed., Philippa Gander, ed. (San Jose State Univ., Moffett Field, CA.), Julie Evans, R. Curtis Graeber (Deutsche Forschungsanstalt fuer Luft- und Raumfahrt, Cologne, Germany, F.R.), Elizabeth Hackett (San Jose State Univ., CA.), Lanny Keil, Hartmut Maab (Deutsche Forschungsanstalt fuer Luft- und Raumfahrt, Cologne, Germany, F.R.), Wolfgang Raabe (Deutsche Forschungsanstalt fuer Luft- und Raumfahrt, Cologne, Germany, F.R.), Mark Rosekind (Stanford Univ., Palo Alto, CA.), and Mike Rountree (Stanford Univ., Palo Alto, CA.) et al Dec. 1991 74 p
(RTOP 505-64-13)
(NASA-TM-103874; A-91186; NAS 1.15:103874) Avail: CASI HC A04/MF A01

Long-duration space missions require adaptation to work-rest schedules which are substantially shifted with respect to earth. Astronauts are expected to work in two-shift operations and the environmental synchronizers (zeitgebers) in a spacecraft differ significantly from those on earth. A study on circadian rhythms, sleep, and performance was conducted by exposing four subjects to 6 deg head-down tilt bedrest (to simulate the effects of the weightless condition) and imposing a 12-h shift (6 h delay per day for two days). Bright light was tested in a cross-over design as a countermeasure for achieving faster resynchronization and regaining stable conditions for sleep and circadian rhythmicity. Data collection included objective sleep recording, temperature, heart rate, and excretion of hormones and electrolytes as well as performance and responses to questionnaires. Even without a shift in the sleep-wake cycle, the sleep quantity, circadian amplitudes and 24 h means decreased in many functions under bedrest conditions. During the shift days, sleepiness and fatigue increased, and alertness decreased. However, sleep quantity was regained, and resynchronization was completed within seven days after the shift for almost all functions, irrespective of whether light was administered during day-time or night-time hours. The time of day of light exposure surprisingly appeared not to have a discriminatory effect on the resynchronization speed under shift and bedrest conditions. The results indicate that simulated weightlessness alters circadian rhythms and sleep, and that schedule changes induce additional physiological disruption with decreased subjective alertness and increased fatigue. Because of their operational implications, these phenomena deserve additional investigation. Author

53 BEHAVIORAL SCIENCES

Includes psychological factors; individual and group behavior; crew training and evaluation; and psychiatric research.

N92-30254# Logicon Technical Services, Inc., Dayton, OH.
REVIEW OF PSYCHOPHYSICALLY-BASED IMAGE QUALITY METRICS Final Report, Jun. 1990 - May 1991
Jennie J. Gallimore Sep. 1991 47 p Prepared in cooperation with Wright State Univ., Dayton, OH
(Contract F33615-89-C-0532)
(AD-A251053; AL-TR-1991-0153) Avail: CASI HC A03/MF A01

There have been many advances in imaging technologies resulting in a variety of techniques for generation, coding for transmission, image processing, decoding, and display of information. In addition to the development of techniques, investigators have recognized the need for quantitative measures of image distortion and/or image quality corresponding to observer performance and observer impressions of the images. The purpose of this report is to review current psychophysically based measures of image quality for possible application to compressed or transmitted sensory imagery. This report briefly reviews human vision models, image quality metrics, empirical modelling approaches to image quality, discusses current research needs, and provides recommendations for immediate application to compressed digital images. GRA

N92-30306*# Bolt, Beranek, and Newman, Inc., Cambridge, MA. Systems and Technologies.
A PRINCIPLED APPROACH TO THE MEASUREMENT OF SITUATION AWARENESS IN COMMERCIAL AVIATION
Yvette J. Tenney, Marilyn Jager Adams, Richard W. Pew, A. W. F. Huggins, and William H. Rogers Washington NASA Jul. 1992 32 p
(Contract NAS1-18788; RTOP 505-64-13-21)
(NASA-CR-4451; NAS 1.26:4451; BBN-7451) Avail: CASI HC A03/MF A01

The issue of how to support situation awareness among crews of modern commercial aircraft is becoming especially important with the introduction of automation in the form of sophisticated flight management computers and expert systems designed to assist the crew. In this paper, cognitive theories are discussed that have relevance for the definition and measurement of situation awareness. These theories suggest that comprehension of the flow of events is an active process that is limited by the modularity of attention and memory constraints, but can be enhanced by expert knowledge and strategies. Three implications of this perspective for assessing and improving situation awareness are considered: (1) Scenario variations are proposed that tax awareness by placing demands on attention; (2) Experimental tasks and probes are described for assessing the cognitive processes

that underlie situation awareness; and (3) The use of computer-based human performance models to augment the measures of situation awareness derived from performance data is explored. Finally, two potential example applications of the proposed assessment techniques are described, one concerning spatial awareness using wide field of view displays and the other emphasizing fault management in aircraft systems. Author

N92-30320# Texas Univ., Houston. Dept. of Neurobiology and Anatomy.
ANALYSIS AND SYNTHESIS OF ADAPTIVE NEURAL ELEMENTS AND ASSEMBLES Annual Report, 1 Oct. 1990 - 30 Sep. 1991
John H. Byrne 17 Feb. 1992 15 p
(Grant AF-AFOSR-0027-91)
(AD-A248467; AFOSR-92-0212TR) Avail: CASI HC A03/MF A01

Between 1 Oct. 1990 and 30 Sep. 1991, progress was made in six areas. First, voltage-clamp experiments investigated the modulation of the voltage-dependent K(+) current (IK,v) by serotonin (5-HT). Second, a computer program that is a general-purpose Simulator for Neural Networks and Action Potentials (SNNAP) was developed. Third, extensions were made to the single-cell model of associative learning by incorporating Hodgkin-Huxley type membrane currents, descriptions of the modulation of membrane currents by 5-HT, and a model of intracellular Ca2(+) diffusion. Fourth, SNNAP was used to investigate the role of interneurons in determining the intensity and duration of motor neuron responses that mediate the tail-withdrawal reflex. Fifth, experiments characterized the synaptic interactions among the neurons of a central pattern generator (CPG) that underlies aspects of feeding behavior. Sixth, SNNAP was used to begin simulating the neurons and synaptic connections of the feeding CPG. In addition, work on the model of the bursting neuron R15 was completed. GRA

N92-30325# North Carolina Univ., Chapel Hill.
SPATIOTEMPORAL CHARACTERISTICS OF HUMAN VISUAL LOCALIZATION Final Report, 1 Oct. 1990 - 31 Dec. 1991
Christina A. Burbeck 28 Feb. 1992 62 p
(Grant AF-AFOSR-0058-91)
(AD-A248494; AFOSR-92-0203TR) Avail: CASI HC A04/MF A01

Psychophysical studies of the processes underlying relative localization in human vision were conducted. Specifically, the focus of this granting period was characterizing the spatial characteristics of the units that encode spatial location. Evidence was found for a higher-order scaled representation of position in which the size of position integration areas scales with the distance being encoded. This scaling of the position integration areas was found to account well for the increase in separation discrimination thresholds with increasing separation. The position integration areas were shown not to integrate luminance, but were shown to depend on an initial spatial organization of the scene. The time course of the position integration was also investigated. Additional studies investigated the relationship between position integration and the Muller-Lyer illusion, and the effect of the spatial frequency of a masking stimulus (presented at termination of the separation discrimination stimulus) on separation discrimination thresholds. GRA

N92-30336# Stanford Univ., CA. Dept. of Psychology.
INDUCED PICTORIAL REPRESENTATIONS Annual Technical Report, 1 Feb. 1991 - 31 Jan. 1992
Barbara G. Tversky 28 Feb. 1992 11 p
(Grant AF-AFOSR-0076-89)
(AD-A248560; AFOSR-92-0231TR) Avail: CASI HC A03/MF A01

On many occasions, such as giving directions, spatial situations are described in words rather than depicted. In comprehending such descriptions, people form mental representations of the situation described by the discourse as well as representations of the text. This project investigates spatial mental models induced by words for large-scale and for immediate environments. The results simultaneously elucidate spatial thinking, text comprehension, and text construction. The experiments using large-scale environments focus on the comprehension and production of various kinds of descriptive text. The experiments using immediate environments focus on on-line use of spatial mental models and updating under changes in point of view. New research is expanding both projects, including investigations of construction of mental models. GRA

N92-30488# Federal Aviation Administration, Atlantic City, NJ.
TECHNICAL TRAINING FOR NATIONAL SIMULATOR EVALUATION SPECIALIST
Theos D. McKinney, Jr. Jun. 1992 36 p
(NASA-CR-190429; NAS 1.26:190429; DOT/FAA/CT-TN92/14)
Avail: CASI HC A03/MF A01

The technical training needs of the Federal Aviation Administration (FAA) specialists who evaluate and qualify FAA recognized flight training simulators and devices are examined. The need for this training is established, and sources and methodologies are recommended for initial, maintenance, and update courses. Author

N92-30613# Hahnemann Medical Coll. and Hospital, Philadelphia, PA. Dept. of Physiology and Biophysics.
CORTICAL MECHANISMS OF ATTENTION, DISCRIMINATION, AND MOTOR RESPONSE TO SOMAESTHETIC STIMULI Annual Report, 1 Apr. 1990 - 31 Mar. 1991
John K. Chapin 1 Dec. 1991 7 p
(Grant AF-AFOSR-0266-90)
(AD-A247228; AFOSR-92-0108TR) Avail: CASI HC A02/MF A01

The overall aim of this research is to investigate the neural circuit mechanisms of attentional and discriminative processing of somatosensory stimuli which are cues for limb movement. These issues are being addressed mainly through use of multi-single neuron recording techniques, which we have recently developed. In the past granting period this approach has been used to record from ensembles of single neurons through microwire electrode arrays chronically implanted in the forepaw/forelimb areas of the somatosensory (SI) and motor (MI) cortices in awake behaving rats. These animals are trained to place their forepaw on a bar and move it up or down immediately upon detecting a vibratory stimulus imposed on the bar. Initially, only neurons in the SI responded to the sensory cue. After the rat learned to perform to criterion in the task, however, neurons in the MI cortex also responded at relatively short latency to the sensory cue. This suggests that transmission through a trans-cortical sensorimotor loop can be enhanced through training. Additional progress has been made on several other projects which provide necessary background information for this investigation. GRA

N92-30679# Harvard Univ., Cambridge, MA.
PSYCHOPHYSICAL STUDIES OF VISUAL CORTICAL FUNCTION Final Technical Report, 1 Sep. 1988 - 31 Aug. 1991
Ken Nakayama 12 Jan. 1992 7 p
(Grant AF-AFOSR-0330-90)
(AD-A246962; AFOSR-92-0096TR) Avail: CASI HC A02/MF A01

Our goal was to understand visual cortical function using psychophysical techniques. In particular, we examined visual attention, visual search, visual surface representation, and color filling-in. In visual attention, we found evidence to suggest two components of focal attention, a transient and a sustained process. We also provided evidence for the role of attention in saccadic eye movements by showing rapid deployment of attention in the gap paradigm. In visual search, we found a particular situation where increasing distractor number led to decreasing reaction times, suggesting a different role for attention in such tasks. In visual surface representation, we outlined the role of surface encoding (border ownership, modal and amodal completion, transparency) in many visual tasks. From these studies we

postulated the principle of generic image sampling, a hypothesis which provides a geometric tool to understand visual surface learning. We also have investigated the perception of depth from unpaired points (DaVinci stereopsis), showing that such points lead to depth and subjective contours. In color filling-in, we have explored spatial-temporal dynamics and have created a neural model. GRA

54 MAN/SYSTEM TECHNOLOGY AND LIFE SUPPORT

Includes human engineering; biotechnology; and space suits and protective clothing.

For related information see also *16 Space Transportation.*

N92-30381*# National Aeronautics and Space Administration. Marshall Space Flight Center, Huntsville, AL.
ASSESSMENT OF A HEAD-MOUNTED MINIATURE MONITOR Final Report
J. P. Hale, II Jun. 1992 32 p
(Proj. 89-07)
(NASA-TM-103587; NAS 1.15:103587) Avail: CASI HC A03/MF A01

Two experiments were conducted to assess the capabilities and limitations of the Private Eye, a miniature, head-mounted monitor. The first experiment compared the Private Eye with a cathode ray tube (CRT) and hard copy in both a constrained and unconstrained work envelope. The task was a simulated maintenance and assembly task that required frequent reference to the displayed information. A main effect of presentation media indicated faster placement times using the CRT as compared with hard copy. There were no significant differences between the Private Eye and either the CRT or hard copy for identification, placement, or total task times. The goal of the second experiment was to determine the effects of various local visual parameters on the ability of the user to accurately perceive the information of the Private Eye. The task was an interactive video game. No significant performance differences were found under either bright or dark ambient illumination environments nor with either visually simple or complex task backgrounds. Glare reflected off of the bezel surrounding the monitor did degrade performance. It was concluded that this head-mounted, miniature monitor could serve a useful role for in situ operations, especially in microgravity environments. Author

N92-30592# Aeronautical Systems Div., Wright-Patterson AFB, OH.
KC-135 CREW REDUCTION FEASIBILITY DEMONSTRATION SIMULATION STUDY. VOLUME 1: FUNCTION ANALYSIS AND FUNCTION REALLOCATION Final Report, Oct. 1990 - Jan. 1991
G. F. Ward, Ross A. Dudley, John A. Hassoun, Edward R. Hughes, and Justin D. Rueb Jun. 1991 123 p
(AD-A252265; ASD-TR-91-5005-Vol-1) Avail: CASI HC A06/MF A01

A function analysis of the four-person crew KC-135 and function reallocation to a three-person crew were completed in support of the KC-135 Avionics Modernization Program. This report is volume one of a three-volume technical report. This effort provided a distribution of functions between automation concepts and the remaining three crewmembers. The function redistribution and automation concepts served as a baseline for a crew station design group to design a cockpit configuration for a three-person crew KC-135 (Vol 2). This configuration was then implemented in a simulator at the Crew Station Evaluation Facility (CSEF) for a comprehensive man-in-the-loop simulation evaluation (Vol 3). The function analysis and reallocation were the first step towards modifying the KC-135 cockpit and will be instrumental in future KC-135 efforts. GRA

N92-30615# Naval Research Lab., Washington, DC.
EYE/SENSOR PROTECTION AGAINST LASER IRRADIATION ABLATIVE MIRROR DEVICES: A MATERIALS ASSESSMENT
Michael E. Boyle, Robert F. Cozzens, and Douglas B. Chrisey 17 Apr. 1992 50 p
(AD-A248787; NRL/MR/4440-92-6964) Avail: CASI HC A03/MF A01

The potential of the ablative mirror concept as an eye/sensor protection system is assessed from a materials science perspective. Realistic operating parameters for the ablative mirror device are determined through examinations of the critical device components. Using these operational parameters and a derived model of laser-surface interactions, the response of different mirror materials is examined. Based on the measured material responses from research literature and our calculated values, we conclude that the ablative mirror concept is not a feasible method of eye protection using typical mirror materials (assuming a device optical gain of 105 and a minimum material reflectivity of 70 percent). Analysis of the interaction between laser irradiation and material surfaces resulted in the identification of a number of important material parameters that can be used to guide material development and identify promising new mirror materials. Areas for future research are also suggested. GRA

N92-30718# Naval Postgraduate School, Monterey, CA.
INTRODUCTION TO HUMAN FACTORS AND WIDE AREA NETWORKING M.S. Thesis
John G. Clarke Mar. 1992 122 p
(AD-A252310) Avail: CASI HC A06/MF A02

The Human-Systems Interaction Course taught at the Naval Postgraduate School is an introduction to the human-systems interface, that part of the system which the human uses to provide input to and receive feedback from the system. This thesis will provide a basic introduction to those which must be considered when designing today's complex military systems. Additionally, this thesis will provide an introduction to the Internet - a worldwide network of computers and smaller networks. Students will use the Internet to gather information, access remote programs, and communicate with other personnel around the world. This is only an introduction to both of these complex topics. GRA

N92-30844# Biodynamic Research Corp., San Antonio, TX.
ADAPTING THE ADAM MANIKIN TECHNOLOGY FOR INJURY PROBABILITY ASSESSMENT Final Report, 5 Jul. 1991 - 19 Feb. 1992
J. H. Raddin, Jr., W. R. Scott, J. B. Bomar, H. L. Smith, and J. V. Benedict 19 Feb. 1992 251 p
(Contract F41624-91-C-6003)
(AD-A252332; AL-TR-1992-0062) Avail: CASI HC A12/MF A03

An approach is presented for the general definition of regional injury human impact criteria with particular attention to the articulated ADAM test manikin and the escape environment. A review of literature and ejection injury data confirmed that injuries of greatest interest were those to the head, neck, thoracolumbar spine, and proximal extremities. A substantial literature review was pursued, demonstrating consistent findings of strain rate-dependent injury behavior over a wide range of injury types and body regions. Building upon previous work on the Dynamic Response Index, a comprehensive proposal is advanced for the conceptual definition of regional viscoelastic strain models for injury probability assessment. The proposed form for a head injury criterion assesses both translation and angular acceleration stress in terms of viscoelastic strain while also incorporating a means to account for their interaction. The neck criterion is based on a viscoelastic strain model of axial stress in association with shear and moment effects. The thoracolumbar spine criterion also proposes an extension of the prior DRI approach to account for interacting effects of moments and shear stresses. Approaches for the proximal extremities are formulated in a similar fashion. An outline is proposed for quantitative formulation and validation of the concept. GRA

N92-31166*# National Aeronautics and Space Administration. Ames Research Center, Moffett Field, CA.
WASTE STREAMS IN A TYPICAL CREWED SPACE HABITAT: AN UPDATE
M. A. Golub and T. Wydeven Feb. 1992 15 p
(RTOP 591-34-31)
(NASA-TM-103888; A-91224; NAS 1.15:103888) Avail: CASI HC A03/MF A01

A compilation of generation rates and chemical compositions of potential waste streams in a typical crewed space habitat, reported in a prior NASA Technical Memorandum and a related journal article, was updated. This report augments that compilation by the inclusion of the following new data: those data uncovered since completion of the prior report; those obtained from Soviet literature relevant to life support issues; and those for various minor human body wastes not presented previously (saliva, flatus, hair, finger- and toenails, dried skin and skin secretions, tears, and semen), but included here for purposes of completeness. These waste streams complement those discussed previously: toilet waste (urine, feces, etc.), hygiene water (laundry, shower/handwash, dishwasher water and cleansing agents), trash, humidity condensate, perspiration and respiration water, trace contaminants, and dust generation. This report also reproduces the latest information on the environmental control and life support system design parameters for Space Station Freedom. Author

55 SPACE BIOLOGY

Includes exobiology; planetary biology; and extraterrestrial life.

No abstracts in this category.

59 MATHEMATICAL AND COMPUTER SCIENCES (GENERAL)

N92-30311*# Institute for Computer Applications in Science and Engineering, Hampton, VA.
COMPILER ANALYSIS FOR IRREGULAR PROBLEMS IN FORTRAN D Final Report
Reinhard vonHanxleden (Rice Univ., Houston, TX.), Ken Kennedy (Rice Univ., Houston, TX.), Charles Koelbel (Rice Univ., Houston, TX.), Raja Das, and Joel Saltz Jun. 1992 22 p Prepared for presentation at the 5th Workshop on Languages and Compilers for Parallel Computing, New Haven, CT, Aug. 1992 Submitted for publication
(Contract NAS1-18605; RTOP 505-90-52-01)
(NASA-CR-189664; ICASE-92-22; NAS 1.26:189664) Avail: CASI HC A03/MF A01

We developed a dataflow framework which provides a basis for rigorously defining strategies to make use of runtime preprocessing methods for distributed memory multiprocessors. In many programs, several loops access the same off-processor memory locations. Our runtime support gives us a mechanism for tracking and reusing copies of off-processor data. A key aspect of our compiler analysis strategy is to determine when it is safe to reuse copies of off-processor data. Another crucial function of the compiler analysis is to identify situations which allow runtime preprocessing overheads to be amortized. This dataflow analysis will make it possible to effectively use the results of interprocedural analysis in our efforts to reduce interprocessor communication and the need for runtime preprocessing. Author

N92-30489*# Institute for Computer Applications in Science and Engineering, Hampton, VA.
SEMIANNUAL FINAL REPORT, 1 OCTOBER 1991 - 31 MARCH 1992
May 1992 49 p
(Contract NAS1-18605; RTOP 505-90-52-01)
(NASA-CR-189660; NAS 1.26:189660) Avail: CASI HC A03/MF A01

A summary of research conducted at the Institute for Computer Applications in Science and Engineering in applied mathematics, numerical analysis, and computer science during the period 1 Oct. 1991 through 31 Mar. 1992 is presented. Author

N92-30600# Office of Science and Technology, Washington, DC.
GRAND CHALLENGES 1993: HIGH PERFORMANCE COMPUTING AND COMMUNICATIONS. A REPORT BY THE COMMITTEE ON PHYSICAL, MATHEMATICAL, AND ENGINEERING SCIENCES TO SUPPLEMENT THE PRESIDENT'S FISCAL YEAR 1993 BUDGET
Jan. 1992 80 p
(PB92-160530) Avail: CASI HC A05/MF A01

The report describes the Presidential initiative in High Performance Computing and Communications. This initiative is well-coordinated, interagency research and development effort designed to sustain and extend U.S. leadership in all advanced areas of computing and networking. The initiative, which represents over four years of planning, not only provides a farsighted vision for investment in technology but also recognizes the importance of human resources and applications that serve major national needs. GRA

N92-30907*# National Aeronautics and Space Administration. Langley Research Center, Hampton, VA.
DELAUNAY TRIANGULATION AND COMPUTATIONAL FLUID DYNAMICS MESHES
Mary-Anne K. Posenau and David M. Mount (Maryland Univ., College Park.) Aug. 1992 10 p Presented at the 4th Canadian Conference on Computational Geometry, Aug. 1992
(RTOP 505-90-53-02)
(NASA-TM-107663; NAS 1.15:107663) Avail: CASI HC A02/MF A01

In aerospace computational fluid dynamics (CFD) calculations, the Delaunay triangulation of suitable quadrilateral meshes can lead to unsuitable triangulated meshes. Here, we present case studies which illustrate the limitations of using structured grid generation methods which produce points in a curvilinear coordinate system for subsequent triangulations for CFD applications. We discuss conditions under which meshes of quadrilateral elements may not produce a Delaunay triangulation suitable for CFD calculations, particularly with regard to high aspect ratio, skewed quadrilateral elements. Author

60 COMPUTER OPERATIONS AND HARDWARE

Includes hardware for computer graphics, firmware, and data processing.

For components see *33 Electronics and Electrical Engineering.*

N92-30432# Universiteit Twente, Enschede (Netherlands). Tele-Informatics and Open Systems Group.
ON THE USE OF PRE-DEFINED IMPLEMENTATION CONSTRUCTS IN DISTRIBUTED SYSTEMS DESIGN
Luis FerreiraPires, Marten vanSinderen, and Chris A. Vissers Feb. 1992 13 p Presented at 3rd Workshop on Future Trends of Distributed Computing Systems in the 1990's, Taipei, China, 14-16 Apr. 1992 Sponsored in part by EEC
(Memo-INF-92-08; TIOS-92/08; ISSN-0924-3755; ETN-92-91782)
Copyright Avail: CASI HC A03/MF A01

The concept of Predefined Implementation Constructs (PDICs),

as a method for distributed system design, is introduced. The selection and use of PDICs is discussed and the applicability of this method is shown on the basis of a middle size design example: the implementation of a sliding window protocol. ESA

N92-30541*# National Aeronautics and Space Administration. Langley Research Center, Hampton, VA.
PRINTER PORT INTERFACE Patent Application
Jerry H. Tucker, inventor (to NASA) and Ann B. Yadlowsky, inventor (to NASA) (National Academy of Sciences - National Research Council, Hampton, VA.) 1 Jun. 1992 13 p
(NASA-Case-LAR-13950-1; NAS 1.71:LAR-13950-1; US-Patent-Appl-SN-891604) Avail: CASI HC A03/MF A01

A printer port interface is provided which converts the printer port on a personal computer to a general purpose bus so that a number of external devices or microprocessor peripheral integrated circuits may be connected to a personal computer via the printer port on the personal computer. This interface enables the printer port to emulate a simple 8 bit microprocessor. The interface device connects the external device to the personal computer and in write mode, received data from the personal computer, signals the external device to accept the information, and sends the data to the external device and in read mode signals the external device to provide data, receives data from the external device and sends the data in amounts which do not exceed the input limits of the printer port to the personal computer. NASA

N92-30564# Department of the Navy, Washington, DC.
LASER OPTICAL MOUSE Patent Application
Frank J. Snow, inventor (to Navy) 15 Aug. 1992 16 p
(AD-D015307; US-Patent-Appl-SN-756261; Navy-Case-73056) Avail: CASI HC A03/MF A01

An apparatus for determining distance coordinates along two orthogonal axes for a computer system, where the coordinates represent the position of a cursor on a screen of a display unit of the computer system is presented. The apparatus includes a pair of velocity detectors and an operating device such as a central processing unit (CPU). When the velocity detectors are moved by an operator, each of the velocity detectors detects velocities along a respective one of the orthogonal axes. The detected velocities are converted into moving distances representative of the coordinates through a calculation of the operating device. GRA

N92-30698# Universiteit Twente, Enschede (Netherlands). Dept. of Computer Science.
HIGH LEVEL SYNTHESIS OF CONTROLPATH MICROARCHITECTURES
A. J. W. M. tenBerg Dec. 1991 23 p
(Memo-INF-91-86; ISSN-0924-3755; ETN-92-91637) Copyright Avail: CASI HC A03/MF A01

A synthesis strategy for the construction of the optimal microarchitecture for a controlpath of an instruction set processor is presented. Input to the system is the behavioral specification of a controlpath. This specification is in the finite state machine from which it is mapped initially onto a single programmed logic array microarchitecture. The synthesis strategy then applies a sequence of decompositions on this initial microarchitecture. This strategy follows a decision scheme until all design objectives are met. It transforms the initial architecture to a complex microarchitecture of several programmed logic arrays and read only memories. In case it is impossible to meet the design objectives, the system constructs a microarchitecture which comes as close as possible to given design objectives. Design objectives are allowed in floorplan dimensions and delay. In the applied strategy, a number of known optimization methods for specific microarchitectures are integrated. This synthesis method explores a larger part of the design space than other controlpath synthesis methods. Other methods are bound to one microarchitecture which they optimize. This system is not only flexible in microarchitecture construction but also open for extension by other optimizations. ESA

N92-30701# Institut National Polytechnique, Grenoble (France).
ARCHITECTURE FOR THE HIGH PERFORMANCE IMPLANTATION OF COMMUNICATION TRANSPORT LEVEL PROTOCOLS Ph.D. Thesis [ARCHITECTURE POUR L'IMPLANTATION HAUTES PERFORMANCES DES PROTOCOLES DE COMMUNICATION DE NIVEAU TRANSPORT]
Christophe Diot 1991 176 p In FRENCH
(ETN-92-91666) Avail: CASI HC A09/MF A02

Using the transputer microprocessor, a high performance implementation of Open System Interconnection (OSI) transport protocol, class 4, is realized. The efficient use of a transputer based environment (using OCCAM as development language) for protocol implementation is demonstrated. The structure of the protocol implementation was designed to minimize data transfers (using dedicated data structures) and to reduce treatment time spent in system tasks (an optimized operating system was developed for memory and timer management). The performance analysis results show that it is possible to raise performance of 5000 TSDU per second, and permit the definition of a set of multitransputers high performance architectures. These architectures will be integrated in an evaluation platform dedicated to 'transfer' protocol implantation. The availability of general purpose protocols (such as TP4 or TCP) for new applications type is discussed. ESA

N92-30712# General Accounting Office, Washington, DC.
COMPUTER SECURITY: AGENCIES REPORTED HAVING IMPLEMENTED MOST SYSTEM SECURITY CONTROLS
Apr. 1992 19 p
(GAO/IMTEC-92-45; B-238954) Avail: CASI HC A03/MF A01

The Computer Security Act of 1987 (P.L. 100-235) requires federal agencies to identify systems that contain sensitive information and to develop and implement plans to safeguard these systems. This report responds to your request that we determine the progress that agencies have made in implementing security controls for sensitive systems since our May 1990 report. For 18 of the systems that we reviewed in our earlier report, the percentage of controls implemented increased from 78 percent in January 1990 to 92 percent in January 1992. In addition, agencies have implemented 88 percent of applicable controls for the 9 new systems reviewed. Agency officials responsible for developing, reviewing, and implementing security plans stated that some controls have not yet been implemented because (1) the systems are undergoing changes that may affect existing security controls, (2) the agencies are improving security controls, and (3) one new system is in the early stages of development. Most agencies continue to believe that security planning is useful in heightening awareness about system-specific security. Also, most of the agency officials we interviewed who participate in assistance visits, as well as security officials at the Office of Management and Budget and the National Institute of Standards and Technology agree that the visits strengthened management commitment to computer security. Author

N92-30724*# Research Inst. for Advanced Computer Science, Moffett Field, CA.
SPARSE DISTRIBUTED MEMORY AND RELATED MODELS
Pentti Kanerva Apr. 1992 55 p Submitted for publication
(Contract NCC2-387)
(NASA-CR-190553; NAS 1.26:190553; RIACS-TR-92.10) Avail: CASI HC A04/MF A01

Described here is sparse distributed memory (SDM) as a neural-net associative memory. It is characterized by two weight matrices and by a large internal dimension - the number of hidden units is much larger than the number of input or output units. The first matrix, A, is fixed and possibly random, and the second matrix, C, is modifiable. The SDM is compared and contrasted to (1) computer memory, (2) correlation-matrix memory, (3) feet-forward artificial neural network, (4) cortex of the cerebellum, (5) Marr and Albus models of the cerebellum, and (6) Albus' cerebellar model arithmetic computer (CMAC). Several variations of the basic SDM design are discussed: the selected-coordinate and hyperplane

designs of Jaeckel, the pseudorandom associative neural memory of Hassoun, and SDM with real-valued input variables by Prager and Fallside. SDM research conducted mainly at the Research Institute for Advanced Computer Science (RIACS) in 1986-1991 is highlighted. Author

61 COMPUTER PROGRAMMING AND SOFTWARE

Includes computer programs, routines, alogorithms, and specific applications, e.g., CAD/CAM.

N92-30260# Cornell Univ., Ithaca, NY.
A PROGRAM OF CONTINUING RESEARCH ON REPRESENTING, MANIPULATING, AND REASONING ABOUT PHYSICAL OBJECTS Final Technical Report, 1 May 1989 - 30 Sep. 1991
John E. Hopcroft 30 Sep. 1991 14 p
(Contract N00014-89-J-1946)
(AD-A251089) Avail: CASI HC A03/MF A01

The Cornell Computer Science Modeling and Simulation Project was founded on the belief that electronic prototypes would have a significant impact on our nation's technological growth. From the project's inception, members of the research team have focused their attention on the investigation of fundamental computer science principles that underlie real-world representations. Our overriding objective is to develop a science base that supports electronic simulation systems to be used in computer-aided design and engineering analysis. To this end, we are carrying out a broad-based research program to develop the underlying methodology that supports representation, editing, and simulation of objects, tasks, and systems. In our original proposal, we stressed three areas of research: solid modeler robustness, user-friendly modeling systems, and control of complex objects. Results in each of these areas are summarized. GRA

N92-30296*# Nebraska Univ., Lincoln. Dept. of Electrical Engineering.
[MODELING OF VIDEO TRAFFIC IN PACKET NETWORKS, LOW RATE VIDEO COMPRESSION, AND THE DEVELOPMENT OF A LOSSY+LOSSLESS IMAGE COMPRESSION ALGORITHM] Semiannual Status Report, 15 Dec. 1991 - 15 Jun. 1992
K. Sayood, Y. C. Chen, and X. Wang 23 Jul. 1992 44 p
(Grant NAG5-1612)
(NASA-CR-190546; NAS 1.26:190546) Avail: CASI HC A03/MF A01

During this reporting period we have worked on three somewhat different problems. These are modeling of video traffic in packet networks, low rate video compression, and the development of a lossy + lossless image compression algorithm, which might have some application in browsing algorithms. The lossy + lossless scheme is an extension of work previously done under this grant. It provides a simple technique for incorporating browsing capability. The low rate coding scheme is also a simple variation on the standard discrete cosine transform (DCT) coding approach. In spite of its simplicity, the approach provides surprisingly high quality reconstructions. The modeling approach is borrowed from the speech recognition literature, and seems to be promising in that it provides a simple way of obtaining an idea about the second order behavior of a particular coding scheme. Details about these are presented. Author

N92-30299*# Texas Univ., Austin. Dept. of Electrical and Computer Engineering.
SURVIVABLE ALGORITHMS AND REDUNDANCY MANAGEMENT IN NASA'S DISTRIBUTED COMPUTING SYSTEMS Final Report, 1 May 1990 - 30 Apr. 1992
Miroslaw Malek 1992 36 p
(Grant NAG9-426)
(NASA-CR-189827; NAS 1.26:189827) Avail: CASI HC A03/MF A01

The design of survivable algorithms requires a solid foundation for executing them. While hardware techniques for fault-tolerant computing are relatively well understood, fault-tolerant operating systems, as well as fault-tolerant applications (survivable algorithms), are, by contrast, little understood, and much more work in this field is required. We outline some of our work that contributes to the foundation of ultrareliable operating systems and fault-tolerant algorithm design. We introduce our consensus-based framework for fault-tolerant system design. This is followed by a description of a hierarchical partitioning method for efficient consensus. A scheduler for redundancy management is introduced, and application-specific fault tolerance is described. We give an overview of our hybrid algorithm technique, which is an alternative to the formal approach given. Author

N92-30351# Technische Univ., Delft (Netherlands). Faculty of Technical Mathematics and Information.
A SURVEY ON PIVOT RULES FOR LINEAR PROGRAMMING
Tamas Terlaky (Eoetvoes Lorand Univ., Budapest, Hungary) and Shuzhong Zhang (Groningen Rijksuniv., Netherlands) 1991 35 p
(Contract OTKA-2115)
(Rept-91-99; ISSN-0922-5641; ETN-92-91849) Copyright Avail: CASI HC A03/MF A01

Various pivot rules of the simplex method or its variants that were developed in the last two decades, starting from the appearance of the minimal index rule of Bland, are surveyed. Particular attention is given to the fitness property of simplex type pivot rules. Three classes of recently developed pivot rules for linear programming are discussed: essentially combinatorial pivot rules. Namely, these rules only use labeling and signs of the variables. These include: minimal index type rules and recursive rules; pivot rules which can be considered in fact as variants or generalizations or specializations of Lemke's method and are closely related to parametric programming; and pivot rules with the common feature that they all have close connections to certain interior point methods. Some open problems for further study are mentioned. ESA

N92-30352# Technische Univ., Delft (Netherlands). Faculty of Technical Mathematics and Information.
ON THE MAGNIFICATION OF CANTOR SETS AND THEIR LIMIT MODELS
Tim Bedford and Albert M. Fisher (Yale Univ., New Haven, CT.) 1991 31 p
(Rept-91-100; ISSN-0922-5641; ETN-92-91850) Copyright Avail: CASI HC A03/MF A01

For a cookie-cutter Cantor set C, the limits of sequences of closed subsets of the set of real numbers obtained by arbitrarily high magnifications around different points of C are considered. It is shown that a well defined set of limit models exists for the infinitesimal scenery in the Cantor set. If C bar is a C(sup 1 + gamma) diffeomorphic copy of C then the set of limit models of C bar is the same as that of C. Furthermore, every limit model is made of Cantor sets which are C(sup 1 + gamma) diffeomorphic with C (for some gamma greater than 0), but not all such C(sup 1 + gamma) copies of C occur in the limit models. The relation between this approach to the asymptotic structure of a Cantor set and Sullivans 'scale function' are considered. An alternative definition of a fractal is proposed. ESA

N92-30353# Technische Univ., Delft (Netherlands). Faculty of Technical Mathematics and Information.
DEGENERACY IN INTERIOR POINT METHODS FOR LINEAR PROGRAMMING
O. Gueler, D. denHertog, C. Roos, Tamas Terlaky (Eoetvoes Lorand Univ., Budapest, Hungary), and T. Tsuchiya (Tokyo Univ., Japan) Dec. 1991 36 p Sponsored by Shell
(Contract OTKA-2116)
(Rept-91-102; ISSN-0922-5641; ETN-92-91852) Copyright Avail: CASI HC A03/MF A01

The various theoretical and practical issues related to degeneracy of IPM's (Interior Point Methods) for linear programming are surveyed. Results which for the most part already appeared in the literature are surveyed. The effect of degeneracy in the convergence of IPM's and on the trajectories followed by the algorithms are considered together with the effect of degeneracy in numerical performance and on finding basic solutions. ESA

N92-30356# Technische Univ., Delft (Netherlands). Faculty of Technical Mathematics and Information.
CONTROLLING USER INTERFACE OBJECTS THROUGH PRE- AND POSTCONDITIONS
James D. Foley (Georgia Inst. of Tech., Atlanta.), Daniel F. Gieskens, and Charles A. P. G. vanderMast 1992 10 p Sponsored in part by Sun Microsystems, Inc.
(Grant NSF IRI-88-13179)
(Rept-92-04; ISSN-0922-5641; ETN-92-91856) Copyright Avail: CASI HC A02/MF A01

The workings of pre- and postconditions and the system supporting this mechanism are shown. The enhancement of a user interface design tool with this mechanism to support a better prototyping environment is discussed. User interface objects (i.e., windows, menus, buttons, sliders, etc.) were augmented with preconditions that determine their visibility and their enabled/disabled status and postconditions that are asserted when certain actions are performed in the object. Postconditions are associated with each functionally different action on the object. Attaching pre- and postconditions to interface objects provides several useful features, such as selective enabling of controls, rapid prototyping, and automatic generation of explanations and help text. ESA

N92-30357# Technische Univ., Delft (Netherlands). Faculty of Technical Mathematics and Information.
THE REMBRANDT SYSTEM FOR MULTI-CRITERIA DECISION ANALYSIS VIA PAIRWISE COMPARISONS OR DIRECT RATING
F. A. Lootsma 1992 32 p
(Rept-92-05; ISSN-0922-5641; ETN-92-91857) Copyright Avail: CASI HC A03/MF A01

Research results and the practical experience in the REMBRANDT system for multicriteria decision analysis are consolidated using ratio estimation in magnitudes or deci-Bells to rate alternatives which are non dominated. The decision alternatives are judged via a method of pairwise comparison, or via direct rating. In the basic pairwise comparison step, the decision maker is asked to state whether he has a weak, strict, strong, or very strong preference to one of two alternatives presented to him, or whether he is indifferent between the two. Direct rating is practically the assignment of grades. The impact scores of the alternatives under the respective criteria via logarithmic regression are estimated, and the final scores of the alternatives are computed via the geometric mean aggregation rule. The REMBRANDT system was designed for decision making in groups. It does not force the group members to abstain sometimes from giving this comparative judgement. Moreover, it analyzes not only the individual opinions, but it also suggests a group compromise solution, taking into account the relative power position of the group members. ESA

N92-30359# Technische Univ., Delft (Netherlands). Faculty of Technical Mathematics and Information.
A FORMAL TRANSFORMATION FROM THE BSI/VDM-SL CONCRETE SYNTAX TO THE CORE ABSTRACT SYNTAX
Nico Plat and Hans Toetenel 1992 96 p
(Rept-92-07; ISSN-0922-5641; ETN-92-91859) Copyright Avail: CASI HC A05/MF A01

The increasing use of VDM (Vienna Development Method) and the growing number of dialects in use have led to the recognition of the need for a standard for VDM-SL (Specification Language). One specific component of the standards for VDM-SL is defined: the 'syntax mapping' which translates a VDM specification expressed in terms of the concrete syntax into a specification expressed in terms of the so called core abstract syntax, which is used by the dynamic semantics of the language. ESA

N92-30377# Wisconsin Univ., Madison. Dept. of Engineering Mechanics.
NEW TRANSIENT AND PSEUDO-TRANSIENT ALGORITHMS FOR VISCOELASTIC MATERIALS Final Technical Report, 15 Dec. 1988 - 14 Jun. 1991
David S. Malkus 4 Mar. 1992 8 p
(Grant AF-AFOSR-0220-89)
(AD-A250642; AFOSR-92-0271TR) Avail: CASI HC A02/MF A01

The principal investigator, D. S. Malkus, his post-doctoral associate, and Ph.D. students worked on three projects related to AFOSR research: (1) Planar viscoelastic flows of fluids with integral constitutive equations. The purpose of the project was to develop new algorithms for flows of non-Newtonian fluids and use them to study polymer-processing flows; (2) Simulation and analysis of differential infrared thermographic stress analysis--SPATE. A consistent thermodynamic theory of viscoplasticity was developed and methods for the experimental determination of model parameters were proposed. The consequence of viscoplastic behavior on differential thermography was studied, by simulating the SPATE stress analysis system. (3) Optimal mass in the finite element method. The purpose of the project was to explore the feasibility and usefulness of quadrature-based optimal mass matrix lumping techniques for higher-order finite element schemes, where they often produce indefinite but diagonal mass matrices. GRA

N92-30379*# Cornell Univ., Ithaca, NY. Dept. of Computer Science.
HOW TO SECURELY REPLICATE SERVICES
Michael Reiter and Kenneth Birman 15 Jun. 1992 28 p
(Grant NAG2-593)
(NASA-CR-190476; NAS 1.26:190476; CU-TR-92-1287) Avail: CASI HC A03/MF A01

A method is presented for constructing replicated services that retain their availability and integrity despite several servers and clients corrupted by an intruder, in addition to others failing benignly. More precisely, a service is replicated by n servers in such a way that a correct client will accept a correct server's response if, for some prespecified parameter k, at least k servers are correct and fewer than k servers are corrupt. The issue of maintaining causality among client requests is also addressed. A security breach resulting from an intruder's ability to effect a violation of causality in the sequence of requests processed by the service is illustrated. An approach to counter this problem is proposed that requires fewer than k servers to be corrupt and that is live if at least k+b servers are correct, where b is the assumed maximum total number of corrupt servers in any system run. An important and novel feature of these schemes is that the client need not be able to identify or authenticate even a single server. Instead, the client is required only to possess at most two public keys for the service. The practicality of these schemes is illustrated through a discussion of several issues pertinent to their implementation and use, and their intended role in a secure version of the Isis system is also described. Author

N92-30428# Center for Mathematics and Computer Science, Amsterdam (Netherlands). Dept. of Computer Science.
LAZY AND INCREMENTAL PROGRAM GENERATION
J. Heering, P. Klint (Amsterdam Univ., Netherlands), and J. Rekers Apr. 1991 15 p Revised Sponsored in part by Commission of the European Communities and Netherlands Organization for Applied Scientific Research TNO
(CWI-CS-R9124; CWI-CS-R8749-Rev; ETN-92-91552) Copyright Avail: CASI HC A03/MF A01

Current program generators usually operate in a 'greedy' manner in the sense that a program must be generated in its entirety before it can be used. If generation time is scarce, or if the input to the generator is subject to modification, it may be better to be more cautious and to generate only those parts of the program that are indispensable for processing the particular data at hand.

This is called 'lazy program generation'. Another closely related strategy is 'incremental program generation'. When its input is modified, an incremental generator will try to make a corresponding modification in its output rather than generate a completely new program. The advantage of using a combination of both strategies in program generators that have to operate in a highly dynamic and/or interactive environment is addressed. ESA

N92-30429# Center for Mathematics and Computer Science, Amsterdam (Netherlands). Dept. of Numerical Mathematics.
ADAPTIVE MULTIGRID APPLIED TO A BIPOLAR TRANSISTOR PROBLEM
J. Molenaar Aug. 1991 21 p
(CWI-NM-R9115; ISSN-0169-0388; ETN-92-91662) Copyright Avail: CASI HC A03/MF A01

An adaptive multigrid method is presented for the solution of the steady two dimensional semiconductor equations. The discretization is made in an adaptive grid by means of the mixed finite element method on rectangles. The integrals involved are approximated by means of the trapezoidal rule in order to obtain a generalization in two dimensions of the well known Scharfetter/Gummel scheme. The use of the trapezoidal rule is shown not to influence the accuracy of the discretization. The discrete equations thus obtained are solved by means of an algorithm. A Vanka type relaxation is used as a smoother, and a local damping of the restricted residual is introduced in order to be able to use very coarse grids. The relative truncation error between coarse and fine grids is used as a refinement criterion for constructing adaptive grids. The relative truncation errors for the semiconductor equations is studied, and the way they can be incorporated into a practical grid adaptation scheme is given. Results are shown for a realistic bipolar transitor problem. ESA

N92-30433# Universiteit Twente, Enschede (Netherlands). Dept. of Computer Science.
A COMPUTATIONAL PROOF OF SOUNDNESS
Stef Joosten and Jan Kuper 28 Jan. 1992 11 p
(Memo-INF-92-09; ISSN-0924-3755; ETN-92-91783) Copyright Avail: CASI HC A03/MF A01

A formal system called CFL is studied. This system contains clauses, atoms and terms, and two rules of derivation: the substitution rule and the cut rule. CFL is interpreted in predicate logic, and the soundness of derivation is proved in this interpretation. The proof is fully computational. ESA

N92-30435# Technische Univ., Delft (Netherlands). Faculty of Technical Mathematics and Information.
ACHIEVABLE POTENTIAL REDUCTIONS IN THE METHOD OF KOJIMA ET AL. IN THE CASE OF LINEAR PROGRAMMING
C. Roos and J.-P. Vial (Geneva Univ., Switzerland) Nov. 1991 13 p
(Grant FNSRS-1-467-0-86)
(Rept-91-78; ISSN-0922-5641; ETN-92-91828) Copyright Avail: CASI HC A03/MF A01

The proposal of a primal-dual interior point method, based on potential reduction, for solving the linear complementarity problem, and the derivation of an O(square root of n(L)) iteration bound, is addressed. In the derivation of this bound, equal step sizes were used in the primal and the dual space, and it was shown that taking the step size equal to 0.4 the potential reduction is at least 0.2. Specialization to the case of linear programming is carried out and it is shown that the latter constant can be improved to 0.267. Admitting different step sizes in both spaces, a further improvement of this constant to 0.345 is possible. For the case of equal step sizes, duality gap is shown to be monotonically decreasing. ESA

N92-30443# Utrecht State Univ. (Netherlands). Dept. of Computer Science.
COMPUTING AND VERIFYING DEPTH ORDERS
Mark deBerg, Mark Overmars, and Otfried Schwarzkopf (Freie Univ., Berlin, Germany, F.R.) Nov. 1991 16 p Sponsored by Netherlands Organization for Applied Scientific Research TNO (Contract ECC-3075)
(RUU-CS-91-41; ISSN-0924-3275; ETN-92-91807) Avail: CASI HC A03/MF A01

A depth order in a set of objects is an order such that object a comes before object a' in the order when a lies behind a', or, in other words, when a is (partially) hidden by a'. Efficient algorithms for the computation and verification of depth orders of sets of n rods in three dimensional space are presented. The algorithms run in time O(n(sup 4/(3 + epsilon))), for any fixed epsilon greater than 0. If all rods are axis parallel, or more generally, have only a constant number of different orientations, then the sorting algorithm runs in O(n(log cubed)n) time and the verification takes O(n(log squared)n) time. The algorithms can be generalized to handle triangles and other polygons instead of rods. They are based on a general framework for computing and verifying linear extensions of implicitly defined binary relations. ESA

N92-30444# Utrecht State Univ. (Netherlands). Dept. of Computer Science.
CLASSIFYING TERMINATION OF TERM REWRITING
H. Zantema Nov. 1991 14 p
(RUU-CS-91-42; ISSN-0924-3275; ETN-92-91808) Avail: CASI HC A03/MF A01

A classification of types of termination of term rewriting systems built on properties in the semantic level in which terms are interpreted is proposed. It can be considered as a generalization of polynomial interpretations. ESA

N92-30445# Utrecht State Univ. (Netherlands). Dept. of Computer Science.
A PROTOCOL SCHEME FOR A CLASS OF MINIMUM DELAY ROUTING ALGORITHMS
Petra J. M. vanHaaften Nov. 1991 31 p
(Contract EEC-3075)
(RUU-CS-91-43; ISSN-0924-3275; ETN-92-91809) Avail: CASI HC A03/MF A01

Protocols and proofs of correctness are given for a class of minimum delay algorithms. A general scheme is given for the protocols which provide a distributed implementation of the algorithms that belong to the described class. A proof scheme for these protocols is given. Example algorithms are given; for each algorithm, a protocol that implements that algorithm is shown and a correctness proof for the protocol is given. ESA

N92-30455# Technische Univ., Delft (Netherlands). Faculty of Technical Mathematics and Information.
IRI'S POLYNOMIALITY PROOF FOR THE IRI-IMAI METHOD RECAST
D. denHertog, C. Roos, and T. Terlaky Oct. 1991 18 p Sponsored by Shell
(Contract OTKA-2116)
(Rept-91-74; ISSN-0922-5641; ETN-92-91824) Copyright Avail: CASI HC A03/MF A01

A paper which showed that the Iri-Imai method converges in O(nL) iterations to an optimal solution is rewritten in the standard notation. In the method it was proved that in each iteration the (multiplicative) barrier function is reduced by (at least) some constant factor (smaller than one). Specialization to the case that the feasible region is a cone is done and the Iri-Imai method, when applying a line search, is shown to yield the optimal solution in one step. ESA

N92-30476# National Aerospace Lab., Amsterdam (Netherlands). Informatics Div.
DEVELOPMENT ENVIRONMENT FOR DIGITAL SIMULATION MODELS OF MULTIBODY SYSTEMS
R. J. P. Groothuizen, A. A. tenDam, and H. deJong 28 Aug. 1989 13 p Presented at the 4th ECMI Meeting on Industrial Mathematics, Saint Wolfgang, Austria, 29 May - 2 Jun. 1989
(Contract NIVR-428-02704-N)
(NLR-TP-89327-U; ETN-92-91528) Avail: CASI HC A03/MF A01

Requirements for an environment for development, verification,

and validation of digital simulation models of multibody systems are formulated. A realization of such an environment is described. ESA

N92-30478# Technische Univ., Eindhoven (Netherlands). Dept. of Mathematics and Computing Science.
STRONG DYNAMIC INPUT-OUTPUT DECOUPLING: FROM LINEARITY TO NONLINEARITY
H. J. C. Huijberts and H. Nijmeijer (Universiteit Twente, Enschede, Netherlands) Feb. 1992 12 p Presented at the IFAC Symposium on Nonlinear Control Systems Design, Bordeaux, France, 1992
(Memo-COSOR-92-04; ISSN-0926-4493; ETN-92-91800) Avail: CASI HC A03/MF A01

The Strong Dynamic Input Output Decoupling Problem (SDIODP) for nonlinear systems is studied. Given a generically satisfied assumption, the solvability of the SDIODP around an equilibrium point is shown to be equivalent to the solvability of the same problem for the linearization of the system around this equilibrium point. The Singh compensator, a dynamic state feedback of minimal order that solves the SDIODP, is introduced. Given the assumption mentioned above, the linearization of the Singh compensator around an equilibrium point is shown to be a Singh commensator for the linearization of the original nonlinear system around this equilibrium point. Author

N92-30479# Utrecht State Univ. (Netherlands). Dept. of Computer Science.
MAINTENANCE OF 2- AND 3-CONNECTED COMPONENTS OF GRAPHS. PART 1: 2- AND 3-EDGE-CONNECTED COMPONENTS
J. A. LaPoutre, J. vanLeeuwen, and M. H. Overmars Jul. 1990 39 p Presented at the French-Israeli Conference on Combinatorics and Algorithms, Jerusalem, Israel, Nov. 1988 Sponsored in part by Commission of the European Communities
(RUU-CS-90-26-Pt-1; ISSN-0924-3275; ETN-92-91801) Avail: CASI HC A03/MF A01

A data structure to efficiently maintain the 2 and 3 edge connected components of a graph, under insertions of edges in the graph, is presented. Starting from an 'empty' graph of n nodes, the insertion of e edges takes O(n x log(n) + e) time in total. The data structure allows the insertions of nodes also (in the same time bounds, taking n as the final number of nodes). Moreover, at any moment, the data structure can answer the following type of query in O(1) time: given two nodes in the graph, are these nodes 2 or 3 edge connected. ESA

N92-30480# Utrecht State Univ. (Netherlands). Dept. of Computer Science.
MAINTENANCE OF 2- AND 3-CONNECTED COMPONENTS OF GRAPHS. PART 2: 2- AND 3-EDGE-CONNECTED COMPONENTS AND 2-VERTEX-CONNECTED COMPONENTS
J. A. LaPoutre Oct. 1990 77 p Sponsored in part by Commission of the European Communities
(RUU-CS-90-27-Pt-2; ISSN-0924-3275; ETN-92-91802) Avail: CASI HC A05/MF A01

Data structures and algorithms to efficiently maintain the 2 and 3 edge connected components and the 2 vertex connected components of graph, under insertions of edges in the graph, are presented. At any moment, the data structure can answer the following type of query: given two nodes in the graph, are these nodes 2 or 3 edge connected or 2 vertex connected. Starting from an 'empty' graph of n nodes, the algorithms run in O((n + m).alpha(m,n)) time, where m is the total number of queries and edge insertions. The data structure also allows for insertions of nodes. A linear time algorithm is presented for maintaining the 2 edge connected components in case the initial graph is connected. ESA

N92-30484# Technische Univ., Delft (Netherlands). Faculty of Technical Mathematics and Information.
COMPONENT CONSTRUCTION: PRACTICAL GUIDELINES FOR THE CONSTRUCTION OF REUSABLE COMPONENTS
Haikuan Li, J. vanKatwijk, and J. vanZeijl 1991 85 p
(Rept-91-89; ISSN-0922-5641; ETN-92-91839) Copyright Avail: CASI HC A05/MF A01

Several points are considered for guiding reusable component construction. A set of language constructs is verified and a group of suggestions about the reusable component construction is provided. A method of frame based component construction is introduced and the documentation of the reusable components is presented. During the discussion some examples are given in C or C++ which are chosen for reusable component contruction in the project. ESA

N92-30485# Technische Univ., Delft (Netherlands). Faculty of Technical Mathematics and Information.
THE SEMANTICS OF THE DUPLEX PROGRAMMING ENVIRONMENT
Haikuan Li and Jan vanKatwijk 1991 47 p
(Rept-91-91; ISSN-0922-5641; ETN-92-91841) Copyright Avail: CASI HC A03/MF A01

The semantics of the Duplex programming environment is described with a set of objects, axioms, and transformation rules. Based on the description, some theorems are proved and an operation generation is specified. The syntax of the software components is appended. ESA

N92-30492# Technische Univ., Delft (Netherlands). Faculty of Technical Mathematics and Information.
THE DUPLEX PROGRAMMING ENVIRONMENT
Haikuan Li and Jan vanKatwijk 1991 41 p
(Rept-91-90; ISSN-0922-5641; ETN-92-91840) Copyright Avail: CASI HC A03/MF A01

The Duplex programming environment supports both functional and structural reuse by means of both object-oriented programming and structure-oriented programming. In this environment, different kinds of components are used to represent either objects or the glue to compose new objects out of existing ones. Since partial specification is used, the experiences with component composition can be accumulated. In terms of generic abstract data types, a conventional program unit can be generalized free from both data and operations, which, however, is usually committed in most conventional programming languages. By specifying the relationship between a single component and the component base, virtual operations can be used in programming, which overcomes the difficulty to reuse generic components. An operation generator is employed to transform any virtual operation into its implementation. ESA

N92-30493# Grenoble-1 Univ. (France). Lab. de Genie Informatique.
CONFIGURATION ALGORITHMS FOR HIERARCHICAL SUPERNODE MACHINES [ALGORITHMES DE CONFIGURATION DES MACHINES HIERARCHIQUES SUPERNODES]
Leon Mugwaneza, Traian Muntean, and Ibrahima Sakho May 1991 17 p In FRENCH
(IMAG-RR-853-I; ETN-92-91472) Avail: CASI HC A03/MF A01

Algorithms for the control of interconnection networks are analyzed and presented. Parallel machines have recently been designed folllowing two approaches: fixed interconnection networks between processors and reconfigurable interconnection networks based on programmable switch devices. Reconfigurable parallel machines using crossbar switches are limited to tens of processors. For massively parallel machines, multistage interconnection networks are used. Supernodes are based on a switching device built as a rearrangeable three stage Clos network. ESA

N92-30512# European Space Agency, Paris (France).
GENERALIZED PROJECTED GRADIENT-TYPE ITERATIVE METHOD FOR PARAMETRIC AND FUNCTIONAL OPTIMIZATION OF DYNAMICAL SYSTEMS SUBJECT TO CONSTRAINTS
Claude Aumasson (Office National d'Etudes et de Recherches Aerospatiales, Paris, France) and Philippe Landiech (Office

National d'Etudes et de Recherches Aerospatiales, Paris, France) Mar. 1992 113 p Transl. into ENGLISH of Methode Iterative de Type Gradient Projete Generalise pour l'Optimisation Parametrique et Fonctionnelle de Systemes Dynmaniques Soumis a des Contraintes (Paris, France, ONERA), 1988 95 p Original language document was announced as N89-29063
(ESA-TT-1166; ONERA-NT-1988-9; ETN-92-91707) Avail: CASI HC A06/MF A02

The generalized projected gradient method applied to the functional and parametric optimization of nonlinear dynamical systems subject to constraints is described. Special attention is given to the inclusion of the constraints. The theoretical aspects of the method are described. The following topics are discussed: the calculations of the cost and constraint sensitivites to variations in the control laws and parameters, the choice of objectives in constraint adjustment at each iteration and the determination of the optimal variations of control laws and corresponding parameters. The use of the method on a simple example of trajectory optimization, for which the analytical solution is also known, is shown. A more complicated example of application is discussed. ESA

N92-30522# Sandia National Labs., Albuquerque, NM.
COMPUTING WITH FAULTY SHARED MEMORY
Y. Afek (Tel-Aviv Univ., Israel), D. S. Greenberg, M. Merritt, and G. Taubenfeld (Bell Telephone Labs., Inc., Murray Hill, NJ.) Feb. 1992 15 p Presented at the 11th Annual Association of Computing Machinery Symposium on Principles of Distributed Computing, Vancouver, Ottawa, 10-12 Aug. 1992
(Contract DE-AC04-76DP-00789)
(DE92-011663; SAND-92-0362C; CONF-920867-1) Avail: CASI HC A03/MF A01

This paper addresses problems of synchronization and coordination in the context of faulty shared memory. We present algorithms for the consensus problem, and for reliable shared memory objects, from collections of read/write registers, 2-processor binary test-and-set objects, and read-modify-write registers, some of which may be faulty. DOE

N92-30543*# National Aeronautics and Space Administration. Pasadena Office, CA.
ENCYCLOPEDIA OF SOFTWARE COMPONENTS Patent Application
Lloyd VanWarren, inventor (to NASA) (Jet Propulsion Lab., California Inst. of Tech., Pasadena.) and Brian C. Beckman, inventor (to NASA) (Jet Propulsion Lab., California Inst. of Tech., Pasadena.) 13 Nov. 1991 52 p
(Contract NAS7-918)
(NASA-Case-NPO-18435-1-CU; NAS 1.71:NPO-18435-1-CU; US-Patent-Appl-SN-792501) Avail: CASI HC A04/MF A01

Intelligent browsing through a collection of reusable software components is facilitated with a computer having a video monitor and a user input interface such as a keyboard or a mouse for transmitting user selections, by presenting a picture of encyclopedia volumes with respective visible labels referring to types of software, in accordance with a metaphor in which each volume includes a page having a list of general topics under the software type of the volume and pages having lists of software components for each one of the generic topics, altering the picture to open one of the volumes in response to an initial user selection specifying the one volume to display on the monitor a picture of the page thereof having the list of general topics and altering the picture to display the page thereof having a list of software components under one of the general topics in response to a next user selection specifying the one general topic, and then presenting a picture of a set of different informative plates depicting different types of information about one of the software components in response to a further user selection specifying the one component. NASA

N92-30550# Mitre Corp., Bedford, MA.
INTEGRATING COMMERCIAL OFF-THE-SHELF TOOLS FOR CUSTOM SOFTWARE DEVELOPMENT
D. S. Blodgett and D. J. Phair Jun. 1992 36 p
(Contract F19628-89-C-0001)
(AD-A252462) Avail: CASI HC A03/MF A01

Fourth-generation, object-driven languages (4GL's) (i.e., Hypermedia) have been used effectively in requirements analysis prototyping and human-machine interface development and have served as a front end to more complex applications. This paper describes the process of evaluating, selecting, and integrating 4GL tools for specific applications running on a variety of microcomputer platforms. To explore these different options, we present an example of a computer-based training system created in a 4GL and describe how numerous commercial off-the-shelf software tools were integrated for added functionality. The logical extension to the current suite of Hypermedia products is tools capable of producing device-independent source code, which in turn is capable of being compiled into stand-alone applications. The impact of using a set of nonhomogeneous tools will be discussed in terms of source code control, supportability, and tool enhanceability. GRA

N92-30555# Duke Univ., Durham, NC.
IMPLEMENTATION OF PARALLEL ALGORITHMS Quarterly Report, 1 Jan. - 31 Mar. 1992
John H. Reif 31 Mar. 1992 9 p
(Contract N00014-91-J-1985)
(AD-A248826) Avail: CASI HC A02/MF A01

Work is progressing in the design of a new, general intermediate representation for parallel code. We wish to provide a single compilation target that is executable on a wide variety of parallel machines and vector processors. The representation we are designing is an extension of VCODE, due to Blelloch at CMU, which is particularly suitable as a target only for data-parallel language. VCODE provides a rich set of vector operations, including powerful segmented prefix computations and permutation operations, which run efficiently on a wide range of architectures. However, VCODE provides only sequential control, which limits its application strictly to data-parallel programming. We have extended VCODE to form a new language called AVCODE which has operations for process creation, communication, and synchronization. AVCODE provides an avenue for efficiently targeting a parallel language to a number of different hardware systems through a single intermediate language. GRA

N92-30579# National Inst. of Standards and Technology, Gaithersburg, MD. Computing and Applied Mathematics Lab.
A BOUSSINESQ ALGORITHM FOR BOUYANT CONVECTION IN POLYGONAL DOMAINS
K. B. McGrattan, R. G. Rehm, H. C. Tang, and H. R. Baum Apr. 1992 27 p
(PB92-187137; NISTIR-4831) Avail: CASI HC A03/MF A01

A 2-D Boussinesq model describing heat-driven buoyant convection in a polygonal enclosure is presented. The hydrodynamics are based on the time-dependent Navier-Stokes equations with constant velocity and thermal conductivity; no turbulence model or other empirical parameters are introduced. The polygonal domain is mapped via a Schwarz-Christoffel transformation onto a rectangle. A finite difference scheme, second-order in space and first order in time, is used to integrate the evolution equations, and an elliptic solver is used to solve the pressure equation. Computational results for high Reynolds numbers are presented through the use of Lagrangian particles which allow one to visualize the flow patterns. Author

N92-30629# Maryland Univ. Baltimore County, Catonsville. Dept. of Electrical Engineering.
IMPLEMENTATION SCHEME FOR RECURSION IN SPECTRAL DIMENSION Final Report, Sep. 1990 - Mar. 1991
Chein-I. Chang Mar. 1992 34 p
(Contract DAAD05-90-P-8392)
(AD-A248945; CRDEC-CR-120) Avail: CASI HC A03/MF A01

Developing recursive detection algorithms for thermal image processing is very important for real-time implementation. In previous work for CRDEC, a first order autoregressive time series

was used to model the background of thermal image which led to the further development of a recursive algorithm in time frames. In this report, we revisit this work and present an alternative approach to developing a recursive algorithm for thermal image target detection. The new approach uses Kalman filter theory, which has proven to be very powerful in real-time processing because of its recursive nature. The previous algorithm was designed for a single spectral band. In reality, however, the characteristics of the vapor cloud and background may vary from band to band in spectral domain; thus, it is practical to extend the earlier and the Kalman filtering approaches to cover multiple spectral bands. To alleviate the difficulty of processing multiple bands, two suboptimal models (separable spectral correlation and separable spectral-Markov spatial correlation) are also proposed for the background. GRA

N92-30631# Naval Postgraduate School, Monterey, CA.
DETECTING POTENTIAL SYNCHRONIZATION CONSTRAINT DEADLOCKS FROM FORMAL SYSTEM SPECIFICATIONS M.S. Thesis
Jeffrey M. Schweiger Mar. 1992 81 p
(AD-A249019) Avail: CASI HC A05/MF A01

This thesis describes a conceptual design for a software tool for automatic detection of synchronization constraint deadlock from the formal specification of a distributed system. The formal specification language Spec is used to define the distributed system. The basic algorithm used is introduced using a graphical representation, and its operation illustrated via an example. GRA

N92-30723*# Research Inst. for Advanced Computer Science, Moffett Field, CA.
GAUSSIAN WINDOWS: A TOOL FOR EXPLORING MULTIVARIATE DATA
Louis A. Jaeckel Sep. 1990 63 p
(Contracts NCC2-408; NCC2-387)
(NASA-CR-190559; NAS 1.26:190559; RIACS-TR-90.41) Avail: CASI HC A04/MF A01

Presented here is a method for interactively exploring a large set of quantitative multivariate data, in order to estimate the shape of the underlying density function. It is assumed that the density function is more or less smooth, but no other specific assumptions are made concerning its structure. The local structure of the data in a given region may be examined by viewing the data through a Gaussian window, whose location and shape are chosen by the user. A Gaussian window is defined by giving each data point a weight based on a multivariate Gaussian function. The weighted sample mean and sample covariance matrix are then computed, using the weights attached to the data points. These quantities are used to compute an estimate of the shape of the density function in the window region. The local structure of the data is described by a method similar to the method of principal components. By taking many such local views of the data, we can form an idea of the structure of the data set. The method is applicable in any number of dimensions. The method can be used to find and describe simple structural features such as peaks, valleys, and saddle points in the density function, and also extended structures in higher dimensions. With some practice, we can apply our geometrical intuition to these structural features in any number of dimensions, so that we can think about and describe the structure of the data. Since the computations involved are relatively simple, the method can easily be implemented on a small computer.
Author

N92-30820# Pennsylvania Univ., Philadelphia.
VISUAL PERCEPTION OF DEPTH FROM OCCLUSION: A NEURAL NETWORK MODEL Progress Report, period ending 1 Jan. 1992
Leif H. Findel 1 Jan. 1992 11 p
(Contract N00014-90-J-1864)
(AD-A249035) Avail: CASI HC A03/MF A01

During this period, we have made substantial progress in understanding how objects are discriminated by the visual system. A number of papers describing our results are enclosed. Major goals of the project have been accomplished in several areas: (1) completion of a beta release version of a novel neural network simulator, NEXUS; (2) development of a parallel version of the NEXUS simulator which allows anatomically interconnected networks to be simultaneously simulated on different workstations linked by ethernet connections; (3) continuing research using our model of how the visual system extracts depth-from-occlusion; and (4) development of related cortically-based models of color visual processing and texture discrimination. Color and texture are used to detect contours in images, and these contours can then be used by our depth-from-occlusion model to determine the relative depth of the colored or textured surfaces. GRA

N92-30886# Oak Ridge National Lab., TN.
GRAPHICAL-BASED CONSTRUCTION OF COMBINATORIAL GEOMETRIES FOR RADIATION TRANSPORT AND SHIELDING APPLICATIONS
T. J. Burns 1992 12 p Presented at the Nuclear Technologies for Space Exploration, Jackson, WY, 16-19 Aug. 1992
(Contract DE-AC05-84OR-21400)
(DE92-014453; CONF-920803-6) Avail: CASI HC A03/MF A01

A graphical-based code system is being developed at ORNL to manipulate combinatorial geometries for radiation transport and shielding applications. The current version (basically a combinatorial geometry debugger) consists of two parts: a FORTRAN-based 'view' generator and a Microsoft Windows application for displaying the geometry. Options and features of both modules are discussed. Examples illustrating the various options available are presented. The potential for utilizing the images produced using the debugger as a visualization tool for the output of the radiation transport codes is discussed as is the future direction of the development.
DOE

N92-30892# Sandia National Labs., Albuquerque, NM.
AN OVERVIEW OF THE COMPUTER AIDED DEFINITION SYSTEM FOR DESIGN DEFINITION AT SANDIA NATIONAL LABORATORIES, LIVERMORE FY1991 UPDATE
B. E. Koopmann Sep. 1991 59 p
(Contract DE-AC04-76DR-00789)
(DE92-015991; SAND-91-8231) Avail: CASI HC A04/MF A01

Sandia National Laboratories, Livermore, is continuing to process the upgrading and enhancing of its Computer Aided Definition System to incorporate new hardware capabilities and software functionality to meet our design definition mission. The original report, published in August 1988, detailed the current configuration and design concepts. Although many of the concepts are still valid, several new hardware capabilities are now available and significant software advances have been made since that report was published. This report describes the updated system configuration and revised concepts for the early 1990's. DOE

N92-30905# Stanford Univ., CA. Systems Optimization Lab.
A STRICTLY IMPROVING LINEAR PROGRAMMING ALGORITHM BASED ON A SERIES OF PHASE 1 PROBLEMS
S. A. Leichner, G. B. Dantzig, and J. W. Davis Apr. 1992 22 p
(Contract DE-FG03-92ER-25116)
(DE92-015905; SU-SOL-92-2) Avail: CASI HC A03/MF A01

When used on degenerate problems, the simplex method often takes a number of degenerate steps at a particular vertex before moving to the next. In theory (although rarely in practice), the simplex method can actually cycle at such a degenerate point. Instead of trying to modify the simplex method to avoid degenerate steps, we have developed a new linear programming algorithm that is completely impervious to degeneracy. This new method solves the Phase II problem of finding an optimal solution by solving a series of Phase I feasibility problems. Strict improvement is attained at each iteration in the Phase I algorithm, and the Phase II sequence of feasibility problems has linear convergence in the number of Phase I problems. When tested on the 30 smallest NETLIB linear programming test problems, the computational results for the new Phase II algorithm were over 15 percent faster than the simplex method; on some problems, it was almost two times faster, and on one problem it was four times faster. DOE

N92-30950# CEP Systemes, Paris (France).
ILS, CE, CALS? FROM DESIGN TO OPERATION [ILS, CE, CALS? DU CONCEPT A LA MISE EN OEUVRE]
1991 140 p In ENGLISH and FRENCH Conference held in Paris, France, 12 Dec. 1991
(ETN-92-91717) Avail: CASI HC A07/MF A02

The use of integrated logistic support (ILS), concurrent engineering (CE), and computer aided acquisition and logistic support (CALS) in different industrial domains is discussed. The applicability of CALS in Europe is analyzed. The most important aspects leading the way to the automation of concurrent engineering are underlined. Quality assurance and basic principles of integrated logistics are discussed. The main tasks accomplished in preparing the arrival of the first A320 are underlined. An integrated logistics support approach involving weapons and weapon subsystems is analyzed. The development of reliability centered maintenance in the nuclear industry is reviewed. The integration efforts between flight crews and ground maintenance personnel to prepare for the A320 are summarized. For individual titles, see N92-30951 through N92-30957.

N92-30951# CEP Systemes, Paris (France).
FIRST CONCLUSIONS OF A MANUFACTURER GROUP ON THE APPLICABILITY OF CALS IN EUROPE [PREMIERES CONCLUSIONS D'UN GROUPE D'INDUSTRIELS SUR L'APPLICABILITE DE CALS EN EUROPE]
J. M. Vital *In* CEP Systemes, ILS, CE, CALS? From Design to Operation 1991 33 p In FRENCH (For primary document see N92-30950 21-61)
Avail: CASI HC A03/MF A02

The applicability of a computer aided acquisition and logistics support (CALS) in Europe is discussed. The fundamental concepts of CALS are summarized. The purpose of the research performed was to improve the management costs of: weapon systems, time delays, and system quality. Different phases and means of information exchanges are considered. The NATO organizational scheme, including groups, subgroups, and the countries involved, for CALS study is given. The following topics are included: legal and contract rules, data exchange standards, network architecture, operation aspects and tests, present CALS approach, risk assessment, and control. Recommmendations for a low cost, fast, and efficient weapon acquisition system, in the scope of an integrated logistic support, are given. The results of the working group revealed that CALS phase 1 is applicable in Europe. ESA

N92-30952# Mentor Graphics (France).
CONCURRENT ENGINEERING [L'INGENIERIE CONCOURANTE]
M. LeBoulbar *In* CEP Systemes, ILS, CE, CALS? From Design to Operation 1991 12 p (For primary document see N92-30950 21-61)
Avail: CASI HC A03/MF A02

The most important aspects concerning the automation of concurrent engineering are discussed. Concurrent engineering consists of a systematic approach during the product and process design phases, which takes into account simultaneously the production, exploitation, and support constraints. The following topics were discussed: the technology trends of the 80's, the design automation problems, the design time reduction, experiences with pilot projects, and the consulting relationships. Customer partnering, technology exchange, continuous process improvement, and product integration were analyzed. Methods of top down design, system design, and design environments are described. ESA

N92-30953# GIAT Industries (France).
QUALITY ASSURANCE AND ILS [L'ASSURANCE QUALITE ET LE SLI]
J. C. Mallet *In* CEP Systemes, ILS, CE, CALS? From Design to Operation 1991 8 p In FRENCH (For primary document see N92-30950 21-61)
Avail: CASI HC A02/MF A02

The concepts of assurance quality and Integrated Logistic Support (ILS) are defined. The several steps required to reach a satisfactory integrated logistic support are as follows: understand the customer requirements; describe the work stations; develop, integrate, and validate different components for the workstations; verify the good conditions of the workstations; and insure the coherence between main and support systems. The main steps and methods of the quality assurance of the integrated logistic support are drawn. The different tasks and development phases involving design and operation of the main and support systems are listed. ESA

N92-30954# Air Inter, Lignes Aeriennes Interieures, Paris (France).
PREPARATION FOR A NEW PLANE (A 320): EXPERIENCE REVIEWED [PREPARATION A L'ACCUEIL D'UN NOUVEAU AVION (A 320): RETOUR D'EXPERIENCE]
D. Boubel *In* CEP Systemes, ILS, CE, CALS? From Design to Operation 1991 56 p In FRENCH (For primary document see N92-30950 21-61)
Avail: CASI HC A04/MF A02

The main tasks accomplished in preparation for a new A320 plane are presented. The topics discussed are: fleet age of international airlines; the IT fleet age on the 01/01/92; A-320 delivery schedule; maintenance policy and program development; airplane control and technical documentation; material supply, maintenance operations, and required tools; computer aided monitoring and control for the plane and the turbine; the ACARS program; the maintenance teams and places; cooperation with flight crew; results; and technical, economic and human improvements. ESA

N92-30955# GIAT Industries (France).
PRACTICAL APPLICATION OF THE ILS: PRACTICAL INTEGRATION, DESIGN, AND LOGISTICS [APPLICATION PRATIQUE DU SLI: INTEGRATION PRATIQUE, CONCEPTION, ET LOGISTIQUE]
B. Dumez *In* CEP Systemes, ILS, CE, CALS? From Design to Operation 1991 9 p In FRENCH (For primary document see N92-30950 21-61)
Avail: CASI HC A02/MF A02

An Integrated Logistics Support (ILS) approach involving weapons and weapon subsystems is analyzed. The influence of the logistics on the design of the equipment and the logistic support is considered. The different aspects involved in the synchronization between design and logistics include the phases of the product life, documentation, weapon subsystem conditions, integrated logistics support concept, and states of the support subsystems. Fifteen tasks of the method applied on logistics support are listed, and engineering techniques involved in the functional analysis, cost analysis and maintenance analysis are included. The basic principles of a project design is scheduled. ESA

N92-30956# Electricite de France, Chatou. Dept. Surveillance Diagnostic et Maintenance.
DEVELOPMENT OF A RELIABILITY MAINTENANCE OPTIMIZATION METHOD [DEVELOPPEMENT D'UNE METHODOLOGIE D'OPTIMISATION DE LA MAINTENANCE PAR LA FIABILITE] **c81**
J. P. Jacquot *In* CEP Systemes, ILS, CE, CALS? From Design to Operation 1991 9 p In FRENCH (For primary document see N92-30950 21-61)
Avail: CASI HC A02/MF A02

The development of reliability centered maintenance in the nuclear industry is reviewed. Qualitative methods were used in a pilot study. The method takes into account failure operational consequences and is based on the use of a special logistics for maintenance task selection and on the experience review analysis. The results are compared with those from the present base program, and confirm the benefits expected by this method.
ESA

N92-30957# Air Inter, Lignes Aeriennes Interieures, Paris (France). Centre d'Instruction de Personnel Navigant.
FLIGHT CREW INTEGRATION IN THE MAINTENANCE CHAIN OF A COMMERCIAL AIRCRAFT (A 320) [INTEGRATION DE L'EQUIPAGE DANS LA CHAINE DE MAINTENANCE D'UN AVION COMMERCIAL (A 320)] **c81**
C. Rafin and G. Raffin *In* CEP Systemes, ILS, CE, CALS? From Design to Operation 1991 9 p In FRENCH (For primary document see N92-30950 21-61)
Avail: CASI HC A02/MF A02

An integration of flight crews and maintenance teams was carried out for the acquisition of an A-320. The characteristics of the aircraft are underlined. Personnel training, meetings, implementation of maintenance and management computer systems were put into practice. Real time computer systems for the management of technical data and an aircraft communication addressing and reporting system were implemented. The following topics are included: the operation of a radio-telephone network and the flight crew technical tasks. The objectives of the company concerning the integration of several different sections and personnel were achieved. The successful operation and safety of the A-320 was reached thanks to the information exchanges between flight crews and ground supporting systems and teams. ESA

N92-30960*# Old Dominion Univ., Norfolk, VA. Dept. of Computer Science.
BUILDING A GENERALIZED DISTRIBUTED SYSTEM MODEL Progress Report, 1 Feb. - 31 Jul. 1992
R. Mukkamala Jul. 1992 124 p
(Grant NAG1-1114)
(NASA-CR-190489; NAS 1.26:190489) Avail: CASI HC A06/MF A02

The key elements in the second year (1991-92) of our project are: (1) implementation of the distributed system prototype; (2) successful passing of the candidacy examination and a PhD proposal acceptance by the funded student; (3) design of storage efficient schemes for replicated distributed systems; and (4) modeling of gracefully degrading reliable computing systems. In the third year of the project (1992-93), we propose to: (1) complete the testing of the prototype; (2) enhance the functionality of the modules by enabling the experimentation with more complex protocols; (3) use the prototype to verify the theoretically predicted performance of locking protocols, etc.; and (4) work on issues related to real-time distributed systems. This should result in efficient protocols for these systems. Author

N92-31154*# Research Inst. for Computing and Information Systems, Houston, TX.
DEMONSTRATION OF A 3D VISION ALGORITHM FOR SPACE APPLICATIONS
Rui J. P. deFigueiredo, ed. (Rice Univ., Houston, TX.) 1987 29 p
(Contract NCC9-16; RICIS Proj. AI-05)
(NASA-CR-190646; NAS 1.26:190646) Avail: CASI HC A03/MF A01

This paper reports an extension of the MIAG algorithm for recognition and motion parameter determination of general 3-D polyhedral objects based on model matching techniques and using movement invariants as features of object representation. Results of tests conducted on the algorithm under conditions simulating space conditions are presented. Author

N92-30271*# Texas A&M Univ., College Station. Dept. of Mechanical Engineering.
COMPUTER VISION IN MICROSTRUCTURAL ANALYSIS
Malur N. Srinivasan, W. Massarweh, and C. L. Hough *In* NASA. Langley Research Center, National Educators' Workshop: Update 1991. Standard Experiments in Engineering Materials Science and Technology Jun. 1992 p 131-139 (For primary document see N92-30263 21-29)
Avail: CASI HC A02/MF A03

N92-30289*# Ventura Coll., CA. Dept. of Engineering.
COMPUTER INTEGRATED LABORATORY TESTING
Charles C. Dahl *In* NASA. Langley Research Center, National Educators' Workshop: Update 1991. Standard Experiments in Engineering Materials Science and Technology Jun. 1992 p 363-365 (For primary document see N92-30263 21-29)
Avail: CASI HC A01/MF A03

62 COMPUTER SYSTEMS

Includes computer networks and special application computer systems.

N92-30363# Sandia National Labs., Albuquerque, NM.
THREE-DIMENSIONAL SHOCK WAVE PHYSICS SIMULATIONS ON MASSIVELY PARALLEL SUPERCOMPUTERS
D. R. Gardner and H. E. Fang 1992 5 p Presented at the 1992 Summer Computer Simulation Conference, Reno, NV, 27-30 Jul. 1992
(Contract DE-AC04-76DP-00789)
(DE92-008679; SAND-92-0404C; CONF-920771-1) Avail: CASI HC A01/MF A01

Three applications of massively parallel computing to weapons development at Sandia National Laboratories are briefly described, including armor/antiarmor simulations. The numerical modeling of penetrator-armor interactions requires detailed, three-dimensional simulation of complex interactions of exotic materials at high speeds. Massively parallel version of CTH and MESA, Eulerian hydrocodes developed in part for armor/antiarmor simulations, are being developed for popular architectures. The codes include models for elastic-plastic material deformation, fracture, and high explosives. Typical armor/antiarmor penetration simulations conducted on massively parallel computers with these codes are presented. The associated speedups as the simulation size is increased indicate that high parallel efficiencies can be achieved for realistic problems. These simulations demonstrate that massively parallel hydrocodes can provide highly-detailed, three-dimensional simulations of armor/antiarmor systems. DOE

N92-30401# Sandia National Labs., Albuquerque, NM.
SCALABLE PARALLEL MOLECULAR DYNAMICS ON MIMD SUPERCOMPUTERS
S. Plimpton and G. Heffelfinger 1992 7 p Presented at the Scalable High Performance Computing Conference, Williamsburg, VA, 26-29 Apr. 1992
(Contract DE-AC04-76DP-00789)
(DE92-015041; SAND-91-2786C; CONF-9204106-5) Avail: CASI HC A02/MF A01

We present two parallel algorithms suitable for molecular dynamics simulations over a wide range of sizes, from a few hundred to millions of atoms. One of the algorithms is optimally scalable, offering performance proportional to N/P where N is the number of atoms (or molecules) and P is the number of processors. The implementation of the algorithms on three MIMD parallel computers (nCUBE 2, Intel Gamma, and Intel Delta) and their performance on a standard benchmark problem as compared to vector and SIMD implementations are discussed. We also briefly describe the integration of one of the algorithms into a widely-used code appropriate for modeling defect dynamics in metals via the Embedded Atom Method. DOE

N92-30482# Utrecht State Univ. (Netherlands). Dept. of Computer Science.
A BIBLIOGRAPHY ON NETWORK FLOW PROBLEMS (2ND EDITION)
Marinus Veldhorst Oct. 1991 25 p
(Contract EEC-3075)
(RUU-CS-91-38; ISSN-0924-3275; ETN-92-91804) Avail: CASI HC A03/MF A01

A bibliography which compiles results interesting from the viewpoint of algorithms, especially combinatorial algorithms, is presented. Concentration is on the maximum flow and the minimum

cost flow problems with integral capacities and linear cost functions with integral coefficients. Results that are not published in regular journals or proceedings of conferences, are only included either when considered important from a historic point of view or when they constitute the current state of the art. For the other varieties and subclasses of the network flow problem the bibliography is certainly not complete, but nevertheless it aims to give a rather broad entrance to the scientific literature on these problems.
ESA

N92-30526# California Univ., San Diego, La Jolla. Dept. of Electrical and Computer Engineering.
CAN STOCHASTIC MODELLING AND ANALYSIS OF MULTISTAGE INTERCONNECTION NETWORKS LEAD TO EFFICIENT USAGE OF REDUNDANCY FOR FAULT-TOLERANT DESIGN?
Amiya Bhattacharya 1992 8 p
(Contract N00014-91-J-1017)
(AD-A250635) Avail: CASI HC A02/MF A01

The rapid growth in device density achieved by very large scale integration technology over the past decade had the attention of researchers centered around the design of array processors. The systolic arrays had been designed for a wide variety of applications, and consequently formal strategies for mapping algorithms onto processor arrays were developed. Use of spare or temporarily idle processing elements to achieve fault tolerance became an attractive aspect of VLSI array processing. The goal was to accomplish the designated task in case of transient or permanent failure of one or more processors, and to achieve a graceful degradation as far as possible. However, formal mapping techniques have not been extended to capture the issues of redundancy mapping. Moreover, processor interconnection topology like shuffle-exchange or butterfly networks, which require global communication links, were not considered to be practical for large on-chip design.
GRA

N92-30557# Carnegie-Mellon Univ., Pittsburgh, PA. Dept. of Electrical and Computer Engineering.
EXPLOITING RESOURCE PARALLELISM FOR INTEGRATED FAULT MONITORING AND RECOVERY Progress Report
John P. Shen 20 Mar. 1992 2 p
(Contract N00014-91-J-1518)
(AD-A248843) Avail: CASI HC A01/MF A01

Most emerging high-performance processors, such as superscalar, and very large instruction word (VLIW) processors, possess substantial fine-grain parallelism in the form of multiple pipeline stages, multiple functional units, and multiple buses. The objective of the proposed research is to develop a new method, called integrated monitoring, which effectively exploits the dynamic availability of parallel resources, e.g. delay slots in the pipe stages or idling functional units, for concurrently detecting program execution errors. Such an approach alleviates the need of a separate and dedicated hardware monitor, and minimizes or eliminates the performance penalty incurred for fault monitoring.
GRA

N92-30596# Massachusetts Inst. of Tech., Cambridge. Dept. of Mathematics.
VLSI DESIGN, PARALLEL COMPUTATION, AND DISTRIBUTED COMPUTING Final Report, 1 Feb. - 30 Sep. 1991
Tom Leighton 30 Sep. 1991 14 p
(Grant AF-AFOSR-0271-89)
(AD-A252349; AFOSR-92-0540TR) Avail: CASI HC A03/MF A01

Research efforts have centered in the areas of parallel and distributed computing, network architecture, combinatorial algorithms, and complexity theory. Significant progress has been made on the development of efficient sorting circuits, network management protocols for high speed networks, distributed graph algorithms and data structures, improved algorithms for packet routing and sorting in parallel machines, algorithms for reconfiguring networks around faults, improved approximation algorithms for a variety of NP-hard optimization problems, VLSI design, and algorithms for combinatorial problems such as multicommodity flow.
GRA

N92-30677*# National Aeronautics and Space Administration. Langley Research Center, Hampton, VA.
AN EXTENSION TO SCHNEIDER'S GENERAL PARADIGM FOR FAULT-TOLERANT CLOCK SYNCHRONIZATION
Paul S. Miner Jun. 1992 56 p
(RTOP 505-64-10-05)
(NASA-TM-107634; NAS 1.15:107634) Avail: CASI HC A04/MF A01

In 1987, Schneider presented a general paradigm that provides a single proof of a number of fault tolerant clock synchronization algorithms. His proof was subsequently subjected to the rigor of mechanical verification by Shankar. However, both Schneider and Shankar assumed a condition Shankar refers to as a bounded delay. This condition states that the elapsed time between synchronization events (i.e., the time that the local process applies an adjustment to its logical clock) is bounded. This property is really a result of the algorithm and should not be assumed in a proof of correctness. This paper remedies this by providing a proof of this property in the context of the general paradigm proposed by Schneider. The argument given is a generalization of Welch and Lynch's proof of a related property for their algorithm.
Author

N92-30696# Center for Mathematics and Computer Science, Amsterdam (Netherlands). Dept. of Computer Science.
THE GKS INPUT MODEL IN MANIFOLD
Dirk Soede, Farhad Arbab, Ivan Herman, and Paul J. W. tenHagen May 1991 23 p Sponsored by Netherlands Organization for Applied Scientific Research TNO
(CWI-CS-R9127; ETN-92-91553) Copyright Avail: CASI HC A03/MF A01

The specification of the Graphic Kernel System (GKS) input model in MANIFOLD is described. The communication patterns implied by the GKS input model are reviewed, and the suitability of the MANIFOLD language as a tool for defining complex dynamic interaction patterns that are common in nontrivial user interfaces is evaluated. The GKS input model is also adopted by all more recent International Standards Organization (ISO) graphics standard documents. A more formal scrutiny of the intercommunication of the components of this model, excluding the implementation details of their functionality, is instructive in itself. It can reveal directions for improvement of its shortcomings and for generalization of its strengths for the ongoing effort to define the functionality of future graphics packages. MANIFOLD is a language for describing interprocess communications. Processes in MANIFOLD communicate by means of buffered streams and by reacting to events raised asynchronously by other processes. Experience shows that MANIFOLD is a promising tool for describing systems of cooperating parallel processes. The MANIFOLD specification of the GKS input model offers a very flexible way to structure user defined logical input devices. It is simple and modular enough to allow easy extensions to include more functionality by local modifications. As such, it can serve as a basis for possible extensions and enhancements envisioned for future graphics packages.
ESA

N92-30812# Fermi National Accelerator Lab., Batavia, IL.
NETWORK LOAD OF X TERMINALS AT CDF
F. Abar, C. OReilly, and E. Wicklund Mar. 1992 9 p
(Contract DE-AC02-76CH-03000)
(DE92-011704; FNAL-TM-1773) Avail: CASI HC A02/MF A01

As an aid to planning future usage of X terminals, the authors measured the network bandwidth used by X terminals on a single Ethernet in a typical application environment at Fermilab. The objectives were twofold. The first objective was to identify the impact of adding one more X terminal onto the CDF Ethernet. The second objective was to determine the maximum number of X terminals allowable on the CDF network. The findings reveal that an X terminal in this environment used, on average, 431 +/-

45 bytes/second. This is quite small compared to the utilizable bandwidth of the thinwire Ethernet network (375 Kilobytes/second, equivalent to 30 percent of total bandwidth). This amounts to an averaged load of .034 percent on the network per X terminal. This paper addresses the network load solely. It does not address the loads imposed by X terminals on the memory and CPU of the host systems. DOE

N92-31111# Sandia National Labs., Albuquerque, NM.
CHOICE COORDINATION WITH MULTIPLE ALTERNATIVES
D. S. Greenberg, G. Taubenfeld (Bell Telephone Labs., Inc., Murray Hill, NJ.), and D. W. Wang (Delaware Univ., Newark.) 31 Jan. 1992 10 p Presented at the 11th Annual Association of Computing Machinery (ACM) Symposium on Principles of Distributed Computing, Vancouver, British Columbia, 10-12 Aug. 1992
(Contract DE-AC04-76DP-00789)
(DE92-011656; SAND-92-0330C; CONF-920867-2) Avail: CASI HC A02/MF A01

The Choice Coordination Problem with kappa alternatives (kappa-CCP) was introduced by Rabin in 1982. The goal is to design a wait-free protocol for n asynchronous processes which causes all correct processes to agree on one out of kappa possible alternatives. Each of the kappa alternatives has an associated shared register, and a solution to the kappa-CCP requires that a special symbol be written in exactly one shared register. All correct processes must eventually halt with a pointer to the register containing the special symbol. The difficulty arises from the fact that each process may have a different naming convention for the registers. Protocols requiring the least number of symbols are considered optimal. We gave a brief overview of our results. DOE

N92-31158*# Computational Logic, Inc., Austin, TX.
VERIFYING THE INTERACTIVE CONVERGENCE CLOCK SYNCHRONIZATION ALGORITHM USING THE BOYER-MOORE THEOREM PROVER Final Report
William D. Young Apr. 1992 46 p
(Contract NAS1-18878; RTOP 505-64-10-05)
(NASA-CR-189649; NAS 1.26:189649) Avail: CASI HC A03/MF A01

The application of formal methods to the analysis of computing systems promises to provide higher and higher levels of assurance as the sophistication of our tools and techniques increases. Improvements in tools and techniques come about as we pit the current state of the art against new and challenging problems. A promising area for the application of formal methods is in real-time and distributed computing. Some of the algorithms in this area are both subtle and important. In response to this challenge and as part of an ongoing attempt to verify an implementation of the Interactive Convergence Clock Synchronization Algorithm (ICCSA), we decided to undertake a proof of the correctness of the algorithm using the Boyer-Moore theorem prover. This paper describes our approach to proving the ICCSA using the Boyer-Moore prover. Author

63 CYBERNETICS

Includes feedback and control theory, artificial intelligence, robotics and expert systems.

For related information see also *54 Man/System Technology and Life Support.*

N92-30314*# National Aeronautics and Space Administration. Lyndon B. Johnson Space Center, Houston, TX.
A SPACE-TIME NEURAL NETWORK FOR PROCESSING BOTH SPACIAL AND TEMPORAL DATA Patent Application
James A. Villarreal, inventor (to NASA) and Robert O. Shelton, inventor (to NASA) 26 Dec. 1991 59 p
(NASA-Case-MSC-21874-1; NAS 1.71:MSC-21874-1; US-Patent-Appl-SN-813556) Avail: CASI HC A04/MF A01

Neural networks are computing systems modeled after the paradigm of the biological brain. For years, researchers using various forms of neural networks have attempted to model the brain's information processing and decision-making capabilities. Neural network algorithms have impressively demonstrated the capability of modeling spatial information. On the other hand, the application of parallel distributed models to the processing of temporal data has been severely restricted. The invention introduces a novel technique which adds the dimension of time to the well known back-propagation neural network algorithm. In the space-time neural network disclosed herein, the synaptic weights between two artificial neurons (processing elements) are replaced with an adaptable-adjustable filter. Instead of a single synaptic weight, the invention provides a plurality of weights representing not only association, but also temporal dependencies. In this case, the synaptic weights are the coefficients to the adaptable digital filters. Novelty is believed to lie in the disclosure of a processing element and a network of the processing elements which are capable of processing temporal as well as spacial data. NASA

N92-30322# University of Southern California, Los Angeles.
PRACTICAL METHOD'S FOR ROBUST MULTIVARIABLE CONTROL Final Report, 1 Aug. 1989 - 31 Oct. 1991
Michael G. Safonov and Edmond A. Jonckheere 31 Dec. 1991 9 p
(Grant AF-AFOSR-0398-89)
(AD-A248473) Avail: CASI HC A02/MF A01

The theme of the research was making modern control theory work. The product of the research has been theory, algorithms, and software applicable to multivariable feedback control problems in which there are design constraints requiring robust attainment of stability and control performance objectives in the face of both structured and unstructured uncertainty. Advances in the past two years have included relative-error methods for system identification, model reduction and control, better algorithms for H- and H2 control computations, and new results on the analysis of stability robustness in the presence of several uncertain real parameters. Although the research was aimed primarily at developing basic concepts, theory, and methodology for robust control design, the theory that is emerging from the research is already beginning to play a significant role in facilitating the control design process in a variety of aerospace engineering applications where robust performance is prerequisite, including aircraft stability augmentation systems, highly maneuverable aircraft design, missile guidance systems, and precision pointing and tracking systems. GRA

N92-30334# California Univ., Santa Barbara. Dept. of Electrical and Computer Engineering.
NUMERICAL METHODS FOR CLOSED-LOOP CONTROL Final Report, 15 Dec. 1988 - 14 Jun. 1991
Alan J. Laub 14 Jun. 1991 27 p
(Grant AF-AFOSR-0167-89)
(AD-A248481; AFOSR-92-0185TR) Avail: CASI HC A03/MF A01

The primary objective of this research was to develop algorithms for large scale computational problems arising in control, filtering, and system theory. The work has concentrated on matrix Riccati equations which are absolutely fundamental, but a range of other topics in control design were also attacked. GRA

N92-30335# Illinois Univ., Urbana. Coordinated Science Lab.
NONLINEAR SYSTEM DESIGN: ADAPTIVE FEEDBACK LINEARIZATION WITH UNMODELED DYNAMICS Final Report, 1 Oct. 1989 - 30 Sep. 1991
Peter V. Kokotovic 30 Sep. 1991 44 p
(Grant AF-AFOSR-0011-90)
(AD-A248484; AFOSR-92-0215TR) Avail: CASI HC A03/MF A01

The main goal of this research is to develop a unified geometric-asymptotic-adaptive methodology for feedback design of nonlinear control systems. Such a methodology is needed because the existing differential geometric results are restrictive and often violated by small modeling errors. Effects of these errors can be analyzed asymptotically by singular perturbation methods,

which however, are still lacking a clear geometric interpretation. Neither geometric, nor perturbational problem formulations can cope with large parametric uncertainty, for which an adaptive approach seems suitable. Conversely, both geometric and asymptotic techniques are to be merged into a methodology which eliminates their individual shortcomings. GRA

N92-30451# Technische Univ., Delft (Netherlands). Faculty of Technical Mathematics and Information.
JOINT QUEUE LENGTH AND RESPONSE TIME DISTRIBUTIONS IN A GENERAL PREEMPTIVE FEEDBACK QUEUE
D. H. J. Epema 1991 22 p
(Rept-91-66; ISSN-0922-5641; ETN-92-91816) Copyright Avail: CASI HC A03/MF A01

A general single server preemptive time sharing model with multiple queues, priorities and feedback, which included the ordinary preemptive policy and Bernoulli feedback, is considered. In the model, there is a finite or countably infinite number K of queues, jobs arrive according to a Poisson process at every queue, and the service time in every queue is generally distributed. Upon completion of a job in queue k, m(sub l) jobs are fed back to queue l, i = 1, 2,..., K, with a probability depending on k, m(sub 1) ,..., m(sub K). Jobs in queue k have preemptive priority over jobs in queue l, when k is less than l. The generating functions of the joint queue length probabilities in stationary state at departure, joint departure and preemption, output, and random instants are derived, along with the Laplace-Stieltjes transform of the total response time of a linear sequence of jobs, for any sequence of their priorities. As a special case, the two queue system is treated. ESA

N92-30710*# National Aeronautics and Space Administration. Ames Research Center, Moffett Field, CA.
COLLECTED NOTES FROM THE BENCHMARKS AND METRICS WORKSHOP
Mark E. Drummond (Sterling Federal Systems, Inc., Moffett Field, CA.), Leslie P. Kaelbling (Teleos Research, Palo Alto, CA.), and Stanley J. Rosenschein (Teleos Research, Palo Alto, CA.) Mar. 1991 61 p Workshop held at Moffett Field, CA, 25 Jun. 1990
(DARPA Order 7382)
(NASA-TM-107910; FIA-91-06; NAS 1.15:107910) Avail: CASI HC A04/MF A01

In recent years there has been a proliferation of proposals in the artificial intelligence (AI) literature for integrated agent architectures. Each architecture offers an approach to the general problem of constructing an integrated agent. Unfortunately, the ways in which one architecture might be considered better than another are not always clear. There has been a growing realization that many of the positive and negative aspects of an architecture become apparent only when experimental evaluation is performed and that to progress as a discipline, we must develop rigorous experimental methods. In addition to the intrinsic intellectual interest of experimentation, rigorous performance evaluation of systems is also a crucial practical concern to our research sponsors. DARPA, NASA, and AFOSR (among others) are actively searching for better ways of experimentally evaluating alternative approaches to building intelligent agents. One tool for experimental evaluation involves testing systems on benchmark tasks in order to assess their relative performance. As part of a joint DARPA and NASA funded project, NASA-Ames and Teleos Research are carrying out a research effort to establish a set of benchmark tasks and evaluation metrics by which the performance of agent architectures may be determined. As part of this project, we held a workshop on Benchmarks and Metrics at the NASA Ames Research Center on June 25, 1990. The objective of the workshop was to foster early discussion on this important topic. We did not achieve a consensus, nor did we expect to. Collected here is some of the information that was exchanged at the workshop. Given here is an outline of the workshop, a list of the participants, notes taken on the white-board during open discussions, position papers/notes from some participants, and copies of slides used in the presentations. Author

N92-30778*# Texas A&M Univ., College Station. Dept. of Mechanical Engineering.
TRAC PERFORMANCE ESTIMATES Final Report
L. Everett 22 Jul. 1992 30 p
(Grant NAG9-362)
(NASA-CR-190530; NAS 1.26:190530) Avail: CASI HC A03/MF A01

This report documents the performance characteristics of a Targeting Reflective Alignment Concept (TRAC) sensor. The performance will be documented for both short and long ranges. For long ranges, the sensor is used without the flat mirror attached to the target. To better understand the capabilities of the TRAC based sensors, an engineering model is required. The model can be used to better design the system for a particular application. This is necessary because there are many interrelated design variables in application. These include lense parameters, camera, and target configuration. The report presents first an analytical development of the performance, and second an experimental verification of the equations. In the analytical presentation it is assumed that the best vision resolution is a single pixel element. The experimental results suggest however that the resolution is better than 1 pixel. Hence the analytical results should be considered worst case conditions. The report also discusses advantages and limitations of the TRAC sensor in light of the performance estimates. Finally the report discusses potential improvements. Author

N92-31148# Polish Academy of Sciences, Warsaw. Inst. Podstawowych Problemow Techniki.
ON TWO METHODS OF DETERMINING THE ELLIPSES AND ELLIPSOIDS OF POSITIONING ACCURACY OF ROBOT MANIPULATORS
Zbigniew Kotulski and Wojciech Szczepanski 1992 34 p
(ISSN-0208-5658) Avail: CASI HC A03/MF A01

When analyzing the problem of the positioning accuracy of robot manipulators it is important to know how large may random deviations of the hand be from the desired position if the joint positioning errors possess a normal distribution. Two methods of determining the ellipses and ellipsoids of probability concentration are compared. The first is based on the standard procedure of the probability calculus. The second approximate method consists in finding at first the polygon or polyhedron of the positioning accuracy, and then in finding the ellipse or ellipsoid of the principal axes and second order moments coinciding with those of the polygon or polyhedron respectively. Examples of application demonstrate that these two methods give very close results. Author

64 NUMERICAL ANALYSIS

Includes iteration, difference equations, and numerical approximation.

N92-30243# Naval Research Lab., Washington, DC.
A LOCAL INTERPOLATOR DERIVED FROM THE DISCRETE FOURIER TRANSFORM Final Report
Robert L. Lucke 30 Apr. 1992 18 p
(AD-A251066; NRL/FR/6521-92-9392) Avail: CASI HC A03/MF A01

The discrete Fourier transform is used to obtain an analog of the Nyquist reconstruction formula for a limited number of data points. The resulting interpolator, when applied to the center of a slide window (rather than applied globally, as is usually done with Fourier-related techniques), can extend good interpolation performance to lower data sampling rates than is possible with polynomial interpolators. GRA

N92-30339# Maryland Univ., College Park. Inst. for Physical Science and Technology.
SPECIAL FINITE ELEMENT METHODS FOR A CLASS OF SECOND ORDER ELLIPTIC PROBLEMS WITH ROUGH COEFFICIENTS Final Report

Ivo Babuska, Gabriel Caloz (Rennes Univ., France), and John E. Osborn Jan. 1992 72 p Sponsored in part by Maryland Univ.; and by Swiss National Science Foundation
(Contract N00014-90-J-1030; NSF CCR-88-20279; NSF DMS-84-10324)
(AD-A248900; BN-1130; MD92-08-1B-GC-JED; MU-TR-92-06) Avail: CASI HC A04/MF A01

In this paper we consider the approximate solution of a class of second order elliptic equations with rough coefficients. Problems of the type considered arise in the analysis of unidirectional composites, where the coefficients represent the properties of the material. We present several methods for this class of problem, and show that they have the same accuracy as usual methods have for problems with smooth coefficients. We refer to the methods as special finite elements methods because they are of finite element type but employ special shape functions, chosen to effectively model the unknown solution. GRA

N92-30347# California Univ., Los Angeles. Dept. of Mathematics.
ALGORITHM TO SOLVE NONLINEAR TIME DEPENDENT PROBLEMS OF ENGINEERING AND PHYSICS Final Report, 1 May 1989 - 31 Oct. 1991
Stanley Osher 31 Oct. 1991 2 p
(Grant AF-AFOSR-0341-89)
(AD-A250641; AFOSR-92-0425TR) Avail: CASI HC A01/MF A01

A triangle based nonoscillatory shock capturing algorithm was developed and applied successfully to immiscible oil recovery problems. Chevron researchers are now using this successfully for real problems. GRA

N92-30350# Technische Univ., Delft (Netherlands). Faculty of Technical Mathematics and Information.
ON REAL AND COMPLEX ZEROS OF ORTHOGONAL POLYNOMIALS IN A DISCRETE SOBOLEV SPACE
H. G. Meijer 1991 25 p
(Rept-91-98; ISSN-0922-5641; ETN-92-91848) Copyright Avail: CASI HC A03/MF A01

A study on the zeros of given polynomials orthogonal with respect to a given inner product is presented. Starting with the Sobolev inner product the tangent theorem for real zeros is explored. The existence of complex zeros is addressed. ESA

N92-30360# Technische Univ., Delft (Netherlands). Faculty of Technical Mathematics and Information.
DIFFERENTIAL EQUATIONS FOR SYMMETRIC GENERALIZED ULTRASPHERICAL POLYNOMIALS
Roelof Koekoek 1992 28 p
(Rept-92-08; ISSN-0922-5641; ETN-92-91860) Copyright Avail: CASI HC A03/MF A01

A study which looks for differential equations satisfied by given generalized Jacobi polynomials which are orthogonal on the interval (1,1) with respect to the given weight function is presented. The definition and some properties of the classical ultraspherical polynomials are given. ESA

N92-30371# Technische Univ., Delft (Netherlands). Faculty of Technical Mathematics and Information.
A THREE-VALUED CUMULATIVE SEMANTICS FOR TMS
Cees Witteveen 1991 19 p
(Rept-91-69; ISSN-0922-5641; ETN-92-91819) Copyright Avail: CASI HC A03/MF A01

The three valued, well founded or skeptical semantics for Truth Maintenance Systems (TMS) can be used to define a cumulative inference relation. This result improves on the results obtained by Makinson and Brewka, who also obtained a cumulative semantics for TMS but had to introduce a more complex extension of the stable model semantics, while the skeptical semantics is a straightforward generalization of the 2 valued stable model semantics. Moreover, the entailment relation induced is computationally tractable. ESA

N92-30375# New York Univ., New York. Inst. of Mathematical Sciences.
SOLAR FLARE MDH Annual Report, 1 Jan. - 31 Dec. 1991
Henry R. Strauss 31 Dec. 1991 7 p
(Grant AF-AFOSR-0044-91)
(AD-A250639; AFOSR-92-0288TR) Avail: CASI HC A02/MF A01

The following research problems were investigated in this program of theoretical solar plasma physics. (1) Three Dimensional Reconnection: A model with axially bounded magnetic flux tubes has been suggested as a source of coronal heating. Numerical simulations have supported this theory. (2) Fast Reconnection: A reconnection rate for the driven reconnection of solar coronal loops and other axially bounded magnetic fields has been obtained. (3) Approximate Equilibrium States: Equilibrium states appropriate for coronal flux tubes and for the magnetic tail of the magnetosphere have been constructed analytically and numerically. (4) Boundary Conditions: A full solution for plane symmetry has been obtained for standing plasma waves with a discontinuous anchoring conductivity. (5) Alfven Waves: It has been shown that highly energetic ions can resonantly destabilize Alfven waves but the effect of Kelvin Helmholtz turbulence prevents further Alfven wave growth, limiting them to a small fraction of the beam energy. (6) Ballooning Modes: The general ballooning equations have been developed. Very simple configurations have been found to be always unstable. GRA

N92-30410# Pittsburgh Univ., PA. Dept. of Mathematics and Statistics.
ON IMPASSE POINTS OF QUASILINEAR DIFFERENTIAL ALGEBRAIC EQUATIONS
Patrick J. Rabier and Werner C. Rheinboldt Jun. 1992 33 p
(Contract N00014-90-J-1025; AF-AFOSR-0094-90; NSF CCR-89-07654)
(AD-A252643; ICMA-92-171) Avail: CASI HC A03/MF A01

This paper presents a mathematical characterization of the impasse points of quasilinear DAE's $A(x) = G(x)$, where then $A(x)$ is a n x n matrix having constant but not full r less than n in the domain of interest. We show that a reduction procedure permits reduction of the DEA to a quasilinear ODE $A1(xi)xi' = G1(xi)$ Rr and that impasse points correspond to special singularities of the reduced ODE. Impasse points of higher index DAE's can also be defined; the only difference is that the above reduction procedure takes more than one step. GRA

N92-30434# Technische Univ., Delft (Netherlands). Faculty of Technical Mathematics and Information.
POSITIVITY FOR A STRONGLY COUPLED ELLIPTIC SYSTEM BY GREEN FUNCTION ESTIMATES
Guido Sweers 1991 22 p
(Rept-91-77; ISSN-0922-5641; ETN-92-91827) Copyright Avail: CASI HC A03/MF A01

A study aiming to show the existence of a positive constant for an elliptic system is presented. Pointwise estimates for the Green functions are needed for the proof. The two sided estimate needed for Green functions in the two dimensional domains is derived. Elliptic operators are proved only for those with constant coefficients in front of the derivatives. Regularity assumptions are stated. ESA

N92-30436# Technische Univ., Delft (Netherlands). Faculty of Technical Mathematics and Information.
REAL CUBIC SYSTEMS WITH FOUR LINE INVARIANTS
Robert E. Kooij 1991 21 p
(Rept-91-79; ISSN-0922-5641; ETN-92-91829) Copyright Avail: CASI HC A03/MF A01

The number of limit cycles for real cubic systems of differential equations on the plane which possess four line invariants is studied. Both the relative positions of the four line invariants and their types (i.e., real or complex lines) are shown to influence the number of limit cycles. ESA

N92-30437# Technische Univ., Delft (Netherlands). Faculty of Technical Mathematics and Information.
GMRESR: A FAMILY OF NESTED GMRES METHODS
H. A. vanderVorst and C. Vuik (Utrecht State Univ., Netherlands) 1991 19 p
(Rept-91-80; ISSN-0922-5641; ETN-92-91830) Copyright Avail: CASI HC A03/MF A01

A study which proposes an iterative solution method for unsymmetric linear systems, in which the preconditioner is updated from step to step, is presented. Variants of the GMRES (Generalized Minimal Residual) algorithm, in which a preconditioner is constructed per iteration step by a suitable iteration process, e.g., by GMRES itself, are suggested. ESA

N92-30446# Utrecht State Univ. (Netherlands). Dept. of Computer Science.
RESTRICTIONS OF GRAPH PARTITION PROBLEMS, PART 1
Hans L. Bodlaender and Klaus Jansen (Trier Univ., Trier-Tarforst, Germany, F.R.) Nov. 1991 20 p
(Contract EEC-3075)
(RUU-CS-91-44-Pt-1; ISSN-0924-3275; ETN-92-91810) Avail: CASI HC A03/MF A01

The problems in partitioning a given graph into k independent sets or cliques of bounded size k' are analyzed for several classes of graphs. The computational complexity of both problems restricted to cographs, split graphs, bipartite graphs and interval graphs given general or constant k and k', is investigated. The assignment problem for operations in a branching flow graph to processors, each with a limit in the number of executable operations is shown to equal the problem of partitioning into independent sets, restricted to cographs. A job assignment problem given intervals for each job and k machines, each executing at most k' jobs, equals the problem to partition into independent sets restricted to interval graphs. Both problems are shown to be NP complete. ESA

N92-30447# Utrecht State Univ. (Netherlands). Dept. of Computer Science.
POINT LOCATION IN FAT SUBDIVISIONS
Mark H. Overmars Nov. 1991 9 p Sponsored in part by Netherlands Organization for Applied Scientific Researchm TNO
(Contract EEC-3075)
(RUU-CS-91-40; ISSN-0924-3275; ETN-92-91806) Avail: CASI HC A02/MF A01

The point location problem in fat subdivisions in d dimensional space is studied. Subdivisions are called fat if no cell has long and skinny parts. It is shown that point location queries in such subdivisions can be performed in a very simple way in time O(log(sup d - 1)n) with a data structure using O(log(sup d - 1)n) storage. The problem is also studied in the situation where the largest cell is only a factor R larger than the smallest cell. In this case, a solution with only O(log R) query time using linear storage, is obtained. ESA

N92-30449# Utrecht State Univ. (Netherlands). Dept. of Computer Science.
LINEAR PLANAR AUGMENTATION ALGORITHMS FOR OUTERPLANAR GRAPHS
Goos Kant Dec. 1991 23 p
(Contract EEC-3075)
(RUU-CS-91-47; ISSN-0924-3275; ETN-92-91813) Avail: CASI HC A03/MF A01

A study which shows that for outerplanar graphs G, the problem of augmenting G by adding a minimum number of edges such that the augmented graph G' is planar and bridge connected, biconnected or triconnected can be solved in linear time and space, is presented. ESA

N92-30450# Utrecht State Univ. (Netherlands). Dept. of Computer Science.
KAYLES ON SPECIAL CLASSES OF GRAPHS: AN APPLICATION OF SPRAGUE-GRUNDY THEORY
Hans L. Bodlaender Dec. 1991 19 p
(RUU-CS-91-49; ISSN-0924-3275; ETN-92-91815) Avail: CASI HC A03/MF A01

Kayles is the game where two players alternately choose a vertex that has not been chosen before, nor is adjacent to an already chosen vertex from a given graph. The last player that choses a vertex wins the game. With help of Sprague-Grundy theory, it is shown that the problem to determine which player has a winning strategy for a given graph, can be solved in 0(n cubed) time on interval graphs, on circular arc graphs, and on permutation graphs, and in O(n(sup 1.631)) time on cographs. For general graphs, the problem is known to be PSPACE complete, and can be solved in time. ESA

N92-30456# Technische Univ., Delft (Netherlands). Faculty of Technical Mathematics and Information.
THE FORMAL POWER OF AGs WITH RESPECT TO THEIR UNDERLYING CFGs
J. P. M. deVreught 1991 23 p
(Rept-91-75; ISSN-0922-5641; ETN-92-91825) Copyright Avail: CASI HC A03/MF A01

The consequence of having an acyclic Context Free Grammar (CFG) as underlying grammar for an Attribute Grammar (AG) is investigated. The formal powers of AGs with underlying cyclic or acyclic CFG differ considerably. AGs with an acyclic CFG are strictly less powerful than AGs with an underlying possibly cyclic CFG. ESA

N92-30457# Technische Univ., Delft (Netherlands). Faculty of Technical Mathematics and Information.
BIFURCATION OF LIMIT CYCLES IN A PARTICULAR CLASS OF QUADRATIC SYSTEMS
W. T. vanHorssen and J. W. Reyn 1991 31 p
(Rept-91-76; ISSN-0922-5641; ETN-92-91826) Copyright Avail: CASI HC A03/MF A01

Within the class of quadratic perturbations, it is shown analytically or numerically how many limit cycles can be bifurcated at first order out of the periodic orbits surrounding the center of the quadratic system: x(dot) = x(1 - x - ay) and y(dot) = y(-1 + ax + y), where a is greater than 1 and less than infinity. ESA

N92-30458# Utrecht State Univ. (Netherlands). Dept. of Computer Science.
ON THE COMPLEXITY OF THE MAXIMUM CUT PROBLEM
Hans L. Bodlaender and Klaus Jansen (Trier Univ., Trier-Tarforst, Germany, F.R.) Oct. 1991 21 p
(Contract EEC-3075)
(RUU-CS-91-39; ISSN-0924-3275; ETN-92-91805) Avail: CASI HC A03/MF A01

The complexity of the combinatorial simple maxcut problem is investigated for several special classes of graphs. This problem is shown to be NP complete when restricted to one of the following classes: chordal graphs, undirected path graphs, split graphs, tripartite graphs, and graphs that are the complement of a bipartite graph. The problem can be solved in polynomial time, when restricted to graphs with bounded treewidth, or cographs. Large classes of graphs that can be seen as generalizations of classes of graphs with bounded treewidth and of the class of the cographs, and allow polynomial time algorithms for the simple maxcut problem, are given. ESA

N92-30459# Technische Univ., Delft (Netherlands). Faculty of Technical Mathematics and Information.
THE FUNCTIONS PSI(x) AND BETA(x) AND SOME INEQUALITIES FOR INTEGRALS (THEOREMS 1-16)
H. vanHaeringen 1992 55 p Submitted for publication
(Rept-92-09; ISSN-0922-5641; ETN-92-91861) Copyright Avail: CASI HC A04/MF A01

The definition of the psi(x) and beta(x) functions is shown and some useful relations are given. More complicated inequalities involving beta(x) are shown. Theorems to derive inequalities for some particular classes of integrals are formulated and proved. ESA

N92-30461# Technische Univ., Delft (Netherlands). Faculty of Technical Mathematics and Information.
FURTHER EXPERIENCES WITH GMRESR
C. Vuik 1992 13 p Presented at the Copper Mountain Conference on Iterative Methods, Copper Mountain, CO, Apr. 1992
(Rept-92-12; ISSN-0922-5641; ETN-92-91864) Copyright Avail: CASI HC A03/MF A01

A variant of the GMRES (Generalized Minimal Residual) method, a popular method for the iterative solution of sparse linear systems with an unsymmetric nonsingular matrix, is proposed. The variant, GMRESR, allows a different precondtioner to be taken in each iteration step. Some properties of this approach are discussed and illustrated with numerical experiments. GMRESR is compared with GMRES, Bi-CGSTAB and FGMRES. ESA

N92-30464# Technische Univ., Delft (Netherlands). Faculty of Technical Mathematics and Information.
ON THE THUE MORSE MEASURE
F. M. Dekking 1992 10 p
(Rept-92-16; ISSN-0922-5641; ETN-92-91867) Copyright Avail: CASI HC A02/MF A01

A precise description of the Thue Morse measure and the Fibonacci measure is obtained. More generally, an equipartition result for ergodic measures in substitution dynamical systems generated by substitutions of constant length is proved. ESA

N92-30473# Grenoble-1 Univ. (France). Lab. ARTEMIS.
RECURSIVE MODELS FOR SYNCHRONOUS SEQUENTIAL DEVICES
Solange Coupet and Laurence Pierre (Provence Univ., Marseille, France) Jul. 1991 21 p Sponsored in part by Commission of the European Communities
(IMAG-RR-855-I; ETN-92-91473) Avail: CASI HC A03/MF A01

In the framework of formal verification of hardware, inductive methods are of great interest. The Bayer-Moore theorem prover is used frequently. In order to model and verify synchronous sequential circuits with this system, an appropriate underlying denotational semantics for such devices must first be designed. A natural modeling of a sequential circuit is a set of higher order (possibly mutually) recursive functions associated with the state variables, which expresses their current values in terms of the past values of the primary inputs and the state variable. However, this model does not quite fit the principles of the Bayer-Moore system. Therefore another representation in which the circuit is modeled by a unique first order tail recursive function with the state variables as parameters is defined. These two models are presented with illustrative examples, and their equivalence is proved mathematically. ESA

N92-30483# Technische Univ., Delft (Netherlands). Faculty of Technical Mathematics and Information.
FINITE VOLUME DISCRETIZATION OF THE CONVECTION-DIFFUSION EQUATION IN GENERAL COORDINATES
P. Wesseling 1991 19 p
(Rept-91-72; ISSN-0922-5641; ETN-92-91822) Copyright Avail: CASI HC A03/MF A01

Finite volume discretizations of the convection-diffusion equation in general coordinates in two dimensions are presented. The diffusion coefficient is piecewise continuous. The coordinate system is assumed to result from a piecewise bilinear boundary fitted mapping of a physical domain on a rectangle. Exact (approximately) discretization for constant and linear functions, despite the irregularity of the equations in general coordinates, is shown. ESA

N92-30490# Technische Univ., Delft (Netherlands). Faculty of Technical Mathematics and Information.
REAL POLYNOMIAL SYSTEMS OF DEGREE n WITH n+1 LINE INVARIANTS
Robert E. Kooij 1991 18 p
(Rept-91-86; ISSN-0922-5641; ETN-92-91836) Copyright Avail: CASI HC A03/MF A01

The number of limit cycles for special classes of real polynomial systems of differential equations in the plane is studied. For real polynomial systems of degree n, which poses n + 1 line invariants, it is shown that both the relative positions of the n + 1 line invariants and their types (i.e., real or complex) influence the number of limit cycles. ESA

N92-30491# Technische Univ., Delft (Netherlands). Faculty of Technical Mathematics and Information.
ABOUT DIFFERENCE EQUATIONS, ALGEBRAS AND DISCRETE EVENTS
Geert Jan Olsder 1991 33 p
(Rept-91-87; ISSN-0922-5641; ETN-92-91837) Copyright Avail: CASI HC A03/MF A01

An introduction to the theory of discrete event dynamic systems is given. Discrete Event Dynamic Systems (DEDS) are nonlinear in the conventional algebra, but are linear in the max-plus algebra. Duplicates of many concepts and results, within the conventional linear algebra and linear systems theory, exist in the max-plus algebra and the theory of DEDS. The motivation to study DEDS comes from the description of flows in networks. Such networks are for instance related to computer systems, traffic systems, and flexible manufacturing in production planning. ESA

N92-30511# Institut des Hautes Etudes Scientifiques, Bures-sur-Yvette (France).
QUANTUM WEYL GROUP AND UNIVERSAL QUANTUM R-MATRIX FOR AFFINE LIE ALGEBRA A1
S. Levendorskii, Y. Soibelman, and V. Stukopin Feb. 1992 16 p
(PB92-178276; IHES/M/92/10) Avail: CASI HC A03/MF A01

In the paper titled 'Quantum Groups', V. Drinfeld indicated a general form for universal quantum R-matrix; for the case sl(2), the author gave an explicit formula for the case sl(n). Other authors offered a formula for universal R-matrix for arbitrary finite-dimensional simple Lie algebra G. The main result of the paper is the analog of that formula for R for affine Lie algebra A1. Author

N92-30516*# Institute for Computer Applications in Science and Engineering, Hampton, VA.
A COMPUTATIONAL ALGORITHM FOR CRACK DETERMINATION: THE MULTIPLE CRACK CASE Final Report
Kurt Bryan and Michael Vogelius (Rutgers - The State Univ., New Brunswick, NJ.) Jun. 1992 41 p Submitted for publication
(Contracts NAS1-18605; NAS1-19480; NSF DMS-89-02532; AF-AFOSR-89-NM-605; RTOP 505-90-52-01)
(NASA-CR-189665; ICASE-92-24; NAS 1.26:189665) Avail: CASI HC A03/MF A01

An algorithm for recovering a collection of linear cracks in a homogeneous electrical conductor from boundary measurements of voltages induced by specified current fluxes is developed. The technique is a variation of Newton's method and is based on taking weighted averages of the boundary data. The method also adaptively changes the applied current flux at each iteration to maintain maximum sensitivity to the estimated locations of the cracks. Author

N92-30517# Technische Univ., Delft (Netherlands). Faculty of Technical Mathematics and Information.
SYNCHRONIZED CONTINUOUS FLOW SYSTEMS
Geert Jan Olsder 1991 18 p
(Rept-91-88; ISSN-0922-5641; ETN-92-91838) Copyright Avail: CASI HC A03/MF A01

Continuous analogs of the descriptions of discrete event dynamic systems and/or timed Petri nets are given. The synchronization aspects of such systems are thus shown to be more basic than their discrete character. Various theorems in the context of discrete event systems have their logical counterparts within the continuous setting. ESA

N92-30533# California Univ., Berkeley.
DYNAMICS OF DEFORMABLE BODIES Final Report, 1 Jan. - 31 Dec. 1991
Jerrold E. Marsden 31 Dec. 1991 2 p
(Grant AF-AFOSR-0133-91)
(AD-A252333; AFOSR-92-0541TR) Avail: CASI HC A01/MF A01

The main achievement in this grant was the development of a scientific understanding of the role of variational principles in symplectic and energy momentum integrators, and using this structure to study the energy oscillation properties of symplectic integrators. The role of locking phenomena that comes up in the numerical solution of structural dynamics problems was also investigated. GRA

N92-30566# Mound Lab., Miamisburg, OH.
OPERATIONAL SURFACES FOR THE RECTANGLE AND TRIANGLE
G. L. Silver 1 Jun. 1992 41 p
(Contract DE-AC04-88DP-43495)
(DE92-015165; MLM-3748) Avail: CASI HC A03/MF A01

Operational surfaces for rectangles and the triangle with center point are illustrated. Equations are derived that interrelate response values for data in rectangular array. Equations for three-dimensional interpolation in the rectangular prism are included. DOE

N92-30568# Yale Univ., New Haven, CT. Dept. of Computer Science.
ON THE RAPID EVALUATION OF TRIGONOMETRIC SERIES
A. Dutt and V. Rokhlin Mar. 1992 33 p
(Contract N00014-89-J-1527; NSF DMS-90-12751)
(AD-A249029; YaleU/DCS/RR-893) Avail: CASI HC A03/MF A01

A group of algorithms is presented generalizing the Fast Fourier Transform (FFT) to the case of non-integer frequencies and non-equispaced nodes on the interval -pi to pi. The schemes of this paper are based on a combination of certain analytical considerations with the classical Fast Fourier Transform, and generalize both the forward and backward FFT's. Each of the algorithms requires O(N x log(N) + N x log(1/epsilon)) arithmetic operations, where epsilon is the precision of computations and N is the number of nodes. The efficiency of the approach is illustrated by several numerical examples. Author (GRA)

N92-30597# Army Armament Research, Development and Engineering Center, Watervliet, NY.
SOLVING THE EULER EQUATIONS USING ADAPTIVE MESH MOTION AND REFINEMENT Final Report
David C. Arney, Rupak Biswas, and Joseph E. Flaherty Apr. 1992 26 p
(AD-A252364; ARCCB-TR-92018) Avail: CASI HC A03/MF A01

We use an adaptive mesh moving and refinement finite volume method to solve the transient Euler equations of compressible flow in one and two space dimensions. Numerical solutions are generated by a MacCormack scheme with Davis's artificial viscosity model. Richardson's extrapolation is used to calculate estimates of the local discretization error which can be used to control mesh motion and refinement. Questions regarding the optimal combination of adaptive strategies and the characterization of the initial mesh are investigated. Results indicate that local mesh refinement with and without mesh moving provide dramatic improvements in accuracy over uniform mesh solutions; that mesh motion provides good results on relatively fine initial meshes; that each problem has an optimal initial mesh and that it is more efficient to begin with a coarser than optimal mesh and refine rather than starting with too fine a mesh; and that a combination of both the adaptive strategies produced the most accurate solutions. GRA

N92-30608# Argonne National Lab., IL.
APPLICATION OF AUTOMATED DEDUCTION TO THE SEARCH FOR SINGLE AXIOMS FOR EXPONENT GROUPS
W. McCune and L. Wos 11 Feb. 1992 6 p Presented at the LPAR-1992, St. Petersburg (Russian Federation), 15-20 Jul. 1992
(Contract W-31-109-eng-38)
(DE92-015271; ANL/CP-75803; CONF-9207101-1) Avail: CASI HC A02/MF A01

We present new results in axiomatic group theory obtained by using automated deduction programs. The results include single axioms, some with the identity and others without, for groups of exponents 3, 4, 5, and 7, and a general form for single axioms for groups of odd exponents. The results were obtained by using the programs in three separate ways: as a symbolic calculator, to search for proofs, and to search for counterexamples. We also touch on relations between logic programming and automated reasoning. DOE

N92-30618# Army Armament Research, Development and Engineering Center, Watervliet, NY.
ANALYTICAL SOLUTION OF ELASTIC-PLASTIC THICK-WALLED CYLINDERS WITH GENERAL HARDENING Final Report
Peter C. Chen Mar. 1992 20 p Presented at the 9th Army Conference on Applied Mathematics and Computing, Minneapolis, MN, 18-21 Jun. 1991
(AD-A249491; ARCCB-TR-92010) Avail: CASI HC A03/MF A01

This report presents an analytical solution for the elastic-plastic behavior of thick-walled cylinders under internal pressure. The general hardening law employed in this investigation is a piecewise linear representation of arbitrary stress-strain curves in uniaxial form. Closed-form analytical solutions are developed for the stresses, the elastic and plastic strains, and the displacements by using Tresca's yield criterion and its associated flow rule. Experimental data obtained from cylinders made of either SAE 1045 steel, OFHC copper, or aluminum alloy 1100 are used to determine the material constants. Numerical results for partially-plastic and fully-plastic cylinders are presented for the radial distributions of plastic hoop strain, radial, and tangential stresses. GRA

N92-30638# Virginia Polytechnic Inst. and State Univ., Blacksburg. Dept. of Mathematics.
COMPUTATIONAL METHODS FOR MODELING AND ACTIVE CONTROL OF DISTRIBUTED PARAMETER SYSTEMS Final Report, 1 Dec. 1988 - 30 Nov. 1991
J. A. Burns and E. M. Cliff 1 Mar. 1992 12 p
(Grant AF-AFOSR-0001-89)
(AD-A248559; AFOSR-92-0239TR) Avail: CASI HC A03/MF A01

This research has developed a number of new results for the modeling and control of spatially continuous dynamic processes. The work includes developing numerical methods for implementing controller designs for those linear and nonlinear partial differential equations that describe the dynamics of fluid/structure systems and thermo-mechanical alloys. GRA

N92-30689# Center for Mathematics and Computer Science, Amsterdam (Netherlands). Dept. of Operations Research, Statistics, and System Theory.
THE TWO-DIMENSIONAL RANDOM WALK: ITS HITTING PROCESS AND ITS CLASSIFICATION
J. W. Cohen Dec. 1990 35 p Sponsored by Netherlands Organization for the Advancement of Research
(CWI-BS-R9003; ETN-92-91640) Copyright Avail: CASI HC A03/MF A01

An analysis by which a detailed classification of the states of a two dimensional random walk in the lattice N by N in R(sub 2) can be obtained, is developed. The technique is illustrated for the two dimensional analogon of the imbedded queue length process of the M/G/1 queue. The hitting point process with the coordinate axes plays an essential role in the analysis. Next to the process the hitting point process of a similar type of random walk on the lattice in the upper half plane is studied. The classification is obtained for the case with non zero drift on the interior of the

state space. The developed technique can also be applied by using results from fluctuation theory to random walks, for which the first moments of the various components of the one step displacement vectors do not exist. The zero drift case is discussed and for the positive recurrent case several state probabilities are evaluated. ESA

N92-30700# Center for Mathematics and Computer Science, Amsterdam (Netherlands). Dept. of Numerical Mathematics.
PARALLEL ASPECTS OF SOME SPECTRAL PROBLEMS IN LINEAR ALGEBRA
Alexander N. Malyshev (Akademiya Nauk SSSR, Novosibirsk.) Jul. 1991 41 p
(CWI-NM-R9113; ETN-92-91661) Copyright Avail: CASI HC A03/MF A01

Unsymmetric eigenvalue problems with guaranteed accuracy are investigated. An algorithm is studied for computing deflating subspaces of the regular linear matrix pencil on parallel computing systems. The problem of separation of the matrix spectrum by the imagery axis is discussed. The algorithm was implemented in a portable way suitable for shared memory parallel computers. Applications of the developed code are made to the solution of the Lyapunov and the Riccati equations. ESA

N92-30716*# Institute for Computer Applications in Science and Engineering, Hampton, VA. Div. of Applied Mathematics.
RESOLUTION PROPERTIES OF THE FOURIER METHOD FOR DISCONTINUOUS WAVES Final Report
David Gottlieb and Chi-Wang Shu Jun. 1992 17 p Submitted for publication
(Contracts NAS1-18605; NAG1-1145; N00014-91-J-4016; DAAL03-91-G-0123; AF-AFOSR-90-0093; RTOP 505-90-52-01) (NASA-CR-189668; ICASE-92-27; NAS 1.26:189668) Avail: CASI HC A03/MF A01

In this paper we discuss the wave-resolution properties of the Fourier approximations of a wave function with discontinuities. It is well known that a minimum of two points per wave is needed to resolve a periodic wave function using Fourier expansions. For Chebyshev approximations of a wave function, a minimum of pi points per wave is needed. Here we obtain an estimate for the minimum number of points per wave to resolve a discontinuous wave based on its Fourier coefficients. In our recent work on overcoming the Gibbs phenomenon, we have shown that the Fourier coefficients of a discontinuous function contain enough information to reconstruct with exponential accuracy the coefficient of a rapidly converging Gegenbauer expansion. We therefore study the resolution properties of a Gegenbauer expansion where both the number of terms and the order increase. Author

N92-30776# Naval Research Lab., Washington, DC.
SOME MODEL THEORY OF FREE GROUPS AND FREE ALGEBRAS
Anthony Gaglione and Dennis Spellman 30 Apr. 1992 34 p
(AD-A249425; NRL/MR/4440-92-6967) Avail: CASI HC A03/MF A01

The subject of this paper is group theory and logic with an emphasis on groups. The concept of a group is one of the most powerful and unifying of all concepts in mathematics. Moreover in addition to turning up in every branch of mathematics, groups have endless applications in science. Wherever there is symmetry, there is a group. The Lorentz transformations of relativity from a Lie group are based on continuous rotation of an object in space-time. Finite groups underlie the structure of all crystals and are indispensable in chemistry, quantum mechanics, and particle physics. The famous eight fold way, which classifies the family of subatomic particles known as hadrons, is a Lie group. In view of the great elegance and utility of groups, it is understandable that mathematicians study them and their properties, which is precisely what this paper does. There is, of course, no way to predict what other practical application this material will have. We do, however, know that groups lie at the very heart of the structure of the universe. GRA

N92-30789# Institut des Hautes Etudes Scientifiques, Bures-sur-Yvette (France).
DIMENSION BOUNDS FOR QUOTIENT SPACES
D. Fried Mar. 1992 9 p
(PB92-177997; IHES/M/92/16) Avail: CASI HC A02/MF A01

The dimension of the quotient space of a compact metrizable space X by a closed equivalence relation R, dim(X/R), is estimated in terms of a neighborhood basis for R in X x X. The finite dimensionality for Gromov's semi-Markovian spaces and for expansive dynamical systems are proven. GRA

N92-30790# Institut des Hautes Etudes Scientifiques, Bures-sur-Yvette (France).
NON-HOLONOMIC FILTRATION: ALGEBRAIC AND GEOMETRIC ASPECTS OF NON-INTEGRABILITY
V. Lychagin and V. Rubtsov Feb. 1992 29 p
(PB92-178003; IHES/M/92/9) Avail: CASI HC A03/MF A01

Various algebraic and geometric applications of a spectral sequence approach to non-integrability are presented. GRA

N92-30843# Army Research Office, Research Triangle Park, NC.
TRANSACTIONS OF THE 9TH ARMY CONFERENCE ON APPLIED MATHEMATICS AND COMPUTING Technical Report, Jan. 1991 - Feb. 1992
Mar. 1992 766 p Conference held in Minneapolis, MN, 18-21 Jun. 1991
(AD-A252140; ARO-92-1) Avail: CASI HC A99/MF A02

The Ninth Army Conference on Applied Mathematics and Computing was held at the Army High Performance Computing Research Center (AHPCRC), at the University of Minnesota, on 18-21 June 1991. The Sponsor of these annual meetings is the Army Mathematics Steering Committee (AMSC). Its members would like to thank Professor George Sell, Director of APHCRC, for serving as chairperson on local arrangements. He along with his staff personnel are to be commended for coordinating the many details needed to conduct this successful scientific meeting. The participants of the conference were treated to an Open House on 17 June, with tours of the facilities and a demonstration of the visualization and graphic facilities. The conference was very well attended with more than one hundred participants, including about forty scientists from the Army laboratories. The technical program consisted of five special sessions scheduled on topics such as Smart Materials Design of Real-Time Control, Probabilistic Algorithms, and Large-Scale Optimization. The conference featured more than forty contributed papers presented in nine technical sessions. In addition there were seven invited speakers, whose names are listed below together with the titles of their talks. GRA

N92-31128# Carnegie-Mellon Univ., Pittsburgh, PA. Dept. of Mathematics.
SOME MATHEMATICAL PROBLEMS IN CONTINUUM MECHANICS Final Technical Report, 30 Sep. 1988 - 29 Jun. 1991
William J. Hrusa 16 Jul. 1991 7 p
(Grant AF-AFOSR-0265-88)
(AD-A250352; Rept-1-52150; AFOSR-92-0351TR) Avail: CASI HC A02/MF A01

Research efforts were focused on problems in viscoelasticity, thermoelasticity, and thermoviscoelasticity. Results were obtained concerning existence, stability, and formation of singularities for classical solutions of various initial-boundary value problems. Some work was also performed on developing models of integrals for thermoviscoelastic materials. GRA

N92-31134# International Centre for Theoretical Physics, Trieste (Italy).
FIXED POINT ITERATIONS FOR A CLASS OF NONLINEAR MAPPINGS IN CERTAIN BANACH SPACES
C. E. Chidume Dec. 1991 10 p
(DE92-630235; IC-91/398) Avail: CASI HC A02/MF A01

It is proven that both the Mann iteration method and the

Ishikawa iteration method converge strongly, in real Banach spaces with a certain property, to the unique fixed point of nonlinear mappings belonging to Class C. DOE

N92-31135# International Centre for Theoretical Physics, Trieste (Italy).
HEAT FLOW OF p-HARMONIC MAPS WITH VALUES INTO SPHERES
Yunmei Chen (Florida Univ., Gainesville.) and Min-Chun Hong Dec. 1991 15 p
(DE92-630236; IC-91/399) Avail: CASI HC A03/MF A01

The global existence of weak solutions for the heat flow of p-harmonic maps of closed Riemannian manifolds into spheres is proved. DOE

N92-31140# Army Armament Research, Development and Engineering Center, Watervliet, NY.
WRAPPABILITY OF CURVES ON SURFACES Final Report
Royce W. Soanes Mar. 1992 22 p Presented at the 8th Army Conference on Applied Mathematics and Computing, Ithaca, NY, 19-22 Jun. 1990
(AD-A250004; ARCCB-TR-92012) Avail: CASI HC A03/MF A01

In this report, conditions are derived under which a path on a general smooth surface is wrappable or capable of receiving an essentially one-dimensional flexible filament under tension that clings to the surface throughout its length and does not slip. Wrappability considerations are of practical importance in the fabrication of filament-wound composite pressure vessels, for instance. The general wrappability conditions derived are applied to two special cases: general cylinders and general surfaces of revolution. GRA

N92-31189# Sandia National Labs., Albuquerque, NM.
COMPONENT-WISE ERROR BOUNDS FOR LINEAR EQUATIONS
Joseph F. Grcar Jun. 1992 22 p
(Contract DE-AC04-76DR-00789)
(DE92-016000; SAND-92-8548) Avail: CASI HC A03/MF A01

Error bounds are derived for individual unknowns in linear equations. These bounds suggest a new condition number that is insensitive to both row and column scaling of the coefficient matrix. The new error bounds and condition numbers can be evaluated easily, without limiting processes. This work complements that of Oettli, Prager, and Skeel concerning component-wise error analysis. DOE

65 STATISTICS AND PROBABILITY

Includes data sampling and smoothing; Monte Carlo method; and stochastic processes.

N92-30355# Technische Univ., Delft (Netherlands). Faculty of Technical Mathematics and Information.
THE DOMAIN OF ATTRACTION OF THE ALPHA-SUM OPERATOR FOR TYPE 2 AND TYPE 3 DISTRIBUTIONS
Gerard Hooghiemstra and Priscilla E. Greenwood (British Columbia Univ., Vancouver.) 1992 18 p
(Rept-92-02; ISSN-0922-5641; ETN-92-91854) Copyright Avail: CASI HC A03/MF A01

It is shown that for F a member of the set D(Psi sub gamma) and for F a member of the set D(empty set), the type 2, and type 3 domains, there exists norming constants a(sub n) greater than 0 and b(sub n) a member of set R such that a(sub n, exp -1)(X(sub n) - b(sub n)/1 - alpha)) has a nondegenerate limit distribution. The method of proof is based on weak convergence of Markov processes with an entrance boundary. The proof uses monotonicity properties of the involved Markov processes and tightness of the sequence X(sub n)(t) for fixed positive t. Starting from the tightness, a full proof of weak convergence is given. The proof of individual tightness is then given. ESA

N92-30452# Technische Univ., Delft (Netherlands). Faculty of Technical Mathematics and Information.
SCALE SENSITIVITY AND RANK PRESERVATION IN A MULTIPLICATIVE VARIANT OF THE AHP AND SMART
F. A. Lootsma 1991 34 p
(Rept-91-67; ISSN-0922-5641; ETN-92-91817) Copyright Avail: CASI HC A03/MF A01

A number of geometric scales based on psychological arguments are used in Analytic Hierarchy Process (AHP). These scales are only used at the first evaluation level, when the alternatives under each of the criteria are compared separately. The impact scores are estimated by logarithmic regression since the airwise comparisons are frequently incomplete. The rank order of the impact scores appears to be invariant when geometric scales are employed. The delicate aggregation step is improved by the geometric mean aggreggation rule and by a new definition of the relative importance of the critreria. At the second evaluation level there is demonstrated to be only one geometric scale to qualify the relative importance of the criteria. The rank order of the final scores of the alternatives does therefore not depend on the geometric scale employed to calculate the impact scores at the first level. The multiplicative AHP is shown to be a multiplicative version of the Simple Multi Attribute Rating Technique (SMART), a popular offspring of Multi Attribute Utility Theory (MAUT), to be used when the choice of an alternative has a riskless outcome. In fact, the mutiplicative AHP is concerned with ratios of intervals on the dimension of desirability, whereas SMART analyzes differences of the corresponding orders of magnitude. ESA

N92-30460# Technische Univ., Delft (Netherlands). Faculty of Technical Mathematics and Information.
SOME INEQUALITIES FOR VARIANCES
H. vanHaeringen 1992 50 p
(Rept-92-10; ISSN-0922-5641; ETN-92-91862) Copyright Avail: CASI HC A03/MF A01

A number of inequalities involving variances are derived. In particular, let h(t) be a density function on (0, infinity), consisting of a positive linear combination of different negative exponential functions. Then the associated variance, provided finite, decreases (increases) when h(t) is multiplied by a nonnegative function omega(t) that is non increasing (non decreasing) and not identically constant. This statement does not hold in general when h(t) is such a density function on (a, infinity) if a does not equal 0, or in (0, a) if a is less than infinity. ESA

N92-30481# Utrecht State Univ. (Netherlands). Dept. of Computer Science.
THE SUM OF WEIGHTED BALLS
Jop F. Sibeyn (Hebrew Univ., Jerusalem, Israel) Oct. 1991 16 p Sponsored by Netherlands Foundation for Computing Science
(Contract EEC-3075)
(RUU-CS-91-37; ISSN-0924-3275; ETN-92-91803) Avail: CASI HC A03/MF A01

The problem of randomly distributing balls over n holes is considered. The weight of the balls is given by a random variable. This problem models several problems from computer science, most importantly randomized load balancing. The distribution of the sums of the weights of the balls in the holes is analyzed using the Chernoff bound and the Hoeffding inequality. Often O(n x log(n)) balls are enough to assure good balancing of the weights. If the expected weight of the balls is much smaller than their maximal weight, it is very useful to gather balls to superballs. An analysis based on the moment generating function of the ball weights is given. The moment generating function of the probability pass function of the sum of weights is derived. From this moment generating function it is easy to derive moments and variance. ESA

N92-30562# Oregon State Univ., Corvallis. Dept. of Statistics.
IMPROVEMENT OF PERFORMANCE OF VARIABLE PROBABILITY SAMPLING STRATEGIES
W. S. Overton and S. V. Stehman 1992 8 p Presented at

the ASA Environmental Statistics Winter Conference, Alexandria, VA, 1-3 Jan. 1991 Prepared in cooperation with State Univ. of New York, Syracuse
(PB92-180264; EPA/600/A-92/107) Avail: CASI HC A02/MF A01

The precision of estimators used with variable probability sampling may be improved either at the design stage or at the analysis stage following selection of the sample. Improvement at the analysis stage is obtained by employing a Horvitz-Thompson difference estimator, which may improve precision even when the response variable is negatively correlated with the inclusion probabilities. In general, optimization of the Horvitz-Thompson difference estimator is achieved by employing bootstrapping to facsimile populations constructed from the sample data: in some cases, optimization can be achieved analytically. This strategy focuses sampling considerations on population description in order to improve the facsimile population representation of the real population under study. Author

N92-30633# North Carolina Univ., Chapel Hill. Dept. of Statistics.
RESEARCH IN STOCHASTIC ANALYSIS AND ITS APPLICATIONS Final Report, 1 Jun. - 30 Sep. 1991
Stamatis Cambanis, Gopinath Kallianpur, and R. R. Leadbetter 18 Dec. 1991 61 p
(Contract DAAL03-91-G-0176)
(AD-A249482; ARO-29016.1-MA) Avail: CASI HC A04/MF A01

Research was conducted in the area of stochastic analysis and its applications in engineering, neurophysiology, and oceanography. A list of the main areas of research activity is as follows: infinite dimensional stochastic differential equations; stochastic partial differential equations; nonlinear filtering; random fields; point processes and random measures; exchangeable processes; nonstationary processes; Gaussian and non-Gaussian processes; wavelet approximation of random signals; sampling designs for time series; random measures associated with high levels; limit theorems for random measures; and parameter estimation under dependence. GRA

N92-30699# Center for Mathematics and Computer Science, Amsterdam (Netherlands). Dept. of Computer Science.
COMBINATORICS AND KOLMOGOROV COMPLEXITY
Ming Li (Waterloo Univ., Ontario) and Paul M. B. Vitanyi 17 May 1991 13 p Presented at the IEEE 6th Structures in Complexity Theory Conference, Chicago, IL, Jun. 1991 Submitted for publication Sponsored in part by Natural Sciences and Engineering Research Council
(Grants NSERC-OGP-0036747; NSERC-OGP-0046506)
(CWI-CS-R9125; ETN-92-91638) Copyright Avail: CASI HC A03/MF A01

The combinatorial properties of finite sequences with high Kolmogorov complexity are investigated. The utility of a Kolmogorov complexity method in combinatorial theory is demonstrated by several examples. Kolmogorov established a notion of complexity (self information) of finite objects which is essentially finitary and combinatorial. Martin-Loef established that the proper definition of finite random sequences corresponds to finite sequences having about maximal Kolmogorov complexity. It is useful to determine the exact form in which certain combinatorial properties hold for high complexity finite sequences. ESA

N92-30771# Florida State Univ., Tallahassee. Dept. of Statistics.
MARKOV CHAIN SIMULATIONS OF BINARY MATRICES
William B. Krebs Jan. 1992 20 p
(Contract DAAL03-90-G-0103)
(AD-A249265; ARO-27868.14-MA) Avail: CASI HC A03/MF A01

We consider Markov chains to simulate graphs with a fixed degree sequence and binary matrices with fixed row and column sums. By means of a combinatorial construction, we bound the subdominant eigenvalues of the chains. Under certain additional conditions, we show that the bounds are polynomial functions of the degree sequences and the row and column sums, respectively. GRA

N92-30803# Argonne National Lab., IL.
QUANTIFICATION AND REDUCTION OF THE UNCERTAINTY IN MASS BALANCE MODELS BY MONTE CARLO ANALYSIS OF PRIOR DATA
B. M. Lesht 1991 29 p Presented at the Approaches to Reducing Uncertainty in Mass Balance Models for Toxics: Lake Ontario Study, Buffalo, NY, 3 Feb. - 5 Mar. 1992
(Contract W-31109-eng-38)
(DE92-010278; ANL/CP-75636; CONF-920291-1) Avail: CASI HC A03/MF A01

The general objective of this workshop is to investigate and discuss methods by which uncertainties in mass balance models for toxics in the Great Lakes may be reduced. As described by the workshop prospectus, this paper is focused on problems of reducing (and quantifying) uncertainty as it relates to: in situ field observations/system response; measurements for the establishment of initial conditions; boundary conditions; calibration/confirmation data sets; and model post-audit data sets. I have taken this description to refer not only to the evaluation of uncertainty in the field observations themselves, but also to the uncertainty associated with the analyses of in situ observations as they interact in the overall modeling process. Thus, I will be concerned here with quantification and reduction of uncertainty: (1) as they may be applied to descriptions of the system that is being modeled; and (2) as they may be associated with model simulations. DOE

N92-31185# Los Alamos National Lab., NM.
A FAILURE-TO-RESTORE UNAVAILABILITY MODEL FOR PERIODICALLY PERFORMED MAINTENANCE
T. F. Bott Jun. 1992 32 p
(Contract W-7405-eng-36)
(DE92-015902; LA-12266-MS) Avail: CASI HC A03/MF A01

This paper presents a simple mathematical model of the entire restoration/surveillance action that ties together the individual probabilities of errors found in human reliability analyses into an estimate of the unavailability of a component arising from failure to be restored after maintenance. This model accounts for failure to restore surveillance frequency, probability of failing to discover an error during surveillance, and probability of incorrect restoration of the tested component after surveillance. DOE

66 SYSTEMS ANALYSIS

Includes mathematical modeling; network analysis; and operations research.

N92-30419# Messerschmitt-Boelkow-Blohm G.m.b.H., Munich (Germany, F.R.).
OPERATIONS AND LOGISTICS TASKS IN THE COLUMBUS DEVELOPMENT PROGRAM
C. Koopmann (Erno Raumfahrttechnik G.m.b.H. Bremen, Germany, F.R.), T. Knudson (European Space Agency. European Space Research and Technology Center, ESTEC, Noordwijk, Netherlands), and Mike C. Attwood (Erno Raumfahrttechnik G.m.b.H. Bremen, Germany, F.R.) 1991 11 p Presented at the 4th Logistics Symposium, Cocoa Beach, FL, 4-6 Nov. 1991 Previously announced in IAA as A92-24367
(MBB-UO-0166-91-PUB; ETN-92-91894) Avail: CASI HC A03/MF A01

Operations and logistics activities in European space programs from the early beginnings via Spacelab to Columbus are reviewed. For the Columbus development production program the major results of the operations and logistics task are described. These tasks cover all necessary activities from requirement definition, through analyses, planning, procedure and application software development and verification for ground operations, flight

operations and logistics. General information about the contractual and organization setup for the performance of operations and logistics tasks within the Columbus program is also provided. Additional details on logistics tasks concerning methods used and tools employed, as well as resulting documentation, are included. ESA

N92-30420# Messerschmitt-Boelkow-Blohm G.m.b.H., Munich (Germany, F.R.).
ADOPTION OF THE LSA S/W DILSA FOR THE COLUMBUS LSA TASKS
Mike C. Attwood (Erno Raumfahrttechnik G.m.b.H. Bremen, Germany, F.R.) and W. Pabst (Erno Raumfahrttechnik G.m.b.H. Bremen, Germany, F.R.) 1991 13 p Presented at the 4th Logistics Symposium, Cocoa Beach, FL, 4-6 Nov. 1991 Previously announced in IAA as A92-24352
(MBB-UO-0168-91-PUB; ETN-92-91896) Avail: CASI HC A03/MF A01

A system and flight configuration level Logistics Support Analysis (LSA) in accordance with Columbus specific implementation guidelines using a computerized tool and S/W (software) is presented. The approach towards performing the LSA, the front end analysis activities performed, the market survey of commercially available LSA S/W and associated personal computer/mainframe test activities, are described. The tailoring process with the LSA S/W product 'DILSA' which was necessary in order to comply with the Columbus specific LSA and Management and Technical Information System (MATIS) requirements is detailed. The selected data record and summary reports as well as the applicable LSA processes are presented. ESA

N92-30442# Messerschmitt-Boelkow-Blohm G.m.b.H., Munich (Germany, F.R.).
COLUMBUS LOGISTICS TRANSPORTATION AND GROUND PROCESSING
Mike C. Attwood (Erno Raumfahrttechnik G.m.b.H. Bremen, Germany, F.R.), Manfred Nordhoff (Erno Raumfahrttechnik G.m.b.H. Bremen, Germany, F.R.), and Horst Goerlich (Erno Raumfahrttechnik G.m.b.H. Bremen, Germany, F.R.) 1991 13 p Presented at the 4th Logistics Symposium, Cocoa Beach, FL, 4-6 Nov. 1991 Previously announced in IAA as A92-24371
(MBB-UO-0167-91-PUB; ETN-92-91895) Avail: CASI HC A03/MF A01

Handling and transportation, and ground processing for the Columbus Man Tended Free Flyer (MTFF) and the Attached Pressurized Module (APM) are described. Handling and transportation to the launch sites in configurations as close as possible to the launch configurations presents a challenge to transportation methods and scenarios, and requires an innovative infrastructure. Ground processing checkout activities at the launch sites need to be organized and timelined in a way to have existing launch site facilities and capabilities support the MTFF/APM needs, and to meet the scheduled launch date. ESA

N92-30891# Los Alamos National Lab., NM.
JOINT STABILIZING PROJECTS IN DEFENSE
G. H. Canavan, J. C. Browne, and R. J. Joseph Jun. 1992 16 p
(Contract W-7405-eng-36)
(DE92-015977; LA-12302-MS) Avail: CASI HC A03/MF A01

Joint defensive projects could increase stability and decrease the alert rates of strategic forces. Areas include the defense of the U.S., Commonwealth of Independent States (CIS), and their allies against third world threats; protection against each other's accidental or unauthorized launches; and defense against intentional attacks. The most promising area appears to be defining interfaces for the handover of satellite warning and trajectory information, which applies to most phases of theater defense and mutual protection. DOE

N92-30898*# National Aeronautics and Space Administration. Lewis Research Center, Cleveland, OH.
A SIMPLIFIED DYNAMIC MODEL OF THE T700 TURBOSHAFT ENGINE
Ahmet Duyar (Florida Atlantic Univ., Boca Raton.), Zhen Gu (Florida Atlantic Univ., Boca Raton.), and Jonathan S. Litt Jun. 1992 22 p Presented at the 48th American Helicopter Society Annual Forum, Washington, DC, 3-5 Jun. 1992; sponsored by the American Helicopter Society
(Grant NAG3-1198; DA Proj. 1L1-61102-AH-45)
(NASA-TM-105805; E-7235; NAS 1.15:105805; AVSCOM-TR-92-C-024; RTOP 505-62-0K) Avail: CASI HC A03/MF A01

A simplified open-loop dynamic model of the T700 turboshaft engine, valid within the normal operating range of the engine, is developed. This model is obtained by linking linear state space models obtained at different engine operating points. Each linear model is developed from a detailed nonlinear engine simulation using a multivariable system identification and realization method. The simplified model may be used with a model-based real time diagnostic scheme for fault detection and diagnostics, as well as for open loop engine dynamics studies and closed loop control analysis utilizing a user generated control law. Author

67 THEORETICAL MATHEMATICS

Includes topology and number theory.

N92-30642# Boston Univ., MA. Center for Polymer Studies.
FRACTAL AND MULTIFRACTAL APPROACHES TO CLUSTERING PHENOMENA Final Report, 1 Oct. 1990 - 30 Sep. 1991
H. E. Stanley 30 Sep. 1991 20 p
(Contract N00014-91-J-1133)
(AD-A249481) Avail: CASI HC A03/MF A01

Recently considerable efforts were made in understanding the dynamics of non-equilibrium interface growth in the context of a variety of fractal clustering models. Many recent investigations have concentrated on the dynamic scaling properties of interfaces obtained in experiments and in various cluster growth models. Particular attention has been devoted to the scaling properties of the rms interface width. It is widely believed that many such problems belong to the same universality class as the Kardar-Parisi-Zhang (KPZ) equation. There have recently appeared several experiments on surface growth. Recently Zhang suggested that the anomalous roughening found in experiments can be explained by an uncorrelated 'noise' obeying a power-law distribution. GRA

N92-31194# Army Armament Research, Development and Engineering Center, Watervliet, NY.
MULTIFRACTAL ANALYSIS OF CHAOTIC POINT SETS Final Report
L. V. Meisel and M. A. Johnson Apr. 1992 38 p
(AD-A250756; ARCCB-TR-92015) Avail: CASI HC A03/MF A01

It is generally acknowledged that nonlinear systems exhibit important features that cannot be understood, controlled, or exploited without addressing their behavior in a non-linear form. We describe qualitative and quantitative techniques for the description of nonlinear dynamic systems. These techniques are illustrated through the analysis of symmetric chaos. GRA

70 PHYSICS (GENERAL)

For precision time and time interval (PTTI) see *35 Instrumentation and Photography;* for geophysics, astrophysics or solar physics see *46 Geophysics, 90 Astrophysics,* or *92 Solar Physics.*

N92-30498# National Inst. for Fusion Science, Nagoya (Japan).
ROLE OF COMPRESSIBILITY ON DRIVEN MAGNETIC RECONNECTION
T. Sato, T. Hayashi, K. Watanabe, R. Horiuchi, M. Tanaka, N. Sawairi (Hiroshima Univ., Japan), and K. Kusano (Hiroshima Univ., Japan) Aug. 1991 32 p
(NIFS-105; ISSN-0915-633X) Avail: CASI HC A03/MF A01

Whether it is induced by an ideal (current driven) instability or by an external force, plasma flow causes a change in the magnetic field configuration and often gives rise to a current intensification locally, resulting in a fast driven reconnection there. Many dramatic phenomena in magnetically confined plasmas such as magnetospheric substorms, solar flares, MHD self-organization, and tokamak sawtooth crash, may be attributed to this fast driven reconnection. Using a fourth order MHD simulation code, it is confirmed that compressibility of the plasma plays a crucial role in leading to a fast (MHD time scale) driven reconnection. This indicates that the incompressible representation is not always applicable to the study of the global dynamical behavior of a magnetically confined plasma. Author

N92-30549# Washington State Univ., Pullman. Dept. of Chemistry.
THEORETICAL STUDY OF PHASE-SHIFTED QUANTUM BEATS IN TIME-RESOLVED LUMINESCENCE SPECTRA FROM A BIASED ASYMMETRIC DOUBLE QUANTUM WELL
Y. Ohtsuki, Lakshmi N. Pandey, and Thomas F. George Jun. 1992 14 p
(Contract N00014-90-J-1193)
(AD-A252422; WSU/92/85; TR-85) Avail: CASI HC A02/MF A01

Analytical expressions have been developed for time-dependent luminescence intensities for a practically feasible asymmetric double quantum well under bias. They were numerically demonstrated to elucidate the characteristic of phase-shifted quantum beats. It is clear analytically as well as numerically that the magnitude of the tunneling interaction can be quantitatively estimated by the beat modulation depth. GRA

N92-30850# California Univ., San Diego, La Jolla. Dept. of Physics.
DISORDER AND TRANSPORT IN HIGHLY CORRELATED SYSTEMS Annual Report, 1 Apr. 1991 - 31 Mar. 1992
Ivan K. Schuller 31 Mar. 1992 8 p
(Contract N00014-91-J-1438)
(AD-A249969) Avail: CASI HC A02/MF A01

This grant was a new start dedicated to studies of disorder and transport in highly correlated electron systems, mostly superconductors. These studies are most conveniently accomplished in thin film structures. Thin films useful in these types of studies present a number of structural and chemical defects at length scales comparable to interatomic spacing. This disorder may have strong effects on the physical properties and so quantitative structural and chemical characterization is a must. The developments in the past year have been beyond expectations. We have developed all the growth and structural characterization techniques useful for the preparation of high and low temperature superconducting films and superlattices. These have been applied to the growth and characterization of films which were used in a number of physical property studies. One particularly interesting highlight was the study of the enhancement of superconductivity by light illumination. GRA

N92-30983# National Inst. for Fusion Science, Nagoya (Japan).
THE ROLE OF STOCHASTICITY IN SAWTOOTH OSCILLATION
Allan J. Lichtenberg (California Univ., Berkeley.), Kimitaka Itoh, Sanae-I. Itoh, and Atsushi Fukuyama (Okayama Univ., Japan) Aug. 1991 79 p
(NIFS-103) Avail: CASI HC A05/MF A01

Stochastization of field lines, resulting from the interaction of the fundamental m/n = 1/1 helical mode with other periodicities, plays an important role in sawtooth oscillations. The time scale for the stochastic temperature diffusion is shown to be sufficiently fast to account for the fast sawtooth crash. The enhanced electron and ion viscosity, arising from the stochastic field lines, are calculated. The enhanced electron viscosity always leads to an initial increase in the growth rate of the mode, the magnetic trigger. The enhanced ion viscosity can ultimately lead to mode stabilization before a complete temperature redistribution or flux reconnection has occurred. A dynamical model is introduced to calculate the path of the sawtooth oscillation through a parameter space of shear and amplitude of the helical perturbation, including a stochastic trigger to an enhanced growth rate, stabilization by ion viscosity, and a prescription for flux reconnection at the end of the growth phase. Our model predicts that four types of the sawtooth oscillations are possible even for a plasma with monotonic q(r) profile. There are two types of rearrangement of the magnetic configuration: a partial-magnetic reconnection, in which the safety factor on axis q(0) value oscillates around 0.7 with delta q(0) approx. equal to 0.05; and a full magnetic reconnection, for which q(0) oscillated between 1 and about 0.8. In a partial reconnection the temperature flattening is rapid and can be either limited to an annulus near the q = 1 rational surface, which then gradually propagates to the axis, or the temperature on axis T(sub e)(0) can rapidly decay, when the stochastic region invades the geometrical axis. With a full magnetic reconnection, T(sub e)(0) collapses rapidly when stochasticity is present or slowly without stochasticity. The main features of the model are compared with experimental observations. In particular, they may explain the sudden growth of the helical perturbation, the magnetic trigger, the fast time scale of the temperature collapse, a partial temperature collapse, and the persistence of an m/n = 1/1 island throughout the sawtooth cycle. Author

N92-31131# Notre Dame Univ., IN.
SINGLE-ELECTRON CHARGING EFFECTS
S. T. Ruggiero 15 Dec. 1991 10 p
(Contract DE-FG02-88ER-45373)
(DE92-015287; DOE/ER-45373/4) Avail: CASI HC A02/MF A01

The status of our project on single-electron tunneling is, again, excellent. As outlined in our original proposal, a key goal for this project has been the development of a scanning tunneling instrument for the purpose of imaging individual particles and tunneling into these particles at high magnetic fields. Further progress is discussed. DOE

N92-30286*# Iowa State Univ. of Science and Technology, Ames. Dept. of Materials Science and Engineering.
DEMONSTRATION OF MAGNETIC DOMAIN BOUNDARY MOVEMENT USING AN EASILY ASSEMBLED VIDEOCAM-MICROSCOPE SYSTEM
John W. Patterson *In* NASA. Langley Research Center, National Educators' Workshop: Update 1991. Standard Experiments in Engineering Materials Science and Technology Jun. 1992 p 309-312 (For primary document see N92-30263 21-29)
Avail: CASI HC A01/MF A03

N92-31079*# Bulgarian Academy of Sciences, Sofia. Inst. of Electronics.
ANALYTICAL ESTIMATES OF THE PP-ALGORITHM AT LOW NUMBER OF DOPPLER PERIODS PER PULSE LENGTH
M. D. Angelova, E. V. Stoykova, and D. V. Stoyanov *In* NASA. Langley Research Center, 16th International Laser Radar Conference, Part 2 Jul. 1992 p 629-632 (For primary document see N92-31013 21-35)
Avail: CASI HC A01/MF A03

71 ACOUSTICS

Includes sound generation, transmission and attenuation. For noise pollution see *45 Environmental Pollution.*

N92-30801# International Centre for Theoretical Physics, Trieste (Italy).
QUANTUM MECHANICS IN GRASSMANN SPACE
N. Mankoc-Borstnik Oct. 1991 22 p
(DE92-622377; IC-91/371) Avail: CASI HC A03/MF A01

The representations of the infinitesimal operators of Lorentz rotations and translation and the corresponding carriers for a scalar, spinor and vector case in the Grassmann space as well as the eigenfunctions of the Hamilton function for a free particle, are presented. Functions are orthogonalized. The mass appears after compactification from 5 to 4 dimensions in the ordinary space-time, while in the Grassmann space the particle lives in five dimensions, so that a boost can be performed. DOE

N92-30890# Allied-Signal Aerospace Co., Kansas City, MO.
CHARACTERIZING ULTRASONIC TRANSDUCERS USING PATTERN RECOGNITION TECHNIQUES
J. W. Ekis Apr. 1992 68 p
(Contract DE-AC04-76DP-00613)
(DE92-015845; KCP-613-4664) Avail: CASI HC A04/MF A01

This project's goal was to develop an automated ultrasonic transducer characterization system. A computer-based test system collected the test data for each of the given transducers. This data set was then processed by a number of pattern recognition algorithms. The results from these classifications placed the transducers into groups of similar units. All the transducers in a group will have similar performance characteristics. Each group was isolated from the others. DOE

N92-30966# Office National d'Etudes et de Recherches Aerospatiales, Paris (France). Direction de la Physique Generale.
RESOLUTION OF THE THREE-DIMENSIONAL PARABOLIC EQUATION APPLIED TO ACOUSTIC PROPAGATION AT LOW ALTITUDES Final Report [RESOLUTION DE L'EQUATION PARABOLIQUE TRIDIMENSIONNELLE APPLIQUEE A LA PROPAGATION ACOUSTIQUE A BASSE ALTITUDE. RAPPORT FINAL]
Y. Delrieux and P. Malbequi May 1991 40 p In FRENCH
(Contract DRET-89-001-118)
(ONERA-RF-17/3641-PY; ETN-92-91669) Avail: CASI HC A03/MF A01

The numerical calculation of the three dimensional parabolic equation is carried out. The finite difference method is applied. The matrix system to be solved depending on the range is separated into two three diagonal systems, by the method of alternating directions. The limiting conditions associated with the parabolic equation are taken into account. The accuracy of the finite difference method is compared with the analytical solution for a propagating configuration in the presence of a uniform wind. Calculations taking into account the presence of obstacles and wind are presented. Differences of the acoustic field are observed by comparing two and three dimensional calculations in and near the obstacle's shaded region. ESA

N92-30979*# National Aeronautics and Space Administration. Langley Research Center, Hampton, VA.
THE OPTIMIZATION OF FORCE INPUTS FOR ACTIVE STRUCTURAL ACOUSTIC CONTROL USING A NEURAL NETWORK
R. H. Cabell (Virginia Polytechnic Inst. and State Univ., Blacksburg.), H. C. Lester, and R. J. Silcox Jun. 1992 9 p Proposed for presentation at the 1992 International Congress on Noise Control Engineering (INTER-NOISE 92), Toronto, Ontario, 20-22 Jul. 1992
(RTOP 535-03-11-03)
(NASA-TM-107627; NAS 1.15:107627) Avail: CASI HC A02/MF A01

This paper investigates the use of a neural network to determine which force actuators, of a multi-actuator array, are best activated in order to achieve structural-acoustic control. The concept is demonstrated using a cylinder/cavity model on which the control forces, produced by piezoelectric actuators, are applied with the objective of reducing the interior noise. A two-layer neural network is employed and the back propagation solution is compared with the results calculated by a conventional, least-squares optimization analysis. The ability of the neural network to accurately and efficiently control actuator activation for interior noise reduction is demonstrated. Author

N92-31151 British Broadcasting Corp., Kingswood (England). Engineering Div.
AN INVESTIGATION OF THE EFFECTS OF BOUNDARY CONSTRAINTS ON THE SOUND INSULATIONS OF LIGHTWEIGHT, DOUBLE LEAF PARTITIONS
G. D. Plumb 1992 13 p
(BBC-RD-1992/4) Copyright Avail: Issuing Activity

The sound insulation of a metal-framed, double lead partition (measured in the Research Department Transmission Suite) was considerably lower when the two leaves of the partition were built into common, rather than independent, surrounding walls. The purpose of the work described in this report was to investigate whether this shortfall in sound insulation was caused by the mechanical coupling of the two leaves of the partition at its perimeter. To investigate the nature of any coupling between the two leaves, the vibration isolation was measured between the two leaves of the test partition, with the two leaves built into either common surrounding walls or into independent walls. Contour plots of the vibration isolation between the two leaves of the partition, for both boundary conditions, revealed the extent of the coupling at the perimeters of the leaves. The amount of coupling observed was sufficient to explain the differences in the sound insulation between the two conditions. Author

N92-31173 British Broadcasting Corp., Kingswood (England). Engineering Div.
OPTIMUM METHODS FOR THE MEASUREMENT OF THE ABSORPTION COEFFICIENTS OF MATERIALS
G. D. Plumb 1992 19 p
(BBC-RD-1992/3) Copyright Avail: Issuing Activity

For the measurement of the absorption coefficients of materials in a reverberation room, the method currently used by the BBC differs from the ISO-Standard method, in the use of additional diffusion in the room and in the distribution of the sample. For the ISO-Standard method, adequate diffusion is achieved by using additional diffusing elements in the reverberation room, whereas the BBC method relies on the distribution of the sample. In this Report, ISO-Standard absorption coefficient measurements are shown to be more appropriate to the design of heavily treated rooms. Absorption coefficient measurements made using the BBC method are more appropriate to the design of sparsely treated rooms. To ensure that measurements at low frequency in the old reverberation room at Research Department are as reliable as possible, the existing BBC method for the measurement of the absorption coefficients of subdivided samples will continue to be used; additional diffusing elements are not then required. If the sample cannot, or would not usually be subdivided, additional diffusing elements will be installed. The ISO-Standard method for the measurement of the absorption coefficients of materials will be used in the new reverberation room. The use of the ISO-Standard method should reduce the influence of 'edge effects' on the measured absorption coefficients. Author

72 ATOMIC AND MOLECULAR PHYSICS

Includes atomic structure, electron properties, and molecular spectra.

N92-30236# Academy of Sciences of the Ukrainian SSR, Kiev. Inst. Teoreticheskoj Fiziki.
SPIN AMPLITUDES OF pp-SCATTERING IN A UNITARIZED SUPERCRITICAL POMERON MODEL

E. S. Martynov 1991 12 p
(DE92-624639; ITP-91-12) Avail: CASI HC A03/MF A01

Spin amplitudes of elastic pp-scattering in a supercritical pomeron model unitarized by a quasi-eikonal method are calculated. It is shown that in this model the proton polarization at small transferred moments decreases as 1/ln(exp 2)s and at fixed ones - as 1/lns. Polarization oscillates both by the energy and by the transferred momentum, decreasing exponentially with increasing of the latter. DOE

N92-30240# State Univ. of New York, Buffalo. Dept. of Chemistry.
CHEMISTRY WITHIN VAN DER WAALS CLUSTER OF UNSATURATED MOLECULES: OBSERVATION OF CATIONIC POLYMERIZATION
Stephanie Gumina, M. T. Coolbaugh, Gopal Vaidyanathan, and James F. Garvey 1 Jun. 1992 8 p
(Contract N00014-88-K-0483)
(AD-A250929; TR-35) Avail: CASI HC A02/MF A01

We present the observation of intracluster ion-molecule polymerization reactions within clusters containing molecules which possess double or triple carbon-carbon bonds. This effect is borne out by the observation of unusual magic numbers in the cluster ion distribution only under expansion conditions which favor the production of large neutral clusters. These magic numbers are rationalized in terms of the production of covalently bonded cyclic molecular ions which terminate the cationic polymerization process. GRA

N92-30255# State Univ. of New York, Buffalo. Dept. of Chemistry.
PHOTODYNAMICS WITHIN (CH3OH)(nCr(CO)6) HETEROCLUSTERS: OBSERVATION OF AN ISOTOPE EFFECT
William R. Peifer and James F. Garvey 1 Jun. 1992 24 p
(Contract N00014-88-K-0483)
(AD-A251058; TR-26) Avail: CASI HC A03/MF A01

We have recently examined the multiphoton dissociation and ionization dynamics of mixed van der Waals heteroclusters of Cr(CO)6 solvated by methanol, and have inferred from photoion fragmentation branching ratios that CD3OD is more efficient than CH3OH in relaxing excess internal energy of the nascent photoion via intracluster energy transfer. Multiphoton ionization is suggested to proceed via single-photon photodissociation of the solvated Cr(CO)6, followed by two-photon ionization of the coordinatively unsaturated photoproduct. Excess energy in the internal modes of the nascent photoion appears to be disposed of via non-statistical, mode-specific transfer to the internal degrees of freedom of an adjacent solvent molecule within the cluster. Photoionization using laser power densities on the order of 1012 to 1013 W/sq cm is accompanied by extensive intracluster bimolecular chemistry. GRA

N92-30259# Cornell Univ., Ithaca, NY. Dept. of Chemistry.
VIBRATIONALLY INDUCED ROTATIONAL AXIS SWITCHING: A NOVEL MECHANISM FOR VIBRATIONAL MODE-COUPLING
H. Li, Gregory S. Ezra, and Laura A. Philips 29 May 1992 37 p
(Contract N00014-90-J-1971)
(AD-A251085; TR-5) Avail: CASI HC A03/MF A01

High resolution IR spectra of small- to medium-sized molecules such as 2 fluoroethanol (2FE) show that the effective density of coupled states is often greater than that obtained by a direct count of vibrational states. A novel mechanism for rotation-vibration interaction, vibrationally induced rotational axis switching (VIRAS), is proposed as a possible explanation for these discrepancies. VIRAS has its origin in centrifugal distortion, and is physically distinct from Coriolis coupling. In the case of 2FE, we explicitly treat the coupling of overall rotation with large-amplitude internal rotation about the C-C bond. Assuming a uniform coupling of all dark vibration torsion states to the bright state, we predict a density of coupled states in good agreement with that observed in the C-H stretching region at 2980/cm. GRA

N92-30261# State Univ. of New York, Buffalo. Dept. of Chemistry.
MAGIC NUMBERS IN MOLECULAR CLUSTERS: A PROBE FOR CHEMICAL REACTIVITY
James F. Garvey and M. T. Coolbaugh 1 Jun. 1992 34 p
(Contract N00014-88-K-0483)
(AD-A251096; TR-33) Avail: CASI HC A03/MF A01

When neutral van der Waals clusters, produced in a supersonic expansion, are ionized the resulting cluster ion distribution can exhibit dramatic intensity anomalies for very specific cluster sizes. These 'magic numbers' typically result from a particulary stable cluster ion geometry generated by the completion of a full solvent shell around a central ion core. We will review our current work which employs magic numbers as a probe, not only of cluster ion structure, but also of chemical reactivity within these species. That is, the appearance of certain magic numbers can be attributed to unique cluster reactions occurring between the ion and the solvating molecules within the cluster. GRA

N92-30331# Academy of Sciences of the Ukrainian SSR, Kiev. Inst. Teoreticheskoj Fiziki.
SCALE SYMMETRY OF QUANTUM SOLITONS
N. M. Chepilko, K. Fujii, and A. P. Kobushkin 1991 13 p
(DE92-624560; ITP-91-8) Avail: CASI HC A03/MF A01

A collective-coordinate Lagrangian for a rotating and vibrating quantum soliton in the nonlinear sigma model is shown to possess a symmetry under scale transformation of the chiral field. Using this symmetry, an integrodifferential equation for the chiral angle is obtained. A consistency condition between this equation and the Schroedinger equation for the quantum soliton is also discussed. At limiting cases (a vibrating, but not rotating soliton; or a rotating, but not vibrating soliton) the integrodifferential ones and the chiral angle become independent of the solution of the Schroedinger equation. DOE

N92-30333# Washington State Univ., Pullman. Dept. of Chemistry.
SPONTANEOUS DECAY OF AN ATOM NEAR A PHASE CONJUGATOR
Henk F. Arnoldus and Thomas F. George Mar. 1992 64 p
(Contract N00014-90-J-1193)
(AD-A248298; WSU/DC/91-TR-81) Avail: CASI HC A04/MF A01

Relaxation of the density operator of an atom near a four-wave mixing phase conjugator (PC) is studied. The relaxation operator Tau can be expressed in the Cartesian components of the atomic dipole operator and correlation functions of the vacuum electromagnetic field. We evaluate these correlation functions in terms of the Fresnel coefficients for reflection and transmission of a polarized monochromatic plane wave. Our expression for Tau includes both linear and nonlinear interactions in the medium, and it reduces to well-known results in the limits of a pure dielectric, a mirror, and empty space. The example of a model two-state atom in combination with a model PC is worked out in detail. From the rate equations for the populations of the levels we infer that the relaxation acquires a contribution from both ordinary spontaneous decay and stimulated transitions which are induced by the PC. It is shown that an atom in its ground state has a finite probability of being excited, and that the excited state has a finite population in the long-time limit. We also work out the case of a degenerate two-level atom in combination with a realistic model of a transparent PC, and it is shown that our present results for the transition rates are consistent with earlier calculations of the fluorescence yield. GRA

N92-30337# Paris II Univ., Orsay (France). Lab. de Physico-chimie Des Rayonnements.
MEASUREMENT OF RADIATIVE LIFETIMES OF VIBRATIONAL STATES OF SIMPLE IONS Final Report, Sep. 1987 - Oct. 1991
Rose Marx and Gerard Mauclaire 31 Dec. 1991 9 p
(Grant AF-AFOSR-0390-87)
(AD-A248567; AFOSR-92-0196TR) Avail: CASI HC A02/MF A01

A differentially pumped, triple cell, FT/ICR machine, where production of the ions, storage in a high vacuum trap for variable relaxation times, and chemical monitoring of the internal energy content of the ions are separated as well in space as in time, was shown to be well suited for experimental determination of radiative lifetime of ions. The monitor ion technique relies on the availability of energetically appropriate ion molecule processes, usually charge or proton transfer reactions. When several levels are populated, only overall lifetimes can be experimentally determined. Correction of the raw data, for radiative cascade, is needed to get individual lifetimes. The reliability of this technique was demonstrated for NO(+) (X, v = 1-4) where accurate ab-initio calculations exist. For HCl(+)/DCl(+) (X, v = l), the agreement with theoretical calculation is reasonable. For polyatomic ions our method can only indicate the presence and measure the relaxation rate of the amount of energy needed to drive the monitor reaction. However this proved quite valuable in the case of the acetone ion, revealing the unexpected possibility to store a substantial amount of internal energy for milliseconds. For some triatomic and tetratomic ions like HCO(+), H2O(+), and NH3(+), our preliminary results have to be confirmed and completed with the newly improved experimental set-up. Reduction of collisional quenching in the relaxation cell by a double differential pumping will allow measurements of lifetimes up to approximately one second. Improvement of the detection sensitivity and reduction of mass discrimination in a large mass range, due to the upgrading of the detection console and to a better control of the ions motion, will increase the accuracy and hopefully allow analysis of multiexponential decays. GRA

N92-30364# Nationaal Inst. voor Kernfysica en Hoge Energiefysica, Amsterdam (Netherlands).
RESCATTERING IN NEUTRINO/ANTINEUTRINO: DEUTERON REACTIONS
A. G. Tenner and N. N. Nikolaev (Landau Inst. for Theoretical Physics, Moscow, USSR) Aug. 1991 27 p
(NIKHEF-H/91-22; ETN-92-91620) Avail: CASI HC A03/MF A01

Rescattering phenomenon in the deuteron by means of the analysis of neutrino/antineutrino deuteron interactions is studied. Values of the rescattering fraction in dependence on various parameters are presented. The charged and negative hadron multiplicities of rescatter and non rescatter events are evaluated. A special study is made of strange particle events. Production rates of specific particles (e.g., negative, strange) are compared for rescattering and non rescattering reactions in their dependence on rapidity. ESA

N92-30403# Gosudarstvennyi Komitet po Ispolzovaniyu Atomnoi Energii, Serpukhov (USSR). Inst. Fiziki Vysokikh Ehnergij.
LINEAR ESTIMATES OF STRUCTURE FUNCTIONS FROM DEEP INELASTIC LEPTON-NUCLEON SCATTERING DATA, PART 1
V. B. Anikeev and V. P. Zhigunov 1991 34 p
(DE92-627288; IHEP-ONF-91-74-Pt-1) Avail: CASI HC A03/MF A01

This paper concerns the linear estimation of structure functions from muon(electron)-nucleon scattering. The expressions obtained for the structure functions estimate provide correct analysis of the random error and the bias. The bias arises because of the finite number of experimental data and the finite resolution of experiment. The approach suggested may become useful for data handling from experiments at HERA. DOE

N92-30404# Gosudarstvennyi Komitet po Ispolzovaniyu Atomnoi Energii, Serpukhov (USSR). Inst. Fiziki Vysokikh Ehnergij.
SEARCH FOR LIGHT NEUTRAL SCALAR AND PSEUDOSCALAR PARTICLES IN pFe INTERACTIONS AT 70 GeV [POISK LEGKIKH NEJTRAL'NYKH SKALYARNYKH I PSEVDOSKALYARNYKH CHASTITS V PFE-VZAIMODEJSTVIVAKH PRI EHNERGII 70 GEHV]
V. B. Anikeev, N. S. Bamburov, and N. I. Bozhko 1991 25 p In RUSSIAN Submitted for publication
(DE92-627317; IFVE-ONF-91-139) Avail: CASI HC A03/MF A01

A search has been performed for weakly interacting neutral light scalar and pseudoscalar particles in a proton beam dump experiment. No positive signal is observed. Limits on the mass and lifetime of these particles are set in the frame of the Standard Model and its minimal supersymmetric extension. The Higgs particle of the SU(2L) x U(1) Standard Model is excluded for masses in the range 1 MeV less than m less than 80 MeV at 95 percent CL. Limits on the Peccei Quinn like axions are also derived. DOE

N92-30415# Nationaal Inst. voor Kernfysica en Hoge Energiefysica, Amsterdam (Netherlands).
ON THE FACTORISATION THEOREM IN BOSON-GLUON FUSION AT HADRON COLLIDERS
F. Anselmo (European Organization for Nuclear Research, Geneva, Switzerland), B. vanEijk (European Organization for Nuclear Research, Geneva, Switzerland), and G. Bordes (College de France, Paris.) 1991 16 p Sponsored by Netherlands Organization for Applied Scientific Research TNO
(NIKHEF-H/91-16; ETN-92-91614) Avail: CASI HC A03/MF A01

An 'improved' tree level description of the calculation of the O(alpha squared (alpha(sub s))) boson gluon fusion processes is presented focusing on heavy fermions in the final state, and the singular structure of the expression for the matrix elements squared is analyzed in detail. At lowest order, that is O(alpha squared), contributions from for instance W bottom scattering, where the bottom quark flux is taken from the bottom quark distribution function in the proton, are deemed to give non negligible contributions to the heavy flavor cross sections. Adding O(alpha squared) and O(alpha squared (alpha(sub s))) cross sections will lead to a typical double counting of Feynman graphs and a solution to this problem by subtracting the collinear singularity in the W gluon fusion process is presented. The results obtained are finite and, although virtual corrections were not explicitly taken into account, are expected to be valid for almost full phase space. Similar conclusions can be drawn in the case where the charged weak current is replaced by the neutral weak current. ESA

N92-30500# National Inst. for Fusion Science, Nagoya (Japan).
EFFECTS OF FAST IONS AND AN EXTERNAL INDUCTIVE ELECTRIC FIELD ON THE NEOCLASSICAL PARALLEL FLOW, CURRENT, AND ROTATION IN GENERAL TOROIDAL SYSTEMS
Noriyoshi Nakajima and Masao Okamoto May 1992 25 p
(NIFS-150; ISSN-0915-633X) Avail: CASI HC A03/MF A01

Effects of external momentum sources, i.e., fast ions produced by the neutral beam injection and an external inductive electric field, on the neoclassical ion parallel flow, current, and rotation are analytically investigated for a simple plasma in general toroidal systems. It is shown that the contribution of the external sources to the ion parallel flow becomes large as the collision frequency of thermal ions increases because of the momentum conservation of Coulomb collisions and sharply decreasing viscosity coefficients with collision frequency. As a result, the beam-driven parallel flow of thermal ions becomes comparable to that of electrons in the Pfirsh-Schlueter collisionality regime, whereas in the 1/nu or banana regime it is smaller than that of electrons by the order of sq. root of (m sub 3/m sub i)(m sub 3 and m sub i are electron and ion masses). This beam-driven ion parallel flow can not produce a large beam-driven current because of the cancellation with electron parallel flow, but produces a large toroidal rotation of ions. As both electrons and ions approach the Pfirsh-Schlueter collisionality regime, the contribution of thermodynamical forces becomes negligibly small and the large toroidal rotation of ions is predominated by the beam-driven component in the non-axisymmetric configuration with large helical ripples. Author

N92-30501# National Inst. for Fusion Science, Nagoya (Japan).
NEGATIVE ION EXTRACTION CHARACTERISTICS OF A LARGE NEGATIVE ION SOURCE WITH DOUBLE-MAGNETIC FILTER CONFIGURATION
Y. Takeiri, A. Ando, O. Kaneko, Y. Oka, and T. Kuroda May 1992 32 p
(NIFS-151; ISSN-0915-633X) Avail: CASI HC A03/MF A01

A multi-ampere hydrogen negative ion source with a large extraction area of 25 cm x 25 cm was developed. This negative ion source is a volume-production-type bucket ion source which is operated with double-magnetic filter configuration. In this configuration, the fast electrons, which produce the vibrationally excited molecules, are trapped near the chamber wall by the cusp field, which is the first magnetic filter. In the central region of the arc chamber, there exist only the thermal electrons with low temperature. As a result, the negative ions are produced in the central region by dissociative attachment. A rod magnetic filter in front of the plasma grid, which is the second magnetic filter, is utilized for reducing the population of the electrons in the vicinity of the plasma grid, which are extracted together with the negative ions. By this structure the extracted electron current can be controlled independently of the H(-) ion current. So far, a 1.4A of H(-) ion current was obtained with the energy of 34 keV. Negative ion extraction characteristics of this ion source, such as the arc power dependence and the gas pressure dependence, are presented. Author

N92-30510# National Inst. for Fusion Science, Nagoya (Japan).
RAPID CHANGE OF HYDROGEN NEUTRAL ENERGY DISTRIBUTION AT L/H-TRANSITION IN JFT-2M H-MODE
Y. Miura (Japan Atomic Energy Research Inst., Tokai.), F. Okano (Japan Atomic Energy Research Inst., Tokai.), N. Suzuki (Japan Atomic Energy Research Inst., Tokai.), M. Mori (Japan Atomic Energy Research Inst., Tokai.), K. Hoshino (Japan Atomic Energy Research Inst., Tokai.), H. Maeda (Japan Atomic Energy Research Inst., Tokai.), T. Takizuka (Japan Atomic Energy Research Inst., Tokai.), Sanae-I. Itoh, and K. Itoh Feb. 1992 21 p Submitted for publication
(NIFS-134; ISSN-0915-633X) Avail: CASI HC A03/MF A01

Rapid changes of the main ion energy distribution at transitions from L to H, H to L and during edge localized modes (ELMs) are studied with the time of flight neutral measurement on the JFT-2M tokamak. At the L to H transition, 200-400 microns prior to the start of H (sub alpha) drop, an increase of the high energy outflux above an energy of 200eV is observed. An energy of more than 200eV for hydrogen corresponds to the collisionless condition upsilon * (sub 1) less than 1 just inside the separtrix. The change of the energy distribution precedes that of the H (sub alpha) signal and is also found for ELMs and the H to L transition. Author

N92-30572# National Inst. for Fusion Science, Nagoya (Japan).
PRODUCTION OF NEGATIVE HYDROGEN IONS IN A LARGE MULTICUSP ION SOURCE WITH DOUBLE-MAGNETIC FILTER CONFIGURATION
A. Ando, Y. Takeiri, O. Kaneko, Y. Oka, M. Wada, and T. Kuroda May 1992 41 p
(NIFS-149; ISSN-0915-633X) Avail: CASI HC A03/MF A01

The production of the negative hydrogen ions in a large multicusp ion source has been investigated in a double-magnetic filter (DMF) configuration. In the DMF configuration, the energetic electrons are trapped by the mirror of a magnetic multicusp field, and only the thermal electrons are present in the center of the arc chamber. A large amount of H(-) ions of more than 1 x 10(exp 12) cm(exp -3) are produced in the center region. The electron current extracted with the H(-) ions can be suppressed by a magnetic filter field in front of a plasma grid without affecting the H(-) ion current. The experimental data obtained in the DMF configuration are compared with those obtained in a single-magnetic filter (SMF) configuration. In the SMF configuration, the energetic electrons are present in the center region, and the magnetic filter in front of a plasma grid reduces the electron density and temperature, which results in the reduction of the H(-) ion current as well as the electron current. The extracted electron current and the optimum gas pressure for the H(-) ion current are lower in the DMF configuration than those in the SMF configuration. Author

N92-30580 Tel-Aviv Univ. (Israel). School of Physics and Astronomy.
POLARIZATION EFFECTS IN PI(+) ABSORPTION IN He-3 M.S. Thesis
Sharon MayTal-Beck Oct. 1990 98 p
(ITN-92-85164) Copyright Avail: Tel-Aviv Univ., Exact Sciences Library, Ramat Aviv, 69978, Israel

The polarization of protons resulting from pi(+) absorption in He-3 was measured at bombarding energies of 120 MeV and 250 MeV. Only protons coming from absorption in a quasi deuteron were detected, using kinematical restraints both in the set-up of the experiment and in the analysis of the data. The system was tested by measuring the polarization of protons resulting from the pi(+)d yields pp reaction, and the results agree with previous measurements. There is a significant discrepancy between the experimental results and theoretical predictions. The polarization measurements show sensitivity to the nuclear density, and thus can be sensitive to short-range correlations between nucleons. Author (ISA)

N92-30586# Lawrence Livermore National Lab., CA.
PROGRAM RELAX: A CODE DESIGNED TO CALCULATE ATOMIC RELAXATION SPECTRA OF X RAYS AND ELECTRONS
D. E. Cullen 20 Mar. 1992 19 p
(Contract W-7405-eng-48)
(DE92-013751; UCRL-ID-110438) Avail: CASI HC A03/MF A01

The code RELAX is designed to calculate atomic relaxation spectra of x-rays and electrons due to bound-bound transitions. This calculation is based on the atomic transition data contained in the Livermore Evaluated Atomic Data Library (EADL). The results produced by this code for fluorescence yield vs. atomic number (Z) have been published elsewhere. DOE

N92-30606# Oregon Univ., Eugene.
INTERMITTENCY, MULTIFRACTALITY, AND HADRONIC COLLISIONS
R. C. Hwa Sep. 1991 10 p Presented at the Ringberg Workshop on Multiparticle Production, Fluctuations and Fractal Structure, Schloss Ringberg (Germany), 25-28 Jun. 1991
(Contracts DE-FG06-91ER-40637; DE-FG06-85ER-40224)
(DE92-014595; DOE/ER-40637/4; OITS-474; CONF-9106340-2)
Avail: CASI HC A02/MF A01

We discuss the properties of the G moments as a means of determining the multifractal features of the intermittency phenomena in multiparticle production. We then summarize ECCO, a Monte Carlo code for simulating hadronic collisions in the framework of the Geometrical Branching Model. It is shown that ECCO can reproduce the intermittency data. DOE

N92-30610# Pennsylvania State Univ., University Park. Dept. of Physics.
THEORETICAL STUDIES IN ELEMENTARY PARTICLE PHYSICS
J. Collins 1991 9 p
(Contract DE-FG02-90ER-40577)
(DE92-015295; DOE/ER-40577/2) Avail: CASI HC A02/MF A01

This report discusses research in: spin physics; transverse polarization and jet production; fundamental QCD; intermediate vector boson production; and hadron collisions. DOE

N92-30611# Washington Univ., Seattle. Dept. of Physics.
NUCLEAR THEORY PROGRESS REPORT, APRIL 1991 - APRIL 1992
1992 31 p
(Contract DE-FG06-88ER-40427)

(DE92-015349; DOE/ER-40427/14-N92) Avail: CASI HC A03/MF A01

This report discusses research in nuclear theory on the following topics: nuclear astrophysics; quantum chromodynamics; quark matter; symmetry breaking; heavy ion reactions; hadronic form factors; neutrino processes; nuclear structure; weak interaction physics; and other related topics. DOE

N92-30625# Illinois Univ., Urbana. Lab. of Physics.
RESEARCH ON ELEMENTARY PARTICLE PHYSICS
L. E. Holloway and T. A. OHalloran May 1992 53 p
(Contract DE-FG02-91ER-40677)
(DE92-014622; DOE/ER-40677/1-Pt-2) Avail: CASI HC A04/MF A01

This report describes the activities of the University of Illinois Experimental High Energy Physics Group. The physicists in the University of Illinois High Energy Physics Group are engaged in a wide variety of experiments at current and future accelerator laboratories. These include: (1) The CDF experiment at the Fermilab Tevetron P(bar)-p collider; (2) Design and developmental work for the SDC group at SSCL; (3) Experiments at the wide band photon beam at Fermilab; (4) The SLD experiment at SLAC and design studies for a (tau)-charm factor; (5) CP violation experiments at Fermilab; (6) The HiRes cosmic ray experiment at Dugway Proving Grounds, Utah; (7) Computational facilities; and (8) Electronics systems development. DOE

N92-30680# Georgia Univ., Athens.
FUNDAMENTAL STUDIES OF CARBON, NH, AND OXYGEN RINGS AND OTHER HIGH ENERGY DENSITY MOLECULAR SYSTEMS Final Technical Report, 1 Apr. 1988 - 31 Oct. 1991
Henry F. Schaefer, III, Ian L. Alberts, Neil A. Burton, Randall D. Davy, and Brian J. Salter-Duke 30 Dec. 1991 17 p
(Grant AF-AFOSR-0167-88)
(AD-A246963; AFOSR-92-0097TR) Avail: CASI HC A03/MF A01

The object of this research is to characterize the molecular structures, energetics, spectroscopic properties, and elementary chemical reactions of the oxygen ring molecules O4 through O12 and related species including (NH)(sub n) and C(sub n). The approach used will exploit recent developments in ab initio molecular quantum mechanics. GRA

N92-30681# Cornell Univ., Ithaca, NY. Dept. of Chemistry.
VACUUM ULTRAVIOLET STUDIES OF MOLECULAR DYNAMICS Final Report, 1988 - 1991
Paul L. Houston 15 Jan. 1992 9 p
(Grant AF-AFOSR-0162-89)
(AD-A246964; AFOSR-92-0098TR) Avail: CASI HC A02/MF A01

This research grant used tunable vacuum ultraviolet radiation generated by four-wave mixing to probe collisional energy transfer, reactive encounters, and photodissociations. Translation to vibration/rotation energy transfer was examined in the H + CO system to learn how the extent of transfer depends on the collision energy and to determine the vibrational and rotational distribution of the product. The quenching of S(1D) by N2 was studied to learn the branching ratio for quenching to each of the 3p0, 3p1, and 3p2 components as well as to determine the rates of equilibration among these components. Photodissociations of OCS, C02, and C3O2 at 157 nm were studied to learn the distribution of energy in the S, 0, and CO products and to investigate vector correlations and velocity distributions of these products. This integrated program of molecular dynamics studies using vacuum ultraviolet radiation has enhanced our knowledge both of the chemical physics of these basic processes and of the interaction of high energy photons with small molecules likely to be found in the upper atmosphere. GRA

N92-30687# Nationaal Inst. voor Kernfysica en Hoge Energiefysica, Amsterdam (Netherlands).
TWO-LOOP QCD CORRECTIONS TO THE COEFFICIENT FUNCTIONS OF THE DEEP INELASTIC STRUCTURE FUNCTIONS F2 AND F(SUB L)
S. A. Larin (Academy of Sciences, USSR, Moscow) and J. A. M. Vermaseren 1991 11 p
(NIKHEF-H/91-17; ETN-92-91615) Avail: CASI HC A03/MF A01

Analytic two loop perturbative Quantum Chromodynamic (QCD) corrections in the leading twist approximation to the coefficient functions of the operator product expansion for the second to tenth moments of the nonsinglet and singlet deep inelastic structure function F2 and F(sub L) are presented. ESA

N92-30697# Nationaal Inst. voor Kernfysica en Hoge Energiefysica, Amsterdam (Netherlands).
NON-PERTURBATIVE EFFECTS IN HIGH-ENERGY ELECTROWEAK INTERACTIONS
F. R. Klinkhamer Oct. 1991 6 p Presented at the Joint International Lepton-Photon Symposium and Europhysics Conference on High Energy Physics, Geneva, Switzerland, 1991 Submitted for publication Sponsored by Royal Netherlands Academy of Arts and Sciences
(NIKHEF-H/91-24; ETN-92-91622) Avail: CASI HC A02/MF A01

A semiclassical calculation shows threshold like behavior for nonperturbative electroweak effects at a parton center of mass energy close to the sphaleron energy E(sub s) approximately 10 TeV. The existing instanton calculations for one particular nonperturbative effect (B + L violation) are reviewed and the calculation of threshold energy is discussed. ESA

N92-30750# Rutherford Appleton Lab., Chilton (England).
REMARKS ON THE EXOTIC U-MESON
Hong-Mo Chan and Sheung Tsun Tsou (Oxford Univ., England) Dec. 1991 12 p
(RAL-91-090; ETN-92-91719) Avail: CASI HC A03/MF A01

In expectation of imminent result from the hyperon beam experiment concerning the exotic U-meson at 3.1 GeV, a detailed program of experimental tests to check the suggestion that U is qqq(bar)q(bar) 'M-diquonium' state is proposed. Apart from some very characteristic decay modes, the U is expected to occur together with several analogous states with various quantum numbers to which it is intimately related. ESA

N92-30780 Tel-Aviv Univ. (Israel). School of Physics and Astronomy.
POLARIZATION EFFECTS IN PI(+) ABSORPTION IN He-4 M.S. Thesis
Jaime L. S. Aclander Oct. 1990 102 p
(ITN-92-85163) Copyright Avail: Tel-Aviv Univ., Exact Sciences Library, Ramat Aviv, 69978, Israel

The polarization of protons resulting from pi(+) absorption in He-4 was measured at bombarding energies of 120 MeV and 250 MeV. Only protons coming from absorption in a quasi-deuteron were analyzed by limiting the recoiling momenta of the remaining particles to 150 MeV/c. The system was tested by measuring the polarization of protons from the pi(+)d yields a proton-antiproton reaction and the results agree with previous measurements. The results are compared with similar measurements done with He-3. Compared with the polarization from absorption on the deuteron at bombarding energies below and above the delta resonance the differences observed for He-4 are larger than for He-3. This effect could be related to the density of the absorbing nucleon pair. There is a large discrepancy between the experimental results and theoretical predictions. Author (ISA)

N92-30782 Tel-Aviv Univ. (Israel). Dept. of Physics and Astronomy.
SPONTANEOUS EMISSION FROM AN ATOM IN MOTION NEAR AN INFINITE CONDUCTING PLANE M.S. Thesis

Amir Komem Apr. 1991 75 p In HEBREW
(ITN-92-85169) Copyright Avail: Tel-Aviv Univ., Exact Sciences Library, Ramat Aviv, 69978, Israel

The problem considered is that of a two-level atom in motion, spontaneously emitting near an infinite perfectly conducting plane. The change in the atom-plane relative position causes a time dependence of the spontaneous emission decay rate and of the Lamb shift. We calculate the decay rate and the Lamb shift by solving the Schroedinger equations using the Wigner-Weisskopf approximation. The Hamiltonians were formulated by the image method, which replaced the plane with the atom's image, so the problem became that of two correlated moving atoms in free space. We also calculate the excitation probabilities of the atoms and the electromagnetic modes with time. The calculation shows a non-exponential decay rate depending on atom-plane distance, changing with time. The Lamb shift, too, depends upon this distance. For a stationary atom (v = 0) we get the well-known results of Morawitz, Milonni and Knight, and Philpott; for a large atom-plane distance we get the free-space results. We also considered the moving atom's spontaneous emission in free space. We derived the well-known results with an additional ((v/c) squared) term, due to the non-relativistic calculations done. Author (ISA)

N92-30791# Illinois Univ., Urbana. Dept. of Physics.
RESEARCH ON ELEMENTARY PARTICLE PHYSICS. TASK P: STUDIES IN THEORY AND PHENOMENOLOGY OF ELEMENTARY PARTICLES, PART 1
May 1992 4 p
(Contract DE-FG02-91ER-40677)
(DE92-014428; DOE/ER-40677/1-Pt-1) Avail: CASI HC A01/MF A01

Over the last year, work has focused on two areas: the phenomenology of quark-gluon differentiation in jets, and theoretical studies involving Dirac-like equations for various systems. Substantive progress has been made in both areas. A paper comparing details of the Lund and Herwig simulations for quark and gluon jets has been written and accepted by Physical Review D. A paper describing a new type of Dirac equation for the relativistic harmonic oscillator, and finding solutions thereof, has been written and submitted for publication. DOE

N92-30798# International Centre for Theoretical Physics, Trieste (Italy).
MULTIPLE SCATTERING THEORY OF X RAY ABSORPTION. A REVIEW
L. Fonda Nov. 1991 38 p
(DE92-622374; IC-91/367) Avail: CASI HC A03/MF A01

We review the basic elements of the theory of x-ray absorption using the tools provided by the theory of multiple scattering. A momentum space approach of clear physical insight is used for the final formulas expressing EXAFS and XANES, i.e. the structures appearing in the absorption coefficient above the edge of a deep core level threshold, and are given in terms of eigenstates of the photoelectron momentum. A simple graphic representation is given for the multiple scattering function. DOE

N92-30826# Argonne National Lab., Idaho Falls, ID.
CLUSTER ASSEMBLY OF HIERARCHICAL NANOSTRUCTURES
R. W. Siegel Feb. 1992 10 p Presented at the Annual Fall Meeting of the Materials Research Society, Boston, MA, 2-6 Dec. 1991
(Contract W-31-109-eng-38)
(DE92-010498; ANL/CP-73759; CONF-911202-68) Avail: CASI HC A02/MF A01

In the past few years, atom clusters with diameters in the range of 2-20 nano-m of a variety of materials, including both metals and ceramics, have been synthesized by evaporation and condensation in high-purity gases and subsequently consolidated in situ under ultrahigh vacuum conditions to create nanophase materials. These new utlrafine-grained materials have properties that are often significantly different and considerably improved relative to those of their coarser-grained counterparts owing to both their small grain-size scale and the large percentage of their atoms in grain boundary environments. Since their properties can be engineered during the synthesis and processing steps, cluster-assembled materials appear to have significant potential for the introduction of a hierarchy of both structure and properties. Some of the recent research on nanophase materials related to properties and scale are reviewed and some of the possibilities for synthesizing hierarchical nanostructures via cluster assembly are considered. DOE

N92-30841# Indiana Univ., Bloomington. Dept. of Physics.
THEORETICAL PARTICLE PHYSICS
S. A. Gottlieb, A. W. Hendry, V. A. Kostelecky, and D. B. Lichtenberg Apr. 1992 30 p
(Contract DE-FG02-91ER-40661)
(DE92-014531; DOE/ER-40661/2) Avail: CASI HC A03/MF A01

We have carried out research in lattice gauge theory, superstring theory, supersymmetry, the solar neutrino puzzle, QCD perturbation theory, and phenomenological models of hadrons. In this report, we summarize our work in each of these areas. DOE

N92-30845# Utah Univ., Salt Lake City. Dept. of Chemistry.
UNDERSTANDING HETEROLYTIC BOND CLEAVAGE
J. Simons and P. B. Armentrout 31 May 1992 36 p
(Contract N00014-89-J-1497)
(AD-A252336; TR-29) Avail: CASI HC A03/MF A01

When considering the fragmentation of a single bond, the attractive singlet and repulsive triplet potential energy curves of the prototype H2 - 2 H dissociation often come to mind. For species in which homolytic bond cleavage is energetically favored, such comparisons are reasonable. For other species where heterolytic cleavage gives lower-energy products, the H2 analogy is inappropriate. This paper offers a qualitative theoretical treatment of the singlet and triplet potential energy curves that arise when a single bond formed by an electron pair is cleaved either homolytically or heterolytically. This analysis is shown to provide insight into several problems involving transition metal systems: transition metal carbonyls, metal ion-ligand complexes, and transition metal dimers. GRA

N92-30853# Oak Ridge National Lab., TN.
EVIDENCE FOR INTERFERENCE BETWEEN RESONANT AND NONRESONANT TRANSFER AND EXCITATION
M. Benhenni, S. M. Shafroth, J. K. Swenson, M. Schulz, J. P. Giese, H. Schone, C. R. Vane, P. F. Dittner, and S. Datz 1991 6 p Presented at the 17th International Conference on the Physics of Electronic and Atomic Collisions, Brisbane (Australia), 10-16 Jul. 1991
(Contracts DE-AC05-84OR-21400; DE-FG05-87ER-40361)
(DE92-011779; CONF-910746-5) Avail: CASI HC A02/MF A01

The first angular distribution measurements of Auger electrons arising from transfer and excitation Auger (TE) processes were performed at O(5+) projective energies of 8 MeV, where the resonant (RTE) and the nonresonant (NTE) transfer and excitation have equal contributions in populating the (1s2s2p(sup 2))(sup 3)D state, and at 13 MeV where RTE is predominant and at 6 MeV where NTE is more significant. The TE angular distributions are strongly forward peaked along the beam direction. The data were fitted to w(theta(sub p)) =C(1 + a(sub 2)P(sub 2)(cos(theta)(sub p)) + a(sub 4)P(sub 4)(cos(theta)p)) and the magnetic substrate population probabilities were inferred. DOE

N92-30967# National Inst. for Fusion Science, Nagoya (Japan).
LINE-EMISSION CROSS SECTIONS FOR THE CHARGE-EXCHANGE REACTION BETWEEN FULLY STRIPPED CARBON AND ATOMIC HYDROGEN IN TOKAMAK PLASMA
K. Ida and T. Kato Jan. 1992 22 p Submitted for publication
(NIFS-129) Avail: CASI HC A03/MF A01

Line-emission cross sections of the charge-exchange reaction between fully stripped carbon and atomic hydrogen are measured in the energy range of 18-38 keV/amu in tokamak plasmas. The

energy dependence of the emission cross sections for the transition of Delta n = 8-7 and Delta n = 7-6 and their ratios are compared with theoretical calculations. Author

N92-30990# National Inst. for Fusion Science, Nagoya (Japan).
STUDY OF Au(-) PRODUCTION IN A PLASMA-SPUTTER TYPE NEGATIVE ION SOURCE Ph.D. Thesis - Nagoya Univ.
Yushirou Okabe Oct. 1991 76 p Sponsored in part by the Ministry of Education, Science and Culture, Japan
(NIFS-115) Avail: CASI HC A05/MF A01

A negative ion source of plasma-sputter type has been constructed for the purpose of studying physical processes which take place in the ion source. Negative ions of gold are produced on the gold target which is immersed in an argon discharge plasma and biased negatively with respect to the plasma. The work function of the target surface was lowered by the deposition of Cs on the target. An in-situ method has been developed to determine the work function of the target surface in the ion source under discharge conditions by measuring the photoelectron currents induced by two lasers (He-Ne, Ar(sup +) laser) simultaneously injected onto the target. The reflectivity at each wavelength on a cesiated gold surface was measured and taken into account in deriving the work function from the photoelectron current measured. The dependence of the Au(sup -) production rate, defined as the ratio of Au(sup -) current to the target current, on the work function of the target surface was obtained from simultaneous measurements of both target surface work function and Au(sup -) production rate while the Cs coverage was changed due to the plasma ion sputtering. The observed minimum work function of a cesiated gold surface in an argon plasma was 1.3 eV, when the negative ion production rate took the maximum value. The production rate increased monotonically and saturated when the surface work function was reduced from 1.9 eV to 1.3 eV. This range of the change in the work function was limited by the wave lengths of lasers used for the determination of the work function. The dependence of Au(sup -) production rate on the incident ion energy was deduced by changing the target bias voltage while the work function was kept constant. The production rate increased with the target bias voltage, and showed a similar dependence on the incident ion energy as the sputtering rate of gold with Ar(sup +) bombardment. The dependence of Au(sup -) production rate on the number of the incident ion was studied by changing the plasma discharge current, while the work function was again kept constant. Author

N92-31137# EG and G Rocky Flats, Inc., Golden, CO.
A METHOD FOR THE PRODUCTION OF WEAKLY ACIDIC CATION EXCHANGE RESINS
H. Heller, F. Werner, A. Mitschker, H. V. Diehl, and A. Schaefer Dec. 1991 10 p Transl. into ENGLISH of European Patent Application No. 0-406-648-A1, (1991)
(Contract DE-AC34-90DP-62349)
(DE92-015314; RFP-Trans-523) Avail: CASI HC A02/MF A01

The invention relates to a nonpolluting method for the production of weakly acidic cation exchange resins by saponification of cross-linked acrylonitrile bead polymers, with an alkaline saponification agent at elevated temperature, according to which method the bead polymer and alkaline saponification agent are jointly added only at elevated temperature. DOE

N92-31147# EG and G Rocky Flats, Inc., Golden, CO.
A METHOD FOR PRODUCTION OF NEW ANION EXCHANGERS
G. Behrendt and H. D. Hunger Dec. 1991 6 p Transl. into ENGLISH of German Patent No. DD-284-416-A5, (1990)
(Contract DE-AC34-90DP-62349)
(DE92-015313; RFP-Trans-524) Avail: CASI HC A02/MF A01

The invention relates to a method for the production of new anion exchangers that can be used in molecular biology, genetic engineering, biotechnology, and phytopathology. According to the invention, halogen-containing polyurethanes are reacted with one or more tertiary amines. By the method, polyurethane shapes with positive surface charges are produced from preformed shapes, with preservation of the form and properties thereof. The products have thermally stable bonds with biomolecules together with high binding capacity. DOE

N92-31201# Los Alamos National Lab., NM.
DIFFUSE NEUTRON SCATTERING SIGNATURES OF ROUGH FILMS
R. Pynn and M. Lujan, Jr. 1992 10 p Presented at the 1992 SPIE International Symposium on Optical Applied Science and Engineering, San Diego, CA, 19-24 Jul. 1992
(Contract W-7405-eng-36)
(DE92-015208; LA-UR-92-1478; CONF-920792-3) Avail: CASI HC A02/MF A01

Patterns of diffuse neutron scattering from thin films are calculated from a perturbation expansion based on the distorted-wave Born approximation. Diffuse fringes can be categorized into three types: those that occur at constant values of the incident or scattered neutron wavevectors, and those for which the neutron wavevector transfer perpendicular to the film is constant. The variation of intensity along these fringes can be used to deduce the spectrum of surface roughness for the film and the degree of correlation between the film's rough surfaces. DOE

N92-31205# Technische Univ. Munich, Garching (Germany, F.R.). Physikdepartment.
NEUTRON SOURCE MUNICH FRM-2
Mar. 1992 44 p
(Contract DE-AC05-84OR-21400)
(DE92-015300; ORNL/tr-92/17) Avail: CASI HC A03/MF A01

This report will provide an overview of the progress and the present stage of development of the 'Neutron Source Munich FRM-II' project. The objective of this project is to create a modern high-flux neutron source which is needed for a broad spectrum of research- and application-oriented studies with thermal and cold neutrons. With the realization of the FRM-II project, it will be possible to contribute greatly to improving the desperately needed neutron supply in Germany. DOE

73 NUCLEAR AND HIGH-ENERGY PHYSICS

Includes elementary and nuclear particles; and reactor theory.

For space radiation see *93 Space Radiation.*

N92-30398# Brookhaven National Lab., Upton, NY.
EFFECTS OF HIGH BEAM RATES ON TPC'S
A. Etkin, S. E. Eiseman, K. J. Foley, R. W. Hackenburg, R. S. Longacre, W. A. Love, T. W. Morris, E. D. Platner, A. C. Saulys, and S. J. Lindenbaum (City Coll. of the City Univ. of New York, NY.) Feb. 1992 13 p Presented at the 6th International Wire Chamber Conference: Wire Chambers - Recent Trends and Alternative Techniques, Vienna (Austria), 17-21 Feb. 1992
(Contracts DE-AC02-76CH-00016; DE-AC02-83ER-40107; DE-FG03-88ER-40424; DE-FG02-88ER-40413; DE-AC03-76SF-00098; DE-FG05-87ER-40309)
(DE92-014594; BNL-47201; CONF-920219-4) Avail: CASI HC A03/MF A01

The TPC's (Time Projection Chamber) used in E-810 at the AGS (Alternating Gradient Synchrotron) were exposed to silicon ion fluxes equivalent to more than 10(exp 7) minimum ionizing particles per second to measure the distortion of the electric field caused by positive ions in the drift region. Results of these tests are presented and the consequences for the TPC based experiment at RHIC (Relativistic Heavy Ion Collider) are discussed. DOE

N92-30589# Fermi National Accelerator Lab., Batavia, IL.
MAGNETIC FIELD MEASUREMENTS OF FERMILAB/GENERAL DYNAMICS BUILT FULL SCALE SSC COLLIDER DIPOLE MAGNETS
S. Delchamps, M. Bleadon, R. Bossert, J. Carson, S. Gourlay, R.

Hanft, W. Koska, M. Kuchnir, M. Lamm, and P. Mazur et al Apr. 1992 8 p Presented at the International Industrial Symposium on the Super Collider, New Orleans, LA, 4-6 Mar. 1992
(Contract DE-AC02-76CH-03000)
(DE92-014612; FNAL/C-92/106; SSCL-Preprint-102; CONF-920331-33) Avail: CASI HC A02/MF A01

This paper presents preliminary results of magnetic field measurements made on a series of 50 mm aperture 15 m long SSC collider dipole magnets designed and manufactured at Fermi National Accelerator Laboratory (Fermilab) for use in the Superconducting Super Collider Laboratory (SSCL) Accelerator System String Test. The magnets were assembled by Fermilab and General Dynamics personnel, and were tested at the Magnet Test Facility (MTF) at Fermilab. Measurements of the dipole field angle, dipole field strength, and field shape parameters at various stages in magnet construction and testing are described. DOE

N92-30624# Sandia National Labs., Albuquerque, NM.
THE RADLAC BEAM PROPAGATION EXPERIMENT
C. A. Frost, S. L. Shope, M. G. Mazarakis, J. W. Poukey, J. S. Wagner, B. N. Turman, C. E. Crist, D. R. Welch (Mission Research Corp., Albuquerque, NM.), and K. W. Struve (Mission Research Corp., Albuquerque, NM.) 1992 9 p Presented at the Charged Particle Beam Conference, Silver Springs, MD, 25-27 Jun. 1991
(Contract DE-AC04-76DP-00789)
(DE92-014620; SAND-92-0819C; CONF-9106276-9) Avail: CASI HC A02/MF A01

The most recent RADLAC experiments studied propagation and hose stability of a high current beam propagating in the atmosphere, and confirmed the convective nature of the hose instability. The unique combination of high beam current and extremely small initial perturbation, allowed saturation of the hose instability to be observed for the first time. Data on high current propagation was needed because the current scaling is more complex than energy scaling. It was important to collect data at atmospheric pressure to insure that subtle air chemistry effects such as avalanche did not distort the experiment. With this philosophy, the results should be directly scalable to applications at higher energy. DOE

N92-30646# Superconducting Super Collider Lab., Dallas, TX.
DESIGNING, FABRICATING AND TESTING COST EFFECTIVE STRUCTURAL COMPOSITE FOR THE SSCL MAGNETS
F. Nobrega May 1992 10 p Presented at the International ACMLC Conference, Orlando, FL, 6-8 May 1992
(Contract DE-AC35-89ER-40486)
(DE92-013469; SSCL-Preprint-77; CONF-9205155-1) Avail: CASI HC A02/MF A01

The Superconducting Super Collider (SSC) is a proton-proton particle accelerator used to study the fundamental forces and particles of nature. When completed in 1999, it will be the world's largest particle accelerator with a total collision energy of 40 TeV. One of the most important components of the collider is the superconducting magnets. They are used to bend and focus the particle beam around the ring. Magnet designs involve sharp bending of the superconducting niobium-titanium copper cable used in making coils. The end turns of the coils are supported with end spacers and saddles made of composite materials. This paper addresses the design, fabrication, testing and cost of these coil end parts. DOE

N92-30725# Nationaal Inst. voor Kernfysica en Hoge Energiefysica, Amsterdam (Netherlands).
VDHW-RELATED MEMO'S
Nils Dobbe 1991 27 p In DUTCH
(LINO-1991-5; ETN-92-91740) Avail: CASI HC A03/MF A01

Internal memorandums concerning the Video Highway (VDHW) system for the NIKHEF particle accelerator were collected. The performances of the present VDHW system were measured. The relay boxes for the VDHW were adapted. Buffer amplifiers were designed and tested for the VDHW console. For individual titles, see N92-30726 through N92-30728.

N92-30726# Nationaal Inst. voor Kernfysica en Hoge Energiefysica, Amsterdam (Netherlands).
MEASUREMENT REPORT ON THE PRESENT VIDEO HIGHWAY SYSTEM OF MEA [MEETRAPPORT OVER: HUIDIG VIDEO HIGHWAY SYSTEEM VAN MEA]
O. Straman and Nils Dobbe *In its* VDHW-Related Memos 1991 p 7-16 In DUTCH (For primary document see N92-30725 21-73)
Avail: CASI HC A02/MF A01

Measurements were carried out in order to document the performances of the present Video Highway (VDHW) system. This permits adaptation of the VDHW system to modifications in the accelerometer configuration. The step response of the prodlines as well as their direct current resistance were determined. The damping due to a parasitic resistance was calculated. ESA

N92-30727# Nationaal Inst. voor Kernfysica en Hoge Energiefysica, Amsterdam (Netherlands).
TUNABLE RELAY BOX (DESIGN AND TESTING) [TUNEABLE RELAISKASTJE]
In its VDHW-Related Memos 1991 p 17-21 In DUTCH (For primary document see N92-30725 21-73)
Avail: CASI HC A01/MF A01

The present relay boxes for the Video Highway (VDHW) were adapted in order to obtain a 100 signal transmission. A variable series resistance which cancels the cable resistance of the prodline was used. The perturbation of the characteristic impedance of the cable is reduced to a minimum with the help of strip lines. The signal is not deformed by the presence of the relay boxes which perturbed the 50 ohm characteristic cable impedance of the prodline. ESA

N92-30728# Nationaal Inst. voor Kernfysica en Hoge Energiefysica, Amsterdam (Netherlands).
CONSOLE DRIVER
In its VDHW-Related Memos 1991 p 22-25 In DUTCH (For primary document see N92-30725 21-73)
Avail: CASI HC A01/MF A01

Buffer amplifiers were designed for the Video Highway (VDHW) console driver. The signal specifications of the console driver were measured. The response of the common mode signal was determined. ESA

N92-30786# Superconducting Super Collider Lab., Dallas, TX.
MAGNETIC MEASUREMENT INSTRUMENTATION DEVELOPMENTS AT THE SSC
Z. R. Wolf, W. C. Li, M. W. Coles, P. F. Pellissier, J. E. Dryer, R. Z. Fuzesy, and T. R. Gathright Mar. 1992 8 p Presented at the International Industrial Symposium on the Super Collider, New Orleans, LA, 4-6 Mar. 1992
(Contract DE-AC35-89ER-40486)
(DE92-013969; SSCL-Preprint-51; CONF-920331-28) Avail: CASI HC A02/MF A01

We review the developments in magnetic measurement instrumentation that have taken place at the Superconducting Super Collider (SSC) Laboratory. The primary developments have been stretched wire systems for superconducting dipole and quadrupole alignment and field integral measurement, and our support of the 'mole' that is being developed by Brookhaven National Laboratory (BNL). DOE

N92-30811# Superconducting Super Collider Lab., Dallas, TX.
APPLICATION OF SUPERCONDUCTING CAVITIES TO THE COLLIDER RINGS OF THE SSC
G. Schaffer Mar. 1992 3 p Presented at the 3rd European Particle Accelerator Conference, Berlin, Fed. Republic of Germany, 24-28 Mar. 1992
(Contract DE-AC35-89ER-40486)
(DE92-011692; SSCL-Preprint-80; CONF-920315-16) Avail: CASI HC A01/MF A01

The rf parameters of the SSC collider rings are briefly characterized by 20 MV peak rf voltage, 3.9 MeV acceleration per turn, and 2 MW rf power ring at a multiple of the 60 MHz bunch

frequency of the proton beam injector. 360 or 480 MHz are preferred frequency choices. In the references design, a normal conducting accelerating structure is foreseen which would operate with gradients of typically 1 MV/m. In contrast to this, superconducting cavities can generate fields of 5 MV/m, or possibly more. In combination with a low R/Q-value, the total stored energy in the rf structure could be increased by an order of magnitude. This would help to reduce the undesired effects of transient beam loading, of rf generator noise, and of imperfections in the generator feedforward current, resulting in reduced phase modulation of the particle bunches at the collision area. For 70 mA circulating beam current, eight superconducting single-cell cavities would be required per ring, instead of 32 to 40 single-cell normalconducting cavities. The savings in tunnel space, and a lower coupling impedance would allow a later upgrade of the beam current to and beyond 200 mA, if desired, for a higher collider luminosity. DOE

N92-30839# Superconducting Super Collider Lab., Dallas, TX.
CONCEPTUAL DESIGN OF THE SSC CRYOGENIC TRANSFER LINES
B. Zhang and V. Ganni Mar. 1992 8 p Presented at the International Industrial Symposium on the Super Collider, New Orleans, LA, 4-6 Mar. 1992
(Contract DE-AC35-89ER-40486)
(DE92-013964; SSCL-Preprint-26; CONF-920331-29) Avail: CASI HC A02/MF A01

The SSC cryogenic system requires transfer lines for transporting cryogens between above-ground refrigeration plants and below-ground subcoolers. The transfer lines will be built in modules for convenience in fabrication, handling, and assembly. Each module of the transfer line consists of a vacuum vessel which encloses a bundle of seven cryogenic circuits at 4 K, 20 K, and 80 K. The cryostat includes an 80 K shield and a multilayer insulation (MLI) system for reduction of the heat leaks into the 20 K and 4 K circuits. Heat leaks through various paths are estimated and presented in conjunction with the basic system requirements. Discussions are provided on the design criteria, constraints, and thermal contraction handling techniques. DOE

N92-30840# Superconducting Super Collider Lab., Dallas, TX.
A DYNAMIC MODEL FOR BEAM TUBE VACUUM EFFECTS ON THE SSC CRYOGENIC SYSTEM
R. H. Carcagno, W. E. Schiesser, H. J. Shih, X. Xu, and A. Yuecel Mar. 1992 8 p Presented at the International Industrial Symposium on the Super Collider, New Orleans, LA, 4-6 Mar. 1992
(Contract DE-AC35-89ER-40486)
(DE92-013967; SSCL-Preprint-33; CONF-920331-25) Avail: CASI HC A02/MF A01

The dynamic interaction between the beam-gas scattering induced energy deposition and the SSC cryogenic system is studied by integrating a cryogenic system dynamic simulator with an adsorption model and a beam-gas scattering and energy deposition model. Simulation results are obtained for a 1 km long SSC arc section where the beam tube pressure in one of the dipoles is increased up to 150 times its nominal operating pressure. The beam-gas scattering induced heat loads arising from such high pressure perturbations can be very high locally, but do not overload the cryogenic system. They are more likely to induce a magnet quench as they result in coil temperatures that largely exceed the desired operating limit. Simulations are also carried out for the case where a large external heat load of 1 W/m is imposed on the coldmass of a half-cell in the section. Results show that the coldmass temperatures rise significantly with the added heat load but the energy deposition in the coldmass due to beam-gas scattering remains low despite the increase in the beam tube temperature. DOE

N92-30881# Superconducting Super Collider Lab., Dallas, TX.
EMITTANCE GROWTH CAUSED BY MAGNET VIBRATIONS IN SSC
G. V. Stupakov Mar. 1992 13 p Presented at the International Industrial Symposium on the Super Collider, New Orleans, LA, 4-6 Mar. 1992
(Contract DE-AC35-89ER-40486)
(DE92-014186; SSCL-516; CONF-920331-19) Avail: CASI HC A03/MF A01

Magnet vibrations may be caused by ground motions in the collider. The vibrations can be characterized as high-frequency (in the range of Hz or tens of Hz) noise. High-frequency noise resonates with the betatron oscillations causing fast emittance growth of the beam. Analytical results indicate a tolerable vibration level that is not harmful for the beams. Estimations for the ambient low-frequency noise show that in typical conditions it is of no danger for the collider. DOE

N92-31198# California Univ., Berkeley. Lawrence Berkeley Lab.
PHYSICS OF THE STAR EXPERIMENT AT THE RELATIVISTIC HEAVY ION COLLIDER
J. W. Harris Jan. 1992 8 p Presented at the 8th Winter Workshop on Nuclear Dynamics, Jackson Hole, WY, 18-25 Jan. 1992
(Contract DE-AC03-76SF-00098)
(DE92-014481; LBL-32121; CONF-920113-5) Avail: CASI HC A02/MF A01

An overview of the STAR experiment at the Relativistic Heavy Ion Collider is presented. The experiment will concentrate on the measurement of particle production and jet production at midrapidity in a search for the Quark-Gluon Plasma. These hadronic observables will be studied on an event-by-event basis to determine the thermodynamics of single events and to identify special and unusual events. The physics addressed by STAR is discussed. DOE

N92-31219# Fermi National Accelerator Lab., Batavia, IL.
RECENT EXPERIMENTAL STUDIES ON HADRON SHOWERS PRODUCED IN HIGH ENERGY MUON-NUCLEUS INTERACTIONS
J. Morfin May 1992 17 p Presented at the 21st International Symposium on Multiparticle Dynamics, Wuhan (China), 23-27 Sep. 1991
(Contract DE-AC02-76CH-03000)
(DE92-016002; FNAL/C-92/129-E; CONF-9109221-6) Avail: CASI HC A03/MF A01

The Fermilab Tevatron Muon Experiment has analyzed the hadron showers of events resulting from the scattering of a muon beam (less than E(sub mu) greater than or = 490 GeV) off H2, D2, and Xenon targets. The topics which will be discussed are: (1) space-time evolution of the hadronization process; (2) leading hadron distributions in the shadowing region; and (3) rates and characteristics of 3-jet events. DOE

74 OPTICS

Includes light phenomena; and optical devices.
For lasers see *36 Lasers and Masers.*

N92-30233# ERG Systems, Inc., Saint James, NY.
FULL SURFACE TESTING OF GRAZING INCIDENCE MIRRORS Quarterly Report, 12 Dec. 1991 - 11 Mar. 1992
John Remo 10 Mar. 1992 45 p
(Contract N00014-90-C-0246)
(AD-A248851) Avail: CASI HC A03/MF A01

The tasks accomplished are as follows: the integration of the optical interferometer head, including the Oriel microstepper and the NEAT scanning stage; the integration of the electronic hardware, including the charge coupled device (CCD) camera, the frame buffer, the Oriel microstepper controller and the NEAT scanning stage controller; the integration of the software, including data acquisition and storage, Oriel microstepper control, NEAT scanning stage control, subaperture phase measurement and synthesis of full-surface phase measurement; and initial testing of the complete integrated system, hardware and software, with

presentation of experimental results of first full-surface measurement tests. GRA

N92-30248# PCO, Inc., Chatsworth, CA.
FIBER OPTIC BASED SIGNAL PROCESSING Final Report, Jun. 1985 - Apr. 1991
Bor U. Chen Dec. 1991 183 p
(Contract F30602-87-C-0015)
(AD-A247857; RL-TR-91-369) Avail: CASI HC A09/MF A02

The objective of this project was to determine the theoretical performance and design latitude available from optical fiber based signal processors in accomplishing filtering, coded sequence generation, and matrix multiplication functions. Towards this goal the contractor has completed the study, design, fabrication and testing aspects of the coded sequence generator. The study and design facets of the filter and matrix multiplier functions also have been accomplished but the fabrication and testing aspects of the processors have not been done. This report extends the art of fiber based signal processors, points the way towards further work and has produced a significant patent (included) and numerous open literature publications. Author (GRA)

N92-30312*# National Aeronautics and Space Administration. Langley Research Center, Hampton, VA.
OFF-SURFACE INFRARED FLOW VISUALIZATION Patent Application
Gregory S. Manuel, inventor (to NASA), Clifford J. Obara, inventor (to NASA) (Lockheed Engineering and Sciences Co., Hampton, VA.), Kamran Daryabeigi, inventor (to NASA), and David W. Alderfer, inventor (to NASA) 16 Dec. 1991 8 p
(NASA-Case-LAR-14568-1; NAS 1.71:LAR-14568-1; US-Patent-Appl-SN-808302) Avail: CASI HC A02/MF A01

A method for visualizing off-surface flows is provided which consists of releasing a gas with infrared absorbing and emitting characteristics into a fluid flow and imaging the flow with an infrared imaging system. This method allows for visualization of off-surface fluid flow in-flight. The novelty of this method is found in providing an apparatus for flow visualization which is contained within the aircraft so as not to disrupt the airflow around the aircraft, is effective at various speeds and altitudes, and is longer-lasting than previous methods of flow visualization. NASA

N92-30343# Phillips Lab., Hanscom AFB, MA.
LIDAR MEASUREMENT OF OPTICAL TURBULENCE: THEORY OF THE CROSSED PATH TECHNIQUE Interim Scientific Report
Robert R. Beland and J. Krause-Polstorff 8 Jul. 1991 44 p
(AD-A248938; AD-E200981; PL-TR-91-2139; ERP-1089) Avail: CASI HC A03/MF A01

The existing measurement capabilities of optical turbulence for IR/optical wavelengths are reviewed. It is shown that no capability exists for simultaneous high spatial and temporal resolution measurements of optical turbulence along an optical path. A general formulation of the remote sensing of optical turbulence is presented, emphasizing the importance of the altitude weighting function, dynamic range requirements, and numerical issues. A new approach to lidar remote sensing of turbulence is presented that uses two lidar beams that are viewed by two receivers along a crossed path. The geometric aspects of this theory are discussed and followed by a quantitative formulation based on the Rytov approximation. The approach is similar to the binary star and crossed laser beam methods that have appeared in the literature. The method is based on the intensity covariance of two backscattered spots viewed along crossed paths. The effects of backscatter spot size and receiver averaging are presented. It is shown that the technique is sensitive to the inner scale and is insensitive to the presence of both backscattering spots in both receiver fields of view. The effects of diffraction, turbulence broadening, and beam wander are discussed. Criteria are presented for all these effects in the design of a practical system. GRA

N92-30504# Tuebingen Univ. (Germany, F.R.). Inst. fuer Astronomie.
THEORY AND MEASUREMENT OF THE ENERGY AND RISETIME RESOLUTION OF SCINTILLATION DETECTORS IN HARD X RAY AREA Thesis [THEORIE UND MESSUNG DER ENERGIE- UND RISETIMEAUFLOESUNG AN SZINTILLATIONS-DETEKTOREN IM HARTEN ROENTGENBEREICH]
Juergen Schneider Jul. 1990 83 p In GERMAN
(ETN-92-91687) Avail: CASI HC A05/MF A01

Several scintillation detectors are examined, and the measurement results are compared in order to increase the energy resolution. The uniformity of each detector was estimated by scanning of the detector surface with a monochromatic x-ray source and by measuring the photon peak location in the energy spectrum at each grid point. Computer programs were developed to record energy and rise-time spectral data and to minimize the background radiation effect. A Southampton detector, a four photomultiplier detector, and a Phoswhich detector were studied. The half value width and the center of gravity location in the distributions are found to be strongly dependent on the preamplifier time constant. It is assumed that an improvement of the analog summation of the preamplifier output signal and a reduction of the absorption losses in the detector angles will improve the energy resolution by 20. ESA

N92-30507# Institut Franco-Allemand de Recherches, Saint-Louis (France).
DOPPLER PHOTOGRAPHY: LASER METHODS ON THE FLOW MEASUREMENT TECHNIQUE [DOPPLERBILD-PHOTOGRAPHIE: LASERMETHODEN IN DER STROEMUNGSMESSTECHNIK]
F. Seiler, J. Srulijes, A. George, and B. Ruck, ed. 1990 32 p In GERMAN Original contains color illustrations
(ISL-PU-303/90; ISBN-3-921-681-01-4; ETN-92-91713) Copyright Avail: CASI HC A03/MF A01

A Michelson interferometer with arms of varied lengths which allows the detection of diffusion light frequency variations in light phase alterations and their transformation in lighting intensity fluctuations is described. The Doppler photography considers the frequency changes of the diffusion light from the different points of a surface. Additionally, the Doppler photograpy is developed by photographing the local variations of lighting intensities, and works without polarization optics. Experiments were carried out with continuous laser (CO2 and cool air radiation) and pulsed laser (warm air radiation and swirl). Photographs of stationary flow phenomena were obtained. Strongly unstationary three dimensional flows were also observed. These flows are unavailable with usual velocity measuring methods. Doppler photography is shown to be less expensive and accurate than laser velocimetry. ESA

N92-30535# Nebraska Univ., Lincoln. Dept. of Chemistry.
EFFECTS OF THE ORIENTATIONAL PAIR CORRELATION ON SECOND ORDER NONLINEAR OPTICAL COEFFICIENTS
C. H. Wang 1 Jun. 1992 22 p
(Contract N00014-90-J-1494)
(AD-A252490; TR-13) Avail: CASI HC A02/MF A01

The orientational order parameter associated with the second order nonlinear optical (NLO) coefficient is calculated by using a statistical mechanics method that includes the angular dependent intermolecular interaction potential. It is shown that in addition to the alignment of dipoles due to the poling field, the orientational pair correlation (OPC) factor is also important in determining the orientational order parameter. When OPC is included, the order parameter becomes a function of the NLO chromorphore concentration. The concentration dependent part of the order parameter is shown to be proportional to the Kirkwood g-factor associated with the orientational correlation of the electric dipoles. In the weak field limit, it is shown that the ratio of two nonlinear optical coefficients, X33/X31, remains equal to 3, independent of the specific nature of the anisotropic intermolecular potential. GRA

N92-30536# Nebraska Univ., Lincoln. Dept. of Chemistry.
DEPOLARIZED LIGHT SCATTERING AND DYNAMIC SHEAR COMPLIANCE OF VISCOELASTIC LIQUIDS
C. H. Wang 1 Jun. 1992 24 p
(Contract N00014-90-J-1494)
(AD-A252491; TR-15) Avail: CASI HC A02/MF A01

Efforts are made to relate the depolarized light scattering spectral power density to the dynamic shear compliance spectrum of a viscoelastic liquid. Generalized Langevin equations are used to describe the dynamics and coupling of reorientation and translational motions. It is shown that in the presence of the coupling, the depolarized scattering spectrum consists of two components: one is associated with the reorientational motion, and the other with the viscoelastic relaxation of the solution. Methods to obtain the dynamic shear compliance from the depolarized light scattering spectrum are described. It is also shown that in the limit of very slow reorientational motion, the depolarized light scattering spectrum is proportional to the imaginary part of the dynamic compliance spectrum, a result predicted by the Pockels photoelastic law. GRA

N92-30581 Tel-Aviv Univ. (Israel). School of Physics and Astronomy.
OPTICAL ISOLATORS IN HIGH POWER LASERS BASED ON HIGH REFLECTIVITY PHASE CONJUGATE MIRRORS M.S. Thesis
Sharon Atzmon May 1990 91 p In HEBREW Prepared in cooperation with Soreq Research Establishment, Israel Atomic Energy Commission, Yavneh
(IA-1452; ITN-92-85170) Copyright Avail: Tel-Aviv Univ., Exact Sciences Library, Ramat Aviv, 69978, Israel

The purpose of this thesis is to characterize a new type of non-linear optical isolator (NLI). NLI operation is based on stimulated Brillouin Scattering (SBS). It allows high transmission of light below a predetermined power threshold but provides high reflectivity and low transmission to suprathreshold light. In application to advanced laser system design, forward propagating light is transmitted whereas backward propagating light is blocked. The advantages of these isolators are relative insensitivity to the polarization of the incident light beams, fast response time (nanoseconds), and totally passive operation. The dependence of the NLI threshold and transmission on incident pulse energy, the type of SBS material, the interaction geometry (focal length of lenses), and the laser pulse duration was experimentally and theoretically examined. The NLI was incorporated into an advanced phase-conjugated multiple-pass amplifier (PCMPA). The gain of the PCMPA was measured along with the influence of the isolator on pulse shape in time and space. The experimental set-up included a low-power Nd:YAG oscillator that provided single longitudinal mode (SLM) pulses of 17 nS duration with energy of 1.5-2.0 mJ per pulse and a multiple-pass Nd:glass amplifier 1.9 cm in diameter and 43 cm long. Multiple passes were obtained through the use of a phase conjugated mirror and the NLI. Theoretical predictions of NLI performance were found to agree with experimental results. Of particular importance was the finding that for incident energies above threshold, the NLI transmitted energy just equal to the threshold energy itself. This conclusion was found to be valid despite experimentally imposed threshold variations of an order of magnitude and incident energies up to 100 times above threshold. Author (ISA)

N92-30783# Washington Univ., Seattle. Applied Physics Lab.
NUMERICAL SIMULATIONS OF LIGHT SCATTERING FROM ROUGH ONE-DIMENSIONAL GOLD SURFACES
Eric I. Thorsos 14 Feb. 1992 14 p
(Contract MIPR-153-91)
(AD-A249794; ARO-29288.1-GS) Avail: CASI HC A03/MF A01

During 1991, Kevin O'Donnell at Georgia Tech made new measurements of light scattering from gold surfaces, which were well characterized and known to be nearly one-dimensional (1-D). In anticipation of these new data, numerical simulations of the scattering experiments were undertaken in this project for comparison with the data and with results of other investigators. GRA

N92-30975*# Virginia Polytechnic Inst. and State Univ., Blacksburg. Dept. of Electrical Engineering.
SINGLE MODE VARIABLE-SENSITIVITY FIBER OPTIC SENSORS
K. A. Murphy, B. R. Fogg, M. F. Gunther, and R. O. Claus 1992 6 p
(Grant NAG1-1348)
(NASA-CR-190492; NAS 1.26:190492) Avail: CASI HC A02/MF A01

We review spatially-weighted optical fiber sensors that filter specific vibration modes from one dimensional beams placed in clamped-free and clamped-clamped configurations. The sensitivity of the sensor is varied along the length of the fiber by tapering circular-core, dual-mode optical fibers. Selective vibration mode suppression on the order of 10 dB was obtained. We describe experimental results and propose future extensions to single mode sensor applications. Author

N92-31126# International Society for Optical Engineering, Bellingham, WA.
SOL-GEL OPTICS: PROCEEDINGS SPIE-THE INTERNATIONAL SOCIETY FOR OPTICAL ENGINEERING Final Report, 1 Jul. 1990 - 30 Jun. 1991
John D. Mackenzie and Donald R. Ulrich Mar. 1992 512 p Conference held in San Diego, CA, 11-13 Jul. 1990
(Grant AF-AFOSR-0295-90)
(AD-A249986; AFOSR-92-0254TR) Avail: CASI HC A22/MF A04

This conference produced the first proceedings on sol-gel optics. The proceedings include reports on the attempts to fabricate semiconductor-in-glass quantum-well confinement lenses. The successful preparation of organic dyes-in-oxides laser elements is discussed, as well as research on the fabrication of grooved glass discs through the mechanical patterning of the soft gels. GRA

N92-31149# Polish Academy of Sciences, Warsaw. Inst. Podstawowych Problemow Techniki.
A TOLERANCE APPROACH TO VISUAL SHAPE PERCEPTION AND IMAGE MATCHING ANALYSIS FOR MODELING OF MICRO-HETEROGENEOUS MATERIALS
Czeslaw Wozniak 1992 67 p
(ISSN-0208-5658) Avail: CASI HC A04/MF A01

The aim of this paper is twofold. First, we propose a mathematical model of how the visible shapes of illuminated material objects are perceived. The leading assumption is that the visual shape perception depends not only on the received two dimensional images, but also on certain 'higher level knowledge' about the viewed objects ('we perceive what we expect to perceive'). The model obtained is represented by the image tolerance relation between the expected and received monochromatic images. On this basis the perceptable shapes of objects can be determined. The second aim of this paper is to show how the proposed image tolerance analysis can be applied to the formation of the representative distributions of constituents for certain micro-heterogeneous material structures. Author

N92-31187# Superconducting Super Collider Lab., Dallas, TX.
OPTICAL TRANSDUCERS FOR SCINTILLATING FIBER READOUT
H. Fenker May 1992 7 p Presented at the International Conference on Radiation Tolerant Scintillators and Detectors, Tallahassee, FL, 28 Apr. - 2 May 1992 Submitted for publication
(Contract DE-AC35-89ER-40486)
(DE92-015963; SSCL-Preprint-120) Avail: CASI HC A02/MF A01

Characteristics of optical-to-electronic transducers which are currently on the market or which will soon be available are discussed in the context of particle detectors using scintillating and wavelength-shifting fibers. It is shown that the most promising

avenue for progress in detector development is via the use of solid state transducers, and that these would benefit from the development of long-wavelength light emitters. DOE

N92-31195# Oak Ridge Y-12 Plant, TN.
AN X RAY MICROPROBE BASED UPON A CLOSE-COUPLED FOCAL-SPOT/GLASS CAPILLARY ARRANGEMENT
D. A. Carpenter and M. A. Taylor Mar. 1992 5 p Presented at the Annual Meeting of the Electron Microscopy Society of America, Boston, MA, 16-21 Aug. 1992
(Contract DE-AC05-84OS-21400)
(DE92-011886; Y/DW-1139; CONF-920819-11) Avail: CASI HC A01/MF A01

As an alternative to aperture optics, the authors describe a microprobe based upon a radiographic microfocus x-ray tube and glass capillary optics. High intensities were obtained by placing the capillary very near the microfocal spot to maximize the acceptance angle. The total reflection of x-rays through the capillary reduced the 1/r(exp 2) losses associated with aperture optics. The beam characteristics and minimum detection limits of the latest version of the microprobe are presented along with examples of applications. DOE

N92-31213# Department of the Navy, Washington, DC.
FIBER OPTIC MICHELSON SENSOR AND ARRAYS WITH PASSIVE ELIMINATION OF POLARIZATION FADING AND SOURCE FEEDBACK ISOLATION Patent Application
Alan D. Kersey, inventor (to Navy) 31 Jan. 1992 29 p
(AD-D015290; US-Patent-Appl-SN-828630; Navy-Case-73519)
Avail: CASI HC A03/MF A01

A fiber optic Michelson interferometric sensor system with passive elimination of polarization fading and source feedback isolation is disclosed. In a preferred embodiment, an optical source provides light of a first polarization state to a polarization selective element. Output light from the polarization selective element passes through a length of optical fiber into a Michelson interferometric sensor which utilizes a Faraday rotator/mirror assembly, that is coupled to distal ends of sensing and reference arms of the Michelson interferometer, to provide for the passive elimination of polarization fading. The polarization selective element at the output of the optical source provides isolation of the optical source from the Michelson interferometric sensor. GRA

N92-31051*# Centre National de la Recherche Scientifique, Verrieres-Le Buisson (France).
OPTICS OF THE OZONE LIDAR ELSA
J. Porteneuve *In* NASA. Langley Research Center, 16th International Laser Radar Conference, Part 2 Jul. 1992 p 525-527 (For primary document see N92-31013 21-35)
Avail: CASI HC A01/MF A03

N92-31060*# National Aeronautics and Space Administration. Langley Research Center, Hampton, VA.
COMPARISON OF EYE-SAFE SOLID STATE LASER DIAL WITH PASSIVE GAS FILTER CORRELATION MEASUREMENTS FROM AIRCRAFT AND SPACECRAFT
Robert V. Hess, Leo D. Staton, H. Andrew Wallio, and Liang-Guo Wang (College of William and Mary, Williamsburg, VA.) *In its* 16th International Laser Radar Conference, Part 2 Jul. 1992 p 559-562 (For primary document see N92-31013 21-35)
Avail: CASI HC A01/MF A03

75 PLASMA PHYSICS

Includes magnetohydrodynamics and plasma fusion.

For ionospheric plasmas see *46 Geophysics*. For space plasmas see *90 Astrophysics*.

N92-30366# Oak Ridge National Lab., TN.
GYRO-LANDAU FLUID MODEL OF TOKAMAK CORE FLUCTUATIONS
J. N. Leboeuf, B. A. Carreras, N. Dominguez, C. L. Hedrick, K. L. Sidikman, V. E. Lynch, J. B. Drake, and D. W. Walker 1992 27 p Presented at the Numerical Tokamak Project Workshop, Santa Fe, NM, 8-9 Apr. 1992
(Contract DE-AC05-84OR-21400)
(DE92-013277; CONF-9204132-1-Extd-Abst) Avail: CASI HC A03/MF A01

Dissipative trapped electron modes (DTEM) may be one of the causes of deterioration of confinement in tokamak and stellarator plasmas. We have implemented a fluid model to study DTEM turbulence in slab geometry. The electron dynamics include in addition to the adiabatic part, a non-adiabatic piece modeled with an i-delta-type response. The ion dynamics include Landau damping and FLR corrections through Landau fluid approximate techniques and Pade approximants for gamma(sub 0)(b) = I(sub 0)(b)e(exp -b). The model follows from the gyrokinetic equation. Evolution equations, which closely resemble those used in standard reduced MHD, are presented since these are better suited to non-linear calculations. The numerical results of radially resolved calculations are discussed. A recently developed hybrid model, which consists of a gyrokinetic implementation for the ions using particles and the same description for the electron dynamics as in the fluid model, is also presented. DOE

N92-30384# National Inst. for Fusion Science, Nagoya (Japan).
MAGNETIC SURFACE BREAKING IN 3D MHD EQUILIBRIA OF L = 2 HELIOTRON
Takaya Hayashi, Akira Takei, and Tetsuya Sato Jan. 1992 31 p Submitted for publication
(NIFS-130; ISSN-0915-633X) Avail: CASI HC A03/MF A01

Magnetic surface breaking due to the finite pressure effect is analyzed for 3-D magnetohydrodynamic equilibria of I = 2 Heliotron configuration. Characteristics of magnetic island formation are extensively surveyed. It is found that the well-hill criterion which was predicted by the local analysis is not always applicable for all cases. Author

N92-30385# National Inst. for Fusion Science, Nagoya (Japan).
FIELD LINE DIVERSION PROPERTIES OF FINITE BETA HELIAS EQUILIBRIA
T. Hayashi, U. Schwenn (Max-Planck-Inst. fuer Plasmaphysik, Munich, Germany, F.R.), and E. Strumberger (Max-Planck-Inst. fuer Plasmaphysik, Munich, Germany, F.R.) Mar. 1992 16 p Submitted for publication Original contains color illustrations
(NIFS-137; ISSN-0915-633X) Avail: CASI HC A03/MF A01

The diversion properties of the magnetic field outside the last closed magnetic surface of the Helias stellarator configuration are investigated for the finite beta-equilibrium. The results support a divertor concept which has been developed from the diversion properties of the corresponding vacuum field. Cross-field transport is simulated by a simplified scrape-off layer (SOL) model. Author

N92-30430# National Inst. for Fusion Science, Nagoya (Japan).
TRITIUM CONTENT OF A DT PELLET IN INERTIAL CONFINEMENT FUSION
S. Kawata (Nagaoka Technological Univ., Japan) and H. Nakashima (Kyushu Univ., Fukuoka, Japan) Oct. 1991 17 p Sponsored in part by the Scientific Research Fund of the Ministry of Education and Culture in Japan
(NIFS-113; ISSN-0915-633X) Avail: CASI HC A03/MF A01

A numerical and an analytical estimations, and a one-dimensional hydrodynamic simulation present that the 30 percent order of reduction of the tritium content in a DT pellet can bring the sufficient energy output in a deuterium-tritium (DT) inertial confinement fusion reactor. In other words, the tritium content can be reduced significantly without a significant reduction in the DT fusion energy output. This new result also means that the tritium inventory can be reduced significantly before and during the reactor operation of a DD reaction to the DT reaction. Author

N92-30431# National Inst. for Fusion Science, Nagoya (Japan).
RECOMBINING PROCESSES IN A COOLING PLASMA BY MIXING OF INITIALLY HEATED GAS
Utaro Furukane (Ehime Univ., Matsuyama, Japan), Kuninori Sato,

Ken Takiyama (Hiroshima Univ., Japan), and Toshiatsu Oda (Hiroshima Univ., Japan) Mar. 1992 34 p Submitted for publication
(NIFS-142; ISSN-0915-633X) Avail: CASI HC A03/MF A01

A numerical investigation of recombining process in a high temperature plasma in a quasi-steady state is made in a gas contact cooling, in which the initial temperature effect of contact gas heated up by the hot plasma is considered as well as the gas cooling due to the surrounding neutral particles freely coming into the plasma. The calculation has shown that the electron temperature relaxes in accord with experimental results and that the occurrence of recombining region and the inverted populations almost agree with the experimental ones. Author

N92-30497# National Inst. for Fusion Science, Nagoya (Japan).
DYNAMIC ANALYSIS OF COMPACT HELICAL SYSTEM POWER SUPPLY AND DESIGNS OF ITS UPGRADE
S. Tanahashi and S. Yamada Sep. 1991 24 p
(NIFS-Tech-2; ISSN-0915-6356) Avail: CASI HC A03/MF A01

Computed dynamic waveforms are compared with measured ones for the power supply of the Compact Helical System (CHS) during 1.5T operation and found to be in good agreement. On the basis of these results, designs for the upgraded power supply for 2T operation are discussed in two cases - with and without power consumption for additional heating. In the former case, the additional heating power is supplied from the AC generator that powers the CHS coils. Electric voltages and currents in the electric circuit are shown for both cases. These designs show the possibility for 2T operation by the addition of some components without changing the ratings of existing components. Author

N92-30499# National Inst. for Fusion Science, Nagoya (Japan).
PLASMA PARAMETER ESTIMATIONS FOR THE LARGE HELICAL DEVICE BASED ON THE GYRO-REDUCED BOHM SCALING
Masao Okamoto, Noriyshi Nakajima, and Hideo Sugama Oct. 1991 25 p Sponsored in part by Ministry of Education, Science and Culture
(NIFS-114; ISSN-0915-633X) Avail: CASI HC A03/MF A01

A model of a gyro-reduced Bohm scaling law is incorporated into a 1-D transport code to predict plasma parameters for the Large Helical Device (LHD). The transport code calculations reproduce well the LDH empirical scaling law and basic parameters and profiles of the LHD plasma are calculated. The amounts of toroidal currents (bootstrap current and beam-driven current) are also estimated. Author

N92-30576# Oak Ridge National Lab., TN.
PROBLEMS WITH THE CONCEPT OF PLASMA EQUILIBRIUM IN TOKAMAKS
B. A. Carreras 1992 24 p Presented at the Real Academia De Ciencias Exactas, Fisicas Y Naturales, Madrid (Spain), 14 Feb. 1992
(Contract DE-AC05-84OR-21400)
(DE92-014454; CONF-9202112-1) Avail: CASI HC A03/MF A01

The equilibrium condition for a magnetically confined plasma is normally formulated in terms of macroscopic equations. In these equations, the plasma pressure is assumed to be a function of the magnetic flux with continuous derivatives. However, in three-dimensional systems this is not necessarily the case. Here, we look at the case of an intrinsically three-dimensional realistic tokamak, and we discuss the possible interconnection between the equilibrium and anomalous transport. DOE

N92-30591# Argonne National Lab., IL.
MHD CONSIDERATIONS FOR A SELF-COOLED LIQUID LITHIUM BLANKET
D. K. Sze, R. F. Mattas, A. B. Hull, B. F. Picologlou, and D. L. Smith Mar. 1992 9 p Presented at the 10th Topical Meeting on Technology of Fusion Energy, Boston, MA, 7-12 Jun. 1992
(Contract W-31-109-eng-38)
(DE92-014864; ANL/CP-75362; CONF-920607-15) Avail: CASI HC A02/MF A01

The magnetohydrodynamic (MHD) effects can present a feasibility issue for a self-cooled liquid metal blanket of magnetically confined fusion reactors, especially the inboard regime of a tokamak. This pressure drop can be significantly reduced by using an insulated wall structure. A self-healing insulating coating has been identified, which will reduce the pressure drop by more than a factor of 10. The future research direction to further quantify the performance of this coating is also outlined. DOE

N92-30612# Wisconsin Univ., Madison. Dept. of Physics.
LOCKED MODES AND MAGNETIC FIELD ERRORS IN MST
A. F. Almagri, S. Assadi, S. C. Prager, J. S. Sarff, and D. W. Kerst Jun. 1992 24 p
(Contract DE-FG02-85ER-53198)
(DE92-015379; DOE/ER-53198/197) Avail: CASI HC A03/MF A01

In the MST reversed field pinch, magnetic oscillations become stationary (locked) in the lab frame as a result of a process involving interactions between the modes, sawteeth, and field errors. Several helical modes become phase locked to each other to form a rotating localized disturbance; the disturbance locks to an impulsive field error generated at a sawtooth crash; the error fields grow monotonically after locking (perhaps due to an unstable interaction between the modes and field error), and over the tens of milliseconds of growth confinement degrades; and the discharge eventually terminates. Field error control has been partially successful in eliminating locking. DOE

N92-30620# Naval Research Lab., Washington, DC.
INTERACTION OF ULTRA-HIGH LASER FIELDS WITH BEAMS AND PLASMAS Interim Report
Eric Esarey and Phillip Sprangle 29 Apr. 1992 33 p
(AD-A249502; NRL/MR/4790-92-6949) Avail: CASI HC A03/MF A01

The nonlinear interaction of ultra-intense laser pulses with electron beams and plasmas displays a wide variety of new phenomena. Advances in laser science have made possible compact terawatt lasers capable of generating subpicosecond pulses at ultra-high powers (equal to or more than 1 TW) and intensities (equal to or more than 1018 W/sq cm). These ultrahigh intensities result in highly relativistic nonlinear electron dynamics. This paper briefly addresses a number of phenomena including the following: (1) laser excitation of large amplitude plasma waves (wakefields); (2) relativistic optical guiding of laser pulses in plasmas; (3) optical guiding by preformed plasma channels; (4) laser frequency amplification by ionization fronts and plasma waves; (5) relativistic harmonic generation; (6) stimulated backscattering from plasmas and electron beams; (7) nonlinear Thomson scattering from plasmas and electron beams; and (8) cooling of electron beams by intense lasers. Potential applications of these effects are also discussed. GRA

N92-30746# Canadian Fusion Fuels Technology Project, Mississauga (Ontario).
BOUNDARY PLASMA TRANSPORT STUDIES ON TFTR
C. S. Pitcher and P. C. Stangeby Nov. 1991 56 p
(Contract DE-FG05-90ER-54091)
(DE92-011942; DOE/ER-54091/1; CFFTP-G-91112) Avail: CASI HC A04/MF A01

In this report we summarize the experimental and theoretical investigations supported under the DOE Transport Initiative Contract on the subject of Boundary Plasma Transport Studies on TFTR. This work can be logically separated into two areas of investigations and therefore the report included here is divided into two parts. First, in Section I, detailed boundary plasma data obtained from TFTR in an ohmic density scan has been compared with results from the LIM Impurity Production and Transport Code. Second, in Section II, experimental results taken with the newly-purchased (specifically for this initiative) intensified CCD camera are presented, which, after comparison with simple

modeling, reveals a new and important effect that has implications for limiter and divertor plate design. DOE

N92-30806# Los Alamos National Lab., NM.
NEUTRON TIME-OF-FLIGHT ION TEMPERATURE DIAGNOSTIC FOR INERTIAL CONFINEMENT FUSION EXPERIMENTS
R. E. Chrien, D. F. Simmons, and D. L. Holmberg 1992 12 p Presented at the 9th Topical Conference on High-Temperature Plasma Diagnostics, Santa Fe, NM, 15-19 Mar. 1992
(Contract W-7405-eng-36)
(DE92-011365; LA-UR-92-875; CONF-920362-19) Avail: CASI HC A03/MF A01

We are constructing a T(sub i) diagnostic for low neutron yield (5 x 10(exp 7) to above 10(exp 9)) d-d and d-t targets in the Nova facility at Livermore. The diagnostic measures the neutron energy spread with 960 scintillator-photomultiplier detectors located 28 m from the target and operates in the single-hit mode. Each detector can measure a single neutron arrival with time resolution of 1 nano-s or better. The arrival time distribution is constructed from the results of typically 200-500 detector measurements. The ion temperature is determined from the spread in neutron energy (Delta)E(sub n) proportional to T(sub i)(sup (1/2)), which is related to the arrival time spread by (Delta)t/t = -(1/2)(Delta)E(sub n)/E(sub n). Each neutron arrival is detected by using a photomultiplier tube to observe the recoil proton from elastic scattering in a fast plastic scintillator. The timing electronics for each channel consist of a novel constant fraction-like discriminator and a multiple hit time-to-digital converter (TDC). The overall system design, together with single channel performance data, is presented. DOE

N92-30810# Oak Ridge National Lab., TN.
DENSITY PROFILE MEASUREMENT USING A MULTICHANNEL DIFLUOROMETHANE LASER INTERFEROMETER SYSTEM ON ATF
C. H. Ma, L. R. Baylor, D. P. Hutchinson, M. Murakami, and J. B. Wilgen 1992 10 p Presented at the 9th Topical Conference on High-Temperature Plasma Diagnostics, Santa Fe, NM, 15-19 Mar. 1992
(Contract DE-AC05-84OR-21400)
(DE92-011691; CONF-920362-23) Avail: CASI HC A02/MF A01

Recent results of the electron density profile measurement on the Advanced Toroidal Facility (ATF) are presented. A multichannel difluoromethane laser interferometer system has been routinely employed to study density evolution in ECH as well as neutral-beam-heated plasma discharges with gas fueling and pellet injection. A chordal inversion code has been developed, and has been used successfully to reconstruct the asymmetric density profiles. Cross-correlation of density profile measurements among FIR interferometer, Thomson scattering, the heavy-ion beam probe, and the fast reciprocating Langmuir probe has been achieved. Radial density profiles measured by the four diagnostics are generally in good agreement and are hollow profiles under most experimental conditions. DOE

N92-30824# Lawrence Livermore National Lab., CA.
REMOTE EXPERIMENTAL SITE CONCEPT FOR DIAGNOSTIC COLLABORATIONS IN FUSION
T. A. Casper Aug. 1991 8 p Presented at the Workshop on Diagnostics for Comtemporary Fusion Experiments, Varenna, Italy, 27 Aug. - 6 Sep. 1991
(Contract W-7405-eng-48)
(DE92-010437; UCRL-CR-107774; CONF-910857-9) Avail: CASI HC A02/MF A01

The next generation of tokamaks, ITER or BPX, will be characterized by an even greater emphasis on joint operation and experimentation. With anticipation of an increased number and diversity of collaborations, especially in the area of diagnostics, we are preparing for such shared facilities by developing a systematic approach to remote, joint physics operation involving experimental teams at several locations. The local area network of computers used for control and data acquisition on present and future experiments can be extended over a wide area network to provide a mechanism for remote operation of subsystems (e.g. diagnostics) required for physics experiments. The technology required for high bandwidth (greater than or equal to 45 Mbps) connections between multiple sites either exists or will be available over the next few years. With the rapid development of high performance workstations, network interfaces, distributed computing, and video conferencing, we can proceed with the development of a system of control and analysis sites to provide for consistent, efficient, and continuing collaborations. Early establishment of such sites could also enhance existing joint design and development efforts. DOE

N92-30833# Texas Univ., Austin. Inst. for Fusion Studies.
LOW-FREQUENCY FLUCTUATIONS IN PLASMA MAGNETIC FIELDS
S. Cable and T. Tajima Feb. 1992 84 p
(Contract DE-FG05-80ET-53088)
(DE92-012139; DOE/ET-53088/541; IFSR-541) Avail: CASI HC A05/MF A01

It is shown that even a non-magnetized plasma with temperature T sustains zero-frequency magnetic fluctuations in thermal equilibrium. Fluctuations in electric and magnetic fields, as well as in densities, are computed. Four cases are studied: a cold, gaseous, isotropic, non-magnetized plasma; a cold, gaseous plasma in a uniform magnetic field; a warm, gaseous plasma described by kinetic theory; and a degenerate electron plasma. For the simple gaseous plasma, the fluctuation strength of the magnetic field as a function of frequency and wavenumber is calculated with the aid of the fluctuation-dissipation theorem. This calculation is done for both collisional and collisionless plasmas. The magnetic field fluctuation spectrum of each plasma has a large zero-frequency peak. The peak is a Dirac delta function in the collisionless plasma and is broadened into a Lorentzian curve in the collisional plasma. The plasma causes a low frequency cutoff in the typical black-body radiation spectrum, and the energy under the discovered peak approximates the energy lost in this cutoff. When the imposed magnetic field is weak, the magnetic field wave vector fluctuation spectra of the two lowest modes are independent of the strength of the imposed field. Further, these modes contain finite energy even when the imposed field is zero. It is the energy of these modes which forms the non-magnetized zero-frequency peak of the isotropic plasma. In deriving these results, a simple relationship between the dispersion relation and the fluctuation power spectrum of electromagnetic waves if found. The warm plasma is shown, by kinetic theory, to exhibit a zero-frequency peak in its magnetic field fluctuation spectrum as well. For the degenerate plasma, we find that electric field fluctuations and number density fluctuations vanish at zero frequency; however, the magnetic field power spectrum diverges at zero frequency. DOE

N92-30880# Texas Univ., Austin. Inst. for Fusion Studies.
TWO DIMENSIONAL ASPECTS OF TOROIDAL DRIFT WAVES IN THE BALLOONING REPRESENTATION
Y. Z. Zhang, S. M. Mahajan, and X. D. Zhang May 1992 14 p
(Contracts DE-FG05-80ET-53088; DE-FG05-88ER-53266)
(DE92-014028; DOE/ET-53088/550; IFSR-550) Avail: CASI HC A03/MF A01

By systematically doing the higher order theory, the predictions of the conventional ballooning theory (CBT) are examined for non-ideal systems. For the complex solvability condition to be satisfied, radial variation of the lowest order mode amplitude needs to be invoked. It turns out, however, that even this procedure with its concomitant modifications of eigenvalues and eigenstructures, is not sufficient to justify the predictions of many CBT solutions; only a small set of CBT solutions could be put on a firm footing. To demonstrate our general conclusions, theoretical and numerical results are presented for system of fluid drift waves non-adiabatic electron response. DOE

N92-30884# Texas Univ., Austin. Inst. for Fusion Studies.
THE RAYLEIGH-TAYLOR INSTABILITY IN AN EXPANDING PLASMA
S. Cable and T. Tajima May 1992 24 p
(Contract DE-FG05-80ET-53088)
(DE92-013883; DOE/ET-53088/544; IFSR-544) Avail: CASI HC A03/MF A01

In a number of fluid systems, overall fluid expansion has a retarding effect on the growth of Rayleigh-Taylor (RT) instabilities: the growth of RT instabilities relative to the expansion of the fluid is slowed and is often sub-exponential. We give two new analytical examples of this phenomena of reduced growth or stabilization: one with incompressible fluids and one with an adiabatic fluid. Confirmation of this phenomenon is also obtained from a new MHD code constructed specifically for modeling fluids undergoing nearly homogenous (but not necessarily isotropic) expansion or contraction. In the code, expansion is included by making each point of the computational grid co-moving with a predetermined overall expansion, which is equivalent to using an expanding metric. DOE

N92-30900# Colorado Univ., Boulder. Dept. of Astrophysical, Planetary, and Atmospheric Sciences.
COLLISIONAL AND CHAOTIC TRANSPORT OF ENERGETIC PARTICLES IN TOROIDAL PLASMA
J. R. Cary and S. G. Shasharina Apr. 1992 10 p
(Contract DE-FG02-85ER-53207)
(DE92-014589; DOE/ER-53207/7) Avail: CASI HC A02/MF A01

We carried out investigations in the area of confinement plasma physics. We developed an accurate theory for the trapping/detrapping process in tokamaks with ripple and stellarators. We determined the alpha particle distribution. The distribution was determined for situations where both types of transport, collisional and collisionless chaotic (ripple), are present. DOE

N92-30984# National Inst. for Fusion Science, Nagoya (Japan).
X RAY RADIATION FROM HOT DENSE PLASMAS AND ATOMIC PROCESSES
Oct. 1991 188 p
(NIFS-Proc-9) Avail: CASI HC A09/MF A02

Given here are papers from a conference on x-ray radiation from hot-dense plasmas and atomic processes. A statistical method to evaluate the opacity of hot, high-Z plasmas is considered by taking account of a line group steming from the same transitions in different charge states.The structure of the line group is described and used to model effective line profiles in numerically treating radiation transport in fluid codes. Dispersion of line spread is obtained by a statistical method with the use of the averaged electron configuration of ions. The validity of the method is studied by reducing the Saha equilibrium relation in the local thermodynamic equilibrium limit. Other topics discussed include practical inertial confinement fusion and its numerical modeling, radiation transport dependence on modeling in laser-produced plasmas, atomic and radiative processes in tokamak plasmas, the thermal structure of astrophysical plasmas, and atomic physics and plasma simulation. Author

N92-30985# National Inst. for Fusion Science, Nagoya (Japan).
BETA LIMIT OF RESISTIVE PLASMA IN TORSATRON/HELIOTRON
K. Itoh, K. Ichiguchi, and Sanae-I. Itoh Feb. 1992 23 p Submitted for publication
(NIFS-131) Avail: CASI HC A03/MF A01

Stability against the interchange mode in the Torsatron/Heliotron device is investigated, taking into account the effects of the resistivity, current diffusivity, ion viscosity, and thermal diffusivity. Critical beta for the low-mode-number stability is found at the finite beta value. For the range plasma parameters of the present experiments, the resistive mode and current diffusive mode set comparable critical beta values, which are consistent with experimental observations. In future high temperature plasmas, the current diffusive mode determines the stability limit for the global mode. Author

N92-30991# National Inst. for Fusion Science, Nagoya (Japan).
A STEADY STATE TOKAMAK OPERATION BY USE OF MAGNETIC MONOPOLES
K. Narihara Dec. 1991 27 p
(DE92-799109; NIFS-126) Avail: CASI HC A03/MF A01

A steady state tokamak operation based on a magnetic monopole generates the needed loop voltage. The monopole circuit is enclosed by a series of solenoid coils in which the magnetic field is feedback controlled so that the force on the circuit balance against the mechanical friction. The driving power is supplied through the current sources of poloidal, ohmic, and solenoid coils. The current drive efficiency is same as that of the ohmic current drive. Author

N92-30992# National Inst. for Fusion Science, Nagoya (Japan).
EDGE POLOIDAL ROTATION PROFILES OF H-MODE PLASMAS IN THE JFT-2M TOKAMAK
K. Ida, S. Hidekuma, M. Kojima, Y. Miura (Japan Atomic Energy Research Inst., Naka.), S. Tsuji (Japan Atomic Energy Research Inst., Naka.), K. Hoshino (Japan Atomic Energy Research Inst., Naka.), M. Mori (Japan Atomic Energy Research Inst., Naka.), N. Suzuki (Japan Atomic Energy Research Inst., Naka.), and T. Yamauchi (Japan Atomic Energy Research Inst., Naka.) et al Dec. 1991 37 p
(DE92-799107; NIFS-124) Avail: CASI HC A03/MF A01

Parameter dependence of the radial structure of the edge poloidal rotation is studied with spectroscopic measurements for L- and H-mode plasmas in the JFT-2M tokamak. The peak of poloidal flow in the electron diamagnetic direction suddenly appears near the plasma edge in H-mode. No critical normalized ion collisionality for the transition of L- to H-mode is observed. The size of the poloidal flow in H-mode has no dependence on poloidal gyro-radius. Author

N92-30993# National Inst. for Fusion Science, Nagoya (Japan).
KINETIC APPROACH TO LONG WAVE LENGTH MODES IN ROTATING PLASMAS
T. Yamagishi (Fukui Inst. of Tech., Japan) Mar. 1992 31 p Submitted for publication
(NIFS-138) Avail: CASI HC A03/MF A01

Stability of low frequency long wave length modes is studied by a kinetic approach in rotating Maxwellian plasmas. In the rigid rotator model, the centrifugal force due to the plasma rotation strongly destabilizes the ballooning modes particularly when the Mach number is close to unity. The fluid flow shear weakly stabilizes the ballooning mode. Energetic particles are effective to stabilize the ballooning mode particularly in the high-Beta region even in the rotating plasmas. The electric potential induced from the radial electric field increases the particle trapping rate for e(Phi) greater than 0. For Phi less than 0 as in tokamaks, electron trapping rate increases, which destabilizes the dissipative trapped electron mode. Author

N92-30994# National Inst. for Fusion Science, Nagoya (Japan).
THREE-DIMENSIONAL MHD EQUILIBRIUM IN THE PRESENCE OF BOOTSTRAP CURRENT FOR LARGE HELICAL DEVICE (LHD)
K. Watanabe (Kyoto Univ., Japan), N. Nakajima, M. Okamoto, Y. Nakamura, and M. Wakatani (Kyoto Univ., Japan) Mar. 1992 44 p Submitted for publication
(NIFS-139) Avail: CASI HC A03/MF A01

Three-dimensional MHD equilibria including the bootstrap current self-consistently are studied for the Large Helical Device (LHD). Magnitude of the bootstrap current is sensitive to the magnetic axis position or Shafranov shift in LHD, which is proportional to the plasma pressure and inversely proportional to the rotational transform. Since the bootstrap current enhances the rotational transform and reduces Shafranov shift, the self-consistent MHD equilibrium is crucial to estimate the bootstrap

current. Total bootstrap current easily exceeds 100 kA for LHD plasmas with (beta) approx. greater than 1 percent under the assumption that both electrons and ions belong to the rare-collisional 1/upsilon regime in the whole plasma region, where (Beta) is a volume averaged beta value. Effects of the vertical field, the quadrupole field and the pressure profile on the bootstrap current are also investigated. Author

N92-30995# National Inst. for Fusion Science, Nagoya (Japan).
NEW METHOD OF ERROR ELIMINATION IN POTENTIAL PROFILE MEASUREMENT OF TOKAMAK PLASMAS BY HIGH VOLTAGE HEAVY ION BEAM PROBES
Y. Hamada, K. Masai, Y. Kawasumi, H. Iguchi, and A. Fujisawa Apr. 1992 33 p Submitted for publication
(NIFS-143) Avail: CASI HC A03/MF A01

The measurement of a potential profile in tokamak plasmas by heavy ion beam probe (HIBP) in a single shot is usually difficult, because as primary beam is swept through plasma cross-section, the secondary beam hits the input slit of an energy analyzer with a large variation in entrance angles (in-plane and out-of-plane). In this paper, a new method (the application of fast toroidal sweeps of the primary or the secondary beam at the analyzer or at an entrance to a tokamak) is proposed to eliminate the error due to the change in the entrance angle. In addition, results of a new calibration method of HIBP in tokamaks (electron stripping by neutral gas) are presented. Author

N92-31002# Wisconsin Univ., Madison. Center for Plasma Theory and Computation.
PRESSURE PROFILES, RESONANT PFIRSCH-SCHLUETER CURRENTS, THERMAL INSTABILITIES, AND MAGNETIC ISLAND FORMATION
C. C. Hegna and J. D. Callen Jun. 1992 23 p
(Contract DE-FG02-86ER-53218)
(DE92-015166; UW-CPTC-92-2) Avail: CASI HC A03/MF A01

A prescription for constructing the plasma pressure profile in the vicinity of an equilibrium magnetic island is derived by solving a sourced pressure diffusion equation near the island region. For pressure sources and sinks that are relatively constant in space, it is found that the plasma pressure profile is insensitive to pressure sources; thus, the pressure profile can be constructed by assuming that the net pressure flux across any topologically toroidal magnetic surface is constant. This construction of the pressure profile is also valid for magnetic islands that are slowly evolving in time. By coupling the pressure evolution equation with the magnetostatic equilibrium equations, the theory is applied to the case of self-consistent construction of pressure-gradient-driven magnetic islands. In particular, we address the question of resonant Pfirsch-Schlueter current induced magnetic islands and the role of thermal effects on nonlinear magnetic islands. DOE

N92-31114# Oak Ridge National Lab., TN.
CRITERIA AND DESIGN TRADE-OFF ISSUES FOR ITER
D. E. Post (Princeton Univ., NJ.) and N. A. Uckan 1992 8 p Presented at the Topical Meeting on the Technology of Fusion Energy, Boston, MA, 7-12 Jul. 1992
(Contracts DE-AC05-84OR-21400; DE-AC02-76CH-03073)
(DE92-011786; CONF-920772-1) Avail: CASI HC A02/MF A01

While the determination of the optimum parameters for a tokamak involves the complex trade-off of a large number of engineering and physics constraints, the overall dimensions are actually determined by a relatively simple set of criteria. These criteria are based on the tokamak radial build and elementary physics and engineering requirements, including guidelines for nT(tau)(sub E), the aspect ratio, the edge safety factor, the plasma elongation, the size of the neutron shield, and the peak field at the toroidal field coil. Two of these parameters, the aspect ratio and plasma elongation, can be chosen so as to optimize the design parameters and minimize the size and cost of the tokamak. The ITER design point of R approximately = 6 m and a approximately = 2 m follows from these constraints and the parameter choices for aspect ratio and elongation. DOE

N92-31116# Lodestar Research Corp., Boulder, CO.
FUNDAMENTAL STUDIES OF FUSION PLASMAS
R. E. Aamodt, P. J. Catto, D. A. Dippolito, J. R. Myra, and D. A. Russell 26 May 1992 34 p
(Contract DE-FG02-88ER-53263)
(DE92-015077; DOE/ER-53263/22; LRC-92-32) Avail: CASI HC A03/MF A01

The major portion of this program is devoted to critical ICH phenomena. The topics include edge physics, fast wave propagation, ICH induced high frequency instabilities, and a preliminary antenna design for Ignitor. This research was strongly coordinated with the world's experimental and design teams at JET, Culham, ORNL, and Ignitor. The results have been widely publicized at both general scientific meetings and topical workshops including the specialty workshop on ICRF design and physics sponsored by Lodestar in April 1992. The combination of theory, empirical modeling, and engineering design in this program makes this research particularly important for the design of future devices and for the understanding and performance projections of present tokamak devices. Additionally, the development of a diagnostic of runaway electrons on TEXT has proven particularly useful for the fundamental understanding of energetic electron confinement. This work has led to a better quantitative basis for quasilinear theory and the role of magnetic vs. electrostatic field fluctuations on electron transport. An APS invited talk was given on this subject and collaboration with PPPL personnel was also initiated. Ongoing research on these topics will continue for the remainder of the contract period and the strong collaborations are expected to continue, enhancing both the relevance of the work and its immediate impact on areas needing critical understanding. DOE

N92-31118# Lawrence Livermore National Lab., CA.
SPECTROSCOPIC DIAGNOSIS OF LONG-SCALE-LENGTH EXPLODING-FOIL PLASMA IN THE PRESENCE OF AN INTENSE RADIATION FIELD
T. D. Shepard, C. J. Keane, L. J. Suter, and J. Abdallah (Los Alamos National Lab., NM.) Mar. 1992 15 p Presented at the 9th Topical Conference on High-Temperature Plasma Diagnostics, Santa Fe, NM, 15-19 Mar. 1992
(Contract W-7405-eng-48)
(DE92-014718; UCRL-JC-109355; CONF-920362-33) Avail: CASI HC A03/MF A01

An effective technique for measuring the local electron temperature and density of a laser-produced plasma involves analysis of the emission and/or absorption spectrum from an impurity dopant. Spatial resolution can be obtained by depositing the impurity in the form of a small microdot on or slightly below the surface of the foil, so that it remains spatially confined while the plasma evolves. However, when an intense high-energy radiation field is present, the ionization balance, level population, and resulting spectrum produced by the impurity may be significantly perturbed. We are currently using several computer models to study the effects of such a radiation field for experimental conditions that could be obtained using the Nova laser facility, and are concentrating on the behavior of line intensity ratios that are typically used for density and temperature diagnosis. The goal of the work presented in this paper is to design an experiment that can be conducted on Nova to determine the feasibility of spectroscopic diagnosis when an intense high-energy radiation field is present. DOE

N92-31197# Oak Ridge National Lab., TN.
RESULTS OF THE HEAVY ION BEAM PROBE MEASUREMENTS ON THE ADVANCED TOROIDAL FACILITY
S. C. Aceto (Rensselaer Polytechnic Inst., Troy, NY.), J. G. Schwelberger (Rensselaer Polytechnic Inst., Troy, NY.), K. A. Connor (Rensselaer Polytechnic Inst., Troy, NY.), J. J. Zielinski (Rensselaer Polytechnic Inst., Troy, NY.), J. C. Glowienka, R. C. Isler, M. Murakami, J. D. Bell, and T. Uckan 1992 5 p Presented at the 14th International Conference on Plasma and 19th EPS Conference on Controlled Fusion and Plasma Physics, Innsbruck (Austria), 29 Jun. - 3 Jul. 1992

(Contract DE-AC05-84OR-21400)
(DE92-014461; CONF-920610-1) Avail: CASI HC A01/MF A01

A heavy ion beam probe (HIBP) has been used to measure radial potential and density profiles in the Advanced Toroidal Facility (ATF). It has also been used to measure density and potential fluctuations at multipole radial locations. These measurements have been primarily made during ECH discharges, although some data have been obtained during neutral-beam-heated discharges.
DOE

76 SOLID-STATE PHYSICS

Includes superconductivity.

For related information, see also *33 Electronics and Electrical Engineering* and *36 Lasers and Masers.*

N92-30247# Midwest Research Inst., Golden, CO.
RESEARCH ON POLYCRYSTALLINE THIN FILM SUBMODULES BASED ON CuInSe2 MATERIALS
A. Catalano, R. Arya, L. Carr, B. Fieselmann, T. Lommasson, R. Podlesny, L. Russell, S. Skibo, A. Rothwarf, and R. Birkmire May 1992 73 p Prepared in cooperation with Solarex Corp., Newtown, PA
(Contract DE-AC02-83CH-10093)
(DE92-010584; NREL/TP-413-4906) Avail: CASI HC A04/MF A01

This report describes progress during the first year of a three-year research program to develop 12 percent-efficient CuInSe2 (CIS) submodules with area greater than 900 sq cm. To meet this objective, the program was divided into five tasks: (1) windows, contacts, substrates; (2) absorber material; (3) device structure; (4) submodule design and encapsulation; and (5) process optimization. In the first year of the program, work was concentrated on the first three tasks with an objective to demonstrate a 9 percent-efficient CIS solar cell. DOE

N92-30252# Stanford Univ., CA. Physics Lab.
TUNNELING ACOUSTIC MICROSCOPY Technical Report, 1 Apr. 1991 - 31 Mar. 1992
C. F. Quate and B. T. Khuri-Yakub May 1992 7 p
(Contract N00014-90-J-1635)
(AD-A251028; SU-GL-4959) Avail: CASI HC A02/MF A01

We have microfabricated an integrated 1 GHz ultrasonic transducer and sharp silicon tip for use as a scanning near-field acoustic microscope probe. The silicon tip, which has a 500 A radius of curvature, is microfabricated using a batch fabrication process compatible with integrated circuit manufacturing techniques. The ZnO ultrasonic transducer is integrally fabricated at the base of the tip to allow sound waves to be transmitted longitudinally down the tip. The microscope is configured such that the tip is brought into close proximity of a sample which has a receiving acoustic transducer. Two-dimensional imaging is accomplished by raster scanning the tip over the sample while feeding back on the total transmitted acoustic power to keep the tip/sample separation constant. GRA

N92-30405# Academy of Sciences of the Ukrainian SSR, Kiev. Inst. Teoreticheskoj Fiziki.
ON THE TEMPERATURE ROLE IN THE TUNNELING PROCESS AT THE COLD FUSION
B. E. Grinyuk and I. V. Simenog 1991 12 p
(DE92-627497; ITP-91-25) Avail: CASI HC A03/MF A01

The temperature dependence of the hydrogen isotopes cold fusion tunneling rate is estimated using a model of screened Coulomb interaction potential between the isotopes. The temperature dependences for the logarithm of the tunneling rate are calculated for pp-, pd-, pt-, and dd-processes at different screening radii. The probable role of pp-reactions is discussed.
DOE

N92-30406# Rutgers - The State Univ., Piscataway, NJ. Dept. of Mechanics and Materials Science.
FERROELECTRIC AND PIEZOELECTRIC PROPERTIES OF ODD-NUMBERED NYLONS Technical Report, 1 Jun. 1991 - 31 May 1992
J. I. Scheinbeim, B. A. Newman, B. Zhang-Mei, and J. W. Lee Jun. 1992 15 p
(Contract N00014-80-C-0795)
(AD-A252270; TR-26) Avail: CASI HC A02/MF A01

Recent discoveries in our laboratory of a new class of ferroelectric polymers--the odd-numbered nylons--led to another important discovery: a mechanism for the stabilization of the remanent polarization in these materials to their crystalline melting point. As the piezoelectric response of ferroelectric polymers is as stable as their remanent polarization, we have produced a set of high temperature stable piezoelectric polymers which can easily operate in a temperature range up to approximately 250 C. In addition, we have now begun to examine new types of piezoelectric polymer films consisting of co-electroprocessed layers of odd-numbered nylon film and poly(vinylidene fluoride) PVF film, which are shown to exhibit a significantly enhanced response, compared to that of either component. Enhanced response is also observed for blended powders of PVF 2 and a copolymer of vinylidene fluoride and tri-fluoroethylene. GRA

N92-30505# Technische Univ., Berlin (Germany, F.R.). Fachbereich Elektrotechnik.
EXAMINATIONS OF THE MICROWAVE PHOTOELECTRIC CONDUCTIVITY OF a-Si:H MULTILAYER SYSTEMS FOR IN SITU CHARACTERIZATION Ph.D. Thesis [UNTERSUCHUNGEN DER MIKROWELLENPHOTOLEITFAEHIGKEIT VON A-SI:H-MEHRSCHICHTSYSTEMEN ZUR IN-SITU CHARAKTERISIERUNG]
Heinz-Christoph Neitzert 1991 144 p In GERMAN
(ETN-92-91688) Avail: CASI HC A07/MF A02

A contactless estimation of electronic transport properties of semiconductors is achieved to depict the boundary surfaces between differently doped silicon layers or between crystalline and amorphous hydrogen silicon (a-Si:H). A plasma enhanced chemical vapor deposition was chosen as a manufacturing process. The kinetics of excess charge carriers in semiconductor layers was tracked. The influence of p-doping on the TRMC (Transient Microwave Photoelectric Conductivity) transients was examined by varying the diborane concentration in the process gas. The hydrogen distribution in a-Si:H layers was obtained through a nuclear reaction analysis and its dependence on the n-doping by introduction of phosphine was characterized by infrared transmission spectrum. The TRMC amplitude of the excitation intensity is shown to be independent of temperature and a good correlation was found between TRMC signals and defect density measurements at room temperature. ESA

N92-30527# Utah Univ., Salt Lake City. Dept. of Materials Science and Engineering.
DECOMPOSITION STUDIES OF TERTIARYBUTYLDIMETHYLANTIMONY
D. S. Cao, C. H. Chen, C. W. Hill, S. H. Li, and G. B. Stringfellow 22 May 1992 23 p
(Contract N00014-91-J-1447)
(AD-A250670; TR-21) Avail: CASI HC A03/MF A01

The vapor pressure, decomposition temperature, decomposition products, and decomposition reaction order are reported for a novel organometallic vapor-phase epitaxy (OMVPE) Sb precursor, tertiarybutyldimethylantimony (TBDMSb, C4H9(CH3)2Sb). The TBDMSb vapor pressure is 7.3 torr at 23 C. The 50 percent decomposition temperature is 300 C for both He and D2 ambients in a flow tube reactor with a residence time of approximately 3.2 seconds at 300 C. The decomposition products are primarily C4H10, C4H8, and TMSb in both ambients. The overall decomposition reaction is first order. The decomposition mechanism is believed to be homolysis followed by recombination and disproportionation reactions for C4H9 and (CH3)2Sb groups. Added trimethylgallium (TMGa) has no measurable effect on either

the pyrolysis rate or the products. Apparently, TMGa and TBDMSb do not interact during pyrolysis, nor do they form a room temperature adduct. No room temperature adduct between TMGA and TBDMSb was formed. It is believed that TBDMSB is a promising Sb precursor for low temperature OMVPE growth. GRA

N92-30574# Oak Ridge National Lab., TN.
IN SITU TEM STUDIES OF THE EFFECT OF MISFIT STRAIN ON THE KINETICS OF Si(SUB 1-x)Ge(SUB x) SOLID PHASE EPITAXY: TEMPERATURE CALIBRATION AND SURFACE EFFECTS
David C. Paine (Brown Univ., Providence, RI.), David J. Howard (Brown Univ., Providence, RI.), and N. Evans 1992 3 p Presented at the Annual Meeting of the Electron Microscopy Society of America, Boston, MA, 16-21 Aug. 1992
(Contracts DE-AC05-84OR-21400; DE-AC05-76OR-00033)
(DE92-011689; CONF-920819-15-Extd-Abst) Avail: CASI HC A01/MF A01

While in situ TEM studies have proven useful for the direct observation of solid-state reaction mechanisms, such studies rarely provide quantitative kinetic data. This limitation is due to problems associated with the accurate measurement of local sample temperature, assessment of beam heating and damage, and minimization of thin-film effects. Sinclair et al have proposed a technique for establishing the temperature of a sample during in situ TEM annealing experiments in which the well-characterized Si (001) solid phase epitaxy amorphous-crystalline transformation rate is used to estimate the temperature in an adjacent (but not contiguous) region of the specimen. We have used this in situ technique to determine the activation energy for strained solid phase epitaxy of Si(sub 1-x)Ge(sub x)(x = 5.4, 11.6, and 17 percent.) DOE

N92-30577# Oak Ridge National Lab., TN.
ION CHANNELING AND SPECTROSCOPIC ELLIPSOMETRY EXAMINATIONS OF THIN-FILM SiO2/EPI-Si STRUCTURES
A. T. Fiory (Bell Telephone Labs., Inc., Murray Hill, NJ.), P. K. Roy (Bell Telephone Labs., Inc., Allentown, PA.), and G. E. Jellison, Jr. Apr. 1992 6 p Presented at the Material Research Society Spring Meeting, San Francisco, CA, 27 Apr. - 2 May 1992
(Contract DE-AC05-84OR-21400)
(DE92-015129; CONF-920402-24) Avail: CASI HC A02/MF A01

Rutherford backscattering ion-channeling spectrometry (RBS) and 2- channel spectroscopic polarization modulation ellipsometry (2-C SPME) were combined in a study of 3- to 16-nm SiO2 films to discern possible differences between conventional MOS oxides, modified surface preparation, and stack-oxide processes which combine chemical vapor deposition with furnace oxidation. An excess silicon scattering is observed by RBS, which suggests atomic displacements associated with interfacial roughness and strain in the crystalline Si. Ellipsometry observes an increase in refractive index with decreasing film thickness, which is consistent with interfacial roughness or Si strain. The various preparation methods for device-quality MOS oxides yielded essentially equivalent results and film densities close to bulk fused SiO2. DOE

N92-30585# Sandia National Labs., Albuquerque, NM.
NEW INSIGHTS INTO RADIATION-INDUCED OXIDE-TRAP CHARGE THROUGH THERMALLY-STIMULATED-CURRENT (TSC) MEASUREMENT AND ANALYSIS
D. M. Fleetwood, S. L. Miller, R. A. Reber, Jr., P. J. McWhorter, and P. S. Winokur 1992 5 p Presented at the Nuclear and Space Radiation Effects Conference, New Orleans, LA, 13-17 Jul. 1992
(Contract DE-AC04-76DP-00789)
(DE92-009054; SAND-92-0344C; CONF-920716-4) Avail: CASI HC A01/MF A01

In this summary, we re-evaluate estimates of trapped-hole energies inferred from TSC measurements and transistor annealing studies. Improved estimates of the trapped-hole 'attempt-to-escape' frequency (upsilon sub A) and a quantitative treatment of (Schottky) electric-field induced barrier lowering strongly suggest that previous estimates of trapped-hole energies in TSC and transistor annealing studies are too low. Moreover, we show that TSC measurements can be modeled analytically from first principles, and the resulting model can accurately predict TSC measurements under arbitrary heating conditions. Finally, we evaluate the dependence of electron trapping in irradiated SiO2 on dose and on electric field during irradiation. DOE

N92-30595# Rutgers - The State Univ., Piscataway, NJ. Dept. of Mechanics and Materials Science.
FERROELECTRIC POLARIZATION MECHANISMS IN NYLON 11 Technical Report, 1 Jun. 1991 - 31 May 1992
B. A. Newman, J. I. Scheinbeim, and J. W. Lee Jun. 1992 29 p
(Contract N00014-80-C-0795)
(AD-A252269; TR-25) Avail: CASI HC A03/MF A01

The combined results of piezoelectric coefficient (d31, e31) measurements, FTIR spectroscopy, and x-ray diffraction studies of three dimensionally oriented Nylon 11 films reveal that the polarization occurs in the crystalline regions. In addition, the orientation of dipoles in a poled Nylon 11 film is not altered by a high temperature annealing treatment (185 C). This unique, high temperature stability of dipole orientation in the crystalline regions provides a method to investigate the polarization mechanism for poled Nylon 11 films. Our results indicate that the difference in observed x-ray diffraction patterns from unpoled and poled films results from an initial 90 deg field induced dipole reorientation mechanism. Further dipole orientation appears to result from a 180 C switching mechanism. GRA

N92-30634# Notre Dame Univ., IN. Dept. of Physics.
STUDIES OF ORDERING IN SEMICONDUCTING AND OTHER ALLOYS Final Report
Kathie E. Newman 1991 7 p
(Contract N00014-89-J-1198)
(AD-A249483) Avail: CASI HC A02/MF A01

New ordered compounds derived from semiconductor and metallic alloys for special values of the composition x were studied. The types of ordered compounds were cataloged. A goal was to determine the stability of the new ordered states for both low and high temperatures. The properties of both the new stable and metastable compounds (e.g., band gaps) were determined. Finally, the validity of a micro-structure model of metastable alloys was tested. We have determined the structural properties of a number of new ordered compounds using a valence-force-field (VFF) model of strain. Specifically, we have determined such quantities as strain energies, bond lengths, and dimensions of unit cells. GRA

N92-30684# Oak Ridge National Lab., TN.
LIFETIMES OF LOW SPIN STATES IN THE SUPERDEFORMED BAND OF Hg-192
I. Y. Lee, C. Baktash, D. M. Cullen, J. D. Garrett, N. R. Johnson, F. K. McGowan, D. F. Winchell, and C. H. Yu (Tennessee Univ., Knoxville.) 1992 1 p Presented at the International Conference on Nuclear Structure at High Angular Momentum, Ottawa, Ontario, 18-21 May 1992
(Contract DE-AC05-84OR-21400)
(DE92-011066; CONF-9205108-3) Avail: CASI HC A01/MF A01

The gamma cascades of superdeformed (SD) Hg nuclei depopulate suddenly into normal deformed (ND) states at I approximately equal to 10. So far the linking transitions have not been observed and the depopulation mechanism is not fully understood. This process involves such properties as the barrier penetration probability, level densities, and gamma transition strengths of SD and ND states. One important factor is the competition between the collective E2 decay along the SD band and the statistical decay to the NC states which can be determined if the lifetime and the intensity of the gamma rays are known. DOE

N92-30748# Midwest Research Inst., Golden, CO.
RESEARCH ON DEFECTS AND TRANSPORT IN AMORPHOUS SILICON-BASED SEMICONDUCTORS
E. A. Schiff (Syracuse Univ., NY.), H. Antoniadis (Syracuse Univ., NY.), J. K. Lee (Syracuse Univ., NY.), and Q. Wang (Syracuse Univ., NY.) Apr. 1992 16 p
(Contract DE-AC02-83CH-10093)
(DE92-001223; NREL/TP-451-4751) Avail: CASI HC A03/MF A01

This report describes the results from research on two topics: (1) the effects of light-soaking on the electron drift mobility in a-Si:H, and (2) modulated electron spin resonance measurements and their relationship to the electronic correlation energy of the D center in a-Si:H. Both of these projects were undertaken to better determine where the 'standard' model for a-Si:H breaks down. The standard model is reasonably successful in accounting for the most elementary 'deep trapping' aspects of electron and hole transport in a-Si:H, and it accounts adequately for the sub-band-gap optical properties. However, it is much less clear whether it provides a sufficient basis for understanding several effects which are crucial in operating solar cells: electron and hole mobilities and recombination in the presence of light-bias and space-charge. In the standard model, one would not expect significant effects on drift mobilities due to light-soaking, which would be envisioned as simply increasing the D-center density. Similarly, in the standard model one would not anticipate a significant temperature dependence to electron spin resonance, because essentially all spins are already detected. Discussions in the available literature on the evidence regarding both effects were inconclusive. The work reported here sets considerably more stringent constraints on the magnitude of the two effects. DOE

N92-30772# Michigan Univ., Ann Arbor.
STUDIES OF PHONONS AND ELECTRONIC EXCITATIONS IN SEMICONDUCTOR HETEROSTRUCTURES Final Report, 1 Feb. 1990 - 31 Jan. 1992
R. Merlin 31 Mar. 1992 15 p
(Contract DAAL03-89-K-0047)
(AD-A249406; ARO-26195.14-PH) Avail: CASI HC A03/MF A01

This report deals with the following areas: (1) screening non-linearities and coupled intersubband-cyclotron modes in quantum-well structures; (2) the pressure dependence of two-magnon scattering in antiferromagnetic insulators; and (3) sequential resonant tunneling in superlattices. The studies are primarily experimental and focus on the technique of Raman scattering. GRA

N92-30781 Tel-Aviv Univ. (Israel). Dept. of Physics and Astronomy.
ANOMALOUS HOPPING CONDUCTIVITY IN AMORPHOUS INDIUM-OXIDE FILMS M.S. Thesis
Haim Shmuelli Jun. 1990 75 p
(ITN-92-85166) Copyright Avail: Tel-Aviv Univ., Exact Sciences Library, Ramat Aviv, 69978, Israel

Metals in which a high amount of disorder is introduced - through impurities, defects, etc. - change their electronic properties dramatically, owing to the transition of electronic states from extended to localized. The aim of this work was to measure the electronic properties and to explore the influence of weak magnetic fields on the VRH conductivity in thin films at very low temperatures. Thin films of 460 A amorphous In(x)O(y) were fabricated and measured. From resistance vs. temperature data, a crossover from the Efros-Shklovskii or the 'Coulomb-gap' regime to a new regime was found at about 3 K. This was supported by magnetoresistance (MR) studies in the same range of temperatures. The MR data are strongly negative and linear in magnetic fields (up to 4.5 tesla). This is in qualitative agreement with some theoretical predictions. Yet no theory can explain the R vs. T data, having a temperature dependence of R proportional to exp((T(sub 0)/T) to the power 0.7). Author (ISA)

N92-30846# North Carolina State Univ., Raleigh.
ATOMIC LAYER EPITAXY GROUP 4 MATERIALS: SURFACE PROCESSES, THIN FILMS, DEVICES, AND THEIR CHARACTERIZATION Semiannual Report, 1 Jan. - 30 Jun. 1992
Robert F. Davis, Salah Bedair, Nadia El-Masry, and Jeffrey T. Glass Jan. 1992 35 p
(Contract N00014-91-J-1416)
(AD-A252352) Avail: CASI HC A03/MF A01

Research concerned with the atomic layer epitaxy (ALE) of silicon carbide (SiC), diamond (C) and cerium dioxide (CeO2) has been conducted within this reporting period. Equipment for the deposition of each of these materials, as well as experimental procedures for the conduct of the studies are in various stages of design, development, and employment. Layer-by-layer deposition of Si and C from the precursors of Si2H6 and C2H4, respectively, and the resulting deposition of monocrystalline beta-SiC (100) has been achieved on Si(100) substrates. Rotation of the heated (820-980 C) sample under the individual source gases and a heated W filament located between these gases allowed a monolayer/cycle deposition to be achieved. Surface science related equipment and associated ultra-high vacuum systems are now being assembled to investigate and determine the chemical routes to achieve ALE of SiC by self-terminating chemical adsorption. Hexamethyldisilane species have been introduced into a hot filament CVD system in an attempt to nucleate diamond on an atomic scale on silicon substrate surfaces. The organosilicic layer formed was characterized by x-ray diffraction, Auger and x-ray photoelectron spectroscopies. The subsequent diamond nucleation and growth under various conditions was investigated. It is found that the nucleation density is very high under reverse dc biasing conditions. The structure of these particles is diamond-like in nature as revealed by Raman spectroscopy and scanning electron microscopy. GRA

N92-30854# Lawrence Livermore National Lab., CA.
TRANSIENT PHOTOCONDUCTIVITY OF LOW TEMPERATURE GaAs GROWN BY MOLECULAR BEAM EPITAXY TERAHERTZ RADAR APPLICATIONS
J. D. Morse, R. P. Mariella, Jr., and C. F. McConaghy 1991 7 p Presented at the DARPA/Rome Laboratory Symposium on Photonics Systems for Antenna Applications, Monterey, CA, 10-12 Dec. 1991
(Contract W-7405-eng-48)
(DE92-011848; UCRL-JC-108738; CONF-911267-3) Avail: CASI HC A02/MF A01

Optoelectronic sampling techniques have been utilized to characterize transient photoconductivity in low temperature (LT) GaAs grown by molecular beam epitaxy (MBE). Metal-semiconductor-metal (MSM) photoconductive devices have been fabricated on LT-GaAs layers grown at a calibrated substrate temperature of 190 C. Results from on-chip photoconductive sampling measurements demonstrate the ability to generate, propagate, and detect photocurrent pulses of approximately 4 ps duration, which is limited by the optoelectronic measurement system. A carrier mobility of 120 cm(exp 2)/V-s has been estimated from these results, which is a factor of 5-10 times larger than alternative materials used for picosecond photoconductivity. This translates to improved sensitivity for emission and detection of terahertz pulses of electromagnetic (EM) radiation. DOE

N92-30885# Lawrence Livermore National Lab., CA.
STRUCTURAL AND MAGNETIC PROPERTIES OF RBa2Cu2NbO8 (R = La, Pr, AND Nd)
H. B. Radousky, J. C. OBrien, M. Bennahmias, P. Klavins (California Univ., Davis.), and C. A. Smith (California Univ., Davis.) Apr. 1992 6 p Presented at the Material Research Society Spring Meeting, San Francisco, CA, 27 Apr. - 2 May 1992
(Contract W-7405-eng-48)
(DE92-014780; UCRL-JC-109064; CONF-920402-14) Avail: CASI HC A02/MF A01

PrBa2Cu2NbO8 (PrBCNO) is an insulating analog to the YBa2Cu3O7 (YUBCO) system, which is interesting as a thin film

buffer layer in YBCO/PrBCNO/YBCO tunnel junctions as well as a potential high (Tc) superconductor if proper doping could be achieved. PrBCNO has a similar structure to PrBCO, with NbO2 planes replacing the CuO chains. Single phase polycrystalline samples of RBCNO have been synthesized with R = La, Pr, and Nd. Attempts to synthesize this structure with the smaller ions Y and Gd have been unsuccessful. The PrBCNO samples show a signature in the magnetization of a magnetic ordering at 12 K. No such magnetic phase transition is observed down to 2 K in the NdBCNO material. DOE

N92-30895# Harry Diamond Labs., Adelphi, MD.
DOUBLE-SIDED WAFER ALIGNMENT TECHNIQUES Final Report, 17 Oct. 1990 - 1 Feb. 1991
Timothy J. Mermagen and Bruce R. Geil Apr. 1992 14 p
(AD-A250757; HDL-TM-92-5) Avail: CASI HC A03/MF A01

A project was undertaken by the Harry Diamond Laboratories to develop a double-sided wafer alignment technique by which special-purpose devices could be fabricated using in-house equipment. The approach developed was inexpensive and did not require infrared alignment methods for viewing through the wafer. A double-sided alignment technique with two different accuracies was developed for use on an ordinary optical mask aligner. These methods were highly successful and are in active use today. GRA

N92-30999# Argonne National Lab., IL.
YBa2Cu(3-x)Co(x)O(y): A SUBSTRATE MATERIAL FOR YBCO SUPERCONDUCTORS
J. D. Vienna, U. Balachandran, R. B. Poeppel, W. Cermignani, and J. A. Taylor Apr. 1992 7 p Presented at the Material Research Society Spring Meeting, San Francisco, CA, 27 Apr. - 2 May 1992
(Contract W-31-109-eng-38)
(DE92-015182; ANL/CP-74758; CONF-920402-28) Avail: CASI HC A02/MF A01

The physical properties of the ceramic YBa(sub 2)Cu(sub (3-x))Co(sub x)O(sub y) have been investigated in order to evaluate its usefulness as a substrate material for YBCO superconductors. YBa(sub 2)Cu(sub (3-x))Co(sub x)O(sub y) has been found to be thermally and chemically compatible with 123 and displays adequate electrical properties for a substrate material. A material with the nominal composition of YBa(sub 2)Cu(sub 2.2)Co(sub 0.8)O(sub 7) was investigated, extensively. The mechanical properties of this material were found to be poor, e.g., tensile strength was only 60 MPa. A semiconductor-like behavior was observed with a room-temperature resistivity of 70 m(Omega).cm and a resistivity equal to 4 (times) 10(exp 6) m(Omega).cm at 77 K. DOE

N92-31000# Sandia National Labs., Albuquerque, NM.
PULSED MICROWAVE PROCESSING OF HIGH-T(SUB c) SUPERCONDUCTING FILMS
R. B. James (Sandia National Labs., Livermore, CA.), K. F. McCarty (Sandia National Labs., Livermore, CA.), T. A. Friedmann (Sandia National Labs., Livermore, CA.), R. H. Stulen (Sandia National Labs., Livermore, CA.), D. S. Ginley (Sandia National Labs., Livermore, CA.), R. A. Alvarez (Lawrence Livermore National Lab., CA.), A. K. Stamper, X. J. Bao, and T. E. Schlesinger 1992 7 p Presented at the Material Research Society Spring Meeting, San Francisco, CA, 27 Apr. - 2 May 1992
(Contract DE-AC04-76DP-00789)
(DE92-014950; SAND-92-1183C; CONF-920402-22) Avail: CASI HC A02/MF A01

We have used 2.0-microsec microwave pulses at a frequency of 2.856 GHz to rapidly heat thin amorphous yttrium-barium-copper-oxide (YBCO) films deposited onto silicon substrates. The samples were irradiated inside a WR-284 waveguide by single-pass TE(sub 10) pulses in a traveling wave geometry. X-ray diffractometry studies show that an amorphous-to-crystalline phase transition occurs for incident pulse powers exceeding about 6 MW, in which case the amorphous YBCO layer is converted to Y2BaCuO5. Microscopy of the irradiated film reveals that the phase transition is brought about by melting of the YBCO precursor film and crystallization of the molten layer upon solidification. Time-resolved in situ experiments of the microwave reflectivity (R) and transmissivity (T) show that there is an abrupt change in R for microwave pulse powers exceeding the melt threshold, so that measurements of R and T can be used to monitor the onset of surface melting. DOE

N92-31190# Argonne National Lab., IL.
GRAIN BOUNDARY WEAK LINKS IN HIGH-Tc SUPERCONDUCTORS
D. Shi, S. Sengupta, K. C. Goretta, S. Salem-Sugua, Jr., M. Smith, and Y. N. Lwin Apr. 1992 6 p Presented at the Material Research Society Spring Meeting, San Francisco, CA, 27 Apr. - 2 May 1992
(Contract W-31-109-eng-38)
(DE92-016192; ANL/CP-76267; CONF-920402-32) Avail: CASI HC A02/MF A01

The transport critical current density (Jc) for high-(Tc) thin films, bicrystals, and bulk ceramics is shown to be determined by magnetic field penetration into the grain boundaries. The gross grain orientations may not in all cases be an important factor in determining this penetration. The parameter (lambda(sub G)/lambda(sub J)(exp 2)) can characterize the strength of the grain boundary coupling, which depends mainly on the crystal coherence and connectivity at the boundary area. DOE

N92-31191# International Centre for Theoretical Physics, Trieste (Italy).
ELASTIC CONSTANTS OF CRYSTALS NEAR MELTING VIA DENSITY FUNCTIONAL THEORY. EFFECT OF THREE-BODY CORRELATIONS
M. Ferconi Nov. 1991 12 p
(DE92-630567; IC-91/378) Avail: CASI HC A03/MF A01

Analytical expressions are presented for the elastic constants of a monatomic classical crystal at melting from the long wavelength limit of the renormalized phonon frequencies obtained via a density functional approach. Within this method a relationship is established between the elastic constants of the hot crystal and the two- and three-body direct correlation functions together with their first and second derivatives of its liquid near freezing. It is also shown that in the crystallized classical one-component plasma, the longitudinal vibrations have the correct long waves behavior. DOE

N92-31200# Los Alamos National Lab., NM.
FINE SCALE MESOSTRUCTURES IN SUPERCONDUCTING AND OTHER MATERIALS
J. A. Krumhansl 1992 15 p Presented at the Lattice Effects in High (Tc) Superconductors, Santa Fe, NM, 13-15 Jan. 1992
(Contract W-7405-eng-36)
(DE92-015207; LA-UR-92-1485; CONF-920141-7) Avail: CASI HC A03/MF A01

We review experimental and theoretical literature on mesoscale features and structures in a variety of displacively transforming materials. These include twinning in martensites and the much finer scale tweed; both may have significant effects on both normal and superconducting properties. Elastic properties are particularly strongly affected. Recent x-ray neutron experiments suggest them in hi-(Tc) materials. DOE

N92-31217# Los Alamos National Lab., NM.
ON THE STRAIN-RATE DEPENDENCE OF DYNAMIC RECRYSTALLIZATION IN COPPER POLYCRYSTALS
Shuh Rong Chen and U. F. Kocks 1992 7 p Presented at the Recrystallization 1992, San Sebastian, Spain, 31 Aug. - 4 Sep. 1992
(Contract W-7405-eng-36)
(DE92-011363; LA-UR-92-897; CONF-920857-1) Avail: CASI HC A02/MF A01

The observed strain-rate dependence of stress strain curves with and without dynamic recrystallization is analyzed. It is found to be incompatible with models of a strictly time-dependent, 'simultaneous static' recrystallization. The activation energy of

dynamic recrystallization is strongly stress dependent: similar, but not identical, to that of dynamic recovery. A new criterion for the transition from single-peak to double-peak behavior is proposed. DOE

N92-31220# Los Alamos National Lab., NM.
OXIDATION OF GALLIUM ARSENIDE Patent Application
Mark A. Hoffbauer, inventor (to DOE) and Jon B. Cross, inventor (to DOE) 16 Nov. 1991 19 p
(Contract W-7405-eng-36)
(DE92-016208; US-Patent-Appl-SN-614413) Avail: CASI HC A03/MF A01

An invention related to gallium arsenide semiconductors and, more particularly, to the oxidation of surface layers of gallium arsenide semiconductors for semiconductor device fabrication is presented. DOE

N92-30280*# North Carolina Agricultural and Technical State Univ., Greensboro. Dept. of Manufacturing Systems.
MECHANISM OF SLIP AND TWINNING
Mansur Rastani *In* NASA. Langley Research Center, National Educators' Workshop: Update 1991. Standard Experiments in Engineering Materials Science and Technology Jun. 1992 p 235-243 (For primary document see N92-30263 21-29)
Avail: CASI HC A02/MF A03

77 THERMODYNAMICS AND STATISTICAL PHYSICS

Includes quantum mechanics; theoretical physics; and Bose and Fermi statistics.

For related information see also *25 Inorganic and Physical Chemistry* and *34 Fluid Mechanics and Heat Transfer.*

N92-30235# Naval Postgraduate School, Monterey, CA.
MIXED AND FORCED CONVECTION FROM AN ARRAY OF DISCRETE HEAT SOURCES IN A VERTICAL CHANNEL. M.S. Thesis
James D. Syring Mar. 1992 87 p
(AD-A248853) Avail: CASI HC A05/MF A01

Mixed and forced convection liquid cooling of discrete heat sources in a vertical channel was investigated. Ten heat sources were flush mounted to one of the plexiglass channel walls, while the opposite wall was insulated. Measurements of heater surface temperatures were made for a channel Reynolds number range of 500-7300 and heat flux range of 510-2700 W/m(exp 2). Temperature patterns on the heated surface were visualized using liquid crystals. Effects of flow pulsations were also investigated in the 0-1.25 Hz range. GRA

N92-30242# Florida Agricultural and Mechanical Univ., Tallahassee. Dept. of Physics.
ANALYTICAL METHODS USING SLATER-TYPE ORBITALS IN QUANTUM CHEMISTRY Final Report, 1 Oct. 1988 - 30 Sep. 1991
H. W. Jones and C. A. Weatherford Mar. 1992 89 p
(Contract F49620-89-C-0007)
(AD-A251044) Avail: CASI HC A05/MF A01

Our main concern is with the development of a Slater-type orbital (STO) multicenter molecular integral package for use with standard ab initio quantum chemistry codes such as the Columbus code and Alchemy. Significant advances have been made toward this goal. A new strategy has been adopted: (1) program all molecular integrals in Mathematics (a computer algebra language that can give arbitrary precision with our alpha-function method); and (2) using assured accurate results as a guide, use FORTRAN to obtain speed and acceptable accuracy. We believe that this dual thrust will finally crack the 'intractable' problem of STO multicenter integrals. Applications will soon be made to real molecules. GRA

N92-30421# Messerschmitt-Boelkow-Blohm G.m.b.H., Munich (Germany, F.R.).
A PROCESSING ENVIRONMENT FOR TEST AND SIMULATION DATA OF THERMODYNAMIC SYSTEMS
R. Mueller (Erno Raumfahrttechnik G.m.b.H. Bremen, Germany, F.R.) and G. Kleinert-Alvarado (Erno Raumfahrttechnik G.m.b.H. Bremen, Germany, F.R.) 1991 8 p Presented at the 4th European Symposium on Space Environmental Control Systems, Florence, Italy, 21-25 Oct. 1991 Previously announced as N92-26963
(MBB-UO-0169-91-PUB; ETN-92-91897) Avail: CASI HC A02/MF A01

The characteristics of a data processing environment established to support the development of advanced, fast responding systems and components, are described. The environment consists of a data acquisition system, a mainframe data processing computer, data transfer networks and several programs. It is ideally suited for the development of fast heat exchangers and has been already used within the first development phases of the Hermes water evaporator assembly and ammonia boiler assembly. Emphasis is on the description of the data acquisition system, the interconnection of the elements and the data processing after testing. Requirements, boundary conditions and further activities are outlined. ESA

N92-30799# International Centre for Theoretical Physics, Trieste (Italy).
FROM A WORLD-SHEET SUPERSYMMETRY TO THE DIRAC EQUATION
N. Mankoc-Borstnik Oct. 1991 16 p
(DE92-622375; IC-91/369) Avail: CASI HC A03/MF A01

Starting from a classical action for a point particle with a local world-sheet supersymmetry, the Dirac equation follows with operators vector-alpha, vector-beta or vector-gamma being defined in the Grassmann space as differential operators and having all the properties of the corresponding Dirac matrices except that vector-alpha and vector-beta are anti-Hermitian rather than Hermitian. Such a particle interacts with an external field as expected. DOE

N92-30800# International Centre for Theoretical Physics, Trieste (Italy).
FROM A PARTICLE WITH A WORLD-LINE SUPERSYMMETRY TO THE DIRAC-LIKE EQUATION
N. Mankoc-Borstnik Oct. 1991 20 p
(DE92-622376; IC-91/370) Avail: CASI HC A03/MF A01

It is shown that the classical action for a particle with a local world-line supersymmetry lead after quantization to the Dirac-like equation which is defined by operators vector-alpha and circumflex-beta fulfilling the same anticommutation relations as the corresponding Dirac matrices, except that these operators are not Hermitian. They even (anti)commute with the Hermitian conjugate operators. It is shown also that the four current is the analog of the classical relativistic four current. DOE

N92-30825# California Univ., Berkeley. Lawrence Berkeley Lab.
EXAMPLE OF A QUANTUM FIELD THEORY BASED ON A NONLINEAR LIE ALGEBRA
K. Schoutens (State Univ. of New York, Stony Brook.), A. Sevrin, and P. vanNieuwenhuizen (European Organization for Nuclear Research, Geneva, Switzerland) Nov. 1991 42 p Presented at the Conference on Gauge Theories: Past and Future, Ann Arbor, MI, 16-18 May 1991
(Contract DE-AC03-76SF-00098)
(DE92-010475; LBL-31382; CONF-9105239-2; ITP-SB-91-34; UCB-PTH-91/52) Avail: CASI HC A03/MF A01

In this contribution to Tini Veltman's Festschrift we shall give a paedagogical account of our work on a new class of gauge theories called W gravities. They contain higher spin gauge fields, but the usual no-go theorems for interacting field theories with spins exceeding two do not apply since these theories are in two dimensions. It is, of course, well known that ghost-free interacting

massless spin 2 fields ('the metric') are gauge fields, and correspond to the geometrical notion of general coordinate transformations in general relativity, but it is yet unknown what extension of these ideas is introduced by the presence of massless higher spin gauge fields. A parallel with supergravity may be drawn: there the presence of massless spin 3/2 fields (gravitinos) corresponds to local fermi-bose symmetries of which these gravitinos are the gauge fields. Their geometrical meaning becomes only clear if one introduces superspace (with bosonic and fermionic coordinates): they correspond to local transformations of the fermionic coordinates. For W gravity one might speculate on a kind of W-superspace with extra bosonic coordinates. DOE

N92-31133# International Centre for Theoretical Physics, Trieste (Italy).
COEXISTENCE OF UNIQUELY ERGODIC SUBSYSTEMS OF INTERVAL MAPPING
Xiangdong Ye Oct. 1991 17 p
(DE92-630231; IC-91/340) Avail: CASI HC A03/MF A01

It is shown that uniquely ergodic subsystems of interval mapping also coexist in the same way as minimal sets do. To do this we give some notations in section 2. In section 3, we define D-function of a uniquely ergodic system and show its basic properties. We prove the coexistence of uniquely ergodic subsystems of interval mapping in section 4. Lastly we give the examples of uniquely ergodic systems with given D-functions in section 5. DOE

N92-31136# International Centre for Theoretical Physics, Trieste (Italy).
STOCHASTIC STRINGS, TOPOLOGY, AND SPACE-TIME CONFINEMENT
K. Namsrai Sep. 1991 7 p
(DE92-630239; IC-91/329) Avail: CASI HC A02/MF A01

Stochastic space-time caused by random strings is considered. By using a conform-like transformation of the metric we reconstruct 'gravitational' theory and derive its consequences. Such an approach permits us to find natural quark confinement due to induced gravitation and to take into account topological structure of space-time in any physical quantity. DOE

N92-31145# International Centre for Theoretical Physics, Trieste (Italy).
ONE-LOOP INTEGRATION FOR THE AXIAL GAUGE WITH GENERALIZED PRESCRIPTION
A. I. Alekseev Oct. 1991 10 p
(DE92-630241; IC-91/360) Avail: CASI HC A02/MF A01

A prescription for the axial singularities which recovers, in a particular case, the well-known PV-prescription is introduced. For massless one-loop integrals of the propagator type in axial gauge, the simple relations between integrals are derived. These relations permit one to reduce all n-dimensional integrals to one nontrivial integral. General expression for the integrals in the c-prescription is derived. A problem of the prescription regeneration as a result of one-loop integration is considered. DOE

N92-31203# International Centre for Theoretical Physics, Trieste (Italy).
GINSBURG CRITERION FOR AN EQUILIBRIUM SUPERRADIANT MODEL IN THE DYNAMIC APPROACH
M. Trache Oct. 1991 9 p
(DE92-630566; IC-91/330) Avail: CASI HC A02/MF A01

Some critical properties of an equilibrium superradiant model are discussed, taking into account the quantum fluctuations of the field variables. The critical region is calculated using the Ginsburg criterion, underlining the role of the atomic concentration as a control parameter of the phase transition. DOE

N92-30288*# Maryland Univ., College Park. Materials and Nuclear Engineering Unit.
STRUCTURE, PROCESSING, AND PROPERTIES OF POTATOES
Isabel K. Lloyd, Kimberly R. Kolos, Edmond C. Menegaux, Huy Luo, Richard H. McCuen, and Thomas M. Regan *In* NASA. Langley Research Center, National Educators' Workshop: Update 1991. Standard Experiments in Engineering Materials Science and Technology Jun. 1992 p 331-359 Sponsored in part by NSF (For primary document see N92-30263 21-29)
Avail: CASI HC A03/MF A03

80 SOCIAL SCIENCES (GENERAL)

Includes educational matters.

N92-30908*# Winthrop Group, Inc., Cambridge, MA.
ROCKET PROPULSION RESEARCH AT LEWIS RESEARCH CENTER Final Report
Virginia P. Dawson Jul. 1992 8 p Presented at the 28th Joint Propulsion Conference and Exhibit, Nashville, TN, 6-8 Jul. 1992; sponsored by AIAA, SAE, ASME, and ASEE Prepared for NASA. Lewis Research Center
(Contract NASw-3920; RTOP 506-42-00)
(NASA-CR-189187; E-7119; NAS 1.26:189187; AIAA Paper 92-3123) Avail: CASI HC A02/MF A01

A small contingent of engineers at NASA LeRC pioneered the basic research on liquid propellants for rockets shortly after World War 2. Carried on through the 1950s, this work influenced the important early decisions made by Abe Silverstein when he took charge of the Office of Space Flight Programs for NASA. He strongly supported the development of liquid hydrogen as a propulsion fuel in the face of resistance from Wernher von Braun. Members of the LeRC staff played an important role in bringing liquid hydrogen technology to the point of reliability through their management of the Centaur Program. This paper demonstrates how the personality and engineering intuition of Abe Silverstein shaped the Centaur program and left a lasting imprint on the laboratory research tradition. Many of the current leaders of LeRC received their first hands-on engineering experience when they worked on the Centaur program in the 1960s. Author

N92-30278*# Oak Ridge National Lab., TN. Metals and Ceramics Div.
SCIENCE IN ACTION: AN INTERDISCIPLINARY SCIENCE EDUCATION PROGRAM
Linda L. Horton *In* NASA. Langley Research Center, National Educators' Workshop: Update 1991. Standard Experiments in Engineering Materials Science and Technology Jun. 1992 p 213-216 (For primary document see N92-30263 21-29)
(Contract DE-AC05-84OR-21400)
Avail: CASI HC A01/MF A03

N92-30281*# Oak Ridge National Lab., TN. Metals and Ceramics Div.
THE MICROSCOPIC WORLD: A DEMONSTRATION OF ELECTRON MICROSCOPY FOR YOUNGER STUDENTS
Linda L. Horton *In* NASA. Langley Research Center, National Educators' Workshop: Update 1991. Standard Experiments in Engineering Materials Science and Technology Jun. 1992 p 247-249 (For primary document see N92-30263 21-29)
(Contract DE-AC05-84OR-21400)
Avail: CASI HC A01/MF A03

81 ADMINISTRATION AND MANAGEMENT

Includes management planning and research.

N92-30349# Pacific Northwest Lab., Richland, WA.
COMPRESSION PLANNING FOR CONTINUOUS IMPROVEMENT IN QUALITY PROGRAMS
Yolanda A. Willis (Willis Consulting, Pittsburgh, PA.) and Frank C. Hood Apr. 1992 7 p Presented at the International High Level Radioactive Waste Management (IHLRWM) Conference: Promoting Understanding Through Education and Communication, Las Vegas, NV, 12-16 Apr. 1992

(Contract DE-AC06-76RL-01830)
(DE92-012331; PNL-SA-20246; CONF-920430-83) Avail: CASI HC A02/MF A01

This paper describes an innovative approach to planning and prioritizing. The approach, 'Compression Planning,' conserves time for the planners while building commitment to continuous improvement and implementation of the plan. Beginning May 1990, 'Compression Planning' was applied to the first organization-wide effort at training integration for regulatory compliance at Battelle Pacific Northwest laboratory (PNL), a multi-program national laboratory. Various applications of this methodology have been used at PNL for programs since then. DOE

N92-30463# Technische Univ., Delft (Netherlands). Faculty of Technical Mathematics and Information.
PAIRWISE COMPARISON OF CONCESSIONS IN NEGOTIATION PROCESSES
F. A. Lootsma, J. M. Sluijs, and S. Y. Wang 1992 14 p Presented at the IFAC Workshop on Support Systems for Decision and Negociation Processes, Warsaw, Poland, 24-26 Jun. 1992
(Rept-92-15; ISSN-0922-5641; ETN-92-91866) Copyright Avail: CASI HC A03/MF A01

Starting off with a pairwise comparison method to evaluate the possible deals between two parties in conflict, the approach is generalized and the case of three parties in conflict is considered. The basic step is the subjective evaluation of a deal where each party offers exactly one concession. The tradeoff benefits and costs are judged in verbal terms which are subsequently converted into numerical values in a discrete geometric scale. Although the number of plausible geometric scales is large, the information to be used by a mediator appears to be scale independent. The approach is illustrated by the results of an exploratory project aiming at a balanced CO2 emission reduction in Poland, Brazil and The Netherlands. The success of the method depends largely on the information processing support. Given the limitations of human imagination and human judgment, the method is not likely to be effective in a conflict between four or more parties, although it can be easily be generalized. ESA

N92-30682# Naval Postgraduate School, Monterey, CA.
DE-CERTS: A DECISION SUPPORT SYSTEM FOR A COMPARATIVE EVALUATION METHOD FOR RISK MANAGEMENT METHODOLOGIES AND TOOLS M.S. Thesis
Leonard A. Crump, Jr. and James G. Pound Sep. 1991 154 p
(AD-A246965) Avail: CASI HC A08/MF A02

A new approach was recently proposed to effectively and objectively evaluate risk management methodologies and tools for their suitability to a given organizational situation. The proposed approach, known as CERTS, is based on defining suitability in terms of criteria which in turn are described in terms of attributes and metrics. Using the Analytic Hierarchy Process, this thesis develops the CERTS approach into a Decision Support System, that could be used easily and effectively by organizations for selecting a risk management methodology or tool. The thesis also applies the developed DSS to three case studies to gain insights on the applicability of the DSS. GRA

N92-30889# Sandia National Labs., Albuquerque, NM.
ATTITUDINAL AND SITUATIONAL DIFFERENCES BETWEEN NATIONAL LABORATORY INVENTORS AND INVENTOR-ENTREPRENEURS
Mark Allen, Suleiman Kassicieh (New Mexico Univ., Albuquerque.), Raymond Radosevich (New Mexico Univ., Albuquerque.), and Jonathon Soderstrom (Martin Marietta Energy Systems, Inc., Oak Ridge, TN.) 1992 14 p Presented at the Technology Transfer Society (TTS) Conference, Atlanta, GA, 24-26 Jun. 1992
(Contract DE-AC04-76DP-00789)
(DE92-015768; SAND-92-1102C; CONF-9206151-3) Avail: CASI HC A03/MF A01

This paper reports the phase-one results of a planned longitudinal study of the incidence of entrepreneurship among inventors who were employees of national laboratories. A survey of 192 inventors employed by national laboratories and 24 ex-employee inventors who became entrepreneurs provided data for comparison of situational and attitudinal variables. Significant differences in attitudes (as measured by the Entrepreneurial Attitude Orientation Scale) were found between inventors who have not become entrepreneurs and those who have. The differences in perceptions of situational variables between the two groups was significant for only two of the seven dimensions tested. DOE

N92-30959*# Office of Space Science and Applications, Washington, DC.
SPACE SCIENCE AND APPLICATIONS: STRATEGIC PLAN 1991
6 Apr. 1991 68 p
(NASA-TM-107811; NAS 1.15:107811) Avail: CASI HC A04/MF A01

The Office of Space Science and Applications (OSSA) 1991 Strategic Plan reflects a transitional year in which we respond to changes and focus on carrying out a vital space science program and strengthening our research base to reap the benefits of current and future missions. The Plan is built on interrelated, complementary strategies for the core space science program, for Mission to Planet Earth, and for Mission from Planet Earth. Each strategy has its own unique themes and mission priorities, but they share a common set of principles and a common goal - leadership through the achievement of excellence. Discussed here is the National Space Policy; an overview of OSSA activities, goals, and objectives; and the implications of the OSSA space science and applications strategy. Author

N92-30974*# National Academy of Sciences - National Research Council, Washington, DC. Task Group on Priorities in Space Research.
SETTING PRIORITIES FOR SPACE RESEARCH: OPPORTUNITIES AND IMPERATIVES
John A. Dutton (Pennsylvania State Univ., University Park.), Philip H. Abelson (American Association for the Advancement of Science, Washington, DC.), Steven V. W. Beckwith (Cornell Univ., Ithaca, NY.), William P. Bishop (Desert Research Inst., Reno, NV.), Radford Byerly, Jr. (Committee on Science, Space and Technology, U.S. House), Lawson Crowe (Colorado Univ., Boulder.), Peter Dews (Harvard Medical School, Boston, MA.), Owen K. Garriott (Teledyne Brown Engineering, Huntsville, AL.), Jonathan Lunine (Lunar and Planetary Inst., Houston, TX.), and Molly K. Macauley (Resources for the Future, Inc., Washington, DC.) 1992 75 p
(Contract NASw-4627)
(NASA-CR-190519; NAS 1.26:190519) Avail: CASI HC A04/MF A01

This report represents the first phase of a study by a task group convened by the Space Studies Board to ascertain whether it should attempt to develop a methodology for recommending priorities among the various initiatives in space research (that is, scientific activities concerned with phenomena in space or utilizing observations from space). The report argues that such priority statements by the space research community are both necessary and desirable and would contribute to the formulation and implementation of public policy. The report advocates the establishment of priorities to enhance effective management of the nation's scientific research program in space. It argues that scientific objectives and purposes should determine how and under what circumstances scientific research should be done. The report does not take a position on the controversy between advocates of manned space exploration and those who favor the exclusive use of unmanned space vehicles. Nor does the report address questions about the value or appropriateness of Space Station Freedom or proposals to establish a permanent manned Moon base or to undertake a manned mission to Mars. These issues lie beyond the charge to the task group. Author

N92-31209# Naval Postgraduate School, Monterey, CA.
MANAGING THE CONTRACT CLOSEOUT PROCESS M.S. Thesis
Janet J. Patton Mar. 1992 204 p
(AD-A250701) Avail: CASI HC A10/MF A03

The primary objective of this thesis was to review the closeout process within DoD activities and determine how the process might be made more efficient. Secondary objectives include identifying the problems in the current process and determining the impact of failure to close out contracts in the time frame stated in the Federal Acquisition Regulation (FAR). Finally, a Contract Closeout Process Summary has been developed as a by-product of this thesis. This guide can be utilized as a training aid or procedures manual. GRA

N92-30956# Electricite de France, Chatou. Dept. Surveillance Diagnostic et Maintenance.
DEVELOPMENT OF A RELIABILITY MAINTENANCE OPTIMIZATION METHOD [DEVELOPPEMENT D'UNE METHODOLOGIE D'OPTIMISATION DE LA MAINTENANCE PAR LA FIABILITE]
J. P. Jacquot *In* CEP Systemes, ILS, CE, CALS? From Design to Operation 1991 9 p In FRENCH (For primary document see N92-30950 21-61)
Avail: CASI HC A02/MF A02

N92-30957# Air Inter, Lignes Aeriennes Interieures, Paris (France). Centre d'Instruction de Personnel Navigant.
FLIGHT CREW INTEGRATION IN THE MAINTENANCE CHAIN OF A COMMERCIAL AIRCRAFT (A 320) [INTEGRATION DE L'EQUIPAGE DANS LA CHAINE DE MAINTENANCE D'UN AVION COMMERCIAL (A 320)]
C. Rafin and G. Raffin *In* CEP Systemes, ILS, CE, CALS? From Design to Operation 1991 9 p In FRENCH (For primary document see N92-30950 21-61)
Avail: CASI HC A02/MF A02

82 DOCUMENTATION AND INFORMATION SCIENCE

Includes information management; information storage and retrieval technology; technical writing; graphic arts; and micrography.

For computer documentation see *61 Computer Programming and Software.*

N92-30234# Naval Postgraduate School, Monterey, CA.
INFORMATION SYSTEMS: HOW THEY AFFECT AND ARE AFFECTED BY ORGANIZATION STRUCTURE M.S. Thesis
Steven W. Smith Mar. 1992 73 p
(AD-A248852) Avail: CASI HC A04/MF A01

This thesis identifies the impacts of organizational structure on the implementation/operation of management information systems, as well as the impact of information technology upon organizational structure. The conclusion is that academic researchers have identified not only key elements of organizational structure to facilitate successful information system implementation, but also human factors involved. There is no absolute choice for an information system; only a best fit for matching an information system and an organization's structure. GRA

N92-30324# Carnegie-Mellon Univ., Pittsburgh, PA. School of Computer Science.
INFORMATION PROCESSING RESEARCH Final Report, Jul. 1987 - Jul. 1990
Allen Newell and Scott E. Fahlman 3 Jan. 1992 148 p
(Contract F33615-87-C-1499)
(AD-A248492; WL-TR-91-1121) Avail: CASI HC A07/MF A02

This report documents a broad program of basic and applied information processing research conducted by Carnegie Mellon's School of Computer Science. The Information Processing Technology Office of the Defense Advanced Research Projects Agency (DARPA) Supported this work during the period 15 Jul. 1987 - 14 Jul. 1990 and extended the contract to 31 Dec. 1990. Chapters 1 through 7 present in detail our seven major research areas: Artificial Intelligence, Image Understanding, Reliable Distributed Systems, Programming Environments, Reasoning About Programs, Uniform Workstation Interfaces, and Very Large Scale Integration. Sections in each chapter present the area's general research context, the specific problems we addressed, our contributions and their significance, and a bibliography for each chapter. GRA

N92-30386*# National Aeronautics and Space Administration. Langley Research Center, Hampton, VA.
STORAGE CONTROL SYSTEM Patent Application
Kenneth D. Wright, II, inventor (to NASA) and David L. Gray, inventor (to NASA) 27 Nov. 1991 108 p
(NASA-Case-LAR-14651-1; NAS 1.71:LAR-14651-1; US-Patent-Appl-SN-799571) Avail: CASI HC A06/MF A02

A storage control system is presented which includes an apparatus and method for user control of a storage interface to operate a storage medium to store data obtained by a real-time data acquisition system. Digital data received in serial format from the data acquisition system is first converted to a parallel format and then provided to the storage interface. The operation of the storage interface is controlled in accordance with instructions based on user control input from a user. Also, a user status output is displayed in accordance with storage data obtained from the storage interface. By allowing the user to control and monitor the operation of the storage interface, a stand-alone, user-controllable data storage system is provided for storing the digital data obtained by a real-time data acquisition system. NASA

N92-30486# Technische Univ., Delft (Netherlands). Faculty of Technical Mathematics and Information.
INFORMATIZATION IN PUBLIC ADMINISTRATION (EGPA-RESEARCH PROJECT 1991). LARGE SCALE INFORMATION SYSTEMS IN THE NETHERLANDS
B. K. Brussaard and W. G. vandenBerg 1991 37 p
(Rept-91-92; ISSN-0922-5641; ETN-92-91842) Copyright Avail: CASI HC A03/MF A01

Case studies for analysis of two information systems are presented: VIASU (Dutch acronym for electronic Videotext information on general and specific financial allocations) and SAGITTA (Dutch acronym for system for automatic processing of import declarations). Both systems made use of data communication facilities and services offered by the Dutch public telephone and telecommunication system. Their study proved that technical size and complexity interact heavily with administrative constraints and idiosyncracies. In both systems analyzed, this amalgamation of variables decided the end results. ESA

N92-30487# Technische Univ., Delft (Netherlands). Faculty of Technical Mathematics and Information.
INFORMATIZATION IN PUBLIC ADMINISTRATION (EGPA-RESEARCH PROJECT 1991). LARGE SCALE INFORMATION SYSTEMS (COMPARATIVE ANALYSIS IN 8 EUROPEAN COUNTRIES)
B. K. Brussaard 1991 21 p
(Rept-91-93; ISSN-0922-5641; ETN-92-91843) Copyright Avail: CASI HC A03/MF A01

A study reporting on an international comparative analysis of large scale Information Systems (IS) in Public Administration (PA) in Western Europe is presented. The objective of the study is to find ways and means of describing these systems with a view to potential sources of success and failure. Researchers in the eight participating countries each analyzed two systems, of which one was considered to be a relative success and the other a relative failure. Use was made of a previously agreed list of research items. Some tentative conclusions are drawn about the applied methods, such as difficulties encountered and other aspects to be considered in possible further research. ESA

N92-30509# Science Applications International Corp., San Diego, CA. Foreign Applied Sciences Assessment Center.
SOVIET APPLIED INFORMATION SCIENCES IN A TIME OF CHANGE
J. Bengston, R. R. Cronin, and R. B. Davidson Jul. 1991 91 p
(PB92-173020) Avail: CASI HC A05/MF A01

The current state of the information sciences in the Soviet Union and the effects of information science capabilities upon other areas of Soviet science and technology are characterized. Estimates are given of the likely effect of the political and social reforms underway in the Soviet Union on the future Soviet progress in the information sciences and, at a more general level, in science and technology. As in other areas of science, Soviet researchers are better in the theoretical aspects of the information sciences than in the applications. Moreover, the Soviets are unable to match either the quality or quanities of the tools of the applied information sciences that are produced in the West. Soviet scientists remain unable to produce computers of any size in the desired quantities. The lack of capable computers is a serious impediment to computer-aided design of very large-scale integrated circuits, while the Soviet microelectronics industry lacks both automated test equipment and automated controls for processing equipment.
Author

N92-30584# Naval Postgraduate School, Monterey, CA.
THE EFFECT OF INFORMATION SYSTEMS ON MIDDLE MANAGEMENT IN THE AEROSPACE INDUSTRY: THE WESTCO CASE M.S. Thesis
Steven L. Gaudreau Mar. 1992 51 p
(AD-A249017) Avail: CASI HC A04/MF A01

This is a case study involving a company in the Aerospace Industry. The case attempts to analyze the trends of decentralization in an organizational structure. Additionally, the analysis will probe the effects these trends are having on middle management positions. The time frame of this thesis includes economic recession and a significant strategy shift due to current world situations. Organizational strategy, culture, subcultures, mission priorities, and education are just a few of the elements that will be reviewed as contributors to these issues. GRA

N92-30636# Navy Personnel Research and Development Center, San Diego, CA.
REVIEWING THE TECHNICAL REPORT
Carmen Fendelman and Linda L. Oestreich Mar. 1992 14 p
(AD-A249494; ILCEP-West Mono-4-Rev-1) Avail: CASI HC A03/MF A01

This report is one of a series of monographs issued by the Interlaboratory Committee on Editing and Publishing (ILCEP). The committee comprises senior publication managers and editors at Navy and Marine Corps scientific and technical research activities. This monograph examines the process of reviewing a technical report. The material is based on ILCEP members' combined experience in the publications field. The discussion is offered to all persons concerned with technical reporting to provide them with more information about the purposes and techniques of the review process. The authors hope that this information will help technical writers and reviewers understand this important step in the dissemination of technical information. GRA

N92-30819# Rome Lab., Griffiss AFB, NY.
THE EVOLVING DATA DICTIONARY
Patrick K. McCabe Feb. 1992 16 p
(AF Proj. 4594)
(AD-A249030; RL-TM-92-8) Avail: CASI HC A03/MF A01

System Analysts have used a variety of techniques to define, implement, and document information systems. As databases grew large, it became increasingly difficult, if not impossible, to determine what data elements were used by what applications. In many cases, as needs changed, it was easier to build a new application with unique data elements than it was to try and find existing data elements that could be used. Data dictionaries were built to solve this problem. Originally hardcopy references, data dictionaries are evolving into fully automated, in-line active control mechanisms. Data dictionary functionality continues to evolve in the direction of heterogeneous system access support and information management. GRA

N92-31001# Pacific Northwest Lab., Richland, WA.
CAN'T JUSTIFY AN IMAGING SYSTEM? HOW ABOUT A CAR?
V. L. Berndt May 1992 23 p Presented at the Association of Records Managers and Administrators Region 10 Conference, Anchorage, AK, 27-29 May 1992
(Contract DE-AC06-76RL-01830)
(DE92-015156; PNL-SA-19807; CONF-9205191-1) Avail: CASI HC A03/MF A01

This paper discusses the evaluation process of an imaging system, identifying areas of concern and opportunity in considering the two main automated alternatives, and explains why a micrographic CAR system might best serve your immediate needs. This will include: (1) examining your current systems; (2) identifying problems associated with paper and microfiche; (3) describing primary advantages of both electronic imaging and micrographic CAR; (4) providing reasons for choosing either an electronic imaging system or a micrographic CAR system; (5) disadvantages to a micrographic CAR system; (6) concerns about electronic imaging; (7) presenting ways to make a micrographic CAR system work for you; and (8) defining the rewards of a micrographic CAR system.
DOE

N92-31132# Westinghouse Savannah River Co., Aiken, SC.
CONSIDERATIONS FOR IMAGING SYSTEM IMPLEMENTATION IN A NETWORKED ENVIRONMENT
B. J. Hudson 1991 12 p Presented at the Westinghouse Computer Symposium, Monroeville, PA, 21-22 Oct. 1991
(Contract DE-AC09-89SR-18035)
(DE92-015338; WSRC-MS-91-392; CONF-9110344-9) Avail: CASI HC A03/MF A01

Information storage and retrieval systems that utilize raster images are increasing in popularity on a wide variety of platforms. Image systems typically involve the transmission of data files in the 100 KiloByte to 1 MegaByte range to users on specialized workstations who expect retrieval in a matter of seconds. The results of the pilot study outlines the potential for the sharing of image information among various platforms and systems, and sets expectations regarding the level of integration. DOE

N92-30277*# Oak Ridge National Lab., TN. Committee on Terminology.
STANDARD TERMINOLOGY IN THE LABORATORY AND CLASSROOM
Richard A. Strehlow *In* NASA. Langley Research Center, National Educators' Workshop: Update 1991. Standard Experiments in Engineering Materials Science and Technology Jun. 1992 p 197-210 (For primary document see N92-30263 21-29)
(Contract DE-AC05-84OR-21400)
Avail: CASI HC A03/MF A03

83 ECONOMICS AND COST ANALYSIS

Includes cost effectiveness studies.

No abstracts in this category.

84 LAW, POLITICAL SCIENCE AND SPACE POLICY

Includes NASA appropriation hearings; aviation law; space law and policy; international law; international cooperation; and patent policy.

N92-31169# Committee on Appropriations (U.S. Senate).
DEPARTMENTS OF VETERANS AFFAIRS AND HOUSING AND URBAN DEVELOPMENT, AND INDEPENDENT AGENCIES APPROPRIATION BILL, 1993
Barbara Mikulski Washington GPO 1992 203 p Report to accompany H.R. 5679 presented by the Committee on

Appropriations, 102d Congress, 2d Session, 3 Aug. 1992 (S-Rept-102-356; GPO-57-805) Avail: CASI HC A10/MF A03; Document Room, Senate, Washington, DC 20510 HC; SOD HC

The Committee on Appropriations examines bill H.R. 5679 for making appropriations for the Department of Veterans Affairs and Housing and Urban Development for the fiscal year ending Sept. 30, 1993. The report presents various amendments, explanations and the contents of the bill to the Senate. For individual title, see N92-31170.

N92-31170# Committee on Appropriations (U.S. Senate).
NATIONAL AERONAUTICS AND SPACE ADMINISTRATION
In its Departments of Veterans Affairs and Housing and Urban Development, and Independent Agencies Appropriation Bill, 1993 1992 p 138-154 (For primary document see N92-31169 21-84)
Avail: CASI HC A03/MF A03; Document Room, Senate, Washington, DC 20510 HC; SOD HC

A subsection of bill H.R. 5679 is presented that covers NASA funding for research facilities and the areas of research to be explored with these allocations. Various NASA programs are explained and the Appropriations Committee's recommendations towards the use of funding is presented. H.A.

85 URBAN TECHNOLOGY AND TRANSPORTATION

Includes applications of space technology to urban problems; technology transfer; technology assessment; and surface and mass transportation.

For related information see also *03 Air Transportation and Safety, 16 Space Transportation,* and *44 Energy Production and Conversion.*

N92-30575# Oak Ridge National Lab., TN.
SPINOFFS FROM R AND D INVESTMENTS
M. A. Brown and C. R. Wilson 1992 10 p Presented at the Technology Transfer Society (TTS) Conference, Atlanta, GA, 24-26 Jun. 1992
(Contract DE-AC05-84OR-21400)
(DE92-014450; CONF-9206151-2) Avail: CASI HC A02/MF A01

This paper examines spinoff benefits that result from R&D projects, and categorizes them in terms of the dimensions of market and technical newness. These dimensions are discussed with reference to two types of spinoffs: (1) alternative market applications (when the results of an R&D project are subsequently applied to a market or use that differs from the originally intended application) and (2) second-generation technologies (when the technology was the subject of an R&D). Examples from the Department of Energy's Energy-Related Inventions Program are integrated into the results of a literature review to illustrate key concepts, including core technologies, degrees of market and technology newness, technology robustness, and the nature of connections linking spinoffs to prior R&D projects. The paper concludes by examining some of the implications that potential economic benefits from spinoffs present for technology managers and R&D evaluators. DOE

88 SPACE SCIENCES (GENERAL)

N92-31222*# Lunar and Planetary Inst., Houston, TX.
TWENTY-THIRD LUNAR AND PLANETARY SCIENCE CONFERENCE Press Abstracts
1992 61 p Conference held in Houston, TX, 16-20 Mar. 1992 Sponsored by NASA. Johnson Space Center
(NASA-CR-190178; NAS 1.26:190178; LPI-Contrib-781) Avail: CASI HC A04/MF A01

Presented here is a collection of papers from the Twenty-Third Lunar and Planetary Science Conference that were chosen for having the greatest potential interest for the general reading public. The presentations avoid jargon and unnecessarily complex terms. Topics covered include electron microscopy studies of a circumstellar rock, the fractal analysis of lava flows, volcanic activity on Venus, the isotopic signature of recent solar wind nitrogen, and the implications of impact crater distribution on Venus. For individual titles, see N92-31223 through N92-31237.

N92-31223*# Washington Univ., Saint Louis, MO. Center for the Space Sciences.
TEM STUDIES OF A CIRCUMSTELLAR ROCK **c90**
Thomas J. Bernatowicz, Sachiko Amari (Chicago Univ., IL.), and Roy S. Lewis (Chicago Univ., IL.) *In* Lunar and Planetary Inst., Twenty-Third Lunar and Planetary Science Conference 1992 p 1-3 (For primary document see N92-31222 21-88)
Avail: CASI HC A01/MF A01

Reported here is the discovery of crystals of titanium carbide in a grain of silicon carbide which formed as a circumstellar dust particle in the atmosphere of a carbon-rich star. Just as in the case of terrestrial rocks, whose assemblage of minerals gives us clues to the composition and conditions of the environment in which they formed, the titanium carbide crystals and their textural relationship to the silicon carbide give us important clues to the nature of the stellar atmosphere in which they formed. From microscopic studies of the relationships between the atomic planes of the silicon carbide and the titanium carbide, we can show that the titanium carbide cannot have existed as already-formed crystals in a gas around which silicon carbide subsequently condensed. An alternative possibility is that both minerals grew quickly and simultaneously from condensing gas in the rapidly cooling and expanding stellar atmosphere. Other microscopic features of the silicon carbide, such as abundant atomic layer disorder and crystal twinning, similarly suggest rapid grain growth. However, another possibility is that the titanium carbide grew inside of the silicon carbide by diffusion of titanium atoms. Our calculations suggest that this scenario is less likely, given the relatively short times (a year or less) for which stellar condensates can be expected to be exposed to temperatures high enough to make diffusion sufficiently rapid. Author

N92-31224*# Hawaii Univ., Honolulu. Inst. of Planetary Geosciences.
FRACTAL ANALYSIS: A NEW REMOTE SENSING TOOL FOR LAVA FLOWS **c91**
B. C. Bruno, G. J. Taylor, S. K. Rowland, P. G. Lucey, and S. Self *In* Lunar and Planetary Inst., Twenty-Third Lunar and Planetary Science Conference 1992 p 4-6 (For primary document see N92-31222 21-88)
Avail: CASI HC A01/MF A01

Many important quantitative parameters have been developed that relate to the rheology and eruption and emplacement mechanics of lavas. This research centers on developing additional, unique parameters, namely the fractal properties of lava flows, to add to this matrix of properties. There are several methods of calculating the fractal dimension of a lava flow margin. We use the 'structured walk' or 'divider' method. In this method, we measure the length of a given lava flow margin by walking rods of different lengths along the margin. Since smaller rod lengths transverse more smaller-scaled features in the flow margin, the apparent length of the flow outline will increase as the length of the measuring rod decreases. By plotting the apparent length of the flow outline as a function of the length of the measuring rod on a log-log plot, fractal behavior can be determined. A linear trend on a log-log plot indicates that the data are fractal. The fractal dimension can then be calculated from the slope of the linear least squares fit line to the data. We use this 'structured walk' method to calculate the fractal dimension of many lava flows using a wide range of rod lengths, from 1/8 to 16 meters, in field studies of the Hawaiian islands. We also use this method to calculate fractal dimensions from aerial photographs of lava flows, using lengths ranging from 20 meters to over 2 kilometers. Finally, we applied this method to

orbital images of extraterrestrial lava flows on Venus, Mars, and the Moon, using rod lengths up to 60 kilometers. Author

N92-31225*# POD Associates, Inc., Albuquerque, NM.
ENVIRONMENT MODELLING IN NEAR EARTH SPACE: PRELIMINARY LDEF RESULTS **c18**
C. R. Coombs, D. R. Atkinson, J. D. Wagner, L. B. Crowell, M. Allbrooks, and A. J. Watts *In* Lunar and Planetary Inst., Twenty-Third Lunar and Planetary Science Conference 1992 p 7-11 (For primary document see N92-31222 21-88)
Avail: CASI HC A01/MF A01

Hypervelocity impacts by space debris cause not only local cratering or penetrations, but also cause large areas of damage in coated, painted or laminated surfaces. Features examined in these analyses display interesting morphological characteristics, commonly exhibiting a concentric ringed appearance. Virtually all features greater than 0.2 mm in diameter possess a spall zone in which all of the paint was removed from the aluminum surface. These spall zones vary in size from approximately 2 - 5 crater diameters. The actual craters in the aluminum substrate vary from central pits without raised rims, to morphologies more typical of craters formed in aluminum under hypervelocity laboratory conditions for the larger features. Most features also possess what is referred to as a 'shock zone' as well. These zones vary in size from approximately 1 - 20 crater diameters. In most cases, only the outer-most layer of paint was affected by this impact related phenomenon. Several impacts possess ridge-like structures encircling the area in which this outer-most paint layer was removed. In many ways, such features resemble the lunar impact basins, but on an extremely reduced scale. Overall, there were no noticeable penetrations, bulges or spallation features on the backside of the tray. On Row 12, approximately 85 degrees from the leading edge (RAM direction), there was approximately one impact per 15 cm(exp 2). On the trailing edge, there was approximately one impact per 72 cm(exp 2). Currently, craters on four aluminum experiment trays from Bay E09, directly on the leading edge are being measured and analyzed. Preliminary results have produced more than 2200 craters on approximately 1500 cm(exp 2) - or approximately 1 impact per 0.7 cm(exp 2). Author

N92-31226*# Lunar and Planetary Inst., Houston, TX.
GLOBAL SCALE CONCENTRATIONS OF VOLCANIC ACTIVITY ON VENUS: A SUMMARY OF THREE 23RD LUNAR AND PLANETARY SCIENCE CONFERENCE ABSTRACTS. 1: VENUS VOLCANISM: GLOBAL DISTRIBUTION AND CLASSIFICATION FROM MAGELLAN DATA. 2: A MAJOR GLOBAL-SCALE CONCENTRATION OF VOLCANIC ACTIVITY IN THE BETA-ATLA-THEMIS REGION OF VENUS. 3: TWO GLOBAL CONCENTRATIONS OF VOLCANISM ON VENUS: GEOLOGIC ASSOCIATIONS AND IMPLICATIONS FOR GLOBAL PATTERN OF UPWELLING AND DOWNWELLING **c91**
L. S. Crumpler, Jayne C. Aubele, James W. Head, J. Guest, and R. S. Saunders *In its* Twenty-Third Lunar and Planetary Science Conference 1992 p 12-14 (For primary document see N92-31222 21-88)
Avail: CASI HC A01/MF A01

As part of the analysis of data from the Magellan Mission, we have compiled a global survey of the location, dimensions, and subsidiary notes of all identified volcanic features on Venus. More than 90 percent of the surface area was examined and the final catalog comprehensively identifies 1548 individual volcanic features larger than approximately 20 km in diameter. Volcanic features included are large volcanoes, intermediate volcanoes, fields of small shield volcanoes, calderas, large lava channels, and lava floods as well as unusual features first noted on Venus such as coronae, arachnoids, and novae. Author

N92-31227*# University of Northeast Louisiana, Monroe. Dept. of Geosciences.
DURATION AND RATES OF DISCHARGE: MAJA VALLES, MARS **c91**
R. A. DeHon and E. A. Pani *In* Lunar and Planetary Inst., Twenty-Third Lunar and Planetary Science Conference 1992 p 15-18 (For primary document see N92-31222 21-88)
Avail: CASI HC A01/MF A01

The 1600 km-long Maja Valles outflow system of Mars consists of three major divisions including the upper valley on Lunae Planum, the canyon section across Xanthe Terra, and the lower valley across western Chryse Planitia. Although water released from the source in Juventae Chasma could reach the terminus of the present day valley system in central Chryse Planitia within 44 hours, the original outflow did not traverse the Martian surface in a direct path. It ponded along its course on northern Lunae Planum and near the western edge of Chryse Planitia significantly prolonging the lifetime of surface flow. Calculation of pond volumes and discharge rates through various parts of the channel system indicates that water flowed through this system for nearly a (terrestrial) year. Discharge rates from the various basins along the Maja channels and the maximum flow rates within the various channels are calculated. With this data, it is possible to place reasonable estimates of the minimum length of time required to drain the various impoundments and the duration of flow in various parts of the channel system. The results of these calculations are discussed. Author

N92-31228*# Rensselaer Polytechnic Inst., Troy, NY. Dept. of Earth and Environmental Sciences.
THE FIRST IDENTIFICATION OF A MAINBELT ASTEROID SOURCE FOR A METEORITE CLASS E-TYPE APOLLO ASTEROID (3103) 1982BB: A LINK BETWEEN THE HUNGARIA ASTEROID ZONE AND THE AUBRITE METEORITES **c90**
M. J. Gaffey, K. L. Reed, and M. S. Kelley *In* Lunar and Planetary Inst., Twenty-Third Lunar and Planetary Science Conference 1992 p 19-23 (For primary document see N92-31222 21-88)
(Grants NAGw-642; NSF AST-90-12180)
Avail: CASI HC A01/MF A01

One of the major goals of asteroid investigators has been to determine the source bodies of the meteorites, and, thus, to provide the needed spatial context. However, despite careful investigation of many of these asteroids, no specific mainbelt asteroidal parent bodies for particular meteorites have yet been identified. Results are reported that represent the first direct link of a set of meteorites (the aubrites or enstatite achondrites) back to a particular source region in the asteroid belt (the Hungaria zone of the innermost belt located at a heliocentric distance of about 1.9 AU (1.9 times the Earth's distance from the Sun)). Since most asteroids in the belt are still located near their original heliocentric formation distances, this link allows the composition and temperature of the solar nebula to be determined at a specific distance from the Sun during the time of planetesimal formation. Orbital considerations suggest that 3103 could be derived from the Hungaria zone. However, the spectral gype of 3103 makes such a source probable. The Hungaria zone is the only region of the asteroid belt where E-type asteroids are common. E-type objects constitute about 55 percent of the classified Hungaria population. Although a more detailed investigation of the dynamical evolution of this object is needed, it appears highly probable that 3103 1982BB was derived from the Hungaria region of the innermost asteroid belt, that it is a fragment of the collisional breakup of an E-object near 1.9 AU, and escaped the mainbelt via the nu sup 16 resonance. Author

N92-31229*# Harvard Univ., Cambridge, MA. Center for Isotope Geochemistry.
THE (146,147)Sm-(142,143)Nd SYSTEMATICS OF EARLY TERRESTRIAL DIFFERENTIATION AND THE LOST CONTINENTS OF THE EARLY EARTH **c46**
Charles L. Harper, Jr. and Stein B. Jacobsen *In* Lunar and Planetary Inst., Twenty-Third Lunar and Planetary Science Conference 1992 p 24-28 (For primary document see N92-31222 21-88)
Avail: CASI HC A01/MF A01

The very early history of the Earth has been one of the great enduring puzzles in the history of geology. We report evidence which clearly can be described as a vestige of a beginning, because

the evidence that we report cannot be interpreted in any other way except as a geochemical signal of processes active in the very early history of the Earth. The evidence itself is a very small anomaly in the abundance of SM-146. The primary aims of this study were to: (1) verify the existence of the 'lost continents' of the Hadean era; and (2) determine their mean age. Author

N92-31230*# California Inst. of Tech., Pasadena. Div. of Geological and Planetary Sciences.
PRESOLAR (?) CORUNDUM IN THE ORGUEIL METEORITE **c90**
G. R. Huss, I. D. Hutcheon, G. J. Wasserburg, and J. Stone *In* Lunar and Planetary Inst., Twenty-Third Lunar and Planetary Science Conference 1992 p 29-33 (For primary document see N92-31222 21-88)
Avail: CASI HC A01/MF A01

The discovery in chondritic meteorites of diamond, SiC, and poorly crystallized graphite that formed around other stars demonstrated conclusively that presolar dust survived the formation of the solar system to be incorporated into meteorites. The presolar nature of these grains is shown by the highly unusual isotopic compositions of their constituent elements. To date, all recognized types of presolar grains have been carbon rich and apparently formed around carbon stars, those with C/O greater than 1. The discovery of the first oxygen-rich grain with isotopic characteristics consistent with a presolar origin is reported. Oxygen-rich grains presumably form only around stars with C/O less than 1. Author

N92-31231*# California Univ., San Diego. Dept. of Chemistry.
ON THE ISOTOPIC SIGNATURE OF RECENT SOLAR-WIND NITROGEN **c92**
Y. Kim, J. S. Kim, K. Marti, and J. F. Kerridge *In* Lunar and Planetary Inst., Twenty-Third Lunar and Planetary Science Conference 1992 p 34-35 (For primary document see N92-31222 21-88)
Avail: CASI HC A01/MF A01

One of the most intriguing discoveries yielded by the Apollo samples was evidence pointing towards a significant long-term change in the composition of the sun. Such a change, of the size inferred from the lunar sample data, is inconsistent with present theories of solar evolution. Consequently, there is much interest in exploring this phenomenon as closely as possible, to determine exactly what compositional changes have taken place and whether those changes really did take place in the sun, or whether the cause lies elsewhere. The reason why we can use the moon to analyze the elements in the sun is that the sun emits a stream of ions, known as the solar wind, whose composition, on average, is believed to be the same as that in the surface regions of the sun. When the solar-wind ions hit the surface of the moon, many of them penetrate a short distance into the dust grains lying on the lunar surface. Thus, after a grain has sat on the lunar surface for a while, it has a rim of material that is partly lunar and partly solar in composition. For most chemical elements, the difference between lunar and solar composition is so sufficiently small that the solar elements cannot be detected, but for a handful of elements that are missing from the moon, their solar 'signature' can be observed in samples of lunar soil brought back by the astronauts. Among those elements is nitrogen, the most common element in the air we breathe, but very rare indeed on the moon. Our analytical techniques are not sophisticated enough yet to enable us to analyze individual lunar soil grains for nitrogen, much less to zero in on just the nitrogen in the surface of such a grain. Consequently we are forced to analyze samples consisting of many different grains, each of which could have experienced its own individual history. This makes it difficult to identify the nitrogen implanted in grain surfaces, and also to define the age of a sample. Author

N92-31232*# Lunar and Planetary Inst., Houston, TX.
CONSTRAINTS ON THE PUTATIVE COMPANIONS TO PSR1257+12 **c90**
R. Malhotra, D. Black, A. Eck, and A. Jackson *In its* Twenty-Third Lunar and Planetary Science Conference 1992 p 36 (For primary document see N92-31222 21-88)
Avail: CASI HC A01/MF A01

The radio pulsar PSR1257+12 was first observed about two years ago at the Arecibo radio telescope. It has a pulse period of 6.2 milliseconds which makes it one of only a handful of known objects of this type that spin at a dizzying rate of several hundred times per second. Routine follow-up monitoring of this object has continued since its discovery. The pulsar's discoverer has recently reported that a standard analysis of the time-of-arrival measurements of the radio pulses from PSR1257+12 showed that after accounting for the usual features of millisecond pulsars, there remained a residual in the signal which appeared to be a superposition of two components, one with a period of 98 days and the other with a period of 66 days. This was interpreted as being due to the presence of two low mass companions in orbit about the pulsar. The amplitude of the individual components in the residuals then gives a measure of the masses of the companions, up to a factor 1/sin i where i is the inclination of the orbital plane to the plane of the sky, so that a lower limit of the companion masses is well defined. The work reported in this paper tests the validity of this interpretation through orbital dynamics. Author

N92-31233*# Southern Methodist Univ., Dallas, TX. Dept. of Geological Sciences.
THE THERMAL ENGINE OF VENUS: IMPLICATIONS FROM THE IMPACT CRATER DISTRIBUTION **c91**
Roger J. Phillips *In* Lunar and Planetary Inst., Twenty-Third Lunar and Planetary Science Conference 1992 p 37-39 (For primary document see N92-31222 21-88)
Avail: CASI HC A01/MF A01

Questions concerning the state of Venus' volcanological activity are currently under investigation. These questions were raised by the imaging radar and altimetric data obtained by the Magellan spacecraft, which began mapping Venus in Sept. 1990. Clues about the answers to these questions are provided by the nature and distribution of impact craters on the surface of Venus. Statistical tests show that the distribution of craters on Venus cannot be distinguished from a completely spatially random population. Further, the majority of craters look relatively pristine; only about 5 percent of the observed craters appear to be embayed or flooded by lavas. The simplest interpretation of these observations is a model in which the impact craters lie on a surface that has been undisturbed by volcanological and tectonic processes since the time the surface was formed. Counting up the number of craters and estimating the rate at which meteoroids strike the surface then gives an age for the venusian surface of 500 million years; in this model the volcanic activity since that time has been essentially nil. This scenario is described as a 'production' model, or perhaps more appropriately, a 'catastrophic' model. Author

N92-31234*# Scripps Institution of Oceanography, La Jolla, CA.
IS THE VENUSIAN LITHOSPHERE SUBDUCTING? **c91**
David T. Sandwell and Gerald Schubert (California Univ., Los Angeles.) *In* Lunar and Planetary Inst., Twenty-Third Lunar and Planetary Science Conference 1992 p 40-46 (For primary document see N92-31222 21-88)
Avail: CASI HC A02/MF A01

Using data collected by the Magellan spacecraft, we are exploring the hypothesis that the cooler and more rigid outer layer of Venus (i.e., the lithosphere) is sinking (subducting) into the interior of Venus. If this process is occurring, it provides a mechanism for cooling the interior of Venus and also for recycling the lighter crustal rocks back into the interior. In addition, since subduction zones drive the plate tectonic motion on the Earth, evidence for lithospheric subduction on Venus raises the possibility of limited plate tectonic-like activity on Venus. Author

N92-31235*# Jet Propulsion Lab., California Inst. of Tech., Pasadena.
SCIENCE QUESTIONS FOR THE MAGELLAN CONTINUING MISSION **c91**

R. S. Saunders and E. R. Stofan *In* Lunar and Planetary Inst., Twenty-Third Lunar and Planetary Science Conference 1992 p 47-48 (For primary document see N92-31222 21-88)
Avail: CASI HC A01/MF A01

Magellan has completed two mapping cycles around the planet Venus, returning high resolution synthetic aperture images and altimetry data of over 95 percent of the planet's surface. Venus is dominated by low lying volcanic plains with an impact crater population indicating an average surface age of about 500 million years. Highland regions either tend to be characterized by volcanic shield complexes and rifting or by complex ridged terrain. Successful as the primary mission of Magellan has been, significant scientific questions remain to be addressed with imaging and gravity data that will be collected over the next several years. Author

N92-31236*# RAND Corp., Santa Monica, CA.
GASPRA'S SHAPE AND SURFACE FEATURES: COMPARISON TO SMALL SATELLITES **c90**
P. C. Thomas, M. E. Davies, D. Simonelli (Cornell Univ., Ithaca, NY.), J. Veverka (Cornell Univ., Ithaca, NY.), and M. J. S. Belton (Kitt Peak National Observatory, Tucson, AZ.) *In* Lunar and Planetary Inst., Twenty-Third Lunar and Planetary Science Conference 1992 p 49-52 (For primary document see N92-31222 21-88)
Avail: CASI HC A01/MF A01

The several thousand asteroids constitute the second largest population of substantial solid objects in the solar system (there are probably more comets), and have been studied from the Earth for nearly two centuries. Asteroids are important members of the solar system for several reasons, among them: (1) they contain the materials that reflect the processes going on early in the time of planet formation; (2) their impacts have been the major external influences on the surface of some terrestrial planets; and (3) their impacts on Earth have probably had major effects on biologic evolution. This paper examines and describes the asteroid Gaspra, and compares it to small satellites. Author

N92-31237*# National Astronomy and Ionosphere Center, Arecibo, Puerto Rico.
DISCOVERY OF TWO PLANETS AROUND A MILLISECOND PULSAR **c91**
A. Wolszczan *In* Lunar and Planetary Inst., Twenty-Third Lunar and Planetary Science Conference 1992 p 53-55 Sponsored in part by NSF Prepared in cooperation with Arecibo Ionospheric Observatory, Puerto Rico (For primary document see N92-31222 21-88)
Avail: CASI HC A01/MF A01

By timing the arrival of radio signals from a rapidly spinning pulsar at the Arecibo Observatory's radio/radar telescope, the most convincing evidence so far for a planetary system outside our own has been found: two or possibly three planets that orbit the neutron star called PSR1257+12. This finding indicates that planet formation may be a more common process than previously anticipated and that the formation of disks of gas and dust that are sufficiently massive to condense into Earth-sized planets orbiting their central bodies can take place under surprisingly diverse conditions. Author

89 ASTRONOMY

Includes radio, gamma-ray, and infrared astronomy, and astrometry.

N92-30686*# National Aeronautics and Space Administration, Washington, DC.
HUBBLE SPACE TELESCOPE. UPDATE: 18 MONTHS IN ORBIT
Apr. 1990 19 p LIMITED REPRODUCIBILITY: More than 20 percent of this document may be affected by color photographs Original contains color illustrations
(NASA-TM-107962; NAS 1.15:107962) Avail: CASI HC A03/MF A01; 16 functional color pages

In April 1990, Space Shuttle Discovery launched the Hubble Space Telescope (HST). An 18 month in-orbit update of the operations and performance of the HST is presented. Numerous color photographs are shown of objects already observed, and mission plans are presented for future observations by the HST. H.A.

N92-30714# Real Inst. y Observatorio de la Armada, San Fernando (Spain).
CARLSBERG MERIDIAN CATALOGUE LA PALMA. NUMBER 5: OBSERVATIONS OF POSITIONS OF STARS AND PLANETS: MAY 1988 TO DEC. 1989
1991 309 p Prepared in cooperation with Copenhagen Observatory, Denmark and Royal Greenwich Observatory, Cambridge, England
(ISBN-84-7469-052-8; ETN-92-91706) Avail: CASI HC A14/MF A03

Positions and magnitudes of 16693 stars north of declination -45 degrees, 15004 proper motions, and 2847 positions and magnitudes of 66 solar system objects obtained with the Carslberg Automatic Meridian Circle on La Palma during the period May 1988 to December 1989 are given. The positions of the stars are for the epoch of observations and the equinox J2000.0, and are in a system close to that of the FK5. The limiting magnitude is m sub v = 14.8. The catalog comprises the following stars: 3883 international reference stars; 1158 faint reference stars in the fields of about 200 benchmark radio sources; 2271 G-K stars within 300 pc; 1234 A5-G0 near the north galactic pole; 1242 stars from an unbiased sample of K-M dwarfs; and 1082 stars in nearby O-B associations. The observations of Callisto, Titan, Uranus, Neptune, Pluto, and 61 minor planets are included. The mean error of a catalog position in the zenith is 0.07 seconds in right ascension and declination, and 0.04 m in magnitude. The mean error of the order motions, derived by combining the position in this catalog with those at earlier epochs, is typically 0.002 seconds per year. ESA

N92-30862# Lawrence Livermore National Lab., CA.
MODELING OF UV LINES FROM CATACLYSMIC VARIABLE WINDS
P. A. Vitello and I. Shlosman (Kentucky Univ., Lexington.) Mar. 1992 6 p Presented at the 10th International Colloqium on Ultra Violet and X Ray Spectroscopy of Astrophysical and Laboratory Plasmas, Berkeley, CA, 3-5 Feb. 1992
(Contract W-7405-eng-48)
(DE92-013443; UCRL-JC-110303; CONF-9202103-2) Avail: CASI HC A02/MF A01

Ultraviolet resonance lines appear to be powerful tools for diagnostics and study of the outflows from cataclysmic variable stars. The origin of these winds and their geometry are not known at present. In order to compare observed lines from the IUE database with synthetic line profiles from accretion disk winds, we have developed a numerical radiation transfer model for 3D non-radial, rotating winds from an accretion disk. Using this model we have studied line spectra from a number of cataclysmic variables. We find that good fits to observed spectra can be obtained using disk winds for mass loss rates much smaller than the accretion rates. DOE

90 ASTROPHYSICS

Includes cosmology; celestial mechanics; space plasmas; and interstellar and interplanetary gases and dust.

For related information see also *75 Plasma Physics.*

N92-30506# Technische Univ., Berlin (Germany, F.R.). Inst. fuer Astronomie und Astrophysik.

[ACTIVITIES REPORT OF THE INSTITUTE FOR ASTRONOMY AND ASTROPHYSICS AT TECHNICAL UNIVERSITY OF BERLIN (GERMANY, F.R.)] Annual Report, 1989 [INSTITUT FUER ASTRONOMIE UND ASTROPHYSIK DER TECHNISCHEN UNIVERSITAET BERLIN. JAHRESBERICHT FUER DAS JAHR 1989]

K. Beuermann 1990 8 p In GERMAN

(MITT-11; ETN-92-91689) Avail: CASI HC A02/MF A01

Activities, computer installations, and conferences of the institute are reviewed. Scientific projects and achievements are presented in the following areas: solar system; cataclysmic variable and x-ray double stars; extragalactic x-ray sources; development, growth and annihilation of stellar dust; chemistry of dust formation; and dust shells and winds. Dissertation, thesis, and publication titles are given. ESA

N92-30578# Los Alamos National Lab., NM.

CONSTRAINTS ON THE NUCLEAR MATTER EQUATION OF STATE FROM PULSAR GLITCHES

B. Link, R. I. Epstein, and K. A. VanRiper 27 Apr. 1992 9 p Presented at the Physics of Isolated Pulsars Workshop, Taos, NM, 23-28 Feb. 1992

(Contract W-7405-eng-36)

(DE92-015142; LA-UR-92-1610; CONF-9202117-2) Avail: CASI HC A02/MF A01

We study the post-glitch response of four pulsars to obtain lower limits on the total moment of inertia of the inner crust superfluid. In contrast to previous work, our constraints are independent of the form of the crust-superfluid coupling. We conclude that the superfluid must comprise (approx. gt) 0.8 percent of the total moment of inertia of the star. This constraint rules out the softest equations of state. DOE

N92-30609# Los Alamos National Lab., NM.

RAPID COOLING AND STRUCTURE OF NEUTRON STARS

K. A. VanRiper and J. M. Lattimer 1992 9 p Presented at the Physics of Isolated Pulsars Workshop, Taos, NM, 23-28 Feb. 1992

(Contract W-7405-eng-36)

(DE92-015279; LA-UR-92-1508; CONF-9202117-3) Avail: CASI HC A02/MF A01

This report discusses the following topics on neutron stars: direct URCA neutrino emission; thermal evolution models; analytic model for diffusion through the crust; and core superfluidity. DOE

N92-30622# Fermi National Accelerator Lab., Batavia, IL.

DARK MATTER AND COSMOLOGY

D. N. Schramm Mar. 1992 17 p Presented at the 2nd International Workshop on Theoretical and Phenomenological Aspects of Underground Physics, Toledo (Spain), 9-13 Sep. 1991 Prepared in cooperation with Chicago Univ., IL

(Contracts DE-AC02-76CH-03000; DE-FG02-91ER-40606)

(DE92-013023; FNAL/C-92/88-A; CONF-9109182-3) Avail: CASI HC A03/MF A01

The cosmological dark matter problem is reviewed. The Big Bang nucleosynthesis constraints on the baryon density are compared with the densities implied by visible matter, dark halos, dynamics of clusters, gravitational lenses, large-scale velocity flows, and the omega = 1 flatness/inflation argument. It is shown that (1) the majority of baryons are dark; and (2) non-baryonic dark matter is probably required on large scales. It is also noted that halo dark matter could be either baryonic or non-baryonic. Descrimination between 'cold' and 'hot' non-baryonic candidates is shown to depend on the assumed 'seeds' that stimulate structure formation. Gaussian density fluctuations, such as those induced by quantum fluctuations, favor cold dark matter, whereas topological defects such as strings, textures or domain walls may work equally or better with hot dark matter. A possible connection between cold dark matter, globular cluster ages, and the Hubble constant is mentioned. Recent large-scale structure measurements, coupled with microwave anisotropy limits, are shown to raise some questions for the previously favored density fluctuation picture. Accelerator and underground limits on dark matter candidates are also reviewed. DOE

N92-30705# Los Alamos National Lab., NM.

FLUCTUATION-DISSIPATION THEOREM IN GENERAL RELATIVITY AND THE COSMOLOGICAL CONSTANT

E. Mottola 1992 14 p Presented at the Workshop on Time Asymmetry, Mazagon, Spain, 30 Sep. - 4 Oct. 1991

(Contract W-7405-eng-36)

(DE92-013542; LA-UR-92-1238; CONF-9109371-2) Avail: CASI HC A03/MF A01

Vacuum fluctuations are an essential feature of quantum field theory. Yet, the smallness of the scalar curvature of our universe suggests that the zero-point energy associated with these fluctuations does not curve spacetime. A possible way out of this paradox is suggested by the fact that microscopic fluctuations are generally accompanied by dissipative behavior in macroscopic systems. The intimate relation between the two is expressed by a fluctuation-dissipation theorem which extends to general relativity. The connection between quantum fluctuations and dissipation suggests a mechanism for the conversion of coherent stresses in the curvature of space into ordinary matter or radiation, thereby relaxing the effective cosmological 'constant' to zero over time. The expansion of the universe may be the effect of this time-asymmetric relaxation process. DOE

N92-30855# Lawrence Livermore National Lab., CA.

HEATING AND MOMENTUM DEPOSITION IN HOT STARS

J. I. Castor Dec. 1991 16 p Presented at the International Astronomical Union Conference on Nonlinear Phenomena in Stellar Variability, Buenos Aires (Argentina), 23 Jul. - 1 Aug. 1991

(Contract W-7405-eng-48)

(DE92-011850; UCRL-JC-109222; CONF-9107218-2) Avail: CASI HC A03/MF A01

The coronae of hot stars are compared with those of the sun and other cool stars, and some important distinctions are drawn. Principal among these are that the hot star coronae readily radiate away any deposited energy, and that the overriding concern is how the momentum is deposited that drives their very vigorous winds. The features of radiatively driven winds are reviewed, with particular attention to their evidently very complex, and presently poorly known, spatial and temporal structure. Some possible explanations for the structure are considered. DOE

N92-30856# Los Alamos National Lab., NM.

NUCLEAR STRUCTURE CALCULATIONS FOR ASTROPHYSICAL APPLICATIONS

P. Moeller (Mainz Univ., Germany, F.R.), K. L. Kratz (Mainz Univ., Germany, F.R.), and J. R. Nix 13 Mar. 1992 18 p Presented at the Exotic Nuclei, South Crimea (USSR), 1-5 Oct. 1991

(Contract W-7405-eng-36)

(DE92-011495; LA-UR-92-980; CONF-9110360-1) Avail: CASI HC A03/MF A01

Here we present calculated results on such diverse properties as nuclear energy levels, ground-state masses and shapes, beta-decay properties, and fission-barrier heights. Our approach to these calculations is to use a unified theoretical framework within which the above properties can all be studied. The results are obtained in the macroscopic-microscopic approach in which a microscopic nuclear-structure single-particle model with extensions is combined with a macroscopic model, such as the liquid drop model. In this model, the total potential energy of the nucleus may be calculated as a function of shape. The maxima and minima in this function correspond to such features as the ground state, fission saddle points, and shape-isomeric states. Various transition

rate matrix elements are determined from wave-functions calculated in the single-particle model with pairing and other relevant residual interactions taken into account. DOE

N92-30973 Arizona Univ., Tucson.
THE ORIGINS OF HOT SUBDWARF STARS Ph.D. Thesis
Rex Anderson Saffer 1991 220 p
Avail: Univ. Microfilms Order No. DA9208034

High signal-to-noise optical spectrophotometry of a sample of field subluminous B stars drawn largely from the Palomar Green ultraviolet excess survey is analyzed with a new grid of model atmospheres and synthetic spectra. The stellar effective temperatures, surface gravities, and photospheric helium abundances are determined simultaneously from a detailed analysis of hydrogen and helium absorption line profiles. The derived temperatures and gravities place the subluminous B stars in the theoretical H-R diagram along and bounded below by theoretical sequences of the zero-age extended horizontal branch, lending strong support to the hypothesis that these stars are composed of helium-burning cores of 0.5 solar mass overlain by very thin layers of hydrogen of less than 0.02 solar mass. Various scenarios for their past evolutionary history are examined in the context of their probable future evolution into white dwarfs of lower than average mass. The derived distances above the Galactic plane support a scale height for the population of z(sub 0) = 285 pc, consistent with the identification of their progenitor stars as members of the old disk population. Radial velocities of sdB and sdO stars are analyzed to infer their kinematic characteristics. The results for the sdB stars are inconclusive, but for the sdO stars the results also are consistent with the population belonging to the older part of the thin disk. Dissert. Abstr.

N92-31108# Los Alamos National Lab., NM.
NONLINEAR RR LYRAE MODELS WITH NEW LIVERMORE OPACITIES
J. A. Guzik and A. N. Cox 1992 4 p Presented at the International Astronomical Union (IAU) Meeting, Mito, Japan, 6-10 Jan. 1992
(Contract W-7405-eng-36)
(DE92-011158; LA-UR-92-879; CONF-920184-2) Avail: CASI HC A01/MF A01

Recently it was shown that a 20 percent opacity decrease in the 20,000-30,000 K region, as indicated by the new Livermore OPAL opacities, reconciles the discrepancy between pulsation and evolution masses of double-mode RR Lyrae variables. Nonlinear hydrodynamic calculations were performed for RR Lyrae models of mass 0.75 solar mass, 51 solar luminosity, and Z = 0.0001 (Osterhoff II type) including this opacity decrease. The Stellingwerf periodic relaxation method was used to converge the models to a limit cycle, and the Floquet matrix eigenvalues calculated to search for a tendency of the fundamental mode to grow from the full-amplitude overtone solution, and the overtone mode to grow from the full-amplitude fundamental solution, thereby predicting double-mode behavior. Models of T(sub eff) less than 7000 K with the opacity decrease have positive fundamental-mode growth rates in the overtone solution, in contrast to earlier results, and models with T(sub eff) less than 7000 have positive 1st overtone growth rates in the fundamental-mode behavior was not found. DOE

N92-31223*# Washington Univ., Saint Louis, MO. Center for the Space Sciences.
TEM STUDIES OF A CIRCUMSTELLAR ROCK
Thomas J. Bernatowicz, Sachiko Amari (Chicago Univ., IL.), and Roy S. Lewis (Chicago Univ., IL.) *In* Lunar and Planetary Inst., Twenty-Third Lunar and Planetary Science Conference 1992 p 1-3 (For primary document see N92-31222 21-88)
Avail: CASI HC A01/MF A01

N92-31228*# Rensselaer Polytechnic Inst., Troy, NY. Dept. of Earth and Environmental Sciences.
THE FIRST IDENTIFICATION OF A MAINBELT ASTEROID SOURCE FOR A METEORITE CLASS E-TYPE APOLLO ASTEROID (3103) 1982BB: A LINK BETWEEN THE HUNGARIA ASTEROID ZONE AND THE AUBRITE METEORITES
M. J. Gaffey, K. L. Reed, and M. S. Kelley *In* Lunar and Planetary Inst., Twenty-Third Lunar and Planetary Science Conference 1992 p 19-23 (For primary document see N92-31222 21-88)
(Grants NAGw-642; NSF AST-90-12180)
Avail: CASI HC A01/MF A01

N92-31230*# California Inst. of Tech., Pasadena. Div. of Geological and Planetary Sciences.
PRESOLAR (?) CORUNDUM IN THE ORGUEIL METEORITE
G. R. Huss, I. D. Hutcheon, G. J. Wasserburg, and J. Stone *In* Lunar and Planetary Inst., Twenty-Third Lunar and Planetary Science Conference 1992 p 29-33 (For primary document see N92-31222 21-88)
Avail: CASI HC A01/MF A01

N92-31232*# Lunar and Planetary Inst., Houston, TX.
CONSTRAINTS ON THE PUTATIVE COMPANIONS TO PSR1257+12
R. Malhotra, D. Black, A. Eck, and A. Jackson *In its* Twenty-Third Lunar and Planetary Science Conference 1992 p 36 (For primary document see N92-31222 21-88)
Avail: CASI HC A01/MF A01

N92-31236*# RAND Corp., Santa Monica, CA.
GASPRA'S SHAPE AND SURFACE FEATURES: COMPARISON TO SMALL SATELLITES
P. C. Thomas, M. E. Davies, D. Simonelli (Cornell Univ., Ithaca, NY.), J. Veverka (Cornell Univ., Ithaca, NY.), and M. J. S. Belton (Kitt Peak National Observatory, Tucson, AZ.) *In* Lunar and Planetary Inst., Twenty-Third Lunar and Planetary Science Conference 1992 p 49-52 (For primary document see N92-31222 21-88)
Avail: CASI HC A01/MF A01

91 LUNAR AND PLANETARY EXPLORATION

Includes planetology; and manned and unmanned flights. For spacecraft design or space stations see *18 Spacecraft Design, Testing and Performance.*

N92-30302*# National Aeronautics and Space Administration. Lewis Research Center, Cleveland, OH.
ELECTRICAL AND CHEMICAL INTERACTIONS AT MARS WORKSHOP, PART 1 Final Report
1992 31 p Workshop held in Cleveland, OH, 19-20 Nov. 1991
(RTOP 506-41-41)
(NASA-CP-10093; E-7016-1; NAS 1.55:10093) Avail: CASI HC A03/MF A01

The Electrical and Chemical Interactions at Mars Workshop, hosted by NASA Lewis Research Center on November 19 and 20, 1991, was held with the following objectives in mind: (1) to identify issues related to electrical and chemical interactions between systems and their local environments on Mars, and (2) to recommend means of addressing those issues, including the dispatch of robotic spacecraft to Mars to acquire necessary information. The workshop began with presentations about Mars' surface and orbital environments, Space Exploration Initiative (SEI) systems, environmental interactions, modeling and analysis, and plans for exploration. Participants were then divided into two working groups: one to examine the surface of Mars; and the other, the orbit of Mars. The working groups were to identify issues relating to environmental interactions; to state for each issue what is known and what new knowledge is needed; and to recommend ways to fulfill the need. Issues were prioritized within each working

group using the relative severity of effects as a criterion. Described here are the two working groups' contributions. A bibliography of materials used during the workshop and suggested reference materials is included. Author

N92-30921*# California Inst. of Tech., Pasadena. Seismological Lab.
IMPACT EROSION OF TERRESTRIAL PLANETARY ATMOSPHERES
Thomas J. Ahrens 5 Aug. 1992 50 p
(Grant NAG5-198)
(NASA-CR-190605; NAS 1.26:190605) Avail: CASI HC A03/MF A01

I review current ideas about the nature of the planetesimals - composition, size distribution, and the planetary encounter velocity. Previous papers on accretion and erosion of planetary atmospheres as a result of multiple impacts are reviewed. Finally, the effects of blowing off a substantial fraction of the atmosphere from a terrestrial planet due to a single giant body impact are discussed. Author

N92-31224*# Hawaii Univ., Honolulu. Inst. of Planetary Geosciences.
FRACTAL ANALYSIS: A NEW REMOTE SENSING TOOL FOR LAVA FLOWS
B. C. Bruno, G. J. Taylor, S. K. Rowland, P. G. Lucey, and S. Self *In* Lunar and Planetary Inst., Twenty-Third Lunar and Planetary Science Conference 1992 p 4-6 (For primary document see N92-31222 21-88)
Avail: CASI HC A01/MF A01

N92-31226*# Lunar and Planetary Inst., Houston, TX.
GLOBAL SCALE CONCENTRATIONS OF VOLCANIC ACTIVITY ON VENUS: A SUMMARY OF THREE 23RD LUNAR AND PLANETARY SCIENCE CONFERENCE ABSTRACTS. 1: VENUS VOLCANISM: GLOBAL DISTRIBUTION AND CLASSIFICATION FROM MAGELLAN DATA. 2: A MAJOR GLOBAL-SCALE CONCENTRATION OF VOLCANIC ACTIVITY IN THE BETA-ATLA-THEMIS REGION OF VENUS. 3: TWO GLOBAL CONCENTRATIONS OF VOLCANISM ON VENUS: GEOLOGIC ASSOCIATIONS AND IMPLICATIONS FOR GLOBAL PATTERN OF UPWELLING AND DOWNWELLING
L. S. Crumpler, Jayne C. Aubele, James W. Head, J. Guest, and R. S. Saunders *In its* Twenty-Third Lunar and Planetary Science Conference 1992 p 12-14 (For primary document see N92-31222 21-88)
Avail: CASI HC A01/MF A01

N92-31227*# University of Northeast Louisiana, Monroe. Dept. of Geosciences.
DURATION AND RATES OF DISCHARGE: MAJA VALLES, MARS
R. A. DeHon and E. A. Pani *In* Lunar and Planetary Inst., Twenty-Third Lunar and Planetary Science Conference 1992 p 15-18 (For primary document see N92-31222 21-88)
Avail: CASI HC A01/MF A01

N92-31233*# Southern Methodist Univ., Dallas, TX. Dept. of Geological Sciences.
THE THERMAL ENGINE OF VENUS: IMPLICATIONS FROM THE IMPACT CRATER DISTRIBUTION
Roger J. Phillips *In* Lunar and Planetary Inst., Twenty-Third Lunar and Planetary Science Conference 1992 p 37-39 (For primary document see N92-31222 21-88)
Avail: CASI HC A01/MF A01

N92-31234*# Scripps Institution of Oceanography, La Jolla, CA.
IS THE VENUSIAN LITHOSPHERE SUBDUCTING?
David T. Sandwell and Gerald Schubert (California Univ., Los Angeles.) *In* Lunar and Planetary Inst., Twenty-Third Lunar and Planetary Science Conference 1992 p 40-46 (For primary document see N92-31222 21-88)
Avail: CASI HC A02/MF A01

N92-31235*# Jet Propulsion Lab., California Inst. of Tech., Pasadena.
SCIENCE QUESTIONS FOR THE MAGELLAN CONTINUING MISSION
R. S. Saunders and E. R. Stofan *In* Lunar and Planetary Inst., Twenty-Third Lunar and Planetary Science Conference 1992 p 47-48 (For primary document see N92-31222 21-88)
Avail: CASI HC A01/MF A01

N92-31237*# National Astronomy and Ionosphere Center, Arecibo, Puerto Rico.
DISCOVERY OF TWO PLANETS AROUND A MILLISECOND PULSAR
A. Wolszczan *In* Lunar and Planetary Inst., Twenty-Third Lunar and Planetary Science Conference 1992 p 53-55 Sponsored in part by NSF Prepared in cooperation with Arecibo Ionospheric Observatory, Puerto Rico (For primary document see N92-31222 21-88)
Avail: CASI HC A01/MF A01

92 SOLAR PHYSICS

Includes solar activity, solar flares, solar radiation and sunspots.

For related information see *93 Space Radiation.*

N92-30797# Oak Ridge National Lab., TN.
NEW SHORTWAVE SOLAR RADIOMETER WITH INFORMATION-BASED SPARSE SAMPLING
M. L. Simpson, C. L. Carnal, M. N. Ericson, D. D. Falter, K. G. Falter, G. E. Jellison, Jr., R. C. Kryter, S. R. Maddox, J. K. Munro, and J. M. Rochelle et al 1991 31 p Presented at the ARM Science Team Conference, Denver, CO, 26-30 Oct. 1991
(Contract DE-AC05-84OR-21400)
(DE92-010483; CONF-9110336-2) Avail: CASI HC A03/MF A01

A new concept for a real-time shortwave solar radiometer is presented, based on the premise that high resolution measurements of the shortwave solar spectrum are needed only in wavelength regions where the atmospheric physics are changing rapidly with respect to lambda. The design features holographic optical elements (HOE's) for nonuniform sampling of the spectrum, customized photocells, and temperature-compensated monolithic wide dynamic range amplifiers. Preliminary results show full spectrum reconstruction accuracies to less than 3 percent with a 10:1 reduction in the number of photocells required. DOE

N92-31162*# Southwest Research Inst., San Antonio, TX. Instrumentation and Space Research Div.
DYNAMICS AND ENERGETICS OF THE SOLAR CORONA Final Technical Report, Sep. 1989 - Aug. 1992
R. S. Steinolfson Aug. 1992 6 p
(Grant NAGw-2087; SwRI Proj. 15-3619)
(NASA-CR-190664; NAS 1.26:190664) Avail: CASI HC A02/MF A01

The primary objective of this research program is to improve our understanding of the dynamics and energetics of the solar corona both in the quiescent dynamic equilibrium state when coronal structure is dominated by the equatorial streamer belt and in the eruptive state when coronal plasma is ejected into the interplanetary medium. Numerical solutions of the time-dependent magnetohydrodynamic (MHD) equations and comparisons of the computed results with observations form the core of the approach to achieving this objective. Some of the specific topics that have been studied are: (1) quiescent coronal streamers in an atmosphere dominated by a dipole magnetic field at large radii, (2) the formation of coronal mass ejections (CMEs) in quiescent streamers due to the emergence of new magnetic flux and due to photospheric shear motion, (3) MHD shock formation near the leading edge of CMEs, (4) coronal magnetic arcade eruption as a result of applied photospheric shear motion, and (5) the three-dimensional structure of CMEs. Author

N92-31168*# Alabama Univ., Huntsville.
FNAS: THE MAGNETIC CONFIGURATION LEADING TO SOLAR FLARES Semiannual Report
Juan M. Fontenla 7 Jul. 1992 48 p
(Grant NAG8-874)
(NASA-CR-190522; NAS 1.26:190522) Avail: CASI HC A03/MF A01

We present a method for solving plasma magnetohydrodynamic (MHD) problems arising from the interaction of plasmas with magnetic fields in stellar atmospheres. Our approach, in contrast to previous methods, is not based on solving equations for the magnetic field and plasma velocity but rather studies the evolution of the electric current and density (and the related gas pressure). We have applied the method to several studies involving linearized departures from static, current-free equilibria. The applications show explicit solutions for cases found in astrophysics and to problems encountered with earlier studies where the gas pressure was neglected. The method is particularly well suited for studying situations which involve a transition between high and low plasma-beta regions. It shows precisely how electric currents, and magnetic free-energy, build up in the plasma as a result of the slow stressing of a potential magnetic field configuration. The method also demonstrates how transverse-current waves, a mix of Alfven and magneto-acoustic modes, propagate in a low-beta plasma for any density stratification and background field geometry. Author

N92-31199# Washington Univ., Seattle.
SOLAR NEUTRINOS: THEORETICAL STATUS
W. C. Haxton 1991 12 p Presented at the 2nd Astrofundamental Physics Topics International Workshop on Theoretical and Phenomenological Aspects of Underground Physics, Erice, Italy, 1-8 Sep. 1991 and Toledo, Spain, 9-13 Sep. 1991
(Contracts DE-FG06-88ER-40427; DE-FG06-90ER-40561)
(DE92-014014; DOE/ER-40427/37-N91; CONF-9109378-1; CONF-9109182-4) Avail: CASI HC A03/MF A01

I review the standard solar model, the disparities between its predictions and the solar neutrino flux measurements of the Homestake and Kamioka 2 collaborations, and possible particle physics resolutions of this puzzle. The effects of matter, including density fluctuations and turbulence, on solar neutrino oscillations are explained by building analogies with more familiar atomic physics phenomena. These and other mechanisms are considered as possible explanations for time variations in the solar neutrino flux. Finally, I consider possible outcomes and implications of the SAGE/GALLEX gallium experiments. DOE

N92-31206# Midwest Research Inst., Golden, CO.
SHINING ON: A PRIMER ON SOLAR RADIATION DATA
M. A. Dunlap, ed. and G. Cook, ed. May 1992 27 p
(Contract DE-AC02-83CH-10093)
(DE92-010555; NREL/TP-463-4856) Avail: CASI HC A03/MF A01

This document is a primer on solar radiation data. General uses of solar energy are presented. The manner in which solar radiation data is used to aid engineers in optimizing the use of solar thermal conversion and photovoltaic conversion is discussed. Methods for acquiring and assimilating the solar radiation data are illustrated. This would include the design and use of pyranometers and pyrheliometers. Seasonal and geographical variations in solar flux reaching the earth are evaluated. Other uses of compiled data include the determination of meteorological impacts of atmospheric disturbances such as volcano eruptions. DOE

N92-31231*# California Univ., San Diego. Dept. of Chemistry.
ON THE ISOTOPIC SIGNATURE OF RECENT SOLAR-WIND NITROGEN
Y. Kim, J. S. Kim, K. Marti, and J. F. Kerridge *In* Lunar and Planetary Inst., Twenty-Third Lunar and Planetary Science Conference 1992 p 34-35 (For primary document see N92-31222 21-88)
Avail: CASI HC A01/MF A01

93 SPACE RADIATION

Includes cosmic radiation; and inner and outer earth's radiation belts.

For biological effects of radiation see *52 Aerospace Medicine*. For theory see *73 Nuclear and High-Energy Physics*.

N92-30627# Los Alamos National Lab., NM.
ULTRA HIGH ENERGY GAMMA RAYS AND OBSERVATIONS WITH CYGNUS/MILAGRO
D. D. Weeks and G. B. Yodh 1992 14 p Presented at the Physics of Isolated Pulsars Workshop, Taos, NM, 23-28 Feb. 1992
(Contract W-7405-eng-36)
(DE92-015243; LA-UR-92-1545; CONF-9202117-1) Avail: CASI HC A03/MF A01

This talk discusses high-energy observations of the Crab pulsar/nebula and the pulsar in the x ray binary, Hercules X-1, and makes the case for continued observations with ground-based gamma ray detectors. The CYGNUS Air Shower Array has a wide field of view and monitors several astrophysical gamma-ray sources at the same time, many of which are prime objects observed by the Compton Gamma Ray Observatory (GRO) and air Cerenkov telescopes. This array and the future MILAGRO Water Cerenkov Detector can perform observations that are simultaneous with similar experiments to provide confirmation of emission, and can measure source spectra at a range of high energies previously unexplored. DOE

N92-30706# Los Alamos National Lab., NM.
THE ESCAPE OF GREATER MeV PHOTONS FROM COSMOLOGICAL GAMMA-RAY BURSTS
E. E. Fenimore, R. I. Epstein, and C. Ho 1992 11 p Presented at the Recent Advanced in High Energy Astronomy, Toulouse, France, 17-22 Mar. 1992
(Contract W-7405-eng-36)
(DE92-013545; LA-UR-92-1231; CONF-9203151-1) Avail: CASI HC A03/MF A01

The recent BATSE result indicates that gamma-ray bursts may be at cosmological distances. As such one must reconcile the high photon densities with the observations of spectra to energies well above the pair production threshold. We have investigated two models of relativistic flows that could provide the requiste beaming to allow the escape of 100 MeV photons: a stationary relativistic wind with a photosphere and a relativistic expanding shell. For typical cosmological gamma-ray burst parameters, the expanding shell model requires a Lorentz factor (gamma) of only 10(exp 2) compared with 3(10)(exp 2) to 10(exp 3) for the relativistic wind. For the expanding shell model, events separated in time at the central source produce peaks observed to be separated by the same time. However, the shape and duration of the peaks are determined by the expansion. The expansion can occur over a much longer time (by gamma(exp 2)) then the duration that the observer sees so gamma-ray burst could be larger than 10(exp 2) light-seconds. We have made two crucial assumptions that require further study. The spectrum was assumed to a be a power law and a two component power law or a power law with a high-energy cut-off would decrease the required gamma. The expanding shell model uses an infinitely thin emitting surface and one with a finite thickness could increase the required gamma. DOE

N92-30828# Fermi National Accelerator Lab., Batavia, IL.
IDEAS FOR A LONG-BASELINE NEUTRINO DETECTOR
R. Bernstein Feb. 1992 12 p Presented at the Workshop on Long-Baseline Neutrino Oscillations, Batavia, IL, 17-20 Nov. 1991
(Contract DE-AC02-76CH-03000)
(DE92-010650; FNAL/C-92/63; CONF-9111141-5) Avail: CASI HC A03/MF A01

The Atmospheric Neutrino Deficit defines a region in (Delta)m(sup 2)-sin(sup 2)2(theta) space which ought to be conclusively tested in a long-baseline experiment. This talk sets out a region to cover (which may change as more data is analyzed)

and translates that region into an L/E. I present exclusion curves for different experiments based on their distance and their precision; I conclude that an experiment which can detect oscillations down to 1 percent located at 1200 km will cleanly test the allowed region from Kamioka and IMB. I then describe the techniques which can perform such a measurement and outline both a detector capable of performing such an experiment and some of the systematic problems we might expect. DOE

99 GENERAL

N92-30327# Research and Development Labs., Culver City, CA.
THE 1991 SUMMER FACULTY RESEARCH PROGRAM (SFRP), VOLUME 4 ATORY Report, 30 Sep. 1990 - 30 Sep. 1991
Gary Moore 9 Jan. 1992 662 p
(Contract F49620-90-C-0076)
(AD-A248766; AFOSR-92-0170TR-Vol-4) Avail: CASI HC A99/MF A06

The purpose of this program are as follows: (1) to develop the basis for continuing research of interest to the Air Force at the institution of the faculty member; (2) to stimulate continuing relations among faculty members and professional peers in the Air Force; (3) to enhance the research interests and capabilities of scientific and engineering educators; and (4) to provide follow-on funding for research of particular promise that was started at an Air Force laboratory under the Summer Faculty Research Program. During the summer of 1991, 170 university faculty conducted research at Air Force laboratories for a period of 10 weeks. Each participant provided a report of their research, and these reports are consolidated into this annual report. GRA

N92-30733*# National Aeronautics and Space Administration. Langley Research Center, Hampton, VA.
RESEARCH AND TECHNOLOGY, 1991. LANGLEY RESEARCH CENTER
Feb. 1992 283 p Original contains color illustrations
(NASA-TM-4331; L-17018; NAS 1.15:4331) Avail: CASI HC A13/MF A03; 28 functional color pages

The mission of the NASA Langley Research Center is to increase the knowledge and capability of the United States in a full range of aeronautics disciplines and in selected space disciplines. This mission will be accomplished by performing innovative research relevant to national needs and Agency goals, transferring technology to users in a timely manner, and providing development support to other United States Government agencies, industry, and other NASA centers. Highlights are given of the major accomplishments and applications that have been made during the past year. The highlights illustrate both the broad range of the research and technology (R&T) activities at NASA Langley Research Center and the contributions of this work toward maintaining United States leadership in aeronautics and space research. Author

N92-30768# Aeronautical Research Labs., Melbourne (Australia).
[ACTIVITIES OF THE AERONAUTICAL RESEARCH LABORATORY] Annual Report, 1990-1991
1991 60 p Original contains color illustrations
Avail: CASI HC A04/MF A01; 35 functional color pages

The annual report of the Aeronautical Research Laboratory (Australia) is given. Topics covered include research in flight mechanics, propulsion, aircraft materials, aircraft structures, aircraft systems, and corporate services. Author

N92-30996 Institut d'Aeronomie Spatiale de Belgique, Brussels.
ASTRONAUTICS 1977-1990 [ASTRONAUTIQUE 1977-1990]
J. Vercheval 1991 300 p In FRENCH
(Aeronomica-Acta-F-42-1991; ETN-92-91705) Avail: Institut d'Aeronomie Spatiale de Belgique, 3 Avenue Circulaire, B-1180 Brussels, Belgium

The annual activities in the field of astronautics from 1977 until 1990 are described. Emphasis is placed on the scientific missions as well as the manned flights. An alphabetical list of satellites with their orbital elements and other essential data are pointed out in each annual balance. ESA

Typical Subject Index Listing

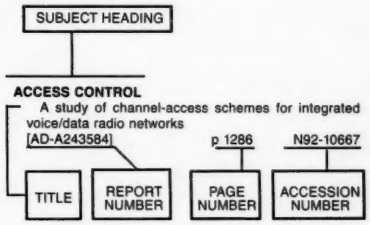

The subject heading is a key to the subject content of the document. Titles, report numbers, and accession numbers of pertinent documents are provided under each subject heading. When the title is insufficiently descriptive of the document content, a title extension has been added, separated from the title by three hyphens. The report number helps to indicate the type of document cited (e.g., NASA report, NASA translation, NASA contractor report). The accession number is the number by which the document abstracts are arranged in this journal and by which the document is sold or requested. The page number helps you locate the the citation in the abstract section. The titles, with title extensions if present, are arranged under each subject heading in ascending accession number order. The subject headings have been selected from the latest revision of the *NASA Thesaurus*.

A

A-320 AIRCRAFT
Preparation for a new plane (A 320): Experience reviewed p 3697 N92-30954
Flight crew integration in the maintenance chain of a commercial aircraft (A 320) p 3698 N92-30957

ABEL FUNCTION
Some model theory of free groups and free algebras [AD-A249425] p 3706 N92-30776

ABLATION
Ablative shielding for hypervelocity projectiles [NASA-CASE-MSC-21884-1] p 3602 N92-30539

ABLATIVE MATERIALS
Eye/sensor protection against laser irradiation ablative mirror devices: A materials assessment [AD-A248787] p 3688 N92-30615

ABSORPTION
Polarization effects in pi(+) absorption in He-3 [ITN-92-85164] p 3714 N92-30580
Polarization effects in pi(+) absorption in He-4 [ITN-92-85163] p 3715 N92-30780

ABSORPTION SPECTRA
Vibrational overtone spectroscopy of gaseous metallocenes [AD-A251088] p 3593 N92-30245
Microscopic theory of THG and electro-absorption in conjugated polymers [DE92-014786] p 3604 N92-30792
Infrared investigations of pristine, doped and partially-doped polypyrrole [AD-A250644] p 3605 N92-30838

ABSORPTION SPECTROSCOPY
Comparison of eye-safe solid state laser DIAL with passive gas filter correlation measurements from aircraft and spacecraft p 3647 N92-31060
Spectroscopic method for Earth-satellite-Earth laser long-path absorption measurements using Retroreflector In Space (RIS) p 3652 N92-31088

ABSORPTIVITY
Optimum methods for the measurement of the absorption coefficients of materials [BBC-RD-1992/3] p 3711 N92-31173

AC GENERATORS
Dynamic analysis of compact helical system power supply and designs of its upgrade [NIFS-TECH-2] p 3723 N92-30497

ACCELERATED LIFE TESTS
In-service evaluation of 2090 aluminum-lithium alloy on F/A-18 aircraft [AD-A248472] p 3607 N92-30321

ACCELERATION (PHYSICS)
Tolerance of beta blocked hypertensives during orthostatic and altitude stresses [AD-A249904] p 3685 N92-30745

ACCELEROMETERS
Development of and flight results from the Space Acceleration Measurement System (SAMS) [NASA-TM-105652] p 3588 N92-30301

ACCRETION DISKS
Modeling of UV lines from cataclysmic variable winds [DE92-013443] p 3739 N92-30862

ACETYLENE
Photodissociation of azulene under UV-laser irradiation at 325 nm [AD-A251093] p 3613 N92-30246
Synthesis and reactivity of 1-methyl-e-ethynylpyridinium triflate [AD-A250638] p 3602 N92-30346
Thermoset precursor to monolithic carbon glass prepared by the Pd/Cu-catalyzed alkynylation of polyphenylenes [AD-A249920] p 3605 N92-30816
Computational simulation of diamond chemical vapor deposition in premixed C2H2/O2/H2 and CH4/O2 strained flames [DE92-012144] p 3606 N92-30857

ACID RAIN
Status of selected air pollution control programs, February 1992 [PB92-171966] p 3673 N92-30561

ACIDS
A method for the production of weakly acidic cation exchange resins [DE92-015314] p 3717 N92-31137

ACOUSTIC DUCTS
Resonant instability of supersonic shear layers p 3632 N92-30661

ACOUSTIC EMISSION
Five experiments in materials science for less than $10.00 p 3611 N92-30283
Wave propagation and vibration of fibre-reinforced laminates [AD-A252101] p 3590 N92-30528
Prediction of coincidence frequencies for a thin-walled, fluid-filled pipe [MRL-TN-600] p 3664 N92-30963
An investigation of the effects of boundary constraints on the sound insulations of lightweight, double leaf partitions [BBC-RD-1992/4] p 3711 N92-31151

ACOUSTIC FATIGUE
Acoustic fatigue life prediction for nonlinear structures with multiple resonant modes [NASA-CR-190471] p 3664 N92-30988

ACOUSTIC FREQUENCIES
Optimum methods for the measurement of the absorption coefficients of materials [BBC-RD-1992/3] p 3711 N92-31173

ACOUSTIC MEASUREMENT
Digital bottom mapping [AD-D015238] p 3682 N92-30413
Optimum methods for the measurement of the absorption coefficients of materials [BBC-RD-1992/3] p 3711 N92-31173

ACOUSTIC MICROSCOPES
Tunneling acoustic microscopy [AD-A251028] p 3727 N92-30252

ACOUSTIC PROPAGATION
Resolution of the three-dimensional parabolic equation applied to acoustic propagation at low altitudes [ONERA-RF-17/3641-PY] p 3711 N92-30966

ACOUSTIC PROPERTIES
Prediction of coincidence frequencies for a thin-walled, fluid-filled pipe [MRL-TN-600] p 3664 N92-30963

ACOUSTIC VELOCITY
Active control of pressure, sound and velocity of centrifugal pumps [AD-A249446] p 3659 N92-30640

ACOUSTICS
Wave propagation and vibration of fibre-reinforced laminates [AD-A252101] p 3590 N92-30528
Remote sensing for the Lincoln Sea Winterover Experiment [AD-A252117] p 3667 N92-30545
Combustion diagnostics by photo-deflection spectroscopy [AD-A250802] p 3594 N92-30645
Prediction of coincidence frequencies for a thin-walled, fluid-filled pipe [MRL-TN-600] p 3664 N92-30963

ACOUSTO-OPTICS
Remote sensing for the Lincoln Sea Winterover Experiment [AD-A252117] p 3667 N92-30545
Acousto-optic filtering of lidar signals p 3650 N92-31077

ACRYLONITRILES
A method for the production of weakly acidic cation exchange resins [DE92-015314] p 3717 N92-31137

ACTIVATION
Epoxides as activators for grafting of poly(tetrahydrofuran) from poly(methylphenylsilylene) [AD-A251086] p 3601 N92-30244

ACTIVATION ANALYSIS
Analysis, review, and documentation of the activation data from LDEF material [NASA-CR-184356] p 3596 N92-31161

ACTIVE CONTROL
Computational methods for modeling and active control of distributed parameter systems [AD-A248559] p 3705 N92-30638
Active control of pressure, sound and velocity of centrifugal pumps [AD-A249446] p 3659 N92-30640
The optimization of force inputs for active structural acoustic control using a neural network [NASA-TM-107627] p 3711 N92-30979
Cryogenic Magnetic Bearing Test Facility (CMBTF) [NASA-CR-189087] p 3582 N92-31164

ACTIVITY (BIOLOGY)
Photoinitiated electron transfer in multichromophoric species: Synthetic tetrads and pentads featuring diquinone moieties [DE92-013472] p 3683 N92-30368

ACTS
The ACTS multibeam antenna [NASA-TM-105645] p 3587 N92-30383
Personal communications via ACTS satellite HBR transponders p 3618 N92-30929
A personal communications network using a Ka-band satellite p 3619 N92-30934

ACTUATORS
An electromechanical actuation system for an expendable launch vehicle [NASA-TM-105774] p 3586 N92-30310
Relaxor ferroelectrics for electrostrictive transducer [AD-A248671] p 3624 N92-30598
Nonlinear stability and control study of highly maneuverable high performance aircraft, phase 2 [NASA-CR-190667] p 3583 N92-30922
The optimization of force inputs for active structural acoustic control using a neural network [NASA-TM-107627] p 3711 N92-30979
An analytical and experimental investigation of flutter suppression via piezoelectric actuation [NASA-TM-107653] p 3580 N92-31174

ADA (PROGRAMMING LANGUAGE)
A model of the ADA avionics real-time system: An example of the benefits of the hardware/software codesign approach in development of real-time systems
[AD-A248893] p 3581 N92-30524
Development statistics for the UH-1 Ada feasibility study
[AD-A252404] p 3584 N92-30547
EASAMS' Ariane 5 on-board software experience
[D308/TN/001] p 3586 N92-30715
ADAPTIVE CONTROL
Nonlinear stability and control study of highly maneuverable high performance aircraft, phase 2
[NASA-CR-190667] p 3583 N92-30922
ADDING CIRCUITS
Repetitive High Energy Pulsed Power (RHEPP) temperature monitoring system utilizing Luxtron fluoroptic sensors and thermocouples technical reference manual
[DE92-013461] p 3637 N92-30893
ADDITIVES
High-temperature ignition of propane with MTBE as an additive: Shock-tube experiments and modeling
[DE92-006679] p 3594 N92-30749
Infrared investigations of pristine, doped and partially-doped polypyrrole
[AD-A250644] p 3605 N92-30838
ADDUCTS
Studies of thermal decomposition of the 1:1 R3Al:en adduct (R = Me, Et; en = ethylenediamine): Synthesis and structure of a novel intermediate Al((HNCH2CH2NH)AlMe2)3
[AD-A251061] p 3603 N92-30623
ADENOSINE TRIPHOSPHATE
The properties of the uptake system for glycine in synaptic vesicles
[ISSN-0800-4412] p 3683 N92-31152
ADHESIVE BONDING
Ultrasound NDE of adhesive bond integrity: A quantitative measure
[AD-A248845] p 3661 N92-30599
Laser induced reaction for pre-bond surface preparation of aluminum alloys
[AD-A249916] p 3598 N92-30872
ADIABATIC CONDITIONS
Development of a modular transient cycle analysis program for the adiabatic diesel and other compound diesel engines
[AD-A249022] p 3658 N92-30538
ADRENAL GLAND
Secretory mechanisms in opiocortin cells during cold stress
[AD-A252317] p 3685 N92-30719
ADSORBENTS
Study of the surface properties of ceramic materials by chromatography
[DE92-011129] p 3604 N92-30695
ADSORPTION
Study of the surface properties of ceramic materials by chromatography
[DE92-011129] p 3604 N92-30695
High resolution electron energy loss studies of surface vibrations
[DE92-014608] p 3626 N92-30901
ADVANCED VERY HIGH RESOLUTION RADIOMETER
Vegetation conditions and yield indicators. Part 1: Main report
[BCRS-91-26-PT-1] p 3667 N92-30471
ECLIPS at LMD: Preliminary results of phase 2
p 3643 N92-31038
AERIAL PHOTOGRAPHY
Fractal analysis: A new remote sensing tool for lava flows p 3736 N92-31224
AERODYNAMIC CHARACTERISTICS
Influence of structural and aerodynamic modeling on flutter analysis and structural optimization
[AD-A248487] p 3583 N92-30323
Joint computational and experimental aerodynamics research on a hypersonic vehicle
[DE92-013439] p 3574 N92-30367
Two-dimensional aerodynamic characteristics of several polygon-shaped cross-sectional models applicable to helicopter fuselages
[NASA-TP-3233] p 3574 N92-30394
Lewis icing research tunnel test of the aerodynamic effects of aircraft ground deicing/anti-icing fluids
[NASA-TP-3238] p 3577 N92-30395
Vortex flow aerodynamics
[AGARD-AR-299] p 3576 N92-30947
A demonstration of passive blade twist control using extension-twist coupling
[NASA-TM-107642] p 3664 N92-31155
Extension of the integral equation formulation of linearized time dependent subsonic flow
[AD-A250654] p 3577 N92-31171
AERODYNAMIC COEFFICIENTS
Preliminary subsonic aerodynamic model for simulation studies of the HL-20 lifting body
[NASA-TM-4302] p 3583 N92-31175
AERODYNAMIC HEATING
Space station trash removal system
[NASA-CASE-MSC-21723-1] p 3588 N92-30315
AERODYNAMIC LOADS
Yaw dynamics of horizontal axis wind turbines
[DE92-001245] p 3670 N92-30837
Vortex flow aerodynamics
[AGARD-AR-299] p 3576 N92-30947
AERODYNAMICS
Selection of opening model for parachute scaling studies
[AD-A250882] p 3573 N92-30239
Ultra high bypass Nacelle aerodynamics inlet flow-through high angle of attack distortion test
[NASA-CR-189149] p 3574 N92-30298
Research and technology, 1991. Langley Research Center
[NASA-TM-4331] p 3744 N92-30733
Yaw dynamics of horizontal axis wind turbines
[DE92-001245] p 3670 N92-30837
Nonlinear stability and control study of highly maneuverable high performance aircraft, phase 2
[NASA-CR-190667] p 3583 N92-30922
Nonlinear aerodynamics and the design of wing tips
[NASA-CR-190649] p 3577 N92-31157
AEROELASTIC RESEARCH WINGS
Extension of the integral equation formulation of linearized time dependent subsonic flow
[AD-A250654] p 3577 N92-31171
AEROELASTICITY
Modeling and analysis methodology for aeroelastically tailored chordwise deformable wings
[NASA-CR-189620] p 3579 N92-30304
Influence of structural and aerodynamic modeling on flutter analysis and structural optimization
[AD-A248487] p 3583 N92-30323
MBB-LAGRANGE: A general structural reliability and optimization structural system
[MBB/FW321/S/PUB/467] p 3662 N92-30423
Composite beam analysis linear analysis of naturally curved and twisted anisotropic beams
[AD-A252652] p 3663 N92-30766
An analytical and experimental investigation of flutter suppression via piezoelectric actuation
[NASA-TM-107653] p 3580 N92-31174
AERONAUTICAL ENGINEERING
Numerical optimization in Germany: A non-exhaustive survey on current activities with emphasis on aeronautics
[MBB/FE211/S/PUB/474] p 3573 N92-30675
AERONAUTICAL SATELLITES
Characteristics of a future aeronautical satellite communications system p 3618 N92-30932
Aeronautical Mobile Satellite Service (AMSS) capacity analysis and protocol performance simulation results
[DOT/FAA/CT-TN90/64] p 3622 N92-31212
AERONOMY
The United States Antarctic Program
[NSF-90-97] p 3676 N92-30708
AEROSOLS
Processing aerosols and filaments in a TM010 microwave cavity at 2.45 GHz
[DE92-013536] p 3615 N92-30703
Linkage of anthropogenic aerosol to clouds and climate
[DE92-013574] p 3674 N92-30707
Tropospheric and stratospheric wind profiling with a direct detection Doppler lidar p 3639 N92-31018
A compact high repetition rate CO2 coherent Doppler lidar p 3639 N92-31022
Phase noise in pulsed Doppler lidar and limitations on achievable single-shot velocity accuracy
p 3639 N92-31024
Multiple scattering technique lidar
p 3641 N92-31031
Analytical multiple scattering correction to the Mie theory: Application to the analysis of the lidar signal
p 3642 N92-31036
Advanced Raman water vapor lidar
p 3643 N92-31040
Measurement of aerosol profiles using high-spectral-resolution Rayleigh-Mie lidar
p 3644 N92-31046
Multiple scattering wavelength dependent backscattering of kaolin dust in the IR: Measurements and theory p 3648 N92-31064
Aureole lidar: Design, operation, and comparison with in-situ measurements p 3648 N92-31065
Effect of atmospheric extinction on laser rangefinder performance at 1.54 and 0.6 microns
p 3648 N92-31066
A considerable effect of stratospheric aerosol on lidar-detected ozone profile and a three-wavelength inversion technique for both ozone and aerosol
p 3651 N92-31080
Measurements of the backscattering phase matrices of crystal clouds with a polarization lidar
p 3651 N92-31083
Lidar sounding of ozone and aerosols
p 3652 N92-31085
Airborne water vapor DIAL research: System development and field measurements
p 3653 N92-31093
Aerosol extinction measurements with CO2-lidar
p 3655 N92-31105
Trace gas and aerosol transports into and out of the Amazon Basin
[NASA-CR-190624] p 3674 N92-31153
Ultrafine aerosol size distributions and sulfuric acid vapor pressures: Implications for new particle formation in the atmosphere
[DE92-015217] p 3675 N92-31183
AEROSPACE ENGINEERING
The 1991 Summer Faculty Research Program (SFRP), volume 4 atory
[AD-A248766] p 3744 N92-30327
Wiring for aerospace applications
[NASA-TM-105777] p 3623 N92-30427
Semiannual final report, 1 October 1991 - 31 March 1992
[NASA-CR-189660] p 3689 N92-30489
Trends in aeropropulsion research and their impact on engineering education
[NASA-TM-105682] p 3583 N92-31172
AEROSPACE ENVIRONMENTS
Electrical and chemical interactions at Mars Workshop, part 1
[NASA-CP-10093] p 3741 N92-30302
AEROSPACE INDUSTRY
The effect of information systems on middle management in the aerospace industry: The Westco case
[AD-A249017] p 3735 N92-30584
AEROSPACE MEDICINE
Aerospace medicine and biology: A continuing bibliography with indexes (supplement 363)
[NASA-SP-7011(363)] p 3685 N92-30987
AEROSPACE SYSTEMS
A description of the research for period 3 of a research program on the planning and control for space robotic manipulators
[NASA-CR-190243] p 3660 N92-30738
AEROSPACE VEHICLES
Development of software to improve AC power quality on large spacecraft
[NASA-CR-190569] p 3589 N92-30989
Advanced electromagnetic methods for aerospace vehicles
[NASA-CR-190650] p 3621 N92-31156
AGING (MATERIALS)
Five experiments in materials science for less than $10.00 p 3611 N92-30283
Isothermal aging effects on PMR-15 resin
[NASA-TM-105648] p 3593 N92-30986
AGRICULTURE
Development of the cultivated landscape of north west Germany under the human influence
[ETN-92-91730] p 3669 N92-30968
AIR
Temperature effect on the Langmuir-Blodgett polymerization of 2-pentadecylaniline
[AD-A250803] p 3601 N92-30250
AIR BREATHING ENGINES
Trends in aeropropulsion research and their impact on engineering education
[NASA-TM-105682] p 3583 N92-31172
AIR CARGO
Organic Matrix Composite Helicopter Internal/External Cargo Pallet System (OMC INTEX)
[AD-A251127] p 3580 N92-30878
AIR CONDUCTIVITY
Infrared investigations of pristine, doped and partially-doped polypyrrole
[AD-A250644] p 3605 N92-30838
AIR DEFENSE
Stealth: A revolutionary change to air warfare
[AD-A249880] p 3617 N92-30869
National airspace system. Air defense and law enforcement surveillance operational concept NAS-SR-135
[DOT/FAA/SE-92/3] p 3579 N92-31211
AIR FLOW
Method of measuring cross-flow vortices by use of an array of hot-film sensors
[NASA-CASE-LAR-14824-1-SB] p 3628 N92-30390

AIR LAW
National airspace system. Air defense and law enforcement surveillance operational concept NAS-SR-135
[DOT/FAA/SE-92/3] p 3579 N92-31211
AIR POLLUTION
Reducing greenhouse gas emissions in Czechoslovakia
[DE92-012354] p 3672 N92-30374
Development and testing of an air quality model for Mexico City
[DE92-011238] p 3673 N92-30520
Status of selected air pollution control programs, February 1992
[PB92-171966] p 3673 N92-30561
Report of the Great Lakes Air Toxics Research Priorities Workshop
[PB92-166933] p 3673 N92-30602
A portable lidar using a diode-pumped YAG laser p 3654 N92-31098
Lidar observation of marine mixed layer p 3655 N92-31104
The environmental dilemma of fossil fuels
[DE92-014887] p 3674 N92-31121
AIR QUALITY
Development and testing of an air quality model for Mexico City
[DE92-011238] p 3673 N92-30520
Airborne lidar mapping of vertical ozone distributions in support of the 1990 Clean Air Act Amendments p 3654 N92-31101
AIR TRANSPORTATION
The Eurofar program: An European overview on advanced VTOL civil transportation system
[MBB-UD-0611-91-PUB] p 3578 N92-30418
The allocation of cargo to channel missions
[DE92-013234] p 3578 N92-30565
Allocation and recovery of federal airport and airway costs, 1991
[AD-A249436] p 3585 N92-30777
AIR WATER INTERACTIONS
Boundary layer structure over the ocean observed by LEANDRE 1 during a tramontane event p 3638 N92-31014
AIRBORNE EQUIPMENT
Boundary layer structure over the ocean observed by LEANDRE 1 during a tramontane event p 3638 N92-31014
A compact high repetition rate CO2 coherent Doppler lidar p 3639 N92-31022
Simplified signal processing for an airborne CO2 Doppler lidar p 3639 N92-31023
Airborne lidar and radiometric observations of PBL- and low clouds p 3642 N92-31037
ECLIPS at LMD: Preliminary results of phase 2 p 3643 N92-31038
Airborne remote sensing of tropospheric water vapor using a near infrared DIAL system p 3644 N92-31042
Airborne water vapor DIAL research: System development and field measurements p 3653 N92-31093
Airborne lidar mapping of vertical ozone distributions in support of the 1990 Clean Air Act Amendments p 3654 N92-31101
AIRBORNE LASERS
Theoretical simulation of a 2 micron airborne solid state laser anemometer p 3647 N92-31059
AIRBORNE RADAR
Aureole lidar: Design, operation, and comparison with in-situ measurements p 3648 N92-31065
AIRCRAFT ACCIDENT INVESTIGATION
Examination of aircraft warning and caution lights after shock testing
[NLR-TP-89284-U] p 3578 N92-30474
Aircraft accident report: Explosive decompression - loss of cargo door in flight, United Airlines Flight 811, Boeing 747-122, N4713U, Honolulu, Hawaii, February 24, 1989
[PB92-910402] p 3578 N92-31159
AIRCRAFT ACCIDENTS
Aircraft accident report: Explosive decompression - loss of cargo door in flight, United Airlines Flight 811, Boeing 747-122, N4713U, Honolulu, Hawaii, February 24, 1989
[PB92-910402] p 3578 N92-31159
AIRCRAFT COMMUNICATION
Proceedings of the Workshop on Advanced Network and Technology Concepts for Mobile, Micro, and Personal Communications
[NASA-CR-190459] p 3617 N92-30923
AIRCRAFT CONFIGURATIONS
High speed research system study. Advanced flight deck configuration effects
[NASA-CR-189650] p 3581 N92-30965
Extension of the integral equation formulation of linearized time dependent subsonic flow
[AD-A250654] p 3577 N92-31171
AIRCRAFT CONSTRUCTION MATERIALS
Low-velocity impact loading on fibre reinforced aluminum laminates (ARALL) and other aircraft sheet materials
[ETN-92-91613] p 3590 N92-30414
Activities of the Aeronautical Research Laboratory p 3744 N92-30768
Organic Matrix Composite Helicopter Internal/External Cargo Pallet System (OMC INTEX)
[AD-A251127] p 3580 N92-30878
AIRCRAFT CONTROL
On-line analysis capabilities developed to support the AFW wind-tunnel tests
[NASA-TM-107651] p 3580 N92-30752
High speed research system study. Advanced flight deck configuration effects
[NASA-CR-189650] p 3581 N92-30965
Preliminary subsonic aerodynamic model for simulation studies of the HL-20 lifting body
[NASA-TM-4302] p 3583 N92-31175
AIRCRAFT DESIGN
Numerical investigations in three-dimensional internal flows
[NASA-CR-190498] p 3628 N92-30380
MBB-LAGRANGE: A general structural reliability and optimization structural system
[MBB/FW321/S/PUB/467] p 3662 N92-30423
Multidisciplinary optimization of fiber composite aircraft structures
[MBB/FW321/S/PUB/476] p 3579 N92-30424
High speed research system study. Advanced flight deck configuration effects
[NASA-CR-189650] p 3581 N92-30965
AIRCRAFT DETECTION
National airspace system. Air defense and law enforcement surveillance operational concept NAS-SR-135
[DOT/FAA/SE-92/3] p 3579 N92-31211
AIRCRAFT ENGINES
Statistics on aircraft gas turbine engine rotor failures that occurred in US commercial aviation during 1989
[DOT/FAA/CT-92/5] p 3581 N92-30303
Trends in aeropropulsion research and their impact on engineering education
[NASA-TM-105682] p 3583 N92-31172
AIRCRAFT EQUIPMENT
Evaluation of head impact kinematics for passengers seated behind interior walls
[AD-A252651] p 3578 N92-30551
A cable detection lidar system for helicopters p 3648 N92-31068
AIRCRAFT GUIDANCE
High speed research system study. Advanced flight deck configuration effects
[NASA-CR-189650] p 3581 N92-30965
AIRCRAFT HAZARDS
A cable detection lidar system for helicopters p 3648 N92-31068
AIRCRAFT INDUSTRY
Research and technology, 1991. Langley Research Center
[NASA-TM-4331] p 3744 N92-30733
AIRCRAFT INSTRUMENTS
The rise of active-element phased-array radar
[RAND-P-7747-RGS] p 3616 N92-30755
AIRCRAFT LANDING
Trial of a slant visual range measuring device p 3644 N92-31043
AIRCRAFT MAINTENANCE
Model analysis and expert system development for planning and scheduling teleoperations for aircraft turnaround functions, volume 1
[AD-A251037] p 3573 N92-30253
Model analysis and expert system development for planning and scheduling teleoperations for aircraft turnaround functions. Volume 2: Top user's guide
[AD-A251083] p 3573 N92-30258
Laser induced fluorescence detection of gums in jet fuels
[AD-A252685] p 3607 N92-30767
Flight crew integration in the maintenance chain of a commercial aircraft (A 320) p 3698 N92-30957
GNAS Maintenance Control Center (GMCC) Design Qualification Test and Evaluation (DQT/E) test procedures
[DOT/FAA/CT-TN91/40] p 3585 N92-30976
AIRCRAFT MODELS
Model analysis and expert system development for planning and scheduling teleoperations for aircraft turnaround functions, volume 1
[AD-A251037] p 3573 N92-30253
Model analysis and expert system development for planning and scheduling teleoperations for aircraft turnaround functions. Volume 2: Top user's guide
[AD-A251083] p 3573 N92-30258
Two-dimensional aerodynamic characteristics of several polygon-shaped cross-sectional models applicable to helicopter fuselages
[NASA-TP-3233] p 3574 N92-30394
AIRCRAFT PILOTS
Introduction to cognitive processes of expert pilots
[DOT/FAA/RD-92/12] p 3578 N92-30980
AIRCRAFT PRODUCTION
High-speed civil transport issues and technology program
[NASA-CR-186020] p 3580 N92-31208
AIRCRAFT SAFETY
Evaluation of head impact kinematics for passengers seated behind interior walls
[AD-A252651] p 3578 N92-30551
Aircraft accident report: Explosive decompression - loss of cargo door in flight, United Airlines Flight 811, Boeing 747-122, N4713U, Honolulu, Hawaii, February 24, 1989
[PB92-910402] p 3578 N92-31159
AIRCRAFT STABILITY
Nonlinear stability and control study of highly maneuverable high performance aircraft, phase 2
[NASA-CR-190667] p 3583 N92-30922
Vortex flow aerodynamics
[AGARD-AR-299] p 3576 N92-30947
AIRCRAFT STRUCTURES
In-service evaluation of 2090 aluminum-lithium alloy on F/A-18 aircraft
[AD-A248472] p 3607 N92-30321
MBB-LAGRANGE: A general structural reliability and optimization structural system
[MBB/FW321/S/PUB/467] p 3662 N92-30423
Multidisciplinary optimization of fiber composite aircraft structures
[MBB/FW321/S/PUB/476] p 3579 N92-30424
Activities of the Aeronautical Research Laboratory p 3744 N92-30768
AIRFOILS
Numerical calculations of two-dimensional single and multi-material flow fields with CCICE
[DE92-015778] p 3636 N92-30903
AIRLINE OPERATIONS
A principled approach to the measurement of situation awareness in commercial aviation
[NASA-CR-4451] p 3686 N92-30306
AIRPORTS
Potential airfield sites in Antarctica for wheeled aircraft
[AD-A249503] p 3584 N92-30621
Allocation and recovery of federal airport and airway costs, 1991
[AD-A249436] p 3585 N92-30777
GNAS Maintenance Control Center (GMCC) Design Qualification Test and Evaluation (DQT/E) test procedures
[DOT/FAA/CT-TN91/40] p 3585 N92-30976
Trial of a slant visual range measuring device p 3644 N92-31043
AIRSPEED
Theoretical simulation of a 2 micron airborne solid state laser anemometer p 3647 N92-31059
ALASKA
Ice thickness observations, North American Arctic and subarctic, 1972-1973 and 1973-1974, part 8
[AD-A250830] p 3681 N92-30238
ALERTNESS
Light as a chronobiologic countermeasure for long-duration space operations
[NASA-TM-103874] p 3686 N92-31167
ALGEBRA
On impasse points of quasilinear differential algebraic equations
[AD-A252643] p 3702 N92-30410
Quantum Weyl Group and universal quantum R-matrix for affine Lie algebra A1
[PB92-178276] p 3704 N92-30511
Parallel aspects of some spectral problems in linear algebra
[CWI-NM-R9113] p 3706 N92-30700
Non-holonomic filtration: Algebraic and geometric aspects of non-integrability
[PB92-178003] p 3706 N92-30790
ALGORITHMS
Modeling of video traffic in packet networks, low rate video compression, and the development of a lossy+lossless image compression algorithm
[NASA-CR-190546] p 3691 N92-30296
Survivable algorithms and redundancy management in NASA's distributed computing systems
[NASA-CR-189827] p 3691 N92-30299
A space-time neural network for processing both spacial and temporal data
[NASA-CASE-MSC-21874-1] p 3700 N92-30314
Algorithm to solve nonlinear time dependent problems of engineering and physics
[AD-A250641] p 3702 N92-30347

A survey on pivot rules for linear programming
[REPT-91-99] p 3691 N92-30351
Degeneracy in interior point methods for linear programming
[REPT-91-102] p 3691 N92-30353
New transient and pseudo-transient algorithms for viscoelastic materials
[AD-A250642] p 3692 N92-30377
How to securely replicate services
[NASA-CR-190476] p 3692 N92-30379
Achievable potential reductions in the method of Kojima et al. in the case of linear programming
[REPT-91-78] p 3693 N92-30435
GMRESR: A family of nested GMRES methods
[REPT-91-80] p 3703 N92-30437
Computing and verifying depth orders
[RUU-CS-91-41] p 3693 N92-30443
Classifying termination of term rewriting
[RUU-CS-91-42] p 3693 N92-30444
A protocol scheme for a class of minimum delay routing algorithms
[RUU-CS-91-43] p 3693 N92-30445
Linear planar augmentation algorithms for outerplanar graphs
[RUU-CS-91-47] p 3703 N92-30449
A multigrid method for a discretization of the incompressible Navier-Stokes equations in general coordinates
[REPT-91-73] p 3629 N92-30454
Iri's polynomiality proof for the Iri-Imai method recast
[REPT-91-74] p 3693 N92-30455
Further experiences with GMRESR
[REPT-92-12] p 3704 N92-30461
A robust multigrid method for a discretization of the incompressible Navier-Stokes equations in general coordinates
[REPT-92-14] p 3629 N92-30462
Maintenance of 2- and 3-connected components of graphs. Part 1: 2- and 3-edge-connected components
[RUU-CS-90-26-PT-1] p 3694 N92-30479
Maintenance of 2- and 3-connected components of graphs. Part 2: 2- and 3-edge-connected components and 2-vertex-connected components
[RUU-CS-90-27-PT-2] p 3694 N92-30480
A bibliography on network flow problems (2nd edition)
[RUU-CS-91-38] p 3698 N92-30482
Configuration algorithms for hierarchical supernode machines
[IMAG-RR-853-I] p 3694 N92-30493
On the potential use of the terminal Doppler weather radar gust front detection algorithm on the WSR-88D system. Part 1: Impacts of radar system differences
[DOT/FAA/NR-92/8,I] p 3678 N92-30495
On the potential use of the terminal Doppler weather radar gust front detection algorithm on the WSR-88D system. Part 2: Detecting non-gust front convergent weather phenomena
[DOT/FAA/NR-92/8,II] p 3678 N92-30496
A computational algorithm for crack determination: The multiple crack case
[NASA-CR-189665] p 3704 N92-30516
Computing with faulty shared memory
[DE92-011663] p 3695 N92-30522
Alignment of a 3-D sensor and a 2-D sensor measuring azimuth and elevation
[AD-A252120] p 3636 N92-30530
Implementation of parallel algorithms
[AD-A248826] p 3695 N92-30555
Doppler mean velocity estimation: Small sample analysis and a new estimator
[AD-A249024] p 3678 N92-30559
On the rapid evaluation of trigonometric series
[AD-A249029] p 3705 N92-30568
A gridless Euler/Navier-Stokes solution algorithm for complex two-dimensional applications
[NASA-TM-107631] p 3575 N92-30570
VLSI design, parallel computation, and distributed computing
[AD-A252349] p 3699 N92-30596
Clouds: Their prediction and simulation
[AD-A250643] p 3679 N92-30643
An extension to Schneider's general paradigm for fault-tolerant clock synchronization
[NASA-TM-107634] p 3699 N92-30677
Implicit upwind-Euler solution algorithms for unstructured-grid applications
[NASA-TM-107645] p 3575 N92-30691
Parallel aspects of some spectral problems in linear algebra
[CWI-NM-R9113] p 3706 N92-30700
Contribution of parallelism to solving a load distribution problem in electric networks
[ETN-92-91668] p 3625 N92-30702
Transactions of the 9th Army Conference on Applied Mathematics and Computing
[AD-A252140] p 3706 N92-30843
Characterizing ultrasonic transducers using pattern recognition techniques
[DE92-015845] p 3711 N92-30890
A strictly improving linear programming algorithm based on a series of Phase 1 problems
[DE92-015905] p 3696 N92-30905
Field studies in geophysical diffraction tomography
[DE92-015084] p 3677 N92-31009
Time and wavelength domain algorithms for chemical analysis by laser radar p 3650 N92-31075
Demonstration of a 3D vision algorithm for space applications
[NASA-CR-190646] p 3698 N92-31154
Verifying the interactive convergence clock synchronization algorithm using the Boyer-Moore theorem prover
[NASA-CR-189649] p 3700 N92-31158

ALIGNMENT
Alignment of a 3-D sensor and a 2-D sensor measuring azimuth and elevation
[AD-A252120] p 3636 N92-30530
Effects of the orientational pair correlation on second order nonlinear optical coefficients
[AD-A252490] p 3720 N92-30535
Double-sided wafer alignment techniques
[AD-A250757] p 3730 N92-30895

ALKALI METALS
Perforated monolayers
[DE92-011632] p 3593 N92-30344

ALKALIES
A method for the production of weakly acidic cation exchange resins
[DE92-015314] p 3717 N92-31137

ALKYL COMPOUNDS
Approaches to polymer curing and imaging via the in situ generation of a catalyst
[AD-A249917] p 3606 N92-30873
From minerals to materials: A facile synthetic route to preceramic polymers for aluminum oxide
[AD-A250351] p 3606 N92-31141

ALKYLATION
Synthesis and reactivity of 1-methyl-e-ethynylpyridinium triflate
[AD-A250638] p 3602 N92-30346

ALKYNES
Thermoset precursor to monolithic carbon glass prepared by the Pd/Cu-catalyzed alkynylation of polyphenylenes
[AD-A249920] p 3605 N92-30816

ALLOCATIONS
Allocation and recovery of federal airport and airway costs, 1991
[AD-A249436] p 3585 N92-30777

ALLOYS
Mechanism of slip and twinning p 3610 N92-30280

ALTERNATING CURRENT
Development of software to improve AC power quality on large spacecraft
[NASA-CR-190569] p 3589 N92-30989

ALTERNATING DIRECTION IMPLICIT METHODS
A boundary element alternating method for two-dimensional mixed-mode fracture problems
[NASA-CR-4460] p 3661 N92-30309
Fast methods to numerically integrate the Reynolds equation for gas fluid films
[NASA-TM-105415] p 3660 N92-30722

ALTIMETRY
Altimetry and lidar using AlGaAs lasers modulated with pseudo-random codes p 3641 N92-31030

ALTITUDE
Water vapor variance measurements using a Raman lidar p 3643 N92-31041

ALTITUDE SIMULATION
The use of tympanometry to detect aerotitis media in hypobaric chamber operations
[AD-A248963] p 3684 N92-30328

ALUMINUM
A comparative EIS study on cermet and platinum anodes for the electrolytic production of aluminum
[DE92-015091] p 3599 N92-31010
Eulerian simulation of the perforation of aluminum plates by nondeforming projectiles
[DE92-011515] p 3664 N92-31123
Environment modelling in near Earth space: Preliminary LDEF results p 3588 N92-31225

ALUMINUM ALLOYS
In-service evaluation of 2090 aluminum-lithium alloy on F/A-18 aircraft
[AD-A248472] p 3607 N92-30321
Low-velocity impact loading on fibre reinforced aluminum laminates (ARALL) and other aircraft sheet materials
[ETN-92-91613] p 3590 N92-30414
MBE grown copper-aluminum alloy films
[AD-A252486] p 3597 N92-30534
Effects of impurities on the mechanical behaviour of primary and secondary cast aluminum alloys
[PB92-180652] p 3598 N92-30785
Nondestructive characterization of two-phase metal-matrix materials
[AD-A249912] p 3592 N92-30815
NDE characterization of the microstructure and mechanical properties of Al-Li alloys
[DE92-012154] p 3598 N92-30858
Process modeling and development for three axisymmetric net shape forgings
[DE92-012111] p 3598 N92-30865
Laser induced reaction for pre-bond surface preparation of aluminum alloys
[AD-A249916] p 3598 N92-30872
Mechanical behavior and processing of aluminum metal matrix composites
[AD-A249918] p 3592 N92-30874
Environmental fatigue of an Al-Li-Cu alloy. Part 2: Microscopic hydrogen cracking processes
[NASA-TM-107620] p 3664 N92-31214
Environmental fatigue of an Al-Li-Cu alloy. Part 3: Modeling of crack tip hydrogen damage
[NASA-TM-107619] p 3665 N92-31215
Thermodynamic evaporation of highly volatile components in the vacuum degassing of melted aluminum alloys
[DE92-015315] p 3600 N92-31218

ALUMINUM COATINGS
Corrosion of high density kinetic energy penetrator materials
[AD-A249439] p 3597 N92-30759

ALUMINUM GALLIUM ARSENIDES
Development of ultra-low noise, high sensitivity planar metal grating coupled AlGaAs/GaAs multiquantum well IR detectors for focal plane array staring IR sensor systems
[AD-A246122] p 3590 N92-30318
Innovative techniques for the production of low cost 2-D laser diode arrays supplies or services and prices/costs
[AD-A252665] p 3656 N92-30552
Altimetry and lidar using AlGaAs lasers modulated with pseudo-random codes p 3641 N92-31030
Injection seeded single mode alexandrite ring laser for lidar applications p 3646 N92-31057

ALUMINUM GRAPHITE COMPOSITES
Method of bonding carbon-carbon and metal matrix composite structures
[AD-D015299] p 3591 N92-30573

ALUMINUM NITRIDES
Studies of thermal decomposition of the 1:1 R3Al:en adduct (R = Me, Et; en = ethylenediamine): Synthesis and structure of a novel intermediate Al((HNCH2CH2NH)AlMe2)3
[AD-A251061] p 3603 N92-30623
Impurity segregation to grain boundaries and defects in AlN
[DE92-011667] p 3599 N92-31112

ALUMINUM OXIDES
A comparative EIS study on cermet and platinum anodes for the electrolytic production of aluminum
[DE92-015091] p 3599 N92-31010
From minerals to materials: A facile synthetic route to preceramic polymers for aluminum oxide
[AD-A250351] p 3606 N92-31141
Presolar (?) corundum in the Orgueil meteorite p 3738 N92-31230

ALUMINUM-LITHIUM ALLOYS
In-service evaluation of 2090 aluminum-lithium alloy on F/A-18 aircraft
[AD-A248472] p 3607 N92-30321

AMAZON REGION (SOUTH AMERICA)
Trace gas and aerosol transports into and out of the Amazon Basin
[NASA-CR-190624] p 3674 N92-31153

AMBIENT TEMPERATURE
Effect of volatility and oxygenates on driveability at intermediate ambient temperatures
[AD-A248902] p 3607 N92-30341

AMINES
A method for production of new anion exchangers
[DE92-015313] p 3717 N92-31147

AMINO ACIDS
The properties of the uptake system for glycine in synaptic vesicles
[ISSN-0800-4412] p 3683 N92-31152

AMORPHOUS MATERIALS
Anomalous hopping conductivity in amorphous indium-oxide films
[ITN-92-85166] p 3729 N92-30781

AMORPHOUS SEMICONDUCTORS
Research on defects and transport in amorphous silicon-based semiconductors
[DE92-001223] p 3729 N92-30748

AMORPHOUS SILICON
Examinations of the microwave photoelectric conductivity of a-Si:H multilayer systems for in situ characterization
[ETN-92-91688] p 3727 N92-30505
Perspective on photovoltaic amorphous silicon
[DE92-010581] p 3670 N92-30519
In situ TEM studies of the effect of misfit strain on the kinetics of Si(sub 1-x)Ge(sub x) solid phase epitaxy: Temperature calibration and surface effects
[DE92-011689] p 3728 N92-30574
Research on defects and transport in amorphous silicon-based semiconductors
[DE92-001223] p 3729 N92-30748
AMPLIFICATION
Role of compressibility on driven magnetic reconnection
[NIFS-105] p 3710 N92-30498
Optical isolators in high power lasers based on high reflectivity phase conjugate mirrors
[IA-1452] p 3721 N92-30581
AMPLIFIER DESIGN
VDHW-related memo's
[LINO-1991-5] p 3718 N92-30725
Console driver p 3718 N92-30728
ANALOG CIRCUITS
VDHW-related memo's
[LINO-1991-5] p 3718 N92-30725
Measurement report on the present Video Highway System of MEA p 3718 N92-30726
ANALOG TO DIGITAL CONVERTERS
Full surface testing of grazing incidence mirrors
[AD-A248851] p 3719 N92-30233
An automated system for creep testing
p 3611 N92-30282
ANCHORS (FASTENERS)
Evaluation of grounding and mooring points for Army aircraft
[AD-A250749] p 3579 N92-31193
ANGLE OF ATTACK
Ultra high bypass Nacelle aerodynamics inlet flow-through high angle of attack distortion test
[NASA-CR-189149] p 3574 N92-30298
ANGLES (GEOMETRY)
Waveguide polarizer using localized surface plasmons
[AD-D015258] p 3614 N92-30348
ANGULAR ACCELERATION
Adapting the ADAM manikin technology for injury probability assessment
[AD-A252332] p 3688 N92-30844
ANGULAR DISTRIBUTION
Evidence for interference between resonant and nonresonant transfer and excitation
[DE92-011779] p 3716 N92-30853
ANHYDRIDES
Polyimides containing the cyclobutene-3,4-dione moiety
[NASA-CASE-LAR-14753-1] p 3601 N92-30313
ANILINE
Temperature effect on the Langmuir-Blodgett polymerization of 2-pentadecylaniline
[AD-A250803] p 3601 N92-30250
ANIMALS
Field studies in geophysical diffraction tomography
[DE92-015084] p 3677 N92-31009
ANIONS
A method for production of new anion exchangers
[DE92-015313] p 3717 N92-31147
ANISOTROPY
Anisotropic silicon etching techniques
[MBB-Z-0413-91-PUB] p 3594 N92-30422
Quantitative non-destructive evaluation of high-temperature superconducting materials
[DE92-011615] p 3661 N92-30693
ANNEALING
Tempered glass and thermal shock of ceramic materials p 3607 N92-30265
Be-Cu precipitation hardening experiment
p 3601 N92-30276
Heat-treating of materials p 3601 N92-30292
In situ TEM studies of the effect of misfit strain on the kinetics of Si(sub 1-x)Ge(sub x) solid phase epitaxy: Temperature calibration and surface effects
[DE92-011689] p 3728 N92-30574
Superconductivity and magnetism in rapidly solidified perovskites
[DE92-014081] p 3597 N92-30588
Thermally activated rejuvenation of ferroelectric properties in electrically fatigued lead zirconate titanate ceramics
[DE92-012634] p 3605 N92-30830
ANNUAL VARIATIONS
Shining on: A primer on solar radiation data
[DE92-010555] p 3743 N92-31206
ANODES
A comparative EIS study on cermet and platinum anodes for the electrolytic production of aluminum
[DE92-015091] p 3599 N92-31010
ANODIZING
Laser induced reaction for pre-bond surface preparation of aluminum alloys
[AD-A249916] p 3598 N92-30872
ANOMALIES
The (146,147)Sm-(142,143)Nd systematics of early terrestrial differentiation and the lost continents of the early Earth p 3678 N92-31229
ANTARCTIC REGIONS
Potential airfield sites in Antarctica for wheeled aircraft
[AD-A249503] p 3584 N92-30621
The United States Antarctic Program
[NSF-90-97] p 3676 N92-30708
Antarctic ice charts, 1989 - 1990: Analysis Atlas
[AD-A249730] p 3669 N92-31179
ANTENNA ARRAYS
Compact range test applications, phase 2
[AD-A248790] p 3615 N92-30583
Performance of ground-based high-frequency receiving arrays with electrically-small ground planes
[AD-A250489] p 3621 N92-31130
ANTENNA DESIGN
Double-loop frequency-selected surfaces for multifrequency division multiplexing in a dual-reflector antenna
[NASA-CASE-NPO-18701-1-CU] p 3614 N92-30391
Fundamental studies of fusion plasmas
[DE92-015077] p 3726 N92-31116
ANTENNA RADIATION PATTERNS
Antenna pattern measurement facilities
[AD-A248964] p 3584 N92-30329
On the radial component of the electric field for a monopole phased array antenna focused in the near zone
[AD-A249441] p 3616 N92-30761
ANTENNAS
A conceptual design of a large aperture microwave radiometer geostationary platform
[NASA-TM-107577] p 3588 N92-30736
Advanced electromagnetic methods for aerospace vehicles
[NASA-CR-190650] p 3621 N92-31156
ANTIFERROMAGNETISM
Studies of phonons and electronic excitations in semiconductor heterostructures
[AD-A249406] p 3729 N92-30772
ANTIMISSILE DEFENSE
Joint stabilizing projects in defense
[DE92-015977] p 3709 N92-30891
ANTIMONY
Decomposition studies of tertiarybutyldimethylantimony
[AD-A250670] p 3727 N92-30527
ANTINEUTRINOS
Rescattering in neutrino/antineutrino: Deuteron reactions
[NIKHEF-H/91-22] p 3713 N92-30364
ANTIPROTONS
Polarization effects in pi(+) absorption in He-4
[ITN-92-85163] p 3715 N92-30780
APERTURES
Transverse pattern modification in a stable apertured laser resonator
[ITN-92-85171] p 3656 N92-30582
A conceptual design of a large aperture microwave radiometer geostationary platform
[NASA-TM-107577] p 3588 N92-30736
On the radial component of the electric field for a monopole phased array antenna focused in the near zone
[AD-A249441] p 3616 N92-30761
Lidar measurements using large liquid mirror telescopes p 3652 N92-31087
APEXES
Maintenance of 2- and 3-connected components of graphs. Part 2: 2- and 3-edge-connected components and 2-vertex-connected components
[RUU-CS-90-27-PT-2] p 3694 N92-30480
APOLLO ASTEROIDS
The first identification of a mainbelt asteroid source for a meteorite Class E-type Apollo asteroid (3103) 1982BB: A link between the Hungaria asteroid zone and the Aubrite meteorites p 3737 N92-31228
APPLICATIONS OF MATHEMATICS
Semiannual final report, 1 October 1991 - 31 March 1992
[NASA-CR-189660] p 3689 N92-30489
APPLICATIONS PROGRAMS (COMPUTERS)
Analytical methods using Slater-type orbitals in quantum chemistry
[AD-A251044] p 3731 N92-30242
Fast methods to numerically integrate the Reynolds equation for gas fluid films
[NASA-TM-105415] p 3660 N92-30722
Real gas flow parameters for NASA Langley 22-inch Mach 20 helium tunnel
[NASA-CR-4462] p 3635 N92-30751
Metal matrix composite analyzer (METCAN) user's manual, version 4.0
[NASA-TM-105244] p 3592 N92-30779
APPROPRIATIONS
Departments of Veterans Affairs and Housing and Urban Development, and Independent Agencies Appropriation Bill, 1993
[S-REPT-102-356] p 3735 N92-31169
National Aeronautics and Space Administration
p 3736 N92-31170
APPROXIMATION
Lidar multiple scattering: Dependence on atmospheric parameters p 3647 N92-31061
AQUIFERS
Flow of fresh and salt water in an aquifer with injection from the top
[REPT-91-68] p 3629 N92-30453
ARC CHAMBERS
Negative ion extraction characteristics of a large negative ion source with double-magnetic filter configuration
[NIFS-151] p 3714 N92-30501
Production of negative hydrogen ions in a large multicusp ion source with double-magnetic filter configuration
[NIFS-149] p 3714 N92-30572
ARC WELDING
Impact testing of welded samples
p 3608 N92-30268
ARCHAEOLOGY
Remote-sensing survey of the Atchafalaya Basin Main Channel, Atchafalaya Channel training project, Saints Martin and Mary Parishes, Louisiana
[AD-A249915] p 3669 N92-31139
ARCHITECTURE (COMPUTERS)
On the use of pre-defined implementation constructs in distributed systems design
[MEMO-INF-92-08] p 3689 N92-30432
Configuration algorithms for hierarchical supernode machines
[IMAG-RR-853-I] p 3694 N92-30493
A model of the ADA avionics real-time system: An example of the benefits of the hardware/software codesign approach in development of real-time systems
[AD-A248893] p 3581 N92-30524
Implementation of parallel algorithms
[AD-A248826] p 3695 N92-30555
VLSI design, parallel computation, and distributed computing
[AD-A252349] p 3699 N92-30596
High level synthesis of controlpath microarchitectures
[MEMO-INF-91-86] p 3690 N92-30698
Architecture for the high performance implantation of communication transport level protocols
[ETN-92-91666] p 3690 N92-30701
Collected notes from the Benchmarks and Metrics Workshop
[NASA-TM-107910] p 3701 N92-30710
Network load of X terminals at CDF
[DE92-011704] p 3699 N92-30812
An overview of the computer aided definition system for design definition at Sandia National Laboratories, Livermore FY1991 update
[DE92-015991] p 3696 N92-30892
ARCTIC REGIONS
Ice thickness observations, North American Arctic and subarctic, 1972-1973 and 1973-1974, part 8
[AD-A250830] p 3681 N92-30238
Laboratory simulation of fluid dynamical process related to winter arctic leads
[AD-A252266] p 3682 N92-30593
Optics of the ozone lidar ELSA p 3645 N92-31051
Operation, maintenance and research activities at the Norwegian Seismic Array (NORSAR), the Norwegian Regional Seismic Array (NORESS), and the Arctic Regional Seismic Array (ARCESS)
[AD-A250403] p 3677 N92-31142
ARGON
High-temperature ignition of propane with MTBE as an additive: Shock-tube experiments and modeling
[DE92-006679] p 3594 N92-30749
ARIANE LAUNCH VEHICLE
EASAMS' Ariane 5 on-board software experience
[D308/TN/001] p 3586 N92-30715
ARMED FORCES (UNITED STATES)
The 1991 Summer Faculty Research Program (SFRP), volume 4 atory
[AD-A248766] p 3744 N92-30327

ARMOR
Development of diagnostics for electromagnetic armor applications
[AD-A251074] p 3587 N92-30257
Three-dimensional shock wave physics simulations on massively parallel supercomputers
[DE92-008679] p 3698 N92-30363
AROMATIC COMPOUNDS
Polymerization of 1-bromo-4-lithiobenzene in THF. A route to soluble polyphenylenes
[AD-A249926] p 3604 N92-30794
ARRAYS
Method of measuring cross-flow vortices by use of an array of hot-film sensors
[NASA-CASE-LAR-14824-1-SB] p 3628 N92-30390
ARTIFICIAL INTELLIGENCE
Analysis and synthesis of adaptive neural elements and assemblies
[AD-A248467] p 3687 N92-30320
Information processing research
[AD-A248492] p 3734 N92-30324
Application of automated deduction to the search for single axioms for exponent groups
[DE92-015271] p 3705 N92-30608
Collected notes from the Benchmarks and Metrics Workshop
[NASA-TM-107910] p 3701 N92-30710
Sparse distributed memory and related models
[NASA-CR-190553] p 3690 N92-30724
ASSURANCE
Quality assurance and ILS p 3697 N92-30953
ASTEROID BELTS
The first identification of a mainbelt asteroid source for a meteorite Class E-type Apollo asteroid (3103) 1982BB: A link between the Hungaria asteroid zone and the Aubrite meteorites p 3737 N92-31228
Gaspra's shape and surface features: Comparison to small satellites p 3739 N92-31236
ASTEROIDS
The first identification of a mainbelt asteroid source for a meteorite Class E-type Apollo asteroid (3103) 1982BB: A link between the Hungaria asteroid zone and the Aubrite meteorites p 3737 N92-31228
Gaspra's shape and surface features: Comparison to small satellites p 3739 N92-31236
ASTRONOMICAL CATALOGS
Carlsberg meridian catalogue La Palma. Number 5: Observations of positions of stars and planets: May 1988 to Dec. 1989
[ISBN-84-7469-052-8] p 3739 N92-30714
ASTRONOMICAL MODELS
Dark matter and cosmology
[DE92-013023] p 3740 N92-30622
ASTRONOMICAL PHOTOGRAPHY
Hubble Space Telescope. Update: 18 months in orbit
[NASA-TM-107962] p 3739 N92-30686
ASTROPHYSICS
Activities report of the Institute for Astronomy and Astrophysics at Technical University of Berlin (Germany, F.R.)
[MITT-11] p 3740 N92-30506
The United States Antarctic Program
[NSF-90-97] p 3676 N92-30708
Nuclear structure calculations for astrophysical applications
[DE92-011495] p 3740 N92-30856
ASYMMETRY
GMRESR: A family of nested GMRES methods
[REPT-91-80] p 3703 N92-30437
Tropical cyclone asymmetries as revealed by recent satellite microwave brightness temperatures
[AD-A249873] p 3679 N92-30867
ASYMPTOTIC METHODS
Nonlinear system design: Adaptive feedback linearization with unmodeled dynamics
[AD-A248484] p 3700 N92-30335
A dynamic subgrid-scale eddy viscosity model p 3630 N92-30649
ATCHAFALAYA RIVER BASIN (LA)
Remote-sensing survey of the Atchafalaya Basin Main Channel, Atchafalaya Channel training project, Saints Martin and Mary Parishes, Louisiana
[AD-A249915] p 3669 N92-31139
ATLANTIC OCEAN
A statistical comparison of AUTEC and Eleuthera Island wind data for the period 1 April 1989 through 30 March 1990
[AD-A248898] p 3679 N92-31003
ATMOSPHERIC BOUNDARY LAYER
Boundary layer structure over the ocean observed by LEANDRE 1 during a tramontane event p 3638 N92-31014
Aureole lidar: Design, operation, and comparison with in-situ measurements p 3648 N92-31065
Lidar analysis techniques for use in the atmospheric boundary layer p 3649 N92-31069
A portable lidar using a diode-pumped YAG laser p 3654 N92-31098
Lidar observation of marine mixed layer p 3655 N92-31104
ATMOSPHERIC CHEMISTRY
Studies of atmospheric molecules by multiphoton spectroscopy
[DE92-012668] p 3672 N92-30345
Development and testing of an air quality model for Mexico City
[DE92-011238] p 3673 N92-30520
Towards the development of a global inventory for black carbon emissions
[DE92-013514] p 3674 N92-30647
ATMOSPHERIC CIRCULATION
Development and testing of an air quality model for Mexico City
[DE92-011238] p 3673 N92-30520
Small satellite radiation budget instrumentation
[DE92-011134] p 3677 N92-31008
Low-level atmospheric flows studied by pulsed Doppler lidar p 3638 N92-31015
Simplified signal processing for an airborne CO2 Doppler lidar p 3639 N92-31023
Coherent summation of spatially distorted Doppler lidar signals using a two-dimensional heterodyne detector array p 3654 N92-31096
ATMOSPHERIC COMPOSITION
Chemielectron and photoelectron spectroscopic studies of importance in the upper atmosphere
[AD-A248838] p 3675 N92-30556
Towards the development of a global inventory for black carbon emissions
[DE92-013514] p 3674 N92-30647
Advanced Raman water vapor lidar p 3643 N92-31040
Lidar analysis techniques for use in the atmospheric boundary layer p 3649 N92-31069
Development of a Raman lidar simulation tool p 3649 N92-31072
Measurement capabilities of giant lidars for middle and upper atmospheric applications p 3651 N92-31084
The ENEA CO2 lidar/DIAL station activity in a tropospheric remote sensing program p 3655 N92-31103
Trace gas and aerosol transports into and out of the Amazon Basin
[NASA-CR-190624] p 3674 N92-31153
ATMOSPHERIC CORRECTION
On the remote sensing of water quality using the optical airborne scanner CAESAR
[BCRS-90-30] p 3666 N92-30466
ATMOSPHERIC DENSITY
A range-resolved bistatic lidar using a high-sensitive CCD-camera p 3640 N92-31027
ATMOSPHERIC EFFECTS
A study of atmospheric optical scattering parameters at 1.5 and 2 micron region for solid state Doppler lidar applications p 3648 N92-31067
ATMOSPHERIC IONIZATION
Chemielectron and photoelectron spectroscopic studies of importance in the upper atmosphere
[AD-A248838] p 3675 N92-30556
ATMOSPHERIC LASERS
Effect of atmospheric extinction on laser rangefinder performance at 1.54 and 0.6 microns p 3648 N92-31066
ATMOSPHERIC MODELS
Regional-scale analysis and forecasting (RAP) report
[AD-A248384] p 3678 N92-30262
Development and testing of an air quality model for Mexico City
[DE92-011238] p 3673 N92-30520
Laboratory scaled simulation of lidar cloud sounding experiments p 3645 N92-31047
Effect of atmospheric extinction on laser rangefinder performance at 1.54 and 0.6 microns p 3648 N92-31066
DIAL simulations for satellite water vapor profile measurements within the BEST project p 3653 N92-31092
The environmental dilemma of fossil fuels
[DE92-014887] p 3674 N92-31121
ATMOSPHERIC MOISTURE
Water vapor variance measurements using a Raman lidar p 3643 N92-31041
Airborne remote sensing of tropospheric water vapor using a near infrared DIAL system p 3644 N92-31042
Comparison of eye-safe solid state laser DIAL with passive gas filter correlation measurements from aircraft and spacecraft p 3647 N92-31060
Performance modeling of daytime Raman lidar systems for profiling atmospheric water vapor p 3653 N92-31090
BELINDA: Broadband Emission Lidar with Narrowband Determination of Absorption. A new concept for measuring water vapor and temperature profiles p 3653 N92-31091
DIAL simulations for satellite water vapor profile measurements within the BEST project p 3653 N92-31092
Alexandrite lidar for the atmospheric water vapor detection and development of powerful tunable sources in IR p 3653 N92-31094
ATMOSPHERIC OPTICS
Lidar sounding of ozone and aerosols p 3652 N92-31085
ATMOSPHERIC PHYSICS
Effect of wave-particle interaction on the outflow of ions at high latitudes
[NASA-CR-190560] p 3677 N92-30962
Tropospheric and stratospheric wind profiling with a direct detection Doppler lidar p 3639 N92-31018
Raman lidar measurements of water vapor and aerosol/clouds during the FIRE/SPECTRE field campaign p 3652 N92-31089
ATMOSPHERIC PRESSURE
The use of tympanometry to detect aerotitis media in hypobaric chamber operations
[AD-A248963] p 3684 N92-30328
Wavemeter measurements of frequency stability of an injection seeded alexandrite laser for pressure and temperature lidar p 3645 N92-31049
ATMOSPHERIC RADIATION
Small satellite radiation budget instrumentation
[DE92-011134] p 3677 N92-31008
ATMOSPHERIC SCATTERING
Effect of atmospheric extinction on laser rangefinder performance at 1.54 and 0.6 microns p 3648 N92-31066
A study of atmospheric optical scattering parameters at 1.5 and 2 micron region for solid state Doppler lidar applications p 3648 N92-31067
A considerable effect of stratospheric aerosol on lidar-detected ozone profile and a three-wavelength inversion technique for both ozone and aerosol p 3651 N92-31080
ATMOSPHERIC SOUNDING
Measurement of aerosol profiles using high-spectral-resolution Rayleigh-Mie lidar p 3644 N92-31046
Laboratory scaled simulation of lidar cloud sounding experiments p 3645 N92-31047
An alexandrite regenerative amplifier for water vapor and temperature measurements p 3645 N92-31048
Tunable Electro-optic modulators for lidar systems and atmospheric applications p 3646 N92-31056
Time and polarization dependent double scattering calculations of lidar returns from water clouds p 3647 N92-31063
Lidar sounding of ozone and aerosols p 3652 N92-31085
ATMOSPHERIC TEMPERATURE
Wavemeter measurements of frequency stability of an injection seeded alexandrite laser for pressure and temperature lidar p 3645 N92-31049
ATMOSPHERIC TURBULENCE
Phase noise in pulsed Doppler lidar and limitations on achievable single-shot velocity accuracy p 3639 N92-31024
ATOMIC CLOCKS
Modeling fast modulation effects in cesium atomic clocks
[AD-A252649] p 3636 N92-30412
ATOMIC EXCITATIONS
Spontaneous emission from an atom in motion near an infinite conducting plane
[ITN-92-85169] p 3715 N92-30782
Evidence for interference between resonant and nonresonant transfer and excitation
[DE92-011779] p 3716 N92-30853
ATOMIC PHYSICS
Atomic layer epitaxy group 4 materials: Surface processes, thin films, devices, and their characterization
[AD-A252352] p 3729 N92-30846
X ray radiation from hot dense plasmas and atomic processes
[NIFS-PROC-9] p 3725 N92-30984
Solar neutrinos: Theoretical status
[DE92-014014] p 3743 N92-31199
ATOMIC SPECTRA
Program RELAX: A code designed to calculate atomic relaxation spectra of x rays and electrons
[DE92-013751] p 3714 N92-30586
ATOMIC STRUCTURE
Determination of pair potentials by analysis of diffuse scattering of the local field in Pd3V and Ni3V
[ESA-TT-1228] p 3597 N92-30513

Microscopic theory of THG and electro-absorption in conjugated polymers
[DE92-014786] p 3604 N92-30792
High-resolution imaging in the scanning transmission electron microscope
[DE92-010647] p 3637 N92-30827
Development of practical MO techniques for prediction of the properties and behavior of materials
[AD-A247218] p 3598 N92-30864
Electron scattering and electromagnetic response properties of metal clusters
[DE92-014715] p 3621 N92-31007
Theoretical study of phase stability in Ni-Al and Ni-Ti alloys
[DE92-014776] p 3599 N92-31119
Self-consistent-field KKR-CPA calculations in the atomic-sphere approximations
[DE92-011525] p 3600 N92-31138
Proceedings of the 181st Electrochemical Society, Inc. Meeting Program
[AD-A249729] p 3596 N92-31178

ATOMS
Spontaneous decay of an atom near a phase conjugator
[AD-A248298] p 3712 N92-30333
Line-emission cross sections for the charge-exchange reaction between fully stripped carbon and atomic hydrogen in tokamak plasma
[NIFS-129] p 3716 N92-30967

ATTENTION
Cortical mechanisms of attention, discrimination, and motor response to somaesthetic stimuli
[AD-A247228] p 3687 N92-30613

ATTENUATION COEFFICIENTS
Lidar measurements of cloud extinction coefficient distribution and its forward scattering phase function according to multiply scattered lidar returns
p 3651 N92-31082

ATTITUDE CONTROL
Alignment of a 3-D sensor and a 2-D sensor measuring azimuth and elevation
[AD-A252120] p 3636 N92-30530

AUGER SPECTROSCOPY
Interaction of atomic hydrogen with the surface methyl group on Si(100): Removal of surface carbon
[AD-A249062] p 3595 N92-30821
Atomic layer epitaxy group 4 materials: Surface processes, thin films, devices, and their characterization
[AD-A252352] p 3729 N92-30846

AUGMENTATION
Linear planar augmentation algorithms for outerplanar graphs
[RUU-CS-91-47] p 3703 N92-30449

AUSTENITIC STAINLESS STEELS
Investigation of joining techniques for advanced austenitic alloys
[DE92-015545] p 3599 N92-30888

AUTOMATIC CONTROL
An automated system for creep testing
p 3611 N92-30282
Application of automated deduction to the search for single axioms for exponent groups
[DE92-015271] p 3705 N92-30608
Growth and evaluation of nonlinear optical materials for laser applications: Barium borate, lithium borate, and silver gallium selenide
[AD-A248861] p 3624 N92-30617
Concurrent engineering p 3697 N92-30952

AUTOMOBILE ENGINES
Nondestructive testing of ceramics for vehicular advanced heat engines
[DE92-010471] p 3604 N92-30744

AUTOMOBILE FUELS
Effect of volatility and oxygenates on driveability at intermediate ambient temperatures
[AD-A248902] p 3607 N92-30341

AVIONICS
A model of the ADA avionics real-time system: An example of the benefits of the hardware/software codesign approach in development of real-time systems
[AD-A248893] p 3581 N92-30524

AXES OF ROTATION
Vibrationally induced rotational axis switching: A novel mechanism for vibrational mode-coupling
[AD-A251085] p 3712 N92-30259

AXIAL FLOW
Numerical study of axial turbulent flow over long cylinders
[AD-A250801] p 3635 N92-30831

AXIOMS
Application of automated deduction to the search for single axioms for exponent groups
[DE92-015271] p 3705 N92-30608

AXISYMMETRIC FLOW
A study of the topology of dissipating motions in direct numerical simulations of time-developing compressible and incompressible mixing layers p 3632 N92-30658

AZIMUTH
Alignment of a 3-D sensor and a 2-D sensor measuring azimuth and elevation
[AD-A252120] p 3636 N92-30530

AZINES
Photoinitiated electron transfer in multichromophoric species: Synthetic tetrads and pentads featuring diquinone moieties
[DE92-013472] p 3683 N92-30368

AZULENE
Photodissociation of azulene under UV-laser irradiation at 325 nm
[AD-A251093] p 3613 N92-30246

B

B STARS
The origins of hot subdwarf stars
p 3741 N92-30973

BACKGROUND RADIATION
High background photon counting lidar
p 3649 N92-31071
Acousto-optic filtering of lidar signals
p 3650 N92-31077

BACKSCATTERING
Generation of stimulated backscattered harmonic radiation from intense laser interactions with beams and plasmas
[AD-A248782] p 3656 N92-30614
Subgrid-scale backscatter in transitional and turbulent flows p 3630 N92-30650
Numerical simulations of light scattering from rough one-dimensional gold surfaces
[AD-A249794] p 3721 N92-30783
Doppler lidar wind measurement with the edge technique p 3638 N92-31017
Tropospheric and stratospheric wind profiling with a direct detection Doppler lidar p 3639 N92-31018
Phase noise in pulsed Doppler lidar and limitations on achievable single-shot velocity accuracy
p 3639 N92-31024
Multiple scattering technique lidar
p 3641 N92-31031
Measurement of multiple scattering effects with a polarization Raman elastic-backscatter lidar
p 3641 N92-31033
Determining water cloud particle sizes from lidar depolarization measurements and time dependent multiple scattering coefficients p 3641 N92-31034
Multiple scattering lidar returns from stratus clouds
p 3642 N92-31035
Airborne lidar and radiometric observations of PBL- and low clouds p 3642 N92-31037
ECLIPS at LMD: Preliminary results of phase 2
p 3643 N92-31038
The 2nd phase of the LEANDRE program: Water-vapor DIAL measurement p 3643 N92-31039
Lidar depolarization by nonspherical particles: Potential of combined depolarization/backscattering measurements for PSC's characterization p 3644 N92-31044
Lidar multiple scattering: Dependence on atmospheric parameters p 3647 N92-31061
Verification measurement of a polarization Raman elastic-backscatter lidar p 3647 N92-31062
Time and polarization dependent double scattering calculations of lidar returns from water clouds
p 3647 N92-31063
Multiple scattering wavelength dependent backscattering of kaolin dust in the IR: Measurements and theory p 3648 N92-31064
Aureole lidar: Design, operation, and comparison with in-situ measurements p 3648 N92-31065
A variable phase function approach for the inversion of lidar return signals p 3649 N92-31073
A comparison of lidar inversion methods for cirrus applications p 3649 N92-31074
Measurements of the backscattering phase matrices of crystal clouds with a polarization lidar
p 3651 N92-31083

BACKWARD WAVE TUBES
Backward-wave oscillator investigations in the Raman Regime
[AD-A250738] p 3622 N92-30332

BACKWARD WAVES
Backward-wave oscillator investigations in the Raman Regime
[AD-A250738] p 3622 N92-30332

BACTERIA
Comparison of epifluorescent viable bacterial count methods
[NASA-TM-103592] p 3683 N92-30305

BALANCE
Quantification and reduction of the uncertainty in mass balance models by Monte Carlo analysis of prior data
[DE92-010278] p 3708 N92-30803

BALLOONING MODES
Kinetic approach to long wave length modes in rotating plasmas
[NIFS-138] p 3725 N92-30993

BALLS
The sum of weighted balls
[RUU-CS-91-37] p 3707 N92-30481

BANACH SPACE
Fixed point iterations for a class of nonlinear mappings in certain Banach spaces
[DE92-630235] p 3706 N92-31134

BANDWIDTH
Bandwidth efficient CCSDS coding standard proposals
[NASA-CR-190317] p 3587 N92-30709
Network load of X terminals at CDF
[DE92-011704] p 3699 N92-30812
Ground-based Doppler lidar of increased laser instability: Conception and design p 3650 N92-31078

BARIUM
Growth and evaluation of nonlinear optical materials for laser applications: Barium borate, lithium borate, and silver gallium selenide
[AD-A248861] p 3624 N92-30617

BARYONS
Dark matter and cosmology
[DE92-013023] p 3740 N92-30622

BASE FLOW
Low order dynamical models for mixing layers
p 3633 N92-30662

BAYS (STRUCTURAL UNITS)
Development of and flight results from the Space Acceleration Measurement System (SAMS)
[NASA-TM-105652] p 3588 N92-30301

BEAM INJECTION
Dynamic analysis of compact helical system power supply and designs of its upgrade
[NIFS-TECH-2] p 3723 N92-30497
Density profile measurement using a multichannel difluoromethane laser interferometer system on ATF
[DE92-011691] p 3724 N92-30810
Application of superconducting cavities to the collider rings of the SSC
[DE92-011692] p 3718 N92-30811
Results of the heavy ion beam probe measurements on the Advanced Toroidal Facility
[DE92-014461] p 3726 N92-31197

BEAMS (RADIATION)
Numerical simulation of the electromagnetic instability of an intense beam in a quadrupole focusing system
[AD-A252275] p 3614 N92-30407
Beam technologies for integrated processing
[AD-A252647] p 3612 N92-30411
Application of superconducting cavities to the collider rings of the SSC
[DE92-011692] p 3718 N92-30811
Emittance growth caused by magnet vibrations in SSC
[DE92-014186] p 3719 N92-30681
Performance of ground-based high-frequency receiving arrays with electrically-small ground planes
[AD-A250489] p 3621 N92-31130

BEAMS (SUPPORTS)
An experiment on the use of disposable plastics as a reinforcement in concrete beams p 3593 N92-30287
Vehicle/guideway interaction for high speed vehicles on flexible guideway
[DE92-013057] p 3660 N92-30860
Thrust test fixture
[AD-D015259] p 3585 N92-31192

BEAT FREQUENCIES
Theoretical study of phase-shifted quantum beats in time-resolved luminescence spectra from a biased asymmetric double quantum well
[AD-A252422] p 3710 N92-30549

BEND TESTS
Measuring the Weibull modulus of microscope slides
p 3612 N92-30294
Effect of bending on the room-temperature tensile strengths of structural ceramics
[DE92-015196] p 3603 N92-30626
Filler metal development for Hastelloy alloy XR
[DE92-782044] p 3600 N92-31163

BENDING
Measuring the Weibull modulus of microscope slides
p 3612 N92-30294

BENZENE
Synthesis of cresols and xylenols from benzene and methanol
[DE91-002143] p 3596 N92-30882

BERYL
An alexandrite regenerative amplifier for water vapor and temperature measurements p 3645 N92-31048

Wavemeter measurements of frequency stability of an injection seeded alexandrite laser for pressure and temperature lidar p 3645 N92-31049
Injection seeded single mode alexandrite ring laser for lidar applications p 3646 N92-31057

BERYLLIUM
Proceedings of a Beryllium Technology Workshop
[DE92-012312] p 3598 N92-30834

BETATRONS
Emittance growth caused by magnet vibrations in SSC
[DE92-014186] p 3719 N92-30881

BIBLIOGRAPHIES
A bibliography on network flow problems (2nd edition)
[RUU-CS-91-38] p 3698 N92-30482
Aerospace medicine and biology: A continuing bibliography with indexes (supplement 363)
[NASA-SP-7011(363)] p 3685 N92-30987

BICRYSTALS
Grain boundary weak links in high-Tc superconductors
[DE92-016192] p 3730 N92-31190

BIG BANG COSMOLOGY
Dark matter and cosmology
[DE92-013023] p 3740 N92-30622

BINARY ALLOYS
Cu-Zn binary phase diagram and diffusion couples
p 3600 N92-30269
Theoretical study of phase stability in Ni-Al and Ni-Ti alloys
[DE92-014776] p 3599 N92-31119

BIOASTRONAUTICS
Aerospace medicine and biology: A continuing bibliography with indexes (supplement 363)
[NASA-SP-7011(363)] p 3685 N92-30987

BIOLOGICAL EFFECTS
Aerospace medicine and biology: A continuing bibliography with indexes (supplement 363)
[NASA-SP-7011(363)] p 3685 N92-30987
Effects of microwave radiation on humans: Monkeys exposed to 1.25 GHz pulsed microwaves
[AD-A249997] p 3686 N92-31127

BIOLOGICAL MODELS (MATHEMATICS)
The revised International Commission on Radiological Protection (ICRP) dosimetric model for the human respiratory tract
[DE92-015092] p 3685 N92-31011

BIOPOLYMERS
Laser mass spectrometry for biopolymers
[DE92-015238] p 3597 N92-31184

BIOSPHERE
The sustainable biosphere initiative: An ecological research agenda p 3673 N92-30425

BIOTECHNOLOGY
Nanoscience and nanotechnology
[AD-A250376] p 3626 N92-30851

BIPOLAR TRANSISTORS
Adaptive multigrid applied to a bipolar transistor problem
[CWI-NM-R9115] p 3693 N92-30429

BIRDS
Habitat model for the Florida Scrub Jay on John F. Kennedy Space Center
[NASA-TM-107543] p 3673 N92-30494

BIREFRINGENCE
Depolarized light scattering and dynamic shear compliance of viscoelastic liquids
[AD-A252491] p 3721 N92-30536

BISMUTH ALLOYS
Experiments with the low melting indium-bismuth alloy system p 3601 N92-30272

BLANKETS (FISSION REACTORS)
MHD considerations for a self-cooled liquid lithium blanket
[DE92-014864] p 3723 N92-30591

BLOOD PRESSURE
Tolerance of beta blocked hypertensives during orthostatic and altitude stresses
[AD-A249904] p 3685 N92-30745

BLUNT BODIES
Two-dimensional aerodynamic characteristics of several polygon-shaped cross-sectional models applicable to helicopter fuselages
[NASA-TP-3233] p 3574 N92-30394

BODY CENTERED CUBIC LATTICES
Mechanism of slip and twinning p 3610 N92-30280
Theoretical study of phase stability in Ni-Al and Ni-Ti alloys
[DE92-014776] p 3599 N92-31119
Stability of metallic superlattices
[DE92-011526] p 3600 N92-31124

BODY KINEMATICS
Evaluation of head impact kinematics for passengers seated behind interior walls
[AD-A252651] p 3578 N92-30551

BODY TEMPERATURE
Secretory mechanisms in opiocortin cells during cold stress
[AD-A252317] p 3685 N92-30719

BODY-WING CONFIGURATIONS
An experimental study of the relationship between velocity and pressure fluctuations in a wing-body junction
[AD-A249628] p 3577 N92-31122

BOEING AIRCRAFT
Lewis icing research tunnel test of the aerodynamic effects of aircraft ground deicing/anti-icing fluids
[NASA-TP-3238] p 3577 N92-30395

BOEING 747 AIRCRAFT
Implicit upwind-Euler solution algorithms for unstructured-grid applications
[NASA-TM-107645] p 3575 N92-30691
Aircraft accident report: Explosive decompression - loss of cargo door in flight, United Airlines Flight 811, Boeing 747-122, N4713U, Honolulu, Hawaii, February 24, 1989
[PB92-910402] p 3578 N92-31159

BONDING
Chemistry within van der Waals cluster of unsaturated molecules: Observation of cationic polymerization
[AD-A250929] p 3712 N92-30240

BORN APPROXIMATION
Diffuse neutron scattering signatures of rough films
[DE92-015208] p 3717 N92-31201

BOSONS
On the factorisation theorem in boson-gluon fusion at hadron colliders
[NIKHEF-H/91-16] p 3713 N92-30415
Theoretical studies in elementary particle physics
[DE92-015295] p 3714 N92-30610

BOUNDARIES
Demonstration of magnetic domain boundary movement using an easily assembled videocam-microscope system
p 3611 N92-30286
Validation of three-dimensional incompressible spatial direct numerical simulation code: A comparison with linear stability and parabolic stability equation theories for boundary-layer transition on a flat plate
[NASA-TP-3205] p 3573 N92-30295
Investigation of the interface phenomena due to interaction of high intensity stress waves with geologic boundaries
[AD-A248992] p 3675 N92-30525
Boundary plasma transport studies on TFTR
[DE92-011942] p 3723 N92-30746
Numerical study of axial turbulent flow over long cylinders
[AD-A250801] p 3635 N92-30831
An investigation of the effects of boundary constraints on the sound insulations of lightweight, double leaf partitions
[BBC-RD-1992/4] p 3711 N92-31151

BOUNDARY CONDITIONS
Validation of three-dimensional incompressible spatial direct numerical simulation code: A comparison with linear stability and parabolic stability equation theories for boundary-layer transition on a flat plate
[NASA-TP-3205] p 3573 N92-30295
Kinetic theory and boundary conditions for flows of highly inelastic spheres
[DE92-012645] p 3629 N92-30438

BOUNDARY ELEMENT METHOD
A boundary element alternating method for two-dimensional mixed-mode fracture problems
[NASA-CR-4460] p 3661 N92-30309

BOUNDARY INTEGRAL METHOD
A computational algorithm for crack determination: The multiple crack case
[NASA-CR-189665] p 3704 N92-30516

BOUNDARY LAYER EQUATIONS
Calculation of viscous hypersonic flows in chemical non-equilibrium
[MBB/FE211/S/PUB/466] p 3634 N92-30674
Numerical study of axial turbulent flow over long cylinders
[AD-A250801] p 3635 N92-30831

BOUNDARY LAYER FLOW
The effects of free stream turbulence and surface curvature on boundary layer flow and heat transfer
[AD-A248846] p 3630 N92-30616
Low Reynolds number kappa-epsilon modeling with the aid of direct simulation data p 3631 N92-30655
One-equation near-wall turbulence modeling with the aid of direct simulation data p 3631 N92-30656

BOUNDARY LAYER SEPARATION
Intersecting shock-wave/turbulent boundary-layer interactions at Mach 8.3
[NASA-TM-103909] p 3635 N92-30765
An experimental study of the relationship between velocity and pressure fluctuations in a wing-body junction
[AD-A249628] p 3577 N92-31122

BOUNDARY LAYER TRANSITION
Validation of three-dimensional incompressible spatial direct numerical simulation code: A comparison with linear stability and parabolic stability equation theories for boundary-layer transition on a flat plate
[NASA-TP-3205] p 3573 N92-30295

BOUNDARY LAYERS
Validation of three-dimensional incompressible spatial direct numerical simulation code: A comparison with linear stability and parabolic stability equation theories for boundary-layer transition on a flat plate
[NASA-TP-3205] p 3573 N92-30295

BOUNDARY VALUE PROBLEMS
Component-wise error bounds for linear equations
[DE92-016000] p 3707 N92-31189

BOUSSINESQ APPROXIMATION
A Boussinesq algorithm for bouyant convection in polygonal domains
[PB92-187137] p 3695 N92-30579

BRANCHING (MATHEMATICS)
Bifurcation of limit cycles in a particular class of quadratic systems
[REPT-91-76] p 3703 N92-30457

BREADBOARD MODELS
Software breadboard study
[NASA-CR-190473] p 3625 N92-30757

BREMSSTRAHLUNG
Search for light neutral scalar and pseudoscalar particles in pFe interactions at 70 GeV
[DE92-627317] p 3713 N92-30404

BRIGHTNESS TEMPERATURE
Tropical cyclone asymmetries as revealed by recent satellite microwave brightness temperatures
[AD-A249873] p 3679 N92-30867
Estimation of vertical profile of soil moisture through multifrequency microwave data analysis
p 3669 N92-30919

BRILLOUIN EFFECT
Interaction physics for megajoule laser fusion targets
[DE92-014796] p 3656 N92-30400
Optical isolators in high power lasers based on high reflectivity phase conjugate mirrors
[IA-1452] p 3721 N92-30581

BRINES
Flow of fresh and salt water in an aquifer with injection from the top
[REPT-91-68] p 3629 N92-30453

BRITTLE MATERIALS
Ceramic processing: Experimental design and optimization p 3607 N92-30267
Mechanical properties of brittle materials
p 3612 N92-30290
Measuring the Weibull modulus of microscope slides
p 3612 N92-30294

BRITTLENESS
Recent improvements in size effects correlations for DBTT and upper shelf energy of ferritic steels
[DE92-014703] p 3599 N92-30877

BROADBAND
BELINDA: Broadband Emission Lidar with Narrowband Determination of Absorption. A new concept for measuring water vapor and temperature profiles
p 3653 N92-31091

BROADCASTING
Technical and economic feasibility of integrated video service by satellite
[NASA-CR-189210] p 3614 N92-30300
The RadioSat (sm) network p 3620 N92-30942
Broadcast satellite service: The international dimension p 3621 N92-30946

BROKEN SYMMETRY
Nuclear theory progress report, April 1991 - April 1992
[DE92-015349] p 3714 N92-30611
Theoretical particle physics
[DE92-014531] p 3716 N92-30841

BROMIDES
Effects of pyridostigmine bromide on A-10 pilots during execution of a simulated mission; performance
[AD-A252309] p 3685 N92-30605

BROMINATION
Polymerization of 1-bromo-4-lithiobenzene in THF. A route to soluble polyphenylenes
[AD-A249926] p 3604 N92-30794

BROWNIAN MOVEMENTS
Low-frequency fluctuations in plasma magnetic fields
[DE92-012139] p 3724 N92-30833

BUBBLES
Measuring the surface tension of soap bubbles
p 3612 N92-30293

BUCKMINSTERFULLERENE
First-principles computational studies of alkali-doped C60 fullerides
[AD-A249018] p 3624 N92-30630

BUDGETING
Departments of Veterans Affairs and Housing and Urban Development, and Independent Agencies Appropriation Bill, 1993
[S-REPT-102-356] p 3735 N92-31169
National Aeronautics and Space Administration p 3736 N92-31170

BUOYANCY
Laboratory simulation of fluid dynamical process related to winter arctic leads
[AD-A252266] p 3682 N92-30593
Generation of large-scale density fluctuations by buoyancy p 3634 N92-30671

BUTENES
High-temperature ignition of propane with MTBE as an additive: Shock-tube experiments and modeling
[DE92-006679] p 3594 N92-30749

BUTTES
Inter- and intra-plate deformation at North American plate boundaries
[NASA-CR-190485] p 3676 N92-30961

BYPASSES
Ultra high bypass Nacelle aerodynamics inlet flow-through high angle of attack distortion test
[NASA-CR-189149] p 3574 N92-30298

C

C-135 AIRCRAFT
KC-135 crew reduction feasibility demonstration simulation study. Volume 1: Function analysis and function reallocation
[AD-A252265] p 3688 N92-30592
A reduced gravity fiber pulling apparatus
[NASA-TM-103594] p 3612 N92-30971

CABLES (ROPES)
Cable compliance
[NASA-TP-3216] p 3612 N92-30378

CALIBRATING
Results of the 1989 experiment with a polarimetric multifrequency SAR
[BCRS-91-33] p 3614 N92-30361
Airborne remote sensing of tropospheric water vapor using a near infrared DIAL system p 3644 N92-31042

CALIFORNIA
Evaporation duct effects at millimeter wavelengths
[AD-A250239] p 3617 N92-30876

CALORIMETERS
Mechanical design and finite element analysis of the SDC central calorimeter
[DE92-011197] p 3655 N92-31109

CAMBER
Modeling and analysis methodology for aeroelastically tailored chordwise deformable wings
[NASA-CR-189620] p 3579 N92-30304

CAMERAS
A stroboscopic technique for using CCD cameras in flow visualization systems for continuous viewing and stop action photography
[NASA-TM-107648] p 3637 N92-30737
Initial laboratory evaluation of color video cameras
[DE92-010399] p 3637 N92-30822
A range-resolved bistatic lidar using a high-sensitive CCD-camera p 3640 N92-31027

CANADA
Ice thickness observations, North American Arctic and subarctic, 1972-1973 and 1973-1974, part 8
[AD-A250830] p 3681 N92-30238

CANOPIES
Selection of opening model for parachute scaling studies
[AD-A250882] p 3573 N92-30239

CANOPIES (VEGETATION)
Habitat model for the Florida Scrub Jay on John F. Kennedy Space Center
[NASA-TM-107543] p 3673 N92-30494
Altimetry and lidar using AlGaAs lasers modulated with pseudo-random codes p 3641 N92-31030

CANYONS
Duration and rates of discharge: Maja Valles, Mars p 3737 N92-31227

CAPACITORS
New insights into radiation-induced oxide-trap charge through Thermally-Stimulated-Current (TSC) measurement and analysis
[DE92-009054] p 3728 N92-30585
Testing of double-layer capacitors for high reliability applications
[DE92-011384] p 3626 N92-30607

CARBON
Chemistry within van der Waals cluster of unsaturated molecules: Observation of cationic polymerization
[AD-A250929] p 3712 N92-30240
Towards the development of a global inventory for black carbon emissions
[DE92-013514] p 3674 N92-30647
Fundamental studies of carbon, NH, and oxygen rings and other high energy density molecular systems
[AD-A246963] p 3715 N92-30680
Interaction of atomic hydrogen with the surface methyl group on Si(100): Removal of surface carbon
[AD-A249062] p 3595 N92-30821
Line-emission cross sections for the charge-exchange reaction between fully stripped carbon and atomic hydrogen in tokamak plasma
[NIFS-129] p 3716 N92-30967
Proceedings of the 181st Electrochemical Society, Inc. Meeting Program
[AD-A249729] p 3596 N92-31178
A miniature carbon furnace for mass spectroscopy
[DE92-014460] p 3597 N92-31196

CARBON DIOXIDE
Studies of atmospheric molecules by multiphoton spectroscopy
[DE92-012668] p 3672 N92-30345
Reducing greenhouse gas emissions in Czechoslovakia
[DE92-012354] p 3672 N92-30374

CARBON DIOXIDE CONCENTRATION
Oceanic CO2 measurements for the WOCE hydrographic survey in the Pacific Ocean, 1990-1991: Shore based analyses during legs 1-3
[DE92-013064] p 3682 N92-30861
The environmental dilemma of fossil fuels
[DE92-014887] p 3674 N92-31121

CARBON DIOXIDE LASERS
Transverse pattern modification in a stable apertured laser resonator
[ITN-92-85171] p 3656 N92-30582
Atmospheric wind sensing with a 1 and 2 micron coherent lidar p 3639 N92-31019
A compact high repetition rate CO2 coherent Doppler lidar p 3639 N92-31022
Simplified signal processing for an airborne CO2 Doppler lidar p 3639 N92-31023
A comparison of Ultra-Sensitive Coherent Detection (USCD) and heterodyne detection for a wind sensing application p 3640 N92-31025
Coherent CO2 lidar: A superior system for observing clouds? p 3644 N92-31045
HgCdTe photomixers for CO2 laser radar systems p 3654 N92-31100
The ENEA CO2 lidar/DIAL station activity in a tropospheric remote sensing program p 3655 N92-31103
Aerosol extinction measurements with CO2-lidar p 3655 N92-31105

CARBON FIBERS
Influence of various carbon fibre types on the mechanical performance and damage tolerance of composites
[MBB/FE202/S/PUB/477] p 3591 N92-30690
Supercritical fluid extraction: A new process for producing high-performance, low-cost carbon fibers
[AD-A249407] p 3595 N92-30773
Precursor structure-fiber property relationships in polyacrylonitrile-based carbon fibers
[AD-A249888] p 3592 N92-30871

CARBON-CARBON COMPOSITES
Method of bonding carbon-carbon and metal matrix composite structures
[AD-D015299] p 3591 N92-30573
The effect of neutron irradiation on the structure and properties of carbon-carbon composite materials
[DE92-011670] p 3592 N92-30809
Evaluation of characterization techniques for carbon-carbon composites
[AD-A252693] p 3593 N92-31005

CARBONATES
Research issues in molten carbonate fuel cells: Pressurization
[DE92-011755] p 3671 N92-31113

CARBONIZATION
Precursor structure-fiber property relationships in polyacrylonitrile-based carbon fibers
[AD-A249888] p 3592 N92-30871

CARBOXYLIC ACIDS
From minerals to materials: A facile synthetic route to preceramic polymers for aluminum oxide
[AD-A250351] p 3606 N92-31141

CARDIOVASCULAR SYSTEM
Feasibility of a walk test to assess the cardiorespiratory fitness of Naval personnel
[AD-A250650] p 3684 N92-30603
Exercise behavior among Navy runners and non-runners
[AD-A250651] p 3685 N92-30644

CARGO
The allocation of cargo to channel missions
[DE92-013234] p 3578 N92-30565

CARGO AIRCRAFT
Organic Matrix Composite Helicopter Internal/External Cargo Pallet System (OMC INTEX)
[AD-A251127] p 3580 N92-30878

CARRIER MOBILITY
Examinations of the microwave photoelectric conductivity of a-Si:H multilayer systems for in situ characterization
[ETN-92-91688] p 3727 N92-30505

CARTESIAN COORDINATES
Minimization of deviations of gear real tooth surfaces determined by coordinate measurements
[NASA-TM-105718] p 3660 N92-30948

CAST ALLOYS
Effects of impurities on the mechanical behaviour of primary and secondary cast aluminum alloys
[PB92-180652] p 3598 N92-30785

CATACLYSMIC VARIABLES
Modeling of UV lines from cataclysmic variable winds
[DE92-013443] p 3739 N92-30862

CATALOGS (PUBLICATIONS)
Global scale concentrations of volcanic activity on Venus: A summary of three 23rd Lunar and Planetary Science Conference abstracts. 1: Venus volcanism: Global distribution and classification from Magellan data. 2: A major global-scale concentration of volcanic activity in the Beta-Atla-Themis region of Venus. 3: Two global concentrations of volcanism on Venus: Geologic associations and implications for global pattern of upwelling and downwelling p 3737 N92-31226

CATALYSIS
A pulse combustion-based VOC destruction technique
[DE92-013563] p 3594 N92-30369
Design of a high activity and selectivity alcohol catalyst
[DE92-013918] p 3594 N92-30717
Surface-mediated photocatalysis
[AD-A249906] p 3595 N92-30793
Synthesis of cresols and xylenols from benzene and methanol
[DE91-002143] p 3596 N92-30882
Methane to liquid
[DE92-001277] p 3596 N92-30883
A novel process for methanol synthesis
[DE92-015798] p 3608 N92-30904

CATALYSTS
Design of a high activity and selectivity alcohol catalyst
[DE92-013918] p 3594 N92-30717
Approaches to polymer curing and imaging via the in situ generation of a catalyst
[AD-A249917] p 3606 N92-30873
The development of precipitated iron catalysts with improved stability
[DE92-014625] p 3596 N92-31006

CATHODE RAY TUBES
Assessment of a head-mounted miniature monitor
[NASA-TM-103587] p 3688 N92-30381

CATHODES
RF vacuum microelectronics
[AD-A249814] p 3626 N92-30836

CATIONS
Chemistry within van der Waals cluster of unsaturated molecules: Observation of cationic polymerization
[AD-A250929] p 3712 N92-30240
Epoxides as activators for grafting of poly(tetrahydrofuran) from poly(methylphenylsilylene)
[AD-A251086] p 3601 N92-30244
Evidence for interference between resonant and nonresonant transfer and excitation
[DE92-011779] p 3716 N92-30853
A method for the production of weakly acidic cation exchange resins
[DE92-015314] p 3717 N92-31137

CAUCHY PROBLEM
Flow of fresh and salt water in an aquifer with injection from the top
[REPT-91-68] p 3629 N92-30453

CAVITIES
Numerical simulation of crater formation heating by laser beam. Analysis of radiation exchanges in the cavity
[ESA-TT-1234] p 3657 N92-30997

CAVITY FLOW
Numerical solution of a three-dimensional cubic cavity flow by using the Boltzmann equation
[NASA-TM-105693] p 3627 N92-30297

CAVITY RESONATORS
Dielectric behavior of semiconductors at microwave frequencies p 3610 N92-30275
Processing aerosols and filaments in a TM010 microwave cavity at 2.45 GHz
[DE92-013536] p 3615 N92-30703
Application of superconducting cavities to the collider rings of the SSC
[DE92-011692] p 3718 N92-30811

CEILINGS (METEOROLOGY)
Airborne lidar and radiometric observations of PBL- and low clouds p 3642 N92-31037
CENTAUR LAUNCH VEHICLE
Rocket propulsion research at Lewis Research Center [NASA-CR-189187] p 3732 N92-30908
CENTRAL NERVOUS SYSTEM
The properties of the uptake system for glycine in synaptic vesicles [ISSN-0800-4412] p 3683 N92-31152
CENTRIFUGAL PUMPS
Active control of pressure, sound and velocity of centrifugal pumps [AD-A249446] p 3659 N92-30640
CERAMICS
Structural ceramics p 3607 N92-30264
Tempered glass and thermal shock of ceramic materials p 3607 N92-30265
Ceramic processing: Experimental design and optimization p 3607 N92-30267
Mechanism of slip and twinning p 3610 N92-30280
Measuring the Weibull modulus of microscope slides p 3612 N92-30294
Transformation toughening of ceramics [AD-A248903] p 3601 N92-30342
Nondestructive evaluation of ceramic components by gamma ray CT [DE92-626843] p 3602 N92-30402
Creep and slow crack growth mechanisms related to macroscopic creep behavior of a silicon nitride ceramic at elevated temperatures [DE92-015195] p 3663 N92-30567
Effect of bending on the room-temperature tensile strengths of structural ceramics [DE92-015196] p 3603 N92-30626
Study of the surface properties of ceramic materials by chromatography [DE92-011129] p 3604 N92-30695
Processing aerosols and filaments in a TM010 microwave cavity at 2.45 GHz [DE92-013536] p 3615 N92-30703
Nondestructive testing of ceramics for vehicular advanced heat engines [DE92-010471] p 3604 N92-30744
Pressure densification [AD-A249438] p 3604 N92-30758
Cluster assembly of hierarchical nanostructures [DE92-010498] p 3716 N92-30826
Thermally activated rejuvenation of ferroelectric properties in electrically fatigued lead zirconate titanate ceramics [DE92-012634] p 3605 N92-30830
Theory of sublinear power dependence for microwave heating in some ceramic materials [DE92-015147] p 3606 N92-30847
YBa2Cu(3-x)Co(x)O(y): A substrate material for YBCO superconductors [DE92-015182] p 3730 N92-30999
Impurity segregation to grain boundaries and defects in AlN [DE92-011667] p 3599 N92-31112
Grain boundary weak links in high-Tc superconductors [DE92-016192] p 3730 N92-31190
CEREBELLUM
Sparse distributed memory and related models [NASA-CR-190553] p 3690 N92-30724
CEREBRAL CORTEX
Cortical mechanisms of attention, discrimination, and motor response to somaesthetic stimuli [AD-A247228] p 3687 N92-30613
Psychophysical studies of visual cortical function [AD-A246962] p 3687 N92-30679
CERENKOV COUNTERS
Ultra high energy gamma rays and observations with CYGNUS/MILAGRO [DE92-015243] p 3743 N92-30627
CERIUM
Atomic layer epitaxy group 4 materials: Surface processes, thin films, devices, and their characterization [AD-A252352] p 3729 N92-30846
CERMETS
A comparative EIS study on cermet and platinum anodes for the electrolytic production of aluminum [DE92-015091] p 3599 N92-31010
CESIUM
Modeling fast modulation effects in cesium atomic clocks [AD-A252649] p 3636 N92-30412
CHANNEL FLOW
Subgrid-scale backscatter in transitional and turbulent flows p 3630 N92-30650
A subgrid-scale model based on the second-order velocity structure function p 3631 N92-30651
Structure of three-dimensional turbulent boundary layers p 3631 N92-30654
Low Reynolds number kappa-epsilon modeling with the aid of direct simulation data p 3631 N92-30655
One-equation near-wall turbulence modeling with the aid of direct simulation data p 3631 N92-30656
The structure of turbulent channel flow with passive scalar transport p 3632 N92-30657
Continuous wavelet analysis of coherent structures p 3634 N92-30673
Numerical study of axial turbulent flow over long cylinders [AD-A250801] p 3635 N92-30831
Duration and rates of discharge: Maja Valles, Mars p 3737 N92-31227
CHAOS
Multifractal analysis of chaotic point sets [AD-A250756] p 3709 N92-31194
CHARACTERIZATION
Evaluation of characterization techniques for carbon-carbon composites [AD-A252693] p 3593 N92-31005
CHARGE COUPLED DEVICES
Full surface testing of grazing incidence mirrors [AD-A248851] p 3719 N92-30233
A stroboscopic technique for using CCD cameras in flow visualization systems for continuous viewing and stop action photography [NASA-TM-107648] p 3637 N92-30737
Boundary plasma transport studies on TFTR [DE92-011942] p 3723 N92-30746
New shortwave solar radiometer with information-based sparse sampling [DE92-010483] p 3742 N92-30797
Focused ion beam implantation [AD-A249662] p 3627 N92-31004
A range-resolved bistatic lidar using a high-sensitive CCD-camera p 3640 N92-31027
CHARGE EXCHANGE
Rapid change of hydrogen neutral energy distribution at L/H-transition in JFT-2M H-mode [NIFS-134] p 3714 N92-30510
Chemielectron and photoelectron spectroscopic studies of importance in the upper atmosphere [AD-A248838] p 3675 N92-30556
CHARGE TRANSFER
Measurement of radiative lifetimes of vibrational states of simple ions [AD-A248567] p 3712 N92-30337
Line-emission cross sections for the charge-exchange reaction between fully stripped carbon and atomic hydrogen in tokamak plasma [NIFS-129] p 3716 N92-30967
Proceedings of the 181st Electrochemical Society, Inc. Meeting Program [AD-A249729] p 3596 N92-31178
CHARPY IMPACT TEST
Recent improvements in size effects correlations for DBTT and upper shelf energy of ferritic steels [DE92-014703] p 3599 N92-30877
CHARTS
Antarctic ice charts, 1989 - 1990: Analysis Atlas [AD-A249730] p 3669 N92-31179
CHELATES
Studies of thermal decomposition of the 1:1 R3Al:en adduct (R = Me, Et; en = ethylenediamine): Synthesis and structure of a novel intermediate Al((HNCH2CH2NH)AlMe2)3 [AD-A251061] p 3603 N92-30623
CHEMICAL ANALYSIS
Perforated monolayers [DE92-011632] p 3593 N92-30344
Time and wavelength domain algorithms for chemical analysis by laser radar p 3650 N92-31075
From minerals to materials: A facile synthetic route to preceramic polymers for aluminum oxide [AD-A250351] p 3606 N92-31141
Filler metal development for Hastelloy alloy XR [DE92-782044] p 3600 N92-31163
CHEMICAL BONDS
Chemistry within van der Waals cluster of unsaturated molecules: Observation of cationic polymerization [AD-A250929] p 3712 N92-30240
Vibrationally induced rotational axis switching: A novel mechanism for vibrational mode-coupling [AD-A251085] p 3712 N92-30259
Understanding heterolytic bond cleavage [AD-A252336] p 3716 N92-30845
A method for production of new anion exchangers [DE92-015313] p 3717 N92-31147
CHEMICAL COMPOSITION
Electrical and chemical interactions at Mars Workshop, part 1 [NASA-CP-10093] p 3741 N92-30302
Time and wavelength domain algorithms for chemical analysis by laser radar p 3650 N92-31075
Waste streams in a typical crewed space habitat: An update [NASA-TM-103888] p 3689 N92-31166
On the isotopic signature of recent solar-wind nitrogen p 3738 N92-31231
CHEMICAL ENERGY
Photoinitiated electron transfer in multichromophoric species: Synthetic tetrads and pentads featuring diquinone moieties [DE92-013472] p 3683 N92-30368
CHEMICAL EXPLOSIONS
Fragment hazard zone analyses for explosive test facilities [DE92-015391] p 3613 N92-30887
Modeling initiation of explosives by projectile impact [DE92-015210] p 3608 N92-31202
CHEMICAL PROPERTIES
Study of the surface properties of ceramic materials by chromatography [DE92-011129] p 3604 N92-30695
Development of practical MO techniques for prediction of the properties and behavior of materials [AD-A247218] p 3598 N92-30864
CHEMICAL REACTIONS
Hyperspectral gas analysis system (HyGAS), phase 1 [AD-A251026] p 3593 N92-30241
Turbulent reacting flows and supersonic combustion [AD-A251065] p 3593 N92-30256
Magic numbers in molecular clusters: A probe for chemical reactivity [AD-A251096] p 3712 N92-30261
A pulse combustion-based VOC destruction technique [DE92-013563] p 3594 N92-30369
Fundamental studies of carbon, NH, and oxygen rings and other high energy density molecular systems [AD-A246963] p 3715 N92-30680
High-temperature ignition of propane with MTBE as an additive: Shock-tube experiments and modeling [DE92-006679] p 3594 N92-30749
Development of practical MO techniques for prediction of the properties and behavior of materials [AD-A247218] p 3598 N92-30864
CHEMICAL REACTORS
The development of precipitated iron catalysts with improved stability [DE92-014625] p 3596 N92-31006
CHEMICAL WARFARE
Effects of pyridostigmine bromide on A-10 pilots during execution of a simulated mission; performance [AD-A252309] p 3685 N92-30605
CHLOROFLUOROCARBONS
Status of selected air pollution control programs, February 1992 [PB92-171966] p 3673 N92-30561
CHLOROPHYLLS
Event-scale relationships between surface velocity, temperature and chlorophyll in the coastal ocean, as seen by satellite [NASA-CR-190266] p 3682 N92-30739
Electrochemical and optical studies of model photosynthetic systems [DE92-010657] p 3683 N92-30829
CHLOROPRENE RESINS
Stress-strain characteristics of rubber-like materials: Experiment and analysis p 3607 N92-30285
CHROMATOGRAPHY
Study of the surface properties of ceramic materials by chromatography [DE92-011129] p 3604 N92-30695
CHROMIUM ALLOYS
Investigation of joining techniques for advanced austenitic alloys [DE92-015545] p 3599 N92-30888
CHROMIUM STEELS
Investigation of joining techniques for advanced austenitic alloys [DE92-015545] p 3599 N92-30888
CIRCADIAN RHYTHMS
Neurophysiological analysis of circadian rhythm entrainment [AD-A248466] p 3684 N92-30319
Melatonin, the pineal gland and circadian rhythms [AD-A250640] p 3684 N92-30376
Control of circadian behavior by transplanted suprachiasmatic nuclei [AD-A250442] p 3686 N92-31143
Light as a chronobiologic countermeasure for long-duration space operations [NASA-TM-103874] p 3686 N92-31167
CIRCUITS
Backward-wave oscillator investigations in the Raman Regime [AD-A250738] p 3622 N92-30332
Dynamic analysis of compact helical system power supply and designs of its upgrade [NIFS-TECH-2] p 3723 N92-30497

VLSI design, parallel computation, and distributed computing
[AD-A252349] p 3699 N92-30596
The temperature dependence of a large dynamic range photodetector structure
[AD-A247667] p 3624 N92-30683
Properties of CMOS devices and circuits fabricated on high-resistivity, detector-grade silicon
[DE92-011727] p 3626 N92-30813
RF vacuum microelectronics
[AD-A249814] p 3626 N92-30836

CITIES
A one-class classifier for identifying urban areas in remotely-sensed data
[DE92-013539] p 3667 N92-30704

CIVIL AVIATION
The Eurofar program: An European overview on advanced VTOL civil transportation system
[MBB-UD-0611-91-PUB] p 3578 N92-30418
Aircraft accident report: Explosive decompression - loss of cargo door in flight, United Airlines Flight 811, Boeing 747-122, N4713U, Honolulu, Hawaii, February 24, 1989
[PB92-910402] p 3578 N92-31159
High-speed civil transport issues and technology program
[NASA-CR-186020] p 3580 N92-31208

CLADDING
Waveguide polarizer using localized surface plasmons
[AD-D015258] p 3614 N92-30348

CLASSIFICATIONS
The use of TM data for identification of land cover and for detection of land use changes in the Atlantic zone of Costa Rica
[BCRS-91-36] p 3666 N92-30362
Classifying termination of term rewriting
[RUU-CS-91-42] p 3693 N92-30444
The two-dimensional random walk: Its hitting process and its classification
[CWI-BS-R9003] p 3705 N92-30689
A one-class classifier for identifying urban areas in remotely-sensed data
[DE92-013539] p 3667 N92-30704

CLAYS
Multiple scattering wavelength dependent backscattering of kaolin dust in the IR: Measurements and theory p 3648 N92-31064

CLEAN ENERGY
The status of renewable energy technology
[DE92-011386] p 3670 N92-30808

CLEAVAGE
Understanding heterolytic bond cleavage
[AD-A252336] p 3716 N92-30845

CLIMATE
The environmental dilemma of fossil fuels
[DE92-014887] p 3674 N92-31121

CLIMATE CHANGE
Small satellite radiation budget instrumentation
[DE92-011134] p 3677 N92-31008
The environmental dilemma of fossil fuels
[DE92-014887] p 3674 N92-31121

CLIMATOLOGY
Evaporation duct effects at millimeter wavelengths
[AD-A250239] p 3617 N92-30876
A statistical comparison of AUTEC and Eleuthera Island wind data for the period 1 April 1989 through 30 March 1990
[AD-A248898] p 3679 N92-31003
Lidar analysis techniques for use in the atmospheric boundary layer p 3649 N92-31069

CLIMBING FLIGHT
Numerical methods for the simulation of complex multi-body flows with applications for the integrated Space Shuttle vehicle p 3576 N92-30741
Application of the Chimera overlapped grid scheme to simulation of Space Shuttle ascent flows p 3576 N92-30742

CLOCKS
An extension to Schneider's general paradigm for fault-tolerant clock synchronization
[NASA-TM-107634] p 3699 N92-30677
Verifying the interactive convergence clock synchronization algorithm using the Boyer-Moore theorem prover
[NASA-CR-189649] p 3700 N92-31158

CLOSED ECOLOGICAL SYSTEMS
Integration mockup and process material management system
[NASA-CR-184319] p 3613 N92-30754

CLOUD COVER
Multiple scattering lidar returns from stratus clouds p 3642 N92-31035
Airborne lidar and radiometric observations of PBL- and low clouds p 3642 N92-31037

CLOUD PHYSICS
Clouds: Their prediction and simulation
[AD-A250643] p 3679 N92-30643

CLOUDS (METEOROLOGY)
Clouds: Their prediction and simulation
[AD-A250643] p 3679 N92-30643
Multiple scattering effects on spaceborne lidar p 3641 N92-31032
Determining water cloud particle sizes from lidar depolarization measurements and time dependent multiple scattering coefficients p 3641 N92-31034
ECLIPS at LMD: Preliminary results of phase 2 p 3643 N92-31038
Water vapor variance measurements using a Raman lidar p 3643 N92-31041
Coherent CO2 lidar: A superior system for observing clouds? p 3644 N92-31045
Time and polarization dependent double scattering calculations of lidar returns from water clouds p 3647 N92-31063
Measurements of the backscattering phase matrices of crystal clouds with a polarization lidar p 3651 N92-31083

CLUMPS
Fractal and multifractal approaches to clustering phenomena
[AD-A249481] p 3709 N92-30642

CLUSTERS
Magic numbers in molecular clusters: A probe for chemical reactivity
[AD-A251096] p 3712 N92-30261
Electron scattering and electromagnetic response properties of metal clusters
[DE92-014715] p 3621 N92-31007

CLUTTER
Maximum likelihood detection of electro-optic moving targets
[AD-A249442] p 3616 N92-30762
Multifrequency measurements of radar ground clutter at 42 sites. Volume 3: Appendix E
[AD-A246988] p 3616 N92-30863

CMOS
Properties of CMOS devices and circuits fabricated on high-resistivity, detector-grade silicon
[DE92-011727] p 3626 N92-30813

COASTAL CURRENTS
Event-scale relationships between surface velocity, temperature and chlorophyll in the coastal ocean, as seen by satellite
[NASA-CR-190266] p 3682 N92-30739

COASTAL WATER
Interpretation of optical remote sensing data over coastal waters
[BCRS-91-27] p 3667 N92-30472
Event-scale relationships between surface velocity, temperature and chlorophyll in the coastal ocean, as seen by satellite
[NASA-CR-190266] p 3682 N92-30739

COASTS
Evaporation duct effects at millimeter wavelengths
[AD-A250239] p 3617 N92-30876

COATING
A shear sensitive monomer-polymer laminate structure and method of using same
[NASA-CASE-LAR-14654-1] p 3662 N92-30317

COATINGS
Fabrication of multifilament conductors: CVD processing of high Tc superconducting composite fibers
[NASA-CR-184344] p 3591 N92-30711

COCKPIT SIMULATORS
KC-135 crew reduction feasibility demonstration simulation study. Volume 1: Function analysis and function reallocation
[AD-A252265] p 3688 N92-30592

COCKPITS
High speed research system study. Advanced flight deck configuration effects
[NASA-CR-189650] p 3581 N92-30965

CODE DIVISION MULTIPLE ACCESS
Personal communications via ACTS satellite HBR transponders p 3618 N92-30929
The ELLIPSO (tm) system: Elliptical low orbits for mobile communications and other optimum system elements p 3618 N92-30930
A personal communications network using a Ka-band satellite p 3619 N92-30934
Capacity and interference in a PCS system p 3619 N92-30937
Direct sequence spread spectrum CDMA in shared spectrum applications p 3619 N92-30939

CODING
Review of psychophysically-based image quality metrics
[AD-A251053] p 3686 N92-30254
Modeling of video traffic in packet networks, low rate video compression, and the development of a lossy+lossless image compression algorithm
[NASA-CR-190546] p 3691 N92-30296
Bandwidth efficient CCSDS coding standard proposals
[NASA-CR-190317] p 3587 N92-30709

COEFFICIENT OF FRICTION
Solid lubrication of laser grown fluorinated diamond thin films
[AD-A249485] p 3603 N92-30635

COEFFICIENTS
Special finite element methods for a class of second order elliptic problems with rough coefficients
[AD-A248900] p 3701 N92-30339
Effects of the orientational pair correlation on second order nonlinear optical coefficients
[AD-A252490] p 3720 N92-30535
Coefficients of the second viscosity in bulk liquid helium
[AD-A252421] p 3629 N92-30548

COGNITION
Induced pictorial representations
[AD-A248560] p 3687 N92-30336
Introduction to cognitive processes of expert pilots
[DOT/FAA/RD-92/12] p 3578 N92-30980

COHERENT RADAR
Diversity imaging techniques in lidar p 3640 N92-31026
Coherent CO2 lidar: A superior system for observing clouds? p 3644 N92-31045

COHERENT RADIATION
Generation of stimulated backscattered harmonic radiation from intense laser interactions with beams and plasmas
[AD-A248782] p 3656 N92-30614

COHERENT SCATTERING
Search for light neutral scalar and pseudoscalar particles in pFe interactions at 70 GeV
[DE92-627317] p 3713 N92-30404

COLD PLASMAS
Low-frequency fluctuations in plasma magnetic fields
[DE92-012139] p 3724 N92-30833

COLD TOLERANCE
Secretory mechanisms in opiocortin cells during cold stress
[AD-A252317] p 3685 N92-30719

COLLIMATION
Antenna pattern measurement facilities
[AD-A248964] p 3584 N92-30329
The ACTS multibeam antenna
[NASA-TM-105645] p 3587 N92-30383

COLLISION AVOIDANCE
A cable detection lidar system for helicopters p 3648 N92-31068

COLLISIONAL PLASMAS
Low-frequency fluctuations in plasma magnetic fields
[DE92-012139] p 3724 N92-30833
Collisional and chaotic transport of energetic particles in toroidal plasma
[DE92-014589] p 3725 N92-30900

COLLISIONLESS PLASMAS
Low-frequency fluctuations in plasma magnetic fields
[DE92-012139] p 3724 N92-30833

COLLISIONS
Impact erosion of terrestrial planetary atmospheres
[NASA-CR-190605] p 3742 N92-30921

COLLOIDS
Transformation toughening of ceramics
[AD-A248903] p 3601 N92-30342
Photochemical solar energy conversion utilizing semiconductors localized in membrane-mimetic systems
[DE92-011115] p 3670 N92-30694

COLOR
A method of making a single layer multi-color luminescent display
[NASA-CASE-LAR-14811-1] p 3622 N92-30389
Psychophysical studies of visual cortical function
[AD-A246962] p 3687 N92-30679
Two-color infrared digital imaging for determination of in-cylinder temperature and species during compression and combustion periods of DI diesel engine
[AD-A249812] p 3595 N92-30835

COLOR TELEVISION
Initial laboratory evaluation of color video cameras
[DE92-010399] p 3637 N92-30822

COLUMBUS SPACE STATION
Operations and logistics tasks in the Columbus development program
[MBB-UO-0166-91-PUB] p 3708 N92-30419
Adoption of the LSA S/W DILSA for the Columbus LSA tasks
[MBB-UO-0168-91-PUB] p 3709 N92-30420
Columbus logistics transportation and ground processing
[MBB-UO-0167-91-PUB] p 3709 N92-30442

COMBINATORIAL ANALYSIS
Kayles on special classes of graphs: An application of Sprague-Grundy theory
[RUU-CS-91-49] p 3703 N92-30450

On the complexity of the maximum cut problem
[RUU-CS-91-39] p 3703 N92-30458
Combinatorics and Kolmogorov complexity
[CWI-CS-R9125] p 3708 N92-30699
Markov chain simulations of binary matrices
[AD-A249265] p 3708 N92-30771
Graphical-based construction of combinatorial geometries for radiation transport and shielding applications
[DE92-014453] p 3696 N92-30886

COMBUSTIBLE FLOW
Turbulent reacting flows and supersonic combustion
[AD-A251065] p 3593 N92-30256
Combustion diagnostics by photo-deflection spectroscopy
[AD-A250802] p 3594 N92-30645

COMBUSTION
A new unsteady mixing model to predict NO(x) production during rapid mixing in a dual-stage combustor
[NASA-CR-189155] p 3581 N92-30569
Combustion diagnostics by photo-deflection spectroscopy
[AD-A250802] p 3594 N92-30645
The influence of Lewis number and nonhomogeneous mixture on premixed turbulent flame structure
p 3597 N92-30669
Two-color infrared digital imaging for determination of in-cylinder temperature and species during compression and combustion periods of DI diesel engine
[AD-A249812] p 3595 N92-30835

COMBUSTION CHAMBERS
A pulse combustion-based VOC destruction technique
[DE92-013563] p 3594 N92-30369
A new unsteady mixing model to predict NO(x) production during rapid mixing in a dual-stage combustor
[NASA-CR-189155] p 3581 N92-30569
Two-color infrared digital imaging for determination of in-cylinder temperature and species during compression and combustion periods of DI diesel engine
[AD-A249812] p 3595 N92-30835

COMBUSTION CHEMISTRY
A pulse combustion-based VOC destruction technique
[DE92-013563] p 3594 N92-30369
Laminar flamelet modeling of turbulent diffusion flames p 3633 N92-30667
Statistics for laminar flamelet modeling
p 3597 N92-30668

COMBUSTION CONTROL
Advanced concepts for controlled combustion in engines
[AD-A249911] p 3595 N92-30814

COMBUSTION EFFICIENCY
A new unsteady mixing model to predict NO(x) production during rapid mixing in a dual-stage combustor
[NASA-CR-189155] p 3581 N92-30569

COMBUSTION PHYSICS
A new unsteady mixing model to predict NO(x) production during rapid mixing in a dual-stage combustor
[NASA-CR-189155] p 3581 N92-30569
Advanced concepts for controlled combustion in engines
[AD-A249911] p 3595 N92-30814
Computational simulation of diamond chemical vapor deposition in premixed C2H2/O2/H2 and CH4/O2 strained flames
[DE92-012144] p 3606 N92-30857

COMBUSTION PRODUCTS
Towards the development of a global inventory for black carbon emissions
[DE92-013514] p 3674 N92-30647
Advanced concepts for controlled combustion in engines
[AD-A249911] p 3595 N92-30814
Two-color infrared digital imaging for determination of in-cylinder temperature and species during compression and combustion periods of DI diesel engine
[AD-A249812] p 3595 N92-30835

COMET RENDEZVOUS ASTEROID FLYBY MISSION
Software breadboard study
[NASA-CR-190473] p 3625 N92-30757

COMETS
Impact erosion of terrestrial planetary atmospheres
[NASA-CR-190605] p 3742 N92-30921

COMMERCE
Attitudinal and situational differences between national laboratory inventors and inventor-entrepreneurs
[DE92-015768] p 3733 N92-30889

COMMERCIAL AIRCRAFT
Statistics on aircraft gas turbine engine rotor failures that occurred in US commercial aviation during 1989
[DOT/FAA/CT-92/5] p 3581 N92-30303
A principled approach to the measurement of situation awareness in commercial aviation
[NASA-CR-4451] p 3686 N92-30306

COMMUNICATING
EHF (28/19 GHz) personal communications satellite terminal development p 3619 N92-30935

COMMUNICATION NETWORKS
The ACTS multibeam antenna
[NASA-TM-105645] p 3587 N92-30383
A paradigm for asynchronous communication and its application to concurrent constraint programming
[RUU-CS-91-46] p 3615 N92-30448
Grand challenges 1993: High performance computing and communications. A report by the Committee on Physical, Mathematical, and Engineering Sciences to supplement the President's fiscal year 1993 budget
[PB92-160530] p 3689 N92-30600
Architecture for the high performance implantation of communication transport level protocols
[ETN-92-91666] p 3690 N92-30701
Network load of X terminals at CDF
[DE92-011704] p 3699 N92-30812
Proceedings of the Workshop on Advanced Network and Technology Concepts for Mobile, Micro, and Personal Communications
[NASA-CR-190459] p 3617 N92-30923
Leo satellite-based telecommunication network concepts p 3617 N92-30926
A personal communications network using a Ka-band satellite p 3619 N92-30934
Cellular: Toward personal communications
p 3619 N92-30936
Capacity and interference in a PCS system
p 3619 N92-30937
The Pan-European Digital Cellular (GSM) System
p 3619 N92-30938
Direct sequence spread spectrum CDMA in shared spectrum applications p 3619 N92-30939
Toward a North American standard for mobile data services p 3620 N92-30940

COMMUNICATION SATELLITES
Proceedings of the Workshop on Advanced Network and Technology Concepts for Mobile, Micro, and Personal Communications
[NASA-CR-190459] p 3617 N92-30923
Design of the American Mobile Satellite System
p 3617 N92-30925
Ka-band mobile and personal systems development at JPL p 3618 N92-30928
EHF (28/19 GHz) personal communications satellite terminal development p 3619 N92-30935
National transportable telecommunications capability
p 3620 N92-30943

COMPANION STARS
Constraints on the putative companions to PSR1257+12 p 3738 N92-31232

COMPARISON
The REMBRANDT system for multi-criteria decision analysis via pairwise comparisons or direct rating
[REPT-92-05] p 3692 N92-30357
Pairwise comparison of concessions in negotiation processes
[REPT-92-15] p 3733 N92-30463
Informatization in public administration (EGPA-research project 1991). Large scale information systems (comparative analysis in 8 European countries)
[REPT-91-93] p 3734 N92-30487
Contribution of parallelism to solving a load distribution problem in electric networks
[ETN-92-91668] p 3625 N92-30702
Transfer soldering evaluation
[DE92-015160] p 3627 N92-31144

COMPENSATORS
Strong dynamic input-output decoupling: From linearity to nonlinearity
[MEMO-COSOR-92-04] p 3694 N92-30478

COMPILERS
Compiler analysis for irregular problems in FORTRAN D
[NASA-CR-189664] p 3689 N92-30311

COMPLEX NUMBERS
Real polynomial systems of degree n with n+1 line invariants
[REPT-91-86] p 3704 N92-30490

COMPLEXITY
On the complexity of the maximum cut problem
[RUU-CS-91-39] p 3703 N92-30458
Combinatorics and Kolmogorov complexity
[CWI-CS-R9125] p 3708 N92-30699

COMPOSITE MATERIALS
National Educators' Workshop: Update 1991. Standard Experiments in Engineering Materials Science and Technology
[NASA-CP-3151] p 3608 N92-30263
Modeling and analysis methodology for aeroelastically tailored chordwise deformable wings
[NASA-CR-189620] p 3579 N92-30304
Special finite element methods for a class of second order elliptic problems with rough coefficients
[AD-A248900] p 3701 N92-30339
Low-velocity impact loading on fibre reinforced aluminum laminates (ARALL) and other aircraft sheet materials
[ETN-92-91613] p 3590 N92-30414
Molecular weight dependence of domain structure in silica-siloxane molecular composites
[DE92-015046] p 3603 N92-30544
Ultrasound NDE of adhesive bond integrity: A quantitative measure
[AD-A248845] p 3661 N92-30599
Center for Composites Manufacturing Science, Reliability, and Maintainability Technology
[AD-A248661] p 3591 N92-30639
Influence of various carbon fibre types on the mechanical performance and damage tolerance of composites
[MBB/FE202/S/PUB/477] p 3591 N92-30690
A demonstration of passive blade twist control using extension-twist coupling
[NASA-TM-107642] p 3664 N92-31155
Advanced electromagnetic methods for aerospace vehicles
[NASA-CR-190650] p 3621 N92-31156

COMPOSITE STRUCTURES
An experiment on the use of disposable plastics as a reinforcement in concrete beams p 3593 N92-30287
Multidisciplinary optimization of fiber composite aircraft structures
[MBB/FW321/S/PUB/476] p 3579 N92-30424
Center for Composites Manufacturing Science, Reliability, and Maintainability Technology
[AD-A248661] p 3591 N92-30639
Designing, fabricating and testing cost effective structural composite for the SSCL magnets
[DE92-013469] p 3718 N92-30646
Nonlinear stress analysis of composite-jacketed steel cylinders subjected to high internal pressure
[AD-A249500] p 3663 N92-30802
Organic Matrix Composite Helicopter Internal/External Cargo Pallet System (OMC INTEX)
[AD-A251127] p 3580 N92-30878
Evaluation of characterization techniques for carbon-carbon composites
[AD-A252693] p 3593 N92-31005
Wrappability of curves on surfaces
[AD-A250004] p 3707 N92-31140

COMPOSITE WRAPPING
Wrappability of curves on surfaces
[AD-A250004] p 3707 N92-31140

COMPRESSIBILITY
Role of compressibility on driven magnetic reconnection
[NIFS-105] p 3710 N92-30498

COMPRESSIBILITY EFFECTS
Interaction of isotropic turbulence with a shock wave
[AD-A250409] p 3635 N92-30852

COMPRESSIBLE FLOW
Algorithm to solve nonlinear time dependent problems of engineering and physics
[AD-A250641] p 3702 N92-30347
Solving the Euler equations using adaptive mesh motion and refinement
[AD-A252364] p 3705 N92-30597
On the subgrid-scale modeling of compressible turbulence p 3631 N92-30652
Modeling the turbulent kinetic energy equation for compressible, homogeneous turbulence
p 3631 N92-30653
Interaction of isotropic turbulence with a shock wave
[AD-A250409] p 3635 N92-30852
Navier-Stokes analysis and experimental data comparison of compressible flow within ducts
[NASA-TM-105796] p 3582 N92-30972

COMPRESSIBLE FLUIDS
Continuum approaches for describing solid-liquid flow
[AD-A249028] p 3629 N92-30560

COMPRESSION TESTS
Influence of various carbon fibre types on the mechanical performance and damage tolerance of composites
[MBB/FE202/S/PUB/477] p 3591 N92-30690
Assessment of an improved multiaxial strength theory based on creep-rupture data for type 316 stainless steel
[DE92-010431] p 3663 N92-30823
Interface friction, lubricants, and their influence on metal flow
[DE92-012112] p 3606 N92-30866

COMPRESSIVE STRENGTH
Structure, processing, and properties of potatoes
p 3611 N92-30288
Precursor structure-fiber property relationships in polyacrylonitrile-based carbon fibers
[AD-A249888] p 3592 N92-30871

COMPRESSORS
Small engine components test facility compressor testing cell at NASA Lewis Research Center
[NASA-TM-105685] p 3584 N92-30508
Repetitive High Energy Pulsed Power (RHEPP) temperature monitoring system utilizing Luxtron fluoroptic sensors and thermocouples technical reference manual
[DE92-013461] p 3637 N92-30893
Navier-Stokes analysis and experimental data comparison of compressible flow within ducts
[NASA-TM-105796] p 3582 N92-30972
COMPUTATION
Computing and verifying depth orders
[RUU-CS-91-41] p 3693 N92-30443
Point location in fat subdivisions
[RUU-CS-91-40] p 3703 N92-30447
Implementation of parallel algorithms
[AD-A248826] p 3695 N92-30555
Grand challenges 1993: High performance computing and communications. A report by the Committee on Physical, Mathematical, and Engineering Sciences to supplement the President's fiscal year 1993 budget
[PB92-160530] p 3689 N92-30600
Transactions of the 9th Army Conference on Applied Mathematics and Computing
[AD-A252140] p 3706 N92-30843
COMPUTATIONAL CHEMISTRY
Analytical methods using Slater-type orbitals in quantum chemistry
[AD-A251044] p 3731 N92-30242
Fundamental studies of carbon, NH, and oxygen rings and other high energy density molecular systems
[AD-A246963] p 3715 N92-30680
Computational simulation of diamond chemical vapor deposition in premixed C2H2/O2/H2 and CH4/O2 strained flames
[DE92-012144] p 3606 N92-30857
Development of practical MO techniques for prediction of the properties and behavior of materials
[AD-A247218] p 3598 N92-30864
COMPUTATIONAL FLUID DYNAMICS
Navier-Stokes computations of a viscous optimized waverider
[NASA-CR-189658] p 3574 N92-30392
A multigrid method for a discretization of the incompressible Navier-Stokes equations in general coordinates
[REPT-91-73] p 3629 N92-30454
Development of a modular transient cycle analysis program for the adiabatic diesel and other compound diesel engines
[AD-A249022] p 3658 N92-30538
A gridless Euler/Navier-Stokes solution algorithm for complex two-dimensional applications
[NASA-TM-107631] p 3575 N92-30570
A Boussinesq algorithm for bouyant convection in polygonal domains
[PB92-187137] p 3695 N92-30579
Monte Carlo particle simulation of low-density fluid flow on MIMD supercomputers
[DE92-014618] p 3630 N92-30607
Low order dynamical models for mixing layers
p 3633 N92-30662
Numerical simulation of low Prandtl number turbulent mixing p 3633 N92-30663
Length scales and dissipation of fine eddies in a mixing layer p 3633 N92-30664
Geometry of premixed flames in three-dimensional turbulence p 3633 N92-30666
Calculation of viscous hypersonic flows in chemical non-equilibrium
[MBB/FE211/S/PUB/466] p 3634 N92-30674
Numerical optimization in Germany: A non-exhaustive survey on current activities with emphasis on aeronautics
[MBB/FE211/S/PUB/474] p 3573 N92-30675
CFD contributions during hypersonic airplane intake design
[MBB/FE213/S/PUB/459] p 3575 N92-30676
Implicit upwind-Euler solution algorithms for unstructured-grid applications
[NASA-TM-107645] p 3575 N92-30691
MATGRID, a program for generation of C-H and C-O topology grids around wing/body configurations: Software description document
[FFA-TN-1990-20] p 3575 N92-30713
Numerical methods for the simulation of complex multi-body flows with applications for the integrated Space Shuttle vehicle
[NASA-CR-190045] p 3575 N92-30740
Numerical methods for the simulation of complex multi-body flows with applications for the integrated Space Shuttle vehicle p 3576 N92-30741
Application of the Chimera overlapped grid scheme to simulation of Space Shuttle ascent flows
p 3576 N92-30742
Delaunay triangulation and computational fluid dynamics meshes
[NASA-TM-107663] p 3689 N92-30907
Navier-Stokes analysis and experimental data comparison of compressible flow within ducts
[NASA-TM-105796] p 3582 N92-30972
Development of a 3-D upwind PNS code for chemically reacting hypersonic flowfields
[NASA-CR-190182] p 3576 N92-30977
A CFD validation roadmap for hypersonic flows
[NASA-TM-103935] p 3636 N92-30982
COMPUTATIONAL GEOMETRY
Graphical-based construction of combinatorial geometries for radiation transport and shielding applications
[DE92-014453] p 3696 N92-30886
COMPUTATIONAL GRIDS
Finite volume discretization of the incompressible Navier-Stokes equations in general coordinates on staggered grids
[REPT-91-71] p 3628 N92-30373
Progress in unstructured-grid methods development for unsteady aerodynamic applications
[NASA-TM-107643] p 3574 N92-30393
Adaptive multigrid applied to a bipolar transistor problem
[CWI-NM-R9115] p 3693 N92-30429
A multigrid method for a discretization of the incompressible Navier-Stokes equations in general coordinates
[REPT-91-73] p 3629 N92-30454
Finite volume discretization of the convection-diffusion equation in general coordinates
[REPT-91-72] p 3704 N92-30483
Operational surfaces for the rectangle and triangle
[DE92-015165] p 3705 N92-30566
Solving the Euler equations using adaptive mesh motion and refinement
[AD-A252364] p 3705 N92-30597
A dynamic subgrid-scale eddy viscosity model
p 3630 N92-30649
Subgrid-scale backscatter in transitional and turbulent flows p 3630 N92-30650
On the subgrid-scale modeling of compressible turbulence p 3631 N92-30652
Statistics for laminar flamelet modeling
p 3597 N92-30668
CFD contributions during hypersonic airplane intake design
[MBB/FE213/S/PUB/459] p 3575 N92-30676
Implicit upwind-Euler solution algorithms for unstructured-grid applications
[NASA-TM-107645] p 3575 N92-30691
Numerical methods for the simulation of complex multi-body flows with applications for the integrated Space Shuttle vehicle
[NASA-CR-190045] p 3575 N92-30740
Application of the Chimera overlapped grid scheme to simulation of Space Shuttle ascent flows
p 3576 N92-30742
Trajectory fitting in function space with application to analytic modeling of surfaces
[NASA-TP-3232] p 3576 N92-30747
Direct simulation of high-speed mixing layers
[NASA-TP-3186] p 3576 N92-30909
Minimization of deviations of gear real tooth surfaces determined by coordinate measurements
[NASA-TM-105718] p 3660 N92-30948
COMPUTER AIDED DESIGN
A program of continuing research on representing, manipulating, and reasoning about physical objects
[AD-A251089] p 3691 N92-30260
Controlling user interface objects through pre- and postconditions
[REPT-92-04] p 3692 N92-30356
MBB-LAGRANGE: A general structural reliability and optimization structural system
[MBB/FW321/S/PUB/467] p 3662 N92-30423
Lazy and incremental program generation
[CWI-CS-R9124] p 3692 N92-30428
Development environment for digital simulation models of multibody systems
[NLR-TP-89327-U] p 3693 N92-30476
Soviet applied information sciences in a time of change
[PB92-173020] p 3734 N92-30509
Reliability in the design phase
[DE92-012217] p 3661 N92-30763
An overview of the computer aided definition system for design definition at Sandia National Laboratories, Livermore FY1991 update
[DE92-015991] p 3696 N92-30892
ILS, CE, CALS? From design to operation
[ETN-92-91717] p 3697 N92-30950
First conclusions of a manufacturer group on the applicability of CALS in Europe p 3697 N92-30951
Concurrent engineering p 3697 N92-30952
Practical application of the ILS: Practical integration, design, and logistics p 3697 N92-30955
Thermohydraulic modeling of nuclear thermal rockets: The KLAXON code
[DE92-015274] p 3589 N92-31204
COMPUTER AIDED MANUFACTURING
Center for Composites Manufacturing Science, Reliability, and Maintainability Technology
[AD-A248661] p 3591 N92-30639
COMPUTER AIDED MAPPING
Digital bottom mapping
[AD-D015238] p 3682 N92-30413
COMPUTER AIDED TOMOGRAPHY
Nondestructive evaluation of ceramic components by gamma ray CT
[DE92-626843] p 3602 N92-30402
COMPUTER ASSISTED INSTRUCTION
Integrating commercial off-the-shelf tools for custom software development
[AD-A252462] p 3695 N92-30550
Quality assurance and ILS p 3697 N92-30953
COMPUTER GRAPHICS
Computing and verifying depth orders
[RUU-CS-91-41] p 3693 N92-30443
The GKS input model in MANIFOLD
[CWI-CS-R9127] p 3699 N92-30696
Gaussian windows: A tool for exploring multivariate data
[NASA-CR-190559] p 3696 N92-30723
Graphical-based construction of combinatorial geometries for radiation transport and shielding applications
[DE92-014453] p 3696 N92-30886
An overview of the computer aided definition system for design definition at Sandia National Laboratories, Livermore FY1991 update
[DE92-015991] p 3696 N92-30892
COMPUTER INFORMATION SECURITY
How to securely replicate services
[NASA-CR-190476] p 3692 N92-30379
DE-CERTS: A decision support system for a comparative evaluation method for risk management methodologies and tools
[AD-A246965] p 3733 N92-30682
Computer security: Agencies reported having implemented most system security controls
[GAO/IMTEC-92-45] p 3690 N92-30712
COMPUTER NETWORKS
A bibliography on network flow problems (2nd edition)
[RUU-CS-91-38] p 3698 N92-30482
Can stochastic modelling and analysis of multistage interconnection networks lead to efficient usage of redundancy for fault-tolerant design?
[AD-A250635] p 3699 N92-30526
VLSI design, parallel computation, and distributed computing
[AD-A252349] p 3699 N92-30596
Introduction to human factors and wide area networking
[AD-A252310] p 3688 N92-30718
Network load of X terminals at CDF
[DE92-011704] p 3699 N92-30812
Visual perception of depth from occlusion: A neural network model
[AD-A249035] p 3696 N92-30820
An overview of the computer aided definition system for design definition at Sandia National Laboratories, Livermore FY1991 update
[DE92-015991] p 3696 N92-30892
Choice coordination with multiple alternatives
[DE92-011656] p 3700 N92-31111
COMPUTER PROGRAMMING
Information processing research
[AD-A248492] p 3734 N92-30324
Lazy and incremental program generation
[CWI-CS-R9124] p 3692 N92-30428
Classifying termination of term rewriting
[RUU-CS-91-42] p 3693 N92-30444
A paradigm for asynchronous communication and its application to concurrent constraint programming
[RUU-CS-91-46] p 3615 N92-30448
The formal power of AGs with respect to their underlying CFGs
[REPT-91-75] p 3703 N92-30456
Recursive models for synchronous sequential devices
[IMAG-RR-855-I] p 3704 N92-30473
Component construction: Practical guidelines for the construction of reusable components
[REPT-91-89] p 3694 N92-30484
The semantics of the Duplex programming environment
[REPT-91-91] p 3694 N92-30485
Integrating commercial off-the-shelf tools for custom software development
[AD-A252462] p 3695 N92-30550

Detecting potential synchronization constraint deadlocks from formal system specifications
[AD-A249019] p 3696 N92-30631
Development of software to improve AC power quality on large spacecraft
[NASA-CR-190569] p 3589 N92-30989

COMPUTER PROGRAMS
Selection of opening model for parachute scaling studies
[AD-A250882] p 3573 N92-30239
Finite element analysis of laminated composite axisymmetric solids. Volume 1: Theory and applications
[AD-A250808] p 3590 N92-30251
A model of the ADA avionics real-time system: An example of the benefits of the hardware/software codesign approach in development of real-time systems
[AD-A248893] p 3581 N92-30524
Encyclopedia of software components
[NASA-CASE-NPO-18435-1-CU] p 3695 N92-30543
Development statistics for the UH-1 Ada feasibility study
[AD-A252404] p 3584 N92-30547
Modelling of heavily loaded lubricated contacts
[AD-A248807] p 3659 N92-30554
Program RELAX: A code designed to calculate atomic relaxation spectra of x rays and electrons
[DE92-013751] p 3714 N92-30586
Application of automated deduction to the search for single axioms for exponent groups
[DE92-015271] p 3705 N92-30608
EASAMS' Ariane 5 on-board software experience
[D308/TN/001] p 3586 N92-30715
Reliability in the design phase
[DE92-012217] p 3661 N92-30763
Two-color infrared digital imaging for determination of in-cylinder temperature and species during compression and combustion periods of DI diesel engine
[AD-A249812] p 3595 N92-30835
Development of practical MO techniques for prediction of the properties and behavior of materials
[AD-A247218] p 3598 N92-30864
Graphical-based construction of combinatorial geometries for radiation transport and shielding applications
[DE92-014453] p 3696 N92-30886
Characterizing ultrasonic transducers using pattern recognition techniques
[DE92-015845] p 3711 N92-30890
Numerical calculations of two-dimensional single and multi-material flow fields with CCICE
[DE92-015778] p 3636 N92-30903
Development of software to improve AC power quality on large spacecraft
[NASA-CR-190569] p 3589 N92-30989
Altimetry and lidar using AlGaAs lasers modulated with pseudo-random codes p 3641 N92-31030
Nonlinear aerodynamics and the design of wing tips
[NASA-CR-190649] p 3577 N92-31157

COMPUTER STORAGE DEVICES
Storage control system
[NASA-CASE-LAR-14651-1] p 3734 N92-30386
Computing with faulty shared memory
[DE92-011663] p 3695 N92-30522
Analysis of a digital RF memory in a signal-delay application
[DE92-013457] p 3626 N92-30764

COMPUTER SYSTEMS DESIGN
How to securely replicate services
[NASA-CR-190476] p 3692 N92-30379
A processing environment for test and simulation data of thermodynamic systems
[MBB-UO-0169-91-PUB] p 3731 N92-30421
On the use of pre-defined implementation constructs in distributed systems design
[MEMO-INF-92-08] p 3689 N92-30432
Component construction: Practical guidelines for the construction of reusable components
[REPT-91-89] p 3694 N92-30484
Foreign surveillance radar upgrade analysis
[AD-A249440] p 3616 N92-30760
Building a generalized distributed system model
[NASA-CR-190489] p 3698 N92-30960

COMPUTER SYSTEMS PERFORMANCE
Architecture for the high performance implantation of communication transport level protocols
[ETN-92-91666] p 3690 N92-30701

COMPUTER SYSTEMS PROGRAMS
The REMBRANDT system for multi-criteria decision analysis via pairwise comparisons or direct rating
[REPT-92-05] p 3692 N92-30357

COMPUTER TECHNIQUES
Information systems: How they affect and are affected by organization structure
[AD-A248852] p 3734 N92-30234
An experiment on the use of disposable plastics as a reinforcement in concrete beams p 3593 N92-30287
Semiannual final report, 1 October 1991 - 31 March 1992
[NASA-CR-189660] p 3689 N92-30489
Can stochastic modelling and analysis of multistage interconnection networks lead to efficient usage of redundancy for fault-tolerant design?
[AD-A250635] p 3699 N92-30526
Implementation of parallel algorithms
[AD-A248826] p 3695 N92-30555
Exploiting resource parallelism for integrated fault monitoring and recovery
[AD-A248843] p 3699 N92-30557
Gaussian windows: A tool for exploring multivariate data
[NASA-CR-190559] p 3696 N92-30723
Can't justify an imaging system? How about a CAR?
[DE92-015156] p 3735 N92-31001

COMPUTER VISION
Computer vision in microstructural analysis
p 3609 N92-30271
Visual perception of depth from occlusion: A neural network model
[AD-A249035] p 3696 N92-30820
Demonstration of a 3D vision algorithm for space applications
[NASA-CR-190646] p 3698 N92-31154

COMPUTERIZED SIMULATION
A program of continuing research on representing, manipulating, and reasoning about physical objects
[AD-A251089] p 3691 N92-30260
Regional-scale analysis and forecasting (RAP) report
[AD-A248384] p 3678 N92-30262
An experiment on the use of disposable plastics as a reinforcement in concrete beams p 3593 N92-30287
Validation of three-dimensional incompressible spatial direct numerical simulation code: A comparison with linear stability and parabolic stability equation theories for boundary-layer transition on a flat plate
[NASA-TP-3205] p 3573 N92-30295
Design and simulation of latent heat storage units
[DE91-002145] p 3670 N92-30330
Numerical simulation of the electromagnetic instability of an intense beam in a quadrupole focusing system
[AD-A252275] p 3614 N92-30407
A processing environment for test and simulation data of thermodynamic systems
[MBB-UO-0169-91-PUB] p 3731 N92-30421
Tritium content of a DT pellet in inertial confinement fusion
[NIFS-113] p 3722 N92-30430
Resonance and control response tests using a control simulation device
[MBB-UD-0608-91-PUB] p 3583 N92-30439
Flexible space-based robot modelling and real-time simulation
[NLR-TP-89364-U] p 3658 N92-30477
Dynamic analysis of compact helical system power supply and designs of its upgrade
[NIFS-TECH-2] p 3723 N92-30497
Intermittency, multifractality, and hadronic collisions
[DE92-014595] p 3714 N92-30606
Monte Carlo particle simulation of low-density fluid flow on MIMD supercomputers
[DE92-014618] p 3630 N92-30607
Clouds: Their prediction and simulation
[AD-A250643] p 3679 N92-30643
Studying Turbulence Using Numerical Simulation Databases. 3: Proceedings of the 1990 Summer Program
[NASA-CR-189475] p 3630 N92-30648
Resonant instability of supersonic shear layers
p 3632 N92-30661
Numerical simulation of low Prandtl number turbulent mixing p 3633 N92-30663
Length scales and dissipation of fine eddies in a mixing layer p 3633 N92-30664
A fractal transition in the two dimensional shear layer
p 3633 N92-30665
Geometry of premixed flames in three-dimensional turbulence p 3633 N92-30666
Laminar flamelet modeling of turbulent diffusion flames p 3633 N92-30667
Statistics for laminar flamelet modeling
p 3597 N92-30668
Generation of large-scale density fluctuations by buoyancy p 3634 N92-30671
Interscale energy transfer in numerically simulated turbulence p 3634 N92-30672
Numerical methods for the simulation of complex multi-body flows with applications for the integrated Space Shuttle vehicle
[NASA-CR-190045] p 3575 N92-30740
Numerical methods for the simulation of complex multi-body flows with applications for the integrated Space Shuttle vehicle p 3576 N92-30741
Analysis of a digital RF memory in a signal-delay application
[DE92-013457] p 3626 N92-30764
Numerical simulations of light scattering from rough one-dimensional gold surfaces
[AD-A249794] p 3721 N92-30783
Quantification and reduction of the uncertainty in mass balance models by Monte Carlo analysis of prior data
[DE92-010278] p 3708 N92-30803
Numerical simulation of the dynamic behavior of the polymeric gels
[DE92-011358] p 3605 N92-30804
Visual perception of depth from occlusion: A neural network model
[AD-A249035] p 3696 N92-30820
Interaction of isotropic turbulence with a shock wave
[AD-A250409] p 3635 N92-30852
Computational simulation of diamond chemical vapor deposition in premixed C2H2/O2/H2 and CH4/O2 strained flames
[DE92-012144] p 3606 N92-30857
Numerical calculations of two-dimensional single and multi-material flow fields with CCICE
[DE92-015778] p 3636 N92-30903
Direct simulation of high-speed mixing layers
[NASA-TP-3186] p 3576 N92-30909
Altimetry and lidar using AlGaAs lasers modulated with pseudo-random codes p 3641 N92-31030
Theoretical simulation of a 2 micron airborne solid state laser anemometer p 3647 N92-31059
Development of a Raman lidar simulation tool
p 3649 N92-31072
Performance modeling of daytime Raman lidar systems for profiling atmospheric water vapor
p 3653 N92-31090
DIAL simulations for satellite water vapor profile measurements within the BEST project
p 3653 N92-31092
Eulerian simulation of the perforation of aluminum plates by nondeforming projectiles
[DE92-011515] p 3664 N92-31123
Demonstration of a 3D vision algorithm for space applications
[NASA-CR-190646] p 3698 N92-31154
Real-time simulation model of the HL-20 lifting body
[NASA-TM-107580] p 3586 N92-31160

COMPUTERS
Computer integrated laboratory testing
p 3611 N92-30289
Soviet applied information sciences in a time of change
[PB92-173020] p 3734 N92-30509
A model of the ADA avionics real-time system: An example of the benefits of the hardware/software codesign approach in development of real-time systems
[AD-A248893] p 3581 N92-30524

CONCATENATED CODES
Bandwidth efficient CCSDS coding standard proposals
[NASA-CR-190317] p 3587 N92-30709

CONCENTRATION (COMPOSITION)
Laser induced fluorescence detection of gums in jet fuels
[AD-A252685] p 3607 N92-30767

CONCENTRATORS
Uniform flux dish concentrators for photovoltaic application
[DE92-010566] p 3671 N92-30896

CONCRETE STRUCTURES
An experiment on the use of disposable plastics as a reinforcement in concrete beams p 3593 N92-30287

CONCURRENT PROCESSING
A paradigm for asynchronous communication and its application to concurrent constraint programming
[RUU-CS-91-46] p 3615 N92-30448
The GKS input model in MANIFOLD
[CWI-CS-R9127] p 3699 N92-30696

CONDITIONS
Vegetation conditions and yield indicators. Part 1: Main report
[BCRS-91-26-PT-1] p 3667 N92-30471

CONDUCTING POLYMERS
Synthesis of orthogonally fused conducting oligomers for molecular electronic devices
[AD-A249929] p 3605 N92-30796
Polyphosphazenes bearing polymerizable pyrrole, thiophene and furan side groups: Synthesis and chemical oxidation
[AD-A249747] p 3607 N92-31207

CONDUCTORS
A computational algorithm for crack determination: The multiple crack case
[NASA-CR-189665] p 3704 N92-30516

CONFERENCES
National Educators' Workshop: Update 1991. Standard Experiments in Engineering Materials Science and Technology
[NASA-CP-3151] p 3608 N92-30263
Electrical and chemical interactions at Mars Workshop, part 1
[NASA-CP-10093] p 3741 N92-30302
Studying Turbulence Using Numerical Simulation Databases. 3: Proceedings of the 1990 Summer Program
[NASA-CR-189475] p 3630 N92-30648
Collected notes from the Benchmarks and Metrics Workshop
[NASA-TM-107910] p 3701 N92-30710
Proceedings of a Beryllium Technology Workshop
[DE92-012312] p 3598 N92-30834
Transactions of the 9th Army Conference on Applied Mathematics and Computing
[AD-A252140] p 3706 N92-30843
Proceedings of the Workshop on Advanced Network and Technology Concepts for Mobile, Micro, and Personal Communications
[NASA-CR-190459] p 3617 N92-30923
X ray radiation from hot dense plasmas and atomic processes
[NIFS-PROC-9] p 3725 N92-30984
Sixteenth International Laser Radar Conference, part 2
[NASA-CP-3158-PT-2] p 3637 N92-31013
Proceedings, phenomenology and applications of high temperature superconductors
[DE92-011133] p 3627 N92-31107
Sol-gel optics: Proceedings SPIE-The International Society for Optical Engineering
[AD-A249986] p 3721 N92-31126
Proceedings of the Sylvia Beach Language Comprehension Conference
[AD-A250488] p 3621 N92-31129
Proceedings of the 181st Electrochemical Society, Inc. Meeting Program
[AD-A249729] p 3596 N92-31178
Twenty-Third Lunar and Planetary Science Conference
[NASA-CR-190178] p 3736 N92-31222
CONFINEMENT
Collisional and chaotic transport of energetic particles in toroidal plasma
[DE92-014589] p 3725 N92-30900
Stochastic strings, topology, and space-time confinement
[DE92-630239] p 3732 N92-31136
CONICAL SCANNING
Conically scanned lidar telescope using holographic optical elements p 3645 N92-31050
CONIFERS
Habitat model for the Florida Scrub Jay on John F. Kennedy Space Center
[NASA-TM-107543] p 3673 N92-30494
CONJUGATION
Microscopic theory of THG and electro-absorption in conjugated polymers
[DE92-014786] p 3604 N92-30792
CONSERVATION EQUATIONS
Development of a 3-D upwind PNS code for chemically reacting hypersonic flowfields
[NASA-CR-190182] p 3576 N92-30977
CONSOLES
Console driver p 3718 N92-30728
CONSTITUTIVE EQUATIONS
Process modeling and development for three axisymmetric net shape forgings
[DE92-012111] p 3598 N92-30865
CONSTRAINTS
Restrictions of graph partition problems, part 1
[RUU-CS-91-44-PT-1] p 3703 N92-30446
A paradigm for asynchronous communication and its application to concurrent constraint programming
[RUU-CS-91-46] p 3615 N92-30448
Generalized projected gradient-type iterative method for parametric and functional optimization of dynamical systems subject to constraints
[ESA-TT-1166] p 3694 N92-30512
CONSTRUCTION
Potential airfield sites in Antarctica for wheeled aircraft
[AD-A249503] p 3584 N92-30621
Design and construction of a Helmholtz coil magnetic test cell
[AD-A249944] p 3585 N92-30849
Graphical-based construction of combinatorial geometries for radiation transport and shielding applications
[DE92-014453] p 3696 N92-30886
CONSTRUCTION MATERIALS
Structural ceramics p 3607 N92-30264
CONTAMINANTS
Laser induced fluorescence detection of gums in jet fuels
[AD-A252685] p 3607 N92-30767
CONTEXT FREE LANGUAGES
The formal power of AGs with respect to their underlying CFGs
[REPT-91-75] p 3703 N92-30456
CONTINENTS
The (146,147)Sm-(142,143)Nd systematics of early terrestrial differentiation and the lost continents of the early Earth p 3678 N92-31229
CONTINUOUS WAVE LASERS
A range-resolved bistatic lidar using a high-sensitive CCD-camera p 3640 N92-31027
CONTINUUM FLOW
Continuum approaches for describing solid-liquid flow
[AD-A249028] p 3629 N92-30560
CONTINUUM MECHANICS
Some mathematical problems in continuum mechanics
[AD-A250352] p 3706 N92-31128
CONTINUUM MODELING
Continuum approaches for describing solid-liquid flow
[AD-A249028] p 3629 N92-30560
A study of discrete and continuum joint modeling techniques
[DE92-012631] p 3663 N92-30859
CONTRACT MANAGEMENT
Managing the contract closeout process
[AD-A250701] p 3733 N92-31209
CONTRACTS
Managing the contract closeout process
[AD-A250701] p 3733 N92-31209
CONTROL
Preliminary dynamic tests of a flight-type ejector
[NASA-TM-105814] p 3582 N92-30998
CONTROL EQUIPMENT
An electromechanical actuation system for an expendable launch vehicle
[NASA-TM-105774] p 3586 N92-30310
Control and augmentation of passive porosity through transpiration control
[NASA-CASE-LAR-14682-1] p 3628 N92-30387
CONTROL SYSTEMS DESIGN
Numerical methods for closed-loop control
[AD-A248481] p 3700 N92-30334
Nonlinear system design: Adaptive feedback linearization with unmodeled dynamics
[AD-A248484] p 3700 N92-30335
Storage control system
[NASA-CASE-LAR-14651-1] p 3734 N92-30386
Resonance and control response tests using a control simulation device
[MBB-UD-0608-91-PUB] p 3583 N92-30439
Computer security: Agencies reported having implemented most system security controls
[GAO/IMTEC-92-45] p 3690 N92-30712
A description of the research for period 3 of a research program on the planning and control for space robotic manipulators
[NASA-CR-190243] p 3660 N92-30738
CONTROL THEORY
Practical method's for robust multivariable control
[AD-A248473] p 3700 N92-30322
Numerical methods for closed-loop control
[AD-A248481] p 3700 N92-30334
On-line analysis capabilities developed to support the AFW wind-tunnel tests
[NASA-TM-107651] p 3580 N92-30752
A simplified dynamic model of the T700 turboshaft engine
[NASA-TM-105805] p 3709 N92-30898
Nonlinear stability and control study of highly maneuverable high performance aircraft, phase 2
[NASA-CR-190667] p 3583 N92-30922
Real-time simulation model of the HL-20 lifting body
[NASA-TM-107580] p 3586 N92-31160
CONTROLLED FUSION
Fundamental studies of fusion plasmas
[DE92-015077] p 3726 N92-31116
CONTROLLERS
Computational methods for modeling and active control of distributed parameter systems
[AD-A248559] p 3705 N92-30638
Microgravity vibration isolation: Optimal preview and feedback control
[NASA-TM-105673] p 3613 N92-30692
On-line analysis capabilities developed to support the AFW wind-tunnel tests
[NASA-TM-107651] p 3580 N92-30752
CONVECTION
Finite volume discretization of the convection-diffusion equation in general coordinates
[REPT-91-72] p 3704 N92-30483
Direct coupling method for time-accurate solution of incompressible Navier-Stokes equations
[NASA-CR-189177] p 3636 N92-30894
Direct simulation of high-speed mixing layers
[NASA-TP-3186] p 3576 N92-30909
On the existence of convectively produced gravity waves p 3638 N92-31016
CONVECTIVE FLOW
A Boussinesq algorithm for bouyant convection in polygonal domains
[PB92-187137] p 3695 N92-30579
CONVECTIVE HEAT TRANSFER
Mixed and forced convection from an array of discrete heat sources in a vertical channel
[AD-A248853] p 3731 N92-30235
Transport phenomena in welds
[DE92-013404] p 3659 N92-30587
Laboratory simulation of fluid dynamical process related to winter arctic leads
[AD-A252266] p 3682 N92-30593
CONVERGENCE
Degeneracy in interior point methods for linear programming
[REPT-91-102] p 3691 N92-30353
Verifying the interactive convergence clock synchronization algorithm using the Boyer-Moore theorem prover
[NASA-CR-189649] p 3700 N92-31158
CONVOLUTION INTEGRALS
High-resolution processing of long-pulse-lidar data p 3651 N92-31081
COOL STARS
Heating and momentum deposition in hot stars
[DE92-011850] p 3740 N92-30855
COOLING
Rapid cooling and structure of neutron stars
[DE92-015279] p 3740 N92-30609
COOLING SYSTEMS
Thermal energy storage
[DE92-014942] p 3672 N92-31176
COPPER
Cu-Zn binary phase diagram and diffusion couples p 3600 N92-30269
Nucleation and growth of diamond on carbon-implanted single crystal copper
[AD-A249021] p 3594 N92-30632
On the strain-rate dependence of dynamic recrystallization in copper polycrystals
[DE92-011363] p 3730 N92-31217
COPPER ALLOYS
MBE grown copper-aluminum alloy films
[AD-A252486] p 3597 N92-30534
X ray scattering studies of non-equilibrium ordering processes
[DE92-014006] p 3598 N92-30787
Environmental fatigue of an Al-Li-Cu alloy. Part 2: Microscopic hydrogen cracking processes
[NASA-TM-107620] p 3664 N92-31214
Environmental fatigue of an Al-Li-Cu alloy. Part 3: Modeling of crack tip hydrogen damage
[NASA-TM-107619] p 3665 N92-31215
COPPER SELENIDES
Research on polycrystalline thin film submodules based on CuInSe2 materials
[DE92-010584] p 3727 N92-30247
CORONARY ARTERY DISEASE
Optimal ECG electrode sites and criteria for detection of asymptomatic coronary artery disease, update 1990. Multilead ECG changes at rest, with exercise, and with coronary angioplasty
[AD-A248613] p 3684 N92-30523
CORRECTION
Two-loop QCD corrections to the coefficient functions of the deep inelastic structure functions F2 and F(sub L)
[NIKHEF-H/91-17] p 3715 N92-30687
Analytical multiple scattering correction to the Mie theory: Application to the analysis of the lidar signal p 3642 N92-31036
CORRELATION
Effects of the orientational pair correlation on second order nonlinear optical coefficients
[AD-A252490] p 3720 N92-30535
Comparison of eye-safe solid state laser DIAL with passive gas filter correlation measurements from aircraft and spacecraft p 3647 N92-31060
Elastic constants of crystals near melting via density functional theory. Effect of three-body correlations
[DE92-630567] p 3730 N92-31191
CORRELATION COEFFICIENTS
Effects of the orientational pair correlation on second order nonlinear optical coefficients
[AD-A252490] p 3720 N92-30535
CORROSION
Corrosion of high density kinetic energy penetrator materials
[AD-A249439] p 3597 N92-30759

A comparative EIS study on cermet and platinum anodes for the electrolytic production of aluminum
[DE92-015091] p 3599 N92-31010
Reflector development for XUV free-electron laser oscillators
[DE92-015212] p 3657 N92-31182
COSINE SERIES
Modeling of video traffic in packet networks, low rate video compression, and the development of a lossy+lossless image compression algorithm
[NASA-CR-190546] p 3691 N92-30296
COSMIC RAY SHOWERS
Ultra high energy gamma rays and observations with CYGNUS/MILAGRO
[DE92-015243] p 3743 N92-30627
COSMIC RAYS
Ideas for a long-baseline neutrino detector
[DE92-010650] p 3743 N92-30828
COSMOLOGY
Fluctuation-dissipation theorem in general relativity and the cosmological constant
[DE92-013542] p 3740 N92-30705
The escape of greater MeV photons from cosmological gamma-ray bursts
[DE92-013545] p 3743 N92-30706
COST ANALYSIS
Allocation and recovery of federal airport and airway costs, 1991
[AD-A249436] p 3585 N92-30777
COST EFFECTIVENESS
Technical and economic feasibility of integrated video service by satellite
[NASA-CR-189210] p 3614 N92-30300
Designing, fabricating and testing cost effective structural composite for the SSCL magnets
[DE92-013469] p 3718 N92-30646
Allocation and recovery of federal airport and airway costs, 1991
[AD-A249436] p 3585 N92-30777
COST ESTIMATES
Allocation and recovery of federal airport and airway costs, 1991
[AD-A249436] p 3585 N92-30777
COUNTING
Comparison of epifluorescent viable bacterial count methods
[NASA-TM-103592] p 3683 N92-30305
COUPLED MODES
Vibrationally induced rotational axis switching: A novel mechanism for vibrational mode-coupling
[AD-A251085] p 3712 N92-30259
Studies of phonons and electronic excitations in semiconductor heterostructures
[AD-A249406] p 3729 N92-30772
COUPLING
Vibrationally induced rotational axis switching: A novel mechanism for vibrational mode-coupling
[AD-A251085] p 3712 N92-30259
COVARIANCE
Gaussian windows: A tool for exploring multivariate data
[NASA-CR-190559] p 3696 N92-30723
CRAB NEBULA
Ultra high energy gamma rays and observations with CYGNUS/MILAGRO
[DE92-015243] p 3743 N92-30627
CRACK CLOSURE
FASTRAN-2: A fatigue crack growth structural analysis program
[NASA-TM-104159] p 3664 N92-30964
CRACK PROPAGATION
Linear elastic fracture mechanics primer
[NASA-TM-103591] p 3662 N92-30416
Crack growth processes at elevated temperatures in advanced materials
[AD-A249023] p 3662 N92-30558
Creep and slow crack growth mechanisms related to macroscopic creep behavior of a silicon nitride ceramic at elevated temperatures
[DE92-015195] p 3663 N92-30567
Investigation of joining techniques for advanced austenitic alloys
[DE92-015545] p 3599 N92-30888
FASTRAN-2: A fatigue crack growth structural analysis program
[NASA-TM-104159] p 3664 N92-30964
Environmental fatigue of an Al-Li-Cu alloy. Part 2: Microscopic hydrogen cracking processes
[NASA-TM-107620] p 3664 N92-31214
Environmental fatigue of an Al-Li-Cu alloy. Part 3: Modeling of crack tip hydrogen damage
[NASA-TM-107619] p 3665 N92-31215
CRACK TIPS
Linear elastic fracture mechanics primer
[NASA-TM-103591] p 3662 N92-30416
Crack growth processes at elevated temperatures in advanced materials
[AD-A249023] p 3662 N92-30558
FASTRAN-2: A fatigue crack growth structural analysis program
[NASA-TM-104159] p 3664 N92-30964
Environmental fatigue of an Al-Li-Cu alloy. Part 2: Microscopic hydrogen cracking processes
[NASA-TM-107620] p 3664 N92-31214
Environmental fatigue of an Al-Li-Cu alloy. Part 3: Modeling of crack tip hydrogen damage
[NASA-TM-107619] p 3665 N92-31215
CRACKS
A boundary element alternating method for two-dimensional mixed-mode fracture problems
[NASA-CR-4460] p 3661 N92-30309
A computational algorithm for crack determination: The multiple crack case
[NASA-CR-189665] p 3704 N92-30516
FASTRAN-2: A fatigue crack growth structural analysis program
[NASA-TM-104159] p 3664 N92-30964
CRASHWORTHINESS
Evaluation of head impact kinematics for passengers seated behind interior walls
[AD-A252651] p 3578 N92-30551
CRATERING
Environment modelling in near Earth space: Preliminary LDEF results p 3588 N92-31225
CRATERS
Environment modelling in near Earth space: Preliminary LDEF results p 3588 N92-31225
CRAY COMPUTERS
Monte Carlo particle simulation of low-density fluid flow on MIMD supercomputers
[DE92-014618] p 3630 N92-30607
CREEP PROPERTIES
An automated system for creep testing
p 3611 N92-30282
Creep and slow crack growth mechanisms related to macroscopic creep behavior of a silicon nitride ceramic at elevated temperatures
[DE92-015195] p 3663 N92-30567
CREEP RUPTURE STRENGTH
Assessment of an improved multiaxial strength theory based on creep-rupture data for type 316 stainless steel
[DE92-010431] p 3663 N92-30823
CREEP TESTS
An automated system for creep testing
p 3611 N92-30282
Filler metal development for Hastelloy alloy XR
[DE92-782044] p 3600 N92-31163
CRESOLS
Synthesis of cresols and xylenols from benzene and methanol
[DE91-002143] p 3596 N92-30882
CREW WORKSTATIONS
KC-135 crew reduction feasibility demonstration simulation study. Volume 1: Function analysis and function reallocation
[AD-A252265] p 3688 N92-30592
CRITICAL POINT
A study of the topology of dissipating motions in direct numerical simulations of time-developing compressible and incompressible mixing layers p 3632 N92-30658
CRITICAL TEMPERATURE
A study of enhancing critical current densities (J(sub c)) and critical temperature (T(sub c)) of high-temperature superconductors
[NASA-TM-103595] p 3627 N92-30902
Ginsburg criterion for an equilibrium superradiant model in the dynamic approach
[DE92-630566] p 3732 N92-31203
CROP GROWTH
Vegetation conditions and yield indicators. Part 1: Main report
[BCRS-91-26-PT-1] p 3667 N92-30471
CROP IDENTIFICATION
Results of the 1989 experiment with a polarimetric multifrequency SAR
[BCRS-91-33] p 3614 N92-30361
CAESAR: Evaluation of the dual-look concept
[BCRS-91-10] p 3666 N92-30467
CROSS CORRELATION
A statistical comparison of AUTEC and Eleuthera Island wind data for the period 1 April 1989 through 30 March 1990
[AD-A248898] p 3679 N92-31003
CROSS COUPLING
Thermoset precursor to monolithic carbon glass prepared by the Pd/Cu-catalyzed alkynylation of polyphenylenes
[AD-A249920] p 3605 N92-30816
CROSS FLOW
Method of measuring cross-flow vortices by use of an array of hot-film sensors
[NASA-CASE-LAR-14824-1-SB] p 3628 N92-30390
Structure of three-dimensional turbulent boundary layers p 3631 N92-30654
CROSS SECTIONS
Two-dimensional aerodynamic characteristics of several polygon-shaped cross-sectional models applicable to helicopter fuselages
[NASA-TP-3233] p 3574 N92-30394
CROSSED FIELDS
Field line diversion properties of finite beta helias equilibria
[NIFS-137] p 3722 N92-30385
CROSSLINKING
Molecular weight dependence of domain structure in silica-siloxane molecular composites
[DE92-015046] p 3603 N92-30544
Approaches to polymer curing and imaging via the in situ generation of a catalyst
[AD-A249917] p 3606 N92-30873
A method for the production of weakly acidic cation exchange resins
[DE92-015314] p 3717 N92-31137
CRYOGENIC EQUIPMENT
Cryogenic Magnetic Bearing Test Facility (CMBTF)
[NASA-CR-189087] p 3582 N92-31164
CRYOGENIC FLUIDS
Conceptual design of the SSC cryogenic transfer lines
[DE92-013964] p 3719 N92-30839
CRYOGENICS
Conceptual design of the SSC cryogenic transfer lines
[DE92-013964] p 3719 N92-30839
A dynamic model for beam tube vacuum effects on the SSC cryogenic system
[DE92-013967] p 3719 N92-30840
CRYOLITE
A comparative EIS study on cermet and platinum anodes for the electrolytic production of aluminum
[DE92-015091] p 3599 N92-31010
CRYOSTATS
Conceptual design of the SSC cryogenic transfer lines
[DE92-013964] p 3719 N92-30839
CRYPTOGRAPHY
How to securely replicate services
[NASA-CR-190476] p 3692 N92-30379
CRYSTAL DEFECTS
Mechanism of slip and twinning p 3610 N92-30280
On the temperature role in the tunneling process at the cold fusion
[DE92-627497] p 3727 N92-30405
Disorder and transport in highly correlated systems
[AD-A249969] p 3710 N92-30850
Impurity segregation to grain boundaries and defects in AlN
[DE92-011667] p 3599 N92-31112
CRYSTAL GROWTH
Growth and evaluation of nonlinear optical materials for laser applications: Barium borate, lithium borate, and silver gallium selenide
[AD-A248861] p 3624 N92-30617
Method of synthesizing high quality, doped diamond and diamonds and devices obtained therefrom
[AD-D015267] p 3604 N92-30685
CRYSTAL STRUCTURE
Mechanism of slip and twinning p 3610 N92-30280
Shock-induced martensitic transformation of highly oriented graphite to diamond
[DE92-014787] p 3602 N92-30399
Structural and magnetic properties of RBa2Cu2NbO8 (R = La, Pr, and Nd)
[DE92-014780] p 3729 N92-30885
YBa2Cu(3-x)Co(x)O(y): A substrate material for YBCO superconductors
[DE92-015182] p 3730 N92-30999
Stabilization of face-centered-cubic titanium
[DE92-011530] p 3600 N92-31125
Self-consistent-field KKR-CPA calculations in the atomic-sphere approximations
[DE92-011525] p 3600 N92-31138
Fine scale mesostructures in superconducting and other materials
[DE92-015207] p 3730 N92-31200
CRYSTAL SURFACES
Nucleation and growth of diamond on carbon-implanted single crystal copper
[AD-A249021] p 3594 N92-30632
Vector analysis of ice fabric data
[AD-A250832] p 3682 N92-30832
CRYSTALLINITY
First-principles computational studies of alkali-doped C60 fullerides
[AD-A249018] p 3624 N92-30630

High-resolution imaging in the scanning transmission electron microscope
[DE92-010647] p 3637 N92-30827

CRYSTALLITES
Nucleation and growth of diamond on carbon-implanted single crystal copper
[AD-A249021] p 3594 N92-30632

CRYSTALLIZATION
X ray scattering studies of non-equilibrium ordering processes
[DE92-014006] p 3598 N92-30787

CRYSTALS
Growth and evaluation of nonlinear optical materials for laser applications: Barium borate, lithium borate, and silver gallium selenide
[AD-A248861] p 3624 N92-30617
Measurements of the backscattering phase matrices of crystal clouds with a polarization lidar
p 3651 N92-31083
Elastic constants of crystals near melting via density functional theory. Effect of three-body correlations
[DE92-630567] p 3730 N92-31191
TEM studies of a circumstellar rock
p 3736 N92-31223

CUBIC EQUATIONS
Real cubic systems with four line invariants
[REPT-91-79] p 3702 N92-30436

CULTURAL RESOURCES
Remote-sensing survey of the Atchafalaya Basin Main Channel, Atchafalaya Channel training project, Saints Martin and Mary Parishes, Louisiana
[AD-A249915] p 3669 N92-31139

CURING
Approaches to polymer curing and imaging via the in situ generation of a catalyst
[AD-A249917] p 3606 N92-30873

CURRENT DENSITY
A study of enhancing critical current densities (J(sub c)) and critical temperature (T(sub c)) of high-temperature superconductors
[NASA-TM-103595] p 3627 N92-30902
Spectroscopic diagnosis of long-scale-length exploding-foil plasma in the presence of an intense radiation field
[DE92-014718] p 3726 N92-31118
Grain boundary weak links in high-Tc superconductors
[DE92-016192] p 3730 N92-31190

CURRENT DISTRIBUTION
New insights into radiation-induced oxide-trap charge through Thermally-Stimulated-Current (TSC) measurement and analysis
[DE92-009054] p 3728 N92-30585

CURVE FITTING
Trajectory fitting in function space with application to analytic modeling of surfaces
[NASA-TP-3232] p 3576 N92-30747

CURVED BEAMS
Composite beam analysis linear analysis of naturally curved and twisted anisotropic beams
[AD-A252652] p 3663 N92-30766

CYCLES
The formal power of AGs with respect to their underlying CFGs
[REPT-91-75] p 3703 N92-30456
Bifurcation of limit cycles in a particular class of quadratic systems
[REPT-91-76] p 3703 N92-30457
Development of hardness cycles for fiber bound materials, using DSC: From laboratory specimens to complex high duty structural members
[MBB-Z-0409-91-PUB] p 3592 N92-30969

CYCLIC LOADS
FASTRAN-2: A fatigue crack growth structural analysis program
[NASA-TM-104159] p 3664 N92-30964

CYCLONES
On the potential use of the terminal Doppler weather radar gust front detection algorithm on the WSR-88D system. Part 2: Detecting non-gust front convergent weather phenomena
[DOT/FAA/NR-92/8,II] p 3678 N92-30496
Tropical cyclone asymmetries as revealed by recent satellite microwave brightness temperatures
[AD-A249873] p 3679 N92-30867

CYCLOTRON RESONANCE
Magnetospheric structure and dynamics: A multisatellite approach
[AD-A252326] p 3676 N92-30720

CYLINDERS
Analytical solution of elastic-plastic thick-walled cylinders with general hardening
[AD-A249491] p 3705 N92-30618
Nonlinear stress analysis of composite-jacketed steel cylinders subjected to high internal pressure
[AD-A249500] p 3663 N92-30802

CYLINDRICAL BODIES
Numerical study of axial turbulent flow over long cylinders
[AD-A250801] p 3635 N92-30831

CZECHOSLOVAKIA
Reducing greenhouse gas emissions in Czechoslovakia
[DE92-012354] p 3672 N92-30374

D

DAMAGE
Environment modelling in near Earth space: Preliminary LDEF results p 3588 N92-31225

DAMAGE ASSESSMENT
Low-velocity impact loading on fibre reinforced aluminum laminates (ARALL) and other aircraft sheet materials
[ETN-92-91613] p 3590 N92-30414
Environmental fatigue of an Al-Li-Cu alloy. Part 3: Modeling of crack tip hydrogen damage
[NASA-TM-107619] p 3665 N92-31215

DAMPING
Low Reynolds number kappa-epsilon modeling with the aid of direct simulation data p 3631 N92-30655

DARK MATTER
Dark matter and cosmology
[DE92-013023] p 3740 N92-30622

DATA ACQUISITION
An automated system for creep testing
p 3611 N92-30282
Three-dimensional laser window formation
[NASA-RP-1280] p 3585 N92-30307
Storage control system
[NASA-CASE-LAR-14651-1] p 3734 N92-30386
A processing environment for test and simulation data of thermodynamic systems
[MBB-UO-0169-91-PUB] p 3731 N92-30421
Development statistics for the UH-1 Ada feasibility study
[AD-A252404] p 3584 N92-30547
Remote experimental site concept for diagnostic collaborations in fusion
[DE92-010437] p 3724 N92-30824
Characterizing ultrasonic transducers using pattern recognition techniques
[DE92-015845] p 3711 N92-30890
Repetitive High Energy Pulsed Power (RHEPP) temperature monitoring system utilizing Luxtron fluoroptic sensors and thermocouples technical reference manual
[DE92-013461] p 3637 N92-30893
Hydrologic modelling and use of remotely sensed data at CWPRS p 3669 N92-30918
Digital methods for analysis of satellite imagery
p 3669 N92-30920
First conclusions of a manufacturer group on the applicability of CALS in Europe p 3697 N92-30951
Shining on: A primer on solar radiation data
[DE92-010555] p 3743 N92-31206

DATA BASE MANAGEMENT SYSTEMS
The evolving data dictionary
[AD-A249030] p 3735 N92-30819
Considerations for imaging system implementation in a networked environment
[DE92-015338] p 3735 N92-31132

DATA BASES
Regional-scale analysis and forecasting (RAP) report
[AD-A248384] p 3678 N92-30262
Wiring for aerospace applications
[NASA-TM-105777] p 3623 N92-30427
Studying Turbulence Using Numerical Simulation Databases. 3: Proceedings of the 1990 Summer Program
[NASA-CR-189475] p 3630 N92-30648
Numerical methods for the simulation of complex multi-body flows with applications for the integrated Space Shuttle vehicle p 3576 N92-30741
A CFD validation roadmap for hypersonic flows
[NASA-TM-103935] p 3636 N92-30982
Chemistry for protection of the environment, 8th International Conference proceedings
[DE92-014317] p 3674 N92-31181

DATA COMPRESSION
Modeling of video traffic in packet networks, low rate video compression, and the development of a lossy+lossless image compression algorithm
[NASA-CR-190546] p 3691 N92-30296
METEODEC/METEOCRYPT: A demonstration of data compression and encryption for operational remote-sensing
[NLR-TP-89294-U] p 3667 N92-30475

DATA FLOW ANALYSIS
A protocol scheme for a class of minimum delay routing algorithms
[RUU-CS-91-43] p 3693 N92-30445
A bibliography on network flow problems (2nd edition)
[RUU-CS-91-38] p 3698 N92-30482
About difference equations, algebras and discrete events
[REPT-91-87] p 3704 N92-30491
High level synthesis of controlpath microarchitectures
[MEMO-INF-91-86] p 3690 N92-30698

DATA MANAGEMENT
Geographic information system and its applications
p 3668 N92-30915

DATA PROCESSING
Computer integrated laboratory testing
p 3611 N92-30289
Development of and flight results from the Space Acceleration Measurement System (SAMS)
[NASA-TM-105652] p 3588 N92-30301
Compiler analysis for irregular problems in FORTRAN D
[NASA-CR-189664] p 3689 N92-30311
Information processing research
[AD-A248492] p 3734 N92-30324
A processing environment for test and simulation data of thermodynamic systems
[MBB-UO-0169-91-PUB] p 3731 N92-30421
Preparations for the ERS-1 and TOPEX/Poseidon satellite altimetry missions
[BCRS-90-28] p 3666 N92-30465
Interpretation of optical remote sensing data over coastal waters
[BCRS-91-27] p 3667 N92-30472
Altimeter and gravity data analysis
[NASA-CR-190478] p 3676 N92-30756
Geographic information system and its applications
p 3668 N92-30915
Estimation of vertical profile of soil moisture through multifrequency microwave data analysis
p 3669 N92-30919

DATA PROCESSING EQUIPMENT
A high speed signal processing system for a diode-pumped YAG lidar p 3646 N92-31054

DATA REDUCTION
On-line analysis capabilities developed to support the AFW wind-tunnel tests
[NASA-TM-107651] p 3580 N92-30752
Quantification and reduction of the uncertainty in mass balance models by Monte Carlo analysis of prior data
[DE92-010278] p 3708 N92-30803
Numerical calculations of two-dimensional single and multi-material flow fields with CCICE
[DE92-015778] p 3636 N92-30903

DATA RETRIEVAL
Geographic information system and its applications
p 3668 N92-30915

DATA SAMPLING
A local interpolator derived from the discrete Fourier transform
[AD-A251066] p 3701 N92-30243
A high speed signal processing system for a diode-pumped YAG lidar p 3646 N92-31054

DATA STORAGE
Storage control system
[NASA-CASE-LAR-14651-1] p 3734 N92-30386
Considerations for imaging system implementation in a networked environment
[DE92-015338] p 3735 N92-31132

DATA STRUCTURES
Linear planar augmentation algorithms for outerplanar graphs
[RUU-CS-91-47] p 3703 N92-30449
Maintenance of 2- and 3-connected components of graphs. Part 1: 2- and 3-edge-connected components
[RUU-CS-90-26-PT-1] p 3694 N92-30479
Maintenance of 2- and 3-connected components of graphs. Part 2: 2- and 3-edge-connected components and 2-vertex-connected components
[RUU-CS-90-27-PT-2] p 3694 N92-30480
Gaussian windows: A tool for exploring multivariate data
[NASA-CR-190559] p 3696 N92-30723
Geographic information system and its applications
p 3668 N92-30915

DATA SYSTEMS
The MARCOR GPS mobile data system
p 3620 N92-30944

DATA TRANSFER (COMPUTERS)
A protocol scheme for a class of minimum delay routing algorithms
[RUU-CS-91-43] p 3693 N92-30445
Printer port interface
[NASA-CASE-LAR-13950-1] p 3690 N92-30541
Architecture for the high performance implantation of communication transport level protocols
[ETN-92-91666] p 3690 N92-30701

DATA TRANSMISSION
Printer port interface
[NASA-CASE-LAR-13950-1] p 3690 N92-30541

Analysis of a digital RF memory in a signal-delay application
[DE92-013457] p 3626 N92-30764

DAYTIME
Interferometers adaptations to lidars
p 3645 N92-31052
Performance modeling of daytime Raman lidar systems for profiling atmospheric water vapor
p 3653 N92-31090

DECAY RATES
Spontaneous emission from an atom in motion near an infinite conducting plane
[ITN-92-85169] p 3715 N92-30782

DECISION MAKING
A space-time neural network for processing both spacial and temporal data
[NASA-CASE-MSC-21874-1] p 3700 N92-30314
The REMBRANDT system for multi-criteria decision analysis via pairwise comparisons or direct rating
[REPT-92-05] p 3692 N92-30357
Scale sensitivity and rank preservation in a multiplicative variant of the AHP and SMART
[REPT-91-67] p 3707 N92-30452
Introduction to cognitive processes of expert pilots
[DOT/FAA/RD-92/12] p 3578 N92-30980

DECISION THEORY
Scale sensitivity and rank preservation in a multiplicative variant of the AHP and SMART
[REPT-91-67] p 3707 N92-30452

DECODERS
Bandwidth efficient CCSDS coding standard proposals
[NASA-CR-190317] p 3587 N92-30709

DECODING
Bandwidth efficient CCSDS coding standard proposals
[NASA-CR-190317] p 3587 N92-30709

DECOMPOSITION
Decomposition studies of tertiarybutyldimethylantimony
[AD-A250670] p 3727 N92-30527

DECOUPLING
Strong dynamic input-output decoupling: From linearity to nonlinearity
[MEMO-COSOR-92-04] p 3694 N92-30478

DEDUCTION
Application of automated deduction to the search for single axioms for exponent groups
[DE92-015271] p 3705 N92-30608

DEEP SPACE
Software breadboard study
[NASA-CR-190473] p 3625 N92-30757

DEFECTS
Characterization and analysis of defects in nonlinear optical molecular composite films
[AD-A252118] p 3661 N92-30529
Research on defects and transport in amorphous silicon-based semiconductors
[DE92-001223] p 3729 N92-30748

DEFENSE PROGRAM
Joint stabilizing projects in defense
[DE92-015977] p 3709 N92-30891
Managing the contract closeout process
[AD-A250701] p 3733 N92-31209

DEFORMATION
Modeling and analysis methodology for aeroelastically tailored chordwise deformable wings
[NASA-CR-189620] p 3579 N92-30304
Signal matching by dynamic programming
[REPT-92-01] p 3614 N92-30354
On recrystallization in metal matrix composites
[DE92-011364] p 3590 N92-30521
Dynamics of deformable bodies
[AD-A252333] p 3705 N92-30533
Inter- and intra-plate deformation at North American plate boundaries
[NASA-CR-190485] p 3676 N92-30961

DEGASSING
Thermodynamic evaporation of highly volatile components in the vacuum degassing of melted aluminum alloys
[DE92-015315] p 3600 N92-31218

DEGRADATION
Isothermal aging effects on PMR-15 resin
[NASA-TM-105648] p 3593 N92-30986
Performance of ground-based high-frequency receiving arrays with electrically-small ground planes
[AD-A250489] p 3621 N92-31130

DEHYDRATION
Design of a high activity and selectivity alcohol catalyst
[DE92-013918] p 3594 N92-30717

DEICING
Lewis icing research tunnel test of the aerodynamic effects of aircraft ground deicing/anti-icing fluids
[NASA-TP-3238] p 3577 N92-30395

DELAMINATING
Finite element analysis of laminated composite axisymmetric solids. Volume 1: Theory and applications
[AD-A250808] p 3590 N92-30251
Influence of various carbon fibre types on the mechanical performance and damage tolerance of composites
[MBB/FE202/S/PUB/477] p 3591 N92-30690

DELAY CIRCUITS
Analysis of a digital RF memory in a signal-delay application
[DE92-013457] p 3626 N92-30764

DENSE PLASMAS
X ray radiation from hot dense plasmas and atomic processes
[NIFS-PROC-9] p 3725 N92-30984

DENSIFICATION
Pressure densification
[AD-A249438] p 3604 N92-30758

DENSITY MEASUREMENT
Density profile measurement using a multichannel difluoromethane laser interferometer system on ATF
[DE92-011691] p 3724 N92-30810

DEPOLARIZATION
Measurement of multiple scattering effects with a polarization Raman elastic-backscatter lidar
p 3641 N92-31033
Determining water cloud particle sizes from lidar depolarization measurements and time dependent multiple scattering coefficients p 3641 N92-31034
Lidar depolarization by nonspherical particles: Potential of combined depolarization/backscattering measurements for PSC's characterization p 3644 N92-31044
Verification measurement of a polarization Raman elastic-backscatter lidar p 3647 N92-31062

DEPOSITION
Waveguide polarizer using localized surface plasmons
[AD-D015258] p 3614 N92-30348
A method of making a single layer multi-color luminescent display
[NASA-CASE-LAR-14811-1] p 3622 N92-30389

DESIGN ANALYSIS
Fiber optic based signal processing
[AD-A247857] p 3720 N92-30248
Designing, engineering, and testing wood structures
p 3593 N92-30270
Modeling and analysis methodology for aeroelastically tailored chordwise deformable wings
[NASA-CR-189620] p 3579 N92-30304
Practical method's for robust multivariable control
[AD-A248473] p 3700 N92-30322
Influence of structural and aerodynamic modeling on flutter analysis and structural optimization
[AD-A248487] p 3583 N92-30323
Composite beam analysis linear analysis of naturally curved and twisted anisotropic beams
[AD-A252652] p 3663 N92-30766
Yaw dynamics of horizontal axis wind turbines
[DE92-001245] p 3670 N92-30837
Practical application of the ILS: Practical integration, design, and logistics p 3697 N92-30955
Research issues in molten carbonate fuel cells: Pressurization
[DE92-011755] p 3671 N92-31113
Nonlinear aerodynamics and the design of wing tips
[NASA-CR-190649] p 3577 N92-31157

DESORPTION
Atomic layer epitaxy group 4 materials: Surface processes, thin films, devices, and their characterization
[AD-A252352] p 3729 N92-30846
Laser mass spectrometry for biopolymers
[DE92-015238] p 3597 N92-31184

DETECTION
Detecting potential synchronization constraint deadlocks from formal system specifications
[AD-A249019] p 3696 N92-30631
Maximum likelihood detection of electro-optic moving targets
[AD-A249442] p 3616 N92-30762
A simplified dynamic model of the T700 turboshaft engine
[NASA-TM-105805] p 3709 N92-30898
A cable detection lidar system for helicopters
p 3648 N92-31068
Measurements of fugitive hydrocarbon emissions with a tunable infrared DIAL p 3655 N92-31102

DEUTERIUM
Tritium content of a DT pellet in inertial confinement fusion
[NIFS-113] p 3722 N92-30430
High field optical-pumping spin-exchange polarized deuterium source
[DE92-010274] p 3657 N92-30848

DEUTERIUM COMPOUNDS
Photodynamics within (CH3OH)(nCr(CO)6) heteroclusters: Observation of an isotope effect
[AD-A251058] p 3712 N92-30255

DEUTERONS
Rescattering in neutrino/antineutrino: Deuteron reactions
[NIKHEF-H/91-22] p 3713 N92-30364

DIAL SATELLITE
DIAL simulations for satellite water vapor profile measurements within the BEST project
p 3653 N92-31092

DIAMOND FILMS
Solid lubrication of laser grown fluorinated diamond thin films
[AD-A249485] p 3603 N92-30635
Method of synthesizing high quality, doped diamond and diamonds and devices obtained therefrom
[AD-D015267] p 3604 N92-30685

DIAMONDS
Shock-induced martensitic transformation of highly oriented graphite to diamond
[DE92-014787] p 3602 N92-30399
Innovative techniques for the production of low cost 2-D laser diode arrays supplies or services and prices/costs
[AD-A252665] p 3656 N92-30552
Nucleation and growth of diamond on carbon-implanted single crystal copper
[AD-A249021] p 3594 N92-30632
Method of synthesizing high quality, doped diamond and diamonds and devices obtained therefrom
[AD-D015267] p 3604 N92-30685
Atomic layer epitaxy group 4 materials: Surface processes, thin films, devices, and their characterization
[AD-A252352] p 3729 N92-30846
Computational simulation of diamond chemical vapor deposition in premixed C2H2/O2/H2 and CH4/O2 strained flames
[DE92-012144] p 3606 N92-30857
Presolar (?) corundum in the Orgueil meteorite
p 3738 N92-31230

DIATOMIC GASES
Numerical solution of a three-dimensional cubic cavity flow by using the Boltzmann equation
[NASA-TM-105693] p 3627 N92-30297

DICTIONARIES
The evolving data dictionary
[AD-A249030] p 3735 N92-30819

DIELECTRIC PROPERTIES
Dielectric behavior of semiconductors at microwave frequencies p 3610 N92-30275
Relaxor ferroelectrics for electrostrictive transducer
[AD-A248671] p 3624 N92-30598

DIELECTRICS
Dielectric behavior of semiconductors at microwave frequencies p 3610 N92-30275
Spontaneous decay of an atom near a phase conjugator
[AD-A248298] p 3712 N92-30333
Radiation, scattering, and guidance of electromagnetic fields by arbitrarily shaped structures embedded in layered dielectric media
[AD-A252621] p 3615 N92-30408

DIESEL ENGINES
Development of a modular transient cycle analysis program for the adiabatic diesel and other compound diesel engines
[AD-A249022] p 3658 N92-30538
Advanced concepts for controlled combustion in engines
[AD-A249911] p 3595 N92-30814
Two-color infrared digital imaging for determination of in-cylinder temperature and species during compression and combustion periods of DI diesel engine
[AD-A249812] p 3595 N92-30835

DIFFERENCE EQUATIONS
About difference equations, algebras and discrete events
[REPT-91-87] p 3704 N92-30491

DIFFERENTIAL EQUATIONS
Differential equations for symmetric generalized ultraspherical polynomials
[REPT-92-08] p 3702 N92-30360
On impasse points of quasilinear differential algebraic equations
[AD-A252643] p 3702 N92-30410
Real cubic systems with four line invariants
[REPT-91-79] p 3702 N92-30436
Bifurcation of limit cycles in a particular class of quadratic systems
[REPT-91-76] p 3703 N92-30457
Real polynomial systems of degree n with n+1 line invariants
[REPT-91-86] p 3704 N92-30490
On the rapid evaluation of trigonometric series
[AD-A249029] p 3705 N92-30568
Non-holonomic filtration: Algebraic and geometric aspects of non-integrability
[PB92-178003] p 3706 N92-30790

Heat flow of p-harmonic maps with values into spheres
[DE92-630236] p 3707 N92-31135
DIFFERENTIAL GEOMETRY
Non-holonomic filtration: Algebraic and geometric aspects of non-integrability
[PB92-178003] p 3706 N92-30790
Wrappability of curves on surfaces
[AD-A250004] p 3707 N92-31140
DIFFRACTION
Field studies in geophysical diffraction tomography
[DE92-015084] p 3677 N92-31009
Multiple scattering lidar returns from stratus clouds
p 3642 N92-31035
DIFFUSE RADIATION
Surface-mediated photocatalysis
[AD-A249906] p 3595 N92-30793
Numerical simulation of crater formation heating by laser beam. Analysis of radiation exchanges in the cavity
[ESA-TT-1234] p 3657 N92-30997
DIFFUSION
Five experiments in materials science for less than $10.00 p 3611 N92-30283
Finite volume discretization of the convection-diffusion equation in general coordinates
[REPT-91-72] p 3704 N92-30483
Direct coupling method for time-accurate solution of incompressible Navier-Stokes equations
[NASA-CR-189177] p 3636 N92-30894
The role of stochasticity in sawtooth oscillation
[NIFS-103] p 3710 N92-30983
Pressure profiles, resonant Pfirsch-Schlueter currents, thermal instabilities, and magnetic island formation
[DE92-015166] p 3726 N92-31002
DIFFUSION FLAMES
Laminar flamelet modeling of turbulent diffusion flames p 3633 N92-30667
DIFLUORO COMPOUNDS
Density profile measurement using a multichannel difluoromethane laser interferometer system on ATF
[DE92-011691] p 3724 N92-30810
DIGITAL COMPUTERS
Digital bottom mapping
[AD-D015238] p 3682 N92-30413
Computing with faulty shared memory
[DE92-011663] p 3695 N92-30522
DIGITAL DATA
Storage control system
[NASA-CASE-LAR-14651-1] p 3734 N92-30386
Two-color infrared digital imaging for determination of in-cylinder temperature and species during compression and combustion periods of DI diesel engine
[AD-A249812] p 3595 N92-30835
Broadcast satellite service: The international dimension p 3621 N92-30946
DIGITAL FILTERS
A space-time neural network for processing both spacial and temporal data
[NASA-CASE-MSC-21874-1] p 3700 N92-30314
DIGITAL SIMULATION
Development environment for digital simulation models of multibody systems
[NLR-TP-89327-U] p 3693 N92-30476
DIGITAL SYSTEMS
Analysis of a digital RF memory in a signal-delay application
[DE92-013457] p 3626 N92-30764
The Pan-European Digital Cellular (GSM) System
p 3619 N92-30938
Toward a North American standard for mobile data services p 3620 N92-30940
DIGITAL TECHNIQUES
Digital methods for analysis of satellite imagery
p 3669 N92-30920
Simplified signal processing for an airborne CO2 Doppler lidar p 3639 N92-31023
DIMENSIONAL STABILITY
The effect of neutron irradiation on the structure and properties of carbon-carbon composite materials
[DE92-011670] p 3592 N92-30809
DIMERS
Studies of thermal decomposition of the 1:1 R3Al:en adduct (R = Me, Et; en = ethylenediamine): Synthesis and structure of a novel intermediate Al((HNCH2CH2NH)AlMe2)3
[AD-A251061] p 3603 N92-30623
DIOXIDES
Atomic layer epitaxy group 4 materials: Surface processes, thin films, devices, and their characterization
[AD-A252352] p 3729 N92-30846
DIRAC EQUATION
Research on elementary particle physics. Task P: Studies in theory and phenomenology of elementary particles, part 1
[DE92-014428] p 3716 N92-30791
From a world-sheet supersymmetry to the Dirac equation
[DE92-622375] p 3731 N92-30799
From a particle with a world-line supersymmetry to the Dirac-like equation
[DE92-622376] p 3731 N92-30800
DIRECT BROADCAST SATELLITES
Direct broadcast satellite-radio: Portable and mobile reception trade-offs p 3621 N92-30945
DISCONTINUITY
Resolution properties of the Fourier method for discontinuous waves
[NASA-CR-189668] p 3706 N92-30716
DISCRETE FUNCTIONS
A local interpolator derived from the discrete Fourier transform
[AD-A251066] p 3701 N92-30243
On the rapid evaluation of trigonometric series
[AD-A249029] p 3705 N92-30568
DISCRIMINATION
Cortical mechanisms of attention, discrimination, and motor response to somaesthetic stimuli
[AD-A247228] p 3687 N92-30613
DISPLACEMENT
Investigation of the interface phenomena due to interaction of high intensity stress waves with geologic boundaries
[AD-A248992] p 3675 N92-30525
Wave propagation and vibration of fibre-reinforced laminates
[AD-A252101] p 3590 N92-30528
A geodetic laser radar rangefinder with 10(exp -7) resolution p 3641 N92-31029
DISPLACEMENT MEASUREMENT
A geodetic laser radar rangefinder with 10(exp -7) resolution p 3641 N92-31029
DISPLAY DEVICES
Assessment of a head-mounted miniature monitor
[NASA-TM-103587] p 3688 N92-30381
An overview of the computer aided definition system for design definition at Sandia National Laboratories, Livermore FY1991 update
[DE92-015991] p 3696 N92-30892
DISSIPATION
Length scales and dissipation of fine eddies in a mixing layer p 3633 N92-30664
Quantum transport, noise and non-linear dissipative effects in one- and two-dimensional systems and associated sub-micron and nanostructure devices
[AD-A250895] p 3627 N92-31210
DISSOCIATION
Understanding heterolytic bond cleavage
[AD-A252336] p 3716 N92-30845
DISTILLATION
Synthesis of cresols and xylenols from benzene and methanol
[DE91-002143] p 3596 N92-30882
DISTORTION
Ultra high bypass Nacelle aerodynamics inlet flow-through high angle of attack distortion test
[NASA-CR-189149] p 3574 N92-30298
Coherent summation of spatially distorted Doppler lidar signals using a two-dimensional heterodyne detector array p 3654 N92-31096
DISTRIBUTED PARAMETER SYSTEMS
Computational methods for modeling and active control of distributed parameter systems
[AD-A248559] p 3705 N92-30638
Building a generalized distributed system model
[NASA-CR-190489] p 3698 N92-30960
DISTRIBUTED PROCESSING
Survivable algorithms and redundancy management in NASA's distributed computing systems
[NASA-CR-189827] p 3691 N92-30299
A space-time neural network for processing both spacial and temporal data
[NASA-CASE-MSC-21874-1] p 3700 N92-30314
On the use of pre-defined implementation constructs in distributed systems design
[MEMO-INF-92-08] p 3689 N92-30432
Computing with faulty shared memory
[DE92-011663] p 3695 N92-30522
VLSI design, parallel computation, and distributed computing
[AD-A252349] p 3699 N92-30596
Network load of X terminals at CDF
[DE92-011704] p 3699 N92-30812
Building a generalized distributed system model
[NASA-CR-190489] p 3698 N92-30960
Choice coordination with multiple alternatives
[DE92-011656] p 3700 N92-31111
DIVERTERS
Field line diversion properties of finite beta helias equilibria
[NIFS-137] p 3722 N92-30385
Review of high Z materials for PSI applications
[NIFS-152] p 3602 N92-30502
DIVIDERS
Fractal analysis: A new remote sensing tool for lava flows p 3736 N92-31224
DIVING (UNDERWATER)
Remote-sensing survey of the Atchafalaya Basin Main Channel, Atchafalaya Channel training project, Saints Martin and Mary Parishes, Louisiana
[AD-A249915] p 3669 N92-31139
DOCUMENT STORAGE
Can't justify an imaging system? How about a CAR?
[DE92-015156] p 3735 N92-31001
DOCUMENTATION
Reviewing the technical report
[AD-A249494] p 3735 N92-30636
DOCUMENTS
Reviewing the technical report
[AD-A249494] p 3735 N92-30636
DOPED CRYSTALS
Evaluation of doped polyethylene oxide as solid electrolyte for polymer batteries
[AD-A249501] p 3624 N92-30619
Method of synthesizing high quality, doped diamond and diamonds and devices obtained therefrom
[AD-D015267] p 3604 N92-30685
Infrared investigations of pristine, doped and partially-doped polypyrrole
[AD-A250644] p 3605 N92-30838
DOPPLER EFFECT
Doppler photography: Laser methods on the flow measurement technique
[ISL-PU-303/90] p 3720 N92-30507
Doppler lidar wind measurement with the edge technique p 3638 N92-31017
Tropospheric and stratospheric wind profiling with a direct detection Doppler lidar p 3639 N92-31018
DOPPLER RADAR
Feasibility of extracting current profile information from HF-radar surface current measurements, part 1 and 2
[BCRS-91-23-PT-1-2] p 3682 N92-30470
On the potential use of the terminal Doppler weather radar gust front detection algorithm on the WSR-88D system. Part 1: Impacts of radar system differences
[DOT/FAA/NR-92/8,I] p 3678 N92-30495
On the potential use of the terminal Doppler weather radar gust front detection algorithm on the WSR-88D system. Part 2: Detecting non-gust front convergent weather phenomena
[DOT/FAA/NR-92/8,II] p 3678 N92-30496
Doppler mean velocity estimation: Small sample analysis and a new estimator
[AD-A249024] p 3678 N92-30559
Sixteenth International Laser Radar Conference, part 2
[NASA-CP-3158-PT-2] p 3637 N92-31013
Doppler lidar wind measurement with the edge technique p 3638 N92-31017
Tropospheric and stratospheric wind profiling with a direct detection Doppler lidar p 3639 N92-31018
Design of a near-IR coherent lidar for high spatial and velocity resolution wind measurement
p 3639 N92-31020
A pulsed CO2 Doppler lidar for boundary layer monitoring p 3639 N92-31021
A compact high repetition rate CO2 coherent Doppler lidar p 3639 N92-31022
Simplified signal processing for an airborne CO2 Doppler lidar p 3639 N92-31023
Phase noise in pulsed Doppler lidar and limitations on achievable single-shot velocity accuracy
p 3639 N92-31024
Coherent CO2 lidar: A superior system for observing clouds? p 3644 N92-31045
Pulsed laser spectral measurement using a Fabry-Perot interferometer: Limits to resolution p 3646 N92-31055
Tm,Ho:YAG laser with tunable range of 2.08-2.12 microns and its applications to spectroscopy
p 3646 N92-31058
Theoretical simulation of a 2 micron airborne solid state laser anemometer p 3647 N92-31059
A study of atmospheric optical scattering parameters at 1.5 and 2 micron region for solid state Doppler lidar applications p 3648 N92-31067
Ground-based Doppler lidar of increased laser instability: Conception and design p 3650 N92-31078
Analytical estimates of the PP-algorithm at low number of Doppler periods per pulse length
p 3650 N92-31079
High-resolution processing of long-pulse-lidar data
p 3651 N92-31081
Coherent summation of spatially distorted Doppler lidar signals using a two-dimensional heterodyne detector array p 3654 N92-31096
The role of laser coherence in long-range vibration measurements p 3654 N92-31097

DRAINAGE
Satellite and Radar Data Use in Rainfall-Runoff Models p 3667 N92-30910
Remote sensing satellite data use in run-off studies p 3668 N92-30914
SCS method of runoff estimation using remote sensing techniques p 3668 N92-30916
Digital methods for analysis of satellite imagery p 3669 N92-30920
Duration and rates of discharge: Maja Valles, Mars p 3737 N92-31227

DRIFT RATE
Tests of the performance of different gas mixtures in microstrip gas counters [NIKHEF-H/91-23] p 3636 N92-30365

DROPS (LIQUIDS)
Waveguide polarizer using localized surface plasmons [AD-D015258] p 3614 N92-30348
Liquid droplet radiator: Design concepts and development logic [MBB-UO-0165-91-PUB] p 3613 N92-30441
Multiple scattering lidar returns from stratus clouds p 3642 N92-31035

DRUGS
Effects of pyridostigmine bromide on A-10 pilots during execution of a simulated mission; performance [AD-A252309] p 3685 N92-30605
Tolerance of beta blocked hypertensives during orthostatic and altitude stresses [AD-A249904] p 3685 N92-30745

DUCTED FLOW
Direct coupling method for time-accurate solution of incompressible Navier-Stokes equations [NASA-CR-189177] p 3636 N92-30894
Navier-Stokes analysis and experimental data comparison of compressible flow within ducts [NASA-TM-105796] p 3582 N92-30972

DUCTS
Direct coupling method for time-accurate solution of incompressible Navier-Stokes equations [NASA-CR-189177] p 3636 N92-30894
Navier-Stokes analysis and experimental data comparison of compressible flow within ducts [NASA-TM-105796] p 3582 N92-30972

DUST
Multiple scattering wavelength dependent backscattering of kaolin dust in the IR: Measurements and theory p 3648 N92-31064

DYE LASERS
Generation of a sodium guidestar using a high power dye laser [DE92-012696] p 3657 N92-31115

DYNAMIC CHARACTERISTICS
Scalable parallel molecular dynamics on MIMD supercomputers [DE92-015041] p 3698 N92-30401
Depolarized light scattering and dynamic shear compliance of viscoelastic liquids [AD-A252491] p 3721 N92-30536
Fractal and multifractal approaches to clustering phenomena [AD-A249481] p 3709 N92-30642
Nonequilibrium behavior of carriers in semiconductors subjected to strong space-time varying fields [AD-A246961] p 3624 N92-30678
A demonstration of passive blade twist control using extension-twist coupling [NASA-TM-107642] p 3664 N92-31155
On the strain-rate dependence of dynamic recrystallization in copper polycrystals [DE92-011363] p 3730 N92-31217

DYNAMIC CONTROL
A demonstration of passive blade twist control using extension-twist coupling [NASA-TM-107642] p 3664 N92-31155

DYNAMIC LOADS
Evaluation of grounding and mooring points for Army aircraft [AD-A250749] p 3579 N92-31193

DYNAMIC MODELS
Selection of opening model for parachute scaling studies [AD-A250882] p 3573 N92-30239
A dynamic model for beam tube vacuum effects on the SSC cryogenic system [DE92-013967] p 3719 N92-30840
Vehicle/guideway interaction for high speed vehicles on flexible guideway [DE92-013057] p 3660 N92-30860
Process modeling and development for three axisymmetric net shape forgings [DE92-012111] p 3598 N92-30865
A simplified dynamic model of the T700 turboshaft engine [NASA-TM-105805] p 3709 N92-30898

DYNAMIC PROGRAMMING
Signal matching by dynamic programming [REPT-92-01] p 3614 N92-30354

DYNAMIC RANGE
The temperature dependence of a large dynamic range photodetector structure [AD-A247667] p 3624 N92-30683
Lidar receivers for picosecond remote sensing p 3650 N92-31076
The role of laser coherence in long-range vibration measurements p 3654 N92-31097

DYNAMIC RESPONSE
Numerical simulation of the dynamic behavior of the polymeric gels [DE92-011358] p 3605 N92-30804
Adapting the ADAM manikin technology for injury probability assessment [AD-A252332] p 3688 N92-30844
Acoustic fatigue life prediction for nonlinear structures with multiple resonant modes [NASA-CR-190471] p 3664 N92-30988

DYNAMIC STABILITY
Constraints on the putative companions to PSR1257+12 p 3738 N92-31232

DYNAMIC STRUCTURAL ANALYSIS
Dynamics of deformable bodies [AD-A252333] p 3705 N92-30533
Acoustic fatigue life prediction for nonlinear structures with multiple resonant modes [NASA-CR-190471] p 3664 N92-30988

DYNAMIC TESTS
Development of hardness cycles for fiber bound materials, using DSC: From laboratory specimens to complex high duty structural members [MBB-Z-0409-91-PUB] p 3592 N92-30969
Preliminary dynamic tests of a flight-type ejector [NASA-TM-105814] p 3582 N92-30998

DYNAMICAL SYSTEMS
On the Thue Morse measure [REPT-92-16] p 3704 N92-30464
Strong dynamic input-output decoupling: From linearity to nonlinearity [MEMO-COSOR-92-04] p 3694 N92-30478
About difference equations, algebras and discrete events [REPT-91-87] p 3704 N92-30491
Generalized projected gradient-type iterative method for parametric and functional optimization of dynamical systems subject to constraints [ESA-TT-1166] p 3694 N92-30512
Synchronized continuous flow systems [REPT-91-88] p 3704 N92-30517
A numerical evaluation of the dynamical systems approach to wall layer turbulence p 3632 N92-30660
Low order dynamical models for mixing layers p 3633 N92-30662
Dimension bounds for quotient spaces [PB92-177997] p 3706 N92-30789

E

E GLASS
A reduced gravity fiber pulling apparatus [NASA-TM-103594] p 3612 N92-30971

EAR
The use of tympanometry to detect aerotitis media in hypobaric chamber operations [AD-A248963] p 3684 N92-30328

EARLY WARNING SYSTEMS
National airspace system. Air defense and law enforcement surveillance operational concept NAS-SR-135 [DOT/FAA/SE-92/3] p 3579 N92-31211

EARTH (PLANET)
The (146,147)Sm-(142,143)Nd systematics of early terrestrial differentiation and the lost continents of the early Earth p 3678 N92-31229

EARTH ATMOSPHERE
The RADLAC beam propagation experiment [DE92-014620] p 3718 N92-30624
On the existence of convectively produced gravity waves p 3638 N92-31016
Advanced Raman water vapor lidar p 3643 N92-31040
Raman lidar measurements of water vapor and aerosol/clouds during the FIRE/SPECTRE field campaign p 3652 N92-31089
The environmental dilemma of fossil fuels [DE92-014887] p 3674 N92-31121

EARTH MAGNETOSPHERE
Magnetospheric structure and dynamics: A multisatellite approach [AD-A252326] p 3676 N92-30720

EARTH OBSERVING SYSTEM (EOS)
Spectroscopic method for Earth-satellite-Earth laser long-path absorption measurements using Retroreflector In Space (RIS) p 3652 N92-31088

EARTH ORBITAL ENVIRONMENTS
Analysis, review, and documentation of the activation data from LDEF material [NASA-CR-184356] p 3596 N92-31161

EARTH ORBITS
Leo satellite-based telecommunication network concepts p 3617 N92-30926

EARTH RESOURCES
The sustainable biosphere initiative: An ecological research agenda p 3673 N92-30425

EARTH SCIENCES
The United States Antarctic Program [NSF-90-97] p 3676 N92-30708

EARTH TERMINALS
EHF (28/19 GHz) personal communications satellite terminal development p 3619 N92-30935

EARTHQUAKES
Inter- and intra-plate deformation at North American plate boundaries [NASA-CR-190485] p 3676 N92-30961

ECOLOGY
The sustainable biosphere initiative: An ecological research agenda p 3673 N92-30425

ECONOMIC ANALYSIS
Technical and economic feasibility of integrated video service by satellite [NASA-CR-189210] p 3614 N92-30300
Reducing greenhouse gas emissions in Czechoslovakia [DE92-012354] p 3672 N92-30374
The effect of information systems on middle management in the aerospace industry: The Westco case [AD-A249017] p 3735 N92-30584
Towards the development of a global inventory for black carbon emissions [DE92-013514] p 3674 N92-30647

ECONOMIC DEVELOPMENT
Spinoffs from R and D investments [DE92-014450] p 3736 N92-30575
The status of renewable energy technology [DE92-011386] p 3670 N92-30808
Fuel cell systems program plan: Fiscal year 1992 [DE92-015985] p 3672 N92-31188
Fuel cells [DE92-001282] p 3672 N92-31221

ECONOMIC IMPACT
Reducing greenhouse gas emissions in Czechoslovakia [DE92-012354] p 3672 N92-30374

ECONOMICS
Spinoffs from R and D investments [DE92-014450] p 3736 N92-30575

ECOSYSTEMS
The sustainable biosphere initiative: An ecological research agenda p 3673 N92-30425

EDDY VISCOSITY
A dynamic subgrid-scale eddy viscosity model p 3630 N92-30649
Low Reynolds number kappa-epsilon modeling with the aid of direct simulation data p 3631 N92-30655
One-equation near-wall turbulence modeling with the aid of direct simulation data p 3631 N92-30656

EDGE DETECTION
Doppler lidar wind measurement with the edge technique p 3638 N92-31017

EDGE DISLOCATIONS
Mechanism of slip and twinning p 3610 N92-30280

EDGES
Maintenance of 2- and 3-connected components of graphs. Part 1: 2- and 3-edge-connected components [RUU-CS-90-26-PT-1] p 3694 N92-30479
Maintenance of 2- and 3-connected components of graphs. Part 2: 2- and 3-edge-connected components and 2-vertex-connected components [RUU-CS-90-27-PT-2] p 3694 N92-30480

EDITING
Reviewing the technical report [AD-A249494] p 3735 N92-30636

EDUCATION
National Educators' Workshop: Update 1991. Standard Experiments in Engineering Materials Science and Technology [NASA-CP-3151] p 3608 N92-30263
Science in action: An interdisciplinary science education program p 3610 N92-30278
The microscopic world: A demonstration of electron microscopy for younger students p 3610 N92-30281
Five experiments in materials science for less than $10.00 p 3611 N92-30283
An experiment on the use of disposable plastics as a reinforcement in concrete beams p 3593 N92-30287

Structure, processing, and properties of potatoes
p 3611 N92-30288
Computer integrated laboratory testing
p 3611 N92-30289
Heat-treating of materials p 3601 N92-30292
Technical training for national simulator evaluation specialist
[NASA-CR-190429] p 3687 N92-30488
Trends in aeropropulsion research and their impact on engineering education
[NASA-TM-105682] p 3583 N92-31172

EFFECTS
Information systems: How they affect and are affected by organization structure
[AD-A248852] p 3734 N92-30234
Anisotropic silicon etching techniques
[MBB-Z-0413-91-PUB] p 3594 N92-30422

EFFICIENCY
Perspective on photovoltaic amorphous silicon
[DE92-010581] p 3670 N92-30519
The allocation of cargo to channel missions
[DE92-013234] p 3578 N92-30565
Introduction to the efficiency of fuel cells
[MBB-Z-0412-91-PUB] p 3671 N92-30970

EIGENVALUES
Parallel aspects of some spectral problems in linear algebra
[CWI-NM-R9113] p 3706 N92-30700
Markov chain simulations of binary matrices
[AD-A249265] p 3708 N92-30771

EIGENVECTORS
Multiple scattering theory of x ray absorption. A review
[DE92-622374] p 3716 N92-30798
Quantum mechanics in Grassmann space
[DE92-622377] p 3711 N92-30801

EIKONAL EQUATION
Spin amplitudes of pp-scattering in a unitarized supercritical pomeron model
[DE92-624639] p 3711 N92-30236

EJECTION
Adapting the ADAM manikin technology for injury probability assessment
[AD-A252332] p 3688 N92-30844

EJECTION SEATS
Adapting the ADAM manikin technology for injury probability assessment
[AD-A252332] p 3688 N92-30844

EJECTORS
Preliminary dynamic tests of a flight-type ejector
[NASA-TM-105814] p 3582 N92-30998

ELASTIC ANISOTROPY
Composite beam analysis linear analysis of naturally curved and twisted anisotropic beams
[AD-A252652] p 3663 N92-30766

ELASTIC PROPERTIES
Laboratory experiments from the toy store
p 3609 N92-30274
A demonstration of passive blade twist control using extension-twist coupling
[NASA-TM-107642] p 3664 N92-31155
Elastic constants of crystals near melting via density functional theory. Effect of three-body correlations
[DE92-630567] p 3730 N92-31191
Fine scale mesostructures in superconducting and other materials
[DE92-015207] p 3730 N92-31200

ELASTIC SCATTERING
Spin amplitudes of pp-scattering in a unitarized supercritical pomeron model
[DE92-624639] p 3711 N92-30236
Verification measurement of a polarization Raman elastic-backscatter lidar p 3647 N92-31062

ELASTIC WAVES
Investigation of the interface phenomena due to interaction of high intensity stress waves with geologic boundaries
[AD-A248992] p 3675 N92-30525

ELASTOMERS
Flexible heating head for induction heating apparatus and method
[NASA-CASE-LAR-14679-2] p 3621 N92-31150

ELASTOPLASTICITY
Analytical solution of elastic-plastic thick-walled cylinders with general hardening
[AD-A249491] p 3705 N92-30618

ELECTRIC ARCS
Wiring for aerospace applications
[NASA-TM-105777] p 3623 N92-30427

ELECTRIC BATTERIES
Evaluation of doped polyethylene oxide as solid electrolyte for polymer batteries
[AD-A249501] p 3624 N92-30619
Electric Vehicle Site Operator Program
[DE92-014591] p 3626 N92-30842

ELECTRIC CONTACTS
Printed transformer process/product improvements
[DE92-014760] p 3624 N92-30590

ELECTRIC CURRENT
Dynamic analysis of compact helical system power supply and designs of its upgrade
[NIFS-TECH-2] p 3723 N92-30497
One-dimensional subband effects in the conductance of multiple quantum wires in Si-MOSFET's
p 3625 N92-30731
Grain boundary weak links in high-Tc superconductors
[DE92-016192] p 3730 N92-31190

ELECTRIC DIPOLES
A new class of ferroelectric polymers: The odd-numbered nylons
[AD-A252268] p 3603 N92-30594

ELECTRIC FIELDS
On the temperature role in the tunneling process at the cold fusion
[DE92-627497] p 3727 N92-30405
The electric field dependence of the laser induced holographic grating relaxation of photorefractive polymer
[AD-A252641] p 3602 N92-30409
Effects of fast ions and an external inductive electric field on the neoclassical parallel flow, current, and rotation in general toroidal systems
[NIFS-150] p 3713 N92-30500
Rapid change of hydrogen neutral energy distribution at L/H-transition in JFT-2M H-mode
[NIFS-134] p 3714 N92-30510
On the radial component of the electric field for a monopole phased array antenna focused in the near zone
[AD-A249441] p 3616 N92-30761

ELECTRIC GENERATORS
Dynamic analysis of compact helical system power supply and designs of its upgrade
[NIFS-TECH-2] p 3723 N92-30497
Introduction to the efficiency of fuel cells
[MBB-Z-0412-91-PUB] p 3671 N92-30970
Fuel cell systems program plan: Fiscal year 1992
[DE92-015985] p 3672 N92-31188

ELECTRIC MOTOR VEHICLES
Electric Vehicle Site Operator Program
[DE92-014591] p 3626 N92-30842

ELECTRIC POWER SUPPLIES
Development of software to improve AC power quality on large spacecraft
[NASA-CR-190569] p 3589 N92-30989

ELECTRIC PROPULSION
A conceptual design of a large aperture microwave radiometer geostationary platform
[NASA-TM-107577] p 3588 N92-30736

ELECTRICAL FAULTS
Comparison of signal processing methods for estimation of network impedance for remote protection
[ETN-92-91686] p 3623 N92-30503
Printed transformer process/product improvements
[DE92-014760] p 3624 N92-30590

ELECTRICAL GROUNDING
Performance of ground-based high-frequency receiving arrays with electrically-small ground planes
[AD-A250489] p 3621 N92-31130

ELECTRICAL IMPEDANCE
Comparison of signal processing methods for estimation of network impedance for remote protection
[ETN-92-91686] p 3623 N92-30503

ELECTRICAL INSULATION
Wiring for aerospace applications
[NASA-TM-105777] p 3623 N92-30427

ELECTRICAL MEASUREMENT
Effects of high beam rates on TPC's
[DE92-014594] p 3717 N92-30398
A computational algorithm for crack determination: The multiple crack case
[NASA-CR-189665] p 3704 N92-30516
Voltammetric measurement of oxygen in single neurons using platinized carbon ring electrodes
[AD-A252191] p 3683 N92-30531
New insights into radiation-induced oxide-trap charge through Thermally-Stimulated-Current (TSC) measurement and analysis
[DE92-009054] p 3728 N92-30585

ELECTRICAL PROPERTIES
Electrical and chemical interactions at Mars Workshop, part 1
[NASA-CP-10093] p 3741 N92-30302
Absolute Seebeck thermoelectric characteristics: Principles, significance, and applications
[DE92-013684] p 3622 N92-30370
Ferroelectric and piezoelectric properties of odd-numbered nylons
[AD-A252270] p 3727 N92-30406
Thermally activated rejuvenation of ferroelectric properties in electrically fatigued lead zirconate titanate ceramics
[DE92-012634] p 3605 N92-30830
YBa2Cu(3-x)Co(x)O(y): A substrate material for YBCO superconductors
[DE92-015182] p 3730 N92-30999

ELECTRICAL RESISTANCE
Measurement report on the present Video Highway System of MEA p 3718 N92-30726
Tunable relay box (design and testing)
p 3718 N92-30727

ELECTRICAL RESISTIVITY
Anomalous hopping conductivity in amorphous indium-oxide films
[ITN-92-85166] p 3729 N92-30781
Properties of CMOS devices and circuits fabricated on high-resistivity, detector-grade silicon
[DE92-011727] p 3626 N92-30813
Polyphosphazenes bearing polymerizable pyrrole, thiophene and furan side groups: Synthesis and chemical oxidation
[AD-A249747] p 3607 N92-31207

ELECTRO-OPTICAL EFFECT
Microscopic theory of THG and electro-absorption in conjugated polymers
[DE92-014786] p 3604 N92-30792

ELECTRO-OPTICS
The electric field dependence of the laser induced holographic grating relaxation of photorefractive polymer
[AD-A252641] p 3602 N92-30409
Maximum likelihood detection of electro-optic moving targets
[AD-A249442] p 3616 N92-30762

ELECTROACOUSTIC TRANSDUCERS
Tunneling acoustic microscopy
[AD-A251028] p 3727 N92-30252

ELECTROCARDIOGRAPHY
Optimal ECG electrode sites and criteria for detection of asymptomatic coronary artery disease, update 1990. Multilead ECG changes at rest, with exercise, and with coronary angioplasty
[AD-A248613] p 3684 N92-30523

ELECTROCHEMICAL CELLS
Infrared investigations of pristine, doped and partially-doped polypyrrole
[AD-A250644] p 3605 N92-30838

ELECTROCHEMICAL OXIDATION
Electrooxidation of soluble alpha,alpha-coupled thiophene oligomers
[AD-A249928] p 3605 N92-30817
Infrared investigations of pristine, doped and partially-doped polypyrrole
[AD-A250644] p 3605 N92-30838

ELECTROCHEMISTRY
On the temperature role in the tunneling process at the cold fusion
[DE92-627497] p 3727 N92-30405
Template-synthesis: A method for enhancing the ionic and electronic conductivity in electronically conductive polymers
[AD-A248806] p 3603 N92-30553
Photochemical solar energy conversion utilizing semiconductors localized in membrane-mimetic systems
[DE92-011115] p 3670 N92-30694
Electrooxidation of soluble alpha,alpha-coupled thiophene oligomers
[AD-A249928] p 3605 N92-30817
Electrochemical and optical studies of model photosynthetic systems
[DE92-010657] p 3683 N92-30829
A comparative EIS study on cermet and platinum anodes for the electrolytic production of aluminum
[DE92-015091] p 3599 N92-31010
Proceedings of the 181st Electrochemical Society, Inc. Meeting Program
[AD-A249729] p 3596 N92-31178

ELECTRODES
Optimal ECG electrode sites and criteria for detection of asymptomatic coronary artery disease, update 1990. Multilead ECG changes at rest, with exercise, and with coronary angioplasty
[AD-A248613] p 3684 N92-30523
Voltammetric measurement of oxygen in single neurons using platinized carbon ring electrodes
[AD-A252191] p 3683 N92-30531
Testing of double-layer capacitors for high reliability applications
[DE92-011384] p 3626 N92-30807

ELECTRODYNAMICS
A new matrix formulation of classical electrodynamics. Part 1: Vacuum
[AD-A249643] p 3616 N92-30721

ELECTROLYSIS
A comparative EIS study on cermet and platinum anodes for the electrolytic production of aluminum
[DE92-015091] p 3599 N92-31010
ELECTROLYTES
Numerical simulation of the dynamic behavior of the polymeric gels
[DE92-011358] p 3605 N92-30804
Ni-H2 cell separator matrix engineering
[NASA-CR-190055] p 3671 N92-30949
Fuel cell systems program plan: Fiscal year 1992
[DE92-015985] p 3672 N92-31188
Fuel cells
[DE92-001282] p 3672 N92-31221
ELECTROMAGNETIC FIELDS
Spontaneous decay of an atom near a phase conjugator
[AD-A248298] p 3712 N92-30333
Waveguide polarizer using localized surface plasmons
[AD-D015258] p 3614 N92-30348
Radiation, scattering, and guidance of electromagnetic fields by arbitrarily shaped structures embedded in layered dielectric media
[AD-A252621] p 3615 N92-30408
Transverse pattern modification in a stable apertured laser resonator
[ITN-92-85171] p 3656 N92-30582
Repetitive High Energy Pulsed Power (RHEPP) temperature monitoring system utilizing Luxtron fluoroptic sensors and thermocouples technical reference manual
[DE92-013461] p 3637 N92-30893
Advanced electromagnetic methods for aerospace vehicles
[NASA-CR-190650] p 3621 N92-31156
ELECTROMAGNETIC INTERACTIONS
Generation of stimulated backscattered harmonic radiation from intense laser interactions with beams and plasmas
[AD-A248782] p 3656 N92-30614
Advanced electromagnetic methods for aerospace vehicles
[NASA-CR-190650] p 3621 N92-31156
ELECTROMAGNETIC INTERFERENCE
Compact range test applications, phase 2
[AD-A248790] p 3615 N92-30583
Quantum interference and confinement effects in narrow channel Si-MOSFET's
[ETN-92-91742] p 3625 N92-30729
ELECTROMAGNETIC NOISE
Quantum transport, noise and non-linear dissipative effects in one- and two-dimensional systems and associated sub-micron and nanostructure devices
[AD-A250895] p 3627 N92-31210
ELECTROMAGNETIC PROPERTIES
Electron scattering and electromagnetic response properties of metal clusters
[DE92-014715] p 3621 N92-31007
ELECTROMAGNETIC PULSES
Pulsed microwave processing of high-T(sub c) superconducting films
[DE92-014950] p 3730 N92-31000
ELECTROMAGNETIC RADIATION
Transverse pattern modification in a stable apertured laser resonator
[ITN-92-85171] p 3656 N92-30582
Electron scattering and electromagnetic response properties of metal clusters
[DE92-014715] p 3621 N92-31007
ELECTROMAGNETIC SCATTERING
Radiation, scattering, and guidance of electromagnetic fields by arbitrarily shaped structures embedded in layered dielectric media
[AD-A252621] p 3615 N92-30408
Finite difference time domain modeling of steady state scattering from jet engines with moving turbine blades
[NASA-CR-190290] p 3582 N92-30753
ELECTROMAGNETISM
Dynamic analysis of compact helical system power supply and designs of its upgrade
[NIFS-TECH-2] p 3723 N92-30497
A new matrix formulation of classical electrodynamics. Part 1: Vacuum
[AD-A249643] p 3616 N92-30721
Advanced electromagnetic methods for aerospace vehicles
[NASA-CR-190650] p 3621 N92-31156
ELECTROMECHANICAL DEVICES
An electromechanical actuation system for an expendable launch vehicle
[NASA-TM-105774] p 3586 N92-30310
Nanoscience and nanotechnology
[AD-A250376] p 3626 N92-30851
ELECTROMECHANICS
An electromechanical actuation system for an expendable launch vehicle
[NASA-TM-105774] p 3586 N92-30310
ELECTRON BEAMS
Interaction of ultra-high laser fields with beams and plasmas
[AD-A249502] p 3723 N92-30620
Reflector development for XUV free-electron laser oscillators
[DE92-015212] p 3657 N92-31182
ELECTRON CYCLOTRON HEATING
Results of the heavy ion beam probe measurements on the Advanced Toroidal Facility
[DE92-014461] p 3726 N92-31197
ELECTRON DENSITY PROFILES
Density profile measurement using a multichannel difluoromethane laser interferometer system on ATF
[DE92-011691] p 3724 N92-30810
ELECTRON DIFFUSION
Tests of the performance of different gas mixtures in microstrip gas counters
[NIKHEF-H/91-23] p 3636 N92-30365
ELECTRON DISTRIBUTION
Magnetospheric structure and dynamics: A multisatellite approach
[AD-A252326] p 3676 N92-30720
ELECTRON ENERGY
Photoinitiated electron transfer in multichromophoric species: Synthetic tetrads and pentads featuring diquinone moieties
[DE92-013472] p 3683 N92-30368
Rapid change of hydrogen neutral energy distribution at L/H-transition in JFT-2M H-mode
[NIFS-134] p 3714 N92-30510
Production of negative hydrogen ions in a large multicusp ion source with double-magnetic filter configuration
[NIFS-149] p 3714 N92-30572
Research on defects and transport in amorphous silicon-based semiconductors
[DE92-001223] p 3729 N92-30748
High resolution electron energy loss studies of surface vibrations
[DE92-014608] p 3626 N92-30901
Spectroscopic diagnosis of long-scale-length exploding-foil plasma in the presence of an intense radiation field
[DE92-014718] p 3726 N92-31118
ELECTRON MICROSCOPES
The microscopic world: A demonstration of electron microscopy for younger students p 3610 N92-30281
High-resolution imaging in the scanning transmission electron microscope
[DE92-010647] p 3637 N92-30827
Single-electron charging effects
[DE92-015287] p 3710 N92-31131
ELECTRON MICROSCOPY
In situ TEM studies of the effect of misfit strain on the kinetics of Si(sub 1-x)Ge(sub x) solid phase epitaxy: Temperature calibration and surface effects
[DE92-011689] p 3728 N92-30574
TEM studies of a circumstellar rock
p 3736 N92-31223
ELECTRON MOBILITY
Tests of the performance of different gas mixtures in microstrip gas counters
[NIKHEF-H/91-23] p 3636 N92-30365
ELECTRON ORBITALS
Development of practical MO techniques for prediction of the properties and behavior of materials
[AD-A247218] p 3598 N92-30864
ELECTRON PARAMAGNETIC RESONANCE
Research on defects and transport in amorphous silicon-based semiconductors
[DE92-001223] p 3729 N92-30748
Evidence for interference between resonant and nonresonant transfer and excitation
[DE92-011779] p 3716 N92-30853
ELECTRON PLASMA
Production of negative hydrogen ions in a large multicusp ion source with double-magnetic filter configuration
[NIFS-149] p 3714 N92-30572
Interaction of ultra-high laser fields with beams and plasmas
[AD-A249502] p 3723 N92-30620
Low-frequency fluctuations in plasma magnetic fields
[DE92-012139] p 3724 N92-30833
ELECTRON SCATTERING
Non-perturbative effects in high-energy electroweak interactions
[NIKHEF-H/91-24] p 3715 N92-30697
Electron scattering and electromagnetic response properties of metal clusters
[DE92-014715] p 3621 N92-31007
ELECTRON SPECTROSCOPY
Interaction of atomic hydrogen with the surface methyl group on Si(100): Removal of surface carbon
[AD-A249062] p 3595 N92-30821
Atomic layer epitaxy group 4 materials: Surface processes, thin films, devices, and their characterization
[AD-A252352] p 3729 N92-30846
ELECTRON STATES
Studies of ordering in semiconducting and other alloys
[AD-A249483] p 3728 N92-30634
Self-consistent-field KKR-CPA calculations in the atomic-sphere approximations
[DE92-011525] p 3600 N92-31138
ELECTRON TRANSFER
Photoinitiated electron transfer in multichromophoric species: Synthetic tetrads and pentads featuring diquinone moieties
[DE92-013472] p 3683 N92-30368
Nonequilibrium behavior of carriers in semiconductors subjected to strong space-time varying fields
[AD-A246961] p 3624 N92-30678
Photochemical solar energy conversion utilizing semiconductors localized in membrane-mimetic systems
[DE92-011115] p 3670 N92-30694
Electrochemical and optical studies of model photosynthetic systems
[DE92-010657] p 3683 N92-30829
Evidence for interference between resonant and nonresonant transfer and excitation
[DE92-011779] p 3716 N92-30853
ELECTRON TRANSITIONS
Program RELAX: A code designed to calculate atomic relaxation spectra of x rays and electrons
[DE92-013751] p 3714 N92-30586
ELECTRON TUNNELING
Single-electron charging effects
[DE92-015287] p 3710 N92-31131
ELECTRONIC EQUIPMENT
A program of continuing research on representing, manipulating, and reasoning about physical objects
[AD-A251089] p 3691 N92-30260
ELECTRONS
Program RELAX: A code designed to calculate atomic relaxation spectra of x rays and electrons
[DE92-013751] p 3714 N92-30586
Understanding heterolytic bond cleavage
[AD-A252336] p 3716 N92-30845
Evidence for interference between resonant and nonresonant transfer and excitation
[DE92-011779] p 3716 N92-30853
Electron scattering and electromagnetic response properties of metal clusters
[DE92-014715] p 3621 N92-31007
ELECTRORETINOGRAPHY
Effects of microwave radiation on humans: Monkeys exposed to 1.25 GHz pulsed microwaves
[AD-A249997] p 3686 N92-31127
ELECTROSTATICS
Magnetospheric structure and dynamics: A multisatellite approach
[AD-A252326] p 3676 N92-30720
ELECTROSTRICTION
Relaxor ferroelectrics for electrostrictive transducer
[AD-A248671] p 3624 N92-30598
ELEMENTARY EXCITATIONS
Scale symmetry of quantum solitons
[DE92-624560] p 3712 N92-30331
ELEMENTARY PARTICLE INTERACTIONS
Linear estimates of structure functions from deep inelastic lepton-nucleon scattering data, part 1
[DE92-627288] p 3713 N92-30403
Search for light neutral scalar and pseudoscalar particles in pFe interactions at 70 GeV
[DE92-627317] p 3713 N92-30404
ELEMENTARY PARTICLES
Scale symmetry of quantum solitons
[DE92-624560] p 3712 N92-30331
Research on elementary particle physics
[DE92-014622] p 3715 N92-30625
ELLIPSES
On two methods of determining the ellipses and ellipsoids of positioning accuracy of robot manipulators
[ISSN-0208-5658] p 3701 N92-31148
ELLIPSOMETERS
Ion channeling and spectroscopic ellipsometry examinations of thin-film SiO2/epi-Si structures
[DE92-015129] p 3728 N92-30577
ELLIPSOMETRY
Ion channeling and spectroscopic ellipsometry examinations of thin-film SiO2/epi-Si structures
[DE92-015129] p 3728 N92-30577
Ellipsometric study of oxide films formed on LDEF metal samples
[AD-A249856] p 3599 N92-31110
ELLIPTIC DIFFERENTIAL EQUATIONS
Special finite element methods for a class of second order elliptic problems with rough coefficients
[AD-A248900] p 3701 N92-30339

Global existence for a semilinear elliptic-parabolic PDE system
[REPT-91-70] p 3628 N92-30372

ELLIPTIC FUNCTIONS
Positivity for a strongly coupled elliptic system by Green function estimates
[REPT-91-77] p 3702 N92-30434

ELLIPTICAL ORBITS
The ELLIPSO (tm) system: Elliptical low orbits for mobile communications and other optimum system elements
p 3618 N92-30930

EMBRITTLEMENT
Recent improvements in size effects correlations for DBTT and upper shelf energy of ferritic steels
[DE92-014703] p 3599 N92-30877

EMISSION
Towards the development of a global inventory for black carbon emissions
[DE92-013514] p 3674 N92-30647
Line-emission cross sections for the charge-exchange reaction between fully stripped carbon and atomic hydrogen in tokamak plasma
[NIFS-129] p 3716 N92-30967

EMISSION SPECTRA
Theoretical study of phase-shifted quantum beats in time-resolved luminescence spectra from a biased asymmetric double quantum well
[AD-A252422] p 3710 N92-30549
High background photon counting lidar
p 3649 N92-31071
Time and wavelength domain algorithms for chemical analysis by laser radar p 3650 N92-31075

EMITTANCE
Nonlinear analysis of a grating free-electron laser
[AD-A248833] p 3656 N92-30743
Emittance growth caused by magnet vibrations in SSC
[DE92-014186] p 3719 N92-30881

EMITTERS
High efficiency thermal to electric energy conversion using selective emitters and spectrally tuned solar cells
[NASA-TM-105755] p 3670 N92-30426

ENERGETIC PARTICLES
Collisional and chaotic transport of energetic particles in toroidal plasma
[DE92-014589] p 3725 N92-30900

ENERGY BUDGETS
Small satellite radiation budget instrumentation
[DE92-011134] p 3677 N92-31008

ENERGY CONSERVATION
Reducing greenhouse gas emissions in Czechoslovakia
[DE92-012354] p 3672 N92-30374
The status of renewable energy technology
[DE92-011386] p 3670 N92-30808

ENERGY CONSUMPTION
Reducing greenhouse gas emissions in Czechoslovakia
[DE92-012354] p 3672 N92-30374

ENERGY CONVERSION
High efficiency thermal to electric energy conversion using selective emitters and spectrally tuned solar cells
[NASA-TM-105755] p 3670 N92-30426
Design of a high activity and selectivity alcohol catalyst
[DE92-013918] p 3594 N92-30717
Magnetic bearings for free-piston Stirling engines
[NASA-TM-105730] p 3660 N92-30734
The status of renewable energy technology
[DE92-011386] p 3670 N92-30808
A novel process for methanol synthesis
[DE92-015798] p 3608 N92-30904

ENERGY CONVERSION EFFICIENCY
High efficiency thermal to electric energy conversion using selective emitters and spectrally tuned solar cells
[NASA-TM-105755] p 3670 N92-30426
Fuel cell systems program plan: Fiscal year 1992
[DE92-015985] p 3672 N92-31188

ENERGY DISSIPATION
A study of the topology of dissipating motions in direct numerical simulations of time-developing compressible and incompressible mixing layers p 3632 N92-30658
High resolution electron energy loss studies of surface vibrations
[DE92-014608] p 3626 N92-30901

ENERGY LEVELS
Nuclear structure calculations for astrophysical applications
[DE92-011495] p 3740 N92-30856

ENERGY POLICY
Reducing greenhouse gas emissions in Czechoslovakia
[DE92-012354] p 3672 N92-30374

ENERGY SOURCES
The status of renewable energy technology
[DE92-011386] p 3670 N92-30808

ENERGY SPECTRA
Theory and measurement of the energy and risetime resolution of scintillation detectors in hard x ray area
[ETN-92-91687] p 3720 N92-30504

ENERGY STORAGE
Design and simulation of latent heat storage units
[DE91-002145] p 3670 N92-30330

ENERGY TECHNOLOGY
Spinoffs from R and D investments
[DE92-014450] p 3736 N92-30575
The status of renewable energy technology
[DE92-011386] p 3670 N92-30808
Introduction to the efficiency of fuel cells
[MBB-Z-0412-91-PUB] p 3671 N92-30970

ENERGY TRANSFER
Photoinitiated electron transfer in multichromophoric species: Synthetic tetrads and pentads featuring diquinone moieties
[DE92-013472] p 3683 N92-30368
Solar flare MDH
[AD-A250639] p 3702 N92-30375
Interscale energy transfer in numerically simulated turbulence p 3634 N92-30672
Vacuum ultraviolet studies of molecular dynamics
[AD-A246964] p 3715 N92-30681

ENGINE AIRFRAME INTEGRATION
Navier-Stokes computations of a viscous optimized waverider
[NASA-CR-189658] p 3574 N92-30392

ENGINE DESIGN
Development of a modular transient cycle analysis program for the adiabatic diesel and other compound diesel engines
[AD-A249022] p 3658 N92-30538

ENGINE FAILURE
Statistics on aircraft gas turbine engine rotor failures that occurred in US commercial aviation during 1989
[DOT/FAA/CT-92/5] p 3581 N92-30303

ENGINE INLETS
Numerical investigations in three-dimensional internal flows
[NASA-CR-190498] p 3628 N92-30380
Navier-Stokes analysis and experimental data comparison of compressible flow within ducts
[NASA-TM-105796] p 3582 N92-30972

ENGINE MONITORING INSTRUMENTS
Laser induced fluorescence detection of gums in jet fuels
[AD-A252685] p 3607 N92-30767

ENGINE TESTING LABORATORIES
Future aerospace ground test facility requirements for the Arnold Engineering Development Center
p 3585 N92-30897

ENGINE TESTS
Small engine components test facility compressor testing cell at NASA Lewis Research Center
[NASA-TM-105685] p 3584 N92-30508
Ringless piston experiments. Natural gas engine technology advancements
[PB92-164466] p 3659 N92-30601

ENGINEERING MANAGEMENT
Concurrent engineering p 3697 N92-30952

ENTRAINMENT
Neurophysiological analysis of circadian rhythm entrainment
[AD-A248466] p 3684 N92-30319

ENVIRONMENT EFFECTS
Reducing greenhouse gas emissions in Czechoslovakia
[DE92-012354] p 3672 N92-30374
Habitat model for the Florida Scrub Jay on John F. Kennedy Space Center
[NASA-TM-107543] p 3673 N92-30494
Small satellite radiation budget instrumentation
[DE92-011134] p 3677 N92-31008

ENVIRONMENT MODELS
Electrical and chemical interactions at Mars Workshop, part 1
[NASA-CP-10093] p 3741 N92-30302
Development and testing of an air quality model for Mexico City
[DE92-011238] p 3673 N92-30520
Airborne lidar mapping of vertical ozone distributions in support of the 1990 Clean Air Act Amendments
p 3654 N92-31101

ENVIRONMENT POLLUTION
Chemistry for protection of the environment, 8th International Conference proceedings
[DE92-014317] p 3674 N92-31181

ENVIRONMENT PROTECTION
Status of selected air pollution control programs, February 1992
[PB92-171966] p 3673 N92-30561
National ocean pollution program: Summary of Federal programs and projects: FY 1989 update
[PB92-187012] p 3673 N92-30563
Report of the Great Lakes Air Toxics Research Priorities Workshop
[PB92-166933] p 3673 N92-30602
Chemistry for protection of the environment, 8th International Conference proceedings
[DE92-014317] p 3674 N92-31181

ENVIRONMENTAL CHEMISTRY
Chemistry for protection of the environment, 8th International Conference proceedings
[DE92-014317] p 3674 N92-31181

ENVIRONMENTAL CONTROL
Integration mockup and process material management system
[NASA-CR-184319] p 3613 N92-30754
Waste streams in a typical crewed space habitat: An update
[NASA-TM-103888] p 3689 N92-31166

ENVIRONMENTAL MONITORING
The sustainable biosphere initiative: An ecological research agenda p 3673 N92-30425

ENVIRONMENTAL SURVEYS
Global scale concentrations of volcanic activity on Venus: A summary of three 23rd Lunar and Planetary Science Conference abstracts. 1: Venus volcanism: Global distribution and classification from Magellan data. 2: A major global-scale concentration of volcanic activity in the Beta-Atla-Themis region of Venus. 3: Two global concentrations of volcanism on Venus: Geologic associations and implications for global pattern of upwelling and downwelling p 3737 N92-31226

ENVIRONMENTAL TESTS
Testing of double-layer capacitors for high reliability applications
[DE92-011384] p 3626 N92-30807

ENZYMES
Methane to liquid
[DE92-001277] p 3596 N92-30883

EPITAXY
In situ TEM studies of the effect of misfit strain on the kinetics of Si(sub 1-x)Ge(sub x) solid phase epitaxy: Temperature calibration and surface effects
[DE92-011689] p 3728 N92-30574
Atomic layer epitaxy group 4 materials: Surface processes, thin films, devices, and their characterization
[AD-A252352] p 3729 N92-30846

EPOXY COMPOUNDS
Epoxides as activators for grafting of poly(tetrahydrofuran) from poly(methylphenylsilylene)
[AD-A251086] p 3601 N92-30244

EPOXY MATRIX COMPOSITES
Organic Matrix Composite Helicopter Internal/External Cargo Pallet System (OMC INTEX)
[AD-A251127] p 3580 N92-30878

EQUATIONS OF MOTION
The Rayleigh-Taylor instability in an expanding plasma
[DE92-013883] p 3725 N92-30884

EQUATIONS OF STATE
Constraints on the nuclear matter equation of state from pulsar glitches
[DE92-015142] p 3740 N92-30578

ERGODIC PROCESS
On the Thue Morse measure
[REPT-92-16] p 3704 N92-30464
Coexistence of uniquely ergodic subsystems of interval mapping
[DE92-630231] p 3732 N92-31133

EROSION
Impact erosion of terrestrial planetary atmospheres
[NASA-CR-190605] p 3742 N92-30921

ERROR ANALYSIS
Regional-scale analysis and forecasting (RAP) report
[AD-A248384] p 3678 N92-30262
Linear estimates of structure functions from deep inelastic lepton-nucleon scattering data, part 1
[DE92-627288] p 3713 N92-30403
Locked modes and magnetic field errors in MST
[DE92-015379] p 3723 N92-30612
New method of error elimination in potential profile measurement of tokamak plasmas by high voltage heavy ion beam probes
[NIFS-143] p 3726 N92-30995
On two methods of determining the ellipses and ellipsoids of positioning accuracy of robot manipulators
[ISSN-0208-5658] p 3701 N92-31148
A failure-to-restore unavailability model for periodically performed maintenance
[DE92-015902] p 3708 N92-31185
Component-wise error bounds for linear equations
[DE92-016000] p 3707 N92-31189

ERROR CORRECTING CODES
METEODEC/METEOCRYPT: A demonstration of data compression and encryption for operational remote-sensing
[NLR-TP-89294-U] p 3667 N92-30475

ERRORS
Alignment of a 3-D sensor and a 2-D sensor measuring azimuth and elevation
[AD-A252120] p 3636 N92-30530
Locked modes and magnetic field errors in MST
[DE92-015379] p 3723 N92-30612
A simplified dynamic model of the T700 turboshaft engine
[NASA-TM-105805] p 3709 N92-30898
ERS-1 (ESA SATELLITE)
Preparations for the ERS-1 and TOPEX/Poseidon satellite altimetry missions
[BCRS-90-28] p 3666 N92-30465
ESTERS
Approaches to polymer curing and imaging via the in situ generation of a catalyst
[AD-A249917] p 3606 N92-30873
ESTIMATES
Linear estimates of structure functions from deep inelastic lepton-nucleon scattering data, part 1
[DE92-627288] p 3713 N92-30403
Positivity for a strongly coupled elliptic system by Green function estimates
[REPT-91-77] p 3702 N92-30434
Plasma parameter estimations for the large helical device based on the gyro-reduced Bohm scaling
[NIFS-114] p 3723 N92-30499
SCS method of runoff estimation using remote sensing techniques p 3668 N92-30916
Remote sensing for rainfall estimation: SAC experience p 3668 N92-30917
Analytical estimates of the PP-algorithm at low number of Doppler periods per pulse length
p 3650 N92-31079
ESTIMATING
Pairwise comparison of concessions in negotiation processes
[REPT-92-15] p 3733 N92-30463
Use of INSAT data in rainfall estimation
p 3668 N92-30912
ETALONS
Interferometers adaptations to lidars
p 3645 N92-31052
ETCHING
Anisotropic silicon etching techniques
[MBB-Z-0413-91-PUB] p 3594 N92-30422
ETHERS
Design of a high activity and selectivity alcohol catalyst
[DE92-013918] p 3594 N92-30717
High-temperature ignition of propane with MTBE as an additive: Shock-tube experiments and modeling
[DE92-008679] p 3594 N92-30749
Polymerization of 1-bromo-4-lithiobenzene in THF. A route to soluble polyphenylenes
[AD-A249926] p 3604 N92-30794
ETHYLENEDIAMINE
Studies of thermal decomposition of the 1:1 R3Al:en adduct (R = Me, Et; en = ethylenediamine): Synthesis and structure of a novel intermediate Al((HNCH2CH2NH)AlMe2)3
[AD-A251061] p 3603 N92-30623
EULER EQUATIONS OF MOTION
Computation of unsteady transonic flows using an implicit centered Euler solver without artificial viscosity
[ESA-TT-1235] p 3575 N92-30514
Calculation of viscous hypersonic flows in chemical non-equilibrium
[MBB/FE211/S/PUB/466] p 3634 N92-30674
CFD contributions during hypersonic airplane intake design
[MBB/FE213/S/PUB/459] p 3575 N92-30676
EUROPEAN SPACE PROGRAMS
Operations and logistics tasks in the Columbus development program
[MBB-UO-0166-91-PUB] p 3708 N92-30419
EUSTACHIAN TUBES
The use of tympanometry to detect aerotitis media in hypobaric chamber operations
[AD-A248963] p 3684 N92-30328
EUTECTICS
Experiments with the low melting indium-bismuth alloy system p 3601 N92-30272
EVALUATION
CAESAR: Evaluation of the dual-look concept
[BCRS-91-10] p 3666 N92-30467
EVAPORATION
Evaporation duct effects at millimeter wavelengths
[AD-A250239] p 3617 N92-30876
Thermodynamic evaporation of highly volatile components in the vacuum degassing of melted aluminum alloys
[DE92-015315] p 3600 N92-31218
EVAPORATORS
Progress in the development of the Hermes evaporators
[MBB-UO-0164-91-PUB] p 3587 N92-30440
EXCIMER LASERS
Tunable solid state lasers based on molecular ions
[AD-A249423] p 3656 N92-30774
Laser induced reaction for pre-bond surface preparation of aluminum alloys
[AD-A249916] p 3598 N92-30872
Advanced Raman water vapor lidar
p 3643 N92-31040
EXERCISE PHYSIOLOGY
Optimal ECG electrode sites and criteria for detection of asymptomatic coronary artery disease, update 1990. Multilead ECG changes at rest, with exercise, and with coronary angioplasty
[AD-A248613] p 3684 N92-30523
Exercise behavior among Navy runners and non-runners
[AD-A250651] p 3685 N92-30644
EXHAUST EMISSION
Status of selected air pollution control programs, February 1992
[PB92-171966] p 3673 N92-30561
EXHAUST GASES
Reducing greenhouse gas emissions in Czechoslovakia
[DE92-012354] p 3672 N92-30374
Numerical investigations in the backflow region of a vacuum plume
[NASA-CR-190515] p 3589 N92-30981
EXHAUST NOZZLES
Navier-Stokes analysis and experimental data comparison of compressible flow within ducts
[NASA-TM-105796] p 3582 N92-30972
Preliminary dynamic tests of a flight-type ejector
[NASA-TM-105814] p 3582 N92-30998
EXOBIOLOGY
Aerospace medicine and biology: A continuing bibliography with indexes (supplement 363)
[NASA-SP-7011(363)] p 3685 N92-30987
EXOTHERMIC REACTIONS
Advanced concepts for controlled combustion in engines
[AD-A249911] p 3595 N92-30814
EXPENDABLE STAGES (SPACECRAFT)
An electromechanical actuation system for an expendable launch vehicle
[NASA-TM-105774] p 3586 N92-30310
EXPERIMENT DESIGN
Ceramic processing: Experimental design and optimization p 3607 N92-30267
A senior manufacturing laboratory for determining injection molding process capability
p 3609 N92-30273
Be-Cu precipitation hardening experiment
p 3601 N92-30276
Determining significant material properties: A discovery approach p 3607 N92-30279
Five experiments in materials science for less than $10.00 p 3611 N92-30283
Isotropic thin-walled pressure vessel experiment
p 3611 N92-30284
Stress-strain characteristics of rubber-like materials: Experiment and analysis p 3607 N92-30285
Demonstration of magnetic domain boundary movement using an easily assembled videocam-microscope system
p 3611 N92-30286
Ideas for a long-baseline neutrino detector
[DE92-010650] p 3743 N92-30828
Spectroscopic diagnosis of long-scale-length exploding-foil plasma in the presence of an intense radiation field
[DE92-014718] p 3726 N92-31118
EXPERIMENTATION
National Educators' Workshop: Update 1991. Standard Experiments in Engineering Materials Science and Technology
[NASA-CP-3151] p 3608 N92-30263
Tempered glass and thermal shock of ceramic materials p 3607 N92-30265
Elementary metallography p 3600 N92-30266
Designing, engineering, and testing wood structures
p 3593 N92-30270
Remote experimental site concept for diagnostic collaborations in fusion
[DE92-010437] p 3724 N92-30824
EXPERT SYSTEMS
Model analysis and expert system development for planning and scheduling teleoperations for aircraft turnaround functions, volume 1
[AD-A251037] p 3573 N92-30253
Model analysis and expert system development for planning and scheduling teleoperations for aircraft turnaround functions. Volume 2: Top user's guide
[AD-A251083] p 3573 N92-30258
A principled approach to the measurement of situation awareness in commercial aviation
[NASA-CR-4451] p 3686 N92-30306
EXPLOSIONS
Spectroscopic diagnosis of long-scale-length exploding-foil plasma in the presence of an intense radiation field
[DE92-014718] p 3726 N92-31118
EXPLOSIVE DECOMPRESSION
Aircraft accident report: Explosive decompression - loss of cargo door in flight, United Airlines Flight 811, Boeing 747-122, N4713U, Honolulu, Hawaii, February 24, 1989
[PB92-910402] p 3578 N92-31159
EXPLOSIVES
Fragment hazard zone analyses for explosive test facilities
[DE92-015391] p 3613 N92-30887
Modeling initiation of explosives by projectile impact
[DE92-015210] p 3608 N92-31202
EXPONENTIAL FUNCTIONS
Some inequalities for variances
[REPT-92-10] p 3707 N92-30460
EXPONENTS
Application of automated deduction to the search for single axioms for exponent groups
[DE92-015271] p 3705 N92-30608
EXPOSURE
Secretory mechanisms in opiocortin cells during cold stress
[AD-A252317] p 3685 N92-30719
Isothermal aging effects on PMR-15 resin
[NASA-TM-105648] p 3593 N92-30986
The revised International Commission on Radiological Protection (ICRP) dosimetric model for the human respiratory tract
[DE92-015092] p 3685 N92-31011
Effects of microwave radiation on humans: Monkeys exposed to 1.25 GHz pulsed microwaves
[AD-A249997] p 3686 N92-31127
EXTINCTION
Aerosol extinction measurements with CO2-lidar
p 3655 N92-31105
EXTRACTION
Supercritical fluid extraction: A new process for producing high-performance, low-cost carbon fibers
[AD-A249407] p 3595 N92-30773
EXTRASOLAR PLANETS
Discovery of two planets around a millisecond pulsar
p 3739 N92-31237
EXTREME ULTRAVIOLET RADIATION
Reflector development for XUV free-electron laser oscillators
[DE92-015212] p 3657 N92-31182
EXTREMELY HIGH FREQUENCIES
The ACTS multibeam antenna
[NASA-TM-105645] p 3587 N92-30383
Personal communications via ACTS satellite HBR transponders p 3618 N92-30929
Characteristics of a future aeronautical satellite communications system p 3618 N92-30932
An integrated Ka/Ku-band payload for personal, mobile and private business communications
p 3619 N92-30933
A personal communications network using a Ka-band satellite p 3619 N92-30934
EHF (28/19 GHz) personal communications satellite terminal development p 3619 N92-30935
EXTRUDING
Laboratory experiments from the toy store
p 3609 N92-30274
Processing aerosols and filaments in a TM010 microwave cavity at 2.45 GHz
[DE92-013536] p 3615 N92-30703
EYE (ANATOMY)
Psychophysical studies of visual cortical function
[AD-A246962] p 3687 N92-30679
EYE PROTECTION
Eye/sensor protection against laser irradiation ablative mirror devices: A materials assessment
[AD-A248787] p 3688 N92-30615

F

F 2 REGION
The calculation of mid-latitude meridional neutral winds from an improved servo model approximation method
[AD-A249874] p 3676 N92-30868
F-15 AIRCRAFT
Thrust stand evaluation of engine performance improvement algorithms in an F-15 airplane
[NASA-TM-104252] p 3581 N92-30518

F-18 AIRCRAFT
In-service evaluation of 2090 aluminum-lithium alloy on F/A-18 aircraft
[AD-A248472] p 3607 N92-30321
FABRICATION
Hybridization of detector array and integrated circuit for readout
[NASA-CASE-NPO-18062-1-CU] p 3623 N92-30542
Designing, fabricating and testing cost effective structural composite for the SSCL magnets
[DE92-013469] p 3718 N92-30646
Properties of CMOS devices and circuits fabricated on high-resistivity, detector-grade silicon
[DE92-011727] p 3626 N92-30813
Double-sided wafer alignment techniques
[AD-A250757] p 3730 N92-30895
Sol-gel optics: Proceedings SPIE-The International Society for Optical Engineering
[AD-A249986] p 3721 N92-31126
FABRY-PEROT INTERFEROMETERS
Measurement of aerosol profiles using high-spectral-resolution Rayleigh-Mie lidar
p 3644 N92-31046
Interferometers adaptations to lidars
p 3645 N92-31052
Pulsed laser spectral measurement using a Fabry-Perot interferometer: Limits to resolution p 3646 N92-31055
FACE CENTERED CUBIC LATTICES
Mechanism of slip and twinning p 3610 N92-30280
Determination of pair potentials by analysis of diffuse scattering of the local field in Pd3V and Ni3V
[ESA-TT-1228] p 3597 N92-30513
Stabilization of face-centered-cubic titanium
[DE92-011530] p 3600 N92-31125
FACTORIZATION
On the factorisation theorem in boson-gluon fusion at hadron colliders
[NIKHEF-H/91-16] p 3713 N92-30415
FADING
Fiber optic Michelson sensor and arrays with passive elimination of polarization fading and source feedback isolation
[AD-D015290] p 3722 N92-31213
FAILURE
Statistics on aircraft gas turbine engine rotor failures that occurred in US commercial aviation during 1989
[DOT/FAA/CT-92/5] p 3581 N92-30303
FAILURE ANALYSIS
Ultrasound NDE of adhesive bond integrity: A quantitative measure
[AD-A248845] p 3661 N92-30599
Effect of bending on the room-temperature tensile strengths of structural ceramics
[DE92-015196] p 3603 N92-30626
Nonlinear stress analysis of composite-jacketed steel cylinders subjected to high internal pressure
[AD-A249500] p 3663 N92-30802
Assessment of an improved multiaxial strength theory based on creep-rupture data for type 316 stainless steel
[DE92-010431] p 3663 N92-30823
A failure-to-restore unavailability model for periodically performed maintenance
[DE92-015902] p 3708 N92-31185
FAR ULTRAVIOLET RADIATION
Vacuum ultraviolet studies of molecular dynamics
[AD-A246964] p 3715 N92-30681
VUV production from a ferrite-driven flash-pumped system
[DE92-011362] p 3657 N92-30805
FAST FOURIER TRANSFORMATIONS
On the rapid evaluation of trigonometric series
[AD-A249029] p 3705 N92-30568
FATIGUE (MATERIALS)
Five experiments in materials science for less than $10.00 p 3611 N92-30283
Linear elastic fracture mechanics primer
[NASA-TM-103591] p 3662 N92-30416
Thermally activated rejuvenation of ferroelectric properties in electrically fatigued lead zirconate titanate ceramics
[DE92-012634] p 3605 N92-30830
FASTRAN-2: A fatigue crack growth structural analysis program
[NASA-TM-104159] p 3664 N92-30964
FATIGUE LIFE
Acoustic fatigue life prediction for nonlinear structures with multiple resonant modes
[NASA-CR-190471] p 3664 N92-30988
FAULT TOLERANCE
How to securely replicate services
[NASA-CR-190476] p 3692 N92-30379
Computing with faulty shared memory
[DE92-011663] p 3695 N92-30522
Can stochastic modelling and analysis of multistage interconnection networks lead to efficient usage of redundancy for fault-tolerant design?
[AD-A250635] p 3699 N92-30526
Exploiting resource parallelism for integrated fault monitoring and recovery
[AD-A248843] p 3699 N92-30557
An extension to Schneider's general paradigm for fault-tolerant clock synchronization
[NASA-TM-107634] p 3699 N92-30677
FEASIBILITY ANALYSIS
Hyperspectral gas analysis system (HyGAS), phase 1
[AD-A251026] p 3593 N92-30241
Model analysis and expert system development for planning and scheduling teleoperations for aircraft turnaround functions, volume 1
[AD-A251037] p 3573 N92-30253
Model analysis and expert system development for planning and scheduling teleoperations for aircraft turnaround functions. Volume 2: Top user's guide
[AD-A251083] p 3573 N92-30258
Development statistics for the UH-1 Ada feasibility study
[AD-A252404] p 3584 N92-30547
Design feasibility study of a Space Station Freedom truss
[NASA-TM-105558] p 3659 N92-30571
KC-135 crew reduction feasibility demonstration simulation study. Volume 1: Function analysis and function reallocation
[AD-A252265] p 3688 N92-30592
The status of renewable energy technology
[DE92-011386] p 3670 N92-30808
Extension of the integral equation formulation of linearized time dependent subsonic flow
[AD-A250654] p 3577 N92-31171
FEDERAL BUDGETS
Departments of Veterans Affairs and Housing and Urban Development, and Independent Agencies Appropriation Bill, 1993
[S-REPT-102-356] p 3735 N92-31169
FEEDBACK
Joint queue length and response time distributions in a general preemptive feedback queue
[REPT-91-66] p 3701 N92-30451
Fiber optic Michelson sensor and arrays with passive elimination of polarization fading and source feedback isolation
[AD-D015290] p 3722 N92-31213
FEEDBACK CONTROL
Practical method's for robust multivariable control
[AD-A248473] p 3700 N92-30322
Numerical methods for closed-loop control
[AD-A248481] p 3700 N92-30334
Nonlinear system design: Adaptive feedback linearization with unmodeled dynamics
[AD-A248484] p 3700 N92-30335
Microgravity vibration isolation: Optimal preview and feedback control
[NASA-TM-105673] p 3613 N92-30692
A simplified dynamic model of the T700 turboshaft engine
[NASA-TM-105805] p 3709 N92-30898
FEEDFORWARD CONTROL
Microgravity vibration isolation: Optimal preview and feedback control
[NASA-TM-105673] p 3613 N92-30692
FERRITES
VUV production from a ferrite-driven flash-pumped system
[DE92-011362] p 3657 N92-30805
FERROELECTRICITY
Ferroelectric and piezoelectric properties of odd-numbered nylons
[AD-A252270] p 3727 N92-30406
A new class of ferroelectric polymers: The odd-numbered nylons
[AD-A252268] p 3603 N92-30594
Ferroelectric polarization mechanisms in Nylon 11
[AD-A252269] p 3728 N92-30595
Relaxor ferroelectrics for electrostrictive transducer
[AD-A248671] p 3624 N92-30598
Thermally activated rejuvenation of ferroelectric properties in electrically fatigued lead zirconate titanate ceramics
[DE92-012634] p 3605 N92-30830
FEYNMAN DIAGRAMS
Search for light neutral scalar and pseudoscalar particles in pFe interactions at 70 GeV
[DE92-627317] p 3713 N92-30404
FIBER COMPOSITES
Finite element analysis of laminated composite axisymmetric solids. Volume 1: Theory and applications
[AD-A250808] p 3590 N92-30251
Low-velocity impact loading on fibre reinforced aluminum laminates (ARALL) and other aircraft sheet materials
[ETN-92-91613] p 3590 N92-30414
Multidisciplinary optimization of fiber composite aircraft structures
[MBB/FW321/S/PUB/476] p 3579 N92-30424
Wave propagation and vibration of fibre-reinforced laminates
[AD-A252101] p 3590 N92-30528
Development of hardness cycles for fiber bound materials, using DSC: From laboratory specimens to complex high duty structural members
[MBB-Z-0409-91-PUB] p 3592 N92-30969
FIBER OPTICS
Fiber optic based signal processing
[AD-A247857] p 3720 N92-30248
Fiber-optic Raman spectroscopy at the Savannah River Site: Uses and techniques
[DE92-013971] p 3596 N92-30899
Single mode variable-sensitivity fiber optic sensors
[NASA-CR-190492] p 3721 N92-30975
Optical transducers for scintillating fiber readout
[DE92-015963] p 3721 N92-31187
Fiber optic Michelson sensor and arrays with passive elimination of polarization fading and source feedback isolation
[AD-D015290] p 3722 N92-31213
FIBER ORIENTATION
Multidisciplinary optimization of fiber composite aircraft structures
[MBB/FW321/S/PUB/476] p 3579 N92-30424
FIBERS
Template-synthesis: A method for enhancing the ionic and electronic conductivity in electronically conductive polymers
[AD-A248806] p 3603 N92-30553
FIELD EFFECT TRANSISTORS
The temperature dependence of a large dynamic range photodetector structure
[AD-A247667] p 3624 N92-30683
Quantum interference and confinement effects in narrow channel Si-MOSFET's
[ETN-92-91742] p 3625 N92-30729
One-dimensional subband effects in the conductance of multiple quantum wires in Si-MOSFET's
p 3625 N92-30731
Enhancement of weak localization in a Si lateral superlattice device p 3625 N92-30732
Focused ion beam implantation
[AD-A249662] p 3627 N92-31004
FIELD EMISSION
RF vacuum microelectronics
[AD-A249814] p 3626 N92-30836
FIELD OF VIEW
Interferometers adaptations to lidars
p 3645 N92-31052
FIELD STRENGTH
Data report, 92-2. Magnetic results, 1985-1990
p 3675 N92-30417
High field optical-pumping spin-exchange polarized deuterium source
[DE92-010274] p 3657 N92-30848
FIELD THEORY (ALGEBRA)
Quantum Weyl Group and universal quantum R-matrix for affine Lie algebra A1
[PB92-178276] p 3704 N92-30511
FIELD THEORY (PHYSICS)
From a world-sheet supersymmetry to the Dirac equation
[DE92-622375] p 3731 N92-30799
From a particle with a world-line supersymmetry to the Dirac-like equation
[DE92-622376] p 3731 N92-30800
Quantum mechanics in Grassmann space
[DE92-622377] p 3711 N92-30801
Example of a quantum field theory based on a nonlinear Lie algebra
[DE92-010475] p 3731 N92-30825
One-loop integration for the axial gauge with generalized prescription
[DE92-630241] p 3732 N92-31145
Ginsburg criterion for an equilibrium superradiant model in the dynamic approach
[DE92-630566] p 3732 N92-31203
FIGHTER AIRCRAFT
Effects of pyridostigmine bromide on A-10 pilots during execution of a simulated mission; performance
[AD-A252309] p 3685 N92-30605
Research and technology, 1991. Langley Research Center
[NASA-TM-4331] p 3744 N92-30733
Nonlinear stability and control study of highly maneuverable high performance aircraft, phase 2
[NASA-CR-190667] p 3583 N92-30922

FILAMENT WINDING
Wrappability of curves on surfaces
[AD-A250004] p 3707 N92-31140
FILLERS
Molecular weight dependence of domain structure in silica-siloxane molecular composites
[DE92-015046] p 3603 N92-30544
Filler metal development for Hastelloy alloy XR
[DE92-782044] p 3600 N92-31163
FILTERS
Fiber optic based signal processing
[AD-A247857] p 3720 N92-30248
Negative ion extraction characteristics of a large negative ion source with double-magnetic filter configuration
[NIFS-151] p 3714 N92-30501
FILTRATION
Non-holonomic filtration: Algebraic and geometric aspects of non-integrability
[PB92-178003] p 3706 N92-30790
FINITE DIFFERENCE THEORY
Validation of three-dimensional incompressible spatial direct numerical simulation code: A comparison with linear stability and parabolic stability equation theories for boundary-layer transition on a flat plate
[NASA-TP-3205] p 3573 N92-30295
A Boussinesq algorithm for bouyant convection in polygonal domains
[PB92-187137] p 3695 N92-30579
Finite difference time domain modeling of steady state scattering from jet engines with moving turbine blades
[NASA-CR-190290] p 3582 N92-30753
Direct coupling method for time-accurate solution of incompressible Navier-Stokes equations
[NASA-CR-189177] p 3636 N92-30894
Resolution of the three-dimensional parabolic equation applied to acoustic propagation at low altitudes
[ONERA-RF-17/3641-PY] p 3711 N92-30966
FINITE ELEMENT METHOD
Finite element analysis of laminated composite axisymmetric solids. Volume 1: Theory and applications
[AD-A250808] p 3590 N92-30251
Influence of structural and aerodynamic modeling on flutter analysis and structural optimization
[AD-A248487] p 3583 N92-30323
Special finite element methods for a class of second order elliptic problems with rough coefficients
[AD-A248900] p 3701 N92-30339
MBB-LAGRANGE: A general structural reliability and optimization structural system
[MBB/FW321/S/PUB/467] p 3662 N92-30423
Ultrasound NDE of adhesive bond integrity: A quantitative measure
[AD-A248845] p 3661 N92-30599
Numerical simulation of the dynamic behavior of the polymeric gels
[DE92-011358] p 3605 N92-30804
A study of discrete and continuum joint modeling techniques
[DE92-012631] p 3663 N92-30859
Cross sectional constants and stress distributions of thin-walled sections
[AD-A249886] p 3663 N92-30870
Numerical analysis of the losipescu specimen for composite materials
[NASA-CR-190658] p 3592 N92-30906
Mechanical design and finite element analysis of the SDC central calorimeter
[DE92-011197] p 3655 N92-31109
An analytical and experimental investigation of flutter suppression via piezoelectric actuation
[NASA-TM-107653] p 3580 N92-31174
FINITE VOLUME METHOD
Finite volume discretization of the incompressible Navier-Stokes equations in general coordinates on staggered grids
[REPT-91-71] p 3628 N92-30373
Finite volume discretization of the convection-diffusion equation in general coordinates
[REPT-91-72] p 3704 N92-30483
Computation of unsteady transonic flows using an implicit centered Euler solver without artificial viscosity
[ESA-TT-1235] p 3575 N92-30514
Solving the Euler equations using adaptive mesh motion and refinement
[AD-A252364] p 3705 N92-30597
FIRE CONTROL
The rise of active-element phased-array radar
[RAND-P-7747-RGS] p 3616 N92-30755
FISCHER-TROPSCH PROCESS
The development of precipitated iron catalysts with improved stability
[DE92-014825] p 3596 N92-31006
FISSURES (GEOLOGY)
A study of discrete and continuum joint modeling techniques
[DE92-012631] p 3663 N92-30859
FIXTURES
Mechanical properties of brittle materials
p 3612 N92-30290
Thrust test fixture
[AD-D015259] p 3585 N92-31192
FLAME PROPAGATION
Geometry of premixed flames in three-dimensional turbulence p 3633 N92-30666
The influence of Lewis number and nonhomogeneous mixture on premixed turbulent flame structure
p 3597 N92-30669
Pre-mixed flame simulations for non-unity Lewis numbers p 3597 N92-30670
FLAME TEMPERATURE
Pre-mixed flame simulations for non-unity Lewis numbers p 3597 N92-30670
FLAMES
Statistics for laminar flamelet modeling
p 3597 N92-30668
FLAT CONDUCTORS
Spontaneous emission from an atom in motion near an infinite conducting plane
[ITN-92-85169] p 3715 N92-30782
FLAT PLATES
Validation of three-dimensional incompressible spatial direct numerical simulation code: A comparison with linear stability and parabolic stability equation theories for boundary-layer transition on a flat plate
[NASA-TP-3205] p 3573 N92-30295
FLAVOR (PARTICLE PHYSICS)
Remarks on the exotic U-meson
[RAL-91-090] p 3715 N92-30750
FLEXIBLE BODIES
Vehicle/guideway interaction for high speed vehicles on flexible guideway
[DE92-013057] p 3660 N92-30860
Flexible heating head for induction heating apparatus and method
[NASA-CASE-LAR-14679-2] p 3621 N92-31150
Extension of the integral equation formulation of linearized time dependent subsonic flow
[AD-A250654] p 3577 N92-31171
FLEXIBLE WINGS
On-line analysis capabilities developed to support the AFW wind-tunnel tests
[NASA-TM-107651] p 3580 N92-30752
FLIGHT CHARACTERISTICS
Technical evaluation report on the Flight Mechanics Panel Symposium on Piloted Simulation Effectiveness
[AGARD-AR-315] p 3584 N92-30769
Real-time simulation model of the HL-20 lifting body
[NASA-TM-107580] p 3586 N92-31160
Preliminary subsonic aerodynamic model for simulation studies of the HL-20 lifting body
[NASA-TM-4302] p 3583 N92-31175
FLIGHT CONDITIONS
Helicopter nighttime parking test results - UH-1
[DOT/FAA/CT-TN92/1] p 3580 N92-31165
FLIGHT CONTROL
Real-time simulation model of the HL-20 lifting body
[NASA-TM-107580] p 3586 N92-31160
An analytical and experimental investigation of flutter suppression via piezoelectric actuation
[NASA-TM-107653] p 3580 N92-31174
Preliminary subsonic aerodynamic model for simulation studies of the HL-20 lifting body
[NASA-TM-4302] p 3583 N92-31175
FLIGHT CREWS
Optimal ECG electrode sites and criteria for detection of asymptomatic coronary artery disease, update 1990. Multilead ECG changes at rest, with exercise, and with coronary angioplasty
[AD-A248613] p 3684 N92-30523
KC-135 crew reduction feasibility demonstration simulation study. Volume 1: Function analysis and function reallocation
[AD-A252265] p 3688 N92-30592
Tolerance of beta blocked hypertensives during orthostatic and altitude stresses
[AD-A249904] p 3685 N92-30745
Flight crew integration in the maintenance chain of a commercial aircraft (A 320) p 3698 N92-30957
FLIGHT MANAGEMENT SYSTEMS
A principled approach to the measurement of situation awareness in commercial aviation
[NASA-CR-4451] p 3686 N92-30306
EASAMS' Ariane 5 on-board software experience
[D308/TN/001] p 3586 N92-30715
FLIGHT MECHANICS
Numerical optimization in Germany: A non-exhaustive survey on current activities with emphasis on aeronautics
[MBB/FE211/S/PUB/474] p 3573 N92-30675
Activities of the Aeronautical Research Laboratory
p 3744 N92-30768
Technical evaluation report on the Flight Mechanics Panel Symposium on Piloted Simulation Effectiveness
[AGARD-AR-315] p 3584 N92-30769
FLIGHT SAFETY
Statistics on aircraft gas turbine engine rotor failures that occurred in US commercial aviation during 1989
[DOT/FAA/CT-92/5] p 3581 N92-30303
A cable detection lidar system for helicopters
p 3648 N92-31068
FLIGHT SIMULATION
KC-135 crew reduction feasibility demonstration simulation study. Volume 1: Function analysis and function reallocation
[AD-A252265] p 3688 N92-30592
Numerical methods for the simulation of complex multi-body flows with applications for the integrated Space Shuttle vehicle p 3576 N92-30741
Technical evaluation report on the Flight Mechanics Panel Symposium on Piloted Simulation Effectiveness
[AGARD-AR-315] p 3584 N92-30769
Preliminary subsonic aerodynamic model for simulation studies of the HL-20 lifting body
[NASA-TM-4302] p 3583 N92-31175
FLIGHT SIMULATORS
Technical training for national simulator evaluation specialist
[NASA-CR-190429] p 3687 N92-30488
Development statistics for the UH-1 Ada feasibility study
[AD-A252404] p 3584 N92-30547
Technical evaluation report on the Flight Mechanics Panel Symposium on Piloted Simulation Effectiveness
[AGARD-AR-315] p 3584 N92-30769
Evaluation of microwave landing system approaches in a wide-body transport simulator
[NASA-CR-4450] p 3579 N92-30978
FLIGHT TESTS
Joint computational and experimental aerodynamics research on a hypersonic vehicle
[DE92-013439] p 3574 N92-30367
Organic Matrix Composite Helicopter Internal/External Cargo Pallet System (OMC INTEX)
[AD-A251127] p 3580 N92-30878
Airborne water vapor DIAL research: System development and field measurements
p 3653 N92-31093
Helicopter nighttime parking test results - UH-1
[DOT/FAA/CT-TN92/1] p 3580 N92-31165
FLIGHT TRAINING
Technical training for national simulator evaluation specialist
[NASA-CR-190429] p 3687 N92-30488
Technical evaluation report on the Flight Mechanics Panel Symposium on Piloted Simulation Effectiveness
[AGARD-AR-315] p 3584 N92-30769
FLOW CHARACTERISTICS
Continuum approaches for describing solid-liquid flow
[AD-A249028] p 3629 N92-30560
Real gas flow parameters for NASA Langley 22-inch Mach 20 helium tunnel
[NASA-CR-4462] p 3635 N92-30751
Studies on the melt flow rate of the SRM 1473: A low density polyethylene resin
[PB92-181080] p 3604 N92-30788
Direct simulation of high-speed mixing layers
[NASA-TP-3186] p 3576 N92-30909
FLOW DEFLECTION
Combustion diagnostics by photo-deflection spectroscopy
[AD-A250802] p 3594 N92-30645
FLOW DISTORTION
A fractal transition in the two dimensional shear layer
p 3633 N92-30665
FLOW DISTRIBUTION
Ultra high bypass Nacelle aerodynamics inlet flow-through high angle of attack distortion test
[NASA-CR-189149] p 3574 N92-30298
Joint computational and experimental aerodynamics research on a hypersonic vehicle
[DE92-013439] p 3574 N92-30367
A Boussinesq algorithm for bouyant convection in polygonal domains
[PB92-187137] p 3695 N92-30579
MATGRID, a program for generation of C-H and C-O topology grids around wing/body configurations: Software description document
[FFA-TN-1990-20] p 3575 N92-30713

Application of the Chimera overlapped grid scheme to simulation of Space Shuttle ascent flows
p 3576 N92-30742
Intersecting shock-wave/turbulent boundary-layer interactions at Mach 8.3
[NASA-TM-103909] p 3635 N92-30765
Numerical study of axial turbulent flow over long cylinders
[AD-A250801] p 3635 N92-30831
Numerical calculations of two-dimensional single and multi-material flow fields with CCICE
[DE92-015778] p 3636 N92-30903
Navier-Stokes analysis and experimental data comparison of compressible flow within ducts
[NASA-TM-105796] p 3582 N92-30972

FLOW EQUATIONS
Progress in unstructured-grid methods development for unsteady aerodynamic applications
[NASA-TM-107643] p 3574 N92-30393
Solving the Euler equations using adaptive mesh motion and refinement
[AD-A252364] p 3705 N92-30597

FLOW MEASUREMENT
Three-dimensional laser window formation
[NASA-RP-1280] p 3585 N92-30307
Method of measuring cross-flow vortices by use of an array of hot-film sensors
[NASA-CASE-LAR-14824-1-SB] p 3628 N92-30390
Doppler photography: Laser methods on the flow measurement technique
[ISL-PU-303/90] p 3720 N92-30507
Combustion diagnostics by photo-deflection spectroscopy
[AD-A250802] p 3594 N92-30645

FLOW STABILITY
Resonant instability of supersonic shear layers
p 3632 N92-30661

FLOW VELOCITY
A subgrid-scale model based on the second-order velocity structure function p 3631 N92-30651
Studies on the melt flow rate of the SRM 1473: A low density polyethylene resin
[PB92-181080] p 3604 N92-30788

FLOW VISUALIZATION
Off-surface infrared flow visualization
[NASA-CASE-LAR-14568-1] p 3720 N92-30312
A shear sensitive monomer-polymer laminate structure and method of using same
[NASA-CASE-LAR-1465^{4}-1] p 3662 N92-30317
Doppler photography: Laser methods on the flow measurement technique
[ISL-PU-303/90] p 3720 N92-30507
A stroboscopic technique for using CCD cameras in flow visualization systems for continuous viewing and stop action photography
[NASA-TM-107648] p 3637 N92-30737
An experimental study of the relationship between velocity and pressure fluctuations in a wing-body junction
[AD-A249628] p 3577 N92-31122

FLUCTUATION THEORY
The two-dimensional random walk: Its hitting process and its classification
[CWI-BS-R9003] p 3705 N92-30689

FLUENCE
Evidence for the dependence of the sputter yield of graphite on ion bombardment fluence
[AD-A252500] p 3623 N92-30537
The effect of neutron irradiation on the structure and properties of carbon-carbon composite materials
[DE92-011670] p 3592 N92-30809

FLUID DYNAMICS
Validation of three-dimensional incompressible spatial direct numerical simulation code: A comparison with linear stability and parabolic stability equation theories for boundary-layer transition on a flat plate
[NASA-TP-3205] p 3573 N92-30295
Laboratory simulation of fluid dynamical process related to winter arctic leads
[AD-A252266] p 3682 N92-30593
Generation of large-scale density fluctuations by buoyancy p 3634 N92-30671
Continuous wavelet analysis of coherent structures
p 3634 N92-30673
Numerical study of axial turbulent flow over long cylinders
[AD-A250801] p 3635 N92-30831
Direct coupling method for time-accurate solution of incompressible Navier-Stokes equations
[NASA-CR-189177] p 3636 N92-30894

FLUID FILMS
Fast methods to numerically integrate the Reynolds equation for gas fluid films
[NASA-TM-105415] p 3660 N92-30722

FLUID FLOW
Off-surface infrared flow visualization
[NASA-CASE-LAR-14568-1] p 3720 N92-30312
Progress in unstructured-grid methods development for unsteady aerodynamic applications
[NASA-TM-107643] p 3574 N92-30393
Flow of fresh and salt water in an aquifer with injection from the top
[REPT-91-68] p 3629 N92-30453
Generation of large-scale density fluctuations by buoyancy p 3634 N92-30671
Numerical calculations of two-dimensional single and multi-material flow fields with CCICE
[DE92-015778] p 3636 N92-30903
Thermohydraulic modeling of nuclear thermal rockets: The KLAXON code
[DE92-015274] p 3589 N92-31204
Fractal analysis: A new remote sensing tool for lava flows p 3736 N92-31224

FLUORESCENCE
Spontaneous decay of an atom near a phase conjugator
[AD-A248298] p 3712 N92-30333
Program RELAX: A code designed to calculate atomic relaxation spectra of x rays and electrons
[DE92-013751] p 3714 N92-30586
Fluorescence lidar multi-color imaging of vegetation
p 3640 N92-31028

FLUTTER ANALYSIS
Influence of structural and aerodynamic modeling on flutter analysis and structural optimization
[AD-A248487] p 3583 N92-30323
On-line analysis capabilities developed to support the AFW wind-tunnel tests
[NASA-TM-107651] p 3580 N92-30752
An analytical and experimental investigation of flutter suppression via piezoelectric actuation
[NASA-TM-107653] p 3580 N92-31174

FLUX PINNING
Proceedings, phenomenology and applications of high temperature superconductors
[DE92-011133] p 3627 N92-31107

FLYBY MISSIONS
Gaspra's shape and surface features: Comparison to small satellites p 3739 N92-31236

FOCAL PLANE DEVICES
Development of ultra-low noise, high sensitivity planar metal grating coupled AlGaAs/GaAs multiquantum well IR detectors for focal plane array staring IR sensor systems
[AD-A246122] p 3590 N92-30318

FOCUSING
Numerical simulation of the electromagnetic instability of an intense beam in a quadrupole focusing system
[AD-A252275] p 3614 N92-30407

FOG
Trial of a slant visual range measuring device
p 3644 N92-31043
Dense fog on the highway: Visual range monitoring in cars? p 3655 N92-31106

FOILS
Spectroscopic diagnosis of long-scale-length exploding-foil plasma in the presence of an intense radiation field
[DE92-014718] p 3726 N92-31118

FORCED CONVECTION
Mixed and forced convection from an array of discrete heat sources in a vertical channel
[AD-A248853] p 3731 N92-30235

FOREST MANAGEMENT
Monitoring of Dutch forest with LANDSAT-TM
[BCRS-91-21] p 3666 N92-30468

FORESTS
Monitoring of Dutch forest with LANDSAT-TM
[BCRS-91-21] p 3666 N92-30468
Registration of windfall damage in the eastern Hunsrueck Plateau (Federal Republic of Germany) utilizing LANDSAT-TM-data: A landscape-ecological analysis for practical forestry
[ESA-TT-1253] p 3667 N92-30515
Development of the cultivated landscape of north west Germany under the human influence
[ETN-92-91730] p 3669 N92-30968
Fluorescence lidar multi-color imaging of vegetation
p 3640 N92-31028

FORGING
Process modeling and development for three axisymmetric net shape forgings
[DE92-012111] p 3598 N92-30865
Interface friction, lubricants, and their influence on metal flow
[DE92-012112] p 3606 N92-30866

FORM FACTORS
Lidar measurements using large liquid mirror telescopes p 3652 N92-31087

FORMALISM
A computational proof of soundness
[MEMO-INF-92-09] p 3693 N92-30433

FORTRAN
Compiler analysis for irregular problems in FORTRAN D
[NASA-CR-189664] p 3689 N92-30311

FORWARD SCATTERING
Lidar measurements of cloud extinction coefficient distribution and its forward scattering phase function according to multiply scattered lidar returns
p 3651 N92-31082

FOSSIL FUELS
The environmental dilemma of fossil fuels
[DE92-014887] p 3674 N92-31121

FOSSILS
Field studies in geophysical diffraction tomography
[DE92-015084] p 3677 N92-31009

FOUR-WAVE MIXING
Vacuum ultraviolet studies of molecular dynamics
[AD-A246964] p 3715 N92-30681

FOURIER ANALYSIS
On the rapid evaluation of trigonometric series
[AD-A249029] p 3705 N92-30568
Resolution properties of the Fourier method for discontinuous waves
[NASA-CR-189668] p 3706 N92-30716

FOURIER SERIES
Validation of three-dimensional incompressible spatial direct numerical simulation code: A comparison with linear stability and parabolic stability equation theories for boundary-layer transition on a flat plate
[NASA-TP-3205] p 3573 N92-30295
Resolution properties of the Fourier method for discontinuous waves
[NASA-CR-189668] p 3706 N92-30716

FOURIER TRANSFORMATION
A local interpolator derived from the discrete Fourier transform
[AD-A251066] p 3701 N92-30243
Optimal shear correction factors in hierarchical plate modelling
[AD-A248899] p 3662 N92-30338
High-resolution processing of long-pulse-lidar data
p 3651 N92-31081

FRACTALS
On the magnification of Cantor sets and their limit models
[REPT-91-100] p 3691 N92-30352
Dense modifiable interconnections utilizing photorefractive volume holograms
[AD-A252193] p 3637 N92-30546
Fractal and multifractal approaches to clustering phenomena
[AD-A249481] p 3709 N92-30642
A fractal transition in the two dimensional shear layer
p 3633 N92-30665
Multifractal analysis of chaotic point sets
[AD-A250756] p 3709 N92-31194
Fractal analysis: A new remote sensing tool for lava flows p 3736 N92-31224

FRACTIONATION
Supercritical fluid extraction: A new process for producing high-performance, low-cost carbon fibers
[AD-A249407] p 3595 N92-30773

FRACTURE MECHANICS
National Educators' Workshop: Update 1991. Standard Experiments in Engineering Materials Science and Technology
[NASA-CP-3151] p 3608 N92-30263
A boundary element alternating method for two-dimensional mixed-mode fracture problems
[NASA-CR-4460] p 3661 N92-30309
Linear elastic fracture mechanics primer
[NASA-TM-103591] p 3662 N92-30416
Quantitative non-destructive evaluation of high-temperature superconducting materials
[DE92-011615] p 3681 N92-30693

FRACTURE STRENGTH
Transformation toughening of ceramics
[AD-A248903] p 3601 N92-30342
Linear elastic fracture mechanics primer
[NASA-TM-103591] p 3662 N92-30416
Crack growth processes at elevated temperatures in advanced materials
[AD-A249023] p 3662 N92-30558

FRACTURING
A boundary element alternating method for two-dimensional mixed-mode fracture problems
[NASA-CR-4460] p 3661 N92-30309

FRAGMENTATION
Understanding heterolytic bond cleavage
[AD-A252336] p 3716 N92-30845
Fragment hazard zone analyses for explosive test facilities
[DE92-015391] p 3613 N92-30887

FRAGMENTS
Statistics on aircraft gas turbine engine rotor failures that occurred in US commercial aviation during 1989
[DOT/FAA/CT-92/5] p 3581 N92-30303
Fragment hazard zone analyses for explosive test facilities
[DE92-015391] p 3613 N92-30887
FRAMES
Thrust test fixture
[AD-D015259] p 3585 N92-31192
FREE ELECTRON LASERS
Nonlinear analysis of a grating free-electron laser
[AD-A248833] p 3656 N92-30743
Reflector development for XUV free-electron laser oscillators
[DE92-015212] p 3657 N92-31182
FREE ENERGY
FNAS: The magnetic configuration leading to solar flares
[NASA-CR-190522] p 3743 N92-31168
FREE FLOW
The effects of free stream turbulence and surface curvature on boundary layer flow and heat transfer
[AD-A248846] p 3630 N92-30616
FREE MOLECULAR FLOW
Numerical investigations in the backflow region of a vacuum plume
[NASA-CR-190515] p 3589 N92-30981
FREE WING AIRCRAFT
Direct simulation of high-speed mixing layers
[NASA-TP-3186] p 3576 N92-30909
FREE-PISTON ENGINES
Magnetic bearings for free-piston Stirling engines
[NASA-TM-105730] p 3660 N92-30734
FREQUENCIES
Doppler mean velocity estimation: Small sample analysis and a new estimator
[AD-A249024] p 3678 N92-30559
FREQUENCY ASSIGNMENT
Direct broadcast satellite-radio: Portable and mobile reception trade-offs p 3621 N92-30945
FREQUENCY DIVISION MULTIPLE ACCESS
The ELLIPSO (tm) system: Elliptical low orbits for mobile communications and other optimum system elements p 3618 N92-30930
An integrated Ka/Ku-band payload for personal, mobile and private business communications p 3619 N92-30933
A personal communications network using a Ka-band satellite p 3619 N92-30934
FREQUENCY HOPPING
The Pan-European Digital Cellular (GSM) System p 3619 N92-30938
FREQUENCY REUSE
Capacity and interference in a PCS system p 3619 N92-30937
FREQUENCY STABILITY
Wavemeter measurements of frequency stability of an injection seeded alexandrite laser for pressure and temperature lidar p 3645 N92-31049
Ground-based Doppler lidar of increased laser instability: Conception and design p 3650 N92-31078
The role of laser coherence in long-range vibration measurements p 3654 N92-31097
FRESH WATER
Flow of fresh and salt water in an aquifer with injection from the top
[REPT-91-68] p 3629 N92-30453
FRICTION
Process modeling and development for three axisymmetric net shape forgings
[DE92-012111] p 3598 N92-30865
Interface friction, lubricants, and their influence on metal flow
[DE92-012112] p 3606 N92-30866
FRICTION REDUCTION
Interface friction, lubricants, and their influence on metal flow
[DE92-012112] p 3606 N92-30866
FRONTS (METEOROLOGY)
On the potential use of the terminal Doppler weather radar gust front detection algorithm on the WSR-88D system. Part 1: Impacts of radar system differences
[DOT/FAA/NR-92/8,I] p 3678 N92-30495
On the potential use of the terminal Doppler weather radar gust front detection algorithm on the WSR-88D system. Part 2: Detecting non-gust front convergent weather phenomena
[DOT/FAA/NR-92/8,II] p 3678 N92-30496
FUEL CELLS
Introduction to the efficiency of fuel cells
[MBB-Z-0412-91-PUB] p 3671 N92-30970
Research issues in molten carbonate fuel cells: Pressurization
[DE92-011755] p 3671 N92-31113
Fuel cell systems program plan: Fiscal year 1992
[DE92-015985] p 3672 N92-31188
Fuel cells
[DE92-001282] p 3672 N92-31221
FUEL COMBUSTION
Effect of volatility and oxygenates on driveability at intermediate ambient temperatures
[AD-A248902] p 3607 N92-30341
Advanced concepts for controlled combustion in engines
[AD-A249911] p 3595 N92-30814
FUEL PRODUCTION
Emissions of greenhouse gases from the use of transportation fuels and electricity
[DE92-012102] p 3674 N92-30770
Methane to liquid
[DE92-001277] p 3596 N92-30883
FUEL SYSTEMS
Laser induced fluorescence detection of gums in jet fuels
[AD-A252685] p 3607 N92-30767
Solar-hydrogen energy system for solar belt countries and use of remote sensing p 3668 N92-30913
FULLERENES
Proceedings of the 181st Electrochemical Society, Inc. Meeting Program
[AD-A249729] p 3596 N92-31178
FUNCTION SPACE
Trajectory fitting in function space with application to analytic modeling of surfaces
[NASA-TP-3232] p 3576 N92-30747
FUNCTIONAL ANALYSIS
Development statistics for the UH-1 Ada feasibility study
[AD-A252404] p 3584 N92-30547
KC-135 crew reduction feasibility demonstration simulation study. Volume 1: Function analysis and function reallocation
[AD-A252265] p 3688 N92-30592
FUNCTIONAL DESIGN SPECIFICATIONS
Software breadboard study
[NASA-CR-190473] p 3625 N92-30757
FUNCTIONS (MATHEMATICS)
The functions psi(x) and beta(x) and some inequalities for integrals (theorems 1-16)
[REPT-92-09] p 3703 N92-30459
Gaussian windows: A tool for exploring multivariate data
[NASA-CR-190559] p 3696 N92-30723
Coexistence of uniquely ergodic subsystems of interval mapping
[DE92-630231] p 3732 N92-31133
Elastic constants of crystals near melting via density functional theory. Effect of three-body correlations
[DE92-630567] p 3730 N92-31191
FURANS
Polyphosphazenes bearing polymerizable pyrrole, thiophene and furan side groups: Synthesis and chemical oxidation
[AD-A249747] p 3607 N92-31207
FURNACES
Ultrafine aerosol size distributions and sulfuric acid vapor pressures: Implications for new particle formation in the atmosphere
[DE92-015217] p 3675 N92-31183
A miniature carbon furnace for mass spectroscopy
[DE92-014460] p 3597 N92-31196
FUSELAGES
Two-dimensional aerodynamic characteristics of several polygon-shaped cross-sectional models applicable to helicopter fuselages
[NASA-TP-3233] p 3574 N92-30394
FUSION REACTORS
MHD considerations for a self-cooled liquid lithium blanket
[DE92-014864] p 3723 N92-30591
Criteria and design trade-off issues for ITER
[DE92-011786] p 3726 N92-31114

G

GALLIUM ARSENIDES
Hybridization of detector array and integrated circuit for readout
[NASA-CASE-NPO-18062-1-CU] p 3623 N92-30542
Transient photoconductivity of low temperature GaAs grown by molecular beam epitaxy terahertz radar applications
[DE92-011848] p 3729 N92-30854
Focused ion beam implantation
[AD-A249662] p 3627 N92-31004
Oxidation of gallium arsenide
[DE92-016208] p 3731 N92-31220
GALLIUM SELENIDES
Growth and evaluation of nonlinear optical materials for laser applications: Barium borate, lithium borate, and silver gallium selenide
[AD-A248861] p 3624 N92-30617
GAME THEORY
Kayles on special classes of graphs: An application of Sprague-Grundy theory
[RUU-CS-91-49] p 3703 N92-30450
GAMMA RAY ASTRONOMY
Ultra high energy gamma rays and observations with CYGNUS/MILAGRO
[DE92-015243] p 3743 N92-30627
GAMMA RAY BURSTS
The escape of greater MeV photons from cosmological gamma-ray bursts
[DE92-013545] p 3743 N92-30706
GAMMA RAY SPECTRA
Lifetimes of low spin states in the superdeformed band of Hg-192
[DE92-011066] p 3728 N92-30684
GAMMA RAYS
Nondestructive evaluation of ceramic components by gamma ray CT
[DE92-626843] p 3602 N92-30402
Ultra high energy gamma rays and observations with CYGNUS/MILAGRO
[DE92-015243] p 3743 N92-30627
Lifetimes of low spin states in the superdeformed band of Hg-192
[DE92-011066] p 3728 N92-30684
GAS ANALYSIS
Hyperspectral gas analysis system (HyGAS), phase 1
[AD-A251026] p 3593 N92-30241
GAS BEARINGS
Fast methods to numerically integrate the Reynolds equation for gas fluid films
[NASA-TM-105415] p 3660 N92-30722
Magnetic bearings for free-piston Stirling engines
[NASA-TM-105730] p 3660 N92-30734
GAS COMPOSITION
A variable phase function approach for the inversion of lidar return signals p 3649 N92-31073
GAS COOLING
Recombining processes in a cooling plasma by mixing of initially heated gas
[NIFS-142] p 3722 N92-30431
GAS DETECTORS
Hyperspectral gas analysis system (HyGAS), phase 1
[AD-A251026] p 3593 N92-30241
Tests of the performance of different gas mixtures in microstrip gas counters
[NIKHEF-H/91-23] p 3636 N92-30365
Optimization of the microstrip gas counter
[NIKHEF-H/91-21] p 3637 N92-30688
GAS FLOW
Algorithm to solve nonlinear time dependent problems of engineering and physics
[AD-A250641] p 3702 N92-30347
Processing aerosols and filaments in a TM010 microwave cavity at 2.45 GHz
[DE92-013536] p 3615 N92-30703
Real gas flow parameters for NASA Langley 22-inch Mach 20 helium tunnel
[NASA-CR-4462] p 3635 N92-30751
GAS GUNS
Development of diagnostics for electromagnetic armor applications
[AD-A251074] p 3587 N92-30257
GAS MIXTURES
Tests of the performance of different gas mixtures in microstrip gas counters
[NIKHEF-H/91-23] p 3636 N92-30365
GAS TRANSPORT
Trace gas and aerosol transports into and out of the Amazon Basin
[NASA-CR-190624] p 3674 N92-31153
GAS TUNGSTEN ARC WELDING
Transport phenomena in welds
[DE92-013404] p 3659 N92-30587
Phase transformations in weldments: New materials and new perspectives
[DE92-016231] p 3600 N92-31177
GAS TURBINE ENGINES
Statistics on aircraft gas turbine engine rotor failures that occurred in US commercial aviation during 1989
[DOT/FAA/CT-92/5] p 3581 N92-30303
Small engine components test facility compressor testing cell at NASA Lewis Research Center
[NASA-TM-105685] p 3584 N92-30508
A new unsteady mixing model to predict NO(x) production during rapid mixing in a dual-stage combustor
[NASA-CR-189155] p 3581 N92-30569

GASEOUS FUELS
Emissions of greenhouse gases from the use of transportation fuels and electricity
[DE92-012102] p 3674 N92-30770
Introduction to the efficiency of fuel cells
[MBB-Z-0412-91-PUB] p 3671 N92-30970
GASOLINE
Effect of volatility and oxygenates on driveability at intermediate ambient temperatures
[AD-A248902] p 3607 N92-30341
GAUGE INVARIANCE
One-loop integration for the axial gauge with generalized prescription
[DE92-630241] p 3732 N92-31145
GAUGE THEORY
Example of a quantum field theory based on a nonlinear Lie algebra
[DE92-010475] p 3731 N92-30825
GEAR TEETH
Minimization of deviations of gear real tooth surfaces determined by coordinate measurements
[NASA-TM-105718] p 3660 N92-30948
GEARS
Development of a full-scale transmission testing procedure to evaluate advanced lubricants
[NASA-TP-3265] p 3658 N92-30396
Minimization of deviations of gear real tooth surfaces determined by coordinate measurements
[NASA-TM-105718] p 3660 N92-30948
GELS
Numerical simulation of the dynamic behavior of the polymeric gels
[DE92-011358] p 3605 N92-30804
From minerals to materials: A facile synthetic route to preceramic polymers for aluminum oxide
[AD-A250351] p 3606 N92-31141
GENE EXPRESSION
Neurophysiological analysis of circadian rhythm entrainment
[AD-A248466] p 3684 N92-30319
GENERAL AVIATION AIRCRAFT
Tolerance of beta blocked hypertensives during orthostatic and altitude stresses
[AD-A249904] p 3685 N92-30745
GENETICS
Control of circadian behavior by transplanted suprachiasmatic nuclei
[AD-A250442] p 3686 N92-31143
GEOCHEMISTRY
Trace element and isotope geochemistry of geothermal fluids, East Rift Zone, Kilauea, Hawaii
[DE92-014586] p 3671 N92-31117
The (146,147)Sm-(142,143)Nd systematics of early terrestrial differentiation and the lost continents of the early Earth p 3678 N92-31229
GEODESIC LINES
Wrappability of curves on surfaces
[AD-A250004] p 3707 N92-31140
GEODESY
Inter- and intra-plate deformation at North American plate boundaries
[NASA-CR-190485] p 3676 N92-30961
A geodetic laser radar rangefinder with 10(exp -7) resolution p 3641 N92-31029
GEOGRAPHIC INFORMATION SYSTEMS
Geographic information system and its applications p 3668 N92-30915
GEOLOGICAL FAULTS
A study of discrete and continuum joint modeling techniques
[DE92-012631] p 3663 N92-30859
GEOLOGICAL SURVEYS
Inter- and intra-plate deformation at North American plate boundaries
[NASA-CR-190485] p 3676 N92-30961
GEOLOGY
Investigation of the interface phenomena due to interaction of high intensity stress waves with geologic boundaries
[AD-A248992] p 3675 N92-30525
GEOMAGNETISM
Data report, 92-2. Magnetic results, 1985-1990 p 3675 N92-30417
GEOMETRICAL OPTICS
The diffraction of short free surface water waves, a uniform expansion
[REPT-92-06] p 3628 N92-30358
GEOMETRY
Computing and verifying depth orders
[RUU-CS-91-41] p 3693 N92-30443
Point location in fat subdivisions
[RUU-CS-91-40] p 3703 N92-30447
GEOPHYSICAL FLUIDS
Trace element and isotope geochemistry of geothermal fluids, East Rift Zone, Kilauea, Hawaii
[DE92-014586] p 3671 N92-31117
GEOPHYSICAL OBSERVATORIES
Data report, 92-2. Magnetic results, 1985-1990 p 3675 N92-30417
Registration of windfall damage in the eastern Hunsrueck Plateau (Federal Republic of Germany) utilizing LANDSAT-TM-data: A landscape-ecological analysis for practical forestry
[ESA-TT-1253] p 3667 N92-30515
GEOPHYSICS
Field studies in geophysical diffraction tomography
[DE92-015084] p 3677 N92-31009
GEOPOTENTIAL
Altimeter and gravity data analysis
[NASA-CR-190478] p 3676 N92-30756
GEOSAT SATELLITES
Preparations for the ERS-1 and TOPEX/Poseidon satellite altimetry missions
[BCRS-90-28] p 3666 N92-30465
GEOTHERMAL RESOURCES
Trace element and isotope geochemistry of geothermal fluids, East Rift Zone, Kilauea, Hawaii
[DE92-014586] p 3671 N92-31117
GERMAN SPACE PROGRAM
Activities report of the Institute for Astronomy and Astrophysics at Technical University of Berlin (Germany, F.R.)
[MITT-11] p 3740 N92-30506
GERMANIUM
Dielectric behavior of semiconductors at microwave frequencies p 3610 N92-30275
GIBBS PHENOMENON
Resolution properties of the Fourier method for discontinuous waves
[NASA-CR-189668] p 3706 N92-30716
GIMBALS
Quick acting gimbal joint
[NASA-CASE-MSC-21918-1] p 3658 N92-30316
GLASS
Tempered glass and thermal shock of ceramic materials p 3607 N92-30265
Measuring the Weibull modulus of microscope slides p 3612 N92-30294
Three-dimensional laser window formation
[NASA-RP-1280] p 3585 N92-30307
GLASS FIBERS
A reduced gravity fiber pulling apparatus
[NASA-TM-103594] p 3612 N92-30971
GLASS LASERS
Sol-gel optics: Proceedings SPIE-The International Society for Optical Engineering
[AD-A249986] p 3721 N92-31126
GLASS TRANSITION TEMPERATURE
Polyimides containing the cyclobutene-3,4-dione moiety
[NASA-CASE-LAR-14753-1] p 3601 N92-30313
GLASSY CARBON
Thermoset precursor to monolithic carbon glass prepared by the Pd/Cu-catalyzed alkynylation of polyphenylenes
[AD-A249920] p 3605 N92-30816
GLINT
Glint errors derived from the partial derivatives of the echo signal phase for a distributed scatterer
[AD-A249499] p 3615 N92-30637
GLOBAL AIR POLLUTION
Trace gas and aerosol transports into and out of the Amazon Basin
[NASA-CR-190624] p 3674 N92-31153
GLOBAL POSITIONING SYSTEM
The MARCOR GPS mobile data system p 3620 N92-30944
Inter- and intra-plate deformation at North American plate boundaries
[NASA-CR-190485] p 3676 N92-30961
GLUONS
On the factorisation theorem in boson-gluon fusion at hadron colliders
[NIKHEF-H/91-16] p 3713 N92-30415
Research on elementary particle physics. Task P: Studies in theory and phenomenology of elementary particles, part 1
[DE92-014428] p 3716 N92-30791
Physics of the STAR experiment at the relativistic heavy ion collider
[DE92-014481] p 3719 N92-31198
GLYCINE
The properties of the uptake system for glycine in synaptic vesicles
[ISSN-0800-4412] p 3683 N92-31152
GOLD
Numerical simulations of light scattering from rough one-dimensional gold surfaces
[AD-A249794] p 3721 N92-30783
Study of Au(-) production in a plasma-sputter type negative ion source
[NIFS-115] p 3717 N92-30990
GOLD ALLOYS
X ray scattering studies of non-equilibrium ordering processes
[DE92-014006] p 3598 N92-30787
GOVERNMENT/INDUSTRY RELATIONS
Attitudinal and situational differences between national laboratory inventors and inventor-entrepreneurs
[DE92-015768] p 3733 N92-30889
GOVERNMENTS
Computer security: Agencies reported having implemented most system security controls
[GAO/IMTEC-92-45] p 3690 N92-30712
GRAFTING
Epoxides as activators for grafting of poly(tetrahydrofuran) from poly(methylphenylsilylene)
[AD-A251086] p 3601 N92-30244
GRAIN BOUNDARIES
Quantitative non-destructive evaluation of high-temperature superconducting materials
[DE92-011615] p 3661 N92-30693
Cluster assembly of hierarchical nanostructures
[DE92-010498] p 3716 N92-30826
Theory of sublinear power dependence for microwave heating in some ceramic materials
[DE92-015147] p 3606 N92-30847
Impurity segregation to grain boundaries and defects in AlN
[DE92-011667] p 3599 N92-31112
Grain boundary weak links in high-Tc superconductors
[DE92-016192] p 3730 N92-31190
GRAIN SIZE
Cluster assembly of hierarchical nanostructures
[DE92-010498] p 3716 N92-30826
GRAMMARS
The formal power of AGs with respect to their underlying CFGs
[REPT-91-75] p 3703 N92-30456
Proceedings of the Sylvia Beach Language Comprehension Conference
[AD-A250488] p 3621 N92-31129
GRANULAR MATERIALS
Kinetic theory and boundary conditions for flows of highly inelastic spheres
[DE92-012645] p 3629 N92-30438
GRAPH THEORY
VLSI design, parallel computation, and distributed computing
[AD-A252349] p 3699 N92-30596
GRAPHIC ARTS
Induced pictorial representations
[AD-A248560] p 3687 N92-30336
Maintenance of 2- and 3-connected components of graphs. Part 1: 2- and 3-edge-connected components
[RUU-CS-90-26-PT-1] p 3694 N92-30479
GRAPHITE
Shock-induced martensitic transformation of highly oriented graphite to diamond
[DE92-014787] p 3602 N92-30399
Evidence for the dependence of the sputter yield of graphite on ion bombardment fluence
[AD-A252500] p 3623 N92-30537
Presolar (?) corundum in the Orgueil meteorite p 3738 N92-31230
GRAPHITE-EPOXY COMPOSITES
Numerical analysis of the Iosipescu specimen for composite materials
[NASA-CR-190658] p 3592 N92-30906
GRAPHS (CHARTS)
Restrictions of graph partition problems, part 1
[RUU-CS-91-44-PT-1] p 3703 N92-30446
Linear planar augmentation algorithms for outerplanar graphs
[RUU-CS-91-47] p 3703 N92-30449
Kayles on special classes of graphs: An application of Sprague-Grundy theory
[RUU-CS-91-49] p 3703 N92-30450
On the complexity of the maximum cut problem
[RUU-CS-91-39] p 3703 N92-30458
Maintenance of 2- and 3-connected components of graphs. Part 1: 2- and 3-edge-connected components
[RUU-CS-90-26-PT-1] p 3694 N92-30479
Maintenance of 2- and 3-connected components of graphs. Part 2: 2- and 3-edge-connected components and 2-vertex-connected components
[RUU-CS-90-27-PT-2] p 3694 N92-30480
GRATINGS (SPECTRA)
Development of ultra-low noise, high sensitivity planar metal grating coupled AlGaAs/GaAs multiquantum well IR detectors for focal plane array staring IR sensor systems
[AD-A246122] p 3590 N92-30318
The electric field dependence of the laser induced holographic grating relaxation of photorefractive polymer
[AD-A252641] p 3602 N92-30409
Nonlinear analysis of a grating free-electron laser
[AD-A248833] p 3656 N92-30743

GRAVITATION
Altimeter and gravity data analysis
[NASA-CR-190478] p 3676 N92-30756
GRAVITATION THEORY
Example of a quantum field theory based on a nonlinear Lie algebra
[DE92-010475] p 3731 N92-30825
Stochastic strings, topology, and space-time confinement
[DE92-630239] p 3732 N92-31136
GRAVITATIONAL EFFECTS
A reduced gravity fiber pulling apparatus
[NASA-TM-103594] p 3612 N92-30971
GRAVITATIONAL FIELDS
Altimeter and gravity data analysis
[NASA-CR-190478] p 3676 N92-30756
GRAVITY ANOMALIES
Altimeter and gravity data analysis
[NASA-CR-190478] p 3676 N92-30756
GRAVITY WAVES
On the existence of convectively produced gravity waves p 3638 N92-31016
Atmospheric measurements using the LAMP lidar during the LADIMAS campaign p 3652 N92-31086
GRAZING INCIDENCE
Full surface testing of grazing incidence mirrors
[AD-A248851] p 3719 N92-30233
GREAT LAKES (NORTH AMERICA)
Report of the Great Lakes Air Toxics Research Priorities Workshop
[PB92-166933] p 3673 N92-30602
Quantification and reduction of the uncertainty in mass balance models by Monte Carlo analysis of prior data
[DE92-010278] p 3708 N92-30803
GREEN'S FUNCTIONS
Positivity for a strongly coupled elliptic system by Green function estimates
[REPT-91-77] p 3702 N92-30434
GREENHOUSE EFFECT
Reducing greenhouse gas emissions in Czechoslovakia
[DE92-012354] p 3672 N92-30374
Emissions of greenhouse gases from the use of transportation fuels and electricity
[DE92-012102] p 3674 N92-30770
The environmental dilemma of fossil fuels
[DE92-014887] p 3674 N92-31121
GRID GENERATION (MATHEMATICS)
Solving the Euler equations using adaptive mesh motion and refinement
[AD-A252364] p 3705 N92-30597
MATGRID, a program for generation of C-H and C-O topology grids around wing/body configurations: Software description document
[FFA-TN-1990-20] p 3575 N92-30713
Numerical methods for the simulation of complex multi-body flows with applications for the integrated Space Shuttle vehicle
[NASA-CR-190045] p 3575 N92-30740
Application of the Chimera overlapped grid scheme to simulation of Space Shuttle ascent flows
p 3576 N92-30742
Trajectory fitting in function space with application to analytic modeling of surfaces
[NASA-TP-3232] p 3576 N92-30747
Delaunay triangulation and computational fluid dynamics meshes
[NASA-TM-107663] p 3689 N92-30907
GROUND CREWS
Flight crew integration in the maintenance chain of a commercial aircraft (A 320) p 3698 N92-30957
GROUND EFFECT (COMMUNICATIONS)
Multifrequency measurements of radar ground clutter at 42 sites. Volume 3: Appendix E
[AD-A246988] p 3616 N92-30863
GROUND STATE
Spontaneous decay of an atom near a phase conjugator
[AD-A248298] p 3712 N92-30333
GROUND STATIONS
ECLIPS at LMD: Preliminary results of phase 2
p 3643 N92-31038
GROUND SUPPORT SYSTEMS
Columbus logistics transportation and ground processing
[MBB-UO-0167-91-PUB] p 3709 N92-30442
Preparation for a new plane (A 320): Experience reviewed p 3697 N92-30954
GROUND TESTS
Resonance and control response tests using a control simulation device
[MBB-UD-0608-91-PUB] p 3583 N92-30439
Compact range test applications, phase 2
[AD-A248790] p 3615 N92-30583
Future aerospace ground test facility requirements for the Arnold Engineering Development Center
p 3585 N92-30897
GROUND TRUTH
Remote sensing for rainfall estimation: SAC experience p 3668 N92-30917
GROUND WATER
Global existence for a semilinear elliptic-parabolic PDE system
[REPT-91-70] p 3628 N92-30372
GROUND WAVE PROPAGATION
High frequency communications under adverse conditions
[AD-A252199] p 3615 N92-30532
GROUND WIND
Methodology investigation, implement remote sensing
[AD-A248901] p 3678 N92-30340
GROUP THEORY
Application of automated deduction to the search for single axioms for exponent groups
[DE92-015271] p 3705 N92-30608
Some model theory of free groups and free algebras
[AD-A249425] p 3706 N92-30776
GUMS (SUBSTANCES)
Laser induced fluorescence detection of gums in jet fuels
[AD-A252685] p 3607 N92-30767
GUNN DIODES
Focused ion beam implantation
[AD-A249662] p 3627 N92-31004
GUSTS
On the potential use of the terminal Doppler weather radar gust front detection algorithm on the WSR-88D system. Part 1: Impacts of radar system differences
[DOT/FAA/NR-92/8,I] p 3678 N92-30495
On the potential use of the terminal Doppler weather radar gust front detection algorithm on the WSR-88D system. Part 2: Detecting non-gust front convergent weather phenomena
[DOT/FAA/NR-92/8,II] p 3678 N92-30496

H

HABITATS
Habitat model for the Florida Scrub Jay on John F. Kennedy Space Center
[NASA-TM-107543] p 3673 N92-30494
HADRONS
On the factorisation theorem in boson-gluon fusion at hadron colliders
[NIKHEF-H/91-16] p 3713 N92-30415
Intermittency, multifractality, and hadronic collisions
[DE92-014595] p 3714 N92-30606
Theoretical studies in elementary particle physics
[DE92-015295] p 3714 N92-30610
Recent experimental studies on hadron showers produced in high energy muon-nucleus interactions
[DE92-016002] p 3719 N92-31219
HAMILTONIAN FUNCTIONS
Ginsburg criterion for an equilibrium superradiant model in the dynamic approach
[DE92-630566] p 3732 N92-31203
HAMSTERS
Control of circadian behavior by transplanted suprachiasmatic nuclei
[AD-A250442] p 3686 N92-31143
HARDENING (MATERIALS)
Analytical solution of elastic-plastic thick-walled cylinders with general hardening
[AD-A249491] p 3705 N92-30618
HARDNESS
Be-Cu precipitation hardening experiment
p 3601 N92-30276
Development of hardness cycles for fiber bound materials, using DSC: From laboratory specimens to complex high duty structural members
[MBB-Z-0409-91-PUB] p 3592 N92-30969
HARMONIC OSCILLATORS
Research on elementary particle physics. Task P: Studies in theory and phenomenology of elementary particles, part 1
[DE92-014428] p 3716 N92-30791
HARMONIC RADIATION
Generation of stimulated backscattered harmonic radiation from intense laser interactions with beams and plasmas
[AD-A248782] p 3656 N92-30614
HASTELLOY (TRADEMARK)
Filler metal development for Hastelloy alloy XR
[DE92-782044] p 3600 N92-31163
HAZARDS
Fragment hazard zone analyses for explosive test facilities
[DE92-015391] p 3613 N92-30887
HEAD (ANATOMY)
Evaluation of head impact kinematics for passengers seated behind interior walls
[AD-A252651] p 3578 N92-30551
Adapting the ADAM manikin technology for injury probability assessment
[AD-A252332] p 3688 N92-30844
HEART
Optimal ECG electrode sites and criteria for detection of asymptomatic coronary artery disease, update 1990. Multilead ECG changes at rest, with exercise, and with coronary angioplasty
[AD-A248613] p 3684 N92-30523
Feasibility of a walk test to assess the cardiorespiratory fitness of Naval personnel
[AD-A250650] p 3684 N92-30603
Tolerance of beta blocked hypertensives during orthostatic and altitude stresses
[AD-A249904] p 3685 N92-30745
HEART DISEASES
Optimal ECG electrode sites and criteria for detection of asymptomatic coronary artery disease, update 1990. Multilead ECG changes at rest, with exercise, and with coronary angioplasty
[AD-A248613] p 3684 N92-30523
HEART FUNCTION
Feasibility of a walk test to assess the cardiorespiratory fitness of Naval personnel
[AD-A250650] p 3684 N92-30603
HEART RATE
Feasibility of a walk test to assess the cardiorespiratory fitness of Naval personnel
[AD-A250650] p 3684 N92-30603
Tolerance of beta blocked hypertensives during orthostatic and altitude stresses
[AD-A249904] p 3685 N92-30745
HEAT EXCHANGERS
A processing environment for test and simulation data of thermodynamic systems
[MBB-UO-0169-91-PUB] p 3731 N92-30421
Progress in the development of the Hermes evaporators
[MBB-UO-0164-91-PUB] p 3587 N92-30440
Liquid droplet radiator: Design concepts and development logic
[MBB-UO-0165-91-PUB] p 3613 N92-30441
HEAT MEASUREMENT
Two-color infrared digital imaging for determination of in-cylinder temperature and species during compression and combustion periods of DI diesel engine
[AD-A249812] p 3595 N92-30835
HEAT OF COMBUSTION
Two-color infrared digital imaging for determination of in-cylinder temperature and species during compression and combustion periods of DI diesel engine
[AD-A249812] p 3595 N92-30835
HEAT RADIATORS
Liquid droplet radiator: Design concepts and development logic
[MBB-UO-0165-91-PUB] p 3613 N92-30441
HEAT SINKS
Innovative techniques for the production of low cost 2-D laser diode arrays supplies or services and prices/costs
[AD-A252665] p 3656 N92-30552
HEAT SOURCES
Mixed and forced convection from an array of discrete heat sources in a vertical channel
[AD-A248853] p 3731 N92-30235
HEAT STORAGE
Design and simulation of latent heat storage units
[DE91-002145] p 3670 N92-30330
Thermal energy storage
[DE92-014942] p 3672 N92-31176
HEAT TRANSFER
Introductory heat-transfer p 3601 N92-30291
Design and simulation of latent heat storage units
[DE91-002145] p 3670 N92-30330
The structure of turbulent channel flow with passive scalar transport p 3632 N92-30657
Intersecting shock-wave/turbulent boundary-layer interactions at Mach 8.3
[NASA-TM-103909] p 3635 N92-30765
Two-color infrared digital imaging for determination of in-cylinder temperature and species during compression and combustion periods of DI diesel engine
[AD-A249812] p 3595 N92-30835
Conceptual design of the SSC cryogenic transfer lines
[DE92-013964] p 3719 N92-30839
HEAT TRANSMISSION
Heat flow of p-harmonic maps with values into spheres
[DE92-630236] p 3707 N92-31135
HEAT TREATMENT
Heat-treating of materials p 3601 N92-30292

HEATING
Method and apparatus for preloading a joint by remotely operable means
[NASA-CASE-MSC-21940-1] p 3659 N92-30540
Heating and momentum deposition in hot stars
[DE92-011850] p 3740 N92-30855
HEATING EQUIPMENT
Flexible heating head for induction heating apparatus and method
[NASA-CASE-LAR-14679-2] p 3621 N92-31150
HEAVY IONS
Effects of high beam rates on TPC's
[DE92-014594] p 3717 N92-30398
New method of error elimination in potential profile measurement of tokamak plasmas by high voltage heavy ion beam probes
[NIFS-143] p 3726 N92-30995
Results of the heavy ion beam probe measurements on the Advanced Toroidal Facility
[DE92-014461] p 3726 N92-31197
Physics of the STAR experiment at the relativistic heavy ion collider
[DE92-014481] p 3719 N92-31198
HELICAL WINDINGS
Dynamic analysis of compact helical system power supply and designs of its upgrade
[NIFS-TECH-2] p 3723 N92-30497
HELICOPTER CONTROL
Resonance and control response tests using a control simulation device
[MBB-UD-0608-91-PUB] p 3583 N92-30439
HELICOPTER DESIGN
Organic Matrix Composite Helicopter Internal/External Cargo Pallet System (OMC INTEX)
[AD-A251127] p 3580 N92-30878
Advanced electromagnetic methods for aerospace vehicles
[NASA-CR-190650] p 3621 N92-31156
HELICOPTER ENGINES
A simplified dynamic model of the T700 turboshaft engine
[NASA-TM-105805] p 3709 N92-30898
HELICOPTER PROPELLER DRIVE
Development of a full-scale transmission testing procedure to evaluate advanced lubricants
[NASA-TP-3265] p 3658 N92-30396
HELICOPTERS
Two-dimensional aerodynamic characteristics of several polygon-shaped cross-sectional models applicable to helicopter fuselages
[NASA-TP-3233] p 3574 N92-30394
A cable detection lidar system for helicopters
p 3648 N92-31068
HELIOTRONS
Magnetic surface breaking in 3D MHD equilibria of I = 2 heliotron
[NIFS-130] p 3722 N92-30384
Dynamic analysis of compact helical system power supply and designs of its upgrade
[NIFS-TECH-2] p 3723 N92-30497
Plasma parameter estimations for the large helical device based on the gyro-reduced Bohm scaling
[NIFS-114] p 3723 N92-30499
Beta limit of resistive plasma in torsatron/heliotron
[NIFS-131] p 3725 N92-30985
Three-dimensional MHD equilibrium in the presence of bootstrap current for Large Helical Device (LHD)
[NIFS-139] p 3725 N92-30994
HELIPORTS
Helicopter nighttime parking test results - UH-1
[DOT/FAA/CT-TN92/1] p 3580 N92-31165
HELIUM
Real gas flow parameters for NASA Langley 22-inch Mach 20 helium tunnel
[NASA-CR-4462] p 3635 N92-30751
HELIUM ISOTOPES
Polarization effects in pi(+) absorption in He-3
[ITN-92-85164] p 3714 N92-30580
Polarization effects in pi(+) absorption in He-4
[ITN-92-85163] p 3715 N92-30780
HERMES MANNED SPACEPLANE
Progress in the development of the Hermes evaporators
[MBB-UO-0164-91-PUB] p 3587 N92-30440
Flexible space-based robot modelling and real-time simulation
[NLR-TP-89364-U] p 3658 N92-30477
HERMITIAN POLYNOMIAL
From a particle with a world-line supersymmetry to the Dirac-like equation
[DE92-622376] p 3731 N92-30800
HETEROCYCLIC COMPOUNDS
Synthesis of orthogonally fused conducting oligomers for molecular electronic devices
[AD-A249929] p 3605 N92-30796
Electrooxidation of soluble alpha,alpha-coupled thiophene oligomers
[AD-A249928] p 3605 N92-30817
HETERODYNING
A comparison of Ultra-Sensitive Coherent Detection (USCD) and heterodyne detection for a wind sensing application p 3640 N92-31025
Coherent summation of spatially distorted Doppler lidar signals using a two-dimensional heterodyne detector array p 3654 N92-31096
The role of laser coherence in long-range vibration measurements p 3654 N92-31097
HETEROGENEITY
Electrochemical and optical studies of model photosynthetic systems
[DE92-010657] p 3683 N92-30829
HIERARCHIES
Scale sensitivity and rank preservation in a multiplicative variant of the AHP and SMART
[REPT-91-67] p 3707 N92-30452
DE-CERTS: A decision support system for a comparative evaluation method for risk management methodologies and tools
[AD-A246965] p 3733 N92-30682
Cluster assembly of hierarchical nanostructures
[DE92-010498] p 3716 N92-30826
HIGH ENERGY INTERACTIONS
Rescattering in neutrino/antineutrino: Deuteron reactions
[NIKHEF-H/91-22] p 3713 N92-30364
On the factorisation theorem in boson-gluon fusion at hadron colliders
[NIKHEF-H/91-16] p 3713 N92-30415
Intermittency, multifractality, and hadronic collisions
[DE92-014595] p 3714 N92-30606
Theoretical studies in elementary particle physics
[DE92-015295] p 3714 N92-30610
Research on elementary particle physics
[DE92-014622] p 3715 N92-30625
Non-perturbative effects in high-energy electroweak interactions
[NIKHEF-H/91-24] p 3715 N92-30697
Recent experimental studies on hadron showers produced in high energy muon-nucleus interactions
[DE92-016002] p 3719 N92-31219
HIGH FREQUENCIES
Comparison of high temperature, high frequency core loss and dynamic B-H loops of a 2V-49Fe-49Co and a grain oriented 3Si-Fe alloy
[NASA-TM-105791] p 3623 N92-30397
High frequency communications under adverse conditions
[AD-A252199] p 3615 N92-30532
RF vacuum microelectronics
[AD-A249814] p 3626 N92-30836
HIGH POWER LASERS
Optical isolators in high power lasers based on high reflectivity phase conjugate mirrors
[IA-1452] p 3721 N92-30581
Injection seeded single mode alexandrite ring laser for lidar applications p 3646 N92-31057
High background photon counting lidar
p 3649 N92-31071
Generation of a sodium guidestar using a high power dye laser
[DE92-012696] p 3657 N92-31115
HIGH PRESSURE
Nonlinear stress analysis of composite-jacketed steel cylinders subjected to high internal pressure
[AD-A249500] p 3663 N92-30802
HIGH RESOLUTION
High-resolution imaging in the scanning transmission electron microscope
[DE92-010647] p 3637 N92-30827
High resolution electron energy loss studies of surface vibrations
[DE92-014608] p 3626 N92-30901
Diversity imaging techniques in lidar
p 3640 N92-31026
A geodetic laser radar rangefinder with 10(exp -7) resolution p 3641 N92-31029
Pulsed laser spectral measurement using a Fabry-Perot interferometer: Limits to resolution p 3646 N92-31055
High-resolution processing of long-pulse-lidar data
p 3651 N92-31081
HIGH REYNOLDS NUMBER
Numerical simulation of low Prandtl number turbulent mixing p 3633 N92-30663
HIGH SPEED
High speed research system study. Advanced flight deck configuration effects
[NASA-CR-189650] p 3581 N92-30965
HIGH SPEED PHOTOGRAPHY
Debris/ice/TPS assessment and integrated photographic analysis for Shuttle Mission STS-45
[NASA-TM-107545] p 3586 N92-30382
HIGH STRENGTH
Structural ceramics p 3607 N92-30264
HIGH TEMPERATURE
Structural ceramics p 3607 N92-30264
Comparison of high temperature, high frequency core loss and dynamic B-H loops of a 2V-49Fe-49Co and a grain oriented 3Si-Fe alloy
[NASA-TM-105791] p 3623 N92-30397
High-temperature ignition of propane with MTBE as an additive: Shock-tube experiments and modeling
[DE92-006679] p 3594 N92-30749
Metal matrix composite analyzer (METCAN) user's manual, version 4.0
[NASA-TM-105244] p 3592 N92-30779
HIGH TEMPERATURE PLASMAS
Interaction physics for megajoule laser fusion targets
[DE92-014796] p 3656 N92-30400
Recombining processes in a cooling plasma by mixing of initially heated gas
[NIFS-142] p 3722 N92-30431
X ray radiation from hot dense plasmas and atomic processes
[NIFS-PROC-9] p 3725 N92-30984
Beta limit of resistive plasma in torsatron/heliotron
[NIFS-131] p 3725 N92-30985
HIGH TEMPERATURE RESEARCH
Nondestructive testing of ceramics for vehicular advanced heat engines
[DE92-010471] p 3604 N92-30744
HIGH TEMPERATURE SUPERCONDUCTORS
Quantitative non-destructive evaluation of high-temperature superconducting materials
[DE92-011615] p 3661 N92-30693
Fabrication of multifilament conductors: CVD processing of high Tc superconducting composite fibers
[NASA-CR-184344] p 3591 N92-30711
Structural and magnetic properties of RBa2Cu2NbO8 (R = La, Pr, and Nd)
[DE92-014780] p 3729 N92-30885
A study of enhancing critical current densities (J(sub c)) and critical temperature (T(sub c)) of high-temperature superconductors
[NASA-TM-103595] p 3627 N92-30902
YBa2Cu(3-x)Co(x)O(y): A substrate material for YBCO superconductors
[DE92-015182] p 3730 N92-30999
Proceedings, phenomenology and applications of high temperature superconductors
[DE92-011133] p 3627 N92-31107
Grain boundary weak links in high-Tc superconductors
[DE92-016192] p 3730 N92-31190
HIGH TEMPERATURE TESTS
Crack growth processes at elevated temperatures in advanced materials
[AD-A249023] p 3662 N92-30558
Assessment of an improved multiaxial strength theory based on creep-rupture data for type 316 stainless steel
[DE92-010431] p 3663 N92-30823
HIGH VACUUM
Thermodynamic evaporation of highly volatile components in the vacuum degassing of melted aluminum alloys
[DE92-015315] p 3600 N92-31218
HIGH VOLTAGES
Data analysis support for the Shuttle Potential and Return Electron Experiment (SPREE) on the Tethered Satellite System 1 (TSS-1) flight
[AD-A248943] p 3588 N92-30628
Repetitive High Energy Pulsed Power (RHEPP) temperature monitoring system utilizing Luxtron fluoroptic sensors and thermocouples technical reference manual
[DE92-013461] p 3637 N92-30893
New method of error elimination in potential profile measurement of tokamak plasmas by high voltage heavy ion beam probes
[NIFS-143] p 3726 N92-30995
HIGHLY MANEUVERABLE AIRCRAFT
Nonlinear stability and control study of highly maneuverable high performance aircraft, phase 2
[NASA-CR-190667] p 3583 N92-30922
HIGHWAYS
Dense fog on the highway: Visual range monitoring in cars? p 3655 N92-31106
HISTOGRAMS
Airborne lidar and radiometric observations of PBL- and low clouds p 3642 N92-31037
HISTORIES
Rocket propulsion research at Lewis Research Center
[NASA-CR-189187] p 3732 N92-30908
HOLES (ELECTRON DEFICIENCIES)
New insights into radiation-induced oxide-trap charge through Thermally-Stimulated-Current (TSC) measurement and analysis
[DE92-009054] p 3728 N92-30585

Research on defects and transport in amorphous silicon-based semiconductors
[DE92-001223] p 3729 N92-30748
HOLOGRAPHY
The electric field dependence of the laser induced holographic grating relaxation of photorefractive polymer
[AD-A252641] p 3602 N92-30409
Dense modifiable interconnections utilizing photorefractive volume holograms
[AD-A252193] p 3637 N92-30546
Conically scanned lidar telescope using holographic optical elements p 3645 N92-31050
HOMOGENEOUS TURBULENCE
Modeling the turbulent kinetic energy equation for compressible, homogeneous turbulence
p 3631 N92-30653
Interscale energy transfer in numerically simulated turbulence p 3634 N92-30672
New insights into large eddy simulation
[AD-A249424] p 3635 N92-30775
HOOKS
Evaluation of grounding and mooring points for Army aircraft
[AD-A250749] p 3579 N92-31193
HORMONE METABOLISMS
Melatonin, the pineal gland and circadian rhythms
[AD-A250640] p 3684 N92-30376
HORMONES
Melatonin, the pineal gland and circadian rhythms
[AD-A250640] p 3684 N92-30376
Secretory mechanisms in opiocortin cells during cold stress
[AD-A252317] p 3685 N92-30719
HOT ISOSTATIC PRESSING
Pressure densification
[AD-A249438] p 3604 N92-30758
HOT PRESSING
Creep and slow crack growth mechanisms related to macroscopic creep behavior of a silicon nitride ceramic at elevated temperatures
[DE92-015195] p 3663 N92-30567
HOT STARS
Heating and momentum deposition in hot stars
[DE92-011850] p 3740 N92-30855
HOT WORKING
Interface friction, lubricants, and their influence on metal flow
[DE92-012112] p 3606 N92-30866
HUBBLE SPACE TELESCOPE
Hubble Space Telescope. Update: 18 months in orbit
[NASA-TM-107962] p 3739 N92-30686
HUMAN BEHAVIOR
Exercise behavior among Navy runners and non-runners
[AD-A250651] p 3685 N92-30644
HUMAN BEINGS
Effects of microwave radiation on humans: Monkeys exposed to 1.25 GHz pulsed microwaves
[AD-A249997] p 3686 N92-31127
HUMAN BODY
Waste streams in a typical crewed space habitat: An update
[NASA-TM-103888] p 3689 N92-31166
HUMAN FACTORS ENGINEERING
Information systems: How they affect and are affected by organization structure
[AD-A248852] p 3734 N92-30234
Cable compliance
[NASA-TP-3216] p 3612 N92-30378
Integrating commercial off-the-shelf tools for custom software development
[AD-A252462] p 3695 N92-30550
Introduction to human factors and wide area networking
[AD-A252310] p 3688 N92-30718
HUMAN PERFORMANCE
A principled approach to the measurement of situation awareness in commercial aviation
[NASA-CR-4451] p 3686 N92-30306
Introduction to cognitive processes of expert pilots
[DOT/FAA/RD-92/12] p 3578 N92-30980
A failure-to-restore unavailability model for periodically performed maintenance
[DE92-015902] p 3708 N92-31185
HUMIDITY MEASUREMENT
The 2nd phase of the LEANDRE program: Water-vapor DIAL measurement p 3643 N92-31039
HYDROCARBONS
Measurements of fugitive hydrocarbon emissions with a tunable infrared DIAL p 3655 N92-31102
From minerals to materials: A facile synthetic route to preceramic polymers for aluminum oxide
[AD-A250351] p 3606 N92-31141
HYDRODYNAMICS
The diffraction of short free surface water waves, a uniform expansion
[REPT-92-06] p 3628 N92-30358
Tritium content of a DT pellet in inertial confinement fusion
[NIFS-113] p 3722 N92-30430
Feasibility of extracting current profile information from HF-radar surface current measurements, part 1 and 2
[BCRS-91-23-PT-1-2] p 3682 N92-30470
Numerical calculations of two-dimensional single and multi-material flow fields with CCICE
[DE92-015778] p 3636 N92-30903
HYDROGEN
Review of high Z materials for PSI applications
[NIFS-152] p 3602 N92-30502
Rapid change of hydrogen neutral energy distribution at L/H-transition in JFT-2M H-mode
[NIFS-134] p 3714 N92-30510
HYDROGEN ATOMS
Interaction of atomic hydrogen with the surface methyl group on Si(100): Removal of surface carbon
[AD-A249062] p 3595 N92-30821
HYDROGEN EMBRITTLEMENT
Environmental fatigue of an Al-Li-Cu alloy. Part 2: Microscopic hydrogen cracking processes
[NASA-TM-107620] p 3664 N92-31214
Environmental fatigue of an Al-Li-Cu alloy. Part 3: Modeling of crack tip hydrogen damage
[NASA-TM-107619] p 3665 N92-31215
HYDROGEN IONS
Negative ion extraction characteristics of a large negative ion source with double-magnetic filter configuration
[NIFS-151] p 3714 N92-30501
Production of negative hydrogen ions in a large multicusp ion source with double-magnetic filter configuration
[NIFS-149] p 3714 N92-30572
HYDROGEN PLASMA
Recombining processes in a cooling plasma by mixing of initially heated gas
[NIFS-142] p 3722 N92-30431
HYDROGEN PRODUCTION
Production of negative hydrogen ions in a large multicusp ion source with double-magnetic filter configuration
[NIFS-149] p 3714 N92-30572
Solar-hydrogen energy system for solar belt countries and use of remote sensing p 3668 N92-30913
HYDROGEN-BASED ENERGY
Solar-hydrogen energy system for solar belt countries and use of remote sensing p 3668 N92-30913
HYDROGRAPHY
Oceanic CO2 measurements for the WOCE hydrographic survey in the Pacific Ocean, 1990-1991: Shore based analyses during legs 1-3
[DE92-013064] p 3682 N92-30861
HYDROLOGY
SCS method of runoff estimation using remote sensing techniques p 3668 N92-30916
HYDROLOGY MODELS
Satellite and Radar Data Use in Rainfall-Runoff Models p 3667 N92-30910
Remote sensing satellite data use in run-off studies
p 3668 N92-30914
Hydrologic modelling and use of remotely sensed data at CWPRS p 3669 N92-30918
HYDROLYSIS
A method for the production of weakly acidic cation exchange resins
[DE92-015314] p 3717 N92-31137
HYPERBOLIC DIFFERENTIAL EQUATIONS
Computation of unsteady transonic flows using an implicit centered Euler solver without artificial viscosity
[ESA-TT-1235] p 3575 N92-30514
HYPERGEOMETRIC FUNCTIONS
Differential equations for symmetric generalized ultraspherical polynomials
[REPT-92-08] p 3702 N92-30360
HYPERSONIC FLOW
Joint computational and experimental aerodynamics research on a hypersonic vehicle
[DE92-013439] p 3574 N92-30367
Calculation of viscous hypersonic flows in chemical non-equilibrium
[MBB/FE211/S/PUB/466] p 3634 N92-30674
CFD contributions during hypersonic airplane intake design
[MBB/FE213/S/PUB/459] p 3575 N92-30676
Intersecting shock-wave/turbulent boundary-layer interactions at Mach 8.3
[NASA-TM-103909] p 3635 N92-30765
Development of a 3-D upwind PNS code for chemically reacting hypersonic flowfields
[NASA-CR-190182] p 3576 N92-30977
A CFD validation roadmap for hypersonic flows
[NASA-TM-103935] p 3636 N92-30982
HYPERSONIC INLETS
CFD contributions during hypersonic airplane intake design
[MBB/FE213/S/PUB/459] p 3575 N92-30676
Intersecting shock-wave/turbulent boundary-layer interactions at Mach 8.3
[NASA-TM-103909] p 3635 N92-30765
HYPERSONIC VEHICLES
Joint computational and experimental aerodynamics research on a hypersonic vehicle
[DE92-013439] p 3574 N92-30367
Navier-Stokes computations of a viscous optimized waverider
[NASA-CR-189658] p 3574 N92-30392
CFD contributions during hypersonic airplane intake design
[MBB/FE213/S/PUB/459] p 3575 N92-30676
Research and technology, 1991. Langley Research Center
[NASA-TM-4331] p 3744 N92-30733
Development of a 3-D upwind PNS code for chemically reacting hypersonic flowfields
[NASA-CR-190182] p 3576 N92-30977
HYPERSONIC WIND TUNNELS
Real gas flow parameters for NASA Langley 22-inch Mach 20 helium tunnel
[NASA-CR-4462] p 3635 N92-30751
HYPERTENSION
Tolerance of beta blocked hypertensives during orthostatic and altitude stresses
[AD-A249904] p 3685 N92-30745
HYPERVELOCITY PROJECTILES
Ablative shielding for hypervelocity projectiles
[NASA-CASE-MSC-21884-1] p 3602 N92-30539
HYPOBARIC ATMOSPHERES
The use of tympanometry to detect aerotitis media in hypobaric chamber operations
[AD-A248963] p 3684 N92-30328
HYPOKINESIA
Light as a chronobiologic countermeasure for long-duration space operations
[NASA-TM-103874] p 3686 N92-31167
HYPOTHALAMUS
Secretory mechanisms in opiocortin cells during cold stress
[AD-A252317] p 3685 N92-30719
Control of circadian behavior by transplanted suprachiasmatic nuclei
[AD-A250442] p 3686 N92-31143

I

ICE
Clouds: Their prediction and simulation
[AD-A250643] p 3679 N92-30643
ICE CLOUDS
Multiple scattering lidar returns from stratus clouds
p 3642 N92-31035
Lidar depolarization by nonspherical particles: Potential of combined depolarization/backscattering measurements for PSC's characterization p 3644 N92-31044
ICE FORMATION
Ice thickness observations, North American Arctic and subarctic, 1972-1973 and 1973-1974, part 8
[AD-A250830] p 3681 N92-30238
Debris/ice/TPS assessment and integrated photographic analysis for Shuttle Mission STS-45
[NASA-TM-107545] p 3586 N92-30382
Lewis icing research tunnel test of the aerodynamic effects of aircraft ground deicing/anti-icing fluids
[NASA-TP-3238] p 3577 N92-30395
Vector analysis of ice fabric data
[AD-A250832] p 3682 N92-30832
ICE MAPPING
Antarctic ice charts, 1989 - 1990: Analysis Atlas
[AD-A249730] p 3669 N92-31179
ICE REPORTING
Ice thickness observations, North American Arctic and subarctic, 1972-1973 and 1973-1974, part 8
[AD-A250830] p 3681 N92-30238
IDEAL GAS
Development of a 3-D upwind PNS code for chemically reacting hypersonic flowfields
[NASA-CR-190182] p 3576 N92-30977
IGNITION
High-temperature ignition of propane with MTBE as an additive: Shock-tube experiments and modeling
[DE92-006679] p 3594 N92-30749
Modeling initiation of explosives by projectile impact
[DE92-015210] p 3608 N92-31202
IMAGE ANALYSIS
Computer vision in microstructural analysis
p 3609 N92-30271
Digital methods for analysis of satellite imagery
p 3669 N92-30920

A tolerance approach to visual shape perception and image matching analysis for modeling of micro-heterogeneous materials
[ISSN-0208-5658] p 3721 N92-31149

IMAGE PROCESSING
Review of psychophysically-based image quality metrics
[AD-A251053] p 3686 N92-30254
Modeling of video traffic in packet networks, low rate video compression, and the development of a lossy+lossless image compression algorithm
[NASA-CR-190546] p 3691 N92-30296
The use of TM data for identification of land cover and for detection of land use changes in the Atlantic zone of Costa Rica
[BCRS-91-36] p 3666 N92-30362
Implementation scheme for recursion in spectral dimension
[AD-A248945] p 3695 N92-30629
Maximum likelihood detection of electro-optic moving targets
[AD-A249442] p 3616 N92-30762
High-resolution imaging in the scanning transmission electron microscope
[DE92-010647] p 3637 N92-30827
Digital methods for analysis of satellite imagery p 3669 N92-30920
A range-resolved bistatic lidar using a high-sensitive CCD-camera p 3640 N92-31027
Fluorescence lidar multi-color imaging of vegetation p 3640 N92-31028
Considerations for imaging system implementation in a networked environment
[DE92-015338] p 3735 N92-31132

IMAGE RESOLUTION
Review of psychophysically-based image quality metrics
[AD-A251053] p 3686 N92-30254
Diversity imaging techniques in lidar p 3640 N92-31026

IMAGERY
Review of psychophysically-based image quality metrics
[AD-A251053] p 3686 N92-30254

IMAGING TECHNIQUES
Hyperspectral gas analysis system (HyGAS), phase 1
[AD-A251026] p 3593 N92-30241
Tunneling acoustic microscopy
[AD-A251028] p 3727 N92-30252
Review of psychophysically-based image quality metrics
[AD-A251053] p 3686 N92-30254
Off-surface infrared flow visualization
[NASA-CASE-LAR-14568-1] p 3720 N92-30312
Remote sensing for the Lincoln Sea Winterover Experiment
[AD-A252117] p 3667 N92-30545
High-resolution imaging in the scanning transmission electron microscope
[DE92-010647] p 3637 N92-30827
Two-color infrared digital imaging for determination of in-cylinder temperature and species during compression and combustion periods of DI diesel engine
[AD-A249812] p 3595 N92-30835
Approaches to polymer curing and imaging via the in situ generation of a catalyst
[AD-A249917] p 3606 N92-30873
Can't justify an imaging system? How about a CAR?
[DE92-015156] p 3735 N92-31001
Sixteenth International Laser Radar Conference, part 2
[NASA-CP-3158-PT-2] p 3637 N92-31013
Diversity imaging techniques in lidar p 3640 N92-31026
Fluorescence lidar multi-color imaging of vegetation p 3640 N92-31028
Tunable Electro-optic modulators for lidar systems and atmospheric applications p 3646 N92-31056
A tolerance approach to visual shape perception and image matching analysis for modeling of micro-heterogeneous materials
[ISSN-0208-5658] p 3721 N92-31149

IMPACT DAMAGE
Impact erosion of terrestrial planetary atmospheres
[NASA-CR-190605] p 3742 N92-30921
Modeling initiation of explosives by projectile impact
[DE92-015210] p 3608 N92-31202
The thermal engine of Venus: Implications from the impact crater distribution p 3738 N92-31233

IMPACT TESTS
Impact testing of welded samples p 3608 N92-30268
Low-velocity impact loading on fibre reinforced aluminum laminates (ARALL) and other aircraft sheet materials
[ETN-92-91613] p 3590 N92-30414
Evaluation of head impact kinematics for passengers seated behind interior walls
[AD-A252651] p 3578 N92-30551

IMPEDANCE
A comparative EIS study on cermet and platinum anodes for the electrolytic production of aluminum
[DE92-015091] p 3599 N92-31010

IMPEDANCE MATCHING
Tunable relay box (design and testing) p 3718 N92-30727

IMPELLERS
Active control of pressure, sound and velocity of centrifugal pumps
[AD-A249446] p 3659 N92-30640
Thrust test fixture
[AD-D015259] p 3585 N92-31192

IMPURITIES
Effects of impurities on the mechanical behaviour of primary and secondary cast aluminum alloys
[PB92-180652] p 3598 N92-30785
Impurity segregation to grain boundaries and defects in AlN
[DE92-011667] p 3599 N92-31112
Spectroscopic diagnosis of long-scale-length exploding-foil plasma in the presence of an intense radiation field
[DE92-014718] p 3726 N92-31118

IN-FLIGHT MONITORING
High speed research system study. Advanced flight deck configuration effects
[NASA-CR-189650] p 3581 N92-30965

INCOHERENT SCATTERING
Phase noise in pulsed Doppler lidar and limitations on achievable single-shot velocity accuracy p 3639 N92-31024

INCOMPRESSIBLE FLOW
Validation of three-dimensional incompressible spatial direct numerical simulation code: A comparison with linear stability and parabolic stability equation theories for boundary-layer transition on a flat plate
[NASA-TP-3205] p 3573 N92-30295
A multigrid method for a discretization of the incompressible Navier-Stokes equations in general coordinates
[REPT-91-73] p 3629 N92-30454
A robust multigrid method for a discretization of the incompressible Navier-Stokes equations in general coordinates
[REPT-92-14] p 3629 N92-30462
A study of the topology of dissipating motions in direct numerical simulations of time-developing compressible and incompressible mixing layers p 3632 N92-30658
The Rayleigh-Taylor instability in an expanding plasma
[DE92-013883] p 3725 N92-30884
Direct coupling method for time-accurate solution of incompressible Navier-Stokes equations
[NASA-CR-189177] p 3636 N92-30894
Numerical calculations of two-dimensional single and multi-material flow fields with CCICE
[DE92-015778] p 3636 N92-30903

INDIAN SPACECRAFT
Use of INSAT data in rainfall estimation p 3668 N92-30912

INDIUM ALLOYS
Experiments with the low melting indium-bismuth alloy system p 3601 N92-30272

INDIUM COMPOUNDS
Research on polycrystalline thin film submodules based on CuInSe2 materials
[DE92-010584] p 3727 N92-30247
Anomalous hopping conductivity in amorphous indium-oxide films
[ITN-92-85166] p 3729 N92-30781

INDUCTION HEATING
Flexible heating head for induction heating apparatus and method
[NASA-CASE-LAR-14679-2] p 3621 N92-31150

INDUCTORS
Comparison of high temperature, high frequency core loss and dynamic B-H loops of a 2V-49Fe-49Co and a grain oriented 3Si-Fe alloy
[NASA-TM-105791] p 3623 N92-30397

INDUSTRIAL MANAGEMENT
ILS, CE, CALS? From design to operation
[ETN-92-91717] p 3697 N92-30950
Concurrent engineering p 3697 N92-30952
Flight crew integration in the maintenance chain of a commercial aircraft (A 320) p 3698 N92-30957

INDUSTRIES
Soviet applied information sciences in a time of change
[PB92-173020] p 3734 N92-30509
Cellular: Toward personal communications p 3619 N92-30936

INELASTIC SCATTERING
Linear estimates of structure functions from deep inelastic lepton-nucleon scattering data, part 1
[DE92-627288] p 3713 N92-30403
Two-loop QCD corrections to the coefficient functions of the deep inelastic structure functions F2 and F(sub L)
[NIKHEF-H/91-17] p 3715 N92-30687

INEQUALITIES
The functions psi(x) and beta(x) and some inequalities for integrals (theorems 1-16)
[REPT-92-09] p 3703 N92-30459
Some inequalities for variances
[REPT-92-10] p 3707 N92-30460
The sum of weighted balls
[RUU-CS-91-37] p 3707 N92-30481

INERTIAL CONFINEMENT FUSION
Tritium content of a DT pellet in inertial confinement fusion
[NIFS-113] p 3722 N92-30430
Neutron time-of-flight ion temperature diagnostic for inertial confinement fusion experiments
[DE92-011365] p 3724 N92-30806
X ray radiation from hot dense plasmas and atomic processes
[NIFS-PROC-9] p 3725 N92-30984

INFERENCE
A three-valued cumulative semantics for TMS
[REPT-91-69] p 3702 N92-30371

INFORMATION DISSEMINATION
Information systems: How they affect and are affected by organization structure
[AD-A248852] p 3734 N92-30234
Science in action: An interdisciplinary science education program p 3610 N92-30278
The sustainable biosphere initiative: An ecological research agenda p 3673 N92-30425
Activities report of the Institute for Astronomy and Astrophysics at Technical University of Berlin (Germany, F.R.)
[MITT-11] p 3740 N92-30506
Reviewing the technical report
[AD-A249494] p 3735 N92-30636

INFORMATION FLOW
Compiler analysis for irregular problems in FORTRAN D
[NASA-CR-189664] p 3689 N92-30311

INFORMATION MANAGEMENT
Informatization in public administration (EGPA-research project 1991). Large scale information systems in The Netherlands
[REPT-91-92] p 3734 N92-30486
Informatization in public administration (EGPA-research project 1991). Large scale information systems (comparative analysis in 8 European countries)
[REPT-91-93] p 3734 N92-30487
The evolving data dictionary
[AD-A249030] p 3735 N92-30819

INFORMATION RETRIEVAL
Can't justify an imaging system? How about a CAR?
[DE92-015156] p 3735 N92-31001
Considerations for imaging system implementation in a networked environment
[DE92-015338] p 3735 N92-31132

INFORMATION SYSTEMS
Informatization in public administration (EGPA-research project 1991). Large scale information systems in The Netherlands
[REPT-91-92] p 3734 N92-30486
Informatization in public administration (EGPA-research project 1991). Large scale information systems (comparative analysis in 8 European countries)
[REPT-91-93] p 3734 N92-30487
The effect of information systems on middle management in the aerospace industry: The Westco case
[AD-A249017] p 3735 N92-30584
The evolving data dictionary
[AD-A249030] p 3735 N92-30819
Can't justify an imaging system? How about a CAR?
[DE92-015156] p 3735 N92-31001
Considerations for imaging system implementation in a networked environment
[DE92-015338] p 3735 N92-31132

INFORMATION THEORY
Combinatorics and Kolmogorov complexity
[CWI-CS-R9125] p 3708 N92-30699

INFRARED DETECTORS
Development of ultra-low noise, high sensitivity planar metal grating coupled AlGaAs/GaAs multiquantum well IR detectors for focal plane array staring IR sensor systems
[AD-A246122] p 3590 N92-30318

INFRARED FILTERS
Advanced mobile satellite communications system using Ka and MM-wave bands in Japan's R and D satellite project p 3617 N92-30924

INFRARED IMAGERY
Off-surface infrared flow visualization
[NASA-CASE-LAR-14568-1] p 3720 N92-30312
Two-color infrared digital imaging for determination of in-cylinder temperature and species during compression and combustion periods of DI diesel engine
[AD-A249812] p 3595 N92-30835
Remote sensing for rainfall estimation: SAC experience p 3668 N92-30917
Aerosol extinction measurements with CO2-lidar p 3655 N92-31105

INFRARED INSTRUMENTS
Airborne remote sensing of tropospheric water vapor using a near infrared DIAL system p 3644 N92-31042

INFRARED LASERS
Effect of atmospheric extinction on laser rangefinder performance at 1.54 and 0.6 microns p 3648 N92-31066
Alexandrite lidar for the atmospheric water vapor detection and development of powerful tunable sources in IR p 3653 N92-31094

INFRARED RADAR
A pulsed CO2 Doppler lidar for boundary layer monitoring p 3639 N92-31021
A compact high repetition rate CO2 coherent Doppler lidar p 3639 N92-31022
Simplified signal processing for an airborne CO2 Doppler lidar p 3639 N92-31023
Multiple scattering wavelength dependent backscattering of kaolin dust in the IR: Measurements and theory p 3648 N92-31064
The ENEA CO2 lidar/DIAL station activity in a tropospheric remote sensing program p 3655 N92-31103
Aerosol extinction measurements with CO2-lidar p 3655 N92-31105

INFRARED RADIATION
Off-surface infrared flow visualization
[NASA-CASE-LAR-14568-1] p 3720 N92-30312
Development of ultra-low noise, high sensitivity planar metal grating coupled AlGaAs/GaAs multiquantum well IR detectors for focal plane array staring IR sensor systems
[AD-A246122] p 3590 N92-30318
Alexandrite lidar for the atmospheric water vapor detection and development of powerful tunable sources in IR p 3653 N92-31094
Measurements of fugitive hydrocarbon emissions with a tunable infrared DIAL p 3655 N92-31102

INFRARED RADIOMETERS
Airborne lidar and radiometric observations of PBL- and low clouds p 3642 N92-31037

INFRARED SPECTRA
Vibrationally induced rotational axis switching: A novel mechanism for vibrational mode-coupling
[AD-A251085] p 3712 N92-30259
Infrared investigations of pristine, doped and partially-doped polypyrrole
[AD-A250644] p 3605 N92-30838

INFRARED SPECTROSCOPY
Fiber-optic Raman spectroscopy at the Savannah River Site: Uses and techniques
[DE92-013971] p 3596 N92-30899

INITIATION
Modeling initiation of explosives by projectile impact
[DE92-015210] p 3608 N92-31202

INITIATORS (EXPLOSIVES)
Temperature effect on the Langmuir-Blodgett polymerization of 2-pentadecylaniline
[AD-A250803] p 3601 N92-30250

INJECTION LASERS
Doppler lidar wind measurement with the edge technique p 3638 N92-31017
Wavemeter measurements of frequency stability of an injection seeded alexandrite laser for pressure and temperature lidar p 3645 N92-31049
Injection seeded single mode alexandrite ring laser for lidar applications p 3646 N92-31057

INJECTION MOLDING
A senior manufacturing laboratory for determining injection molding process capability p 3609 N92-30273

INJURIES
Evaluation of head impact kinematics for passengers seated behind interior walls
[AD-A252651] p 3578 N92-30551
Adapting the ADAM manikin technology for injury probability assessment
[AD-A252332] p 3688 N92-30844

INLET FLOW
Ultra high bypass Nacelle aerodynamics inlet flow-through high angle of attack distortion test
[NASA-CR-189149] p 3574 N92-30298

INSTRUCTORS
Technical training for national simulator evaluation specialist
[NASA-CR-190429] p 3687 N92-30488

INSULATION
An investigation of the effects of boundary constraints on the sound insulations of lightweight, double leaf partitions
[BBC-RD-1992/4] p 3711 N92-31151

INSULATORS
A method of making a single layer multi-color luminescent display
[NASA-CASE-LAR-14811-1] p 3622 N92-30389

INTAKE SYSTEMS
Numerical investigations in three-dimensional internal flows
[NASA-CR-190498] p 3628 N92-30380

INTEGRAL EQUATIONS
Extension of the integral equation formulation of linearized time dependent subsonic flow
[AD-A250654] p 3577 N92-31171

INTEGRALS
New transient and pseudo-transient algorithms for viscoelastic materials
[AD-A250642] p 3692 N92-30377
The functions psi(x) and beta(x) and some inequalities for integrals (theorems 1-16)
[REPT-92-09] p 3703 N92-30459
Ginsburg criterion for an equilibrium superradiant model in the dynamic approach
[DE92-630566] p 3732 N92-31203

INTEGRATED CIRCUITS
Tunneling acoustic microscopy
[AD-A251028] p 3727 N92-30252
Hybridization of detector array and integrated circuit for readout
[NASA-CASE-NPO-18062-1-CU] p 3623 N92-30542

INTEGRATORS
Dynamics of deformable bodies
[AD-A252333] p 3705 N92-30533

INTERACTIONS
Electrical and chemical interactions at Mars Workshop, part 1
[NASA-CP-10093] p 3741 N92-30302

INTERFACES
Investigation of the interface phenomena due to interaction of high intensity stress waves with geologic boundaries
[AD-A248992] p 3675 N92-30525
Printer port interface
[NASA-CASE-LAR-13950-1] p 3690 N92-30541

INTERFACIAL ENERGY
Stability of metallic superlattices
[DE92-011526] p 3600 N92-31124

INTERFACIAL TENSION
Measuring the surface tension of soap bubbles p 3612 N92-30293
Transport phenomena in welds
[DE92-013404] p 3659 N92-30587

INTERFERENCE
Capacity and interference in a PCS system p 3619 N92-30937

INTERFEROMETERS
Density profile measurement using a multichannel difluoromethane laser interferometer system on ATF
[DE92-011691] p 3724 N92-30810

INTERFEROMETRY
Fiber optic Michelson sensor and arrays with passive elimination of polarization fading and source feedback isolation
[AD-D015290] p 3722 N92-31213

INTERLAMINAR STRESS
Composite beam analysis linear analysis of naturally curved and twisted anisotropic beams
[AD-A252652] p 3663 N92-30766

INTERMEDIATE FREQUENCIES
Advanced mobile satellite communications system using Ka and MM-wave bands in Japan's R and D satellite project p 3617 N92-30924

INTERMETALLICS
Cu-Zn binary phase diagram and diffusion couples p 3600 N92-30269
Crack growth processes at elevated temperatures in advanced materials
[AD-A249023] p 3662 N92-30558

INTERMOLECULAR FORCES
Magic numbers in molecular clusters: A probe for chemical reactivity
[AD-A251096] p 3712 N92-30261

INTERNAL COMBUSTION ENGINES
Ringless piston experiments. Natural gas engine technology advancements
[PB92-164466] p 3659 N92-30601

INTERNAL ENERGY
Measurement of radiative lifetimes of vibrational states of simple ions
[AD-A248567] p 3712 N92-30337

INTERNAL PRESSURE
Analytical solution of elastic-plastic thick-walled cylinders with general hardening
[AD-A249491] p 3705 N92-30618
Nonlinear stress analysis of composite-jacketed steel cylinders subjected to high internal pressure
[AD-A249500] p 3663 N92-30802

INTERNATIONAL COOPERATION
Informatization in public administration (EGPA-research project 1991). Large scale information systems (comparative analysis in 8 European countries)
[REPT-91-93] p 3734 N92-30487
Joint stabilizing projects in defense
[DE92-015977] p 3709 N92-30891
ILS, CE, CALS? From design to operation
[ETN-92-91717] p 3697 N92-30950
First conclusions of a manufacturer group on the applicability of CALS in Europe p 3697 N92-30951
Preparation for a new plane (A 320): Experience reviewed p 3697 N92-30954

INTERPLANETARY DUST
TEM studies of a circumstellar rock p 3736 N92-31223
Presolar (?) corundum in the Orgueil meteorite p 3738 N92-31230

INTERPLANETARY MEDIUM
Dynamics and energetics of the solar corona
[NASA-CR-190664] p 3742 N92-31162

INTERPOLATION
A local interpolator derived from the discrete Fourier transform
[AD-A251066] p 3701 N92-30243
Regional-scale analysis and forecasting (RAP) report
[AD-A248384] p 3678 N92-30262
Operational surfaces for the rectangle and triangle
[DE92-015165] p 3705 N92-30566

INTERPROCESSOR COMMUNICATION
Compiler analysis for irregular problems in FORTRAN D
[NASA-CR-189664] p 3689 N92-30311
The GKS input model in MANIFOLD
[CWI-CS-R9127] p 3699 N92-30696

INVARIANCE
Theoretical particle physics
[DE92-014531] p 3716 N92-30841

INVARIANT IMBEDDINGS
Real cubic systems with four line invariants
[REPT-91-79] p 3702 N92-30436
Real polynomial systems of degree n with n+1 line invariants
[REPT-91-86] p 3704 N92-30490

INVENTIONS
Polyimides containing the cyclobutene-3,4-dione moiety
[NASA-CASE-LAR-14753-1] p 3601 N92-30313
Quick acting gimbal joint
[NASA-CASE-MSC-21918-1] p 3658 N92-30316
Attitudinal and situational differences between national laboratory inventors and inventor-entrepreneurs
[DE92-015768] p 3733 N92-30889

ION ACCELERATORS
Effects of high beam rates on TPC's
[DE92-014594] p 3717 N92-30398

ION ATOM INTERACTIONS
Evidence for interference between resonant and nonresonant transfer and excitation
[DE92-011779] p 3716 N92-30853

ION BEAMS
Computer-controlled ion beam sputter-deposition of superconducting oxide films
[AD-A248495] p 3601 N92-30326
Effects of high beam rates on TPC's
[DE92-014594] p 3717 N92-30398
Evidence for the dependence of the sputter yield of graphite on ion bombardment fluence
[AD-A252500] p 3623 N92-30537
Study of Au(-) production in a plasma-sputter type negative ion source
[NIFS-115] p 3717 N92-30990
New method of error elimination in potential profile measurement of tokamak plasmas by high voltage heavy ion beam probes
[NIFS-143] p 3726 N92-30995
Focused ion beam implantation
[AD-A249662] p 3627 N92-31004
Results of the heavy ion beam probe measurements on the Advanced Toroidal Facility
[DE92-014461] p 3726 N92-31197

ION CHARGE
Measurement of radiative lifetimes of vibrational states of simple ions
[AD-A248567] p 3712 N92-30337

ION CURRENTS
Effects of fast ions and an external inductive electric field on the neoclassical parallel flow, current, and rotation in general toroidal systems
[NIFS-150] p 3713 N92-30500
Template-synthesis: A method for enhancing the ionic and electronic conductivity in electronically conductive polymers
[AD-A248806] p 3603 N92-30553
Data analysis support for the Shuttle Potential and Return Electron Experiment (SPREE) on the Tethered Satellite System 1 (TSS-1) flight
[AD-A248943] p 3588 N92-30628
ION CYCLOTRON RADIATION
Fundamental studies of fusion plasmas
[DE92-015077] p 3726 N92-31116
ION DISTRIBUTION
Rapid change of hydrogen neutral energy distribution at L/H-transition in JFT-2M H-mode
[NIFS-134] p 3714 N92-30510
ION EXCHANGE RESINS
A method for the production of weakly acidic cation exchange resins
[DE92-015314] p 3717 N92-31137
A method for regenerating ion exchange resin
[DE92-015312] p 3606 N92-31146
ION EXCHANGING
A method for the production of weakly acidic cation exchange resins
[DE92-015314] p 3717 N92-31137
A method for production of new anion exchangers
[DE92-015313] p 3717 N92-31147
ION EXTRACTION
Negative ion extraction characteristics of a large negative ion source with double-magnetic filter configuration
[NIFS-151] p 3714 N92-30501
ION IMPLANTATION
A method of making a single layer multi-color luminescent display
[NASA-CASE-LAR-14811-1] p 3622 N92-30389
Focused ion beam implantation
[AD-A249662] p 3627 N92-31004
ION IRRADIATION
Evidence for the dependence of the sputter yield of graphite on ion bombardment fluence
[AD-A252500] p 3623 N92-30537
ION PRODUCTION RATES
Study of Au(-) production in a plasma-sputter type negative ion source
[NIFS-115] p 3717 N92-30990
ION SHEATHS
Data analysis support for the Shuttle Potential and Return Electron Experiment (SPREE) on the Tethered Satellite System 1 (TSS-1) flight
[AD-A248943] p 3588 N92-30628
ION SOURCES
Negative ion extraction characteristics of a large negative ion source with double-magnetic filter configuration
[NIFS-151] p 3714 N92-30501
Production of negative hydrogen ions in a large multicusp ion source with double-magnetic filter configuration
[NIFS-149] p 3714 N92-30572
Study of Au(-) production in a plasma-sputter type negative ion source
[NIFS-115] p 3717 N92-30990
ION TEMPERATURE
Neutron time-of-flight ion temperature diagnostic for inertial confinement fusion experiments
[DE92-011365] p 3724 N92-30806
IONIC DIFFUSION
Beta limit of resistive plasma in torsatron/heliotron
[NIFS-131] p 3725 N92-30985
IONIC REACTIONS
Chemistry within van der Waals cluster of unsaturated molecules: Observation of cationic polymerization
[AD-A250929] p 3712 N92-30240
IONIZATION
Laser mass spectrometry for biopolymers
[DE92-015238] p 3597 N92-31184
IONIZATION CHAMBERS
Tests of the performance of different gas mixtures in microstrip gas counters
[NIKHEF-H/91-23] p 3636 N92-30365
Optimization of the microstrip gas counter
[NIKHEF-H/91-21] p 3637 N92-30688
IONIZATION POTENTIALS
Chemielectron and photoelectron spectroscopic studies of importance in the upper atmosphere
[AD-A248838] p 3675 N92-30556
IONIZING RADIATION
Effects of high beam rates on TPC's
[DE92-014594] p 3717 N92-30398
IONS
Measurement of radiative lifetimes of vibrational states of simple ions
[AD-A248567] p 3712 N92-30337
Effects of fast ions and an external inductive electric field on the neoclassical parallel flow, current, and rotation in general toroidal systems
[NIFS-150] p 3713 N92-30500
IRON
Search for light neutral scalar and pseudoscalar particles in pFe interactions at 70 GeV
[DE92-627317] p 3713 N92-30404
IRRADIATION
Photodissociation of azulene under UV-laser irradiation at 325 nm
[AD-A251093] p 3613 N92-30246
Interaction physics for megajoule laser fusion targets
[DE92-014796] p 3656 N92-30400
Eye/sensor protection against laser irradiation ablative mirror devices: A materials assessment
[AD-A248787] p 3688 N92-30615
Proceedings of a Beryllium Technology Workshop
[DE92-012312] p 3598 N92-30834
Laser mass spectrometry for biopolymers
[DE92-015238] p 3597 N92-31184
ISCCP PROJECT
Raman lidar measurements of water vapor and aerosol/clouds during the FIRE/SPECTRE field campaign p 3652 N92-31089
ISCHEMIA
Optimal ECG electrode sites and criteria for detection of asymptomatic coronary artery disease, update 1990. Multilead ECG changes at rest, with exercise, and with coronary angioplasty
[AD-A248613] p 3684 N92-30523
ISLANDS
A statistical comparison of AUTEC and Eleuthera Island wind data for the period 1 April 1989 through 30 March 1990
[AD-A248898] p 3679 N92-31003
ISOLATORS
Optical isolators in high power lasers based on high reflectivity phase conjugate mirrors
[IA-1452] p 3721 N92-30581
Fiber optic Michelson sensor and arrays with passive elimination of polarization fading and source feedback isolation
[AD-D015290] p 3722 N92-31213
ISOMERS
The electric field dependence of the laser induced holographic grating relaxation of photorefractive polymer
[AD-A252641] p 3602 N92-30409
ISOTHERMAL PROCESSES
Isothermal aging effects on PMR-15 resin
[NASA-TM-105648] p 3593 N92-30986
ISOTOPE EFFECT
Photodynamics within (CH3OH)(nCr(CO)6) heteroclusters: Observation of an isotope effect
[AD-A251058] p 3712 N92-30255
ISOTOPES
Trace element and isotope geochemistry of geothermal fluids, East Rift Zone, Kilauea, Hawaii
[DE92-014586] p 3671 N92-31117
ISOTROPIC TURBULENCE
Subgrid-scale backscatter in transitional and turbulent flows p 3630 N92-30650
A subgrid-scale model based on the second-order velocity structure function p 3631 N92-30651
Modeling the turbulent kinetic energy equation for compressible, homogeneous turbulence p 3631 N92-30653
Pre-mixed flame simulations for non-unity Lewis numbers p 3597 N92-30670
Interscale energy transfer in numerically simulated turbulence p 3634 N92-30672
New insights into large eddy simulation
[AD-A249424] p 3635 N92-30775
Interaction of isotropic turbulence with a shock wave
[AD-A250409] p 3635 N92-30852
ISOTROPISM
Optimal shear correction factors in hierarchical plate modelling
[AD-A248899] p 3662 N92-30338
ISOTROPY
Isotropic thin-walled pressure vessel experiment p 3611 N92-30284
Generation of large-scale density fluctuations by buoyancy p 3634 N92-30671
ITERATION
Further experiences with GMRESR
[REPT-92-12] p 3704 N92-30461
Numerical analysis of the Iosipescu specimen for composite materials
[NASA-CR-190658] p 3592 N92-30906
Fixed point iterations for a class of nonlinear mappings in certain Banach spaces
[DE92-630235] p 3706 N92-31134
ITERATIVE SOLUTION
A strictly improving linear programming algorithm based on a series of Phase 1 problems
[DE92-015905] p 3696 N92-30905
Fixed point iterations for a class of nonlinear mappings in certain Banach spaces
[DE92-630235] p 3706 N92-31134

J

JACKETS
Nonlinear stress analysis of composite-jacketed steel cylinders subjected to high internal pressure
[AD-A249500] p 3663 N92-30802
JAMMING
High frequency communications under adverse conditions
[AD-A252199] p 3615 N92-30532
JET ENGINE FUELS
Laser induced fluorescence detection of gums in jet fuels
[AD-A252685] p 3607 N92-30767
JET ENGINES
Finite difference time domain modeling of steady state scattering from jet engines with moving turbine blades
[NASA-CR-190290] p 3582 N92-30753
JET FLOW
A new unsteady mixing model to predict NO(x) production during rapid mixing in a dual-stage combustor
[NASA-CR-189155] p 3581 N92-30569
Variational method in the statistical theory of turbulent two-phase flows
[AD-A252263] p 3630 N92-30604
JET PROPULSION
Future aerospace ground test facility requirements for the Arnold Engineering Development Center p 3585 N92-30897
JOINTS (JUNCTIONS)
Quick acting gimbal joint
[NASA-CASE-MSC-21918-1] p 3658 N92-30316
Cable compliance
[NASA-TP-3216] p 3612 N92-30378
Method and apparatus for preloading a joint by remotely operable means
[NASA-CASE-MSC-21940-1] p 3659 N92-30540
Method of bonding carbon-carbon and metal matrix composite structures
[AD-D015299] p 3591 N92-30573
Transfer soldering evaluation
[DE92-015160] p 3627 N92-31144
JOSEPHSON JUNCTIONS
Proceedings, phenomenology and applications of high temperature superconductors
[DE92-011133] p 3627 N92-31107
JOURNAL BEARINGS
Fast methods to numerically integrate the Reynolds equation for gas fluid films
[NASA-TM-105415] p 3660 N92-30722

K

KALMAN FILTERS
Alignment of a 3-D sensor and a 2-D sensor measuring azimuth and elevation
[AD-A252120] p 3636 N92-30530
Implementation scheme for recursion in spectral dimension
[AD-A248945] p 3695 N92-30629
KEYING
METEODEC/METEOCRYPT: A demonstration of data compression and encryption for operational remote-sensing
[NLR-TP-89294-U] p 3667 N92-30475
KINEMATICS
Numerical analysis of the Iosipescu specimen for composite materials
[NASA-CR-190658] p 3592 N92-30906
KINETIC ENERGY
Introductory heat-transfer p 3601 N92-30291
Modeling the turbulent kinetic energy equation for compressible, homogeneous turbulence p 3631 N92-30653
KINETIC EQUATIONS
Modeling the turbulent kinetic energy equation for compressible, homogeneous turbulence p 3631 N92-30653
KINETIC THEORY
Kinetic theory and boundary conditions for flows of highly inelastic spheres
[DE92-012645] p 3629 N92-30438

KINETICS
Temperature effect on the Langmuir-Blodgett polymerization of 2-pentadecylaniline
[AD-A250803] p 3601 N92-30250
Kinetic theory and boundary conditions for flows of highly inelastic spheres
[DE92-012645] p 3629 N92-30438
A new unsteady mixing model to predict NO(x) production during rapid mixing in a dual-stage combustor
[NASA-CR-189155] p 3581 N92-30569
In situ TEM studies of the effect of misfit strain on the kinetics of Si(sub 1-x)Ge(sub x) solid phase epitaxy: Temperature calibration and surface effects
[DE92-011689] p 3728 N92-30574
KNUDSEN FLOW
Numerical investigations in the backflow region of a vacuum plume
[NASA-CR-190515] p 3589 N92-30981
KOLMOGOROFF THEORY
Combinatorics and Kolmogorov complexity
[CWI-CS-R9125] p 3708 N92-30699
KOLMOGOROFF-SMIRNOFF TEST
Combinatorics and Kolmogorov complexity
[CWI-CS-R9125] p 3708 N92-30699

L

LABORATORIES
Computer integrated laboratory testing
p 3611 N92-30289
The 1991 Summer Faculty Research Program (SFRP), volume 4 atory
[AD-A248766] p 3744 N92-30327
Nuclear electric propulsion development and qualification facilities
[NASA-TM-105521] p 3589 N92-30818
Attitudinal and situational differences between national laboratory inventors and inventor-entrepreneurs
[DE92-015768] p 3733 N92-30889
LABYRINTH SEALS
Ringless piston experiments. Natural gas engine technology advancements
[PB92-164466] p 3659 N92-30601
LAKE ICE
Ice thickness observations, North American Arctic and subarctic, 1972-1973 and 1973-1974, part 8
[AD-A250830] p 3681 N92-30238
LAKE TAHOE (CA-NV)
Inter- and intra-plate deformation at North American plate boundaries
[NASA-CR-190485] p 3676 N92-30961
LAMELLA (METALLURGY)
Crack growth processes at elevated temperatures in advanced materials
[AD-A249023] p 3662 N92-30558
LAMINAR FLOW
Statistics for laminar flamelet modeling
p 3597 N92-30668
The influence of Lewis number and nonhomogeneous mixture on premixed turbulent flame structure
p 3597 N92-30669
Nonlinear analysis of a grating free-electron laser
[AD-A248833] p 3656 N92-30743
LAMINATES
Finite element analysis of laminated composite axisymmetric solids. Volume 1: Theory and applications
[AD-A250808] p 3590 N92-30251
A shear sensitive monomer-polymer laminate structure and method of using same
[NASA-CASE-LAR-14654-1] p 3662 N92-30317
Low-velocity impact loading on fibre reinforced aluminum laminates (ARALL) and other aircraft sheet materials
[ETN-92-91613] p 3590 N92-30414
Wave propagation and vibration of fibre-reinforced laminates
[AD-A252101] p 3590 N92-30528
Thermal stress evaluation of a symmetrically laminated composite plate
[AD-A249450] p 3591 N92-30641
Composite beam analysis linear analysis of naturally curved and twisted anisotropic beams
[AD-A252652] p 3663 N92-30766
LAND ICE
Potential airfield sites in Antarctica for wheeled aircraft
[AD-A249503] p 3584 N92-30621
LAND MOBILE SATELLITE SERVICE
Issues for the integration of satellite and terrestrial cellular networks for mobile communications
p 3620 N92-30941
LAND USE
The use of TM data for identification of land cover and for detection of land use changes in the Atlantic zone of Costa Rica
[BCRS-91-36] p 3666 N92-30362
LANDAU DAMPING
Gyro-Landau fluid model of tokamak core fluctuations
[DE92-013277] p 3722 N92-30366
LANDSAT SATELLITES
A one-class classifier for identifying urban areas in remotely-sensed data
[DE92-013539] p 3667 N92-30704
LANGUAGES
Proceedings of the Sylvia Beach Language Comprehension Conference
[AD-A250488] p 3621 N92-31129
LARGE SPACE STRUCTURES
A conceptual design of a large aperture microwave radiometer geostationary platform
[NASA-TM-107577] p 3588 N92-30736
Development of software to improve AC power quality on large spacecraft
[NASA-CR-190569] p 3589 N92-30989
LASER ALTIMETERS
Altimetry and lidar using AlGaAs lasers modulated with pseudo-random codes p 3641 N92-31030
LASER ANEMOMETERS
Theoretical simulation of a 2 micron airborne solid state laser anemometer p 3647 N92-31059
LASER APPLICATIONS
Photodissociation of azulene under UV-laser irradiation at 325 nm
[AD-A251093] p 3613 N92-30246
Three-dimensional laser window formation
[NASA-RP-1280] p 3585 N92-30307
The electric field dependence of the laser induced holographic grating relaxation of photorefractive polymer
[AD-A252641] p 3602 N92-30409
Laser optical mouse
[AD-D015307] p 3690 N92-30564
Growth and evaluation of nonlinear optical materials for laser applications: Barium borate, lithium borate, and silver gallium selenide
[AD-A248861] p 3624 N92-30617
Density profile measurement using a multichannel difluoromethane laser interferometer system on ATF
[DE92-011691] p 3724 N92-30810
Laser induced reaction for pre-bond surface preparation of aluminum alloys
[AD-A249916] p 3598 N92-30872
Tm,Ho:YAG laser with tunable range of 2.08-2.12 microns and its applications to spectroscopy
p 3646 N92-31058
Emerging solid-state laser technology by lidar/DIAL remote sensing p 3653 N92-31095
The role of laser coherence in long-range vibration measurements p 3654 N92-31097
HgCdTe photomixers for CO2 laser radar systems
p 3654 N92-31100
LASER BEAMS
Waveguide polarizer using localized surface plasmons
[AD-D015258] p 3614 N92-30348
Generation of stimulated backscattered harmonic radiation from intense laser interactions with beams and plasmas
[AD-A248782] p 3656 N92-30614
A range-resolved bistatic lidar using a high-sensitive CCD-camera p 3640 N92-31027
LASER CAVITIES
Transverse pattern modification in a stable apertured laser resonator
[ITN-92-85171] p 3656 N92-30582
Reflector development for XUV free-electron laser oscillators
[DE92-015212] p 3657 N92-31182
LASER DOPPLER VELOCIMETERS
Doppler photography: Laser methods on the flow measurement technique
[ISL-PU-303/90] p 3720 N92-30507
LASER DRILLING
Numerical simulation of crater formation heating by laser beam. Analysis of radiation exchanges in the cavity
[ESA-TT-1234] p 3657 N92-30997
LASER FUSION
Interaction physics for megajoule laser fusion targets
[DE92-014796] p 3656 N92-30400
LASER GUIDANCE
Generation of a sodium guidestar using a high power dye laser
[DE92-012696] p 3657 N92-31115
LASER INDUCED FLUORESCENCE
Laser induced fluorescence detection of gums in jet fuels
[AD-A252685] p 3607 N92-30767
Time and wavelength domain algorithms for chemical analysis by laser radar p 3650 N92-31075
LASER MATERIALS
Optical isolators in high power lasers based on high reflectivity phase conjugate mirrors
[IA-1452] p 3721 N92-30581
LASER MODE LOCKING
Locked modes and magnetic field errors in MST
[DE92-015379] p 3723 N92-30612
LASER MODES
Transverse pattern modification in a stable apertured laser resonator
[ITN-92-85171] p 3656 N92-30582
LASER OUTPUTS
Eye/sensor protection against laser irradiation ablative mirror devices: A materials assessment
[AD-A248787] p 3688 N92-30615
Interaction of ultra-high laser fields with beams and plasmas
[AD-A249502] p 3723 N92-30620
The 2nd phase of the LEANDRE program: Water-vapor DIAL measurement p 3643 N92-31039
LASER PLASMA INTERACTIONS
Interaction physics for megajoule laser fusion targets
[DE92-014796] p 3656 N92-30400
Interaction of ultra-high laser fields with beams and plasmas
[AD-A249502] p 3723 N92-30620
LASER PLASMAS
Generation of stimulated backscattered harmonic radiation from intense laser interactions with beams and plasmas
[AD-A248782] p 3656 N92-30614
Spectroscopic diagnosis of long-scale-length exploding-foil plasma in the presence of an intense radiation field
[DE92-014718] p 3726 N92-31118
LASER POWER BEAMING
Method for remotely powering a device such as a lunar rover
[NASA-CASE-LAR-14789-1] p 3658 N92-30388
LASER PUMPING
Generation of stimulated backscattered harmonic radiation from intense laser interactions with beams and plasmas
[AD-A248782] p 3656 N92-30614
A high speed signal processing system for a diode-pumped YAG lidar p 3646 N92-31054
LASER RANGE FINDERS
Effect of atmospheric extinction on laser rangefinder performance at 1.54 and 0.6 microns
p 3648 N92-31066
Dense fog on the highway: Visual range monitoring in cars? p 3655 N92-31106
LASER SPECTROSCOPY
Research studies on extreme ultraviolet and soft x ray lasers
[AD-A249798] p 3657 N92-30784
Tm,Ho:YAG laser with tunable range of 2.08-2.12 microns and its applications to spectroscopy
p 3646 N92-31058
Spectroscopic method for Earth-satellite-Earth laser long-path absorption measurements using Retroreflector In Space (RIS) p 3652 N92-31088
LASER STABILITY
Transverse pattern modification in a stable apertured laser resonator
[ITN-92-85171] p 3656 N92-30582
LASER TARGETS
Interaction physics for megajoule laser fusion targets
[DE92-014796] p 3656 N92-30400
LASER WINDOWS
Three-dimensional laser window formation
[NASA-RP-1280] p 3585 N92-30307
LASERS
Solid lubrication of laser grown fluorinated diamond thin films
[AD-A249485] p 3603 N92-30635
Sixteenth International Laser Radar Conference, part 2
[NASA-CP-3158-PT-2] p 3637 N92-31013
Altimetry and lidar using AlGaAs lasers modulated with pseudo-random codes p 3641 N92-31030
LATENT HEAT
Design and simulation of latent heat storage units
[DE91-002145] p 3670 N92-30330
LATERAL CONTROL
On-line analysis capabilities developed to support the AFW wind-tunnel tests
[NASA-TM-107651] p 3580 N92-30752
LATTICES (MATHEMATICS)
The two-dimensional random walk: Its hitting process and its classification
[CWI-BS-R9003] p 3705 N92-30689
LAUNCH VEHICLES
An electromechanical actuation system for an expendable launch vehicle
[NASA-TM-105774] p 3586 N92-30310
Space transportation systems, launch systems, and propulsion for the Space Exploration Initiative: Results from Project Outreach
[NASA-CR-190345] p 3587 N92-30958

LAUNCHING
Debris/ice/TPS assessment and integrated photographic analysis for Shuttle Mission STS-45
[NASA-TM-107545] p 3586 N92-30382
LAVA
Fractal analysis: A new remote sensing tool for lava flows p 3736 N92-31224
LEAD ALLOYS
Mechanical design and finite element analysis of the SDC central calorimeter
[DE92-011197] p 3655 N92-31109
LEAD ZIRCONATE TITANATES
Thermally activated rejuvenation of ferroelectric properties in electrically fatigued lead zirconate titanate ceramics
[DE92-012634] p 3605 N92-30830
LEADERSHIP
Research and technology, 1991. Langley Research Center
[NASA-TM-4331] p 3744 N92-30733
LEARNING
Dense modifiable interconnections utilizing photorefractive volume holograms
[AD-A252193] p 3637 N92-30546
LEAST SQUARES METHOD
Vector analysis of ice fabric data
[AD-A250832] p 3682 N92-30832
A strictly improving linear programming algorithm based on a series of Phase 1 problems
[DE92-015905] p 3696 N92-30905
LEPTONS
Linear estimates of structure functions from deep inelastic lepton-nucleon scattering data, part 1
[DE92-627288] p 3713 N92-30403
LEWIS NUMBERS
The influence of Lewis number and nonhomogeneous mixture on premixed turbulent flame structure p 3597 N92-30669
Pre-mixed flame simulations for non-unity Lewis numbers p 3597 N92-30670
LIAPUNOV FUNCTIONS
Parallel aspects of some spectral problems in linear algebra
[CWI-NM-R9113] p 3706 N92-30700
LIE GROUPS
Some model theory of free groups and free algebras
[AD-A249425] p 3706 N92-30776
Example of a quantum field theory based on a nonlinear Lie algebra
[DE92-010475] p 3731 N92-30825
LIFE SCIENCES
Aerospace medicine and biology: A continuing bibliography with indexes (supplement 363)
[NASA-SP-7011(363)] p 3685 N92-30987
LIFE SUPPORT SYSTEMS
Waste streams in a typical crewed space habitat: An update
[NASA-TM-103888] p 3689 N92-31166
LIFTING BODIES
Real-time simulation model of the HL-20 lifting body
[NASA-TM-107580] p 3586 N92-31160
LIFTING REENTRY VEHICLES
Preliminary subsonic aerodynamic model for simulation studies of the HL-20 lifting body
[NASA-TM-4302] p 3583 N92-31175
LIGANDS
Studies of thermal decomposition of the 1:1 R3Al:en adduct (R = Me, Et; en = ethylenediamine): Synthesis and structure of a novel intermediate Al((HNCH2CH2NH)AlMe2)3
[AD-A251061] p 3603 N92-30623
LIGHT AMPLIFIERS
Optical isolators in high power lasers based on high reflectivity phase conjugate mirrors
[IA-1452] p 3721 N92-30581
An alexandrite regenerative amplifier for water vapor and temperature measurements p 3645 N92-31048
An ultra-sensitive coherent detector capable of single photon detection for lidar applications p 3646 N92-31053
LIGHT CURVE
Wave propagation and vibration of fibre-reinforced laminates
[AD-A252101] p 3590 N92-30528
LIGHT EMISSION
Wave propagation and vibration of fibre-reinforced laminates
[AD-A252101] p 3590 N92-30528
LIGHT EMITTING DIODES
Assessment of a head-mounted miniature monitor
[NASA-TM-103587] p 3688 N92-30381
LIGHT SCATTERING
Depolarized light scattering and dynamic shear compliance of viscoelastic liquids
[AD-A252491] p 3721 N92-30536
Clouds: Their prediction and simulation
[AD-A250643] p 3679 N92-30643
Numerical simulations of light scattering from rough one-dimensional gold surfaces
[AD-A249794] p 3721 N92-30783
LIGHT TRANSMISSION
Optical isolators in high power lasers based on high reflectivity phase conjugate mirrors
[IA-1452] p 3721 N92-30581
LIMITERS (FUSION REACTORS)
Boundary plasma transport studies on TFTR
[DE92-011942] p 3723 N92-30746
LIMITS (MATHEMATICS)
Bifurcation of limit cycles in a particular class of quadratic systems
[REPT-91-76] p 3703 N92-30457
LINE SPECTRA
Modeling of UV lines from cataclysmic variable winds
[DE92-013443] p 3739 N92-30862
Line-emission cross sections for the charge-exchange reaction between fully stripped carbon and atomic hydrogen in tokamak plasma
[NIFS-129] p 3716 N92-30967
LINEAR ACCELERATORS
The RADLAC beam propagation experiment
[DE92-014620] p 3718 N92-30624
LINEAR ARRAYS
On the radial component of the electric field for a monopole phased array antenna focused in the near zone
[AD-A249441] p 3616 N92-30761
LINEAR EQUATIONS
About difference equations, algebras and discrete events
[REPT-91-87] p 3704 N92-30491
Parallel aspects of some spectral problems in linear algebra
[CWI-NM-R9113] p 3706 N92-30700
Minimization of deviations of gear real tooth surfaces determined by coordinate measurements
[NASA-TM-105718] p 3660 N92-30948
Component-wise error bounds for linear equations
[DE92-016000] p 3707 N92-31189
LINEAR PROGRAMMING
A survey on pivot rules for linear programming
[REPT-91-99] p 3691 N92-30351
Degeneracy in interior point methods for linear programming
[REPT-91-102] p 3691 N92-30353
Achievable potential reductions in the method of Kojima et al. in the case of linear programming
[REPT-91-78] p 3693 N92-30435
Iri's polynomiality proof for the Iri-Imai method recast
[REPT-91-74] p 3693 N92-30455
A strictly improving linear programming algorithm based on a series of Phase 1 problems
[DE92-015905] p 3696 N92-30905
LINEAR QUADRATIC REGULATOR
Microgravity vibration isolation: Optimal preview and feedback control
[NASA-TM-105673] p 3613 N92-30692
LINEAR SYSTEMS
GMRESR: A family of nested GMRES methods
[REPT-91-80] p 3703 N92-30437
Further experiences with GMRESR
[REPT-92-12] p 3704 N92-30461
Contribution of parallelism to solving a load distribution problem in electric networks
[ETN-92-91668] p 3625 N92-30702
LINEARIZATION
Nonlinear system design: Adaptive feedback linearization with unmodeled dynamics
[AD-A248484] p 3700 N92-30335
Global existence for a semilinear elliptic-parabolic PDE system
[REPT-91-70] p 3628 N92-30372
Strong dynamic input-output decoupling: From linearity to nonlinearity
[MEMO-COSOR-92-04] p 3694 N92-30478
LINKAGES
Quick acting gimbal joint
[NASA-CASE-MSC-21918-1] p 3658 N92-30316
LIQUEFACTION
Emissions of greenhouse gases from the use of transportation fuels and electricity
[DE92-012102] p 3674 N92-30770
LIQUID COOLING
Mixed and forced convection from an array of discrete heat sources in a vertical channel
[AD-A248853] p 3731 N92-30235
LIQUID CRYSTALS
A shear sensitive monomer-polymer laminate structure and method of using same
[NASA-CASE-LAR-14654-1] p 3662 N92-30317
LIQUID FLOW
Continuum approaches for describing solid-liquid flow
[AD-A249028] p 3629 N92-30560
LIQUID HELIUM
Coefficients of the second viscosity in bulk liquid helium
[AD-A252421] p 3629 N92-30548
LIQUID LITHIUM
MHD considerations for a self-cooled liquid lithium blanket
[DE92-014864] p 3723 N92-30591
LIQUID METALS
Transport phenomena in welds
[DE92-013404] p 3659 N92-30587
LIQUID PROPELLANT ROCKET ENGINES
Rocket propulsion research at Lewis Research Center
[NASA-CR-189187] p 3732 N92-30908
LIQUID ROCKET PROPELLANTS
Rocket propulsion research at Lewis Research Center
[NASA-CR-189187] p 3732 N92-30908
LIQUID-SOLID INTERFACES
Continuum approaches for describing solid-liquid flow
[AD-A249028] p 3629 N92-30560
LIQUIDS
Prediction of coincidence frequencies for a thin-walled, fluid-filled pipe
[MRL-TN-600] p 3664 N92-30963
LITHIUM ALLOYS
NDE characterization of the microstructure and mechanical properties of Al-Li alloys
[DE92-012154] p 3598 N92-30858
Environmental fatigue of an Al-Li-Cu alloy. Part 2: Microscopic hydrogen cracking processes
[NASA-TM-107620] p 3664 N92-31214
Environmental fatigue of an Al-Li-Cu alloy. Part 3: Modeling of crack tip hydrogen damage
[NASA-TM-107619] p 3665 N92-31215
LITHIUM BORATES
Growth and evaluation of nonlinear optical materials for laser applications: Barium borate, lithium borate, and silver gallium selenide
[AD-A248861] p 3624 N92-30617
LITHOSPHERE
Is the Venusian lithosphere subducting? p 3738 N92-31234
LOAD TESTS
Proceedings of a Beryllium Technology Workshop
[DE92-012312] p 3598 N92-30834
LOADS (FORCES)
Designing, engineering, and testing wood structures p 3593 N92-30270
Control and augmentation of passive porosity through transpiration control
[NASA-CASE-LAR-14682-1] p 3628 N92-30387
Design feasibility study of a Space Station Freedom truss
[NASA-TM-105558] p 3659 N92-30571
LOCAL AREA NETWORKS
Remote experimental site concept for diagnostic collaborations in fusion
[DE92-010437] p 3724 N92-30824
LOGIC CIRCUITS
High level synthesis of controlpath microarchitectures
[MEMO-INF-91-86] p 3690 N92-30698
LOGIC PROGRAMMING
A computational proof of soundness
[MEMO-INF-92-09] p 3693 N92-30433
LOGISTICS
Operations and logistics tasks in the Columbus development program
[MBB-UO-0166-91-PUB] p 3708 N92-30419
Adoption of the LSA S/W DILSA for the Columbus LSA tasks
[MBB-UO-0168-91-PUB] p 3709 N92-30420
Columbus logistics transportation and ground processing
[MBB-UO-0167-91-PUB] p 3709 N92-30442
Quality assurance and ILS p 3697 N92-30953
Practical application of the ILS: Practical integration, design, and logistics p 3697 N92-30955
LOGISTICS MANAGEMENT
ILS, CE, CALS? From design to operation
[ETN-92-91717] p 3697 N92-30950
First conclusions of a manufacturer group on the applicability of CALS in Europe p 3697 N92-30951
Quality assurance and ILS p 3697 N92-30953
Preparation for a new plane (A 320): Experience reviewed p 3697 N92-30954
Practical application of the ILS: Practical integration, design, and logistics p 3697 N92-30955
Flight crew integration in the maintenance chain of a commercial aircraft (A 320) p 3698 N92-30957
LONG DURATION EXPOSURE FACILITY
Ellipsometric study of oxide films formed on LDEF metal samples
[AD-A249856] p 3599 N92-31110

Analysis, review, and documentation of the activation data from LDEF material
[NASA-CR-184356] p 3596 N92-31161
Environment modelling in near Earth space: Preliminary LDEF results p 3588 N92-31225

LONG DURATION SPACE FLIGHT
Light as a chronobiologic countermeasure for long-duration space operations
[NASA-TM-103874] p 3686 N92-31167

LORAN C
The MARCOR GPS mobile data system
p 3620 N92-30944

LORENTZ TRANSFORMATIONS
Quantum mechanics in Grassmann space
[DE92-622377] p 3711 N92-30801

LOW ALTITUDE
Resolution of the three-dimensional parabolic equation applied to acoustic propagation at low altitudes
[ONERA-RF-17/3641-PY] p 3711 N92-30966

LOW COST
Supercritical fluid extraction: A new process for producing high-performance, low-cost carbon fibers
[AD-A249407] p 3595 N92-30773
Performance of ground-based high-frequency receiving arrays with electrically-small ground planes
[AD-A250489] p 3621 N92-31130

LOW DENSITY FLOW
Monte Carlo particle simulation of low-density fluid flow on MIMD supercomputers
[DE92-014618] p 3630 N92-30607

LOW FREQUENCIES
Low-frequency fluctuations in plasma magnetic fields
[DE92-012139] p 3724 N92-30833
Effect of wave-particle interaction on the outflow of ions at high latitudes
[NASA-CR-190560] p 3677 N92-30962

LOW GRAVITY MANUFACTURING
A reduced gravity fiber pulling apparatus
[NASA-TM-103594] p 3612 N92-30971

LOW NOISE
Modification of 95 GHz radar source module for low phase noise operation
[AD-A249793] p 3622 N92-31180

LOW REYNOLDS NUMBER
Mixed and forced convection from an array of discrete heat sources in a vertical channel
[AD-A248853] p 3731 N92-30235
Low Reynolds number kappa-epsilon modeling with the aid of direct simulation data p 3631 N92-30655
Numerical simulation of low Prandtl number turbulent mixing p 3633 N92-30663

LOW TEMPERATURE
Coefficients of the second viscosity in bulk liquid helium
[AD-A252421] p 3629 N92-30548
Anomalous hopping conductivity in amorphous indium-oxide films
[ITN-92-85166] p 3729 N92-30781
Transient photoconductivity of low temperature GaAs grown by molecular beam epitaxy terahertz radar applications
[DE92-011848] p 3729 N92-30854

LOWER ATMOSPHERE
A comparison of lidar inversion methods for cirrus applications p 3649 N92-31074
Lidar measurements using large liquid mirror telescopes p 3652 N92-31087
Airborne water vapor DIAL research: System development and field measurements
p 3653 N92-31093
Aerosol extinction measurements with CO2-lidar
p 3655 N92-31105

LUBRICANT TESTS
Development of a full-scale transmission testing procedure to evaluate advanced lubricants
[NASA-TP-3265] p 3658 N92-30396

LUBRICANTS
Modelling of heavily loaded lubricated contacts
[AD-A248807] p 3659 N92-30554
Interface friction, lubricants, and their influence on metal flow
[DE92-012112] p 3606 N92-30866

LUBRICATING OILS
Development of a full-scale transmission testing procedure to evaluate advanced lubricants
[NASA-TP-3265] p 3658 N92-30396

LUBRICATION
Development of a full-scale transmission testing procedure to evaluate advanced lubricants
[NASA-TP-3265] p 3658 N92-30396
Solid lubrication of laser grown fluorinated diamond thin films
[AD-A249485] p 3603 N92-30635

LUBRICATION SYSTEMS
Modelling of heavily loaded lubricated contacts
[AD-A248807] p 3659 N92-30554

LUMINAIRES
Examination of aircraft warning and caution lights after shock testing
[NLR-TP-89284-U] p 3578 N92-30474

LUMINESCENCE
A method of making a single layer multi-color luminescent display
[NASA-CASE-LAR-14811-1] p 3622 N92-30389
Theoretical study of phase-shifted quantum beats in time-resolved luminescence spectra from a biased asymmetric double quantum well
[AD-A252422] p 3710 N92-30549
Nonlinear RR Lyrae models with new Livermore opacities
[DE92-011158] p 3741 N92-31108

LUNAR COMPOSITION
On the isotopic signature of recent solar-wind nitrogen
p 3738 N92-31231

LUNAR GRAVITATION
A reduced gravity fiber pulling apparatus
[NASA-TM-103594] p 3612 N92-30971

LUNAR GRAVITY SIMULATOR
A reduced gravity fiber pulling apparatus
[NASA-TM-103594] p 3612 N92-30971

LUNAR ROCKS
On the isotopic signature of recent solar-wind nitrogen
p 3738 N92-31231

LUNAR ROVING VEHICLES
Method for remotely powering a device such as a lunar rover
[NASA-CASE-LAR-14789-1] p 3658 N92-30388

LUNAR SOIL
On the isotopic signature of recent solar-wind nitrogen
p 3738 N92-31231

M

MACH NUMBER
Interaction of isotropic turbulence with a shock wave
[AD-A250409] p 3635 N92-30852

MAGELLAN PROJECT (NASA)
Science questions for the Magellan continuing mission
p 3738 N92-31235

MAGNETIC ANOMALIES
Design and construction of a Helmholtz coil magnetic test cell
[AD-A249944] p 3585 N92-30849

MAGNETIC BEARINGS
Magnetic bearings for free-piston Stirling engines
[NASA-TM-105730] p 3660 N92-30734
Cryogenic Magnetic Bearing Test Facility (CMBTF)
[NASA-CR-189087] p 3582 N92-31164

MAGNETIC COILS
Design and construction of a Helmholtz coil magnetic test cell
[AD-A249944] p 3585 N92-30849

MAGNETIC CORES
Comparison of high temperature, high frequency core loss and dynamic B-H loops of a 2V-49Fe-49Co and a grain oriented 3Si-Fe alloy
[NASA-TM-105791] p 3623 N92-30397

MAGNETIC DIPOLES
Magnetic field measurements of Fermilab/General Dynamics built full scale SSC collider dipole magnets
[DE92-014612] p 3717 N92-30589
Magnetic measurement instrumentation developments at the SSC
[DE92-013969] p 3718 N92-30786

MAGNETIC DOMAINS
Demonstration of magnetic domain boundary movement using an easily assembled videocam-microscope system
p 3611 N92-30286

MAGNETIC FIELD CONFIGURATIONS
Solar flare MDH
[AD-A250639] p 3702 N92-30375
Field line diversion properties of finite beta helias equilibria
[NIFS-137] p 3722 N92-30385
Role of compressibility on driven magnetic reconnection
[NIFS-105] p 3710 N92-30498
Pressure profiles, resonant Pfirsch-Schlueter currents, thermal instabilities, and magnetic island formation
[DE92-015166] p 3726 N92-31002
FNAS: The magnetic configuration leading to solar flares
[NASA-CR-190522] p 3743 N92-31168

MAGNETIC FIELD INVERSIONS
Temperature dependence of universal conductance fluctuations in narrow Si inversion layers
p 3625 N92-30730

MAGNETIC FIELD RECONNECTION
Role of compressibility on driven magnetic reconnection
[NIFS-105] p 3710 N92-30498
The role of stochasticity in sawtooth oscillation
[NIFS-103] p 3710 N92-30983

MAGNETIC FIELDS
Demonstration of magnetic domain boundary movement using an easily assembled videocam-microscope system
p 3611 N92-30286
Magnetic surface breaking in 3D MHD equilibria of I = 2 heliotron
[NIFS-130] p 3722 N92-30384
Field line diversion properties of finite beta helias equilibria
[NIFS-137] p 3722 N92-30385
Negative ion extraction characteristics of a large negative ion source with double-magnetic filter configuration
[NIFS-151] p 3714 N92-30501
Problems with the concept of plasma equilibrium in tokamaks
[DE92-014454] p 3723 N92-30576
Magnetic field measurements of Fermilab/General Dynamics built full scale SSC collider dipole magnets
[DE92-014612] p 3717 N92-30589
Locked modes and magnetic field errors in MST
[DE92-015379] p 3723 N92-30612
One-dimensional subband effects in the conductance of multiple quantum wires in Si-MOSFET's
p 3625 N92-30731
Enhancement of weak localization in a Si lateral superlattice device p 3625 N92-30732
Nonlinear analysis of a grating free-electron laser
[AD-A248833] p 3656 N92-30743
Studies of phonons and electronic excitations in semiconductor heterostructures
[AD-A249406] p 3729 N92-30772
Anomalous hopping conductivity in amorphous indium-oxide films
[ITN-92-85166] p 3729 N92-30781
Low-frequency fluctuations in plasma magnetic fields
[DE92-012139] p 3724 N92-30833
Design and construction of a Helmholtz coil magnetic test cell
[AD-A249944] p 3585 N92-30849
Grain boundary weak links in high-Tc superconductors
[DE92-016192] p 3730 N92-31190

MAGNETIC FLUX
Proceedings, phenomenology and applications of high temperature superconductors
[DE92-011133] p 3627 N92-31107

MAGNETIC LEVITATION VEHICLES
Vehicle/guideway interaction for high speed vehicles on flexible guideway
[DE92-013057] p 3660 N92-30860

MAGNETIC MATERIALS
Comparison of high temperature, high frequency core loss and dynamic B-H loops of a 2V-49Fe-49Co and a grain oriented 3Si-Fe alloy
[NASA-TM-105791] p 3623 N92-30397
Fundamental studies of strongly magnetic rare earth-transition metal alloys
[DE92-015916] p 3600 N92-31186

MAGNETIC MEASUREMENT
Data report, 92-2. Magnetic results, 1985-1990
p 3675 N92-30417
Magnetic measurement instrumentation developments at the SSC
[DE92-013969] p 3718 N92-30786
Design and construction of a Helmholtz coil magnetic test cell
[AD-A249944] p 3585 N92-30849

MAGNETIC MONOPOLES
A steady state tokamak operation by use of magnetic monopoles
[DE92-799109] p 3725 N92-30991

MAGNETIC PROPERTIES
Superconductivity and magnetism in rapidly solidified perovskites
[DE92-014081] p 3597 N92-30588
Structural and magnetic properties of RBa2Cu2NbO8 (R = La, Pr, and Nd)
[DE92-014780] p 3729 N92-30885

MAGNETIC STORMS
Magnetospheric structure and dynamics: A multisatellite approach
[AD-A252326] p 3676 N92-30720

MAGNETIC SUSPENSION
Magnetic bearings for free-piston Stirling engines
[NASA-TM-105730] p 3660 N92-30734

MAGNETIC VARIATIONS
Temperature dependence of universal conductance fluctuations in narrow Si inversion layers
p 3625 N92-30730

MAGNETOHYDRODYNAMIC FLOW
Role of compressibility on driven magnetic reconnection
[NIFS-105] p 3710 N92-30498

MAGNETOHYDRODYNAMIC STABILITY
Numerical simulation of the electromagnetic instability of an intense beam in a quadrupole focusing system
[AD-A252275] p 3614 N92-30407
Problems with the concept of plasma equilibrium in tokamaks
[DE92-014454] p 3723 N92-30576
Locked modes and magnetic field errors in MST
[DE92-015379] p 3723 N92-30612
Two dimensional aspects of toroidal drift waves in the ballooning representation
[DE92-014028] p 3724 N92-30880
The Rayleigh-Taylor instability in an expanding plasma
[DE92-013883] p 3725 N92-30884
The role of stochasticity in sawtooth oscillation
[NIFS-103] p 3710 N92-30983
Beta limit of resistive plasma in torsatron/heliotron
[NIFS-131] p 3725 N92-30985
Kinetic approach to long wave length modes in rotating plasmas
[NIFS-138] p 3725 N92-30993
Three-dimensional MHD equilibrium in the presence of bootstrap current for Large Helical Device (LHD)
[NIFS-139] p 3725 N92-30994
Pressure profiles, resonant Pfirsch-Schlueter currents, thermal instabilities, and magnetic island formation
[DE92-015166] p 3726 N92-31002
Criteria and design trade-off issues for ITER
[DE92-011786] p 3726 N92-31114
Fundamental studies of fusion plasmas
[DE92-015077] p 3726 N92-31116

MAGNETOHYDRODYNAMIC WAVES
FNAS: The magnetic configuration leading to solar flares
[NASA-CR-190522] p 3743 N92-31168

MAGNETOHYDRODYNAMICS
Magnetic surface breaking in 3D MHD equilibria of I = 2 heliotron
[NIFS-130] p 3722 N92-30384
Role of compressibility on driven magnetic reconnection
[NIFS-105] p 3710 N92-30498
MHD considerations for a self-cooled liquid lithium blanket
[DE92-014864] p 3723 N92-30591
Three-dimensional MHD equilibrium in the presence of bootstrap current for Large Helical Device (LHD)
[NIFS-139] p 3725 N92-30994
Dynamics and energetics of the solar corona
[NASA-CR-190664] p 3742 N92-31162
FNAS: The magnetic configuration leading to solar flares
[NASA-CR-190522] p 3743 N92-31168

MAGNETOMETERS
Data report, 92-2. Magnetic results, 1985-1990
p 3675 N92-30417

MAGNETOPLASMADYNAMICS
Dynamics and energetics of the solar corona
[NASA-CR-190664] p 3742 N92-31162

MAGNETORESISTIVITY
Quantum interference and confinement effects in narrow channel Si-MOSFET's
[ETN-92-91742] p 3625 N92-30729
Temperature dependence of universal conductance fluctuations in narrow Si inversion layers
p 3625 N92-30730
Enhancement of weak localization in a Si lateral superlattice device p 3625 N92-30732
Anomalous hopping conductivity in amorphous indium-oxide films
[ITN-92-85166] p 3729 N92-30781

MAGNETOSPHERE-IONOSPHERE COUPLING
Effect of wave-particle interaction on the outflow of ions at high latitudes
[NASA-CR-190560] p 3677 N92-30962

MAGNETOSPHERIC INSTABILITY
Role of compressibility on driven magnetic reconnection
[NIFS-105] p 3710 N92-30498

MAGNIFICATION
On the magnification of Cantor sets and their limit models
[REPT-91-100] p 3691 N92-30352

MAGNONS
Studies of phonons and electronic excitations in semiconductor heterostructures
[AD-A249406] p 3729 N92-30772

MAINTAINABILITY
Center for Composites Manufacturing Science, Reliability, and Maintainability Technology
[AD-A248661] p 3591 N92-30639

MAINTENANCE
Potential airfield sites in Antarctica for wheeled aircraft
[AD-A249503] p 3584 N92-30621
Development of a reliability maintenance optimization method p 3697 N92-30956
A failure-to-restore unavailability model for periodically performed maintenance
[DE92-015902] p 3708 N92-31185

MAN ENVIRONMENT INTERACTIONS
Small satellite radiation budget instrumentation
[DE92-011134] p 3677 N92-31008

MAN MACHINE SYSTEMS
Cable compliance
[NASA-TP-3216] p 3612 N92-30378

MAN-COMPUTER INTERFACE
Controlling user interface objects through pre- and postconditions
[REPT-92-04] p 3692 N92-30356
Integrating commercial off-the-shelf tools for custom software development
[AD-A252462] p 3695 N92-30550
Introduction to human factors and wide area networking
[AD-A252310] p 3688 N92-30718

MANAGEMENT ANALYSIS
DE-CERTS: A decision support system for a comparative evaluation method for risk management methodologies and tools
[AD-A246965] p 3733 N92-30682
Preparation for a new plane (A 320): Experience reviewed p 3697 N92-30954

MANAGEMENT INFORMATION SYSTEMS
Information systems: How they affect and are affected by organization structure
[AD-A248852] p 3734 N92-30234
First conclusions of a manufacturer group on the applicability of CALS in Europe p 3697 N92-30951

MANAGEMENT METHODS
Informatization in public administration (EGPA-research project 1991). Large scale information systems in The Netherlands
[REPT-91-92] p 3734 N92-30486
Informatization in public administration (EGPA-research project 1991). Large scale information systems (comparative analysis in 8 European countries)
[REPT-91-93] p 3734 N92-30487
The effect of information systems on middle management in the aerospace industry: The Westco case
[AD-A249017] p 3735 N92-30584

MANAGEMENT PLANNING
Grand challenges 1993: High performance computing and communications. A report by the Committee on Physical, Mathematical, and Engineering Sciences to supplement the President's fiscal year 1993 budget
[PB92-160530] p 3689 N92-30600

MANAGEMENT SYSTEMS
Integration mockup and process material management system
[NASA-CR-184319] p 3613 N92-30754
GNAS Maintenance Control Center (GMCC) Design Qualification Test and Evaluation (DQT/E) test procedures
[DOT/FAA/CT-TN91/40] p 3585 N92-30976

MANIFOLDS (MATHEMATICS)
On impasse points of quasilinear differential algebraic equations
[AD-A252643] p 3702 N92-30410
Non-holonomic filtration: Algebraic and geometric aspects of non-integrability
[PB92-178003] p 3706 N92-30790
Heat flow of p-harmonic maps with values into spheres
[DE92-630236] p 3707 N92-31135

MANIPULATORS
Flexible space-based robot modelling and real-time simulation
[NLR-TP-89364-U] p 3658 N92-30477
A description of the research for period 3 of a research program on the planning and control for space robotic manipulators
[NASA-CR-190243] p 3660 N92-30738
On two methods of determining the ellipses and ellipsoids of positioning accuracy of robot manipulators
[ISSN-0208-5658] p 3701 N92-31148

MANNED SPACE FLIGHT
Astronautics 1977-1990
[AERONOMICA-ACTA-F-42-1991] p 3744 N92-30996

MANNED SPACECRAFT
Real-time simulation model of the HL-20 lifting body
[NASA-TM-107580] p 3586 N92-31160

MANUALS
Managing the contract closeout process
[AD-A250701] p 3733 N92-31209

MANUFACTURING
A senior manufacturing laboratory for determining injection molding process capability
p 3609 N92-30273
Laboratory experiments from the toy store
p 3609 N92-30274
Innovative techniques for the production of low cost 2-D laser diode arrays supplies or services and prices/costs
[AD-A252665] p 3656 N92-30552
Printed transformer process/product improvements
[DE92-014760] p 3624 N92-30590
Pulsed microwave processing of high-T(sub c) superconducting films
[DE92-014950] p 3730 N92-31000
Flexible heating head for induction heating apparatus and method
[NASA-CASE-LAR-14679-2] p 3621 N92-31150

MANY BODY PROBLEM
Ginsburg criterion for an equilibrium superradiant model in the dynamic approach
[DE92-630566] p 3732 N92-31203

MAPPING
A formal transformation from the BSI/VDM-SL concrete syntax to the core abstract syntax
[REPT-92-07] p 3692 N92-30359
Coexistence of uniquely ergodic subsystems of interval mapping
[DE92-630231] p 3732 N92-31133
Fixed point iterations for a class of nonlinear mappings in certain Banach spaces
[DE92-630235] p 3706 N92-31134
Heat flow of p-harmonic maps with values into spheres
[DE92-630236] p 3707 N92-31135
Multifractal analysis of chaotic point sets
[AD-A250756] p 3709 N92-31194

MAPS
Global scale concentrations of volcanic activity on Venus: A summary of three 23rd Lunar and Planetary Science Conference abstracts. 1: Venus volcanism: Global distribution and classification from Magellan data. 2: A major global-scale concentration of volcanic activity in the Beta-Atla-Themis region of Venus. 3: Two global concentrations of volcanism on Venus: Geologic associations and implications for global pattern of upwelling and downwelling p 3737 N92-31226

MARINE METEOROLOGY
The United States Antarctic Program
[NSF-90-97] p 3676 N92-30708
Boundary layer structure over the ocean observed by LEANDRE 1 during a tramontane event
p 3638 N92-31014
Aureole lidar: Design, operation, and comparison with in-situ measurements p 3648 N92-31065

MARKET RESEARCH
The MARCOR GPS mobile data system
p 3620 N92-30944

MARKETING
Spinoffs from R and D investments
[DE92-014450] p 3736 N92-30575
Fuel cell systems program plan: Fiscal year 1992
[DE92-015985] p 3672 N92-31188
Fuel cells
[DE92-001282] p 3672 N92-31221

MARKOV CHAINS
Markov chain simulations of binary matrices
[AD-A249265] p 3708 N92-30771

MARKOV PROCESSES
The domain of attraction of the alpha-sum operator for type 2 and type 3 distributions
[REPT-92-02] p 3707 N92-30355

MARS (PLANET)
Space transportation systems, launch systems, and propulsion for the Space Exploration Initiative: Results from Project Outreach
[NASA-CR-190345] p 3587 N92-30958
Twenty-Third Lunar and Planetary Science Conference
[NASA-CR-190178] p 3736 N92-31222

MARS ENVIRONMENT
Global scale concentrations of volcanic activity on Venus: A summary of three 23rd Lunar and Planetary Science Conference abstracts. 1: Venus volcanism: Global distribution and classification from Magellan data. 2: A major global-scale concentration of volcanic activity in the Beta-Atla-Themis region of Venus. 3: Two global concentrations of volcanism on Venus: Geologic associations and implications for global pattern of upwelling and downwelling p 3737 N92-31226

MARS SURFACE
Electrical and chemical interactions at Mars Workshop, part 1
[NASA-CP-10093] p 3741 N92-30302
Duration and rates of discharge: Maja Valles, Mars
p 3737 N92-31227

MARS VOLCANOES
Global scale concentrations of volcanic activity on Venus: A summary of three 23rd Lunar and Planetary Science Conference abstracts. 1: Venus volcanism: Global distribution and classification from Magellan data. 2: A major global-scale concentration of volcanic activity in the Beta-Atla-Themis region of Venus. 3: Two global concentrations of volcanism on Venus: Geologic associations and implications for global pattern of upwelling and downwelling p 3737 N92-31226
MARTENSITIC TRANSFORMATION
Shock-induced martensitic transformation of highly oriented graphite to diamond
[DE92-014787] p 3602 N92-30399
MASERS
A geodetic laser radar rangefinder with 10(exp -7) resolution p 3641 N92-31029
MASKS
Double-sided wafer alignment techniques
[AD-A250757] p 3730 N92-30895
MASS DISTRIBUTION
Quantification and reduction of the uncertainty in mass balance models by Monte Carlo analysis of prior data
[DE92-010278] p 3708 N92-30803
MASS SPECTROMETERS
Laser mass spectrometry for biopolymers
[DE92-015238] p 3597 N92-31184
MASS SPECTROSCOPY
Chemielectron and photoelectron spectroscopic studies of importance in the upper atmosphere
[AD-A248838] p 3675 N92-30556
Ion channeling and spectroscopic ellipsometry examinations of thin-film SiO2/epi-Si structures
[DE92-015129] p 3728 N92-30577
Laser mass spectrometry for biopolymers
[DE92-015238] p 3597 N92-31184
A miniature carbon furnace for mass spectroscopy
[DE92-014460] p 3597 N92-31196
MASSIVELY PARALLEL PROCESSORS
Three-dimensional shock wave physics simulations on massively parallel supercomputers
[DE92-008679] p 3698 N92-30363
Exploiting resource parallelism for integrated fault monitoring and recovery
[AD-A248843] p 3699 N92-30557
Contribution of parallelism to solving a load distribution problem in electric networks
[ETN-92-91668] p 3625 N92-30702
MATCHING
Signal matching by dynamic programming
[REPT-92-01] p 3614 N92-30354
MATERIAL ABSORPTION
Infrared investigations of pristine, doped and partially-doped polypyrrole
[AD-A250644] p 3605 N92-30838
MATERIALS HANDLING
Integration mockup and process material management system
[NASA-CR-184319] p 3613 N92-30754
Organic Matrix Composite Helicopter Internal/External Cargo Pallet System (OMC INTEX)
[AD-A251127] p 3580 N92-30878
MATERIALS RECOVERY
Determining significant material properties: A discovery approach p 3607 N92-30279
MATERIALS SCIENCE
Structural ceramics p 3607 N92-30264
Elementary metallography p 3600 N92-30266
Ceramic processing: Experimental design and optimization p 3607 N92-30267
Standard terminology in the laboratory and classroom p 3610 N92-30277
Five experiments in materials science for less than $10.00 p 3611 N92-30283
Beam technologies for integrated processing
[AD-A252647] p 3612 N92-30411
MATERIALS TESTS
Ceramic processing: Experimental design and optimization p 3607 N92-30267
Crack growth processes at elevated temperatures in advanced materials
[AD-A249023] p 3662 N92-30558
Influence of various carbon fibre types on the mechanical performance and damage tolerance of composites
[MBB/FE202/S/PUB/477] p 3591 N92-30690
Nondestructive testing of ceramics for vehicular advanced heat engines
[DE92-010471] p 3604 N92-30744
Proceedings of a Beryllium Technology Workshop
[DE92-012312] p 3598 N92-30834
MATHEMATICAL MODELS
Mathematical models of non-linear mechanical and electrical systems and their qualitative behavior
[AD-A248847] p 3622 N92-30249
Modeling and analysis methodology for aeroelastically tailored chordwise deformable wings
[NASA-CR-189620] p 3579 N92-30304
Scale symmetry of quantum solitons
[DE92-624560] p 3712 N92-30331
The diffraction of short free surface water waves, a uniform expansion
[REPT-92-06] p 3628 N92-30358
Modeling fast modulation effects in cesium atomic clocks
[AD-A252649] p 3636 N92-30412
Low-velocity impact loading on fibre reinforced aluminum laminates (ARALL) and other aircraft sheet materials
[ETN-92-91613] p 3590 N92-30414
Joint queue length and response time distributions in a general preemptive feedback queue
[REPT-91-66] p 3701 N92-30451
Flow of fresh and salt water in an aquifer with injection from the top
[REPT-91-68] p 3629 N92-30453
Iri's polynomiality proof for the Iri-Imai method recast
[REPT-91-74] p 3693 N92-30455
Alignment of a 3-D sensor and a 2-D sensor measuring azimuth and elevation
[AD-A252120] p 3636 N92-30530
Development of a modular transient cycle analysis program for the adiabatic diesel and other compound diesel engines
[AD-A249022] p 3658 N92-30538
Modelling of heavily loaded lubricated contacts
[AD-A248807] p 3659 N92-30554
Continuum approaches for describing solid-liquid flow
[AD-A249028] p 3629 N92-30560
Ultrasound NDE of adhesive bond integrity: A quantitative measure
[AD-A248845] p 3661 N92-30599
A numerical evaluation of the dynamical systems approach to wall layer turbulence p 3632 N92-30660
Low order dynamical models for mixing layers p 3633 N92-30662
Geometry of premixed flames in three-dimensional turbulence p 3633 N92-30666
Laminar flamelet modeling of turbulent diffusion flames p 3633 N92-30667
Calculation of viscous hypersonic flows in chemical non-equilibrium
[MBB/FE211/S/PUB/466] p 3634 N92-30674
Numerical optimization in Germany: A non-exhaustive survey on current activities with emphasis on aeronautics
[MBB/FE211/S/PUB/474] p 3573 N92-30675
Non-perturbative effects in high-energy electroweak interactions
[NIKHEF-H/91-24] p 3715 N92-30697
Trajectory fitting in function space with application to analytic modeling of surfaces
[NASA-TP-3232] p 3576 N92-30747
Finite difference time domain modeling of steady state scattering from jet engines with moving turbine blades
[NASA-CR-190290] p 3582 N92-30753
Composite beam analysis linear analysis of naturally curved and twisted anisotropic beams
[AD-A252652] p 3663 N92-30766
Numerical simulation of the dynamic behavior of the polymeric gels
[DE92-011358] p 3605 N92-30804
Low-frequency fluctuations in plasma magnetic fields
[DE92-012139] p 3724 N92-30833
Evaporation duct effects at millimeter wavelengths
[AD-A250239] p 3617 N92-30876
Characterizing ultrasonic transducers using pattern recognition techniques
[DE92-015845] p 3711 N92-30890
Resolution of the three-dimensional parabolic equation applied to acoustic propagation at low altitudes
[ONERA-RF-17/3641-PY] p 3711 N92-30966
Development of software to improve AC power quality on large spacecraft
[NASA-CR-190569] p 3589 N92-30989
Numerical simulation of crater formation heating by laser beam. Analysis of radiation exchanges in the cavity
[ESA-TT-1234] p 3657 N92-30997
Lidar multiple scattering: Dependence on atmospheric parameters p 3647 N92-31061
Correction for nonlinear photon counting effects in lidar systems p 3649 N92-31070
On two methods of determining the ellipses and ellipsoids of positioning accuracy of robot manipulators
[ISSN-0208-5658] p 3701 N92-31148
A tolerance approach to visual shape perception and image matching analysis for modeling of micro-heterogeneous materials
[ISSN-0208-5658] p 3721 N92-31149
Preliminary subsonic aerodynamic model for simulation studies of the HL-20 lifting body
[NASA-TM-4302] p 3583 N92-31175
A failure-to-restore unavailability model for periodically performed maintenance
[DE92-015902] p 3708 N92-31185
Environmental fatigue of an Al-Li-Cu alloy. Part 3: Modeling of crack tip hydrogen damage
[NASA-TM-107619] p 3665 N92-31215
MATRICES
Markov chain simulations of binary matrices
[AD-A249265] p 3708 N92-30771
MATRICES (MATHEMATICS)
On impasse points of quasilinear differential algebraic equations
[AD-A252643] p 3702 N92-30410
A new matrix formulation of classical electrodynamics. Part 1: Vacuum
[AD-A249643] p 3616 N92-30721
Sparse distributed memory and related models
[NASA-CR-190553] p 3690 N92-30724
MATRIX MATERIALS
Center for Composites Manufacturing Science, Reliability, and Maintainability Technology
[AD-A248661] p 3591 N92-30639
Laser mass spectrometry for biopolymers
[DE92-015238] p 3597 N92-31184
MATTER (PHYSICS)
Constraints on the nuclear matter equation of state from pulsar glitches
[DE92-015142] p 3740 N92-30578
MAXIMUM LIKELIHOOD ESTIMATES
Doppler mean velocity estimation: Small sample analysis and a new estimator
[AD-A249024] p 3678 N92-30559
Effect of bending on the room-temperature tensile strengths of structural ceramics
[DE92-015196] p 3603 N92-30626
Maximum likelihood detection of electro-optic moving targets
[AD-A249442] p 3616 N92-30762
MAXWELL EQUATION
Finite difference time domain modeling of steady state scattering from jet engines with moving turbine blades
[NASA-CR-190290] p 3582 N92-30753
MAXWELL FLUIDS
Kinetic approach to long wave length modes in rotating plasmas
[NIFS-138] p 3725 N92-30993
MEASURING INSTRUMENTS
Method of measuring cross-flow vortices by use of an array of hot-film sensors
[NASA-CASE-LAR-14824-1-SB] p 3628 N92-30390
Magnetic measurement instrumentation developments at the SSC
[DE92-013969] p 3718 N92-30786
Results of the heavy ion beam probe measurements on the Advanced Toroidal Facility
[DE92-014461] p 3726 N92-31197
MECHANICAL PROPERTIES
Ceramic processing: Experimental design and optimization p 3607 N92-30267
Mechanical properties of brittle materials p 3612 N92-30290
Influence of various carbon fibre types on the mechanical performance and damage tolerance of composites
[MBB/FE202/S/PUB/477] p 3591 N92-30690
Effects of impurities on the mechanical behaviour of primary and secondary cast aluminum alloys
[PB92-180652] p 3598 N92-30785
Nondestructive characterization of two-phase metal-matrix materials
[AD-A249912] p 3592 N92-30815
NDE characterization of the microstructure and mechanical properties of Al-Li alloys
[DE92-012154] p 3598 N92-30858
Mechanical behavior and processing of aluminum metal matrix composites
[AD-A249918] p 3592 N92-30874
YBa2Cu(3-x)Co(x)O(y): A substrate material for YBCO superconductors
[DE92-015182] p 3730 N92-30999
MECHANICAL SHOCK
Modeling initiation of explosives by projectile impact
[DE92-015210] p 3608 N92-31202
MECHANICAL TWINNING
Mechanism of slip and twinning p 3610 N92-30280
MEDITERRANEAN SEA
Boundary layer structure over the ocean observed by LEANDRE 1 during a tramontane event p 3638 N92-31014
MELTING
Experiments with the low melting indium-bismuth alloy system p 3601 N92-30272
Studies on the melt flow rate of the SRM 1473: A low density polyethylene resin
[PB92-181080] p 3604 N92-30788

Elastic constants of crystals near melting via density functional theory. Effect of three-body correlations
[DE92-630567] p 3730 N92-31191

MELTING POINTS
Experiments with the low melting indium-bismuth alloy system p 3601 N92-30272
Thermoset precursor to monolithic carbon glass prepared by the Pd/Cu-catalyzed alkynylation of polyphenylenes
[AD-A249920] p 3605 N92-30816

MEMBRANES
Analysis and synthesis of adaptive neural elements and assembles
[AD-A248467] p 3687 N92-30320
Photochemical solar energy conversion utilizing semiconductors localized in membrane-mimetic systems
[DE92-011115] p 3670 N92-30694

MEMORY (COMPUTERS)
Computing with faulty shared memory
[DE92-011663] p 3695 N92-30522
Sparse distributed memory and related models
[NASA-CR-190553] p 3690 N92-30724

MENTAL PERFORMANCE
Induced pictorial representations
[AD-A248560] p 3687 N92-30336

MERCURY CADMIUM TELLURIDES
HgCdTe photomixers for CO2 laser radar systems p 3654 N92-31100

MERCURY ISOTOPES
Lifetimes of low spin states in the superdeformed band of Hg-192
[DE92-011066] p 3728 N92-30684

MERIDIONAL FLOW
The calculation of mid-latitude meridional neutral winds from an improved servo model approximation method
[AD-A249874] p 3676 N92-30868

MESOMETEOROLOGY
On the potential use of the terminal Doppler weather radar gust front detection algorithm on the WSR-88D system. Part 2: Detecting non-gust front convergent weather phenomena
[DOT/FAA/NR-92/8,II] p 3678 N92-30496

MESONS
Remarks on the exotic U-meson
[RAL-91-090] p 3715 N92-30750

MESOSCALE PHENOMENA
On the potential use of the terminal Doppler weather radar gust front detection algorithm on the WSR-88D system. Part 2: Detecting non-gust front convergent weather phenomena
[DOT/FAA/NR-92/8,II] p 3678 N92-30496
Low-level atmospheric flows studied by pulsed Doppler lidar p 3638 N92-31015

MESOSPHERE
Sixteenth International Laser Radar Conference, part 2
[NASA-CP-3158-PT-2] p 3637 N92-31013

METAL BONDING
Method of bonding carbon-carbon and metal matrix composite structures
[AD-D015299] p 3591 N92-30573

METAL FATIGUE
Environmental fatigue of an Al-Li-Cu alloy. Part 2: Microscopic hydrogen cracking processes
[NASA-TM-107620] p 3664 N92-31214

METAL FILMS
MBE grown copper-aluminum alloy films
[AD-A252486] p 3597 N92-30534

METAL IONS
Tunable solid state lasers based on molecular ions
[AD-A249423] p 3656 N92-30774

METAL MATRIX COMPOSITES
On recrystallization in metal matrix composites
[DE92-011364] p 3590 N92-30521
Method of bonding carbon-carbon and metal matrix composite structures
[AD-D015299] p 3591 N92-30573
Metal matrix composite analyzer (METCAN) user's manual, version 4.0
[NASA-TM-105244] p 3592 N92-30779
Nondestructive characterization of two-phase metal-matrix materials
[AD-A249912] p 3592 N92-30815
Mechanical behavior and processing of aluminum metal matrix composites
[AD-A249918] p 3592 N92-30874

METAL OXIDE SEMICONDUCTORS
Quantum interference and confinement effects in narrow channel Si-MOSFET's
[ETN-92-91742] p 3625 N92-30729
Temperature dependence of universal conductance fluctuations in narrow Si inversion layers p 3625 N92-30730
One-dimensional subband effects in the conductance of multiple quantum wires in Si-MOSFET's p 3625 N92-30731
Enhancement of weak localization in a Si lateral superlattice device p 3625 N92-30732
Focused ion beam implantation
[AD-A249662] p 3627 N92-31004

METAL PLATES
Eulerian simulation of the perforation of aluminum plates by nondeforming projectiles
[DE92-011515] p 3664 N92-31123

METAL SURFACES
Nucleation and growth of diamond on carbon-implanted single crystal copper
[AD-A249021] p 3594 N92-30632
Laser induced reaction for pre-bond surface preparation of aluminum alloys
[AD-A249916] p 3598 N92-30872
Environment modelling in near Earth space: Preliminary LDEF results p 3588 N92-31225

METAL VAPOR LASERS
Generation of a sodium guidestar using a high power dye laser
[DE92-012696] p 3657 N92-31115

METAL VAPORS
Investigations on atomic-vapor-filter high-spectral-resolution lidar for temperature measurements p 3654 N92-31099

METALLIZING
Hybridization of detector array and integrated circuit for readout
[NASA-CASE-NPO-18062-1-CU] p 3623 N92-30542
Mechanical behavior and processing of aluminum metal matrix composites
[AD-A249918] p 3592 N92-30874

METALLOGRAPHY
Elementary metallography p 3600 N92-30266

METALLOIDS
Studies of ordering in semiconducting and other alloys
[AD-A249483] p 3728 N92-30634

METALLURGY
National Educators' Workshop: Update 1991. Standard Experiments in Engineering Materials Science and Technology
[NASA-CP-3151] p 3608 N92-30263

METALORGANIC CHEMICAL VAPOR DEPOSITION
Fabrication of multifilament conductors: CVD processing of high Tc superconducting composite fibers
[NASA-CR-184344] p 3591 N92-30711

METALS
Mechanism of slip and twinning p 3610 N92-30280
Heat-treating of materials p 3601 N92-30292
Cluster assembly of hierarchical nanostructures
[DE92-010498] p 3716 N92-30826
Electron scattering and electromagnetic response properties of metal clusters
[DE92-014715] p 3621 N92-31007

METASTABLE STATE
Studies of ordering in semiconducting and other alloys
[AD-A249483] p 3728 N92-30634

METEORITE CRATERS
The thermal engine of Venus: Implications from the impact crater distribution p 3738 N92-31233

METEORITES
Ablative shielding for hypervelocity projectiles
[NASA-CASE-MSC-21884-1] p 3602 N92-30539

METEORITIC COMPOSITION
The first identification of a mainbelt asteroid source for a meteorite Class E-type Apollo asteroid (3103) 1982BB: A link between the Hungaria asteroid zone and the Aubrite meteorites p 3737 N92-31228
Presolar (?) corundum in the Orgueil meteorite p 3738 N92-31230

METEOROID PROTECTION
Ablative shielding for hypervelocity projectiles
[NASA-CASE-MSC-21884-1] p 3602 N92-30539

METEOROLOGICAL PARAMETERS
Evaporation duct effects at millimeter wavelengths
[AD-A250239] p 3617 N92-30876
Use of INSAT data in rainfall estimation p 3668 N92-30912
Advanced Raman water vapor lidar p 3643 N92-31040
An alexandrite regenerative amplifier for water vapor and temperature measurements p 3645 N92-31048
Lidar multiple scattering: Dependence on atmospheric parameters p 3647 N92-31061
Lidar analysis techniques for use in the atmospheric boundary layer p 3649 N92-31069

METEOROLOGICAL RADAR
Methodology investigation, implement remote sensing
[AD-A248901] p 3678 N92-30340
On the potential use of the terminal Doppler weather radar gust front detection algorithm on the WSR-88D system. Part 1: Impacts of radar system differences
[DOT/FAA/NR-92/8,I] p 3678 N92-30495
On the potential use of the terminal Doppler weather radar gust front detection algorithm on the WSR-88D system. Part 2: Detecting non-gust front convergent weather phenomena
[DOT/FAA/NR-92/8,II] p 3678 N92-30496
Low-level atmospheric flows studied by pulsed Doppler lidar p 3638 N92-31015
Doppler lidar wind measurement with the edge technique p 3638 N92-31017
Design of a near-IR coherent lidar for high spatial and velocity resolution wind measurement p 3639 N92-31020
A compact high repetition rate CO2 coherent Doppler lidar p 3639 N92-31022
Simplified signal processing for an airborne CO2 Doppler lidar p 3639 N92-31023
A comparison of Ultra-Sensitive Coherent Detection (USCD) and heterodyne detection for a wind sensing application p 3640 N92-31025
Measurement of multiple scattering effects with a polarization Raman elastic-backscatter lidar p 3641 N92-31033
Pulsed laser spectral measurement using a Fabry-Perot interferometer: Limits to resolution p 3646 N92-31055
Tunable Electro-optic modulators for lidar systems and atmospheric applications p 3646 N92-31056
Aureole lidar: Design, operation, and comparison with in-situ measurements p 3648 N92-31065
A study of atmospheric optical scattering parameters at 1.5 and 2 micron region for solid state Doppler lidar applications p 3648 N92-31067
Lidar analysis techniques for use in the atmospheric boundary layer p 3649 N92-31069

METEOROLOGICAL SATELLITES
Use of INSAT data in rainfall estimation p 3668 N92-30912

METEOROLOGY
Development and testing of an air quality model for Mexico City
[DE92-011238] p 3673 N92-30520
Clouds: Their prediction and simulation
[AD-A250643] p 3679 N92-30643
Evaporation duct effects at millimeter wavelengths
[AD-A250239] p 3617 N92-30876
Remote sensing applications to rainfall estimation p 3668 N92-30911
Remote sensing for rainfall estimation: SAC experience p 3668 N92-30917
Airborne lidar and radiometric observations of PBL- and low clouds p 3642 N92-31037
The 2nd phase of the LEANDRE program: Water-vapor DIAL measurement p 3643 N92-31039
Ground-based Doppler lidar of increased laser instability: Conception and design p 3650 N92-31078

METEOSAT SATELLITE
METEODEC/METEOCRYPT: A demonstration of data compression and encryption for operational remote-sensing
[NLR-TP-89294-U] p 3667 N92-30475
ECLIPS at LMD: Preliminary results of phase 2 p 3643 N92-31038

METHANE
Computational simulation of diamond chemical vapor deposition in premixed C2H2/O2/H2 and CH4/O2 strained flames
[DE92-012144] p 3606 N92-30857
Methane to liquid
[DE92-001277] p 3596 N92-30883

METHYL ALCOHOL
Photodynamics within (CH3OH)(nCr(CO)6) heteroclusters: Observation of an isotope effect
[AD-A251058] p 3712 N92-30255
Design of a high activity and selectivity alcohol catalyst
[DE92-013918] p 3594 N92-30717
Synthesis of cresols and xylenols from benzene and methanol
[DE91-002143] p 3596 N92-30882
Methane to liquid
[DE92-001277] p 3596 N92-30883
A novel process for methanol synthesis
[DE92-015798] p 3608 N92-30904

METHYL CHLORIDE
Electrooxidation of soluble alpha,alpha-coupled thiophene oligomers
[AD-A249928] p 3605 N92-30817

METHYL COMPOUNDS
Interaction of atomic hydrogen with the surface methyl group on Si(100): Removal of surface carbon
[AD-A249062] p 3595 N92-30821

METHYLENE
Synthesis and reactivity of 1-methyl-e-ethynylpyridinium triflate
[AD-A250638] p 3602 N92-30346

METRIC SPACE
Dimension bounds for quotient spaces
[PB92-177997] p 3706 N92-30789
Coexistence of uniquely ergodic subsystems of interval mapping
[DE92-630231] p 3732 N92-31133
MEXICO
Development and testing of an air quality model for Mexico City
[DE92-011238] p 3673 N92-30520
MICHELSON INTERFEROMETERS
Doppler photography: Laser methods on the flow measurement technique
[ISL-PU-303/90] p 3720 N92-30507
Fiber optic Michelson sensor and arrays with passive elimination of polarization fading and source feedback isolation
[AD-D015290] p 3722 N92-31213
MICROANALYSIS
An x ray microprobe based upon a close-coupled focal-spot/glass capillary arrangement
[DE92-011886] p 3722 N92-31195
MICROCHANNEL PLATES
Lidar receivers for picosecond remote sensing
p 3650 N92-31076
MICROCLIMATOLOGY
Development and testing of an air quality model for Mexico City
[DE92-011238] p 3673 N92-30520
MICROCOMPUTERS
Integrating commercial off-the-shelf tools for custom software development
[AD-A252462] p 3695 N92-30550
MICROCRACKS
Quantitative non-destructive evaluation of high-temperature superconducting materials
[DE92-011615] p 3661 N92-30693
MICROELECTRONICS
Nanoscience and nanotechnology
[AD-A250376] p 3626 N92-30851
MICROMECHANICS
Transformation toughening of ceramics
[AD-A248903] p 3601 N92-30342
MICROMINIATURIZED ELECTRONIC DEVICES
Nanoscience and nanotechnology
[AD-A250376] p 3626 N92-30851
MICROPOROSITY
Template-synthesis: A method for enhancing the ionic and electronic conductivity in electronically conductive polymers
[AD-A248806] p 3603 N92-30553
MICROPROCESSORS
Architecture for the high performance implantation of communication transport level protocols
[ETN-92-91666] p 3690 N92-30701
MICROSCOPY
Comparison of epifluorescent viable bacterial count methods
[NASA-TM-103592] p 3683 N92-30305
MICROSTRIP ANTENNAS
Radiation, scattering, and guidance of electromagnetic fields by arbitrarily shaped structures embedded in layered dielectric media
[AD-A252621] p 3615 N92-30408
MICROSTRIP DEVICES
Tests of the performance of different gas mixtures in microstrip gas counters
[NIKHEF-H/91-23] p 3636 N92-30365
Optimization of the microstrip gas counter
[NIKHEF-H/91-21] p 3637 N92-30688
MICROSTRUCTURE
Computer vision in microstructural analysis
p 3609 N92-30271
Mechanism of slip and twinning p 3610 N92-30280
Transformation toughening of ceramics
[AD-A248903] p 3601 N92-30342
Crack growth processes at elevated temperatures in advanced materials
[AD-A249023] p 3662 N92-30558
Transport phenomena in welds
[DE92-013404] p 3659 N92-30587
NDE characterization of the microstructure and mechanical properties of Al-Li alloys
[DE92-012154] p 3598 N92-30858
Evaluation of characterization techniques for carbon-carbon composites
[AD-A252693] p 3593 N92-31005
Fundamental studies of strongly magnetic rare earth-transition metal alloys
[DE92-015916] p 3600 N92-31186
MICROWAVE IMAGERY
Tropical cyclone asymmetries as revealed by recent satellite microwave brightness temperatures
[AD-A249873] p 3679 N92-30867
Estimation of vertical profile of soil moisture through multifrequency microwave data analysis
p 3669 N92-30919
Diversity imaging techniques in lidar
p 3640 N92-31026
MICROWAVE LANDING SYSTEMS
Evaluation of microwave landing system approaches in a wide-body transport simulator
[NASA-CR-4450] p 3579 N92-30978
MICROWAVE OSCILLATORS
Backward-wave oscillator investigations in the Raman Regime
[AD-A250738] p 3622 N92-30332
MICROWAVE RADIOMETERS
A conceptual design of a large aperture microwave radiometer geostationary platform
[NASA-TM-107577] p 3588 N92-30736
Remote sensing applications to rainfall estimation
p 3668 N92-30911
MICROWAVES
Processing aerosols and filaments in a TM010 microwave cavity at 2.45 GHz
[DE92-013536] p 3615 N92-30703
Theory of sublinear power dependence for microwave heating in some ceramic materials
[DE92-015147] p 3606 N92-30847
Estimation of vertical profile of soil moisture through multifrequency microwave data analysis
p 3669 N92-30919
Pulsed microwave processing of high-T(sub c) superconducting films
[DE92-014950] p 3730 N92-31000
Effects of microwave radiation on humans: Monkeys exposed to 1.25 GHz pulsed microwaves
[AD-A249997] p 3686 N92-31127
MIDDLE ATMOSPHERE
Atmospheric measurements using the LAMP lidar during the LADIMAS campaign p 3652 N92-31086
MIE SCATTERING
Analytical multiple scattering correction to the Mie theory: Application to the analysis of the lidar signal
p 3642 N92-31036
Time and polarization dependent double scattering calculations of lidar returns from water clouds
p 3647 N92-31063
MILITARY AIRCRAFT
Stealth: A revolutionary change to air warfare
[AD-A249880] p 3617 N92-30869
Evaluation of grounding and mooring points for Army aircraft
[AD-A250749] p 3579 N92-31193
MILITARY HELICOPTERS
Resonance and control response tests using a control simulation device
[MBB-UD-0608-91-PUB] p 3583 N92-30439
MILITARY OPERATIONS
Stealth: A revolutionary change to air warfare
[AD-A249880] p 3617 N92-30869
Joint stabilizing projects in defense
[DE92-015977] p 3709 N92-30891
MILITARY TECHNOLOGY
The rise of active-element phased-array radar
[RAND-P-7747-RGS] p 3616 N92-30755
MILLIMETER WAVES
Radiation, scattering, and guidance of electromagnetic fields by arbitrarily shaped structures embedded in layered dielectric media
[AD-A252621] p 3615 N92-30408
Evaporation duct effects at millimeter wavelengths
[AD-A250239] p 3617 N92-30876
Advanced mobile satellite communications system using Ka and MM-wave bands in Japan's R and D satellite project p 3617 N92-30924
Experimental millimeter-wave personal satellite communications system p 3617 N92-30927
MIMD (COMPUTERS)
Scalable parallel molecular dynamics on MIMD supercomputers
[DE92-015041] p 3698 N92-30401
Monte Carlo particle simulation of low-density fluid flow on MIMD supercomputers
[DE92-014618] p 3630 N92-30607
Contribution of parallelism to solving a load distribution problem in electric networks
[ETN-92-91668] p 3625 N92-30702
MINERALS
From minerals to materials: A facile synthetic route to preceramic polymers for aluminum oxide
[AD-A250351] p 3606 N92-31141
MINIATURE ELECTRONIC EQUIPMENT
Quantum transport, noise and non-linear dissipative effects in one- and two-dimensional systems and associated sub-micron and nanostructure devices
[AD-A250895] p 3627 N92-31210
MINIATURIZATION
Assessment of a head-mounted miniature monitor
[NASA-TM-103587] p 3688 N92-30381
Nanoscience and nanotechnology
[AD-A250376] p 3626 N92-30851
A miniature carbon furnace for mass spectroscopy
[DE92-014460] p 3597 N92-31196
MIRRORS
Full surface testing of grazing incidence mirrors
[AD-A248851] p 3719 N92-30233
Eye/sensor protection against laser irradiation ablative mirror devices: A materials assessment
[AD-A248787] p 3688 N92-30615
TRAC performance estimates
[NASA-CR-190530] p 3701 N92-30778
MISSION PLANNING
Hubble Space Telescope. Update: 18 months in orbit
[NASA-TM-107962] p 3739 N92-30686
MIXING
Recombining processes in a cooling plasma by mixing of initially heated gas
[NIFS-142] p 3722 N92-30431
A new unsteady mixing model to predict NO(x) production during rapid mixing in a dual-stage combustor
[NASA-CR-189155] p 3581 N92-30569
MIXING LAYERS (FLUIDS)
Turbulent reacting flows and supersonic combustion
[AD-A251065] p 3593 N92-30256
A study of the topology of dissipating motions in direct numerical simulations of time-developing compressible and incompressible mixing layers p 3632 N92-30658
Resonant instability of supersonic shear layers
p 3632 N92-30661
Low order dynamical models for mixing layers
p 3633 N92-30662
Length scales and dissipation of fine eddies in a mixing layer p 3633 N92-30664
A fractal transition in the two dimensional shear layer
p 3633 N92-30665
Continuous wavelet analysis of coherent structures
p 3634 N92-30673
Direct simulation of high-speed mixing layers
[NASA-TP-3186] p 3576 N92-30909
MOBILE COMMUNICATION SYSTEMS
Proceedings of the Workshop on Advanced Network and Technology Concepts for Mobile, Micro, and Personal Communications
[NASA-CR-190459] p 3617 N92-30923
Advanced mobile satellite communications system using Ka and MM-wave bands in Japan's R and D satellite project p 3617 N92-30924
Design of the American Mobile Satellite System
p 3617 N92-30925
Ka-band mobile and personal systems development at JPL p 3618 N92-30928
The ELLIPSO (tm) system: Elliptical low orbits for mobile communications and other optimum system elements
p 3618 N92-30930
An integrated Ka/Ku-band payload for personal, mobile and private business communications
p 3619 N92-30933
Cellular: Toward personal communications
p 3619 N92-30936
Capacity and interference in a PCS system
p 3619 N92-30937
The Pan-European Digital Cellular (GSM) System
p 3619 N92-30938
Toward a North American standard for mobile data services p 3620 N92-30940
The RadioSat (sm) network p 3620 N92-30942
National transportable telecommunications capability
p 3620 N92-30943
Broadcast satellite service: The international dimension p 3621 N92-30946
Aeronautical Mobile Satellite Service (AMSS) capacity analysis and protocol performance simulation results
[DOT/FAA/CT-TN90/64] p 3622 N92-31212
MODELS
Adapting the ADAM manikin technology for injury probability assessment
[AD-A252332] p 3688 N92-30844
MODEMS
Toward a North American standard for mobile data services p 3620 N92-30940
MODULATION
Altimetry and lidar using AlGaAs lasers modulated with pseudo-random codes p 3641 N92-31030
MODULATION TRANSFER FUNCTION
Review of psychophysically-based image quality metrics
[AD-A251053] p 3686 N92-30254
MODULATORS
Tunable Electro-optic modulators for lidar systems and atmospheric applications p 3646 N92-31056

MODULUS OF ELASTICITY
Elastic constants of crystals near melting via density functional theory. Effect of three-body correlations
[DE92-630567] p 3730 N92-31191
MOLECULAR BEAM EPITAXY
MBE grown copper-aluminum alloy films
[AD-A252486] p 3597 N92-30534
Transient photoconductivity of low temperature GaAs grown by molecular beam epitaxy terahertz radar applications
[DE92-011848] p 3729 N92-30854
MOLECULAR ELECTRONICS
Extended orthogonally fused conducting oligomers for molecular electronic devices
[AD-A249927] p 3605 N92-30795
Synthesis of orthogonally fused conducting oligomers for molecular electronic devices
[AD-A249929] p 3605 N92-30796
MOLECULAR INTERACTIONS
Chemistry within van der Waals cluster of unsaturated molecules: Observation of cationic polymerization
[AD-A250929] p 3712 N92-30240
Vacuum ultraviolet studies of molecular dynamics
[AD-A246964] p 3715 N92-30681
MOLECULAR IONS
Chemistry within van der Waals cluster of unsaturated molecules: Observation of cationic polymerization
[AD-A250929] p 3712 N92-30240
Tunable solid state lasers based on molecular ions
[AD-A249423] p 3656 N92-30774
MOLECULAR ORBITALS
Analytical methods using Slater-type orbitals in quantum chemistry
[AD-A251044] p 3731 N92-30242
Superconductivity and magnetism in rapidly solidified perovskites
[DE92-014081] p 3597 N92-30588
MOLECULAR ROTATION
Vacuum ultraviolet studies of molecular dynamics
[AD-A246964] p 3715 N92-30681
MOLECULAR SPECTROSCOPY
Tunable Electro-optic modulators for lidar systems and atmospheric applications p 3646 N92-31056
MOLECULAR STRUCTURE
Perforated monolayers
[DE92-011632] p 3593 N92-30344
Fundamental studies of carbon, NH, and oxygen rings and other high energy density molecular systems
[AD-A246963] p 3715 N92-30680
MOLECULAR WEIGHT
Polyimides containing the cyclobutene-3,4-dione moiety
[NASA-CASE-LAR-14753-1] p 3601 N92-30313
Molecular weight dependence of domain structure in silica-siloxane molecular composites
[DE92-015046] p 3603 N92-30544
MOLECULES
Studies of atmospheric molecules by multiphoton spectroscopy
[DE92-012668] p 3672 N92-30345
Scalable parallel molecular dynamics on MIMD supercomputers
[DE92-015041] p 3698 N92-30401
Characterization and analysis of defects in nonlinear optical molecular composite films
[AD-A252118] p 3661 N92-30529
Lidar sounding of ozone and aerosols
p 3652 N92-31085
MOLTEN SALT ELECTROLYTES
Research issues in molten carbonate fuel cells: Pressurization
[DE92-011755] p 3671 N92-31113
MOLTEN SALTS
Research issues in molten carbonate fuel cells: Pressurization
[DE92-011755] p 3671 N92-31113
MOMENTUM TRANSFER
Heating and momentum deposition in hot stars
[DE92-011850] p 3740 N92-30855
MONITORS
Assessment of a head-mounted miniature monitor
[NASA-TM-103587] p 3688 N92-30381
Voltammetric measurement of oxygen in single neurons using platinized carbon ring electrodes
[AD-A252191] p 3683 N92-30531
Exploiting resource parallelism for integrated fault monitoring and recovery
[AD-A248843] p 3699 N92-30557
Repetitive High Energy Pulsed Power (RHEPP) temperature monitoring system utilizing Luxtron fluoroptic sensors and thermocouples technical reference manual
[DE92-013461] p 3637 N92-30893
Airborne lidar and radiometric observations of PBL- and low clouds p 3642 N92-31037
MONKEYS
Effects of microwave radiation on humans: Monkeys exposed to 1.25 GHz pulsed microwaves
[AD-A249997] p 3686 N92-31127
MONOCHROMATIC RADIATION
Spontaneous decay of an atom near a phase conjugator
[AD-A248298] p 3712 N92-30333
MONOMERS
A shear sensitive monomer-polymer laminate structure and method of using same
[NASA-CASE-LAR-14654-1] p 3662 N92-30317
Studies of thermal decomposition of the 1:1 R3Al:en adduct (R = Me, Et; en = ethylenediamine): Synthesis and structure of a novel intermediate Al((HNCH2CH2NH)AlMe2)3
[AD-A251061] p 3603 N92-30623
MONOPOLE ANTENNAS
On the radial component of the electric field for a monopole phased array antenna focused in the near zone
[AD-A249441] p 3616 N92-30761
MONTE CARLO METHOD
Doppler mean velocity estimation: Small sample analysis and a new estimator
[AD-A249024] p 3678 N92-30559
Intermittency, multifractality, and hadronic collisions
[DE92-014595] p 3714 N92-30606
Monte Carlo particle simulation of low-density fluid flow on MIMD supercomputers
[DE92-014618] p 3630 N92-30607
Quantification and reduction of the uncertainty in mass balance models by Monte Carlo analysis of prior data
[DE92-010278] p 3708 N92-30803
Effect of wave-particle interaction on the outflow of ions at high latitudes
[NASA-CR-190560] p 3677 N92-30962
Multiple scattering effects on spaceborne lidar
p 3641 N92-31032
Laboratory scaled simulation of lidar cloud sounding experiments p 3645 N92-31047
Lidar multiple scattering: Dependence on atmospheric parameters p 3647 N92-31061
MOON
Twenty-Third Lunar and Planetary Science Conference
[NASA-CR-190178] p 3736 N92-31222
MOORING
Evaluation of grounding and mooring points for Army aircraft
[AD-A250749] p 3579 N92-31193
MOTION STABILITY
Thrust test fixture
[AD-D015259] p 3585 N92-31192
MOVING TARGET INDICATORS
Maximum likelihood detection of electro-optic moving targets
[AD-A249442] p 3616 N92-30762
MSAT
Design of the American Mobile Satellite System
p 3617 N92-30925
Ka-band mobile and personal systems development at JPL p 3618 N92-30928
The RadioSat (sm) network p 3620 N92-30942
MSM (SEMICONDUCTORS)
Transient photoconductivity of low temperature GaAs grown by molecular beam epitaxy terahertz radar applications
[DE92-011848] p 3729 N92-30854
MULTIBEAM ANTENNAS
The ACTS multibeam antenna
[NASA-TM-105645] p 3587 N92-30383
Characteristics of a future aeronautical satellite communications system p 3618 N92-30932
MULTIGRID METHODS
Adaptive multigrid applied to a bipolar transistor problem
[CWI-NM-R9115] p 3693 N92-30429
A multigrid method for a discretization of the incompressible Navier-Stokes equations in general coordinates
[REPT-91-73] p 3629 N92-30454
A robust multigrid method for a discretization of the incompressible Navier-Stokes equations in general coordinates
[REPT-92-14] p 3629 N92-30462
MULTIPATH TRANSMISSION
Direct sequence spread spectrum CDMA in shared spectrum applications p 3619 N92-30939
Performance of ground-based high-frequency receiving arrays with electrically-small ground planes
[AD-A250489] p 3621 N92-31130
MULTIPHASE FLOW
Continuum approaches for describing solid-liquid flow
[AD-A249028] p 3629 N92-30560
MULTIPHOTON ABSORPTION
Microscopic theory of THG and electro-absorption in conjugated polymers
[DE92-014786] p 3604 N92-30792
MULTIPLE ACCESS
An integrated Ka/Ku-band payload for personal, mobile and private business communications
p 3619 N92-30933
MULTIPLEXING
Double-loop frequency-selected surfaces for multifrequency division multiplexing in a dual-reflector antenna
[NASA-CASE-NPO-18701-1-CU] p 3614 N92-30391
VDHW-related memo's
[LINO-1991-5] p 3718 N92-30725
Measurement report on the present Video Highway System of MEA p 3718 N92-30726
Tunable relay box (design and testing)
p 3718 N92-30727
Console driver p 3718 N92-30728
MULTIPROCESSING (COMPUTERS)
Three-dimensional shock wave physics simulations on massively parallel supercomputers
[DE92-008679] p 3698 N92-30363
A model of the ADA avionics real-time system: An example of the benefits of the hardware/software codesign approach in development of real-time systems
[AD-A248893] p 3581 N92-30524
MULTISENSOR APPLICATIONS
Method of measuring cross-flow vortices by use of an array of hot-film sensors
[NASA-CASE-LAR-14824-1-SB] p 3628 N92-30390
MULTISPECTRAL RADAR
Fluorescence lidar multi-color imaging of vegetation
p 3640 N92-31028
MULTIVARIABLE CONTROL
Practical method's for robust multivariable control
[AD-A248473] p 3700 N92-30322
MULTIVARIATE STATISTICAL ANALYSIS
Gaussian windows: A tool for exploring multivariate data
[NASA-CR-190559] p 3696 N92-30723
MUONS
Recent experimental studies on hadron showers produced in high energy muon-nucleus interactions
[DE92-016002] p 3719 N92-31219
MUTATIONS
Control of circadian behavior by transplanted suprachiasmatic nuclei
[AD-A250442] p 3686 N92-31143
MYOCARDIAL INFARCTION
Optimal ECG electrode sites and criteria for detection of asymptomatic coronary artery disease, update 1990. Multilead ECG changes at rest, with exercise, and with coronary angioplasty
[AD-A248613] p 3684 N92-30523

N

NACELLES
Ultra high bypass Nacelle aerodynamics inlet flow-through high angle of attack distortion test
[NASA-CR-189149] p 3574 N92-30298
NASA PROGRAMS
Studying Turbulence Using Numerical Simulation Databases. 3: Proceedings of the 1990 Summer Program
[NASA-CR-189475] p 3630 N92-30648
Research and technology, 1991. Langley Research Center
[NASA-TM-4331] p 3744 N92-30733
Space science and applications: Strategic plan 1991
[NASA-TM-107811] p 3733 N92-30959
Setting priorities for space research: Opportunities and imperatives
[NASA-CR-190519] p 3733 N92-30974
National Aeronautics and Space Administration
p 3736 N92-31170
NASA SPACE PROGRAMS
Hubble Space Telescope. Update: 18 months in orbit
[NASA-TM-107962] p 3739 N92-30686
NATIONAL AEROSPACE PLANE PROGRAM
Development of a 3-D upwind PNS code for chemically reacting hypersonic flowfields
[NASA-CR-190182] p 3576 N92-30977
NATIONAL AIRSPACE SYSTEM
GNAS Maintenance Control Center (GMCC) Design Qualification Test and Evaluation (DQT/E) test procedures
[DOT/FAA/CT-TN91/40] p 3585 N92-30976
National airspace system. Air defense and law enforcement surveillance operational concept NAS-SR-135
[DOT/FAA/SE-92/3] p 3579 N92-31211

NATURAL GAS
Ringless piston experiments. Natural gas engine technology advancements
[PB92-164466] p 3659 N92-30601
Methane to liquid
[DE92-001277] p 3596 N92-30883
NAVIER-STOKES EQUATION
Joint computational and experimental aerodynamics research on a hypersonic vehicle
[DE92-013439] p 3574 N92-30367
Finite volume discretization of the incompressible Navier-Stokes equations in general coordinates on staggered grids
[REPT-91-71] p 3628 N92-30373
Numerical investigations in three-dimensional internal flows
[NASA-CR-190498] p 3628 N92-30380
Navier-Stokes computations of a viscous optimized waverider
[NASA-CR-189658] p 3574 N92-30392
A multigrid method for a discretization of the incompressible Navier-Stokes equations in general coordinates
[REPT-91-73] p 3629 N92-30454
A robust multigrid method for a discretization of the incompressible Navier-Stokes equations in general coordinates
[REPT-92-14] p 3629 N92-30462
A gridless Euler/Navier-Stokes solution algorithm for complex two-dimensional applications
[NASA-TM-107631] p 3575 N92-30570
A Boussinesq algorithm for bouyant convection in polygonal domains
[PB92-187137] p 3695 N92-30579
Direct coupling method for time-accurate solution of incompressible Navier-Stokes equations
[NASA-CR-189177] p 3636 N92-30894
Navier-Stokes analysis and experimental data comparison of compressible flow within ducts
[NASA-TM-105796] p 3582 N92-30972
NAVIGATION SATELLITES
The MARCOR GPS mobile data system
p 3620 N92-30944
Broadcast satellite service: The international dimension p 3621 N92-30946
NEAR INFRARED RADIATION
Design of a near-IR coherent lidar for high spatial and velocity resolution wind measurement
p 3639 N92-31020
Airborne remote sensing of tropospheric water vapor using a near infrared DIAL system p 3644 N92-31042
NEBULAE
Impact erosion of terrestrial planetary atmospheres
[NASA-CR-190605] p 3742 N92-30921
NECK (ANATOMY)
Adapting the ADAM manikin technology for injury probability assessment
[AD-A252332] p 3688 N92-30844
NEGATIVE IONS
Negative ion extraction characteristics of a large negative ion source with double-magnetic filter configuration
[NIFS-151] p 3714 N92-30501
Production of negative hydrogen ions in a large multicusp ion source with double-magnetic filter configuration
[NIFS-149] p 3714 N92-30572
Study of Au(-) production in a plasma-sputter type negative ion source
[NIFS-115] p 3717 N92-30990
NEODYMIUM LASERS
An ultra-sensitive coherent detector capable of single photon detection for lidar applications
p 3646 N92-31053
Laser mass spectrometry for biopolymers
[DE92-015238] p 3597 N92-31184
NETWORK ANALYSIS
A bibliography on network flow problems (2nd edition)
[RUU-CS-91-38] p 3698 N92-30482
About difference equations, algebras and discrete events
[REPT-91-87] p 3704 N92-30491
Can stochastic modelling and analysis of multistage interconnection networks lead to efficient usage of redundancy for fault-tolerant design?
[AD-A250635] p 3699 N92-30526
High level synthesis of controlpath microarchitectures
[MEMO-INF-91-86] p 3690 N92-30698
NETWORK SYNTHESIS
Configuration algorithms for hierarchical supernode machines
[IMAG-RR-853-I] p 3694 N92-30493
NEURAL NETS
A space-time neural network for processing both spacial and temporal data
[NASA-CASE-MSC-21874-1] p 3700 N92-30314
Analysis and synthesis of adaptive neural elements and assembles
[AD-A248467] p 3687 N92-30320
Dense modifiable interconnections utilizing photorefractive volume holograms
[AD-A252193] p 3637 N92-30546
Cortical mechanisms of attention, discrimination, and motor response to somaesthetic stimuli
[AD-A247228] p 3687 N92-30613
Sparse distributed memory and related models
[NASA-CR-190553] p 3690 N92-30724
Visual perception of depth from occlusion: A neural network model
[AD-A249035] p 3696 N92-30820
The optimization of force inputs for active structural acoustic control using a neural network
[NASA-TM-107627] p 3711 N92-30979
NEURONS
Neurophysiological analysis of circadian rhythm entrainment
[AD-A248466] p 3684 N92-30319
Analysis and synthesis of adaptive neural elements and assembles
[AD-A248467] p 3687 N92-30320
Voltammetric measurement of oxygen in single neurons using platinized carbon ring electrodes
[AD-A252191] p 3683 N92-30531
Cortical mechanisms of attention, discrimination, and motor response to somaesthetic stimuli
[AD-A247228] p 3687 N92-30613
Secretory mechanisms in opiocortin cells during cold stress
[AD-A252317] p 3685 N92-30719
NEUROPHYSIOLOGY
Neurophysiological analysis of circadian rhythm entrainment
[AD-A248466] p 3684 N92-30319
Analysis and synthesis of adaptive neural elements and assembles
[AD-A248467] p 3687 N92-30320
Research in stochastic analysis and its applications
[AD-A249482] p 3708 N92-30633
NEUROTRANSMITTERS
Neurophysiological analysis of circadian rhythm entrainment
[AD-A248466] p 3684 N92-30319
The properties of the uptake system for glycine in synaptic vesicles
[ISSN-0800-4412] p 3683 N92-31152
NEUTRAL ATMOSPHERES
The calculation of mid-latitude meridional neutral winds from an improved servo model approximation method
[AD-A249874] p 3676 N92-30868
NEUTRAL BEAMS
Dynamic analysis of compact helical system power supply and designs of its upgrade
[NIFS-TECH-2] p 3723 N92-30497
Line-emission cross sections for the charge-exchange reaction between fully stripped carbon and atomic hydrogen in tokamak plasma
[NIFS-129] p 3716 N92-30967
NEUTRAL PARTICLES
Search for light neutral scalar and pseudoscalar particles in pFe interactions at 70 GeV
[DE92-627317] p 3713 N92-30404
NEUTRINOS
Rescattering in neutrino/antineutrino: Deuteron reactions
[NIKHEF-H/91-22] p 3713 N92-30364
Rapid cooling and structure of neutron stars
[DE92-015279] p 3740 N92-30609
Ideas for a long-baseline neutrino detector
[DE92-010650] p 3743 N92-30828
Solar neutrinos: Theoretical status
[DE92-014014] p 3743 N92-31199
NEUTRON COUNTERS
Neutron time-of-flight ion temperature diagnostic for inertial confinement fusion experiments
[DE92-011365] p 3724 N92-30806
NEUTRON DIFFRACTION
Diffuse neutron scattering signatures of rough films
[DE92-015208] p 3717 N92-31201
NEUTRON IRRADIATION
The effect of neutron irradiation on the structure and properties of carbon-carbon composite materials
[DE92-011670] p 3592 N92-30809
NEUTRON SCATTERING
Determination of pair potentials by analysis of diffuse scattering of the local field in Pd3V and Ni3V
[ESA-TT-1228] p 3597 N92-30513
Molecular weight dependence of domain structure in silica-siloxane molecular composites
[DE92-015046] p 3603 N92-30544
Diffuse neutron scattering signatures of rough films
[DE92-015208] p 3717 N92-31201
NEUTRON SOURCES
Neutron Source Munich FRM-2
[DE92-015300] p 3717 N92-31205
NEUTRON STARS
Rapid cooling and structure of neutron stars
[DE92-015279] p 3740 N92-30609
Discovery of two planets around a millisecond pulsar
p 3739 N92-31237
NEWTON METHODS
A computational algorithm for crack determination: The multiple crack case
[NASA-CR-189665] p 3704 N92-30516
NEWTONIAN FLUIDS
Lewis icing research tunnel test of the aerodynamic effects of aircraft ground deicing/anti-icing fluids
[NASA-TP-3238] p 3577 N92-30395
NICKEL ALLOYS
Stabilization of face-centered-cubic titanium
[DE92-011530] p 3600 N92-31125
NICKEL HYDROGEN BATTERIES
Ni-H2 cell separator matrix engineering
[NASA-CR-190055] p 3671 N92-30949
NIGHT
Helicopter nighttime parking test results - UH-1
[DOT/FAA/CT-TN92/1] p 3580 N92-31165
NIOBIUM
Potassium Rankine cycle power conversion systems for lunar-Mars surface power
[DE92-015102] p 3589 N92-31012
NITROGEN
Verification measurement of a polarization Raman elastic-backscatter lidar p 3647 N92-31062
NITROGEN ISOTOPES
On the isotopic signature of recent solar-wind nitrogen
p 3738 N92-31231
NOAA SATELLITES
Vegetation conditions and yield indicators. Part 1: Main report
[BCRS-91-26-PT-1] p 3667 N92-30471
NOISE GENERATORS
Prediction of coincidence frequencies for a thin-walled, fluid-filled pipe
[MRL-TN-600] p 3664 N92-30963
NOISE MEASUREMENT
Active control of pressure, sound and velocity of centrifugal pumps
[AD-A249446] p 3659 N92-30640
NOISE REDUCTION
Active control of pressure, sound and velocity of centrifugal pumps
[AD-A249446] p 3659 N92-30640
Phase noise in pulsed Doppler lidar and limitations on achievable single-shot velocity accuracy
p 3639 N92-31024
An investigation of the effects of boundary constraints on the sound insulations of lightweight, double leaf partitions
[BBC-RD-1992/4] p 3711 N92-31151
NOISE SPECTRA
Active control of pressure, sound and velocity of centrifugal pumps
[AD-A249446] p 3659 N92-30640
NONDESTRUCTIVE TESTS
Nondestructive evaluation of ceramic components by gamma ray CT
[DE92-626843] p 3602 N92-30402
A computational algorithm for crack determination: The multiple crack case
[NASA-CR-189665] p 3704 N92-30516
Ultrasound NDE of adhesive bond integrity: A quantitative measure
[AD-A248845] p 3661 N92-30599
Quantitative non-destructive evaluation of high-temperature superconducting materials
[DE92-011615] p 3661 N92-30693
Nondestructive testing of ceramics for vehicular advanced heat engines
[DE92-010471] p 3604 N92-30744
NDE characterization of the microstructure and mechanical properties of Al-Li alloys
[DE92-012154] p 3598 N92-30858
NONEQUILIBRIUM CONDITIONS
Calculation of viscous hypersonic flows in chemical non-equilibrium
[MBB/FE211/S/PUB/466] p 3634 N92-30674
X ray scattering studies of non-equilibrium ordering processes
[DE92-014006] p 3598 N92-30787
NONHOLONOMIC EQUATIONS
Non-holonomic filtration: Algebraic and geometric aspects of non-integrability
[PB92-178003] p 3706 N92-30790
NONLINEAR EVOLUTION EQUATIONS
Low order dynamical models for mixing layers
p 3633 N92-30662

NONLINEAR FILTERS
Research in stochastic analysis and its applications
[AD-A249482] p 3708 N92-30633
NONLINEAR OPTICS
The electric field dependence of the laser induced holographic grating relaxation of photorefractive polymer
[AD-A252641] p 3602 N92-30409
Characterization and analysis of defects in nonlinear optical molecular composite films
[AD-A252118] p 3661 N92-30529
Effects of the orientational pair correlation on second order nonlinear optical coefficients
[AD-A252490] p 3720 N92-30535
Research studies on extreme ultraviolet and soft x ray lasers
[AD-A249798] p 3657 N92-30784
NONLINEAR SYSTEMS
Nonlinear system design: Adaptive feedback linearization with unmodeled dynamics
[AD-A248484] p 3700 N92-30335
Strong dynamic input-output decoupling: From linearity to nonlinearity
[MEMO-COSOR-92-04] p 3694 N92-30478
Nondestructive characterization of two-phase metal-matrix materials
[AD-A249912] p 3592 N92-30815
Example of a quantum field theory based on a nonlinear Lie algebra
[DE92-010475] p 3731 N92-30825
Acoustic fatigue life prediction for nonlinear structures with multiple resonant modes
[NASA-CR-190471] p 3664 N92-30988
Nonlinear RR Lyrae models with new Livermore opacities
[DE92-011158] p 3741 N92-31108
Fixed point iterations for a class of nonlinear mappings in certain Banach spaces
[DE92-630235] p 3706 N92-31134
Multifractal analysis of chaotic point sets
[AD-A250756] p 3709 N92-31194
NONLINEARITY
Mathematical models of non-linear mechanical and electrical systems and their qualitative behavior
[AD-A248847] p 3622 N92-30249
Characterization and analysis of defects in nonlinear optical molecular composite films
[AD-A252118] p 3661 N92-30529
Effects of the orientational pair correlation on second order nonlinear optical coefficients
[AD-A252490] p 3720 N92-30535
Growth and evaluation of nonlinear optical materials for laser applications: Barium borate, lithium borate, and silver gallium selenide
[AD-A248861] p 3624 N92-30617
Interaction of ultra-high laser fields with beams and plasmas
[AD-A249502] p 3723 N92-30620
Generation of large-scale density fluctuations by buoyancy p 3634 N92-30671
Nonlinear analysis of a grating free-electron laser
[AD-A248833] p 3656 N92-30743
New insights into large eddy simulation
[AD-A249424] p 3635 N92-30775
Nonlinear stress analysis of composite-jacketed steel cylinders subjected to high internal pressure
[AD-A249500] p 3663 N92-30802
Nonlinear stability and control study of highly maneuverable high performance aircraft, phase 2
[NASA-CR-190667] p 3583 N92-30922
Correction for nonlinear photon counting effects in lidar systems p 3649 N92-31070
Nonlinear aerodynamics and the design of wing tips
[NASA-CR-190649] p 3577 N92-31157
Preliminary subsonic aerodynamic model for simulation studies of the HL-20 lifting body
[NASA-TM-4302] p 3583 N92-31175
NONUNIFORM PLASMAS
Collisional and chaotic transport of energetic particles in toroidal plasma
[DE92-014589] p 3725 N92-30900
NORMAL DENSITY FUNCTIONS
The sum of weighted balls
[RUU-CS-91-37] p 3707 N92-30481
NOSES (FOREBODIES)
High speed research system study. Advanced flight deck configuration effects
[NASA-CR-189650] p 3581 N92-30965
NOWCASTING
On the potential use of the terminal Doppler weather radar gust front detection algorithm on the WSR-88D system. Part 2: Detecting non-gust front convergent weather phenomena
[DOT/FAA/NR-92/8,II] p 3678 N92-30496
NOZZLE FLOW
Real gas flow parameters for NASA Langley 22-inch Mach 20 helium tunnel
[NASA-CR-4462] p 3635 N92-30751
Numerical investigations in the backflow region of a vacuum plume
[NASA-CR-190515] p 3589 N92-30981
Preliminary dynamic tests of a flight-type ejector
[NASA-TM-105814] p 3582 N92-30998
NOZZLE GEOMETRY
Finite element analysis of laminated composite axisymmetric solids. Volume 1: Theory and applications
[AD-A250808] p 3590 N92-30251
NUCLEAR ASTROPHYSICS
Nuclear theory progress report, April 1991 - April 1992
[DE92-015349] p 3714 N92-30611
NUCLEAR DEFORMATION
Lifetimes of low spin states in the superdeformed band of Hg-192
[DE92-011066] p 3728 N92-30684
NUCLEAR DEVICES
Boundary plasma transport studies on TFTR
[DE92-011942] p 3723 N92-30746
Criteria and design trade-off issues for ITER
[DE92-011786] p 3726 N92-31114
NUCLEAR ELECTRIC PROPULSION
NEP systems engineering efforts in FY-92: Plans and status
[NASA-TM-105775] p 3588 N92-30308
Nuclear electric propulsion development and qualification facilities
[NASA-TM-105521] p 3589 N92-30818
NUCLEAR FUSION
On the temperature role in the tunneling process at the cold fusion
[DE92-627497] p 3727 N92-30405
On the factorisation theorem in boson-gluon fusion at hadron colliders
[NIKHEF-H/91-16] p 3713 N92-30415
Dark matter and cosmology
[DE92-013023] p 3740 N92-30622
NUCLEAR INTERACTIONS
Rescattering in neutrino/antineutrino: Deuteron reactions
[NIKHEF-H/91-22] p 3713 N92-30364
NUCLEAR MODELS
Non-perturbative effects in high-energy electroweak interactions
[NIKHEF-H/91-24] p 3715 N92-30697
Nuclear structure calculations for astrophysical applications
[DE92-011495] p 3740 N92-30856
NUCLEAR PHYSICS
Intermittency, multifractality, and hadronic collisions
[DE92-014595] p 3714 N92-30606
Physics of the STAR experiment at the relativistic heavy ion collider
[DE92-014481] p 3719 N92-31198
NUCLEAR POWER PLANTS
Fiber-optic Raman spectroscopy at the Savannah River Site: Uses and techniques
[DE92-013971] p 3596 N92-30899
Development of a reliability maintenance optimization method p 3697 N92-30956
NUCLEAR PROPULSION
Thermohydraulic modeling of nuclear thermal rockets: The KLAXON code
[DE92-015274] p 3589 N92-31204
NUCLEAR REACTIONS
Search for light neutral scalar and pseudoscalar particles in pFe interactions at 70 GeV
[DE92-627317] p 3713 N92-30404
Nuclear theory progress report, April 1991 - April 1992
[DE92-015349] p 3714 N92-30611
NUCLEAR REACTORS
NEP systems engineering efforts in FY-92: Plans and status
[NASA-TM-105775] p 3588 N92-30308
Method for remotely powering a device such as a lunar rover
[NASA-CASE-LAR-14789-1] p 3658 N92-30388
NUCLEAR RESEARCH AND TEST REACTORS
Neutron Source Munich FRM-2
[DE92-015300] p 3717 N92-31205
NUCLEAR ROCKET ENGINES
Thermohydraulic modeling of nuclear thermal rockets: The KLAXON code
[DE92-015274] p 3589 N92-31204
NUCLEAR SCATTERING
Rescattering in neutrino/antineutrino: Deuteron reactions
[NIKHEF-H/91-22] p 3713 N92-30364
Two-loop QCD corrections to the coefficient functions of the deep inelastic structure functions F2 and F(sub L)
[NIKHEF-H/91-17] p 3715 N92-30687
NUCLEAR STRUCTURE
Nuclear theory progress report, April 1991 - April 1992
[DE92-015349] p 3714 N92-30611
Nuclear structure calculations for astrophysical applications
[DE92-011495] p 3740 N92-30856
NUCLEATION
Nucleation and growth of diamond on carbon-implanted single crystal copper
[AD-A249021] p 3594 N92-30632
NUCLEIC ACIDS
Laser mass spectrometry for biopolymers
[DE92-015238] p 3597 N92-31184
NUCLEONS
Linear estimates of structure functions from deep inelastic lepton-nucleon scattering data, part 1
[DE92-627288] p 3713 N92-30403
Constraints on the nuclear matter equation of state from pulsar glitches
[DE92-015142] p 3740 N92-30578
NUMERICAL ANALYSIS
Numerical methods for closed-loop control
[AD-A248481] p 3700 N92-30334
Semiannual final report, 1 October 1991 - 31 March 1992
[NASA-CR-189660] p 3689 N92-30489
Computational methods for modeling and active control of distributed parameter systems
[AD-A248559] p 3705 N92-30638
A numerical evaluation of the dynamical systems approach to wall layer turbulence p 3632 N92-30660
Numerical calculations of two-dimensional single and multi-material flow fields with CCICE
[DE92-015778] p 3636 N92-30903
Dynamics and energetics of the solar corona
[NASA-CR-190664] p 3742 N92-31162
Thermohydraulic modeling of nuclear thermal rockets: The KLAXON code
[DE92-015274] p 3589 N92-31204
NUMERICAL CONTROL
Computer-controlled ion beam sputter-deposition of superconducting oxide films
[AD-A248495] p 3601 N92-30326
NUMERICAL FLOW VISUALIZATION
A multigrid method for a discretization of the incompressible Navier-Stokes equations in general coordinates
[REPT-91-73] p 3629 N92-30454
NUMERICAL INTEGRATION
Fast methods to numerically integrate the Reynolds equation for gas fluid films
[NASA-TM-105415] p 3660 N92-30722
One-loop integration for the axial gauge with generalized prescription
[DE92-630241] p 3732 N92-31145
NUMERICAL WEATHER FORECASTING
Regional-scale analysis and forecasting (RAP) report
[AD-A248384] p 3678 N92-30262
NYLON (TRADEMARK)
Ferroelectric and piezoelectric properties of odd-numbered nylons
[AD-A252270] p 3727 N92-30406
A new class of ferroelectric polymers: The odd-numbered nylons
[AD-A252268] p 3603 N92-30594
Ferroelectric polarization mechanisms in Nylon 11
[AD-A252269] p 3728 N92-30595

O

OBJECT-ORIENTED PROGRAMMING
The Duplex programming environment
[REPT-91-90] p 3694 N92-30492
OCCLUSION
Visual perception of depth from occlusion: A neural network model
[AD-A249035] p 3696 N92-30820
OCEAN BOTTOM
Digital bottom mapping
[AD-D015238] p 3682 N92-30413
OCEAN CURRENTS
Feasibility of extracting current profile information from HF-radar surface current measurements, part 1 and 2
[BCRS-91-23-PT-1-2] p 3682 N92-30470
Oceanic CO2 measurements for the WOCE hydrographic survey in the Pacific Ocean, 1990-1991: Shore based analyses during legs 1-3
[DE92-013064] p 3682 N92-30861
OCEAN MODELS
Laboratory simulation of fluid dynamical process related to winter arctic leads
[AD-A252266] p 3682 N92-30593

OCEAN SURFACE
Event-scale relationships between surface velocity, temperature and chlorophyll in the coastal ocean, as seen by satellite
[NASA-CR-190266] p 3682 N92-30739
Boundary layer structure over the ocean observed by LEANDRE 1 during a tramontane event
p 3638 N92-31014
Airborne lidar and radiometric observations of PBL- and low clouds p 3642 N92-31037
OCEANOGRAPHIC PARAMETERS
Remote sensing for the Lincoln Sea Winterover Experiment
[AD-A252117] p 3667 N92-30545
OCEANOGRAPHY
Preparations for the ERS-1 and TOPEX/Poseidon satellite altimetry missions
[BCRS-90-28] p 3666 N92-30465
Research in stochastic analysis and its applications
[AD-A249482] p 3708 N92-30633
Oceanic CO2 measurements for the WOCE hydrographic survey in the Pacific Ocean, 1990-1991: Shore based analyses during legs 1-3
[DE92-013064] p 3682 N92-30861
Multiple scattering effects on spaceborne lidar
p 3641 N92-31032
OCEANS
Remote sensing for the Lincoln Sea Winterover Experiment
[AD-A252117] p 3667 N92-30545
National ocean pollution program: Summary of Federal programs and projects: FY 1989 update
[PB92-187012] p 3673 N92-30563
Altimeter and gravity data analysis
[NASA-CR-190478] p 3676 N92-30756
OIL RECOVERY
Algorithm to solve nonlinear time dependent problems of engineering and physics
[AD-A250641] p 3702 N92-30347
OILS
Algorithm to solve nonlinear time dependent problems of engineering and physics
[AD-A250641] p 3702 N92-30347
Ringless piston experiments. Natural gas engine technology advancements
[PB92-164466] p 3659 N92-30601
OLIGOMERS
Extended orthogonally fused conducting oligomers for molecular electronic devices
[AD-A249927] p 3605 N92-30795
Synthesis of orthogonally fused conducting oligomers for molecular electronic devices
[AD-A249929] p 3605 N92-30796
Thermoset precursor to monolithic carbon glass prepared by the Pd/Cu-catalyzed alkynylation of polyphenylenes
[AD-A249920] p 3605 N92-30816
Electrooxidation of soluble alpha,alpha-coupled thiophene oligomers
[AD-A249928] p 3605 N92-30817
ON-LINE SYSTEMS
On-line analysis capabilities developed to support the AFW wind-tunnel tests
[NASA-TM-107651] p 3580 N92-30752
ONBOARD DATA PROCESSING
Technical and economic feasibility of integrated video service by satellite
[NASA-CR-189210] p 3614 N92-30300
An integrated Ka/Ku-band payload for personal, mobile and private business communications
p 3619 N92-30933
OPACITY
Nonlinear RR Lyrae models with new Livermore opacities
[DE92-011158] p 3741 N92-31108
OPERATING COSTS
Allocation and recovery of federal airport and airway costs, 1991
[AD-A249436] p 3585 N92-30777
OPERATING SYSTEMS (COMPUTERS)
Survivable algorithms and redundancy management in NASA's distributed computing systems
[NASA-CR-189827] p 3691 N92-30299
A model of the ADA avionics real-time system: An example of the benefits of the hardware/software codesign approach in development of real-time systems
[AD-A248893] p 3581 N92-30524
OPERATIONAL PROBLEMS
Stealth: A revolutionary change to air warfare
[AD-A249880] p 3617 N92-30869
OPERATIONS RESEARCH
Operations and logistics tasks in the Columbus development program
[MBB-UO-0166-91-PUB] p 3708 N92-30419
OPERATORS (MATHEMATICS)
From a world-sheet supersymmetry to the Dirac equation
[DE92-622375] p 3731 N92-30799
From a particle with a world-line supersymmetry to the Dirac-like equation
[DE92-622376] p 3731 N92-30800
Quantum mechanics in Grassmann space
[DE92-622377] p 3711 N92-30801
Heat flow of p-harmonic maps with values into spheres
[DE92-630236] p 3707 N92-31135
OPTICAL COMMUNICATION
Fiber optic based signal processing
[AD-A247857] p 3720 N92-30248
OPTICAL FIBERS
Fiber optic based signal processing
[AD-A247857] p 3720 N92-30248
Single mode variable-sensitivity fiber optic sensors
[NASA-CR-190492] p 3721 N92-30975
Optical transducers for scintillating fiber readout
[DE92-015963] p 3721 N92-31187
OPTICAL FILTERS
Initial laboratory evaluation of color video cameras
[DE92-010399] p 3637 N92-30822
Acousto-optic filtering of lidar signals
p 3650 N92-31077
OPTICAL MATERIALS
Eye/sensor protection against laser irradiation ablative mirror devices: A materials assessment
[AD-A248787] p 3688 N92-30615
Growth and evaluation of nonlinear optical materials for laser applications: Barium borate, lithium borate, and silver gallium selenide
[AD-A248861] p 3624 N92-30617
OPTICAL MEASUREMENT
Three-dimensional laser window formation
[NASA-RP-1280] p 3585 N92-30307
Lidar measurement of optical turbulence: Theory of the crossed path technique
[AD-A248938] p 3720 N92-30343
Laser optical mouse
[AD-D015307] p 3690 N92-30564
OPTICAL MEASURING INSTRUMENTS
Lidar measurement of optical turbulence: Theory of the crossed path technique
[AD-A248938] p 3720 N92-30343
Eye/sensor protection against laser irradiation ablative mirror devices: A materials assessment
[AD-A248787] p 3688 N92-30615
Linkage of anthropogenic aerosol to clouds and climate
[DE92-013574] p 3674 N92-30707
Single mode variable-sensitivity fiber optic sensors
[NASA-CR-190492] p 3721 N92-30975
OPTICAL MICROSCOPES
Demonstration of magnetic domain boundary movement using an easily assembled videocam-microscope system
p 3611 N92-30286
OPTICAL PATHS
Lidar measurement of optical turbulence: Theory of the crossed path technique
[AD-A248938] p 3720 N92-30343
Spectroscopic method for Earth-satellite-Earth laser long-path absorption measurements using Retroreflector In Space (RIS) p 3652 N92-31088
OPTICAL POLARIZATION
Fiber optic Michelson sensor and arrays with passive elimination of polarization fading and source feedback isolation
[AD-D015290] p 3722 N92-31213
OPTICAL PROPERTIES
Interpretation of optical remote sensing data over coastal waters
[BCRS-91-27] p 3667 N92-30472
Ion channeling and spectroscopic ellipsometry examinations of thin-film SiO2/epi-Si structures
[DE92-015129] p 3728 N92-30577
Multiple scattering effects on spaceborne lidar
p 3641 N92-31032
Lidar measurements of cloud extinction coefficient distribution and its forward scattering phase function according to multiply scattered lidar returns
p 3651 N92-31082
OPTICAL PUMPING
VUV production from a ferrite-driven flash-pumped system
[DE92-011362] p 3657 N92-30805
High field optical-pumping spin-exchange polarized deuterium source
[DE92-010274] p 3657 N92-30848
OPTICAL RADAR
Lidar measurement of optical turbulence: Theory of the crossed path technique
[AD-A248938] p 3720 N92-30343
Sixteenth International Laser Radar Conference, part 2
[NASA-CP-3158-PT-2] p 3637 N92-31013
Boundary layer structure over the ocean observed by LEANDRE 1 during a tramontane event
p 3638 N92-31014
Low-level atmospheric flows studied by pulsed Doppler lidar p 3638 N92-31015
On the existence of convectively produced gravity waves p 3638 N92-31016
Doppler lidar wind measurement with the edge technique p 3638 N92-31017
Tropospheric and stratospheric wind profiling with a direct detection Doppler lidar p 3639 N92-31018
Atmospheric wind sensing with a 1 and 2 micron coherent lidar p 3639 N92-31019
Design of a near-IR coherent lidar for high spatial and velocity resolution wind measurement
p 3639 N92-31020
A pulsed CO2 Doppler lidar for boundary layer monitoring p 3639 N92-31021
A compact high repetition rate CO2 coherent Doppler lidar p 3639 N92-31022
Simplified signal processing for an airborne CO2 Doppler lidar p 3639 N92-31023
Phase noise in pulsed Doppler lidar and limitations on achievable single-shot velocity accuracy
p 3639 N92-31024
A comparison of Ultra-Sensitive Coherent Detection (USCD) and heterodyne detection for a wind sensing application p 3640 N92-31025
Diversity imaging techniques in lidar
p 3640 N92-31026
A range-resolved bistatic lidar using a high-sensitive CCD-camera p 3640 N92-31027
Fluorescence lidar multi-color imaging of vegetation
p 3640 N92-31028
A geodetic laser radar rangefinder with 10(exp -7) resolution p 3641 N92-31029
Altimetry and lidar using AlGaAs lasers modulated with pseudo-random codes p 3641 N92-31030
Multiple scattering technique lidar
p 3641 N92-31031
Multiple scattering effects on spaceborne lidar
p 3641 N92-31032
Measurement of multiple scattering effects with a polarization Raman elastic-backscatter lidar
p 3641 N92-31033
Determining water cloud particle sizes from lidar depolarization measurements and time dependent multiple scattering coefficients p 3641 N92-31034
Multiple scattering lidar returns from stratus clouds
p 3642 N92-31035
Analytical multiple scattering correction to the Mie theory: Application to the analysis of the lidar signal
p 3642 N92-31036
Airborne lidar and radiometric observations of PBL- and low clouds p 3642 N92-31037
ECLIPS at LMD: Preliminary results of phase 2
p 3643 N92-31038
The 2nd phase of the LEANDRE program: Water-vapor DIAL measurement p 3643 N92-31039
Advanced Raman water vapor lidar
p 3643 N92-31040
Water vapor variance measurements using a Raman lidar p 3643 N92-31041
Airborne remote sensing of tropospheric water vapor using a near infrared DIAL system p 3644 N92-31042
Trial of a slant visual range measuring device
p 3644 N92-31043
Lidar depolarization by nonspherical particles: Potential of combined depolarization/backscattering measurements for PSC's characterization p 3644 N92-31044
Coherent CO2 lidar: A superior system for observing clouds? p 3644 N92-31045
Measurement of aerosol profiles using high-spectral-resolution Rayleigh-Mie lidar
p 3644 N92-31046
Laboratory scaled simulation of lidar cloud sounding experiments p 3645 N92-31047
An alexandrite regenerative amplifier for water vapor and temperature measurements p 3645 N92-31048
Wavemeter measurements of frequency stability of an injection seeded alexandrite laser for pressure and temperature lidar p 3645 N92-31049
Conically scanned lidar telescope using holographic optical elements p 3645 N92-31050
Optics of the ozone lidar ELSA p 3645 N92-31051
Interferometers adaptations to lidars
p 3645 N92-31052
An ultra-sensitive coherent detector capable of single photon detection for lidar applications
p 3646 N92-31053
A high speed signal processing system for a diode-pumped YAG lidar p 3646 N92-31054

Pulsed laser spectral measurement using a Fabry-Perot interferometer: Limits to resolution p 3646 N92-31055
Tunable Electro-optic modulators for lidar systems and atmospheric applications p 3646 N92-31056
Injection seeded single mode alexandrite ring laser for lidar applications p 3646 N92-31057
Tm,Ho:YAG laser with tunable range of 2.08-2.12 microns and its applications to spectroscopy p 3646 N92-31058
Theoretical simulation of a 2 micron airborne solid state laser anemometer p 3647 N92-31059
Comparison of eye-safe solid state laser DIAL with passive gas filter correlation measurements from aircraft and spacecraft p 3647 N92-31060
Lidar multiple scattering: Dependence on atmospheric parameters p 3647 N92-31061
Verification measurement of a polarization Raman elastic-backscatter lidar p 3647 N92-31062
Time and polarization dependent double scattering calculations of lidar returns from water clouds p 3647 N92-31063
Multiple scattering wavelength dependent backscattering of kaolin dust in the IR: Measurements and theory p 3648 N92-31064
Aureole lidar: Design, operation, and comparison with in-situ measurements p 3648 N92-31065
A study of atmospheric optical scattering parameters at 1.5 and 2 micron region for solid state Doppler lidar applications p 3648 N92-31067
A cable detection lidar system for helicopters p 3648 N92-31068
Lidar analysis techniques for use in the atmospheric boundary layer p 3649 N92-31069
Correction for nonlinear photon counting effects in lidar systems p 3649 N92-31070
High background photon counting lidar p 3649 N92-31071
Development of a Raman lidar simulation tool p 3649 N92-31072
A variable phase function approach for the inversion of lidar return signals p 3649 N92-31073
A comparison of lidar inversion methods for cirrus applications p 3649 N92-31074
Time and wavelength domain algorithms for chemical analysis by laser radar p 3650 N92-31075
Lidar receivers for picosecond remote sensing p 3650 N92-31076
Acousto-optic filtering of lidar signals p 3650 N92-31077
Ground-based Doppler lidar of increased laser instability: Conception and design p 3650 N92-31078
A considerable effect of stratospheric aerosol on lidar-detected ozone profile and a three-wavelength inversion technique for both ozone and aerosol p 3651 N92-31080
High-resolution processing of long-pulse-lidar data p 3651 N92-31081
Lidar measurements of cloud extinction coefficient distribution and its forward scattering phase function according to multiply scattered lidar returns p 3651 N92-31082
Measurements of the backscattering phase matrices of crystal clouds with a polarization lidar p 3651 N92-31083
Measurement capabilities of giant lidars for middle and upper atmospheric applications p 3651 N92-31084
Lidar sounding of ozone and aerosols p 3652 N92-31085
Atmospheric measurements using the LAMP lidar during the LADIMAS campaign p 3652 N92-31086
Lidar measurements using large liquid mirror telescopes p 3652 N92-31087
Performance modeling of daytime Raman lidar systems for profiling atmospheric water vapor p 3653 N92-31090
BELINDA: Broadband Emission Lidar with Narrowband Determination of Absorption. A new concept for measuring water vapor and temperature profiles p 3653 N92-31091
DIAL simulations for satellite water vapor profile measurements within the BEST project p 3653 N92-31092
Airborne water vapor DIAL research: System development and field measurements p 3653 N92-31093
Alexandrite lidar for the atmospheric water vapor detection and development of powerful tunable sources in IR p 3653 N92-31094
Emerging solid-state laser technology by lidar/DIAL remote sensing p 3653 N92-31095
Coherent summation of spatially distorted Doppler lidar signals using a two-dimensional heterodyne detector array p 3654 N92-31096
A portable lidar using a diode-pumped YAG laser p 3654 N92-31098
Investigations on atomic-vapor-filter high-spectral-resolution lidar for temperature measurements p 3654 N92-31099
HgCdTe photomixers for CO2 laser radar systems p 3654 N92-31100
Airborne lidar mapping of vertical ozone distributions in support of the 1990 Clean Air Act Amendments p 3654 N92-31101
Measurements of fugitive hydrocarbon emissions with a tunable infrared DIAL p 3655 N92-31102
The ENEA CO2 lidar/DIAL station activity in a tropospheric remote sensing program p 3655 N92-31103
Lidar observation of marine mixed layer p 3655 N92-31104
Aerosol extinction measurements with CO2-lidar p 3655 N92-31105
Dense fog on the highway: Visual range monitoring in cars? p 3655 N92-31106

OPTICAL SCANNERS
Full surface testing of grazing incidence mirrors [AD-A248851] p 3719 N92-30233
On the remote sensing of water quality using the optical airborne scanner CAESAR [BCRS-90-30] p 3666 N92-30466
CAESAR: Evaluation of the dual-look concept [BCRS-91-10] p 3666 N92-30467
Interpretation of optical remote sensing data over coastal waters [BCRS-91-27] p 3667 N92-30472

OPTICAL SLANT RANGE
Trial of a slant visual range measuring device p 3644 N92-31043

OPTICAL THICKNESS
A comparison of lidar inversion methods for cirrus applications p 3649 N92-31074

OPTICAL WAVEGUIDES
Waveguide polarizer using localized surface plasmons [AD-D015258] p 3614 N92-30348

OPTIMAL CONTROL
Generalized projected gradient-type iterative method for parametric and functional optimization of dynamical systems subject to constraints [ESA-TT-1166] p 3694 N92-30512
Microgravity vibration isolation: Optimal preview and feedback control [NASA-TM-105673] p 3613 N92-30692

OPTIMIZATION
MBB-LAGRANGE: A general structural reliability and optimization structural system [MBB/FW321/S/PUB/467] p 3662 N92-30423
Multidisciplinary optimization of fiber composite aircraft structures [MBB/FW321/S/PUB/476] p 3579 N92-30424
Numerical optimization in Germany: A non-exhaustive survey on current activities with emphasis on aeronautics [MBB/FE211/S/PUB/474] p 3573 N92-30675
Optimization of the microstrip gas counter [NIKHEF-H/91-21] p 3637 N92-30688
Transactions of the 9th Army Conference on Applied Mathematics and Computing [AD-A252140] p 3706 N92-30843
Development of a reliability maintenance optimization method p 3697 N92-30956
Nonlinear aerodynamics and the design of wing tips [NASA-CR-190649] p 3577 N92-31157

OPTOELECTRONIC DEVICES
Transient photoconductivity of low temperature GaAs grown by molecular beam epitaxy terahertz radar applications [DE92-011848] p 3729 N92-30854
Tunable Electro-optic modulators for lidar systems and atmospheric applications p 3646 N92-31056
Multiple scattering wavelength dependent backscattering of kaolin dust in the IR: Measurements and theory p 3648 N92-31064

ORBIT PERTURBATION
Altimeter and gravity data analysis [NASA-CR-190478] p 3676 N92-30756
Constraints on the putative companions to PSR1257+12 p 3738 N92-31232

ORBITAL MECHANICS
Correlative measurement opportunities between ATLAS-1 and UARS experiments [NASA-TM-107630] p 3679 N92-30735
Constraints on the putative companions to PSR1257+12 p 3738 N92-31232

ORBITS
Coexistence of uniquely ergodic subsystems of interval mapping [DE92-630231] p 3732 N92-31133

ORDER-DISORDER TRANSFORMATIONS
Determination of pair potentials by analysis of diffuse scattering of the local field in Pd3V and Ni3V [ESA-TT-1228] p 3597 N92-30513
X ray scattering studies of non-equilibrium ordering processes [DE92-014006] p 3598 N92-30787
Theoretical study of phase stability in Ni-Al and Ni-Ti alloys [DE92-014776] p 3599 N92-31119
Self-consistent-field KKR-CPA calculations in the atomic-sphere approximations [DE92-011525] p 3600 N92-31138

ORGANIC COMPOUNDS
Perforated monolayers [DE92-011632] p 3593 N92-30344
A pulse combustion-based VOC destruction technique [DE92-013563] p 3594 N92-30369
Extended orthogonally fused conducting oligomers for molecular electronic devices [AD-A249927] p 3605 N92-30795
Synthesis of orthogonally fused conducting oligomers for molecular electronic devices [AD-A249929] p 3605 N92-30796

ORGANIC LASERS
Sol-gel optics: Proceedings SPIE-The International Society for Optical Engineering [AD-A249986] p 3721 N92-31126

ORGANIC MATERIALS
Surface-mediated photocatalysis [AD-A249906] p 3595 N92-30793

ORGANIC SEMICONDUCTORS
Surface-mediated photocatalysis [AD-A249906] p 3595 N92-30793

ORGANIZING
Information systems: How they affect and are affected by organization structure [AD-A248852] p 3734 N92-30234
Preparation for a new plane (A 320): Experience reviewed p 3697 N92-30954
Flight crew integration in the maintenance chain of a commercial aircraft (A 320) p 3698 N92-30957

ORGANOMETALLIC COMPOUNDS
Vibrational overtone spectroscopy of gaseous metallocenes [AD-A251088] p 3593 N92-30245
Studies of thermal decomposition of the 1:1 R3Al:en adduct (R = Me, Et; en = ethylenediamine): Synthesis and structure of a novel intermediate Al((HNCH2CH2NH)AlMe2)3 [AD-A251061] p 3603 N92-30623
Extended orthogonally fused conducting oligomers for molecular electronic devices [AD-A249927] p 3605 N92-30795

ORGUEIL METEORITE
Presolar (?) corundum in the Orgueil meteorite p 3738 N92-31230

ORTHOGONALITY
On real and complex zeros of orthogonal polynomials in a discrete Sobolev space [REPT-91-98] p 3702 N92-30350

ORTHOSTATIC TOLERANCE
Tolerance of beta blocked hypertensives during orthostatic and altitude stresses [AD-A249904] p 3685 N92-30745

OSCILLATIONS
The role of stochasticity in sawtooth oscillation [NIFS-103] p 3710 N92-30983

OSCILLATORS
Design of a near-IR coherent lidar for high spatial and velocity resolution wind measurement p 3639 N92-31020
A pulsed CO2 Doppler lidar for boundary layer monitoring p 3639 N92-31021
Modification of 95 GHz radar source module for low phase noise operation [AD-A249793] p 3622 N92-31180
Reflector development for XUV free-electron laser oscillators [DE92-015212] p 3657 N92-31182

OXIDATION
Ion channeling and spectroscopic ellipsometry examinations of thin-film SiO2/epi-Si structures [DE92-015129] p 3728 N92-30577
Photodegradation effects in materials exposed to high flux solar and solar simulated radiation [DE91-002147] p 3596 N92-30879
Methane to liquid [DE92-001277] p 3596 N92-30883
Polyphosphazenes bearing polymerizable pyrrole, thiophene and furan side groups: Synthesis and chemical oxidation [AD-A249747] p 3607 N92-31207
Oxidation of gallium arsenide [DE92-016208] p 3731 N92-31220

OXIDATION-REDUCTION REACTIONS
Electrooxidation of soluble alpha,alpha-coupled thiophene oligomers [AD-A249928] p 3605 N92-30817

OXIDE FILMS
Computer-controlled ion beam sputter-deposition of superconducting oxide films
[AD-A248495] p 3601 N92-30326
Evaluation of doped polyethylene oxide as solid electrolyte for polymer batteries
[AD-A249501] p 3624 N92-30619
Anomalous hopping conductivity in amorphous indium-oxide films
[ITN-92-85166] p 3729 N92-30781
Ellipsometric study of oxide films formed on LDEF metal samples
[AD-A249856] p 3599 N92-31110
OXYGEN
Voltammetric measurement of oxygen in single neurons using platinized carbon ring electrodes
[AD-A252191] p 3683 N92-30531
Fundamental studies of carbon, NH, and oxygen rings and other high energy density molecular systems
[AD-A246963] p 3715 N92-30680
High-temperature ignition of propane with MTBE as an additive: Shock-tube experiments and modeling
[DE92-006679] p 3594 N92-30749
Computational simulation of diamond chemical vapor deposition in premixed C2H2/O2/H2 and CH4/O2 strained flames
[DE92-012144] p 3606 N92-30857
OXYGEN CONSUMPTION
Voltammetric measurement of oxygen in single neurons using platinized carbon ring electrodes
[AD-A252191] p 3683 N92-30531
Feasibility of a walk test to assess the cardiorespiratory fitness of Naval personnel
[AD-A250650] p 3684 N92-30603
OXYGEN IONS
Evidence for interference between resonant and nonresonant transfer and excitation
[DE92-011779] p 3716 N92-30853
OZONE
Sixteenth International Laser Radar Conference, part 2
[NASA-CP-3158-PT-2] p 3637 N92-31013
Optics of the ozone lidar ELSA p 3645 N92-31051
A variable phase function approach for the inversion of lidar return signals p 3649 N92-31073
A considerable effect of stratospheric aerosol on lidar-detected ozone profile and a three-wavelength inversion technique for both ozone and aerosol p 3651 N92-31080
Measurement capabilities of giant lidars for middle and upper atmospheric applications p 3651 N92-31084
Lidar sounding of ozone and aerosols p 3652 N92-31085
Airborne lidar mapping of vertical ozone distributions in support of the 1990 Clean Air Act Amendments p 3654 N92-31101
OZONOMETRY
Optics of the ozone lidar ELSA p 3645 N92-31051
A variable phase function approach for the inversion of lidar return signals p 3649 N92-31073
OZONOSPHERE
Optics of the ozone lidar ELSA p 3645 N92-31051

P

PACIFIC OCEAN
Oceanic CO2 measurements for the WOCE hydrographic survey in the Pacific Ocean, 1990-1991: Shore based analyses during legs 1-3
[DE92-013064] p 3682 N92-30861
PACKAGING
Innovative techniques for the production of low cost 2-D laser diode arrays supplies or services and prices/costs
[AD-A252665] p 3656 N92-30552
PACKET TRANSMISSION
Modeling of video traffic in packet networks, low rate video compression, and the development of a lossy+lossless image compression algorithm
[NASA-CR-190546] p 3691 N92-30296
PAINTS
Environment modelling in near Earth space: Preliminary LDEF results p 3588 N92-31225
PAIR PRODUCTION
The escape of greater MeV photons from cosmological gamma-ray bursts
[DE92-013545] p 3743 N92-30706
PAKISTAN
Solar-hydrogen energy system for solar belt countries and use of remote sensing p 3668 N92-30913
PALEOBIOLOGY
Field studies in geophysical diffraction tomography
[DE92-015084] p 3677 N92-31009
PARABOLIC DIFFERENTIAL EQUATIONS
Global existence for a semilinear elliptic-parabolic PDE system
[REPT-91-70] p 3628 N92-30372
Flow of fresh and salt water in an aquifer with injection from the top
[REPT-91-68] p 3629 N92-30453
Resolution of the three-dimensional parabolic equation applied to acoustic propagation at low altitudes
[ONERA-RF-17/3641-PY] p 3711 N92-30966
PARABOLIC REFLECTORS
Antenna pattern measurement facilities
[AD-A248964] p 3584 N92-30329
Uniform flux dish concentrators for photovoltaic application
[DE92-010566] p 3671 N92-30896
PARACHUTE FABRICS
Selection of opening model for parachute scaling studies
[AD-A250882] p 3573 N92-30239
PARACHUTES
Selection of opening model for parachute scaling studies
[AD-A250882] p 3573 N92-30239
PARALLEL FLOW
Effects of fast ions and an external inductive electric field on the neoclassical parallel flow, current, and rotation in general toroidal systems
[NIFS-150] p 3713 N92-30500
PARALLEL PROCESSING (COMPUTERS)
Three-dimensional shock wave physics simulations on massively parallel supercomputers
[DE92-008679] p 3698 N92-30363
Scalable parallel molecular dynamics on MIMD supercomputers
[DE92-015041] p 3698 N92-30401
Configuration algorithms for hierarchical supernode machines
[IMAG-RR-853-I] p 3694 N92-30493
Implementation of parallel algorithms
[AD-A248826] p 3695 N92-30555
Exploiting resource parallelism for integrated fault monitoring and recovery
[AD-A248843] p 3699 N92-30557
VLSI design, parallel computation, and distributed computing
[AD-A252349] p 3699 N92-30596
The GKS input model in MANIFOLD
[CWI-CS-R9127] p 3699 N92-30696
PARALLEL PROGRAMMING
Configuration algorithms for hierarchical supernode machines
[IMAG-RR-853-I] p 3694 N92-30493
Implementation of parallel algorithms
[AD-A248826] p 3695 N92-30555
The GKS input model in MANIFOLD
[CWI-CS-R9127] p 3699 N92-30696
PARAMETER IDENTIFICATION
Comparison of signal processing methods for estimation of network impedance for remote protection
[ETN-92-91686] p 3623 N92-30503
PARAMETERIZATION
Plasma parameter estimations for the large helical device based on the gyro-reduced Bohm scaling
[NIFS-114] p 3723 N92-30499
PARAMETRIC AMPLIFIERS
Comparison of eye-safe solid state laser DIAL with passive gas filter correlation measurements from aircraft and spacecraft p 3647 N92-31060
PARSING ALGORITHMS
The formal power of AGs with respect to their underlying CFGs
[REPT-91-75] p 3703 N92-30456
PARTIAL DIFFERENTIAL EQUATIONS
Solving the Euler equations using adaptive mesh motion and refinement
[AD-A252364] p 3705 N92-30597
Research in stochastic analysis and its applications
[AD-A249482] p 3708 N92-30633
PARTICLE ACCELERATOR TARGETS
Search for light neutral scalar and pseudoscalar particles in pFe interactions at 70 GeV
[DE92-627317] p 3713 N92-30404
On the temperature role in the tunneling process at the cold fusion
[DE92-627497] p 3727 N92-30405
Recent experimental studies on hadron showers produced in high energy muon-nucleus interactions
[DE92-016002] p 3719 N92-31219
PARTICLE ACCELERATORS
Research on elementary particle physics
[DE92-014622] p 3715 N92-30625
Optimization of the microstrip gas counter
[NIKHEF-H/91-21] p 3637 N92-30688
PARTICLE BEAMS
The RADLAC beam propagation experiment
[DE92-014620] p 3718 N92-30624
Optimization of the microstrip gas counter
[NIKHEF-H/91-21] p 3637 N92-30688
PARTICLE COLLISIONS
Intermittency, multifractality, and hadronic collisions
[DE92-014595] p 3714 N92-30606
Theoretical studies in elementary particle physics
[DE92-015295] p 3714 N92-30610
Optimization of the microstrip gas counter
[NIKHEF-H/91-21] p 3637 N92-30688
Application of superconducting cavities to the collider rings of the SSC
[DE92-011692] p 3718 N92-30811
Mechanical design and finite element analysis of the SDC central calorimeter
[DE92-011197] p 3655 N92-31109
Physics of the STAR experiment at the relativistic heavy ion collider
[DE92-014481] p 3719 N92-31198
PARTICLE ENERGY
Polarization effects in pi(+) absorption in He-3
[ITN-92-85164] p 3714 N92-30580
Polarization effects in pi(+) absorption in He-4
[ITN-92-85163] p 3715 N92-30780
PARTICLE INTERACTIONS
Spin amplitudes of pp-scattering in a unitarized supercritical pomeron model
[DE92-624639] p 3711 N92-30236
The escape of greater MeV photons from cosmological gamma-ray bursts
[DE92-013545] p 3743 N92-30706
Remarks on the exotic U-meson
[RAL-91-090] p 3715 N92-30750
PARTICLE MOTION
Spin amplitudes of pp-scattering in a unitarized supercritical pomeron model
[DE92-624639] p 3711 N92-30236
Scalable parallel molecular dynamics on MIMD supercomputers
[DE92-015041] p 3698 N92-30401
Investigation of the interface phenomena due to interaction of high intensity stress waves with geologic boundaries
[AD-A248992] p 3675 N92-30525
A dynamic model for beam tube vacuum effects on the SSC cryogenic system
[DE92-013967] p 3719 N92-30840
PARTICLE PRODUCTION
Physics of the STAR experiment at the relativistic heavy ion collider
[DE92-014481] p 3719 N92-31198
PARTICLE SIZE DISTRIBUTION
Cluster assembly of hierarchical nanostructures
[DE92-010498] p 3716 N92-30826
Determining water cloud particle sizes from lidar depolarization measurements and time dependent multiple scattering coefficients p 3641 N92-31034
Lidar depolarization by nonspherical particles: Potential of combined depolarization/backscattering measurements for PSC's characterization p 3644 N92-31044
Lidar sounding of ozone and aerosols p 3652 N92-31085
Ultrafine aerosol size distributions and sulfuric acid vapor pressures: Implications for new particle formation in the atmosphere
[DE92-015217] p 3675 N92-31183
PARTICLE THEORY
Stochastic strings, topology, and space-time confinement
[DE92-630239] p 3732 N92-31136
PARTICULATES
Status of selected air pollution control programs, February 1992
[PB92-171966] p 3673 N92-30561
PARTITIONS (MATHEMATICS)
Restrictions of graph partition problems, part 1
[RUU-CS-91-44-PT-1] p 3703 N92-30446
PARTONS
Physics of the STAR experiment at the relativistic heavy ion collider
[DE92-014481] p 3719 N92-31198
PATTERN RECOGNITION
A one-class classifier for identifying urban areas in remotely-sensed data
[DE92-013539] p 3667 N92-30704
Characterizing ultrasonic transducers using pattern recognition techniques
[DE92-015845] p 3711 N92-30890
PAYLOADS
An integrated Ka/Ku-band payload for personal, mobile and private business communications p 3619 N92-30933

PELLETS
Tritium content of a DT pellet in inertial confinement fusion
[NIFS-113] p 3722 N92-30430
PENETRATION
Eulerian simulation of the perforation of aluminum plates by nondeforming projectiles
[DE92-011515] p 3664 N92-31123
Environment modelling in near Earth space: Preliminary LDEF results p 3588 N92-31225
PERCEPTION
Attitudinal and situational differences between national laboratory inventors and inventor-entrepreneurs
[DE92-015768] p 3733 N92-30889
PERFORMANCE PREDICTION
A principled approach to the measurement of situation awareness in commercial aviation
[NASA-CR-4451] p 3686 N92-30306
NEP systems engineering efforts in FY-92: Plans and status
[NASA-TM-105775] p 3588 N92-30308
Thrust stand evaluation of engine performance improvement algorithms in an F-15 airplane
[NASA-TM-104252] p 3581 N92-30518
Modelling of heavily loaded lubricated contacts
[AD-A248807] p 3659 N92-30554
TRAC performance estimates
[NASA-CR-190530] p 3701 N92-30778
Acoustic fatigue life prediction for nonlinear structures with multiple resonant modes
[NASA-CR-190471] p 3664 N92-30988
Performance modeling of daytime Raman lidar systems for profiling atmospheric water vapor
p 3653 N92-31090
Preliminary subsonic aerodynamic model for simulation studies of the HL-20 lifting body
[NASA-TM-4302] p 3583 N92-31175
Aeronautical Mobile Satellite Service (AMSS) capacity analysis and protocol performance simulation results
[DOT/FAA/CT-TN90/64] p 3622 N92-31212
PERFORMANCE TESTS
Full surface testing of grazing incidence mirrors
[AD-A248851] p 3719 N92-30233
Tests of the performance of different gas mixtures in microstrip gas counters
[NIKHEF-H/91-23] p 3636 N92-30365
On the potential use of the terminal Doppler weather radar gust front detection algorithm on the WSR-88D system. Part 1: Impacts of radar system differences
[DOT/FAA/NR-92/8,I] p 3678 N92-30495
Compact range test applications, phase 2
[AD-A248790] p 3615 N92-30583
Collected notes from the Benchmarks and Metrics Workshop
[NASA-TM-107910] p 3701 N92-30710
VDHW-related memo's
[LINO-1991-5] p 3718 N92-30725
Measurement report on the present Video Highway System of MEA p 3718 N92-30726
Console driver p 3718 N92-30728
New shortwave solar radiometer with information-based sparse sampling
[DE92-010483] p 3742 N92-30797
Testing of double-layer capacitors for high reliability applications
[DE92-011384] p 3626 N92-30807
Initial laboratory evaluation of color video cameras
[DE92-010399] p 3637 N92-30822
Characterizing ultrasonic transducers using pattern recognition techniques
[DE92-015845] p 3711 N92-30890
EHF (28/19 GHz) personal communications satellite terminal development p 3619 N92-30935
Direct sequence spread spectrum CDMA in shared spectrum applications p 3619 N92-30939
GNAS Maintenance Control Center (GMCC) Design Qualification Test and Evaluation (DQT/E) test procedures
[DOT/FAA/CT-TN91/40] p 3585 N92-30976
Effect of atmospheric extinction on laser rangefinder performance at 1.54 and 0.6 microns
p 3648 N92-31066
A study of atmospheric optical scattering parameters at 1.5 and 2 micron region for solid state Doppler lidar applications p 3648 N92-31067
Cryogenic Magnetic Bearing Test Facility (CMBTF)
[NASA-CR-189087] p 3582 N92-31164
Evaluation of grounding and mooring points for Army aircraft
[AD-A250749] p 3579 N92-31193
PERIODIC VARIATIONS
The role of stochasticity in sawtooth oscillation
[NIFS-103] p 3710 N92-30983
PERIPHERAL EQUIPMENT (COMPUTERS)
Laser optical mouse
[AD-D015307] p 3690 N92-30564
PERMITTIVITY
Evaluation of doped polyethylene oxide as solid electrolyte for polymer batteries
[AD-A249501] p 3624 N92-30619
PEROVSKITES
Superconductivity and magnetism in rapidly solidified perovskites
[DE92-014081] p 3597 N92-30588
PERSONAL COMPUTERS
Printer port interface
[NASA-CASE-LAR-13950-1] p 3690 N92-30541
PERSONNEL
Exercise behavior among Navy runners and non-runners
[AD-A250651] p 3685 N92-30644
Attitudinal and situational differences between national laboratory inventors and inventor-entrepreneurs
[DE92-015768] p 3733 N92-30889
PERSONNEL MANAGEMENT
Flight crew integration in the maintenance chain of a commercial aircraft (A 320) p 3698 N92-30957
PERTURBATION THEORY
Non-perturbative effects in high-energy electroweak interactions
[NIKHEF-H/91-24] p 3715 N92-30697
Theoretical particle physics
[DE92-014531] p 3716 N92-30841
PETRI NETS
Synchronized continuous flow systems
[REPT-91-88] p 3704 N92-30517
PHARMACOLOGY
Tolerance of beta blocked hypertensives during orthostatic and altitude stresses
[AD-A249904] p 3685 N92-30745
PHASE DIAGRAMS
Cu-Zn binary phase diagram and diffusion couples
p 3600 N92-30269
Be-Cu precipitation hardening experiment
p 3601 N92-30276
PHASE ERROR
Glint errors derived from the partial derivatives of the echo signal phase for a distributed scatterer
[AD-A249499] p 3615 N92-30637
PHASE LOCKED SYSTEMS
Mathematical models of non-linear mechanical and electrical systems and their qualitative behavior
[AD-A248847] p 3622 N92-30249
PHASE MODULATION
Modeling fast modulation effects in cesium atomic clocks
[AD-A252649] p 3636 N92-30412
PHASE SHIFT
Mathematical models of non-linear mechanical and electrical systems and their qualitative behavior
[AD-A248847] p 3622 N92-30249
Theoretical study of phase-shifted quantum beats in time-resolved luminescence spectra from a biased asymmetric double quantum well
[AD-A252422] p 3710 N92-30549
PHASE TRANSFORMATIONS
Structure, processing, and properties of potatoes
p 3611 N92-30288
Transformation toughening of ceramics
[AD-A248903] p 3601 N92-30342
Theoretical study of phase stability in Ni-Al and Ni-Ti alloys
[DE92-014776] p 3599 N92-31119
Stabilization of face-centered-cubic titanium
[DE92-011530] p 3600 N92-31125
Phase transformations in weldments: New materials and new perspectives
[DE92-016231] p 3600 N92-31177
Fine scale mesostructures in superconducting and other materials
[DE92-015207] p 3730 N92-31200
PHASE VELOCITY
Investigation of the interface phenomena due to interaction of high intensity stress waves with geologic boundaries
[AD-A248992] p 3675 N92-30525
PHASED ARRAYS
The rise of active-element phased-array radar
[RAND-P-7747-RGS] p 3616 N92-30755
On the radial component of the electric field for a monopole phased array antenna focused in the near zone
[AD-A249441] p 3616 N92-30761
Operation, maintenance and research activities at the Norwegian Seismic Array (NORSAR), the Norwegian Regional Seismic Array (NORESS), and the Arctic Regional Seismic Array (ARCESS)
[AD-A250403] p 3677 N92-31142
PHENOLS
Synthesis of cresols and xylenols from benzene and methanol
[DE91-002143] p 3596 N92-30882
PHENOMENOLOGY
Proceedings, phenomenology and applications of high temperature superconductors
[DE92-011133] p 3627 N92-31107
PHONONS
Studies of phonons and electronic excitations in semiconductor heterostructures
[AD-A249406] p 3729 N92-30772
High resolution electron energy loss studies of surface vibrations
[DE92-014608] p 3626 N92-30901
PHOSPHORS
A method of making a single layer multi-color luminescent display
[NASA-CASE-LAR-14811-1] p 3622 N92-30389
Tunable solid state lasers based on molecular ions
[AD-A249423] p 3656 N92-30774
PHOSPHORUS
Polyphosphazenes bearing polymerizable pyrrole, thiophene and furan side groups: Synthesis and chemical oxidation
[AD-A249747] p 3607 N92-31207
PHOTICS
Neurophysiological analysis of circadian rhythm entrainment
[AD-A248466] p 3684 N92-30319
PHOTOACOUSTIC SPECTROSCOPY
Combustion diagnostics by photo-deflection spectroscopy
[AD-A250802] p 3594 N92-30645
PHOTOCHEMICAL REACTIONS
Photoinitiated electron transfer in multichromophoric species: Synthetic tetrads and pentads featuring diquinone moieties
[DE92-013472] p 3683 N92-30368
Photochemical solar energy conversion utilizing semiconductors localized in membrane-mimetic systems
[DE92-011115] p 3670 N92-30694
Surface-mediated photocatalysis
[AD-A249906] p 3595 N92-30793
Synthesis of cresols and xylenols from benzene and methanol
[DE91-002143] p 3596 N92-30882
PHOTOCONDUCTIVITY
Transient photoconductivity of low temperature GaAs grown by molecular beam epitaxy terahertz radar applications
[DE92-011848] p 3729 N92-30854
PHOTODIODES
HgCdTe photomixers for CO2 laser radar systems
p 3654 N92-31100
Optical transducers for scintillating fiber readout
[DE92-015963] p 3721 N92-31187
PHOTODISSOCIATION
Photodissociation of azulene under UV-laser irradiation at 325 nm
[AD-A251093] p 3613 N92-30246
Photodynamics within (CH3OH)(nCr(CO)6) heteroclusters: Observation of an isotope effect
[AD-A251058] p 3712 N92-30255
Vacuum ultraviolet studies of molecular dynamics
[AD-A246964] p 3715 N92-30681
PHOTOELECTRIC EFFECT
Study of Au(-) production in a plasma-sputter type negative ion source
[NIFS-115] p 3717 N92-30990
PHOTOELECTRIC EMISSION
Multiple scattering theory of x ray absorption. A review
[DE92-622374] p 3716 N92-30798
PHOTOELECTROCHEMISTRY
Anisotropic silicon etching techniques
[MBB-Z-0413-91-PUB] p 3594 N92-30422
PHOTOELECTRON SPECTROSCOPY
Chemielectron and photoelectron spectroscopic studies of importance in the upper atmosphere
[AD-A248838] p 3675 N92-30556
PHOTOIONIZATION
Photodynamics within (CH3OH)(nCr(CO)6) heteroclusters: Observation of an isotope effect
[AD-A251058] p 3712 N92-30255
Studies of atmospheric molecules by multiphoton spectroscopy
[DE92-012668] p 3672 N92-30345
PHOTOLYSIS
Photodegradation effects in materials exposed to high flux solar and solar simulated radiation
[DE91-002147] p 3596 N92-30879
PHOTOMETERS
Development of ultra-low noise, high sensitivity planar metal grating coupled AlGaAs/GaAs multiquantum well IR detectors for focal plane array staring IR sensor systems
[AD-A246122] p 3590 N92-30318
The temperature dependence of a large dynamic range photodetector structure
[AD-A247667] p 3624 N92-30683

Acousto-optic filtering of lidar signals
p 3650 N92-31077
HgCdTe photomixers for CO2 laser radar systems
p 3654 N92-31100

PHOTOMULTIPLIER TUBES
Correction for nonlinear photon counting effects in lidar systems p 3649 N92-31070
Lidar receivers for picosecond remote sensing
p 3650 N92-31076

PHOTON DENSITY
The escape of greater MeV photons from cosmological gamma-ray bursts
[DE92-013545] p 3743 N92-30706

PHOTONS
Photodissociation of azulene under UV-laser irradiation at 325 nm
[AD-A251093] p 3613 N92-30246
The escape of greater MeV photons from cosmological gamma-ray bursts
[DE92-013545] p 3743 N92-30706
An ultra-sensitive coherent detector capable of single photon detection for lidar applications
p 3646 N92-31053
Correction for nonlinear photon counting effects in lidar systems p 3649 N92-31070
High background photon counting lidar
p 3649 N92-31071
Lidar measurements using large liquid mirror telescopes p 3652 N92-31087

PHOTOPEAK
Theory and measurement of the energy and risetime resolution of scintillation detectors in hard x ray area
[ETN-92-91687] p 3720 N92-30504

PHOTOSYNTHESIS
Electrochemical and optical studies of model photosynthetic systems
[DE92-010657] p 3683 N92-30829

PHOTOVOLTAIC CELLS
Solar-hydrogen energy system for solar belt countries and use of remote sensing p 3668 N92-30913

PHOTOVOLTAIC CONVERSION
Uniform flux dish concentrators for photovoltaic application
[DE92-010566] p 3671 N92-30896
Shining on: A primer on solar radiation data
[DE92-010555] p 3743 N92-31206

PHOTOVOLTAIC EFFECT
Examinations of the microwave photoelectric conductivity of a-Si:H multilayer systems for in situ characterization
[ETN-92-91688] p 3727 N92-30505

PHYSICAL EXERCISE
Optimal ECG electrode sites and criteria for detection of asymptomatic coronary artery disease, update 1990. Multilead ECG changes at rest, with exercise, and with coronary angioplasty
[AD-A248613] p 3684 N92-30523
Exercise behavior among Navy runners and non-runners
[AD-A250651] p 3685 N92-30644

PHYSICAL FITNESS
Feasibility of a walk test to assess the cardiorespiratory fitness of Naval personnel
[AD-A250650] p 3684 N92-30603
Exercise behavior among Navy runners and non-runners
[AD-A250651] p 3685 N92-30644

PHYSICAL OPTICS
An x ray microprobe based upon a close-coupled focal-spot/glass capillary arrangement
[DE92-011886] p 3722 N92-31195

PHYSICAL PROPERTIES
Properties of CMOS devices and circuits fabricated on high-resistivity, detector-grade silicon
[DE92-011727] p 3626 N92-30813
Proceedings of a Beryllium Technology Workshop
[DE92-012312] p 3598 N92-30834
Stabilization of face-centered-cubic titanium
[DE92-011530] p 3600 N92-31125
Proceedings of the 181st Electrochemical Society, Inc. Meeting Program
[AD-A249729] p 3596 N92-31178

PHYSIOLOGICAL EFFECTS
Effects of pyridostigmine bromide on A-10 pilots during execution of a simulated mission; performance
[AD-A252309] p 3685 N92-30605

PHYSIOLOGICAL RESPONSES
Cortical mechanisms of attention, discrimination, and motor response to somaesthetic stimuli
[AD-A247228] p 3687 N92-30613
Control of circadian behavior by transplanted suprachiasmatic nuclei
[AD-A250442] p 3686 N92-31143
Light as a chronobiologic countermeasure for long-duration space operations
[NASA-TM-103874] p 3686 N92-31167

PHYSIOLOGY
Fluorescence lidar multi-color imaging of vegetation
p 3640 N92-31028

PIEZOELECTRICITY
Ferroelectric and piezoelectric properties of odd-numbered nylons
[AD-A252270] p 3727 N92-30406
A new class of ferroelectric polymers: The odd-numbered nylons
[AD-A252268] p 3603 N92-30594
Ferroelectric polarization mechanisms in Nylon 11
[AD-A252269] p 3728 N92-30595
The optimization of force inputs for active structural acoustic control using a neural network
[NASA-TM-107627] p 3711 N92-30979
An analytical and experimental investigation of flutter suppression via piezoelectric actuation
[NASA-TM-107653] p 3580 N92-31174

PILOT ERROR
Introduction to cognitive processes of expert pilots
[DOT/FAA/RD-92/12] p 3578 N92-30980

PILOT PERFORMANCE
Effects of pyridostigmine bromide on A-10 pilots during execution of a simulated mission; performance
[AD-A252309] p 3685 N92-30605
Helicopter nighttime parking test results - UH-1
[DOT/FAA/CT-TN92/1] p 3580 N92-31165

PILOT TRAINING
Technical evaluation report on the Flight Mechanics Panel Symposium on Piloted Simulation Effectiveness
[AGARD-AR-315] p 3584 N92-30769
Introduction to cognitive processes of expert pilots
[DOT/FAA/RD-92/12] p 3578 N92-30980

PINEAL GLAND
Melatonin, the pineal gland and circadian rhythms
[AD-A250640] p 3684 N92-30376

PIONS
Polarization effects in pi(+) absorption in He-3
[ITN-92-85164] p 3714 N92-30580
Polarization effects in pi(+) absorption in He-4
[ITN-92-85163] p 3715 N92-30780

PIPELINING (COMPUTERS)
Exploiting resource parallelism for integrated fault monitoring and recovery
[AD-A248843] p 3699 N92-30557

PIPES (TUBES)
Conceptual design of the SSC cryogenic transfer lines
[DE92-013964] p 3719 N92-30839
Prediction of coincidence frequencies for a thin-walled, fluid-filled pipe
[MRL-TN-600] p 3664 N92-30963

PISTONS
Ringless piston experiments. Natural gas engine technology advancements
[PB92-164466] p 3659 N92-30601

PLAINS
Duration and rates of discharge: Maja Valles, Mars
p 3737 N92-31227

PLANAR STRUCTURES
Development of ultra-low noise, high sensitivity planar metal grating coupled AlGaAs/GaAs multiquantum well IR detectors for focal plane array staring IR sensor systems
[AD-A246122] p 3590 N92-30318

PLANE WAVES
Spontaneous decay of an atom near a phase conjugator
[AD-A248298] p 3712 N92-30333

PLANETARY ATMOSPHERES
Impact erosion of terrestrial planetary atmospheres
[NASA-CR-190605] p 3742 N92-30921

PLANETARY BOUNDARY LAYER
On the existence of convectively produced gravity waves p 3638 N92-31016
A pulsed CO2 Doppler lidar for boundary layer monitoring p 3639 N92-31021
Airborne lidar and radiometric observations of PBL- and low clouds p 3642 N92-31037
Analytical estimates of the PP-algorithm at low number of Doppler periods per pulse length
p 3650 N92-31079

PLANETARY COMPOSITION
The first identification of a mainbelt asteroid source for a meteorite Class E-type Apollo asteroid (3103) 1982BB: A link between the Hungaria asteroid zone and the Aubrite meteorites p 3737 N92-31228

PLANETARY EVOLUTION
Impact erosion of terrestrial planetary atmospheres
[NASA-CR-190605] p 3742 N92-30921
The first identification of a mainbelt asteroid source for a meteorite Class E-type Apollo asteroid (3103) 1982BB: A link between the Hungaria asteroid zone and the Aubrite meteorites p 3737 N92-31228
The (146,147)Sm-(142,143)Nd systematics of early terrestrial differentiation and the lost continents of the early Earth p 3678 N92-31229
The thermal engine of Venus: Implications from the impact crater distribution p 3738 N92-31233
Is the Venusian lithosphere subducting?
p 3738 N92-31234
Gaspra's shape and surface features: Comparison to small satellites p 3739 N92-31236
Discovery of two planets around a millisecond pulsar
p 3739 N92-31237

PLANETARY GEOLOGY
The (146,147)Sm-(142,143)Nd systematics of early terrestrial differentiation and the lost continents of the early Earth p 3678 N92-31229
The thermal engine of Venus: Implications from the impact crater distribution p 3738 N92-31233

PLANETARY MAPPING
Global scale concentrations of volcanic activity on Venus: A summary of three 23rd Lunar and Planetary Science Conference abstracts. 1: Venus volcanism: Global distribution and classification from Magellan data. 2: A major global-scale concentration of volcanic activity in the Beta-Atla-Themis region of Venus. 3: Two global concentrations of volcanism on Venus: Geologic associations and implications for global pattern of upwelling and downwelling p 3737 N92-31226

PLANETARY MASS
Discovery of two planets around a millisecond pulsar
p 3739 N92-31237

PLANETARY ORBITS
Carlsberg meridian catalogue La Palma. Number 5: Observations of positions of stars and planets: May 1988 to Dec. 1989
[ISBN-84-7469-052-8] p 3739 N92-30714

PLANETARY SURFACES
Gaspra's shape and surface features: Comparison to small satellites p 3739 N92-31236

PLANETARY SYSTEMS
Discovery of two planets around a millisecond pulsar
p 3739 N92-31237

PLANNING
Compression planning for continuous improvement in quality programs
[DE92-012331] p 3732 N92-30349
The allocation of cargo to channel missions
[DE92-013234] p 3578 N92-30565

PLANT DESIGN
Small engine components test facility compressor testing cell at NASA Lewis Research Center
[NASA-TM-105685] p 3584 N92-30508

PLASMA COMPOSITION
Boundary plasma transport studies on TFTR
[DE92-011942] p 3723 N92-30746
Spectroscopic diagnosis of long-scale-length exploding-foil plasma in the presence of an intense radiation field
[DE92-014718] p 3726 N92-31118

PLASMA CONTROL
Role of compressibility on driven magnetic reconnection
[NIFS-105] p 3710 N92-30498
Plasma parameter estimations for the large helical device based on the gyro-reduced Bohm scaling
[NIFS-114] p 3723 N92-30499
MHD considerations for a self-cooled liquid lithium blanket
[DE92-014864] p 3723 N92-30591
Locked modes and magnetic field errors in MST
[DE92-015379] p 3723 N92-30612
Boundary plasma transport studies on TFTR
[DE92-011942] p 3723 N92-30746
The Rayleigh-Taylor instability in an expanding plasma
[DE92-013883] p 3725 N92-30884
Collisional and chaotic transport of energetic particles in toroidal plasma
[DE92-014589] p 3725 N92-30900
Kinetic approach to long wave length modes in rotating plasmas
[NIFS-138] p 3725 N92-30993
Three-dimensional MHD equilibrium in the presence of bootstrap current for Large Helical Device (LHD)
[NIFS-139] p 3725 N92-30994
Criteria and design trade-off issues for ITER
[DE92-011786] p 3726 N92-31114

PLASMA CURRENTS
Effects of fast ions and an external inductive electric field on the neoclassical parallel flow, current, and rotation in general toroidal systems
[NIFS-150] p 3713 N92-30500
Pressure profiles, resonant Pfirsch-Schlueter currents, thermal instabilities, and magnetic island formation
[DE92-015166] p 3726 N92-31002

PLASMA DENSITY
Results of the heavy ion beam probe measurements on the Advanced Toroidal Facility
[DE92-014461] p 3726 N92-31197

PLASMA DIAGNOSTICS
Neutron time-of-flight ion temperature diagnostic for inertial confinement fusion experiments
[DE92-011365] p 3724 N92-30806
Density profile measurement using a multichannel difluoromethane laser interferometer system on ATF
[DE92-011691] p 3724 N92-30810
Remote experimental site concept for diagnostic collaborations in fusion
[DE92-010437] p 3724 N92-30824
Spectroscopic diagnosis of long-scale-length exploding-foil plasma in the presence of an intense radiation field
[DE92-014718] p 3726 N92-31118

PLASMA DRIFT
Two dimensional aspects of toroidal drift waves in the ballooning representation
[DE92-014028] p 3724 N92-30880

PLASMA DYNAMICS
Field line diversion properties of finite beta helias equilibria
[NIFS-137] p 3722 N92-30385
Plasma parameter estimations for the large helical device based on the gyro-reduced Bohm scaling
[NIFS-114] p 3723 N92-30499
The Rayleigh-Taylor instability in an expanding plasma
[DE92-013883] p 3725 N92-30884

PLASMA EQUILIBRIUM
Magnetic surface breaking in 3D MHD equilibria of I = 2 heliotron
[NIFS-130] p 3722 N92-30384
Field line diversion properties of finite beta helias equilibria
[NIFS-137] p 3722 N92-30385
Problems with the concept of plasma equilibrium in tokamaks
[DE92-014454] p 3723 N92-30576
Pressure profiles, resonant Pfirsch-Schlueter currents, thermal instabilities, and magnetic island formation
[DE92-015166] p 3726 N92-31002

PLASMA HEATING
Fundamental studies of fusion plasmas
[DE92-015077] p 3726 N92-31116
Results of the heavy ion beam probe measurements on the Advanced Toroidal Facility
[DE92-014461] p 3726 N92-31197

PLASMA JETS
Study of Au(-) production in a plasma-sputter type negative ion source
[NIFS-115] p 3717 N92-30990

PLASMA OSCILLATIONS
Locked modes and magnetic field errors in MST
[DE92-015379] p 3723 N92-30612

PLASMA PHYSICS
Plasma parameter estimations for the large helical device based on the gyro-reduced Bohm scaling
[NIFS-114] p 3723 N92-30499
The Rayleigh-Taylor instability in an expanding plasma
[DE92-013883] p 3725 N92-30884
The role of stochasticity in sawtooth oscillation
[NIFS-103] p 3710 N92-30983
Dynamics and energetics of the solar corona
[NASA-CR-190664] p 3742 N92-31162

PLASMA POTENTIALS
New method of error elimination in potential profile measurement of tokamak plasmas by high voltage heavy ion beam probes
[NIFS-143] p 3726 N92-30995

PLASMA PRESSURE
Pressure profiles, resonant Pfirsch-Schlueter currents, thermal instabilities, and magnetic island formation
[DE92-015166] p 3726 N92-31002

PLASMA TURBULENCE
Gyro-Landau fluid model of tokamak core fluctuations
[DE92-013277] p 3722 N92-30366

PLASMA WAVES
Solar flare MDH
[AD-A250639] p 3702 N92-30375
Interaction of ultra-high laser fields with beams and plasmas
[AD-A249502] p 3723 N92-30620
Magnetospheric structure and dynamics: A multisatellite approach
[AD-A252326] p 3676 N92-30720
Two dimensional aspects of toroidal drift waves in the ballooning representation
[DE92-014028] p 3724 N92-30880
Effect of wave-particle interaction on the outflow of ions at high latitudes
[NASA-CR-190560] p 3677 N92-30962
Fundamental studies of fusion plasmas
[DE92-015077] p 3726 N92-31116

PLASMAS (PHYSICS)
Role of compressibility on driven magnetic reconnection
[NIFS-105] p 3710 N92-30498
Production of negative hydrogen ions in a large multicusp ion source with double-magnetic filter configuration
[NIFS-149] p 3714 N92-30572
Boundary plasma transport studies on TFTR
[DE92-011942] p 3723 N92-30746
VUV production from a ferrite-driven flash-pumped system
[DE92-011362] p 3657 N92-30805
Line-emission cross sections for the charge-exchange reaction between fully stripped carbon and atomic hydrogen in tokamak plasma
[NIFS-129] p 3716 N92-30967
The role of stochasticity in sawtooth oscillation
[NIFS-103] p 3710 N92-30983
Kinetic approach to long wave length modes in rotating plasmas
[NIFS-138] p 3725 N92-30993
Three-dimensional MHD equilibrium in the presence of bootstrap current for Large Helical Device (LHD)
[NIFS-139] p 3725 N92-30994
New method of error elimination in potential profile measurement of tokamak plasmas by high voltage heavy ion beam probes
[NIFS-143] p 3726 N92-30995
FNAS: The magnetic configuration leading to solar flares
[NASA-CR-190522] p 3743 N92-31168
Physics of the STAR experiment at the relativistic heavy ion collider
[DE92-014481] p 3719 N92-31198

PLASMONS
Waveguide polarizer using localized surface plasmons
[AD-D015258] p 3614 N92-30348

PLASTIC DEFORMATION
FASTRAN-2: A fatigue crack growth structural analysis program
[NASA-TM-104159] p 3664 N92-30964

PLASTIC PROPERTIES
Laboratory experiments from the toy store p 3609 N92-30274

PLASTICS
Determining significant material properties: A discovery approach p 3607 N92-30279
An experiment on the use of disposable plastics as a reinforcement in concrete beams p 3593 N92-30287

PLATE THEORY
Optimal shear correction factors in hierarchical plate modelling
[AD-A248899] p 3662 N92-30338

PLATES (STRUCTURAL MEMBERS)
Thermal stress evaluation of a symmetrically laminated composite plate
[AD-A249450] p 3591 N92-30641
An analytical and experimental investigation of flutter suppression via piezoelectric actuation
[NASA-TM-107653] p 3580 N92-31174

PLATES (TECTONICS)
A geodetic laser radar rangefinder with 10(exp -7) resolution p 3641 N92-31029
Is the Venusian lithosphere subducting? p 3738 N92-31234

PLATING
Printed transformer process/product improvements
[DE92-014760] p 3624 N92-30590

PLATINUM
A comparative EIS study on cermet and platinum anodes for the electrolytic production of aluminum
[DE92-015091] p 3599 N92-31010

PLOTTING
Fractal analysis: A new remote sensing tool for lava flows p 3736 N92-31224

PLUMES
Numerical investigations in the backflow region of a vacuum plume
[NASA-CR-190515] p 3589 N92-30981

POINTS (MATHEMATICS)
Point location in fat subdivisions
[RUU-CS-91-40] p 3703 N92-30447

POLAR METEOROLOGY
Lidar depolarization by nonspherical particles: Potential of combined depolarization/backscattering measurements for PSC's characterization p 3644 N92-31044

POLAR REGIONS
Effect of wave-particle interaction on the outflow of ions at high latitudes
[NASA-CR-190560] p 3677 N92-30962

POLARIMETERS
Modification of 95 GHz radar source module for low phase noise operation
[AD-A249793] p 3622 N92-31180

POLARIZATION (CHARGE SEPARATION)
Ferroelectric polarization mechanisms in Nylon 11
[AD-A252269] p 3728 N92-30595

POLARIZATION (SPIN ALIGNMENT)
Spin amplitudes of pp-scattering in a unitarized supercritical pomeron model
[DE92-624639] p 3711 N92-30236
Polarization effects in pi(+) absorption in He-3
[ITN-92-85164] p 3714 N92-30580
Theoretical studies in elementary particle physics
[DE92-015295] p 3714 N92-30610
Polarization effects in pi(+) absorption in He-4
[ITN-92-85163] p 3715 N92-30780
High field optical-pumping spin-exchange polarized deuterium source
[DE92-010274] p 3657 N92-30848

POLARIZATION (WAVES)
Results of the 1989 experiment with a polarimetric multifrequency SAR
[BCRS-91-33] p 3614 N92-30361

POLARIZATION CHARACTERISTICS
Measurements of the backscattering phase matrices of crystal clouds with a polarization lidar p 3651 N92-31083

POLARIZED LIGHT
Verification measurement of a polarization Raman elastic-backscatter lidar p 3647 N92-31062
Time and polarization dependent double scattering calculations of lidar returns from water clouds p 3647 N92-31063
Fiber optic Michelson sensor and arrays with passive elimination of polarization fading and source feedback isolation
[AD-D015290] p 3722 N92-31213

POLARIZERS
Waveguide polarizer using localized surface plasmons
[AD-D015258] p 3614 N92-30348

POLICIES
Setting priorities for space research: Opportunities and imperatives
[NASA-CR-190519] p 3733 N92-30974

POLLUTION CONTROL
Status of selected air pollution control programs, February 1992
[PB92-171966] p 3673 N92-30561
Report of the Great Lakes Air Toxics Research Priorities Workshop
[PB92-166933] p 3673 N92-30602
Fiber-optic Raman spectroscopy at the Savannah River Site: Uses and techniques
[DE92-013971] p 3596 N92-30899
Chemistry for protection of the environment, 8th International Conference proceedings
[DE92-014317] p 3674 N92-31181

POLLUTION MONITORING
Report of the Great Lakes Air Toxics Research Priorities Workshop
[PB92-166933] p 3673 N92-30602
Linkage of anthropogenic aerosol to clouds and climate
[DE92-013574] p 3674 N92-30707
A portable lidar using a diode-pumped YAG laser p 3654 N92-31098
Lidar observation of marine mixed layer p 3655 N92-31104

POLLUTION TRANSPORT
Lidar observation of marine mixed layer p 3655 N92-31104
Trace gas and aerosol transports into and out of the Amazon Basin
[NASA-CR-190624] p 3674 N92-31153

POLOIDAL FLUX
Edge poloidal rotation profiles of H-mode plasmas in the JFT-2M tokamak
[DE92-799107] p 3725 N92-30992

POLYACETYLENE
Microscopic theory of THG and electro-absorption in conjugated polymers
[DE92-014786] p 3604 N92-30792

POLYACRYLONITRILE
Precursor structure-fiber property relationships in polyacrylonitrile-based carbon fibers
[AD-A249888] p 3592 N92-30871

POLYAMIDE RESINS
A new class of ferroelectric polymers: The odd-numbered nylons
[AD-A252268] p 3603 N92-30594

POLYCARBONATES
A study of discrete and continuum joint modeling techniques
[DE92-012631] p 3663 N92-30859

POLYCRYSTALS
Research on polycrystalline thin film submodules based on CuInSe2 materials
[DE92-010584] p 3727 N92-30247
On the strain-rate dependence of dynamic recrystallization in copper polycrystals
[DE92-011363] p 3730 N92-31217

POLYETHYLENES
Evaluation of doped polyethylene oxide as solid electrolyte for polymer batteries
[AD-A249501] p 3624 N92-30619
Studies on the melt flow rate of the SRM 1473: A low density polyethylene resin
[PB92-181080] p 3604 N92-30788
POLYGONS
Two-dimensional aerodynamic characteristics of several polygon-shaped cross-sectional models applicable to helicopter fuselages
[NASA-TP-3233] p 3574 N92-30394
POLYIMIDE RESINS
Isothermal aging effects on PMR-15 resin
[NASA-TM-105648] p 3593 N92-30986
POLYIMIDES
Polyimides containing the cyclobutene-3,4-dione moiety
[NASA-CASE-LAR-14753-1] p 3601 N92-30313
Approaches to polymer curing and imaging via the in situ generation of a catalyst
[AD-A249917] p 3606 N92-30873
POLYMER CHEMISTRY
Infrared investigations of pristine, doped and partially-doped polypyrrole
[AD-A250644] p 3605 N92-30838
POLYMERIC FILMS
Ferroelectric and piezoelectric properties of odd-numbered nylons
[AD-A252270] p 3727 N92-30406
Characterization and analysis of defects in nonlinear optical molecular composite films
[AD-A252118] p 3661 N92-30529
POLYMERIZATION
Chemistry within van der Waals cluster of unsaturated molecules: Observation of cationic polymerization
[AD-A250929] p 3712 N92-30240
Epoxides as activators for grafting of poly(tetrahydrofuran) from poly(methylphenylsilylene)
[AD-A251086] p 3601 N92-30244
Temperature effect on the Langmuir-Blodgett polymerization of 2-pentadecylaniline
[AD-A250803] p 3601 N92-30250
Synthesis and reactivity of 1-methyl-e-ethynylpyridinium triflate
[AD-A250638] p 3602 N92-30346
Polymerization of 1-bromo-4-lithiobenzene in THF. A route to soluble polyphenylenes
[AD-A249926] p 3604 N92-30794
POLYMERS
The electric field dependence of the laser induced holographic grating relaxation of photorefractive polymer
[AD-A252641] p 3602 N92-30409
Template-synthesis: A method for enhancing the ionic and electronic conductivity in electronically conductive polymers
[AD-A248806] p 3603 N92-30553
POLYNOMIALS
A local interpolator derived from the discrete Fourier transform
[AD-A251066] p 3701 N92-30243
On real and complex zeros of orthogonal polynomials in a discrete Sobolev space
[REPT-91-98] p 3702 N92-30350
Achievable potential reductions in the method of Kojima et al. in the case of linear programming
[REPT-91-78] p 3693 N92-30435
Iri's polynomiality proof for the Iri-Imai method recast
[REPT-91-74] p 3693 N92-30455
Real polynomial systems of degree n with n+1 line invariants
[REPT-91-86] p 3704 N92-30490
POLYNUCLEOTIDES
Laser mass spectrometry for biopolymers
[DE92-015238] p 3597 N92-31184
POLYPEPTIDES
Laser mass spectrometry for biopolymers
[DE92-015238] p 3597 N92-31184
POLYSILANES
Epoxides as activators for grafting of poly(tetrahydrofuran) from poly(methylphenylsilylene)
[AD-A251086] p 3601 N92-30244
POLYURETHANE RESINS
A method for production of new anion exchangers
[DE92-015313] p 3717 N92-31147
POMERANCHUK THEOREM
Spin amplitudes of pp-scattering in a unitarized supercritical pomeron model
[DE92-624639] p 3711 N92-30236
POMERONS
Spin amplitudes of pp-scattering in a unitarized supercritical pomeron model
[DE92-624639] p 3711 N92-30236
POPULATION INVERSION
Recombining processes in a cooling plasma by mixing of initially heated gas
[NIFS-142] p 3722 N92-30431
POPULATIONS
Comparison of epifluorescent viable bacterial count methods
[NASA-TM-103592] p 3683 N92-30305
Improvement of performance of variable probability sampling strategies
[PB92-180264] p 3707 N92-30562
POROSITY
Perforated monolayers
[DE92-011632] p 3593 N92-30344
Control and augmentation of passive porosity through transpiration control
[NASA-CASE-LAR-14682-1] p 3628 N92-30387
POROUS MATERIALS
Control and augmentation of passive porosity through transpiration control
[NASA-CASE-LAR-14682-1] p 3628 N92-30387
PORTABLE EQUIPMENT
Direct broadcast satellite-radio: Portable and mobile reception trade-offs p 3621 N92-30945
A portable lidar using a diode-pumped YAG laser p 3654 N92-31098
POSEIDON SATELLITE
Preparations for the ERS-1 and TOPEX/Poseidon satellite altimetry missions
[BCRS-90-28] p 3666 N92-30465
POSITION (LOCATION)
Point location in fat subdivisions
[RUU-CS-91-40] p 3703 N92-30447
The MARCOR GPS mobile data system p 3620 N92-30944
POSITION ERRORS
Glint errors derived from the partial derivatives of the echo signal phase for a distributed scatterer
[AD-A249499] p 3615 N92-30637
On two methods of determining the ellipses and ellipsoids of positioning accuracy of robot manipulators
[ISSN-0208-5658] p 3701 N92-31148
POSITION INDICATORS
Laser optical mouse
[AD-D015307] p 3690 N92-30564
POSITION SENSING
Carlsberg meridian catalogue La Palma. Number 5: Observations of positions of stars and planets: May 1986 to Dec. 1989
[ISBN-84-7469-052-8] p 3739 N92-30714
POTASSIUM
First-principles computational studies of alkali-doped C60 fullerides
[AD-A249018] p 3624 N92-30630
Potassium Rankine cycle power conversion systems for lunar-Mars surface power
[DE92-015102] p 3589 N92-31012
POTATOES
Structure, processing, and properties of potatoes p 3611 N92-30288
POTENTIAL ENERGY
Understanding heterolytic bond cleavage
[AD-A252336] p 3716 N92-30845
POTENTIAL FIELDS
FNAS: The magnetic configuration leading to solar flares
[NASA-CR-190522] p 3743 N92-31168
POTENTIOMETERS
An automated system for creep testing p 3611 N92-30282
POWDER (PARTICLES)
From minerals to materials: A facile synthetic route to preceramic polymers for aluminum oxide
[AD-A250351] p 3606 N92-31141
POWER AMPLIFIERS
Method for remotely powering a device such as a lunar rover
[NASA-CASE-LAR-14789-1] p 3658 N92-30388
Experimental millimeter-wave personal satellite communications system p 3617 N92-30927
Design of a near-IR coherent lidar for high spatial and velocity resolution wind measurement p 3639 N92-31020
A pulsed CO2 Doppler lidar for boundary layer monitoring p 3639 N92-31021
POWER CONVERTERS
Magnetic bearings for free-piston Stirling engines
[NASA-TM-105730] p 3660 N92-30734
POWER SUPPLIES
Wiring for aerospace applications
[NASA-TM-105777] p 3623 N92-30427
PRANDTL NUMBER
Numerical simulation of low Prandtl number turbulent mixing p 3633 N92-30663
PRECIPITATION (CHEMISTRY)
The development of precipitated iron catalysts with improved stability
[DE92-014625] p 3596 N92-31006
Trace element and isotope geochemistry of geothermal fluids, East Rift Zone, Kilauea, Hawaii
[DE92-014586] p 3671 N92-31117
PRECIPITATION HARDENING
Be-Cu precipitation hardening experiment p 3601 N92-30276
PRECONDITIONING
Controlling user interface objects through pre- and postconditions
[REPT-92-04] p 3692 N92-30356
PREDICTION ANALYSIS TECHNIQUES
Joint computational and experimental aerodynamics research on a hypersonic vehicle
[DE92-013439] p 3574 N92-30367
Comparison of signal processing methods for estimation of network impedance for remote protection
[ETN-92-91686] p 3623 N92-30503
A new unsteady mixing model to predict NO(x) production during rapid mixing in a dual-stage combustor
[NASA-CR-189155] p 3581 N92-30569
New insights into radiation-induced oxide-trap charge through Thermally-Stimulated-Current (TSC) measurement and analysis
[DE92-009054] p 3728 N92-30585
Variational method in the statistical theory of turbulent two-phase flows
[AD-A252263] p 3630 N92-30604
Numerical methods for the simulation of complex multi-body flows with applications for the integrated Space Shuttle vehicle p 3576 N92-30741
Reliability in the design phase
[DE92-012217] p 3661 N92-30763
NDE characterization of the microstructure and mechanical properties of Al-Li alloys
[DE92-012154] p 3598 N92-30858
A study of discrete and continuum joint modeling techniques
[DE92-012631] p 3663 N92-30859
PREDICTIONS
Prediction of coincidence frequencies for a thin-walled, fluid-filled pipe
[MRL-TN-600] p 3664 N92-30963
PREMIXED FLAMES
Geometry of premixed flames in three-dimensional turbulence p 3633 N92-30666
The influence of Lewis number and nonhomogeneous mixture on premixed turbulent flame structure p 3597 N92-30669
Pre-mixed flame simulations for non-unity Lewis numbers p 3597 N92-30670
Computational simulation of diamond chemical vapor deposition in premixed C2H2/O2/H2 and CH4/O2 strained flames
[DE92-012144] p 3606 N92-30857
PREMIXING
Statistics for laminar flamelet modeling p 3597 N92-30668
PREPROCESSING
Compiler analysis for irregular problems in FORTRAN D
[NASA-CR-189664] p 3689 N92-30311
PRESIDENTIAL REPORTS
Grand challenges 1993: High performance computing and communications. A report by the Committee on Physical, Mathematical, and Engineering Sciences to supplement the President's fiscal year 1993 budget
[PB92-160530] p 3689 N92-30600
PRESSURE CHAMBERS
The use of tympanometry to detect aerotitis media in hypobaric chamber operations
[AD-A248963] p 3684 N92-30328
PRESSURE DISTRIBUTION
Isotropic thin-walled pressure vessel experiment p 3611 N92-30284
Pressure profiles, resonant Pfirsch-Schlueter currents, thermal instabilities, and magnetic island formation
[DE92-015166] p 3726 N92-31002
PRESSURE EFFECTS
Magnetic surface breaking in 3D MHD equilibria of l = 2 heliotron
[NIFS-130] p 3722 N92-30384
The structure of turbulent channel flow with passive scalar transport p 3632 N92-30657
Research issues in molten carbonate fuel cells: Pressurization
[DE92-011755] p 3671 N92-31113
PRESSURE GRADIENTS
Structure of three-dimensional turbulent boundary layers p 3631 N92-30654

PRESSURE MEASUREMENT
Wavemeter measurements of frequency stability of an injection seeded alexandrite laser for pressure and temperature lidar p 3645 N92-31049
An experimental study of the relationship between velocity and pressure fluctuations in a wing-body junction
[AD-A249628] p 3577 N92-31122
PRESSURE OSCILLATIONS
An experimental study of the relationship between velocity and pressure fluctuations in a wing-body junction
[AD-A249628] p 3577 N92-31122
PRESSURE REDUCTION
MHD considerations for a self-cooled liquid lithium blanket
[DE92-014864] p 3723 N92-30591
PRESSURE VESSELS
Isotropic thin-walled pressure vessel experiment p 3611 N92-30284
Conceptual design of the SSC cryogenic transfer lines
[DE92-013964] p 3719 N92-30839
Recent improvements in size effects correlations for DBTT and upper shelf energy of ferritic steels
[DE92-014703] p 3599 N92-30877
PRESSURIZING
Research issues in molten carbonate fuel cells: Pressurization
[DE92-011755] p 3671 N92-31113
PRESTRESSING
Method and apparatus for preloading a joint by remotely operable means
[NASA-CASE-MSC-21940-1] p 3659 N92-30540
PRINTED CIRCUITS
Printed transformer process/product improvements
[DE92-014760] p 3624 N92-30590
Transfer soldering evaluation
[DE92-015160] p 3627 N92-31144
PRINTERS
Printer port interface
[NASA-CASE-LAR-13950-1] p 3690 N92-30541
PRIORITIES
Compression planning for continuous improvement in quality programs
[DE92-012331] p 3732 N92-30349
Space science and applications: Strategic plan 1991
[NASA-TM-107811] p 3733 N92-30959
Setting priorities for space research: Opportunities and imperatives
[NASA-CR-190519] p 3733 N92-30974
PROBABILITY DENSITY FUNCTIONS
Some inequalities for variances
[REPT-92-10] p 3707 N92-30460
Statistics for laminar flamelet modeling p 3597 N92-30668
A statistical comparison of AUTEC and Eleuthera Island wind data for the period 1 April 1989 through 30 March 1990
[AD-A248898] p 3679 N92-31003
PROBABILITY THEORY
The sum of weighted balls
[RUU-CS-91-37] p 3707 N92-30481
Improvement of performance of variable probability sampling strategies
[PB92-180264] p 3707 N92-30562
Combinatorics and Kolmogorov complexity
[CWI-CS-R9125] p 3708 N92-30699
Foreign surveillance radar upgrade analysis
[AD-A249440] p 3616 N92-30760
Transactions of the 9th Army Conference on Applied Mathematics and Computing
[AD-A252140] p 3706 N92-30843
Adapting the ADAM manikin technology for injury probability assessment
[AD-A252332] p 3688 N92-30844
A statistical comparison of AUTEC and Eleuthera Island wind data for the period 1 April 1989 through 30 March 1990
[AD-A248898] p 3679 N92-31003
A failure-to-restore unavailability model for periodically performed maintenance
[DE92-015902] p 3708 N92-31185
PROBLEM SOLVING
Elementary metallography p 3600 N92-30266
Algorithm to solve nonlinear time dependent problems of engineering and physics
[AD-A250641] p 3702 N92-30347
Restrictions of graph partition problems, part 1
[RUU-CS-91-44-PT-1] p 3703 N92-30446
PROCEDURES
Computer integrated laboratory testing p 3611 N92-30289
Managing the contract closeout process
[AD-A250701] p 3733 N92-31209
PROCESS CONTROL (INDUSTRY)
A senior manufacturing laboratory for determining injection molding process capability p 3609 N92-30273
Printed transformer process/product improvements
[DE92-014760] p 3624 N92-30590
A statistical rationale for establishing process quality control limits using fixed sample size, for critical current verification of SSC superconducting wire
[DE92-014844] p 3661 N92-31120
PROCESSING
Structural ceramics p 3607 N92-30264
PRODUCT DEVELOPMENT
Encyclopedia of software components
[NASA-CASE-NPO-18435-1-CU] p 3695 N92-30543
Technical evaluation report on the Flight Mechanics Panel Symposium on Piloted Simulation Effectiveness
[AGARD-AR-315] p 3584 N92-30769
Future aerospace ground test facility requirements for the Arnold Engineering Development Center p 3585 N92-30897
Preparation for a new plane (A 320): Experience reviewed p 3697 N92-30954
PRODUCTION ENGINEERING
Beam technologies for integrated processing
[AD-A252647] p 3612 N92-30411
Innovative techniques for the production of low cost 2-D laser diode arrays supplies or services and prices/costs
[AD-A252665] p 3656 N92-30552
Effects of impurities on the mechanical behaviour of primary and secondary cast aluminum alloys
[PB92-180652] p 3598 N92-30785
PRODUCTION PLANNING
Concurrent engineering p 3697 N92-30952
PROFILES
Feasibility of extracting current profile information from HF-radar surface current measurements, part 1 and 2
[BCRS-91-23-PT-1-2] p 3682 N92-30470
PROGRAMMED INSTRUCTION
High level synthesis of controlpath microarchitectures
[MEMO-INF-91-86] p 3690 N92-30698
PROGRAMMING LANGUAGES
A formal transformation from the BSI/VDM-SL concrete syntax to the core abstract syntax
[REPT-92-07] p 3692 N92-30359
The semantics of the Duplex programming environment
[REPT-91-91] p 3694 N92-30485
Integrating commercial off-the-shelf tools for custom software development
[AD-A252462] p 3695 N92-30550
Implementation of parallel algorithms
[AD-A248826] p 3695 N92-30555
The GKS input model in MANIFOLD
[CWI-CS-R9127] p 3699 N92-30696
PROJECT MANAGEMENT
Practical application of the ILS: Practical integration, design, and logistics p 3697 N92-30955
Development of a reliability maintenance optimization method p 3697 N92-30956
PROJECT PLANNING
A description of the research for period 3 of a research program on the planning and control for space robotic manipulators
[NASA-CR-190243] p 3660 N92-30738
Future aerospace ground test facility requirements for the Arnold Engineering Development Center p 3585 N92-30897
Space science and applications: Strategic plan 1991
[NASA-TM-107811] p 3733 N92-30959
Fuel cell systems program plan: Fiscal year 1992
[DE92-015985] p 3672 N92-31188
High-speed civil transport issues and technology program
[NASA-CR-186020] p 3580 N92-31208
PROJECTILES
Fragment hazard zone analyses for explosive test facilities
[DE92-015391] p 3613 N92-30887
Eulerian simulation of the perforation of aluminum plates by nondeforming projectiles
[DE92-011515] p 3664 N92-31123
Modeling initiation of explosives by projectile impact
[DE92-015210] p 3608 N92-31202
PROPAGATION MODES
Transverse pattern modification in a stable apertured laser resonator
[ITN-92-85171] p 3656 N92-30582
PROPANE
High-temperature ignition of propane with MTBE as an additive: Shock-tube experiments and modeling
[DE92-006679] p 3594 N92-30749
PROPELLERS
Thrust test fixture
[AD-D015259] p 3585 N92-31192
PROPERTIES
Scale sensitivity and rank preservation in a multiplicative variant of the AHP and SMART
[REPT-91-67] p 3707 N92-30452
PROPULSION
Thrust stand evaluation of engine performance improvement algorithms in an F-15 airplane
[NASA-TM-104252] p 3581 N92-30518
Activities of the Aeronautical Research Laboratory p 3744 N92-30768
Trends in aeropropulsion research and their impact on engineering education
[NASA-TM-105682] p 3583 N92-31172
PROPULSION SYSTEM CONFIGURATIONS
NEP systems engineering efforts in FY-92: Plans and status
[NASA-TM-105775] p 3588 N92-30308
Nuclear electric propulsion development and qualification facilities
[NASA-TM-105521] p 3589 N92-30818
PROPULSION SYSTEM PERFORMANCE
Nuclear electric propulsion development and qualification facilities
[NASA-TM-105521] p 3589 N92-30818
PROSTHETIC DEVICES
Cable compliance
[NASA-TP-3216] p 3612 N92-30378
PROTECTIVE COATINGS
MHD considerations for a self-cooled liquid lithium blanket
[DE92-014864] p 3723 N92-30591
PROTOCOL (COMPUTERS)
A protocol scheme for a class of minimum delay routing algorithms
[RUU-CS-91-43] p 3693 N92-30445
Architecture for the high performance implantation of communication transport level protocols
[ETN-92-91666] p 3690 N92-30701
Building a generalized distributed system model
[NASA-CR-190489] p 3698 N92-30960
Choice coordination with multiple alternatives
[DE92-011656] p 3700 N92-31111
PROTON BEAMS
A dynamic model for beam tube vacuum effects on the SSC cryogenic system
[DE92-013967] p 3719 N92-30840
PROTON SCATTERING
Neutron time-of-flight ion temperature diagnostic for inertial confinement fusion experiments
[DE92-011365] p 3724 N92-30806
PROTONS
Spin amplitudes of pp-scattering in a unitarized supercritical pomeron model
[DE92-624639] p 3711 N92-30236
Polarization effects in pi(+) absorption in He-3
[ITN-92-85164] p 3714 N92-30580
Polarization effects in pi(+) absorption in He-4
[ITN-92-85163] p 3715 N92-30780
PROTOPLANETS
Impact erosion of terrestrial planetary atmospheres
[NASA-CR-190605] p 3742 N92-30921
The first identification of a mainbelt asteroid source for a meteorite Class E-type Apollo asteroid (3103) 1982BB: A link between the Hungaria asteroid zone and the Aubrite meteorites p 3737 N92-31228
PROTOTYPES
A program of continuing research on representing, manipulating, and reasoning about physical objects
[AD-A251089] p 3691 N92-30260
Resonance and control response tests using a control simulation device
[MBB-UD-0608-91-PUB] p 3583 N92-30439
Progress in the development of the Hermes evaporators
[MBB-UO-0164-91-PUB] p 3587 N92-30440
EASAMS' Ariane 5 on-board software experience
[D308/TN/001] p 3586 N92-30715
PSEUDONOISE
High frequency communications under adverse conditions
[AD-A252199] p 3615 N92-30532
PSYCHOPHYSICS
Review of psychophysically-based image quality metrics
[AD-A251053] p 3686 N92-30254
Spatiotemporal characteristics of human visual localization
[AD-A248494] p 3687 N92-30325
PSYCHOPHYSIOLOGY
Psychophysical studies of visual cortical function
[AD-A246962] p 3687 N92-30679
PULLING
A reduced gravity fiber pulling apparatus
[NASA-TM-103594] p 3612 N92-30971

PULSARS
Constraints on the nuclear matter equation of state from pulsar glitches
[DE92-015142] p 3740 N92-30578
Ultra high energy gamma rays and observations with CYGNUS/MILAGRO
[DE92-015243] p 3743 N92-30627
Constraints on the putative companions to PSR1257+12 p 3738 N92-31232
PULSE AMPLITUDE MODULATION
Backward-wave oscillator investigations in the Raman Regime
[AD-A250738] p 3622 N92-30332
PULSE COMMUNICATION
Toward a North American standard for mobile data services p 3620 N92-30940
PULSE DOPPLER RADAR
Low-level atmospheric flows studied by pulsed Doppler lidar p 3638 N92-31015
PULSE DURATION
Optical isolators in high power lasers based on high reflectivity phase conjugate mirrors
[IA-1452] p 3721 N92-30581
PULSE RATE
Feasibility of a walk test to assess the cardiorespiratory fitness of Naval personnel
[AD-A250650] p 3684 N92-30603
PULSED LASERS
Interaction of ultra-high laser fields with beams and plasmas
[AD-A249502] p 3723 N92-30620
Doppler lidar wind measurement with the edge technique p 3638 N92-31017
Tropospheric and stratospheric wind profiling with a direct detection Doppler lidar p 3639 N92-31018
A range-resolved bistatic lidar using a high-sensitive CCD-camera p 3640 N92-31027
Multiple scattering lidar returns from stratus clouds p 3642 N92-31035
Pulsed laser spectral measurement using a Fabry-Perot interferometer: Limits to resolution p 3646 N92-31055
Effect of atmospheric extinction on laser rangefinder performance at 1.54 and 0.6 microns p 3648 N92-31066
PULSES
A pulse combustion-based VOC destruction technique
[DE92-013563] p 3594 N92-30369
PURIFICATION
A method for regenerating ion exchange resin
[DE92-015312] p 3606 N92-31146
PYRIDINES
Effects of pyridostigmine bromide on A-10 pilots during execution of a simulated mission; performance
[AD-A252309] p 3685 N92-30605
Resonance Raman spectroscopic studies of trans dioxorhenium(V)tetrapyridyl species
[AD-A249919] p 3595 N92-30875
PYROLYTIC GRAPHITE
Shock-induced martensitic transformation of highly oriented graphite to diamond
[DE92-014787] p 3602 N92-30399
PYRROLES
Template-synthesis: A method for enhancing the ionic and electronic conductivity in electronically conductive polymers
[AD-A248806] p 3603 N92-30553
Infrared investigations of pristine, doped and partially-doped polypyrrole
[AD-A250644] p 3605 N92-30838
Polyphosphazenes bearing polymerizable pyrrole, thiophene and furan side groups: Synthesis and chemical oxidation
[AD-A249747] p 3607 N92-31207

Q

Q FACTORS
Processing aerosols and filaments in a TM010 microwave cavity at 2.45 GHz
[DE92-013536] p 3615 N92-30703
QUADRATIC EQUATIONS
Bifurcation of limit cycles in a particular class of quadratic systems
[REPT-91-76] p 3703 N92-30457
QUADRUPOLES
Numerical simulation of the electromagnetic instability of an intense beam in a quadrupole focusing system
[AD-A252275] p 3614 N92-30407
Magnetic measurement instrumentation developments at the SSC
[DE92-013969] p 3718 N92-30786
QUALIFICATIONS
Nuclear electric propulsion development and qualification facilities
[NASA-TM-105521] p 3589 N92-30818
QUALITY CONTROL
Impact testing of welded samples p 3608 N92-30268
A senior manufacturing laboratory for determining injection molding process capability p 3609 N92-30273
Compression planning for continuous improvement in quality programs
[DE92-012331] p 3732 N92-30349
NDE characterization of the microstructure and mechanical properties of Al-Li alloys
[DE92-012154] p 3598 N92-30858
The Pan-European Digital Cellular (GSM) System p 3619 N92-30938
First conclusions of a manufacturer group on the applicability of CALS in Europe p 3697 N92-30951
Quality assurance and ILS p 3697 N92-30953
A statistical rationale for establishing process quality control limits using fixed sample size, for critical current verification of SSC superconducting wire
[DE92-014844] p 3661 N92-31120
QUANTITATIVE ANALYSIS
Tolerance of beta blocked hypertensives during orthostatic and altitude stresses
[AD-A249904] p 3685 N92-30745
QUANTUM CHEMISTRY
Analytical methods using Slater-type orbitals in quantum chemistry
[AD-A251044] p 3731 N92-30242
Spontaneous decay of an atom near a phase conjugator
[AD-A248298] p 3712 N92-30333
QUANTUM CHROMODYNAMICS
On the factorisation theorem in boson-gluon fusion at hadron colliders
[NIKHEF-H/91-16] p 3713 N92-30415
Theoretical studies in elementary particle physics
[DE92-015295] p 3714 N92-30610
Nuclear theory progress report, April 1991 - April 1992
[DE92-015349] p 3714 N92-30611
Two-loop QCD corrections to the coefficient functions of the deep inelastic structure functions F2 and F(sub L)
[NIKHEF-H/91-17] p 3715 N92-30687
Theoretical particle physics
[DE92-014531] p 3716 N92-30841
Physics of the STAR experiment at the relativistic heavy ion collider
[DE92-014481] p 3719 N92-31198
QUANTUM EFFICIENCY
Development of ultra-low noise, high sensitivity planar metal grating coupled AlGaAs/GaAs multiquantum well IR detectors for focal plane array staring IR sensor systems
[AD-A246122] p 3590 N92-30318
An ultra-sensitive coherent detector capable of single photon detection for lidar applications p 3646 N92-31053
QUANTUM ELECTRODYNAMICS
Quantum interference and confinement effects in narrow channel Si-MOSFET's
[ETN-92-91742] p 3625 N92-30729
QUANTUM ELECTRONICS
One-dimensional subband effects in the conductance of multiple quantum wires in Si-MOSFET's p 3625 N92-30731
Quantum transport, noise and non-linear dissipative effects in one- and two-dimensional systems and associated sub-micron and nanostructure devices
[AD-A250895] p 3627 N92-31210
QUANTUM MECHANICS
From a world-sheet supersymmetry to the Dirac equation
[DE92-622375] p 3731 N92-30799
Quantum mechanics in Grassmann space
[DE92-622377] p 3711 N92-30801
QUANTUM THEORY
Development of ultra-low noise, high sensitivity planar metal grating coupled AlGaAs/GaAs multiquantum well IR detectors for focal plane array staring IR sensor systems
[AD-A246122] p 3590 N92-30318
Quantum Weyl Group and universal quantum R-matrix for affine Lie algebra A1
[PB92-178276] p 3704 N92-30511
Theoretical study of phase-shifted quantum beats in time-resolved luminescence spectra from a biased asymmetric double quantum well
[AD-A252422] p 3710 N92-30549
Fluctuation-dissipation theorem in general relativity and the cosmological constant
[DE92-013542] p 3740 N92-30705
From a world-sheet supersymmetry to the Dirac equation
[DE92-622375] p 3731 N92-30799
Quantum mechanics in Grassmann space
[DE92-622377] p 3711 N92-30801
Example of a quantum field theory based on a nonlinear Lie algebra
[DE92-010475] p 3731 N92-30825
Low-frequency fluctuations in plasma magnetic fields
[DE92-012139] p 3724 N92-30833
One-loop integration for the axial gauge with generalized prescription
[DE92-630241] p 3732 N92-31145
Elastic constants of crystals near melting via density functional theory. Effect of three-body correlations
[DE92-630567] p 3730 N92-31191
QUANTUM WELLS
Theoretical study of phase-shifted quantum beats in time-resolved luminescence spectra from a biased asymmetric double quantum well
[AD-A252422] p 3710 N92-30549
Studies of phonons and electronic excitations in semiconductor heterostructures
[AD-A249406] p 3729 N92-30772
Sol-gel optics: Proceedings SPIE-The International Society for Optical Engineering
[AD-A249986] p 3721 N92-31126
QUARK MODELS
Remarks on the exotic U-meson
[RAL-91-090] p 3715 N92-30750
Stochastic strings, topology, and space-time confinement
[DE92-630239] p 3732 N92-31136
QUARKS
Theoretical studies in elementary particle physics
[DE92-015295] p 3714 N92-30610
Two-loop QCD corrections to the coefficient functions of the deep inelastic structure functions F2 and F(sub L)
[NIKHEF-H/91-17] p 3715 N92-30687
Remarks on the exotic U-meson
[RAL-91-090] p 3715 N92-30750
Research on elementary particle physics. Task P: Studies in theory and phenomenology of elementary particles, part 1
[DE92-014428] p 3716 N92-30791
Theoretical particle physics
[DE92-014531] p 3716 N92-30841
Physics of the STAR experiment at the relativistic heavy ion collider
[DE92-014481] p 3719 N92-31198
QUARTZ CRYSTALS
Computer-controlled ion beam sputter-deposition of superconducting oxide films
[AD-A248495] p 3601 N92-30326
QUASI-STEADY STATES
Recombining processes in a cooling plasma by mixing of initially heated gas
[NIFS-142] p 3722 N92-30431
QUEUEING THEORY
Joint queue length and response time distributions in a general preemptive feedback queue
[REPT-91-66] p 3701 N92-30451
Foreign surveillance radar upgrade analysis
[AD-A249440] p 3616 N92-30760
QUOTIENTS
Dimension bounds for quotient spaces
[PB92-177997] p 3706 N92-30789

R

RADAR
Transient photoconductivity of low temperature GaAs grown by molecular beam epitaxy terahertz radar applications
[DE92-011848] p 3729 N92-30854
Modification of 95 GHz radar source module for low phase noise operation
[AD-A249793] p 3622 N92-31180
RADAR DATA
Satellite and Radar Data Use in Rainfall-Runoff Models p 3667 N92-30910
RADAR DETECTION
On the potential use of the terminal Doppler weather radar gust front detection algorithm on the WSR-88D system. Part 1: Impacts of radar system differences
[DOT/FAA/NR-92/8,I] p 3678 N92-30495
On the potential use of the terminal Doppler weather radar gust front detection algorithm on the WSR-88D system. Part 2: Detecting non-gust front convergent weather phenomena
[DOT/FAA/NR-92/8,II] p 3678 N92-30496
Remote sensing for rainfall estimation: SAC experience p 3668 N92-30917
RADAR FILTERS
Investigations on atomic-vapor-filter high-spectral-resolution lidar for temperature measurements p 3654 N92-31099
RADAR IMAGERY
Diversity imaging techniques in lidar p 3640 N92-31026

Science questions for the Magellan continuing mission
p 3738 N92-31235

RADAR MEASUREMENT
Lidar measurement of optical turbulence: Theory of the crossed path technique
[AD-A248938] p 3720 N92-30343
Glint errors derived from the partial derivatives of the echo signal phase for a distributed scatterer
[AD-A249499] p 3615 N92-30637
Satellite and Radar Data Use in Rainfall-Runoff Models p 3667 N92-30910
Doppler lidar wind measurement with the edge technique p 3638 N92-31017
Design of a near-IR coherent lidar for high spatial and velocity resolution wind measurement
p 3639 N92-31020
A range-resolved bistatic lidar using a high-sensitive CCD-camera p 3640 N92-31027
Determining water cloud particle sizes from lidar depolarization measurements and time dependent multiple scattering coefficients p 3641 N92-31034
Analytical multiple scattering correction to the Mie theory: Application to the analysis of the lidar signal
p 3642 N92-31036
Airborne lidar and radiometric observations of PBL- and low clouds p 3642 N92-31037
Measurement of aerosol profiles using high-spectral-resolution Rayleigh-Mie lidar
p 3644 N92-31046
Laboratory scaled simulation of lidar cloud sounding experiments p 3645 N92-31047
Wavemeter measurements of frequency stability of an injection seeded alexandrite laser for pressure and temperature lidar p 3645 N92-31049
Multiple scattering wavelength dependent backscattering of kaolin dust in the IR: Measurements and theory p 3648 N92-31064
Lidar measurements of cloud extinction coefficient distribution and its forward scattering phase function according to multiply scattered lidar returns
p 3651 N92-31082
Atmospheric measurements using the LAMP lidar during the LADIMAS campaign p 3652 N92-31086
Lidar measurements using large liquid mirror telescopes p 3652 N92-31087
Raman lidar measurements of water vapor and aerosol/clouds during the FIRE/SPECTRE field campaign p 3652 N92-31089
Performance modeling of daytime Raman lidar systems for profiling atmospheric water vapor
p 3653 N92-31090
BELINDA: Broadband Emission Lidar with Narrowband Determination of Absorption. A new concept for measuring water vapor and temperature profiles
p 3653 N92-31091
DIAL simulations for satellite water vapor profile measurements within the BEST project
p 3653 N92-31092
Airborne water vapor DIAL research: System development and field measurements
p 3653 N92-31093
Alexandrite lidar for the atmospheric water vapor detection and development of powerful tunable sources in IR p 3653 N92-31094
Emerging solid-state laser technology by lidar/DIAL remote sensing p 3653 N92-31095
Coherent summation of spatially distorted Doppler lidar signals using a two-dimensional heterodyne detector array p 3654 N92-31096
The role of laser coherence in long-range vibration measurements p 3654 N92-31097
A portable lidar using a diode-pumped YAG laser
p 3654 N92-31098
Investigations on atomic-vapor-filter high-spectral-resolution lidar for temperature measurements p 3654 N92-31099
HgCdTe photomixers for CO2 laser radar systems
p 3654 N92-31100
Airborne lidar mapping of vertical ozone distributions in support of the 1990 Clean Air Act Amendments
p 3654 N92-31101
Measurements of fugitive hydrocarbon emissions with a tunable infrared DIAL p 3655 N92-31102
The ENEA CO2 lidar/DIAL station activity in a tropospheric remote sensing program
p 3655 N92-31103
Lidar observation of marine mixed layer
p 3655 N92-31104
Aerosol extinction measurements with CO2-lidar
p 3655 N92-31105
Dense fog on the highway: Visual range monitoring in cars? p 3655 N92-31106

RADAR NETWORKS
Remote sensing for rainfall estimation: SAC experience p 3668 N92-30917

RADAR RECEIVERS
Aureole lidar: Design, operation, and comparison with in-situ measurements p 3648 N92-31065

RADAR SCATTERING
Glint errors derived from the partial derivatives of the echo signal phase for a distributed scatterer
[AD-A249499] p 3615 N92-30637
Laboratory scaled simulation of lidar cloud sounding experiments p 3645 N92-31047
Verification measurement of a polarization Raman elastic-backscatter lidar p 3647 N92-31062
Time and polarization dependent double scattering calculations of lidar returns from water clouds
p 3647 N92-31063
Multiple scattering wavelength dependent backscattering of kaolin dust in the IR: Measurements and theory p 3648 N92-31064
Aureole lidar: Design, operation, and comparison with in-situ measurements p 3648 N92-31065

RADAR TARGETS
Glint errors derived from the partial derivatives of the echo signal phase for a distributed scatterer
[AD-A249499] p 3615 N92-30637
Analysis of a digital RF memory in a signal-delay application
[DE92-013457] p 3626 N92-30764

RADAR TRACKING
The rise of active-element phased-array radar
[RAND-P-7747-RGS] p 3616 N92-30755

RADIAL DISTRIBUTION
Analytical solution of elastic-plastic thick-walled cylinders with general hardening
[AD-A249491] p 3705 N92-30618

RADIANCE
Ginsburg criterion for an equilibrium superradiant model in the dynamic approach
[DE92-630566] p 3732 N92-31203

RADIANT HEATING
Theory of sublinear power dependence for microwave heating in some ceramic materials
[DE92-015147] p 3606 N92-30847

RADIATION COUNTERS
Correction for nonlinear photon counting effects in lidar systems p 3649 N92-31070
High background photon counting lidar
p 3649 N92-31071

RADIATION DAMAGE
The effect of neutron irradiation on the structure and properties of carbon-carbon composite materials
[DE92-011670] p 3592 N92-30809
Recent improvements in size effects correlations for DBTT and upper shelf energy of ferritic steels
[DE92-014703] p 3599 N92-30877

RADIATION DETECTORS
Ultra high energy gamma rays and observations with CYGNUS/MILAGRO
[DE92-015243] p 3743 N92-30627
Ideas for a long-baseline neutrino detector
[DE92-010650] p 3743 N92-30828
An ultra-sensitive coherent detector capable of single photon detection for lidar applications
p 3646 N92-31053
Optical transducers for scintillating fiber readout
[DE92-015963] p 3721 N92-31187

RADIATION DISTRIBUTION
Two-color infrared digital imaging for determination of in-cylinder temperature and species during compression and combustion periods of DI diesel engine
[AD-A249812] p 3595 N92-30835
Spectroscopic diagnosis of long-scale-length exploding-foil plasma in the presence of an intense radiation field
[DE92-014718] p 3726 N92-31118

RADIATION DOSAGE
The revised International Commission on Radiological Protection (ICRP) dosimetric model for the human respiratory tract
[DE92-015092] p 3685 N92-31011
Analysis, review, and documentation of the activation data from LDEF material
[NASA-CR-184356] p 3596 N92-31161

RADIATION EFFECTS
New insights into radiation-induced oxide-trap charge through Thermally-Stimulated-Current (TSC) measurement and analysis
[DE92-009054] p 3728 N92-30585
The effect of neutron irradiation on the structure and properties of carbon-carbon composite materials
[DE92-011670] p 3592 N92-30809
Recent improvements in size effects correlations for DBTT and upper shelf energy of ferritic steels
[DE92-014703] p 3599 N92-30877
Effects of microwave radiation on humans: Monkeys exposed to 1.25 GHz pulsed microwaves
[AD-A249997] p 3686 N92-31127
Analysis, review, and documentation of the activation data from LDEF material
[NASA-CR-184356] p 3596 N92-31161

RADIATION MEASUREMENT
Ideas for a long-baseline neutrino detector
[DE92-010650] p 3743 N92-30828
Analysis, review, and documentation of the activation data from LDEF material
[NASA-CR-184356] p 3596 N92-31161
Solar neutrinos: Theoretical status
[DE92-014014] p 3743 N92-31199

RADIATION PROTECTION
The revised International Commission on Radiological Protection (ICRP) dosimetric model for the human respiratory tract
[DE92-015092] p 3685 N92-31011

RADIATION SHIELDING
Graphical-based construction of combinatorial geometries for radiation transport and shielding applications
[DE92-014453] p 3696 N92-30886

RADIATION TOLERANCE
The revised International Commission on Radiological Protection (ICRP) dosimetric model for the human respiratory tract
[DE92-015092] p 3685 N92-31011

RADIATION TRANSPORT
Graphical-based construction of combinatorial geometries for radiation transport and shielding applications
[DE92-014453] p 3696 N92-30886

RADIATIVE HEAT TRANSFER
Liquid droplet radiator: Design concepts and development logic
[MBB-UO-0165-91-PUB] p 3613 N92-30441
Heating and momentum deposition in hot stars
[DE92-011850] p 3740 N92-30855

RADIATIVE LIFETIME
Measurement of radiative lifetimes of vibrational states of simple ions
[AD-A248567] p 3712 N92-30337

RADIATIVE TRANSFER
Clouds: Their prediction and simulation
[AD-A250643] p 3679 N92-30643
Modeling of UV lines from cataclysmic variable winds
[DE92-013443] p 3739 N92-30862
Raman lidar measurements of water vapor and aerosol/clouds during the FIRE/SPECTRE field campaign p 3652 N92-31089

RADICALS
Approaches to polymer curing and imaging via the in situ generation of a catalyst
[AD-A249917] p 3606 N92-30873

RADIO COMMUNICATION
High frequency communications under adverse conditions
[AD-A252199] p 3615 N92-30532
Experimental millimeter-wave personal satellite communications system p 3617 N92-30927
Cellular: Toward personal communications
p 3619 N92-30936
National transportable telecommunications capability
p 3620 N92-30943

RADIO EQUIPMENT
The RadioSat (sm) network p 3620 N92-30942
The MARCOR GPS mobile data system
p 3620 N92-30944
Broadcast satellite service: The international dimension p 3621 N92-30946

RADIO FREQUENCIES
Analysis of a digital RF memory in a signal-delay application
[DE92-013457] p 3626 N92-30764
Multifrequency measurements of radar ground clutter at 42 sites. Volume 3: Appendix E
[AD-A246988] p 3616 N92-30863

RADIO FREQUENCY HEATING
Dynamic analysis of compact helical system power supply and designs of its upgrade
[NIFS-TECH-2] p 3723 N92-30497
Fundamental studies of fusion plasmas
[DE92-015077] p 3726 N92-31116

RADIO RECEIVERS
Experimental millimeter-wave personal satellite communications system p 3617 N92-30927

RADIO SIGNALS
Discovery of two planets around a millisecond pulsar
p 3739 N92-31237

RADIO TRANSMISSION
Direct broadcast satellite-radio: Portable and mobile reception trade-offs p 3621 N92-30945

RADIOACTIVE DECAY
Spontaneous decay of an atom near a phase conjugator
[AD-A248298] p 3712 N92-30333

RADIOACTIVE ISOTOPES
The revised International Commission on Radiological Protection (ICRP) dosimetric model for the human respiratory tract
[DE92-015092] p 3685 N92-31011
RADIOBIOLOGY
The revised International Commission on Radiological Protection (ICRP) dosimetric model for the human respiratory tract
[DE92-015092] p 3685 N92-31011
RADIOGRAPHY
An x ray microprobe based upon a close-coupled focal-spot/glass capillary arrangement
[DE92-011886] p 3722 N92-31195
RADIOMETERS
New shortwave solar radiometer with information-based sparse sampling
[DE92-010483] p 3742 N92-30797
Remote sensing for rainfall estimation: SAC experience p 3668 N92-30917
Comparison of eye-safe solid state laser DIAL with passive gas filter correlation measurements from aircraft and spacecraft p 3647 N92-31060
RAIL TRANSPORTATION
Vehicle/guideway interaction for high speed vehicles on flexible guideway
[DE92-013057] p 3660 N92-30860
RAIN
Satellite and Radar Data Use in Rainfall-Runoff Models p 3667 N92-30910
Remote sensing applications to rainfall estimation p 3668 N92-30911
Use of INSAT data in rainfall estimation p 3668 N92-30912
Remote sensing satellite data use in run-off studies p 3668 N92-30914
Remote sensing for rainfall estimation: SAC experience p 3668 N92-30917
RAMAN LASERS
Alexandrite lidar for the atmospheric water vapor detection and development of powerful tunable sources in IR p 3653 N92-31094
RAMAN SPECTRA
Interaction physics for megajoule laser fusion targets
[DE92-014796] p 3656 N92-30400
Resonance Raman spectroscopic studies of trans dioxorhenium(V)tetrapyridyl species
[AD-A249919] p 3595 N92-30875
Measurement of multiple scattering effects with a polarization Raman elastic-backscatter lidar p 3641 N92-31033
Advanced Raman water vapor lidar p 3643 N92-31040
Water vapor variance measurements using a Raman lidar p 3643 N92-31041
Verification measurement of a polarization Raman elastic-backscatter lidar p 3647 N92-31062
RAMAN SPECTROSCOPY
Electrochemical and optical studies of model photosynthetic systems
[DE92-010657] p 3683 N92-30829
Fiber-optic Raman spectroscopy at the Savannah River Site: Uses and techniques
[DE92-013971] p 3596 N92-30899
Development of a Raman lidar simulation tool p 3649 N92-31072
RANDOM PROCESSES
Combinatorics and Kolmogorov complexity
[CWI-CS-R9125] p 3708 N92-30699
RANDOM VARIABLES
The sum of weighted balls
[RUU-CS-91-37] p 3707 N92-30481
RANDOM WALK
The two-dimensional random walk: Its hitting process and its classification
[CWI-BS-R9003] p 3705 N92-30689
RANGEFINDING
Compact range test applications, phase 2
[AD-A248790] p 3615 N92-30583
Doppler lidar wind measurement with the edge technique p 3638 N92-31017
A geodetic laser radar rangefinder with 10(exp -7) resolution p 3641 N92-31029
Atmospheric measurements using the LAMP lidar during the LADIMAS campaign p 3652 N92-31086
RANKINE CYCLE
Potassium Rankine cycle power conversion systems for lunar-Mars surface power
[DE92-015102] p 3589 N92-31012
RANKINE-HUGONIOT RELATION
Shock-induced martensitic transformation of highly oriented graphite to diamond
[DE92-014787] p 3602 N92-30399
RAPID QUENCHING (METALLURGY)
Superconductivity and magnetism in rapidly solidified perovskites
[DE92-014081] p 3597 N92-30588
RAPID TRANSIT SYSTEMS
Vehicle/guideway interaction for high speed vehicles on flexible guideway
[DE92-013057] p 3660 N92-30860
RARE EARTH ALLOYS
Fundamental studies of strongly magnetic rare earth-transition metal alloys
[DE92-015916] p 3600 N92-31186
RAREFIED GAS DYNAMICS
Numerical solution of a three-dimensional cubic cavity flow by using the Boltzmann equation
[NASA-TM-105693] p 3627 N92-30297
RASTER SCANNING
Tunneling acoustic microscopy
[AD-A251028] p 3727 N92-30252
Considerations for imaging system implementation in a networked environment
[DE92-015338] p 3735 N92-31132
RATES (PER TIME)
High-temperature ignition of propane with MTBE as an additive: Shock-tube experiments and modeling
[DE92-006679] p 3594 N92-30749
RATINGS
The REMBRANDT system for multi-criteria decision analysis via pairwise comparisons or direct rating
[REPT-92-05] p 3692 N92-30357
Scale sensitivity and rank preservation in a multiplicative variant of the AHP and SMART
[REPT-91-67] p 3707 N92-30452
RATS
Cortical mechanisms of attention, discrimination, and motor response to somaesthetic stimuli
[AD-A247228] p 3687 N92-30613
RAYLEIGH SCATTERING
Investigations on atomic-vapor-filter high-spectral-resolution lidar for temperature measurements p 3654 N92-31099
RAYLEIGH-RITZ METHOD
Variational method in the statistical theory of turbulent two-phase flows
[AD-A252263] p 3630 N92-30604
REACTING FLOW
Turbulent reacting flows and supersonic combustion
[AD-A251065] p 3593 N92-30256
Development of a 3-D upwind PNS code for chemically reacting hypersonic flowfields
[NASA-CR-190182] p 3576 N92-30977
REACTION KINETICS
A pulse combustion-based VOC destruction technique
[DE92-013563] p 3594 N92-30369
Statistics for laminar flamelet modeling p 3597 N92-30668
High-temperature ignition of propane with MTBE as an additive: Shock-tube experiments and modeling
[DE92-006679] p 3594 N92-30749
Development of practical MO techniques for prediction of the properties and behavior of materials
[AD-A247218] p 3598 N92-30864
A novel process for methanol synthesis
[DE92-015798] p 3608 N92-30904
REACTIVITY
Magic numbers in molecular clusters: A probe for chemical reactivity
[AD-A251096] p 3712 N92-30261
REACTOR DESIGN
Potassium Rankine cycle power conversion systems for lunar-Mars surface power
[DE92-015102] p 3589 N92-31012
Criteria and design trade-off issues for ITER
[DE92-011786] p 3726 N92-31114
REACTOR MATERIALS
Review of high Z materials for PSI applications
[NIFS-152] p 3602 N92-30502
The effect of neutron irradiation on the structure and properties of carbon-carbon composite materials
[DE92-011670] p 3592 N92-30809
Recent improvements in size effects correlations for DBTT and upper shelf energy of ferritic steels
[DE92-014703] p 3599 N92-30877
Potassium Rankine cycle power conversion systems for lunar-Mars surface power
[DE92-015102] p 3589 N92-31012
READING
Proceedings of the Sylvia Beach Language Comprehension Conference
[AD-A250488] p 3621 N92-31129
READOUT
Hybridization of detector array and integrated circuit for readout
[NASA-CASE-NPO-18062-1-CU] p 3623 N92-30542
Optical transducers for scintillating fiber readout
[DE92-015963] p 3721 N92-31187
REAL GASES
Real gas flow parameters for NASA Langley 22-inch Mach 20 helium tunnel
[NASA-CR-4462] p 3635 N92-30751
REAL TIME OPERATION
Storage control system
[NASA-CASE-LAR-14651-1] p 3734 N92-30386
Flexible space-based robot modelling and real-time simulation
[NLR-TP-89364-U] p 3658 N92-30477
A model of the ADA avionics real-time system: An example of the benefits of the hardware/software codesign approach in development of real-time systems
[AD-A248893] p 3581 N92-30524
Implementation scheme for recursion in spectral dimension
[AD-A248945] p 3695 N92-30629
On-line analysis capabilities developed to support the AFW wind-tunnel tests
[NASA-TM-107651] p 3580 N92-30752
New shortwave solar radiometer with information-based sparse sampling
[DE92-010483] p 3742 N92-30797
Transactions of the 9th Army Conference on Applied Mathematics and Computing
[AD-A252140] p 3706 N92-30843
Repetitive High Energy Pulsed Power (RHEPP) temperature monitoring system utilizing Luxtron fluoroptic sensors and thermocouples technical reference manual
[DE92-013461] p 3637 N92-30893
Building a generalized distributed system model
[NASA-CR-190489] p 3698 N92-30960
Real-time simulation model of the HL-20 lifting body
[NASA-TM-107580] p 3586 N92-31160
RECEIVERS
Direct broadcast satellite-radio: Portable and mobile reception trade-offs p 3621 N92-30945
Altimetry and lidar using AlGaAs lasers modulated with pseudo-random codes p 3641 N92-31030
Lidar receivers for picosecond remote sensing p 3650 N92-31076
Acousto-optic filtering of lidar signals p 3650 N92-31077
RECOMMENDATIONS
The sustainable biosphere initiative: An ecological research agenda p 3673 N92-30425
Setting priorities for space research: Opportunities and imperatives
[NASA-CR-190519] p 3733 N92-30974
National Aeronautics and Space Administration p 3736 N92-31170
RECONNAISSANCE
The rise of active-element phased-array radar
[RAND-P-7747-RGS] p 3616 N92-30755
RECOVERY VEHICLES
Emissions of greenhouse gases from the use of transportation fuels and electricity
[DE92-012102] p 3674 N92-30770
RECRYSTALLIZATION
On recrystallization in metal matrix composites
[DE92-011364] p 3590 N92-30521
On the strain-rate dependence of dynamic recrystallization in copper polycrystals
[DE92-011363] p 3730 N92-31217
RECTANGLES
Operational surfaces for the rectangle and triangle
[DE92-015165] p 3705 N92-30566
RECURSIVE FUNCTIONS
Recursive models for synchronous sequential devices
[IMAG-RR-855-I] p 3704 N92-30473
RECYCLING
Determining significant material properties: A discovery approach p 3607 N92-30279
Review of high Z materials for PSI applications
[NIFS-152] p 3602 N92-30502
REDUCED GRAVITY
Development of and flight results from the Space Acceleration Measurement System (SAMS)
[NASA-TM-105652] p 3588 N92-30301
Microgravity vibration isolation: Optimal preview and feedback control
[NASA-TM-105673] p 3613 N92-30692
A reduced gravity fiber pulling apparatus
[NASA-TM-103594] p 3612 N92-30971
REDUNDANCY
Survivable algorithms and redundancy management in NASA's distributed computing systems
[NASA-CR-189827] p 3691 N92-30299
REFLECTANCE
Optical isolators in high power lasers based on high reflectivity phase conjugate mirrors
[IA-1452] p 3721 N92-30581
Reflector development for XUV free-electron laser oscillators
[DE92-015212] p 3657 N92-31182

Shining on: A primer on solar radiation data
[DE92-010555] p 3743 N92-31206

REFLECTOR ANTENNAS
Double-loop frequency-selected surfaces for multifrequency division multiplexing in a dual-reflector antenna
[NASA-CASE-NPO-18701-1-CU] p 3614 N92-30391

REFLECTORS
A conceptual design of a large aperture microwave radiometer geostationary platform
[NASA-TM-107577] p 3588 N92-30736
Reflector development for XUV free-electron laser oscillators
[DE92-015212] p 3657 N92-31182

REFRACTIVITY
The electric field dependence of the laser induced holographic grating relaxation of photorefractive polymer
[AD-A252641] p 3602 N92-30409
Determining water cloud particle sizes from lidar depolarization measurements and time dependent multiple scattering coefficients p 3641 N92-31034

REFRACTORY MATERIALS
Crack growth processes at elevated temperatures in advanced materials
[AD-A249023] p 3662 N92-30558
Nondestructive testing of ceramics for vehicular advanced heat engines
[DE92-010471] p 3604 N92-30744

REFRACTORY METAL ALLOYS
Potassium Rankine cycle power conversion systems for lunar-Mars surface power
[DE92-015102] p 3589 N92-31012

REGENERATION (ENGINEERING)
Advanced mobile satellite communications system using Ka and MM-wave bands in Japan's R and D satellite project p 3617 N92-30924
A method for regenerating ion exchange resin
[DE92-015312] p 3606 N92-31146

REGENERATORS
Thermal energy storage
[DE92-014942] p 3672 N92-31176

REGGE POLES
Remarks on the exotic U-meson
[RAL-91-090] p 3715 N92-30750

REGRESSION ANALYSIS
Filler metal development for Hastelloy alloy XR
[DE92-782044] p 3600 N92-31163

REGULATIONS
Computer security: Agencies reported having implemented most system security controls
[GAO/IMTEC-92-45] p 3690 N92-30712

REINFORCEMENT (STRUCTURES)
An experiment on the use of disposable plastics as a reinforcement in concrete beams p 3593 N92-30287
Mechanical behavior and processing of aluminum metal matrix composites
[AD-A249918] p 3592 N92-30874

REINFORCING FIBERS
Wave propagation and vibration of fibre-reinforced laminates
[AD-A252101] p 3590 N92-30528

RELATIVISTIC ELECTRON BEAMS
Nonlinear analysis of a grating free-electron laser
[AD-A248833] p 3656 N92-30743

RELATIVISTIC PARTICLES
Effects of high beam rates on TPC's
[DE92-014594] p 3717 N92-30398

RELATIVITY
Fluctuation-dissipation theorem in general relativity and the cosmological constant
[DE92-013542] p 3740 N92-30705
Stochastic strings, topology, and space-time confinement
[DE92-630239] p 3732 N92-31136

RELAXATION (MECHANICS)
Program RELAX: A code designed to calculate atomic relaxation spectra of x rays and electrons
[DE92-013751] p 3714 N92-30586

RELAY SATELLITES
SHARP system for personal communications p 3618 N92-30931

RELIABILITY
Statistical theory on reliability
[AD-A250809] p 3660 N92-30237
NEP systems engineering efforts in FY-92: Plans and status
[NASA-TM-105775] p 3588 N92-30308
Testing of double-layer capacitors for high reliability applications
[DE92-011384] p 3626 N92-30807
Development of a reliability maintenance optimization method p 3697 N92-30956
Transfer soldering evaluation
[DE92-015160] p 3627 N92-31144

RELIABILITY ANALYSIS
Statistical theory on reliability
[AD-A250809] p 3660 N92-30237
Reliability in the design phase
[DE92-012217] p 3661 N92-30763
NDE characterization of the microstructure and mechanical properties of Al-Li alloys
[DE92-012154] p 3598 N92-30858
A failure-to-restore unavailability model for periodically performed maintenance
[DE92-015902] p 3708 N92-31185

RELIABILITY ENGINEERING
MBB-LAGRANGE: A general structural reliability and optimization structural system
[MBB/FW321/S/PUB/467] p 3662 N92-30423
Reliability in the design phase
[DE92-012217] p 3661 N92-30763

REMOTE CONTROL
Method and apparatus for preloading a joint by remotely operable means
[NASA-CASE-MSC-21940-1] p 3659 N92-30540
Remote experimental site concept for diagnostic collaborations in fusion
[DE92-010437] p 3724 N92-30824

REMOTE SENSING
Methodology investigation, implement remote sensing
[AD-A248901] p 3678 N92-30340
The use of TM data for identification of land cover and for detection of land use changes in the Atlantic zone of Costa Rica
[BCRS-91-36] p 3666 N92-30362
On the remote sensing of water quality using the optical airborne scanner CAESAR
[BCRS-90-30] p 3666 N92-30466
CAESAR: Evaluation of the dual-look concept
[BCRS-91-10] p 3666 N92-30467
Monitoring of Dutch forest with LANDSAT-TM
[BCRS-91-21] p 3666 N92-30468
Feasibility of extracting current profile information from HF-radar surface current measurements, part 1 and 2
[BCRS-91-23-PT-1-2] p 3682 N92-30470
Vegetation conditions and yield indicators. Part 1: Main report
[BCRS-91-26-PT-1] p 3667 N92-30471
Interpretation of optical remote sensing data over coastal waters
[BCRS-91-27] p 3667 N92-30472
Registration of windfall damage in the eastern Hunsrueck Plateau (Federal Republic of Germany) utilizing LANDSAT-TM-data: A landscape-ecological analysis for practical forestry
[ESA-TT-1253] p 3667 N92-30515
Remote sensing for the Lincoln Sea Winterover Experiment
[AD-A252117] p 3667 N92-30545
A one-class classifier for identifying urban areas in remotely-sensed data
[DE92-013539] p 3667 N92-30704
Fiber-optic Raman spectroscopy at the Savannah River Site: Uses and techniques
[DE92-013971] p 3596 N92-30899
Satellite and Radar Data Use in Rainfall-Runoff Models p 3667 N92-30910
Remote sensing applications to rainfall estimation p 3668 N92-30911
Use of INSAT data in rainfall estimation p 3668 N92-30912
Solar-hydrogen energy system for solar belt countries and use of remote sensing p 3668 N92-30913
Remote sensing satellite data use in run-off studies p 3668 N92-30914
Geographic information system and its applications p 3668 N92-30915
SCS method of runoff estimation using remote sensing techniques p 3668 N92-30916
Remote sensing for rainfall estimation: SAC experience p 3668 N92-30917
Hydrologic modelling and use of remotely sensed data at CWPRS p 3669 N92-30918
Estimation of vertical profile of soil moisture through multifrequency microwave data analysis p 3669 N92-30919
Digital methods for analysis of satellite imagery p 3669 N92-30920
Field studies in geophysical diffraction tomography
[DE92-015084] p 3677 N92-31009
Sixteenth International Laser Radar Conference, part 2
[NASA-CP-3158-PT-2] p 3637 N92-31013
Atmospheric wind sensing with a 1 and 2 micron coherent lidar p 3639 N92-31019
Airborne remote sensing of tropospheric water vapor using a near infrared DIAL system p 3644 N92-31042
Conically scanned lidar telescope using holographic optical elements p 3645 N92-31050
Tm,Ho:YAG laser with tunable range of 2.08-2.12 microns and its applications to spectroscopy p 3646 N92-31058
Development of a Raman lidar simulation tool p 3649 N92-31072
Lidar receivers for picosecond remote sensing p 3650 N92-31076
Measurement capabilities of giant lidars for middle and upper atmospheric applications p 3651 N92-31084
Airborne water vapor DIAL research: System development and field measurements p 3653 N92-31093
Emerging solid-state laser technology by lidar/DIAL remote sensing p 3653 N92-31095
The ENEA CO2 lidar/DIAL station activity in a tropospheric remote sensing program p 3655 N92-31103
Remote-sensing survey of the Atchafalaya Basin Main Channel, Atchafalaya Channel training project, Saints Martin and Mary Parishes, Louisiana
[AD-A249915] p 3669 N92-31139
Fractal analysis: A new remote sensing tool for lava flows p 3736 N92-31224
Science questions for the Magellan continuing mission p 3738 N92-31235

REMOTELY PILOTED VEHICLES
Thrust test fixture
[AD-D015259] p 3585 N92-31192

REPORTS
Activities report of the Institute for Astronomy and Astrophysics at Technical University of Berlin (Germany, F.R.)
[MITT-11] p 3740 N92-30506
Astronautics 1977-1990
[AERONOMICA-ACTA-F-42-1991] p 3744 N92-30996

RESEARCH AND DEVELOPMENT
Beam technologies for integrated processing
[AD-A252647] p 3612 N92-30411
Operations and logistics tasks in the Columbus development program
[MBB-UO-0166-91-PUB] p 3708 N92-30419
Soviet applied information sciences in a time of change
[PB92-173020] p 3734 N92-30509
Spinoffs from R and D investments
[DE92-014450] p 3736 N92-30575
Center for Composites Manufacturing Science, Reliability, and Maintainability Technology
[AD-A248661] p 3591 N92-30639
Research and technology, 1991. Langley Research Center
[NASA-TM-4331] p 3744 N92-30733
National Aeronautics and Space Administration p 3736 N92-31170
Trends in aeropropulsion research and their impact on engineering education
[NASA-TM-105682] p 3583 N92-31172

RESEARCH FACILITIES
Research and technology, 1991. Langley Research Center
[NASA-TM-4331] p 3744 N92-30733
Activities of the Aeronautical Research Laboratory p 3744 N92-30768
National Aeronautics and Space Administration p 3736 N92-31170

RESEARCH MANAGEMENT
A program of continuing research on representing, manipulating, and reasoning about physical objects
[AD-A251089] p 3691 N92-30260
The 1991 Summer Faculty Research Program (SFRP), volume 4 atory
[AD-A248766] p 3744 N92-30327
Research on elementary particle physics
[DE92-014622] p 3715 N92-30625
Neutron Source Munich FRM-2
[DE92-015300] p 3717 N92-31205
Fuel cells
[DE92-001282] p 3672 N92-31221

RESEARCH PROJECTS
The 1991 Summer Faculty Research Program (SFRP), volume 4 atory
[AD-A248766] p 3744 N92-30327
Grand challenges 1993: High performance computing and communications. A report by the Committee on Physical, Mathematical, and Engineering Sciences to supplement the President's fiscal year 1993 budget
[PB92-160530] p 3689 N92-30600

RESEARCH VEHICLES
Joint computational and experimental aerodynamics research on a hypersonic vehicle
[DE92-013439] p 3574 N92-30367

RESIDUAL STRESS
Analytical solution of elastic-plastic thick-walled cylinders with general hardening
[AD-A249491] p 3705 N92-30618

RESIN MATRIX COMPOSITES
Nonlinear stress analysis of composite-jacketed steel cylinders subjected to high internal pressure
[AD-A249500] p 3663 N92-30802
RESINS
Studies on the melt flow rate of the SRM 1473: A low density polyethylene resin
[PB92-181080] p 3604 N92-30788
RESOLUTION
Resolution properties of the Fourier method for discontinuous waves
[NASA-CR-189668] p 3706 N92-30716
RESOLUTION CELL
Analytical estimates of the PP-algorithm at low number of Doppler periods per pulse length
p 3650 N92-31079
RESONANCE
Resonance Raman spectroscopic studies of trans dioxorhenium(V)tetrapyridyl species
[AD-A249919] p 3595 N92-30875
RESONANCE LINES
Modeling of UV lines from cataclysmic variable winds
[DE92-013443] p 3739 N92-30862
RESONANCE TESTING
Resonance and control response tests using a control simulation device
[MBB-UD-0608-91-PUB] p 3583 N92-30439
Optimum methods for the measurement of the absorption coefficients of materials
[BBC-RD-1992/3] p 3711 N92-31173
RESONANT FREQUENCIES
Prediction of coincidence frequencies for a thin-walled, fluid-filled pipe
[MRL-TN-600] p 3664 N92-30963
RESONANT TUNNELING
Studies of phonons and electronic excitations in semiconductor heterostructures
[AD-A249406] p 3729 N92-30772
RESONANT VIBRATION
Resonance Raman spectroscopic studies of trans dioxorhenium(V)tetrapyridyl species
[AD-A249919] p 3595 N92-30875
RESPIRATION
Feasibility of a walk test to assess the cardiorespiratory fitness of Naval personnel
[AD-A250650] p 3684 N92-30603
RESPONSE TIME (COMPUTERS)
Joint queue length and response time distributions in a general preemptive feedback queue
[REPT-91-66] p 3701 N92-30451
RETROREFLECTORS
Spectroscopic method for Earth-satellite-Earth laser long-path absorption measurements using Retroreflector In Space (RIS) p 3652 N92-31088
REUSE
Component construction: Practical guidelines for the construction of reusable components
[REPT-91-89] p 3694 N92-30484
The Duplex programming environment
[REPT-91-90] p 3694 N92-30492
REVERBERATION
Optimum methods for the measurement of the absorption coefficients of materials
[BBC-RD-1992/3] p 3711 N92-31173
REVERSE FIELD PINCH
Locked modes and magnetic field errors in MST
[DE92-015379] p 3723 N92-30612
REYNOLDS EQUATION
Fast methods to numerically integrate the Reynolds equation for gas fluid films
[NASA-TM-105415] p 3660 N92-30722
REYNOLDS NUMBER
One-equation near-wall turbulence modeling with the aid of direct simulation data p 3631 N92-30656
Direct numerical simulations of stably-stratified sheared turbulence: Implications for oceanic mixing
p 3632 N92-30659
Generation of large-scale density fluctuations by buoyancy p 3634 N92-30671
RHEOLOGY
Lewis icing research tunnel test of the aerodynamic effects of aircraft ground deicing/anti-icing fluids
[NASA-TP-3238] p 3577 N92-30395
Fractal analysis: A new remote sensing tool for lava flows p 3736 N92-31224
RICCATI EQUATION
Numerical methods for closed-loop control
[AD-A248481] p 3700 N92-30334
Parallel aspects of some spectral problems in linear algebra
[CWI-NM-R9113] p 3706 N92-30700
RICHARDSON NUMBER
Direct numerical simulations of stably-stratified sheared turbulence: Implications for oceanic mixing
p 3632 N92-30659
RIEMANN MANIFOLD
Heat flow of p-harmonic maps with values into spheres
[DE92-630236] p 3707 N92-31135
RING LASERS
Injection seeded single mode alexandrite ring laser for lidar applications p 3646 N92-31057
RINGS
Ringless piston experiments. Natural gas engine technology advancements
[PB92-164466] p 3659 N92-30601
RISK
DE-CERTS: A decision support system for a comparative evaluation method for risk management methodologies and tools
[AD-A246965] p 3733 N92-30682
ROBOT ARMS
Cable compliance
[NASA-TP-3216] p 3612 N92-30378
Flexible space-based robot modelling and real-time simulation
[NLR-TP-89364-U] p 3658 N92-30477
On two methods of determining the ellipses and ellipsoids of positioning accuracy of robot manipulators
[ISSN-0208-5658] p 3701 N92-31148
ROBOT CONTROL
A description of the research for period 3 of a research program on the planning and control for space robotic manipulators
[NASA-CR-190243] p 3660 N92-30738
ROBOT DYNAMICS
Flexible space-based robot modelling and real-time simulation
[NLR-TP-89364-U] p 3658 N92-30477
A description of the research for period 3 of a research program on the planning and control for space robotic manipulators
[NASA-CR-190243] p 3660 N92-30738
ROBOT SENSORS
Demonstration of a 3D vision algorithm for space applications
[NASA-CR-190646] p 3698 N92-31154
ROBOTICS
Cable compliance
[NASA-TP-3216] p 3612 N92-30378
Collected notes from the Benchmarks and Metrics Workshop
[NASA-TM-107910] p 3701 N92-30710
A description of the research for period 3 of a research program on the planning and control for space robotic manipulators
[NASA-CR-190243] p 3660 N92-30738
ROCK MECHANICS
A study of discrete and continuum joint modeling techniques
[DE92-012631] p 3663 N92-30859
ROCKET ENGINE DESIGN
Rocket propulsion research at Lewis Research Center
[NASA-CR-189187] p 3732 N92-30908
ROCKET EXHAUST
Numerical investigations in the backflow region of a vacuum plume
[NASA-CR-190515] p 3589 N92-30981
ROCKS
Investigation of the interface phenomena due to interaction of high intensity stress waves with geologic boundaries
[AD-A248992] p 3675 N92-30525
A study of discrete and continuum joint modeling techniques
[DE92-012631] p 3663 N92-30859
TEM studies of a circumstellar rock
p 3736 N92-31223
RODS
Fractal analysis: A new remote sensing tool for lava flows p 3736 N92-31224
ROOM TEMPERATURE
On the temperature role in the tunneling process at the cold fusion
[DE92-627497] p 3727 N92-30405
ROOT-MEAN-SQUARE ERRORS
Analytical estimates of the PP-algorithm at low number of Doppler periods per pulse length
p 3650 N92-31079
ROTARY WINGS
Development of a full-scale transmission testing procedure to evaluate advanced lubricants
[NASA-TP-3265] p 3658 N92-30396
Composite beam analysis linear analysis of naturally curved and twisted anisotropic beams
[AD-A252652] p 3663 N92-30766
Development of hardness cycles for fiber bound materials, using DSC: From laboratory specimens to complex high duty structural members
[MBB-Z-0409-91-PUB] p 3592 N92-30969
A demonstration of passive blade twist control using extension-twist coupling
[NASA-TM-107642] p 3664 N92-31155
ROTATING PLASMAS
Effects of fast ions and an external inductive electric field on the neoclassical parallel flow, current, and rotation in general toroidal systems
[NIFS-150] p 3713 N92-30500
Edge poloidal rotation profiles of H-mode plasmas in the JFT-2M tokamak
[DE92-799107] p 3725 N92-30992
Kinetic approach to long wave length modes in rotating plasmas
[NIFS-138] p 3725 N92-30993
ROTOR BLADES
A demonstration of passive blade twist control using extension-twist coupling
[NASA-TM-107642] p 3664 N92-31155
ROTOR DYNAMICS
Cryogenic Magnetic Bearing Test Facility (CMBTF)
[NASA-CR-189087] p 3582 N92-31164
ROTORS
Statistics on aircraft gas turbine engine rotor failures that occurred in US commercial aviation during 1989
[DOT/FAA/CT-92/5] p 3581 N92-30303
Yaw dynamics of horizontal axis wind turbines
[DE92-001245] p 3670 N92-30837
RUBBER
Stress-strain characteristics of rubber-like materials: Experiment and analysis p 3607 N92-30285
RULES
A survey on pivot rules for linear programming
[REPT-91-99] p 3691 N92-30351
RUNGE-KUTTA METHOD
Validation of three-dimensional incompressible spatial direct numerical simulation code: A comparison with linear stability and parabolic stability equation theories for boundary-layer transition on a flat plate
[NASA-TP-3205] p 3573 N92-30295
RUNWAYS
Potential airfield sites in Antarctica for wheeled aircraft
[AD-A249503] p 3584 N92-30621
RUPTURING
Measuring the Weibull modulus of microscope slides
p 3612 N92-30294

S

SACCADIC EYE MOVEMENTS
Psychophysical studies of visual cortical function
[AD-A246962] p 3687 N92-30679
SAFETY
Optimal ECG electrode sites and criteria for detection of asymptomatic coronary artery disease, update 1990. Multilead ECG changes at rest, with exercise, and with coronary angioplasty
[AD-A248613] p 3684 N92-30523
Fragment hazard zone analyses for explosive test facilities
[DE92-015391] p 3613 N92-30887
SAFETY DEVICES
A cable detection lidar system for helicopters
p 3648 N92-31068
SALINITY
Laboratory simulation of fluid dynamical process related to winter arctic leads
[AD-A252266] p 3682 N92-30593
SALT SPRAY TESTS
Corrosion of high density kinetic energy penetrator materials
[AD-A249439] p 3597 N92-30759
SAMARIUM ISOTOPES
The (146,147)Sm-(142,143)Nd systematics of early terrestrial differentiation and the lost continents of the early Earth p 3678 N92-31229
SAMPLES
Comparison of epifluorescent viable bacterial count methods
[NASA-TM-103592] p 3683 N92-30305
In situ TEM studies of the effect of misfit strain on the kinetics of Si(sub 1-x)Ge(sub x) solid phase epitaxy: Temperature calibration and surface effects
[DE92-011689] p 3728 N92-30574
SAMPLING
Improvement of performance of variable probability sampling strategies
[PB92-180264] p 3707 N92-30562
New shortwave solar radiometer with information-based sparse sampling
[DE92-010483] p 3742 N92-30797
Transient photoconductivity of low temperature GaAs grown by molecular beam epitaxy terahertz radar applications
[DE92-011848] p 3729 N92-30854

Oceanic CO2 measurements for the WOCE hydrographic survey in the Pacific Ocean, 1990-1991: Shore based analyses during legs 1-3
[DE92-013064] p 3682 N92-30861
Phase noise in pulsed Doppler lidar and limitations on achievable single-shot velocity accuracy
p 3639 N92-31024
Ultrafine aerosol size distributions and sulfuric acid vapor pressures: Implications for new particle formation in the atmosphere
[DE92-015217] p 3675 N92-31183

SAN FRANCISCO (CA)
Inter- and intra-plate deformation at North American plate boundaries
[NASA-CR-190485] p 3676 N92-30961

SATELLITE ALTIMETRY
Preparations for the ERS-1 and TOPEX/Poseidon satellite altimetry missions
[BCRS-90-28] p 3666 N92-30465
Altimeter and gravity data analysis
[NASA-CR-190478] p 3676 N92-30756

SATELLITE ANTENNAS
The ACTS multibeam antenna
[NASA-TM-105645] p 3587 N92-30383
Characteristics of a future aeronautical satellite communications system p 3618 N92-30932

SATELLITE COMMUNICATION
The ACTS multibeam antenna
[NASA-TM-105645] p 3587 N92-30383
Advanced mobile satellite communications system using Ka and MM-wave bands in Japan's R and D satellite project p 3617 N92-30924
Leo satellite-based telecommunication network concepts p 3617 N92-30926
Experimental millimeter-wave personal satellite communications system p 3617 N92-30927
The ELLIPSO (tm) system: Elliptical low orbits for mobile communications and other optimum system elements
p 3618 N92-30930
SHARP system for personal communications
p 3618 N92-30931
Characteristics of a future aeronautical satellite communications system p 3618 N92-30932
An integrated Ka/Ku-band payload for personal, mobile and private business communications
p 3619 N92-30933
A personal communications network using a Ka-band satellite p 3619 N92-30934
EHF (28/19 GHz) personal communications satellite terminal development p 3619 N92-30935
National transportable telecommunications capability
p 3620 N92-30943
Aeronautical Mobile Satellite Service (AMSS) capacity analysis and protocol performance simulation results
[DOT/FAA/CT-TN90/64] p 3622 N92-31212

SATELLITE DESIGN
Design of the American Mobile Satellite System
p 3617 N92-30925

SATELLITE IMAGERY
Monitoring of Dutch forest with LANDSAT-TM
[BCRS-91-21] p 3666 N92-30468
Satellite and Radar Data Use in Rainfall-Runoff Models p 3667 N92-30910
Digital methods for analysis of satellite imagery
p 3669 N92-30920

SATELLITE INSTRUMENTS
Small satellite radiation budget instrumentation
[DE92-011134] p 3677 N92-31008
A comparison of Ultra-Sensitive Coherent Detection (USCD) and heterodyne detection for a wind sensing application p 3640 N92-31025

SATELLITE NETWORKS
The ACTS multibeam antenna
[NASA-TM-105645] p 3587 N92-30383
Design of the American Mobile Satellite System
p 3617 N92-30925
Leo satellite-based telecommunication network concepts p 3617 N92-30926
Ka-band mobile and personal systems development at JPL p 3618 N92-30928
Issues for the integration of satellite and terrestrial cellular networks for mobile communications
p 3620 N92-30941

SATELLITE OBSERVATION
Satellite and Radar Data Use in Rainfall-Runoff Models p 3667 N92-30910
Remote sensing satellite data use in run-off studies
p 3668 N92-30914
DIAL simulations for satellite water vapor profile measurements within the BEST project
p 3653 N92-31092

SATELLITE POWER TRANSMISSION
Method for remotely powering a device such as a lunar rover
[NASA-CASE-LAR-14789-1] p 3658 N92-30388

SATELLITE TRACKING
The MARCOR GPS mobile data system
p 3620 N92-30944

SATELLITE TRANSMISSION
Leo satellite-based telecommunication network concepts p 3617 N92-30926
Personal communications via ACTS satellite HBR transponders p 3618 N92-30929

SATELLITE-BORNE INSTRUMENTS
Remote sensing applications to rainfall estimation
p 3668 N92-30911

SATURATION
Theory of sublinear power dependence for microwave heating in some ceramic materials
[DE92-015147] p 3606 N92-30847

SAWTOOTH WAVEFORMS
The role of stochasticity in sawtooth oscillation
[NIFS-103] p 3710 N92-30983

SCALARS
The structure of turbulent channel flow with passive scalar transport p 3632 N92-30657

SCALE MODELS
Direct numerical simulations of stably-stratified sheared turbulence: Implications for oceanic mixing
p 3632 N92-30659
Supercritical fluid extraction: A new process for producing high-performance, low-cost carbon fibers
[AD-A249407] p 3595 N92-30773
Laboratory scaled simulation of lidar cloud sounding experiments p 3645 N92-31047

SCALING LAWS
Selection of opening model for parachute scaling studies
[AD-A250882] p 3573 N92-30239
Plasma parameter estimations for the large helical device based on the gyro-reduced Bohm scaling
[NIFS-114] p 3723 N92-30499
Fractal and multifractal approaches to clustering phenomena
[AD-A249481] p 3709 N92-30642

SCANNING TUNNELING MICROSCOPY
Tunneling acoustic microscopy
[AD-A251028] p 3727 N92-30252
The microscopic world: A demonstration of electron microscopy for younger students p 3610 N92-30281
Single-electron charging effects
[DE92-015287] p 3710 N92-31131

SCATTERING
Multiple scattering theory of x ray absorption. A review
[DE92-622374] p 3716 N92-30798
Resonance Raman spectroscopic studies of trans dioxorhenium(V)tetrapyridyl species
[AD-A249919] p 3595 N92-30875
Altimetry and lidar using AlGaAs lasers modulated with pseudo-random codes p 3641 N92-31030
Multiple scattering effects on spaceborne lidar
p 3641 N92-31032
Determining water cloud particle sizes from lidar depolarization measurements and time dependent multiple scattering coefficients p 3641 N92-31034
Modification of 95 GHz radar source module for low phase noise operation
[AD-A249793] p 3622 N92-31180
Diffuse neutron scattering signatures of rough films
[DE92-015208] p 3717 N92-31201

SCATTERING AMPLITUDE
Spin amplitudes of pp-scattering in a unitarized supercritical pomeron model
[DE92-624639] p 3711 N92-30236

SCATTERING COEFFICIENTS
Multiple scattering technique lidar
p 3641 N92-31031
Laboratory scaled simulation of lidar cloud sounding experiments p 3645 N92-31047
A comparison of lidar inversion methods for cirrus applications p 3649 N92-31074

SCATTERING CROSS SECTIONS
Numerical simulations of light scattering from rough one-dimensional gold surfaces
[AD-A249794] p 3721 N92-30783
Multiple scattering theory of x ray absorption. A review
[DE92-622374] p 3716 N92-30798
Development of a Raman lidar simulation tool
p 3649 N92-31072

SCATTERING FUNCTIONS
Multiple scattering theory of x ray absorption. A review
[DE92-622374] p 3716 N92-30798
Determining water cloud particle sizes from lidar depolarization measurements and time dependent multiple scattering coefficients p 3641 N92-31034
Lidar measurements of cloud extinction coefficient distribution and its forward scattering phase function according to multiply scattered lidar returns
p 3651 N92-31082

SCHEDULING
Model analysis and expert system development for planning and scheduling teleoperations for aircraft turnaround functions, volume 1
[AD-A251037] p 3573 N92-30253
Model analysis and expert system development for planning and scheduling teleoperations for aircraft turnaround functions. Volume 2: Top user's guide
[AD-A251083] p 3573 N92-30258
Compression planning for continuous improvement in quality programs
[DE92-012331] p 3732 N92-30349
Joint queue length and response time distributions in a general preemptive feedback queue
[REPT-91-66] p 3701 N92-30451

SCHOOLS
Computer vision in microstructural analysis
p 3609 N92-30271
Experiments with the low melting indium-bismuth alloy system p 3601 N92-30272
Determining significant material properties: A discovery approach p 3607 N92-30279

SCHROEDINGER EQUATION
Spontaneous emission from an atom in motion near an infinite conducting plane
[ITN-92-85169] p 3715 N92-30782

SCHWARZ-CHRISTOFFEL TRANSFORMATION
A Boussinesq algorithm for bouyant convection in polygonal domains
[PB92-187137] p 3695 N92-30579

SCIENCE
Science in action: An interdisciplinary science education program p 3610 N92-30278

SCIENTIFIC SATELLITES
Remote sensing for the Lincoln Sea Winterover Experiment
[AD-A252117] p 3667 N92-30545
Astronautics 1977-1990
[AERONOMICA-ACTA-F-42-1991] p 3744 N92-30996

SCIENTISTS
Science in action: An interdisciplinary science education program p 3610 N92-30278

SCINTILLATION
Theory and measurement of the energy and risetime resolution of scintillation detectors in hard x ray area
[ETN-92-91687] p 3720 N92-30504

SCINTILLATION COUNTERS
Mechanical design and finite element analysis of the SDC central calorimeter
[DE92-011197] p 3655 N92-31109
Optical transducers for scintillating fiber readout
[DE92-015963] p 3721 N92-31187

SEA BREEZE
On the potential use of the terminal Doppler weather radar gust front detection algorithm on the WSR-88D system. Part 2: Detecting non-gust front convergent weather phenomena
[DOT/FAA/NR-92/8,II] p 3678 N92-30496
Low-level atmospheric flows studied by pulsed Doppler lidar p 3638 N92-31015

SEA ICE
Ice thickness observations, North American Arctic and subarctic, 1972-1973 and 1973-1974, part 8
[AD-A250830] p 3681 N92-30238
Remote sensing for the Lincoln Sea Winterover Experiment
[AD-A252117] p 3667 N92-30545
Laboratory simulation of fluid dynamical process related to winter arctic leads
[AD-A252266] p 3682 N92-30593
Vector analysis of ice fabric data
[AD-A250832] p 3682 N92-30832
Antarctic ice charts, 1989 - 1990: Analysis Atlas
[AD-A249730] p 3669 N92-31179

SEA WATER
Oceanic CO2 measurements for the WOCE hydrographic survey in the Pacific Ocean, 1990-1991: Shore based analyses during legs 1-3
[DE92-013064] p 3682 N92-30861

SEASAT SATELLITES
Preparations for the ERS-1 and TOPEX/Poseidon satellite altimetry missions
[BCRS-90-28] p 3666 N92-30465

SEAT BELTS
Evaluation of head impact kinematics for passengers seated behind interior walls
[AD-A252651] p 3578 N92-30551

SEATS
Evaluation of head impact kinematics for passengers seated behind interior walls
[AD-A252651] p 3578 N92-30551

SECRETIONS
Waste streams in a typical crewed space habitat: An update
[NASA-TM-103888] p 3689 N92-31166

SECULAR VARIATIONS
Data report, 92-2. Magnetic results, 1985-1990
p 3675 N92-30417
SEEBECK EFFECT
Absolute Seebeck thermoelectric characteristics: Principles, significance, and applications
[DE92-013684] p 3622 N92-30370
SEISMIC WAVES
Operation, maintenance and research activities at the Norwegian Seismic Array (NORSAR), the Norwegian Regional Seismic Array (NORESS), and the Arctic Regional Seismic Array (ARCESS)
[AD-A250403] p 3677 N92-31142
SEISMOLOGY
Inter- and intra-plate deformation at North American plate boundaries
[NASA-CR-190485] p 3676 N92-30961
Field studies in geophysical diffraction tomography
[DE92-015084] p 3677 N92-31009
Operation, maintenance and research activities at the Norwegian Seismic Array (NORSAR), the Norwegian Regional Seismic Array (NORESS), and the Arctic Regional Seismic Array (ARCESS)
[AD-A250403] p 3677 N92-31142
SELECTIVE SURFACES
Double-loop frequency-selected surfaces for multifrequency division multiplexing in a dual-reflector antenna
[NASA-CASE-NPO-18701-1-CU] p 3614 N92-30391
SELF CONSISTENT FIELDS
Self-consistent-field KKR-CPA calculations in the atomic-sphere approximations
[DE92-011525] p 3600 N92-31138
SEMANTICS
A three-valued cumulative semantics for TMS
[REPT-91-69] p 3702 N92-30371
A computational proof of soundness
[MEMO-INF-92-09] p 3693 N92-30433
A paradigm for asynchronous communication and its application to concurrent constraint programming
[RUU-CS-91-46] p 3615 N92-30448
Recursive models for synchronous sequential devices
[IMAG-RR-855-I] p 3704 N92-30473
The semantics of the Duplex programming environment
[REPT-91-91] p 3694 N92-30485
The Duplex programming environment
[REPT-91-90] p 3694 N92-30492
SEMICONDUCTOR DEVICES
Enhancement of weak localization in a Si lateral superlattice device p 3625 N92-30732
Oxidation of gallium arsenide
[DE92-016208] p 3731 N92-31220
SEMICONDUCTOR DIODES
Innovative techniques for the production of low cost 2-D laser diode arrays supplies or services and prices/costs
[AD-A252665] p 3656 N92-30552
A high speed signal processing system for a diode-pumped YAG lidar p 3646 N92-31054
SEMICONDUCTOR LASERS
Innovative techniques for the production of low cost 2-D laser diode arrays supplies or services and prices/costs
[AD-A252665] p 3656 N92-30552
A high speed signal processing system for a diode-pumped YAG lidar p 3646 N92-31054
Injection seeded single mode alexandrite ring laser for lidar applications p 3646 N92-31057
Tm,Ho:YAG laser with tunable range of 2.08-2.12 microns and its applications to spectroscopy
p 3646 N92-31058
High background photon counting lidar
p 3649 N92-31071
SEMICONDUCTORS (MATERIALS)
Dielectric behavior of semiconductors at microwave frequencies p 3610 N92-30275
Development of ultra-low noise, high sensitivity planar metal grating coupled AlGaAs/GaAs multiquantum well IR detectors for focal plane array staring IR sensor systems
[AD-A246122] p 3590 N92-30318
Waveguide polarizer using localized surface plasmons
[AD-D015258] p 3614 N92-30348
Adaptive multigrid applied to a bipolar transistor problem
[CWI-NM-R9115] p 3693 N92-30429
Hybridization of detector array and integrated circuit for readout
[NASA-CASE-NPO-18062-1-CU] p 3623 N92-30542
Ion channeling and spectroscopic ellipsometry examinations of thin-film SiO2/epi-Si structures
[DE92-015129] p 3728 N92-30577
New insights into radiation-induced oxide-trap charge through Thermally-Stimulated-Current (TSC) measurement and analysis
[DE92-009054] p 3728 N92-30585
Studies of ordering in semiconducting and other alloys
[AD-A249483] p 3728 N92-30634
Nonequilibrium behavior of carriers in semiconductors subjected to strong space-time varying fields
[AD-A246961] p 3624 N92-30678
Method of synthesizing high quality, doped diamond and diamonds and devices obtained therefrom
[AD-D015267] p 3604 N92-30685
Photochemical solar energy conversion utilizing semiconductors localized in membrane-mimetic systems
[DE92-011115] p 3670 N92-30694
Studies of phonons and electronic excitations in semiconductor heterostructures
[AD-A249406] p 3729 N92-30772
Polymerization of 1-bromo-4-lithiobenzene in THF. A route to soluble polyphenylenes
[AD-A249926] p 3604 N92-30794
Oxidation of gallium arsenide
[DE92-016208] p 3731 N92-31220
SENSITIVITY
Scale sensitivity and rank preservation in a multiplicative variant of the AHP and SMART
[REPT-91-67] p 3707 N92-30452
SENSORS
TRAC performance estimates
[NASA-CR-190530] p 3701 N92-30778
SENSORY PERCEPTION
Cortical mechanisms of attention, discrimination, and motor response to somaesthetic stimuli
[AD-A247228] p 3687 N92-30613
SEPARATED FLOW
Active control of pressure, sound and velocity of centrifugal pumps
[AD-A249446] p 3659 N92-30640
Vortex flow aerodynamics
[AGARD-AR-299] p 3576 N92-30947
SEPARATORS
Ni-H2 cell separator matrix engineering
[NASA-CR-190055] p 3671 N92-30949
SEQUENCING
On the Thue Morse measure
[REPT-92-16] p 3704 N92-30464
SEQUENTIAL ANALYSIS
Recursive models for synchronous sequential devices
[IMAG-RR-855-I] p 3704 N92-30473
SEROTONIN
Analysis and synthesis of adaptive neural elements and assembles
[AD-A248467] p 3687 N92-30320
SERVOCONTROL
An analytical and experimental investigation of flutter suppression via piezoelectric actuation
[NASA-TM-107653] p 3580 N92-31174
SERVOMECHANISMS
The calculation of mid-latitude meridional neutral winds from an improved servo model approximation method
[AD-A249874] p 3676 N92-30868
An analytical and experimental investigation of flutter suppression via piezoelectric actuation
[NASA-TM-107653] p 3580 N92-31174
SET THEORY
On the magnification of Cantor sets and their limit models
[REPT-91-100] p 3691 N92-30352
The domain of attraction of the alpha-sum operator for type 2 and type 3 distributions
[REPT-92-02] p 3707 N92-30355
Dimension bounds for quotient spaces
[PB92-177997] p 3706 N92-30789
Multifractal analysis of chaotic point sets
[AD-A250756] p 3709 N92-31194
SHAPE MEMORY ALLOYS
Method and apparatus for preloading a joint by remotely operable means
[NASA-CASE-MSC-21940-1] p 3659 N92-30540
SHAPES
Process modeling and development for three axisymmetric net shape forgings
[DE92-012111] p 3598 N92-30865
A tolerance approach to visual shape perception and image matching analysis for modeling of micro-heterogeneous materials
[ISSN-0208-5658] p 3721 N92-31149
Fractal analysis: A new remote sensing tool for lava flows p 3736 N92-31224
Gaspra's shape and surface features: Comparison to small satellites p 3739 N92-31236
SHEAR FLOW
Direct numerical simulations of stably-stratified sheared turbulence: Implications for oceanic mixing
p 3632 N92-30659
Interscale energy transfer in numerically simulated turbulence p 3634 N92-30672
SHEAR LAYERS
Resonant instability of supersonic shear layers
p 3632 N92-30661
A fractal transition in the two dimensional shear layer
p 3633 N92-30665
SHIP HULLS
The diffraction of short free surface water waves, a uniform expansion
[REPT-92-06] p 3628 N92-30358
Cross sectional constants and stress distributions of thin-walled sections
[AD-A249886] p 3663 N92-30870
SHIPS
Lidar observation of marine mixed layer
p 3655 N92-31104
SHOCK TESTS
Examination of aircraft warning and caution lights after shock testing
[NLR-TP-89284-U] p 3578 N92-30474
SHOCK TUBES
High-temperature ignition of propane with MTBE as an additive: Shock-tube experiments and modeling
[DE92-006679] p 3594 N92-30749
SHOCK WAVE INTERACTION
Intersecting shock-wave/turbulent boundary-layer interactions at Mach 8.3
[NASA-TM-103909] p 3635 N92-30765
Interaction of isotropic turbulence with a shock wave
[AD-A250409] p 3635 N92-30852
SHOCK WAVE PROFILES
Shock-induced martensitic transformation of highly oriented graphite to diamond
[DE92-014787] p 3602 N92-30399
Investigation of the interface phenomena due to interaction of high intensity stress waves with geologic boundaries
[AD-A248992] p 3675 N92-30525
SHOCK WAVE PROPAGATION
Investigation of the interface phenomena due to interaction of high intensity stress waves with geologic boundaries
[AD-A248992] p 3675 N92-30525
SHOCK WAVES
Algorithm to solve nonlinear time dependent problems of engineering and physics
[AD-A250641] p 3702 N92-30347
Three-dimensional shock wave physics simulations on massively parallel supercomputers
[DE92-008679] p 3698 N92-30363
Interaction of isotropic turbulence with a shock wave
[AD-A250409] p 3635 N92-30852
SHORT WAVE RADIATION
Research studies on extreme ultraviolet and soft x ray lasers
[AD-A249798] p 3657 N92-30784
New shortwave solar radiometer with information-based sparse sampling
[DE92-010483] p 3742 N92-30797
SHOT NOISE
Phase noise in pulsed Doppler lidar and limitations on achievable single-shot velocity accuracy
p 3639 N92-31024
SIDE-LOOKING RADAR
Results of the 1989 experiment with a polarimetric multifrequency SAR
[BCRS-91-33] p 3614 N92-30361
SIGNAL ANALYSIS
Signal matching by dynamic programming
[REPT-92-01] p 3614 N92-30354
SIGNAL ANALYZERS
Fiber optic based signal processing
[AD-A247857] p 3720 N92-30248
SIGNAL DETECTION
Optimal ECG electrode sites and criteria for detection of asymptomatic coronary artery disease, update 1990. Multilead ECG changes at rest, with exercise, and with coronary angioplasty
[AD-A248613] p 3684 N92-30523
Remote sensing for the Lincoln Sea Winterover Experiment
[AD-A252117] p 3667 N92-30545
Operation, maintenance and research activities at the Norwegian Seismic Array (NORSAR), the Norwegian Regional Seismic Array (NORESS), and the Arctic Regional Seismic Array (ARCESS)
[AD-A250403] p 3677 N92-31142
SIGNAL DISTORTION
Signal matching by dynamic programming
[REPT-92-01] p 3614 N92-30354
Comparison of signal processing methods for estimation of network impedance for remote protection
[ETN-92-91686] p 3623 N92-30503
SIGNAL MEASUREMENT
Doppler mean velocity estimation: Small sample analysis and a new estimator
[AD-A249024] p 3678 N92-30559
Compact range test applications, phase 2
[AD-A248790] p 3615 N92-30583

SIGNAL MIXING
Technical and economic feasibility of integrated video service by satellite
[NASA-CR-189210] p 3614 N92-30300
SIGNAL PROCESSING
Fiber optic based signal processing
[AD-A247857] p 3720 N92-30248
Comparison of signal processing methods for estimation of network impedance for remote protection
[ETN-92-91686] p 3623 N92-30503
Optimal ECG electrode sites and criteria for detection of asymptomatic coronary artery disease, update 1990. Multilead ECG changes at rest, with exercise, and with coronary angioplasty
[AD-A248613] p 3684 N92-30523
VDHW-related memo's
[LINO-1991-5] p 3718 N92-30725
Measurement report on the present Video Highway System of MEA p 3718 N92-30726
Tunable relay box (design and testing) p 3718 N92-30727
Console driver p 3718 N92-30728
Field studies in geophysical diffraction tomography
[DE92-015084] p 3677 N92-31009
Simplified signal processing for an airborne CO2 Doppler lidar p 3639 N92-31023
Diversity imaging techniques in lidar p 3640 N92-31026
Multiple scattering technique lidar p 3641 N92-31031
Multiple scattering effects on spaceborne lidar p 3641 N92-31032
Determining water cloud particle sizes from lidar depolarization measurements and time dependent multiple scattering coefficients p 3641 N92-31034
Analytical multiple scattering correction to the Mie theory: Application to the analysis of the lidar signal p 3642 N92-31036
A high speed signal processing system for a diode-pumped YAG lidar p 3646 N92-31054
Operation, maintenance and research activities at the Norwegian Seismic Array (NORSAR), the Norwegian Regional Seismic Array (NORESS), and the Arctic Regional Seismic Array (ARCESS)
[AD-A250403] p 3677 N92-31142
SIGNAL TO NOISE RATIOS
Initial laboratory evaluation of color video cameras
[DE92-010399] p 3637 N92-30822
Phase noise in pulsed Doppler lidar and limitations on achievable single-shot velocity accuracy p 3639 N92-31024
Diversity imaging techniques in lidar p 3640 N92-31026
Comparison of eye-safe solid state laser DIAL with passive gas filter correlation measurements from aircraft and spacecraft p 3647 N92-31060
Analytical estimates of the PP-algorithm at low number of Doppler periods per pulse length p 3650 N92-31079
Coherent summation of spatially distorted Doppler lidar signals using a two-dimensional heterodyne detector array p 3654 N92-31096
SIGNATURES
Diffuse neutron scattering signatures of rough films
[DE92-015208] p 3717 N92-31201
SILICON
Tunneling acoustic microscopy
[AD-A251028] p 3727 N92-30252
Dielectric behavior of semiconductors at microwave frequencies p 3610 N92-30275
Anisotropic silicon etching techniques
[MBB-Z-0413-91-PUB] p 3594 N92-30422
Quantum interference and confinement effects in narrow channel Si-MOSFET's
[ETN-92-91742] p 3625 N92-30729
Temperature dependence of universal conductance fluctuations in narrow Si inversion layers p 3625 N92-30730
Interaction of atomic hydrogen with the surface methyl group on Si(100): Removal of surface carbon
[AD-A249062] p 3595 N92-30821
Development of advanced silicon solar cells for Space Station Freedom
[NASA-CR-189215] p 3672 N92-31216
SILICON CARBIDES
Nondestructive characterization of two-phase metal-matrix materials
[AD-A249912] p 3592 N92-30815
Atomic layer epitaxy group 4 materials: Surface processes, thin films, devices, and their characterization
[AD-A252352] p 3729 N92-30846
TEM studies of a circumstellar rock p 3736 N92-31223
Presolar (?) corundum in the Orgueil meteorite p 3738 N92-31230
SILICON NITRIDES
Creep and slow crack growth mechanisms related to macroscopic creep behavior of a silicon nitride ceramic at elevated temperatures
[DE92-015195] p 3663 N92-30567
Effect of bending on the room-temperature tensile strengths of structural ceramics
[DE92-015196] p 3603 N92-30626
SILICON OXIDES
Ion channeling and spectroscopic ellipsometry examinations of thin-film SiO2/epi-Si structures
[DE92-015129] p 3728 N92-30577
SILICON RADIATION DETECTORS
Properties of CMOS devices and circuits fabricated on high-resistivity, detector-grade silicon
[DE92-011727] p 3626 N92-30813
SILOXANES
Molecular weight dependence of domain structure in silica-siloxane molecular composites
[DE92-015046] p 3603 N92-30544
SILVICULTURE
Development of the cultivated landscape of north west Germany under the human influence
[ETN-92-91730] p 3669 N92-30968
SIMD (COMPUTERS)
Contribution of parallelism to solving a load distribution problem in electric networks
[ETN-92-91668] p 3625 N92-30702
SIMPLEX METHOD
A survey on pivot rules for linear programming
[REPT-91-99] p 3691 N92-30351
SIMULATION
A model of the ADA avionics real-time system: An example of the benefits of the hardware/software codesign approach in development of real-time systems
[AD-A248893] p 3581 N92-30524
Laboratory simulation of fluid dynamical process related to winter arctic leads
[AD-A252266] p 3682 N92-30593
Pre-mixed flame simulations for non-unity Lewis numbers p 3597 N92-30670
Laboratory scaled simulation of lidar cloud sounding experiments p 3645 N92-31047
Aeronautical Mobile Satellite Service (AMSS) capacity analysis and protocol performance simulation results
[DOT/FAA/CT-TN90/64] p 3622 N92-31212
SINGLE CRYSTALS
Growth and evaluation of nonlinear optical materials for laser applications: Barium borate, lithium borate, and silver gallium selenide
[AD-A248861] p 3624 N92-30617
Nucleation and growth of diamond on carbon-implanted single crystal copper
[AD-A249021] p 3594 N92-30632
A study of enhancing critical current densities (J(sub c)) and critical temperature (T(sub c)) of high-temperature superconductors
[NASA-TM-103595] p 3627 N92-30902
SINGULARITY (MATHEMATICS)
On impasse points of quasilinear differential algebraic equations
[AD-A252643] p 3702 N92-30410
Some mathematical problems in continuum mechanics
[AD-A250352] p 3706 N92-31128
One-loop integration for the axial gauge with generalized prescription
[DE92-630241] p 3732 N92-31145
SINTERING
Pressure densification
[AD-A249438] p 3604 N92-30758
Cluster assembly of hierarchical nanostructures
[DE92-010498] p 3716 N92-30826
SKIN (STRUCTURAL MEMBER)
Control and augmentation of passive porosity through transpiration control
[NASA-CASE-LAR-14682-1] p 3628 N92-30387
SKIN FRICTION
Numerical study of axial turbulent flow over long cylinders
[AD-A250801] p 3635 N92-30831
SKY WAVES
High frequency communications under adverse conditions
[AD-A252199] p 3615 N92-30532
SLATER ORBITALS
Analytical methods using Slater-type orbitals in quantum chemistry
[AD-A251044] p 3731 N92-30242
SLEEP
Light as a chronobiologic countermeasure for long-duration space operations
[NASA-TM-103874] p 3686 N92-31167
SLIDING FRICTION
Modelling of heavily loaded lubricated contacts
[AD-A248807] p 3659 N92-30554
Eulerian simulation of the perforation of aluminum plates by nondeforming projectiles
[DE92-011515] p 3664 N92-31123
SLOPES
Fractal analysis: A new remote sensing tool for lava flows p 3736 N92-31224
SLURRIES
The development of precipitated iron catalysts with improved stability
[DE92-014625] p 3596 N92-31006
SMART STRUCTURES
The optimization of force inputs for active structural acoustic control using a neural network
[NASA-TM-107627] p 3711 N92-30979
SMOOTHING
Trajectory fitting in function space with application to analytic modeling of surfaces
[NASA-TP-3232] p 3576 N92-30747
SNAILS
Voltammetric measurement of oxygen in single neurons using platinized carbon ring electrodes
[AD-A252191] p 3683 N92-30531
SNOW
Multiple scattering lidar returns from stratus clouds p 3642 N92-31035
SOAPS
Measuring the surface tension of soap bubbles p 3612 N92-30293
A method for the production of weakly acidic cation exchange resins
[DE92-015314] p 3717 N92-31137
SOBOLEV SPACE
On real and complex zeros of orthogonal polynomials in a discrete Sobolev space
[REPT-91-98] p 3702 N92-30350
SOCIAL FACTORS
Pairwise comparison of concessions in negotiation processes
[REPT-92-15] p 3733 N92-30463
SODIUM
Generation of a sodium guidestar using a high power dye laser
[DE92-012696] p 3657 N92-31115
SOFTWARE ENGINEERING
Information processing research
[AD-A248492] p 3734 N92-30324
A formal transformation from the BSI/VDM-SL concrete syntax to the core abstract syntax
[REPT-92-07] p 3692 N92-30359
On the use of pre-defined implementation constructs in distributed systems design
[MEMO-INF-92-08] p 3689 N92-30432
Development environment for digital simulation models of multibody systems
[NLR-TP-89327-U] p 3693 N92-30476
Encyclopedia of software components
[NASA-CASE-NPO-18435-1-CU] p 3695 N92-30543
EASAMS' Ariane 5 on-board software experience
[D308/TN/001] p 3586 N92-30715
SOFTWARE REUSE
Encyclopedia of software components
[NASA-CASE-NPO-18435-1-CU] p 3695 N92-30543
SOFTWARE TOOLS
Adoption of the LSA S/W DILSA for the Columbus LSA tasks
[MBB-UO-0168-91-PUB] p 3709 N92-30420
MBB-LAGRANGE: A general structural reliability and optimization structural system
[MBB/FW321/S/PUB/467] p 3662 N92-30423
Development environment for digital simulation models of multibody systems
[NLR-TP-89327-U] p 3693 N92-30476
Component construction: Practical guidelines for the construction of reusable components
[REPT-91-89] p 3694 N92-30484
The semantics of the Duplex programming environment
[REPT-91-91] p 3694 N92-30485
The Duplex programming environment
[REPT-91-90] p 3694 N92-30492
Encyclopedia of software components
[NASA-CASE-NPO-18435-1-CU] p 3695 N92-30543
Integrating commercial off-the-shelf tools for custom software development
[AD-A252462] p 3695 N92-30550
Detecting potential synchronization constraint deadlocks from formal system specifications
[AD-A249019] p 3696 N92-30631
Collected notes from the Benchmarks and Metrics Workshop
[NASA-TM-107910] p 3701 N92-30710
MATGRID, a program for generation of C-H and C-O topology grids around wing/body configurations: Software description document
[FFA-TN-1990-20] p 3575 N92-30713

On-line analysis capabilities developed to support the AFW wind-tunnel tests
[NASA-TM-107651] p 3580 N92-30752
SOIL MECHANICS
Evaluation of grounding and mooring points for Army aircraft
[AD-A250749] p 3579 N92-31193
SOIL MOISTURE
Estimation of vertical profile of soil moisture through multifrequency microwave data analysis p 3669 N92-30919
SOIL SCIENCE
Chemistry for protection of the environment, 8th International Conference proceedings
[DE92-014317] p 3674 N92-31181
SOILS
Investigation of the interface phenomena due to interaction of high intensity stress waves with geologic boundaries
[AD-A248992] p 3675 N92-30525
SCS method of runoff estimation using remote sensing techniques p 3668 N92-30916
SOL-GEL PROCESSES
Sol-gel optics: Proceedings SPIE-The International Society for Optical Engineering
[AD-A249986] p 3721 N92-31126
SOLAR CELLS
Research on polycrystalline thin film submodules based on CuInSe2 materials
[DE92-010584] p 3727 N92-30247
Waveguide polarizer using localized surface plasmons
[AD-D015258] p 3614 N92-30348
High efficiency thermal to electric energy conversion using selective emitters and spectrally tuned solar cells
[NASA-TM-105755] p 3670 N92-30426
Examinations of the microwave photoelectric conductivity of a-Si:H multilayer systems for in situ characterization
[ETN-92-91688] p 3727 N92-30505
Perspective on photovoltaic amorphous silicon
[DE92-010581] p 3670 N92-30519
A conceptual design of a large aperture microwave radiometer geostationary platform
[NASA-TM-107577] p 3588 N92-30736
Research on defects and transport in amorphous silicon-based semiconductors
[DE92-001223] p 3729 N92-30748
Development of advanced silicon solar cells for Space Station Freedom
[NASA-CR-189215] p 3672 N92-31216
SOLAR COLLECTORS
Uniform flux dish concentrators for photovoltaic application
[DE92-010566] p 3671 N92-30896
SOLAR CORONA
Solar flare MDH
[AD-A250639] p 3702 N92-30375
Dynamics and energetics of the solar corona
[NASA-CR-190664] p 3742 N92-31162
SOLAR ENERGY
Shining on: A primer on solar radiation data
[DE92-010555] p 3743 N92-31206
SOLAR ENERGY CONVERSION
Photochemical solar energy conversion utilizing semiconductors localized in membrane-mimetic systems
[DE92-011115] p 3670 N92-30694
Solar-hydrogen energy system for solar belt countries and use of remote sensing p 3668 N92-30913
Thermal energy storage
[DE92-014942] p 3672 N92-31176
Shining on: A primer on solar radiation data
[DE92-010555] p 3743 N92-31206
SOLAR FLARES
Solar flare MDH
[AD-A250639] p 3702 N92-30375
FNAS: The magnetic configuration leading to solar flares
[NASA-CR-190522] p 3743 N92-31168
SOLAR FLUX
Solar neutrinos: Theoretical status
[DE92-014014] p 3743 N92-31199
SOLAR NEUTRINOS
Theoretical particle physics
[DE92-014531] p 3716 N92-30841
Solar neutrinos: Theoretical status
[DE92-014014] p 3743 N92-31199
SOLAR OSCILLATIONS
Solar neutrinos: Theoretical status
[DE92-014014] p 3743 N92-31199
SOLAR PHYSICS
Solar flare MDH
[AD-A250639] p 3702 N92-30375
SOLAR RADIATION
New shortwave solar radiometer with information-based sparse sampling
[DE92-010483] p 3742 N92-30797
Photodegradation effects in materials exposed to high flux solar and solar simulated radiation
[DE91-002147] p 3596 N92-30879
Nonlinear RR Lyrae models with new Livermore opacities
[DE92-011158] p 3741 N92-31108
Shining on: A primer on solar radiation data
[DE92-010555] p 3743 N92-31206
SOLAR WIND
Twenty-Third Lunar and Planetary Science Conference
[NASA-CR-190178] p 3736 N92-31222
On the isotopic signature of recent solar-wind nitrogen p 3738 N92-31231
SOLDERING
Transfer soldering evaluation
[DE92-015160] p 3627 N92-31144
SOLID ELECTROLYTES
Evaluation of doped polyethylene oxide as solid electrolyte for polymer batteries
[AD-A249501] p 3624 N92-30619
SOLID LUBRICANTS
Solid lubrication of laser grown fluorinated diamond thin films
[AD-A249485] p 3603 N92-30635
SOLID STATE
Heat-treating of materials p 3601 N92-30292
In situ TEM studies of the effect of misfit strain on the kinetics of Si(sub 1-x)Ge(sub x) solid phase epitaxy: Temperature calibration and surface effects
[DE92-011689] p 3728 N92-30574
Initial laboratory evaluation of color video cameras
[DE92-010399] p 3637 N92-30822
A compact high repetition rate CO2 coherent Doppler lidar p 3639 N92-31022
SOLID STATE DEVICES
Double-sided wafer alignment techniques
[AD-A250757] p 3730 N92-30895
SOLID STATE LASERS
Tunable solid state lasers based on molecular ions
[AD-A249423] p 3656 N92-30774
Doppler lidar wind measurement with the edge technique p 3638 N92-31017
Atmospheric wind sensing with a 1 and 2 micron coherent lidar p 3639 N92-31019
An alexandrite regenerative amplifier for water vapor and temperature measurements p 3645 N92-31048
Comparison of eye-safe solid state laser DIAL with passive gas filter correlation measurements from aircraft and spacecraft p 3647 N92-31060
A study of atmospheric optical scattering parameters at 1.5 and 2 micron region for solid state Doppler lidar applications p 3648 N92-31067
Alexandrite lidar for the atmospheric water vapor detection and development of powerful tunable sources in IR p 3653 N92-31094
Emerging solid-state laser technology by lidar/DIAL remote sensing p 3653 N92-31095
SOLID SURFACES
Control and augmentation of passive porosity through transpiration control
[NASA-CASE-LAR-14682-1] p 3628 N92-30387
SOLID-SOLID INTERFACES
Eulerian simulation of the perforation of aluminum plates by nondeforming projectiles
[DE92-011515] p 3664 N92-31123
SOLIDIFICATION
Experiments with the low melting indium-bismuth alloy system p 3601 N92-30272
Superconductivity and magnetism in rapidly solidified perovskites
[DE92-014081] p 3597 N92-30588
Phase transformations in weldments: New materials and new perspectives
[DE92-016231] p 3600 N92-31177
SOLIDS
Finite element analysis of laminated composite axisymmetric solids. Volume 1: Theory and applications
[AD-A250808] p 3590 N92-30251
SOLIDS FLOW
Kinetic theory and boundary conditions for flows of highly inelastic spheres
[DE92-012645] p 3629 N92-30438
SOLITARY WAVES
Scale symmetry of quantum solitons
[DE92-624560] p 3712 N92-30331
SONAR
Relaxor ferroelectrics for electrostrictive transducer
[AD-A248671] p 3624 N92-30598
SOUND TRANSDUCERS
Tunneling acoustic microscopy
[AD-A251028] p 3727 N92-30252
SOUND WAVES
A pulse combustion-based VOC destruction technique
[DE92-013583] p 3594 N92-30369
Prediction of coincidence frequencies for a thin-walled, fluid-filled pipe
[MRL-TN-600] p 3664 N92-30963
SOUNDING
Methodology investigation, implement remote sensing
[AD-A248901] p 3678 N92-30340
SOURCE PROGRAMS
Integrating commercial off-the-shelf tools for custom software development
[AD-A252462] p 3695 N92-30550
SPACE CHARGE
Thermally activated rejuvenation of ferroelectric properties in electrically fatigued lead zirconate titanate ceramics
[DE92-012634] p 3605 N92-30830
SPACE DEBRIS
Space station trash removal system
[NASA-CASE-MSC-21723-1] p 3588 N92-30315
Debris/ice/TPS assessment and integrated photographic analysis for Shuttle Mission STS-45
[NASA-TM-107545] p 3586 N92-30382
Environment modelling in near Earth space: Preliminary LDEF results p 3588 N92-31225
SPACE EXPLORATION
Electrical and chemical interactions at Mars Workshop, part 1
[NASA-CP-10093] p 3741 N92-30302
Space transportation systems, launch systems, and propulsion for the Space Exploration Initiative: Results from Project Outreach
[NASA-CR-190345] p 3587 N92-30958
Space science and applications: Strategic plan 1991
[NASA-TM-107811] p 3733 N92-30959
Setting priorities for space research: Opportunities and imperatives
[NASA-CR-190519] p 3733 N92-30974
SPACE LABORATORIES
Correlative measurement opportunities between ATLAS-1 and UARS experiments
[NASA-TM-107630] p 3679 N92-30735
SPACE LOGISTICS
Integration mockup and process material management system
[NASA-CR-184319] p 3613 N92-30754
SPACE MISSIONS
Debris/ice/TPS assessment and integrated photographic analysis for Shuttle Mission STS-45
[NASA-TM-107545] p 3586 N92-30382
Software breadboard study
[NASA-CR-190473] p 3625 N92-30757
SPACE PLASMAS
X ray radiation from hot dense plasmas and atomic processes
[NIFS-PROC-9] p 3725 N92-30984
SPACE POWER REACTORS
Nuclear electric propulsion development and qualification facilities
[NASA-TM-105521] p 3589 N92-30818
Potassium Rankine cycle power conversion systems for lunar-Mars surface power
[DE92-015102] p 3589 N92-31012
Thermohydraulic modeling of nuclear thermal rockets: The KLAXON code
[DE92-015274] p 3589 N92-31204
SPACE PROCESSING
Integration mockup and process material management system
[NASA-CR-184319] p 3613 N92-30754
SPACE PROGRAMS
Space science and applications: Strategic plan 1991
[NASA-TM-107811] p 3733 N92-30959
SPACE SHUTTLE BOOSTERS
Numerical methods for the simulation of complex multi-body flows with applications for the integrated Space Shuttle vehicle p 3576 N92-30741
SPACE SHUTTLE MAIN ENGINE
Cryogenic Magnetic Bearing Test Facility (CMBTF)
[NASA-CR-189087] p 3582 N92-31164
SPACE SHUTTLE ORBITERS
Development of and flight results from the Space Acceleration Measurement System (SAMS)
[NASA-TM-105652] p 3588 N92-30301
Data analysis support for the Shuttle Potential and Return Electron Experiment (SPREE) on the Tethered Satellite System 1 (TSS-1) flight
[AD-A248943] p 3588 N92-30628
SPACE SHUTTLES
Correlative measurement opportunities between ATLAS-1 and UARS experiments
[NASA-TM-107630] p 3679 N92-30735
Numerical methods for the simulation of complex multi-body flows with applications for the integrated Space Shuttle vehicle
[NASA-CR-190045] p 3575 N92-30740

Numerical methods for the simulation of complex multi-body flows with applications for the integrated Space Shuttle vehicle p 3576 N92-30741
Application of the Chimera overlapped grid scheme to simulation of Space Shuttle ascent flows p 3576 N92-30742

SPACE STATION FREEDOM
Design feasibility study of a Space Station Freedom truss
[NASA-TM-105558] p 3659 N92-30571
Integration mockup and process material management system
[NASA-CR-184319] p 3613 N92-30754
Waste streams in a typical crewed space habitat: An update
[NASA-TM-103888] p 3689 N92-31166
Development of advanced silicon solar cells for Space Station Freedom
[NASA-CR-189215] p 3672 N92-31216

SPACE STATION POWER SUPPLIES
Development of advanced silicon solar cells for Space Station Freedom
[NASA-CR-189215] p 3672 N92-31216

SPACE STATIONS
Space station trash removal system
[NASA-CASE-MSC-21723-1] p 3588 N92-30315

SPACE TRANSPORTATION
Research and technology, 1991. Langley Research Center
[NASA-TM-4331] p 3744 N92-30733

SPACE TRANSPORTATION SYSTEM
Space transportation systems, launch systems, and propulsion for the Space Exploration Initiative: Results from Project Outreach
[NASA-CR-190345] p 3587 N92-30958

SPACE WEAPONS
Corrosion of high density kinetic energy penetrator materials
[AD-A249439] p 3597 N92-30759
Joint stabilizing projects in defense
[DE92-015977] p 3709 N92-30891

SPACE-TIME FUNCTIONS
Fluctuation-dissipation theorem in general relativity and the cosmological constant
[DE92-013542] p 3740 N92-30705
Stochastic strings, topology, and space-time confinement
[DE92-630239] p 3732 N92-31136

SPACEBORNE ASTRONOMY
Hubble Space Telescope. Update: 18 months in orbit
[NASA-TM-107962] p 3739 N92-30686

SPACEBORNE EXPERIMENTS
Microgravity vibration isolation: Optimal preview and feedback control
[NASA-TM-105673] p 3613 N92-30692
Analysis, review, and documentation of the activation data from LDEF material
[NASA-CR-184356] p 3596 N92-31161

SPACECRAFT CHARGING
Data analysis support for the Shuttle Potential and Return Electron Experiment (SPREE) on the Tethered Satellite System 1 (TSS-1) flight
[AD-A248943] p 3588 N92-30628

SPACECRAFT DESIGN
Integration mockup and process material management system
[NASA-CR-184319] p 3613 N92-30754
Real-time simulation model of the HL-20 lifting body
[NASA-TM-107580] p 3586 N92-31160

SPACECRAFT LAUNCHING
Space transportation systems, launch systems, and propulsion for the Space Exploration Initiative: Results from Project Outreach
[NASA-CR-190345] p 3587 N92-30958

SPACECRAFT POWER SUPPLIES
Magnetic bearings for free-piston Stirling engines
[NASA-TM-105730] p 3660 N92-30734
Development of software to improve AC power quality on large spacecraft
[NASA-CR-190569] p 3589 N92-30989

SPACECRAFT PROPULSION
NEP systems engineering efforts in FY-92: Plans and status
[NASA-TM-105775] p 3588 N92-30308
Space transportation systems, launch systems, and propulsion for the Space Exploration Initiative: Results from Project Outreach
[NASA-CR-190345] p 3587 N92-30958

SPACECRAFT SHIELDING
Ablative shielding for hypervelocity projectiles
[NASA-CASE-MSC-21884-1] p 3602 N92-30539

SPACECRAFT STRUCTURES
Research and technology, 1991. Langley Research Center
[NASA-TM-4331] p 3744 N92-30733

SPACECRAFT TEMPERATURE
Progress in the development of the Hermes evaporators
[MBB-UO-0164-91-PUB] p 3587 N92-30440

SPACELAB
Development of and flight results from the Space Acceleration Measurement System (SAMS)
[NASA-TM-105652] p 3588 N92-30301

SPACERS
Design feasibility study of a Space Station Freedom truss
[NASA-TM-105558] p 3659 N92-30571
Designing, fabricating and testing cost effective structural composite for the SSCL magnets
[DE92-013469] p 3718 N92-30646

SPALLATION
Environment modelling in near Earth space: Preliminary LDEF results p 3588 N92-31225

SPATIAL DISTRIBUTION
Spatiotemporal characteristics of human visual localization
[AD-A248494] p 3687 N92-30325
Induced pictorial representations
[AD-A248560] p 3687 N92-30336

SPATIAL RESOLUTION
Initial laboratory evaluation of color video cameras
[DE92-010399] p 3637 N92-30822
A geodetic laser radar rangefinder with 10(exp -7) resolution p 3641 N92-31029

SPECIES DIFFUSION
Cu-Zn binary phase diagram and diffusion couples p 3600 N92-30269

SPECIFIC HEAT
Structure, processing, and properties of potatoes p 3611 N92-30288
Introductory heat-transfer p 3601 N92-30291
Thermal energy storage
[DE92-014942] p 3672 N92-31176

SPECIFICATIONS
Detecting potential synchronization constraint deadlocks from formal system specifications
[AD-A249019] p 3696 N92-30631

SPECIMENS
Development of hardness cycles for fiber bound materials, using DSC: From laboratory specimens to complex high duty structural members
[MBB-Z-0409-91-PUB] p 3592 N92-30969

SPECTRA
Non-holonomic filtration: Algebraic and geometric aspects of non-integrability
[PB92-178003] p 3706 N92-30790

SPECTRAL BANDS
Implementation scheme for recursion in spectral dimension
[AD-A248945] p 3695 N92-30629

SPECTRAL EMISSION
VUV production from a ferrite-driven flash-pumped system
[DE92-011362] p 3657 N92-30805

SPECTRAL RESOLUTION
Measurement of aerosol profiles using high-spectral-resolution Rayleigh-Mie lidar p 3644 N92-31046
Interferometers adaptations to lidars p 3645 N92-31052
Investigations on atomic-vapor-filter high-spectral-resolution lidar for temperature measurements p 3654 N92-31099

SPECTRAL SIGNATURES
Interpretation of optical remote sensing data over coastal waters
[BCRS-91-27] p 3667 N92-30472
A one-class classifier for identifying urban areas in remotely-sensed data
[DE92-013539] p 3667 N92-30704

SPECTROMETERS
Optical transducers for scintillating fiber readout
[DE92-015963] p 3721 N92-31187

SPECTROPHOTOMETRY
The origins of hot subdwarf stars p 3741 N92-30973

SPECTROSCOPIC ANALYSIS
Vibrational overtone spectroscopy of gaseous metallocenes
[AD-A251088] p 3593 N92-30245

SPECTROSCOPY
Vibrational overtone spectroscopy of gaseous metallocenes
[AD-A251088] p 3593 N92-30245
Studies of atmospheric molecules by multiphoton spectroscopy
[DE92-012668] p 3672 N92-30345
Combustion diagnostics by photo-deflection spectroscopy
[AD-A250802] p 3594 N92-30645
Fundamental studies of carbon, NH, and oxygen rings and other high energy density molecular systems
[AD-A246963] p 3715 N92-30680
Surface-mediated photocatalysis
[AD-A249906] p 3595 N92-30793
Resonance Raman spectroscopic studies of trans dioxorhenium(V)tetrapyridyl species
[AD-A249919] p 3595 N92-30875
Ellipsometric study of oxide films formed on LDEF metal samples
[AD-A249856] p 3599 N92-31110

SPECTRUM ANALYSIS
Hyperspectral gas analysis system (HyGAS), phase 1
[AD-A251026] p 3593 N92-30241
Theoretical study of phase-shifted quantum beats in time-resolved luminescence spectra from a biased asymmetric double quantum well
[AD-A252422] p 3710 N92-30549
Modeling of UV lines from cataclysmic variable winds
[DE92-013443] p 3739 N92-30862
Water vapor variance measurements using a Raman lidar p 3643 N92-31041
Pulsed laser spectral measurement using a Fabry-Perot interferometer: Limits to resolution p 3646 N92-31055

SPECULAR REFLECTION
Numerical simulation of crater formation heating by laser beam. Analysis of radiation exchanges in the cavity
[ESA-TT-1234] p 3657 N92-30997

SPEECH RECOGNITION
Modeling of video traffic in packet networks, low rate video compression, and the development of a lossy+lossless image compression algorithm
[NASA-CR-190546] p 3691 N92-30296

SPHERES
Heat flow of p-harmonic maps with values into spheres
[DE92-630236] p 3707 N92-31135

SPIN DYNAMICS
Theoretical studies in elementary particle physics
[DE92-015295] p 3714 N92-30610
Studies of ordering in semiconducting and other alloys
[AD-A249483] p 3728 N92-30634

SPIN EXCHANGE
High field optical-pumping spin-exchange polarized deuterium source
[DE92-010274] p 3657 N92-30848

SPINE
Adapting the ADAM manikin technology for injury probability assessment
[AD-A252332] p 3688 N92-30844

SPONTANEOUS EMISSION
Spontaneous emission from an atom in motion near an infinite conducting plane
[ITN-92-85169] p 3715 N92-30782

SPOT (FRENCH SATELLITE)
Technical and economic feasibility of integrated video service by satellite
[NASA-CR-189210] p 3614 N92-30300

SPREAD SPECTRUM TRANSMISSION
High frequency communications under adverse conditions
[AD-A252199] p 3615 N92-30532
Direct sequence spread spectrum CDMA in shared spectrum applications p 3619 N92-30939

SPUTTERING
Computer-controlled ion beam sputter-deposition of superconducting oxide films
[AD-A248495] p 3601 N92-30326
Review of high Z materials for PSI applications
[NIFS-152] p 3602 N92-30502
Evidence for the dependence of the sputter yield of graphite on ion bombardment fluence
[AD-A252500] p 3623 N92-30537
Study of Au(-) production in a plasma-sputter type negative ion source
[NIFS-115] p 3717 N92-30990

STABILITY
Numerical simulation of the electromagnetic instability of an intense beam in a quadrupole focusing system
[AD-A252275] p 3614 N92-30407
New insights into large eddy simulation
[AD-A249424] p 3635 N92-30775
The development of precipitated iron catalysts with improved stability
[DE92-014625] p 3596 N92-31006
Theoretical study of phase stability in Ni-Al and Ni-Ti alloys
[DE92-014776] p 3599 N92-31119
Stability of metallic superlattices
[DE92-011526] p 3600 N92-31124

STABILITY AUGMENTATION
Practical method's for robust multivariable control
[AD-A248473] p 3700 N92-30322

STABILITY TESTS
Nonlinear stability and control study of highly maneuverable high performance aircraft, phase 2
[NASA-CR-190667] p 3583 N92-30922
STABILIZATION
Stabilization of face-centered-cubic titanium
[DE92-011530] p 3600 N92-31125
STAINLESS STEELS
Solid lubrication of laser grown fluorinated diamond thin films
[AD-A249485] p 3603 N92-30635
Assessment of an improved multiaxial strength theory based on creep-rupture data for type 316 stainless steel
[DE92-010431] p 3663 N92-30823
Photodegradation effects in materials exposed to high flux solar and solar simulated radiation
[DE91-002147] p 3596 N92-30879
Investigation of joining techniques for advanced austenitic alloys
[DE92-015545] p 3599 N92-30888
Potassium Rankine cycle power conversion systems for lunar-Mars surface power
[DE92-015102] p 3589 N92-31012
STANDARDIZATION
Standard terminology in the laboratory and classroom
p 3610 N92-30277
The Pan-European Digital Cellular (GSM) System
p 3619 N92-30938
STANDARDS
Standard terminology in the laboratory and classroom
p 3610 N92-30277
The GKS input model in MANIFOLD
[CWI-CS-R9127] p 3699 N92-30696
Assessment of an improved multiaxial strength theory based on creep-rupture data for type 316 stainless steel
[DE92-010431] p 3663 N92-30823
Toward a North American standard for mobile data services p 3620 N92-30940
Optimum methods for the measurement of the absorption coefficients of materials
[BBC-RD-1992/3] p 3711 N92-31173
STAR FORMATION
Constraints on the putative companions to PSR1257+12 p 3738 N92-31232
STARS
TEM studies of a circumstellar rock
p 3736 N92-31223
STATISTICAL ANALYSIS
Statistical theory on reliability
[AD-A250809] p 3660 N92-30237
Regional-scale analysis and forecasting (RAP) report
[AD-A248384] p 3678 N92-30262
Statistics on aircraft gas turbine engine rotor failures that occurred in US commercial aviation during 1989
[DOT/FAA/CT-92/5] p 3581 N92-30303
Development statistics for the UH-1 Ada feasibility study
[AD-A252404] p 3584 N92-30547
Improvement of performance of variable probability sampling strategies
[PB92-180264] p 3707 N92-30562
Statistics for laminar flamelet modeling
p 3597 N92-30668
Event-scale relationships between surface velocity, temperature and chlorophyll in the coastal ocean, as seen by satellite
[NASA-CR-190266] p 3682 N92-30739
A statistical rationale for establishing process quality control limits using fixed sample size, for critical current verification of SSC superconducting wire
[DE92-014844] p 3661 N92-31120
A failure-to-restore unavailability model for periodically performed maintenance
[DE92-015902] p 3708 N92-31185
STATISTICAL CORRELATION
Variational method in the statistical theory of turbulent two-phase flows
[AD-A252263] p 3630 N92-30604
STATISTICAL DISTRIBUTIONS
The domain of attraction of the alpha-sum operator for type 2 and type 3 distributions
[REPT-92-02] p 3707 N92-30355
STEADY STATE
Adaptive multigrid applied to a bipolar transistor problem
[CWI-NM-R9115] p 3693 N92-30429
Finite difference time domain modeling of steady state scattering from jet engines with moving turbine blades
[NASA-CR-190290] p 3582 N92-30753
A steady state tokamak operation by use of magnetic monopoles
[DE92-799109] p 3725 N92-30991
STEELS
Nonlinear stress analysis of composite-jacketed steel cylinders subjected to high internal pressure
[AD-A249500] p 3663 N92-30802
Process modeling and development for three axisymmetric net shape forgings
[DE92-012111] p 3598 N92-30865
Recent improvements in size effects correlations for DBTT and upper shelf energy of ferritic steels
[DE92-014703] p 3599 N92-30877
STELLAR ATMOSPHERES
The origins of hot subdwarf stars
p 3741 N92-30973
FNAS: The magnetic configuration leading to solar flares
[NASA-CR-190522] p 3743 N92-31168
TEM studies of a circumstellar rock
p 3736 N92-31223
STELLAR CORES
Rapid cooling and structure of neutron stars
[DE92-015279] p 3740 N92-30609
STELLAR CORONAS
Heating and momentum deposition in hot stars
[DE92-011850] p 3740 N92-30855
STELLAR ENVELOPES
Twenty-Third Lunar and Planetary Science Conference
[NASA-CR-190178] p 3736 N92-31222
TEM studies of a circumstellar rock
p 3736 N92-31223
STELLAR EVOLUTION
Rapid cooling and structure of neutron stars
[DE92-015279] p 3740 N92-30609
The origins of hot subdwarf stars
p 3741 N92-30973
TEM studies of a circumstellar rock
p 3736 N92-31223
On the isotopic signature of recent solar-wind nitrogen
p 3738 N92-31231
STELLAR LUMINOSITY
The origins of hot subdwarf stars
p 3741 N92-30973
STELLAR MASS
The origins of hot subdwarf stars
p 3741 N92-30973
Nonlinear RR Lyrae models with new Livermore opacities
[DE92-011158] p 3741 N92-31108
Constraints on the putative companions to PSR1257+12 p 3738 N92-31232
STELLAR MASS EJECTION
Dynamics and energetics of the solar corona
[NASA-CR-190664] p 3742 N92-31162
STELLAR MODELS
Rapid cooling and structure of neutron stars
[DE92-015279] p 3740 N92-30609
Modeling of UV lines from cataclysmic variable winds
[DE92-013443] p 3739 N92-30862
Nonlinear RR Lyrae models with new Livermore opacities
[DE92-011158] p 3741 N92-31108
Solar neutrinos: Theoretical status
[DE92-014014] p 3743 N92-31199
STELLAR ORBITS
Carlsberg meridian catalogue La Palma. Number 5: Observations of positions of stars and planets: May 1988 to Dec. 1989
[ISBN-84-7469-052-8] p 3739 N92-30714
STELLAR PHYSICS
Activities report of the Institute for Astronomy and Astrophysics at Technical University of Berlin (Germany, F.R.)
[MITT-11] p 3740 N92-30506
STELLAR SPECTRA
Modeling of UV lines from cataclysmic variable winds
[DE92-013443] p 3739 N92-30862
STELLAR STRUCTURE
Rapid cooling and structure of neutron stars
[DE92-015279] p 3740 N92-30609
STELLAR TEMPERATURE
Heating and momentum deposition in hot stars
[DE92-011850] p 3740 N92-30855
STELLAR WINDS
Modeling of UV lines from cataclysmic variable winds
[DE92-013443] p 3739 N92-30862
STELLARATORS
Field line diversion properties of finite beta helias equilibria
[NIFS-137] p 3722 N92-30385
Three-dimensional MHD equilibrium in the presence of bootstrap current for Large Helical Device (LHD)
[NIFS-139] p 3725 N92-30994
Pressure profiles, resonant Pfirsch-Schlueter currents, thermal instabilities, and magnetic island formation
[DE92-015166] p 3726 N92-31002
STEREOSCOPY
CAESAR: Evaluation of the dual-look concept
[BCRS-91-10] p 3666 N92-30467
STIFFNESS
In-service evaluation of 2090 aluminum-lithium alloy on F/A-18 aircraft
[AD-A248472] p 3607 N92-30321
Relaxor ferroelectrics for electrostrictive transducer
[AD-A248671] p 3624 N92-30598
STIMULATED EMISSION
Ginsburg criterion for an equilibrium superradiant model in the dynamic approach
[DE92-630566] p 3732 N92-31203
STIRLING ENGINES
Magnetic bearings for free-piston Stirling engines
[NASA-TM-105730] p 3660 N92-30734
STOCHASTIC PROCESSES
Comparison of signal processing methods for estimation of network impedance for remote protection
[ETN-92-91686] p 3623 N92-30503
Can stochastic modelling and analysis of multistage interconnection networks lead to efficient usage of redundancy for fault-tolerant design?
[AD-A250635] p 3699 N92-30526
Research in stochastic analysis and its applications
[AD-A249482] p 3708 N92-30633
The role of stochasticity in sawtooth oscillation
[NIFS-103] p 3710 N92-30983
Stochastic strings, topology, and space-time confinement
[DE92-630239] p 3732 N92-31136
STOKES LAW OF RADIATION
Measurements of the backscattering phase matrices of crystal clouds with a polarization lidar
p 3651 N92-31083
STOPPING
Classifying termination of term rewriting
[RUU-CS-91-42] p 3693 N92-30444
STOVL AIRCRAFT
Preliminary dynamic tests of a flight-type ejector
[NASA-TM-105814] p 3582 N92-30998
STRAIN DISTRIBUTION
Isotropic thin-walled pressure vessel experiment
p 3611 N92-30284
Numerical analysis of the Iosipescu specimen for composite materials
[NASA-CR-190658] p 3592 N92-30906
Inter- and intra-plate deformation at North American plate boundaries
[NASA-CR-190485] p 3676 N92-30961
STRAIN RATE
Laboratory experiments from the toy store
p 3609 N92-30274
Creep and slow crack growth mechanisms related to macroscopic creep behavior of a silicon nitride ceramic at elevated temperatures
[DE92-015195] p 3663 N92-30567
Adapting the ADAM manikin technology for injury probability assessment
[AD-A252332] p 3688 N92-30844
Inter- and intra-plate deformation at North American plate boundaries
[NASA-CR-190485] p 3676 N92-30961
On the strain-rate dependence of dynamic recrystallization in copper polycrystals
[DE92-011363] p 3730 N92-31217
STRANGENESS
Rescattering in neutrino/antineutrino: Deuteron reactions
[NIKHEF-H/91-22] p 3713 N92-30364
Physics of the STAR experiment at the relativistic heavy ion collider
[DE92-014481] p 3719 N92-31198
STRATEGY
ILS, CE, CALS? From design to operation
[ETN-92-91717] p 3697 N92-30950
STRATOCUMULUS CLOUDS
Airborne lidar and radiometric observations of PBL- and low clouds p 3642 N92-31037
STRATOSPHERE
Tropospheric and stratospheric wind profiling with a direct detection Doppler lidar p 3639 N92-31018
A considerable effect of stratospheric aerosol on lidar-detected ozone profile and a three-wavelength inversion technique for both ozone and aerosol
p 3651 N92-31080
A portable lidar using a diode-pumped YAG laser
p 3654 N92-31098
STRATUS CLOUDS
Multiple scattering lidar returns from stratus clouds
p 3642 N92-31035
STREAK CAMERAS
A geodetic laser radar rangefinder with 10(exp -7) resolution p 3641 N92-31029
STRESS ANALYSIS
Finite element analysis of laminated composite axisymmetric solids. Volume 1: Theory and applications
[AD-A250808] p 3590 N92-30251

Stress-strain characteristics of rubber-like materials: Experiment and analysis p 3607 N92-30285
New transient and pseudo-transient algorithms for viscoelastic materials
[AD-A250642] p 3692 N92-30377
A dynamic subgrid-scale eddy viscosity model p 3630 N92-30649
Nonlinear stress analysis of composite-jacketed steel cylinders subjected to high internal pressure
[AD-A249500] p 3663 N92-30802

STRESS CONCENTRATION
FASTRAN-2: A fatigue crack growth structural analysis program
[NASA-TM-104159] p 3664 N92-30964

STRESS CORROSION CRACKING
Environmental fatigue of an Al-Li-Cu alloy. Part 2: Microscopic hydrogen cracking processes
[NASA-TM-107620] p 3664 N92-31214
Environmental fatigue of an Al-Li-Cu alloy. Part 3: Modeling of crack tip hydrogen damage
[NASA-TM-107619] p 3665 N92-31215

STRESS DISTRIBUTION
Isotropic thin-walled pressure vessel experiment p 3611 N92-30284
A shear sensitive monomer-polymer laminate structure and method of using same
[NASA-CASE-LAR-14654-1] p 3662 N92-30317
Linear elastic fracture mechanics primer
[NASA-TM-103591] p 3662 N92-30416
Cross sectional constants and stress distributions of thin-walled sections
[AD-A249886] p 3663 N92-30870
Numerical analysis of the Iosipescu specimen for composite materials
[NASA-CR-190658] p 3592 N92-30906

STRESS FUNCTIONS
Thermal stress evaluation of a symmetrically laminated composite plate
[AD-A249450] p 3591 N92-30641

STRESS INTENSITY FACTORS
A boundary element alternating method for two-dimensional mixed-mode fracture problems
[NASA-CR-4460] p 3661 N92-30309
Linear elastic fracture mechanics primer
[NASA-TM-103591] p 3662 N92-30416
FASTRAN-2: A fatigue crack growth structural analysis program
[NASA-TM-104159] p 3664 N92-30964

STRESS PROPAGATION
Investigation of the interface phenomena due to interaction of high intensity stress waves with geologic boundaries
[AD-A248992] p 3675 N92-30525
Wave propagation and vibration of fibre-reinforced laminates
[AD-A252101] p 3590 N92-30528

STRESS-STRAIN RELATIONSHIPS
Finite element analysis of laminated composite axisymmetric solids. Volume 1: Theory and applications
[AD-A250808] p 3590 N92-30251
Isotropic thin-walled pressure vessel experiment p 3611 N92-30284
Stress-strain characteristics of rubber-like materials: Experiment and analysis p 3607 N92-30285
Analytical solution of elastic-plastic thick-walled cylinders with general hardening
[AD-A249491] p 3705 N92-30618
On the strain-rate dependence of dynamic recrystallization in copper polycrystals
[DE92-011363] p 3730 N92-31217

STRESS-STRAIN-TIME RELATIONS
Investigation of the interface phenomena due to interaction of high intensity stress waves with geologic boundaries
[AD-A248992] p 3675 N92-30525

STRESSES
Designing, engineering, and testing wood structures p 3593 N92-30270
On recrystallization in metal matrix composites
[DE92-011364] p 3590 N92-30521
In situ TEM studies of the effect of misfit strain on the kinetics of Si(sub 1-x)Ge(sub x) solid phase epitaxy: Temperature calibration and surface effects
[DE92-011689] p 3728 N92-30574

STRING THEORY
Stochastic strings, topology, and space-time confinement
[DE92-630239] p 3732 N92-31136

STRIP TRANSMISSION LINES
Tunable relay box (design and testing) p 3718 N92-30727

STROBOSCOPES
A stroboscopic technique for using CCD cameras in flow visualization systems for continuous viewing and stop action photography
[NASA-TM-107648] p 3637 N92-30737

STRUCTURAL ANALYSIS
National Educators' Workshop: Update 1991. Standard Experiments in Engineering Materials Science and Technology
[NASA-CP-3151] p 3608 N92-30263
Multidisciplinary optimization of fiber composite aircraft structures
[MBB/FW321/S/PUB/476] p 3579 N92-30424
Design feasibility study of a Space Station Freedom truss
[NASA-TM-105558] p 3659 N92-30571
Continuous wavelet analysis of coherent structures p 3634 N92-30673
Metal matrix composite analyzer (METCAN) user's manual, version 4.0
[NASA-TM-105244] p 3592 N92-30779
Cross sectional constants and stress distributions of thin-walled sections
[AD-A249886] p 3663 N92-30870
Structural and magnetic properties of RBa2Cu2NbO8 (R = La, Pr, and Nd)
[DE92-014780] p 3729 N92-30885
FASTRAN-2: A fatigue crack growth structural analysis program
[NASA-TM-104159] p 3664 N92-30964

STRUCTURAL DESIGN
Modeling and analysis methodology for aeroelastically tailored chordwise deformable wings
[NASA-CR-189620] p 3579 N92-30304
The diffraction of short free surface water waves, a uniform expansion
[REPT-92-06] p 3628 N92-30358
MBB-LAGRANGE: A general structural reliability and optimization structural system
[MBB/FW321/S/PUB/467] p 3662 N92-30423
Multidisciplinary optimization of fiber composite aircraft structures
[MBB/FW321/S/PUB/476] p 3579 N92-30424
Composite beam analysis linear analysis of naturally curved and twisted anisotropic beams
[AD-A252652] p 3663 N92-30766
Mechanical behavior and processing of aluminum metal matrix composites
[AD-A249918] p 3592 N92-30874
Vortex flow aerodynamics
[AGARD-AR-299] p 3576 N92-30947
FASTRAN-2: A fatigue crack growth structural analysis program
[NASA-TM-104159] p 3664 N92-30964

STRUCTURAL ENGINEERING
Designing, engineering, and testing wood structures p 3593 N92-30270

STRUCTURAL MEMBERS
Development of hardness cycles for fiber bound materials, using DSC: From laboratory specimens to complex high duty structural members
[MBB-Z-0409-91-PUB] p 3592 N92-30969

STRUCTURAL RELIABILITY
Center for Composites Manufacturing Science, Reliability, and Maintainability Technology
[AD-A248661] p 3591 N92-30639

STRUCTURAL STABILITY
The optimization of force inputs for active structural acoustic control using a neural network
[NASA-TM-107627] p 3711 N92-30979

STRUCTURAL VIBRATION
Prediction of coincidence frequencies for a thin-walled, fluid-filled pipe
[MRL-TN-600] p 3664 N92-30963
Acoustic fatigue life prediction for nonlinear structures with multiple resonant modes
[NASA-CR-190471] p 3664 N92-30988

STUDENTS
Elementary metallography p 3600 N92-30266
Computer vision in microstructural analysis p 3609 N92-30271
Experiments with the low melting indium-bismuth alloy system p 3601 N92-30272
A senior manufacturing laboratory for determining injection molding process capability p 3609 N92-30273
Laboratory experiments from the toy store p 3609 N92-30274
Be-Cu precipitation hardening experiment p 3601 N92-30276
Science in action: An interdisciplinary science education program p 3610 N92-30278
Determining significant material properties: A discovery approach p 3607 N92-30279

SUBARCTIC REGIONS
Ice thickness observations, North American Arctic and subarctic, 1972-1973 and 1973-1974, part 8
[AD-A250830] p 3681 N92-30238

SUBDUCTION (GEOLOGY)
Is the Venusian lithosphere subducting? p 3738 N92-31234

SUBDWARF STARS
The origins of hot subdwarf stars p 3741 N92-30973

SUBLIMATION
Numerical simulation of crater formation heating by laser beam. Analysis of radiation exchanges in the cavity
[ESA-TT-1234] p 3657 N92-30997

SUBMERGED BODIES
Thrust test fixture
[AD-D015259] p 3585 N92-31192

SUBMINIATURIZATION
Quantum transport, noise and non-linear dissipative effects in one- and two-dimensional systems and associated sub-micron and nanostructure devices
[AD-A250895] p 3627 N92-31210

SUBREFLECTORS
Double-loop frequency-selected surfaces for multifrequency division multiplexing in a dual-reflector antenna
[NASA-CASE-NPO-18701-1-CU] p 3614 N92-30391

SUBSONIC FLOW
Extension of the integral equation formulation of linearized time dependent subsonic flow
[AD-A250654] p 3577 N92-31171

SUBSONIC SPEED
Preliminary subsonic aerodynamic model for simulation studies of the HL-20 lifting body
[NASA-TM-4302] p 3583 N92-31175

SUBSTRATES
Research on polycrystalline thin film submodules based on CuInSe2 materials
[DE92-010584] p 3727 N92-30247
A method of making a single layer multi-color luminescent display
[NASA-CASE-LAR-14811-1] p 3622 N92-30389
YBa2Cu(3-x)Co(x)O(y): A substrate material for YBCO superconductors
[DE92-015182] p 3730 N92-30999

SULFUR DIOXIDES
Status of selected air pollution control programs, February 1992
[PB92-171966] p 3673 N92-30561
Towards the development of a global inventory for black carbon emissions
[DE92-013514] p 3674 N92-30647

SULFURIC ACID
Temperature effect on the Langmuir-Blodgett polymerization of 2-pentadecylaniline
[AD-A250803] p 3601 N92-30250
Ultrafine aerosol size distributions and sulfuric acid vapor pressures: Implications for new particle formation in the atmosphere
[DE92-015217] p 3675 N92-31183

SUN
Heating and momentum deposition in hot stars
[DE92-011850] p 3740 N92-30855
On the isotopic signature of recent solar-wind nitrogen p 3738 N92-31231

SUPERCOMPUTERS
Three-dimensional shock wave physics simulations on massively parallel supercomputers
[DE92-008679] p 3698 N92-30363
Scalable parallel molecular dynamics on MIMD supercomputers
[DE92-015041] p 3698 N92-30401
Monte Carlo particle simulation of low-density fluid flow on MIMD supercomputers
[DE92-014618] p 3630 N92-30807

SUPERCONDUCTING FILMS
Computer-controlled ion beam sputter-deposition of superconducting oxide films
[AD-A248495] p 3601 N92-30326
Disorder and transport in highly correlated systems
[AD-A249969] p 3710 N92-30850
Pulsed microwave processing of high-T(sub c) superconducting films
[DE92-014950] p 3730 N92-31000
Proceedings, phenomenology and applications of high temperature superconductors
[DE92-011133] p 3627 N92-31107

SUPERCONDUCTING MAGNETS
Magnetic field measurements of Fermilab/General Dynamics built full scale SSC collider dipole magnets
[DE92-014612] p 3717 N92-30589
Designing, fabricating and testing cost effective structural composite for the SSCL magnets
[DE92-013469] p 3718 N92-30646
Magnetic measurement instrumentation developments at the SSC
[DE92-013969] p 3718 N92-30786
Emittance growth caused by magnet vibrations in SSC
[DE92-014186] p 3719 N92-30881

SUPERCONDUCTING SUPER COLLIDER
Magnetic field measurements of Fermilab/General Dynamics built full scale SSC collider dipole magnets
[DE92-014612] p 3717 N92-30589

Designing, fabricating and testing cost effective structural composite for the SSCL magnets
[DE92-013469] p 3718 N92-30646
Magnetic measurement instrumentation developments at the SSC
[DE92-013969] p 3718 N92-30786
Application of superconducting cavities to the collider rings of the SSC
[DE92-011692] p 3718 N92-30811
Conceptual design of the SSC cryogenic transfer lines
[DE92-013964] p 3719 N92-30839
A dynamic model for beam tube vacuum effects on the SSC cryogenic system
[DE92-013967] p 3719 N92-30840
Emittance growth caused by magnet vibrations in SSC
[DE92-014186] p 3719 N92-30881
Mechanical design and finite element analysis of the SDC central calorimeter
[DE92-011197] p 3655 N92-31109
A statistical rationale for establishing process quality control limits using fixed sample size, for critical current verification of SSC superconducting wire
[DE92-014844] p 3661 N92-31120

SUPERCONDUCTIVITY
Superconductivity and magnetism in rapidly solidified perovskites
[DE92-014081] p 3597 N92-30588
First-principles computational studies of alkali-doped C60 fullerides
[AD-A249018] p 3624 N92-30630
Fabrication of multifilament conductors: CVD processing of high Tc superconducting composite fibers
[NASA-CR-184344] p 3591 N92-30711
Application of superconducting cavities to the collider rings of the SSC
[DE92-011692] p 3718 N92-30811
Fine scale mesostructures in superconducting and other materials
[DE92-015207] p 3730 N92-31200

SUPERCONDUCTORS
Superconductivity and magnetism in rapidly solidified perovskites
[DE92-014081] p 3597 N92-30588
First-principles computational studies of alkali-doped C60 fullerides
[AD-A249018] p 3624 N92-30630
Disorder and transport in highly correlated systems
[AD-A249969] p 3710 N92-30850
A study of enhancing critical current densities (J(sub c)) and critical temperature (T(sub c)) of high-temperature superconductors
[NASA-TM-103595] p 3627 N92-30902
A statistical rationale for establishing process quality control limits using fixed sample size, for critical current verification of SSC superconducting wire
[DE92-014844] p 3661 N92-31120
Fine scale mesostructures in superconducting and other materials
[DE92-015207] p 3730 N92-31200

SUPERCRITICAL FLUIDS
Supercritical fluid extraction: A new process for producing high-performance, low-cost carbon fibers
[AD-A249407] p 3595 N92-30773

SUPERFLUIDITY
Constraints on the nuclear matter equation of state from pulsar glitches
[DE92-015142] p 3740 N92-30578
Rapid cooling and structure of neutron stars
[DE92-015279] p 3740 N92-30609

SUPERHIGH FREQUENCIES
The ACTS multibeam antenna
[NASA-TM-105645] p 3587 N92-30383
Radiation, scattering, and guidance of electromagnetic fields by arbitrarily shaped structures embedded in layered dielectric media
[AD-A252621] p 3615 N92-30408
Software breadboard study
[NASA-CR-190473] p 3625 N92-30757
Multifrequency measurements of radar ground clutter at 42 sites. Volume 3: Appendix E
[AD-A246988] p 3616 N92-30863
An integrated Ka/Ku-band payload for personal, mobile and private business communications
p 3619 N92-30933

SUPERLATTICES
Enhancement of weak localization in a Si lateral superlattice device p 3625 N92-30732
Disorder and transport in highly correlated systems
[AD-A249969] p 3710 N92-30850
Stability of metallic superlattices
[DE92-011526] p 3600 N92-31124

SUPERSONIC COMBUSTION
Turbulent reacting flows and supersonic combustion
[AD-A251065] p 3593 N92-30256

SUPERSONIC FLOW
Turbulent reacting flows and supersonic combustion
[AD-A251065] p 3593 N92-30256

SUPERSONIC JET FLOW
Resonant instability of supersonic shear layers
p 3632 N92-30661

SUPERSONIC SPEED
Navier-Stokes computations of a viscous optimized waverider
[NASA-CR-189658] p 3574 N92-30392

SUPERSONIC TRANSPORTS
A new unsteady mixing model to predict NO(x) production during rapid mixing in a dual-stage combustor
[NASA-CR-189155] p 3581 N92-30569
High-speed civil transport issues and technology program
[NASA-CR-186020] p 3580 N92-31208

SUPERSYMMETRY
From a world-sheet supersymmetry to the Dirac equation
[DE92-622375] p 3731 N92-30799
From a particle with a world-line supersymmetry to the Dirac-like equation
[DE92-622376] p 3731 N92-30800
Theoretical particle physics
[DE92-014531] p 3716 N92-30841

SUPPORT SYSTEMS
Adoption of the LSA S/W DILSA for the Columbus LSA tasks
[MBB-UO-0168-91-PUB] p 3709 N92-30420
Scale sensitivity and rank preservation in a multiplicative variant of the AHP and SMART
[REPT-91-67] p 3707 N92-30452
DE-CERTS: A decision support system for a comparative evaluation method for risk management methodologies and tools
[AD-A246965] p 3733 N92-30682

SURFACE GEOMETRY
Wrappability of curves on surfaces
[AD-A250004] p 3707 N92-31140

SURFACE PROPERTIES
Full surface testing of grazing incidence mirrors
[AD-A248851] p 3719 N92-30233
Study of the surface properties of ceramic materials by chromatography
[DE92-011129] p 3604 N92-30695
Surface-mediated photocatalysis
[AD-A249906] p 3595 N92-30793
Vector analysis of ice fabric data
[AD-A250832] p 3682 N92-30832
High resolution electron energy loss studies of surface vibrations
[DE92-014608] p 3626 N92-30901

SURFACE REACTIONS
Magnetic surface breaking in 3D MHD equilibria of I = 2 heliotron
[NIFS-130] p 3722 N92-30384
Interaction of atomic hydrogen with the surface methyl group on Si(100): Removal of surface carbon
[AD-A249062] p 3595 N92-30821

SURFACE ROUGHNESS
Evidence for the dependence of the sputter yield of graphite on ion bombardment fluence
[AD-A252500] p 3623 N92-30537
Diffuse neutron scattering signatures of rough films
[DE92-015208] p 3717 N92-31201

SURFACE TEMPERATURE
Mixed and forced convection from an array of discrete heat sources in a vertical channel
[AD-A248853] p 3731 N92-30235
Event-scale relationships between surface velocity, temperature and chlorophyll in the coastal ocean, as seen by satellite
[NASA-CR-190266] p 3682 N92-30739

SURFACE TREATMENT
Laser induced reaction for pre-bond surface preparation of aluminum alloys
[AD-A249916] p 3598 N92-30872

SURFACE WATER
Duration and rates of discharge: Maja Valles, Mars
p 3737 N92-31227

SURFACE WAVES
The diffraction of short free surface water waves, a uniform expansion
[REPT-92-06] p 3628 N92-30358

SURVEILLANCE
A failure-to-restore unavailability model for periodically performed maintenance
[DE92-015902] p 3708 N92-31185
National airspace system. Air defense and law enforcement surveillance operational concept NAS-SR-135
[DOT/FAA/SE-92/3] p 3579 N92-31211

SURVEILLANCE RADAR
The rise of active-element phased-array radar
[RAND-P-7747-RGS] p 3616 N92-30755
Foreign surveillance radar upgrade analysis
[AD-A249440] p 3616 N92-30760

SURVEYS
Oceanic CO2 measurements for the WOCE hydrographic survey in the Pacific Ocean, 1990-1991: Shore based analyses during legs 1-3
[DE92-013064] p 3682 N92-30861
Attitudinal and situational differences between national laboratory inventors and inventor-entrepreneurs
[DE92-015768] p 3733 N92-30889
Remote-sensing survey of the Atchafalaya Basin Main Channel, Atchafalaya Channel training project, Saints Martin and Mary Parishes, Louisiana
[AD-A249915] p 3669 N92-31139

SWITCHES
Nonequilibrium behavior of carriers in semiconductors subjected to strong space-time varying fields
[AD-A246961] p 3624 N92-30678

SWITCHING
Vibrationally induced rotational axis switching: A novel mechanism for vibrational mode-coupling
[AD-A251085] p 3712 N92-30259
A new class of ferroelectric polymers: The odd-numbered nylons
[AD-A252268] p 3603 N92-30594

SWITCHING THEORY
Configuration algorithms for hierarchical supernode machines
[IMAG-RR-853-I] p 3694 N92-30493

SYMMETRY
Scale symmetry of quantum solitons
[DE92-624560] p 3712 N92-30331
Some model theory of free groups and free algebras
[AD-A249425] p 3706 N92-30776

SYNAPSES
The properties of the uptake system for glycine in synaptic vesicles
[ISSN-0800-4412] p 3683 N92-31152

SYNCHRONISM
Detecting potential synchronization constraint deadlocks from formal system specifications
[AD-A249019] p 3696 N92-30631
An extension to Schneider's general paradigm for fault-tolerant clock synchronization
[NASA-TM-107634] p 3699 N92-30677
Verifying the interactive convergence clock synchronization algorithm using the Boyer-Moore theorem prover
[NASA-CR-189649] p 3700 N92-31158

SYNCHRONIZED OSCILLATORS
Mathematical models of non-linear mechanical and electrical systems and their qualitative behavior
[AD-A248847] p 3622 N92-30249

SYNCHRONOUS PLATFORMS
A conceptual design of a large aperture microwave radiometer geostationary platform
[NASA-TM-107577] p 3588 N92-30736
SHARP system for personal communications
p 3618 N92-30931

SYNCHROTRONS
Effects of high beam rates on TPC's
[DE92-014594] p 3717 N92-30398
Recent experimental studies on hadron showers produced in high energy muon-nucleus interactions
[DE92-016002] p 3719 N92-31219

SYNTAX
A formal transformation from the BSI/VDM-SL concrete syntax to the core abstract syntax
[REPT-92-07] p 3692 N92-30359
Proceedings of the Sylvia Beach Language Comprehension Conference
[AD-A250488] p 3621 N92-31129

SYNTHESIS (CHEMISTRY)
Synthesis and reactivity of 1-methyl-e-ethynylpyridinium triflate
[AD-A250638] p 3602 N92-30346
Template-synthesis: A method for enhancing the ionic and electronic conductivity in electronically conductive polymers
[AD-A248806] p 3603 N92-30553
Infrared investigations of pristine, doped and partially-doped polypyrrole
[AD-A250644] p 3605 N92-30838
Computational simulation of diamond chemical vapor deposition in premixed C2H2/O2/H2 and CH4/O2 strained flames
[DE92-012144] p 3606 N92-30857
Synthesis of cresols and xylenols from benzene and methanol
[DE91-002143] p 3596 N92-30882
Methane to liquid
[DE92-001277] p 3596 N92-30883
A novel process for methanol synthesis
[DE92-015798] p 3608 N92-30904

The development of precipitated iron catalysts with improved stability
[DE92-014625] p 3596 N92-31006
A method for the production of weakly acidic cation exchange resins
[DE92-015314] p 3717 N92-31137
A method for production of new anion exchangers
[DE92-015313] p 3717 N92-31147
Proceedings of the 181st Electrochemical Society, Inc. Meeting Program
[AD-A249729] p 3596 N92-31178
Polyphosphazenes bearing polymerizable pyrrole, thiophene and furan side groups: Synthesis and chemical oxidation
[AD-A249747] p 3607 N92-31207

SYNTHETIC APERTURE RADAR
Results of the 1989 experiment with a polarimetric multifrequency SAR
[BCRS-91-33] p 3614 N92-30361

SYNTHETIC FIBERS
Ni-H2 cell separator matrix engineering
[NASA-CR-190055] p 3671 N92-30949

SYSTEM IDENTIFICATION
A simplified dynamic model of the T700 turboshaft engine
[NASA-TM-105805] p 3709 N92-30898

SYSTEMS ANALYSIS
Adoption of the LSA S/W DILSA for the Columbus LSA tasks
[MBB-UO-0168-91-PUB] p 3709 N92-30420
Classifying termination of term rewriting
[RUU-CS-91-42] p 3693 N92-30444
Pairwise comparison of concessions in negotiation processes
[REPT-92-15] p 3733 N92-30463
Informatization in public administration (EGPA-research project 1991). Large scale information systems in The Netherlands
[REPT-91-92] p 3734 N92-30486
The evolving data dictionary
[AD-A249030] p 3735 N92-30819
Multifractal analysis of chaotic point sets
[AD-A250756] p 3709 N92-31194

SYSTEMS ENGINEERING
Model analysis and expert system development for planning and scheduling teleoperations for aircraft turnaround functions. Volume 2: Top user's guide
[AD-A251083] p 3573 N92-30258
A program of continuing research on representing, manipulating, and reasoning about physical objects
[AD-A251089] p 3691 N92-30260
Survivable algorithms and redundancy management in NASA's distributed computing systems
[NASA-CR-189827] p 3691 N92-30299
NEP systems engineering efforts in FY-92: Plans and status
[NASA-TM-105775] p 3588 N92-30308
A model of the ADA avionics real-time system: An example of the benefits of the hardware/software codesign approach in development of real-time systems
[AD-A248893] p 3581 N92-30524
Can stochastic modelling and analysis of multistage interconnection networks lead to efficient usage of redundancy for fault-tolerant design?
[AD-A250635] p 3699 N92-30526
Introduction to human factors and wide area networking
[AD-A252310] p 3688 N92-30718
Tunable relay box (design and testing)
p 3718 N92-30727
Electric Vehicle Site Operator Program
[DE92-014591] p 3626 N92-30842
Ka-band mobile and personal systems development at JPL p 3618 N92-30928
Direct broadcast satellite-radio: Portable and mobile reception trade-offs p 3621 N92-30945
Concurrent engineering p 3697 N92-30952

SYSTEMS INTEGRATION
Computer integrated laboratory testing
p 3611 N92-30289
Beam technologies for integrated processing
[AD-A252647] p 3612 N92-30411
Integration mockup and process material management system
[NASA-CR-184319] p 3613 N92-30754
Issues for the integration of satellite and terrestrial cellular networks for mobile communications
p 3620 N92-30941
Practical application of the ILS: Practical integration, design, and logistics p 3697 N92-30955

SYSTEMS MANAGEMENT
The effect of information systems on middle management in the aerospace industry: The Westco case
[AD-A249017] p 3735 N92-30584

SYSTEMS SIMULATION
Development environment for digital simulation models of multibody systems
[NLR-TP-89327-U] p 3693 N92-30476
High level synthesis of controlpath microarchitectures
[MEMO-INF-91-86] p 3690 N92-30698
A dynamic model for beam tube vacuum effects on the SSC cryogenic system
[DE92-013967] p 3719 N92-30840

T

TANTALUM ALLOYS
Potassium Rankine cycle power conversion systems for lunar-Mars surface power
[DE92-015102] p 3589 N92-31012

TARGET ACQUISITION
Maximum likelihood detection of electro-optic moving targets
[AD-A249442] p 3616 N92-30762
TRAC performance estimates
[NASA-CR-190530] p 3701 N92-30778

TARGET RECOGNITION
TRAC performance estimates
[NASA-CR-190530] p 3701 N92-30778

TARGETS
Alignment of a 3-D sensor and a 2-D sensor measuring azimuth and elevation
[AD-A252120] p 3636 N92-30530
Maximum likelihood detection of electro-optic moving targets
[AD-A249442] p 3616 N92-30762

TASKS
Compression planning for continuous improvement in quality programs
[DE92-012331] p 3732 N92-30349
Operations and logistics tasks in the Columbus development program
[MBB-UO-0166-91-PUB] p 3708 N92-30419

TAYLOR INSTABILITY
The Rayleigh-Taylor instability in an expanding plasma
[DE92-013883] p 3725 N92-30884

TEA LASERS
A compact high repetition rate CO2 coherent Doppler lidar p 3639 N92-31022

TECHNICAL WRITING
Reviewing the technical report
[AD-A249494] p 3735 N92-30636

TECHNOLOGIES
Soviet applied information sciences in a time of change
[PB92-173020] p 3734 N92-30509

TECHNOLOGY ASSESSMENT
Structural ceramics p 3607 N92-30264
Technical and economic feasibility of integrated video service by satellite
[NASA-CR-189210] p 3614 N92-30300
NEP systems engineering efforts in FY-92: Plans and status
[NASA-TM-105775] p 3588 N92-30308
The Eurofar program: An European overview on advanced VTOL civil transportation system
[MBB-UD-0611-91-PUB] p 3578 N92-30418
Wiring for aerospace applications
[NASA-TM-105777] p 3623 N92-30427
Soviet applied information sciences in a time of change
[PB92-173020] p 3734 N92-30509
Grand challenges 1993: High performance computing and communications. A report by the Committee on Physical, Mathematical, and Engineering Sciences to supplement the President's fiscal year 1993 budget
[PB92-160530] p 3689 N92-30600
Report of the Great Lakes Air Toxics Research Priorities Workshop
[PB92-166933] p 3673 N92-30602
Numerical optimization in Germany: A non-exhaustive survey on current activities with emphasis on aeronautics
[MBB/FE211/S/PUB/474] p 3573 N92-30675
Hubble Space Telescope. Update: 18 months in orbit
[NASA-TM-107962] p 3739 N92-30686
Nondestructive testing of ceramics for vehicular advanced heat engines
[DE92-010471] p 3604 N92-30744
Technical evaluation report on the Flight Mechanics Panel Symposium on Piloted Simulation Effectiveness
[AGARD-AR-315] p 3584 N92-30769
The status of renewable energy technology
[DE92-011386] p 3670 N92-30808
Adapting the ADAM manikin technology for injury probability assessment
[AD-A252332] p 3688 N92-30844
Cellular: Toward personal communications
p 3619 N92-30936
Introduction to the efficiency of fuel cells
[MBB-Z-0412-91-PUB] p 3671 N92-30970
Emerging solid-state laser technology by lidar/DIAL remote sensing p 3653 N92-31095
Advanced electromagnetic methods for aerospace vehicles
[NASA-CR-190650] p 3621 N92-31156
Trends in aeropropulsion research and their impact on engineering education
[NASA-TM-105682] p 3583 N92-31172

TECHNOLOGY TRANSFER
Spinoffs from R and D investments
[DE92-014450] p 3736 N92-30575
Proceedings of a Beryllium Technology Workshop
[DE92-012312] p 3598 N92-30834
Dense fog on the highway: Visual range monitoring in cars? p 3655 N92-31106

TECHNOLOGY UTILIZATION
Concurrent engineering p 3697 N92-30952
Demonstration of a 3D vision algorithm for space applications
[NASA-CR-190646] p 3698 N92-31154

TECTONICS
A study of discrete and continuum joint modeling techniques
[DE92-012631] p 3663 N92-30859
A geodetic laser radar rangefinder with 10(exp -7) resolution p 3641 N92-31029
The thermal engine of Venus: Implications from the impact crater distribution p 3738 N92-31233
Is the Venusian lithosphere subducting?
p 3738 N92-31234

TELECOMMUNICATION
Proceedings of the Workshop on Advanced Network and Technology Concepts for Mobile, Micro, and Personal Communications
[NASA-CR-190459] p 3617 N92-30923
Leo satellite-based telecommunication network concepts p 3617 N92-30926

TELEMETRY
Bandwidth efficient CCSDS coding standard proposals
[NASA-CR-190317] p 3587 N92-30709

TELEOPERATORS
Model analysis and expert system development for planning and scheduling teleoperations for aircraft turnaround functions, volume 1
[AD-A251037] p 3573 N92-30253
Model analysis and expert system development for planning and scheduling teleoperations for aircraft turnaround functions. Volume 2: Top user's guide
[AD-A251083] p 3573 N92-30258

TELEPHONES
Issues for the integration of satellite and terrestrial cellular networks for mobile communications
p 3620 N92-30941
National transportable telecommunications capability
p 3620 N92-30943

TELESCOPES
Doppler lidar wind measurement with the edge technique p 3638 N92-31017
Fluorescence lidar multi-color imaging of vegetation
p 3640 N92-31028
Conically scanned lidar telescope using holographic optical elements p 3645 N92-31050
Lidar measurements using large liquid mirror telescopes p 3652 N92-31087
Generation of a sodium guidestar using a high power dye laser
[DE92-012696] p 3657 N92-31115

TELEVISION SYSTEMS
Demonstration of magnetic domain boundary movement using an easily assembled videocam-microscope system
p 3611 N92-30286

TEMPERATE REGIONS
The calculation of mid-latitude meridional neutral winds from an improved servo model approximation method
[AD-A249874] p 3676 N92-30868

TEMPERATURE CONTROL
Ni-H2 cell separator matrix engineering
[NASA-CR-190055] p 3671 N92-30949

TEMPERATURE DEPENDENCE
On the temperature role in the tunneling process at the cold fusion
[DE92-627497] p 3727 N92-30405
Coefficients of the second viscosity in bulk liquid helium
[AD-A252421] p 3629 N92-30548
Thermal stress evaluation of a symmetrically laminated composite plate
[AD-A249450] p 3591 N92-30641
The temperature dependence of a large dynamic range photodetector structure
[AD-A247667] p 3624 N92-30683
Temperature dependence of universal conductance fluctuations in narrow Si inversion layers
p 3625 N92-30730

The properties of the uptake system for glycine in synaptic vesicles
[ISSN-0800-4412] p 3683 N92-31152
Ultrafine aerosol size distributions and sulfuric acid vapor pressures: Implications for new particle formation in the atmosphere
[DE92-015217] p 3675 N92-31183
Fine scale mesostructures in superconducting and other materials
[DE92-015207] p 3730 N92-31200

TEMPERATURE EFFECTS
Temperature effect on the Langmuir-Blodgett polymerization of 2-pentadecylaniline
[AD-A250803] p 3601 N92-30250
Comparison of high temperature, high frequency core loss and dynamic B-H loops of a 2V-49Fe-49Co and a grain oriented 3Si-Fe alloy
[NASA-TM-105791] p 3623 N92-30397
Recombining processes in a cooling plasma by mixing of initially heated gas
[NIFS-142] p 3722 N92-30431
Modelling of heavily loaded lubricated contacts
[AD-A248807] p 3659 N92-30554
Metal matrix composite analyzer (METCAN) user's manual, version 4.0
[NASA-TM-105244] p 3592 N92-30779
Testing of double-layer capacitors for high reliability applications
[DE92-011384] p 3626 N92-30807
Isothermal aging effects on PMR-15 resin
[NASA-TM-105648] p 3593 N92-30986

TEMPERATURE MEASUREMENT
Mixed and forced convection from an array of discrete heat sources in a vertical channel
[AD-A248853] p 3731 N92-30235
In situ TEM studies of the effect of misfit strain on the kinetics of Si(sub 1-x)Ge(sub x) solid phase epitaxy: Temperature calibration and surface effects
[DE92-011689] p 3728 N92-30574
Combustion diagnostics by photo-deflection spectroscopy
[AD-A250802] p 3594 N92-30645
Repetitive High Energy Pulsed Power (RHEPP) temperature monitoring system utilizing Luxtron fluoroptic sensors and thermocouples technical reference manual
[DE92-013461] p 3637 N92-30893
An alexandrite regenerative amplifier for water vapor and temperature measurements p 3645 N92-31048
Wavemeter measurements of frequency stability of an injection seeded alexandrite laser for pressure and temperature lidar p 3645 N92-31049
BELINDA: Broadband Emission Lidar with Narrowband Determination of Absorption. A new concept for measuring water vapor and temperature profiles p 3653 N92-31091
Investigations on atomic-vapor-filter high-spectral-resolution lidar for temperature measurements p 3654 N92-31099

TEMPERATURE PROFILES
BELINDA: Broadband Emission Lidar with Narrowband Determination of Absorption. A new concept for measuring water vapor and temperature profiles p 3653 N92-31091

TEMPERING
Tempered glass and thermal shock of ceramic materials p 3607 N92-30265

TEMPLATES
Template-synthesis: A method for enhancing the ionic and electronic conductivity in electronically conductive polymers
[AD-A248806] p 3603 N92-30553

TEMPORAL DISTRIBUTION
Spatiotemporal characteristics of human visual localization
[AD-A248494] p 3687 N92-30325
Event-scale relationships between surface velocity, temperature and chlorophyll in the coastal ocean, as seen by satellite
[NASA-CR-190266] p 3682 N92-30739

TENSILE CREEP
Filler metal development for Hastelloy alloy XR
[DE92-782044] p 3600 N92-31163

TENSILE STRENGTH
Effect of bending on the room-temperature tensile strengths of structural ceramics
[DE92-015196] p 3603 N92-30626

TENSILE TESTS
Stress-strain characteristics of rubber-like materials: Experiment and analysis p 3607 N92-30285
Mechanical properties of brittle materials p 3612 N92-30290
Effect of bending on the room-temperature tensile strengths of structural ceramics
[DE92-015196] p 3603 N92-30626
Assessment of an improved multiaxial strength theory based on creep-rupture data for type 316 stainless steel
[DE92-010431] p 3663 N92-30823

TENSORS
Finite volume discretization of the incompressible Navier-Stokes equations in general coordinates on staggered grids
[REPT-91-71] p 3628 N92-30373
Finite volume discretization of the convection-diffusion equation in general coordinates
[REPT-91-72] p 3704 N92-30483

TERMINAL BALLISTICS
Development of diagnostics for electromagnetic armor applications
[AD-A251074] p 3587 N92-30257

TERMINOLOGY
Standard terminology in the laboratory and classroom p 3610 N92-30277

TERMS
Classifying termination of term rewriting
[RUU-CS-91-42] p 3693 N92-30444

TERNARY SYSTEMS
Studies of ordering in semiconducting and other alloys
[AD-A249483] p 3728 N92-30634

TERRAIN
Low-level atmospheric flows studied by pulsed Doppler lidar p 3638 N92-31015
Science questions for the Magellan continuing mission p 3738 N92-31235

TERRESTRIAL PLANETS
Impact erosion of terrestrial planetary atmospheres
[NASA-CR-190605] p 3742 N92-30921

TEST EQUIPMENT
Computer integrated laboratory testing p 3611 N92-30289
Design and construction of a Helmholtz coil magnetic test cell
[AD-A249944] p 3585 N92-30849

TEST FACILITIES
Antenna pattern measurement facilities
[AD-A248964] p 3584 N92-30329
Small engine components test facility compressor testing cell at NASA Lewis Research Center
[NASA-TM-105685] p 3584 N92-30508
Compact range test applications, phase 2
[AD-A248790] p 3615 N92-30583
Nuclear electric propulsion development and qualification facilities
[NASA-TM-105521] p 3589 N92-30818
Fragment hazard zone analyses for explosive test facilities
[DE92-015391] p 3613 N92-30887
Future aerospace ground test facility requirements for the Arnold Engineering Development Center p 3585 N92-30897
Cryogenic Magnetic Bearing Test Facility (CMBTF)
[NASA-CR-189087] p 3582 N92-31164

TEST RANGES
Antenna pattern measurement facilities
[AD-A248964] p 3584 N92-30329

TEST STANDS
Development of diagnostics for electromagnetic armor applications
[AD-A251074] p 3587 N92-30257
Development of a full-scale transmission testing procedure to evaluate advanced lubricants
[NASA-TP-3265] p 3658 N92-30396
Thrust stand evaluation of engine performance improvement algorithms in an F-15 airplane
[NASA-TM-104252] p 3581 N92-30518

TESTS
A processing environment for test and simulation data of thermodynamic systems
[MBB-UO-0169-91-PUB] p 3731 N92-30421
Ideas for a long-baseline neutrino detector
[DE92-010650] p 3743 N92-30828

TETHERED SATELLITES
Data analysis support for the Shuttle Potential and Return Electron Experiment (SPREE) on the Tethered Satellite System 1 (TSS-1) flight
[AD-A248943] p 3588 N92-30628

TETRAD THEORY
Photoinitiated electron transfer in multichromophoric species: Synthetic tetrads and pentads featuring diquinone moieties
[DE92-013472] p 3683 N92-30368

TETRAETHYL ORTHOSILICATE
Molecular weight dependence of domain structure in silica-siloxane molecular composites
[DE92-015046] p 3603 N92-30544

TETRAHYDROFURAN
Epoxides as activators for grafting of poly(tetrahydrofuran) from poly(methylphenylsilylene)
[AD-A251086] p 3601 N92-30244
Polymerization of 1-bromo-4-lithiobenzene in THF. A route to soluble polyphenylenes
[AD-A249926] p 3604 N92-30794

TEXTURES
Vector analysis of ice fabric data
[AD-A250832] p 3682 N92-30832

THEMATIC MAPPERS (LANDSAT)
Monitoring of Dutch forest with LANDSAT-TM
[BCRS-91-21] p 3666 N92-30468
Registration of windfall damage in the eastern Hunsrueck Plateau (Federal Republic of Germany) utilizing LANDSAT-TM-data: A landscape-ecological analysis for practical forestry
[ESA-TT-1253] p 3667 N92-30515

THEMATIC MAPPING
The use of TM data for identification of land cover and for detection of land use changes in the Atlantic zone of Costa Rica
[BCRS-91-36] p 3666 N92-30362

THEOREM PROVING
Computing and verifying depth orders
[RUU-CS-91-41] p 3693 N92-30443
Linear planar augmentation algorithms for outerplanar graphs
[RUU-CS-91-47] p 3703 N92-30449
Kayles on special classes of graphs: An application of Sprague-Grundy theory
[RUU-CS-91-49] p 3703 N92-30450
Strong dynamic input-output decoupling: From linearity to nonlinearity
[MEMO-COSOR-92-04] p 3694 N92-30478
An extension to Schneider's general paradigm for fault-tolerant clock synchronization
[NASA-TM-107634] p 3699 N92-30677
The two-dimensional random walk: Its hitting process and its classification
[CWI-BS-R9003] p 3705 N92-30689
Resolution properties of the Fourier method for discontinuous waves
[NASA-CR-189668] p 3706 N92-30716
Verifying the interactive convergence clock synchronization algorithm using the Boyer-Moore theorem prover
[NASA-CR-189649] p 3700 N92-31158

THEOREMS
A three-valued cumulative semantics for TMS
[REPT-91-69] p 3702 N92-30371
On the factorisation theorem in boson-gluon fusion at hadron colliders
[NIKHEF-H/91-16] p 3713 N92-30415
Computing and verifying depth orders
[RUU-CS-91-41] p 3693 N92-30443
Restrictions of graph partition problems, part 1
[RUU-CS-91-44-PT-1] p 3703 N92-30446
Point location in fat subdivisions
[RUU-CS-91-40] p 3703 N92-30447
On the complexity of the maximum cut problem
[RUU-CS-91-39] p 3703 N92-30458
On the Thue Morse measure
[REPT-92-16] p 3704 N92-30464
Synchronized continuous flow systems
[REPT-91-88] p 3704 N92-30517
The two-dimensional random walk: Its hitting process and its classification
[CWI-BS-R9003] p 3705 N92-30689
A new matrix formulation of classical electrodynamics. Part 1: Vacuum
[AD-A249643] p 3616 N92-30721

THEORETICAL PHYSICS
Theoretical studies in elementary particle physics
[DE92-015295] p 3714 N92-30610
Nuclear theory progress report, April 1991 - April 1992
[DE92-015349] p 3714 N92-30611
Research on elementary particle physics
[DE92-014622] p 3715 N92-30625
Research on elementary particle physics. Task P: Studies in theory and phenomenology of elementary particles, part 1
[DE92-014428] p 3716 N92-30791
Theoretical particle physics
[DE92-014531] p 3716 N92-30841
Solar neutrinos: Theoretical status
[DE92-014014] p 3743 N92-31199

THERMAL BLOOMING
An ultra-sensitive coherent detector capable of single photon detection for lidar applications p 3646 N92-31053

THERMAL CONDUCTIVITY
Impurity segregation to grain boundaries and defects in AlN
[DE92-011667] p 3599 N92-31112

THERMAL DECOMPOSITION
Studies of thermal decomposition of the 1:1 R3Al:en adduct (R = Me, Et; en = ethylenediamine): Synthesis and structure of a novel intermediate Al((HNCH2CH2NH)AlMe2)3
[AD-A251061] p 3603 N92-30623
THERMAL DEGRADATION
Photodegradation effects in materials exposed to high flux solar and solar simulated radiation
[DE91-002147] p 3596 N92-30879
THERMAL DIFFUSION
A method of making a single layer multi-color luminescent display
[NASA-CASE-LAR-14811-1] p 3622 N92-30389
Rapid cooling and structure of neutron stars
[DE92-015279] p 3740 N92-30609
THERMAL DIFFUSIVITY
Beta limit of resistive plasma in torsatron/heliotron
[NIFS-131] p 3725 N92-30985
THERMAL ENERGY
High efficiency thermal to electric energy conversion using selective emitters and spectrally tuned solar cells
[NASA-TM-105755] p 3670 N92-30426
Magnetic bearings for free-piston Stirling engines
[NASA-TM-105730] p 3660 N92-30734
THERMAL EXPANSION
Hybridization of detector array and integrated circuit for readout
[NASA-CASE-NPO-18062-1-CU] p 3623 N92-30542
THERMAL INSTABILITY
Pressure profiles, resonant Pfirsch-Schlueter currents, thermal instabilities, and magnetic island formation
[DE92-015166] p 3726 N92-31002
THERMAL MAPPING
Implementation scheme for recursion in spectral dimension
[AD-A248945] p 3695 N92-30629
THERMAL PROTECTION
Debris/ice/TPS assessment and integrated photographic analysis for Shuttle Mission STS-45
[NASA-TM-107545] p 3586 N92-30382
THERMAL SHOCK
Tempered glass and thermal shock of ceramic materials p 3607 N92-30265
THERMAL STABILITY
A new class of ferroelectric polymers: The odd-numbered nylons
[AD-A252268] p 3603 N92-30594
Ferroelectric polarization mechanisms in Nylon 11
[AD-A252269] p 3728 N92-30595
THERMAL STRESSES
Thermal stress evaluation of a symmetrically laminated composite plate
[AD-A249450] p 3591 N92-30641
THERMOCHEMISTRY
The influence of Lewis number and nonhomogeneous mixture on premixed turbulent flame structure
p 3597 N92-30669
THERMOCOUPLES
Absolute Seebeck thermoelectric characteristics: Principles, significance, and applications
[DE92-013684] p 3622 N92-30370
Repetitive High Energy Pulsed Power (RHEPP) temperature monitoring system utilizing Luxtron fluoroptic sensors and thermocouples technical reference manual
[DE92-013461] p 3637 N92-30893
THERMODYNAMIC PROPERTIES
Search for light neutral scalar and pseudoscalar particles in pFe interactions at 70 GeV
[DE92-627317] p 3713 N92-30404
YBa2Cu(3-x)Co(x)O(y): A substrate material for YBCO superconductors
[DE92-015182] p 3730 N92-30999
Theoretical study of phase stability in Ni-Al and Ni-Ti alloys
[DE92-014776] p 3599 N92-31119
Stability of metallic superlattices
[DE92-011526] p 3600 N92-31124
Thermodynamic evaporation of highly volatile components in the vacuum degassing of melted aluminum alloys
[DE92-015315] p 3600 N92-31218
THERMODYNAMICS
Structure, processing, and properties of potatoes
p 3611 N92-30288
Introductory heat-transfer p 3601 N92-30291
New transient and pseudo-transient algoritims for viscoelastic materials
[AD-A250642] p 3692 N92-30377
A processing environment for test and simulation data of thermodynamic systems
[MBB-UO-0169-91-PUB] p 3731 N92-30421
Thermohydraulic modeling of nuclear thermal rockets: The KLAXON code
[DE92-015274] p 3589 N92-31204
Thermodynamic evaporation of highly volatile components in the vacuum degassing of melted aluminum alloys
[DE92-015315] p 3600 N92-31218
THERMOELASTICITY
Some mathematical problems in continuum mechanics
[AD-A250352] p 3706 N92-31128
THERMOELECTRIC POWER GENERATION
Absolute Seebeck thermoelectric characteristics: Principles, significance, and applications
[DE92-013684] p 3622 N92-30370
High efficiency thermal to electric energy conversion using selective emitters and spectrally tuned solar cells
[NASA-TM-105755] p 3670 N92-30426
THERMOELECTRICITY
Absolute Seebeck thermoelectric characteristics: Principles, significance, and applications
[DE92-013684] p 3622 N92-30370
THERMOGRAPHY
New transient and pseudo-transient algorithms for viscoelastic materials
[AD-A250642] p 3692 N92-30377
THERMOGRAVIMETRY
Evaluation of doped polyethylene oxide as solid electrolyte for polymer batteries
[AD-A249501] p 3624 N92-30619
THERMOHYDRAULICS
Thermohydraulic modeling of nuclear thermal rockets: The KLAXON code
[DE92-015274] p 3589 N92-31204
THERMOREGULATION
Secretory mechanisms in opiocortin cells during cold stress
[AD-A252317] p 3685 N92-30719
THERMOSPHERE
Measurement capabilities of giant lidars for middle and upper atmospheric applications p 3651 N92-31084
THERMOVISCOELASTICITY
Some mathematical problems in continuum mechanics
[AD-A250352] p 3706 N92-31128
THICK PLATES
Optimal shear correction factors in hierarchical plate modelling
[AD-A248899] p 3662 N92-30338
THICKNESS
Ice thickness observations, North American Arctic and subarctic, 1972-1973 and 1973-1974, part 8
[AD-A250830] p 3681 N92-30238
THIN FILMS
Research on polycrystalline thin film submodules based on CuInSe2 materials
[DE92-010584] p 3727 N92-30247
A shear sensitive monomer-polymer laminate structure and method of using same
[NASA-CASE-LAR-14654-1] p 3662 N92-30317
Perforated monolayers
[DE92-011632] p 3593 N92-30344
High efficiency thermal to electric energy conversion using selective emitters and spectrally tuned solar cells
[NASA-TM-105755] p 3670 N92-30426
Perspective on photovoltaic amorphous silicon
[DE92-010581] p 3670 N92-30519
Ion channeling and spectroscopic ellipsometry examinations of thin-film SiO2/epi-Si structures
[DE92-015129] p 3728 N92-30577
Solid lubrication of laser grown fluorinated diamond thin films
[AD-A249485] p 3603 N92-30635
Fabrication of multifilament conductors: CVD processing of high Tc superconducting composite fibers
[NASA-CR-184344] p 3591 N92-30711
Fast methods to numerically integrate the Reynolds equation for gas fluid films
[NASA-TM-105415] p 3660 N92-30722
Anomalous hopping conductivity in amorphous indium-oxide films
[ITN-92-85166] p 3729 N92-30781
Atomic layer epitaxy group 4 materials: Surface processes, thin films, devices, and their characterization
[AD-A252352] p 3729 N92-30846
Disorder and transport in highly correlated systems
[AD-A249969] p 3710 N92-30850
Pulsed microwave processing of high-T(sub c) superconducting films
[DE92-014950] p 3730 N92-31000
Ellipsometric study of oxide films formed on LDEF metal samples
[AD-A249856] p 3599 N92-31110
Grain boundary weak links in high-Tc superconductors
[DE92-016192] p 3730 N92-31190
Diffuse neutron scattering signatures of rough films
[DE92-015208] p 3717 N92-31201
THIN WALLS
Isotropic thin-walled pressure vessel experiment
p 3611 N92-30284
Cross sectional constants and stress distributions of thin-walled sections
[AD-A249886] p 3663 N92-30670
THREE DIMENSIONAL BODIES
Three-dimensional laser window formation
[NASA-RP-1280] p 3585 N92-30307
Demonstration of a 3D vision algorithm for space applications
[NASA-CR-190646] p 3698 N92-31154
THREE DIMENSIONAL BOUNDARY LAYER
Structure of three-dimensional turbulent boundary layers p 3631 N92-30654
THREE DIMENSIONAL FLOW
Numerical solution of a three-dimensional cubic cavity flow by using the Boltzmann equation
[NASA-TM-105693] p 3627 N92-30297
Numerical investigations in three-dimensional internal flows
[NASA-CR-190498] p 3628 N92-30380
Development of a 3-D upwind PNS code for chemically reacting hypersonic flowfields
[NASA-CR-190182] p 3576 N92-30977
An experimental study of the relationship between velocity and pressure fluctuations in a wing-body junction
[AD-A249628] p 3577 N92-31122
THREE DIMENSIONAL MODELS
Three-dimensional shock wave physics simulations on massively parallel supercomputers
[DE92-008679] p 3698 N92-30363
Resolution of the three-dimensional parabolic equation applied to acoustic propagation at low altitudes
[ONERA-RF-17/3641-PY] p 3711 N92-30966
Three-dimensional MHD equilibrium in the presence of bootstrap current for Large Helical Device (LHD)
[NIFS-139] p 3725 N92-30994
THREE DIMENSIONAL MOTION
Three-dimensional shock wave physics simulations on massively parallel supercomputers
[DE92-008679] p 3698 N92-30363
THRUST
Preliminary dynamic tests of a flight-type ejector
[NASA-TM-105814] p 3582 N92-30998
Thrust test fixture
[AD-D015259] p 3585 N92-31192
THRUST LOADS
Thrust stand evaluation of engine performance improvement algorithms in an F-15 airplane
[NASA-TM-104252] p 3581 N92-30518
THRUST VECTOR CONTROL
An electromechanical actuation system for an expendable launch vehicle
[NASA-TM-105774] p 3586 N92-30310
THYRISTORS
Dynamic analysis of compact helical system power supply and designs of its upgrade
[NIFS-TECH-2] p 3723 N92-30497
THYROID GLAND
Secretory mechanisms in opiocortin cells during cold stress
[AD-A252317] p 3685 N92-30719
TIDES
Atmospheric measurements using the LAMP lidar during the LADIMAS campaign p 3652 N92-31086
TILT ROTOR AIRCRAFT
The Eurofar program: An European overview on advanced VTOL civil transportation system
[MBB-UD-0611-91-PUB] p 3578 N92-30418
TIMBER IDENTIFICATION
Monitoring of Dutch forest with LANDSAT-TM
[BCRS-91-21] p 3666 N92-30468
TIME DEPENDENCE
Progress in unstructured-grid methods development for unsteady aerodynamic applications
[NASA-TM-107643] p 3574 N92-30393
Theoretical study of phase-shifted quantum beats in time-resolved luminescence spectra from a biased asymmetric double quantum well
[AD-A252422] p 3710 N92-30549
Finite difference time domain modeling of steady state scattering from jet engines with moving turbine blades
[NASA-CR-190290] p 3582 N92-30753
Determining water cloud particle sizes from lidar depolarization measurements and time dependent multiple scattering coefficients p 3641 N92-31034
Time and polarization dependent double scattering calculations of lidar returns from water clouds
p 3647 N92-31063
Extension of the integral equation formulation of linearized time dependent subsonic flow
[AD-A250654] p 3577 N92-31171
TIME DIVISION MULTIPLE ACCESS
Direct sequence spread spectrum CDMA in shared spectrum applications p 3619 N92-30939

TIME LAG
First conclusions of a manufacturer group on the applicability of CALS in Europe p 3697 N92-30951
TIME MEASUREMENT
Verifying the interactive convergence clock synchronization algorithm using the Boyer-Moore theorem prover
[NASA-CR-189649] p 3700 N92-31158
TIME OF FLIGHT SPECTROMETERS
Neutron time-of-flight ion temperature diagnostic for inertial confinement fusion experiments
[DE92-011365] p 3724 N92-30806
TIME SERIES ANALYSIS
Implementation scheme for recursion in spectral dimension
[AD-A248945] p 3695 N92-30629
Research in stochastic analysis and its applications
[AD-A249482] p 3708 N92-30633
TIME SHARING
Joint queue length and response time distributions in a general preemptive feedback queue
[REPT-91-66] p 3701 N92-30451
TIME TEMPERATURE PARAMETER
A study of enhancing critical current densities (J(sub c)) and critical temperature (T(sub c)) of high-temperature superconductors
[NASA-TM-103595] p 3627 N92-30902
TITANIUM ALLOYS
Stabilization of face-centered-cubic titanium
[DE92-011530] p 3600 N92-31125
TITANIUM CARBIDES
TEM studies of a circumstellar rock
p 3736 N92-31223
TOKAMAK DEVICES
Gyro-Landau fluid model of tokamak core fluctuations
[DE92-013277] p 3722 N92-30366
Role of compressibility on driven magnetic reconnection
[NIFS-105] p 3710 N92-30498
Review of high Z materials for PSI applications
[NIFS-152] p 3602 N92-30502
Rapid change of hydrogen neutral energy distribution at L/H-transition in JFT-2M H-mode
[NIFS-134] p 3714 N92-30510
Problems with the concept of plasma equilibrium in tokamaks
[DE92-014454] p 3723 N92-30576
MHD considerations for a self-cooled liquid lithium blanket
[DE92-014864] p 3723 N92-30591
Boundary plasma transport studies on TFTR
[DE92-011942] p 3723 N92-30746
Remote experimental site concept for diagnostic collaborations in fusion
[DE92-010437] p 3724 N92-30824
Line-emission cross sections for the charge-exchange reaction between fully stripped carbon and atomic hydrogen in tokamak plasma
[NIFS-129] p 3716 N92-30967
The role of stochasticity in sawtooth oscillation
[NIFS-103] p 3710 N92-30983
X ray radiation from hot dense plasmas and atomic processes
[NIFS-PROC-9] p 3725 N92-30984
A steady state tokamak operation by use of magnetic monopoles
[DE92-799109] p 3725 N92-30991
Edge poloidal rotation profiles of H-mode plasmas in the JFT-2M tokamak
[DE92-799107] p 3725 N92-30992
Kinetic approach to long wave length modes in rotating plasmas
[NIFS-138] p 3725 N92-30993
New method of error elimination in potential profile measurement of tokamak plasmas by high voltage heavy ion beam probes
[NIFS-143] p 3726 N92-30995
Criteria and design trade-off issues for ITER
[DE92-011786] p 3726 N92-31114
Fundamental studies of fusion plasmas
[DE92-015077] p 3726 N92-31116
TOMOGRAPHY
Field studies in geophysical diffraction tomography
[DE92-015084] p 3677 N92-31009
TOPEX
Preparations for the ERS-1 and TOPEX/Poseidon satellite altimetry missions
[BCRS-90-28] p 3666 N92-30465
TOPOGRAPHY
Low-level atmospheric flows studied by pulsed Doppler lidar p 3638 N92-31015
TOPOLOGY
A study of the topology of dissipating motions in direct numerical simulations of time-developing compressible and incompressible mixing layers p 3632 N92-30658
Stochastic strings, topology, and space-time confinement
[DE92-630239] p 3732 N92-31136
TOROIDAL PLASMAS
Effects of fast ions and an external inductive electric field on the neoclassical parallel flow, current, and rotation in general toroidal systems
[NIFS-150] p 3713 N92-30500
Two dimensional aspects of toroidal drift waves in the ballooning representation
[DE92-014028] p 3724 N92-30880
Collisional and chaotic transport of energetic particles in toroidal plasma
[DE92-014589] p 3725 N92-30900
Fundamental studies of fusion plasmas
[DE92-015077] p 3726 N92-31116
TORSIONAL STRESS
Cross sectional constants and stress distributions of thin-walled sections
[AD-A249886] p 3663 N92-30870
TOUGHNESS
Transformation toughening of ceramics
[AD-A248903] p 3601 N92-30342
TOXIC HAZARDS
Quantification and reduction of the uncertainty in mass balance models by Monte Carlo analysis of prior data
[DE92-010278] p 3708 N92-30803
TRACE CONTAMINANTS
Trace gas and aerosol transports into and out of the Amazon Basin
[NASA-CR-190624] p 3674 N92-31153
Waste streams in a typical crewed space habitat: An update
[NASA-TM-103888] p 3689 N92-31166
TRACE ELEMENTS
Trace element and isotope geochemistry of geothermal fluids, East Rift Zone, Kilauea, Hawaii
[DE92-014586] p 3671 N92-31117
TRACKING (POSITION)
TRAC performance estimates
[NASA-CR-190530] p 3701 N92-30778
TRADEOFFS
Pairwise comparison of concessions in negotiation processes
[REPT-92-15] p 3733 N92-30463
TRAINING DEVICES
Integrating commercial off-the-shelf tools for custom software development
[AD-A252462] p 3695 N92-30550
Managing the contract closeout process
[AD-A250701] p 3733 N92-31209
TRAINING SIMULATORS
Technical training for national simulator evaluation specialist
[NASA-CR-190429] p 3687 N92-30488
TRAJECTORIES
Degeneracy in interior point methods for linear programming
[REPT-91-102] p 3691 N92-30353
Trajectory fitting in function space with application to analytic modeling of surfaces
[NASA-TP-3232] p 3576 N92-30747
TRAJECTORY CONTROL
Generalized projected gradient-type iterative method for parametric and functional optimization of dynamical systems subject to constraints
[ESA-TT-1166] p 3694 N92-30512
TRANSDUCERS
Optical transducers for scintillating fiber readout
[DE92-015963] p 3721 N92-31187
Thrust test fixture
[AD-D015259] p 3585 N92-31192
TRANSFER FUNCTIONS
A new matrix formulation of classical electrodynamics. Part 1: Vacuum
[AD-A249643] p 3616 N92-30721
TRANSFORMERS
Comparison of high temperature, high frequency core loss and dynamic B-H loops of a 2V-49Fe-49Co and a grain oriented 3Si-Fe alloy
[NASA-TM-105791] p 3623 N92-30397
Printed transformer process/product improvements
[DE92-014760] p 3624 N92-30590
TRANSIENT RESPONSE
Development of a modular transient cycle analysis program for the adiabatic diesel and other compound diesel engines
[AD-A249022] p 3658 N92-30538
Nonlinear stability and control study of highly maneuverable high performance aircraft, phase 2
[NASA-CR-190667] p 3583 N92-30922
Preliminary dynamic tests of a flight-type ejector
[NASA-TM-105814] p 3582 N92-30998
TRANSISTORS
New insights into radiation-induced oxide-trap charge through Thermally-Stimulated-Current (TSC) measurement and analysis
[DE92-009054] p 3728 N92-30585
TRANSIT TIME
Aeronautical Mobile Satellite Service (AMSS) capacity analysis and protocol performance simulation results
[DOT/FAA/CT-TN90/64] p 3622 N92-31212
TRANSITION FLOW
A fractal transition in the two dimensional shear layer
p 3633 N92-30665
TRANSITION METALS
Tunable solid state lasers based on molecular ions
[AD-A249423] p 3656 N92-30774
Fundamental studies of strongly magnetic rare earth-transition metal alloys
[DE92-015916] p 3600 N92-31186
TRANSITION TEMPERATURE
First-principles computational studies of alkali-doped C60 fullerides
[AD-A249018] p 3624 N92-30630
TRANSMISSION LINES
A cable detection lidar system for helicopters
p 3648 N92-31068
TRANSMISSION LOSS
Evaporation duct effects at millimeter wavelengths
[AD-A250239] p 3617 N92-30876
TRANSMISSIONS (MACHINE ELEMENTS)
Development of a full-scale transmission testing procedure to evaluate advanced lubricants
[NASA-TP-3265] p 3658 N92-30396
TRANSMISSOMETERS
Trial of a slant visual range measuring device
p 3644 N92-31043
TRANSMITTER RECEIVERS
Personal communications via ACTS satellite HBR transponders p 3618 N92-30929
Ground-based Doppler lidar of increased laser instability: Conception and design p 3650 N92-31078
Lidar measurements using large liquid mirror telescopes p 3652 N92-31087
TRANSONIC FLOW
Progress in unstructured-grid methods development for unsteady aerodynamic applications
[NASA-TM-107643] p 3574 N92-30393
Computation of unsteady transonic flows using an implicit centered Euler solver without artificial viscosity
[ESA-TT-1235] p 3575 N92-30514
A gridless Euler/Navier-Stokes solution algorithm for complex two-dimensional applications
[NASA-TM-107631] p 3575 N92-30570
Implicit upwind-Euler solution algorithms for unstructured-grid applications
[NASA-TM-107645] p 3575 N92-30691
Application of the Chimera overlapped grid scheme to simulation of Space Shuttle ascent flows
p 3576 N92-30742
TRANSPIRATION
Control and augmentation of passive porosity through transpiration control
[NASA-CASE-LAR-14682-1] p 3628 N92-30387
TRANSPONDERS
Software breadboard study
[NASA-CR-190473] p 3625 N92-30757
Experimental millimeter-wave personal satellite communications system p 3617 N92-30927
Personal communications via ACTS satellite HBR transponders p 3618 N92-30929
TRANSPORT AIRCRAFT
Potential airfield sites in Antarctica for wheeled aircraft
[AD-A249503] p 3584 N92-30621
Research and technology, 1991. Langley Research Center
[NASA-TM-4331] p 3744 N92-30733
Evaluation of microwave landing system approaches in a wide-body transport simulator
[NASA-CR-4450] p 3579 N92-30978
TRANSPORT PROPERTIES
Absolute Seebeck thermoelectric characteristics: Principles, significance, and applications
[DE92-013684] p 3622 N92-30370
Plasma parameter estimations for the large helical device based on the gyro-reduced Bohm scaling
[NIFS-114] p 3723 N92-30499
Examinations of the microwave photoelectric conductivity of a-Si:H multilayer systems for in situ characterization
[ETN-92-91688] p 3727 N92-30505
Transport phenomena in welds
[DE92-013404] p 3659 N92-30587
The structure of turbulent channel flow with passive scalar transport p 3632 N92-30657
Nonequilibrium behavior of carriers in semiconductors subjected to strong space-time varying fields
[AD-A246961] p 3624 N92-30678

Event-scale relationships between surface velocity, temperature and chlorophyll in the coastal ocean, as seen by satellite
[NASA-CR-190266] p 3682 N92-30739
Disorder and transport in highly correlated systems
[AD-A249969] p 3710 N92-30850

TRANSPORT THEORY
Collisional and chaotic transport of energetic particles in toroidal plasma
[DE92-014589] p 3725 N92-30900

TRANSPORTATION
Columbus logistics transportation and ground processing
[MBB-UO-0167-91-PUB] p 3709 N92-30442
Emissions of greenhouse gases from the use of transportation fuels and electricity
[DE92-012102] p 3674 N92-30770

TRANSPUTERS
Architecture for the high performance implantation of communication transport level protocols
[ETN-92-91666] p 3690 N92-30701

TRAPPED PARTICLES
Gyro-Landau fluid model of tokamak core fluctuations
[DE92-013277] p 3722 N92-30366
Kinetic approach to long wave length modes in rotating plasmas
[NIFS-138] p 3725 N92-30993

TRAVELING WAVES
Research studies on extreme ultraviolet and soft x ray lasers
[AD-A249798] p 3657 N92-30784

TREES (PLANTS)
Registration of windfall damage in the eastern Hunsrueck Plateau (Federal Republic of Germany) utilizing LANDSAT-TM-data: A landscape-ecological analysis for practical forestry
[ESA-TT-1253] p 3667 N92-30515
Fluorescence lidar multi-color imaging of vegetation
p 3640 N92-31028
Altimetry and lidar using AlGaAs lasers modulated with pseudo-random codes p 3641 N92-31030

TRENDS
The effect of information systems on middle management in the aerospace industry: The Westco case
[AD-A249017] p 3735 N92-30584

TRIANGLES
Operational surfaces for the rectangle and triangle
[DE92-015165] p 3705 N92-30566

TRIANGULATION
Delaunay triangulation and computational fluid dynamics meshes
[NASA-TM-107663] p 3689 N92-30907
Inter- and intra-plate deformation at North American plate boundaries
[NASA-CR-190485] p 3676 N92-30961

TRIBOLOGY
Modelling of heavily loaded lubricated contacts
[AD-A248807] p 3659 N92-30554

TRIGONOMETRIC FUNCTIONS
On the rapid evaluation of trigonometric series
[AD-A249029] p 3705 N92-30568

TRITIUM
Tritium content of a DT pellet in inertial confinement fusion
[NIFS-113] p 3722 N92-30430

TROPICAL STORMS
Tropical cyclone asymmetries as revealed by recent satellite microwave brightness temperatures
[AD-A249873] p 3679 N92-30867

TROPOPAUSE
Airborne remote sensing of tropospheric water vapor using a near infrared DIAL system p 3644 N92-31042

TROPOSPHERE
Sixteenth International Laser Radar Conference, part 2
[NASA-CP-3158-PT-2] p 3637 N92-31013
Tropospheric and stratospheric wind profiling with a direct detection Doppler lidar p 3639 N92-31018
Airborne remote sensing of tropospheric water vapor using a near infrared DIAL system p 3644 N92-31042
A variable phase function approach for the inversion of lidar return signals p 3649 N92-31073
Measurement capabilities of giant lidars for middle and upper atmospheric applications p 3651 N92-31084
The ENEA CO2 lidar/DIAL station activity in a tropospheric remote sensing program
p 3655 N92-31103

TRUSSES
Design feasibility study of a Space Station Freedom truss
[NASA-TM-105558] p 3659 N92-30571

TUNABLE LASERS
Tunable solid state lasers based on molecular ions
[AD-A249423] p 3656 N92-30774
Tunable Electro-optic modulators for lidar systems and atmospheric applications p 3646 N92-31056
Tm,Ho:YAG laser with tunable range of 2.08-2.12 microns and its applications to spectroscopy
p 3646 N92-31058
Alexandrite lidar for the atmospheric water vapor detection and development of powerful tunable sources in IR p 3653 N92-31094
Measurements of fugitive hydrocarbon emissions with a tunable infrared DIAL p 3655 N92-31102

TUNING
Acousto-optic filtering of lidar signals
p 3650 N92-31077

TURBIDITY
A comparison of lidar inversion methods for cirrus applications p 3649 N92-31074

TURBINE BLADES
Finite difference time domain modeling of steady state scattering from jet engines with moving turbine blades
[NASA-CR-190290] p 3582 N92-30753
Yaw dynamics of horizontal axis wind turbines
[DE92-001245] p 3670 N92-30837

TURBINE ENGINES
A simplified dynamic model of the T700 turboshaft engine
[NASA-TM-105805] p 3709 N92-30898

TURBINE PUMPS
Cryogenic Magnetic Bearing Test Facility (CMBTF)
[NASA-CR-189087] p 3582 N92-31164

TURBOFAN ENGINES
Thrust stand evaluation of engine performance improvement algorithms in an F-15 airplane
[NASA-TM-104252] p 3581 N92-30518

TURBOSHAFTS
A simplified dynamic model of the T700 turboshaft engine
[NASA-TM-105805] p 3709 N92-30898

TURBULENCE
Studying Turbulence Using Numerical Simulation Databases. 3: Proceedings of the 1990 Summer Program
[NASA-CR-189475] p 3630 N92-30648
On the subgrid-scale modeling of compressible turbulence p 3631 N92-30652
One-equation near-wall turbulence modeling with the aid of direct simulation data p 3631 N92-30656
Direct numerical simulations of stably-stratified sheared turbulence: Implications for oceanic mixing
p 3632 N92-30659
Length scales and dissipation of fine eddies in a mixing layer p 3633 N92-30664
Geometry of premixed flames in three-dimensional turbulence p 3633 N92-30666
Statistics for laminar flamelet modeling
p 3597 N92-30668
Pre-mixed flame simulations for non-unity Lewis numbers p 3597 N92-30670
Generation of large-scale density fluctuations by buoyancy p 3634 N92-30671
Interscale energy transfer in numerically simulated turbulence p 3634 N92-30672
Direct simulation of high-speed mixing layers
[NASA-TP-3186] p 3576 N92-30909
Prediction of coincidence frequencies for a thin-walled, fluid-filled pipe
[MRL-TN-600] p 3664 N92-30963
Evaluation of microwave landing system approaches in a wide-body transport simulator
[NASA-CR-4450] p 3579 N92-30978
Solar neutrinos: Theoretical status
[DE92-014014] p 3743 N92-31199

TURBULENCE EFFECTS
Lidar measurement of optical turbulence: Theory of the crossed path technique
[AD-A248938] p 3720 N92-30343
The effects of free stream turbulence and surface curvature on boundary layer flow and heat transfer
[AD-A248846] p 3630 N92-30616

TURBULENCE MODELS
Variational method in the statistical theory of turbulent two-phase flows
[AD-A252263] p 3630 N92-30604
Studying Turbulence Using Numerical Simulation Databases. 3: Proceedings of the 1990 Summer Program
[NASA-CR-189475] p 3630 N92-30648
A dynamic subgrid-scale eddy viscosity model
p 3630 N92-30649
A subgrid-scale model based on the second-order velocity structure function p 3631 N92-30651
On the subgrid-scale modeling of compressible turbulence p 3631 N92-30652
Modeling the turbulent kinetic energy equation for compressible, homogeneous turbulence
p 3631 N92-30653
One-equation near-wall turbulence modeling with the aid of direct simulation data p 3631 N92-30656
Application of the Chimera overlapped grid scheme to simulation of Space Shuttle ascent flows
p 3576 N92-30742
New insights into large eddy simulation
[AD-A249424] p 3635 N92-30775
Interaction of isotropic turbulence with a shock wave
[AD-A250409] p 3635 N92-30852

TURBULENT BOUNDARY LAYER
The effects of free stream turbulence and surface curvature on boundary layer flow and heat transfer
[AD-A248846] p 3630 N92-30616
A dynamic subgrid-scale eddy viscosity model
p 3630 N92-30649
Structure of three-dimensional turbulent boundary layers p 3631 N92-30654
A numerical evaluation of the dynamical systems approach to wall layer turbulence p 3632 N92-30660
Intersecting shock-wave/turbulent boundary-layer interactions at Mach 8.3
[NASA-TM-103909] p 3635 N92-30765
An experimental study of the relationship between velocity and pressure fluctuations in a wing-body junction
[AD-A249628] p 3577 N92-31122

TURBULENT DIFFUSION
Laminar flamelet modeling of turbulent diffusion flames p 3633 N92-30667

TURBULENT FLOW
Turbulent reacting flows and supersonic combustion
[AD-A251065] p 3593 N92-30256
Variational method in the statistical theory of turbulent two-phase flows
[AD-A252263] p 3630 N92-30604
Studying Turbulence Using Numerical Simulation Databases. 3: Proceedings of the 1990 Summer Program
[NASA-CR-189475] p 3630 N92-30648
A dynamic subgrid-scale eddy viscosity model
p 3630 N92-30649
Subgrid-scale backscatter in transitional and turbulent flows p 3630 N92-30650
A subgrid-scale model based on the second-order velocity structure function p 3631 N92-30651
Structure of three-dimensional turbulent boundary layers p 3631 N92-30654
The structure of turbulent channel flow with passive scalar transport p 3632 N92-30657
Direct numerical simulations of stably-stratified sheared turbulence: Implications for oceanic mixing
p 3632 N92-30659
A numerical evaluation of the dynamical systems approach to wall layer turbulence p 3632 N92-30660
Length scales and dissipation of fine eddies in a mixing layer p 3633 N92-30664
The influence of Lewis number and nonhomogeneous mixture on premixed turbulent flame structure
p 3597 N92-30669
Continuous wavelet analysis of coherent structures
p 3634 N92-30673
New insights into large eddy simulation
[AD-A249424] p 3635 N92-30775
Numerical study of axial turbulent flow over long cylinders
[AD-A250801] p 3635 N92-30831
Interaction of isotropic turbulence with a shock wave
[AD-A250409] p 3635 N92-30852

TURBULENT HEAT TRANSFER
The effects of free stream turbulence and surface curvature on boundary layer flow and heat transfer
[AD-A248846] p 3630 N92-30616

TURBULENT JETS
Advanced concepts for controlled combustion in engines
[AD-A249911] p 3595 N92-30814

TURBULENT MIXING
Numerical simulation of low Prandtl number turbulent mixing p 3633 N92-30663

TVD SCHEMES
Development of a 3-D upwind PNS code for chemically reacting hypersonic flowfields
[NASA-CR-190182] p 3576 N92-30977

TWINNING
Five experiments in materials science for less than $10.00 p 3611 N92-30283

TWISTED WINGS
A demonstration of passive blade twist control using extension-twist coupling
[NASA-TM-107642] p 3664 N92-31155

TWO DIMENSIONAL BODIES
A tolerance approach to visual shape perception and image matching analysis for modeling of micro-heterogeneous materials
[ISSN-0208-5658] p 3721 N92-31149

TWO DIMENSIONAL FLOW
A gridless Euler/Navier-Stokes solution algorithm for complex two-dimensional applications
[NASA-TM-107631] p 3575 N92-30570
Structure of three-dimensional turbulent boundary layers p 3631 N92-30654
A fractal transition in the two dimensional shear layer p 3633 N92-30665
Geometry of premixed flames in three-dimensional turbulence p 3633 N92-30666
Numerical calculations of two-dimensional single and multi-material flow fields with CCICE
[DE92-015778] p 3636 N92-30903
TWO DIMENSIONAL MODELS
A boundary element alternating method for two-dimensional mixed-mode fracture problems
[NASA-CR-4460] p 3661 N92-30309
Adaptive multigrid applied to a bipolar transistor problem
[CWI-NM-R9115] p 3693 N92-30429
A gridless Euler/Navier-Stokes solution algorithm for complex two-dimensional applications
[NASA-TM-107631] p 3575 N92-30570
A Boussinesq algorithm for bouyant convection in polygonal domains
[PB92-187137] p 3695 N92-30579
Length scales and dissipation of fine eddies in a mixing layer p 3633 N92-30664
TWO PHASE FLOW
Variational method in the statistical theory of turbulent two-phase flows
[AD-A252263] p 3630 N92-30604

U

U.S.S.R.
Soviet applied information sciences in a time of change
[PB92-173020] p 3734 N92-30509
Joint stabilizing projects in defense
[DE92-015977] p 3709 N92-30891
UH-1 HELICOPTER
Development statistics for the UH-1 Ada feasibility study
[AD-A252404] p 3584 N92-30547
Helicopter nighttime parking test results - UH-1
[DOT/FAA/CT-TN92/1] p 3580 N92-31165
ULTRASONIC TESTS
Ultrasound NDE of adhesive bond integrity: A quantitative measure
[AD-A248845] p 3661 N92-30599
Characterizing ultrasonic transducers using pattern recognition techniques
[DE92-015845] p 3711 N92-30890
ULTRASONIC WAVE TRANSDUCERS
Characterizing ultrasonic transducers using pattern recognition techniques
[DE92-015845] p 3711 N92-30890
ULTRAVIOLET LASERS
Photodissociation of azulene under UV-laser irradiation at 325 nm
[AD-A251093] p 3613 N92-30246
Research studies on extreme ultraviolet and soft x ray lasers
[AD-A249798] p 3657 N92-30784
ULTRAVIOLET RADIATION
Measurements of fugitive hydrocarbon emissions with a tunable infrared DIAL p 3655 N92-31102
ULTRAVIOLET SPECTRA
Modeling of UV lines from cataclysmic variable winds
[DE92-013443] p 3739 N92-30862
UNDERGROUND EXPLOSIONS
Investigation of the interface phenomena due to interaction of high intensity stress waves with geologic boundaries
[AD-A248992] p 3675 N92-30525
UNDERWATER ACOUSTICS
Digital bottom mapping
[AD-D015238] p 3682 N92-30413
UNIFORM FLOW
Numerical investigations in three-dimensional internal flows
[NASA-CR-190498] p 3628 N92-30380
UNIQUENESS
Global existence for a semilinear elliptic-parabolic PDE system
[REPT-91-70] p 3628 N92-30372
UNITED STATES
Research and technology, 1991. Langley Research Center
[NASA-TM-4331] p 3744 N92-30733
Joint stabilizing projects in defense
[DE92-015977] p 3709 N92-30891
UNIVERSITY PROGRAM
Research on elementary particle physics
[DE92-014622] p 3715 N92-30625
UNSTEADY AERODYNAMICS
Progress in unstructured-grid methods development for unsteady aerodynamic applications
[NASA-TM-107643] p 3574 N92-30393
Extension of the integral equation formulation of linearized time dependent subsonic flow
[AD-A250654] p 3577 N92-31171
UNSTEADY FLOW
Mixed and forced convection from an array of discrete heat sources in a vertical channel
[AD-A248853] p 3731 N92-30235
UPPER ATMOSPHERE
Chemielectron and photoelectron spectroscopic studies of importance in the upper atmosphere
[AD-A248838] p 3675 N92-30556
Measurement capabilities of giant lidars for middle and upper atmospheric applications p 3651 N92-31084
UPPER ATMOSPHERE RESEARCH SATELLITE (UARS)
Correlative measurement opportunities between ATLAS-1 and UARS experiments
[NASA-TM-107630] p 3679 N92-30735
URANIUM ALLOYS
Corrosion of high density kinetic energy penetrator materials
[AD-A249439] p 3597 N92-30759
URBAN DEVELOPMENT
Departments of Veterans Affairs and Housing and Urban Development, and Independent Agencies Appropriation Bill, 1993
[S-REPT-102-356] p 3735 N92-31169
USER MANUALS (COMPUTER PROGRAMS)
Metal matrix composite analyzer (METCAN) user's manual, version 4.0
[NASA-TM-105244] p 3592 N92-30779
FASTRAN-2: A fatigue crack growth structural analysis program
[NASA-TM-104159] p 3664 N92-30964
USER REQUIREMENTS
Relaxor ferroelectrics for electrostrictive transducer
[AD-A248671] p 3624 N92-30598

V

VACUUM
A new matrix formulation of classical electrodynamics. Part 1: Vacuum
[AD-A249643] p 3616 N92-30721
RF vacuum microelectronics
[AD-A249814] p 3626 N92-30836
Numerical investigations in the backflow region of a vacuum plume
[NASA-CR-190515] p 3589 N92-30981
Thermodynamic evaporation of highly volatile components in the vacuum degassing of melted aluminum alloys
[DE92-015315] p 3600 N92-31218
VACUUM EFFECTS
A dynamic model for beam tube vacuum effects on the SSC cryogenic system
[DE92-013967] p 3719 N92-30840
VACUUM SPECTROSCOPY
Atomic layer epitaxy group 4 materials: Surface processes, thin films, devices, and their characterization
[AD-A252352] p 3729 N92-30846
VACUUM SYSTEMS
A dynamic model for beam tube vacuum effects on the SSC cryogenic system
[DE92-013967] p 3719 N92-30840
VALENCE
Development of practical MO techniques for prediction of the properties and behavior of materials
[AD-A247218] p 3598 N92-30864
VALLEYS
Duration and rates of discharge: Maja Valles, Mars p 3737 N92-31227
VAN DER WAALS FORCES
Magic numbers in molecular clusters: A probe for chemical reactivity
[AD-A251096] p 3712 N92-30261
VAPOR DEPOSITION
Solid lubrication of laser grown fluorinated diamond thin films
[AD-A249485] p 3603 N92-30635
Method of synthesizing high quality, doped diamond and diamonds and devices obtained therefrom
[AD-D015267] p 3604 N92-30685
Corrosion of high density kinetic energy penetrator materials
[AD-A249439] p 3597 N92-30759
Atomic layer epitaxy group 4 materials: Surface processes, thin films, devices, and their characterization
[AD-A252352] p 3729 N92-30846
Computational simulation of diamond chemical vapor deposition in premixed C2H2/O2/H2 and CH4/O2 strained flames
[DE92-012144] p 3606 N92-30857
VAPOR PHASE EPITAXY
Decomposition studies of tertiarybutyldimethylantimony
[AD-A250670] p 3727 N92-30527
VAPOR PHASES
Decomposition studies of tertiarybutyldimethylantimony
[AD-A250670] p 3727 N92-30527
Thermodynamic evaporation of highly volatile components in the vacuum degassing of melted aluminum alloys
[DE92-015315] p 3600 N92-31218
VAPOR PRESSURE
Effect of volatility and oxygenates on driveability at intermediate ambient temperatures
[AD-A248902] p 3607 N92-30341
Thermodynamic evaporation of highly volatile components in the vacuum degassing of melted aluminum alloys
[DE92-015315] p 3600 N92-31218
VARIABILITY
The status of renewable energy technology
[DE92-011386] p 3670 N92-30808
VARIABLE STARS
Nonlinear RR Lyrae models with new Livermore opacities
[DE92-011158] p 3741 N92-31108
VARIANCE (STATISTICS)
Some inequalities for variances
[REPT-92-10] p 3707 N92-30460
VARIATIONAL PRINCIPLES
Dynamics of deformable bodies
[AD-A252333] p 3705 N92-30533
Variational method in the statistical theory of turbulent two-phase flows
[AD-A252263] p 3630 N92-30604
VARIATIONS
Gyro-Landau fluid model of tokamak core fluctuations
[DE92-013277] p 3722 N92-30366
Water vapor variance measurements using a Raman lidar p 3643 N92-31041
VECTOR ANALYSIS
Vector analysis of ice fabric data
[AD-A250832] p 3682 N92-30832
Wrappability of curves on surfaces
[AD-A250004] p 3707 N92-31140
VECTOR PROCESSING (COMPUTERS)
Contribution of parallelism to solving a load distribution problem in electric networks
[ETN-92-91668] p 3625 N92-30702
VEGETATION
Habitat model for the Florida Scrub Jay on John F. Kennedy Space Center
[NASA-TM-107543] p 3673 N92-30494
SCS method of runoff estimation using remote sensing techniques p 3668 N92-30916
VEGETATION GROWTH
Vegetation conditions and yield indicators. Part 1: Main report
[BCRS-91-26-PT-1] p 3667 N92-30471
Development of the cultivated landscape of north west Germany under the human influence
[ETN-92-91730] p 3669 N92-30968
VELOCITY
Combustion diagnostics by photo-deflection spectroscopy
[AD-A250802] p 3594 N92-30645
Generation of large-scale density fluctuations by buoyancy p 3634 N92-30671
VELOCITY DISTRIBUTION
Event-scale relationships between surface velocity, temparature and chlorophyll in the coastal ocean, as seen by satellite
[NASA-CR-190266] p 3682 N92-30739
VELOCITY MEASUREMENT
Doppler mean velocity estimation: Small sample analysis and a new estimator
[AD-A249024] p 3678 N92-30559
Laser optical mouse
[AD-D015307] p 3690 N92-30564
Theoretical simulation of a 2 micron airborne solid state laser anemometer p 3647 N92-31059
An experimental study of the relationship between velocity and pressure fluctuations in a wing-body junction
[AD-A249628] p 3577 N92-31122
VENUS (PLANET)
Twenty-Third Lunar and Planetary Science Conference
[NASA-CR-190178] p 3736 N92-31222

Global scale concentrations of volcanic activity on Venus: A summary of three 23rd Lunar and Planetary Science Conference abstracts. 1: Venus volcanism: Global distribution and classification from Magellan data. 2: A major global-scale concentration of volcanic activity in the Beta-Atla-Themis region of Venus. 3: Two global concentrations of volcanism on Venus: Geologic associations and implications for global pattern of upwelling and downwelling p 3737 N92-31226
The thermal engine of Venus: Implications from the impact crater distribution p 3738 N92-31233
Is the Venusian lithosphere subducting? p 3738 N92-31234
Science questions for the Magellan continuing mission p 3738 N92-31235

VENUS SURFACE
The thermal engine of Venus: Implications from the impact crater distribution p 3738 N92-31233
Is the Venusian lithosphere subducting? p 3738 N92-31234
Science questions for the Magellan continuing mission p 3738 N92-31235

VERTICAL AIR CURRENTS
Linkage of anthropogenic aerosol to clouds and climate
[DE92-013574] p 3674 N92-30707

VERTICAL DISTRIBUTION
Antenna pattern measurement facilities
[AD-A248964] p 3584 N92-30329
Airborne lidar mapping of vertical ozone distributions in support of the 1990 Clean Air Act Amendments p 3654 N92-31101

VERTICAL TAKEOFF AIRCRAFT
The Eurofar program: An European overview on advanced VTOL civil transportation system
[MBB-UD-0611-91-PUB] p 3578 N92-30418

VERY HIGH FREQUENCIES
Multifrequency measurements of radar ground clutter at 42 sites. Volume 3: Appendix E
[AD-A246988] p 3616 N92-30863

VERY LARGE SCALE INTEGRATION
Information processing research
[AD-A248492] p 3734 N92-30324
VLSI design, parallel computation, and distributed computing
[AD-A252349] p 3699 N92-30596

VHSIC (CIRCUITS)
A model of the ADA avionics real-time system: An example of the benefits of the hardware/software codesign approach in development of real-time systems
[AD-A248893] p 3581 N92-30524

VIABILITY
Comparison of epifluorescent viable bacterial count methods
[NASA-TM-103592] p 3683 N92-30305

VIBRATION
Measurement of radiative lifetimes of vibrational states of simple ions
[AD-A248567] p 3712 N92-30337
Emittance growth caused by magnet vibrations in SSC
[DE92-014186] p 3719 N92-30881

VIBRATION DAMPING
Single mode variable-sensitivity fiber optic sensors
[NASA-CR-190492] p 3721 N92-30975
An analytical and experimental investigation of flutter suppression via piezoelectric actuation
[NASA-TM-107653] p 3580 N92-31174

VIBRATION ISOLATORS
Microgravity vibration isolation: Optimal preview and feedback control
[NASA-TM-105673] p 3613 N92-30692
An investigation of the effects of boundary constraints on the sound insulations of lightweight, double leaf partitions
[BBC-RD-1992/4] p 3711 N92-31151

VIBRATION MEASUREMENT
Single mode variable-sensitivity fiber optic sensors
[NASA-CR-190492] p 3721 N92-30975
The role of laser coherence in long-range vibration measurements p 3654 N92-31097
An investigation of the effects of boundary constraints on the sound insulations of lightweight, double leaf partitions
[BBC-RD-1992/4] p 3711 N92-31151

VIBRATION MODE
Vibrationally induced rotational axis switching: A novel mechanism for vibrational mode-coupling
[AD-A251085] p 3712 N92-30259

VIBRATION TESTS
Testing of double-layer capacitors for high reliability applications
[DE92-011384] p 3626 N92-30807

VIBRATIONAL SPECTRA
Vibrational overtone spectroscopy of gaseous metallocenes
[AD-A251088] p 3593 N92-30245
Vibrationally induced rotational axis switching: A novel mechanism for vibrational mode-coupling
[AD-A251085] p 3712 N92-30259
Fiber-optic Raman spectroscopy at the Savannah River Site: Uses and techniques
[DE92-013971] p 3596 N92-30899

VIDEO COMMUNICATION
Technical and economic feasibility of integrated video service by satellite
[NASA-CR-189210] p 3614 N92-30300

VIDEO DATA
Modeling of video traffic in packet networks, low rate video compression, and the development of a lossy+lossless image compression algorithm
[NASA-CR-190546] p 3691 N92-30296

VIDEO EQUIPMENT
VDHW-related memo's
[LINO-1991-5] p 3718 N92-30725
A stroboscopic technique for using CCD cameras in flow visualization systems for continuous viewing and stop action photography
[NASA-TM-107648] p 3637 N92-30737

VIDEO SIGNALS
Measurement report on the present Video Highway System of MEA p 3718 N92-30726
Tunable relay box (design and testing) p 3718 N92-30727
Console driver p 3718 N92-30728

VIDEO TAPE RECORDERS
Demonstration of magnetic domain boundary movement using an easily assembled videocam-microscope system p 3611 N92-30286

VISCOELASTICITY
Depolarized light scattering and dynamic shear compliance of viscoelastic liquids
[AD-A252491] p 3721 N92-30536
Some mathematical problems in continuum mechanics
[AD-A250352] p 3706 N92-31128

VISCOPLASTICITY
New transient and pseudo-transient algorithms for viscoelastic materials
[AD-A250642] p 3692 N92-30377

VISCOSITY
Coefficients of the second viscosity in bulk liquid helium
[AD-A252421] p 3629 N92-30548
Continuous wavelet analysis of coherent structures p 3634 N92-30673

VISCOUS FLOW
Navier-Stokes computations of a viscous optimized waverider
[NASA-CR-189658] p 3574 N92-30392
A gridless Euler/Navier-Stokes solution algorithm for complex two-dimensional applications
[NASA-TM-107631] p 3575 N92-30570
Calculation of viscous hypersonic flows in chemical non-equilibrium
[MBB/FE211/S/PUB/466] p 3634 N92-30674
Direct coupling method for time-accurate solution of incompressible Navier-Stokes equations
[NASA-CR-189177] p 3636 N92-30894

VISIBILITY
Trial of a slant visual range measuring device p 3644 N92-31043
Dense fog on the highway: Visual range monitoring in cars? p 3655 N92-31106

VISUAL DISCRIMINATION
Visual perception of depth from occlusion: A neural network model
[AD-A249035] p 3696 N92-30820

VISUAL FIELDS
Spatiotemporal characteristics of human visual localization
[AD-A248494] p 3687 N92-30325

VISUAL FLIGHT
Helicopter nighttime parking test results - UH-1
[DOT/FAA/CT-TN92/1] p 3580 N92-31165

VISUAL PERCEPTION
Spatiotemporal characteristics of human visual localization
[AD-A248494] p 3687 N92-30325
Induced pictorial representations
[AD-A248560] p 3687 N92-30336
Visual perception of depth from occlusion: A neural network model
[AD-A249035] p 3696 N92-30820
A tolerance approach to visual shape perception and image matching analysis for modeling of micro-heterogeneous materials
[ISSN-0208-5658] p 3721 N92-31149

VISUAL TASKS
Psychophysical studies of visual cortical function
[AD-A246962] p 3687 N92-30679

VOICE COMMUNICATION
Personal communications via ACTS satellite HBR transponders p 3618 N92-30929
The ELLIPSO (tm) system: Elliptical low orbits for mobile communications and other optimum system elements p 3618 N92-30930
A personal communications network using a Ka-band satellite p 3619 N92-30934

VOIDS
Ellipsometric study of oxide films formed on LDEF metal samples
[AD-A249856] p 3599 N92-31110

VOLATILITY
Effect of volatility and oxygenates on driveability at intermediate ambient temperatures
[AD-A248902] p 3607 N92-30341

VOLCANOLOGY
Global scale concentrations of volcanic activity on Venus: A summary of three 23rd Lunar and Planetary Science Conference abstracts. 1: Venus volcanism: Global distribution and classification from Magellan data. 2: A major global-scale concentration of volcanic activity in the Beta-Atla-Themis region of Venus. 3: Two global concentrations of volcanism on Venus: Geologic associations and implications for global pattern of upwelling and downwelling p 3737 N92-31226
The thermal engine of Venus: Implications from the impact crater distribution p 3738 N92-31233

VOLT-AMPERE CHARACTERISTICS
The temperature dependence of a large dynamic range photodetector structure
[AD-A247667] p 3624 N92-30683

VORTEX GENERATORS
Ultra high bypass Nacelle aerodynamics inlet flow-through high angle of attack distortion test
[NASA-CR-189149] p 3574 N92-30298

VORTICES
Method of measuring cross-flow vortices by use of an array of hot-film sensors
[NASA-CASE-LAR-14824-1-SB] p 3628 N92-30390
Studying Turbulence Using Numerical Simulation Databases. 3: Proceedings of the 1990 Summer Program
[NASA-CR-189475] p 3630 N92-30648
A dynamic subgrid-scale eddy viscosity model p 3630 N92-30649
Subgrid-scale backscatter in transitional and turbulent flows p 3630 N92-30650
A subgrid-scale model based on the second-order velocity structure function p 3631 N92-30651
On the subgrid-scale modeling of compressible turbulence p 3631 N92-30652
Direct numerical simulations of stably-stratified sheared turbulence: Implications for oceanic mixing p 3632 N92-30659
Length scales and dissipation of fine eddies in a mixing layer p 3633 N92-30664
Geometry of premixed flames in three-dimensional turbulence p 3633 N92-30666
Continuous wavelet analysis of coherent structures p 3634 N92-30673
New insights into large eddy simulation
[AD-A249424] p 3635 N92-30775
Tropical cyclone asymmetries as revealed by recent satellite microwave brightness temperatures
[AD-A249873] p 3679 N92-30867
Vortex flow aerodynamics
[AGARD-AR-299] p 3576 N92-30947

VORTICITY
A study of the topology of dissipating motions in direct numerical simulations of time-developing compressible and incompressible mixing layers p 3632 N92-30658

VORTICITY EQUATIONS
Numerical study of axial turbulent flow over long cylinders
[AD-A250801] p 3635 N92-30831

VSAT (NETWORK)
Advanced mobile satellite communications system using Ka and MM-wave bands in Japan's R and D satellite project p 3617 N92-30924

W

WAFERS
Double-sided wafer alignment techniques
[AD-A250757] p 3730 N92-30895

WALKING
Feasibility of a walk test to assess the cardiorespiratory fitness of Naval personnel
[AD-A250650] p 3684 N92-30603

WALL FLOW
A subgrid-scale model based on the second-order velocity structure function p 3631 N92-30651
A numerical evaluation of the dynamical systems approach to wall layer turbulence p 3632 N92-30660
Resonant instability of supersonic shear layers p 3632 N92-30661

WALLS
Numerical study of axial turbulent flow over long cylinders
[AD-A250801] p 3635 N92-30831
An investigation of the effects of boundary constraints on the sound insulations of lightweight, double leaf partitions
[BBC-RD-1992/4] p 3711 N92-31151
WARFARE
Stealth: A revolutionary change to air warfare
[AD-A249880] p 3617 N92-30869
WARNING SYSTEMS
Examination of aircraft warning and caution lights after shock testing
[NLR-TP-89284-U] p 3578 N92-30474
A cable detection lidar system for helicopters p 3648 N92-31068
WASTE DISPOSAL
Space station trash removal system
[NASA-CASE-MSC-21723-1] p 3588 N92-30315
Waste streams in a typical crewed space habitat: An update
[NASA-TM-103888] p 3689 N92-31166
Chemistry for protection of the environment, 8th International Conference proceedings
[DE92-014317] p 3674 N92-31181
WASTE ENERGY UTILIZATION
Thermal energy storage
[DE92-014942] p 3672 N92-31176
WASTE HEAT
Liquid droplet radiator: Design concepts and development logic
[MBB-UO-0165-91-PUB] p 3613 N92-30441
Thermal energy storage
[DE92-014942] p 3672 N92-31176
WASTE TREATMENT
Chemistry for protection of the environment, 8th International Conference proceedings
[DE92-014317] p 3674 N92-31181
WASTES
Algorithm to solve nonlinear time dependent problems of engineering and physics
[AD-A250641] p 3702 N92-30347
WATER
Determining water cloud particle sizes from lidar depolarization measurements and time dependent multiple scattering coefficients p 3641 N92-31034
WATER FLOW
Global existence for a semilinear elliptic-parabolic PDE system
[REPT-91-70] p 3628 N92-30372
Remote sensing satellite data use in run-off studies p 3668 N92-30914
Duration and rates of discharge: Maja Valles, Mars p 3737 N92-31227
WATER MANAGEMENT
Hydrologic modelling and use of remotely sensed data at CWPRS p 3669 N92-30918
WATER POLLUTION
National ocean pollution program: Summary of Federal programs and projects: FY 1989 update
[PB92-187012] p 3673 N92-30563
WATER QUALITY
On the remote sensing of water quality using the optical airborne scanner CAESAR
[BCRS-90-30] p 3666 N92-30466
Report of the Great Lakes Air Toxics Research Priorities Workshop
[PB92-166933] p 3673 N92-30602
WATER RESOURCES
Hydrologic modelling and use of remotely sensed data at CWPRS p 3669 N92-30918
WATER RUNOFF
Remote sensing satellite data use in run-off studies p 3668 N92-30914
WATER TUNNEL TESTS
The effects of free stream turbulence and surface curvature on boundary layer flow and heat transfer
[AD-A248846] p 3630 N92-30616
WATER VAPOR
The 2nd phase of the LEANDRE program: Water-vapor DIAL measurement p 3643 N92-31039
Advanced Raman water vapor lidar p 3643 N92-31040
Water vapor variance measurements using a Raman lidar p 3643 N92-31041
Airborne remote sensing of tropospheric water vapor using a near infrared DIAL system p 3644 N92-31042
An alexandrite regenerative amplifier for water vapor and temperature measurements p 3645 N92-31048
Raman lidar measurements of water vapor and aerosol/clouds during the FIRE/SPECTRE field campaign p 3652 N92-31089
BELINDA: Broadband Emission Lidar with Narrowband Determination of Absorption. A new concept for measuring water vapor and temperature profiles p 3653 N92-31091
DIAL simulations for satellite water vapor profile measurements within the BEST project p 3653 N92-31092
Airborne water vapor DIAL research: System development and field measurements p 3653 N92-31093
Alexandrite lidar for the atmospheric water vapor detection and development of powerful tunable sources in IR p 3653 N92-31094
WATERSHEDS
SCS method of runoff estimation using remote sensing techniques p 3668 N92-30916
WAVE DIFFRACTION
The diffraction of short free surface water waves, a uniform expansion
[REPT-92-06] p 3628 N92-30358
WAVE EQUATIONS
A new matrix formulation of classical electrodynamics. Part 1: Vacuum
[AD-A249643] p 3616 N92-30721
WAVE FUNCTIONS
Resolution properties of the Fourier method for discontinuous waves
[NASA-CR-189668] p 3706 N92-30716
Nuclear structure calculations for astrophysical applications
[DE92-011495] p 3740 N92-30856
WAVE PROPAGATION
Transverse pattern modification in a stable apertured laser resonator
[ITN-92-85171] p 3656 N92-30582
The RADLAC beam propagation experiment
[DE92-014620] p 3718 N92-30624
Low-level atmospheric flows studied by pulsed Doppler lidar p 3638 N92-31015
Fundamental studies of fusion plasmas
[DE92-015077] p 3726 N92-31116
WAVE REFLECTION
Validation of three-dimensional incompressible spatial direct numerical simulation code: A comparison with linear stability and parabolic stability equation theories for boundary-layer transition on a flat plate
[NASA-TP-3205] p 3573 N92-30295
WAVE RESISTANCE
The diffraction of short free surface water waves, a uniform expansion
[REPT-92-06] p 3628 N92-30358
WAVE-PARTICLE INTERACTIONS
Effect of wave-particle interaction on the outflow of ions at high latitudes
[NASA-CR-190560] p 3677 N92-30962
WAVEGUIDE LASERS
Waveguide polarizer using localized surface plasmons
[AD-D015258] p 3614 N92-30348
WAVEGUIDES
Backward-wave oscillator investigations in the Raman Regime
[AD-A250738] p 3622 N92-30332
WAVERIDERS
Navier-Stokes computations of a viscous optimized waverider
[NASA-CR-189658] p 3574 N92-30392
WEAK ENERGY INTERACTIONS
Non-perturbative effects in high-energy electroweak interactions
[NIKHEF-H/91-24] p 3715 N92-30697
WEAPON SYSTEMS
Stealth: A revolutionary change to air warfare
[AD-A249880] p 3617 N92-30869
First conclusions of a manufacturer group on the applicability of CALS in Europe p 3697 N92-30951
Practical application of the ILS: Practical integration, design, and logistics p 3697 N92-30955
WEAPONS
Three-dimensional shock wave physics simulations on massively parallel supercomputers
[DE92-008679] p 3698 N92-30363
WEAR TESTS
Development of a full-scale transmission testing procedure to evaluate advanced lubricants
[NASA-TP-3265] p 3658 N92-30396
WEATHER
On the potential use of the terminal Doppler weather radar gust front detection algorithm on the WSR-88D system. Part 2: Detecting non-gust front convergent weather phenomena
[DOT/FAA/NR-92/8,II] p 3678 N92-30496
Airborne lidar and radiometric observations of PBL- and low clouds p 3642 N92-31037
WEATHER FORECASTING
Clouds: Their prediction and simulation
[AD-A250643] p 3679 N92-30643
WEATHER STATIONS
ECLIPS at LMD: Preliminary results of phase 2 p 3643 N92-31038
WEIBULL DENSITY FUNCTIONS
Measuring the Weibull modulus of microscope slides p 3612 N92-30294
Effect of bending on the room-temperature tensile strengths of structural ceramics
[DE92-015196] p 3603 N92-30626
WEIGHT (MASS)
Molecular weight dependence of domain structure in silica-siloxane molecular composites
[DE92-015046] p 3603 N92-30544
WEIGHTING FUNCTIONS
Lidar measurement of optical turbulence: Theory of the crossed path technique
[AD-A248938] p 3720 N92-30343
Differential equations for symmetric generalized ultraspherical polynomials
[REPT-92-08] p 3702 N92-30360
WEIGHTLESSNESS SIMULATION
Light as a chronobiologic countermeasure for long-duration space operations
[NASA-TM-103874] p 3686 N92-31167
WELD STRENGTH
Impact testing of welded samples p 3608 N92-30268
WELDABILITY
Investigation of joining techniques for advanced austenitic alloys
[DE92-015545] p 3599 N92-30888
Filler metal development for Hastelloy alloy XR
[DE92-782044] p 3600 N92-31163
WELDED JOINTS
Impact testing of welded samples p 3608 N92-30268
Transport phenomena in welds
[DE92-013404] p 3659 N92-30587
Investigation of joining techniques for advanced austenitic alloys
[DE92-015545] p 3599 N92-30888
Filler metal development for Hastelloy alloy XR
[DE92-782044] p 3600 N92-31163
Phase transformations in weldments: New materials and new perspectives
[DE92-016231] p 3600 N92-31177
WETTABILITY
Ni-H2 cell separator matrix engineering
[NASA-CR-190055] p 3671 N92-30949
WHITE DWARF STARS
The origins of hot subdwarf stars p 3741 N92-30973
WIND (METEOROLOGY)
Development and testing of an air quality model for Mexico City
[DE92-011238] p 3673 N92-30520
The calculation of mid-latitude meridional neutral winds from an improved servo model approximation method
[AD-A249874] p 3676 N92-30868
A statistical comparison of AUTEC and Eleuthera Island wind data for the period 1 April 1989 through 30 March 1990
[AD-A248898] p 3679 N92-31003
Atmospheric wind sensing with a 1 and 2 micron coherent lidar p 3639 N92-31019
Evaluation of grounding and mooring points for Army aircraft
[AD-A250749] p 3579 N92-31193
WIND DIRECTION
Evaluation of microwave landing system approaches in a wide-body transport simulator
[NASA-CR-4450] p 3579 N92-30978
A statistical comparison of AUTEC and Eleuthera Island wind data for the period 1 April 1989 through 30 March 1990
[AD-A248898] p 3679 N92-31003
WIND EFFECTS
Resolution of the three-dimensional parabolic equation applied to acoustic propagation at low altitudes
[ONERA-RF-17/3641-PY] p 3711 N92-30966
WIND MEASUREMENT
Methodology investigation, implement remote sensing
[AD-A248901] p 3678 N92-30340
The calculation of mid-latitude meridional neutral winds from an improved servo model approximation method
[AD-A249874] p 3676 N92-30868
A statistical comparison of AUTEC and Eleuthera Island wind data for the period 1 April 1989 through 30 March 1990
[AD-A248898] p 3679 N92-31003
Doppler lidar wind measurement with the edge technique p 3638 N92-31017
Ground-based Doppler lidar of increased laser instability: Conception and design p 3650 N92-31078

WIND PROFILES
Methodology investigation, implement remote sensing [AD-A248901] p 3678 N92-30340
Tropospheric and stratospheric wind profiling with a direct detection Doppler lidar p 3639 N92-31018
Pulsed laser spectral measurement using a Fabry-Perot interferometer: Limits to resolution p 3646 N92-31055
WIND SHEAR
Methodology investigation, implement remote sensing [AD-A248901] p 3678 N92-30340
WIND TUNNEL MODELS
An analytical and experimental investigation of flutter suppression via piezoelectric actuation [NASA-TM-107653] p 3580 N92-31174
WIND TUNNEL TESTS
Joint computational and experimental aerodynamics research on a hypersonic vehicle [DE92-013439] p 3574 N92-30367
Two-dimensional aerodynamic characteristics of several polygon-shaped cross-sectional models applicable to helicopter fuselages [NASA-TP-3233] p 3574 N92-30394
Lewis icing research tunnel test of the aerodynamic effects of aircraft ground deicing/anti-icing fluids [NASA-TP-3238] p 3577 N92-30395
The effects of free stream turbulence and surface curvature on boundary layer flow and heat transfer [AD-A248846] p 3630 N92-30616
On-line analysis capabilities developed to support the AFW wind-tunnel tests [NASA-TM-107651] p 3580 N92-30752
Intersecting shock-wave/turbulent boundary-layer interactions at Mach 8.3 [NASA-TM-103909] p 3635 N92-30765
An experimental study of the relationship between velocity and pressure fluctuations in a wing-body junction [AD-A249628] p 3577 N92-31122
A demonstration of passive blade twist control using extension-twist coupling [NASA-TM-107642] p 3664 N92-31155
An analytical and experimental investigation of flutter suppression via piezoelectric actuation [NASA-TM-107653] p 3580 N92-31174
WIND TURBINES
Yaw dynamics of horizontal axis wind turbines [DE92-001245] p 3670 N92-30837
WIND VELOCITY
A statistical comparison of AUTEC and Eleuthera Island wind data for the period 1 April 1989 through 30 March 1990 [AD-A248898] p 3679 N92-31003
WIND VELOCITY MEASUREMENT
Low-level atmospheric flows studied by pulsed Doppler lidar p 3638 N92-31015
Atmospheric wind sensing with a 1 and 2 micron coherent lidar p 3639 N92-31019
Design of a near-IR coherent lidar for high spatial and velocity resolution wind measurement p 3639 N92-31020
A compact high repetition rate CO2 coherent Doppler lidar p 3639 N92-31022
Phase noise in pulsed Doppler lidar and limitations on achievable single-shot velocity accuracy p 3639 N92-31024
A comparison of Ultra-Sensitive Coherent Detection (USCD) and heterodyne detection for a wind sensing application p 3640 N92-31025
WINDS ALOFT
The calculation of mid-latitude meridional neutral winds from an improved servo model approximation method [AD-A249874] p 3676 N92-30868
Tropospheric and stratospheric wind profiling with a direct detection Doppler lidar p 3639 N92-31018
Water vapor variance measurements using a Raman lidar p 3643 N92-31041
WING TIPS
Nonlinear aerodynamics and the design of wing tips [NASA-CR-190649] p 3577 N92-31157
WINGS
Modeling and analysis methodology for aeroelastically tailored chordwise deformable wings [NASA-CR-189620] p 3579 N92-30304
Influence of structural and aerodynamic modeling on flutter analysis and structural optimization [AD-A248487] p 3583 N92-30323
Nonlinear aerodynamics and the design of wing tips [NASA-CR-190649] p 3577 N92-31157
WINTER
Ice thickness observations, North American Arctic and subarctic, 1972-1973 and 1973-1974, part 8 [AD-A250830] p 3681 N92-30238
Laboratory simulation of fluid dynamical process related to winter arctic leads [AD-A252266] p 3682 N92-30593
WIRE
Fabrication of multifilament conductors: CVD processing of high Tc superconducting composite fibers [NASA-CR-184344] p 3591 N92-30711
A statistical rationale for establishing process quality control limits using fixed sample size, for critical current verification of SSC superconducting wire [DE92-014844] p 3661 N92-31120
WIRELESS COMMUNICATION
Direct sequence spread spectrum CDMA in shared spectrum applications p 3619 N92-30939
WIRING
Wiring for aerospace applications [NASA-TM-105777] p 3623 N92-30427
WOOD
Designing, engineering, and testing wood structures p 3593 N92-30270
WORDS (LANGUAGE)
Induced pictorial representations [AD-A248560] p 3687 N92-30336
WORK-REST CYCLE
Light as a chronobiologic countermeasure for long-duration space operations [NASA-TM-103874] p 3686 N92-31167
WORKLOADS (PSYCHOPHYSIOLOGY)
A principled approach to the measurement of situation awareness in commercial aviation [NASA-CR-4451] p 3686 N92-30306
KC-135 crew reduction feasibility demonstration simulation study. Volume 1: Function analysis and function reallocation [AD-A252265] p 3688 N92-30592
WORKSTATIONS
Network load of X terminals at CDF [DE92-011704] p 3699 N92-30812

X

X RAY ABSORPTION
Multiple scattering theory of x ray absorption. A review [DE92-622374] p 3716 N92-30798
X RAY ANALYSIS
An x ray microprobe based upon a close-coupled focal-spot/glass capillary arrangement [DE92-011886] p 3722 N92-31195
X RAY ASTRONOMY
Theory and measurement of the energy and risetime resolution of scintillation detectors in hard x ray area [ETN-92-91687] p 3720 N92-30504
Activities report of the Institute for Astronomy and Astrophysics at Technical University of Berlin (Germany, F.R.) [MITT-11] p 3740 N92-30506
X RAY BINARIES
Ultra high energy gamma rays and observations with CYGNUS/MILAGRO [DE92-015243] p 3743 N92-30627
X RAY FLUORESCENCE
An x ray microprobe based upon a close-coupled focal-spot/glass capillary arrangement [DE92-011886] p 3722 N92-31195
X RAY LASERS
Research studies on extreme ultraviolet and soft x ray lasers [AD-A249798] p 3657 N92-30784
X RAY SCATTERING
X ray scattering studies of non-equilibrium ordering processes [DE92-014006] p 3598 N92-30787
X RAY SPECTROSCOPY
Spectroscopic diagnosis of long-scale-length exploding-foil plasma in the presence of an intense radiation field [DE92-014718] p 3726 N92-31118
X RAY TUBES
An x ray microprobe based upon a close-coupled focal-spot/glass capillary arrangement [DE92-011886] p 3722 N92-31195
X RAYS
Program RELAX: A code designed to calculate atomic relaxation spectra of x rays and electrons [DE92-013751] p 3714 N92-30586
Research studies on extreme ultraviolet and soft x ray lasers [AD-A249798] p 3657 N92-30784
X ray radiation from hot dense plasmas and atomic processes [NIFS-PROC-9] p 3725 N92-30984
XENON FLUORIDE LASERS
Advanced Raman water vapor lidar p 3643 N92-31040

Y

YAG LASERS
Tropospheric and stratospheric wind profiling with a direct detection Doppler lidar p 3639 N92-31018
Design of a near-IR coherent lidar for high spatial and velocity resolution wind measurement p 3639 N92-31020
A comparison of Ultra-Sensitive Coherent Detection (USCD) and heterodyne detection for a wind sensing application p 3640 N92-31025
Fluorescence lidar multi-color imaging of vegetation p 3640 N92-31028
A geodetic laser radar rangefinder with 10(exp -7) resolution p 3641 N92-31029
An ultra-sensitive coherent detector capable of single photon detection for lidar applications p 3646 N92-31053
A high speed signal processing system for a diode-pumped YAG lidar p 3646 N92-31054
Tm,Ho:YAG laser with tunable range of 2.08-2.12 microns and its applications to spectroscopy p 3646 N92-31058
Theoretical simulation of a 2 micron airborne solid state laser anemometer p 3647 N92-31059
A portable lidar using a diode-pumped YAG laser p 3654 N92-31098
YAW
Yaw dynamics of horizontal axis wind turbines [DE92-001245] p 3670 N92-30837
YIELD
Vegetation conditions and yield indicators. Part 1: Main report [BCRS-91-26-PT-1] p 3667 N92-30471
YIELD STRENGTH
Measuring the Weibull modulus of microscope slides p 3612 N92-30294

Z

ZERO POINT ENERGY
Fluctuation-dissipation theorem in general relativity and the cosmological constant [DE92-013542] p 3740 N92-30705
ZINC
Cu-Zn binary phase diagram and diffusion couples p 3600 N92-30269

Typical Personal Author Index Listing

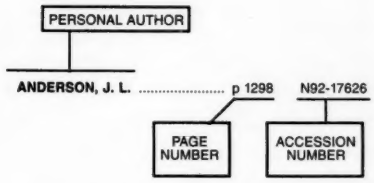

Listings in this index are arranged alphabetically by personal author. The page number helps you locate the citation in the abstract section. The accession number denotes the number by which the citation is identified.

A

AAMODT, R. E. ..... p 3726 N92-31116
ABAR, F. ..... p 3699 N92-30812
ABDALLAH, J. ..... p 3726 N92-31118
ABE, TAKAYUKI ..... p 3683 N92-30531
ABELSON, PHILIP H. ..... p 3733 N92-30974
ABERLE, JAMES T. ..... p 3621 N92-31156
ABHIRAMAN, AGARAM S. ..... p 3592 N92-30871
ABREU, VINCENT J. ..... p 3639 N92-31018
ABREVAYA, H. ..... p 3596 N92-31006
ABSHIRE, JAMES B. ..... p 3641 N92-31030
ACETO, S. C. ..... p 3726 N92-31197
ACHENBACH, J. D. ..... p 3661 N92-30693
ACLANDER, JAIME L. S. ..... p 3715 N92-30780
ADAMS, MARILYN JAGER ..... p 3686 N92-30306
ADAMS, RICHARD J. ..... p 3578 N92-30980
ADDY, HAROLD E., JR. ..... p 3577 N92-30395
ADOLF, D. ..... p 3605 N92-30804
AESCHLIMAN, D. P. ..... p 3574 N92-30367
AFEK, Y. ..... p 3695 N92-30522
AGARWAL, NAVAL K. ..... p 3628 N92-30390
AHRENS, THOMAS J. ..... p 3742 N92-30921
AIKEN, JOHN G. ..... p 3617 N92-30926
ALAM, S. ..... p 3596 N92-30882
ALBERTS, IAN L. ..... p 3715 N92-30680
ALDERFER, DAVID W. ..... p 3720 N92-30312
ALEJANDRO, S. ..... p 3639 N92-31022
p 3639 N92-31024
ALEKSEEV, A. I. ..... p 3732 N92-31145
ALEXANDER, K. B. ..... p 3599 N92-31112
ALKEMADE, J. A. H. ..... p 3614 N92-30354
ALLAIRE, P. E. ..... p 3613 N92-30692
ALLBROOKS, M. ..... p 3588 N92-31225
ALLCOCK, HARRY R. ..... p 3607 N92-31207
ALLEN, DAVID J. ..... p 3607 N92-30285
ALLEN, MARK ..... p 3733 N92-30889
ALLENDORF, M. A. ..... p 3594 N92-30369
ALLMAN, S. L. ..... p 3597 N92-31184
ALMAGRI, A. F. ..... p 3723 N92-30612
ALVAREZ, R. A. ..... p 3730 N92-31000
ALVAREZ, R. J., II ..... p 3644 N92-31046
AMARI, SACHIKO ..... p 3736 N92-31223
AMBROSE, JOHN ..... p 3682 N92-30413
AMIMOTO, SHERWIN ..... p 3640 N92-31025
p 3646 N92-31053
AMINI, ALI ..... p 3675 N92-30525
AMZAJERDIAN, FARZIN ..... p 3648 N92-31067
ANDERSON, K. D. ..... p 3617 N92-30876
ANDERSON, M. S. ..... p 3623 N92-30537
ANDO, A. ..... p 3714 N92-30501
p 3714 N92-30572
ANGELOVA, M. D. ..... p 3650 N92-31078
p 3650 N92-31079
ANIKEEV, V. B. ..... p 3713 N92-30403
p 3713 N92-30404
ANSELMO, F. ..... p 3713 N92-30415
ANSMANN, ALBERT ..... p 3641 N92-31033
p 3647 N92-31062
ANTONIADIS, H. ..... p 3729 N92-30748
APBLETT, ALLEN W. ..... p 3606 N92-31141
ARBAB, FARHAD ..... p 3699 N92-30696
ARMAND, SASAN C. ..... p 3659 N92-30571
ARMENTROUT, P. B. ..... p 3716 N92-30845
ARNEY, DAVID C. ..... p 3705 N92-30597
ARNOLDUS, HENK F. ..... p 3712 N92-30333
ARYA, R. ..... p 3727 N92-30247
ASAI, KAZUHIRO ..... p 3646 N92-31058
ASHURST, WILLIAM T. ..... p 3633 N92-30666
ASSADI, S. ..... p 3723 N92-30612
ASSINK, ROGER A. ..... p 3603 N92-30544
ATKINSON, D. R. ..... p 3588 N92-31225
ATTWOOD, MIKE C. ..... p 3708 N92-30419
p 3709 N92-30420
p 3709 N92-30442
ATZMON, SHARON ..... p 3721 N92-30581
AUBELE, JAYNE C. ..... p 3737 N92-31226
AUCIELLO, ORLANDO H. ..... p 3601 N92-30326
AUGENSTEIN, B. ..... p 3587 N92-30958
AUMASSON, CLAUDE ..... p 3694 N92-30512
AUPOIX, B. ..... p 3631 N92-30653

B

BABUSKA, I. ..... p 3662 N92-30338
BABUSKA, IVO ..... p 3701 N92-30339
BACH, BEVERLY ..... p 3620 N92-30943
BAIR, W. J. ..... p 3685 N92-31011
BAKER, J. ..... p 3673 N92-30602
BAKTASH, C. ..... p 3728 N92-30684
BALACHANDRAN, U. ..... p 3730 N92-30999
BALANIS, CONSTANTINE A. ..... p 3621 N92-31156
BALLARD, THEODORE R. ..... p 3676 N92-30868
BAMBUROV, N. S. ..... p 3713 N92-30404
BANKS, DANIEL W. ..... p 3628 N92-30387
BANTA, ROBERT M. ..... p 3638 N92-31015
BAO, X. J. ..... p 3730 N92-31000
BARAKAT, ABDALLAH R. ..... p 3677 N92-30962
BARBINI, R. ..... p 3655 N92-31103
BARGER, RAYMOND L. ..... p 3576 N92-30747
BARILLOT, PHILIPPE ..... p 3657 N92-30997
BARNES, A. G. ..... p 3584 N92-30769
BARNES, JOHN E. ..... p 3639 N92-31018
BARON, JUDSON R. ..... p 3585 N92-30897
BARON, KESSAG ..... p 3684 N92-30523
BARR, P. K. ..... p 3594 N92-30369
BARRON, ANDREW R. ..... p 3606 N92-31141
BARTEL, T. ..... p 3630 N92-30607
BASCARAN, E. ..... p 3670 N92-30330
BASU, ASIT P. ..... p 3660 N92-30237
BATES, ROY E. ..... p 3681 N92-30238
BATINA, JOHN T. ..... p 3574 N92-30393
p 3575 N92-30570
p 3575 N92-30691
BATY, R. S. ..... p 3636 N92-30903
BAUER, STEVEN X. S. ..... p 3628 N92-30387
BAUGH, D. A. ..... p 3623 N92-30537
BAUGHER, CHARLES R. ..... p 3588 N92-30301
BAUM, H. R. ..... p 3695 N92-30579
BAYLOR, L. R. ..... p 3724 N92-30810
BEAUCAGE, GREG ..... p 3603 N92-30544
BEAVAN, JOHN ..... p 3676 N92-30961
BECKA, G. A. ..... p 3627 N92-31144
BECKMAN, BRIAN C. ..... p 3695 N92-30543
BECKWITH, STEVEN V. W. ..... p 3733 N92-30974
BEDAIR, SALAH ..... p 3729 N92-30846
BEDELL, K. S. ..... p 3627 N92-31107
BEDFORD, TIM ..... p 3691 N92-30352
BEGGS, JOHN H. ..... p 3582 N92-30753
BEHRENDT, G. ..... p 3717 N92-31147
BELAND, ROBERT R. ..... p 3720 N92-30343
BELL, J. D. ..... p 3726 N92-31197
BELTON, M. J. S. ..... p 3739 N92-31236
BEN-DAVID, AVISHAI ..... p 3648 N92-31064
BENEDICT, J. V. ..... p 3688 N92-30844
BENGSTON, J. ..... p 3734 N92-30509
BENHENNI, M. ..... p 3716 N92-30853
BENNAHMIAS, M. ..... p 3729 N92-30885
BENOIST, RODNEY ..... p 3648 N92-31067
BERCAW, R. W. ..... p 3623 N92-30427
BERKHOUT, J. A. A. ..... p 3667 N92-30471
BERKOOZ, GAL ..... p 3632 N92-30660
BERNATOWICZ, THOMAS J. ..... p 3736 N92-31223
BERNDT, V. L. ..... p 3735 N92-31001
BERNSTEIN, R. ..... p 3743 N92-30828
BEUERMANN, K. ..... p 3740 N92-30506
BHANDARI, S. M. ..... p 3668 N92-30917
BHATTACHARYA, AMIYA ..... p 3699 N92-30526
BILELLO, MICHAEL A. ..... p 3681 N92-30238
BILLINGSLEY, J. B. ..... p 3616 N92-30863
BILTOFT, CHRISTOPHER A. ..... p 3678 N92-30340
BIRKMIRE, R. ..... p 3727 N92-30247
BIRMAN, KENNETH ..... p 3692 N92-30379
BIRNIE, STEVEN ANDREW ..... p 3586 N92-30715
BIRTCHER, CRAIG R. ..... p 3621 N92-31156
BISHOP, WILLIAM P. ..... p 3733 N92-30974
BISSINGER, N. C. ..... p 3575 N92-30676
BISSON, S. E. ..... p 3652 N92-31089
BISSONNETTE, L. R. ..... p 3642 N92-31035
BISSONNETTE, LUC R. ..... p 3641 N92-31031
BISWAS, RUPAK ..... p 3705 N92-30597
BLACK, D. ..... p 3738 N92-31232
BLAISDELL, G. A. ..... p 3631 N92-30653
BLANC, JEAN-YVES ..... p 3625 N92-30702
BLANC, PHILIPPE ..... p 3629 N92-30453
BLEADON, M. ..... p 3717 N92-30589
BLODGETT, D. S. ..... p 3695 N92-30550
BLOEMER, MARK J. ..... p 3614 N92-30348
BOCKER, R. P. ..... p 3616 N92-30721
BODALIA, R. ..... p 3601 N92-30250
BODLAENDER, HANS L. ..... p 3703 N92-30446
p 3703 N92-30450
p 3703 N92-30458
BOERMA, J. ..... p 3666 N92-30467
BOESENBERG, J. ..... p 3645 N92-31048
BOGDONOFF, SEYMOUR M. ..... p 3585 N92-30897
BOHEIM, KENNETH B. ..... p 3620 N92-30943
BOHLEN, R. ..... p 3587 N92-30440
BOMAR, J. B. ..... p 3688 N92-30844
BONNEE, W. J. A. ..... p 3578 N92-30474
BONNIER, D. ..... p 3648 N92-31066
BORCHARDT, H. ..... p 3644 N92-31043
BORDES, G. ..... p 3713 N92-30415
BORIS, J. P. ..... p 3635 N92-30775
BORMAN, GARY L. ..... p 3658 N92-30538
BORRA, E. ..... p 3652 N92-31087
BORRI, MARCO ..... p 3663 N92-30766
BOSSERT, R. ..... p 3717 N92-30589
BOTT, T. F. ..... p 3708 N92-31185
BOUBEL, D. ..... p 3697 N92-30954
BOWLES, KENNETH J. ..... p 3593 N92-30986
BOWMAN, C. T. ..... p 3593 N92-30256
BOYLE, MICHAEL E. ..... p 3688 N92-30615
BOZHKO, N. I. ..... p 3713 N92-30404
BRADSHAW, P. ..... p 3630 N92-30616
p 3631 N92-30654
BRAMLETTE, T. T. ..... p 3594 N92-30369
BRASCHE, L. J. H. ..... p 3598 N92-30858
BRATANOV, B. M. ..... p 3650 N92-31078
BRATT, PETER R. ..... p 3654 N92-31100
BREININGER, DAVID R. ..... p 3673 N92-30494
BRICOUT, F. A. ..... p 3596 N92-30882
BRODKIN, JUDITH S. ..... p 3599 N92-31110
BROKOPP, RICHARD A. ..... p 3584 N92-30508
BROOKS, REBECCA B. ..... p 3685 N92-30605
BROWELL, EDWARD V. ..... p 3653 N92-31093
BROWN, G. ..... p 3661 N92-31120
BROWN, M. A. ..... p 3736 N92-30575
BROWN, S. R. ..... p 3663 N92-30859
BROWNE, J. C. ..... p 3709 N92-30891
BRUBAKER, LINDA B. ..... p 3673 N92-30425
BRUECK, EKKES ..... p 3624 N92-30617
BRUNEAU, D. ..... p 3643 N92-31039
BRUNO, B. C. ..... p 3736 N92-31224
BRUSCAGLIONI, P. ..... p 3645 N92-31047
BRUSSAARD, B. K. ..... p 3734 N92-30486
p 3734 N92-30487
BRYAN, KURT ..... p 3704 N92-30516
BUCHMAN, A. ..... p 3598 N92-30872
BUCK, O. ..... p 3598 N92-30858
BUCKLEY, JOHN D. ..... p 3621 N92-31150
BUELL, J. C. ..... p 3633 N92-30664
BUNING, PIETER G. ..... p 3576 N92-30742

BUNNELL, L. ROY p 3607 N92-30265
BURBECK, CHRISTINA A. p 3687 N92-30325
BURCHELL, T. D. p 3592 N92-30809
BURGESON, JOHN C. p 3678 N92-30262
BURKHARDT, R. p 3612 N92-30378
BURNS, J. A. p 3705 N92-30638
BURNS, T. J. p 3696 N92-30886
BURROWS, LINDA M. p 3586 N92-30310
BURTON, NEIL A. p 3715 N92-30680
BUTLER, CAROLYN F. p 3653 N92-31093
BYERLY, RADFORD, JR. p 3733 N92-30974
BYRNE, JOHN H. p 3687 N92-30320

C

CABELL, R. H. p 3711 N92-30979
CABLE, S. p 3724 N92-30833
p 3725 N92-30884
CABOT, WILLIAM H. p 3630 N92-30649
p 3630 N92-30650
p 3631 N92-30651
CAI, Y. p 3660 N92-30860
CAI, ZHIHUA p 3603 N92-30553
CALDWELL, L. M. p 3644 N92-31046
CALLAHAN, D. L. p 3599 N92-31112
CALLEN, J. D. p 3726 N92-31002
CALOZ, GABRIEL p 3701 N92-30339
CAMBANIS, STAMATIS p 3708 N92-30633
CAMPBELL, J. F. p 3576 N92-30947
CANAVAN, G. H. p 3709 N92-30891
CANT, R. S. p 3597 N92-30668
CANTWELL, B. J. p 3632 N92-30658
CAO, D. S. p 3727 N92-30527
CAPBERN, ALAIN p 3648 N92-31068
CAPONE, D. W., II p 3661 N92-31120
CAPPIELLO, M. W. p 3589 N92-31204
CARCAGNO, R. H. p 3719 N92-30840
CARIOU, JEAN-PIERRE p 3647 N92-31059
CARNAL, C. L. p 3742 N92-30797
CARO, J. p 3625 N92-30730
p 3625 N92-30731
p 3625 N92-30732
CARPENTER, D. A. p 3722 N92-31195
CARPENTER, M. H. p 3576 N92-30909
CARPENTER, STEPHEN R. p 3673 N92-30425
CARR, L. p 3727 N92-30247
CARRERAS, B. A. p 3722 N92-30366
p 3723 N92-30576
CARSON, J. p 3717 N92-30589
CARSWELL, A. I. p 3649 N92-31070
CARTER, DONALD I. p 3585 N92-30897
CARY, J. R. p 3725 N92-30900
CASPER, T. A. p 3724 N92-30824
CASSONE, VINCENT M. p 3684 N92-30376
CASTIEL, DAVID p 3618 N92-30930
CASTOR, J. I. p 3740 N92-30855
CATALANO, A. p 3727 N92-30247
CATTO, P. J. p 3726 N92-31116
CERMIGNANI, W. p 3730 N92-30999
CHAN, HONG-MO p 3715 N92-30750
CHAN, KIN PUI p 3654 N92-31096
CHAN, KWAI S. p 3662 N92-30558
CHAN, WILLIAM M. p 3575 N92-30740
p 3576 N92-30741
p 3576 N92-30742
CHANG, CHAU-LYAN p 3573 N92-30295
CHANG, CHEIN-I. p 3695 N92-30629
CHANG, IKE p 3616 N92-30755
CHANG, R. P. p 3594 N92-30632
CHANG, STEPHEN p 3579 N92-30304
CHAPDELAINE, E. R. p 3581 N92-30303
CHAPIN, JOHN K. p 3687 N92-30613
CHASNOV, J. p 3633 N92-30663
CHASNOV, J. R. p 3634 N92-30671
CHAZETTE, P. p 3653 N92-31092
CHEN, B. p 3671 N92-31117
CHEN, BOR U. p 3720 N92-30248
CHEN, C. H. p 3727 N92-30527
p 3597 N92-31184
CHEN, C. J. p 3598 N92-30785
CHEN, J. H. p 3632 N92-30658
CHEN, PETER C. p 3705 N92-30618
p 3663 N92-30802
CHEN, S. S. p 3660 N92-30860
CHEN, SHUH RONG p 3730 N92-31217
CHEN, VICTOR C. p 3615 N92-30637
CHEN, Y. C. p 3691 N92-30296
CHEN, YUNMEI p 3707 N92-31135
CHENG, C. C. p 3595 N92-30821
CHEPILKO, N. M. p 3712 N92-30331
CHIDUME, C. E. p 3706 N92-31134
CHILDS, GWEN V. p 3685 N92-30719
CHING, J. p 3673 N92-30602
CHONG, M. S. p 3632 N92-30658
CHORNOBOY, EDWARD S. p 3678 N92-30559
CHOU, TSU-WEI p 3591 N92-30639
CHOWDHURY, MOSTAFIZ R. p 3593 N92-30287
CHOYKE, W. J. p 3595 N92-30821
CHRIEN, R. E. p 3724 N92-30806
CHRISEY, DOUGLAS B. p 3688 N92-30615
CHRISTENSEN, HEGE p 3683 N92-31152
CHRISTIAN, J. L., JR. p 3623 N92-30427
CHRISTOPHERSON, D. p 3661 N92-31120
CHUBB, DONALD L. p 3670 N92-30426
CHUMBLEY, L. S. p 3598 N92-30858
CHYBA, THOMAS H. p 3653 N92-31093
CIESLAK, M. J. p 3600 N92-31177
CLAFFEY, KERRN J. p 3682 N92-30832
CLARK, B. E. p 3581 N92-30524
CLARK, N. H. p 3626 N92-30807
CLARKE, JOHN G. p 3688 N92-30718
CLAUS, R. O. p 3721 N92-30975
CLEVERS, J. G. P. W. p 3666 N92-30467
CLIFF, E. M. p 3705 N92-30638
COFFEY, H. T. p 3660 N92-30860
COHEN, J. W. p 3705 N92-30689
COLAO, F. p 3655 N92-31103
COLE, J. J. p 3659 N92-30601
COLES, M. W. p 3718 N92-30786
COLLINS, J. p 3714 N92-30610
COLTRIN, M. E. p 3606 N92-30857
COMTE, P. p 3631 N92-30651
CONNERS, TIMOTHY R. p 3581 N92-30518
CONNOR, K. A. p 3726 N92-31197
COOK, G. p 3743 N92-31206
COOKSEY, DAVID L. p 3579 N92-31193
COOLBAUGH, M. T. p 3712 N92-30240
p 3712 N92-30261
COOMBS, C. R. p 3588 N92-31225
COOPER, DANIEL I. p 3649 N92-31069
COPELAND, CARL E. p 3621 N92-31150
CORNWELL, L. R. p 3612 N92-30290
COSTELLO, DANIEL J., JR. p 3587 N92-30709
COTTON, WILLIAM R. p 3679 N92-30643
COUCH, LANA M. p 3585 N92-30897
COULTER, K. P. p 3657 N92-30848
COULTRIP, ROBERT H. p 3621 N92-31150
COUPET, SOLANGE p 3704 N92-30473
COWAN, RICHARD L. p 3601 N92-30276
COX, A. N. p 3741 N92-31108
COZZENS, ROBERT F. p 3688 N92-30615
CRAIG, DOUGLAS F. p 3607 N92-30264
CRIST, C. E. p 3718 N92-30624
CRONIN, R. R. p 3734 N92-30509
CROSS, JON B. p 3731 N92-31220
CROUT, R. L. p 3667 N92-30545
CROWE, LAWSON p 3733 N92-30974
CROWELL, CYNTHIA A. p 3574 N92-30394
CROWELL, L. B. p 3588 N92-31225
CRUMP, LEONARD A., JR. p 3733 N92-30682
CRUMPLER, L. S. p 3737 N92-31226
CRUZ, CHRISTOPHER I. p 3586 N92-31160
p 3583 N92-31175
CRUZ, X. p 3673 N92-30520
CULLEN, D. E. p 3714 N92-30586
CULLEN, D. M. p 3728 N92-30684
CULLEN, VICKY p 3676 N92-30708
CUPITT, L. p 3673 N92-30602
CURWEN, P. W. p 3660 N92-30734
CYMERMAN, A. p 3684 N92-30328

D

DAHIYA, JAI N. p 3610 N92-30275
DAHL, CHARLES C. p 3611 N92-30289
DANDAN, R. A. p 3590 N92-30251
DANDY, D. S. p 3606 N92-30857
DANTZIG, G. B. p 3696 N92-30905
DAO, L. H. p 3605 N92-30817
DARYABEIGI, KAMRAN p 3720 N92-30312
DAS, RAJA p 3689 N92-30311
DATZ, S. p 3716 N92-30853
DAVENPORT, W. J. p 3577 N92-31122
DAVID, S. A. p 3659 N92-30587
DAVIDSON, DAVID L. p 3662 N92-30558
DAVIDSON, R. B. p 3734 N92-30509
DAVIES, M. E. p 3739 N92-31236
DAVIS, FRANCIS L. p 3615 N92-30583
DAVIS, J. BRADLEY p 3586 N92-30382
DAVIS, J. W. p 3696 N92-30905
DAVIS, JOANNA F. p 3604 N92-30794
DAVIS, ROBERT F. p 3601 N92-30326
p 3729 N92-30846
DAVIS, V. A. p 3588 N92-30628
DAVY, RANDALL D. p 3715 N92-30680
DAWSON, DONNA K. p 3580 N92-30878
DAWSON, VIRGINIA P. p 3732 N92-30908
DEAN, RICHARD A. p 3620 N92-30940
DEBERG, MARK p 3693 N92-30443
DEBOER, FRANK S. p 3615 N92-30448
DECKER, HARRY J. p 3658 N92-30396
DEFIGUEIREDO, RUI J. P. p 3698 N92-31154
DEFONTAINE, D. p 3600 N92-31138
DEFOUR, MARTIN p 3648 N92-31068
DEGRAAF, C. p 3625 N92-30731
p 3625 N92-30732
DEHEL, THOMAS F. p 3622 N92-31212
DEHON, R. A. p 3737 N92-31227
DEJONG, H. p 3693 N92-30476
DEKKING, F. M. p 3704 N92-30464
DELANOY, G. A. p 3671 N92-31117
DELCHAMPS, S. p 3717 N92-30589
DELEVA, A. p 3650 N92-31077
DELLIPRISCOLI, FRANCESCO p 3620 N92-30941
DELOMBARD, RICHARD p 3588 N92-30301
DELRE, ENRICO p 3620 N92-30941
DELRIEUX, Y. p 3711 N92-30966
DELUCHI, M. A. p 3674 N92-30770
DELUCIA, R. A. p 3581 N92-30303
DENHERTOG, D. p 3691 N92-30353
p 3693 N92-30455
DENN, FRED M. p 3679 N92-30735
DENTON, NANCY L. p 3611 N92-30284
DESCHOULEPNIKOFF, L. p 3644 N92-31044
DESSOUKY, K. p 3618 N92-30928
DEVALK, C. F. p 3682 N92-30470
DEVINE, J. A. p 3684 N92-30328
DEVREUGHT, J. P. M. p 3703 N92-30456
DEWAR, MICHAEL J. p 3598 N92-30864
DEWEESE, RICHARD p 3578 N92-30551
DEWS, PETER p 3733 N92-30974
DEYOUNG, RUSSELL J. p 3658 N92-30388
DHARCOURT, J. M. p 3662 N92-30338
DIAMOND, P. p 3629 N92-30560
DIAZ, A. p 3605 N92-30817
DICKMAN, J. E. p 3623 N92-30427
DIEHL, H. V. p 3717 N92-31137
DIELEMAN, P. p 3658 N92-30477
DIMOFTE, FLORIN p 3660 N92-30722
DIOT, CHRISTOPHE p 3690 N92-30701
DIPPOLITO, D. A. p 3726 N92-31116
DISILVESTRE, RAYMOND W. p 3643 N92-31040
DISMOND, HARRIET R. p 3637 N92-30737
DITTNER, P. F. p 3716 N92-30853
DIVECHA, AMARNATH P. p 3591 N92-30573
DIX, B. p 3639 N92-31022
DIXIT, S. N. p 3604 N92-30792
DOBBE, NILS p 3718 N92-30725
p 3718 N92-30726
DODGE, JEFFREY A. p 3607 N92-31207
DODIUK, H. p 3598 N92-30872
DOHERTY, MICHAEL P. p 3588 N92-30308
DOHOGNE, CAROLINE A. p 3659 N92-30571
DOMARADZKI, J. A. p 3634 N92-30672
DOMINGUEZ, N. p 3722 N92-30366
DOMOKOS, G. p 3630 N92-30604
DONOVAN, D. P. p 3649 N92-31070
DRAKE, J. B. p 3722 N92-30366
DREISCHUH, T. N. p 3650 N92-31076
p 3651 N92-31081
DRUMMOND, COLIN K. p 3582 N92-30998
DRUMMOND, J. PHILIP p 3576 N92-30909
DRUMMOND, MARK E. p 3701 N92-30710
DRYER, J. E. p 3718 N92-30786
DUBINSKY, RICHARD p 3648 N92-31067
DUBOWSKY, STEVEN p 3660 N92-30738
DUCHARME, STEPHEN p 3602 N92-30409
DUDLEY, ROSS A. p 3688 N92-30592
DUMEZ, B. p 3697 N92-30955
DUNLAP, M. A. p 3743 N92-31206
DURAN, R. S. p 3601 N92-30250
DURAND, P. p 3638 N92-31014
DUTT, A. p 3705 N92-30568
DUTT, D. S. p 3589 N92-30818
DUTTON, JOHN A. p 3733 N92-30974
DUYAR, AHMET p 3709 N92-30898
DYKE, J. M. p 3675 N92-30556

E

EATHERLY, W. P. p 3592 N92-30809
EBERHARD, WYNN L. p 3644 N92-31045
EBERLE, A. p 3575 N92-30676
ECK, A. p 3738 N92-31232
EDDLEMAN, H. p 3674 N92-30647
EDNER, H. p 3640 N92-31028
EFTEKHARI, ABE p 3662 N92-30317
EHRET, G. p 3644 N92-31042
EICHINGER, WILLIAM E. p 3649 N92-31069
EISEMAN, S. E. p 3717 N92-30398
EKIS, J. W. p 3711 N92-30890
EKLUND, E. A. p 3623 N92-30537
EKLUND, J. E. p 3598 N92-30785
EKLUND, W. p 3612 N92-30378
EL-GIZAWY, A. S. p 3598 N92-30865
p 3606 N92-30866

EL-MASRY, NADIA ..... p 3729 N92-30846
EL-SHARAWY, EL-BUDAWY ..... p 3621 N92-31156
ELLESTAD, MYRVIN H. ..... p 3684 N92-30523
ELOURAGINI, S. ..... p 3643 N92-31038
ELOURAGINI, SALEM ..... p 3649 N92-31074
EMBURY, J. D. ..... p 3590 N92-30521
ENG, R. S. ..... p 3646 N92-31056
p 3654 N92-31097
EPEMA, D. H. J. ..... p 3701 N92-30451
EPSTEIN, R. I. ..... p 3740 N92-30578
p 3743 N92-30706
ERICSON, M. N. ..... p 3742 N92-30797
ERICSSON, K. ANDERS ..... p 3578 N92-30980
ERSKINE, D. ..... p 3602 N92-30399
ERWIN, STEVEN C. ..... p 3624 N92-30630
ESAREY, ERIC ..... p 3656 N92-30614
p 3723 N92-30620
ESCHENAUER, H. A. ..... p 3579 N92-30424
ESTABROOK, P. ..... p 3618 N92-30928
ETKIN, A. ..... p 3717 N92-30398
EVANS, J. ..... p 3623 N92-30427
EVANS, JULIE ..... p 3686 N92-31167
EVANS, K. ..... p 3643 N92-31041
p 3652 N92-31089
EVANS, KEITH A. ..... p 3643 N92-31040
EVANS, N. ..... p 3728 N92-30574
EVERETT, L. ..... p 3701 N92-30778
EWING, ANDREW G. ..... p 3683 N92-30531
EZRA, GREGORY S. ..... p 3712 N92-30259

F

FAHLMAN, SCOTT E. ..... p 3734 N92-30324
FALTER, D. D. ..... p 3742 N92-30797
FALTER, K. G. ..... p 3742 N92-30797
FANG, H. E. ..... p 3698 N92-30363
FANG, RUSSELL J. F. ..... p 3618 N92-30929
FANNING, ARTHUR E. ..... p 3585 N92-30897
FARGE, M. ..... p 3634 N92-30673
FARLEY, G. L. ..... p 3592 N92-30906
FARR, STEVEN D. ..... p 3616 N92-30760
FARRELL, PATRICK V. ..... p 3658 N92-30538
FEATHER, J. B. ..... p 3579 N92-30978
FEDERHEN, HERBERT M. ..... p 3615 N92-30532
FEIGELSON, ROBERT S. ..... p 3624 N92-30617
FENDELMAN, CARMEN ..... p 3735 N92-30636
FENDLER, J. H. ..... p 3670 N92-30694
FENIMORE, E. E. ..... p 3743 N92-30706
FENKER, H. ..... p 3721 N92-31187
FENN, ALAN J. ..... p 3616 N92-30761
FENN, MARTA A. ..... p 3653 N92-31093
FENTON, B. C. ..... p 3581 N92-30303
FERBER, M. K. ..... p 3663 N92-30567
FERCONI, M. ..... p 3730 N92-31191
FERNANDO, H. J. ..... p 3682 N92-30593
FERRANDO, WILLIAM A. ..... p 3591 N92-30573
FERRARE, R. ..... p 3643 N92-31041
p 3652 N92-31089
FERRARE, RICHARD A. ..... p 3643 N92-31040
p 3653 N92-31090
FERREIRAPIRES, LUIS ..... p 3689 N92-30432
FERRICK, MICHAEL G. ..... p 3682 N92-30832
FERTALA, REMI ..... p 3648 N92-31068
FERZIGER, J. H. ..... p 3632 N92-30659
p 3633 N92-30667
FETTERER, F. M. ..... p 3667 N92-30545
FIESELMANN, B. ..... p 3727 N92-30247
FIFE, WILMER K. ..... p 3602 N92-30346
FINDEL, LEIF H. ..... p 3696 N92-30820
FINLEY, BRIAN D. ..... p 3588 N92-30301
FIORY, A. T. ..... p 3728 N92-30577
FISCHER, KEN W. ..... p 3639 N92-31018
FISHER, ALBERT M. ..... p 3691 N92-30352
FLAHERTY, JOSEPH E. ..... p 3705 N92-30597
FLAMANT, C. ..... p 3638 N92-31014
FLAMANT, P. ..... p 3638 N92-31014
FLAMANT, P. H. ..... p 3642 N92-31037
p 3643 N92-31038
FLAMANT, PIERRE H. ..... p 3649 N92-31074
FLATT, S. ..... p 3652 N92-31087
FLEETWOOD, D. M. ..... p 3728 N92-30585
FLEMING, D. P. ..... p 3660 N92-30734
FLESIA, C. ..... p 3642 N92-31036
p 3644 N92-31044
FLOOD, DENNIS J. ..... p 3670 N92-30426
FOGG, B. R. ..... p 3721 N92-30975
FOLEY, H. C. ..... p 3594 N92-30717
FOLEY, JAMES D. ..... p 3692 N92-30356
FOLEY, K. J. ..... p 3717 N92-30398
FONDA, L. ..... p 3716 N92-30798
FONTANA, MARIO ..... p 3589 N92-30818
FONTENLA, JUAN M. ..... p 3743 N92-31168
FORNASIER, LUCIANO ..... p 3573 N92-30675
FORTE, V. A., JR. ..... p 3684 N92-30328
FOSSUM, ERIC R. ..... p 3623 N92-30542
FOSTER, DAVID E. ..... p 3658 N92-30538
FOX, MARYE A. ..... p 3595 N92-30793
p 3598 N92-30864
FOX, ROBERT L. ..... p 3621 N92-31150
FRANK, MARK ..... p 3625 N92-30757
FRANKE, JOHN M. ..... p 3637 N92-30737
FRANZEN, WOLFGANG ..... p 3599 N92-31110
FRECHET, JEAN M. ..... p 3606 N92-30873
FREED, C. ..... p 3654 N92-31097
FRELIN, R. ..... p 3639 N92-31022
FRIED, D. ..... p 3706 N92-30789
FRIEDEN, B. R. ..... p 3616 N92-30721
FRIEDMAN, H. ..... p 3657 N92-31115
FRIEDMANN, T. A. ..... p 3730 N92-31000
FROST, C. A. ..... p 3718 N92-30624
FUJII, K. ..... p 3712 N92-30331
FUJISAWA, A. ..... p 3726 N92-30995
FUKUYAMA, ATSUSHI ..... p 3710 N92-30983
FURUKANE, UTARO ..... p 3722 N92-30431
FUZESY, R. Z. ..... p 3718 N92-30786

G

GAFFEY, M. J. ..... p 3737 N92-31228
GAGLIONE, ANTHONY ..... p 3706 N92-30776
GAHL, JOHN ..... p 3622 N92-30332
GALLIMORE, JENNIE J. ..... p 3686 N92-30254
GANDER, PHILIPPA ..... p 3686 N92-31167
GANGLOFF, RICHARD P. ..... p 3664 N92-31214
p 3665 N92-31215
GANNI, V. ..... p 3719 N92-30839
GAO, JIANRONG ..... p 3625 N92-30729
p 3625 N92-30730
p 3625 N92-30731
p 3625 N92-30732
GARBER, T. ..... p 3587 N92-30958
GARDNER, CHESTER S. ..... p 3651 N92-31084
GARDNER, D. R. ..... p 3698 N92-30363
GARDNER, JAMES E. ..... p 3608 N92-30263
GARLOW, R. K. ..... p 3614 N92-30300
GARMAN-DUVALLE, LISSA ..... p 3640 N92-31025
p 3646 N92-31053
GARN, PAUL A. ..... p 3588 N92-30736
GARNER, F. A. ..... p 3599 N92-30877
GARNER, R. C. ..... p 3641 N92-31034
p 3647 N92-31063
GARRETT, J. D. ..... p 3728 N92-30684
GARRIOTT, OWEN K. ..... p 3733 N92-30974
GARRISON, JAMES L. ..... p 3588 N92-30736
GARSTANG, MICHAEL ..... p 3674 N92-31153
GARVEY, JAMES F. ..... p 3712 N92-30240
p 3712 N92-30255
p 3712 N92-30261
GATHRIGHT, T. R. ..... p 3718 N92-30786
GAUDREAU, STEVEN L. ..... p 3735 N92-30584
GAZZA, GEORGE E. ..... p 3604 N92-30758
GEIJBERTS, M. H. J. ..... p 3637 N92-30688
GEIJSBERTS, M. ..... p 3636 N92-30365
GEIL, BRUCE R. ..... p 3730 N92-30895
GENTRY, BRUCE M. ..... p 3638 N92-31017
p 3646 N92-31055
GEORGE, A. ..... p 3720 N92-30507
GEORGE, T. J. ..... p 3671 N92-31113
GEORGE, THOMAS F. ..... p 3712 N92-30333
p 3629 N92-30548
p 3710 N92-30549
GERLACH, D. C. ..... p 3671 N92-31117
GERMANO, MASSIMO ..... p 3630 N92-30649
GERNSBACHER, MORTON A. ..... p 3621 N92-31129
GHIRINGHELLI, GIAN L. ..... p 3663 N92-30766
GIBSON, C. ..... p 3633 N92-30663
GIBSON, GARY G. ..... p 3679 N92-30735
GIESE, J. P. ..... p 3716 N92-30853
GIESKENS, DANIEL F. ..... p 3692 N92-30356
GILBERT, LEWIS E. ..... p 3676 N92-30961
GILL, T. P. S. ..... p 3599 N92-30888
GILLAND, JAMES H. ..... p 3588 N92-30308
GILLESPIE, JAMES B. ..... p 3650 N92-31075
GINLEY, D. S. ..... p 3730 N92-31000
GIRARD, L. ..... p 3652 N92-31087
GLASS, JEFFREY T. ..... p 3729 N92-30846
GLASSMAN, ARTHUR J. ..... p 3583 N92-31172
GLOWIENKA, J. C. ..... p 3726 N92-31197
GOEHRE, C. ..... p 3587 N92-30440
GOERLICH, HORST ..... p 3709 N92-30442
GOINS, RICHARD T. ..... p 3581 N92-30965
GOLDSMITH, J. E. M. ..... p 3652 N92-31089
p 3653 N92-31090
GOLSHAN, NASSER ..... p 3621 N92-30945
GOLUB, M. A. ..... p 3689 N92-31166
GONG, DELI ..... p 3603 N92-30635
GONIS, A. ..... p 3600 N92-31138
GOOD, TOM ..... p 3640 N92-31025
p 3646 N92-31053
GORETTA, K. C. ..... p 3730 N92-31190
GORIN, INNA ..... p 3643 N92-31040
GORMAN, THOMAS M. ..... p 3593 N92-30270
GOTSIS, P. K. ..... p 3592 N92-30779
GOTTLIEB, DAVID ..... p 3706 N92-30716
GOTTLIEB, S. A. ..... p 3716 N92-30841
GOURLAY, S. ..... p 3717 N92-30589
GOWDY, VAN ..... p 3578 N92-30551
GRAEBER, R. CURTIS ..... p 3686 N92-31167
GRANT, WILLIAM B. ..... p 3653 N92-31093
GRASSO, R. J. ..... p 3649 N92-31072
GRAU, RICHARD H. ..... p 3579 N92-31193
GRAY, DAVID L. ..... p 3734 N92-30386
GRAY, F. G. ..... p 3581 N92-30524
GRAY, J. A. ..... p 3594 N92-30749
GRCAR, JOSEPH F. ..... p 3707 N92-31189
GREEN, E. R. ..... p 3590 N92-30528
GREEN, W. A. ..... p 3590 N92-30528
GREENBERG, D. S. ..... p 3695 N92-30522
p 3700 N92-31111
GREENWOOD, PRISCILLA E. ..... p 3707 N92-30355
GRINSTEIN, F. F. ..... p 3635 N92-30775
GRINYUK, B. E. ..... p 3727 N92-30405
GRODSINSKY, C. M. ..... p 3613 N92-30692
GRONSKI, ROBERT S. ..... p 3584 N92-30508
GROOT, J. S. ..... p 3614 N92-30361
GROOTHUIZEN, R. J. P. ..... p 3693 N92-30476
GROSS, ROLF ..... p 3640 N92-31025
p 3646 N92-31053
GROSSMANN, BENOIST ..... p 3648 N92-31068
GROSSMANN, BENOIST E. ..... p 3653 N92-31093
GRUND, CHRISTIAN J. ..... p 3639 N92-31020
GRUNTHANER, FRANK J. ..... p 3623 N92-30542
GU, ZHEN ..... p 3709 N92-30898
GUARINO, V. ..... p 3655 N92-31109
GUAY, J. ..... p 3605 N92-30817
GUELER, O. ..... p 3691 N92-30353
GUEST, J. ..... p 3737 N92-31226
GUEZENNEC, Y. ..... p 3632 N92-30657
p 3634 N92-30673
GUIOCHON, G. ..... p 3604 N92-30695
GUMINA, STEPHANIE ..... p 3712 N92-30240
GUNNINK, J. ..... p 3667 N92-30471
GUNTHER, M. F. ..... p 3721 N92-30975
GUO, D. ..... p 3604 N92-30792
GUPTA, RAJENDRA ..... p 3594 N92-30645
GURDEV, L. L. ..... p 3651 N92-31081
GURIOLI, M. ..... p 3645 N92-31047
GUTLEBEN, H. ..... p 3595 N92-30821
GUTTMAN, C. M. ..... p 3604 N92-30788
GUZIK, J. A. ..... p 3741 N92-31108

H

HACKENBURG, R. W. ..... p 3717 N92-30398
HACKETT, ELIZABETH ..... p 3686 N92-31167
HADJIPANAYIS, G. C. ..... p 3600 N92-31186
HAFIZI, B. ..... p 3656 N92-30743
HAGARD, ARNE ..... p 3655 N92-31105
HAHN, W. ..... p 3655 N92-31106
HALBERSTAM, ISIDORE M. ..... p 3678 N92-30262
HALE, J. P., II ..... p 3688 N92-30381
HALL, M. L. ..... p 3589 N92-31204
HAMADA, Y. ..... p 3726 N92-30995
HAMAMOTO, NAOKAZU ..... p 3617 N92-30924
HAMILTON, M. L. ..... p 3599 N92-30877
HAMMOUD, A. N. ..... p 3623 N92-30427
HAMPTON, R. D. ..... p 3613 N92-30692
HANDSCHUH, R. F. ..... p 3660 N92-30948
HANFT, R. ..... p 3717 N92-30589
HANSEN, A. C. ..... p 3670 N92-30837
HANSON, R. K. ..... p 3593 N92-30256
HARDESTY, R. MICHAEL ..... p 3638 N92-31015
p 3644 N92-31045
HARIS, P. A. T. ..... p 3652 N92-31086
HARLOFF, G. J. ..... p 3582 N92-30972
HARNED, NANCY J. ..... p 3682 N92-30413
HARPER, CHARLES L., JR. ..... p 3678 N92-31229
HARRIMAN, ARTHUR E. ..... p 3685 N92-30605
HARRINGTON, B. C., III ..... p 3672 N92-31221
HARRIS, J. W. ..... p 3719 N92-31198
HARRIS, N. W. ..... p 3646 N92-31056
HARRIS, S. E. ..... p 3657 N92-30784
HARRISON, EDWIN F. ..... p 3679 N92-30735
HARRISON, G. ..... p 3578 N92-30565
HARTJES, F. G. ..... p 3636 N92-30365
p 3637 N92-30688
HARTZHEIM, W. ..... p 3579 N92-30424
HARVEY, J. ..... p 3629 N92-30560
HASSOON, S. ..... p 3593 N92-30245
p 3613 N92-30246
HASSOUN, JOHN A. ..... p 3688 N92-30592
HAWORTH, D. C. ..... p 3597 N92-30669
HAXTON, W. C. ..... p 3743 N92-31199
HAYASHI, T. ..... p 3722 N92-30385
p 3710 N92-30498

HAYASHI, TAKAYA ..... p 3722 N92-30384
HAYES, EDWARD J. ..... p 3619 N92-30933
HEAD, JAMES W. ..... p 3737 N92-31226
HEDIGER, TIMOTHY B. ..... p 3682 N92-30413
HEDMAN, SVEN G. ..... p 3575 N92-30713
HEDRICK, C. L. ..... p 3722 N92-30366
HEEG, JENNIFER ..... p 3580 N92-31174
HEERING, J. ..... p 3692 N92-30428
HEFFELFINGER, G. ..... p 3698 N92-30401
HEFFERNAN, STUART ..... p 3619 N92-30936
HEGNA, C. C. ..... p 3726 N92-31002
HEISER, WILLIAM H. ..... p 3585 N92-30897
HELLER, H. ..... p 3717 N92-31137
HELMICK, RONALD E. ..... p 3636 N92-30530
HENDERSON, SAMMY W. ..... p 3639 N92-31019
HENDERSON, T. R. ..... p 3614 N92-30300
HENDRY, A. W. ..... p 3716 N92-30841
HERMAN, IVAN ..... p 3699 N92-30696
HERMANS, A. J. ..... p 3628 N92-30358
HERRMANN, GUENTER ..... p 3591 N92-30690
HESS, ROBERT V. ..... p 3647 N92-31060
HESSE, PHILIP W. ..... p 3591 N92-30573
HEWETT, MARLE D. ..... p 3580 N92-31208
HEYERS, K. ..... p 3625 N92-30732
HIDEKUMA, S. ..... p 3725 N92-30992
HIGDON, NOAH S. ..... p 3653 N92-31093
HIGGINBOTHAM, SCOTT A. ..... p 3586 N92-30382
HILAND, J. ..... p 3587 N92-30958
HILL, C. W. ..... p 3727 N92-30527
HILL, EUGENE G. ..... p 3577 N92-30395
HILL, N. F. ..... p 3655 N92-31109
HILL, RALPH H. ..... p 3607 N92-30767
HILLENBRAND, CHRISTOPHER F. ..... p 3585 N92-31192
HILLS, S. W. ..... p 3661 N92-30763
HILLSMAN, VERNON S. ..... p 3611 N92-30284
HINKAMP, J. H. ..... p 3679 N92-31003
HISER, H. W. ..... p 3668 N92-30911
HO, C. ..... p 3743 N92-30706
HO, C. M. ..... p 3633 N92-30664
..... p 3634 N92-30673
HO, H. ..... p 3592 N92-30906
HOADLEY, SHERWOOD T. ..... p 3580 N92-30752
HOECKER, D. A. ..... p 3655 N92-31109
HOF, DOUG ..... p 3649 N92-31069
HOFFBAUER, MARK A. ..... p 3731 N92-31220
HOGENDOORN, R. A. ..... p 3667 N92-30475
HOLCOMB, R. S. ..... p 3589 N92-31012
HOLDER, DARRYL ..... p 3585 N92-30849
HOLLAND, MARJORIE M. ..... p 3673 N92-30425
HOLLAND, S. ..... p 3626 N92-30813
HOLLANDSWORTH, CLINTON E. ..... p 3587 N92-30257
HOLLIS, BRIAN R. ..... p 3635 N92-30751
HOLLOWAY, L. E. ..... p 3715 N92-30625
HOLMBERG, D. L. ..... p 3724 N92-30806
HOLT, R. J. ..... p 3657 N92-30848
HOLT, S. E. ..... p 3632 N92-30659
HOLTKAMP, DAVID ..... p 3649 N92-31069
HONG, MIN-CHUN ..... p 3707 N92-31135
HOOD, FRANK C. ..... p 3732 N92-30349
HOOGHIEMSTRA, GERARD ..... p 3707 N92-30355
HOOIE, D. T. ..... p 3672 N92-31221
HOOPER, WILLIAM P. ..... p 3648 N92-31065
HOPCROFT, JOHN E. ..... p 3691 N92-30260
HOPKINS, D. A. ..... p 3592 N92-30779
HORDINSKY, JERRY R. ..... p 3685 N92-30745
HORDUBAY, T. D. ..... p 3655 N92-31109
HORIUCHI, R. ..... p 3710 N92-30498
HORSTMAN, K. C. ..... p 3635 N92-30765
HORTON, LINDA L. ..... p 3610 N92-30278
..... p 3610 N92-30281
HOSHINO, K. ..... p 3714 N92-30510
..... p 3725 N92-30992
HOUGH, C. L. ..... p 3609 N92-30271
HOUSTON, PAUL L. ..... p 3715 N92-30681
HOWARD, DAVID J. ..... p 3728 N92-30574
HRKACH, JEFFREY S. ..... p 3601 N92-30244
HRUSA, WILLIAM J. ..... p 3706 N92-31128
HU, THOMAS S. ..... p 3663 N92-30870
HUANG, QIRONG ..... p 3651 N92-31082
HUBBARD, DAVID C. ..... p 3685 N92-30605
HUBBELL, STEPHEN P. ..... p 3673 N92-30425
HUBER, H. ..... p 3578 N92-30418
HUDDLESTON, R. L. ..... p 3663 N92-30823
HUDSON, B. J. ..... p 3735 N92-31132
HUDSON, J. G. ..... p 3674 N92-30707
HUFF, T. L. ..... p 3683 N92-30305
HUFFAKER, R. MILTON ..... p 3639 N92-31019
HUGGINS, A. W. F. ..... p 3686 N92-30306
HUGHES, EDWARD R. ..... p 3688 N92-30592
HUGHES, W. J. ..... p 3676 N92-30720
HUIJBERTS, H. J. C. ..... p 3694 N92-30478
HUISING, J. ..... p 3666 N92-30362
HULL, A. B. ..... p 3723 N92-30591
HUMMEL, J. R. ..... p 3649 N92-31072
HUMMER, CHARLES R. ..... p 3587 N92-30257
HUNGER, H. D. ..... p 3717 N92-31147
HUPP, JOSEPH T. ..... p 3595 N92-30875
HURRELL, JOHN P. ..... p 3636 N92-30412
HUSH, D. R. ..... p 3667 N92-30704
HUSS, G. R. ..... p 3738 N92-31230
HUTCHEON, I. D. ..... p 3738 N92-31230
HUTCHINSON, D. P. ..... p 3724 N92-30810
HUTT, D. L. ..... p 3642 N92-31035
..... p 3648 N92-31066
HWA, R. C. ..... p 3714 N92-30606
HWANG, DANNY P. ..... p 3627 N92-30297

I

ICHIE, K. ..... p 3641 N92-31029
ICHIGUCHI, K. ..... p 3725 N92-30985
ICHIKAWA, KENICHI ..... p 3606 N92-31146
IDA, K. ..... p 3716 N92-30967
..... p 3725 N92-30992
IDEMIZU, TAKESHI ..... p 3606 N92-31146
IGNATIEV, A. ..... p 3596 N92-30879
IGUCHI, H. ..... p 3726 N92-30995
IMBERT, BEATRICE ..... p 3647 N92-31059
INKOL, ROBERT J. ..... p 3624 N92-30683
INTERRANTE, LEONARD V. ..... p 3603 N92-30623
ISLER, R. C. ..... p 3726 N92-31197
ISMAIL, SYED ..... p 3653 N92-31093
ISOBE, SHUNKICHI ..... p 3617 N92-30924
ITABE, TOSHIKAZU ..... p 3646 N92-31058
ITOH, K. ..... p 3714 N92-30510
..... p 3725 N92-30985
ITOH, KIMITAKA ..... p 3710 N92-30983
ITOH, SANAE-I. ..... p 3714 N92-30510
..... p 3710 N92-30983
..... p 3725 N92-30985
ITSWEIRE, E. C. ..... p 3632 N92-30659

J

JACKSON, A. ..... p 3738 N92-31232
JACKSON, E. BRUCE ..... p 3586 N92-31160
..... p 3583 N92-31175
JACOBS, JAMES A. ..... p 3608 N92-30263
JACOBSEN, STEIN B. ..... p 3678 N92-31229
JACQUOT, J. P. ..... p 3697 N92-30956
JAECKEL, LOUIS A. ..... p 3696 N92-30723
JAMES, R. B. ..... p 3730 N92-31000
JANG, SEI-JOO ..... p 3624 N92-30598
JANKOWSKI, A. F. ..... p 3600 N92-31125
JANSEN, KLAUS ..... p 3703 N92-30446
..... p 3703 N92-30458
JANSSEN, T. J. B. M. ..... p 3625 N92-30731
JANVRIN, BRUCE ..... p 3603 N92-30635
JASINSKI, RACHEL ..... p 3588 N92-30736
JAYNE, DOUGLAS ..... p 3593 N92-30986
JEDREY, T. ..... p 3618 N92-30928
JELINEK, D. A. ..... p 3626 N92-30764
JELLISON, G. E., JR. ..... p 3728 N92-30577
..... p 3742 N92-30797
JENKINS, M. G. ..... p 3663 N92-30567
..... p 3603 N92-30626
JENSEN, D. R. ..... p 3648 N92-31065
JEONG, Y. I. ..... p 3595 N92-30835
JESSON, D. E. ..... p 3637 N92-30827
JIANG, H. ..... p 3595 N92-30835
JIANG, ZHIPING ..... p 3603 N92-30623
JIMENEZ, JAVIER ..... p 3633 N92-30665
JOHANSSON, J. ..... p 3640 N92-31028
JOHNSON, CHRISTOPHER S. ..... p 3595 N92-30875
JOHNSON, D. R. ..... p 3604 N92-30744
JOHNSON, J. P. ..... p 3630 N92-30616
JOHNSON, M. A. ..... p 3709 N92-31194
JOHNSON, N. R. ..... p 3728 N92-30684
JOHNSON, P. M. ..... p 3672 N92-30345
JOHNSON, SAMUEL D. JR. ..... p 3621 N92-31150
JOHNSON, WALTER A. ..... p 3636 N92-30412
JOLLIFFE, B. W. ..... p 3655 N92-31102
JONCKHEERE, EDMOND A. ..... p 3700 N92-30322
JONES, H. W. ..... p 3731 N92-30242
JONES, STEPHEN B. ..... p 3637 N92-30737
JOOSTEN, STEF ..... p 3693 N92-30433
JORGENSEN, G. ..... p 3671 N92-30896
JOSEPH, R. J. ..... p 3709 N92-30891
JOSLIN, RONALD D. ..... p 3573 N92-30295
JUN, CHUL-WON ..... p 3629 N92-30548
JUNG, J. ..... p 3663 N92-30859

K

KACHELMYER, A. L. ..... p 3654 N92-31097
KADISH, K. M. ..... p 3596 N92-31178
KAELBLING, LESLIE P. ..... p 3701 N92-30710
KALLIANPUR, GOPINATH ..... p 3708 N92-30633
KALONJI, G. ..... p 3597 N92-30588
KANEKO, O. ..... p 3714 N92-30501
..... p 3714 N92-30572
KANERVA, PENTTI ..... p 3690 N92-30724
KANO, T. ..... p 3640 N92-31027
KANT, GOOS ..... p 3703 N92-30449
KARL, ROBERT ..... p 3649 N92-31069
KARMARKAN, SUBHASH D. ..... p 3591 N92-30573
KARPLUS, ALAN K. ..... p 3607 N92-30279
KARUZA, SARUNAS K. ..... p 3636 N92-30412
KASSELS, C. G. M. ..... p 3628 N92-30373
KASSICIEH, SULEIMAN ..... p 3733 N92-30889
KATNIK, GREGORY N. ..... p 3586 N92-30382
KATO, T. ..... p 3716 N92-30967
KATZ, I. ..... p 3588 N92-30628
KATZ, J. D. ..... p 3606 N92-30847
KAUL, B. V. ..... p 3651 N92-31083
KAWASUMI, Y. ..... p 3726 N92-30995
KAWATA, S. ..... p 3722 N92-30430
KAZEM, SAYYED M. ..... p 3600 N92-30266
KEANE, C. J. ..... p 3726 N92-31118
KEE, R. J. ..... p 3606 N92-30857
KEELING, C. D. ..... p 3682 N92-30861
KEELTY, J. MALCOLM ..... p 3619 N92-30933
KEICHER, W. E. ..... p 3654 N92-31097
KEIL, LANNY ..... p 3686 N92-31167
KELLER, A. ..... p 3592 N92-30969
KELLER, J. O. ..... p 3594 N92-30369
KELLEY, HENRY L. ..... p 3574 N92-30394
KELLEY, M. S. ..... p 3737 N92-31228
KELLY, P. M. ..... p 3667 N92-30704
KENIK, E. A. ..... p 3599 N92-31112
KENKRE, V. M. ..... p 3606 N92-30847
KENNEDY, KEN ..... p 3689 N92-30311
KENNEDY, KEVIN J. ..... p 3617 N92-30869
KERLEY, J. ..... p 3612 N92-30378
KERRIDGE, J. F. ..... p 3738 N92-31231
KERSEY, ALAN D. ..... p 3722 N92-31213
KERST, D. W. ..... p 3723 N92-30612
KESMODEL, L. L. ..... p 3626 N92-30901
KHURI-YAKUB, B. T. ..... p 3727 N92-30252
KIEMLE, C. ..... p 3644 N92-31042
KIKUCHI, Y. ..... p 3599 N92-30888
KILLINGER, DENNIS ..... p 3653 N92-31095
KILLINGER, DENNIS K. ..... p 3654 N92-31096
KIM, J. ..... p 3632 N92-30657
KIM, J. S. ..... p 3738 N92-31231
KIM, KYUNG-HOON ..... p 3659 N92-30554
KIM, N. H. ..... p 3624 N92-30617
KIM, Y. ..... p 3738 N92-31231
KIMURA, SHIGERU ..... p 3617 N92-30927
KING, WENDELL C. ..... p 3677 N92-31009
KINGON, ANGUS I. ..... p 3601 N92-30326
KINGSTON, R. H. ..... p 3654 N92-31097
KINNEY, E. R. ..... p 3657 N92-30848
KIRCHNER, MARK E. ..... p 3585 N92-30897
KIRKS, KENNETH R. ..... p 3643 N92-31040
KIRLIN, PETER S. ..... p 3591 N92-30711
KITTIVER, CHARLES ..... p 3617 N92-30925
KLAVINS, P. ..... p 3729 N92-30885
KLEIN, R. E. ..... p 3682 N92-30470
KLEINERT-ALVARADO, G. ..... p 3731 N92-30421
KLINKHAMER, F. R. ..... p 3715 N92-30697
KLINT, P. ..... p 3692 N92-30428
KNIPP, DARREN ..... p 3591 N92-30641
KNOSPE, C. R. ..... p 3613 N92-30692
KNUDSON, T. ..... p 3708 N92-30419
KOBUSHKIN, A. P. ..... p 3712 N92-30331
KOCKS, U. F. ..... p 3590 N92-30521
..... p 3730 N92-31217
KOEKOEK, ROELOF ..... p 3702 N92-30360
KOELBEL, CHARLES ..... p 3689 N92-30311
KOENIG, G. G. ..... p 3641 N92-31034
KOEPKE, CZ. ..... p 3656 N92-30774
KOEPPL, ALOIS ..... p 3613 N92-30441
KOFF, BERNARD L. ..... p 3585 N92-30897
KOJIMA, M. ..... p 3725 N92-30992
KOK, JOOST N. ..... p 3615 N92-30448
KOKKE, J. M. M. ..... p 3666 N92-30466
KOKOTOVIC, PETER V. ..... p 3700 N92-30335
KOLAR, STANISLAV ..... p 3672 N92-30374
KOLAROV, G. ..... p 3650 N92-31077
KOLBE, R. L. ..... p 3635 N92-30775
KOLKMAN, H. J. ..... p 3578 N92-30474
KOLOS, KIMBERLY R. ..... p 3611 N92-30288
KOMEM, AMIR ..... p 3715 N92-30782
KOOIJ, ROBERT E. ..... p 3702 N92-30436
..... p 3704 N92-30490
KOOPMANN, B. E. ..... p 3696 N92-30892
KOOPMANN, C. ..... p 3708 N92-30419
KORB, C. L. ..... p 3645 N92-31049
KORB, C. LAURENCE ..... p 3638 N92-31017
KORDES, F. L. G. ..... p 3667 N92-30475
KORNREICH, PHILIPP ..... p 3597 N92-30534
KOSALY, G. ..... p 3633 N92-30667
KOSEFF, J. R. ..... p 3632 N92-30659
KOSKA, W. ..... p 3717 N92-30589

KOSTALOVA, MARIE p 3672 N92-30374
KOSTELECKY, V. A. p 3716 N92-30841
KOTULSKI, ZBIGNIEW p 3701 N92-31148
KOTZIN, MICHAEL p 3619 N92-30938
KOVALEV, V. A. p 3649 N92-31073
KOVESI-DOMOKOS, S. p 3630 N92-30604
KOWALCZYK, R. S. p 3657 N92-30848
KOZOL, J. p 3607 N92-30321
KRAFT, L. ALAN p 3589 N92-30989
KRALL, J. p 3614 N92-30407
KRATZ, K. L. p 3740 N92-30856
KRAUSE-POLSTORFF, J. p 3720 N92-30343
KRCH, GARY D. p 3658 N92-30316
KREBS, WILLIAM B. p 3708 N92-30771
KREPSKI, RICHARD P. p 3601 N92-30272
KRESIN, V. V. p 3621 N92-31007
KRICHBAUMER, W. p 3655 N92-31106
KRISHNAMURTHY, T. p 3661 N92-30309
KROO, ILAN p 3577 N92-31157
KRUEGER, D. A. p 3644 N92-31046
KRUER, W. L. p 3656 N92-30400
KRUMHANSL, J. A. p 3730 N92-31200
KRYTER, R. C. p 3742 N92-30797
KUAN, C. p 3660 N92-30948
KUCHNIR, M. p 3717 N92-30589
KUES, HENRY p 3686 N92-31127
KULLNIG, RUDOLPH p 3603 N92-30623
KUMAR, A. S. p 3599 N92-30877
KUMAR, AJAY p 3576 N92-30909
KUMAR, B. p 3624 N92-30619
KUNHARDT, ERICH E. p 3624 N92-30678
KUNZ, KARL S. p 3582 N92-30753
KUPER, JAN p 3693 N92-30433
KURODA, T. p 3714 N92-30501
p 3714 N92-30572
KUS, M. p 3606 N92-30847
KUSANO, K. p 3710 N92-30498
KUSSOY, M. I. p 3635 N92-30765
KUTSCHLOJENGA, F. J. p 3667 N92-30471
KUWASHIMA, S. p 3646 N92-31054
KUZNETSOV, A. L. p 3651 N92-31083
KWAN, ROBERT K. p 3614 N92-30300
KWON, DAEKEUN p 3603 N92-30623

L

LABONSKI, PAUL A. p 3682 N92-30413
LACY, BOB p 3640 N92-31025
p 3646 N92-31053
LACY, W. J. p 3674 N92-31181
LADERACH, G. E. p 3637 N92-30893
LAIRD, C. E. p 3596 N92-31161
LAKE, RENEE C. p 3664 N92-31155
LAMERS, J. T. p 3666 N92-30467
LAMM, M. p 3717 N92-30589
LANCE, BRIAN p 3659 N92-30554
LANDIECH, PHILIPPE p 3694 N92-30512
LANDRY, CHRISTOPHER C. p 3606 N92-31141
LANGDON, H. SCOTT p 3582 N92-30753
LANKFORD, JAMES p 3662 N92-30558
LAPOUTRE, J. A. p 3694 N92-30479
p 3694 N92-30480
LAPP, M. p 3652 N92-31089
LARIN, S. A. p 3715 N92-30687
LARKIN, MICHAEL J. p 3574 N92-30298
LAROCHELLE, V. p 3648 N92-31066
LARRABEE, JOHN F. p 3616 N92-30863
LATTIMER, J. M. p 3740 N92-30609
LAU, YAU Y. p 3683 N92-30531
LAUB, ALAN J. p 3700 N92-30334
LAUBEN, DAVID N. p 3607 N92-30267
LAUER, V. p 3625 N92-30731
LAVERNIA, E. J. p 3592 N92-30874
LAX, B. p 3646 N92-31056
LEADBETTER, R. R. p 3708 N92-30633
LEBOEUF, J. N. p 3722 N92-30366
LEBOULBAR, M. p 3697 N92-30952
LEE, CHARLES Y.-C. p 3661 N92-30529
LEE, H. p 3624 N92-30617
LEE, H. SANG p 3646 N92-31057
LEE, H.-J. p 3592 N92-30779
LEE, I. Y. p 3728 N92-30684
LEE, J. K. p 3729 N92-30748
LEE, J. W. p 3727 N92-30406
p 3603 N92-30594
p 3728 N92-30595
LEE, JA H. p 3658 N92-30388
LEE, S. p 3635 N92-30852
LEE, SANGSAN p 3630 N92-30650
p 3631 N92-30651
LEE, T. C. p 3670 N92-30330
LEE, WILLIAM C. Y. p 3619 N92-30937
LEI, J. p 3605 N92-30838
LEICHNER, S. A. p 3696 N92-30905
LEIDINGER, BERNHARD J. G. p 3587 N92-30440
LEIDINGER, BERNHARD, J. G. p 3613 N92-30441
LEIGHTON, TOM p 3699 N92-30586
LELE, S. K. p 3632 N92-30661
p 3635 N92-30852
LEMPICKI, A. p 3656 N92-30774
LENTZ, W. J. p 3649 N92-31071
LEONHARDT, TODD A. p 3593 N92-30986
LEOPOLD, RAY J. p 3617 N92-30926
LESHT, B. M. p 3708 N92-30803
LESTER, H. C. p 3711 N92-30979
LEV, VALY p 3619 N92-30938
LEVENDORSKII, S. p 3704 N92-30511
LEVESQUE, ALLEN H. p 3620 N92-30940
LEVI, MARK p 3622 N92-30249
LEVIN, SIMON A. p 3673 N92-30425
LEVINE, H. p 3629 N92-30560
LEVY, MILTON p 3597 N92-30759
LEWICKI, DAVID G. p 3658 N92-30396
LEWIS, D. W. p 3613 N92-30692
LEWIS, ROY S. p 3736 N92-31223
LI, H. p 3712 N92-30259
LI, HAIKUAN p 3694 N92-30484
p 3694 N92-30485
p 3694 N92-30492
LI, MING p 3708 N92-30699
LI, S. H. p 3727 N92-30527
LI, SHUANHU p 3628 N92-30372
LI, W. C. p 3718 N92-30786
LIANG, W. p 3605 N92-30838
LIAW, GOANG-SHIN p 3589 N92-30981
LICHTENBERG, ALLAN J. p 3710 N92-30983
LICHTENBERG, D. B. p 3716 N92-30841
LILLEY, J. R. p 3588 N92-30628
LILLINGTON, DAVID R. p 3672 N92-31216
LIN, K. W. p 3605 N92-30830
LINDENBAUM, S. J. p 3717 N92-30398
LINK, B. p 3740 N92-30578
LISSAK, BOAZ p 3656 N92-30582
LITT, JONATHAN S. p 3709 N92-30898
LITVIN, F. L. p 3660 N92-30948
LIU, CHENG p 3578 N92-30565
LIVINGSTON, JOHN M. p 3654 N92-31101
LLOYD, ISABEL K. p 3611 N92-30288
LOMMASSON, T. p 3727 N92-30247
LONGACRE, R. S. p 3717 N92-30398
LONGHURST, GLEN R. p 3598 N92-30834
LOOTSMA, F. A. p 3692 N92-30357
p 3707 N92-30452
p 3733 N92-30463
LOOYEN, W. J. p 3666 N92-30467
LOPEZ, A. R. p 3636 N92-30903
LOUDEN, B. S. p 3599 N92-30877
LOVE, W. A. p 3717 N92-30398
LOWE, ROLAND A. p 3670 N92-30426
LUBCHENCO, JANE p 3673 N92-30425
LUCAS, S. R. p 3595 N92-30821
LUCEY, P. G. p 3736 N92-31224
LUCKE, ROBERT L. p 3701 N92-30243
LUDWIG, RHEINHOLD p 3661 N92-30599
LUEBBERS, RAYMOND J. p 3582 N92-30753
LUFT, W. p 3670 N92-30519
LUJAN, M., JR. p 3717 N92-31201
LUNDEEN, CALVIN D. p 3608 N92-30268
LUNDIN, C. D. p 3599 N92-30888
LUNINE, JONATHAN p 3733 N92-30974
LUO, HUY p 3611 N92-30288
LUTFI, N. p 3668 N92-30913
LUU, T. T. p 3588 N92-30628
LWIN, Y. N. p 3730 N92-31190
LYCHAGIN, V. p 3706 N92-30790
LYNCH, V. E. p 3722 N92-30366
LYSAK, D. B. p 3652 N92-31086

M

MA, C. H. p 3724 N92-30810
MA, R. J. p 3602 N92-30409
MAAB, HARTMUT p 3686 N92-31167
MACAULEY, MOLLY K. p 3733 N92-30974
MACCRACKEN, M. C. p 3674 N92-31121
MACKENZIE, JOHN D. p 3721 N92-31126
MACMAHON, JAMES A. p 3673 N92-30425
MADDALON, DAL V. p 3628 N92-30390
MADDOX, S. R. p 3742 N92-30797
MADRID, PHILIP p 3607 N92-30267
MAEDA, H. p 3714 N92-30510
MAEDA, M. p 3653 N92-31094
MAHAJAN, S. M. p 3724 N92-30880
MAJTENYI, STEVEN I. p 3675 N92-30525
MAJUMDAR, D. p 3661 N92-30763
MAKAROV, G. S. p 3600 N92-31218
MALBEQUI, P. p 3711 N92-30966
MALEK, MIROSLAW p 3691 N92-30299
MALHOTRA, R. p 3738 N92-31232
MALKUS, DAVID S. p 3692 N92-30377
MALLET, J. C. p 3697 N92-30953
MALSTROM, R. A. p 3596 N92-30899
MALYSHEV, ALEXANDER N. p 3706 N92-30700
MAMAKOS, WILLIAM A. p 3643 N92-31040
MANGALAM, SIVA M. p 3628 N92-30390
MANIZADE, SERDAR S. p 3641 N92-31030
MANKOC-BORSTNIK, N. p 3731 N92-30799
p 3731 N92-30800
p 3711 N92-30801
MANSOUR, N. N. p 3631 N92-30655
p 3631 N92-30656
MANUEL, GREGORY S. p 3720 N92-30312
MARATHE, G. T. p 3669 N92-30920
MAREES, G. p 3666 N92-30466
p 3667 N92-30472
MARGALIT, ELI p 3648 N92-31067
MARIELLA, R. P., JR. p 3729 N92-30854
MARSDEN, JERROLD E. p 3705 N92-30533
MARSHALL, D. B. p 3601 N92-30342
MARTEL, CARLOS p 3633 N92-30665
MARTI, K. p 3738 N92-31231
MARTIN, CHARLES R. p 3603 N92-30553
p 3605 N92-30838
p 3607 N92-31207
MARTIN, JAY K. p 3658 N92-30538
MARTYNOV, E. S. p 3711 N92-30236
MARUYAMA, N. p 3660 N92-30948
MARVIN, JOSEPH G. p 3636 N92-30982
MARX, ROSE p 3712 N92-30337
MASAI, K. p 3726 N92-30995
MASON, MARK W. p 3606 N92-31141
MASSARWEH, W. p 3609 N92-30271
MASSETH, J. p 3660 N92-30948
MATHEW, F. T p 3669 N92-30918
MATSON, PAMELA A. p 3673 N92-30425
MATSUMOTO, H. p 3646 N92-31054
p 3654 N92-31098
MATTAS, R. F. p 3723 N92-30591
MATYJASZEWSKI, KRZYSZTOF p 3601 N92-30244
MAUCLAIRE, GERARD p 3712 N92-30337
MAUREY, J. R. p 3604 N92-30788
MAYFIELD, M. J. p 3672 N92-31221
MAYOR, SHANE D. p 3653 N92-31093
MAYTAL-BECK, SHARON p 3714 N92-30580
MAZARAKIS, M. G. p 3718 N92-30624
MAZUMDAR, S. p 3604 N92-30792
MAZUR, P. p 3717 N92-30589
MCCABE, PATRICK K. p 3735 N92-30819
MCCARTY, K. F. p 3730 N92-31000
MCCLELLAND, H. T. p 3609 N92-30274
MCCLUG, WILLIAM D., JR. p 3659 N92-30554
MCCLUNG, R. W. p 3604 N92-30744
MCCONAGHY, C. F. p 3729 N92-30854
MCCORMICK, M. PATRICK p 3637 N92-31013
MCCOY, JEFFREY H. p 3679 N92-30867
MCCOY, ROBERT A. p 3600 N92-30269
MCCUEN, RICHARD H. p 3611 N92-30288
MCCULLOUGH, ROY L. p 3591 N92-30639
MCCUNE, W. p 3705 N92-30608
MCDONALD, H. p 3659 N92-30640
MCGILL, MATT J. p 3639 N92-31018
MCGOWAN, F. K. p 3728 N92-30684
MCGRATTAN, K. B. p 3695 N92-30579
MCGRAW, SANDRA M. p 3580 N92-30752
MCINTOSH, ROBERT E. p 3622 N92-31180
MCKINNEY, THEOS D., JR. p 3687 N92-30488
MCMURRY, P. H. p 3675 N92-31163
MCNAIR, L. A. p 3673 N92-30520
MCNICHOLL, P. p 3639 N92-31022
p 3639 N92-31024
MCWHORTER, P. J. p 3728 N92-30585
MEEKS, E. p 3606 N92-30857
MEGIE, G. p 3653 N92-31092
MEHTA, RAJEEV p 3661 N92-30529
MEIJER, H. G. p 3702 N92-30350
MEISEL, L. V. p 3709 N92-31194
MELFI, S. H. p 3638 N92-31016
p 3643 N92-31041
p 3652 N92-31089
MELFI, S. HARVEY p 3643 N92-31040
MELILLO, JERRY M. p 3673 N92-30425
MELL, W. E. p 3633 N92-30667
MELNGAILIS, JOHN p 3627 N92-31004
MELNIK, ROBERT E. p 3585 N92-30897
MENAKER, MICHAEL p 3686 N92-31143
MENEGAUX, EDMOND C. p 3611 N92-30288
MENENGER, L. p 3643 N92-31038
MENEVEAU, C. p 3634 N92-30673
MENON, SURESH p 3581 N92-30569
MERCER, STEPHEN C. p 3585 N92-30897
MERLIN, R. p 3729 N92-30772
MERLINI, TEODORO p 3663 N92-30766
MERMAGEN, TIMOTHY J. p 3730 N92-30895
MERRITT, M. p 3695 N92-30522
MEULDIJK, D. p 3667 N92-30471
MICHAELIS, W. p 3653 N92-31091

MICHAELIS, WALFRIED p 3641 N92-31033
p 3647 N92-31062
MICHALSKI, K. A. p 3615 N92-30408
MIDDELHOEK, J. p 3625 N92-30730
MIKULSKI, BARBARA p 3735 N92-31169
MILES, R. N. p 3664 N92-30988
MILLER, FRANK p 3619 N92-30939
MILLER, M. p 3587 N92-30958
MILLER, S. L. p 3728 N92-30585
MILLS, G. A. p 3594 N92-30717
MILSTEIN, LAURENCE B. p 3619 N92-30939
MILTON, M. J. T. p 3655 N92-31102
MINATO, ATSUSHI p 3652 N92-31088
MINER, PAUL S. p 3699 N92-30677
MIRICK, PAUL H. p 3664 N92-31155
MISTRETTA, IGNAZIO p 3620 N92-30941
MITSCHKER, A. p 3717 N92-31137
MITSEV, TS. p 3650 N92-31077
MIURA, Y. p 3714 N92-30510
p 3725 N92-30992
MIZUSHIMA, Y. p 3641 N92-31029
MOELLER, P. p 3740 N92-30856
MOFFAT, R. J. p 3630 N92-30616
MOHAMED, F. A. p 3592 N92-30874
MOHLER, R. R. p 3583 N92-30922
MOIN, P. p 3635 N92-30852
MOIN, PARVIZ p 3630 N92-30649
p 3630 N92-30650
p 3635 N92-30831
MOLENAAR, J. p 3693 N92-30429
MOLIAN, ARUL p 3603 N92-30635
MOLIAN, P. p 3603 N92-30635
MOORE, GARY p 3744 N92-30327
MOOSMUELLER, H. p 3649 N92-31073
MORFIN, J. p 3719 N92-31219
MORI, M. p 3714 N92-30510
p 3725 N92-30992
MORRIS, T. W. p 3717 N92-30398
MORRISH, ART p 3604 N92-30685
MORRISON, J. T. p 3581 N92-30524
MORSE, J. D. p 3729 N92-30854
MORTON, J. p 3592 N92-30906
MOSER, R. p 3632 N92-30658
MOSER, R. D. p 3633 N92-30662
p 3633 N92-30664
MOSER, ROBERT D. p 3635 N92-30831
MOTTLEY, CAROLYN p 3595 N92-30875
MOTTOLA, E. p 3740 N92-30705
MOUNT, DAVID M. p 3689 N92-30907
MUELLER-REMMERS, P. p 3587 N92-30440
MUELLER, HUBERT p 3583 N92-30439
MUELLER, R. p 3731 N92-30421
p 3587 N92-30440
MUENKEL, C. p 3644 N92-31043
MUGNAI, A. p 3644 N92-31044
MUGWANEZA, LEON p 3694 N92-30493
MUKKAMALA, R. p 3698 N92-30960
MUKUNDA, H. S. p 3576 N92-30909
MULDERS, M. A. p 3666 N92-30362
MULLER, M. p 3581 N92-30303
MUNDT, CHRISTIAN p 3634 N92-30674
MUNGAL, M. G. p 3593 N92-30256
MUNRO, J. K. p 3742 N92-30797
MUNTEAN, TRAIAN p 3694 N92-30493
MURAKAMI, M. p 3724 N92-30810
p 3726 N92-31197
MURAOKA, K. p 3653 N92-31094
MURPHY, K. A. p 3721 N92-30975
MURTHY, K. M. SUNDARA p 3618 N92-30931
MURTHY, P. L. N. p 3592 N92-30779
MYERS, I. T. p 3623 N92-30427
MYERS, PHILLIP S. p 3658 N92-30538
MYRA, J. R. p 3726 N92-31116

N

NABOKO, V. N. p 3650 N92-31078
NAEGELI, DAVID W. p 3607 N92-30767
NAEIJE, M. C. p 3666 N92-30465
NAGLER, S. E. p 3598 N92-30787
NAKAJIMA, HAJIME p 3600 N92-31163
NAKAJIMA, N. p 3725 N92-30994
NAKAJIMA, NORIYOSHI p 3713 N92-30500
NAKAJIMA, NORIYSHI p 3723 N92-30499
NAKAMURA, HIROO p 3602 N92-30502
NAKAMURA, Y. p 3725 N92-30994
NAKASHIMA, H. p 3722 N92-30430
NAKAYAMA, KEN p 3687 N92-30679
NAMSRAI, K. p 3732 N92-31136
NARAYANAN, M. S. p 3668 N92-30917
NARIHARA, K. p 3725 N92-30991
NASIATKA, J. p 3655 N92-31109
NAVE, S. E. p 3596 N92-30899
NEITZERT, HEINZ-CHRISTOPH p 3727 N92-30505
NELLIS, W. p 3602 N92-30399
NELSON, HAROLD, JR. p 3579 N92-31211
NEU, C. E. p 3607 N92-30321
NEVES, JOAO C. p 3635 N92-30831
NEWELL, ALLEN p 3734 N92-30324
NEWMAN, B. A. p 3727 N92-30406
p 3603 N92-30594
p 3728 N92-30595
NEWMAN, JAMES C., JR. p 3664 N92-30964
NEWMAN, KATHIE E. p 3728 N92-30634
NEWNAM, B. E. p 3657 N92-31182
NIEDRA, J. M. p 3623 N92-30397
NIELSEN, NORMAN B. p 3654 N92-31101
NIEMI, EUGENE E., JR. p 3573 N92-30239
NIEUWENHUIS, G. J. A. p 3667 N92-30471
NIJMEIJER, H. p 3694 N92-30478
NIKOLAEV, N. N. p 3713 N92-30364
NITSCHKE, F. p 3671 N92-30970
NIX, J. R. p 3740 N92-30856
NIXON, MARK W. p 3664 N92-31155
NOBREGA, F. p 3718 N92-30646
NODA, NOBUAKI p 3602 N92-30502
NOMURA, A. p 3640 N92-31027
NORDHOFF, MANFRED p 3709 N92-30442
NOREEN, GARY K. p 3620 N92-30942
NOTARI, ANTHONY p 3646 N92-31055
p 3646 N92-31057
NOVAKOV, T. p 3674 N92-30647
NTUEN, CELESTINE A. p 3573 N92-30253
p 3573 N92-30258
NUCKOLLS, C. p 3625 N92-30757

O

OBARA, CLIFFORD J. p 3720 N92-30312
OBERKAMPF, W. L. p 3574 N92-30367
OBRIEN, J. C. p 3729 N92-30885
OCONNELL, R. F. p 3627 N92-31210
ODA, TOSHIATSU p 3722 N92-30431
ODONNELL, R. G. p 3664 N92-30963
OESTREICH, LINDA L. p 3735 N92-30636
OFFENBERG, M. p 3625 N92-30731
OGAWA, I. p 3641 N92-31029
OGIHARA, MASAHIRO p 3606 N92-31146
OHALLORAN, T. A. p 3715 N92-30625
OHANDLEY, R. C. p 3597 N92-30588
OHMORI, SHINGO p 3617 N92-30924
OHTSUKI, Y. p 3710 N92-30549
OKA, Y. p 3714 N92-30501
p 3714 N92-30572
OKABE, YUSHIROU p 3717 N92-30990
OKAMOTO, M. p 3725 N92-30994
OKAMOTO, MASAO p 3723 N92-30499
p 3713 N92-30500
OKANO, F. p 3714 N92-30510
OKUMURA, H. p 3646 N92-31054
p 3654 N92-31098
OLIVIER, BERNARD J. p 3603 N92-30544
OLIVIER, LISA D. p 3638 N92-31015
OLSDER, GEERT JAN p 3704 N92-30491
p 3704 N92-30517
OLSEN, C. p 3593 N92-30245
OLSON, ANNETTE M. p 3673 N92-30425
ONG, T. P. p 3594 N92-30632
OOSTERLEE, C. W. p 3628 N92-30373
p 3629 N92-30454
p 3629 N92-30462
OPPENHEIM, A. K. p 3595 N92-30814
ORAN, E. S. p 3635 N92-30775
OREF, I. p 3613 N92-30246
OREILLY, C. p 3699 N92-30812
ORLETSKY, D. p 3587 N92-30958
OROURKE, P. E. p 3596 N92-30899
OSBORN, JOHN E. p 3701 N92-30339
OSBORN, KEVIN p 3659 N92-30554
OSHER, STANLEY p 3702 N92-30347
OSKAM, D. p 3666 N92-30465
OVERMARS, M. H. p 3694 N92-30479
OVERMARS, MARK p 3693 N92-30443
OVERMARS, MARK H. p 3703 N92-30447
OVERTON, W. S. p 3707 N92-30562

P

PABST, W. p 3709 N92-30420
PAINE, DAVID C. p 3728 N92-30574
PALAMIDESSI, CATUSCIA p 3615 N92-30448
PALEVSKY, ALAN p 3626 N92-30836
PALM, STEPHEN P. p 3638 N92-31016
PALMER, L. C. p 3619 N92-30934
PALUCCI, A. p 3655 N92-31103
PAN, W. Y. p 3605 N92-30830
PANDEY, LAKSHMI N. p 3710 N92-30549
PANI, E. A. p 3737 N92-31227
PANNEKOEK, J. G. p 3636 N92-30365
p 3637 N92-30688
PARK, EUI H. p 3573 N92-30253
p 3573 N92-30258
PARK, J. C. p 3679 N92-31003
PARKS, STEVEN J. p 3576 N92-30742
PARMAR, DEVENDRA S. p 3662 N92-30317
PARSONS, E. L. p 3672 N92-31221
PASSAMANTE, ANTHONY P. p 3682 N92-30413
PATTERSON, JOHN W. p 3611 N92-30286
PATTON, JANET J. p 3733 N92-31209
PAUL, LORI p 3617 N92-30923
PEARSON, CHARLES E. p 3669 N92-31139
PEARSON, GUY N. p 3639 N92-31021
PEIFER, WILLIAM R. p 3712 N92-30255
PELLISSIER, P. F. p 3718 N92-30786
PELON, J. p 3638 N92-31014
p 3642 N92-31037
p 3643 N92-31038
p 3643 N92-31039
p 3653 N92-31092
PENG, JIAN p 3621 N92-31156
PENNER, J. E. p 3674 N92-30647
PENNISTON, R. R. p 3624 N92-30590
PENNYCOOK, S. J. p 3637 N92-30827
PERENBOOM, J. A. A. J. p 3625 N92-30731
PEREZ, LANCE C. p 3587 N92-30709
PERRY, A. E. p 3632 N92-30658
PERSSON, ROLF p 3655 N92-31105
PETERS, H. C. p 3682 N92-30470
PETRESKY, J. p 3633 N92-30663
PETRO, ANDREW J. p 3588 N92-30315
PEW, RICHARD W. p 3686 N92-30306
PHAIR, D. J. p 3695 N92-30550
PHAM, H. p 3661 N92-30763
PHILBRICK, C. R. p 3652 N92-31086
PHILIPS, LAURA A. p 3712 N92-30259
PHILLIPS, ROGER J. p 3738 N92-31233
PHILLIPS, W. MORRIS p 3621 N92-31150
PIASCIK, ROBERT S. p 3664 N92-31214
p 3665 N92-31215
PICKERELL, THOMAS p 3579 N92-31211
PICKHOLTZ, RAYMOND L. p 3619 N92-30939
PICOLOGLOU, B. F. p 3723 N92-30591
PIERRE, LAURENCE p 3704 N92-30473
PIKE, COREY p 3619 N92-30935
PINSKI, F. J. p 3599 N92-31119
PIOMELLI, UGO p 3630 N92-30649
p 3630 N92-30650
PITCHER, C. S. p 3723 N92-30746
PLANCHE, O. p 3633 N92-30667
PLAT, NICO p 3692 N92-30359
PLATNER, E. D. p 3717 N92-30398
PLEAS, JOHN p 3684 N92-30603
p 3685 N92-30644
PLIMPTON, S. p 3698 N92-30401
p 3630 N92-30607
PLOCINSKI, DAVID p 3609 N92-30273
PLUMB, G. D. p 3711 N92-31151
p 3711 N92-31173
PODLESNY, R. p 3727 N92-30247
POEPPEL, R. B. p 3730 N92-30999
POHLIG, STEPHEN C. p 3616 N92-30762
POINSOT, T. p 3633 N92-30667
POINSOT, T. J. p 3597 N92-30669
POLLOCK, D. A. p 3661 N92-31120
POLOVTSEVA, E. R. p 3651 N92-31083
PONSARDIN, PATRICK p 3653 N92-31093
POOLE, LAMONT R. p 3641 N92-31032
POOLE, W. J. p 3590 N92-30521
PORTENEUVE, J. p 3645 N92-31051
p 3645 N92-31052
POSENAU, MARY-ANNE K. p 3689 N92-30907
POST, D. E. p 3726 N92-31114
POST, MADISON J. p 3639 N92-31020
POTT, RICHARD p 3669 N92-30968
POTTERVELD, D. H. p 3657 N92-30848
POUKEY, J. W. p 3718 N92-30624
POUND, JAMES G. p 3733 N92-30682
POVINELLI, LOUIS A. p 3583 N92-31172
PRAGER, S. C. p 3723 N92-30612
PRASAD, C. R. p 3645 N92-31049
PRATHER, W. S. p 3596 N92-30899
PRENGLE, H. W., JR. p 3596 N92-30882
PRESSMAN, A. E. p 3667 N92-30545
PRICE, KENT M. p 3614 N92-30300
PRINS, J. J. M. p 3658 N92-30477
PSALTIS, DEMETRI p 3637 N92-30546
PYNN, R. p 3717 N92-31201

Q

QIAO, C. Y. P. p 3599 N92-30888
QIU, JINHUAN p 3651 N92-31080
p 3651 N92-31082
QUAGLIA, P. p 3643 N92-31039
QUATE, C. F. p 3727 N92-30252

QUICK, ROBERT, JR. ..... p 3649 N92-31069

R

RAABE, WOLFGANG ..... p 3686 N92-31167
RABIER, PATRICK J. ..... p 3702 N92-30410
RADDIN, J. H., JR. ..... p 3688 N92-30844
RADELAAR, S. ..... p 3625 N92-30730
p 3625 N92-30731
p 3625 N92-30732
RADOSEVICH, RAYMOND ..... p 3733 N92-30889
RADOUSKY, H. B. ..... p 3729 N92-30885
RAFFIN, G. ..... p 3698 N92-30957
RAFIN, C. ..... p 3698 N92-30957
RAGLAND, WILLIAM ..... p 3593 N92-31005
RAGSDALE, W. A. ..... p 3586 N92-31160
RAJU, I. S. ..... p 3661 N92-30309
RALL, JONATHAN A. R. ..... p 3641 N92-31030
RAMESHA, M. ..... p 3668 N92-30916
RAMOS-IZQUIERDO, LUIS ..... p 3643 N92-31040
RAO, A. V. R. KRISHNA ..... p 3668 N92-30912
RAO, B. M. ..... p 3668 N92-30917
RAO, D. K. ..... p 3660 N92-30734
RAO, K. S. ..... p 3669 N92-30919
RAO, MADHAV ..... p 3603 N92-30635
RAPP, RICHARD H. ..... p 3676 N92-30756
RASTANI, MANSUR ..... p 3610 N92-30280
RAU, Y.-C. ..... p 3652 N92-31086
REBER, R. A., JR. ..... p 3728 N92-30585
RECK, THOMAS ..... p 3623 N92-30503
REDDER, CHRISTOPHER R. ..... p 3678 N92-30262
REED, K. L. ..... p 3737 N92-31228
REED, R. P. ..... p 3622 N92-30370
REGAN, THOMAS M. ..... p 3611 N92-30288
REGEN, S. L. ..... p 3593 N92-30344
REGIER, FRANK A. ..... p 3587 N92-30383
REHFIELD, LAWRENCE W. ..... p 3579 N92-30304
REHM, R. G. ..... p 3695 N92-30579
REICHERT, B. A. ..... p 3582 N92-30972
REICHERT, BRUCE A. ..... p 3583 N92-31172
REIF, JOHN H. ..... p 3695 N92-30555
REITER, MICHAEL ..... p 3692 N92-30379
REKERS, J. ..... p 3692 N92-30428
REMO, JOHN ..... p 3719 N92-30233
RENAUD, J. ..... p 3578 N92-30418
RENGER, W. ..... p 3644 N92-31042
RENZE, KEVIN J. ..... p 3576 N92-30742
REYN, J. W. ..... p 3703 N92-30457
REYNOLDS, W. C. ..... p 3593 N92-30256
REYNOLDS, WILLIAM C. ..... p 3631 N92-30653
RHEE, K. T. ..... p 3595 N92-30835
RHEINBOLDT, WERNER C. ..... p 3702 N92-30410
RHODES, DAVID B. ..... p 3637 N92-30737
RIAHI, D. N. ..... p 3633 N92-30662
RIBEZZO, S. ..... p 3655 N92-31103
RICE, THEODORE R. ..... p 3636 N92-30530
RICHMAN, M. W. ..... p 3629 N92-30438
RIDER, W. J. ..... p 3589 N92-31204
RIFE, M. C. ..... p 3577 N92-31122
ROBERTSON, JAMES B. ..... p 3622 N92-30389
ROBINSON, R. A. ..... p 3655 N92-31102
ROCHELLE, J. M. ..... p 3742 N92-30797
ROCK, P. B. ..... p 3684 N92-30328
RODGERS, E. B. ..... p 3683 N92-30305
RODI, W. ..... p 3631 N92-30655
p 3631 N92-30656
ROGALLO, R. S. ..... p 3634 N92-30671
p 3634 N92-30672
ROGERS, M. ..... p 3632 N92-30658
p 3633 N92-30663
ROGERS, WILLIAM H. ..... p 3686 N92-30306
ROGERSON, G A. ..... p 3590 N92-30528
ROHR, R. ..... p 3587 N92-30440
ROKHLIN, V. ..... p 3705 N92-30568
ROKUGAWA, S. ..... p 3602 N92-30402
ROOS, C. ..... p 3691 N92-30353
p 3693 N92-30435
p 3693 N92-30455
ROOZ, E. ..... p 3670 N92-30330
ROOZEKRANS, J. N. ..... p 3667 N92-30471
ROSE, WILLIAM C. ..... p 3628 N92-30380
ROSEKIND, MARK ..... p 3686 N92-31167
ROSEN, DAVID L. ..... p 3650 N92-31075
ROSENSCHEIN, STANLEY J. ..... p 3701 N92-30710
ROSSONI, P. ..... p 3612 N92-30378
ROTE, D. M. ..... p 3660 N92-30860
ROTEL, M. ..... p 3598 N92-30872
ROTH, MARY ELLEN ..... p 3586 N92-30310
ROTHBLATT, MARTIN ..... p 3620 N92-30944
ROTHWARF, A. ..... p 3727 N92-30247
ROUNTREE, MIKE ..... p 3686 N92-31167
ROUTE, ROGER K. ..... p 3624 N92-30617
ROWLAND, S. K. ..... p 3736 N92-31224
ROY, P. K. ..... p 3728 N92-30577
RUBINSZTAJN, SLAWOMIR ..... p 3602 N92-30346
RUBTSOV, V. ..... p 3706 N92-30790
RUCK, B. ..... p 3720 N92-30507
RUCKER, MICHELLE A. ..... p 3602 N92-30539
RUEB, JUSTIN D. ..... p 3688 N92-30592
RUGGIERO, S. T. ..... p 3710 N92-31131
RUIZ, M. ..... p 3673 N92-30520
RUNYAN, L. JAMES ..... p 3577 N92-30395
RUOFF, R. S. ..... p 3596 N92-31178
RUSAK, BENJAMIN ..... p 3684 N92-30319
RUSSELL, A. G. ..... p 3673 N92-30520
RUSSELL, D. A. ..... p 3726 N92-31116
RUSSELL, L. ..... p 3727 N92-30247
RUTLAND, C. J. ..... p 3597 N92-30668
p 3597 N92-30670
RUTTEN, JAN J. M. M. ..... p 3615 N92-30448
RYAN, DEIRDRE A. ..... p 3582 N92-30753

S

SABNIS, J. S. ..... p 3659 N92-30640
SADEGHI, FARSHID ..... p 3659 N92-30554
SAETRE, HELGE A. ..... p 3684 N92-30523
SAFFER, REX ANDERSON ..... p 3741 N92-30973
SAFONOV, MICHAEL G. ..... p 3700 N92-30322
SAGALYN, PAUL L. ..... p 3599 N92-31110
SAHIRA, KENSHO ..... p 3600 N92-31163
SAITO, Y. ..... p 3640 N92-31027
SAKHO, IBRAHIMA ..... p 3694 N92-30493
SALAMA, KAMEL ..... p 3592 N92-30815
SALEM-SUGUA, S., JR. ..... p 3730 N92-31190
SALEM, J. A. ..... p 3663 N92-30567
SALTER-DUKE, BRIAN J. ..... p 3715 N92-30680
SALTUS, ALLEN R., JR. ..... p 3669 N92-31139
SALTZ, JOEL ..... p 3689 N92-30311
SAMARA, NOAH ..... p 3621 N92-30946
SAMEL, ALEXANDER ..... p 3686 N92-31167
SANDHU, R. S. ..... p 3590 N92-30251
SANDWELL, DAVID T. ..... p 3738 N92-31234
SANSONI, P. ..... p 3645 N92-31047
SARFF, J. S. ..... p 3723 N92-30612
SARGOYTCHEV, S. ..... p 3652 N92-31087
SASADEUSZ, C. L. ..... p 3664 N92-30963
SASANO, YASUHIRO ..... p 3652 N92-31088
SATO, KUNINORI ..... p 3722 N92-30431
SATO, T. ..... p 3710 N92-30498
SATO, TETSUYA ..... p 3722 N92-30384
SAULYS, A. C. ..... p 3717 N92-30398
SAUNDERS, R. S. ..... p 3737 N92-31226
p 3738 N92-31235
SAWAIRI, N. ..... p 3710 N92-30498
SAWICKA, B. D. ..... p 3602 N92-30402
SAYOOD, K. ..... p 3691 N92-30296
SCHAEFER, A. ..... p 3717 N92-31137
SCHAEFER, DALE W. ..... p 3603 N92-30544
SCHAEFER, HENRY F., III ..... p 3715 N92-30680
SCHAFFER, G. ..... p 3718 N92-30811
SCHAMILOGLU, EDL ..... p 3622 N92-30332
SCHEINBEIM, J. I. ..... p 3727 N92-30406
p 3603 N92-30594
p 3728 N92-30595
SCHERBARTH, D. W. ..... p 3655 N92-31109
SCHIESSER, W. E. ..... p 3719 N92-30840
SCHIFF, E. A. ..... p 3729 N92-30748
SCHIFLETT, SAMUEL G. ..... p 3685 N92-30605
SCHILLER, N. H. ..... p 3641 N92-31029
SCHILLING, DONALD L. ..... p 3619 N92-30939
SCHLESINGER, T. E. ..... p 3730 N92-31000
SCHMIDT, FRED ..... p 3618 N92-30932
SCHMIDTKE, KLAUS ..... p 3592 N92-30969
SCHMITZ, J. ..... p 3636 N92-30365
p 3637 N92-30688
SCHNEIDER, JUERGEN ..... p 3720 N92-30504
SCHOLZ, CHRIS ..... p 3676 N92-30961
SCHONE, H. ..... p 3716 N92-30853
SCHOUTENS, K. ..... p 3731 N92-30825
SCHRAMM, D. N. ..... p 3740 N92-30622
SCHUBERT, GERALD ..... p 3738 N92-31234
SCHUELER, D. G. ..... p 3670 N92-30808
SCHUHMACHER, G. ..... p 3579 N92-30424
SCHULLER, IVAN K. ..... p 3710 N92-30850
SCHULTZ, K. I. ..... p 3640 N92-31026
p 3654 N92-31097
SCHULZ, M. ..... p 3716 N92-30853
SCHULZE, CHRISTOPH ..... p 3647 N92-31062
SCHUMM, JEFFRY ..... p 3605 N92-30796
SCHUMM, JEFFRY S. ..... p 3605 N92-30795
SCHUSTER, GREGORY L. ..... p 3658 N92-30388
SCHWAB, C. ..... p 3662 N92-30338
SCHWARZE, G. E. ..... p 3623 N92-30397
SCHWARZKOPF, OTFRIED ..... p 3693 N92-30443
SCHWEIGER, JEFFREY M. ..... p 3696 N92-30631
SCHWEIGER, PAUL S. ..... p 3574 N92-30298
SCHWELBERGER, J. G. ..... p 3726 N92-31197
SCHWEMMER, G. K. ..... p 3645 N92-31049
SCHWEMMER, GEARY K. ..... p 3645 N92-31050
SCHWENDIMANN, P. ..... p 3642 N92-31036
SCHWENN, U. ..... p 3722 N92-30385
SCHWIESOW, R. L. ..... p 3639 N92-31023
SCOTT, W. E. ..... p 3671 N92-30949
SCOTT, W. R. ..... p 3688 N92-30844
SEGAL, A. ..... p 3628 N92-30373
SEGALMAN, D. ..... p 3605 N92-30804
SEIDEL, HELMUT ..... p 3594 N92-30422
SEILER, F. ..... p 3720 N92-30507
SEKAR, B. ..... p 3576 N92-30909
SELF, S. ..... p 3736 N92-31224
SELLMYER, D. J. ..... p 3600 N92-31186
SELVESTER, RONALD H. ..... p 3684 N92-30523
SENDSTAD, O. ..... p 3631 N92-30654
SENGUPTA, LOUISE C. ..... p 3599 N92-31110
SENGUPTA, S. ..... p 3730 N92-31190
SENS, ANNE-SOPHIE ..... p 3575 N92-30514
SENTIS, M. ..... p 3657 N92-30805
SERAFIM, P. ..... p 3656 N92-30743
SETTIMO, FRANCO ..... p 3620 N92-30941
SEUNTJENS, J. M. ..... p 3661 N92-31120
SEVRIN, A. ..... p 3731 N92-30825
SHAFROTH, S. M. ..... p 3716 N92-30853
SHAHINPOOR, M. ..... p 3605 N92-30804
SHAMSUNDAR, N. ..... p 3670 N92-30330
SHAPIRO, RALPH ..... p 3678 N92-30262
SHASHARINA, S. G. ..... p 3725 N92-30900
SHAW, R. W. ..... p 3597 N92-31196
SHE, C. Y. ..... p 3644 N92-31046
SHELTON, ROBERT O. ..... p 3700 N92-30314
p 3659 N92-30540
SHEN, JOHN P. ..... p 3699 N92-30557
SHEPARD, T. D. ..... p 3726 N92-31118
SHI, C. ..... p 3599 N92-30688
SHI, D. ..... p 3730 N92-31190
SHIELD, J. E. ..... p 3598 N92-30858
SHIH, H. J. ..... p 3719 N92-30840
SHIMADA, MASAAKI ..... p 3617 N92-30927
SHIMSKI, JOHN T. ..... p 3658 N92-30396
SHLOSMAN, I. ..... p 3739 N92-30862
SHMUELLI, HAIM ..... p 3729 N92-30781
SHOCK, R. N. ..... p 3596 N92-30883
SHOPE, S. L. ..... p 3718 N92-30624
SHROUT, THOMAS R. ..... p 3624 N92-30598
SHU, CHI-WANG ..... p 3706 N92-30716
SIAHPUSH, A. S. ..... p 3661 N92-30763
SIBEYN, JOP F. ..... p 3707 N92-30481
SICA, R. J. ..... p 3652 N92-31087
SIDIKMAN, K. L. ..... p 3722 N92-30366
SIEGEL, R. W. ..... p 3716 N92-30826
SILCOX, R. J. ..... p 3711 N92-30979
SILLING, S. A. ..... p 3664 N92-31123
SILVER, G. L. ..... p 3705 N92-30566
SILVETTI, S. P. ..... p 3590 N92-30521
SIMENOG, I. V. ..... p 3727 N92-30405
SIMMET, G. ..... p 3644 N92-31042
SIMMONS, D. F. ..... p 3724 N92-30806
SIMONELLI, D. ..... p 3739 N92-31236
SIMONS, J. ..... p 3716 N92-30845
SIMPSON, M. L. ..... p 3742 N92-30797
SIMPSON, R. L. ..... p 3577 N92-31122
SINGH, JAG J. ..... p 3662 N92-30317
SINGH, P. P. ..... p 3600 N92-31138
SINGLETON, J. ..... p 3625 N92-30731
SINGLETON, JEFFREY D. ..... p 3664 N92-31155
SIRBAUGH, J. R. ..... p 3582 N92-30972
SIRCAR, A. K. ..... p 3624 N92-30619
SJOSTEDT, ROB J. ..... p 3580 N92-30878
SKIBO, S. ..... p 3727 N92-30247
SKINNER, WILBERT R. ..... p 3639 N92-31018
SLUIJS, J. M. ..... p 3733 N92-30463
SLUITER, M. ..... p 3599 N92-31119
p 3600 N92-31124
SMITH, C. A. ..... p 3729 N92-30885
SMITH, D. L. ..... p 3723 N92-30591
SMITH, H. L. ..... p 3688 N92-30844
SMITH, J. H. B. ..... p 3576 N92-30947
SMITH, M. ..... p 3730 N92-31190
SMITH, STEVEN W. ..... p 3734 N92-30234
SNAIL, KEITH ..... p 3604 N92-30685
SNAVELY, D. L. ..... p 3593 N92-30245
p 3613 N92-30246
SNOW, FRANK J. ..... p 3690 N92-30564
SNYDER, E. J. ..... p 3623 N92-30537
SOANES, ROYCE W. ..... p 3707 N92-31140
SODERSTROM, JONATHON ..... p 3733 N92-30889
SOEDE, DIRK ..... p 3699 N92-30696
SOH, WOO Y. ..... p 3636 N92-30894
SOHN, P. Y. ..... p 3619 N92-30934
SOHN, PHILIP Y. ..... p 3618 N92-30932
SOIBELMAN, Y. ..... p 3704 N92-30511
SOLAL, FRANCINE ..... p 3597 N92-30513
SOLOMON, JOSEPH C. ..... p 3684 N92-30523
SONDERGAARD, R. ..... p 3632 N92-30658
SORENSEN, CARL D. ..... p 3612 N92-30293
p 3612 N92-30294

SORIA, J. p 3632 N92-30658
SOSA, G. p 3673 N92-30520
SOVEY, J. p 3589 N92-30818
SPELLMAN, DENNIS p 3706 N92-30776
SPIEGEL, F. XAVIER p 3611 N92-30282
p 3611 N92-30283
SPINKS, DEBRA p 3630 N92-30648
SPOWART, M. P. p 3639 N92-31023
SPRANGLE, P. p 3656 N92-30743
SPRANGLE, PHILLIP p 3656 N92-30614
p 3723 N92-30620
SQUIRES, KYLE p 3631 N92-30652
SRINIVAS, M. G. p 3667 N92-30910
p 3668 N92-30914
SRINIVAS, P. p 3668 N92-30916
SRINIVASAN, MALUR N. p 3609 N92-30271
SRULIJES, J. p 3720 N92-30507
ST.CLAIR, TERRY L. p 3601 N92-30313
STAFFORD, B. p 3670 N92-30519
STALEY, O. GLENN p 3643 N92-31040
STAMPER, A. K. p 3730 N92-31000
STANGEBY, P. C. p 3723 N92-30746
STANLEY, H. E. p 3709 N92-30642
STATON, LEO D. p 3647 N92-31060
STAVNES, M. p 3623 N92-30427
STEFANUTTI, L. p 3644 N92-31044
STEHMAN, S. V. p 3707 N92-30562
STEICH, DAVID J. p 3582 N92-30753
STEIN, E. p 3670 N92-30330
STEINHARDT, P. p 3629 N92-30560
STEINOLFSON, R. S. p 3742 N92-31162
STEPHENS, ERIC B. p 3604 N92-30794
p 3605 N92-30816
STERN, A. p 3619 N92-30934
STERN, ALAN p 3618 N92-30932
STEVENS, LINDA T. p 3684 N92-30603
STEVENS, S. SCOTT p 3677 N92-31009
STEVENS, T. D. p 3652 N92-31086
STIEGLER, JAMES O. p 3608 N92-30263
STOCKS, G. M. p 3599 N92-31119
STOFAN, E. R. p 3738 N92-31235
STONE, J. p 3738 N92-31230
STOYANOV, D. V. p 3650 N92-31076
p 3650 N92-31078
p 3650 N92-31079
p 3651 N92-31081
STOYKOVA, E. V. p 3650 N92-31079
STRAMAN, O. p 3718 N92-30726
STRAUSS, HENRY R. p 3702 N92-30375
STREETT, CRAIG L. p 3573 N92-30295
STREHLOW, RICHARD A. p 3610 N92-30277
STREICHER, J. p 3644 N92-31043
p 3655 N92-31106
STREIT, G. p 3673 N92-30520
STRETCH, D. p 3632 N92-30657
STRINGFELLOW, G. B. p 3727 N92-30527
STRIZ, ALFRED G. p 3583 N92-30323
STRIZAK, J. P. p 3592 N92-30809
STRUB, P. TED p 3682 N92-30739
STRUMBERGER, E. p 3722 N92-30385
STRUVE, K. W. p 3718 N92-30624
STUKOPIN, V. p 3704 N92-30511
STULEN, R. H. p 3730 N92-31000
STUMPF, GREGORY J. p 3678 N92-30495
p 3678 N92-30496
STUPAKOV, G. V. p 3719 N92-30881
SUE, M. K. p 3618 N92-30928
SUGAMA, HIDEO p 3723 N92-30499
SUGIMOTO, NOBUO p 3652 N92-31088
SUGITA, T. p 3646 N92-31054
p 3654 N92-31098
SUK, JIRI p 3672 N92-30374
SULLIVAN, JOHN M. p 3661 N92-30599
SUMMERS, C. L. p 3646 N92-31056
SUMMERS, L. G. p 3579 N92-30978
SUN, WEIMIN p 3621 N92-31156
SUTER, L. J. p 3726 N92-31118
SUZUKI, N. p 3714 N92-30510
p 3725 N92-30992
SUZUKI, YOSHIAKI p 3617 N92-30927
SVANBERG, S. p 3640 N92-31028
SWAN, PETER A. p 3617 N92-30926
SWANN, N. R. W. p 3655 N92-31102
SWEERS, GUIDO p 3702 N92-30434
SWENSON, J. K. p 3716 N92-30853
SWENSRUD, R. L. p 3655 N92-31109
SWINK, JAY R. p 3581 N92-30965
SWITHINBANK, CHARLES p 3584 N92-30621
SWYDEN, T. p 3614 N92-30407
SYRING, JAMES D. p 3731 N92-30235
SZCZEPANSKI, WOJCIECH p 3701 N92-31148
SZE, D. K. p 3723 N92-30591
SZE, R. C. p 3657 N92-30805

T

TAJIMA, T. p 3724 N92-30833
p 3725 N92-30884
TAKACS, J. M. p 3602 N92-30409
TAKAHASHI, P. p 3671 N92-31117
TAKAHASHI, YASUHIRO p 3617 N92-30927
TAKASE, Y. p 3603 N92-30594
TAKASHIMA, NARUHISA p 3574 N92-30392
TAKEI, AKIRA p 3722 N92-30384
TAKEICHI, M. p 3641 N92-31029
TAKEIRI, Y. p 3714 N92-30501
p 3714 N92-30572
TAKESHIMA, A. p 3641 N92-31029
TAKEUCHI, N. p 3646 N92-31054
p 3654 N92-31098
TAKIYAMA, KEN p 3722 N92-30431
TAKIZUKA, T. p 3714 N92-30510
TAM, C. K. W. p 3632 N92-30661
TANABE, TETSUO p 3602 N92-30502
TANAHASHI, S. p 3723 N92-30497
TANAKA, M. p 3710 N92-30498
TANAKA, MASATO p 3617 N92-30927
TANG, C. M. p 3614 N92-30407
TANG, H. C. p 3695 N92-30579
TANG, K. p 3597 N92-31184
TANKINS, E. S. p 3607 N92-30321
TANNEHILL, J. C. p 3576 N92-30977
TAUBENFELD, G. p 3695 N92-30522
p 3700 N92-31111
TAYLOR, DANIEL E. p 3585 N92-30777
TAYLOR, G. J. p 3736 N92-31224
TAYLOR, J. A. p 3730 N92-30999
TAYLOR, M. A. p 3722 N92-31195
TAYLOR, R. T. p 3596 N92-30883
TEAGUE, STEVEN M. p 3685 N92-30745
TENBERG, A. J. W. M. p 3690 N92-30698
TENDAM, A. A. p 3693 N92-30476
TENHAGEN, PAUL J. W. p 3699 N92-30696
TENNER, A. G. p 3713 N92-30364
TENNEY, YVETTE J. p 3686 N92-30306
TERLAKY, T. p 3693 N92-30455
TERLAKY, TAMAS p 3691 N92-30351
p 3691 N92-30353
TERRY, P. L. p 3637 N92-30822
THAM, FOOK S. p 3603 N92-30623
THEOPOLD, F. A. p 3653 N92-31091
THERIAULT, J.-M. p 3648 N92-31066
THIES, MARK C. p 3595 N92-30773
THIRUVENGADACHARI, S. p 3668 N92-30916
THOMAS, D. M. p 3671 N92-31117
p 3671 N92-31117
THOMAS, P. C. p 3739 N92-31236
THOMASSEN, K. p 3589 N92-30818
THOMPSON, J. J. p 3607 N92-30321
THORNTON, H. R. p 3612 N92-30290
THORSOS, ERIC I. p 3721 N92-30783
THRO, P.-Y. p 3645 N92-31048
TIEE, JOE p 3649 N92-31069
TIERNEY, J. W. p 3608 N92-30904
TIRKAS, PANAYIOTIS A. p 3621 N92-31156
TOEDTE, R. J. p 3659 N92-30587
TOETENEL, HANS p 3692 N92-30359
TOLLES, WILLIAM M. p 3626 N92-30851
TOMLINSON, J. J. p 3672 N92-31176
TOPORKOV, D. K. p 3657 N92-30848
TOUR, J. M. p 3605 N92-30817
TOUR, JAMES M. p 3604 N92-30794
p 3605 N92-30795
p 3605 N92-30796
p 3605 N92-30816
TRACHE, M. p 3732 N92-31203
TRENT, WILLIAM p 3579 N92-31211
TROUVE, A. p 3597 N92-30668
p 3597 N92-30670
TSAI, M. Y. p 3592 N92-30906
TSE, D. G. p 3659 N92-30640
TSOU, SHEUNG TSUN p 3715 N92-30750
TSUCHIYA, MASAYUKI p 3655 N92-31104
TSUCHIYA, T. p 3691 N92-30353
TSUJI, S. p 3725 N92-30992
TUCKER, D. S. p 3612 N92-30971
TUCKER, JERRY H. p 3690 N92-30541
TURCHI, P. E. A. p 3599 N92-31119
p 3600 N92-31124
TURMAN, B. N. p 3718 N92-30624
TUTTLE, B. A. p 3605 N92-30830
TVERSKY, BARBARA G. p 3687 N92-30336
TYSELL, LARS G. p 3575 N92-30713

U

UCHINO, O. p 3653 N92-31094
UCHIUMI, M. p 3653 N92-31094
UCKAN, N. A. p 3726 N92-31114
UCKAN, T. p 3726 N92-31197
UDO, F. p 3636 N92-30365
p 3637 N92-30688
ULIBARRI, TAMARA A. p 3603 N92-30544
ULRICH, DONALD R. p 3721 N92-31126
UM, CHUNG-IN p 3629 N92-30548
UNRUH, W. P. p 3615 N92-30703
URSIC, JAMES R. p 3677 N92-31009
USUI, S. p 3602 N92-30402
UTHE, EDWARD E. p 3654 N92-31101

V

VAIDYANATHAN, GOPAL p 3712 N92-30240
VALENTIN, R. p 3642 N92-31037
p 3643 N92-31038
VAN SUETENDAEL, RICHARD p 3585 N92-30976
VANDENBERG, W. G. p 3734 N92-30486
VANDENBROEK, A. C. p 3614 N92-30361
VANDERKOOIJ, M. W. A. p 3666 N92-30465
VANDERMAST, CHARLES A. P. G. p 3692 N92-30356
VANDERVORST, H. A. p 3703 N92-30437
VANDIJK, A. p 3667 N92-30471
VANDYKE, LEON S. p 3603 N92-30553
p 3607 N92-31207
VANE, C. R. p 3716 N92-30853
VANEIJK, B. p 3713 N92-30415
VANHAAFTEN, PETRA J. M. p 3693 N92-30445
VANHAERINGEN, H. p 3703 N92-30459
p 3707 N92-30460
VANHORSSEN, W. T. p 3703 N92-30457
VANKAN, J. p 3628 N92-30373
VANKATWIJK, J. p 3694 N92-30484
VANKATWIJK, JAN p 3694 N92-30485
p 3694 N92-30492
VANLEEUWEN, J. p 3694 N92-30479
VANMARTER, T. p 3593 N92-30245
VANNIEUWENHUIZEN, P. p 3731 N92-30825
VANRIPER, K. A. p 3740 N92-30578
p 3740 N92-30609
VANSINDEREN, MARTEN p 3689 N92-30432
VANWARREN, LLOYD p 3695 N92-30543
VANWOERKOM, P. T. L. M. p 3658 N92-30477
VANZEIJL, J. p 3694 N92-30484
VELDHORST, MARINUS p 3698 N92-30482
VENKATACHALAM, P. p 3668 N92-30915
VENN, G. p 3578 N92-30418
VERBLE, ADAS JAMES, JR. p 3613 N92-30754
VERBRUGGEN, A. H. p 3625 N92-30730
VERCHEVAL, J. p 3744 N92-30996
VERHOEF, W. p 3666 N92-30467
p 3667 N92-30471
VERHOFF, VINCENT G. p 3585 N92-30307
VERMASEREN, J. A. M. p 3715 N92-30687
VERMEER, P. L. p 3614 N92-30354
VEVERKA, J. p 3739 N92-31236
VEZIROGLU, T. N. p 3668 N92-30913
VIAL, J.-P. p 3693 N92-30435
VIENNA, J. D. p 3730 N92-30999
VIGIL, M. G. p 3613 N92-30887
VILLARREAL, JAMES A. p 3700 N92-30314
VILSMEIER, JOSEF WALTER p 3591 N92-30690
VISSERS, CHRIS A. p 3689 N92-30432
VITAL, J. M. p 3697 N92-30951
VITANYI, PAUL M. B. p 3708 N92-30699
VITELLO, P. A. p 3739 N92-30862
VLASSE, MARCUS p 3627 N92-30902
VLOT, ARIE p 3590 N92-30414
VOGELIUS, MICHAEL p 3704 N92-30516
VOGT, G. J. p 3615 N92-30703
VOIT, FRANK J. p 3636 N92-30412
VONHANXLEDEN, REINHARD p 3689 N92-30311
VONROEDERN, B. p 3670 N92-30519
VOSS, E. p 3654 N92-31099
VOSS, RALF p 3594 N92-30422
VUIK, C. p 3703 N92-30437
p 3704 N92-30461
VUORINEN, J. J. p 3598 N92-30785

W

WACHINGER, G. p 3592 N92-30969
WADA, M. p 3714 N92-30572
WADAWADIGI, G. p 3576 N92-30977
WAGNER, J. D. p 3588 N92-31225
WAGNER, J. S. p 3718 N92-30624
WAKATANI, M. p 3725 N92-30994
WAKAYAMA, SEAN p 3577 N92-31157
WAKKER, K. F. p 3666 N92-30465
WALEFFE, F. p 3633 N92-30662
WALKER, D. W. p 3722 N92-30366
WALKER, GILBERT H. p 3658 N92-30388

WALKER, M. M. p 3574 N92-30367
WALL, M. A. p 3600 N92-31125
WALLINDER, E. p 3640 N92-31028
WALLIO, H. ANDREW p 3647 N92-31060
WANDINGER, ULLA p 3641 N92-31033
p 3647 N92-31062
WANG, C. H. p 3602 N92-30409
p 3720 N92-30535
p 3721 N92-30536
WANG, D. W. p 3700 N92-31111
WANG, FU-QUAN p 3587 N92-30709
WANG, J.-C. p 3660 N92-30948
WANG, LIANG-GUO p 3647 N92-31060
WANG, Q. p 3729 N92-30748
WANG, S. Y. p 3733 N92-30463
WANG, X. p 3691 N92-30296
WARASHIMA, Y. p 3641 N92-31029
WARD, G. F. p 3688 N92-30592
WASSERBURG, G. J. p 3738 N92-31230
WATANABE, K. p 3710 N92-30498
p 3725 N92-30994
WATANABE, KATSUTOSHI p 3600 N92-31163
WATKINS, B. E. p 3596 N92-30883
WATTS, A. J. p 3588 N92-31225
WEATHERFORD, C. A. p 3731 N92-30242
WEBER, P. G. p 3677 N92-31008
WEEKS, D. D. p 3743 N92-30627
WEIGMAN, BERNARD J. p 3611 N92-30282
WEINER, M. M. p 3621 N92-31130
WEISER, MARTIN W. p 3607 N92-30267
WEISS, ROSANNE M. p 3580 N92-31165
WEISSMAN, P. T. p 3624 N92-30619
WEITKAMP, C. p 3653 N92-31091
p 3654 N92-31099
WEITKAMP, CLAUS p 3641 N92-31033
p 3647 N92-31062
WELCH, D. R. p 3718 N92-30624
WELLBORN, S. R. p 3582 N92-30972
WENDELIN, T. p 3671 N92-30896
WENDER, I. p 3608 N92-30904
WERNAND, M. R. p 3666 N92-30466
p 3667 N92-30472
WERNER, CH. p 3655 N92-31106
WERNER, F. p 3717 N92-31137
WESSELING, P. p 3628 N92-30373
p 3629 N92-30454
p 3629 N92-30462
p 3704 N92-30483
WEST, H. B. p 3671 N92-31117
WESTBROOK, C. K. p 3594 N92-30749
WESTERVELT, R. p 3629 N92-30560
WHITE, C. W. p 3594 N92-30632
WHITE, J. M. p 3667 N92-30704
WHITE, L. W. p 3614 N92-30300
WHITE, T. S. p 3581 N92-30524
WHITELAW, JAMES H. p 3659 N92-30640
WHITEMAN, D. p 3643 N92-31041
p 3652 N92-31089
WHITEMAN, DAVID N. p 3643 N92-31040
WHITEWAY, J. A. p 3649 N92-31070
WICKLUND, E. p 3699 N92-30812
WICKMAN, JERRY L. p 3609 N92-30273
WIDENER, EDWARD L. p 3601 N92-30291
p 3601 N92-30292
WIECZOREK, JOHANNES p 3667 N92-30515
WIEGNER, MATTHIAS p 3647 N92-31061
WIESEMAN, CAROL D. p 3580 N92-30752
WIESERMAN, W. R. p 3623 N92-30397
WILBUR, MATTHEW L. p 3664 N92-31155
WILGEN, J. B. p 3724 N92-30810
WILKERSON, THOMAS D. p 3645 N92-31050
WILLIAMS, M. C. p 3671 N92-31113
WILLIAMS, M. D. p 3673 N92-30520
WILLIAMS, MARC H. p 3577 N92-31171
WILLIAMS, MICHAEL D. p 3658 N92-30388
WILLIAMS, R. S. p 3623 N92-30537
WILLIS, YOLANDA A. p 3732 N92-30349
WILSON, C. R. p 3736 N92-30575
WILSON, CHRISTOPHER D. p 3662 N92-30416
WILSON, D. S. p 3660 N92-30734
WILSON, JOHN C. p 3574 N92-30394
WINCHELL, D. F. p 3728 N92-30684
WINDISCH, C. F., JR. p 3599 N92-31010
WINKER, DAVID M. p 3641 N92-31032
WINOKUR, P. S. p 3728 N92-30585
WITKOWSKI, W. p 3605 N92-30804
WITTEN, ALAN J. p 3677 N92-31009
WITTEVEEN, CEES p 3702 N92-30371
WOLF, Z. R. p 3718 N92-30786
WOLFE, W. E. p 3590 N92-30251
WOLSZCZAN, A. p 3739 N92-31237
WOLTZ, J. p 3661 N92-31120
WOOD, RICHARD M. p 3628 N92-30387
WOOD, WILLIAM B. p 3658 N92-30316
WOODRUFF, ROBERT R. p 3685 N92-30605
WOODS, P. T. p 3655 N92-31102
WOS, L. p 3705 N92-30608
WOZNIAK, CZESLAW p 3721 N92-31149
WRAY, A. A. p 3634 N92-30672
WRIGHT, KENNETH D., II p 3734 N92-30386
WU, R. p 3605 N92-30817
WU, RUILIAN p 3605 N92-30795
p 3605 N92-30796
WU, TE-KAO p 3614 N92-30391
WULFMEYER, V. p 3645 N92-31048
WYDEVEN, T. p 3689 N92-31166

X

XIONG, F. p 3594 N92-30632
XU, X. p 3719 N92-30840

Y

YACTOR, R. J. p 3608 N92-31202
YADLOWSKY, ANN B. p 3690 N92-30541
YAMADA, S. p 3723 N92-30497
YAMAGISHI, SUSUMU p 3655 N92-31104
YAMAGISHI, T. p 3725 N92-30993
YAMAGUCHI, K. p 3640 N92-31027
YAMAGUCHI, S. p 3654 N92-31098
YAMAMOTO, MINORU p 3617 N92-30924
YAMANOUCHI, HIROSHI p 3655 N92-31104
YAMAUCHI, T. p 3725 N92-30992
YATES, J. T., JR. p 3595 N92-30821
YE, XIANGDONG p 3732 N92-31133
YODER, MAX N. p 3590 N92-30318
YODH, G. B. p 3743 N92-30627
YOUNG, A. D. p 3576 N92-30947
YOUNG, J. P. p 3597 N92-31196
YOUNG, L. p 3657 N92-30848
YOUNG, WILLIAM D. p 3700 N92-31158
YU, C. H. p 3728 N92-30684
YUE, C. F. p 3605 N92-30830
YUECEL, A. p 3719 N92-30840

Z

ZABIELSKI, CHESTER V. p 3597 N92-30759
ZACCANTI, G. p 3645 N92-31047
ZACHARIA, T. p 3659 N92-30587
ZAHAVI, J. p 3598 N92-30872
ZANTEMA, H. p 3693 N92-30444
ZEIDMAN, B. p 3657 N92-30848
ZELDIN, MARTEL p 3602 N92-30346
ZEMAN, OTTO p 3631 N92-30652
p 3631 N92-30653
ZGHICHE, A. p 3657 N92-30848
ZHANG-MEI, B. p 3727 N92-30406
ZHANG, B. p 3719 N92-30839
ZHANG, SHUZHONG p 3691 N92-30351
ZHANG, X. D. p 3724 N92-30880
ZHANG, X. Q. p 3602 N92-30409
ZHANG, Y. Z. p 3724 N92-30880
ZHIGUNOV, V. P. p 3713 N92-30403
ZIELINSKI, J. J. p 3726 N92-31197
ZIERTEN, THOMAS A. p 3577 N92-30395
ZISCHKA, PETER J. p 3579 N92-30304
ZOHAR, Y. p 3633 N92-30664
ZOLTANI, C. K. p 3630 N92-30604
ZOTEMANTEL, RAINER p 3662 N92-30423
ZUEV, V. E. p 3652 N92-31085

Typical Corporate Source Index Listing

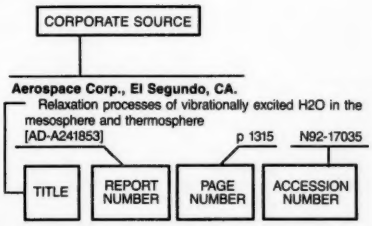

Listings in this index are arranged alphabetically by corporate source. The title of the document provides the user with a brief description of the subject matter. The report number helps to indicate the type of document cited (e.g., NASA report, translation, NASA contractor report). The accession number denotes the number by which the citation is identified. The page number helps you locate the citation in the abstract section. The titles are arranged under each corporate source in ascending accession number order.

A

ACADEMIA SINICA, BEIJING (CHINA).
A considerable effect of stratospheric aerosol on lidar-detected ozone profile and a three-wavelength inversion technique for both ozone and aerosol
p 3651 N92-31080
Lidar measurements of cloud extinction coefficient distribution and its forward scattering phase function according to multiply scattered lidar returns
p 3651 N92-31082

ACADEMY OF SCIENCES OF THE UKRAINIAN SSR, KIEV.
Spin amplitudes of pp-scattering in a unitarized supercritical pomeron model
[DE92-624639] p 3711 N92-30236
Scale symmetry of quantum solitons
[DE92-624560] p 3712 N92-30331
On the temperature role in the tunneling process at the cold fusion
[DE92-627497] p 3727 N92-30405

ACADEMY OF SCIENCES (USSR), TOMSK.
Measurements of the backscattering phase matrices of crystal clouds with a polarization lidar
p 3651 N92-31083
Lidar sounding of ozone and aerosols
p 3652 N92-31085

ADVANCED AVIATION CONCEPTS, JUPITER, FL.
Introduction to cognitive processes of expert pilots
[DOT/FAA/RD-92/12] p 3578 N92-30980

ADVANCED CONTROL TECHNOLOGY, INC., NORTHRIDGE, CA.
Cryogenic Magnetic Bearing Test Facility (CMBTF)
[NASA-CR-189087] p 3582 N92-31164

ADVANCED TECHNOLOGY MATERIALS, INC., DANBURY, CT.
Fabrication of multifilament conductors: CVD processing of high Tc superconducting composite fibers
[NASA-CR-184344] p 3591 N92-30711

ADVISORY GROUP FOR AEROSPACE RESEARCH AND DEVELOPMENT, NEUILLY-SUR-SEINE (FRANCE).
Technical evaluation report on the Flight Mechanics Panel Symposium on Piloted Simulation Effectiveness
[AGARD-AR-315] p 3584 N92-30769
Vortex flow aerodynamics
[AGARD-AR-299] p 3576 N92-30947

AERONAUTICAL RESEARCH INST. OF SWEDEN, STOCKHOLM.
MATGRID, a program for generation of C-H and C-O topology grids around wing/body configurations: Software description document
[FFA-TN-1990-20] p 3575 N92-30713

AERONAUTICAL RESEARCH LABS., MELBOURNE (AUSTRALIA).
Activities of the Aeronautical Research Laboratory
p 3744 N92-30768

AERONAUTICAL SYSTEMS DIV., WRIGHT-PATTERSON AFB, OH.
KC-135 crew reduction feasibility demonstration simulation study. Volume 1: Function analysis and function reallocation
[AD-A252265] p 3688 N92-30592

AEROSPACE CORP., EL SEGUNDO, CA.
Modeling fast modulation effects in cesium atomic clocks
[AD-A252649] p 3636 N92-30412

AEROSPACE CORP., LOS ANGELES, CA.
A comparison of Ultra-Sensitive Coherent Detection (USCD) and heterodyne detection for a wind sensing application p 3640 N92-31025
An ultra-sensitive coherent detector capable of single photon detection for lidar applications
p 3646 N92-31053

AEROSPACE MEDICAL RESEARCH LABS., BROOKS AFB, TX.
Effects of pyridostigmine bromide on A-10 pilots during execution of a simulated mission; performance
[AD-A252309] p 3685 N92-30605

AFRISPACE, INC., WASHINGTON, DC.
Broadcast satellite service: The international dimension p 3621 N92-30946

AIR FORCE ACADEMY, CO.
Future aerospace ground test facility requirements for the Arnold Engineering Development Center
p 3585 N92-30897

AIR FORCE INST. OF TECH., WRIGHT-PATTERSON AFB, OH.
Thermal stress evaluation of a symmetrically laminated composite plate
[AD-A249450] p 3591 N92-30641
Tropical cyclone asymmetries as revealed by recent satellite microwave brightness temperatures
[AD-A249873] p 3679 N92-30867
The calculation of mid-latitude meridional neutral winds from an improved servo model approximation method
[AD-A249874] p 3676 N92-30868

AIR INTER, LIGNES AERIENNES INTERIEURES, PARIS (FRANCE).
Preparation for a new plane (A 320): Experience reviewed p 3697 N92-30954
Flight crew integration in the maintenance chain of a commercial aircraft (A 320) p 3698 N92-30957

ALABAMA A & M UNIV., NORMAL.
Numerical investigations in the backflow region of a vacuum plume
[NASA-CR-190515] p 3589 N92-30981

ALABAMA UNIV., HUNTSVILLE.
FNAS: The magnetic configuration leading to solar flares
[NASA-CR-190522] p 3743 N92-31168

ALLIED-SIGNAL AEROSPACE CO., KANSAS CITY, MO.
Printed transformer process/product improvements
[DE92-014760] p 3624 N92-30590
Process modeling and development for three axisymmetric net shape forgings
[DE92-012111] p 3598 N92-30865
Interface friction, lubricants, and their influence on metal flow
[DE92-012112] p 3606 N92-30866
Characterizing ultrasonic transducers using pattern recognition techniques
[DE92-015845] p 3711 N92-30890
Transfer soldering evaluation
[DE92-015160] p 3627 N92-31144

AMERICAN MOBILE SATELLITE CORP., WASHINGTON, DC.
Design of the American Mobile Satellite System
p 3617 N92-30925

AMES LAB., IA.
NDE characterization of the microstructure and mechanical properties of Al-Li alloys
[DE92-012154] p 3598 N92-30858

ANALYTICAL SERVICES AND MATERIALS, INC., HAMPTON, VA.
A boundary element alternating method for two-dimensional mixed-mode fracture problems
[NASA-CR-4460] p 3661 N92-30309

ARECIBO IONOSPHERIC OBSERVATORY, PUERTO RICO.
Discovery of two planets around a millisecond pulsar
p 3739 N92-31237

ARGONNE NATIONAL LAB., IDAHO FALLS, ID.
Cluster assembly of hierarchical nanostructures
[DE92-010498] p 3716 N92-30826

ARGONNE NATIONAL LAB., IL.
MHD considerations for a self-cooled liquid lithium blanket
[DE92-014864] p 3723 N92-30591
Application of automated deduction to the search for single axioms for exponent groups
[DE92-015271] p 3705 N92-30608
Emissions of greenhouse gases from the use of transportation fuels and electricity
[DE92-012102] p 3674 N92-30770
Quantification and reduction of the uncertainty in mass balance models by Monte Carlo analysis of prior data
[DE92-010278] p 3708 N92-30803
High field optical-pumping spin-exchange polarized deuterium source
[DE92-010274] p 3657 N92-30848
Vehicle/guideway interaction for high speed vehicles on flexible guideway
[DE92-013057] p 3660 N92-30860
YBa2Cu(3-x)Co(x)O(y): A substrate material for YBCO superconductors
[DE92-015182] p 3730 N92-30999
Mechanical design and finite element analysis of the SDC central calorimeter
[DE92-011197] p 3655 N92-31109
Grain boundary weak links in high-Tc superconductors
[DE92-016192] p 3730 N92-31190

ARIZONA STATE UNIV., TEMPE.
Laboratory experiments from the toy store
p 3609 N92-30274
Photoinitiated electron transfer in multichromophoric species: Synthetic tetrads and pentads featuring diquinone moieties
[DE92-013472] p 3683 N92-30368
Laboratory simulation of fluid dynamical process related to winter arctic leads
[AD-A252266] p 3682 N92-30593
Advanced electromagnetic methods for aerospace vehicles
[NASA-CR-190650] p 3621 N92-31156

ARIZONA UNIV., TUCSON.
The origins of hot subdwarf stars
p 3741 N92-30973

ARKANSAS UNIV., FAYETTEVILLE.
Combustion diagnostics by photo-deflection spectroscopy
[AD-A250802] p 3594 N92-30645

ARMY ARMAMENT RESEARCH, DEVELOPMENT AND ENGINEERING CENTER, WATERVLIET, NY.
Solving the Euler equations using adaptive mesh motion and refinement
[AD-A252364] p 3705 N92-30597
Analytical solution of elastic-plastic thick-walled cylinders with general hardening
[AD-A249491] p 3705 N92-30618

Nonlinear stress analysis of composite-jacketed steel cylinders subjected to high internal pressure
[AD-A249500] p 3663 N92-30802
Wrappability of curves on surfaces
[AD-A250004] p 3707 N92-31140
Multifractal analysis of chaotic point sets
[AD-A250756] p 3709 N92-31194

ARMY COLD REGIONS RESEARCH AND ENGINEERING LAB., HANOVER, NH.
Ice thickness observations, North American Arctic and subarctic, 1972-1973 and 1973-1974, part 8
[AD-A250830] p 3681 N92-30238
Potential airfield sites in Antarctica for wheeled aircraft
[AD-A249503] p 3584 N92-30621
Vector analysis of ice fabric data
[AD-A250832] p 3682 N92-30832

ARMY ELECTRONIC PROVING GROUND, FORT HUACHUCA, AZ.
Antenna pattern measurement facilities
[AD-A248964] p 3584 N92-30329
Compact range test applications, phase 2
[AD-A248790] p 3615 N92-30583

ARMY ENGINEER WATERWAYS EXPERIMENT STATION, VICKSBURG, MS.
Evaluation of grounding and mooring points for Army aircraft
[AD-A250749] p 3579 N92-31193

ARMY LAB. COMMAND, WATERTOWN, MA.
Ellipsometric study of oxide films formed on LDEF metal samples
[AD-A249856] p 3599 N92-31110

ARMY MATERIALS TECHNOLOGY LAB., WATERTOWN, MA.
Pressure densification
[AD-A249438] p 3604 N92-30758
Corrosion of high density kinetic energy penetrator materials
[AD-A249439] p 3597 N92-30759

ARMY MISSILE COMMAND, REDSTONE ARSENAL, AL.
Design and construction of a Helmholtz coil magnetic test cell
[AD-A249944] p 3585 N92-30849

ARMY RESEARCH INST. OF ENVIRONMENTAL MEDICINE, NATICK, MA.
The use of tympanometry to detect aerotitis media in hypobaric chamber operations
[AD-A248963] p 3684 N92-30328

ARMY RESEARCH OFFICE, RESEARCH TRIANGLE PARK, NC.
Transactions of the 9th Army Conference on Applied Mathematics and Computing
[AD-A252140] p 3706 N92-30843

ARNOLD ENGINEERING DEVELOPMENT CENTER, ARNOLD AIR FORCE STATION, TN.
Future aerospace ground test facility requirements for the Arnold Engineering Development Center
p 3585 N92-30897

ATMOSPHERIC SCIENCES LAB., WHITE SANDS MISSILE RANGE, NM.
Time and wavelength domain algorithms for chemical analysis by laser radar p 3650 N92-31075

ATOMIC ENERGY OF CANADA LTD., CHALK RIVER (ONTARIO).
Nondestructive evaluation of ceramic components by gamma ray CT
[DE92-626843] p 3602 N92-30402

B

BALL STATE UNIV., MUNCIE, IN.
A senior manufacturing laboratory for determining injection molding process capability
p 3609 N92-30273

BALLISTIC RESEARCH LABS., ABERDEEN PROVING GROUND, MD.
Development of diagnostics for electromagnetic armor applications
[AD-A251074] p 3587 N92-30257
Variational method in the statistical theory of turbulent two-phase flows
[AD-A252263] p 3630 N92-30604

BATTELLE PACIFIC NORTHWEST LABS., RICHLAND, WA.
Tempered glass and thermal shock of ceramic materials p 3607 N92-30265

BELEIDSCOMMISSIE REMOTE SENSING, DELFT (NETHERLANDS).
Results of the 1989 experiment with a polarimetric multifrequency SAR
[BCRS-91-33] p 3614 N92-30361
The use of TM data for identification of land cover and for detection of land use changes in the Atlantic zone of Costa Rica
[BCRS-91-36] p 3666 N92-30362
Preparations for the ERS-1 and TOPEX/Poseidon satellite altimetry missions
[BCRS-90-28] p 3666 N92-30465
On the remote sensing of water quality using the optical airborne scanner CAESAR
[BCRS-90-30] p 3666 N92-30466
CAESAR: Evaluation of the dual-look concept
[BCRS-91-10] p 3666 N92-30467
Monitoring of Dutch forest with LANDSAT-TM
[BCRS-91-21] p 3666 N92-30468
Feasibility of extracting current profile information from HF-radar surface current measurements, part 1 and 2
[BCRS-91-23-PT-1-2] p 3682 N92-30470
Vegetation conditions and yield indicators. Part 1: Main report
[BCRS-91-26-PT-1] p 3667 N92-30471
Interpretation of optical remote sensing data over coastal waters
[BCRS-91-27] p 3667 N92-30472

BIODYNAMIC RESEARCH CORP., SAN ANTONIO, TX.
Adapting the ADAM manikin technology for injury probability assessment
[AD-A252332] p 3688 N92-30844

BIONETICS CORP., COCOA BEACH, FL.
Habitat model for the Florida Scrub Jay on John F. Kennedy Space Center
[NASA-TM-107543] p 3673 N92-30494

BMW-A.G., MUNICH (GERMANY, F. R.).
Dense fog on the highway: Visual range monitoring in cars? p 3655 N92-31106

BOLT, BERANEK, AND NEWMAN, INC., CAMBRIDGE, MA.
A principled approach to the measurement of situation awareness in commercial aviation
[NASA-CR-4451] p 3686 N92-30306

BOSTON UNIV., MA.
Mathematical models of non-linear mechanical and electrical systems and their qualitative behavior
[AD-A248847] p 3622 N92-30249
Fractal and multifractal approaches to clustering phenomena
[AD-A249481] p 3709 N92-30642
Magnetospheric structure and dynamics: A multisatellite approach
[AD-A252326] p 3676 N92-30720
Tunable solid state lasers based on molecular ions
[AD-A249423] p 3656 N92-30774

BOWLING GREEN STATE UNIV., OH.
Vibrational overtone spectroscopy of gaseous metallocenes
[AD-A251088] p 3593 N92-30245
Photodissociation of azulene under UV-laser irradiation at 325 nm
[AD-A251093] p 3613 N92-30246

BRIGHAM YOUNG UNIV., PROVO, UT.
Measuring the surface tension of soap bubbles
p 3612 N92-30293
Measuring the Weibull modulus of microscope slides
p 3612 N92-30294

BRITISH BROADCASTING CORP., KINGSWOOD (ENGLAND).
An investigation of the effects of boundary constraints on the sound insulations of lightweight, double leaf partitions
[BBC-RD-1992/4] p 3711 N92-31151
Optimum methods for the measurement of the absorption coefficients of materials
[BBC-RD-1992/3] p 3711 N92-31173

BROOKHAVEN NATIONAL LAB., UPTON, NY.
Effects of high beam rates on TPC's
[DE92-014594] p 3717 N92-30398

BULGARIAN ACADEMY OF SCIENCES, SOFIA.
Lidar receivers for picosecond remote sensing
p 3650 N92-31076
Acousto-optic filtering of lidar signals
p 3650 N92-31077
Ground-based Doppler lidar of increased laser instability: Conception and design p 3650 N92-31078
Analytical estimates of the PP-algorithm at low number of Doppler periods per pulse length
p 3650 N92-31079
High-resolution processing of long-pulse-lidar data
p 3651 N92-31081

C

CALIFORNIA INST. OF TECH., PASADENA.
Dense modifiable interconnections utilizing photorefractive volume holograms
[AD-A252193] p 3637 N92-30546
Impact erosion of terrestrial planetary atmospheres
[NASA-CR-190605] p 3742 N92-30921
Presolar (?) corundum in the Orgueil meteorite
p 3738 N92-31230

CALIFORNIA UNIV., BERKELEY.
Dynamics of deformable bodies
[AD-A252333] p 3705 N92-30533
Advanced concepts for controlled combustion in engines
[AD-A249911] p 3595 N92-30814

CALIFORNIA UNIV., BERKELEY. LAWRENCE BERKELEY LAB.
Properties of CMOS devices and circuits fabricated on high-resistivity, detector-grade silicon
[DE92-011727] p 3626 N92-30813
Example of a quantum field theory based on a nonlinear Lie algebra
[DE92-010475] p 3731 N92-30825
Physics of the STAR experiment at the relativistic heavy ion collider
[DE92-014481] p 3719 N92-31198

CALIFORNIA UNIV., DAVIS.
Modeling and analysis methodology for aeroelastically tailored chordwise deformable wings
[NASA-CR-189620] p 3579 N92-30304

CALIFORNIA UNIV., IRVINE.
Mechanical behavior and processing of aluminum metal matrix composites
[AD-A249918] p 3592 N92-30874

CALIFORNIA UNIV., LOS ANGELES.
Algorithm to solve nonlinear time dependent problems of engineering and physics
[AD-A250641] p 3702 N92-30347
Evidence for the dependence of the sputter yield of graphite on ion bombardment fluence
[AD-A252500] p 3623 N92-30537

CALIFORNIA UNIV., SAN DIEGO.
On the isotopic signature of recent solar-wind nitrogen
p 3738 N92-31231

CALIFORNIA UNIV., SAN DIEGO, LA JOLLA.
Can stochastic modelling and analysis of multistage interconnection networks lead to efficient usage of redundancy for fault-tolerant design?
[AD-A250635] p 3699 N92-30526
Disorder and transport in highly correlated systems
[AD-A249969] p 3710 N92-30850

CALIFORNIA UNIV., SANTA BARBARA.
Numerical methods for closed-loop control
[AD-A248481] p 3700 N92-30334

CAMBRIDGE UNIV. (ENGLAND).
Statistics for laminar flamelet modeling
p 3597 N92-30668

CANADIAN FUSION FUELS TECHNOLOGY PROJECT, MISSISSAUGA (ONTARIO).
Boundary plasma transport studies on TFTR
[DE92-011942] p 3723 N92-30746

CARNEGIE-MELLON UNIV., PITTSBURGH, PA.
Epoxides as activators for grafting of poly(tetrahydrofuran) from poly(methylphenylsilylene)
[AD-A251086] p 3601 N92-30244
Information processing research
[AD-A248492] p 3734 N92-30324
Exploiting resource parallelism for integrated fault monitoring and recovery
[AD-A248843] p 3699 N92-30557
Some mathematical problems in continuum mechanics
[AD-A250352] p 3706 N92-31128

CENTER FOR MATHEMATICS AND COMPUTER SCIENCE, AMSTERDAM (NETHERLANDS).
Lazy and incremental program generation
[CWI-CS-R9124] p 3692 N92-30428
Adaptive multigrid applied to a bipolar transistor problem
[CWI-NM-R9115] p 3693 N92-30429
The two-dimensional random walk: Its hitting process and its classification
[CWI-BS-R9003] p 3705 N92-30689
The GKS input model in MANIFOLD
[CWI-CS-R9127] p 3699 N92-30896
Combinatorics and Kolmogorov complexity
[CWI-CS-R9125] p 3708 N92-30699
Parallel aspects of some spectral problems in linear algebra
[CWI-NM-R9113] p 3706 N92-30700

CENTRAL WATER AND POWER RESEARCH STATION, POONA (INDIA).
Hydrologic modelling and use of remotely sensed data at CWPRS p 3669 N92-30918

CENTRE D'ETUDES ET DE RECHERCHES, TOULOUSE (FRANCE).
Modeling the turbulent kinetic energy equation for compressible, homogeneous turbulence
p 3631 N92-30653

CENTRE NATIONAL DE LA RECHERCHE SCIENTIFIQUE, VERRIERES-LE BUISSON (FRANCE).
Optics of the ozone lidar ELSA p 3645 N92-31051
Interferometers adaptations to lidars
p 3645 N92-31052

CEP SYSTEMES, PARIS (FRANCE).
ILS, CE, CALS? From design to operation
[ETN-92-91717] p 3697 N92-30950
First conclusions of a manufacturer group on the applicability of CALS in Europe p 3697 N92-30951
CHIBA UNIV. (JAPAN).
A high speed signal processing system for a diode-pumped YAG lidar p 3646 N92-31054
A portable lidar using a diode-pumped YAG laser p 3654 N92-31098
CHICAGO UNIV., IL.
Dark matter and cosmology
[DE92-013023] p 3740 N92-30622
CITY COLL. OF THE CITY UNIV. OF NEW YORK, NY.
Direct sequence spread spectrum CDMA in shared spectrum applications p 3619 N92-30939
CLEMSON UNIV., SC.
Supercritical fluid extraction: A new process for producing high-performance, low-cost carbon fibers
[AD-A249407] p 3595 N92-30773
CLEVELAND METROPOLITAN GENERAL HOSPITAL, OH.
Tolerance of beta blocked hypertensives during orthostatic and altitude stresses
[AD-A249904] p 3685 N92-30745
COASTAL ENVIRONMENTS, INC., BATON ROUGE, LA.
Remote-sensing survey of the Atchafalaya Basin Main Channel, Atchafalaya Channel training project, Saints Martin and Mary Parishes, Louisiana
[AD-A249915] p 3669 N92-31139
COHERENT TECHNOLOGIES, INC., BOULDER, CO.
Atmospheric wind sensing with a 1 and 2 micron coherent lidar p 3639 N92-31019
COLLEGE OF WESTERN NEW ENGLAND, SPRINGFIELD, MA.
Determining significant material properties: A discovery approach p 3607 N92-30279
COLORADO STATE UNIV., FORT COLLINS.
Template-synthesis: A method for enhancing the ionic and electronic conductivity in electronically conductive polymers
[AD-A248806] p 3603 N92-30553
Clouds: Their prediction and simulation
[AD-A250643] p 3679 N92-30643
Infrared investigations of pristine, doped and partially-doped polypyrrole
[AD-A250644] p 3605 N92-30838
Measurement of aerosol profiles using high-spectral-resolution Rayleigh-Mie lidar p 3644 N92-31046
Polyphosphazenes bearing polymerizable pyrrole, thiophene and furan side groups: Synthesis and chemical oxidation
[AD-A249747] p 3607 N92-31207
COLORADO UNIV., BOULDER.
Collisional and chaotic transport of energetic particles in toroidal plasma
[DE92-014589] p 3725 N92-30900
A pulsed CO2 Doppler lidar for boundary layer monitoring p 3639 N92-31021
COMMITTEE ON APPROPRIATIONS (U.S. SENATE).
Departments of Veterans Affairs and Housing and Urban Development, and Independent Agencies Appropriation Bill, 1993
[S-REPT-102-356] p 3735 N92-31169
National Aeronautics and Space Administration p 3736 N92-31170
COMMUNICATIONS RESEARCH CENTRE, OTTAWA (ONTARIO).
An integrated Ka/Ku-band payload for personal, mobile and private business communications p 3619 N92-30933
EHF (28/19 GHz) personal communications satellite terminal development p 3619 N92-30935
COMMUNICATIONS SATELLITE CORP., CLARKSBURG, MD.
Personal communications via ACTS satellite HBR transponders p 3618 N92-30929
COMPUTATIONAL LOGIC, INC., AUSTIN, TX.
Verifying the interactive convergence clock synchronization algorithm using the Boyer-Moore theorem prover
[NASA-CR-189649] p 3700 N92-31158
COMPUTER RESOURCE MANAGEMENT, INC., HERNDON, VA.
National airspace system. Air defense and law enforcement surveillance operational concept NAS-SR-135
[DOT/FAA/SE-92/3] p 3579 N92-31211
COMPUTER TECHNOLOGY ASSOCIATES, INC., MCKEE CITY, NJ.
Aeronautical Mobile Satellite Service (AMSS) capacity analysis and protocol performance simulation results
[DOT/FAA/CT-TN90/64] p 3622 N92-31212
COORDINATING RESEARCH COUNCIL, INC., ATLANTA, GA.
Effect of volatility and oxygenates on driveability at intermediate ambient temperatures
[AD-A248902] p 3607 N92-30341
COPENHAGEN OBSERVATORY (DENMARK).
Carlsberg meridian catalogue La Palma. Number 5: Observations of positions of stars and planets: May 1988 to Dec. 1989
[ISBN-84-7469-052-8] p 3739 N92-30714
CORNELL UNIV., ITHACA, NY.
Vibrationally induced rotational axis switching: A novel mechanism for vibrational mode-coupling
[AD-A251085] p 3712 N92-30259
A program of continuing research on representing, manipulating, and reasoning about physical objects
[AD-A251089] p 3691 N92-30260
How to securely replicate services
[NASA-CR-190476] p 3692 N92-30379
A numerical evaluation of the dynamical systems approach to wall layer turbulence p 3632 N92-30660
Vacuum ultraviolet studies of molecular dynamics
[AD-A246964] p 3715 N92-30681
Approaches to polymer curing and imaging via the in situ generation of a catalyst
[AD-A249917] p 3606 N92-30873

D

DALHOUSIE UNIV., HALIFAX (NOVA SCOTIA).
Neurophysiological analysis of circadian rhythm entrainment
[AD-A248466] p 3684 N92-30319
DANISH METEOROLOGICAL INST., COPENHAGEN.
Data report, 92-2. Magnetic results, 1985-1990 p 3675 N92-30417
DAYTON UNIV., OH.
Evaluation of doped polyethylene oxide as solid electrolyte for polymer batteries
[AD-A249501] p 3624 N92-30619
DAYTON UNIV. RESEARCH INST., OH.
Evaluation of characterization techniques for carbon-carbon composites
[AD-A252693] p 3593 N92-31005
DEFENCE RESEARCH ESTABLISHMENT ATLANTIC, DARTMOUTH (NOVA SCOTIA).
Cross sectional constants and stress distributions of thin-walled sections
[AD-A249886] p 3663 N92-30870
DEFENCE RESEARCH ESTABLISHMENT, OTTAWA (ONTARIO).
The temperature dependence of a large dynamic range photodetector structure
[AD-A247667] p 3624 N92-30683
DEFENCE RESEARCH ESTABLISHMENT VALCARTIER (QUEBEC).
Multiple scattering technique lidar p 3641 N92-31031
Multiple scattering lidar returns from stratus clouds p 3642 N92-31035
Effect of atmospheric extinction on laser rangefinder performance at 1.54 and 0.6 microns p 3648 N92-31066
DELAWARE UNIV., NEWARK.
Center for Composites Manufacturing Science, Reliability, and Maintainability Technology
[AD-A248661] p 3591 N92-30639
Design of a high activity and selectivity alcohol catalyst
[DE92-013918] p 3594 N92-30717
Fundamental studies of strongly magnetic rare earth-transition metal alloys
[DE92-015916] p 3600 N92-31186
DEPARTMENT OF DEFENSE, FORT MEADE, MD.
Toward a North American standard for mobile data services p 3620 N92-30940
DEPARTMENT OF ENERGY, WASHINGTON, DC.
Chemistry for protection of the environment, 8th International Conference proceedings
[DE92-014317] p 3674 N92-31181
Fuel cell systems program plan: Fiscal year 1992
[DE92-015985] p 3672 N92-31188
DEPARTMENT OF THE ARMY, WASHINGTON, DC.
Waveguide polarizer using localized surface plasmons
[AD-D015258] p 3614 N92-30348
DEPARTMENT OF THE NAVY, WASHINGTON, DC.
Digital bottom mapping
[AD-D015238] p 3682 N92-30413
Laser optical mouse
[AD-D015307] p 3690 N92-30564
Method of bonding carbon-carbon and metal matrix composite structures
[AD-D015299] p 3591 N92-30573
Method of synthesizing high quality, doped diamond and diamonds and devices obtained therefrom
[AD-D015267] p 3604 N92-30685
Thrust test fixture
[AD-D015259] p 3585 N92-31192
Fiber optic Michelson sensor and arrays with passive elimination of polarization fading and source feedback isolation
[AD-D015290] p 3722 N92-31213
DESERT RESEARCH INST., RENO, NV.
Linkage of anthropogenic aerosol to clouds and climate
[DE92-013574] p 3674 N92-30707
DEUTSCHE FORSCHUNGS- UND VERSUCHSANSTALT FUER LUFT- UND RAUMFAHRT, OBERPFAFFENHOFEN (GERMANY, F.R.).
Airborne remote sensing of tropospheric water vapor using a near infrared DIAL system p 3644 N92-31042
DEUTSCHE FORSCHUNGSANSTALT FUER LUFT- UND RAUMFAHRT, OBERPFAFFENHOFEN (GERMANY, F.R.).
Trial of a slant visual range measuring device p 3644 N92-31043
DOUGLAS AIRCRAFT CO., INC., LONG BEACH, CA.
High speed research system study. Advanced flight deck configuration effects
[NASA-CR-189650] p 3581 N92-30965
Evaluation of microwave landing system approaches in a wide-body transport simulator
[NASA-CR-4450] p 3579 N92-30978
DUGWAY PROVING GROUND, UT.
Methodology investigation, implement remote sensing
[AD-A248901] p 3678 N92-30340
DUKE UNIV., DURHAM, NC.
Implementation of parallel algorithms
[AD-A248826] p 3695 N92-30555

E

EAST CAROLINA UNIV., GREENVILLE, NC.
An experiment on the use of disposable plastics as a reinforcement in concrete beams p 3593 N92-30287
ECOLE NORMALE SUPERIEURE, PARIS (FRANCE).
Continuous wavelet analysis of coherent structures p 3634 N92-30673
ECOLE POLYTECHNIQUE, PALAISEAU (FRANCE).
Airborne lidar and radiometric observations of PBL- and low clouds p 3642 N92-31037
ECLIPS at LMD: Preliminary results of phase 2 p 3643 N92-31038
A comparison of lidar inversion methods for cirrus applications p 3649 N92-31074
ECOLOGICAL SOCIETY OF AMERICA.
The sustainable biosphere initiative: An ecological research agenda p 3673 N92-30425
EDGERTON, GERMESHAUSEN AND GRIER, INC., IDAHO FALLS, ID.
Reliability in the design phase
[DE92-012217] p 3661 N92-30763
Proceedings of a Beryllium Technology Workshop
[DE92-012312] p 3598 N92-30834
EG AND G ROCKY FLATS, INC., GOLDEN, CO.
A method for the production of weakly acidic cation exchange resins
[DE92-015314] p 3717 N92-31137
A method for regenerating ion exchange resin
[DE92-015312] p 3606 N92-31146
A method for production of new anion exchangers
[DE92-015313] p 3717 N92-31147
EIDGENOESSISCHE TECHNISCHE HOCHSCHULE, ZURICH (SWITZERLAND).
Analytical multiple scattering correction to the Mie theory: Application to the analysis of the lidar signal p 3642 N92-31036
Lidar depolarization by nonspherical particles: Potential of combined depolarization/backscattering measurements for PSC's characterization p 3644 N92-31044
ELECTRICITE DE FRANCE, CHATOU.
Development of a reliability maintenance optimization method p 3697 N92-30956
ELECTROCHEMICAL SOCIETY, INC., PENNINGTON, NJ.
Proceedings of the 181st Electrochemical Society, Inc. Meeting Program
[AD-A249729] p 3596 N92-31178
ELLIOTT-AUTOMATION SPACE AND ADVANCED MILITARY SYSTEMS LTD., CAMBERLEY (ENGLAND).
EASAMS' Ariane 5 on-board software experience
[D308/TN/001] p 3586 N92-30715
ELLIPSAT CORP., WASHINGTON, DC.
The ELLIPSO (tm) system: Elliptical low orbits for mobile communications and other optimum system elements p 3618 N92-30930

ENVIRONMENTAL ANALYSIS AND REMOTE SENSING, DELFT (NETHERLANDS).
Monitoring of Dutch forest with LANDSAT-TM
[BCRS-91-21] p 3666 N92-30468

ENVIRONMENTAL PROTECTION AGENCY, LAS VEGAS, NV.
A variable phase function approach for the inversion of lidar return signals p 3649 N92-31073

ENVIRONMENTAL PROTECTION AGENCY, RESEARCH TRIANGLE PARK, NC.
A model of the ADA avionics real-time system: An example of the benefits of the hardware/software codesign approach in development of real-time systems
[AD-A248893] p 3581 N92-30524
Status of selected air pollution control programs, February 1992
[PB92-171966] p 3673 N92-30561
Report of the Great Lakes Air Toxics Research Priorities Workshop
[PB92-166933] p 3673 N92-30602

ERG SYSTEMS, INC., SAINT JAMES, NY.
Full surface testing of grazing incidence mirrors
[AD-A248851] p 3719 N92-30233

EUROPEAN NUCLEAR ENERGY AGENCY, FRASCATI (ITALY).
The ENEA CO2 lidar/DIAL station activity in a tropospheric remote sensing program
p 3655 N92-31103

EUROPEAN SPACE AGENCY, PARIS (FRANCE).
Generalized projected gradient-type iterative method for parametric and functional optimization of dynamical systems subject to constraints
[ESA-TT-1166] p 3694 N92-30512
Determination of pair potentials by analysis of diffuse scattering of the local field in Pd3V and Ni3V
[ESA-TT-1228] p 3597 N92-30513
Computation of unsteady transonic flows using an implicit centered Euler solver without artificial viscosity
[ESA-TT-1235] p 3575 N92-30514
Registration of windfall damage in the eastern Hunsrueck Plateau (Federal Republic of Germany) utilizing LANDSAT-TM-data: A landscape-ecological analysis for practical forestry
[ESA-TT-1253] p 3667 N92-30515
Numerical simulation of crater formation heating by laser beam. Analysis of radiation exchanges in the cavity
[ESA-TT-1234] p 3657 N92-30997

F

FEDERAL AVIATION ADMINISTRATION, ATLANTIC CITY, NJ.
Technical training for national simulator evaluation specialist
[NASA-CR-190429] p 3687 N92-30488
GNAS Maintenance Control Center (GMCC) Design Qualification Test and Evaluation (DQT/E) test procedures
[DOT/FAA/CT-TN91/40] p 3585 N92-30976
Helicopter nighttime parking test results - UH-1
[DOT/FAA/CT-TN92/1] p 3580 N92-31165

FEDERAL AVIATION ADMINISTRATION, WASHINGTON, DC.
Evaluation of head impact kinematics for passengers seated behind interior walls
[AD-A252651] p 3578 N92-30551
Allocation and recovery of federal airport and airway costs, 1991
[AD-A249436] p 3585 N92-30777

FERMI NATIONAL ACCELERATOR LAB., BATAVIA, IL.
Magnetic field measurements of Fermilab/General Dynamics built full scale SSC collider dipole magnets
[DE92-014612] p 3717 N92-30589
Dark matter and cosmology
[DE92-013023] p 3740 N92-30622
Network load of X terminals at CDF
[DE92-011704] p 3699 N92-30812
Ideas for a long-baseline neutrino detector
[DE92-010650] p 3743 N92-30828
Recent experimental studies on hadron showers produced in high energy muon-nucleus interactions
[DE92-016002] p 3719 N92-31219

FLORENCE UNIV. (ITALY).
Issues for the integration of satellite and terrestrial cellular networks for mobile communications
p 3620 N92-30941
Laboratory scaled simulation of lidar cloud sounding experiments p 3645 N92-31047

FLORIDA AGRICULTURAL AND MECHANICAL UNIV., TALLAHASSEE.
Analytical methods using Slater-type orbitals in quantum chemistry
[AD-A251044] p 3731 N92-30242

FLORIDA STATE UNIV., TALLAHASSEE.
Resonant instability of supersonic shear layers
p 3632 N92-30661
Markov chain simulations of binary matrices
[AD-A249265] p 3708 N92-30771

FLORIDA UNIV., GAINESVILLE.
Temperature effect on the Langmuir-Blodgett polymerization of 2-pentadecylaniline
[AD-A250803] p 3601 N92-30250
Development of ultra-low noise, high sensitivity planar metal grating coupled AlGaAs/GaAs multiquantum well IR detectors for focal plane array staring IR sensor systems
[AD-A246122] p 3590 N92-30318
X ray scattering studies of non-equilibrium ordering processes
[DE92-014006] p 3598 N92-30787

G

G AND C SYSTEMS, INC., SAN JUAN CAPISTRANO, CA.
High-speed civil transport issues and technology program
[NASA-CR-186020] p 3580 N92-31208

GALAXY SCIENTIFIC CORP., MAYS LANDING, NJ.
Statistics on aircraft gas turbine engine rotor failures that occurred in US commercial aviation during 1989
[DOT/FAA/CT-92/5] p 3581 N92-30303

GENERAL ACCOUNTING OFFICE, WASHINGTON, DC.
Computer security: Agencies reported having implemented most system security controls
[GAO/IMTEC-92-45] p 3690 N92-30712

GENERAL MOTORS RESEARCH LABS., WARREN, MI.
The influence of Lewis number and nonhomogeneous mixture on premixed turbulent flame structure
p 3597 N92-30669

GENEVA COLL., BEAVER FALLS, PA.
Experiments with the low melting indium-bismuth alloy system p 3601 N92-30272

GEORGIA INST. OF TECH., ATLANTA.
Precursor structure-fiber property relationships in polyacrylonitrile-based carbon fibers
[AD-A249888] p 3592 N92-30871

GEORGIA UNIV., ATHENS.
Fundamental studies of carbon, NH, and oxygen rings and other high energy density molecular systems
[AD-A246963] p 3715 N92-30680

GIAT INDUSTRIES (FRANCE).
Quality assurance and ILS p 3697 N92-30953
Practical application of the ILS: Practical integration, design, and logistics p 3697 N92-30955

GKSS-FORSCHUNGSZENTRUM GEESTHACHT (GERMANY, F.R.).
Measurement of multiple scattering effects with a polarization Raman elastic-backscatter lidar
p 3641 N92-31033
Verification measurement of a polarization Raman elastic-backscatter lidar p 3647 N92-31062
BELINDA: Broadband Emission Lidar with Narrowband Determination of Absorption. A new concept for measuring water vapor and temperature profiles
p 3653 N92-31091
Investigations on atomic-vapor-filter high-spectral-resolution lidar for temperature measurements p 3654 N92-31099

GOLDSWORTHY ENGINEERING, INC., SPRINGVILLE, UT.
Organic Matrix Composite Helicopter Internal/External Cargo Pallet System (OMC INTEX)
[AD-A251127] p 3580 N92-30878

GOSUDARSTVENNYI KOMITET PO ISPOLZOVANIYU ATOMNOI ENERGII, SERPUKHOV (USSR).
Linear estimates of structure functions from deep inelastic lepton-nucleon scattering data, part 1
[DE92-627288] p 3713 N92-30403
Search for light neutral scalar and pseudoscalar particles in pFe interactions at 70 GeV
[DE92-627317] p 3713 N92-30404

GRENOBLE-1 UNIV. (FRANCE).
Recursive models for synchronous sequential devices
[IMAG-RR-855-I] p 3704 N92-30473
Configuration algorithms for hierarchical supernode machines
[IMAG-RR-853-I] p 3694 N92-30493

GTE GOVERNMENT SYSTEMS CORP., WALTHAM, MA.
Cellular: Toward personal communications
p 3619 N92-30936

H

HAHNEMANN MEDICAL COLL. AND HOSPITAL, PHILADELPHIA, PA.
Cortical mechanisms of attention, discrimination, and motor response to somaesthetic stimuli
[AD-A247228] p 3687 N92-30613

HAMAMATSU PHOTONICS K. K., ICHINO (JAPAN).
A geodetic laser radar rangefinder with 10(exp -7) resolution p 3641 N92-31029

HARRY DIAMOND LABS., ADELPHI, MD.
Double-sided wafer alignment techniques
[AD-A250757] p 3730 N92-30895

HARVARD UNIV., CAMBRIDGE, MA.
Psychophysical studies of visual cortical function
[AD-A246962] p 3687 N92-30679
From minerals to materials: A facile synthetic route to preceramic polymers for aluminum oxide
[AD-A250351] p 3606 N92-31141
The (146,147)Sm-(142,143)Nd systematics of early terrestrial differentiation and the lost continents of the early Earth p 3678 N92-31229

HAWAII UNIV., HONOLULU.
Trace element and isotope geochemistry of geothermal fluids, East Rift Zone, Kilauea, Hawaii
[DE92-014586] p 3671 N92-31117
Fractal analysis: A new remote sensing tool for lava flows p 3736 N92-31224

HELSINKI UNIV. OF TECHNOLOGY, ESPOO (FINLAND).
Effects of impurities on the mechanical behaviour of primary and secondary cast aluminum alloys
[PB92-180652] p 3598 N92-30785

HOUSTON UNIV., TX.
Nondestructive characterization of two-phase metal-matrix materials
[AD-A249912] p 3592 N92-30815

HUGHES STX, INC., LANHAM, MD.
Raman lidar measurements of water vapor and aerosol/clouds during the FIRE/SPECTRE field campaign p 3652 N92-31089

I

IDAHO UNIV., MOSCOW.
Designing, engineering, and testing wood structures
p 3593 N92-30270

IIT RESEARCH INST., LANHAM, MD.
Development statistics for the UH-1 Ada feasibility study
[AD-A252404] p 3584 N92-30547

ILLINOIS UNIV., URBANA.
Nonlinear system design: Adaptive feedback linearization with unmodeled dynamics
[AD-A248484] p 3700 N92-30335
Research on elementary particle physics
[DE92-014622] p 3715 N92-30625
Research on elementary particle physics. Task P: Studies in theory and phenomenology of elementary particles, part 1
[DE92-014428] p 3716 N92-30791

ILLINOIS UNIV., URBANA-CHAMPAIGN.
Measurement capabilities of giant lidars for middle and upper atmospheric applications p 3651 N92-31084

INDIAN INST. OF TECH., BOMBAY.
Satellite and Radar Data Use in Rainfall-Runoff Models p 3667 N92-30910
Remote sensing satellite data use in run-off studies
p 3668 N92-30914
Geographic information system and its applications
p 3668 N92-30915
Estimation of vertical profile of soil moisture through multifrequency microwave data analysis
p 3669 N92-30919
Digital methods for analysis of satellite imagery
p 3669 N92-30920

INDIAN METEOROLOGICAL DEPT., NEW DELHI.
Use of INSAT data in rainfall estimation
p 3668 N92-30912

INDIAN SPACE RESEARCH ORGANIZATION, AHMEDABAD.
Remote sensing for rainfall estimation: SAC experience p 3668 N92-30917

INDIANA UNIV., BLOOMINGTON.
Theoretical particle physics
[DE92-014531] p 3716 N92-30841
High resolution electron energy loss studies of surface vibrations
[DE92-014608] p 3626 N92-30901

INDIANA UNIV.-PURDUE UNIV., INDIANAPOLIS.
Synthesis and reactivity of 1-methyl-e-ethynylpyridinium triflate
[AD-A250638] p 3602 N92-30346

INSTITUT D'AERONOMIE SPATIALE DE BELGIQUE, BRUSSELS.
Astronautics 1977-1990
[AERONOMICA-ACTA-F-42-1991] p 3744 N92-30996
INSTITUT DE MECANIQUE DE GRENOBLE (FRANCE).
A subgrid-scale model based on the second-order velocity structure function p 3631 N92-30651
INSTITUT DES HAUTES ETUDES SCIENTIFIQUES, BURES-SUR-YVETTE (FRANCE).
Quantum Weyl Group and universal quantum R-matrix for affine Lie algebra A1
[PB92-178276] p 3704 N92-30511
Dimension bounds for quotient spaces
[PB92-177997] p 3706 N92-30789
Non-holonomic filtration: Algebraic and geometric aspects of non-integrability
[PB92-178003] p 3706 N92-30790
INSTITUT FRANCO-ALLEMAND DE RECHERCHES, SAINT-LOUIS (FRANCE).
Doppler photography: Laser methods on the flow measurement technique
[ISL-PU-303/90] p 3720 N92-30507
INSTITUT NATIONAL POLYTECHNIQUE, GRENOBLE (FRANCE).
Architecture for the high performance implantation of communication transport level protocols
[ETN-92-91666] p 3690 N92-30701
Contribution of parallelism to solving a load distribution problem in electric networks
[ETN-92-91668] p 3625 N92-30702
INSTITUTE FOR COMPUTER APPLICATIONS IN SCIENCE AND ENGINEERING, HAMPTON, VA.
Compiler analysis for irregular problems in FORTRAN D
[NASA-CR-189664] p 3689 N92-30311
Semiannual final report, 1 October 1991 - 31 March 1992
[NASA-CR-189660] p 3689 N92-30489
A computational algorithm for crack determination: The multiple crack case
[NASA-CR-189665] p 3704 N92-30516
Resolution properties of the Fourier method for discontinuous waves
[NASA-CR-189668] p 3706 N92-30716
INSTITUTE FOR DEFENSE ANALYSES, ALEXANDRIA, VA.
High frequency communications under adverse conditions
[AD-A252199] p 3615 N92-30532
INTERMET TECHNOLOGY, GEORGETOWN, PA.
Experiments with the low melting indium-bismuth alloy system p 3601 N92-30272
INTERNATIONAL CENTRE FOR THEORETICAL PHYSICS, TRIESTE (ITALY).
Multiple scattering theory of x ray absorption. A review
[DE92-622374] p 3716 N92-30798
From a world-sheet supersymmetry to the Dirac equation
[DE92-622375] p 3731 N92-30799
From a particle with a world-line supersymmetry to the Dirac-like equation
[DE92-622376] p 3731 N92-30800
Quantum mechanics in Grassmann space
[DE92-622377] p 3711 N92-30801
Coexistence of uniquely ergodic subsystems of interval mapping
[DE92-630231] p 3732 N92-31133
Fixed point iterations for a class of nonlinear mappings in certain Banach spaces
[DE92-630235] p 3706 N92-31134
Heat flow of p-harmonic maps with values into spheres
[DE92-630236] p 3707 N92-31135
Stochastic strings, topology, and space-time confinement
[DE92-630239] p 3732 N92-31136
One-loop integration for the axial gauge with generalized prescription
[DE92-630241] p 3732 N92-31145
Elastic constants of crystals near melting via density functional theory. Effect of three-body correlations
[DE92-630567] p 3730 N92-31191
Ginsburg criterion for an equilibrium superradiant model in the dynamic approach
[DE92-630566] p 3732 N92-31203
INTERNATIONAL SOCIETY FOR OPTICAL ENGINEERING, BELLINGHAM, WA.
Sol-gel optics: Proceedings SPIE-The International Society for Optical Engineering
[AD-A249986] p 3721 N92-31126
IOWA STATE UNIV. OF SCIENCE AND TECHNOLOGY, AMES.
Demonstration of magnetic domain boundary movement using an easily assembled videocam-microscope system p 3611 N92-30286
Development of a 3-D upwind PNS code for chemically reacting hypersonic flowfields
[NASA-CR-190182] p 3576 N92-30977
ISRAEL INST. OF METALS, HAIFA.
Laser induced reaction for pre-bond surface preparation of aluminum alloys
[AD-A249916] p 3598 N92-30872

J

JAPAN ATOMIC ENERGY RESEARCH INST., TOKYO.
Filler metal development for Hastelloy alloy XR
[DE92-782044] p 3600 N92-31163
JET PROPULSION LAB., CALIFORNIA INST. OF TECH., PASADENA.
Double-loop frequency-selected surfaces for multifrequency division multiplexing in a dual-reflector antenna
[NASA-CASE-NPO-18701-1-CU] p 3614 N92-30391
Hybridization of detector array and integrated circuit for readout
[NASA-CASE-NPO-18062-1-CU] p 3623 N92-30542
Encyclopedia of software components
[NASA-CASE-NPO-18435-1-CU] p 3695 N92-30543
Proceedings of the Workshop on Advanced Network and Technology Concepts for Mobile, Micro, and Personal Communications
[NASA-CR-190459] p 3617 N92-30923
Ka-band mobile and personal systems development at JPL p 3618 N92-30928
Direct broadcast satellite-radio: Portable and mobile reception trade-offs p 3621 N92-30945
Science questions for the Magellan continuing mission p 3738 N92-31235
JOHNS HOPKINS UNIV., BALTIMORE, MD.
Direct numerical simulations of stably-stratified sheared turbulence: Implications for oceanic mixing p 3632 N92-30659

K

KANSAS STATE UNIV., MANHATTAN.
Electric Vehicle Site Operator Program
[DE92-014591] p 3626 N92-30842
KYUSHU UNIV., FUKUOKA (JAPAN).
Alexandrite lidar for the atmospheric water vapor detection and development of powerful tunable sources in IR p 3653 N92-31094

L

LAMONT-DOHERTY GEOLOGICAL OBSERVATORY, PALISADES, NY.
Inter- and intra-plate deformation at North American plate boundaries
[NASA-CR-190485] p 3676 N92-30961
LASER SCIENCE, INC., AMES, IA.
Solid lubrication of laser grown fluorinated diamond thin films
[AD-A249485] p 3603 N92-30635
LAVAL UNIV. (QUEBEC).
Multiple scattering lidar returns from stratus clouds p 3642 N92-31035
Effect of atmospheric extinction on laser rangefinder performance at 1.54 and 0.6 microns p 3648 N92-31066
LAWRENCE LIVERMORE NATIONAL LAB., CA.
Shock-induced martensitic transformation of highly oriented graphite to diamond
[DE92-014787] p 3602 N92-30399
Interaction physics for megajoule laser fusion targets
[DE92-014796] p 3656 N92-30400
Program RELAX: A code designed to calculate atomic relaxation spectra of x rays and electrons
[DE92-013751] p 3714 N92-30586
Towards the development of a global inventory for black carbon emissions
[DE92-013514] p 3674 N92-30647
Microscopic theory of THG and electro-absorption in conjugated polymers
[DE92-014786] p 3604 N92-30792
Remote experimental site concept for diagnostic collaborations in fusion
[DE92-010437] p 3724 N92-30824
Transient photoconductivity of low temperature GaAs grown by molecular beam epitaxy terahertz radar applications
[DE92-011848] p 3729 N92-30854
Heating and momentum deposition in hot stars
[DE92-011850] p 3740 N92-30855
Modeling of UV lines from cataclysmic variable winds
[DE92-013443] p 3739 N92-30862
Methane to liquid
[DE92-001277] p 3596 N92-30883
Structural and magnetic properties of RBa2Cu2NbO8 (R = La, Pr, and Nd)
[DE92-014780] p 3729 N92-30885
Electron scattering and electromagnetic response properties of metal clusters
[DE92-014715] p 3621 N92-31007
Generation of a sodium guidestar using a high power dye laser
[DE92-012696] p 3657 N92-31115
Spectroscopic diagnosis of long-scale-length exploding-foil plasma in the presence of an intense radiation field
[DE92-014718] p 3726 N92-31118
Theoretical study of phase stability in Ni-Al and Ni-Ti alloys
[DE92-014776] p 3599 N92-31119
The environmental dilemma of fossil fuels
[DE92-014887] p 3674 N92-31121
Stability of metallic superlattices
[DE92-011526] p 3600 N92-31124
Stabilization of face-centered-cubic titanium
[DE92-011530] p 3600 N92-31125
Self-consistent-field KKR-CPA calculations in the atomic-sphere approximations
[DE92-011525] p 3600 N92-31138
LEHIGH UNIV., BETHLEHEM, PA.
Perforated monolayers
[DE92-011632] p 3593 N92-30344
LITTON INDUSTRIES, MOORPARK, CA.
A study of atmospheric optical scattering parameters at 1.5 and 2 micron region for solid state Doppler lidar applications p 3648 N92-31067
LODESTAR RESEARCH CORP., BOULDER, CO.
Fundamental studies of fusion plasmas
[DE92-015077] p 3726 N92-31116
LOGICON TECHNICAL SERVICES, INC., DAYTON, OH.
Review of psychophysically-based image quality metrics
[AD-A251053] p 3686 N92-30254
LOS ALAMOS NATIONAL LAB., NM.
Development and testing of an air quality model for Mexico City
[DE92-011238] p 3673 N92-30520
On recrystallization in metal matrix composites
[DE92-011364] p 3590 N92-30521
Constraints on the nuclear matter equation of state from pulsar glitches
[DE92-015142] p 3740 N92-30578
Rapid cooling and structure of neutron stars
[DE92-015279] p 3740 N92-30609
Ultra high energy gamma rays and observations with CYGNUS/MILAGRO
[DE92-015243] p 3743 N92-30627
Processing aerosols and filaments in a TM010 microwave cavity at 2.45 GHz
[DE92-013536] p 3615 N92-30703
A one-class classifier for identifying urban areas in remotely-sensed data
[DE92-013539] p 3667 N92-30704
Fluctuation-dissipation theorem in general relativity and the cosmological constant
[DE92-013542] p 3740 N92-30705
The escape of greater MeV photons from cosmological gamma-ray bursts
[DE92-013545] p 3743 N92-30706
VUV production from a ferrite-driven flash-pumped system
[DE92-011362] p 3657 N92-30805
Neutron time-of-flight ion temperature diagnostic for inertial confinement fusion experiments
[DE92-011365] p 3724 N92-30806
Theory of sublinear power dependence for microwave heating in some ceramic materials
[DE92-015147] p 3606 N92-30847
Nuclear structure calculations for astrophysical applications
[DE92-011495] p 3740 N92-30856
Joint stabilizing projects in defense
[DE92-015977] p 3709 N92-30891
Small satellite radiation budget instrumentation
[DE92-011134] p 3677 N92-31008
Lidar analysis techniques for use in the atmospheric boundary layer p 3649 N92-31069
Proceedings, phenomenology and applications of high temperature superconductors
[DE92-011133] p 3627 N92-31107
Nonlinear RR Lyrae models with new Livermore opacities
[DE92-011158] p 3741 N92-31108
Reflector development for XUV free-electron laser oscillators
[DE92-015212] p 3657 N92-31182
A failure-to-restore unavailability model for periodically performed maintenance
[DE92-015902] p 3708 N92-31185

Fine scale mesostructures in superconducting and other materials
[DE92-015207] p 3730 N92-31200
Diffuse neutron scattering signatures of rough films
[DE92-015208] p 3717 N92-31201
Modeling initiation of explosives by projectile impact
[DE92-015210] p 3608 N92-31202
Thermohydraulic modeling of nuclear thermal rockets: The KLAXON code
[DE92-015274] p 3589 N92-31204
On the strain-rate dependence of dynamic recrystallization in copper polycrystals
[DE92-011363] p 3730 N92-31217
Oxidation of gallium arsenide
[DE92-016208] p 3731 N92-31220

LOUISIANA STATE UNIV., BATON ROUGE.
Quantum transport, noise and non-linear dissipative effects in one- and two-dimensional systems and associated sub-micron and nanostructure devices
[AD-A250895] p 3627 N92-31210

LOWELL UNIV., MA.
Selection of opening model for parachute scaling studies
[AD-A250882] p 3573 N92-30239

LOYOLA COLL., BALTIMORE, MD.
An automated system for creep testing
p 3611 N92-30282
Five experiments in materials science for less than $10.00 p 3611 N92-30283

LUDWIG-MAXIMILIANS-UNIV., MUNICH (GERMANY, F.R.).
Lidar multiple scattering: Dependence on atmospheric parameters p 3647 N92-31061

LUNAR AND PLANETARY INST., HOUSTON, TX.
Twenty-Third Lunar and Planetary Science Conference
[NASA-CR-190178] p 3736 N92-31222
Global scale concentrations of volcanic activity on Venus: A summary of three 23rd Lunar and Planetary Science Conference abstracts. 1: Venus volcanism: Global distribution and classification from Magellan data. 2: A major global-scale concentration of volcanic activity in the Beta-Atla-Themis region of Venus. 3: Two global concentrations of volcanism on Venus: Geologic associations and implications for global pattern of upwelling and downwelling p 3737 N92-31226
Constraints on the putative companions to PSR1257+12 p 3738 N92-31232

LUND INST. OF TECH. (SWEDEN).
Fluorescence lidar multi-color imaging of vegetation
p 3640 N92-31028

M

MARQUETTE UNIV., MILWAUKEE, WI.
Resonance Raman spectroscopic studies of trans dioxorhenium(V)tetrapyridyl species
[AD-A249919] p 3595 N92-30875

MARYLAND UNIV., COLLEGE PARK.
Structure, processing, and properties of potatoes
p 3611 N92-30288
Optimal shear correction factors in hierarchical plate modelling
[AD-A248899] p 3662 N92-30338
Special finite element methods for a class of second order elliptic problems with rough coefficients
[AD-A248900] p 3701 N92-30339
Navier-Stokes computations of a viscous optimized waverider
[NASA-CR-189658] p 3574 N92-30392
Subgrid-scale backscatter in transitional and turbulent flows p 3630 N92-30650

MARYLAND UNIV. BALTIMORE COUNTY, CATONSVILLE.
Implementation scheme for recursion in spectral dimension
[AD-A248945] p 3695 N92-30629

MASSACHUSETTS INST. OF TECH., CAMBRIDGE.
Superconductivity and magnetism in rapidly solidified perovskites
[DE92-014081] p 3597 N92-30588
VLSI design, parallel computation, and distributed computing
[AD-A252349] p 3699 N92-30596
A description of the research for period 3 of a research program on the planning and control for space robotic manipulators
[NASA-CR-190243] p 3660 N92-30738
Focused ion beam implantation
[AD-A249662] p 3627 N92-31004

MASSACHUSETTS INST. OF TECH., LEXINGTON.
Doppler mean velocity estimation: Small sample analysis and a new estimator
[AD-A249024] p 3678 N92-30559
On the radial component of the electric field for a monopole phased array antenna focused in the near zone
[AD-A249441] p 3616 N92-30761
Maximum likelihood detection of electro-optic moving targets
[AD-A249442] p 3616 N92-30762
Multifrequency measurements of radar ground clutter at 42 sites. Volume 3: Appendix E
[AD-A246988] p 3616 N92-30863
Diversity imaging techniques in lidar
p 3640 N92-31026
Tunable Electro-optic modulators for lidar systems and atmospheric applications p 3646 N92-31056
The role of laser coherence in long-range vibration measurements p 3654 N92-31097

MASSACHUSETTS UNIV., AMHERST.
Modification of 95 GHz radar source module for low phase noise operation
[AD-A249793] p 3622 N92-31180

MATERIALS RESEARCH LABS., MARIBYRNONG (AUSTRALIA).
Prediction of coincidence frequencies for a thin-walled, fluid-filled pipe
[MRL-TN-600] p 3664 N92-30963

MAX-PLANCK-INST. FUER METEOROLOGIE, HAMBURG (GERMANY, F.R.).
An alexandrite regenerative amplifier for water vapor and temperature measurements p 3645 N92-31048

MCAT INST., SAN JOSE, CA.
Numerical methods for the simulation of complex multi-body flows with applications for the integrated Space Shuttle vehicle
[NASA-CR-190045] p 3575 N92-30740
Numerical methods for the simulation of complex multi-body flows with applications for the integrated Space Shuttle vehicle p 3576 N92-30741
Application of the Chimera overlapped grid scheme to simulation of Space Shuttle ascent flows
p 3576 N92-30742

MEISEI ELECTRIC CO. LTD., MORIYA (JAPAN).
A range-resolved bistatic lidar using a high-sensitive CCD-camera p 3640 N92-31027

MEMORIAL HEART INST., LONG BEACH, CA.
Optimal ECG electrode sites and criteria for detection of asymptomatic coronary artery disease, update 1990. Multilead ECG changes at rest, with exercise, and with coronary angioplasty
[AD-A248613] p 3684 N92-30523

MENTOR GRAPHICS (FRANCE).
Concurrent engineering p 3697 N92-30952

MESSERSCHMITT-BOELKOW-BLOHM G.M.B.H., MUNICH (GERMANY, F.R.).
The Eurofar program: An European overview on advanced VTOL civil transportation system
[MBB-UD-0611-91-PUB] p 3578 N92-30418
Operations and logistics tasks in the Columbus development program
[MBB-UO-0166-91-PUB] p 3708 N92-30419
Adoption of the LSA S/W DILSA for the Columbus LSA tasks
[MBB-UO-0168-91-PUB] p 3709 N92-30420
A processing environment for test and simulation data of thermodynamic systems
[MBB-UO-0169-91-PUB] p 3731 N92-30421
Anisotropic silicon etching techniques
[MBB-Z-0413-91-PUB] p 3594 N92-30422
MBB-LAGRANGE: A general structural reliability and optimization structural system
[MBB/FW321/S/PUB/467] p 3662 N92-30423
Multidisciplinary optimization of fiber composite aircraft structures
[MBB/FW321/S/PUB/476] p 3579 N92-30424
Resonance and control response tests using a control simulation device
[MBB-UD-0608-91-PUB] p 3583 N92-30439
Progress in the development of the Hermes evaporators
[MBB-UO-0164-91-PUB] p 3587 N92-30440
Liquid droplet radiator: Design concepts and development logic
[MBB-UO-0165-91-PUB] p 3613 N92-30441
Columbus logistics transportation and ground processing
[MBB-UO-0167-91-PUB] p 3709 N92-30442
Calculation of viscous hypersonic flows in chemical non-equilibrium
[MBB/FE211/S/PUB/466] p 3634 N92-30674
Numerical optimization in Germany: A non-exhaustive survey on current activities with emphasis on aeronautics
[MBB/FE211/S/PUB/474] p 3573 N92-30675
CFD contributions during hypersonic airplane intake design
[MBB/FE213/S/PUB/459] p 3575 N92-30676
Influence of various carbon fibre types on the mechanical performance and damage tolerance of composites
[MBB/FE202/S/PUB/477] p 3591 N92-30690
Development of hardness cycles for fiber bound materials, using DSC: From laboratory specimens to complex high duty structural members
[MBB-Z-0409-91-PUB] p 3592 N92-30969
Introduction to the efficiency of fuel cells
[MBB-Z-0412-91-PUB] p 3671 N92-30970

MIAMI UNIV., CORAL GABLES, FL.
Remote sensing applications to rainfall estimation
p 3668 N92-30911

MIAMI UNIV., FL.
Solar-hydrogen energy system for solar belt countries and use of remote sensing p 3668 N92-30913

MIAMI UNIV., OXFORD, OH.
Ni-H2 cell separator matrix engineering
[NASA-CR-190055] p 3671 N92-30949

MICHIGAN UNIV., ANN ARBOR.
Studies of phonons and electronic excitations in semiconductor heterostructures
[AD-A249406] p 3729 N92-30772
Tropospheric and stratospheric wind profiling with a direct detection Doppler lidar p 3639 N92-31018

MICRO CRAFT, INC., HUNTSVILLE, AL.
Integration mockup and process material management system
[NASA-CR-184319] p 3613 N92-30754

MIDWEST RESEARCH INST., GOLDEN, CO.
Research on polycrystalline thin film submodules based on CuInSe2 materials
[DE92-010584] p 3727 N92-30247
Design and simulation of latent heat storage units
[DE91-002145] p 3670 N92-30330
Perspective on photovoltaic amorphous silicon
[DE92-010581] p 3670 N92-30519
Research on defects and transport in amorphous silicon-based semiconductors
[DE92-001223] p 3729 N92-30748
Yaw dynamics of horizontal axis wind turbines
[DE92-001245] p 3670 N92-30837
Photodegradation effects in materials exposed to high flux solar and solar simulated radiation
[DE91-002147] p 3596 N92-30879
Synthesis of cresols and xylenols from benzene and methanol
[DE91-002143] p 3596 N92-30882
Uniform flux dish concentrators for photovoltaic application
[DE92-010566] p 3671 N92-30896
Shining on: A primer on solar radiation data
[DE92-010555] p 3743 N92-31206

MINISTRY OF POSTS AND TELECOMMUNICATIONS, TOKYO (JAPAN).
Advanced mobile satellite communications system using Ka and MM-wave bands in Japan's R and D satellite project p 3617 N92-30924
Experimental millimeter-wave personal satellite communications system p 3617 N92-30927

MINNESOTA UNIV., MINNEAPOLIS.
Ultrafine aerosol size distributions and sulfuric acid vapor pressures: Implications for new particle formation in the atmosphere
[DE92-015217] p 3675 N92-31183

MISSOURI UNIV., COLUMBIA.
Statistical theory on reliability
[AD-A250809] p 3660 N92-30237

MITRE CORP., BEDFORD, MA.
Integrating commercial off-the-shelf tools for custom software development
[AD-A252462] p 3695 N92-30550
Performance of ground-based high-frequency receiving arrays with electrically-small ground planes
[AD-A250489] p 3621 N92-31130

MITRE CORP., MCLEAN, VA.
Continuum approaches for describing solid-liquid flow
[AD-A249028] p 3629 N92-30560

MORGANTOWN TECHNOLOGY CENTER, WV.
Research issues in molten carbonate fuel cells: Pressurization
[DE92-011755] p 3671 N92-31113
Fuel cells
[DE92-001282] p 3672 N92-31221

MOTOROLA, INC., ARLINGTON HEIGHTS, IL.
The Pan-European Digital Cellular (GSM) System
p 3619 N92-30938

MOTOROLA, INC., CHANDLER, AZ.
Software breadboard study
[NASA-CR-190473] p 3625 N92-30757

MOTOROLA, INC., SCHAUMBURG, IL.
Leo satellite-based telecommunication network concepts p 3617 N92-30926

MOUND LAB., MIAMISBURG, OH.
Operational surfaces for the rectangle and triangle
[DE92-015165] p 3705 N92-30566

MULTI-TECHNOLOGY ANALYSIS AND RESEARCH CORP., WASHINGTON, DC.
The MARCOR GPS mobile data system
p 3620 N92-30944

N

NATIONAAL INST. VOOR KERNFYSICA EN HOGE ENERGIEFYSICA, AMSTERDAM (NETHERLANDS).
Rescattering in neutrino/antineutrino: Deuteron reactions
[NIKHEF-H/91-22] p 3713 N92-30364
Tests of the performance of different gas mixtures in microstrip gas counters
[NIKHEF-H/91-23] p 3636 N92-30365
On the factorisation theorem in boson-gluon fusion at hadron colliders
[NIKHEF-H/91-16] p 3713 N92-30415
Two-loop QCD corrections to the coefficient functions of the deep inelastic structure functions F2 and F(sub L)
[NIKHEF-H/91-17] p 3715 N92-30687
Optimization of the microstrip gas counter
[NIKHEF-H/91-21] p 3637 N92-30688
Non-perturbative effects in high-energy electroweak interactions
[NIKHEF-H/91-24] p 3715 N92-30697
VDHW-related memo's
[LINO-1991-5] p 3718 N92-30725
Measurement report on the present Video Highway System of MEA p 3718 N92-30726
Tunable relay box (design and testing)
p 3718 N92-30727
Console driver p 3718 N92-30728

NATIONAL ACADEMY OF SCIENCES - NATIONAL RESEARCH COUNCIL, WASHINGTON, DC.
Setting priorities for space research: Opportunities and imperatives
[NASA-CR-190519] p 3733 N92-30974

NATIONAL AERONAUTICS AND SPACE ADMINISTRATION, WASHINGTON, DC.
Hubble Space Telescope. Update: 18 months in orbit
[NASA-TM-107962] p 3739 N92-30686
Aerospace medicine and biology: A continuing bibliography with indexes (supplement 363)
[NASA-SP-7011(363)] p 3685 N92-30987

NATIONAL AERONAUTICS AND SPACE ADMINISTRATION. AMES RESEARCH CENTER, MOFFETT FIELD, CA.
Low Reynolds number kappa-epsilon modeling with the aid of direct simulation data p 3631 N92-30655
One-equation near-wall turbulence modeling with the aid of direct simulation data p 3631 N92-30656
The structure of turbulent channel flow with passive scalar transport p 3632 N92-30657
A study of the topology of dissipating motions in direct numerical simulations of time-developing compressible and incompressible mixing layers p 3632 N92-30658
Low order dynamical models for mixing layers
p 3633 N92-30662
Numerical simulation of low Prandtl number turbulent mixing p 3633 N92-30663
Length scales and dissipation of fine eddies in a mixing layer p 3633 N92-30664
Interscale energy transfer in numerically simulated turbulence p 3634 N92-30672
Collected notes from the Benchmarks and Metrics Workshop
[NASA-TM-107910] p 3701 N92-30710
Intersecting shock-wave/turbulent boundary-layer interactions at Mach 8.3
[NASA-TM-103909] p 3635 N92-30765
A CFD validation roadmap for hypersonic flows
[NASA-TM-103935] p 3636 N92-30982
Waste streams in a typical crewed space habitat: An update
[NASA-TM-103888] p 3689 N92-31166
Light as a chronobiologic countermeasure for long-duration space operations
[NASA-TM-103874] p 3686 N92-31167

NATIONAL AERONAUTICS AND SPACE ADMINISTRATION. GODDARD SPACE FLIGHT CENTER, GREENBELT, MD.
Cable compliance
[NASA-TP-3216] p 3612 N92-30378
Generation of large-scale density fluctuations by buoyancy p 3634 N92-30671
On the existence of convectively produced gravity waves p 3638 N92-31016
Doppler lidar wind measurement with the edge technique p 3638 N92-31017
Altimetry and lidar using AlGaAs lasers modulated with pseudo-random codes p 3641 N92-31030
Advanced Raman water vapor lidar
p 3643 N92-31040
Water vapor variance measurements using a Raman lidar p 3643 N92-31041
Wavemeter measurements of frequency stability of an injection seeded alexandrite laser for pressure and temperature lidar p 3645 N92-31049
Conically scanned lidar telescope using holographic optical elements p 3645 N92-31050
Pulsed laser spectral measurement using a Fabry-Perot interferometer: Limits to resolution p 3646 N92-31055
Raman lidar measurements of water vapor and aerosol/clouds during the FIRE/SPECTRE field campaign p 3652 N92-31089
Performance modeling of daytime Raman lidar systems for profiling atmospheric water vapor
p 3653 N92-31090

NATIONAL AERONAUTICS AND SPACE ADMINISTRATION. HUGH L. DRYDEN FLIGHT RESEARCH FACILITY, EDWARDS, CA.
Thrust stand evaluation of engine performance improvement algorithms in an F-15 airplane
[NASA-TM-104252] p 3581 N92-30518

NATIONAL AERONAUTICS AND SPACE ADMINISTRATION. LYNDON B. JOHNSON SPACE CENTER, HOUSTON, TX.
A space-time neural network for processing both spacial and temporal data
[NASA-CASE-MSC-21674-1] p 3700 N92-30314
Space station trash removal system
[NASA-CASE-MSC-21723-1] p 3588 N92-30315
Quick acting gimbal joint
[NASA-CASE-MSC-21918-1] p 3658 N92-30316
Debris/ice/TPS assessment and integrated photographic analysis for Shuttle Mission STS-45
[NASA-TM-107545] p 3586 N92-30382
Ablative shielding for hypervelocity projectiles
[NASA-CASE-MSC-21884-1] p 3602 N92-30539
Method and apparatus for preloading a joint by remotely operable means
[NASA-CASE-MSC-21940-1] p 3659 N92-30540

NATIONAL AERONAUTICS AND SPACE ADMINISTRATION. LANGLEY RESEARCH CENTER, HAMPTON, VA.
National Educators' Workshop: Update 1991. Standard Experiments in Engineering Materials Science and Technology
[NASA-CP-3151] p 3608 N92-30263
Validation of three-dimensional incompressible spatial direct numerical simulation code: A comparison with linear stability and parabolic stability equation theories for boundary-layer transition on a flat plate
[NASA-TP-3205] p 3573 N92-30295
Off-surface infrared flow visualization
[NASA-CASE-LAR-14568-1] p 3720 N92-30312
Polyimides containing the cyclobutene-3,4-dione moiety
[NASA-CASE-LAR-14753-1] p 3601 N92-30313
A shear sensitive monomer-polymer laminate structure and method of using same
[NASA-CASE-LAR-14654-1] p 3662 N92-30317
Storage control system
[NASA-CASE-LAR-14651-1] p 3734 N92-30386
Control and augmentation of passive porosity through transpiration control
[NASA-CASE-LAR-14682-1] p 3628 N92-30387
Method for remotely powering a device such as a lunar rover
[NASA-CASE-LAR-14789-1] p 3658 N92-30388
A method of making a single layer multi-color luminescent display
[NASA-CASE-LAR-14811-1] p 3622 N92-30389
Method of measuring cross-flow vortices by use of an array of hot-film sensors
[NASA-CASE-LAR-14824-1-SB] p 3628 N92-30390
Progress in unstructured-grid methods development for unsteady aerodynamic applications
[NASA-TM-107643] p 3574 N92-30393
Two-dimensional aerodynamic characteristics of several polygon-shaped cross-sectional models applicable to helicopter fuselages
[NASA-TP-3233] p 3574 N92-30394
Printer port interface
[NASA-CASE-LAR-13950-1] p 3690 N92-30541
A gridless Euler/Navier-Stokes solution algorithm for complex two-dimensional applications
[NASA-TM-107631] p 3575 N92-30570
An extension to Schneider's general paradigm for fault-tolerant clock synchronization
[NASA-TM-107634] p 3699 N92-30677
Implicit upwind-Euler solution algorithms for unstructured-grid applications
[NASA-TM-107645] p 3575 N92-30691
Research and technology, 1991. Langley Research Center
[NASA-TM-4331] p 3744 N92-30733
Correlative measurement opportunities between ATLAS-1 and UARS experiments
[NASA-TM-107630] p 3679 N92-30735
A conceptual design of a large aperture microwave radiometer geostationary platform
[NASA-TM-107577] p 3588 N92-30736
A stroboscopic technique for using CCD cameras in flow visualization systems for continuous viewing and stop action photography
[NASA-TM-107648] p 3637 N92-30737
Trajectory fitting in function space with application to analytic modeling of surfaces
[NASA-TP-3232] p 3576 N92-30747
On-line analysis capabilities developed to support the AFW wind-tunnel tests
[NASA-TM-107651] p 3580 N92-30752
Delaunay triangulation and computational fluid dynamics meshes
[NASA-TM-107663] p 3689 N92-30907
Direct simulation of high-speed mixing layers
[NASA-TP-3186] p 3576 N92-30909
FASTRAN-2: A fatigue crack growth structural analysis program
[NASA-TM-104159] p 3664 N92-30964
The optimization of force inputs for active structural acoustic control using a neural network
[NASA-TM-107627] p 3711 N92-30979
Sixteenth International Laser Radar Conference, part 2
[NASA-CP-3158-PT-2] p 3637 N92-31013
Multiple scattering effects on spaceborne lidar
p 3641 N92-31032
Comparison of eye-safe solid state laser DIAL with passive gas filter correlation measurements from aircraft and spacecraft p 3647 N92-31060
Airborne water vapor DIAL research: System development and field measurements
p 3653 N92-31093
Flexible heating head for induction heating apparatus and method
[NASA-CASE-LAR-14679-2] p 3621 N92-31150
A demonstration of passive blade twist control using extension-twist coupling
[NASA-TM-107642] p 3664 N92-31155
Real-time simulation model of the HL-20 lifting body
[NASA-TM-107580] p 3586 N92-31160
An analytical and experimental investigation of flutter suppression via piezoelectric actuation
[NASA-TM-107653] p 3580 N92-31174
Preliminary subsonic aerodynamic model for simulation studies of the HL-20 lifting body
[NASA-TM-4302] p 3583 N92-31175
Environmental fatigue of an Al-Li-Cu alloy. Part 2: Microscopic hydrogen cracking processes
[NASA-TM-107620] p 3664 N92-31214
Environmental fatigue of an Al-Li-Cu alloy. Part 3: Modeling of crack tip hydrogen damage
[NASA-TM-107619] p 3665 N92-31215

NATIONAL AERONAUTICS AND SPACE ADMINISTRATION. LEWIS RESEARCH CENTER, CLEVELAND, OH.
Numerical solution of a three-dimensional cubic cavity flow by using the Boltzmann equation
[NASA-TM-105693] p 3627 N92-30297
Development of and flight results from the Space Acceleration Measurement System (SAMS)
[NASA-TM-105652] p 3588 N92-30301
Electrical and chemical interactions at Mars Workshop, part 1
[NASA-CP-10093] p 3741 N92-30302
Three-dimensional laser window formation
[NASA-RP-1280] p 3585 N92-30307
NEP systems engineering efforts in FY-92: Plans and status
[NASA-TM-105775] p 3588 N92-30308
An electromechanical actuation system for an expendable launch vehicle
[NASA-TM-105774] p 3586 N92-30310
The ACTS multibeam antenna
[NASA-TM-105645] p 3587 N92-30383
Lewis icing research tunnel test of the aerodynamic effects of aircraft ground deicing/anti-icing fluids
[NASA-TP-3238] p 3577 N92-30395
Development of a full-scale transmission testing procedure to evaluate advanced lubricants
[NASA-TP-3265] p 3658 N92-30396
Comparison of high temperature, high frequency core loss and dynamic B-H loops of a 2V-49Fe-49Co and a grain oriented 3Si-Fe alloy
[NASA-TM-105791] p 3623 N92-30397
High efficiency thermal to electric energy conversion using selective emitters and spectrally tuned solar cells
[NASA-TM-105755] p 3670 N92-30426
Wiring for aerospace applications
[NASA-TM-105777] p 3623 N92-30427

Small engine components test facility compressor testing cell at NASA Lewis Research Center
[NASA-TM-105685] p 3584 N92-30508
Design feasibility study of a Space Station Freedom truss
[NASA-TM-105558] p 3659 N92-30571
Microgravity vibration isolation: Optimal preview and feedback control
[NASA-TM-105673] p 3613 N92-30692
Fast methods to numerically integrate the Reynolds equation for gas fluid films
[NASA-TM-105415] p 3660 N92-30722
Magnetic bearings for free-piston Stirling engines
[NASA-TM-105730] p 3660 N92-30734
Metal matrix composite analyzer (METCAN) user's manual, version 4.0
[NASA-TM-105244] p 3592 N92-30779
Nuclear electric propulsion development and qualification facilities
[NASA-TM-105521] p 3589 N92-30818
A simplified dynamic model of the T700 turboshaft engine
[NASA-TM-105805] p 3709 N92-30898
Rocket propulsion research at Lewis Research Center
[NASA-CR-189187] p 3732 N92-30908
Characteristics of a future aeronautical satellite communications system p 3618 N92-30932
A personal communications network using a Ka-band satellite p 3619 N92-30934
Minimization of deviations of gear real tooth surfaces determined by coordinate measurements
[NASA-TM-105718] p 3660 N92-30948
Navier-Stokes analysis and experimental data comparison of compressible flow within ducts
[NASA-TM-105796] p 3582 N92-30972
Isothermal aging effects on PMR-15 resin
[NASA-TM-105648] p 3593 N92-30986
Preliminary dynamic tests of a flight-type ejector
[NASA-TM-105814] p 3582 N92-30998
Trends in aeropropulsion research and their impact on engineering education
[NASA-TM-105682] p 3583 N92-31172

NATIONAL AERONAUTICS AND SPACE ADMINISTRATION. MARSHALL SPACE FLIGHT CENTER, HUNTSVILLE, AL.

Comparison of epifluorescent viable bacterial count methods
[NASA-TM-103592] p 3683 N92-30305
Assessment of a head-mounted miniature monitor
[NASA-TM-103587] p 3688 N92-30381
Linear elastic fracture mechanics primer
[NASA-TM-103591] p 3662 N92-30416
A study of enhancing critical current densities (J(sub c)) and critical temperature (T(sub c)) of high-temperature superconductors
[NASA-TM-103595] p 3627 N92-30902
A reduced gravity fiber pulling apparatus
[NASA-TM-103594] p 3612 N92-30971

NATIONAL AERONAUTICS AND SPACE ADMINISTRATION. PASADENA OFFICE, CA.

Double-loop frequency-selected surfaces for multifrequency division multiplexing in a dual-reflector antenna
[NASA-CASE-NPO-18701-1-CU] p 3614 N92-30391
Hybridization of detector array and integrated circuit for readout
[NASA-CASE-NPO-18062-1-CU] p 3623 N92-30542
Encyclopedia of software components
[NASA-CASE-NPO-18435-1-CU] p 3695 N92-30543

NATIONAL AEROSPACE LAB., AMSTERDAM (NETHERLANDS).

Monitoring of Dutch forest with LANDSAT-TM
[BCRS-91-21] p 3666 N92-30468
Examination of aircraft warning and caution lights after shock testing
[NLR-TP-89284-U] p 3578 N92-30474
METEODEC/METEOCRYPT: A demonstration of data compression and encryption for operational remote-sensing
[NLR-TP-89294-U] p 3667 N92-30475
Development environment for digital simulation models of multibody systems
[NLR-TP-89327-U] p 3693 N92-30476
Flexible space-based robot modelling and real-time simulation
[NLR-TP-89364-U] p 3658 N92-30477

NATIONAL ASTRONOMY AND IONOSPHERE CENTER, ARECIBO, PUERTO RICO.

Discovery of two planets around a millisecond pulsar p 3739 N92-31237

NATIONAL CENTER FOR ATMOSPHERIC RESEARCH, BOULDER, CO.

Simplified signal processing for an airborne CO2 Doppler lidar p 3639 N92-31023

NATIONAL COMMUNICATIONS SYSTEM, ARLINGTON, VA.

National transportable telecommunications capability p 3620 N92-30943

NATIONAL DEFENCE RESEARCH ESTABLISHMENT, LINKOEPING (SWEDEN).

Aerosol extinction measurements with CO2-lidar p 3655 N92-31105

NATIONAL INST. FOR ENVIRONMENTAL STUDIES, TSUKUBA (JAPAN).

Spectroscopic method for Earth-satellite-Earth laser long-path absorption measurements using Retroreflector In Space (RIS) p 3652 N92-31088

NATIONAL INST. FOR FUSION SCIENCE, NAGOYA (JAPAN).

Magnetic surface breaking in 3D MHD equilibria of l = 2 heliotron
[NIFS-130] p 3722 N92-30384
Field line diversion properties of finite beta helias equilibria
[NIFS-137] p 3722 N92-30385
Tritium content of a DT pellet in inertial confinement fusion
[NIFS-113] p 3722 N92-30430
Recombining processes in a cooling plasma by mixing of initially heated gas
[NIFS-142] p 3722 N92-30431
Dynamic analysis of compact helical system power supply and designs of its upgrade
[NIFS-TECH-2] p 3723 N92-30497
Role of compressibility on driven magnetic reconnection
[NIFS-105] p 3710 N92-30498
Plasma parameter estimations for the large helical device based on the gyro-reduced Bohm scaling
[NIFS-114] p 3723 N92-30499
Effects of fast ions and an external inductive electric field on the neoclassical parallel flow, current, and rotation in general toroidal systems
[NIFS-150] p 3713 N92-30500
Negative ion extraction characteristics of a large negative ion source with double-magnetic filter configuration
[NIFS-151] p 3714 N92-30501
Review of high Z materials for PSI applications
[NIFS-152] p 3602 N92-30502
Rapid change of hydrogen neutral energy distribution at L/H-transition in JFT-2M H-mode
[NIFS-134] p 3714 N92-30510
Production of negative hydrogen ions in a large multicusp ion source with double-magnetic filter configuration
[NIFS-149] p 3714 N92-30572
Line-emission cross sections for the charge-exchange reaction between fully stripped carbon and atomic hydrogen in tokamak plasma
[NIFS-129] p 3716 N92-30967
The role of stochasticity in sawtooth oscillation
[NIFS-103] p 3710 N92-30983
X ray radiation from hot dense plasmas and atomic processes
[NIFS-PROC-9] p 3725 N92-30984
Beta limit of resistive plasma in torsatron/heliotron
[NIFS-131] p 3725 N92-30985
Study of Au(-) production in a plasma-sputter type negative ion source
[NIFS-115] p 3717 N92-30990
A steady state tokamak operation by use of magnetic monopoles
[DE92-799109] p 3725 N92-30991
Edge poloidal rotation profiles of H-mode plasmas in the JFT-2M tokamak
[DE92-799107] p 3725 N92-30992
Kinetic approach to long wave length modes in rotating plasmas
[NIFS-138] p 3725 N92-30993
Three-dimensional MHD equilibrium in the presence of bootstrap current for Large Helical Device (LHD)
[NIFS-139] p 3725 N92-30994
New method of error elimination in potential profile measurement of tokamak plasmas by high voltage heavy ion beam probes
[NIFS-143] p 3726 N92-30995

NATIONAL INST. OF STANDARDS AND TECHNOLOGY, GAITHERSBURG, MD.

A Boussinesq algorithm for bouyant convection in polygonal domains
[PB92-187137] p 3695 N92-30579
Studies on the melt flow rate of the SRM 1473: A low density polyethylene resin
[PB92-181080] p 3604 N92-30788

NATIONAL MATERIALS ADVISORY BOARD, WASHINGTON, DC.

Beam technologies for integrated processing
[AD-A252647] p 3612 N92-30411

NATIONAL OCEANIC AND ATMOSPHERIC ADMINISTRATION, BOULDER, CO.

Low-level atmospheric flows studied by pulsed Doppler lidar p 3638 N92-31015
Design of a near-IR coherent lidar for high spatial and velocity resolution wind measurement p 3639 N92-31020
Coherent CO2 lidar: A superior system for observing clouds? p 3644 N92-31045

NATIONAL OCEANIC AND ATMOSPHERIC ADMINISTRATION, WASHINGTON, DC.

National ocean pollution program: Summary of Federal programs and projects: FY 1989 update
[PB92-187012] p 3673 N92-30563

NATIONAL PHYSICAL LAB., TEDDINGTON (ENGLAND).

Measurements of fugitive hydrocarbon emissions with a tunable infrared DIAL p 3655 N92-31102

NATIONAL REMOTE SENSING AGENCY, HYDERABAD (INDIA).

SCS method of runoff estimation using remote sensing techniques p 3668 N92-30916

NATIONAL SCIENCE FOUNDATION, WASHINGTON, DC.

The United States Antarctic Program
[NSF-90-97] p 3676 N92-30708

NATIONAL SEVERE STORMS LAB., NORMAN, OK.

On the potential use of the terminal Doppler weather radar gust front detection algorithm on the WSR-88D system. Part 1: Impacts of radar system differences
[DOT/FAA/NR-92/8,I] p 3678 N92-30495
On the potential use of the terminal Doppler weather radar gust front detection algorithm on the WSR-88D system. Part 2: Detecting non-gust front convergent weather phenomena
[DOT/FAA/NR-92/8,II] p 3678 N92-30496

NATIONAL TRANSPORTATION SAFETY BOARD, WASHINGTON, DC.

Aircraft accident report: Explosive decompression - loss of cargo door in flight, United Airlines Flight 811, Boeing 747-122, N4713U, Honolulu, Hawaii, February 24, 1989
[PB92-910402] p 3578 N92-31159

NAVAL AIR DEVELOPMENT CENTER, WARMINSTER, PA.

In-service evaluation of 2090 aluminum-lithium alloy on F/A-18 aircraft
[AD-A248472] p 3607 N92-30321

NAVAL COMMAND, CONTROL AND OCEAN SURVEILLANCE CENTER, SAN DIEGO, CA.

A new matrix formulation of classical electrodynamics. Part 1: Vacuum
[AD-A249643] p 3616 N92-30721

NAVAL HEALTH RESEARCH CENTER, SAN DIEGO, CA.

Feasibility of a walk test to assess the cardiorespiratory fitness of Naval personnel
[AD-A250650] p 3684 N92-30603
Exercise behavior among Navy runners and non-runners
[AD-A250651] p 3685 N92-30644

NAVAL OCEAN SYSTEMS CENTER, SAN DIEGO, CA.

Evaporation duct effects at millimeter wavelengths
[AD-A250239] p 3617 N92-30876

NAVAL OCEANOGRAPHIC AND ATMOSPHERIC RESEARCH LAB., BAY SAINT LOUIS, MS.

Remote sensing for the Lincoln Sea Winterover Experiment
[AD-A252117] p 3667 N92-30545

NAVAL POLAR OCEANOGRAPHY CENTER, WASHINGTON, DC.

Antarctic ice charts, 1989 - 1990: Analysis Atlas
[AD-A249730] p 3669 N92-31179

NAVAL POSTGRADUATE SCHOOL, MONTEREY, CA.

Information systems: How they affect and are affected by organization structure
[AD-A248852] p 3734 N92-30234
Mixed and forced convection from an array of discrete heat sources in a vertical channel
[AD-A248853] p 3731 N92-30235
The effect of information systems on middle management in the aerospace industry: The Westco case
[AD-A249017] p 3735 N92-30584
Detecting potential synchronization constraint deadlocks from formal system specifications
[AD-A249019] p 3696 N92-30631
DE-CERTS: A decision support system for a comparative evaluation method for risk management methodologies and tools
[AD-A246965] p 3733 N92-30682
Introduction to human factors and wide area networking
[AD-A252310] p 3688 N92-30718
High background photon counting lidar p 3649 N92-31071
Managing the contract closeout process
[AD-A250701] p 3733 N92-31209

NAVAL RESEARCH LAB., WASHINGTON, DC.
A local interpolator derived from the discrete Fourier transform
[AD-A251066] p 3701 N92-30243
Numerical simulation of the electromagnetic instability of an intense beam in a quadrupole focusing system
[AD-A252275] p 3614 N92-30407
Generation of stimulated backscattered harmonic radiation from intense laser interactions with beams and plasmas
[AD-A248782] p 3656 N92-30614
Eye/sensor protection against laser irradiation ablative mirror devices: A materials assessment
[AD-A248787] p 3688 N92-30615
Interaction of ultra-high laser fields with beams and plasmas
[AD-A249502] p 3723 N92-30620
Glint errors derived from the partial derivatives of the echo signal phase for a distributed scatterer
[AD-A249499] p 3615 N92-30637
Nonlinear analysis of a grating free-electron laser
[AD-A248833] p 3656 N92-30743
New insights into large eddy simulation
[AD-A249424] p 3635 N92-30775
Some model theory of free groups and free algebras
[AD-A249425] p 3706 N92-30776
Nanoscience and nanotechnology
[AD-A250376] p 3626 N92-30851
Aureole lidar: Design, operation, and comparison with in-situ measurements p 3648 N92-31065

NAVAL SURFACE WEAPONS CENTER, DAHLGREN, VA.
Alignment of a 3-D sensor and a 2-D sensor measuring azimuth and elevation
[AD-A252120] p 3636 N92-30530

NAVAL UNDERSEA WARFARE CENTER, WEST PALM BEACH, FL.
A statistical comparison of AUTEC and Eleuthera Island wind data for the period 1 April 1989 through 30 March 1990
[AD-A248898] p 3679 N92-31003

NAVAL WAR COLL., NEWPORT, RI.
Stealth: A revolutionary change to air warfare
[AD-A249880] p 3617 N92-30869

NAVY PERSONNEL RESEARCH AND DEVELOPMENT CENTER, SAN DIEGO, CA.
Reviewing the technical report
[AD-A249494] p 3735 N92-30636

NEBRASKA UNIV., LINCOLN.
Modeling of video traffic in packet networks, low rate video compression, and the development of a lossy+lossless image compression algorithm
[NASA-CR-190546] p 3691 N92-30296
The electric field dependence of the laser induced holographic grating relaxation of photorefractive polymer
[AD-A252641] p 3602 N92-30409
Effects of the orientational pair correlation on second order nonlinear optical coefficients
[AD-A252490] p 3720 N92-30535
Depolarized light scattering and dynamic shear compliance of viscoelastic liquids
[AD-A252491] p 3721 N92-30536
Electrochemical and optical studies of model photosynthetic systems
[DE92-010657] p 3683 N92-30829

NEVADA UNIV., RENO.
Numerical investigations in three-dimensional internal flows
[NASA-CR-190498] p 3628 N92-30380

NEW MEXICO UNIV., ALBUQUERQUE.
Ceramic processing: Experimental design and optimization p 3607 N92-30267
Backward-wave oscillator investigations in the Raman Regime
[AD-A250738] p 3622 N92-30332

NEW YORK UNIV., NEW YORK.
Solar flare MDH
[AD-A250639] p 3702 N92-30375

NORTH CAROLINA AGRICULTURAL AND TECHNICAL STATE UNIV., GREENSBORO.
Model analysis and expert system development for planning and scheduling teleoperations for aircraft turnaround functions, volume 1
[AD-A251037] p 3573 N92-30253
Model analysis and expert system development for planning and scheduling teleoperations for aircraft turnaround functions. Volume 2: Top user's guide
[AD-A251083] p 3573 N92-30258
Mechanism of slip and twinning p 3610 N92-30280

NORTH CAROLINA STATE UNIV., RALEIGH.
Computer-controlled ion beam sputter-deposition of superconducting oxide films
[AD-A248495] p 3601 N92-30326
Real gas flow parameters for NASA Langley 22-inch Mach 20 helium tunnel
[NASA-CR-4462] p 3635 N92-30751
Atomic layer epitaxy group 4 materials: Surface processes, thin films, devices, and their characterization
[AD-A252352] p 3729 N92-30846

NORTH CAROLINA UNIV., CHAPEL HILL.
Spatiotemporal characteristics of human visual localization
[AD-A248494] p 3687 N92-30325
Research in stochastic analysis and its applications
[AD-A249482] p 3708 N92-30633

NORTHEAST SEMICONDUCTOR, INC., ITHACA, NY.
Innovative techniques for the production of low cost 2-D laser diode arrays supplies or services and prices/costs
[AD-A252665] p 3656 N92-30552

NORTHEASTERN UNIV., BOSTON, MA.
Stress-strain characteristics of rubber-like materials: Experiment and analysis p 3607 N92-30285

NORTHWESTERN UNIV., EVANSTON, IL.
Nucleation and growth of diamond on carbon-implanted single crystal copper
[AD-A249021] p 3594 N92-30632
Quantitative non-destructive evaluation of high-temperature superconducting materials
[DE92-011615] p 3661 N92-30693
Resonance Raman spectroscopic studies of trans dioxorhenium(V)tetrapyridyl species
[AD-A249919] p 3595 N92-30875

NORWEGIAN DEFENCE RESEARCH ESTABLISHMENT, KJELLER.
The properties of the uptake system for glycine in synaptic vesicles
[ISSN-0800-4412] p 3683 N92-31152

NOTRE DAME UNIV., IN.
Studies of ordering in semiconducting and other alloys
[AD-A249483] p 3728 N92-30634
Bandwidth efficient CCSDS coding standard proposals
[NASA-CR-190317] p 3587 N92-30709
Single-electron charging effects
[DE92-015287] p 3710 N92-31131

NOTTINGHAM UNIV. (ENGLAND).
Wave propagation and vibration of fibre-reinforced laminates
[AD-A252101] p 3590 N92-30528

NYMA, INC., GREENBELT, MD.
Advanced Raman water vapor lidar p 3643 N92-31040

O

OAK RIDGE NATIONAL LAB., TN.
Structural ceramics p 3607 N92-30264
Standard terminology in the laboratory and classroom p 3610 N92-30277
Science in action: An interdisciplinary science education program p 3610 N92-30278
The microscopic world: A demonstration of electron microscopy for younger students p 3610 N92-30281
Gyro-Landau fluid model of tokamak core fluctuations
[DE92-013277] p 3722 N92-30366
The allocation of cargo to channel missions
[DE92-013234] p 3578 N92-30565
Creep and slow crack growth mechanisms related to macroscopic creep behavior of a silicon nitride ceramic at elevated temperatures
[DE92-015195] p 3663 N92-30567
In situ TEM studies of the effect of misfit strain on the kinetics of Si(sub 1-x)Ge(sub x) solid phase epitaxy: Temperature calibration and surface effects
[DE92-011689] p 3728 N92-30574
Spinoffs from R and D investments
[DE92-014450] p 3736 N92-30575
Problems with the concept of plasma equilibrium in tokamaks
[DE92-014454] p 3723 N92-30576
Ion channeling and spectroscopic ellipsometry examinations of thin-film SiO2/epi-Si structures
[DE92-015129] p 3728 N92-30577
Transport phenomena in welds
[DE92-013404] p 3659 N92-30587
Effect of bending on the room-temperature tensile strengths of structural ceramics
[DE92-015196] p 3603 N92-30626
Lifetimes of low spin states in the superdeformed band of Hg-192
[DE92-011066] p 3728 N92-30684
Nondestructive testing of ceramics for vehicular advanced heat engines
[DE92-010471] p 3604 N92-30744
New shortwave solar radiometer with information-based sparse sampling
[DE92-010483] p 3742 N92-30797
The effect of neutron irradiation on the structure and properties of carbon-carbon composite materials
[DE92-011670] p 3592 N92-30809
Density profile measurement using a multichannel difluoromethane laser interferometer system on ATF
[DE92-011691] p 3724 N92-30810
Assessment of an improved multiaxial strength theory based on creep-rupture data for type 316 stainless steel
[DE92-010431] p 3663 N92-30823
High-resolution imaging in the scanning transmission electron microscope
[DE92-010647] p 3637 N92-30827
Evidence for interference between resonant and nonresonant transfer and excitation
[DE92-011779] p 3716 N92-30853
Graphical-based construction of combinatorial geometries for radiation transport and shielding applications
[DE92-014453] p 3696 N92-30886
Investigation of joining techniques for advanced austenitic alloys
[DE92-015545] p 3599 N92-30888
Field studies in geophysical diffraction tomography
[DE92-015084] p 3677 N92-31009
Potassium Rankine cycle power conversion systems for lunar-Mars surface power
[DE92-015102] p 3589 N92-31012
Impurity segregation to grain boundaries and defects in AlN
[DE92-011667] p 3599 N92-31112
Criteria and design trade-off issues for ITER
[DE92-011786] p 3726 N92-31114
Thermal energy storage
[DE92-014942] p 3672 N92-31176
Laser mass spectrometry for biopolymers
[DE92-015238] p 3597 N92-31184
A miniature carbon furnace for mass spectroscopy
[DE92-014460] p 3597 N92-31196
Results of the heavy ion beam probe measurements on the Advanced Toroidal Facility
[DE92-014461] p 3726 N92-31197

OAK RIDGE Y-12 PLANT, TN.
An x ray microprobe based upon a close-coupled focal-spot/glass capillary arrangement
[DE92-011886] p 3722 N92-31195

OBSERVATOIRE CANTONAL, NEUCHATEL (SWITZERLAND).
Analytical multiple scattering correction to the Mie theory: Application to the analysis of the lidar signal p 3642 N92-31036
Lidar depolarization by nonspherical particles: Potential of combined depolarization/backscattering measurements for PSC's characterization p 3644 N92-31044

OFFICE NATIONAL D'ETUDES ET DE RECHERCHES AEROSPATIALES, MEUNDON (FRANCE).
Theoretical simulation of a 2 micron airborne solid state laser anemometer p 3647 N92-31059

OFFICE NATIONAL D'ETUDES ET DE RECHERCHES AEROSPATIALES, PARIS (FRANCE).
Resolution of the three-dimensional parabolic equation applied to acoustic propagation at low altitudes
[ONERA-RF-17/3641-PY] p 3711 N92-30966

OFFICE OF SCIENCE AND TECHNOLOGY, WASHINGTON, DC.
Grand challenges 1993: High performance computing and communications. A report by the Committee on Physical, Mathematical, and Engineering Sciences to supplement the President's fiscal year 1993 budget
[PB92-160530] p 3689 N92-30600

OFFICE OF SPACE SCIENCE AND APPLICATIONS, WASHINGTON, DC.
Space science and applications: Strategic plan 1991
[NASA-TM-107811] p 3733 N92-30959

OHIO NORTHERN UNIV., ADA.
Be-Cu precipitation hardening experiment p 3601 N92-30276

OHIO STATE UNIV., COLUMBUS.
Finite element analysis of laminated composite axisymmetric solids. Volume 1: Theory and applications
[AD-A250808] p 3590 N92-30251
Altimeter and gravity data analysis
[NASA-CR-190478] p 3676 N92-30756

OKLAHOMA UNIV., NORMAN.
Influence of structural and aerodynamic modeling on flutter analysis and structural optimization
[AD-A248487] p 3583 N92-30323
On the potential use of the terminal Doppler weather radar gust front detection algorithm on the WSR-88D system. Part 2: Detecting non-gust front convergent weather phenomena
[DOT/FAA/NR-92/8,II] p 3678 N92-30496

OLD DOMINION UNIV., NORFOLK, VA.
Building a generalized distributed system model
[NASA-CR-190489] p 3698 N92-30960

OREGON STATE UNIV., CORVALLIS.
Improvement of performance of variable probability sampling strategies
[PB92-180264] p 3707 N92-30562

Event-scale relationships between surface velocity, temperature and chlorophyll in the coastal ocean, as seen by satellite
[NASA-CR-190266] p 3682 N92-30739
Nonlinear stability and control study of highly maneuverable high performance aircraft, phase 2
[NASA-CR-190667] p 3583 N92-30922

OREGON UNIV., EUGENE.
Intermittency, multifractality, and hadronic collisions
[DE92-014595] p 3714 N92-30606
Proceedings of the Sylvia Beach Language Comprehension Conference
[AD-A250488] p 3621 N92-31129

P

PACIFIC NORTHWEST LAB., RICHLAND, WA.
Compression planning for continuous improvement in quality programs
[DE92-012331] p 3732 N92-30349
Reducing greenhouse gas emissions in Czechoslovakia
[DE92-012354] p 3672 N92-30374
Recent improvements in size effects correlations for DBTT and upper shelf energy of ferritic steels
[DE92-014703] p 3599 N92-30877
Can't justify an imaging system? How about a CAR?
[DE92-015156] p 3735 N92-31001
A comparative EIS study on cermet and platinum anodes for the electrolytic production of aluminum
[DE92-015091] p 3599 N92-31010
The revised International Commission on Radiological Protection (ICRP) dosimetric model for the human respiratory tract
[DE92-015092] p 3685 N92-31011

PACTEL CORP., WALNUT CREEK, CA.
Capacity and interference in a PCS system
p 3619 N92-30937

PARIS II UNIV., ORSAY (FRANCE).
Measurement of radiative lifetimes of vibrational states of simple ions
[AD-A248567] p 3712 N92-30337

PARIS VI UNIV. (FRANCE).
Boundary layer structure over the ocean observed by LEANDRE 1 during a tramontane event
p 3638 N92-31014
The 2nd phase of the LEANDRE program: Water-vapor DIAL measurement p 3643 N92-31039
DIAL simulations for satellite water vapor profile measurements within the BEST project
p 3653 N92-31092

PCO, INC., CHATSWORTH, CA.
Fiber optic based signal processing
[AD-A247857] p 3720 N92-30248

PENNSYLVANIA STATE UNIV., UNIVERSITY PARK.
Voltammetric measurement of oxygen in single neurons using platinized carbon ring electrodes
[AD-A252191] p 3683 N92-30531
Relaxor ferroelectrics for electrostrictive transducer
[AD-A248671] p 3624 N92-30598
Theoretical studies in elementary particle physics
[DE92-015295] p 3714 N92-30610
Finite difference time domain modeling of steady state scattering from jet engines with moving turbine blades
[NASA-CR-190290] p 3582 N92-30753
Atmospheric measurements using the LAMP lidar during the LADIMAS campaign p 3652 N92-31086

PENNSYLVANIA UNIV., PHILADELPHIA.
First-principles computational studies of alkali-doped C60 fullerides
[AD-A249018] p 3624 N92-30630
Visual perception of depth from occlusion: A neural network model
[AD-A249035] p 3696 N92-30820

PHILLIPS LAB., HANSCOM AFB, MA.
Lidar measurement of optical turbulence: Theory of the crossed path technique
[AD-A248938] p 3720 N92-30343
A compact high repetition rate CO2 coherent Doppler lidar p 3639 N92-31022

PHOTOMETRICS, INC., WOBURN, MA.
Phase noise in pulsed Doppler lidar and limitations on achievable single-shot velocity accuracy
p 3639 N92-31024
Determining water cloud particle sizes from lidar depolarization measurements and time dependent multiple scattering coefficients p 3641 N92-31034
Time and polarization dependent double scattering calculations of lidar returns from water clouds
p 3647 N92-31063

PITTSBURGH UNIV., PA.
On impasse points of quasilinear differential algebraic equations
[AD-A252643] p 3702 N92-30410
Interaction of atomic hydrogen with the surface methyl group on Si(100): Removal of surface carbon
[AD-A249062] p 3595 N92-30821
A novel process for methanol synthesis
[DE92-015798] p 3608 N92-30904

POD ASSOCIATES, INC., ALBUQUERQUE, NM.
Environment modelling in near Earth space: Preliminary LDEF results p 3588 N92-31225

POLISH ACADEMY OF SCIENCES, WARSAW.
On two methods of determining the ellipses and ellipsoids of positioning accuracy of robot manipulators
[ISSN-0208-5658] p 3701 N92-31148
A tolerance approach to visual shape perception and image matching analysis for modeling of micro-heterogeneous materials
[ISSN-0208-5658] p 3721 N92-31149

POLITECNICO DI MILANO (ITALY).
Composite beam analysis linear analysis of naturally curved and twisted anisotropic beams
[AD-A252652] p 3663 N92-30766

POLITECNICO DI TORINO (ITALY).
A dynamic subgrid-scale eddy viscosity model
p 3630 N92-30649

POLYTECHNIC UNIV., FARMINGDALE, NY.
Nonequilibrium behavior of carriers in semiconductors subjected to strong space-time varying fields
[AD-A246961] p 3624 N92-30678

PRATT AND WHITNEY AIRCRAFT, EAST HARTFORD, CT.
Ultra high bypass Nacelle aerodynamics inlet flow-through high angle of attack distortion test
[NASA-CR-189149] p 3574 N92-30298

PRC KENTRON, INC., EDWARDS, CA.
High-speed civil transport issues and technology program
[NASA-CR-186020] p 3580 N92-31208

PURDUE UNIV., WEST LAFAYETTE, IN.
Elementary metallography p 3600 N92-30266
Isotropic thin-walled pressure vessel experiment
p 3611 N92-30284
Introductory heat-transfer p 3601 N92-30291
Heat-treating of materials p 3601 N92-30292
Modelling of heavily loaded lubricated contacts
[AD-A248807] p 3659 N92-30554
Extension of the integral equation formulation of linearized time dependent subsonic flow
[AD-A250654] p 3577 N92-31171

Q

QUEST INTEGRATED, INC., KENT, WA.
A new unsteady mixing model to predict NO(x) production during rapid mixing in a dual-stage combustor
[NASA-CR-189155] p 3581 N92-30569

R

RADIO SATELLITE CORP., LONG BEACH, CA.
The RadioSat (sm) network p 3620 N92-30942

RAND CORP., SANTA MONICA, CA.
Space transportation systems, launch systems, and propulsion for the Space Exploration Initiative: Results from Project Outreach
[NASA-CR-190345] p 3587 N92-30958
Gaspra's shape and surface features: Comparison to small satellites p 3739 N92-31236

RAND GRADUATE INST. FOR POLICIES STUDY, SANTA MONICA, CA.
The rise of active-element phased-array radar
[RAND-P-7747-RGS] p 3616 N92-30755

RAYTHEON CO., LEXINGTON, MA.
RF vacuum microelectronics
[AD-A249814] p 3626 N92-30836

REAL INST. Y OBSERVATORIO DE LA ARMADA, SAN FERNANDO (SPAIN).
Carlsberg meridian catalogue La Palma. Number 5: Observations of positions of stars and planets: May 1988 to Dec. 1989
[ISBN-84-7469-052-8] p 3739 N92-30714

RENSSELAER POLYTECHNIC INST., TROY, NY.
Studies of thermal decomposition of the 1:1 R3Al:en adduct (R = Me, Et; en = ethylenediamine): Synthesis and structure of a novel intermediate Al((HNCH2CH2NH)AlMe2)3
[AD-A251061] p 3603 N92-30623
The first identification of a mainbelt asteroid source for a meteorite Class E-type Apollo asteroid (3103) 1982BB: A link between the Hungaria asteroid zone and the Aubrite meteorites p 3737 N92-31228

RESEARCH AND DEVELOPMENT LABS., CULVER CITY, CA.
The 1991 Summer Faculty Research Program (SFRP), volume 4 atory
[AD-A248766] p 3744 N92-30327

RESEARCH INST. FOR ADVANCED COMPUTER SCIENCE, MOFFETT FIELD, CA.
Gaussian windows: A tool for exploring multivariate data
[NASA-CR-190559] p 3696 N92-30723
Sparse distributed memory and related models
[NASA-CR-190553] p 3690 N92-30724

RESEARCH INST. FOR COMPUTING AND INFORMATION SYSTEMS, HOUSTON, TX.
Demonstration of a 3D vision algorithm for space applications
[NASA-CR-190646] p 3698 N92-31154

RESSLER ASSOCIATES, INC., LAUREL, MD.
Advanced Raman water vapor lidar
p 3643 N92-31040

ROCKWELL INTERNATIONAL SCIENCE CENTER, THOUSAND OAKS, CA.
Transformation toughening of ceramics
[AD-A248903] p 3601 N92-30342

ROME LAB., GRIFFISS AFB, NY.
Foreign surveillance radar upgrade analysis
[AD-A249440] p 3616 N92-30760
The evolving data dictionary
[AD-A249030] p 3735 N92-30819

ROYAL GREENWICH OBSERVATORY, CAMBRIDGE (ENGLAND).
Carlsberg meridian catalogue La Palma. Number 5: Observations of positions of stars and planets: May 1988 to Dec. 1989
[ISBN-84-7469-052-8] p 3739 N92-30714

ROYAL NORWEGIAN COUNCIL FOR SCIENTIFIC AND INDUSTRIAL RESEARCH, KJELLER.
Operation, maintenance and research activities at the Norwegian Seismic Array (NORSAR), the Norwegian Regional Seismic Array (NORESS), and the Arctic Regional Seismic Array (ARCESS)
[AD-A250403] p 3677 N92-31142

RUTGERS - THE STATE UNIV., NEW BRUNSWICK, NJ.
Two-color infrared digital imaging for determination of in-cylinder temperature and species during compression and combustion periods of DI diesel engine
[AD-A249812] p 3595 N92-30835

RUTGERS - THE STATE UNIV., PISCATAWAY, NJ.
Ferroelectric and piezoelectric properties of odd-numbered nylons
[AD-A252270] p 3727 N92-30406
A new class of ferroelectric polymers: The odd-numbered nylons
[AD-A252268] p 3603 N92-30594
Ferroelectric polarization mechanisms in Nylon 11
[AD-A252269] p 3728 N92-30595

RUTHERFORD APPLETON LAB., CHILTON (ENGLAND).
Remarks on the exotic U-meson
[RAL-91-090] p 3715 N92-30750

S

SANDIA NATIONAL LABS., ALBUQUERQUE, NM.
Three-dimensional shock wave physics simulations on massively parallel supercomputers
[DE92-008679] p 3698 N92-30363
Joint computational and experimental aerodynamics research on a hypersonic vehicle
[DE92-013439] p 3574 N92-30367
Absolute Seebeck thermoelectric characteristics: Principles, significance, and applications
[DE92-013684] p 3622 N92-30370
Scalable parallel molecular dynamics on MIMD supercomputers
[DE92-015041] p 3698 N92-30401
Computing with faulty shared memory
[DE92-011663] p 3695 N92-30522
Molecular weight dependence of domain structure in silica-siloxane molecular composites
[DE92-015046] p 3603 N92-30544
New insights into radiation-induced oxide-trap charge through Thermally-Stimulated-Current (TSC) measurement and analysis
[DE92-009054] p 3728 N92-30585
Monte Carlo particle simulation of low-density fluid flow on MIMD supercomputers
[DE92-014618] p 3630 N92-30607
The RADLAC beam propagation experiment
[DE92-014620] p 3718 N92-30624
Geometry of premixed flames in three-dimensional turbulence p 3633 N92-30666
High-temperature ignition of propane with MTBE as an additive: Shock-tube experiments and modeling
[DE92-006679] p 3594 N92-30749
Analysis of a digital RF memory in a signal-delay application
[DE92-013457] p 3626 N92-30764
Numerical simulation of the dynamic behavior of the polymeric gels
[DE92-011358] p 3605 N92-30804

Testing of double-layer capacitors for high reliability applications
[DE92-011384] p 3626 N92-30807
The status of renewable energy technology
[DE92-011386] p 3670 N92-30808
Initial laboratory evaluation of color video cameras
[DE92-010399] p 3637 N92-30822
Thermally activated rejuvenation of ferroelectric properties in electrically fatigued lead zirconate titanate ceramics
[DE92-012634] p 3605 N92-30830
Computational simulation of diamond chemical vapor deposition in premixed C2H2/O2/H2 and CH4/O2 strained flames
[DE92-012144] p 3606 N92-30857
A study of discrete and continuum joint modeling techniques
[DE92-012631] p 3663 N92-30859
Fragment hazard zone analyses for explosive test facilities
[DE92-015391] p 3613 N92-30887
Attitudinal and situational differences between national laboratory inventors and inventor-entrepreneurs
[DE92-015768] p 3733 N92-30889
An overview of the computer aided definition system for design definition at Sandia National Laboratories, Livermore FY1991 update
[DE92-015991] p 3696 N92-30892
Repetitive High Energy Pulsed Power (RHEPP) temperature monitoring system utilizing Luxtron fluoroptic sensors and thermocouples technical reference manual
[DE92-013461] p 3637 N92-30893
Numerical calculations of two-dimensional single and multi-material flow fields with CCICE
[DE92-015778] p 3636 N92-30903
Pulsed microwave processing of high-T(sub c) superconducting films
[DE92-014950] p 3730 N92-31000
Choice coordination with multiple alternatives
[DE92-011656] p 3700 N92-31111
Eulerian simulation of the perforation of aluminum plates by nondeforming projectiles
[DE92-011515] p 3664 N92-31123
Phase transformations in weldments: New materials and new perspectives
[DE92-016231] p 3600 N92-31177
Component-wise error bounds for linear equations
[DE92-016000] p 3707 N92-31189

SANDIA NATIONAL LABS., LIVERMORE, CA.
A pulse combustion-based VOC destruction technique
[DE92-013563] p 3594 N92-30369

SANTA BARBARA RESEARCH CENTER, GOLETA, CA.
HgCdTe photomixers for CO2 laser radar systems
p 3654 N92-31100

SCIENCE AND ENGINEERING SERVICES, INC., BURTONSVILLE, MD.
Injection seeded single mode alexandrite ring laser for lidar applications p 3646 N92-31057

SCIENCE AND TECHNOLOGY CORP., EDGEWOOD, MD.
Multiple scattering wavelength dependent backscattering of kaolin dust in the IR: Measurements and theory p 3648 N92-31064

SCIENCE AND TECHNOLOGY CORP., HAMPTON, VA.
Regional-scale analysis and forecasting (RAP) report
[AD-A248384] p 3678 N92-30262

SCIENCE APPLICATIONS INTERNATIONAL CORP., SAN DIEGO, CA.
Soviet applied information sciences in a time of change
[PB92-173020] p 3734 N92-30509

SCIENTIFIC RESEARCH ASSOCIATES, INC., GLASTONBURY, CT.
Active control of pressure, sound and velocity of centrifugal pumps
[AD-A249446] p 3659 N92-30640

SCRIPPS INSTITUTION OF OCEANOGRAPHY, LA JOLLA, CA.
Oceanic CO2 measurements for the WOCE hydrographic survey in the Pacific Ocean, 1990-1991: Shore based analyses during legs 1-3
[DE92-013064] p 3682 N92-30861
Is the Venusian lithosphere subducting?
p 3738 N92-31234

SETS TECHNOLOGY, INC., MILILANI, HI.
Hyperspectral gas analysis system (HyGAS), phase 1
[AD-A251026] p 3593 N92-30241

SHINSHU UNIV., NAGANO (JAPAN).
A range-resolved bistatic lidar using a high-sensitive CCD-camera p 3640 N92-31027

SHIP RESEARCH INST., TOKYO (JAPAN).
Lidar observation of marine mixed layer
p 3655 N92-31104

SOLAREX CORP., NEWTOWN, PA.
Research on polycrystalline thin film submodules based on CuInSe2 materials
[DE92-010584] p 3727 N92-30247

SOREQ RESEARCH ESTABLISHMENT, ISRAEL ATOMIC ENERGY COMMISSION, YAVNEH.
Optical isolators in high power lasers based on high reflectivity phase conjugate mirrors
[IA-1452] p 3721 N92-30581

SOUTH CAROLINA UNIV., COLUMBIA.
Polymerization of 1-bromo-4-lithiobenzene in THF. A route to soluble polyphenylenes
[AD-A249926] p 3604 N92-30794
Extended orthogonally fused conducting oligomers for molecular electronic devices
[AD-A249927] p 3605 N92-30795
Synthesis of orthogonally fused conducting oligomers for molecular electronic devices
[AD-A249929] p 3605 N92-30796
Thermoset precursor to monolithic carbon glass prepared by the Pd/Cu-catalyzed alkynylation of polyphenylenes
[AD-A249920] p 3605 N92-30816
Electrooxidation of soluble alpha,alpha-coupled thiophene oligomers
[AD-A249928] p 3605 N92-30817

SOUTHAMPTON UNIV. (ENGLAND).
Chemielectron and photoelectron spectroscopic studies of importance in the upper atmosphere
[AD-A248838] p 3675 N92-30556

SOUTHEASTERN CENTER FOR ELECTRICAL ENGINEERING EDUCATION, INC., SAINT CLOUD, FL.
Optimal ECG electrode sites and criteria for detection of asymptomatic coronary artery disease, update 1990. Multilead ECG changes at rest, with exercise, and with coronary angioplasty
[AD-A248613] p 3684 N92-30523

SOUTHERN METHODIST UNIV., DALLAS, TX.
The thermal engine of Venus: Implications from the impact crater distribution p 3738 N92-31233

SOUTHWEST RESEARCH INST., SAN ANTONIO, TX.
Crack growth processes at elevated temperatures in advanced materials
[AD-A249023] p 3662 N92-30558
Ringless piston experiments. Natural gas engine technology advancements
[PB92-164466] p 3659 N92-30601
Laser induced fluorescence detection of gums in jet fuels
[AD-A252685] p 3607 N92-30767
Dynamics and energetics of the solar corona
[NASA-CR-190664] p 3742 N92-31162

SPACE AND NAVAL WARFARE SYSTEMS COMMAND, WASHINGTON, DC.
Effects of microwave radiation on humans: Monkeys exposed to 1.25 GHz pulsed microwaves
[AD-A249997] p 3686 N92-31127

SPACE SYSTEMS/LORAL, PALO ALTO, CA.
Technical and economic feasibility of integrated video service by satellite
[NASA-CR-189210] p 3614 N92-30300

SPARTA, INC., LEXINGTON, MA.
Development of a Raman lidar simulation tool
p 3649 N92-31072

SPECTROLAB, INC., SYLMAR, CA.
Development of advanced silicon solar cells for Space Station Freedom
[NASA-CR-189215] p 3672 N92-31216

SRI INTERNATIONAL CORP., MENLO PARK, CA.
Airborne lidar mapping of vertical ozone distributions in support of the 1990 Clean Air Act Amendments
p 3654 N92-31101

STANFORD UNIV., CA.
Tunneling acoustic microscopy
[AD-A251028] p 3727 N92-30252
Turbulent reacting flows and supersonic combustion
[AD-A251065] p 3593 N92-30256
Induced pictorial representations
[AD-A248560] p 3687 N92-30336
The effects of free stream turbulence and surface curvature on boundary layer flow and heat transfer
[AD-A248846] p 3630 N92-30616
Growth and evaluation of nonlinear optical materials for laser applications: Barium borate, lithium borate, and silver gallium selenide
[AD-A248861] p 3624 N92-30617
Studying Turbulence Using Numerical Simulation Databases. 3: Proceedings of the 1990 Summer Program
[NASA-CR-189475] p 3630 N92-30648
On the subgrid-scale modeling of compressible turbulence p 3631 N92-30652
Structure of three-dimensional turbulent boundary layers p 3631 N92-30654
A fractal transition in the two dimensional shear layer
p 3633 N92-30665
Research studies on extreme ultraviolet and soft x ray lasers
[AD-A249798] p 3657 N92-30784
Numerical study of axial turbulent flow over long cylinders
[AD-A250801] p 3635 N92-30831
Interaction of isotropic turbulence with a shock wave
[AD-A250409] p 3635 N92-30852
A strictly improving linear programming algorithm based on a series of Phase 1 problems
[DE92-015905] p 3696 N92-30905
Nonlinear aerodynamics and the design of wing tips
[NASA-CR-190649] p 3577 N92-31157

STATE UNIV. OF NEW YORK, BINGHAMTON.
Acoustic fatigue life prediction for nonlinear structures with multiple resonant modes
[NASA-CR-190471] p 3664 N92-30988

STATE UNIV. OF NEW YORK, BUFFALO.
Chemistry within van der Waals cluster of unsaturated molecules: Observation of cationic polymerization
[AD-A250929] p 3712 N92-30240
Photodynamics within (CH3OH)(nCr(CO)6) heteroclusters: Observation of an isotope effect
[AD-A251058] p 3712 N92-30255
Magic numbers in molecular clusters: A probe for chemical reactivity
[AD-A251096] p 3712 N92-30261

STATE UNIV. OF NEW YORK, STONY BROOK.
Studies of atmospheric molecules by multiphoton spectroscopy
[DE92-012668] p 3672 N92-30345

STATE UNIV. OF NEW YORK, SYRACUSE.
Improvement of performance of variable probability sampling strategies
[PB92-180264] p 3707 N92-30562

STATE UNIV. OF SOUTHEAST MISSOURI, CAPE GIRARDEAU.
Dielectric behavior of semiconductors at microwave frequencies p 3610 N92-30275

SUPERCONDUCTING SUPER COLLIDER LAB., DALLAS, TX.
Designing, fabricating and testing cost effective structural composite for the SSCL magnets
[DE92-013469] p 3718 N92-30646
Magnetic measurement instrumentation developments at the SSC
[DE92-013969] p 3718 N92-30786
Application of superconducting cavities to the collider rings of the SSC
[DE92-011692] p 3718 N92-30811
Conceptual design of the SSC cryogenic transfer lines
[DE92-013964] p 3719 N92-30839
A dynamic model for beam tube vacuum effects on the SSC cryogenic system
[DE92-013967] p 3719 N92-30840
Emittance growth caused by magnet vibrations in SSC
[DE92-014186] p 3719 N92-30881
A statistical rationale for establishing process quality control limits using fixed sample size, for critical current verification of SSC superconducting wire
[DE92-014844] p 3661 N92-31120
Optical transducers for scintillating fiber readout
[DE92-015963] p 3721 N92-31187

SVERDRUP TECHNOLOGY, INC., BROOK PARK, OH.
Direct coupling method for time-accurate solution of incompressible Navier-Stokes equations
[NASA-CR-189177] p 3636 N92-30894

SYRACUSE UNIV., NY.
MBE grown copper-aluminum alloy films
[AD-A252486] p 3597 N92-30534
Photochemical solar energy conversion utilizing semiconductors localized in membrane-mimetic systems
[DE92-011115] p 3670 N92-30694

SYSTEMS SCIENCE AND SOFTWARE, LA JOLLA, CA.
Data analysis support for the Shuttle Potential and Return Electron Experiment (SPREE) on the Tethered Satellite System 1 (TSS-1) flight
[AD-A248943] p 3588 N92-30628

T

TECHNISCHE UNIV., BERLIN (GERMANY, F.R.).
Comparison of signal processing methods for estimation of network impedance for remote protection
[ETN-92-91686] p 3623 N92-30503
Examinations of the microwave photoelectric conductivity of a-Si:H multilayer systems for in situ characterization
[ETN-92-91688] p 3727 N92-30505
Activities report of the Institute for Astronomy and Astrophysics at Technical University of Berlin (Germany, F.R.)
[MITT-11] p 3740 N92-30506

TECHNISCHE UNIV., DELFT (NETHERLANDS).
On real and complex zeros of orthogonal polynomials in a discrete Sobolev space
[REPT-91-98] p 3702 N92-30350

A survey on pivot rules for linear programming
[REPT-91-99] p 3691 N92-30351
On the magnification of Cantor sets and their limit models
[REPT-91-100] p 3691 N92-30352
Degeneracy in interior point methods for linear programming
[REPT-91-102] p 3691 N92-30353
Signal matching by dynamic programming
[REPT-92-01] p 3614 N92-30354
The domain of attraction of the alpha-sum operator for type 2 and type 3 distributions
[REPT-92-02] p 3707 N92-30355
Controlling user interface objects through pre- and postconditions
[REPT-92-04] p 3692 N92-30356
The REMBRANDT system for multi-criteria decision analysis via pairwise comparisons or direct rating
[REPT-92-05] p 3692 N92-30357
The diffraction of short free surface water waves, a uniform expansion
[REPT-92-06] p 3628 N92-30358
A formal transformation from the BSI/VDM-SL concrete syntax to the core abstract syntax
[REPT-92-07] p 3692 N92-30359
Differential equations for symmetric generalized ultraspherical polynomials
[REPT-92-08] p 3702 N92-30360
A three-valued cumulative semantics for TMS
[REPT-91-69] p 3702 N92-30371
Global existence for a semilinear elliptic-parabolic PDE system
[REPT-91-70] p 3628 N92-30372
Finite volume discretization of the incompressible Navier-Stokes equations in general coordinates on staggered grids
[REPT-91-71] p 3628 N92-30373
Low-velocity impact loading on fibre reinforced aluminum laminates (ARALL) and other aircraft sheet materials
[ETN-92-91613] p 3590 N92-30414
Positivity for a strongly coupled elliptic system by Green function estimates
[REPT-91-77] p 3702 N92-30434
Achievable potential reductions in the method of Kojima et al. in the case of linear programming
[REPT-91-78] p 3693 N92-30435
Real cubic systems with four line invariants
[REPT-91-79] p 3702 N92-30436
GMRESR: A family of nested GMRES methods
[REPT-91-80] p 3703 N92-30437
Joint queue length and response time distributions in a general preemptive feedback queue
[REPT-91-66] p 3701 N92-30451
Scale sensitivity and rank preservation in a multiplicative variant of the AHP and SMART
[REPT-91-67] p 3707 N92-30452
Flow of fresh and salt water in an aquifer with injection from the top
[REPT-91-68] p 3629 N92-30453
A multigrid method for a discretization of the incompressible Navier-Stokes equations in general coordinates
[REPT-91-73] p 3629 N92-30454
Iri's polynomiality proof for the Iri-Imai method recast
[REPT-91-74] p 3693 N92-30455
The formal power of AGs with respect to their underlying CFGs
[REPT-91-75] p 3703 N92-30456
Bifurcation of limit cycles in a particular class of quadratic systems
[REPT-91-76] p 3703 N92-30457
The functions psi(x) and beta(x) and some inequalities for integrals (theorems 1-16)
[REPT-92-09] p 3703 N92-30459
Some inequalities for variances
[REPT-92-10] p 3707 N92-30460
Further experiences with GMRESR
[REPT-92-12] p 3704 N92-30461
A robust multigrid method for a discretization of the incompressible Navier-Stokes equations in general coordinates
[REPT-92-14] p 3629 N92-30462
Pairwise comparison of concessions in negotiation processes
[REPT-92-15] p 3733 N92-30463
On the Thue Morse measure
[REPT-92-16] p 3704 N92-30464
Finite volume discretization of the convection-diffusion equation in general coordinates
[REPT-91-72] p 3704 N92-30483
Component construction: Practical guidelines for the construction of reusable components
[REPT-91-89] p 3694 N92-30484
The semantics of the Duplex programming environment
[REPT-91-91] p 3694 N92-30485
Informatization in public administration (EGPA-research project 1991). Large scale information systems in The Netherlands
[REPT-91-92] p 3734 N92-30486
Informatization in public administration (EGPA-research project 1991). Large scale information systems (comparative analysis in 8 European countries)
[REPT-91-93] p 3734 N92-30487
Real polynomial systems of degree n with n+1 line invariants
[REPT-91-86] p 3704 N92-30490
About difference equations, algebras and discrete events
[REPT-91-87] p 3704 N92-30491
The Duplex programming environment
[REPT-91-90] p 3694 N92-30492
Synchronized continuous flow systems
[REPT-91-88] p 3704 N92-30517
Quantum interference and confinement effects in narrow channel Si-MOSFET's
[ETN-92-91742] p 3625 N92-30729
Temperature dependence of universal conductance fluctuations in narrow Si inversion layers
p 3625 N92-30730
One-dimensional subband effects in the conductance of multiple quantum wires in Si-MOSFET's
p 3625 N92-30731
Enhancement of weak localization in a Si lateral superlattice device p 3625 N92-30732

TECHNISCHE UNIV., EINDHOVEN (NETHERLANDS).
Strong dynamic input-output decoupling: From linearity to nonlinearity
[MEMO-COSOR-92-04] p 3694 N92-30478

TECHNISCHE UNIV., HANOVER (GERMANY, F.R.).
Development of the cultivated landscape of north west Germany under the human influence
[ETN-92-91730] p 3669 N92-30968

TECHNISCHE UNIV. MUNICH, GARCHING (GERMANY, F.R.).
Neutron Source Munich FRM-2
[DE92-015300] p 3717 N92-31205

TEL-AVIV UNIV. (ISRAEL).
Polarization effects in pi(+) absorption in He-3
[ITN-92-85164] p 3714 N92-30580
Optical isolators in high power lasers based on high reflectivity phase conjugate mirrors
[IA-1452] p 3721 N92-30581
Transverse pattern modification in a stable apertured laser resonator
[ITN-92-85171] p 3656 N92-30582
Polarization effects in pi(+) absorption in He-4
[ITN-92-85163] p 3715 N92-30780
Anomalous hopping conductivity in amorphous indium-oxide films
[ITN-92-85166] p 3729 N92-30781
Spontaneous emission from an atom in motion near an infinite conducting plane
[ITN-92-85169] p 3715 N92-30782

TELESAT CANADA, GLOUCESTER (ONTARIO).
SHARP system for personal communications
p 3618 N92-30931

TENNESSEE UNIV., KNOXVILLE.
Study of the surface properties of ceramic materials by chromatography
[DE92-011129] p 3604 N92-30695

TEXAS A&M UNIV., COLLEGE STATION.
Computer vision in microstructural analysis
p 3609 N92-30271
Mechanical properties of brittle materials
p 3612 N92-30290
Melatonin, the pineal gland and circadian rhythms
[AD-A250640] p 3684 N92-30376
Radiation, scattering, and guidance of electromagnetic fields by arbitrarily shaped structures embedded in layered dielectric media
[AD-A252621] p 3615 N92-30408
TRAC performance estimates
[NASA-CR-190530] p 3701 N92-30778

TEXAS UNIV., AUSTIN.
Survivable algorithms and redundancy management in NASA's distributed computing systems
[NASA-CR-189827] p 3691 N92-30299
Surface-mediated photocatalysis
[AD-A249906] p 3595 N92-30793
Low-frequency fluctuations in plasma magnetic fields
[DE92-012139] p 3724 N92-30833
Development of practical MO techniques for prediction of the properties and behavior of materials
[AD-A247218] p 3598 N92-30864
Two dimensional aspects of toroidal drift waves in the ballooning representation
[DE92-014028] p 3724 N92-30880
The Rayleigh-Taylor instability in an expanding plasma
[DE92-013883] p 3725 N92-30884

TEXAS UNIV., GALVESTON.
Secretory mechanisms in opiocortin cells during cold stress
[AD-A252317] p 3685 N92-30719

TEXAS UNIV., HOUSTON.
Analysis and synthesis of adaptive neural elements and assembles
[AD-A248467] p 3687 N92-30320

THOMSON-TRT DEFENSE, GUYANCOURT (FRANCE).
A cable detection lidar system for helicopters
p 3648 N92-31068

TOHOKU UNIV., SENDAI (JAPAN).
Tm,Ho:YAG laser with tunable range of 2.08-2.12 microns and its applications to spectroscopy
p 3646 N92-31058

TRW, INC., BEAVERCREEK, OH.
A model of the ADA avionics real-time system: An example of the benefits of the hardware/software codesign approach in development of real-time systems
[AD-A248893] p 3581 N92-30524

TUEBINGEN UNIV. (GERMANY, F.R.).
Theory and measurement of the energy and risetime resolution of scintillation detectors in hard x ray area
[ETN-92-91687] p 3720 N92-30504

U

UNIVERSITEIT TWENTE, ENSCHEDE (NETHERLANDS).
On the use of pre-defined implementation constructs in distributed systems design
[MEMO-INF-92-08] p 3689 N92-30432
A computational proof of soundness
[MEMO-INF-92-09] p 3693 N92-30433
High level synthesis of controlpath microarchitectures
[MEMO-INF-91-86] p 3690 N92-30698

UNIVERSITIES SPACE RESEARCH ASSOCIATION, COLUMBIA, MD.
Raman lidar measurements of water vapor and aerosol/clouds during the FIRE/SPECTRE field campaign p 3652 N92-31089
Performance modeling of daytime Raman lidar systems for profiling atmospheric water vapor
p 3653 N92-31090

UNIVERSITY OF EASTERN KENTUCKY, RICHMOND.
Analysis, review, and documentation of the activation data from LDEF material
[NASA-CR-184356] p 3596 N92-31161

UNIVERSITY OF NORTHEAST LOUISIANA, MONROE.
Duration and rates of discharge: Maja Valles, Mars
p 3737 N92-31227

UNIVERSITY OF SOUTH FLORIDA, TAMPA.
Emerging solid-state laser technology by lidar/DIAL remote sensing p 3653 N92-31095
Coherent summation of spatially distorted Doppler lidar signals using a two-dimensional heterodyne detector array p 3654 N92-31096

UNIVERSITY OF SOUTHERN CALIFORNIA, DOWNEY.
Optimal ECG electrode sites and criteria for detection of asymptomatic coronary artery disease, update 1990. Multilead ECG changes at rest, with exercise, and with coronary angioplasty
[AD-A248613] p 3684 N92-30523

UNIVERSITY OF SOUTHERN CALIFORNIA, LOS ANGELES.
Practical method's for robust multivariable control
[AD-A248473] p 3700 N92-30322

UNIVERSITY OF THE PACIFIC, STOCKTON, CA.
Impact testing of welded samples
p 3608 N92-30268

UNIVERSITY OF WESTERN ONTARIO, LONDON.
Lidar measurements using large liquid mirror telescopes p 3652 N92-31087

UNIVERSITY RESEARCH FOUNDATION, GREENBELT, MD.
Advanced Raman water vapor lidar
p 3643 N92-31040

UOP, INC., DES PLAINES, IL.
The development of precipitated iron catalysts with improved stability
[DE92-014625] p 3596 N92-31006

UTAH STATE UNIV., LOGAN.
Effect of wave-particle interaction on the outflow of ions at high latitudes
[NASA-CR-190560] p 3677 N92-30962

UTAH UNIV., SALT LAKE CITY.
Decomposition studies of tertiarybutyldimethylantimony
[AD-A250670] p 3727 N92-30527
Understanding heterolytic bond cleavage
[AD-A252336] p 3716 N92-30845

UTD, INC., NEWINGTON, VA.
Investigation of the interface phenomena due to interaction of high intensity stress waves with geologic boundaries
[AD-A248992] p 3675 N92-30525

UTRECHT STATE UNIV. (NETHERLANDS).
Computing and verifying depth orders
[RUU-CS-91-41] p 3693 N92-30443
Classifying termination of term rewriting
[RUU-CS-91-42] p 3693 N92-30444
A protocol scheme for a class of minimum delay routing algorithms
[RUU-CS-91-43] p 3693 N92-30445
Restrictions of graph partition problems, part 1
[RUU-CS-91-44-PT-1] p 3703 N92-30446
Point location in fat subdivisions
[RUU-CS-91-40] p 3703 N92-30447
A paradigm for asynchronous communication and its application to concurrent constraint programming
[RUU-CS-91-48] p 3615 N92-30448
Linear planar augmentation algorithms for outerplanar graphs
[RUU-CS-91-47] p 3703 N92-30449
Kayles on special classes of graphs: An application of Sprague-Grundy theory
[RUU-CS-91-49] p 3703 N92-30450
On the complexity of the maximum cut problem
[RUU-CS-91-39] p 3703 N92-30458
Maintenance of 2- and 3-connected components of graphs. Part 1: 2- and 3-edge-connected components
[RUU-CS-90-26-PT-1] p 3694 N92-30479
Maintenance of 2- and 3-connected components of graphs. Part 2: 2- and 3-edge-connected components and 2-vertex-connected components
[RUU-CS-90-27-PT-2] p 3694 N92-30480
The sum of weighted balls
[RUU-CS-91-37] p 3707 N92-30481
A bibliography on network flow problems (2nd edition)
[RUU-CS-91-38] p 3698 N92-30482

V

VALPARAISO UNIV., IN.
Development of software to improve AC power quality on large spacecraft
[NASA-CR-190569] p 3589 N92-30989
VENTURA COLL., CA.
Computer integrated laboratory testing
p 3611 N92-30289
VIRGINIA POLYTECHNIC INST. AND STATE UNIV., BLACKSBURG.
A model of the ADA avionics real-time system: An example of the benefits of the hardware/software codesign approach in development of real-time systems
[AD-A248893] p 3581 N92-30524
Computational methods for modeling and active control of distributed parameter systems
[AD-A248559] p 3705 N92-30638
Numerical analysis of the Iosipescu specimen for composite materials
[NASA-CR-190658] p 3592 N92-30906
Single mode variable-sensitivity fiber optic sensors
[NASA-CR-190492] p 3721 N92-30975
An experimental study of the relationship between velocity and pressure fluctuations in a wing-body junction
[AD-A249628] p 3577 N92-31122
VIRGINIA UNIV., CHARLOTTESVILLE.
Control of circadian behavior by transplanted suprachiasmatic nuclei
[AD-A250442] p 3686 N92-31143
Trace gas and aerosol transports into and out of the Amazon Basin
[NASA-CR-190624] p 3674 N92-31153

W

WASHINGTON STATE UNIV., PULLMAN.
Spontaneous decay of an atom near a phase conjugator
[AD-A248298] p 3712 N92-30333
Coefficients of the second viscosity in bulk liquid helium
[AD-A252421] p 3629 N92-30548
Theoretical study of phase-shifted quantum beats in time-resolved luminescence spectra from a biased asymmetric double quantum well
[AD-A252422] p 3710 N92-30549
WASHINGTON UNIV., SAINT LOUIS, MO.
TEM studies of a circumstellar rock
p 3736 N92-31223
WASHINGTON UNIV., SEATTLE.
Nuclear theory progress report, April 1991 - April 1992
[DE92-015349] p 3714 N92-30611
Laminar flamelet modeling of turbulent diffusion flames p 3633 N92-30667
Numerical simulations of light scattering from rough one-dimensional gold surfaces
[AD-A249794] p 3721 N92-30783
Solar neutrinos: Theoretical status
[DE92-014014] p 3743 N92-31199
WESTINGHOUSE SAVANNAH RIVER CO., AIKEN, SC.
Fiber-optic Raman spectroscopy at the Savannah River Site: Uses and techniques
[DE92-013971] p 3596 N92-30899
Considerations for imaging system implementation in a networked environment
[DE92-015338] p 3735 N92-31132
Thermodynamic evaporation of highly volatile components in the vacuum degassing of melted aluminum alloys
[DE92-015315] p 3600 N92-31218
WINTHROP GROUP, INC., CAMBRIDGE, MA.
Rocket propulsion research at Lewis Research Center
[NASA-CR-189187] p 3732 N92-30908
WISCONSIN UNIV., MADISON.
New transient and pseudo-transient algorithms for viscoelastic materials
[AD-A250642] p 3692 N92-30377
Development of a modular transient cycle analysis program for the adiabatic diesel and other compound diesel engines
[AD-A249022] p 3658 N92-30538
Locked modes and magnetic field errors in MST
[DE92-015379] p 3723 N92-30612
Pre-mixed flame simulations for non-unity Lewis numbers p 3597 N92-30670
Pressure profiles, resonant Pfirsch-Schlueter currents, thermal instabilities, and magnetic island formation
[DE92-015166] p 3726 N92-31002
Effect of atmospheric extinction on laser rangefinder performance at 1.54 and 0.6 microns
p 3648 N92-31066
WORCESTER POLYTECHNIC INST., MA.
Kinetic theory and boundary conditions for flows of highly inelastic spheres
[DE92-012645] p 3629 N92-30438
Ultrasound NDE of adhesive bond integrity: A quantitative measure
[AD-A248845] p 3661 N92-30599
WRIGHT LAB., WRIGHT-PATTERSON AFB, OH.
Characterization and analysis of defects in nonlinear optical molecular composite films
[AD-A252118] p 3661 N92-30529
WRIGHT STATE UNIV., DAYTON, OH.
Review of psychophysically-based image quality metrics
[AD-A251053] p 3686 N92-30254

Y

YALE UNIV., NEW HAVEN, CT.
On the rapid evaluation of trigonometric series
[AD-A249029] p 3705 N92-30568
YORK UNIV. (ONTARIO).
Correction for nonlinear photon counting effects in lidar systems p 3649 N92-31070
YOUNGSTOWN STATE UNIV., OH.
Cu-Zn binary phase diagram and diffusion couples
p 3600 N92-30269

Typical Contract Number Index Listing

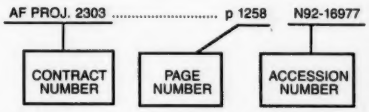

Listings in this index are arranged alphanumerically by contract number. Under each contract number the accession numbers denoting documents that have been produced as a result of research done under that contract are arranged in ascending order. The page number helps to locate the citation in the abstract section. The accession number denotes the number by which the citation is identified.

AC-90-695 ..... p 3619 N92-30934
AF PROJ. 2303 ..... p 3661 N92-30525
AF PROJ. 4594 ..... p 3735 N92-30819
AF-AFOSR-0001-89 ..... p 3705 N92-30638
AF-AFOSR-0011-90 ..... p 3700 N92-30335
AF-AFOSR-0027-91 ..... p 3687 N92-30320
AF-AFOSR-0044-91 ..... p 3702 N92-30375
AF-AFOSR-0045-89 ..... p 3637 N92-30546
AF-AFOSR-0058-91 ..... p 3687 N92-30325
AF-AFOSR-0069-90 ..... p 3624 N92-30678
AF-AFOSR-0076-89 ..... p 3687 N92-30336
AF-AFOSR-0094-90 ..... p 3702 N92-30410
AF-AFOSR-0098-90 ..... p 3686 N92-31143
AF-AFOSR-0104-90 ..... p 3684 N92-30319
AF-AFOSR-0133-91 ..... p 3705 N92-30533
AF-AFOSR-0148-91 ..... p 3598 N92-30872
AF-AFOSR-0151-90 ..... p 3593 N92-30256
AF-AFOSR-0162-89 ..... p 3715 N92-30681
AF-AFOSR-0167-88 ..... p 3715 N92-30680
AF-AFOSR-0167-89 ..... p 3700 N92-30334
AF-AFOSR-0179-89 ..... p 3598 N92-30864
AF-AFOSR-0220-89 ..... p 3692 N92-30377
AF-AFOSR-0226-89 ..... p 3632 N92-30660
AF-AFOSR-0244-90 ..... p 3684 N92-30376
AF-AFOSR-0246-89 ..... p 3630 N92-30616
AF-AFOSR-0249-89 ..... p 3635 N92-30852
AF-AFOSR-0265-88 ..... p 3706 N92-31128
AF-AFOSR-0266-90 ..... p 3687 N92-30613
AF-AFOSR-0269-91 ..... p 3679 N92-30643
AF-AFOSR-0271-89 ..... p 3699 N92-30596
AF-AFOSR-0272-90 ..... p 3621 N92-31129
AF-AFOSR-0295-90 ..... p 3721 N92-31126
AF-AFOSR-0296-91 ..... p 3622 N92-30249
AF-AFOSR-0330-90 ..... p 3687 N92-30679
AF-AFOSR-0341-89 ..... p 3702 N92-30347
AF-AFOSR-0351-89 ..... p 3675 N92-30556
AF-AFOSR-0353-88 ..... p 3590 N92-30528
AF-AFOSR-0390-87 ..... p 3712 N92-30337
AF-AFOSR-0393-89 ..... p 3622 N92-30332
AF-AFOSR-0398-89 ..... p 3700 N92-30322
AF-AFOSR-0406-89 ..... p 3660 N92-30237
AF-AFOSR-89-NM-605 ..... p 3704 N92-30516
AF-AFOSR-90-0093 ..... p 3706 N92-30716
ARPA ORDER 7781 ..... p 3614 N92-30407
ARPA ORDER 8162 ..... p 3626 N92-30836
ATD-91-GNC-7102 ..... p 3580 N92-31208
BCRS PROJ. AO-3.3 ..... p 3667 N92-30472
BCRS PROJ. CO-2.19 ..... p 3667 N92-30471
BCRS PROJ. OP-1.30 ..... p 3682 N92-30470
BCRS PROJ. OP-3.5 ..... p 3666 N92-30465
BCRS PROJ. TE-1.13 ..... p 3666 N92-30467
BCRS PROJ. TE-1.17 ..... p 3614 N92-30361
BCRS PROJ. TO-1.24 ..... p 3666 N92-30466
BCRS PROJ. TO-2.10 ..... p 3666 N92-30362
BCRS PROJ. TO-2.17 ..... p 3666 N92-30468
DA PROJ. 1L1-61102-AH-43 ..... p 3587 N92-30257
p 3630 N92-30604
DA PROJ. 1L1-61102-AH-45 ..... p 3709 N92-30898
DA PROJ. 1L1-62211-A-47-A ..... p 3658 N92-30396
DA PROJ. 1L1-62211-A-47AB ..... p 3664 N92-31155
DA PROJ. 1L1-62211-A-47A ..... p 3660 N92-30948
DA PROJ. 1L2-36003-D-313 ..... p 3574 N92-30394
DA PROJ. 3M1-61102-BS-15 ..... p 3686 N92-31127
DAAA15-89-D-0007 ..... p 3648 N92-31064
DAAD05-90-P-8392 ..... p 3695 N92-30629
DAAE07-84-C-R063 ..... p 3658 N92-30538
DAAJ02-86-C-0009 ..... p 3580 N92-30878
DAAL03-86-G-0193 ..... p 3591 N92-30639
DAAL03-86-G-0194 ..... p 3591 N92-30639
DAAL03-86-K-0170 ..... p 3591 N92-30639
DAAL03-87-K-0123 ..... p 3595 N92-30814
DAAL03-88-K-0096 ..... p 3592 N92-30815
DAAL03-88-K-0103 ..... p 3656 N92-30774
DAAL03-88-K-0108 ..... p 3627 N92-31004
DAAL03-89-K-0027 ..... p 3592 N92-30874
DAAL03-89-K-0047 ..... p 3729 N92-30772
DAAL03-89-K-0067 ..... p 3595 N92-30773
DAAL03-90-G-0103 ..... p 3708 N92-30771
DAAL03-90-G-0232 ..... p 3622 N92-31180
DAAL03-91-C-0041 ..... p 3603 N92-30635
DAAL03-91-G-0103 ..... p 3595 N92-30793
DAAL03-91-G-0123 ..... p 3706 N92-30716
DAAL03-91-G-0176 ..... p 3708 N92-30633
DAAL03-91-G-0188 ..... p 3595 N92-30835
DAAL04-90-C-0024 ..... p 3661 N92-30599
DACA76-91-C-0013 ..... p 3593 N92-30241
DACW29-88-D-0122 ..... p 3669 N92-31139
DAJA45-90-C-0037 ..... p 3663 N92-30766
DARPA ORDER 7382 ..... p 3701 N92-30710
DE-AC02-76CH-00016 ..... p 3717 N92-30398
DE-AC02-76CH-03000 ..... p 3717 N92-30589
p 3740 N92-30622
p 3699 N92-30812
p 3743 N92-30828
p 3719 N92-31219
DE-AC02-76CH-03073 ..... p 3726 N92-31114
DE-AC02-83CH-10093 ..... p 3727 N92-30247
p 3670 N92-30330
p 3670 N92-30519
p 3729 N92-30748
p 3670 N92-30837
p 3596 N92-30879
p 3596 N92-30882
p 3671 N92-30896
p 3743 N92-31206
DE-AC02-83ER-40107 ..... p 3717 N92-30398
DE-AC03-76SF-00098 ..... p 3717 N92-30398
p 3674 N92-30647
p 3626 N92-30813
p 3731 N92-30825
p 3600 N92-31138
p 3719 N92-31198
DE-AC04-76DP-00613 ..... p 3624 N92-30590
p 3598 N92-30865
p 3606 N92-30866
p 3711 N92-30890
p 3627 N92-31144
DE-AC04-76DP-00789 ..... p 3698 N92-30363
p 3574 N92-30367
p 3622 N92-30370
p 3698 N92-30401
p 3695 N92-30522
p 3603 N92-30544
p 3728 N92-30585
p 3630 N92-30607
p 3718 N92-30624
p 3632 N92-30658
p 3626 N92-30764
p 3605 N92-30804
p 3626 N92-30807
p 3670 N92-30808
p 3637 N92-30822
p 3605 N92-30830
p 3663 N92-30859
p 3613 N92-30887
p 3733 N92-30889
p 3637 N92-30893
p 3636 N92-30903
p 3730 N92-31000
p 3700 N92-31111
p 3664 N92-31123
p 3600 N92-31177
DE-AC04-76DR-00789 ..... p 3594 N92-30369
p 3594 N92-30749
p 3606 N92-30857
p 3696 N92-30892
p 3707 N92-31189
DE-AC04-88DP-43495 ..... p 3705 N92-30566
DE-AC05-76OR-00033 ..... p 3728 N92-30574
DE-AC05-84OR-21400 ..... p 3610 N92-30277
p 3610 N92-30278
p 3610 N92-30281
p 3722 N92-30366
p 3578 N92-30565
p 3663 N92-30567
p 3728 N92-30574
p 3736 N92-30575
p 3723 N92-30576
p 3728 N92-30577
p 3659 N92-30587
p 3603 N92-30626
p 3728 N92-30684
p 3604 N92-30744
p 3742 N92-30797
p 3592 N92-30809
p 3724 N92-30810
p 3663 N92-30823
p 3637 N92-30827
p 3716 N92-30853
p 3696 N92-30886
p 3599 N92-30888
p 3677 N92-31009
p 3589 N92-31012
p 3599 N92-31112
p 3726 N92-31114
p 3672 N92-31176
p 3597 N92-31184
p 3597 N92-31196
p 3726 N92-31197
p 3717 N92-31205
DE-AC05-84OS-21400 ..... p 3722 N92-31195
DE-AC06-76RL-01830 ..... p 3607 N92-30265
p 3732 N92-30349
p 3672 N92-30374
p 3599 N92-30877
p 3735 N92-31001
p 3599 N92-31010
p 3685 N92-31011
DE-AC06-87RL-10930 ..... p 3589 N92-30818
DE-AC07-76ID-01570 ..... p 3661 N92-30763
p 3598 N92-30834
DE-AC09-89SR-18035 ..... p 3596 N92-30899
p 3735 N92-31132
p 3600 N92-31218
DE-AC22-87PC-79812 ..... p 3596 N92-31006
DE-AC22-91PC-90185 ..... p 3629 N92-30438
DE-AC34-90DP-62349 ..... p 3717 N92-31137
p 3606 N92-31146
p 3717 N92-31147
DE-AC35-89ER-40486 ..... p 3718 N92-30646
p 3718 N92-30786
p 3718 N92-30811
p 3719 N92-30839
p 3719 N92-30840
p 3719 N92-30881
p 3661 N92-31120
p 3721 N92-31187
DE-FC07-91ID-13074 ..... p 3626 N92-30842
DE-FG02-84ER-13261 ..... p 3683 N92-30829
DE-FG02-84ER-45147 ..... p 3626 N92-30901
DE-FG02-84ER-45174 ..... p 3597 N92-30588
DE-FG02-85ER-13403 ..... p 3593 N92-30344
DE-FG02-85ER-53198 ..... p 3723 N92-30612
DE-FG02-85ER-53207 ..... p 3725 N92-30900
DE-FG02-86ER-13484 ..... p 3661 N92-30693
DE-FG02-86ER-13506 ..... p 3670 N92-30694
DE-FG02-86ER-13590 ..... p 3672 N92-30345
DE-FG02-86ER-45262 ..... p 3600 N92-31186
DE-FG02-86ER-53218 ..... p 3726 N92-31002
DE-FG02-87ER-13791 ..... p 3683 N92-30368
DE-FG02-88ER-40413 ..... p 3717 N92-30398
DE-FG02-88ER-45373 ..... p 3710 N92-31131
DE-FG02-88ER-53263 ..... p 3726 N92-31116
DE-FG02-90ER-40577 ..... p 3714 N92-30610
DE-FG02-90ER-45413 ..... p 3600 N92-31186
DE-FG02-91ER-40606 ..... p 3740 N92-30822
DE-FG02-91ER-40661 ..... p 3716 N92-30841

DE-FG02-91ER-40677 ..... p 3715 N92-30625
p 3716 N92-30791
DE-FG02-91ER-61205 ..... p 3675 N92-31183
DE-FG03-85SF-15799 ..... p 3671 N92-31117
DE-FG03-88ER-40424 ..... p 3717 N92-30398
DE-FG03-90ER-60982 ..... p 3682 N92-30861
DE-FG03-92ER-25116 ..... p 3696 N92-30905
DE-FG05-80ET-53088 ..... p 3724 N92-30833
p 3724 N92-30880
p 3725 N92-30884
DE-FG05-86ER-45280 ..... p 3598 N92-30787
DE-FG05-87ER-40309 ..... p 3717 N92-30398
DE-FG05-87ER-40361 ..... p 3716 N92-30853
DE-FG05-88ER-13859 ..... p 3604 N92-30695
DE-FG05-88ER-53268 ..... p 3724 N92-30880
DE-FG05-90ER-54091 ..... p 3723 N92-30746
DE-FG06-85ER-40224 ..... p 3714 N92-30606
DE-FG06-88ER-40427 ..... p 3714 N92-30611
p 3743 N92-31199
DE-FG06-90ER-40561 ..... p 3743 N92-31199
DE-FG06-91ER-40637 ..... p 3714 N92-30606
DE-FG08-90ER-61012 ..... p 3674 N92-30707
DE-FG22-89PC-89786 ..... p 3608 N92-30904
DE-FG22-90PC-90291 ..... p 3594 N92-30717
DRET-89-001-118 ..... p 3711 N92-30966
DTFA01-80-Y-10524 ..... p 3678 N92-30495
p 3678 N92-30496
DTFA01-84-Z-02030 ..... p 3678 N92-30559
DTFA01-90-C-00042 ..... p 3578 N92-30980
DTFA01-91-Y-01004 ..... p 3579 N92-31211
DTFA02-86-85098 ..... p 3685 N92-30745
DTFA03-89-C-0043 ..... p 3581 N92-30303
ECC-3075 ..... p 3693 N92-30443
EEC-JRC-3444-88-08-ED-ISP-NL . p 3667 N92-30471
EEC-3075 ..... p 3693 N92-30445
p 3703 N92-30446
p 3703 N92-30447
p 3703 N92-30449
p 3703 N92-30458
p 3707 N92-30481
p 3698 N92-30482
ERI PROJ. 3051 ..... p 3576 N92-30977
ESA-7222/87/NL ..... p 3658 N92-30477
ESA-7560/88 ..... p 3667 N92-30475
ESA-7662/88 ..... p 3667 N92-30475
FNSRS-1-467-0-86 ..... p 3693 N92-30435
F04701-88-C-0089 ..... p 3636 N92-30412
F19628-89-C-0001 ..... p 3695 N92-30550
F19628-89-C-0167 ..... p 3678 N92-30262
F19628-90-C-0002 ..... p 3678 N92-30559
p 3616 N92-30761
p 3616 N92-30762
p 3616 N92-30863
F19628-90-C-0133 ..... p 3588 N92-30628
F19628-90-K-0003 ..... p 3676 N92-30720
F30602-81-C-0169 ..... p 3597 N92-30534
F30602-87-C-0015 ..... p 3720 N92-30248
F33615-84-K-2437 ..... p 3594 N92-30645
F33615-85-C-3213 ..... p 3590 N92-30251
F33615-86-C-2623 ..... p 3659 N92-30554
F33615-87-C-1499 ..... p 3734 N92-30324
F33615-87-C-2714 ..... p 3624 N92-30619
F33615-87-C-3228 ..... p 3583 N92-30323
F33615-87-D-0609 ..... p 3684 N92-30523
F33615-87-D-1452 ..... p 3581 N92-30524
F33615-88-C-3400 ..... p 3573 N92-30253
p 3573 N92-30258
F33615-89-C-0532 ..... p 3686 N92-30254
F33615-90-C-2050 ..... p 3607 N92-30767
F33615-90-C-3206 ..... p 3577 N92-31171
F33615-91-C-5618 ..... p 3593 N92-31005
F40650-90-C-0061 ..... p 3585 N92-30897
F41624-91-C-6003 ..... p 3688 N92-30844
F49620-86-C-0008 ..... p 3587 N92-30958
F49620-89-C-0007 ..... p 3731 N92-30242
F49620-89-C-0031 ..... p 3601 N92-30342
F49620-89-C-0032 ..... p 3662 N92-30558
F49620-90-C-0076 ..... p 3744 N92-30327
F49620-91-C-0008 ..... p 3675 N92-30525
GRI-5089-293-1848 ..... p 3659 N92-30601
JPL-958596 ..... p 3625 N92-30757
MDA903-89-C-0003 ..... p 3615 N92-30532
MDA903-89-K-0078 ..... p 3612 N92-30411
MDA972-91-C-0032 ..... p 3626 N92-30836
MDA972-92-C-0028 ..... p 3612 N92-30411
MIPR-107-91 ..... p 3657 N92-30784
MIPR-153-91 ..... p 3721 N92-30783
MITRE RP-91260 ..... p 3621 N92-31130
NAGW-1072 ..... p 3635 N92-30751
NAGW-1251 ..... p 3682 N92-30739
NAGW-2087 ..... p 3742 N92-31162
NAGW-642 ..... p 3737 N92-31228
NAG1-1053 ..... p 3592 N92-30906
NAG1-1081 ..... p 3583 N92-30922
NAG1-1082 ..... p 3621 N92-31156
NAG1-1114 ..... p 3698 N92-30960
NAG1-1145 ..... p 3706 N92-30716
NAG1-1192 ..... p 3574 N92-30392
NAG1-1348 ..... p 3721 N92-30975
NAG1-1350 ..... p 3582 N92-30753
NAG1-745 ..... p 3664 N92-31214
p 3665 N92-31215
NAG1-801 ..... p 3660 N92-30738
NAG1-978 ..... p 3664 N92-30988
NAG2-502 ..... p 3576 N92-30977
NAG2-593 ..... p 3692 N92-30379
NAG3-1053 ..... p 3671 N92-30949
NAG3-1198 ..... p 3709 N92-30898
NAG3-1254 ..... p 3589 N92-30989
NAG5-1546 ..... p 3677 N92-30962
NAG5-1612 ..... p 3691 N92-30296
NAG5-198 ..... p 3742 N92-30921
NAG5-557 ..... p 3587 N92-30709
NAG5-781 ..... p 3676 N92-30756
NAG5-799 ..... p 3676 N92-30961
NAG8-201 ..... p 3589 N92-30981
NAG8-874 ..... p 3743 N92-31168
NAG9-362 ..... p 3701 N92-30778
NAG9-426 ..... p 3691 N92-30299
NASA ORDER H-08071D ..... p 3596 N92-31161
NASW-3920 ..... p 3732 N92-30908
NASW-4627 ..... p 3733 N92-30974
NAS1-18028 ..... p 3579 N92-30978
NAS1-18605 ..... p 3689 N92-30311
p 3689 N92-30489
p 3704 N92-30516
p 3706 N92-30716
NAS1-18754 ..... p 3579 N92-30304
NAS1-18788 ..... p 3686 N92-30306
NAS1-18878 ..... p 3700 N92-31158
NAS1-19317 ..... p 3661 N92-30309
NAS1-19345 ..... p 3581 N92-30965
NAS1-19480 ..... p 3704 N92-30516
NAS10-10285 ..... p 3673 N92-30494
NAS10-11624 ..... p 3673 N92-30494
NAS2-12722 ..... p 3580 N92-31208
NAS3-24672 ..... p 3672 N92-31216
NAS3-25092 ..... p 3614 N92-30300
NAS3-25266 ..... p 3588 N92-30308
p 3636 N92-30894
NAS3-25572 ..... p 3582 N92-30972
NAS3-25952 ..... p 3582 N92-31164
NAS3-26061 ..... p 3574 N92-30298
NAS3-26242 ..... p 3660 N92-30734
NAS7-918 ..... p 3581 N92-30569
p 3614 N92-30391
p 3623 N92-30542
p 3695 N92-30543
p 3617 N92-30923
NAS8-36412 ..... p 3613 N92-30754
NAS8-38485 ..... p 3591 N92-30711
NCC1-106 ..... p 3674 N92-31153
NCC2-387 ..... p 3696 N92-30723
p 3690 N92-30724
NCC2-408 ..... p 3696 N92-30723
NCC2-460 ..... p 3630 N92-30648
NCC2-507 ..... p 3628 N92-30380
NCC2-654 ..... p 3575 N92-30740
NCC2-683 ..... p 3577 N92-31157
NCC9-16 ..... p 3698 N92-31154
NIVR-428-02704-N ..... p 3693 N92-30476
NR PROJ. RR0-4108 ..... p 3685 N92-30719
NSERC-OGP-0036747 ..... p 3708 N92-30699
NSERC-OGP-0046506 ..... p 3708 N92-30699
NSF AST-90-12180 ..... p 3737 N92-31228
NSF CCR-88-20279 ..... p 3701 N92-30339
NSF CCR-89-07654 ..... p 3702 N92-30410
NSF DMS-84-10324 ..... p 3701 N92-30339
NSF DMS-89-02532 ..... p 3704 N92-30516
NSF DMS-90-12751 ..... p 3705 N92-30568
NSF IRI-88-13179 ..... p 3692 N92-30356
N00014-80-C-0795 ..... p 3727 N92-30406
p 3603 N92-30594
p 3728 N92-30595
N00014-82-K-0280 ..... p 3595 N92-30821
N00014-82-K-0612 ..... p 3603 N92-30553
p 3605 N92-30838
p 3607 N92-31207
N00014-86-J-1124 ..... p 3627 N92-31210
N00014-88-K-0016 ..... p 3685 N92-30719
N00014-88-K-0145 ..... p 3635 N92-30831
N00014-88-K-0483 ..... p 3712 N92-30240
p 3712 N92-30255
p 3712 N92-30261
N00014-88-K-0525 ..... p 3601 N92-30326
N00014-88-K-0664 ..... p 3593 N92-30245
p 3613 N92-30246
N00014-89-C-0090 ..... p 3659 N92-30640
N00014-89-J-1198 ..... p 3728 N92-30634
N00014-89-J-1497 ..... p 3716 N92-30845
N00014-89-J-1527 ..... p 3705 N92-30568
N00014-89-J-1848 ..... p 3594 N92-30632
N00014-89-J-1855 ..... p 3592 N92-30871
N00014-89-J-1946 ..... p 3691 N92-30260
N00014-89-J-3062 ..... p 3604 N92-30794
p 3605 N92-30795
p 3605 N92-30796
p 3605 N92-30816
p 3605 N92-30817
N00014-90-C-0246 ..... p 3719 N92-30233
N00014-90-J-1025 ..... p 3702 N92-30410
N00014-90-J-1030 ..... p 3662 N92-30338
p 3701 N92-30339
N00014-90-J-1045 ..... p 3682 N92-30593
N00014-90-J-1161 ..... p 3683 N92-30531
N00014-90-J-1178 ..... p 3623 N92-30537
N00014-90-J-1186 ..... p 3601 N92-30244
N00014-90-J-1193 ..... p 3712 N92-30333
p 3629 N92-30548
p 3710 N92-30549
N00014-90-J-1197 ..... p 3615 N92-30408
N00014-90-J-1494 ..... p 3720 N92-30535
p 3721 N92-30536
N00014-90-J-1635 ..... p 3727 N92-30252
N00014-90-J-1864 ..... p 3696 N92-30820
N00014-90-J-1909 ..... p 3577 N92-31122
N00014-90-J-1971 ..... p 3712 N92-30259
N00014-90-J-1976 ..... p 3632 N92-30658
N00014-90-J-4077 ..... p 3624 N92-30598
N00014-90-J-4092 ..... p 3624 N92-30617
N00014-91-C-0222 ..... p 3656 N92-30552
N00014-91-J-1017 ..... p 3699 N92-30526
N00014-91-J-1035 ..... p 3595 N92-30875
N00014-91-J-1133 ..... p 3709 N92-30642
N00014-91-J-1265 ..... p 3624 N92-30630
N00014-91-J-1338 ..... p 3606 N92-30873
N00014-91-J-1416 ..... p 3729 N92-30846
N00014-91-J-1434 ..... p 3602 N92-30346
N00014-91-J-1438 ..... p 3710 N92-30850
N00014-91-J-1447 ..... p 3727 N92-30527
N00014-91-J-1518 ..... p 3699 N92-30557
N00014-91-J-1655 ..... p 3601 N92-30250
N00014-91-J-1917 ..... p 3603 N92-30623
N00014-91-J-1934 ..... p 3606 N92-31141
N00014-91-J-1976 ..... p 3590 N92-30318
N00014-91-J-1985 ..... p 3695 N92-30555
N00014-91-J-4016 ..... p 3706 N92-30716
N00014-92-J-1413 ..... p 3596 N92-31178
OTKA-2115 ..... p 3691 N92-30351
OTKA-2116 ..... p 3691 N92-30353
p 3693 N92-30455
PROJ. 89-07 ..... p 3688 N92-30381
PROJ. 90-N26 ..... p 3627 N92-30902
RF PROJ. 765353/718266 ..... p 3676 N92-30756
RICIS PROJ. AI-05 ..... p 3698 N92-31154
RTOP 144-50-50 ..... p 3614 N92-30300
RTOP 323-57-4A ..... p 3623 N92-30427
RTOP 324-02-00 ..... p 3581 N92-30569
RTOP 474-46-10 ..... p 3659 N92-30571
RTOP 505-59-00 ..... p 3636 N92-30982
RTOP 505-59-36-01 ..... p 3574 N92-30394
RTOP 505-59-40-10 ..... p 3574 N92-30392
RTOP 505-59-40 ..... p 3635 N92-30765
RTOP 505-59-50-01 ..... p 3573 N92-30295
RTOP 505-59-53-01 ..... p 3576 N92-30747
RTOP 505-59-53-03 ..... p 3637 N92-30737
RTOP 505-62-20 ..... p 3627 N92-30297
RTOP 505-62-30 ..... p 3582 N92-30998
RTOP 505-62-40-06 ..... p 3576 N92-30909
RTOP 505-62-52 ..... p 3636 N92-30894
p 3582 N92-30972
p 3583 N92-31172
RTOP 505-62-84 ..... p 3585 N92-30307
p 3584 N92-30508
RTOP 505-63-36 ..... p 3658 N92-30396
p 3660 N92-30948
p 3664 N92-31155
RTOP 505-63-50-01 ..... p 3608 N92-30263
RTOP 505-63-50-04 ..... p 3664 N92-30964
p 3664 N92-31214
p 3665 N92-31215
RTOP 505-63-50-12 ..... p 3574 N92-30393
p 3575 N92-30570
p 3575 N92-30691
RTOP 505-63-50-15 ..... p 3580 N92-30752
p 3580 N92-31174
RTOP 505-63-53-01 ..... p 3661 N92-30309
RTOP 505-64-10-05 ..... p 3699 N92-30677
p 3700 N92-31158
RTOP 505-64-13-21 ..... p 3686 N92-30306
RTOP 505-64-13 ..... p 3686 N92-31167
RTOP 505-64-20 ..... p 3580 N92-31208
RTOP 505-64-40-01 ..... p 3583 N92-31175
RTOP 505-64-52-01 ..... p 3586 N92-31160
RTOP 505-66-41-66 ..... p 3579 N92-30978
RTOP 505-68-11 ..... p 3577 N92-30395
RTOP 505-90-52-01 ..... p 3689 N92-30311
p 3689 N92-30489

	p 3704	N92-30516
	p 3706	N92-30716
RTOP 505-90-53-02	p 3689	N92-30907
RTOP 506-40-41-02	p 3635	N92-30751
RTOP 506-41-11	p 3670	N92-30426
RTOP 506-41-41	p 3741	N92-30302
	p 3586	N92-30310
RTOP 506-42-00	p 3732	N92-30908
RTOP 506-49-21-02	p 3588	N92-30736
RTOP 510-01-50	p 3592	N92-30779
	p 3593	N92-30986
RTOP 510-02-12-08	p 3579	N92-30304
RTOP 533-02-36	p 3581	N92-30518
RTOP 535-03-10	p 3574	N92-30298
RTOP 535-03-11-03	p 3711	N92-30979
RTOP 590-13-11	p 3660	N92-30734
RTOP 590-13-31	p 3623	N92-30397
RTOP 590-21-11	p 3660	N92-30722
RTOP 590-21-31	p 3582	N92-31164
RTOP 591-34-31	p 3689	N92-31166
RTOP 593-72-00	p 3588	N92-30308
RTOP 618-22-31-02	p 3679	N92-30735
RTOP 650-60-15-01-00	p 3617	N92-30923
RTOP 665-45-20-21	p 3637	N92-31013
RTOP 679-40-00	p 3587	N92-30383
RTOP 694-03-OH	p 3588	N92-30301
SWRI PROJ. 15-3619	p 3742	N92-31162
W-31-109-ENG-38	p 3723	N92-30591
	p 3705	N92-30608
	p 3716	N92-30826
	p 3660	N92-30860
	p 3730	N92-30999
	p 3730	N92-31190
W-31109-ENG-38	p 3674	N92-30770
	p 3708	N92-30803
	p 3657	N92-30848
	p 3655	N92-31109
W-7405-ENG-36	p 3673	N92-30520
	p 3590	N92-30521
	p 3740	N92-30578
	p 3740	N92-30609
	p 3743	N92-30627
	p 3615	N92-30703
	p 3667	N92-30704
	p 3740	N92-30705
	p 3743	N92-30706
	p 3657	N92-30805
	p 3724	N92-30806
	p 3606	N92-30847
	p 3740	N92-30856
	p 3709	N92-30891
	p 3677	N92-31008
	p 3627	N92-31107
	p 3741	N92-31108
	p 3657	N92-31182
	p 3708	N92-31185
	p 3730	N92-31200
	p 3717	N92-31201
	p 3608	N92-31202
	p 3589	N92-31204
	p 3730	N92-31217
	p 3731	N92-31220
W-7405-ENG-48	p 3602	N92-30399
	p 3656	N92-30400
	p 3714	N92-30586
	p 3674	N92-30647
	p 3594	N92-30749
	p 3604	N92-30792
	p 3724	N92-30824
	p 3729	N92-30854
	p 3740	N92-30855
	p 3739	N92-30862
	p 3596	N92-30883
	p 3729	N92-30885
	p 3621	N92-31007
	p 3657	N92-31115
	p 3726	N92-31118
	p 3599	N92-31119
	p 3674	N92-31121
	p 3600	N92-31124
	p 3600	N92-31125
	p 3600	N92-31138
W-7405-ENG-82	p 3598	N92-30858

Typical Report Number Index Listing

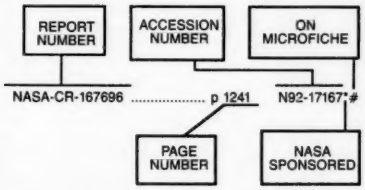

Listings in this index are arranged alphanumerically by report number. The accession number denotes the number by which the citation is identified. The page number helps to locate the citation in the abstract section. An asterisk (*) indicates that the item is a NASA report. A pound sign (#) indicates that the item is available on microfiche.

A-91186 ..... p 3686 N92-31167 * #
A-91224 ..... p 3689 N92-31166 * #
A-92027 ..... p 3635 N92-30765 * #
A-92091 ..... p 3636 N92-30982 * #

AD-A246122 ..... p 3590 N92-30318 #
AD-A246961 ..... p 3624 N92-30678 #
AD-A246962 ..... p 3687 N92-30679 #
AD-A246963 ..... p 3715 N92-30680 #
AD-A246964 ..... p 3715 N92-30681 #
AD-A246965 ..... p 3733 N92-30682 #
AD-A246988 ..... p 3616 N92-30863 #
AD-A247218 ..... p 3598 N92-30864 #
AD-A247228 ..... p 3687 N92-30613 #
AD-A247667 ..... p 3624 N92-30683 #
AD-A247857 ..... p 3720 N92-30248 #
AD-A248298 ..... p 3712 N92-30333 #
AD-A248384 ..... p 3678 N92-30262 #
AD-A248466 ..... p 3684 N92-30319 #
AD-A248467 ..... p 3687 N92-30320 #
AD-A248472 ..... p 3607 N92-30321 #
AD-A248473 ..... p 3700 N92-30322 #
AD-A248481 ..... p 3700 N92-30334 #
AD-A248484 ..... p 3700 N92-30335 #
AD-A248487 ..... p 3583 N92-30323 #
AD-A248492 ..... p 3734 N92-30324 #
AD-A248494 ..... p 3687 N92-30325 #
AD-A248495 ..... p 3601 N92-30326 #
AD-A248559 ..... p 3705 N92-30638 #
AD-A248560 ..... p 3687 N92-30336 #
AD-A248567 ..... p 3712 N92-30337 #
AD-A248613 ..... p 3684 N92-30523 #
AD-A248661 ..... p 3591 N92-30639 #
AD-A248671 ..... p 3624 N92-30598 #
AD-A248766 ..... p 3744 N92-30327 #
AD-A248782 ..... p 3656 N92-30614 #
AD-A248787 ..... p 3688 N92-30615 #
AD-A248790 ..... p 3615 N92-30583 #
AD-A248806 ..... p 3603 N92-30553 #
AD-A248807 ..... p 3659 N92-30554 #
AD-A248826 ..... p 3695 N92-30555 #
AD-A248833 ..... p 3656 N92-30743 #
AD-A248838 ..... p 3675 N92-30556 #
AD-A248843 ..... p 3699 N92-30557 #
AD-A248845 ..... p 3661 N92-30599 #
AD-A248846 ..... p 3630 N92-30616 #
AD-A248847 ..... p 3622 N92-30249 #
AD-A248851 ..... p 3719 N92-30233 #
AD-A248852 ..... p 3734 N92-30234 #
AD-A248853 ..... p 3731 N92-30235 #
AD-A248861 ..... p 3624 N92-30617 #
AD-A248893 ..... p 3581 N92-30524 #
AD-A248898 ..... p 3679 N92-31003 #
AD-A248899 ..... p 3662 N92-30338 #
AD-A248900 ..... p 3701 N92-30339 #

AD-A248901 ..... p 3678 N92-30340 #
AD-A248902 ..... p 3607 N92-30341 #
AD-A248903 ..... p 3601 N92-30342 #
AD-A248938 ..... p 3720 N92-30343 #
AD-A248943 ..... p 3588 N92-30628 #
AD-A248945 ..... p 3695 N92-30629 #
AD-A248963 ..... p 3684 N92-30328 #
AD-A248964 ..... p 3584 N92-30329 #
AD-A248992 ..... p 3675 N92-30525 #
AD-A249017 ..... p 3735 N92-30584 #
AD-A249018 ..... p 3624 N92-30630 #
AD-A249019 ..... p 3696 N92-30631 #
AD-A249021 ..... p 3594 N92-30632 #
AD-A249022 ..... p 3658 N92-30538 #
AD-A249023 ..... p 3662 N92-30558 #
AD-A249024 ..... p 3678 N92-30559 #
AD-A249028 ..... p 3629 N92-30560 #
AD-A249029 ..... p 3705 N92-30568 #
AD-A249030 ..... p 3735 N92-30819 #
AD-A249035 ..... p 3696 N92-30820 #
AD-A249062 ..... p 3595 N92-30821 #
AD-A249265 ..... p 3708 N92-30771 #
AD-A249406 ..... p 3729 N92-30772 #
AD-A249407 ..... p 3595 N92-30773 #
AD-A249423 ..... p 3656 N92-30774 #
AD-A249424 ..... p 3635 N92-30775 #
AD-A249425 ..... p 3706 N92-30776 #
AD-A249436 ..... p 3585 N92-30777 #
AD-A249438 ..... p 3604 N92-30758 #
AD-A249439 ..... p 3597 N92-30759 #
AD-A249440 ..... p 3616 N92-30760 #
AD-A249441 ..... p 3616 N92-30761 #
AD-A249442 ..... p 3616 N92-30762 #
AD-A249446 ..... p 3659 N92-30640 #
AD-A249450 ..... p 3591 N92-30641 #
AD-A249481 ..... p 3709 N92-30642 #
AD-A249482 ..... p 3708 N92-30633 #
AD-A249483 ..... p 3728 N92-30634 #
AD-A249485 ..... p 3603 N92-30635 #
AD-A249491 ..... p 3705 N92-30618 #
AD-A249494 ..... p 3735 N92-30636 #
AD-A249499 ..... p 3615 N92-30637 #
AD-A249500 ..... p 3663 N92-30802 #
AD-A249501 ..... p 3624 N92-30619 #
AD-A249502 ..... p 3723 N92-30620 #
AD-A249503 ..... p 3584 N92-30621 #
AD-A249628 ..... p 3577 N92-31122 #
AD-A249643 ..... p 3616 N92-30721 #
AD-A249662 ..... p 3627 N92-31004 #
AD-A249729 ..... p 3596 N92-31178 #
AD-A249730 ..... p 3669 N92-31179 #
AD-A249747 ..... p 3607 N92-31207 #
AD-A249793 ..... p 3622 N92-31180 #
AD-A249794 ..... p 3721 N92-30783 #
AD-A249798 ..... p 3657 N92-30784 #
AD-A249812 ..... p 3595 N92-30835 #
AD-A249814 ..... p 3626 N92-30836 #
AD-A249856 ..... p 3599 N92-31110 #
AD-A249873 ..... p 3679 N92-30867 #
AD-A249874 ..... p 3676 N92-30868 #
AD-A249880 ..... p 3617 N92-30869 #
AD-A249886 ..... p 3663 N92-30870 #
AD-A249888 ..... p 3592 N92-30871 #
AD-A249904 ..... p 3685 N92-30745 #
AD-A249906 ..... p 3595 N92-30793 #
AD-A249911 ..... p 3595 N92-30814 #
AD-A249912 ..... p 3592 N92-30815 #
AD-A249915 ..... p 3669 N92-31139 #
AD-A249916 ..... p 3598 N92-30872 #
AD-A249917 ..... p 3606 N92-30873 #
AD-A249918 ..... p 3592 N92-30874 #
AD-A249919 ..... p 3595 N92-30875 #
AD-A249920 ..... p 3605 N92-30816 #
AD-A249926 ..... p 3604 N92-30794 #
AD-A249927 ..... p 3605 N92-30795 #
AD-A249928 ..... p 3605 N92-30817 #
AD-A249929 ..... p 3605 N92-30796 #
AD-A249944 ..... p 3585 N92-30849 #
AD-A249969 ..... p 3710 N92-30850 #
AD-A249986 ..... p 3721 N92-31126 #
AD-A249997 ..... p 3686 N92-31127 #
AD-A250004 ..... p 3707 N92-31140 #
AD-A250239 ..... p 3617 N92-30876 #

AD-A250351 ..... p 3606 N92-31141 #
AD-A250352 ..... p 3706 N92-31128 #
AD-A250376 ..... p 3626 N92-30851 #
AD-A250403 ..... p 3677 N92-31142 #
AD-A250409 ..... p 3635 N92-30852 #
AD-A250442 ..... p 3686 N92-31143 #
AD-A250488 ..... p 3621 N92-31129 #
AD-A250489 ..... p 3621 N92-31130 #
AD-A250635 ..... p 3699 N92-30526 #
AD-A250638 ..... p 3602 N92-30346 #
AD-A250639 ..... p 3702 N92-30375 #
AD-A250640 ..... p 3684 N92-30376 #
AD-A250641 ..... p 3702 N92-30347 #
AD-A250642 ..... p 3692 N92-30377 #
AD-A250643 ..... p 3679 N92-30643 #
AD-A250644 ..... p 3605 N92-30838 #
AD-A250650 ..... p 3684 N92-30603 #
AD-A250651 ..... p 3685 N92-30644 #
AD-A250654 ..... p 3577 N92-31171 #
AD-A250670 ..... p 3727 N92-30527 #
AD-A250701 ..... p 3733 N92-31209 #
AD-A250738 ..... p 3622 N92-30332 #
AD-A250749 ..... p 3579 N92-31193 #
AD-A250756 ..... p 3709 N92-31194 #
AD-A250757 ..... p 3730 N92-30895 #
AD-A250801 ..... p 3635 N92-30831 #
AD-A250802 ..... p 3594 N92-30645 #
AD-A250803 ..... p 3601 N92-30250 #
AD-A250808 ..... p 3590 N92-30251 #
AD-A250809 ..... p 3660 N92-30237 #
AD-A250830 ..... p 3681 N92-30238 #
AD-A250832 ..... p 3682 N92-30832 #
AD-A250882 ..... p 3573 N92-30239 #
AD-A250895 ..... p 3627 N92-31210 #
AD-A250929 ..... p 3712 N92-30240 #
AD-A251026 ..... p 3593 N92-30241 #
AD-A251028 ..... p 3727 N92-30252 #
AD-A251037 ..... p 3573 N92-30253 #
AD-A251044 ..... p 3731 N92-30242 #
AD-A251053 ..... p 3686 N92-30254 #
AD-A251058 ..... p 3712 N92-30255 #
AD-A251061 ..... p 3603 N92-30623 #
AD-A251065 ..... p 3593 N92-30256 #
AD-A251066 ..... p 3701 N92-30243 #
AD-A251074 ..... p 3587 N92-30257 #
AD-A251083 ..... p 3573 N92-30258 #
AD-A251085 ..... p 3712 N92-30259 #
AD-A251086 ..... p 3601 N92-30244 #
AD-A251088 ..... p 3593 N92-30245 #
AD-A251089 ..... p 3691 N92-30260 #
AD-A251093 ..... p 3613 N92-30246 #
AD-A251096 ..... p 3712 N92-30261 #
AD-A251127 ..... p 3580 N92-30878 #
AD-A252101 ..... p 3590 N92-30528 #
AD-A252117 ..... p 3667 N92-30545 #
AD-A252118 ..... p 3661 N92-30529 #
AD-A252120 ..... p 3636 N92-30530 #
AD-A252140 ..... p 3706 N92-30843 #
AD-A252191 ..... p 3683 N92-30531 #
AD-A252193 ..... p 3637 N92-30546 #
AD-A252199 ..... p 3615 N92-30532 #
AD-A252263 ..... p 3630 N92-30604 #
AD-A252265 ..... p 3688 N92-30592 #
AD-A252266 ..... p 3682 N92-30593 #
AD-A252268 ..... p 3603 N92-30594 #
AD-A252269 ..... p 3728 N92-30595 #
AD-A252270 ..... p 3727 N92-30406 #
AD-A252275 ..... p 3614 N92-30407 #
AD-A252309 ..... p 3685 N92-30605 #
AD-A252310 ..... p 3688 N92-30718 #
AD-A252317 ..... p 3685 N92-30719 #
AD-A252326 ..... p 3676 N92-30720 #
AD-A252332 ..... p 3688 N92-30844 #
AD-A252333 ..... p 3705 N92-30533 #
AD-A252336 ..... p 3716 N92-30845 #
AD-A252349 ..... p 3699 N92-30596 #
AD-A252352 ..... p 3729 N92-30846 #
AD-A252364 ..... p 3705 N92-30597 #
AD-A252404 ..... p 3584 N92-30547 #
AD-A252421 ..... p 3629 N92-30548 #
AD-A252422 ..... p 3710 N92-30549 #
AD-A252462 ..... p 3695 N92-30550 #
AD-A252486 ..... p 3597 N92-30534 #

AD-A252490 ..... p 3720 N92-30535 #
AD-A252491 ..... p 3721 N92-30536 #
AD-A252500 ..... p 3623 N92-30537 #
AD-A252621 ..... p 3615 N92-30408 #
AD-A252641 ..... p 3602 N92-30409 #
AD-A252643 ..... p 3702 N92-30410 #
AD-A252647 ..... p 3612 N92-30411 #
AD-A252649 ..... p 3636 N92-30412 #
AD-A252651 ..... p 3578 N92-30551 #
AD-A252652 ..... p 3663 N92-30766 #
AD-A252665 ..... p 3656 N92-30552 #
AD-A252685 ..... p 3607 N92-30767 #
AD-A252693 ..... p 3593 N92-31005 #

AD-D015238 ..... p 3682 N92-30413
AD-D015258 ..... p 3614 N92-30348 #
AD-D015259 ..... p 3585 N92-31192 #
AD-D015267 ..... p 3604 N92-30685 #
AD-D015290 ..... p 3722 N92-31213 #
AD-D015299 ..... p 3591 N92-30573
AD-D015307 ..... p 3690 N92-30564 #

AD-E200940 ..... p 3678 N92-30262 #
AD-E200981 ..... p 3720 N92-30343 #
AD-E200987 ..... p 3588 N92-30628 #
AD-E501529 ..... p 3615 N92-30532 #
AD-E951786 ..... p 3585 N92-30849 #

AECL-10461 ..... p 3602 N92-30402 #

AERONOMICA-ACTA-F-42-1991 . p 3744 N92-30996

AFIT/CI/CIA-91-102 ..... p 3591 N92-30641 #
AFIT/CI/CIA-91-117 ..... p 3679 N92-30867 #
AFIT/CI/CIA-91-121 ..... p 3676 N92-30868 #

AFOSR-91-0148 ..... p 3598 N92-30872 #
AFOSR-92-0095TR ..... p 3624 N92-30678 #
AFOSR-92-0096TR ..... p 3687 N92-30679 #
AFOSR-92-0097TR ..... p 3715 N92-30680 #
AFOSR-92-0098TR ..... p 3715 N92-30681 #
AFOSR-92-0108TR ..... p 3687 N92-30613 #
AFOSR-92-0115TR ..... p 3598 N92-30864 #
AFOSR-92-0170TR-VOL-4 ..... p 3744 N92-30327 #
AFOSR-92-0185TR ..... p 3700 N92-30334 #
AFOSR-92-0187TR ..... p 3694 N92-30319 #
AFOSR-92-0196TR ..... p 3712 N92-30337 #
AFOSR-92-0203TR ..... p 3687 N92-30325 #
AFOSR-92-0212TR ..... p 3687 N92-30320 #
AFOSR-92-0215TR ..... p 3700 N92-30335 #
AFOSR-92-0228TR ..... p 3622 N92-30249 #
AFOSR-92-0231TR ..... p 3687 N92-30336 #
AFOSR-92-0235TR ..... p 3675 N92-30525 #
AFOSR-92-0236TR ..... p 3601 N92-30342 #
AFOSR-92-0239TR ..... p 3705 N92-30638 #
AFOSR-92-0241TR ..... p 3662 N92-30558 #
AFOSR-92-0254TR ..... p 3721 N92-31126 #
AFOSR-92-0255TR ..... p 3675 N92-30556 #
AFOSR-92-0258TR ..... p 3630 N92-30616 #
AFOSR-92-0266TR ..... p 3622 N92-30332 #
AFOSR-92-0271TR ..... p 3692 N92-30377 #
AFOSR-92-0280TR ..... p 3679 N92-30643 #
AFOSR-92-0288TR ..... p 3702 N92-30375 #
AFOSR-92-0348TR ..... p 3621 N92-31129 #
AFOSR-92-0351TR ..... p 3706 N92-31128 #
AFOSR-92-0358TR ..... p 3660 N92-30237 #
AFOSR-92-0408TR ..... p 3635 N92-30852 #
AFOSR-92-0410TR ..... p 3686 N92-31143 #
AFOSR-92-0413TR ..... p 3684 N92-30376 #
AFOSR-92-0425TR ..... p 3702 N92-30347 #
AFOSR-92-0456TR ..... p 3593 N92-30256 #
AFOSR-92-0539TR ..... p 3637 N92-30546 #
AFOSR-92-0540TR ..... p 3699 N92-30596 #
AFOSR-92-0541TR ..... p 3705 N92-30533 #

AGARD-AR-299 ..... p 3576 N92-30947 #
AGARD-AR-315 ..... p 3584 N92-30769 #

AIAA PAPER 92-0354 ..... p 3588 N92-30301 * #
AIAA PAPER 92-3123 ..... p 3732 N92-30908 * #
AIAA PAPER 92-3747 ..... p 3581 N92-30518 * #
AIAA PAPER 92-3980 ..... p 3584 N92-30508 * #

AL-TR-1991-0029 ..... p 3684 N92-30523 #
AL-TR-1991-0153 ..... p 3686 N92-30254 #
AL-TR-1992-0005 ..... p 3685 N92-30605 #
AL-TR-1992-0062 ..... p 3688 N92-30844 #

AMSMI/TR-RD-WS-92-1 ..... p 3585 N92-30849 #

ANL-HEP-CP-92-13 ..... p 3655 N92-31109 #

ANL/CP-73759 ..... p 3716 N92-30826 #
ANL/CP-74758 ..... p 3730 N92-30999 #
ANL/CP-74864 ..... p 3660 N92-30860 #
ANL/CP-75202 ..... p 3657 N92-30848 #
ANL/CP-75362 ..... p 3723 N92-30591 #
ANL/CP-75636 ..... p 3708 N92-30803 #
ANL/CP-75803 ..... p 3705 N92-30608 #
ANL/CP-76267 ..... p 3730 N92-31190 #

ANL/ESD/TM-22-VOL-1 ..... p 3674 N92-30770 #

AR-006-858 ..... p 3664 N92-30963

ARCCB-TR-92009 ..... p 3663 N92-30802 #
ARCCB-TR-92010 ..... p 3705 N92-30618 #
ARCCB-TR-92012 ..... p 3707 N92-31140 #
ARCCB-TR-92015 ..... p 3709 N92-31194 #
ARCCB-TR-92018 ..... p 3705 N92-30597 #

ARO-24614.22-MS-UIR ..... p 3591 N92-30639 #
ARO-24615.1-MS-UIE ..... p 3591 N92-30639 #
ARO-24616.1-MS-UIF ..... p 3591 N92-30639 #
ARO-25245.15-EG ..... p 3595 N92-30814 #
ARO-25397.9-MS ..... p 3592 N92-30815 #
ARO-25631.13-PH ..... p 3656 N92-30774 #
ARO-26051.5-EL ..... p 3627 N92-31004 #
ARO-26160.22-PH ..... p 3657 N92-30784 #
ARO-26195.14-PH ..... p 3729 N92-30772 #
ARO-26439.48-MS ..... p 3592 N92-30874 #
ARO-26591.5-MS ..... p 3595 N92-30773 #
ARO-27868.14-MA ..... p 3708 N92-30771 #
ARO-28298.4-CH ..... p 3595 N92-30793 #
ARO-28316.1-EG ..... p 3595 N92-30835 #
ARO-28584.1-GS-EQ ..... p 3622 N92-31180 #
ARO-29016.1-MA ..... p 3708 N92-30633 #
ARO-29043.1-MS-SBI ..... p 3603 N92-30635 #
ARO-29288.1-GS ..... p 3721 N92-30783 #
ARO-92-1 ..... p 3706 N92-30843 #

ASD-TR-91-5005-VOL-1 ..... p 3688 N92-30592 #

ASIAC-1090.10 ..... p 3583 N92-30323 #

AVSCOM-TR-91-C-026 ..... p 3658 N92-30396 * #
AVSCOM-TR-92-B-002 ..... p 3574 N92-30394 * #
AVSCOM-TR-92-C-003 ..... p 3660 N92-30948 * #
AVSCOM-TR-92-C-024 ..... p 3709 N92-30898 * #

B-238954 ..... p 3690 N92-30712 #

BBC-RD-1992/3 ..... p 3711 N92-31173
BBC-RD-1992/4 ..... p 3711 N92-31151

BBN-7451 ..... p 3686 N92-30306 * #

BCRS-90-28 ..... p 3666 N92-30465 #
BCRS-90-30 ..... p 3666 N92-30466 #
BCRS-91-10 ..... p 3666 N92-30467 #
BCRS-91-21 ..... p 3666 N92-30468 #
BCRS-91-23-PT-1-2 ..... p 3682 N92-30470 #
BCRS-91-26-PT-1 ..... p 3667 N92-30471 #
BCRS-91-27 ..... p 3667 N92-30472 #
BCRS-91-33 ..... p 3614 N92-30361 #
BCRS-91-36 ..... p 3666 N92-30362 #

BN-1129 ..... p 3662 N92-30338 #
BN-1130 ..... p 3701 N92-30339 #

BNL-47201 ..... p 3717 N92-30398 #

BRL-TR-3358 ..... p 3587 N92-30257 #
BRL-TR-3362 ..... p 3630 N92-30604 #

CFD-26 ..... p 3576 N92-30977 * #

CFFTP-G-91112 ..... p 3723 N92-30746 #

CIT-61430 ..... p 3637 N92-30546 #

COELMN/PD-90/11 ..... p 3669 N92-31139 #

CONF-9102170-1 ..... p 3598 N92-30858 #
CONF-9104368-1-REV-1 ..... p 3674 N92-30647 #
CONF-9105239-2 ..... p 3731 N92-30825 #
CONF-910572 ..... p 3602 N92-30402 #
CONF-910626-16 ..... p 3674 N92-31121 #
CONF-9106276-9 ..... p 3718 N92-30624 #
CONF-9106340-2 ..... p 3714 N92-30606 #
CONF-9107218-2 ..... p 3740 N92-30855 #
CONF-910746-5 ..... p 3716 N92-30853 #
CONF-9108140 ..... p 3627 N92-31107 #
CONF-9108168-3 ..... p 3604 N92-30792 #
CONF-910857-9 ..... p 3724 N92-30824 #
CONF-9109182-3 ..... p 3740 N92-30622 #
CONF-9109182-4 ..... p 3743 N92-31199 #
CONF-9109221-6 ..... p 3719 N92-31219 #
CONF-9109356-1 ..... p 3657 N92-30848 #
CONF-9109358 ..... p 3674 N92-31181 #
CONF-9109371-2 ..... p 3740 N92-30705 #
CONF-9109378-1 ..... p 3743 N92-31199 #
CONF-9110252-2 ..... p 3599 N92-31119 #
CONF-9110336-2 ..... p 3742 N92-30797 #
CONF-9110344-9 ..... p 3735 N92-31132 #
CONF-9110359-1 ..... p 3637 N92-30827 #
CONF-9110360-1 ..... p 3740 N92-30856 #
CONF-911106-93 ..... p 3626 N92-30813 #
CONF-9111141-5 ..... p 3743 N92-30828 #
CONF-9111209 ..... p 3598 N92-30834 #
CONF-9111226-1 ..... p 3621 N92-31007 #
CONF-911131-3 ..... p 3656 N92-30400 #
CONF-911202-68 ..... p 3716 N92-30826 #
CONF-911202-73 ..... p 3600 N92-31138 #
CONF-911202-75 ..... p 3600 N92-31125 #
CONF-911267-3 ..... p 3729 N92-30854 #
CONF-911296-6 ..... p 3657 N92-30805 #
CONF-920104-23 ..... p 3589 N92-30818 * #
CONF-920113-5 ..... p 3719 N92-31198 #
CONF-920141-7 ..... p 3730 N92-31200 #
CONF-920146-3 ..... p 3599 N92-30877 #
CONF-920184-2 ..... p 3741 N92-31108 #
CONF-9202103-2 ..... p 3739 N92-30862 #
CONF-9202111-2 ..... p 3657 N92-31182 #
CONF-9202112-1 ..... p 3723 N92-30576 #
CONF-9202117-1 ..... p 3743 N92-30627 #
CONF-9202117-2 ..... p 3740 N92-30578 #
CONF-9202117-3 ..... p 3740 N92-30609 #
CONF-920219-4 ..... p 3717 N92-30398 #
CONF-920291-1 ..... p 3708 N92-30803 #
CONF-9203108-1 ..... p 3604 N92-30744 #
CONF-9203127-1 ..... p 3605 N92-30804 #
CONF-9203130-1 ..... p 3600 N92-31124 #
CONF-9203140-1 ..... p 3606 N92-30857 #
CONF-920315-16 ..... p 3718 N92-30811 #
CONF-9203151-1 ..... p 3743 N92-30706 #
CONF-920331-19 ..... p 3719 N92-30881 #
CONF-920331-25 ..... p 3719 N92-30840 #
CONF-920331-28 ..... p 3718 N92-30786 #
CONF-920331-29 ..... p 3719 N92-30839 #
CONF-920331-2 ..... p 3655 N92-31109 #
CONF-920331-33 ..... p 3717 N92-30589 #
CONF-920331-50 ..... p 3661 N92-31120 #
CONF-920362-19 ..... p 3724 N92-30806 #
CONF-920362-23 ..... p 3724 N92-30810 #
CONF-920362-33 ..... p 3726 N92-31118 #
CONF-920402-14 ..... p 3729 N92-30885 #
CONF-920402-15-REV-1 ..... p 3602 N92-30399 #
CONF-920402-20 ..... p 3603 N92-30544 #
CONF-920402-22 ..... p 3730 N92-31000 #
CONF-920402-24 ..... p 3728 N92-30577 #
CONF-920402-28 ..... p 3730 N92-30999 #
CONF-920402-29 ..... p 3606 N92-30847 #
CONF-920402-32 ..... p 3730 N92-31190 #
CONF-920402-5 ..... p 3615 N92-30703 #
CONF-9204106-4 ..... p 3630 N92-30607 #
CONF-9204106-5 ..... p 3698 N92-30401 #
CONF-9204112-1 ..... p 3677 N92-31008 #
CONF-9204131-1 ..... p 3578 N92-30565 #
CONF-9204132-1-EXTD-ABST ..... p 3722 N92-30366 #
CONF-9204151-1 ..... p 3596 N92-30899 #
CONF-920423-4 ..... p 3622 N92-30370 #
CONF-920430-83 ..... p 3732 N92-30349 #
CONF-920445-1 ..... p 3605 N92-30830 #
CONF-920466-11 ..... p 3594 N92-30369 #
CONF-920501-16 ..... p 3685 N92-31011 #
CONF-9205108-3 ..... p 3728 N92-30684 #
CONF-9205115-2 ..... p 3670 N92-30519 #
CONF-920514-4 ..... p 3599 N92-31010 #
CONF-9205141-4 ..... p 3667 N92-30704 #
CONF-9205155-1 ..... p 3718 N92-30646 #
CONF-9205191-1 ..... p 3735 N92-31001 #
CONF-920534-2 ..... p 3574 N92-30367 #
CONF-920574-2 ..... p 3597 N92-31196 #
CONF-920574-3 ..... p 3597 N92-31184 #
CONF-920584-3 ..... p 3596 N92-30883 #
CONF-920607-15 ..... p 3723 N92-30591 #
CONF-920610-1 ..... p 3726 N92-31197 #
CONF-9206114-5 ..... p 3670 N92-30808 #
CONF-9206151-2 ..... p 3736 N92-30575 #
CONF-9206151-3 ..... p 3733 N92-30889 #
CONF-9206155-1 ..... p 3660 N92-30860 #
CONF-9206173-3 ..... p 3600 N92-31177 #
CONF-9206187-1 ..... p 3663 N92-30567 #
CONF-9206187-2 ..... p 3603 N92-30626 #
CONF-920631-16 ..... p 3663 N92-30823 #
CONF-920633-1 ..... p 3663 N92-30859 #
CONF-920669-4 ..... p 3626 N92-30807 #
CONF-920673-3-EXTD-ABST ..... p 3592 N92-30809 #
CONF-920678-4 ..... p 3671 N92-30896 #
CONF-920707-9 ..... p 3594 N92-30749 #
CONF-9207101-1 ..... p 3705 N92-30608 #
CONF-920716-4 ..... p 3728 N92-30585 #
CONF-920771-1 ..... p 3698 N92-30363 #
CONF-920772-1 ..... p 3726 N92-31114 #
CONF-920792-3 ..... p 3717 N92-31201 #
CONF-920793-2 ..... p 3677 N92-31009 #
CONF-920795-1 ..... p 3659 N92-30587 #

CONF-920796-5 ..... p 3608 N92-31202 #
CONF-920801-2 ..... p 3671 N92-31113 #
CONF-920801-4 ..... p 3589 N92-31012 #
CONF-920803-6 ..... p 3696 N92-30886 #
CONF-920803-8 ..... p 3589 N92-31204 #
CONF-920814-1 ..... p 3673 N92-30520 #
CONF-920819-11 ..... p 3722 N92-31195 #
CONF-920819-13 ..... p 3599 N92-31112 #
CONF-920819-15-EXTD-ABST ..... p 3728 N92-30574 #
CONF-920853-3 ..... p 3657 N92-31115 #
CONF-920857-1 ..... p 3730 N92-31217 #
CONF-920857-2 ..... p 3590 N92-30521 #
CONF-920867-1 ..... p 3695 N92-30522 #
CONF-920867-2 ..... p 3700 N92-31111 #

CRC-578 ..... p 3607 N92-30341 #

CRDEC-CR-120 ..... p 3695 N92-30629 #

CRREL-SR-43-PT-8 ..... p 3681 N92-30238 #
CRREL-SR-91-24 ..... p 3584 N92-30621 #

CRREL-92-1 ..... p 3682 N92-30832 #

CSU-TR-68 ..... p 3607 N92-31207 #

CU-TR-92-1287 ..... p 3692 N92-30379 * #

CWI-BS-R9003 ..... p 3705 N92-30689 #

CWI-CS-R8749-REV ..... p 3692 N92-30428 #
CWI-CS-R9124 ..... p 3692 N92-30428 #
CWI-CS-R9125 ..... p 3708 N92-30699 #
CWI-CS-R9127 ..... p 3699 N92-30696 #

CWI-NM-R9113 ..... p 3706 N92-30700 #
CWI-NM-R9115 ..... p 3693 N92-30429 #

DE91-002143 ..... p 3596 N92-30882 #
DE91-002145 ..... p 3670 N92-30330 #
DE91-002147 ..... p 3596 N92-30879 #
DE92-001223 ..... p 3729 N92-30748 #
DE92-001245 ..... p 3670 N92-30837 #
DE92-001277 ..... p 3596 N92-30883 #
DE92-001282 ..... p 3672 N92-31221 #
DE92-004262 ..... p 3589 N92-30818 * #
DE92-006679 ..... p 3594 N92-30749 #
DE92-008679 ..... p 3698 N92-30363 #
DE92-009054 ..... p 3728 N92-30585 #
DE92-010274 ..... p 3657 N92-30848 #
DE92-010278 ..... p 3708 N92-30803 #
DE92-010399 ..... p 3637 N92-30822 #
DE92-010431 ..... p 3663 N92-30823 #
DE92-010437 ..... p 3724 N92-30824 #
DE92-010471 ..... p 3604 N92-30744 #
DE92-010475 ..... p 3731 N92-30825 #
DE92-010483 ..... p 3742 N92-30797 #
DE92-010498 ..... p 3716 N92-30826 #
DE92-010555 ..... p 3743 N92-31206 #
DE92-010566 ..... p 3671 N92-30896 #
DE92-010581 ..... p 3670 N92-30519 #
DE92-010584 ..... p 3727 N92-30247 #
DE92-010647 ..... p 3637 N92-30827 #
DE92-010650 ..... p 3743 N92-30828 #
DE92-010657 ..... p 3683 N92-30829 #
DE92-011066 ..... p 3728 N92-30684 #
DE92-011115 ..... p 3670 N92-30694 #
DE92-011129 ..... p 3604 N92-30695 #
DE92-011133 ..... p 3627 N92-31107 #
DE92-011134 ..... p 3677 N92-31008 #
DE92-011158 ..... p 3741 N92-31108 #
DE92-011197 ..... p 3655 N92-31109 #
DE92-011238 ..... p 3673 N92-30520 #
DE92-011358 ..... p 3605 N92-30804 #
DE92-011362 ..... p 3657 N92-30805 #
DE92-011363 ..... p 3730 N92-31217 #
DE92-011364 ..... p 3590 N92-30521 #
DE92-011365 ..... p 3724 N92-30806 #
DE92-011384 ..... p 3626 N92-30807 #
DE92-011386 ..... p 3670 N92-30808 #
DE92-011495 ..... p 3740 N92-30856 #
DE92-011515 ..... p 3664 N92-31123 #
DE92-011525 ..... p 3600 N92-31138 #
DE92-011526 ..... p 3600 N92-31124 #
DE92-011530 ..... p 3600 N92-31125 #
DE92-011615 ..... p 3661 N92-30693 #
DE92-011632 ..... p 3593 N92-30344 #
DE92-011656 ..... p 3700 N92-31111 #
DE92-011663 ..... p 3695 N92-30522 #
DE92-011667 ..... p 3599 N92-31112 #
DE92-011670 ..... p 3592 N92-30809 #
DE92-011689 ..... p 3728 N92-30574 #
DE92-011691 ..... p 3724 N92-30810 #
DE92-011692 ..... p 3718 N92-30811 #
DE92-011704 ..... p 3699 N92-30812 #
DE92-011727 ..... p 3626 N92-30813 #
DE92-011755 ..... p 3671 N92-31113 #
DE92-011779 ..... p 3716 N92-30853 #
DE92-011786 ..... p 3726 N92-31114 #
DE92-011848 ..... p 3729 N92-30854 #
DE92-011850 ..... p 3740 N92-30855 #
DE92-011886 ..... p 3722 N92-31195 #
DE92-011942 ..... p 3723 N92-30746 #
DE92-012102 ..... p 3674 N92-30770 #
DE92-012111 ..... p 3598 N92-30865 #
DE92-012112 ..... p 3606 N92-30866 #
DE92-012139 ..... p 3724 N92-30833 #
DE92-012144 ..... p 3606 N92-30857 #
DE92-012154 ..... p 3598 N92-30858 #
DE92-012217 ..... p 3661 N92-30763 #
DE92-012312 ..... p 3598 N92-30834 #
DE92-012331 ..... p 3732 N92-30349 #
DE92-012354 ..... p 3672 N92-30374 #
DE92-012631 ..... p 3663 N92-30859 #
DE92-012634 ..... p 3605 N92-30830 #
DE92-012645 ..... p 3629 N92-30438 #
DE92-012668 ..... p 3672 N92-30345 #
DE92-012696 ..... p 3657 N92-31115 #
DE92-013023 ..... p 3740 N92-30622 #
DE92-013057 ..... p 3660 N92-30860 #
DE92-013064 ..... p 3682 N92-30861 #
DE92-013234 ..... p 3578 N92-30565 #
DE92-013277 ..... p 3722 N92-30366 #
DE92-013404 ..... p 3659 N92-30587 #
DE92-013439 ..... p 3574 N92-30367 #
DE92-013443 ..... p 3739 N92-30862 #
DE92-013457 ..... p 3626 N92-30764 #
DE92-013461 ..... p 3637 N92-30893 #
DE92-013469 ..... p 3718 N92-30646 #
DE92-013472 ..... p 3683 N92-30368 #
DE92-013514 ..... p 3674 N92-30647 #
DE92-013536 ..... p 3615 N92-30703 #
DE92-013539 ..... p 3667 N92-30704 #
DE92-013542 ..... p 3740 N92-30705 #
DE92-013545 ..... p 3743 N92-30706 #
DE92-013563 ..... p 3594 N92-30369 #
DE92-013574 ..... p 3674 N92-30707 #
DE92-013684 ..... p 3622 N92-30370 #
DE92-013751 ..... p 3714 N92-30586 #
DE92-013883 ..... p 3725 N92-30884 #
DE92-013918 ..... p 3594 N92-30717 #
DE92-013964 ..... p 3719 N92-30839 #
DE92-013967 ..... p 3719 N92-30840 #
DE92-013969 ..... p 3718 N92-30786 #
DE92-013971 ..... p 3596 N92-30899 #
DE92-014006 ..... p 3598 N92-30787 #
DE92-014014 ..... p 3743 N92-31199 #
DE92-014028 ..... p 3724 N92-30880 #
DE92-014081 ..... p 3597 N92-30588 #
DE92-014186 ..... p 3719 N92-30881 #
DE92-014317 ..... p 3674 N92-31181 #
DE92-014428 ..... p 3716 N92-30791 #
DE92-014450 ..... p 3736 N92-30575 #
DE92-014453 ..... p 3696 N92-30886 #
DE92-014454 ..... p 3723 N92-30576 #
DE92-014460 ..... p 3597 N92-31196 #
DE92-014461 ..... p 3726 N92-31197 #
DE92-014481 ..... p 3719 N92-31198 #
DE92-014531 ..... p 3716 N92-30841 #
DE92-014586 ..... p 3671 N92-31117 #
DE92-014589 ..... p 3725 N92-30900 #
DE92-014591 ..... p 3626 N92-30842 #
DE92-014594 ..... p 3717 N92-30398 #
DE92-014595 ..... p 3714 N92-30606 #
DE92-014608 ..... p 3626 N92-30901 #
DE92-014612 ..... p 3717 N92-30589 #
DE92-014616 ..... p 3630 N92-30607 #
DE92-014620 ..... p 3718 N92-30624 #
DE92-014622 ..... p 3715 N92-30625 #
DE92-014625 ..... p 3596 N92-31006 #
DE92-014703 ..... p 3599 N92-30877 #
DE92-014715 ..... p 3621 N92-31007 #
DE92-014718 ..... p 3726 N92-31118 #
DE92-014760 ..... p 3624 N92-30590 #
DE92-014776 ..... p 3599 N92-31119 #
DE92-014780 ..... p 3729 N92-30885 #
DE92-014786 ..... p 3604 N92-30792 #
DE92-014787 ..... p 3602 N92-30399 #
DE92-014796 ..... p 3656 N92-30400 #
DE92-014844 ..... p 3661 N92-31120 #
DE92-014864 ..... p 3723 N92-30591 #
DE92-014887 ..... p 3674 N92-31121 #
DE92-014942 ..... p 3672 N92-31176 #
DE92-014950 ..... p 3730 N92-31000 #
DE92-015041 ..... p 3698 N92-30401 #
DE92-015046 ..... p 3603 N92-30544 #
DE92-015077 ..... p 3726 N92-31116 #
DE92-015084 ..... p 3677 N92-31009 #
DE92-015091 ..... p 3599 N92-31010 #
DE92-015092 ..... p 3685 N92-31011 #
DE92-015102 ..... p 3589 N92-31012 #
DE92-015129 ..... p 3728 N92-30577 #
DE92-015142 ..... p 3740 N92-30578 #
DE92-015147 ..... p 3606 N92-30847 #
DE92-015156 ..... p 3735 N92-31001 #
DE92-015160 ..... p 3627 N92-31144 #
DE92-015165 ..... p 3705 N92-30566 #
DE92-015166 ..... p 3726 N92-31002 #
DE92-015182 ..... p 3730 N92-30999 #
DE92-015195 ..... p 3663 N92-30567 #
DE92-015196 ..... p 3603 N92-30626 #
DE92-015207 ..... p 3730 N92-31200 #
DE92-015208 ..... p 3717 N92-31201 #
DE92-015210 ..... p 3608 N92-31202 #
DE92-015212 ..... p 3657 N92-31182 #
DE92-015217 ..... p 3675 N92-31183 #
DE92-015238 ..... p 3597 N92-31184 #
DE92-015243 ..... p 3743 N92-30627 #
DE92-015271 ..... p 3705 N92-30608 #
DE92-015274 ..... p 3589 N92-31204 #
DE92-015279 ..... p 3740 N92-30609 #
DE92-015287 ..... p 3710 N92-31131 #
DE92-015295 ..... p 3714 N92-30610 #
DE92-015300 ..... p 3717 N92-31205 #
DE92-015312 ..... p 3606 N92-31146 #
DE92-015313 ..... p 3717 N92-31147 #
DE92-015314 ..... p 3717 N92-31137 #
DE92-015315 ..... p 3600 N92-31218 #
DE92-015338 ..... p 3735 N92-31132 #
DE92-015349 ..... p 3714 N92-30611 #
DE92-015379 ..... p 3723 N92-30612 #
DE92-015391 ..... p 3613 N92-30887 #
DE92-015545 ..... p 3599 N92-30888 #
DE92-015768 ..... p 3733 N92-30889 #
DE92-015778 ..... p 3636 N92-30903 #
DE92-015798 ..... p 3608 N92-30904 #
DE92-015845 ..... p 3711 N92-30890 #
DE92-015902 ..... p 3708 N92-31185 #
DE92-015905 ..... p 3696 N92-30905 #
DE92-015916 ..... p 3600 N92-31186 #
DE92-015963 ..... p 3721 N92-31187 #
DE92-015977 ..... p 3709 N92-30891 #
DE92-015985 ..... p 3672 N92-31188 #
DE92-015991 ..... p 3696 N92-30892 #
DE92-016000 ..... p 3707 N92-31189 #
DE92-016002 ..... p 3719 N92-31219 #
DE92-016192 ..... p 3730 N92-31190 #
DE92-016206 ..... p 3731 N92-31220 #
DE92-016231 ..... p 3600 N92-31177 #
DE92-622374 ..... p 3716 N92-30796 #
DE92-622375 ..... p 3731 N92-30799 #
DE92-622376 ..... p 3731 N92-30800 #
DE92-622377 ..... p 3711 N92-30801 #
DE92-624560 ..... p 3712 N92-30331 #
DE92-624639 ..... p 3711 N92-30236 #
DE92-626843 ..... p 3602 N92-30402 #
DE92-627288 ..... p 3713 N92-30403 #
DE92-627317 ..... p 3713 N92-30404 #
DE92-627497 ..... p 3727 N92-30405 #
DE92-630231 ..... p 3732 N92-31133 #
DE92-630235 ..... p 3706 N92-31134 #
DE92-630236 ..... p 3707 N92-31135 #
DE92-630239 ..... p 3732 N92-31136 #
DE92-630241 ..... p 3732 N92-31145 #
DE92-630566 ..... p 3732 N92-31203 #
DE92-630567 ..... p 3730 N92-31191 #
DE92-782044 ..... p 3600 N92-31163 #
DE92-799107 ..... p 3725 N92-30992 #
DE92-799109 ..... p 3725 N92-30991 #

DLR-FB-90-31 ..... p 3667 N92-30515 #

DOE/ER-13261/6 ..... p 3683 N92-30829 #
DOE/ER-13403/4 ..... p 3593 N92-30344 #
DOE/ER-13484/4 ..... p 3661 N92-30693 #
DOE/ER-13506/37 ..... p 3670 N92-30694 #
DOE/ER-13590/10 ..... p 3672 N92-30345 #
DOE/ER-13791/37 ..... p 3683 N92-30368 #
DOE/ER-13859/31 ..... p 3604 N92-30695 #
DOE/ER-40427/14-N92 ..... p 3714 N92-30611 #
DOE/ER-40427/37-N91 ..... p 3743 N92-31199 #
DOE/ER-40577/2 ..... p 3714 N92-30610 #
DOE/ER-40637/4 ..... p 3714 N92-30606 #
DOE/ER-40661/2 ..... p 3716 N92-30841 #
DOE/ER-40677/1-PT-1 ..... p 3716 N92-30791 #
DOE/ER-40677/1-PT-2 ..... p 3715 N92-30625 #
DOE/ER-45147/7 ..... p 3626 N92-30901 #
DOE/ER-45174/T4 ..... p 3597 N92-30586 #
DOE/ER-45280/T4 ..... p 3598 N92-30787 #
DOE/ER-45373/4 ..... p 3710 N92-31131 #
DOE/ER-45413/2 ..... p 3600 N92-31186 #
DOE/ER-53198/197 ..... p 3723 N92-30612 #
DOE/ER-53207/7 ..... p 3725 N92-30900 #
DOE/ER-53263/22 ..... p 3726 N92-31116 #
DOE/ER-54091/1 ..... p 3723 N92-30746 #
DOE/ER-60982/2 ..... p 3682 N92-30861 #
DOE/ER-61012/2 ..... p 3674 N92-30707 #
DOE/ER-61205/1 ..... p 3675 N92-31183 #

DOE/ET-53088/541 ..... p 3724 N92-30833 #
DOE/ET-53088/544 ..... p 3725 N92-30884 #
DOE/ET-53088/550 ..... p 3724 N92-30880 #

DOE/FE-0260P ..... p 3672 N92-31188 #

DOE/ID-13074/T3 ..... p 3626 N92-30842 #

DOE/METC-C/92/7014 ..... p 3671 N92-31113 #

DOE/METC-92-0276 ..... p 3672 N92-31221 #

DOE/NBM-92001277 ..... p 3596 N92-30883 #

DOE/PC-79812/T2 ..... p 3596 N92-31006 #
DOE/PC-89786/T12 ..... p 3608 N92-30904 #
DOE/PC-90185/T4 ..... p 3629 N92-30438 #
DOE/PC-90291/T5 ..... p 3594 N92-30717 #

DOE/SF-15799/T14 ..... p 3671 N92-31117 #

DOT/FAA/AM-92/19 ..... p 3685 N92-30745 #
DOT/FAA/AM-92/20 ..... p 3578 N92-30551 #

DOT/FAA/CT-TN90/64 ..... p 3622 N92-31212 #
DOT/FAA/CT-TN91/40 ..... p 3585 N92-30976 #
DOT/FAA/CT-TN92/14 ..... p 3687 N92-30488 #
DOT/FAA/CT-TN92/1 ..... p 3580 N92-31165 #

DOT/FAA/CT-92/5 ..... p 3581 N92-30303 #

DOT/FAA/NR-92/8,II ..... p 3678 N92-30496 #
DOT/FAA/NR-92/8,I ..... p 3678 N92-30495 #

DOT/FAA/RD-92/12 ..... p 3578 N92-30980 #

DOT/FAA/SE-92/3 ..... p 3579 N92-31211 #

DPG-FR-91-713 ..... p 3678 N92-30340 #

DREA-TM-92/209 ..... p 3663 N92-30870 #

DREO-TN-91-35 ..... p 3624 N92-30683 #

D308/TN/001 ..... p 3586 N92-30715

E-5808 ..... p 3577 N92-30395 * #
E-6096 ..... p 3585 N92-30307 * #
E-6531 ..... p 3658 N92-30396 * #
E-6571 ..... p 3592 N92-30779 * #
E-6824 ..... p 3660 N92-30722 * #
E-6882 ..... p 3659 N92-30571 * #
E-7000 ..... p 3587 N92-30383 * #
E-7007 ..... p 3593 N92-30986 * #
E-7016-1 ..... p 3741 N92-30302 * #
E-7018 ..... p 3588 N92-30301 * #
E-7041 ..... p 3636 N92-30894 * #
E-7042 ..... p 3613 N92-30692 * #
E-7061 ..... p 3583 N92-31172 * #
E-7064 ..... p 3584 N92-30508 * #
E-7080 ..... p 3627 N92-30297 * #
E-7091 ..... p 3660 N92-30734 * #
E-7115 ..... p 3660 N92-30948 * #
E-7119 ..... p 3732 N92-30908 * #
E-7166 ..... p 3670 N92-30426 * #
E-7202 ..... p 3586 N92-30310 * #
E-7203 ..... p 3588 N92-30308 * #
E-7204 ..... p 3623 N92-30427 * #
E-7221 ..... p 3623 N92-30397 * #
E-7226 ..... p 3582 N92-30972 * #
E-7235 ..... p 3709 N92-30898 * #
E-7245 ..... p 3582 N92-30998 * #

EGG-FSP-10017 ..... p 3598 N92-30834 #

EGG-ME-9968 ..... p 3661 N92-30763 #

EOARD-TR-92-07 ..... p 3598 N92-30872 #

EPA/450/2-91/009 ..... p 3673 N92-30561 #
EPA/600/A-92/107 ..... p 3707 N92-30562 #
EPA/600/R-92/029 ..... p 3673 N92-30602 #

ERP-1089 ..... p 3720 N92-30343 #

ESA-TT-1166 ..... p 3694 N92-30512 #
ESA-TT-1228 ..... p 3597 N92-30513 #
ESA-TT-1234 ..... p 3657 N92-30997 #
ESA-TT-1235 ..... p 3575 N92-30514 #
ESA-TT-1253 ..... p 3667 N92-30515 #

ESD-TR-91-174 ..... p 3616 N92-30762 #
ESD-TR-91-176 ..... p 3616 N92-30863 #
ESD-TR-944 ..... p 3616 N92-30761 #

ETN-92-91472 ..... p 3694 N92-30493 #
ETN-92-91473 ..... p 3704 N92-30473 #
ETN-92-91525 ..... p 3578 N92-30474 #
ETN-92-91526 ..... p 3667 N92-30475 #
ETN-92-91528 ..... p 3693 N92-30476 #
ETN-92-91529 ..... p 3658 N92-30477 #
ETN-92-91552 ..... p 3692 N92-30428 #
ETN-92-91553 ..... p 3699 N92-30696 #
ETN-92-91613 ..... p 3590 N92-30414 #
ETN-92-91614 ..... p 3713 N92-30415 #
ETN-92-91615 ..... p 3715 N92-30687 #
ETN-92-91619 ..... p 3637 N92-30688 #
ETN-92-91620 ..... p 3713 N92-30364 #
ETN-92-91621 ..... p 3636 N92-30365 #
ETN-92-91622 ..... p 3715 N92-30697 #
ETN-92-91637 ..... p 3690 N92-30698 #
ETN-92-91638 ..... p 3708 N92-30699 #
ETN-92-91640 ..... p 3705 N92-30689 #
ETN-92-91661 ..... p 3706 N92-30700 #
ETN-92-91662 ..... p 3693 N92-30429 #
ETN-92-91666 ..... p 3690 N92-30701 #
ETN-92-91668 ..... p 3625 N92-30702 #
ETN-92-91669 ..... p 3711 N92-30966 #
ETN-92-91686 ..... p 3623 N92-30503 #
ETN-92-91687 ..... p 3720 N92-30504 #
ETN-92-91688 ..... p 3727 N92-30505 #
ETN-92-91689 ..... p 3740 N92-30506 #
ETN-92-91704 ..... p 3575 N92-30713 #
ETN-92-91705 ..... p 3744 N92-30996
ETN-92-91706 ..... p 3739 N92-30714 #
ETN-92-91707 ..... p 3694 N92-30512 #
ETN-92-91708 ..... p 3597 N92-30513 #
ETN-92-91709 ..... p 3575 N92-30514 #
ETN-92-91710 ..... p 3667 N92-30515 #
ETN-92-91713 ..... p 3720 N92-30507 #
ETN-92-91716 ..... p 3586 N92-30715
ETN-92-91717 ..... p 3697 N92-30950 #
ETN-92-91719 ..... p 3715 N92-30750 #
ETN-92-91730 ..... p 3669 N92-30968
ETN-92-91740 ..... p 3718 N92-30725 #
ETN-92-91742 ..... p 3625 N92-30729 #
ETN-92-91746 ..... p 3657 N92-30997 #
ETN-92-91782 ..... p 3689 N92-30432 #
ETN-92-91783 ..... p 3693 N92-30433 #
ETN-92-91800 ..... p 3694 N92-30478 #
ETN-92-91801 ..... p 3694 N92-30479 #
ETN-92-91802 ..... p 3694 N92-30480 #
ETN-92-91803 ..... p 3707 N92-30481 #
ETN-92-91804 ..... p 3698 N92-30482 #
ETN-92-91805 ..... p 3703 N92-30458 #
ETN-92-91806 ..... p 3703 N92-30447 #
ETN-92-91807 ..... p 3693 N92-30443 #
ETN-92-91808 ..... p 3693 N92-30444 #
ETN-92-91809 ..... p 3693 N92-30445 #
ETN-92-91810 ..... p 3703 N92-30446 #
ETN-92-91812 ..... p 3615 N92-30448 #
ETN-92-91813 ..... p 3703 N92-30449 #
ETN-92-91815 ..... p 3703 N92-30450 #
ETN-92-91816 ..... p 3701 N92-30451 #
ETN-92-91817 ..... p 3707 N92-30452 #
ETN-92-91818 ..... p 3629 N92-30453 #
ETN-92-91819 ..... p 3702 N92-30371 #
ETN-92-91820 ..... p 3628 N92-30372 #
ETN-92-91821 ..... p 3628 N92-30373 #
ETN-92-91822 ..... p 3704 N92-30483 #
ETN-92-91823 ..... p 3629 N92-30454 #
ETN-92-91824 ..... p 3693 N92-30455 #
ETN-92-91825 ..... p 3703 N92-30456 #
ETN-92-91826 ..... p 3703 N92-30457 #
ETN-92-91827 ..... p 3702 N92-30434 #
ETN-92-91828 ..... p 3693 N92-30435 #
ETN-92-91829 ..... p 3702 N92-30436 #
ETN-92-91830 ..... p 3703 N92-30437 #
ETN-92-91836 ..... p 3704 N92-30490 #
ETN-92-91837 ..... p 3704 N92-30491 #
ETN-92-91838 ..... p 3704 N92-30517 #
ETN-92-91839 ..... p 3694 N92-30484 #
ETN-92-91840 ..... p 3694 N92-30492 #
ETN-92-91841 ..... p 3694 N92-30485 #
ETN-92-91842 ..... p 3734 N92-30486 #
ETN-92-91843 ..... p 3734 N92-30487 #
ETN-92-91848 ..... p 3702 N92-30350 #
ETN-92-91849 ..... p 3691 N92-30351 #
ETN-92-91850 ..... p 3691 N92-30352 #
ETN-92-91852 ..... p 3691 N92-30353 #
ETN-92-91853 ..... p 3614 N92-30354 #
ETN-92-91854 ..... p 3707 N92-30355 #
ETN-92-91856 ..... p 3692 N92-30356 #
ETN-92-91857 ..... p 3692 N92-30357 #
ETN-92-91858 ..... p 3628 N92-30358 #
ETN-92-91859 ..... p 3692 N92-30359 #
ETN-92-91860 ..... p 3702 N92-30360 #
ETN-92-91861 ..... p 3703 N92-30459 #
ETN-92-91862 ..... p 3707 N92-30460 #
ETN-92-91864 ..... p 3704 N92-30461 #
ETN-92-91865 ..... p 3629 N92-30462 #
ETN-92-91866 ..... p 3733 N92-30463 #
ETN-92-91867 ..... p 3704 N92-30464 #
ETN-92-91868 ..... p 3666 N92-30465 #
ETN-92-91869 ..... p 3666 N92-30466 #
ETN-92-91871 ..... p 3666 N92-30467 #
ETN-92-91872 ..... p 3666 N92-30468 #
ETN-92-91874 ..... p 3682 N92-30470 #
ETN-92-91875 ..... p 3667 N92-30471 #
ETN-92-91876 ..... p 3667 N92-30472 #
ETN-92-91881 ..... p 3614 N92-30361 #
ETN-92-91884 ..... p 3666 N92-30362 #
ETN-92-91888 ..... p 3583 N92-30439 #
ETN-92-91890 ..... p 3578 N92-30418 #
ETN-92-91892 ..... p 3587 N92-30440 #
ETN-92-91893 ..... p 3613 N92-30441 #
ETN-92-91894 ..... p 3708 N92-30419 #
ETN-92-91895 ..... p 3709 N92-30442 #
ETN-92-91896 ..... p 3709 N92-30420 #
ETN-92-91897 ..... p 3731 N92-30421 #
ETN-92-91898 ..... p 3592 N92-30969 #
ETN-92-91899 ..... p 3671 N92-30970 #
ETN-92-91900 ..... p 3594 N92-30422 #
ETN-92-91901 ..... p 3662 N92-30423 #
ETN-92-91902 ..... p 3579 N92-30424 #
ETN-92-91904 ..... p 3591 N92-30690 #
ETN-92-91905 ..... p 3634 N92-30674 #
ETN-92-91906 ..... p 3573 N92-30675 #
ETN-92-91907 ..... p 3575 N92-30676 #

FAA/APO-210 ..... p 3585 N92-30777 #
FAA/APO-91-4 ..... p 3585 N92-30777 #

FFA-TN-1990-20 ..... p 3575 N92-30713 #

FIA-91-06 ..... p 3701 N92-30710 * #

FNAL-TM-1773 ..... p 3699 N92-30812 #

FNAL/C-92/106 ..... p 3717 N92-30589 #
FNAL/C-92/129-E ..... p 3719 N92-31219 #
FNAL/C-92/63 ..... p 3743 N92-30828 #
FNAL/C-92/88-A ..... p 3740 N92-30622 #

GAO/IMTEC-92-45 ..... p 3690 N92-30712 #

GETA-91-10 ..... p 3659 N92-30601 #

GIT-E-19-673 ..... p 3592 N92-30871 #

GPO-57-805 ..... p 3735 N92-31169 #

GRI-91/0362 ..... p 3659 N92-30601 #

H-1795 ..... p 3580 N92-31208 * #
H-1842 ..... p 3581 N92-30518 * #

HDL-TM-92-5 ..... p 3730 N92-30895 #

IA-1452 ..... p 3721 N92-30581

IC-91/329 ..... p 3732 N92-31136 #
IC-91/330 ..... p 3732 N92-31203 #
IC-91/340 ..... p 3732 N92-31133 #
IC-91/360 ..... p 3732 N92-31145 #
IC-91/367 ..... p 3716 N92-30798 #
IC-91/369 ..... p 3731 N92-30799 #
IC-91/370 ..... p 3731 N92-30800 #
IC-91/371 ..... p 3711 N92-30801 #
IC-91/378 ..... p 3730 N92-31191 #
IC-91/398 ..... p 3706 N92-31134 #
IC-91/399 ..... p 3707 N92-31135 #

ICASE-92-22 ..... p 3689 N92-30311 * #
ICASE-92-24 ..... p 3704 N92-30516 * #
ICASE-92-27 ..... p 3706 N92-30716 * #

ICMA-92-171 ..... p 3702 N92-30410 #

IDA-P-2598 ..... p 3615 N92-30532 #

IDA/HQ-91-38244 ..... p 3615 N92-30532 #

IFSR-541 ..... p 3724 N92-30833 #
IFSR-544 ..... p 3725 N92-30884 #
IFSR-550 ..... p 3724 N92-30880 #

IFVE-ONF-91-139 ..... p 3713 N92-30404 #

IHEP-ONF-91-74-PT-1 ..... p 3713 N92-30403 #

IHES/M/92/10 ..... p 3704 N92-30511 #
IHES/M/92/16 ..... p 3706 N92-30789 #
IHES/M/92/9 ..... p 3706 N92-30790 #

ILCEP-WEST MONO-4-REV-1 ..... p 3735 N92-30636 #

IMAG-RR-853-I ..... p 3694 N92-30493 #

IMAG-RR-855-I ..... p 3704 N92-30473 #

IS-M-685 ..... p 3598 N92-30858 #

ISBN-3-921-681-01-4 ..... p 3720 N92-30507 #
ISBN-84-7469-052-8 ..... p 3739 N92-30714 #
ISBN-90-5411-006-6 ..... p 3667 N92-30472 #
ISBN-90-5411-008-2 ..... p 3666 N92-30466 #
ISBN-90-5411-009-0 ..... p 3666 N92-30467 #
ISBN-90-5411-012-0 ..... p 3667 N92-30471 #
ISBN-90-5411-013-9 ..... p 3682 N92-30470 #
ISBN-90-5411-015-5 ..... p 3666 N92-30468 #
ISBN-90-5411-016-3 ..... p 3614 N92-30361 #
ISBN-90-5411-017-1 ..... p 3666 N92-30465 #
ISBN-90-5411-026-0 ..... p 3666 N92-30362 #
ISBN-92-835-0669-3 ..... p 3584 N92-30769 #
ISBN-92-835-0670-7 ..... p 3576 N92-30947 #

ISL-PU-303/90 ..... p 3720 N92-30507 #

ISSN-0208-5658 ..... p 3701 N92-31148 #
ISSN-0208-5658 ..... p 3721 N92-31149 #
ISSN-0800-4412 ..... p 3683 N92-31152 #
ISSN-0924-3755 ..... p 3690 N92-30698 #

ITN-92-85163 ..... p 3715 N92-30780
ITN-92-85164 ..... p 3714 N92-30580
ITN-92-85166 ..... p 3729 N92-30781
ITN-92-85169 ..... p 3715 N92-30782
ITN-92-85170 ..... p 3721 N92-30581
ITN-92-85171 ..... p 3656 N92-30582

ITP-SB-91-34 ..... p 3731 N92-30825 #

ITP-91-12 ..... p 3711 N92-30236 #
ITP-91-25 ..... p 3727 N92-30405 #
ITP-91-8 ..... p 3712 N92-30331 #

JAERI-M-91-189 ..... p 3600 N92-31163 #

JPL-PUBL-91-35 ..... p 3617 N92-30923 * #

JPR-9950-1370 ..... p 3625 N92-30757 * #

JSR-91-310 ..... p 3629 N92-30560 #

KCP-613-4501 ..... p 3598 N92-30865 #
KCP-613-4504 ..... p 3606 N92-30866 #
KCP-613-4664 ..... p 3711 N92-30890 #
KCP-613-4701 ..... p 3624 N92-30590 #
KCP-613-4749 ..... p 3627 N92-31144 #

L-16929 ..... p 3576 N92-30909 * #
L-16951 ..... p 3574 N92-30394 * #
L-16956 ..... p 3583 N92-31175 * #
L-17018 ..... p 3744 N92-30733 * #
L-17026 ..... p 3573 N92-30295 * #
L-17054 ..... p 3576 N92-30747 * #
L-17099 ..... p 3608 N92-30263 * #
L-17126-PT-2 ..... p 3637 N92-31013 * #

LA-UR-92-1231 ..... p 3743 N92-30706 #
LA-UR-92-1238 ..... p 3740 N92-30705 #
LA-UR-92-1262 ..... p 3667 N92-30704 #
LA-UR-92-1289 ..... p 3615 N92-30703 #
LA-UR-92-1476 ..... p 3608 N92-31202 #
LA-UR-92-1478 ..... p 3717 N92-31201 #
LA-UR-92-1485 ..... p 3730 N92-31200 #
LA-UR-92-1508 ..... p 3740 N92-30609 #
LA-UR-92-1539 ..... p 3657 N92-31182 #
LA-UR-92-1545 ..... p 3743 N92-30627 #
LA-UR-92-1558 ..... p 3606 N92-30847 #
LA-UR-92-1610 ..... p 3740 N92-30578 #
LA-UR-92-1674 ..... p 3589 N92-31204 #
LA-UR-92-808 ..... p 3673 N92-30520 #
LA-UR-92-875 ..... p 3724 N92-30806 #
LA-UR-92-879 ..... p 3741 N92-31108 #
LA-UR-92-896 ..... p 3657 N92-30805 #
LA-UR-92-897 ..... p 3730 N92-31217 #
LA-UR-92-898 ..... p 3590 N92-30521 #
LA-UR-92-922 ..... p 3627 N92-31107 #
LA-UR-92-949 ..... p 3677 N92-31008 #
LA-UR-92-980 ..... p 3740 N92-30856 #

LA-12286-MS ..... p 3708 N92-31185 #
LA-12302-MS ..... p 3709 N92-30891 #

LBL-31382 ..... p 3731 N92-30825 #
LBL-31596 ..... p 3626 N92-30813 #
LBL-32121 ..... p 3719 N92-31198 #

LINO-1991-5 ..... p 3718 N92-30725 #

LPI-CONTRIB-781 ..... p 3736 N92-31222 * #

LRC-92-32 ..... p 3726 N92-31116 #

MBB-UD-0608-91-PUB ..... p 3583 N92-30439 #
MBB-UD-0611-91-PUB ..... p 3578 N92-30418 #

MBB-UO-0164-91-PUB ..... p 3587 N92-30440 #
MBB-UO-0165-91-PUB ..... p 3613 N92-30441 #
MBB-UO-0166-91-PUB ..... p 3708 N92-30419 #
MBB-UO-0167-91-PUB ..... p 3709 N92-30442 #
MBB-UO-0168-91-PUB ..... p 3709 N92-30420 #
MBB-UO-0169-91-PUB ..... p 3731 N92-30421 #

MBB-Z-0409-91-PUB ..... p 3592 N92-30969 #
MBB-Z-0412-91-PUB ..... p 3671 N92-30970 #
MBB-Z-0413-91-PUB ..... p 3594 N92-30422 #

MBB/FE202/S/PUB/477 ..... p 3591 N92-30690 #
MBB/FE211/S/PUB/466 ..... p 3634 N92-30674 #
MBB/FE211/S/PUB/474 ..... p 3573 N92-30675 #
MBB/FE213/S/PUB/459 ..... p 3575 N92-30676 #

MBB/FW321/S/PUB/467 ..... p 3662 N92-30423 #
MBB/FW321/S/PUB/476 ..... p 3579 N92-30424 #

MC-PY-92-011 ..... p 3613 N92-30754 * #

MCAT-92-009 ..... p 3575 N92-30740 * #

MDC-91K0792 ..... p 3579 N92-30978 * #

MD92-08-1B-GC-JED ..... p 3701 N92-30339 #

MEMO-COSOR-92-04 ..... p 3694 N92-30478 #

MEMO-INF-91-86 ..... p 3690 N92-30698 #
MEMO-INF-92-08 ..... p 3689 N92-30432 #
MEMO-INF-92-09 ..... p 3693 N92-30433 #

MIT-TR-916-VOL-3 ..... p 3616 N92-30863 #

MITT-11 ..... p 3740 N92-30506 #

MLM-3748 ..... p 3705 N92-30566 #

MRL-TN-600 ..... p 3664 N92-30963

MTL-TR-92-15 ..... p 3604 N92-30758 #
MTL-TR-92-17 ..... p 3597 N92-30759 #
MTL-TR-92-2 ..... p 3599 N92-31110 #

MTR-11277 ..... p 3621 N92-31130 #

MU-TR-92-06 ..... p 3701 N92-30339 #

N-3283-AF/NASA ..... p 3587 N92-30958 #

NADC-91078-60 ..... p 3607 N92-30321 #

NAS 1.15:103587 ..... p 3688 N92-30381 * #
NAS 1.15:103591 ..... p 3662 N92-30416 * #
NAS 1.15:103592 ..... p 3683 N92-30305 * #
NAS 1.15:103594 ..... p 3612 N92-30971 * #
NAS 1.15:103595 ..... p 3627 N92-30902 * #
NAS 1.15:103874 ..... p 3686 N92-31167 * #
NAS 1.15:103888 ..... p 3689 N92-31166 * #
NAS 1.15:103909 ..... p 3635 N92-30765 * #
NAS 1.15:103935 ..... p 3636 N92-30982 * #
NAS 1.15:104159 ..... p 3664 N92-30964 * #
NAS 1.15:104252 ..... p 3581 N92-30518 * #
NAS 1.15:105244 ..... p 3592 N92-30779 * #
NAS 1.15:105415 ..... p 3660 N92-30722 * #
NAS 1.15:105521 ..... p 3589 N92-30818 * #
NAS 1.15:105558 ..... p 3659 N92-30571 * #
NAS 1.15:105645 ..... p 3587 N92-30383 * #
NAS 1.15:105648 ..... p 3593 N92-30986 * #
NAS 1.15:105652 ..... p 3588 N92-30301 * #
NAS 1.15:105673 ..... p 3613 N92-30692 * #
NAS 1.15:105682 ..... p 3583 N92-31172 * #
NAS 1.15:105685 ..... p 3584 N92-30508 * #
NAS 1.15:105693 ..... p 3627 N92-30297 * #
NAS 1.15:105718 ..... p 3660 N92-30948 * #
NAS 1.15:105730 ..... p 3660 N92-30734 * #
NAS 1.15:105755 ..... p 3670 N92-30426 * #
NAS 1.15:105774 ..... p 3586 N92-30310 * #
NAS 1.15:105775 ..... p 3588 N92-30308 * #
NAS 1.15:105777 ..... p 3623 N92-30427 * #
NAS 1.15:105791 ..... p 3623 N92-30397 * #
NAS 1.15:105796 ..... p 3582 N92-30972 * #
NAS 1.15:105805 ..... p 3709 N92-30898 * #
NAS 1.15:105814 ..... p 3582 N92-30998 * #
NAS 1.15:107543 ..... p 3673 N92-30494 * #
NAS 1.15:107545 ..... p 3586 N92-30382 * #
NAS 1.15:107577 ..... p 3588 N92-30736 * #
NAS 1.15:107580 ..... p 3586 N92-31160 * #
NAS 1.15:107619 ..... p 3665 N92-31215 * #
NAS 1.15:107620 ..... p 3664 N92-31214 * #
NAS 1.15:107627 ..... p 3711 N92-30979 * #
NAS 1.15:107630 ..... p 3679 N92-30735 * #
NAS 1.15:107631 ..... p 3575 N92-30570 * #
NAS 1.15:107634 ..... p 3699 N92-30677 * #
NAS 1.15:107642 ..... p 3664 N92-31155 * #
NAS 1.15:107643 ..... p 3574 N92-30393 * #
NAS 1.15:107645 ..... p 3575 N92-30691 * #
NAS 1.15:107648 ..... p 3637 N92-30737 * #
NAS 1.15:107651 ..... p 3580 N92-30752 * #
NAS 1.15:107653 ..... p 3580 N92-31174 * #
NAS 1.15:107663 ..... p 3689 N92-30907 * #
NAS 1.15:107811 ..... p 3733 N92-30959 * #
NAS 1.15:107910 ..... p 3701 N92-30710 * #
NAS 1.15:107962 ..... p 3739 N92-30686 * #
NAS 1.15:3238 ..... p 3577 N92-30395 * #
NAS 1.15:4302 ..... p 3583 N92-31175 * #
NAS 1.15:4331 ..... p 3744 N92-30733 * #
NAS 1.21:7011(363) ..... p 3685 N92-30987 *
NAS 1.26:184319 ..... p 3613 N92-30754 * #
NAS 1.26:184344 ..... p 3591 N92-30711 * #
NAS 1.26:184356 ..... p 3596 N92-31161 * #
NAS 1.26:186020 ..... p 3580 N92-31208 * #
NAS 1.26:189087 ..... p 3582 N92-31164 * #
NAS 1.26:189149 ..... p 3574 N92-30298 * #
NAS 1.26:189155 ..... p 3581 N92-30569 * #
NAS 1.26:189177 ..... p 3636 N92-30894 * #
NAS 1.26:189187 ..... p 3732 N92-30908 * #
NAS 1.26:189210 ..... p 3614 N92-30300 * #
NAS 1.26:189215 ..... p 3672 N92-31216 * #
NAS 1.26:189475 ..... p 3630 N92-30648 * #
NAS 1.26:189620 ..... p 3579 N92-30304 * #
NAS 1.26:189649 ..... p 3700 N92-31158 * #
NAS 1.26:189650 ..... p 3581 N92-30965 * #
NAS 1.26:189658 ..... p 3574 N92-30392 * #
NAS 1.26:189660 ..... p 3689 N92-30489 * #
NAS 1.26:189664 ..... p 3689 N92-30311 * #
NAS 1.26:189665 ..... p 3704 N92-30516 * #
NAS 1.26:189668 ..... p 3706 N92-30716 * #
NAS 1.26:189827 ..... p 3691 N92-30299 * #
NAS 1.26:190045 ..... p 3575 N92-30740 * #
NAS 1.26:190055 ..... p 3671 N92-30949 * #
NAS 1.26:190178 ..... p 3736 N92-31222 * #
NAS 1.26:190182 ..... p 3576 N92-30977 * #
NAS 1.26:190243 ..... p 3660 N92-30738 * #
NAS 1.26:190266 ..... p 3682 N92-30739 * #
NAS 1.26:190290 ..... p 3582 N92-30753 * #
NAS 1.26:190317 ..... p 3587 N92-30709 * #
NAS 1.26:190345 ..... p 3587 N92-30958 #
NAS 1.26:190429 ..... p 3687 N92-30488 #
NAS 1.26:190459 ..... p 3617 N92-30923 * #
NAS 1.26:190471 ..... p 3664 N92-30988 * #
NAS 1.26:190473 ..... p 3625 N92-30757 * #
NAS 1.26:190476 ..... p 3692 N92-30379 * #
NAS 1.26:190478 ..... p 3676 N92-30756 * #
NAS 1.26:190485 ..... p 3676 N92-30961 * #
NAS 1.26:190489 ..... p 3698 N92-30960 * #
NAS 1.26:190492 ..... p 3721 N92-30975 * #
NAS 1.26:190498 ..... p 3628 N92-30380 * #
NAS 1.26:190515 ..... p 3589 N92-30981 * #
NAS 1.26:190519 ..... p 3733 N92-30974 * #
NAS 1.26:190522 ..... p 3743 N92-31168 * #
NAS 1.26:190530 ..... p 3701 N92-30778 * #
NAS 1.26:190546 ..... p 3691 N92-30296 * #
NAS 1.26:190553 ..... p 3690 N92-30724 * #
NAS 1.26:190559 ..... p 3696 N92-30723 * #
NAS 1.26:190560 ..... p 3677 N92-30962 * #
NAS 1.26:190569 ..... p 3589 N92-30989 * #
NAS 1.26:190605 ..... p 3742 N92-30921 * #
NAS 1.26:190624 ..... p 3674 N92-31153 * #
NAS 1.26:190646 ..... p 3698 N92-31154 * #
NAS 1.26:190649 ..... p 3577 N92-31157 * #
NAS 1.26:190650 ..... p 3621 N92-31156 * #
NAS 1.26:190658 ..... p 3592 N92-30908 * #
NAS 1.26:190664 ..... p 3742 N92-31162 * #
NAS 1.26:190667 ..... p 3583 N92-30922 * #
NAS 1.26:4450 ..... p 3579 N92-30978 * #
NAS 1.26:4451 ..... p 3686 N92-30306 * #
NAS 1.26:4460 ..... p 3661 N92-30309 * #
NAS 1.26:4462 ..... p 3635 N92-30751 * #
NAS 1.55:10093 ..... p 3741 N92-30302 * #
NAS 1.55:3151 ..... p 3608 N92-30263 * #
NAS 1.55:3158-PT-2 ..... p 3637 N92-31013 * #
NAS 1.60:3186 ..... p 3576 N92-30909 * #
NAS 1.60:3205 ..... p 3573 N92-30295 * #
NAS 1.60:3216 ..... p 3612 N92-30378 * #
NAS 1.60:3232 ..... p 3576 N92-30747 * #
NAS 1.60:3233 ..... p 3574 N92-30394 * #
NAS 1.60:3265 ..... p 3658 N92-30396 * #
NAS 1.61:1280 ..... p 3585 N92-30307 * #
NAS 1.71:LAR-13950-1 ..... p 3690 N92-30541 * #
NAS 1.71:LAR-14568-1 ..... p 3720 N92-30312 * #
NAS 1.71:LAR-14651-1 ..... p 3734 N92-30386 * #
NAS 1.71:LAR-14654-1 ..... p 3662 N92-30317 * #
NAS 1.71:LAR-14682-1 ..... p 3628 N92-30387 * #
NAS 1.71:LAR-14753-1 ..... p 3601 N92-30313 * #
NAS 1.71:LAR-14789-1 ..... p 3658 N92-30388 * #
NAS 1.71:LAR-14811-1 ..... p 3622 N92-30389 * #
NAS 1.71:LAR-14824-1-SB ..... p 3628 N92-30390 * #

NAS 1.71:MSC-21723-1 ..... p 3588 N92-30315 * #
NAS 1.71:MSC-21874-1 ..... p 3700 N92-30314 * #
NAS 1.71:MSC-21884-1 ..... p 3602 N92-30539 * #
NAS 1.71:MSC-21918-1 ..... p 3658 N92-30316 * #
NAS 1.71:MSC-21940-1 ..... p 3659 N92-30540 * #
NAS 1.71:NPO-18062-1-CU ..... p 3623 N92-30542 * #
NAS 1.71:NPO-18435-1-CU ..... p 3695 N92-30543 * #
NAS 1.71:NPO-18701-1-CU ..... p 3614 N92-30391 * #

NASA-CASE-LAR-13950-1 ..... p 3690 N92-30541 * #
NASA-CASE-LAR-14568-1 ..... p 3720 N92-30312 * #
NASA-CASE-LAR-14651-1 ..... p 3734 N92-30386 * #
NASA-CASE-LAR-14654-1 ..... p 3662 N92-30317 * #
NASA-CASE-LAR-14679-2 ..... p 3621 N92-31150 * #
NASA-CASE-LAR-14682-1 ..... p 3628 N92-30387 * #
NASA-CASE-LAR-14753-1 ..... p 3601 N92-30313 * #
NASA-CASE-LAR-14789-1 ..... p 3658 N92-30388 * #
NASA-CASE-LAR-14811-1 ..... p 3622 N92-30389 * #
NASA-CASE-LAR-14824-1-SB ..... p 3628 N92-30390 * #

NASA-CASE-MSC-21723-1 ..... p 3588 N92-30315 * #
NASA-CASE-MSC-21874-1 ..... p 3700 N92-30314 * #
NASA-CASE-MSC-21884-1 ..... p 3602 N92-30539 * #
NASA-CASE-MSC-21918-1 ..... p 3658 N92-30316 * #
NASA-CASE-MSC-21940-1 ..... p 3659 N92-30540 * #

NASA-CASE-NPO-18062-1-CU ..... p 3623 N92-30542 * #
NASA-CASE-NPO-18435-1-CU ..... p 3695 N92-30543 * #
NASA-CASE-NPO-18701-1-CU ..... p 3614 N92-30391 * #

NASA-CP-10093 ..... p 3741 N92-30302 * #
NASA-CP-3151 ..... p 3608 N92-30263 * #
NASA-CP-3158-PT-2 ..... p 3637 N92-31013 * #

NASA-CR-184319 ..... p 3613 N92-30754 * #
NASA-CR-184344 ..... p 3591 N92-30711 * #
NASA-CR-184356 ..... p 3596 N92-31161 * #
NASA-CR-186020 ..... p 3580 N92-31208 * #
NASA-CR-189087 ..... p 3582 N92-31164 * #
NASA-CR-189149 ..... p 3574 N92-30298 * #
NASA-CR-189155 ..... p 3581 N92-30569 * #
NASA-CR-189177 ..... p 3636 N92-30894 * #
NASA-CR-189187 ..... p 3732 N92-30908 * #
NASA-CR-189210 ..... p 3614 N92-30300 * #
NASA-CR-189215 ..... p 3672 N92-31216 * #
NASA-CR-189475 ..... p 3630 N92-30648 * #
NASA-CR-189620 ..... p 3579 N92-30304 * #
NASA-CR-189649 ..... p 3700 N92-31158 * #
NASA-CR-189650 ..... p 3581 N92-30965 * #
NASA-CR-189656 ..... p 3574 N92-30392 * #
NASA-CR-189660 ..... p 3689 N92-30489 * #
NASA-CR-189664 ..... p 3689 N92-30311 * #
NASA-CR-189665 ..... p 3704 N92-30516 * #
NASA-CR-189668 ..... p 3706 N92-30716 * #
NASA-CR-189827 ..... p 3691 N92-30299 * #
NASA-CR-190045 ..... p 3575 N92-30740 * #
NASA-CR-190055 ..... p 3671 N92-30949 * #
NASA-CR-190178 ..... p 3736 N92-31222 * #
NASA-CR-190182 ..... p 3576 N92-30977 * #
NASA-CR-190243 ..... p 3660 N92-30738 * #
NASA-CR-190266 ..... p 3682 N92-30739 * #
NASA-CR-190290 ..... p 3582 N92-30753 * #
NASA-CR-190317 ..... p 3587 N92-30709 * #
NASA-CR-190345 ..... p 3587 N92-30958 * #
NASA-CR-190429 ..... p 3687 N92-30488 #
NASA-CR-190459 ..... p 3617 N92-30923 * #
NASA-CR-190471 ..... p 3664 N92-30988 * #
NASA-CR-190473 ..... p 3625 N92-30757 * #
NASA-CR-190476 ..... p 3692 N92-30379 * #
NASA-CR-190478 ..... p 3676 N92-30756 * #
NASA-CR-190485 ..... p 3676 N92-30961 * #
NASA-CR-190489 ..... p 3698 N92-30960 * #
NASA-CR-190492 ..... p 3721 N92-30975 * #
NASA-CR-190498 ..... p 3628 N92-30380 * #
NASA-CR-190515 ..... p 3589 N92-30981 * #
NASA-CR-190519 ..... p 3733 N92-30974 * #
NASA-CR-190522 ..... p 3743 N92-31168 * #
NASA-CR-190530 ..... p 3701 N92-30778 * #
NASA-CR-190546 ..... p 3691 N92-30296 * #
NASA-CR-190553 ..... p 3690 N92-30724 * #
NASA-CR-190559 ..... p 3696 N92-30723 * #
NASA-CR-190560 ..... p 3677 N92-30962 * #
NASA-CR-190569 ..... p 3589 N92-30989 * #
NASA-CR-190605 ..... p 3742 N92-30921 * #
NASA-CR-190624 ..... p 3674 N92-31153 * #
NASA-CR-190646 ..... p 3698 N92-31154 * #
NASA-CR-190649 ..... p 3577 N92-31157 * #
NASA-CR-190650 ..... p 3621 N92-31156 * #
NASA-CR-190658 ..... p 3592 N92-30906 * #
NASA-CR-190664 ..... p 3742 N92-31162 * #
NASA-CR-190667 ..... p 3583 N92-30922 * #
NASA-CR-4450 ..... p 3579 N92-30978 * #
NASA-CR-4451 ..... p 3686 N92-30306 * #
NASA-CR-4460 ..... p 3661 N92-30309 * #
NASA-CR-4462 ..... p 3635 N92-30751 * #

NASA-RP-1280 ..... p 3585 N92-30307 * #

NASA-SP-7011(363) ..... p 3685 N92-30987 *

NASA-TM-103587 ..... p 3688 N92-30381 * #
NASA-TM-103591 ..... p 3662 N92-30416 * #
NASA-TM-103592 ..... p 3683 N92-30305 * #
NASA-TM-103594 ..... p 3612 N92-30971 * #
NASA-TM-103595 ..... p 3627 N92-30902 * #
NASA-TM-103874 ..... p 3686 N92-31167 * #
NASA-TM-103888 ..... p 3689 N92-31166 * #
NASA-TM-103909 ..... p 3635 N92-30765 * #
NASA-TM-103935 ..... p 3636 N92-30982 * #
NASA-TM-104159 ..... p 3664 N92-30964 * #
NASA-TM-104252 ..... p 3581 N92-30518 * #
NASA-TM-105244 ..... p 3592 N92-30779 * #
NASA-TM-105415 ..... p 3660 N92-30722 * #
NASA-TM-105521 ..... p 3589 N92-30818 * #
NASA-TM-105558 ..... p 3659 N92-30571 * #
NASA-TM-105645 ..... p 3587 N92-30383 * #
NASA-TM-105648 ..... p 3593 N92-30986 * #
NASA-TM-105652 ..... p 3588 N92-30301 * #
NASA-TM-105673 ..... p 3613 N92-30692 * #
NASA-TM-105682 ..... p 3583 N92-31172 * #
NASA-TM-105685 ..... p 3584 N92-30508 * #
NASA-TM-105693 ..... p 3627 N92-30297 * #
NASA-TM-105718 ..... p 3660 N92-30948 * #
NASA-TM-105730 ..... p 3660 N92-30734 * #
NASA-TM-105755 ..... p 3670 N92-30426 * #
NASA-TM-105774 ..... p 3586 N92-30310 * #
NASA-TM-105775 ..... p 3588 N92-30308 * #
NASA-TM-105777 ..... p 3623 N92-30427 * #
NASA-TM-105791 ..... p 3623 N92-30397 * #
NASA-TM-105796 ..... p 3582 N92-30972 * #
NASA-TM-105805 ..... p 3709 N92-30898 * #
NASA-TM-105814 ..... p 3582 N92-30998 * #
NASA-TM-107543 ..... p 3673 N92-30494 * #
NASA-TM-107545 ..... p 3586 N92-30382 * #
NASA-TM-107577 ..... p 3588 N92-30736 * #
NASA-TM-107580 ..... p 3586 N92-31160 * #
NASA-TM-107619 ..... p 3665 N92-31215 * #
NASA-TM-107620 ..... p 3664 N92-31214 * #
NASA-TM-107627 ..... p 3711 N92-30979 * #
NASA-TM-107630 ..... p 3679 N92-30735 * #
NASA-TM-107631 ..... p 3575 N92-30570 * #
NASA-TM-107634 ..... p 3699 N92-30677 * #
NASA-TM-107642 ..... p 3664 N92-31155 * #
NASA-TM-107643 ..... p 3574 N92-30393 * #
NASA-TM-107645 ..... p 3575 N92-30691 * #
NASA-TM-107648 ..... p 3637 N92-30737 * #
NASA-TM-107651 ..... p 3580 N92-30752 * #
NASA-TM-107653 ..... p 3580 N92-31174 * #
NASA-TM-107663 ..... p 3689 N92-30907 * #
NASA-TM-107811 ..... p 3733 N92-30959 * #
NASA-TM-107910 ..... p 3701 N92-30710 * #
NASA-TM-107962 ..... p 3739 N92-30686 * #
NASA-TM-4302 ..... p 3583 N92-31175 * #
NASA-TM-4331 ..... p 3744 N92-30733 * #

NASA-TP-3186 ..... p 3576 N92-30909 * #
NASA-TP-3205 ..... p 3573 N92-30295 * #
NASA-TP-3216 ..... p 3612 N92-30378 * #
NASA-TP-3232 ..... p 3576 N92-30747 * #
NASA-TP-3233 ..... p 3574 N92-30394 * #
NASA-TP-3238 ..... p 3577 N92-30395 * #
NASA-TP-3265 ..... p 3658 N92-30396 * #

NATICK-TR-92/009 ..... p 3573 N92-30239 #

NAVY-CASE-73056 ..... p 3690 N92-30564 #
NAVY-CASE-73519 ..... p 3722 N92-31213 #
NAVY-CASE-73546 ..... p 3604 N92-30685 #

NDRE/PUBL-92/1001 ..... p 3683 N92-31152 #

NHRC-91-28 ..... p 3684 N92-30603 #
NHRC-91-43 ..... p 3685 N92-30644 #

NIFS-PROC-9 ..... p 3725 N92-30984 #

NIFS-TECH-2 ..... p 3723 N92-30497 #

NIFS-103 ..... p 3710 N92-30983 #
NIFS-105 ..... p 3710 N92-30498 #
NIFS-113 ..... p 3722 N92-30430 #
NIFS-114 ..... p 3723 N92-30499 #
NIFS-115 ..... p 3717 N92-30990 #
NIFS-124 ..... p 3725 N92-30992 #
NIFS-126 ..... p 3725 N92-30991 #
NIFS-129 ..... p 3716 N92-30967 #
NIFS-130 ..... p 3722 N92-30384 #
NIFS-131 ..... p 3725 N92-30985 #
NIFS-134 ..... p 3714 N92-30510 #
NIFS-137 ..... p 3722 N92-30385 #
NIFS-138 ..... p 3725 N92-30993 #
NIFS-139 ..... p 3725 N92-30994 #

NIFS-142 ..... p 3722 N92-30431 #
NIFS-143 ..... p 3726 N92-30995 #
NIFS-149 ..... p 3714 N92-30572 #
NIFS-150 ..... p 3713 N92-30500 #
NIFS-151 ..... p 3714 N92-30501 #
NIFS-152 ..... p 3602 N92-30502 #

NIKHEF-H/91-16 ..... p 3713 N92-30415 #
NIKHEF-H/91-17 ..... p 3715 N92-30687 #
NIKHEF-H/91-21 ..... p 3637 N92-30688 #
NIKHEF-H/91-22 ..... p 3713 N92-30364 #
NIKHEF-H/91-23 ..... p 3636 N92-30365 #
NIKHEF-H/91-24 ..... p 3715 N92-30697 #

NISTIR-4627 ..... p 3604 N92-30788 #
NISTIR-4831 ..... p 3695 N92-30579 #

NLR-TP-89284-U ..... p 3578 N92-30474 #
NLR-TP-89294-U ..... p 3667 N92-30475 #
NLR-TP-89327-U ..... p 3693 N92-30476 #
NLR-TP-89364-U ..... p 3658 N92-30477 #

NMAB-461 ..... p 3612 N92-30411 #

NOARL-TN-231 ..... p 3667 N92-30545 #

NRAD-TD-2259 ..... p 3616 N92-30721 #

NREL/TP-253-4278 ..... p 3596 N92-30882 #
NREL/TP-253-4280 ..... p 3670 N92-30330 #
NREL/TP-253-4282 ..... p 3596 N92-30879 #
NREL/TP-412-4796 ..... p 3670 N92-30519 #
NREL/TP-413-4906 ..... p 3727 N92-30247 #
NREL/TP-441-4800 ..... p 3671 N92-30896 #
NREL/TP-442-4822 ..... p 3670 N92-30837 #
NREL/TP-451-4751 ..... p 3729 N92-30748 #
NREL/TP-463-4856 ..... p 3743 N92-31206 #

NRL/FR/6521-92-9392 ..... p 3701 N92-30243 #

NRL/MR/1003-92-6989 ..... p 3626 N92-30851 #
NRL/MR/4400-92-6979 ..... p 3635 N92-30775 #
NRL/MR/4440-92-6786 ..... p 3656 N92-30614 #
NRL/MR/4440-92-6964 ..... p 3688 N92-30615 #
NRL/MR/4440-92-6967 ..... p 3706 N92-30776 #
NRL/MR/4440-92-6978 ..... p 3615 N92-30637 #
NRL/MR/4790-92-6949 ..... p 3723 N92-30620 #
NRL/MR/4790-92-6954 ..... p 3656 N92-30743 #
NRL/MR/4790-92-6984 ..... p 3614 N92-30407 #

NSF-90-97 ..... p 3676 N92-30708 #

NSWCDD/TR-92/181 ..... p 3636 N92-30530 #

NTSB/AAR-90/01 ..... p 3578 N92-31159 #
NTSB/AAR-92/02 ..... p 3578 N92-31159 #

NUWC-NPT-TD-10012 ..... p 3679 N92-31003 #

OITS-474 ..... p 3714 N92-30606 #

ONERA-NT-1988-9 ..... p 3694 N92-30512 #
ONERA-NT-1989-7 ..... p 3597 N92-30513 #
ONERA-NT-1990-5 ..... p 3657 N92-30997 #
ONERA-NT-1990-8 ..... p 3575 N92-30514 #

ONERA-RF-17/3641-PY ..... p 3711 N92-30966 #

ORNL/SUB-88-07685/02 ..... p 3599 N92-30888 #

ORNL/TM-12081 ..... p 3672 N92-31176 #

ORNL/TR-92/17 ..... p 3717 N92-31205 #

OSR-9008 ..... p 3675 N92-30525 #

OSU-ECE-NASA-92-02 ..... p 3583 N92-30922 * #

PB92-160530 ..... p 3689 N92-30600 #
PB92-164466 ..... p 3659 N92-30601 #
PB92-166933 ..... p 3673 N92-30602 #
PB92-171966 ..... p 3673 N92-30561 #
PB92-173020 ..... p 3734 N92-30509 #
PB92-177997 ..... p 3706 N92-30789 #
PB92-178003 ..... p 3708 N92-30790 #
PB92-178276 ..... p 3704 N92-30511 #
PB92-180264 ..... p 3707 N92-30562 #
PB92-180652 ..... p 3598 N92-30785 #
PB92-181080 ..... p 3604 N92-30788 #
PB92-187012 ..... p 3673 N92-30563 #
PB92-187137 ..... p 3695 N92-30579 #
PB92-910402 ..... p 3578 N92-31159 #

PC-86-08 ..... p 3580 N92-30878 #

PL-TR-91-2135 ..... p 3678 N92-30262 #

PL-TR-91-2139 ..... p 3720 N92-30343 #
PL-TR-91-2194 ..... p 3588 N92-30628 #
PL-TR-92-2099 ..... p 3676 N92-30720 #

PNL-SA-19683 ..... p 3599 N92-30877 #
PNL-SA-19807 ..... p 3735 N92-31001 #
PNL-SA-20194 ..... p 3685 N92-31011 #
PNL-SA-20246 ..... p 3732 N92-30349 #
PNL-SA-20305 ..... p 3599 N92-31010 #
PNL-SA-20399 ..... p 3672 N92-30374 #

PWA-6354 ..... p 3574 N92-30298 * #

QUEST-TR-534 ..... p 3581 N92-30569 * #

R/D-6571-AN-01 ..... p 3663 N92-30766 #

RAL-91-090 ..... p 3715 N92-30750 #

RAND-P-7747-RGS ..... p 3616 N92-30755 #

RAY/RD/S-4752 ..... p 3626 N92-30836 #

REPT-1-52150 ..... p 3706 N92-31128 #
REPT-18 ..... p 3602 N92-30409 #
REPT-240-746 ..... p 3672 N92-31216 * #
REPT-524-679 ..... p 3598 N92-30872 #
REPT-91-100 ..... p 3691 N92-30352 #
REPT-91-102 ..... p 3691 N92-30353 #
REPT-91-66 ..... p 3701 N92-30451 #
REPT-91-67 ..... p 3707 N92-30452 #
REPT-91-68 ..... p 3629 N92-30453 #
REPT-91-69 ..... p 3702 N92-30371 #
REPT-91-70 ..... p 3628 N92-30372 #
REPT-91-71 ..... p 3628 N92-30373 #
REPT-91-72 ..... p 3704 N92-30483 #
REPT-91-73 ..... p 3629 N92-30454 #
REPT-91-74 ..... p 3693 N92-30455 #
REPT-91-75 ..... p 3703 N92-30456 #
REPT-91-76 ..... p 3703 N92-30457 #
REPT-91-77 ..... p 3702 N92-30434 #
REPT-91-78 ..... p 3693 N92-30435 #
REPT-91-79 ..... p 3702 N92-30436 #
REPT-91-80 ..... p 3703 N92-30437 #
REPT-91-86 ..... p 3704 N92-30490 #
REPT-91-87 ..... p 3704 N92-30491 #
REPT-91-88 ..... p 3704 N92-30517 #
REPT-91-89 ..... p 3694 N92-30484 #
REPT-91-90 ..... p 3694 N92-30492 #
REPT-91-91 ..... p 3694 N92-30485 #
REPT-91-92 ..... p 3734 N92-30486 #
REPT-91-93 ..... p 3734 N92-30487 #
REPT-91-98 ..... p 3702 N92-30350 #
REPT-91-99 ..... p 3691 N92-30351 #
REPT-92-01 ..... p 3614 N92-30354 #
REPT-92-02 ..... p 3707 N92-30355 #
REPT-92-04 ..... p 3692 N92-30356 #
REPT-92-05 ..... p 3692 N92-30357 #
REPT-92-06 ..... p 3628 N92-30358 #
REPT-92-07 ..... p 3692 N92-30359 #
REPT-92-08 ..... p 3702 N92-30360 #
REPT-92-09 ..... p 3703 N92-30459 #
REPT-92-10 ..... p 3707 N92-30460 #
REPT-92-12 ..... p 3704 N92-30461 #
REPT-92-14 ..... p 3629 N92-30462 #
REPT-92-15 ..... p 3733 N92-30463 #
REPT-92-16 ..... p 3704 N92-30464 #
REPT-92B00026 ..... p 3612 N92-30378 * #

RFP-TRANS-523 ..... p 3717 N92-31137 #
RFP-TRANS-524 ..... p 3717 N92-31147 #
RFP-TRANS-525 ..... p 3606 N92-31146 #

RIACS-TR-90.41 ..... p 3696 N92-30723 * #
RIACS-TR-92.10 ..... p 3690 N92-30724 * #

RL-TM-92-8 ..... p 3735 N92-30819 #

RL-TR-91-369 ..... p 3720 N92-30248 #
RL-TR-92-112 ..... p 3597 N92-30534 #
RL-TR-92-34 ..... p 3616 N92-30760 #

RTOP 505-62-0K ..... p 3709 N92-30898 * #

RUU-CS-90-26-PT-1 ..... p 3694 N92-30479 #
RUU-CS-90-27-PT-2 ..... p 3694 N92-30480 #
RUU-CS-91-37 ..... p 3707 N92-30481 #
RUU-CS-91-38 ..... p 3698 N92-30482 #
RUU-CS-91-39 ..... p 3703 N92-30458 #
RUU-CS-91-40 ..... p 3703 N92-30447 #
RUU-CS-91-41 ..... p 3693 N92-30443 #
RUU-CS-91-42 ..... p 3693 N92-30444 #
RUU-CS-91-43 ..... p 3693 N92-30445 #
RUU-CS-91-44-PT-1 ..... p 3703 N92-30446 #
RUU-CS-91-46 ..... p 3615 N92-30448 #
RUU-CS-91-47 ..... p 3703 N92-30449 #

RUU-CS-91-49 ..... p 3703 N92-30450 #

R92-920036-F ..... p 3659 N92-30640 #

S-REPT-102-356 ..... p 3735 N92-31169 #

SAND-91-1015C ..... p 3622 N92-30370 #
SAND-91-1624 ..... p 3637 N92-30893 #
SAND-91-1730C ..... p 3663 N92-30859 #
SAND-91-2539C ..... p 3603 N92-30544 #
SAND-91-2579 ..... p 3637 N92-30822 #
SAND-91-2650 ..... p 3636 N92-30903 #
SAND-91-2786C ..... p 3698 N92-30401 #
SAND-91-2787C ..... p 3630 N92-30607 #
SAND-91-8231 ..... p 3696 N92-30892 #
SAND-91-8721 ..... p 3594 N92-30749 #
SAND-92-0193C ..... p 3605 N92-30804 #
SAND-92-0243 ..... p 3613 N92-30887 #
SAND-92-0330C ..... p 3700 N92-31111 #
SAND-92-0344C ..... p 3728 N92-30585 #
SAND-92-0362C ..... p 3695 N92-30522 #
SAND-92-0404C ..... p 3698 N92-30363 #
SAND-92-0448 ..... p 3626 N92-30764 #
SAND-92-0493 ..... p 3664 N92-31123 #
SAND-92-0523C ..... p 3670 N92-30808 #
SAND-92-0736C ..... p 3626 N92-30807 #
SAND-92-0819C ..... p 3718 N92-30624 #
SAND-92-0864C ..... p 3605 N92-30830 #
SAND-92-0919C ..... p 3574 N92-30367 #
SAND-92-1102C ..... p 3733 N92-30889 #
SAND-92-1183C ..... p 3730 N92-31000 #
SAND-92-1233C ..... p 3600 N92-31177 #
SAND-92-8429C ..... p 3594 N92-30369 #
SAND-92-8462C ..... p 3606 N92-30857 #
SAND-92-8548 ..... p 3707 N92-31189 #

SC71002.FR ..... p 3601 N92-30342 #

SR-1 ..... p 3678 N92-30262 #
SR-2 ..... p 3676 N92-30720 #

SSCL-PREPRINT-102 ..... p 3717 N92-30589 #
SSCL-PREPRINT-120 ..... p 3721 N92-31187 #
SSCL-PREPRINT-26 ..... p 3719 N92-30839 #
SSCL-PREPRINT-33 ..... p 3719 N92-30840 #
SSCL-PREPRINT-51 ..... p 3718 N92-30786 #
SSCL-PREPRINT-52 ..... p 3661 N92-31120 #
SSCL-PREPRINT-77 ..... p 3718 N92-30646 #
SSCL-PREPRINT-80 ..... p 3718 N92-30811 #

SSCL-516 ..... p 3719 N92-30881 #

SSD-TR-92-15 ..... p 3636 N92-30412 #

SSS-DPR-91-2194 ..... p 3588 N92-30628 #

SU-GL-4959 ..... p 3727 N92-30252 #

SU-SOL-92-2 ..... p 3696 N92-30905 #

SU-TF-54 ..... p 3635 N92-30831 #

SWRI-03-3685 ..... p 3607 N92-30767 #
SWRI-06-2699/3 ..... p 3662 N92-30558 #
SWRI-3178-3.2 ..... p 3659 N92-30601 #

TEC-0005-PHASE-1 ..... p 3593 N92-30241 #

TIOS-92/08 ..... p 3689 N92-30432 #

TR-0091(6925-08)-3 ..... p 3636 N92-30412 #
TR-011 ..... p 3683 N92-30531 #
TR-10 ..... p 3593 N92-30245 #
TR-10 ..... p 3605 N92-30817 #
TR-10 ..... p 3595 N92-30875 #
TR-11 ..... p 3605 N92-30796 #
TR-12 ..... p 3605 N92-30816 #
TR-13 ..... p 3720 N92-30535 #
TR-15 ..... p 3721 N92-30536 #
TR-16 ..... p 3602 N92-30346 #
TR-19 ..... p 3623 N92-30537 #
TR-21 ..... p 3727 N92-30527 #
TR-24 ..... p 3603 N92-30594 #
TR-25 ..... p 3728 N92-30595 #
TR-26 ..... p 3712 N92-30255 #
TR-26 ..... p 3727 N92-30406 #
TR-29 ..... p 3716 N92-30845 #
TR-32 ..... p 3601 N92-30244 #
TR-33 ..... p 3712 N92-30261 #
TR-35 ..... p 3712 N92-30240 #
TR-42 ..... p 3595 N92-30821 #
TR-5 ..... p 3712 N92-30259 #
TR-66 ..... p 3603 N92-30553 #
TR-7 ..... p 3601 N92-30250 #
TR-7 ..... p 3605 N92-30795 #
TR-85 ..... p 3710 N92-30549 #

TR-86 ..... p 3629 N92-30548 #
TR-8 ..... p 3613 N92-30246 #
TR-8 ..... p 3594 N92-30632 #
TR-8 ..... p 3604 N92-30794 #
TR-940 ..... p 3616 N92-30762 #
TR-942 ..... p 3678 N92-30559 #
TR-944 ..... p 3616 N92-30761 #
TR-9 ..... p 3606 N92-30873 #

TRC-EM-CAB-9203 ..... p 3621 N92-31156 * #

UCB-PTH-91/52 ..... p 3731 N92-30825 #

UCRL-CR-107774 ..... p 3724 N92-30824 #

UCRL-ID-110438 ..... p 3714 N92-30586 #

UCRL-JC-106406 ..... p 3674 N92-31121 #
UCRL-JC-107793 ..... p 3600 N92-31125 #
UCRL-JC-108523-REV-1 ..... p 3674 N92-30647 #
UCRL-JC-108738 ..... p 3729 N92-30854 #
UCRL-JC-108753 ..... p 3600 N92-31138 #
UCRL-JC-108775 ..... p 3599 N92-31119 #
UCRL-JC-108838 ..... p 3600 N92-31124 #
UCRL-JC-109064 ..... p 3729 N92-30885 #
UCRL-JC-109212 ..... p 3621 N92-31007 #
UCRL-JC-109222 ..... p 3740 N92-30855 #
UCRL-JC-109293-REV-1 ..... p 3602 N92-30399 #
UCRL-JC-109355 ..... p 3726 N92-31118 #
UCRL-JC-109599 ..... p 3656 N92-30400 #
UCRL-JC-109730 ..... p 3604 N92-30792 #
UCRL-JC-110098 ..... p 3657 N92-31115 #
UCRL-JC-110303 ..... p 3739 N92-30862 #

UDR-TR-91-135 ..... p 3624 N92-30619 #
UDR-TR-92-25 ..... p 3593 N92-31005 #

UM-AERO-92-08 ..... p 3574 N92-30392 * #

US-PATENT-APPL-SN-614413 ..... p 3731 N92-31220 #
US-PATENT-APPL-SN-624014 ..... p 3682 N92-30413
US-PATENT-APPL-SN-724084 ..... p 3591 N92-30573
US-PATENT-APPL-SN-747321 ..... p 3604 N92-30685 #
US-PATENT-APPL-SN-756261 ..... p 3690 N92-30564 #
US-PATENT-APPL-SN-790731 ..... p 3621 N92-31150 * #
US-PATENT-APPL-SN-792501 ..... p 3695 N92-30543 * #
US-PATENT-APPL-SN-799571 ..... p 3734 N92-30386 * #
US-PATENT-APPL-SN-800785 ..... p 3585 N92-31192 #
US-PATENT-APPL-SN-808302 ..... p 3720 N92-30312 * #
US-PATENT-APPL-SN-811279 ..... p 3614 N92-30348 #
US-PATENT-APPL-SN-813556 ..... p 3700 N92-30314 * #
US-PATENT-APPL-SN-822457 ..... p 3658 N92-30388 * #
US-PATENT-APPL-SN-823805 ..... p 3628 N92-30390 * #
US-PATENT-APPL-SN-828630 ..... p 3722 N92-31213 #
US-PATENT-APPL-SN-845090 ..... p 3601 N92-30313 * #
US-PATENT-APPL-SN-849612 ..... p 3662 N92-30317 * #
US-PATENT-APPL-SN-858176 ..... p 3622 N92-30389 * #
US-PATENT-APPL-SN-877966 ..... p 3623 N92-30542 * #
US-PATENT-APPL-SN-887001 ..... p 3588 N92-30315 * #
US-PATENT-APPL-SN-887002 ..... p 3628 N92-30387 * #
US-PATENT-APPL-SN-887674 ..... p 3602 N92-30539 * #
US-PATENT-APPL-SN-891604 ..... p 3690 N92-30541 * #
US-PATENT-APPL-SN-892072 ..... p 3659 N92-30540 * #
US-PATENT-APPL-SN-899536 ..... p 3658 N92-30316 * #
US-PATENT-APPL-SN-909501 ..... p 3614 N92-30391 * #

US-PATENT-CLASS-228-198 ..... p 3591 N92-30573
US-PATENT-CLASS-367-88 ..... p 3682 N92-30413

US-PATENT-5,077,699 ..... p 3682 N92-30413
US-PATENT-5,100,049 ..... p 3591 N92-30573

USAAVSCOM-TR-92-B-010 ..... p 3664 N92-31155 * #
USAAVSCOM-TR-92-D-2 ..... p 3580 N92-30878 #

USAEPG-FR-1420-PHASE-2 ..... p 3615 N92-30583 #

UW-CPTC-92-2 ..... p 3726 N92-31002 #

VAL-6/1991 ..... p 3598 N92-30785 #

VPI-AOE-188 ..... p 3577 N92-31122 #

WES/MP/GL-92-10 ..... p 3579 N92-31193 #

WHC-SA-1402 ..... p 3589 N92-30818 * #

WL-TR-91-1121 ..... p 3734 N92-30324 #
WL-TR-91-2120 ..... p 3659 N92-30554 #
WL-TR-91-2139 ..... p 3624 N92-30619 #
WL-TR-91-3020-VOL-1 ..... p 3590 N92-30251 #
WL-TR-91-3064 ..... p 3583 N92-30323 #
WL-TR-91-3107-VOL-1 ..... p 3573 N92-30253 #
WL-TR-91-3107-VOL-2 ..... p 3573 N92-30258 #
WL-TR-91-3120 ..... p 3577 N92-31171 #
WL-TR-92-1022 ..... p 3581 N92-30524 #

WL-TR-92-2015 ..... p 3607 N92-30767 #
WL-TR-92-2023 ..... p 3594 N92-30645 #
WL-TR-92-3043 ..... p 3590 N92-30528 #
WL-TR-92-4004 ..... p 3661 N92-30529 #
WL-TR-92-4027 ..... p 3593 N92-31005 #

WSRC-MS-91-392 ..... p 3735 N92-31132 #
WSRC-MS-92-131 ..... p 3586 N92-30899 #

WSRC-TR-146 ..... p 3600 N92-31218 #

WSS/CI-92-6 ..... p 3606 N92-30857 #

WSU/DC/91-TR-81 ..... p 3712 N92-30333 #

WSU/92/85 ..... p 3710 N92-30549 #
WSU/92/86 ..... p 3629 N92-30548 #

Y/DW-1139 ..... p 3722 N92-31195 #

YALEU/DCS/RR-893 ..... p 3705 N92-30568 #

Typical Accession Number Index Listing

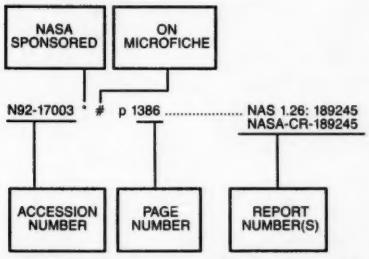

Listings in this index are arranged alphanumerically by accession number. The page number helps to locate the citation in the abstract section. An asterisk (*) indicates that the item is a NASA report. A pound sign (#) indicates that the item is available on microfiche.

N92-30233 # p 3719 ..... AD-A248851
N92-30234 # p 3734 ..... AD-A248852
N92-30235 # p 3731 ..... AD-A248853
N92-30236 # p 3711 ..... DE92-624639
ITP-91-12
N92-30237 # p 3660 ..... AD-A250809
AFOSR-92-0358TR
N92-30238 # p 3681 ..... AD-A250830
CRREL-SR-43-PT-8
N92-30239 # p 3573 ..... AD-A250882
NATICK-TR-92/009
N92-30240 # p 3712 ..... AD-A250929
TR-35
N92-30241 # p 3593 ..... AD-A251026
TEC-0005-PHASE-1
N92-30242 # p 3731 ..... AD-A251044
N92-30243 # p 3701 ..... AD-A251066
NRL/FR/6521-92-9392
N92-30244 # p 3601 ..... AD-A251086
TR-32
N92-30245 # p 3593 ..... AD-A251088
TR-10
N92-30246 # p 3613 ..... AD-A251093
TR-8
N92-30247 # p 3727 ..... DE92-010584
NREL/TP-413-4906
N92-30248 # p 3720 ..... AD-A247857
RL-TR-91-369
N92-30249 # p 3622 ..... AD-A248847
AFOSR-92-0228TR
N92-30250 # p 3601 ..... AD-A250803
TR-7
N92-30251 # p 3590 ..... AD-A250808
WL-TR-91-3020-VOL-1
N92-30252 # p 3727 ..... AD-A251028
SU-GL-4959
N92-30253 # p 3573 ..... AD-A251037
WL-TR-91-3107-VOL-1
N92-30254 # p 3686 ..... AD-A251053
AL-TR-1991-0153
N92-30255 # p 3712 ..... AD-A251058
TR-26
N92-30256 # p 3593 ..... AD-A251065
AFOSR-92-0456TR
N92-30257 # p 3587 ..... AD-A251074
BRL-TR-3358
N92-30258 # p 3573 ..... AD-A251083
WL-TR-91-3107-VOL-2
N92-30259 # p 3712 ..... AD-A251085
TR-5
N92-30260 # p 3691 ..... AD-A251089
N92-30261 # p 3712 ..... AD-A251096
TR-33
N92-30262 # p 3678 ..... AD-A248384
AD-E200940
PL-TR-91-2135
SR-1
N92-30263* # p 3608 ..... L-17099
NAS 1.55:3151
NASA-CP-3151
N92-30264* # p 3607 ..... NO REPORT NUMBER
N92-30265* # p 3607 ..... NO REPORT NUMBER
N92-30266* # p 3600 ..... NO REPORT NUMBER
N92-30267* # p 3607 ..... NO REPORT NUMBER
N92-30268* # p 3608 ..... NO REPORT NUMBER
N92-30269* # p 3600 ..... NO REPORT NUMBER
N92-30270* # p 3593 ..... NO REPORT NUMBER
N92-30271* # p 3609 ..... NO REPORT NUMBER
N92-30272* # p 3601 ..... NO REPORT NUMBER
N92-30273* # p 3609 ..... NO REPORT NUMBER
N92-30274* # p 3609 ..... NO REPORT NUMBER
N92-30275* # p 3610 ..... NO REPORT NUMBER
N92-30276* # p 3601 ..... NO REPORT NUMBER
N92-30277* # p 3610 ..... NO REPORT NUMBER
N92-30278* # p 3610 ..... NO REPORT NUMBER
N92-30279* # p 3607 ..... NO REPORT NUMBER
N92-30280* # p 3610 ..... NO REPORT NUMBER
N92-30281* # p 3610 ..... NO REPORT NUMBER
N92-30282* # p 3611 ..... NO REPORT NUMBER
N92-30283* # p 3611 ..... NO REPORT NUMBER
N92-30284* # p 3611 ..... NO REPORT NUMBER
N92-30285* # p 3607 ..... NO REPORT NUMBER
N92-30286* # p 3611 ..... NO REPORT NUMBER
N92-30287* # p 3593 ..... NO REPORT NUMBER
N92-30288* # p 3611 ..... NO REPORT NUMBER
N92-30289* # p 3611 ..... NO REPORT NUMBER
N92-30290* # p 3612 ..... NO REPORT NUMBER
N92-30291* # p 3601 ..... NO REPORT NUMBER
N92-30292* # p 3601 ..... NO REPORT NUMBER
N92-30293* # p 3612 ..... NO REPORT NUMBER
N92-30294* # p 3612 ..... NO REPORT NUMBER
N92-30295* # p 3573 ..... L-17026
NAS 1.60:3205
NASA-TP-3205
N92-30296* # p 3691 ..... NAS 1.26:190546
NASA-CR-190546
N92-30297* # p 3627 ..... E-7080
NAS 1.15:105693
NASA-TM-105693
N92-30298* # p 3574 ..... NAS 1.26:189149
NASA-CR-189149
PWA-6354
N92-30299* # p 3691 ..... NAS 1.26:189827
NASA-CR-189827
N92-30300* # p 3614 ..... NAS 1.26:189210
NASA-CR-189210
N92-30301* # p 3588 ..... AIAA PAPER 92-0354
E-7018
NAS 1.15:105652
NASA-TM-105652
N92-30302* # p 3741 ..... E-7016-1
NAS 1.55:10093
NASA-CP-10093
N92-30303 # p 3581 ..... DOT/FAA/CT-92/5
N92-30304* # p 3579 ..... NAS 1.26:189620
NASA-CR-189620
N92-30305* # p 3683 ..... NAS 1.15:103592
NASA-TM-103592
N92-30306* # p 3686 ..... BBN-7451
NAS 1.26:4451
NASA-CR-4451
N92-30307* # p 3585 ..... E-6096
NAS 1.61:1280
NASA-RP-1280
N92-30308* # p 3588 ..... E-7203
NAS 1.15:105775
NASA-TM-105775
N92-30309* # p 3661 ..... NAS 1.26:4460
NASA-CR-4460
N92-30310* # p 3586 ..... E-7202
NAS 1.15:105774
NASA-TM-105774
N92-30311* # p 3689 ..... ICASE-92-22
NAS 1.26:189664
NASA-CR-189664
N92-30312* # p 3720 ..... NAS 1.71:LAR-14568-1
NASA-CASE-LAR-14568-1
US-PATENT-APPL-SN-808302
N92-30313* # p 3601 ..... NAS 1.71:LAR-14753-1
NASA-CASE-LAR-14753-1
US-PATENT-APPL-SN-845090
N92-30314* # p 3700 ..... NAS 1.71:MSC-21874-1
NASA-CASE-MSC-21874-1
US-PATENT-APPL-SN-813556
N92-30315* # p 3588 ..... NAS 1.71:MSC-21723-1
NASA-CASE-MSC-21723-1
US-PATENT-APPL-SN-887001
N92-30316* # p 3658 ..... NAS 1.71:MSC-21918-1
NASA-CASE-MSC-21918-1
US-PATENT-APPL-SN-899536
N92-30317* # p 3662 ..... NAS 1.71:LAR-14654-1
NASA-CASE-LAR-14654-1
US-PATENT-APPL-SN-849612
N92-30318 # p 3590 ..... AD-A246122
N92-30319 # p 3684 ..... AD-A248466
AFOSR-92-0187TR
N92-30320 # p 3687 ..... AD-A248467
AFOSR-92-0212TR
N92-30321 # p 3607 ..... AD-A248472
NADC-91078-60
N92-30322 # p 3700 ..... AD-A248473
N92-30323 # p 3583 ..... AD-A248487
ASIAC-1090.10
WL-TR-91-3084
N92-30324 # p 3734 ..... AD-A248492
WL-TR-91-1121
N92-30325 # p 3687 ..... AD-A248494
AFOSR-92-0203TR
N92-30326 # p 3601 ..... AD-A248495
N92-30327 # p 3744 ..... AD-A248766
AFOSR-92-0170TR-VOL-4
N92-30328 # p 3684 ..... AD-A248963
N92-30329 # p 3584 ..... AD-A248964
N92-30330 # p 3670 ..... DE91-002145
NREL/TP-253-4280
N92-30331 # p 3712 ..... DE92-624560
ITP-91-8
N92-30332 # p 3622 ..... AD-A250738
AFOSR-92-0266TR
N92-30333 # p 3712 ..... AD-A248298
WSU/DC/91-TR-81
N92-30334 # p 3700 ..... AD-A248481
AFOSR-92-0185TR
N92-30335 # p 3700 ..... AD-A248484
AFOSR-92-0215TR
N92-30336 # p 3687 ..... AD-A248560
AFOSR-92-0231TR
N92-30337 # p 3712 ..... AD-A248567
AFOSR-92-0196TR
N92-30338 # p 3662 ..... AD-A248899
BN-1129
N92-30339 # p 3701 ..... AD-A248900
BN-1130
MD92-08-1B-GC-JED
MU-TR-92-06
N92-30340 # p 3678 ..... AD-A248901
DPG-FR-91-713
N92-30341 # p 3607 ..... AD-A248902
CRC-578
N92-30342 # p 3601 ..... AD-A248903
AFOSR-92-0236TR
SC71002.FR
N92-30343 # p 3720 ..... AD-A248938
AD-E200981
ERP-1089
PL-TR-91-2139
N92-30344 # p 3593 ..... DE92-011632
DOE/ER-13403/4
N92-30345 # p 3672 ..... DE92-012668
DOE/ER-13590/10
N92-30346 # p 3602 ..... AD-A250638
TR-16
N92-30347 # p 3702 ..... AD-A250641
AFOSR-92-0425TR
N92-30348 # p 3614 ..... AD-D015258
US-PATENT-APPL-SN-811279
N92-30349 # p 3732 ..... CONF-920430-83
DE92-012331
PNL-SA-20246
N92-30350 # p 3702 ..... ETN-92-91848
REPT-91-98

N92-30351 # p 3691 ..... ETN-92-91849
REPT-91-99
N92-30352 # p 3691 ..... ETN-92-91850
REPT-91-100
N92-30353 # p 3691 ..... ETN-92-91852
REPT-91-102
N92-30354 # p 3614 ..... ETN-92-91853
REPT-92-01
N92-30355 # p 3707 ..... ETN-92-91854
REPT-92-02
N92-30356 # p 3692 ..... ETN-92-91856
REPT-92-04
N92-30357 # p 3692 ..... ETN-92-91857
REPT-92-05
N92-30358 # p 3628 ..... ETN-92-91858
REPT-92-06
N92-30359 # p 3692 ..... ETN-92-91859
REPT-92-07
N92-30360 # p 3702 ..... ETN-92-91860
REPT-92-08
N92-30361 # p 3614 ..... BCRS-91-33
ETN-92-91881
ISBN-90-5411-016-3
N92-30362 # p 3666 ..... BCRS-91-36
ETN-92-91884
ISBN-90-5411-026-0
N92-30363 # p 3698 ..... CONF-920771-1
DE92-008679
SAND-92-0404C
N92-30364 # p 3713 ..... ETN-92-91620
NIKHEF-H/91-22
N92-30365 # p 3636 ..... ETN-92-91621
NIKHEF-H/91-23
N92-30366 # p 3722 ... CONF-9204132-1-EXTD-ABST
DE92-013277
N92-30367 # p 3574 ..... CONF-920534-2
DE92-013439
SAND-92-0919C
N92-30368 # p 3683 ..... DE92-013472
DOE/ER-13791/37
N92-30369 # p 3594 ..... CONF-920466-11
DE92-013563
SAND-92-8429C
N92-30370 # p 3622 ..... CONF-920423-4
DE92-013684
SAND-91-1015C
N92-30371 # p 3702 ..... ETN-92-91819
REPT-91-69
N92-30372 # p 3628 ..... ETN-92-91820
REPT-91-70
N92-30373 # p 3628 ..... ETN-92-91821
REPT-91-71
N92-30374 # p 3672 ..... DE92-012354
PNL-SA-20399
N92-30375 # p 3702 ..... AD-A250639
AFOSR-92-0288TR
N92-30376 # p 3684 ..... AD-A250640
AFOSR-92-0413TR
N92-30377 # p 3692 ..... AD-A250642
AFOSR-92-0271TR
N92-30378* # p 3612 ..... NAS 1.60:3216
NASA-TP-3216
REPT-92B00026
N92-30379* # p 3692 ..... CU-TR-92-1287
NAS 1.26:190476
NASA-CR-190476
N92-30380* # p 3628 ..... NAS 1.26:190498
NASA-CR-190498
N92-30381* # p 3688 ..... NAS 1.15:103587
NASA-TM-103587
N92-30382* # p 3586 ..... NAS 1.15:107545
NASA-TM-107545
N92-30383* # p 3587 ..... E-7000
NAS 1.15:105645
NASA-TM-105645
N92-30384 # p 3722 ..... NIFS-130
N92-30385 # p 3722 ..... NIFS-137
N92-30386* # p 3734 ..... NAS 1.71:LAR-14651-1
NASA-CASE-LAR-14651-1
US-PATENT-APPL-SN-799571
N92-30387* # p 3628 ..... NAS 1.71:LAR-14682-1
NASA-CASE-LAR-14682-1
US-PATENT-APPL-SN-887002
N92-30388* # p 3658 ..... NAS 1.71:LAR-14789-1
NASA-CASE-LAR-14789-1
US-PATENT-APPL-SN-822457
N92-30389* # p 3622 ..... NAS 1.71:LAR-14811-1
NASA-CASE-LAR-14811-1
US-PATENT-APPL-SN-858176
N92-30390* # p 3628 ..... NAS 1.71:LAR-14824-1-SB
NASA-CASE-LAR-14824-1-SB
US-PATENT-APPL-SN-823805
N92-30391* # p 3614 ..... NAS 1.71:NPO-18701-1-CU
NASA-CASE-NPO-18701-1-CU
US-PATENT-APPL-SN-909501
N92-30392* # p 3574 ..... NAS 1.26:189658
NASA-CR-189658
UM-AERO-92-08
N92-30393* # p 3574 ..... NAS 1.15:107643
NASA-TM-107643
N92-30394* # p 3574 ..... AVSCOM-TR-92-B-002
L-16951
NAS 1.60:3233
NASA-TP-3233
N92-30395* # p 3577 ..... E-5808
NAS 1.15:3238
NASA-TP-3238
N92-30396* # p 3658 ..... AVSCOM-TR-91-C-026
E-6531
NAS 1.60:3265
NASA-TP-3265
N92-30397* # p 3623 ..... E-7221
NAS 1.15:105791
NASA-TM-105791
N92-30398 # p 3717 ..... BNL-47201
CONF-920219-4
DE92-014594
N92-30399 # p 3602 ..... CONF-920402-15-REV-1
DE92-014787
UCRL-JC-109293-REV-1
N92-30400 # p 3656 ..... CONF-911131-3
DE92-014796
UCRL-JC-109599
N92-30401 # p 3698 ..... CONF-9204106-5
DE92-015041
SAND-91-2786C
N92-30402 # p 3602 ..... AECL-10461
CONF-910572
DE92-626843
N92-30403 # p 3713 ..... DE92-627288
IHEP-ONF-91-74-PT-1
N92-30404 # p 3713 ..... DE92-627317
IFVE-ONF-91-139
N92-30405 # p 3727 ..... DE92-627497
ITP-91-25
N92-30406 # p 3727 ..... AD-A252270
TR-26
N92-30407 # p 3614 ..... AD-A252275
NRL/MR/4790-92-6984
N92-30408 # p 3615 ..... AD-A252621
N92-30409 # p 3602 ..... AD-A252641
REPT-18
N92-30410 # p 3702 ..... AD-A252643
ICMA-92-171
N92-30411 # p 3612 ..... AD-A252647
NMAB-461
N92-30412 # p 3636 ..... AD-A252649
SSD-TR-92-15
TR-0091(6925-08)-3
N92-30413 p 3682 ..... AD-D015238
US-PATENT-APPL-SN-624014
US-PATENT-CLASS-367-88
US-PATENT-5,077,699
N92-30414 # p 3590 ..... ETN-92-91613
N92-30415 # p 3713 ..... ETN-92-91614
NIKHEF-H/91-16
N92-30416* # p 3662 ..... NAS 1.15:103591
NASA-TM-103591
N92-30417 # p 3675 ..... NO REPORT NUMBER
N92-30418 # p 3578 ..... ETN-92-91890
MBB-UD-0611-91-PUB
N92-30419 # p 3708 ..... ETN-92-91894
MBB-UO-0166-91-PUB
N92-30420 # p 3709 ..... ETN-92-91896
MBB-UO-0168-91-PUB
N92-30421 # p 3731 ..... ETN-92-91897
MBB-UO-0169-91-PUB
N92-30422 # p 3594 ..... ETN-92-91900
MBB-Z-0413-91-PUB
N92-30423 # p 3662 ..... ETN-92-91901
MBB/FW321/S/PUB/467
N92-30424 # p 3579 ..... ETN-92-91902
MBB/FW321/S/PUB/476
N92-30425 p 3673 ..... NO REPORT NUMBER
N92-30426* # p 3670 ..... E-7166
NAS 1.15:105755
NASA-TM-105755
N92-30427* # p 3623 ..... E-7204
NAS 1.15:105777
NASA-TM-105777
N92-30428 # p 3692 ..... CWI-CS-R8749-REV
CWI-CS-R9124
ETN-92-91552
N92-30429 # p 3693 ..... CWI-NM-R9115
ETN-92-91662
N92-30430 # p 3722 ..... NIFS-113
N92-30431 # p 3722 ..... NIFS-142
N92-30432 # p 3689 ..... ETN-92-91782
MEMO-INF-92-08
TIOS-92/08
N92-30433 # p 3693 ..... ETN-92-91783
MEMO-INF-92-09
N92-30434 # p 3702 ..... ETN-92-91827
REPT-91-77
N92-30435 # p 3693 ..... ETN-92-91828
REPT-91-78
N92-30436 # p 3702 ..... ETN-92-91829
REPT-91-79
N92-30437 # p 3703 ..... ETN-92-91830
REPT-91-80
N92-30438 # p 3629 ..... DE92-012645
DOE/PC-90185/T4
N92-30439 # p 3583 ..... ETN-92-91888
MBB-UD-0608-91-PUB
N92-30440 # p 3587 ..... ETN-92-91892
MBB-UO-0164-91-PUB
N92-30441 # p 3613 ..... ETN-92-91893
MBB-UO-0165-91-PUB
N92-30442 # p 3709 ..... ETN-92-91895
MBB-UO-0167-91-PUB
N92-30443 # p 3693 ..... ETN-92-91807
RUU-CS-91-41
N92-30444 # p 3693 ..... ETN-92-91808
RUU-CS-91-42
N92-30445 # p 3693 ..... ETN-92-91809
RUU-CS-91-43
N92-30446 # p 3703 ..... ETN-92-91810
RUU-CS-91-44-PT-1
N92-30447 # p 3703 ..... ETN-92-91806
RUU-CS-91-40
N92-30448 # p 3615 ..... ETN-92-91812
RUU-CS-91-46
N92-30449 # p 3703 ..... ETN-92-91813
RUU-CS-91-47
N92-30450 # p 3703 ..... ETN-92-91815
RUU-CS-91-49
N92-30451 # p 3701 ..... ETN-92-91816
REPT-91-66
N92-30452 # p 3707 ..... ETN-92-91817
REPT-91-67
N92-30453 # p 3629 ..... ETN-92-91818
REPT-91-68
N92-30454 # p 3629 ..... ETN-92-91823
REPT-91-73
N92-30455 # p 3693 ..... ETN-92-91824
REPT-91-74
N92-30456 # p 3703 ..... ETN-92-91825
REPT-91-75
N92-30457 # p 3703 ..... ETN-92-91826
REPT-91-76
N92-30458 # p 3703 ..... ETN-92-91805
RUU-CS-91-39
N92-30459 # p 3703 ..... ETN-92-91861
REPT-92-09
N92-30460 # p 3707 ..... ETN-92-91862
REPT-92-10
N92-30461 # p 3704 ..... ETN-92-91864
REPT-92-12
N92-30462 # p 3629 ..... ETN-92-91865
REPT-92-14
N92-30463 # p 3733 ..... ETN-92-91866
REPT-92-15
N92-30464 # p 3704 ..... ETN-92-91867
REPT-92-16
N92-30465 # p 3666 ..... BCRS-90-28
ETN-92-91868
ISBN-90-5411-017-1
N92-30466 # p 3666 ..... BCRS-90-30
ETN-92-91869
ISBN-90-5411-008-2
N92-30467 # p 3666 ..... BCRS-91-10
ETN-92-91871
ISBN-90-5411-009-0
N92-30468 # p 3666 ..... BCRS-91-21
ETN-92-91872
ISBN-90-5411-015-5
N92-30470 # p 3682 ..... BCRS-91-23-PT-1-2
ETN-92-91874
ISBN-90-5411-013-9
N92-30471 # p 3667 ..... BCRS-91-26-PT-1
ETN-92-91875
ISBN-90-5411-012-0
N92-30472 # p 3667 ..... BCRS-91-27
ETN-92-91876
ISBN-90-5411-006-6
N92-30473 # p 3704 ..... ETN-92-91473
IMAG-RR-855-I
N92-30474 # p 3578 ..... ETN-92-91525
NLR-TP-89284-U
N92-30475 # p 3667 ..... ETN-92-91526
NLR-TP-89294-U
N92-30476 # p 3693 ..... ETN-92-91528
NLR-TP-89327-U
N92-30477 # p 3658 ..... ETN-92-91529
NLR-TP-89364-U
N92-30478 # p 3694 ..... ETN-92-91800
MEMO-COSOR-92-04
N92-30479 # p 3694 ..... ETN-92-91801

RUU-CS-90-26-PT-1
N92-30480 # p 3694 ETN-92-91802
RUU-CS-90-27-PT-2
N92-30481 # p 3707 ETN-92-91803
RUU-CS-91-37
N92-30482 # p 3698 ETN-92-91804
RUU-CS-91-38
N92-30483 # p 3704 ETN-92-91822
REPT-91-72
N92-30484 # p 3694 ETN-92-91839
REPT-91-89
N92-30485 # p 3694 ETN-92-91841
REPT-91-91
N92-30486 # p 3734 ETN-92-91842
REPT-91-92
N92-30487 # p 3734 ETN-92-91843
REPT-91-93
N92-30488 # p 3687 DOT/FAA/CT-TN92/14
NAS 1.26:190429
NASA-CR-190429
N92-30489* # p 3689 NAS 1.26:189660
NASA-CR-189660
N92-30490 # p 3704 ETN-92-91836
REPT-91-86
N92-30491 # p 3704 ETN-92-91837
REPT-91-87
N92-30492 # p 3694 ETN-92-91840
REPT-91-90
N92-30493 # p 3694 ETN-92-91472
IMAG-RR-853-I
N92-30494* # p 3673 NAS 1.15:107543
NASA-TM-107543
N92-30495 # p 3678 DOT/FAA/NR-92/8,I
N92-30496 # p 3678 DOT/FAA/NR-92/8,II
N92-30497 # p 3723 NIFS-TECH-2
N92-30498 # p 3710 NIFS-105
N92-30499 # p 3723 NIFS-114
N92-30500 # p 3713 NIFS-150
N92-30501 # p 3714 NIFS-151
N92-30502 # p 3602 NIFS-152
N92-30503 # p 3623 ETN-92-91686
N92-30504 # p 3720 ETN-92-91687
N92-30505 # p 3727 ETN-92-91688
N92-30506 # p 3740 ETN-92-91689
MITT-11
N92-30507 # p 3720 ETN-92-91713
ISBN-3-921-681-01-4
ISL-PU-303/90
N92-30508* # p 3584 AIAA PAPER 92-3980
E-7064
NAS 1.15:105685
NASA-TM-105685
N92-30509 # p 3734 PB92-173020
N92-30510 # p 3714 NIFS-134
N92-30511 # p 3704 IHES/M/92/10
PB92-178276
N92-30512 # p 3694 ESA-TT-1166
ETN-92-91707
ONERA-NT-1988-9
N92-30513 # p 3597 ESA-TT-1228
ETN-92-91708
ONERA-NT-1989-7
N92-30514 # p 3575 ESA-TT-1235
ETN-92-91709
ONERA-NT-1990-8
N92-30515 # p 3667 DLR-FB-90-31
ESA-TT-1253
ETN-92-91710
N92-30516* # p 3704 ICASE-92-24
NAS 1.26:189665
NASA-CR-189665
N92-30517 # p 3704 ETN-92-91838
REPT-91-88
N92-30518* # p 3581 AIAA PAPER 92-3747
H-1842
NAS 1.15:104252
NASA-TM-104252
N92-30519 # p 3670 CONF-9205115-2
DE92-010581
NREL/TP-412-4796
N92-30520 # p 3673 CONF-920814-1
DE92-011238
LA-UR-92-808
N92-30521 # p 3590 CONF-920857-2
DE92-011364
LA-UR-92-898
N92-30522 # p 3695 CONF-920867-1
DE92-011663
SAND-92-0362C
N92-30523 # p 3684 AD-A248613
AL-TR-1991-0029
N92-30524 # p 3581 AD-A248893
WL-TR-92-1022
N92-30525 # p 3675 AD-A248992
AFOSR-92-0235TR
OSR-9008
N92-30526 # p 3699 AD-A250635
N92-30527 # p 3727 AD-A250670
TR-21
N92-30528 # p 3590 AD-A252101
WL-TR-92-3043
N92-30529 # p 3661 AD-A252118
WL-TR-92-4004
N92-30530 # p 3636 AD-A252120
NSWCDD/TR-92/181
N92-30531 # p 3683 AD-A252191
TR-011
N92-30532 # p 3615 AD-A252199
AD-E501529
IDA-P-2598
IDA/HQ-91-38244
N92-30533 # p 3705 AD-A252333
AFOSR-92-0541TR
N92-30534 # p 3597 AD-A252486
RL-TR-92-112
N92-30535 # p 3720 AD-A252490
TR-13
N92-30536 # p 3721 AD-A252491
TR-15
N92-30537 # p 3623 AD-A252500
TR-19
N92-30538 # p 3658 AD-A249022
N92-30539* # p 3602 NAS 1.71:MSC-21884-1
NASA-CASE-MSC-21884-1
US-PATENT-APPL-SN-887674
N92-30540* # p 3659 NAS 1.71:MSC-21940-1
NASA-CASE-MSC-21940-1
US-PATENT-APPL-SN-892072
N92-30541* # p 3690 NAS 1.71:LAR-13950-1
NASA-CASE-LAR-13950-1
US-PATENT-APPL-SN-891604
N92-30542* # p 3623 NAS 1.71:NPO-18062-1-CU
NASA-CASE-NPO-18062-1-CU
US-PATENT-APPL-SN-877966
N92-30543* # p 3695 NAS 1.71:NPO-18435-1-CU
NASA-CASE-NPO-18435-1-CU
US-PATENT-APPL-SN-792501
N92-30544 # p 3603 CONF-920402-20
DE92-015046
SAND-91-2539C
N92-30545 # p 3667 AD-A252117
NOARL-TN-231
N92-30546 # p 3637 AD-A252193
AFOSR-92-0539TR
CIT-61430
N92-30547 # p 3584 AD-A252404
N92-30548 # p 3629 AD-A252421
TR-86
WSU/92/86
N92-30549 # p 3710 AD-A252422
TR-85
WSU/92/85
N92-30550 # p 3695 AD-A252462
N92-30551 # p 3578 AD-A252651
DOT/FAA/AM-92/20
N92-30552 # p 3656 AD-A252665
N92-30553 # p 3603 AD-A248806
TR-66
N92-30554 # p 3659 AD-A248807
WL-TR-91-2120
N92-30555 # p 3695 AD-A248826
N92-30556 # p 3675 AD-A248838
AFOSR-92-0255TR
N92-30557 # p 3699 AD-A248843
N92-30558 # p 3662 AD-A249023
AFOSR-92-0241TR
SWRI-06-2699/3
N92-30559 # p 3678 AD-A249024
TR-942
N92-30560 # p 3629 AD-A249028
JSR-91-310
N92-30561 # p 3673 EPA/450/2-91/009
PB92-171966
N92-30562 # p 3707 EPA/600/A-92/107
PB92-180264
N92-30563 # p 3673 PB92-187012
N92-30564 # p 3690 AD-D015307
NAVY-CASE-73056
US-PATENT-APPL-SN-756261
N92-30565 # p 3578 CONF-9204131-1
DE92-013234
N92-30566 # p 3705 DE92-015165
MLM-3748
N92-30567 # p 3663 CONF-9206187-1
DE92-015195
N92-30568 # p 3705 AD-A249029
YALEU/DCS/RR-893
N92-30569* # p 3581 NAS 1.26:189155
NASA-CR-189155
QUEST-TR-534
N92-30570* # p 3575 NAS 1.15:107631
NASA-TM-107631
N92-30571* # p 3659 E-6882
NAS 1.15:105558
NASA-TM-105558
N92-30572 # p 3714 NIFS-149
N92-30573 p 3591 AD-D015299
US-PATENT-APPL-SN-724084
US-PATENT-CLASS-228-198
US-PATENT-5,100,049
N92-30574 # p 3728 CONF-920819-15-EXTD-ABST
DE92-011689
N92-30575 # p 3736 CONF-9206151-2
DE92-014450
N92-30576 # p 3723 CONF-9202112-1
DE92-014454
N92-30577 # p 3728 CONF-920402-24
DE92-015129
N92-30578 # p 3740 CONF-9202117-2
DE92-015142
LA-UR-92-1610
N92-30579 # p 3695 NISTIR-4831
PB92-187137
N92-30580 p 3714 ITN-92-85164
N92-30581 p 3721 IA-1452
ITN-92-85170
N92-30582 p 3656 ITN-92-85171
N92-30583 # p 3615 AD-A248790
USAEPG-FR-1420-PHASE-2
N92-30584 # p 3735 AD-A249017
N92-30585 # p 3728 CONF-920716-4
DE92-009054
SAND-92-0344C
N92-30586 # p 3714 DE92-013751
UCRL-ID-110438
N92-30587 # p 3659 CONF-920795-1
DE92-013404
N92-30588 # p 3597 DE92-014081
DOE/ER-45174/T4
N92-30589 # p 3717 CONF-920331-33
DE92-014612
FNAL/C-92/106
SSCL-PREPRINT-102
N92-30590 # p 3624 DE92-014760
KCP-613-4701
N92-30591 # p 3723 ANL/CP-75362
CONF-920607-15
DE92-014864
N92-30592 # p 3688 AD-A252265
ASD-TR-91-5005-VOL-1
N92-30593 # p 3682 AD-A252266
N92-30594 # p 3603 AD-A252268
TR-24
N92-30595 # p 3728 AD-A252269
TR-25
N92-30596 # p 3699 AD-A252349
AFOSR-92-0540TR
N92-30597 # p 3705 AD-A252364
ARCCB-TR-92018
N92-30598 # p 3624 AD-A248671
N92-30599 # p 3661 AD-A248845
N92-30600 # p 3689 PB92-160530
N92-30601 # p 3659 GETA-91-10
GRI-91/0362
PB92-164466
SWRI-3178-3.2
N92-30602 # p 3673 EPA/600/R-92/029
PB92-166933
N92-30603 # p 3684 AD-A250650
NHRC-91-28
N92-30604 # p 3630 AD-A252263
BRL-TR-3362
N92-30605 # p 3685 AD-A252309
AL-TR-1992-0005
N92-30606 # p 3714 CONF-9106340-2
DE92-014595
DOE/ER-40637/4
OITS-474
N92-30607 # p 3630 CONF-9204106-4
DE92-014618
SAND-91-2787C
N92-30608 # p 3705 ANL/CP-75803
CONF-9207101-1
DE92-015271
N92-30609 # p 3740 CONF-9202117-3
DE92-015279
LA-UR-92-1508
N92-30610 # p 3714 DE92-015295
DOE/ER-40577/2
N92-30611 # p 3714 DE92-015349
DOE/ER-40427/14-N92
N92-30612 # p 3723 DE92-015379
DOE/ER-53198/197
N92-30613 # p 3687 AD-A247228
AFOSR-92-0108TR
N92-30614 # p 3656 AD-A248782
NRL/MR/4440-92-6786
N92-30615 # p 3688 AD-A248787

NRL/MR/4440-92-6964
N92-30616 # p 3630 ..... AD-A248846
AFOSR-92-0258TR
N92-30617 # p 3624 ..... AD-A248861
N92-30618 # p 3705 ..... AD-A249491
ARCCB-TR-92010
N92-30619 # p 3624 ..... AD-A249501
UDR-TR-91-135
WL-TR-91-2139
N92-30620 # p 3723 ..... AD-A249502
NRL/MR/4790-92-6949
N92-30621 # p 3584 ..... AD-A249503
CRREL-SR-91-24
N92-30622 # p 3740 ..... CONF-9109182-3
DE92-013023
FNAL/C-92/88-A
N92-30623 # p 3603 ..... AD-A251061
N92-30624 # p 3718 ..... CONF-9106276-9
DE92-014620
SAND-92-0819C
N92-30625 # p 3715 ..... DE92-014622
DOE/ER-40677/1-PT-2
N92-30626 # p 3603 ..... CONF-9206187-2
DE92-015196
N92-30627 # p 3743 ..... CONF-9202117-1
DE92-015243
LA-UR-92-1545
N92-30628 # p 3588 ..... AD-A248943
AD-E200987
PL-TR-91-2194
SSS-DPR-91-2194
N92-30629 # p 3695 ..... AD-A248945
CRDEC-CR-120
N92-30630 # p 3624 ..... AD-A249018
N92-30631 # p 3696 ..... AD-A249019
N92-30632 # p 3594 ..... AD-A249021
TR-8
N92-30633 # p 3708 ..... AD-A249482
ARO-29016.1-MA
N92-30634 # p 3728 ..... AD-A249483
N92-30635 # p 3603 ..... AD-A249485
ARO-29043.1-MS-SBI
N92-30636 # p 3735 ..... AD-A249494
ILCEP-WEST MONO-4-REV-1
N92-30637 # p 3615 ..... AD-A249499
NRL/MR/4440-92-6978
N92-30638 # p 3705 ..... AD-A248559
AFOSR-92-0239TR
N92-30639 # p 3591 ..... AD-A248661
ARO-24614.22-MS-UIR
ARO-24615.1-MS-UIE
ARO-24616.1-MS-UIF
N92-30640 # p 3659 ..... AD-A249446
R92-920036-F
N92-30641 # p 3591 ..... AD-A249450
AFIT/CI/CIA-91-102
N92-30642 # p 3709 ..... AD-A249481
N92-30643 # p 3679 ..... AD-A250643
AFOSR-92-0280TR
N92-30644 # p 3685 ..... AD-A250651
NHRC-91-43
N92-30645 # p 3594 ..... AD-A250802
WL-TR-92-2023
N92-30646 # p 3718 ..... CONF-9205155-1
DE92-013469
SSCL-PREPRINT-77
N92-30647 # p 3674 ..... CONF-9104368-1-REV-1
DE92-013514
UCRL-JC-108523-REV-1
N92-30648* # p 3630 ..... NAS 1.26:189475
NASA-CR-189475
N92-30649* # p 3630 ..... NO REPORT NUMBER
N92-30650* # p 3630 ..... NO REPORT NUMBER
N92-30651* # p 3631 ..... NO REPORT NUMBER
N92-30652* # p 3631 ..... NO REPORT NUMBER
N92-30653* # p 3631 ..... NO REPORT NUMBER
N92-30654* # p 3631 ..... NO REPORT NUMBER
N92-30655* # p 3631 ..... NO REPORT NUMBER
N92-30656* # p 3631 ..... NO REPORT NUMBER
N92-30657* # p 3632 ..... NO REPORT NUMBER
N92-30658* # p 3632 ..... NO REPORT NUMBER
N92-30659* # p 3632 ..... NO REPORT NUMBER
N92-30660* # p 3632 ..... NO REPORT NUMBER
N92-30661* # p 3632 ..... NO REPORT NUMBER
N92-30662* # p 3633 ..... NO REPORT NUMBER
N92-30663* # p 3633 ..... NO REPORT NUMBER
N92-30664* # p 3633 ..... NO REPORT NUMBER
N92-30665* # p 3633 ..... NO REPORT NUMBER
N92-30666* # p 3633 ..... NO REPORT NUMBER
N92-30667* # p 3633 ..... NO REPORT NUMBER
N92-30668* # p 3597 ..... NO REPORT NUMBER
N92-30669* # p 3597 ..... NO REPORT NUMBER
N92-30670* # p 3597 ..... NO REPORT NUMBER
N92-30671* # p 3634 ..... NO REPORT NUMBER
N92-30672* # p 3634 ..... NO REPORT NUMBER
N92-30673* # p 3634 ..... NO REPORT NUMBER
N92-30674 # p 3634 ..... ETN-92-91905
MBB/FE211/S/PUB/466
N92-30675 # p 3573 ..... ETN-92-91906
MBB/FE211/S/PUB/474
N92-30676 # p 3575 ..... ETN-92-91907
MBB/FE213/S/PUB/459
N92-30677* # p 3699 ..... NAS 1.15:107634
NASA-TM-107634
N92-30678 # p 3624 ..... AD-A246961
AFOSR-92-0095TR
N92-30679 # p 3687 ..... AD-A246962
AFOSR-92-0096TR
N92-30680 # p 3715 ..... AD-A246963
AFOSR-92-0097TR
N92-30681 # p 3715 ..... AD-A246964
AFOSR-92-0098TR
N92-30682 # p 3733 ..... AD-A246965
N92-30683 # p 3624 ..... AD-A247667
DREO-TN-91-35
N92-30684 # p 3728 ..... CONF-9205108-3
DE92-011066
N92-30685 # p 3604 ..... AD-D015267
NAVY-CASE-73546
US-PATENT-APPL-SN-747321
N92-30686* # p 3739 ..... NAS 1.15:107962
NASA-TM-107962
N92-30687 # p 3715 ..... ETN-92-91615
NIKHEF-H/91-17
N92-30688 # p 3637 ..... ETN-92-91619
NIKHEF-H/91-21
N92-30689 # p 3705 ..... CWI-BS-R9003
ETN-92-91640
N92-30690 # p 3591 ..... ETN-92-91904
MBB/FE202/S/PUB/477
N92-30691* # p 3575 ..... NAS 1.15:107645
NASA-TM-107645
N92-30692* # p 3613 ..... E-7042
NAS 1.15:105673
NASA-TM-105673
N92-30693 # p 3661 ..... DE92-011615
DOE/ER-13484/4
N92-30694 # p 3670 ..... DE92-011115
DOE/ER-13506/37
N92-30695 # p 3604 ..... DE92-011129
DOE/ER-13859/31
N92-30696 # p 3699 ..... CWI-CS-R9127
ETN-92-91553
N92-30697 # p 3715 ..... ETN-92-91622
NIKHEF-H/91-24
N92-30698 # p 3690 ..... ETN-92-91637
ISSN-0924-3755
MEMO-INF-91-86
N92-30699 # p 3708 ..... CWI-CS-R9125
ETN-92-91638
N92-30700 # p 3706 ..... CWI-NM-R9113
ETN-92-91661
N92-30701 # p 3690 ..... ETN-92-91666
N92-30702 # p 3625 ..... ETN-92-91668
N92-30703 # p 3615 ..... CONF-920402-5
DE92-013536
LA-UR-92-1289
N92-30704 # p 3667 ..... CONF-9205141-4
DE92-013539
LA-UR-92-1262
N92-30705 # p 3740 ..... CONF-9109371-2
DE92-013542
LA-UR-92-1238
N92-30706 # p 3743 ..... CONF-9203151-1
DE92-013545
LA-UR-92-1231
N92-30707 # p 3674 ..... DE92-013574
DOE/ER-61012/2
N92-30708 # p 3676 ..... NSF-90-97
N92-30709* # p 3587 ..... NAS 1.26:190317
NASA-CR-190317
N92-30710* # p 3701 ..... FIA-91-06
NAS 1.15:107910
NASA-TM-107910
N92-30711* # p 3591 ..... NAS 1.26:184344
NASA-CR-184344
N92-30712 # p 3690 ..... B-238954
GAO/IMTEC-92-45
N92-30713 # p 3575 ..... ETN-92-91704
FFA-TN-1990-20
N92-30714 # p 3739 ..... ETN-92-91706
ISBN-84-7469-052-8
N92-30715 p 3586 ..... D308/TN/001
ETN-92-91716
N92-30716* # p 3706 ..... ICASE-92-27
NAS 1.26:189668
NASA-CR-189668
N92-30717 # p 3594 ..... DE92-013918
DOE/PC-90291/T5
N92-30718 # p 3688 ..... AD-A252310
N92-30719 # p 3685 ..... AD-A252317
N92-30720 # p 3676 ..... AD-A252326
PL-TR-92-2099
SR-2
N92-30721 # p 3616 ..... AD-A249643
NRAD-TD-2259
N92-30722* # p 3660 ..... E-6824
NAS 1.15:105415
NASA-TM-105415
N92-30723* # p 3696 ..... NAS 1.26:190559
NASA-CR-190559
RIACS-TR-90.41
N92-30724* # p 3690 ..... NAS 1.26:190553
NASA-CR-190553
RIACS-TR-92.10
N92-30725 # p 3718 ..... ETN-92-91740
LINO-1991-5
N92-30726 # p 3718 ..... NO REPORT NUMBER
N92-30727 # p 3718 ..... NO REPORT NUMBER
N92-30728 # p 3718 ..... NO REPORT NUMBER
N92-30729 # p 3625 ..... ETN-92-91742
N92-30730 # p 3625 ..... NO REPORT NUMBER
N92-30731 # p 3625 ..... NO REPORT NUMBER
N92-30732 # p 3625 ..... NO REPORT NUMBER
N92-30733* # p 3744 ..... L-17018
NAS 1.15:4331
NASA-TM-4331
N92-30734* # p 3660 ..... E-7091
NAS 1.15:105730
NASA-TM-105730
N92-30735* # p 3679 ..... NAS 1.15:107630
NASA-TM-107630
N92-30736* # p 3588 ..... NAS 1.15:107577
NASA-TM-107577
N92-30737* # p 3637 ..... NAS 1.15:107648
NASA-TM-107648
N92-30738* # p 3660 ..... NAS 1.26:190243
NASA-CR-190243
N92-30739* # p 3682 ..... NAS 1.26:190266
NASA-CR-190266
N92-30740* # p 3575 ..... MCAT-92-009
NAS 1.26:190045
NASA-CR-190045
N92-30741* # p 3576 ..... NO REPORT NUMBER
N92-30742* # p 3576 ..... NO REPORT NUMBER
N92-30743 # p 3656 ..... AD-A248833
NRL/MR/4790-92-6954
N92-30744 # p 3604 ..... CONF-9203108-1
DE92-010471
N92-30745 # p 3685 ..... AD-A249904
DOT/FAA/AM-92/19
N92-30746 # p 3723 ..... CFFTP-G-91112
DE92-011942
DOE/ER-54091/1
N92-30747* # p 3576 ..... L-17054
NAS 1.60:3232
NASA-TP-3232
N92-30748 # p 3729 ..... DE92-001223
NREL/TP-451-4751
N92-30749 # p 3594 ..... CONF-920707-9
DE92-006679
SAND-91-8721
N92-30750 # p 3715 ..... ETN-92-91719
RAL-91-090
N92-30751* # p 3635 ..... NAS 1.26:4462
NASA-CR-4462
N92-30752* # p 3580 ..... NAS 1.15:107651
NASA-TM-107651
N92-30753* # p 3582 ..... NAS 1.26:190290
NASA-CR-190290
N92-30754* # p 3613 ..... MC-PY-92-011
NAS 1.26:184319
NASA-CR-184319
N92-30755 # p 3616 ..... RAND-P-7747-RGS
N92-30756* # p 3676 ..... NAS 1.26:190478
NASA-CR-190478
N92-30757* # p 3625 ..... JPR-9950-1370
NAS 1.26:190473
NASA-CR-190473
N92-30758 # p 3604 ..... AD-A249438
MTL-TR-92-15
N92-30759 # p 3597 ..... AD-A249439
MTL-TR-92-17
N92-30760 # p 3616 ..... AD-A249440
RL-TR-92-34
N92-30761 # p 3616 ..... AD-A249441
ESD-TR-944
TR-944
N92-30762 # p 3616 ..... AD-A249442
ESD-TR-91-174
TR-940
N92-30763 # p 3661 ..... DE92-012217
EGG-ME-9968
N92-30764 # p 3626 ..... DE92-013457
SAND-92-0448
N92-30765* # p 3635 ..... A-92027
NAS 1.15:103909
NASA-TM-103909

N92-30766 # p 3663 ..... AD-A252652
R/D-6571-AN-01
N92-30767 # p 3607 ..... AD-A252685
SWRI-03-3685
WL-TR-92-2015
N92-30768 # p 3744 ..... NO REPORT NUMBER
N92-30769 # p 3584 ..... AGARD-AR-315
ISBN-92-835-0669-3
N92-30770 # p 3674 ..... ANL/ESD/TM-22-VOL-1
DE92-012102
N92-30771 # p 3708 ..... AD-A249265
ARO-27868.14-MA
N92-30772 # p 3729 ..... AD-A249406
ARO-26195.14-PH
N92-30773 # p 3595 ..... AD-A249407
ARO-26591.5-MS
N92-30774 # p 3656 ..... AD-A249423
ARO-25631.13-PH
N92-30775 # p 3635 ..... AD-A249424
NRL/MR/4400-92-6979
N92-30776 # p 3706 ..... AD-A249425
NRL/MR/4440-92-6967
N92-30777 # p 3585 ..... AD-A249436
FAA/APO-210
FAA/APO-91-4
N92-30778* # p 3701 ..... NAS 1.26:190530
NASA-CR-190530
N92-30779* # p 3592 ..... E-6571
/ NAS 1.15:105244
NASA-TM-105244
N92-30780 p 3715 ..... ITN-92-85163
N92-30781 p 3729 ..... ITN-92-85166
N92-30782 p 3715 ..... ITN-92-85169
N92-30783 # p 3721 ..... AD-A249794
ARO-29288.1-GS
N92-30784 # p 3657 ..... AD-A249798
ARO-26160.22-PH
N92-30785 # p 3598 ..... PB92-180652
VAL-6/1991
N92-30786 # p 3718 ..... CONF-920331-28
DE92-013969
SSCL-PREPRINT-51
N92-30787 # p 3598 ..... DE92-014006
DOE/ER-45280/T4
N92-30788 # p 3604 ..... NISTIR-4627
PB92-181080
N92-30789 # p 3706 ..... IHES/M/92/16
PB92-177997
N92-30790 # p 3706 ..... IHES/M/92/9
PB92-178003
N92-30791 # p 3716 ..... DE92-014428
DOE/ER-40677/1-PT-1
N92-30792 # p 3604 ..... CONF-9108168-3
DE92-014786
UCRL-JC-109730
N92-30793 # p 3595 ..... AD-A249906
ARO-26298.4-CH
N92-30794 # p 3604 ..... AD-A249926
TR-8
N92-30795 # p 3605 ..... AD-A249927
TR-7
N92-30796 # p 3605 ..... AD-A249929
TR-11
N92-30797 # p 3742 ..... CONF-9110336-2
DE92-010483
N92-30798 # p 3716 ..... DE92-622374
IC-91/367
N92-30799 # p 3731 ..... DE92-622375
IC-91/369
N92-30800 # p 3731 ..... DE92-622376
IC-91/370
N92-30801 # p 3711 ..... DE92-622377
IC-91/371
N92-30802 # p 3663 ..... AD-A249500
ARCCB-TR-92009
N92-30803 # p 3708 ..... ANL/CP-75636
CONF-920291-1
DE92-010278
N92-30804 # p 3605 ..... CONF-9203127-1
DE92-011358
SAND-92-0193C
N92-30805 # p 3657 ..... CONF-911296-6
DE92-011362
LA-UR-92-896
N92-30806 # p 3724 ..... CONF-920362-19
DE92-011365
LA-UR-92-875
N92-30807 # p 3626 ..... CONF-920669-4
DE92-011384
SAND-92-0736C
N92-30808 # p 3670 ..... CONF-9206114-5
DE92-011386
SAND-92-0523C
N92-30809 # p 3592 ..... CONF-920673-3-EXTD-ABST
DE92-011670
N92-30810 # p 3724 ..... CONF-920362-23
DE92-011691
N92-30811 # p 3718 ..... CONF-920315-16
DE92-011692
SSCL-PREPRINT-80
N92-30812 # p 3699 ..... DE92-011704
FNAL-TM-1773
N92-30813 # p 3626 ..... CONF-911106-93
DE92-011727
LBL-31596
N92-30814 # p 3595 ..... AD-A249911
ARO-25245.15-EG
N92-30815 # p 3592 ..... AD-A249912
ARO-25397.9-MS
N92-30816 # p 3605 ..... AD-A249920
TR-12
N92-30817 # p 3605 ..... AD-A249928
TR-10
N92-30818* # p 3589 ..... CONF-920104-23
DE92-004262
NAS 1.15:105521
NASA-TM-105521
WHC-SA-1402
N92-30819 # p 3735 ..... AD-A249030
RL-TM-92-8
N92-30820 # p 3696 ..... AD-A249035
N92-30821 # p 3595 ..... AD-A249062
TR-42
N92-30822 # p 3637 ..... DE92-010399
SAND-91-2579
N92-30823 # p 3663 ..... CONF-920631-16
DE92-010431
N92-30824 # p 3724 ..... CONF-910857-9
DE92-010437
UCRL-CR-107774
N92-30825 # p 3731 ..... CONF-9105239-2
DE92-010475
ITP-SB-91-34
LBL-31382
UCB-PTH-91/52
N92-30826 # p 3716 ..... ANL/CP-73759
CONF-911202-68
DE92-010498
N92-30827 # p 3637 ..... CONF-9110359-1
DE92-010647
N92-30828 # p 3743 ..... CONF-9111141-5
DE92-010650
FNAL/C-92/63
N92-30829 # p 3683 ..... DE92-010657
DOE/ER-13261/6
N92-30830 # p 3605 ..... CONF-920445-1
DE92-012634
SAND-92-0864C
N92-30831 # p 3635 ..... AD-A250801
SU-TF-54
N92-30832 # p 3682 ..... AD-A250832
CRREL-92-1
N92-30833 # p 3724 ..... DE92-012139
DOE/ET-53088/541
IFSR-541
N92-30834 # p 3598 ..... CONF-9111209
DE92-012312
EGG-FSP-10017
N92-30835 # p 3595 ..... AD-A249812
ARO-28316.1-EG
N92-30836 # p 3626 ..... AD-A249814
RAY/RD/S-4752
N92-30837 # p 3670 ..... DE92-001245
NREL/TP-442-4822
N92-30838 # p 3605 ..... AD-A250644
N92-30839 # p 3719 ..... CONF-920331-29
DE92-013964
SSCL-PREPRINT-26
N92-30840 # p 3719 ..... CONF-920331-25
DE92-013967
SSCL-PREPRINT-33
N92-30841 # p 3716 ..... DE92-014531
DOE/ER-40661/2
N92-30842 # p 3626 ..... DE92-014591
DOE/ID-13074/T3
N92-30843 # p 3706 ..... AD-A252140
ARO-92-1
N92-30844 # p 3688 ..... AD-A252332
AL-TR-1992-0062
N92-30845 # p 3716 ..... AD-A252336
TR-29
N92-30846 # p 3729 ..... AD-A252352
N92-30847 # p 3606 ..... CONF-920402-29
DE92-015147
LA-UR-92-1558
N92-30848 # p 3657 ..... ANL/CP-75202
CONF-9109356-1
DE92-010274
N92-30849 # p 3585 ..... AD-A249944
AD-E951786
AMSMI/TR-RD-WS-92-1
N92-30850 # p 3710 ..... AD-A249969
N92-30851 # p 3626 ..... AD-A250376
NRL/MR/1003-92-6989
N92-30852 # p 3635 ..... AD-A250409
AFOSR-92-0408TR
N92-30853 # p 3716 ..... CONF-910746-5
DE92-011779
N92-30854 # p 3729 ..... CONF-911267-3
DE92-011848
UCRL-JC-108738
N92-30855 # p 3740 ..... CONF-9107218-2
DE92-011850
UCRL-JC-109222
N92-30856 # p 3740 ..... CONF-9110360-1
DE92-011495
LA-UR-92-980
N92-30857 # p 3608 ..... CONF-9203140-1
DE92-012144
SAND-92-8462C
WSS/CI-92-6
N92-30858 # p 3598 ..... CONF-9102170-1
DE92-012154
IS-M-685
N92-30859 # p 3663 ..... CONF-920633-1
DE92-012631
SAND-91-1730C
N92-30860 # p 3660 ..... ANL/CP-74864
CONF-9206155-1
DE92-013057
N92-30861 # p 3682 ..... DE92-013064
DOE/ER-60982/2
N92-30862 # p 3739 ..... CONF-9202103-2
DE92-013443
UCRL-JC-110303
N92-30863 # p 3616 ..... AD-A246988
ESD-TR-91-176
MIT-TR-916-VOL-3
N92-30864 # p 3598 ..... AD-A247218
AFOSR-92-0115TR
N92-30865 # p 3598 ..... DE92-012111
KCP-613-4501
N92-30866 # p 3606 ..... DE92-012112
KCP-613-4504
N92-30867 # p 3679 ..... AD-A249873
AFIT/CI/CIA-91-117
N92-30868 # p 3676 ..... AD-A249874
AFIT/CI/CIA-91-121
N92-30869 # p 3617 ..... AD-A249880
N92-30870 # p 3663 ..... AD-A249886
DREA-TM-92/209
N92-30871 # p 3592 ..... AD-A249888
GIT-E-19-673
N92-30872 # p 3598 ..... AD-A249916
AFOSR-91-0148
EOARD-TR-92-07
REPT-524-679
N92-30873 # p 3606 ..... AD-A249917
TR-9
N92-30874 # p 3592 ..... AD-A249918
ARO-26439.48-MS
N92-30875 # p 3595 ..... AD-A249919
TR-10
N92-30876 # p 3617 ..... AD-A250239
N92-30877 # p 3599 ..... CONF-920146-3
DE92-014703
PNL-SA-19683
N92-30878 # p 3580 ..... AD-A251127
PC-86-08
USAAVSCOM-TR-92-D-2
N92-30879 # p 3596 ..... DE91-002147
NREL/TP-253-4282
N92-30880 # p 3724 ..... DE92-014028
DOE/ET-53088/550
IFSR-550
N92-30881 # p 3719 ..... CONF-920331-19
DE92-014186
SSCL-516
N92-30882 # p 3596 ..... DE91-002143
NREL/TP-253-4278
N92-30883 # p 3596 ..... CONF-920584-3
DE92-001277
DOE/NBM-92001277
N92-30884 # p 3725 ..... DE92-013883
DOE/ET-53088/544
IFSR-544
N92-30885 # p 3729 ..... CONF-920402-14
DE92-014780
UCRL-JC-109064
N92-30886 # p 3696 ..... CONF-920803-6
DE92-014453
N92-30887 # p 3613 ..... DE92-015391
SAND-92-0243
N92-30888 # p 3599 ..... DE92-015545
ORNL/SUB-88-07685/02
N92-30889 # p 3733 ..... CONF-9206151-3
DE92-015768
SAND-92-1102C

N92-30890 # p 3711 ..... DE92-015845
KCP-613-4664
N92-30891 # p 3709 ..... DE92-015977
LA-12302-MS
N92-30892 # p 3696 ..... DE92-015991
SAND-91-8231
N92-30893 # p 3637 ..... DE92-013461
SAND-91-1624
N92-30894* # p 3636 ..... E-7041
NAS 1.26:189177
NASA-CR-189177
N92-30895 # p 3730 ..... AD-A250757
HDL-TM-92-5
N92-30896 # p 3671 ..... CONF-920678-4
DE92-010566
NREL/TP-441-4800
N92-30897 # p 3585 ..... NO REPORT NUMBER
N92-30898* # p 3709 ..... AVSCOM-TR-92-C-024
E-7235
NAS 1.15:105805
NASA-TM-105805
RTOP 505-62-0K
N92-30899 # p 3596 ..... CONF-9204151-1
DE92-013971
WSRC-MS-92-131
N92-30900 # p 3725 ..... DE92-014589
DOE/ER-53207/7
N92-30901 # p 3626 ..... DE92-014608
DOE/ER-45147/7
N92-30902* # p 3627 ..... NAS 1.15:103595
NASA-TM-103595
N92-30903 # p 3636 ..... DE92-015778
SAND-91-2650
N92-30904 # p 3608 ..... DE92-015798
DOE/PC-89786/T12
N92-30905 # p 3696 ..... DE92-015905
SU-SOL-92-2
N92-30906* # p 3592 ..... NAS 1.26:190658
NASA-CR-190658
N92-30907* # p 3689 ..... NAS 1.15:107663
NASA-TM-107663
N92-30908* # p 3732 ..... AIAA PAPER 92-3123
E-7119
NAS 1.26:189187
NASA-CR-189187
N92-30909* # p 3576 ..... L-16929
NAS 1.60:3186
NASA-TP-3186
N92-30910 # p 3667 ..... NO REPORT NUMBER
N92-30911 # p 3668 ..... NO REPORT NUMBER
N92-30912 # p 3668 ..... NO REPORT NUMBER
N92-30913 # p 3668 ..... NO REPORT NUMBER
N92-30914 # p 3668 ..... NO REPORT NUMBER
N92-30915 # p 3668 ..... NO REPORT NUMBER
N92-30916 # p 3668 ..... NO REPORT NUMBER
N92-30917 # p 3668 ..... NO REPORT NUMBER
N92-30918 # p 3669 ..... NO REPORT NUMBER
N92-30919 # p 3669 ..... NO REPORT NUMBER
N92-30920 # p 3669 ..... NO REPORT NUMBER
N92-30921* # p 3742 ..... NAS 1.26:190605
NASA-CR-190605
N92-30922* # p 3583 ..... NAS 1.26:190667
NASA-CR-190667
OSU-ECE-NASA-92-02
N92-30923* # p 3617 ..... JPL-PUBL-91-35
NAS 1.26:190459
NASA-CR-190459
N92-30924* # p 3617 ..... NO REPORT NUMBER
N92-30925* # p 3617 ..... NO REPORT NUMBER
N92-30926* # p 3617 ..... NO REPORT NUMBER
N92-30927* # p 3617 ..... NO REPORT NUMBER
N92-30928* # p 3618 ..... NO REPORT NUMBER
N92-30929* # p 3618 ..... NO REPORT NUMBER
N92-30930* # p 3618 ..... NO REPORT NUMBER
N92-30931* # p 3618 ..... NO REPORT NUMBER
N92-30932* # p 3618 ..... NO REPORT NUMBER
N92-30933* # p 3619 ..... NO REPORT NUMBER
N92-30934* # p 3619 ..... NO REPORT NUMBER
N92-30935* # p 3619 ..... NO REPORT NUMBER
N92-30936* # p 3619 ..... NO REPORT NUMBER
N92-30937* # p 3619 ..... NO REPORT NUMBER
N92-30938* # p 3619 ..... NO REPORT NUMBER
N92-30939* # p 3619 ..... NO REPORT NUMBER
N92-30940* # p 3620 ..... NO REPORT NUMBER
N92-30941* # p 3620 ..... NO REPORT NUMBER
N92-30942* # p 3620 ..... NO REPORT NUMBER
N92-30943* # p 3620 ..... NO REPORT NUMBER
N92-30944* # p 3620 ..... NO REPORT NUMBER
N92-30945* # p 3621 ..... NO REPORT NUMBER
N92-30946* # p 3621 ..... NO REPORT NUMBER
N92-30947 # p 3576 ..... AGARD-AR-299
ISBN-92-835-0670-7
N92-30948* # p 3660 ..... AVSCOM-TR-92-C-003
E-7115
NAS 1.15:105718
NASA-TM-105718
N92-30949* # p 3671 ..... NAS 1.26:190055
NASA-CR-190055
N92-30950 # p 3697 ..... ETN-92-91717
N92-30951 # p 3697 ..... NO REPORT NUMBER
N92-30952 # p 3697 ..... NO REPORT NUMBER
N92-30953 # p 3697 ..... NO REPORT NUMBER
N92-30954 # p 3697 ..... NO REPORT NUMBER
N92-30955 # p 3697 ..... NO REPORT NUMBER
N92-30956 # p 3697 ..... NO REPORT NUMBER
N92-30957 # p 3698 ..... NO REPORT NUMBER
N92-30958 # p 3587 ..... N-3283-AF/NASA
NAS 1.26:190345
NASA-CR-190345
N92-30959* # p 3733 ..... NAS 1.15:107811
NASA-TM-107811
N92-30960* # p 3698 ..... NAS 1.26:190489
NASA-CR-190489
N92-30961* # p 3676 ..... NAS 1.26:190485
NASA-CR-190485
N92-30962* # p 3677 ..... NAS 1.26:190560
NASA-CR-190560
N92-30963 p 3664 ..... AR-006-858
MRL-TN-600
N92-30964* # p 3664 ..... NAS 1.15:104159
NASA-TM-104159
N92-30965* # p 3581 ..... NAS 1.26:189650
NASA-CR-189650
N92-30966 # p 3711 ..... ETN-92-91669
ONERA-RF-17/3641-PY
N92-30967 # p 3716 ..... NIFS-129
N92-30968 p 3669 ..... ETN-92-91730
N92-30969 # p 3592 ..... ETN-92-91898
MBB-Z-0409-91-PUB
N92-30970 # p 3671 ..... ETN-92-91899
MBB-Z-0412-91-PUB
N92-30971* # p 3612 ..... NAS 1.15:103594
NASA-TM-103594
N92-30972* # p 3582 ..... E-7226
NAS 1.15:105796
NASA-TM-105796
N92-30973 p 3741 ..... NO REPORT NUMBER
N92-30974* # p 3733 ..... NAS 1.26:190519
NASA-CR-190519
N92-30975* # p 3721 ..... NAS 1.26:190492
NASA-CR-190492
N92-30976 # p 3585 ..... DOT/FAA/CT-TN91/40
N92-30977* # p 3576 ..... CFD-26
NAS 1.26:190182
NASA-CR-190182
N92-30978* # p 3579 ..... MDC-91K0792
NAS 1.26:4450
NASA-CR-4450
N92-30979* # p 3711 ..... NAS 1.15:107627
NASA-TM-107627
N92-30980 # p 3578 ..... DOT/FAA/RD-92/12
N92-30981* # p 3589 ..... NAS 1.26:190515
NASA-CR-190515
N92-30982* # p 3636 ..... A-92091
NAS 1.15:103935
NASA-TM-103935
N92-30983 # p 3710 ..... NIFS-103
N92-30984 # p 3725 ..... NIFS-PROC-9
N92-30985 # p 3725 ..... NIFS-131
N92-30986* # p 3593 ..... E-7007
NAS 1.15:105648
NASA-TM-105648
N92-30987* p 3685 ..... NAS 1.21:7011(363)
NASA-SP-7011(363)
N92-30988* # p 3664 ..... NAS 1.26:190471
NASA-CR-190471
N92-30989* # p 3589 ..... NAS 1.26:190569
NASA-CR-190569
N92-30990 # p 3717 ..... NIFS-115
N92-30991 # p 3725 ..... DE92-799109
NIFS-126
N92-30992 # p 3725 ..... DE92-799107
NIFS-124
N92-30993 # p 3725 ..... NIFS-138
N92-30994 # p 3725 ..... NIFS-139
N92-30995 # p 3726 ..... NIFS-143
N92-30996 p 3744 AERONOMICA-ACTA-F-42-1991
ETN-92-91705
N92-30997 # p 3657 ..... ESA-TT-1234
ETN-92-91746
ONERA-NT-1990-5
N92-30998* # p 3582 ..... E-7245
NAS 1.15:105814
NASA-TM-105814
N92-30999 # p 3730 ..... ANL/CP-74758
CONF-920402-28
DE92-015182
N92-31000 # p 3730 ..... CONF-920402-22
DE92-014950
SAND-92-1183C
N92-31001 # p 3735 ..... CONF-9205191-1
DE92-015156
PNL-SA-19807
N92-31002 # p 3726 ..... DE92-015166
UW-CPTC-92-2
N92-31003 # p 3679 ..... AD-A248898
NUWC-NPT-TD-10012
N92-31004 # p 3627 ..... AD-A249662
ARO-26051.5-EL
N92-31005 # p 3593 ..... AD-A252693
UDR-TR-92-25
WL-TR-92-4027
N92-31006 # p 3596 ..... DE92-014625
DOE/PC-79812/T2
N92-31007 # p 3621 ..... CONF-9111226-1
DE92-014715
UCRL-JC-109212
N92-31008 # p 3677 ..... CONF-9204112-1
DE92-011134
LA-UR-92-949
N92-31009 # p 3677 ..... CONF-920793-2
DE92-015084
N92-31010 # p 3599 ..... CONF-920514-4
DE92-015091
PNL-SA-20305
N92-31011 # p 3685 ..... CONF-920501-16
DE92-015092
PNL-SA-20194
N92-31012 # p 3589 ..... CONF-920801-4
DE92-015102
N92-31013* # p 3637 ..... L-17126-PT-2
NAS 1.55:3158-PT-2
NASA-CP-3158-PT-2
N92-31014* # p 3638 ..... NO REPORT NUMBER
N92-31015* # p 3638 ..... NO REPORT NUMBER
N92-31016* # p 3638 ..... NO REPORT NUMBER
N92-31017* # p 3638 ..... NO REPORT NUMBER
N92-31018* # p 3639 ..... NO REPORT NUMBER
N92-31019* # p 3639 ..... NO REPORT NUMBER
N92-31020* # p 3639 ..... NO REPORT NUMBER
N92-31021* # p 3639 ..... NO REPORT NUMBER
N92-31022* # p 3639 ..... NO REPORT NUMBER
N92-31023* # p 3639 ..... NO REPORT NUMBER
N92-31024* # p 3639 ..... NO REPORT NUMBER
N92-31025* # p 3640 ..... NO REPORT NUMBER
N92-31026* # p 3640 ..... NO REPORT NUMBER
N92-31027* # p 3640 ..... NO REPORT NUMBER
N92-31028* # p 3640 ..... NO REPORT NUMBER
N92-31029* # p 3641 ..... NO REPORT NUMBER
N92-31030* # p 3641 ..... NO REPORT NUMBER
N92-31031* # p 3641 ..... NO REPORT NUMBER
N92-31032* # p 3641 ..... NO REPORT NUMBER
N92-31033* # p 3641 ..... NO REPORT NUMBER
N92-31034* # p 3641 ..... NO REPORT NUMBER
N92-31035* # p 3642 ..... NO REPORT NUMBER
N92-31036* # p 3642 ..... NO REPORT NUMBER
N92-31037* # p 3642 ..... NO REPORT NUMBER
N92-31038* # p 3643 ..... NO REPORT NUMBER
N92-31039* # p 3643 ..... NO REPORT NUMBER
N92-31040* # p 3643 ..... NO REPORT NUMBER
N92-31041* # p 3643 ..... NO REPORT NUMBER
N92-31042* # p 3644 ..... NO REPORT NUMBER
N92-31043* # p 3644 ..... NO REPORT NUMBER
N92-31044* # p 3644 ..... NO REPORT NUMBER
N92-31045* # p 3644 ..... NO REPORT NUMBER
N92-31046* # p 3644 ..... NO REPORT NUMBER
N92-31047* # p 3645 ..... NO REPORT NUMBER
N92-31048* # p 3645 ..... NO REPORT NUMBER
N92-31049* # p 3645 ..... NO REPORT NUMBER
N92-31050* # p 3645 ..... NO REPORT NUMBER
N92-31051* # p 3645 ..... NO REPORT NUMBER
N92-31052* # p 3645 ..... NO REPORT NUMBER
N92-31053* # p 3646 ..... NO REPORT NUMBER
N92-31054* # p 3646 ..... NO REPORT NUMBER
N92-31055* # p 3646 ..... NO REPORT NUMBER
N92-31056* # p 3646 ..... NO REPORT NUMBER
N92-31057* # p 3646 ..... NO REPORT NUMBER
N92-31058* # p 3646 ..... NO REPORT NUMBER
N92-31059* # p 3647 ..... NO REPORT NUMBER
N92-31060* # p 3647 ..... NO REPORT NUMBER
N92-31061* # p 3647 ..... NO REPORT NUMBER
N92-31062* # p 3647 ..... NO REPORT NUMBER
N92-31063* # p 3647 ..... NO REPORT NUMBER
N92-31064* # p 3648 ..... NO REPORT NUMBER
N92-31065* # p 3648 ..... NO REPORT NUMBER
N92-31066* # p 3648 ..... NO REPORT NUMBER
N92-31067* # p 3648 ..... NO REPORT NUMBER
N92-31068* # p 3648 ..... NO REPORT NUMBER
N92-31069* # p 3649 ..... NO REPORT NUMBER
N92-31070* # p 3649 ..... NO REPORT NUMBER
N92-31071* # p 3649 ..... NO REPORT NUMBER
N92-31072* # p 3649 ..... NO REPORT NUMBER
N92-31073* # p 3649 ..... NO REPORT NUMBER
N92-31074* # p 3649 ..... NO REPORT NUMBER
N92-31075* # p 3650 ..... NO REPORT NUMBER
N92-31076* # p 3650 ..... NO REPORT NUMBER
N92-31077* # p 3650 ..... NO REPORT NUMBER
N92-31078* # p 3650 ..... NO REPORT NUMBER

N92-31079* # p 3650 ..... NO REPORT NUMBER
N92-31080* # p 3651 ..... NO REPORT NUMBER
N92-31081* # p 3651 ..... NO REPORT NUMBER
N92-31082* # p 3651 ..... NO REPORT NUMBER
N92-31083* # p 3651 ..... NO REPORT NUMBER
N92-31084* # p 3651 ..... NO REPORT NUMBER
N92-31085* # p 3652 ..... NO REPORT NUMBER
N92-31086* # p 3652 ..... NO REPORT NUMBER
N92-31087* # p 3652 ..... NO REPORT NUMBER
N92-31088* # p 3652 ..... NO REPORT NUMBER
N92-31089* # p 3652 ..... NO REPORT NUMBER
N92-31090* # p 3653 ..... NO REPORT NUMBER
N92-31091* # p 3653 ..... NO REPORT NUMBER
N92-31092* # p 3653 ..... NO REPORT NUMBER
N92-31093* # p 3653 ..... NO REPORT NUMBER
N92-31094* # p 3653 ..... NO REPORT NUMBER
N92-31095* # p 3653 ..... NO REPORT NUMBER
N92-31096* # p 3654 ..... NO REPORT NUMBER
N92-31097* # p 3654 ..... NO REPORT NUMBER
N92-31098* # p 3654 ..... NO REPORT NUMBER
N92-31099* # p 3654 ..... NO REPORT NUMBER
N92-31100* # p 3654 ..... NO REPORT NUMBER
N92-31101* # p 3654 ..... NO REPORT NUMBER
N92-31102* # p 3655 ..... NO REPORT NUMBER
N92-31103* # p 3655 ..... NO REPORT NUMBER
N92-31104* # p 3655 ..... NO REPORT NUMBER
N92-31105* # p 3655 ..... NO REPORT NUMBER
N92-31106* # p 3655 ..... NO REPORT NUMBER
N92-31107 # p 3627 ..... CONF-9108140
DE92-011133
LA-UR-92-922
N92-31108 # p 3741 ..... CONF-920184-2
DE92-011158
LA-UR-92-879
N92-31109 # p 3655 ..... ANL-HEP-CP-92-13
CONF-920331-2
DE92-011197
N92-31110 # p 3599 ..... AD-A249856
MTL-TR-92-2
N92-31111 # p 3700 ..... CONF-920867-2
DE92-011656
SAND-92-0330C
N92-31112 # p 3599 ..... CONF-920819-13
DE92-011667
N92-31113 # p 3671 ..... CONF-920801-2
DE92-011755
DOE/METC-C/92/7014
N92-31114 # p 3726 ..... CONF-920772-1
DE92-011786
N92-31115 # p 3657 ..... CONF-920853-3
DE92-012696
UCRL-JC-110098
N92-31116 # p 3726 ..... DE92-015077
DOE/ER-53263/22
LRC-92-32
N92-31117 # p 3671 ..... DE92-014586
DOE/SF-15799/T14
N92-31118 # p 3726 ..... CONF-920362-33
DE92-014718
UCRL-JC-109355
N92-31119 # p 3599 ..... CONF-9110252-2
DE92-014776
UCRL-JC-108775
N92-31120 # p 3661 ..... CONF-920331-50
DE92-014844
SSCL-PREPRINT-52
N92-31121 # p 3674 ..... CONF-910626-16
DE92-014887
UCRL-JC-106406
N92-31122 # p 3577 ..... AD-A249628
VPI-AOE-188
N92-31123 # p 3664 ..... DE92-011515
SAND-92-0493
N92-31124 # p 3600 ..... CONF-9203130-1
DE92-011526
UCRL-JC-108838
N92-31125 # p 3600 ..... CONF-911202-75
DE92-011530
UCRL-JC-107793
N92-31126 # p 3721 ..... AD-A249986
AFOSR-92-0254TR
N92-31127 # p 3686 ..... AD-A249997
N92-31128 # p 3706 ..... AD-A250352
AFOSR-92-0351TR
REPT-1-52150
N92-31129 # p 3621 ..... AD-A250488
AFOSR-92-0348TR
N92-31130 # p 3621 ..... AD-A250489
MTR-11277
N92-31131 # p 3710 ..... DE92-015287
DOE/ER-45373/4
N92-31132 # p 3735 ..... CONF-9110344-9
DE92-015338
WSRC-MS-91-392
N92-31133 # p 3732 ..... DE92-630231
IC-91/340
N92-31134 # p 3706 ..... DE92-630235
IC-91/398
N92-31135 # p 3707 ..... DE92-630236
IC-91/399
N92-31136 # p 3732 ..... DE92-630239
IC-91/329
N92-31137 # p 3717 ..... DE92-015314
RFP-TRANS-523
N92-31138 # p 3600 ..... CONF-911202-73
DE92-011525
UCRL-JC-108753
N92-31139 # p 3669 ..... AD-A249915
COELMN/PD-90/11
N92-31140 # p 3707 ..... AD-A250004
ARCCB-TR-92012
N92-31141 # p 3606 ..... AD-A250351
N92-31142 # p 3677 ..... AD-A250403
N92-31143 # p 3686 ..... AD-A250442
AFOSR-92-0410TR
N92-31144 # p 3627 ..... DE92-015160
KCP-613-4749
N92-31145 # p 3732 ..... DE92-630241
IC-91/360
N92-31146 # p 3606 ..... DE92-015312
RFP-TRANS-525
N92-31147 # p 3717 ..... DE92-015313
RFP-TRANS-524
N92-31148 # p 3701 ..... ISSN-0208-5658
N92-31149 # p 3721 ..... ISSN-0208-5658
N92-31150* # p 3621 ..... NASA-CASE-LAR-14679-2
US-PATENT-APPL-SN-790731
N92-31151 p 3711 ..... BBC-RD-1992/4
N92-31152 # p 3683 ..... ISSN-0800-4412
NDRE/PUBL-92/1001
N92-31153* # p 3674 ..... NAS 1.26:190624
NASA-CR-190624
N92-31154* # p 3698 ..... NAS 1.26:190646
NASA-CR-190646
N92-31155* # p 3664 ..... NAS 1.15:107642
NASA-TM-107642
USAAVSCOM-TR-92-B-010
N92-31156* # p 3621 ..... NAS 1.26:190650
NASA-CR-190650
TRC-EM-CAB-9203
N92-31157* # p 3577 ..... NAS 1.26:190649
NASA-CR-190649
N92-31158* # p 3700 ..... NAS 1.26:189649
NASA-CR-189649
N92-31159 # p 3578 ..... NTSB/AAR-90/01
NTSB/AAR-92/02
PB92-910402
N92-31160* # p 3586 ..... NAS 1.15:107580
NASA-TM-107580
N92-31161* # p 3596 ..... NAS 1.26:184356
NASA-CR-184356
N92-31162* # p 3742 ..... NAS 1.26:190664
NASA-CR-190664
N92-31163 # p 3600 ..... DE92-782044
JAERI-M-91-189
N92-31164* # p 3582 ..... NAS 1.26:189087
NASA-CR-189087
N92-31165 # p 3580 ..... DOT/FAA/CT-TN92/1
N92-31166* # p 3689 ..... A-91224
NAS 1.15:103888
NASA-TM-103888
N92-31167* # p 3686 ..... A-91186
NAS 1.15:103874
NASA-TM-103874
N92-31168* # p 3743 ..... NAS 1.26:190522
NASA-CR-190522
N92-31169 # p 3735 ..... GPO-57-805
S-REPT-102-356
N92-31170 # p 3736 ..... NO REPORT NUMBER
N92-31171 # p 3577 ..... AD-A250654
WL-TR-91-3120
N92-31172* # p 3583 ..... E-7061
NAS 1.15:105682
NASA-TM-105682
N92-31173 p 3711 ..... BBC-RD-1992/3
N92-31174* # p 3580 ..... NAS 1.15:107653
NASA-TM-107653
N92-31175* # p 3583 ..... L-16956
NAS 1.15:4302
NASA-TM-4302
N92-31176 # p 3672 ..... DE92-014942
ORNL/TM-12081
N92-31177 # p 3600 ..... CONF-9206173-3
DE92-016231
SAND-92-1233C
N92-31178 # p 3596 ..... AD-A249729
N92-31179 # p 3669 ..... AD-A249730
N92-31180 # p 3622 ..... AD-A249793
ARO-28584.1-GS-EQ
N92-31181 # p 3674 ..... CONF-9109358
DE92-014317
N92-31182 # p 3657 ..... CONF-9202111-2
DE92-015212
LA-UR-92-1539
N92-31183 # p 3675 ..... DE92-015217
DOE/ER-61205/1
N92-31184 # p 3597 ..... CONF-920574-3
DE92-015238
N92-31185 # p 3708 ..... DE92-015902
LA-12266-MS
N92-31186 # p 3600 ..... DE92-015916
DOE/ER-45413/2
N92-31187 # p 3721 ..... DE92-015963
SSCL-PREPRINT-120
N92-31188 # p 3672 ..... DE92-015985
DOE/FE-0260P
N92-31189 # p 3707 ..... DE92-016000
SAND-92-8548
N92-31190 # p 3730 ..... ANL/CP-76267
CONF-920402-32
DE92-016192
N92-31191 # p 3730 ..... DE92-630567
IC-91/378
N92-31192 # p 3585 ..... AD-D015259
US-PATENT-APPL-SN-800785
N92-31193 # p 3579 ..... AD-A250749
WES/MP/GL-92-10
N92-31194 # p 3709 ..... AD-A250756
ARCCB-TR-92015
N92-31195 # p 3722 ..... CONF-920819-11
DE92-011886
Y/DW-1139
N92-31196 # p 3597 ..... CONF-920574-2
DE92-014460
N92-31197 # p 3726 ..... CONF-920610-1
DE92-014461
N92-31198 # p 3719 ..... CONF-920113-5
DE92-014481
LBL-32121
N92-31199 # p 3743 ..... CONF-9109182-4
CONF-9109378-1
DE92-014014
DOE/ER-40427/37-N91
N92-31200 # p 3730 ..... CONF-920141-7
DE92-015207
LA-UR-92-1485
N92-31201 # p 3717 ..... CONF-920792-3
DE92-015208
LA-UR-92-1478
N92-31202 # p 3608 ..... CONF-920796-5
DE92-015210
LA-UR-92-1476
N92-31203 # p 3732 ..... DE92-630566
IC-91/330
N92-31204 # p 3589 ..... CONF-920803-8
DE92-015274
LA-UR-92-1674
N92-31205 # p 3717 ..... DE92-015300
ORNL/TR-92/17
N92-31206 # p 3743 ..... DE92-010555
NREL/TP-463-4856
N92-31207 # p 3607 ..... AD-A249747
CSU-TR-68
N92-31208* # p 3580 ..... H-1795
NAS 1.26:186020
NASA-CR-186020
N92-31209 # p 3733 ..... AD-A250701
N92-31210 # p 3627 ..... AD-A250895
N92-31211 # p 3579 ..... DOT/FAA/SE-92/3
N92-31212 # p 3622 ..... DOT/FAA/CT-TN90/64
N92-31213 # p 3722 ..... AD-D015290
NAVY-CASE-73519
US-PATENT-APPL-SN-828630
N92-31214* # p 3664 ..... NAS 1.15:107620
NASA-TM-107620
N92-31215* # p 3665 ..... NAS 1.15:107619
NASA-TM-107619
N92-31216* # p 3672 ..... NAS 1.26:189215
NASA-CR-189215
REPT-240-746
N92-31217 # p 3730 ..... CONF-920857-1
DE92-011363
LA-UR-92-897
N92-31218 # p 3600 ..... DE92-015315
WSRC-TR-146
N92-31219 # p 3719 ..... CONF-9109221-6
DE92-016002
FNAL/C-92/129-E
N92-31220 # p 3731 ..... DE92-016208
US-PATENT-APPL-SN-614413
N92-31221 # p 3672 ..... DE92-001282
DOE/METC-92-0276
N92-31222* # p 3736 ..... LPI-CONTRIB-781
NAS 1.26:190178
NASA-CR-190178
N92-31223* # p 3736 ..... NO REPORT NUMBER
N92-31224* # p 3736 ..... NO REPORT NUMBER
N92-31225* # p 3588 ..... NO REPORT NUMBER

N92-31226* # p 3737 ..... NO REPORT NUMBER
N92-31227* # p 3737 ..... NO REPORT NUMBER
N92-31228* # p 3737 ..... NO REPORT NUMBER
N92-31229* # p 3678 ..... NO REPORT NUMBER
N92-31230* # p 3738 ..... NO REPORT NUMBER
N92-31231* # p 3738 ..... NO REPORT NUMBER
N92-31232* # p 3738 ..... NO REPORT NUMBER
N92-31233* # p 3738 ..... NO REPORT NUMBER
N92-31234* # p 3738 ..... NO REPORT NUMBER
N92-31235* # p 3738 ..... NO REPORT NUMBER
N92-31236* # p 3739 ..... NO REPORT NUMBER
N92-31237* # p 3739 ..... NO REPORT NUMBER

Appendix

NASA SCIENTIFIC AND TECHNICAL INFORMATION PROGRAM PRODUCTS AND SERVICES

The NASA Scientific and Technical Information (STI) Program provides for the collection and announcement of aerospace-related reports and literature obtained worldwide through agreements and exchanges. The result of the collection is the comprehensive NASA STI Database that covers aeronautics, space, and supporting disciplines.

The STI Database, documents generated or obtained by NASA, and products and services derived from or supporting the database are made available to the NASA research community and to the public. Descriptions and sources of these items are presented in the following pages.

Scientific and Technical Aerospace Reports (*STAR*) is an abstract journal, listing citations with abstracts for aerospace-related reports obtained from worldwide sources. *STAR* is issued on the 8th and 23rd of each month and announces current documents that have been entered into the NASA STI Database during the previous two weeks. The reports are of the following types:

- NASA, NASA contractor, and NASA grantee reports;
- Reports issued by other U.S. Government agencies, domestic and foreign institutions, universities, and private firms;
- Translations in report form;
- NASA-owned patents and patent applications;
- Other U.S. Government agency and foreign patents and patent applications;
- Domestic and foreign dissertations and theses.

Journal, book, and conference literature, journal translations, and certain foreign dissertations having the same subject scope as *STAR* are announced in a companion journal, *International Aerospace Abstracts* (*IAA*). *IAA* is issued on the 1st and 15th of each month and is available from the American Institute of Aeronautics and Astronautics, Technical Information Service, 555 West 57th Street, 12th Floor, New York, NY 10019.

ELIGIBILITY AND REGISTRATION FOR NASA STI PRODUCTS AND SERVICES

Organizations of the type listed below that have registered with NASA can receive products and services.

- NASA offices and installations, contractors, subcontractors, grantees, and consultants;
- Other U.S. Government agencies and their contractors;
- Libraries in the United States that have arrangements with NASA to maintain collections of NASA documents for public reference;
- Other organizations in the United States having a need for NASA documents in work related to aeronautics and space research;
- Organizations abroad that have established reciprocal documents exchange arrangements with NASA.

The central service points — central points of document acquisition and control within qualified organizations — or individuals are eligible to register for NASA STI products and services. Domestic organizations or individuals may be eligible to receive various classes of NASA publications and services and should address their requests for registration or further information to:

NASA Center for AeroSpace Information
ATTN: Registration Services
P.O. Box 8757
Baltimore, MD 21240-0757
301-621-0390

Organizations abroad should direct requests to:

National Aeronautics and Space Administration
Scientific and Technical Information Program (JTT)
International STI Program
Washington, DC 20546-0001
USA
703-271-5640

SUBJECT SCOPE

The subject scope of *STAR* and *IAA* includes all aspects of aeronautics and space research and development, supporting basic and applied research, and applications. Aerospace aspects of Earth resources, energy development, conservation, oceanography, environmental protection, urban transportation, and other topics of high national priority are also covered.

HOW TO USE *STAR* SUBJECT CATEGORIES

Abstracts in *STAR* are categorized by 10 major subject divisions that are divided further into 76 specific subject categories. The subject divisions and categories are listed in the Table of Contents together with a note for each that defines its scope and provides any cross-references. For example:

16 SPACE TRANSPORTATION
Includes passenger and cargo space transportation, e.g., shuttle operations; and space rescue techniques. For related information see also *03 Air Transportation and Safety* and *18 Spacecraft Design, Testing and Performance.* For space suits see *54 Man/System Technology and Life Support.*

CROSS-REFERENCES

Individual *STAR* abstracts are not ordinarily cross-referenced, except for certain conference reports or book translations that have had separate abstracts written for their component papers or chapters. Citations and abstracts of the components follow immediately after those of the parent document. When the subject content of a component differs sufficiently from the general content of the parent, a cross-reference citation also is printed at the end of the category to which it normally would have been assigned if it were independent.

DOCUMENTS ON MICROFICHE

Documents available on microfiche are designated by a pound sign (#) following the accession number.

LIMITED REPRODUCIBILITY

A note of limited reproducibility appears in the citation, if there are factors affecting the reproducibility of more than 20% of the document. These factors include faint or broken type, color photographs, black and white photographs, foldouts, dot matrix print, or some other factor that limits the reproducibility of the document. This notation also appears on the microfiche header.

COLOR COPIES

An increasing number of NASA scientific and technical reports are being produced with color graphs, charts, illustrations, and photographs. An indication that a document has color pages follows the source and pricing (SAP) information in the *STAR* citation.

Registered users of the NASA Scientific and Technical Information Program will receive ordered documents with color at no additional cost, as long as stock copies of the document are available. Otherwise, an additional fee of $2.00 per color page will be charged. The NASA Center for AeroSpace Information staff will contact registered users to determine individual user's needs.

NASA PATENTS AND PATENT APPLICATIONS

Patents and patent applications owned by NASA are announced in *STAR* under appropriate subject categories and are referenced in the *STAR* indexes. In the Report/Accession Number Index, patents are indexed by the NASA Case Number, and the U.S. Patent Class. Patent applications are indexed by the NASA Case Number and the U.S. Patent Application Serial Number.

Printed copies of patents (which are not microfiched) are available for purchase from the U.S. Patent and Trademark Office.

When ordering patents, the U.S. Patent Number should be used, and payment must be remitted in advance, by money order or check payable to the Commissioner of Patents and Trademarks. Prepaid purchase coupons for ordering are also available from the U.S. Patent and Trademark Office.

NASA patent application specifications are sold in both paper copy and microfiche by the NASA Center for AeroSpace Information (CASI). The N accession number should be used in ordering either paper copy or microfiche from CASI.

The patents and patent applications announced in *STAR* are owned by NASA and are available for royalty-free licensing. Requests for licensing terms and further information should be addressed to:

National Aeronautics and Space Administration
Associate General Counsel for Intellectual Property
Code GP
Washington, DC 20546-0001

SOURCES FOR DOCUMENTS

One or more sources from which a document announced in *STAR* is available to the public is given in each citation. The most commonly indicated sources and their acronyms or abbreviations are listed on page A-6. If the publication is available from a source other than those listed, the publisher and address will be displayed on the availability line or in combination with the corporate source line.

Avail: CASI. Sold by the NASA Center for AeroSpace Information. Prices for hard copy (HC) and microfiche (MF) are indicated by a price code following the letters HC or MF in the *STAR* citation. Current values for the price codes are given in the tables on page A-7.

NOTE ON ORDERING DOCUMENTS: When ordering publications from CASI, use the N accession number or other report number. It is also advisable to cite the title and other bibliographic identification.

Avail: SOD (or GPO). Sold by the Superintendent of Documents, U.S. Government Printing Office, in hard copy.

Avail: BLL (formerly NLL): British Library Lending Division, Boston Spa, Wetherby, Yorkshire, England. Photocopies available from this organization at the price shown. (If none is given, address inquiry to the BLL.)

Avail: DOE Depository Libraries. Organizations in U.S. cities and abroad that maintain collections of Department of Energy reports, usually in microfiche form, are listed in *Energy Research Abstracts.* Services available from the DOE and its de-

positories are described in a booklet, *DOE Technical Information Center - Its Functions and Services* (TID-4660), which may be obtained without charge from the DOE Technical Information Center.

Avail: ESDU. Pricing information on specific data, computer programs, and details on Engineering Sciences Data Unit (ESDU) topic categories can be obtained from ESDU International Ltd. Requesters in North America should use the Virginia address while all other requesters should use the London address, both of which are on page A-6.

Avail: Fachinformationszentrum, Karlsruhe. Gesellschaft für wissenschaftlich-technische Information mbH 7514 Eggenstein-Leopoldshafen 2, Germany.

Avail: HMSO. Publications of Her Majesty's Stationery Office are sold in the U.S. by Pendragon House, Inc. (PHI), Redwood City, CA. The U.S. price (including a service and mailing charge) is given, or a conversion table may be obtained from PHI.

Avail: Issuing Activity, or Corporate Author, or no indication of availability. Inquiries as to the availability of these documents should be addressed to the organization shown in the citation as the corporate author of the document.

Avail: NASA Public Document Rooms. Documents so indicated may be examined at or purchased from the National Aeronautics and Space Administration (JBD-4), Public Documents Room (Room 1H23), Washington, DC 20546-0001, or public document rooms located at NASA installations, and the NASA Pasadena Office at the Jet Propulsion Laboratory.

Avail: NTIS. Sold by the National Technical Information Service. Initially distributed microfiche under the NTIS SRIM (Selected Research Microfiche) are available. For information concerning this service, consult the NTIS Subscription Section, Springfield, VA 22161.

Avail: Univ. Microfilms. Documents so indicated are dissertations selected from *Dissertation Abstracts* and are sold by University Microfilms as xerographic copy (HC) and microfilm. All requests should cite the author and the Order Number as they appear in the citation.

Avail: US Patent and Trademark Office. Sold by Commissioner of Patents and Trademarks, U.S. Patent and Trademark Office, at the standard price of $1.50 each, postage free. (See discussion of NASA patents and patent applications below.)

Avail: (US Sales Only). These foreign documents are available to users within the United States from the National Technical Information Service (NTIS). They are available to users outside the United States through the International Nuclear Information Service (INIS) representative in their country, or by applying directly to the issuing organization.

Avail: USGS. Originals of many reports from the U.S. Geological Survey, which may contain color illustrations, or otherwise may not have the quality of illustrations preserved in the microfiche or facsimile reproduction, may be examined by the public at the libraries of the USGS field offices whose addresses are listed on page A-6. The libraries may be queried concerning the availability of specific documents and the possible utilization of local copying services, such as color reproduction.

FEDERAL DEPOSITORY LIBRARIES: To provide the general public with greater access to U.S. Government publications, Congress established the Federal Depository Library Program under the Government Printing Office (GPO), with 53 regional depositories responsible for permanent retention of material, inter-library loan, and reference services. (These libraries are not sales outlets.) At least one copy of nearly every NASA and NASA-sponsored publication, either in printed or microfiche format, is received and retained by the 53 regional depositories. A list of the regional GPO libraries, appears on page A-8. A local library can contact a regional depository library to help locate specific reports, or direct contact may be made by an individual.

PUBLIC COLLECTION OF NASA DOCUMENTS

An extensive collection of NASA and NASA-sponsored publications is maintianed by the British Library Lending Divison, Boston Spa, Wetherby, Yorkshire, England, for public access. The British Library Lending Division also has available many of the non-NASA publications cited in *STAR*.

European requesters may purchase facsimile copy or microfiche of NASA and NASA-sponsored documents, those identified by both the symbols # and * from ESA—Information Retrieval Service, European Space Agency, 8-10 rue Mario-Nikis, 75738 Paris CEDEX 15, France.

SUBMITTING DOCUMENTS

All users of this abstract service are urged to forward reports to be considered for announcement in *STAR*. This will aid NASA in its efforts to provide the fullest possible coverage of all scientific and technical publications that might support aeronautics and space research and development. If you have prepared relevant reports (other than those you will transmit to NASA, DOD, or DOE through the usual contract- or grant-reporting channels), please send them for consideration to the NASA Center for AeroSpace Information, P.O. Box 8757, Baltimore, MD 21240-0757.

Reprints of journal articles, book chapters, and conference papers are also welcome. These will be considered for announcement in *STAR*'s companion journal, *IAA*.

You may specify a particular source to be included in a report announcement if you wish; otherwise the report will be placed on a public sale at the NASA Center for AeroSpace Information. Copyrighted publications will be announced but not distributed or sold.

PURCHASE OF *STAR*

STAR is publicly available on annual subscription from the NASA Center for AeroSpace Information (CASI) at $114.00.

STAR is available to registered users on annual subscription from the NASA Center for AeroSpace Information, ATTN: Registration Services, P.O. Box 8757, Baltimore, MD 21240-0757.

Microfiche of the abstract sections of *STAR* are available, on annual subscription, from CASI. Annual subscription rates are $216.00 North America; $432.00 foreign.

ADDRESSES OF ORGANIZATIONS

American Institute of Aeronautics and Astronautics
Technical Information Service
555 West 57th Street, 12th Floor
New York, New York 10019

British Library Lending Division,
Boston Spa, Wetherby, Yorkshire,
England

Commissioner of Patents and Trademarks
U.S. Patent and Trademark Office
Washington, DC 20231

Department of Energy
Technical Information Center
P.O. Box 62
Oak Ridge, Tennessee 37830

European Space Agency-Information Retrieval Service
ESRIN
Via Galileo Galilei
00044 Frascati (Rome) Italy

Engineering Sciences Data Unit International
P.O. Box 1633
Manassas, Virginia 22110

Engineering Sciences Data Unit International, Ltd.
251-259 Regent Street
London, W1R 7AD, England

Fachinformationszentrum Karlsruhe
Gesellschaft für wissenschaftlich-technische
Information mbH
7514 Eggenstein-Leopoldshafen 2, Germany

Her Majesty's Stationery Office
P.O. Box 569, S.E. 1
London, England

NASA Center for AeroSpace Information
P.O. Box 8757
Baltimore, Maryland 21240-0757

National Aeronautics and Space Administration
Scientific and Technical Information Program (JTT)
Washington, DC 20546-0001

National Technical Information Service
5285 Port Royal Road
Springfield, Virginia 22161

Pendragon House, Inc.
899 Broadway Avenue
Redwood City, California 94063

Superintendent of Documents
U.S. Government Printing Office
Washington, DC 20402

University Microfilms
A Xerox Company
300 North Zeeb Road
Ann Arbor, Michigan 48106

University Microfilms, Ltd.
Tylers Green
London, England

U.S. Geological Survey Library National Center
MS 950
12201 Sunrise Valley Drive
Reston, Virginia 22092

U.S. Geological Survey Library
2255 North Gemini Drive
Flagstaff, Arizona 86001

U.S. Geological Survey
345 Middlefield Road
Menlo Park, California 94025

U.S. Geological Survey Library
Box 25046
Denver Federal Center, MS914
Denver, Colorado 80225

CASI PRICE TABLES

(Effective October 1, 1991)

STANDARD PRICE DOCUMENTS

PRICE CODE	NORTH AMERICAN PRICE	FOREIGN PRICE
A01	$ 9.00	$ 18.00
A02	12.50	25.00
A03	17.00	34.00
A04-A05	19.00	38.00
A06-A09	26.00	52.00
A10-A13	35.00	70.00
A14-A17	43.00	86.00
A18-A21	50.00	100.00
A22-A25	59.00	118.00
A99	69.00	138.00

MICROFICHE

PRICE CODE	NORTH AMERICAN PRICE	FOREIGN PRICE
A01	$ 9.00	$ 18.00
A02	12.50	25.00
A03	17.00	34.00
A04	19.00	38.00
A06	26.00	52.00
A10	35.00	70.00

IMPORTANT NOTICE

CASI Shipping and Handling Charges
U.S. — ADD $3.00 per TOTAL ORDER
Canada and Mexico — ADD $3.50 per TOTAL ORDER
All Other Countries — ADD $7.50 per TOTAL ORDER
Does NOT apply to orders
requesting CASI RUSH HANDLING.
Contact CASI for charge.

FEDERAL REGIONAL DEPOSITORY LIBRARIES

ALABAMA

AUBURN UNIV. AT MONTGOMERY LIBRARY
Documents Dept.
7300 University Drive
Montgomery, AL 36117-3596
(205) 244-3650 FAX: (205) 244-0678

UNIV. OF ALABAMA
Amelia Gayle Gorgas Library
Govt. Documents
Box 870266
Tuscaloosa, AL 35487-0266
(205) 348-6046 FAX: (205) 348-8833

ARIZONA

DEPT. OF LIBRARY, ARCHIVES, AND PUBLIC RECORDS
Federal Documents
Third Floor State Capitol
1700 West Washington
Phoenix, AZ 85007
(602) 542-4121 FAX: (602) 542-4400; 542-4500

ARKANSAS

ARKANSAS STATE LIBRARY
State Library Services
One Capitol Mall
Little Rock, AR 72201
(501) 682-2869

CALIFORNIA

CALIFORNIA STATE LIBRARY
Govt. Publications Section
914 Capitol Mall - P.O. Box 942837
Sacramento, CA 94237-0001
(916) 322-4572 FAX: (916) 324-8120

COLORADO

UNIV. OF COLORADO - BOULDER
Norlin Library
Govt. Publications
Campus Box 184
Boulder, CO 80309-0184
(303) 492-8834 FAX: (303) 492-2185

DENVER PUBLIC LIBRARY
Govt. Publications Dept. BS/GPD
1357 Broadway
Denver, CO 80203
(303) 571-2135

CONNECTICUT

CONNECTICUT STATE LIBRARY
231 Capitol Avenue
Hartford, CT 06106
(203) 566-4971 FAX: (203) 566-3322

FLORIDA

UNIV. OF FLORIDA LIBRARIES
Documents Dept.
Library West
Gainesville, FL 32611-2048
(904) 392-0366 FAX: (904) 392-7251

GEORGIA

UNIV. OF GEORGIA LIBRARIES
Govt. Documents Dept.
Jackson Street
Athens, GA 30602
(404) 542-8949 FAX: (404) 542-6522

HAWAII

UNIV. OF HAWAII
Hamilton Library
Govt. Documents Collection
2550 The Mall
Honolulu, HI 96822
(808) 948-8230 FAX: (808) 956-5968

IDAHO

UNIV. OF IDAHO LIBRARY
Documents Section
Moscow, ID 83843
(208) 885-6344 FAX: (208) 885-6817

ILLINOIS

ILLINOIS STATE LIBRARY
Reference Dept.
300 South Second
Springfield, IL 62701-1796
(217) 782-7596 FAX: (217) 524-0041

INDIANA

INDIANA STATE LIBRARY
Serials/Documents Section
140 North Senate Avenue
Indianapolis, IN 46204
(317) 232-3678 FAX: (317) 232-3728

IOWA

UNIV. OF IOWA LIBRARIES
Govt. Publications Dept.
Washington & Madison Streets
Iowa City, IA 52242
(319) 335-5926 FAX: (319) 335-5830

KANSAS

UNIV. OF KANSAS
Govt. Documents & Map Library
6001 Malatt Hall
Lawrence, KS 66045-2800
(913) 864-4660 FAX: (913) 864-5380

KENTUCKY

UNIV. OF KENTUCKY LIBRARIES
Govt. Publications/Maps Dept.
Lexington, KY 40506-0039
(606) 257-3139 FAX: (606) 257-1563; 257-8379

LOUISIANA

LOUISIANA STATE UNIV.
Middleton Library
Govt. Documents Dept.
Baton Rouge, LA 70803
(504) 388-2570 FAX: (504) 388-6992

LOUISIANA TECHNICAL UNIV.
Prescott Memorial Library
Govt. Documents Dept.
305 Wisteria Street
Ruston, LA 71270-9985
(318) 257-4962 FAX: (318) 257-2447

MAINE

TRI-STATE DOCUMENTS DEPOSITORY
Raymond H. Fogler Library
Govt. Documents & Microforms Dept.
Univ. of Maine
Orono, ME 04469
(207) 581-1680

MARYLAND

UNIV. OF MARYLAND
Hornbake Library
Govt. Documents/Maps Unit
College Park, MD 20742
(301) 454-3034 FAX: (301) 454-4985

MASSACHUSETTS

BOSTON PUBLIC LIBRARY
Govt. Documents Dept.
666 Boylston Street
Boston, MA 02117
(617) 536-5400 ext. 226
FAX: (617) 267-8273; 267-8248

MICHIGAN

DETROIT PUBLIC LIBRARY
5201 Woodward Avenue
Detroit, MI 48202-4093
(313) 833-1440; 833-1409
FAX: (313) 833-5039

LIBRARY OF MICHIGAN
Govt. Documents Unit
P.O. Box 30007
Lansing, MI 48909
(517) 373-0640 FAX: (517) 373-3381

MINNESOTA

UNIV. OF MINNESOTA
Wilson Library
Govt. Publications Library
309 19th Avenue South
Minneapolis, MN 55455
(612) 624-5073 FAX: (612) 626-9353

MISSISSIPPI

UNIV. OF MISSISSIPPI
J.D. Williams Library
Federal Documents Dept.
106 Old Gym Bldg.
University, MS 38677
(601) 232-5857 FAX: (601) 232-5453

MISSOURI

UNIV. OF MISSOURI - COLUMBIA
Ellis Library
Govt. Documents
Columbia, MO 65201
(314) 882-6733 FAX: (314) 882-8044

MONTANA

UNIV. OF MONTANA
Maureen & Mike Mansfield Library
Documents Div.
Missoula, MT 59812-1195
(406) 243-6700 FAX: (406) 243-2060

NEBRASKA

UNIV. OF NEBRASKA - LINCOLN
D.L. Love Memorial Library
Documents Dept.
Lincoln, NE 68588
(402) 472-2562

NEVADA

UNIV. OF NEVADA
Reno Library
Govt. Publications Dept.
Reno, NV 89557
(702) 784-6579 FAX: (702) 784-1751

NEW JERSEY

NEWARK PUBLIC LIBRARY
U.S. Documents Div.
5 Washington Street - P.O. Box 630
Newark, NJ 07101-0630
(201) 733-7812 FAX: (201) 733-5648

NEW MEXICO

UNIV. OF NEW MEXICO
General Library
Govt. Publications Dept.
Albuquerque, NM 87131-1466
(505) 277-5441 FAX: (505) 277-6019

NEW MEXICO STATE LIBRARY
325 Don Gaspar Avenue
Santa Fe, NM 87503
(505) 827-3826 FAX: (505) 827-3820

NEW YORK

NEW YORK STATE LIBRARY
Documents/Gift & Exchange Section
Federal Depository Program
Cultural Education Center
Albany, NY 12230
(518) 474-5563 FAX: (518) 474-5786

NORTH CAROLINA

UNIV. OF NORTH CAROLINA - CHAPEL HILL
CB#3912, Davis Library
BA/SS Dept.—Documents
Chapel Hill, NC 27599
(919) 962-1151 FAX: (919) 962-0484

NORTH DAKOTA

NORTH DAKOTA STATE UNIV. LIBRARY
Documents Office
Fargo, ND 58105
(701) 237-8886 FAX: (701) 237-7138
In cooperation with Univ. of North Dakota, Chester Fritz Library
Grand Forks

OHIO

STATE LIBRARY OF OHIO
Documents Dept.
65 South Front Street
Columbus, OH 43266
(614) 644-7051 FAX: (614) 752-9178

OKLAHOMA

OKLAHOMA DEPT. OF LIBRARIES
U.S. Govt. Information Div.
200 NE 18th Street
Oklahoma City, OK 73105-3298
(405) 521-2502, ext. 252, 253
FAX: (405) 525-7804

OKLAHOMA STATE UNIV.
Edmon Low Library
Documents Dept.
Stillwater, OK 74078
(405) 744-6546 FAX: (405) 744-5183

OREGON

PORTLAND STATE UNIV.
Millar Library
934 SW Harrison - P.O. Box 1151
Portland, OR 97207
(503) 725-3673 FAX: (503) 725-4527

PENNSYLVANIA

STATE LIBRARY OF PENN.
Govt. Publications Section
Walnut St. & Commonwealth Ave. - P.O. Box 1601
Harrisburg, PA 17105
(717) 787-3752

SOUTH CAROLINA

CLEMSON UNIV.
Cooper Library
Public Documents Unit
Clemson, SC 29634-3001
(803) 656-5174 FAX: (803) 656-3025
In cooperation with Univ. of South Carolina, Thomas Cooper Library, Columbia

TENNESSEE

MEMPHIS STATE UNIV. LIBRARIES
Govt. Documents
Memphis, TN 38152
(901) 678-2586 FAX: (901) 678-2511

TEXAS

TEXAS STATE LIBRARY
United States Documents
P.O. Box 12927 - 1201 Brazos
Austin, TX 78711
(512) 463-5455 FAX: (512) 463-5436

TEXAS TECH. UNIV. LIBRARY
Documents Dept.
Lubbock, TX 79409
(806) 742-2268 FAX: (806) 742-1920

UTAH

UTAH STATE UNIV.
Merrill Library & Learning Resources Center, UMC-3000
Documents Dept.
Logan, UT 84322-3000
(801) 750-2684 FAX: (801) 750-2677

VIRGINIA

UNIV. OF VIRGINIA
Alderman Library
Govt. Documents
Charlottesville, VA 22903-2498
(804) 924-3133 FAX: (804) 924-4337

WASHINGTON

WASHINGTON STATE LIBRARY
Document Section
MS AJ-11
Olympia, WA 98504-0111
(206) 753-4027 FAX: (206) 753-3546

WEST VIRGINIA

WEST VIRGINIA UNIV. LIBRARY
Govt. Documents Section
P.O. Box 6069
Morgantown, WV 26506
(304) 293-3640

WISCONSIN

ST. HIST. SOC. OF WISCONSIN LIBRARY
Govt. Publications Section
816 State Street
Madison, WI 53706
(608) 262-2781 FAX: (608) 262-4711
In cooperation with Univ. of Wisconsin-Madison, Memorial Library

MILWAUKEE PUBLIC LIBRARY
Documents Div.
814 West Wisconsin Avenue
Milwaukee, WI 53233
(414) 278-2167 FAX: (414) 278-2137

*U.S. G.P.O.:1992-342-599:60021

National Aeronautics and
Space Administration
Code JTT
Washington, D.C.
20546-0001

Official Business
Penalty for Private Use, $300

SPECIAL FOURTH-CLASS RATE
POSTAGE & FEES PAID
NASA
PERMIT No. G27

NASA

POSTMASTER: If Undeliverable (Section 158
Postal Manual) Do Not Return